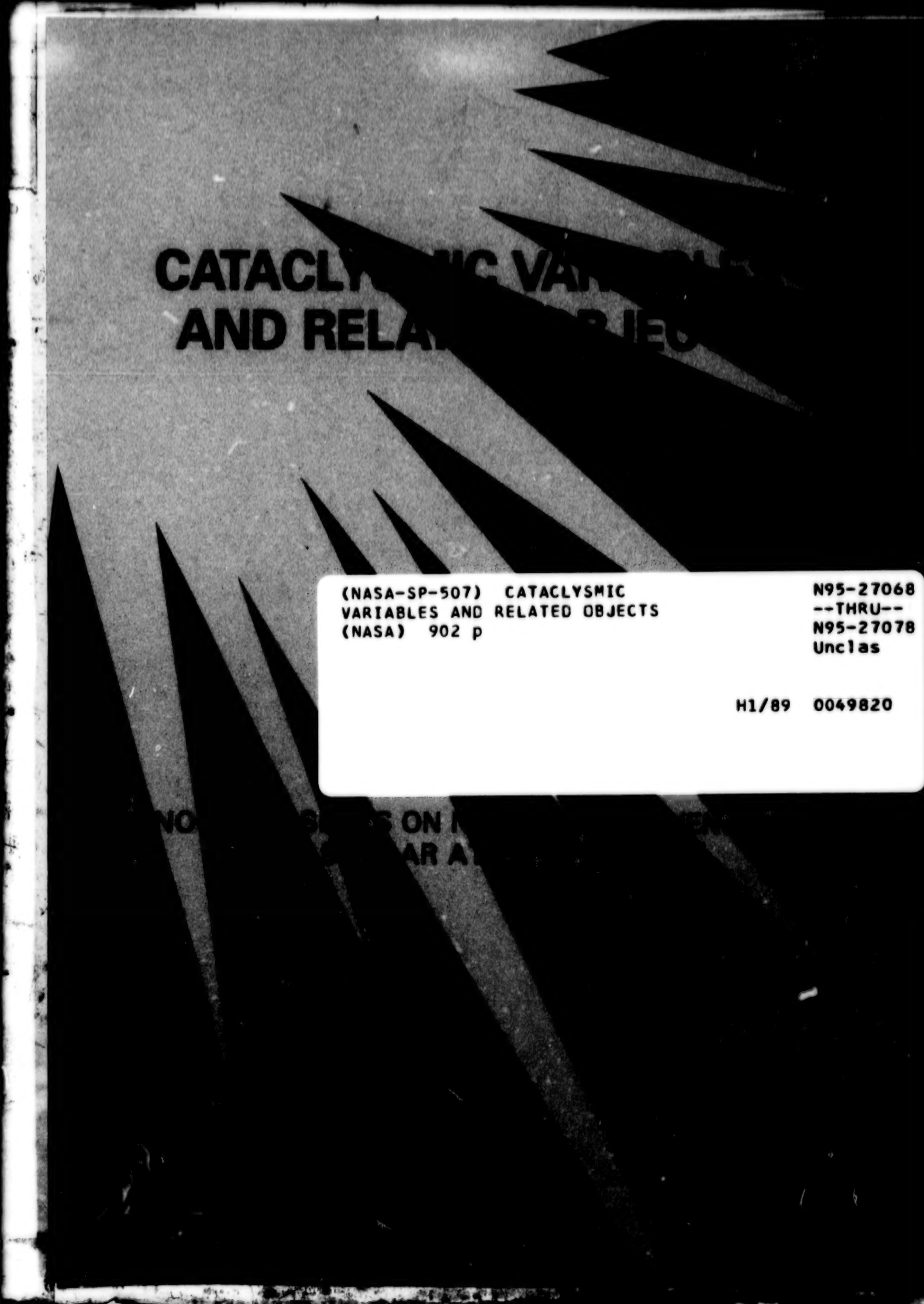


(NASA-SP-507) CATACLYSMIC VARIABLES AND RELATED OBJECTS (NASA) 902 p

N95-27068
--THRU--
N95-27078
Unclas

H1/89 0049820

CATACLYSMIC VARIABLES AND RELATED OBJECTS

Library of Congress Cataloging-in-Publication Data

Hack, Margherita,
Cataclysmic variables and related objects / by Margherita Hack and Constanze la Dous.
p. cm. -- (NASA SP : 507)
"September 1993."
Includes bibliographical references and index.
Supt. of Docs. no.: NAS 1.21:507
1. Cataclysmic variable stars. I. Title II. Series.
QB835.H27 1993 92-7619
523.8'446--dc20 CIP

For sale by the Superintendent of Documents,
U.S. Government Printing Office, Wasington, DC 20402

NASA SP-507

MONOGRAPH SERIES ON NONTHERMAL PHENOMENA
IN STELLAR ATMOSPHERES

CATACLYSMIC VARIABLES AND RELATED OBJECTS

Margherita Hack
Constanze la Dous

Stuart Jordan, Solar Physics
Editor/Organizer and American Coordinator

Richard Thomas, Stellar/Solar
Editor/Organizer and European Coordinator

Leo Goldberg*
Senior Adviser to NASA

Jean-Claude Pecker
Senior Adviser to CNRS

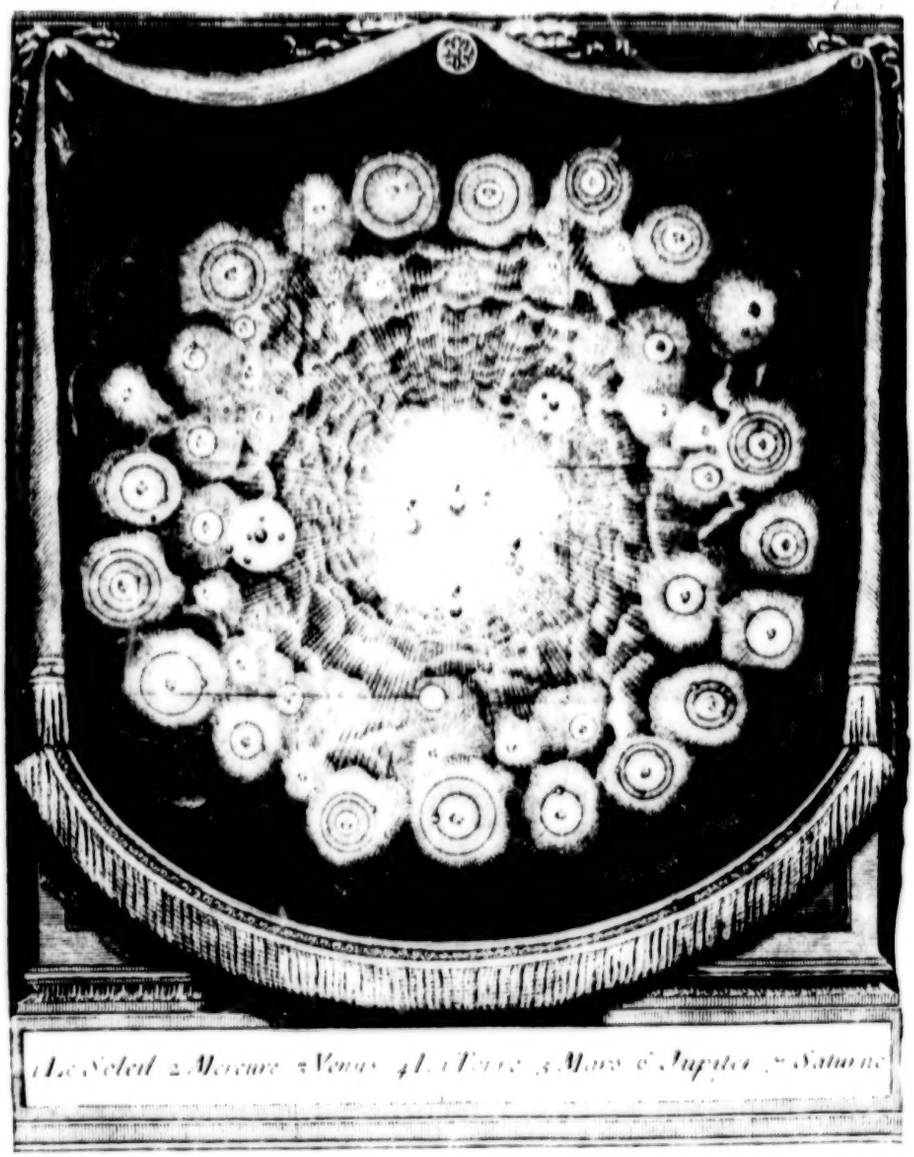


Centre National de la
Recherche Scientifique
Paris, France

1993

NASA
National Aeronautics and
Space Administration
Scientific and Technical
Information Branch
Washington, D.C.

*Deceased 1987



... **Assurons-nous bien du fait, avant que de nous inquiéter de la cause. Il est vrai que cette méthode est bien lente pour la plupart des gens, qui courent natuellement à la cause, et passent par dessus la vérité du fait; mais enfin nous éviterons le ridicule d'avoir trouvé la cause de ce qui n'est point.**

...

...

... **De grands physiciens ont fort bien trouvé pourquoi les lieux souterrains sont chauds en hiver, et froids en été; de plus grands physiciens ont trouve depuis peu que cela n'était pas.**

—Fontenelle, Histoire des Oracles
Chapitre IV, pp. 20 et 23

DEDICATION

in grateful appreciation
we dedicate this series and these volumes

to *Cecilia Payne-Gaposchkin*, who, with Sergei, set the spirit of empirical-theoretical atmospheric modeling by observing:

> "All true variable stars have variable atmospheres, but a variable atmosphere is probably the property of all stars, whether obviously variable in brightness or not [as witness the solar envelope]";

and who, by her intimate knowledge of particular stars, pioneered in the recognition of the fundamental importance of "individuality of stellar atmospheric characteristics."

to *Daniel Chalonge*, who sought, by ingenious meticulous observations, to make quantitative the features of qualitative classical taxonomy, thereby laying the foundations of showing the inadequacy of its two-dimensional, single-region atmospheric, character;

and who always opposed the spirit of a distinguished theoretical colleague's remark:

> "Don't show me those new observations of yours; they inhibit the range of my speculations."

PREFACE

This book, Cataclysmic Variables and Related Objects, is the final volume in the NASA/CNRS monograph series on nonthermal stellar atmospheres. Looking back over the eight volumes, we note with some satisfaction that the series has hewed close to its original objective of emphasizing, to quote from the preface of the first volume, "observational data and possible physical mechanisms, critically examined, much more than formal atmospheric models and detailed computational procedures." Certainly that is the main thrust of this final volume.

At the same time, much has changed over the twelve years since the first volume appeared, both in the rapid advances that have occurred in stellar astronomy as well as in the procedures for producing the books, for which NASA has been responsible. It is only fair to the editors and authors of this final book to note that one consequence of these recent changes in NASA has been a significant and regrettable delay in its date of publication. As the NASA organizer for this series, I can assert that the source of this delay has been almost entirely budgetary and not in the persons who have tried to expedite the process, often with no money; but this is small consolation for editors and authors who worked hard to have their manuscripts ready by 1989, only to have to wait until 1993 to see the book in print. Professionals in the field must admire the patience and forbearance of these astronomers. I certainly do. One consequence of the delay is that the material in this book does not cover the developments of the early 1990s. To the observation that a section covering the last three years could have been added I must say that this would have occasioned even further delays, an alternative clearly to be avoided.

Notwithstanding the delay, this volume contains a rich assembly of data, along with their possible interpretation, on a particularly fascinating class of stellar objects. As has been our experience with previous volumes, we hope that this approach will prove useful to students and researchers worldwide, who are usually more interested in confronting the observations directly than in starting with complex theoretical models as a basis for their own research. NASA will oversee a large distribution of the book in the western hemisphere, and the French CNRS will serve a similar function in the eastern one. To get an overview of the highlights of the book, the French and English summaries provided at the beginning are a good place to start.

Since this monograph series now comes to a end, it is fitting to recognize a number of individuals who have played key roles in its production. There is no question where to begin. Richard N. Thomas, justly famed as the prime mover of early non-LTE theory as applied to optically thick spectral lines, is the father of this series. Highly original and insightful, often iconoclastic, occasionally infuriating, but always stimulating and completely committed to the advancement of astronomy and astronomers, Dick Thomas, as so many of us know him, was the powerful engine behind this series. He inspired and started it. He shepherded its development like a jealous, absolutely dedicated parent. For the final four volumes, he provided a Perspective section, both to relate the objects treated in each book to others across the HR diagram and, in some cases, to suggest alternative viewpoints to those emphasized by the authors. And when in his perception some part of a book was running thin, he participated directly in stimulating a renewed effort to produce volumes that have to date been well received by the worldwide community of astronomers. First and foremost among those we thank is Dick Thomas, without whom there would have been no series.

In France, the valuable collaboration with the CNRS, essential to the international character of the series, was due almost entirely to the efforts of Jean-Claude Pecker, distinguished astronomer, former IAU

PRECEDING PAGE BLANK NOT FILMED

Secretary General, and current member of l'Academie de Sciences, who set up the project from the French end. The constant cooperation of the French government and the enthusiastic participation of a number of the European astronomers who served as editors and authors can often be traced to these initial arrangements. It can truly be said that this particular series, at least, would not have materialized without him.

Those of us closely connected with the series all mourn the loss of Leo Goldberg, who served us all as friend and counsellor (officially as the Senior Advisor to NASA) until his death in 1987. In a project of this nature, some difference of opinion on procedure is bound to occur as the work progresses, and he was especially skilled in helping us all resolve some of the issues that arose. We miss him and are grateful for his contributions.

Beyond the three aforementioned persons are those others without whom the series could not have been produced. They are, of course, the editors and authors of the various volumes. Since the service of science, in this case astronomical science, is the only justification for this project in the broader sense, so it is to the scientists themselves who wrote the text that the greatest collective thanks must be given, for only they had and have the expertise that gives these volumes credibility and value. It is especially noteworthy that all of the editors and authors, without exception, provided their manuscripts - which is to say their valuable time - without compensation from the funding agencies for that purpose, and with no hope of royalties from any book sales that might occur. Their efforts were entirely a service to astronomy, and for that we are all in their debt.

Finally, there is a long list of individuals within NASA who have supported the series in a number of important ways, ranging from the provision of funds for the copy editing and printing to expediting the process itself. As the project has been over twelve years in duration, the list is fairly long, and undoubtedly incomplete; but the following individuals must be included: Dave Bohlin, Jack Brandt, Harold Glaser, Betty Graham, Virginia Kendall, Frank Martin, George Peiper, Karen Simon, Jim Trainor, Kay Voglewede, and Ed Weiler. Most recently, on this book, Erwin Schmerling at NASA Headquarters and Lee Blue and Bob Ferris at the Center for Aerospace Information have been extremely helpful in removing the final obstacles to completing the book on a very restricted budget.

The series has benefitted enormously from the contributions of all of the persons mentioned, and a great many more. It is hoped that the astronomers who use these books will benefit accordingly.

The NASA Series Editor/Organizer
Greenbelt, April 1993

CONTENTS

Chapter	*Page*
Perspective	xiii
Resume	xxix
Summary	lxiii
1 Introduction *Margherita Hack and Constanze la Dous*	1
I. Nomenclature and Classification	1
II. The Big Picture and the Plan of the Book	2
III. General Physical Properties of Cataclysmic Variables	3
IV. Selection Effects	6
V. A Statistical View of Novae, Dwarf Novae, and Nova-like Stars	7
Part I DWARF NOVAE AND NOVA-LIKE STARS *Constanze la Dous*	
2 Dwarf Novae	15
I. Classification	15
II. Photometric Observations	21
III. Spectroscopic Observations	65
3 Nova-like Variables	95
I. Definition and General Characteristics	95
II. UX Ursae Majoris Stars	96
III. Anti-Dwarf Novae	102
IV. DQ Herculis Stars	112
V. Photometric Appearance	125
VI. AM Canum Venaticorum Stars	140
4 Models for Various Aspects of Dwarf Novae and Nova-like Stars	145
I. History of Modeling	145
II. Modern Interpretation	150
III. The Accretion Disc	164
IV. Modeling the Observed Spectra	192
V. The Evolutionary State of Cataclysmic Binaries	214
5 Summary	233
References (Part I)	237

Part II CLASSICAL NOVAE AND RECURRENT NOVAE

6 Classical Novae and Recurrent Novae: General Properties
Margherita Hack, Pierluigi Selvelli, and Hilmar Duerbeck 261

I. Introduction 261
II. Photometric Properties 262
III. Spectroscopic Properties 281
IV. Infrared Observations of Novae 300
V. Ultraviolet Observations of Novae and Recurrent Novae 315
VI. The X-Ray Emission of Novae and Recurrent Novae 342
VII. Final Decline and Nova Envelopes 346
VIII. Radioastronomical Observations of Nova Envelopes 366

7 Models of Classical and Recurrent Novae
Michael Friedjung and Hilmar Duerbeck 371

I. Introduction 371
II. Short History 374
III. Simple Models to Explain Observations 382
IV. Empirical Approach 392
V. Causes of Nova Outbursts 406

8 Typical Examples of Classical Novae
Margherita Hack, Pierluigi Selvelli, Antonio Bianchini, and Hilmar Duerbeck 413

I. Introduction 413
II. V 1500 Cygni: A Very Fast Nova 414
III. V 603 Aql: An Historic Survey 426
IV. CP Pup 438
V. GK Per 1901 443
VI. V 1668 Cygni 1978: a Moderately Fast Nova 460
VII. FH Ser 470
VIII. DQ Her 1934: a Slow Nova 475
IX. The Old Nova T Aur 1891 487
X. RR Pic 490

9 Recurrent Novae
Margherita Hack and Pierluigi Selvelli 511

I. The Known Recurrent Novae 511
II. U Sco 513
III. T Pyxidis 519
IV. RS Ophiuchi 523
V. V 1017 Sagittarii 542
VI. T Coronae Borealis 543
VII. Conclusions 558

10 Summary
Margherita Hack and Michael Friedjung 561

I. The Observations 561
II. The Theories 563

References (Part II) 567

Part III SYMBIOTIC STARS

11 Overview of the Observations of Symbiotic Stars
Roberto Viotti 583

I. Introducing the Symbiotic Stars 583
II. General Overview of the Observations 585
III. The Light History of Symbiotic Stars 585
IV. The Visible Spectrum 592
V. Polarization 603
VI. Infrared Observations 605
VII. Radio Observations 613
VIII. The Ultraviolet Spectrum of Symbiotic Stars 619
IX. X-Ray Observations of Symbiotic Stars 634
X. Summary of the Observations 638

12 Models of Symbiotic Stars
Michael Friedjung 647

I. General Considerations 647
II. History and Overview of Simple Models 647
III. Single Star Models 649
IV. Binary Models 652

13 Discussion on Selected Symbiotic Stars
Roberto Viotti and Margherita Hack 663

I. Introduction 663
II. Z Andromedae and the Diagnostics of the Symbiotic Stars 663
III. The High-Velocity Symbiotic Star AG Draconis 674
IV. The Symbiotic Novae 683
V. R Aquari: A Symbiotic Mira with a Jet 693

14 Summary of Our Present Knowledge about Symbiotic Stars
Michael Friedjung and Roberto Viotti 727

I. Symbiotic Stars as Interactive Binaries 727
II. Nature of the Components of the Symbiotic Systems 728
III. Emission Lines 729
IV. Chemical Composition 729
V. Variability 730
VI. Nebulae 731

References (Part III) 733

15 Perspectives and Unsolved Problems
Michael Friedjung, Margherita Hack, Constanze la Dous, and Roberto Viotti 749

Subject Index 757

Star Index 763

List of Contributing Authors 769

PERSPECTIVE

I. HISTORIC OBSERVATIONAL PERSPECTIVE ON CV-PROTOTYPE STARS

"Star swells up and bursts" (then, more gradually, returns to an essentially unchanged pre-outburst state) was the historic, observation-delineated, abstract/caricature of the phenomena whose episodic occurrence defined the original prototypes of the cataclysmic variable (CV) class of stars—novae and recurrent novae. Such phenomena/stars gave this class, via the Gaposchkins, its descriptive title. Other "similar" varieties of stars, defined by lesser amplitudes and more frequent recurrance of an "outburst", and/or by (variable) spectral features resembling those of some outburst phases, were later added to the CV class. Often, it was/is ambiguous whether some particular star belongs to the CV class via one of its later added varieties, or to some other class, such as the Be, that exhibits overlapping aspects of variability with the CV. Thus the CV class, and its "cousins", strongly stimulate curiosity to identify a thermodynamics able to represent a variety of large-variability aspects of stellar taxonomy/structure/evolution, so more encompassing than Eddington's variety, which was only quasi-adequate for even "equilibrium" stars.

In pre-spectroscopy history, this primary "cataclysmic" observational characteristic of novae/recurrent-novae was: very large (factor 10^2-10^7), transient (weeks through months duration), episodic (decades through centuries recurrence interval), unpredictable, luminosity increases. Later, the introduction of spectroscopic observations showed a mass ejection simultaneously paralleling the luminosity outburst, exhibiting several, often overlapping, evolving sets of large-blue-shifted spectral lines; first absorption, then emission-absorption profiled (P Cyg-type), then wholly emission. Overall, this ensemble of spectral lines (including all varieties introduced by their time variation, which include the forbidden-transition solar coronal lines) presents a symbiotic melange of low- and super-ionized species. Also in parallel evolution, during its premaximum rise the continuum monotonically reddens; post-maximum, it monotonically blues.

Thus, as the variety and breadth of observations evolved, so emerged/evolved the two simultaneous/associated/parallel primary observational characteristics of the nova/recurrent-nova prototype of the CV class: abruptly enhanced luminosity, abruptly appearing ultrathermal mass outflow. But that energy liberation resulting in luminosity enhancement appears to occur sufficiently deeply in the star that it undergoes that diffusive radiative-transfer—not direct—escape which causes the overlying layers to approximate the spectral appearance of a "normal", *supergiant*, stellar atmosphere whose flux/effective temperature evolves in time. So the pre-maximum time-scale of radiation *quality* (color) differs from that of radiation *quantity* (luminosity) via the time-scale of the outward motion of the $t\lambda\sim1$ levels corresponding to the mass outflow. There also evolved an elaboration of the details, and an appreciation of the significance, of the third basic characteristic of the CV class: the time unfolding of the "symbiotic" spectrum, whose pervasiveness across the class, and community with other classes, is today more often emphasized than is that of the *double*-aspect cataclysmic-outburst.

Other "peculiar" stars historically exhibited some variety of mass outflow; other exhibited strong luminosity excess and variability. But at least until the advent of far-UV observations, via space observatories, no variety of stars exhibited, so unambiguously, an association between (apparent) onset of strong mass outflow and strong luminosity variability as did novae/recurrent novae— essentially because of the

PRECEDING PAGE BLANK NOT FILMED

large velocity shifts observeable in their visual-spectral lines, which made their mass outflow, aerodynamic mass loss, unmistakably clear.

WR stars have long shown the clearest such visual-spectral association between unusually large values of both luminosity and mass outflow, but in steady-state values of each (so were historically called the "permanent novae"). P Cygni, once classed as a "nova (Cyg 1600)", and now linked to the Luminous-Blue-Variables, shows large visual-spectral mass outflow, but its twice observed luminosity outbursts were pre-spectral and smaller than novae. Visual-spectral observations of the "envelope/nebulae" of PN stars evince historic mass ejection, but no accompanying luminosity-change measures exist. The Be stars—McLaughlin's "little PN"—are the closest, in such historic empirical association between *enhanced* luminosity and mass outflow, but only *implied* such association, because velocity measures were only of envelope-, not of photospheric-chromospheric-coronal-, matter at those visual-spectral-only epochs, and then only when one painstakingly collected and diagnosed all retrievable historic data (cf Doazan, Volume 2 of this series.

Over the IUE decade, coordinated visual and farUV observations have established, not just implied, for some Be stars, at some epochs, such unambiguous association between changes in (pre-envelope, high-velocity) mass outflow and luminosity—as well as associated changes in other spectral features, which detail the outward evolution of the mass outflow. This latter includes the behavior/role of the envelope as a "regulating-valve" between the mass outflow and mass loss. Far-UV measures also show still existing, high-velocity, pre-envelope mass outflow from the central stars of the PN. One observes, in the far-UV, the same high-velocity outflow from some recurrent novae, decades after outburst. Thus a bridge between CV and other classes exists, in the stellar-structural implication of this primary CV characteristic: episodic, "cataclysmic", energy/mass loss.

For novae/recurrent novae, time-resolution of these two (mass outflow, luminosity variability) aspects of the episodic phenomenon was/is yet insufficient to show which, if either, "begins first", hence might be considered to be the "more fundamental", especially because each differs/evolves with the particular geometrical and spectral region observed. The same ambiguity yet exists in the relative behavior of luminosity and outflow at the *photospheric* level in the Be stars—it and sub-photospheric levels being the essential ones in discussing origin of outburst, in single-star modeling. Other cousins' time-resolution is even less.

In stellar types of the currently defined CV class other than the novae/recurrent novae, such association between mass outflow and luminosity changes has (apparently, according to the authors/material collected in this CV volume) not yet been sufficiently documented in high-resolution detail to synthesize into any unambiguous picture of their relation/interaction/structural resultant. But those "theories"/models of the CV class that a priori vastly subordinate mass ejection to luminosity outburst—or worse, model the CV phenomenon as consisting only of a luminosity outburst without mass outflow, as in some CV theoreticians' speculative models of dwarf novae (contradicted by observation)—obscure useful empirical-thermodynamic information/guidance. Such information, digested without a priori prejudice, broadens our knowledge of the variety/range of mass outflow from stars, and of the relative significance of mass and radiative-energy losses on the modeling of stellar structure/evolution (see Table 1, at the end of this Perspective Chapter).

Of course, one has a diagnostic choice in trying to use "normal", "peculiar", other than CV, and CV stars to gain insight/detailed knowledge of this "now ubiquitous" phenomenon of stellar mass loss and its general relation (if any) to stellar radiative-energy loss. Either one can take literally all the cited links between CV and other stellar types re phenomena of mass outflow and luminosity variability, or one

can insist that CV phenomena are too exceptional to permit CV stars to be included in the variety of single stars. Under the first alternative, one regards the CV stars as simply exhibiting extreme varieties of the mass/energy-loss phenomenon in single-stars. Under the second, one regards the class as indeed exceptional, in having no thermodynamic relation to any variety of single-star mass loss and/or luminosity enhancement; so it must be diagnosed and modeled outside single-star taxonomy.

Especially given the complete reversal of most thinking on single-star mass loss introduced by space-observatory data, one would prefer an observation-based rather than an a priori speculative choice between the above alternatives. So I am surprised at the volume's choosing the later included, less extensively delineated re mass outflow, dwarf novae—rather than the prototype, more observationally detailed, novae/recurrent novae—to introduce the panorama of, and put into perspective, the CV class of stars. Possibly this choice previews/reflects the volume's omission of single-star pictures, and of associated phenomena observed in single-star "cousins", in its discussion of models for CV-type stars. Such a priori modeling restriction implies the a priori exclusion of CV stars/phenomena from being part of the data-basis for understanding the significance of intrinsic mass loss from single stars, and its sometimes strong variability, often associated with that of stellar luminosity, in modeling stellar structure and evolution. *We understand stellar thermodynamics too incompletely to a priori exclude any data or any diagnostic alternatives.*

Such stellar mass loss, historically observed in the visual spectrum of only a few peculiar stars, has now been observed in the nonvisual spectrum of a wide variety of stars from space telescopes, especially in the far-UV. Indeed, mass loss of some size is now recognized to be a property of essentially all stars, paralleling the radiative-loss, but of yet generally unknown origin. Thus the distinguishing aspect of the mass-loss component of the outbursts characistic of CV-prototype stars is not the mass loss itself, but its episodically cataclysmic character—simultaneously parallel to that of the luminosity.

Today, from the standpoint of observational/empirical stellar thermodynamics, it would appear that one can no more construct a nova/recurrent-nova structural model that focuses only on the luminosity outburst than one can construct a "normal" star model that focuses only on luminosity and subordinates mass loss (see again Table 1). Of course, as do the authors of this volume, one can always try to redefine the CV class in terms of speculative models, in which a mass outflow *from* the system is not basic to the configuration producing a "CV system". The problem is how to adapt such speculative-model-based classification to the framework of historic observation-based stellar taxonomy, which is slowly evolving to embrace the higher resolution, visual and nonvisual, observations, and the broader thermodynamics, of today's astronomy—in order to include real-world novae/recurrent novae/"cousins" where mass outflow is apparently basic, and parallel to radiative-energy outflow, in modeling stellar structure/evolution.

II. CV MODELING PERSPECTIVE FROM: SINGLE-STAR INTERPRETATION/REPRESENTATION OF CATACLYSMIC-SYMBIOTIC VARIABILITY; NON-EDDINGTON-THERMODYNAMIC MODELING OF UNIVERSAL STELLAR MASS LOSS AND MULTI-REGIONAL ATMOSPHERIC STRUCTURE; SPECULATIVE BINARY MASS-INTERCHANGE MODELING.

Empirically, thus, arose the historic nova picture, wholly based on the visual-spectral observations/characteristics. According to it, the star abruptly ejects, at ultra-thermal speed (from unknown cause), an outer layer of small (10^{-3}-10^{-6} solar) mass, but very large opacity. Modern far-UV observations suggest modifying this picture only by regarding the outburst as an enhancement, not initiation, of an existing, smaller, mass outflow. To first approximation, the increasing luminosity simply reflects the increasing surface area of an expanding, optically thick, time-constant radiative-flux,

photosphere. To better approximation, the expanding envelope: (i) exhibits a radiative flux that decreases slowly relative to the luminosity increase; (ii) so, during its opaque phase, shows a "photosphere" cooling from "hot" (OB) to "cool" (FG); (iii) decreases its opacity to eventually reveal "hot" non-ejected layers, which become the "photosphere", and whose "T" reflect their radiative flux and radius, during the following "quiet" phase.

If this picture reflects reality, an understanding of the thermodynamics underlying it is invaluable in understanding the origin and outward propagation of stellar mass outflow/loss generally, and its relation to the radiative energy loss/luminosity. An understanding of what fixes the thickness/depth/mass of the expelled layer is an essential step in understanding the size of such mass loss, and its variability. The same is true, relative to what determines that (luminosity, radius) relation, and its time-variation, which produces the slow radiative-flux decrease during the initial expansion/outburst, in order to progress in understanding what produces such strong luminosity (integrated flux) variability.

The evolving line spectrum progressively delineates the several regions of the nova/recurrent-nova variety of those "differentially outflowing/evolving, extended multi-regioned atmospheres" which, even at historic pre-space epochs, were also variously observed in the visual spectra of other varieties of mass-outflowing peculiar stars. With the exception of the Sun, Be stars, and novae, those peculiar stars were mainly supergiants and giants, and these phenomena were considered to be anomalies of "extended atmospheres" of stars off the main sequence (in structure and evolutionary stage). Thanks to eclipse observations of the Sun, a multi-region "supergiant-similar" extended atmospheric structure for main-sequence stars was gradually detailed in pre-space years; solidified by space observations; and attributed to the effects of nonradiative fluxes: energy, for nonradiative heating/thermal extension; mass, for aerodynamic extension. For Be stars and PN, such structure was historically restricted to mass-ejected envelopes. Now, via far-UV observations, a solar-type hot sub-envelope, capped by a very extended cool envelope, atmospheric structure becomes recognized. So we also realize that a similar multi-regioned atmospheric structure, whose mass/energy distribution evolves in time with the varying mass and energy fluxes, may underlie the novae/recurrent-novae third distinguishing characteristic: their time-dependent "symbiotic spectrum". Again, this would link the atmospheric and thermodynamic structure of the CV class to that structure/thermodynamics increasingly identified in a variety of single stars (cf Thomas, Volume 4 of this series).

Such "increasingly popular" multi-regioned structure, resting on admitting a variety of fluxes from a star and adopting a broad nonEquilibrium thermodynamic structural representation for them and their propagation, strongly contrasts to that single-regioned neo-classical one that is produced by only a radiative-energy flux, under that "quasi-Equilibrium" standard modeling introduced by Eddington (1930). So clearly, any diagnostic discussion of such symbiotic spectral features should include consideration of their implications on the several alternatives for atmospheric structure, and on the variety of (nonEquilibrum) thermodynamics required to represent it. Simply applying archaic diagnostics and thermodynamics to current data hardly produces reliable results.

Earlier volumes in this series compared, in varied detail, such alternative models, and some symbiotic features. The latter are too often underemphasized, reflecting evolving controvery on the general presence/effect of dissipative non-radiative energy fluxes (of Volumes 4 and 6 of this series). Nonetheless, single-star models strongly-departing from Eddington-standard ones are generally adopted: (1) nonLTE is routinely included; (2) although theories of its origin and size are controversial, single-star mass outflow and its perturbation on atmospheric models is widely explored; (3) primary incompletness is (a) too often adopting RE and (b) generally ignoring the implications/effects of variability (of Vol-

umes 2, 4, 6, and 7 of this series).

By contrast, Section III of the Introductory Chapter of the present volume presents the symbiotic features, and irregular luminosity variability, as the only common physical properties of CV stars, without commenting on any possible relation of these to multi-regional single-star atmospheres. Also by contrast, the mass-*out*-flow characteristic of whatever stars compose the CV system is treated curiously. It is unmentioned, except to suggest that it may, in some cases, provide the origin of the necessary mass transfer. "Curiously", because if so, the rationale for a close-binary, Roche-instability, vanishes. An episodic cataclysmic outburst is not identified as a possible common *physical* property of CV *stars*, only as something observed in a CV *system*, which the (speculative) basic characteristic of the CV system—a mass *inflow* to the "erupting" star—will explain/model. The role of that multi-regioned atmosphere increasingly found in even "normal" stars, its relation to the observed symbioticity, its modification by the "companion", by *its* multi-regioned structure, and by binary mass exchange—none of these are discussed in the present volume.

The last 40 years' revolution in normal-star models and its space-data support are not much used to re-examine the pre-space mass-interchange picture. On reading this volume, one has the feeling that far-UV observations of the various stellar types are simply collected, without asking their impact on either the need for binary models, or how these data are produced in the binary picture. As one of the authors says: "mainly the mass-interchange model is a (speculative) concept, not yet a model in the sense of using it to predict spectra" (ie, it is not "conceived" from spectral observations). Since "symbioticity"—their designated principal common physical property—is *wholly* spectral, its relation to the model/concept is then somewhat obscure, except in that limited symbioticity arising in the simple (and classical) presence of two stars. If one ignores—as in this volume—a coherent multi-regioned structure of the component stars, a number of the sub- and super-ionized spectral features are not produced by the model. Illustrative of these—because of the stringent conditions to produce them, especially transiently—are the solar-coronal forbidden lines; with their implication of a large expanding volume of gas at low density and with a T_e~1 - 10 x 10^6 K, which is not predicted by these mass-interchange models.

As continously remarked, space-observatory addition of nova/recurrent-nova observations in the far-UV, X-ray, and far-IR spectral regions do not change—only supplement—the historic caricature/picture, which was constructed to simply represent the visual-spectral observations, not to illustrate any theory for the origin of the enhanced mass outflow and luminosity. Because the opacities in some of these added spectral regions exceed that in the visual, these new data simply provide simultaneous observations of a greater range of atmospheric regions—hence of a greater range of symbiotic features. In addition, those far-UV observations of some novae/recurrent novae that show a continuous (smaller) mass outflow at phases other than the eruptive provide continuity to "normal" stars.

Such phenomena and such "peculiar" stars —novae and other mass-outflowing stars— long ago demanded the enlargement of that restricted variety of stellar thermodynamics and structure speculatively imposed by Eddington to describe "normal" stars in the 1920's. By contrast to such "Eddington-normal" stars—which are closed thermodynamic systems (only radiative-energy fluxes) and thermally structured—the novae and other "then-peculiar" stars exhibited aerodynamic mass outflow, ie, nonthermal flux propagation and atmospheric structure. Thus-historic visual-spectral observations of novae during outburst, and of other less strongly changing but brighter stars, "previewed" a multi-regioned outer-atmospheric structure, linked to the occurrance of a mass-outflow, and its sub-atmospheric extension, that was only later observed/inferred, from nonvisual spectra, to be quite general, to some degree, among all stars.

Variability in such mass loss—hence implied in such atmospheric structure—was frequent among such peculiar stars; better delineated today; and observed in many, but not all, stars. The novae variety, with quasi-similarities in some other stars, remains even more peculiar—but not exceptional—in being "catastrophic". So in all "historically mass-loss peculiar", and in normal stars today, a mass-loss parallels a radiative loss. And requires a nonEddington thermodynamics in stronger aspects than simply a nonLTE in microscopic energy states.

The structure of such "variable-mass-loss" peculiar stars is nonthermally time-dependent; instead of being thermal, quiet, and time-independent, as are Eddington-normal stars. So there are at least two gross time-phases for such "peculiar" stars as those in the CV and "cousin" classes: an "eruptive", or at least an "active", phase, exemplified by the novae/recurrent-novae in the CV class, and by the Be stars in the "cousin" classes; and a "quiet" phase exhibited by the novae outside their eruptive phase, by the Be stars during their "normal B" phase, etc. Also the possibility of intermediate phases exists, not yet detailed because of observational incompleteness. So the nonEddington thermodynamics must allow a wide range of time-dependence, hardly with well defined and repetitive "cycles"; time-scales range at least from minutes to centuries; today, our knowledge is only empirical.

The third basic question is how far into the interior must one begin to model this time-dependence, whose character we observe only in the atmosphere. This of course depends on the major problem: the origin of all nonradiative-fluxes, and of their time-dependence. Clearly *all* fluxes, as well as any stellar structure depending on them, must be allowed—a priori—a possible time-dependence. I return to the point in Section III.

The speculative binary mass-interchange model imposes the CV variety of variability to be a surface, not internal, phenomenon; its time-dependence is that of the mass-interchange, filtered by "surface-relaxation" times. Originally, the model produced the mass interchange from Roche instability of a close binary. Some therorists are now apparently willing to accept single-star mass outflow as the mass-source, removing the need for "close/unstable" binarity. Other theorists were long ago willing to accept the (cataclysm energy source) needed mass infall as coming from an enveloping nebula. This latter picture is currently being advocated for the T Tauri stars—giving them also an accretion disk. Because the T Tauri are speculated to be early-stage, and the novae late-stage, evolutionary objects, the origin of the enveloping nebulae poses an interesting problem. In the similar cases of the Be stars (resembling the T Tauri stars) and the PN (resembling the novae), observations suggest the associated nebulae are produced by mass outflow from the star. So here, any time-dependence, producing the observed change in luminosity and mass outflow, would seem related to internal structure rather than to environment. One sees that a priori conjecture to "solve" one problem—the energy for "cataclysmic behavior"—often discords with other data and speculations.

At the pre-space epoch, the fundamental question was whether Eddington-normal and mass-loss-peculiar stars represented two thermodynamically different, but co-existing, types of real-world stars, or whether only one species was real-world, the other being wholly speculative, based on equally speculative, too limited, quasi-Equilibrium, thermodynamics. Contemporary far-UV and X-ray observations show some variety of mass loss to be present in all sufficiently observed stars, even in stars once thought, from their visual spectrum alone, to be Eddington normal. Many of these stars show variable mass loss and luminosity, some even resembling the episodic large-amplitude variety once thought peculiar to novae/recurrent-novae. The same is true for some variety of "symbiotic" effects. So whenever *single-star* modeling is adopted, it must be compatible with two observational requirements: (1) produce a mass loss, which—for some stars/models—is also capable of a variety of types of

variability; (2) produce a symbiotic spectrum, also capable of variability. Note that time-scales cannot be restricted to being "short". Even if one excludes CV time-scales as "uncertain to be single-star", Be time-scales up to decades through centuries are observed.

The above historic caricature/abstract of the historic nova/recurrent nova CV prototype is compatible with such expanded-Eddington thermodynamics mainly because its construction is wholly empirical and non-restrictive. But this alone hardly establishes the picture as either adequate or correct. Specifically, the picture says nothing about the origin of the mass loss, nor of its variability, nor of the associated enhanced luminosity—especially of the "variety of variability". The picture simply postulates a mass ejection of unknown origin, having only empirically specified characteristics; plus an accompanying luminosity increase. Which of the two is basic, or whether they are simply parallel increases in mass- and energy- outflow from the star as a whole, are not considered in this historic picture updated by modern space-based observations.

But current "explanation/modeling" of origin, size, variability of normal-star mass loss is in no better situation. Current "theories" focus on some variety of atmospheric or radiative instability. They do not consider phenomena of the deep interior, whence arises the radiative-outflow, to which the summarized phenomenological associations suggest the mass outflow may be parallel, in origin and in behavior. We note that we can regard the radiative-energy outflow as originating in nuclear interactions that change mass-state populations. Such interactions are unbalanced, producing energy flux and evolving mass-state populations, because the distribution of mass-state populations is strongly nonLTE, and the local environment is "thin" to energy fluxes from such interactions. One kind of completely parallel approach to mass outflow would seek unbalanced increase in local mass concentration—mass creation, not simply its repartition—to produce a mass flux from the central regions. But there are other alternatives, involving cooperative macro-thermodynamic, not just statistical, particle-interactive configurations. All these must be explored, discriminating by observations.

So the "why" of simple mass loss, in parallel to radiative-energy loss, is a question common to all stars. The novae/recurrent novae, the CV class generally, and classes with similar variability characteristics like the Be class, aggrevate the problem/question, but do not change its basic character, replacing closed-system modeling of single stars by open-system modeling, and in a way which permits variability under a variety of amplitudes and time-scales. Eddington was able to produce a variability in luminosity, not in energy generated, under his thermodynamics—so long as he did not require self-consistency in the outer atmosphere—by admiting stellar pulsation. (We recognize that demanding such self-consistency, even in nonvariable stars led to the nonLTE breakdown of Eddington-type atmospheric modeling under his thermodynamics.) But the observed variability in the preceding is far broader than that which such pulsation alone would introduce.

So by itself, via some kind of thermodynamics broader and more real-world than Eddington's, an observed mass loss from some star *now* implies nothing exceptional/peculiar for that star re stellar structure—atmospheric and internal. All stars exhibit mass loss parallel to radiative loss. We simply have not yet produced structural models that represent such parallel loss, both generally, and in a number of varieties, in origin and in size, especially in its relation to the star's energy (possibly mass ?) production. Neither do we yet understand, nor have we yet formulated, the nonEddington, obviously strongly non-Equilibrium, thermodynamics governing this real-world stellar structure/evolution.

Toward this objective, we can only dispassionately collect, and diagnose, all available evidence. Cray-exhaustive computation, speculatively iterating from an Eddington-type quasi-Equilibrium basis, instead of using a

broader observational base to define a thermodynamically better basis for beginning model computation, is simply myopic in trying to represent those data ignored in its formulation. Very clearly, the information on variable, especially cataclysmic, associated luminosity and mass loss is a critical part of this evidence. Particularly, we must put the historically extensive visual-spectral data, and the less extensive nonvisual-spectral observations from space, into the perspective of an (empirical) picture of stellar mass loss relative to radiative energy loss—and of some kind of open-system thermodynamics that enables us to describe it.

III. BRIEF EMPIRICAL-THEORETICAL PERSPECTIVE ON THE RELATION OF STELLAR MASS-LOSS AND RADIATIVE-ENERGY LOSS—ESPECIALLY OF THEIR ASSOCIATED VARIABILITY—TO STELLAR STRUCTURE AND EVOLUTION.

Toward this perspective, I highly abstract: (a) the evolution of our empirical knowledge of stellar mass loss and its variability, and of its association with luminosity and *its* variability, and the association of both with a multi-regional atmospheric structure and symbioticity, from a century of visual-spectral observations of peculiar stars; (b) the speculative directions of explanation/modeling to which it led when theoreticians left unquestioned the applicability of Eddington-type thermodynamics with its modeling of stellar structure/evolution under only a radiative flux; (c) the vistas opened when one removes, from diagnosis of historic-visual-, supplemented by current far-UV-, spectra the myopia imposed by Eddington-type thermodynamics. Throughout, I regard CV data as part of the information-supply on the range of stellar mass loss, its association with radiative-energy loss, and on "multi-region symbioticism"—these mass/energy fluxes representing parallel characteristics of stellar structure and evolution.

The luminosity anomalies of novae/ recurrent novae, and of "related eruptive stars" like P Cygni, were well known, grossly, for centuries; the existence/character of an accompanying mass outflow, for less than a century; the existence of a high-velocity mass outflow outside eruptive epochs, only in the last IUE decade for novae/recurrent-novae and PN, but for a half-century for P Cyg. The mass outflow peculiarity of the WR and Be stars, and the Sun—linked to that of extended, multi-regional atmospheres—became known in the 1860's; of the PN, much later. Studies up through the 1930's focused on *what* were the details of these peculiar-star characteristics/phenomena/structure, relative to what were considered to be "normal" in stars as modeled following Eddington. The basic question remained: does the existence of such peculiar stars, whose observed characteristics violate the thermodynamics imposed by Eddington in normal-star modeling, in any way challenge that normal-star, as well as peculiar-stars modeling (as indeed the space-epoch observations of mass loss in normal stars showed to be the situation)?

Accompanying the pre-space detailing of the mass outflow and multi-regional characteristics of peculiar stars grew an increasing awareness of their link to symbiotic-peculiar stars and phenomena. Earliest interpretation of the link was confined to the easy alternative of "binarity", to which the Eddington focus on only a radiative-energy flux, hence single-regioned atmosphere (photosphere), restricted diagnostics of simultaneous "hot"/"cold" spectra. Then solar eclipse studies, previewing those from space, exhibited undeniably single-star symbioticity—the simultaneous presence of: CO and CN bands; optically-thick Hα, HeI, HeII, lines; [Fe X, XI, XIV], [CIV]. Eventually space-based observations added many intermediate-energy-level lines — notably those resonance lines of CIV--OVI found in the far-UV of WR and other hot stars, and whose subordinate lines had been long-known in the WR visual spectrum. Mrs. Gaposchkin had immediately identified the Sun as symbiotic: WC-6 in the far-UV;GO in the visual. This exhibited single-star symbiosis linked to the atmospheric structural effect of nonradiative fluxes in a banal, faint, feeble mass-flux star; hence showed that Eddington-type thermodynamics broke down, in ways other than simply

thermal nonLTE, in the atmosphere of a star which would be called normal at normal-star distance.

So the question became whether Eddington thermodynamics also broke down in the interior, relative to structure and fluxes produced there. Because peculiar-star phenomena had previewed this atmospheric breakdown, the question was actually two-fold: (i) do Eddington-anomalous peculiar star characteristics—especially mass-flux existence, general flux variability, and atmospheric symbioticity—also imply break down of Eddington-thermodynamics in their interior; (ii) does such breakdown in peculiar stars imply the same for normal stars? Clearly, more detailed peculiar-star studies were required.

In the 1920's, two paths unfolded for stellar-structural studies: one continuing this dilineation of *what*, for peculiar stars; the other, attempting to ask *why*, for normal, and eventually peculiar, stars. The former, and its motivation, is exemplified by Cecilia Payne-Gaposchkin's work; the latter, by Eddington's.

Cecilia Payne-Gaposchkin's application of Saha's equilibrium-ionization approach to a variety of stars in *Stellar Atmospheres* (1925) was pioneering. Apparently as a result of these quasiEquilibrium, Eddington-normal-star studies—comparing their predictions to peculiar star observations—she devoted her next 50 years to assembling the *what* of peculiar stars, especially their variability characteristics. Her and Sergi Gaposchkin's work on stellar intrinsic variability, particularly those in that CV class—whose title and sweep they coined—is a classic in delineating its empirical-thermodynamic character re *what*. Her work also forecast the impact of similar study of the "spectrum-variables", of which the Be class is the proto-example; and of the classification-confusion between Be and CV types for such stars as Z And.

The work's major incompleteness lay in not recognizing a *thermodynamic*-peculiarity paralleling stellar. However, Cecila Payne-Gaposchkin's stimulation of a worldwide ensemble of peculiar-star observers was profound; those around Struve were exemplary. The occasional remarks, spread through the literature, by Cecila Payne-Gaposchkin and Struve on the implications of variability, and of the implications of stellar peculiarity (possibly viewed only as "peculiar phases" of "normality"), on the completeness of normal star "theory"/modeling, underlined their independent disbelief in any "singular" nature of peculiarity and should have attracted greater attention to the need for expanding stellar (nonEquilibrium) thermodynamics than they did.

Eddington's studies (equally the 1920's) of normal-star *why* focused on asking the change in stellar structure if one altered the *isolated* thermodynamic-system character of Emden's (1907) stellar modeling by introducing *only* the radiative-energy flux: by which one observes the star, and from whose existence one concludes a star evolves, in some way, because of such energy loss (assuming energy conservation). Thus he modeled stars as *closed* systems: his "why" focused on the origin—where and how—of the radiative-energy flux. His thermodynamics restricted it to being the *only* flux whose origin is related to the basic structure/evolution of the star — hence about whose origin one must ask in modeling *global* stellar structure.

He localized the radiative-energy flux origin as deep in the interior, asserting that its effect on stellar structure was thus largely independent of details of its production because thermodynamic conditions there (which control the process, if it was thermal) were determined—under his assumed hydrostatic equilibrium—only by the star's mass. A more consequential aspect was the "temperature" distribution fixed by the mode of energy transport to, and ejection from, surface regions. Indeed, under his thermodynamics (linear nonEquilibrium), the star's ability to transport outward the flux conditioned how much it could "stably" produce in its regions of origin; and this, rather than the microscopic details of its production, determined the luminosity's "tran-

sport-allowed" size. Identifying the most efficient *thermal* transport mechanism—to accord with his *imposed* quasi-Equilibrium thermal structure of the star—to be radiative transport, he formalized the process' pervasive astrophysical importance and averted interest in nonthermal mass transport—*for his so defined normal stars*.

So Eddington-type thermodynamics applied to model normal stars had 3 significant characteristics: (1) only energy flux; (2) origin of the flux in the deep interior; (3) size of the flux more determined by what the regions exterior to those of energy origin can transport to, and expel from, the surface than it is by the details of the mechanism of energy production. Characteristic (3) was abstracted by Schwarzschild (1958): (a) "the luminosity of a star is not determined by the rate of energy generation by nuclear processes, but by the radiative-equilibrium condition—(attained) not by adjusting its luminosity but by adjusting its nuclear sources by contraction/expansion"; (b) "(we can) derive *uniquely* the (star's) internal structure from values of the mass, luminosity, radius, and composition of the outer layers—because the (time-) constancy of stars (luminosity and structure) asserts that the stellar interior must be in perfect equilibrium." Peculiar stars long made their disagreement blatant.

If, at our epoch, as observations suggest, progress in stellar modeling requires that we treat a mass flux parallel to a radiative-energy flux, one has two alternatives: follow Eddington's approach to discuss the origin (where, how) of the mass-flux in the way he did for radiative flux, *assuming* that his results on radiative flux are not modified by the existence of the mass flux; or begin wholly anew, asking an associated production of the two fluxes, guided by observations of such association in asking how to proceed. Because the velocities required to transport mass loss of the observed size in "normal" stars are so highly subthermal everywhere below the mid-photosphere, superficially there is no real problem in assuming its presence does not affect Eddington-type modeling of the interior. However, in considering the origin, and depth properties, of significantly large variability—of the type evinced by CV, P Cyg, Be, and PN objects alike—relative to Schwarzschild-like "equilibrium" concepts, problems clearly arise in whole-star (nonEquilibrium) thermodynamic consistency.

In the '30's, as a focus on the *what* of peculiar stars was increasingly paralled by one on *why*, again two paths arose in peculiar-star studies. Most observing astronomers followed Cecilia Payne-Gaposchkin and focused on *what*, to gain further insight, before asking *why* (the orientation of Fontenelle's frontispice in our monograph volumes). Various theoreticians tried the inconsistent approach of retaining Eddington's normal-star thermodynamics to try to model peculiar-star configurations that inherently violated them. Until the advent of space studies, detailed, observation-guided, challenges to such speculation lay mainly in attempts at nonEquilibrium-thermodynamically self-consistent studies of the solar outer atmosphere and mass outflow. Such attempts in studying the PN were handicapped by lack of sufficiently detailed data, and again a too restricted thermodynamics adopted for the modeling.

The *why* focus of such theroticicans, as did Eddington's, differed basically from the *what* in its speculative, rather than an empirical, model orientation. Rather than try to empirically model, under an empirical thermodynamics, all spectral features associated with the mass outflow and its linkage to luminosity, "why" theories followed Eddingtion in their focus on identifying an energy source for the mass outflow, and for the associated luminosity peculiarities. For Be and WR stars, an energy source was sought for the mass outflow; for the CV, subordinating mass outflow to luminosity rise, energy was sought for the latter. Pre-space identification of mass outflow and "cataclysmic" luminosity rise as being something exceptional introduced a search for exceptional configurations to represent peculiar stars. The alternative of searching for a nonEddington thermodynamics under which "peculiar" stars would no longer be peculiar was

followed by only a few of us (of Volume 4 of this series).

The proposed such exceptional configurations ranged from single stars rotating at near-breakup velocity (proposed for Be stars by many, and WR stars by some, speculators)—so producing an (imposed, not observed) equatorial-only mass outflow, to a binary configuration with components sufficiently close (imposed, not observed) to be unstable against mass transfer (CV generally)—so also producing a (accretion) disk around one component. The focus on a search for energy sources, not for a broader thermodynamics—constructed to represent all available observations, modified as these expand—generally persists among speculative theoreticians even in our space-based observational era. Now, mass outflow is normal; and an energy source for it is a common, not exceptional, problem. The only "individual" character of such mass outflow lies in the variety of variabilty and size.

So it is fitting that inability to produce such variability was the historic inadequacy of the equatorial-disk models of Be stars: the inability of that fixed equatorial disk associated with rotation to reproduce their "phase-variability", with its highly individual and variable occurrence and duration. Indeed, such inadequacy to reproduce such variability was a principal reason that its originator, Struve, dropped the rotational-instability theory and a focus on *why* (but in which his disciples persisted) to return to a focus on modeling the *what* of Be atmospheric structure.

To do so, he expanded the class of stars considered, to embrace that variety of "(low-ionization) emission-line-peculiar", "spectrum-variable", stars producing Be-similar envelopes. (Note that unlike the CV, speculatively proposed class of stars satisfying the Roche model, Struve's class—and its subclasses—were defined by observed, not hypothesized, phenomena.) To represent these data, he proposed a solar-similar, multi-region, atmosphere: quiet "chromosphere"; dynamic "corona"; omitting an equatorial disk (possibly prematurely, if one regards a planetary system as a cool, enveloping, atmospheric region). Because this improved model was pre-IUE, it did not include that dissipative non-radiative flux which, with its observed "symbiotic" effect, is a "must" today.

The major virtues of the Struve empirical model over the speculative were: (i) the greater variety of stellar types it embraced, including phenomena observed in many CV phases; (ii) being observation based, it could be modified in accord with new data—eg, those establishing the solar chromosphere-corona as "hot", and low-atmosphere originating. In Volume 2 of this series, Doazan and Thomas introduced such kind of modeling-extension/change, focusing on solar similarity in exo-photospheric but sub-envelope structure, and on variability to incorporate the envelope structure. Later, simultaneous observations in the far-UV and visual produced more detailed inference on the (time, space) structure of the atmosphere as a whole. Such inference was not speculative-concept based; rather, concepts were inferred from the empirically derived structure.

The predictable inadequacy of those attempts at modeling mass-loss-peculiar stars from a thermodynamics based on excluding mass loss emphasizes the futility of retaining Eddington's viewpoint that stellar structure can be adequately modeled by focusing on the origin/propagation of only the energy flux. Those current theoretical attempts to model mass flux as wholly determined by energy fluxes perpetuate Eddington's seeking the structural change in Emden's no-flux models by admitting only the radiative-energy flux, the evidence on mass flux even then provided by peculiar stars to the contrary. Eddington simply handicapped his modeling efforts by including only that energy flux, without asking whether such a priori judgement on its all-importance accorded with observa[illegible]. In the same way, current mass-flux modeling that a priori interprets its observed association with luminosity *uniquely* as causal *may* be also handicapping its efforts. Clearly, analysis of the data on the behavior of such association

under a wide range of variability provides one objective basis for choice between simple association and causality. This is one of the reasons I emphasize the necessity to analyze CV data under *no a priori choice on the cause of variability, or on which fluxes are significant in modeling stellar structure/evolution.*

Too often one errs in trying to compare energy- to mass- flux significance by comparing luminosity to the kinetic energy of the mass outflow [of Table 3-11 of (my) Volume 4 in the series]. With the exception of the novae, the luminosity dominates; even for the WR stars, the kinetic energy is only some 10% of the radiative. But what is actually important, in considering flux effects on stellar structure and evolution is how much of the mass/energy stored in the star such fluxes carry away.

The classical criterion for approximating near-Equilibrium configurations by Equilibrium is that all fluxes of Quantity X must be small relative to the storage of X. Our last few decades' experience with nonLTE modeling demonstrates that such criterion applied to the whole star is insufficient to assess what happens near the boundary. Nonetheless, in trying to make a "whole-star" assessment (addressing internal as well as atmospheric structure/evolution) of the relative significance of mass/energy fluxes, such estimates are illustrative.

So in the Perspective Chapter of the preceeding Volume 7, on the FGK and T Tauri stars, I made such comparison (Table 1 in Volume 7) for a range of stars. I simply followed Schwarzschild (1958) in identifying energy stored (ES) in the star with that potentially useful for nuclear liberation: ES = 0.07 x 10^{20} $M_\odot$ ($\sim 10^{-2}$ $M_\odot$ c^2). I used the data in Table 3-11 of my Series Volume 4. (Newer values for mass loss introduce no difference in the following.). For such variable stars as the Be, where even now values at different phases are not well-determined, I simply gave the range of values in the literature. I did not include, in that Volume 7 table, the novae, because "simultaneous" values, at different phases, are even more uncertain.

If, however, one *approximates* the situation by assuming the times during which the major enhancements of mass and energy fluxes occur to be the same, inclusion of the novae/recurrent novae/dwarf novae may be interesting. So, I reproduce that Volume 7 table with that inclusion, using the data given in Table 1-1 of this CV volume. I give two final columns for these CV stars: one, using total energy-and mass-loss during the whole "cataclysmic episode" without specifying its duration; the other, with its duration taken as one year for novae/recurrent-novae, and 10 days for dwarf novae.

The Volume 7 results were interesting in their showing that, while the ratio of luminosity/energy content predominates over mass loss/mass content [or, equivalently, (stored energy carried away by mass outflow)/stored energy] for cool dwarf, faint, low-mass stars, there is a gradual change to the reverse, as one progresses to hotter, more-luminous, higher-mass stars. The ratio of (luminosity/energy-content) : (mass-loss/mass-content) is 100:1 for the Sun; 1:10 for the WR stars. The supergiants show larger mass-loss effects. Hot dwarfs range from 1000: 1 to comparable; Be stars, 1000:1 to 1:10—how much of the B-star range reflects observational scatter is uncertain. Cool-dwarf data, other than from the Sun, are also uncertain. Also, these luminosity estimates are based on M_V only, so may under-estimate the actual L — but if it is by enough to reverse the above trend, it would be surprising. So the overall indication that one can hardly ignore the mass-loss effect relative to that of the radiative-energy loss remains.

Here, the Table 1, CV-expanded version of these results exhibits the same effect, only reinforced, as might be expected. The larger mass loss is accompanied by smaller ratio of radiative-loss effect to mass-loss effect in diminishing the star's energy storage. The value ranges from 100 for novae/recurrent-novae to 10^4—10^3 for dwarf novae. The comparative order is surprising, but recall that these luminosity estimates are based on visual spectra only. Reliable measures of the far-UV contribution exist only for some novae/recurrent novae. So, these

values simply supplement the usual/historical conclusion (based on mass-loss kinetic energy) that the energy carried away by the mass loss is comparable to the radiative. But what we really need is these kinds of results at the several phases of the outburst, details of phenomena associated with variability.

What I conclude from these comparisons of: historic-visual with space-based non-visual spectral observations of "peculiar" vs "normal" stars, and the adequacy of Eddington-type vs the implications of broader thermodynamics, is that internal as well as atmospheric remodeling needs re-examination from first principles. One finds the origin of the energy for the radiative-energy flux in exothermic "evolution" of nonLTE populations of mass states—except that what sometimes occurs, for extended periods, to produce *very* strong increase in energy liberation, for a variety of stars, is not at all clear. The additional energy required to expel mass from the star is generally (except for novae) small compared with the radiative flux, even though that part of the star's energy storage lost to the star via the mass flux often exceeds that part lost by the radiative-energy flux. But the mass source of the mass flux is something else. That it is simply mass "evaporation" from the star contradicts many observations. That it is simply an outward-accelerating flow requires a modeling of the initiation, variability, and structural change involved. Indeed, it is not observationally unambiguous that the star's mass actually decreases by the mass-outflow amount; vis, that there is not some "mass source", paralleling the radiative-energy source, in the star's interior.

If the later "unconventional" alternative is true, one might see in it an alternative to either "big-bang" cosmology, or the Hoyle-Bondi continuous mass creation in the interstellar medium. This volume is no place for such

TABLE 1. CRUDE COMPARISON OF ENERGY AND MASS LOSSES, TO ENERGY AND MASS STORAGE FOR VARIOUS STELLAR TYPES

Stellar Type	M units 2.10^{33}g	ES units 10^{53}erg	$\dot{M}$ units 6.10^{20}g/s	V_{max} Obsv. units 10^{3}k/s	KE[$\dot{M}$] units 10^{40}erg/s	E[$\dot{M}$] units 10^{40}erg/s	L units 10^{40}erg/s	$\dot{M}$/M units 10^{-15}/s	L\ES units 10^{-15}/s
WR	50-10	7-1.5	10-1	4-2	10^{-1}-10^{-3}	5-1	0.4-0.08	60-30	6-8
Osg	30-10	5-1.5	1-10^{-3}	3-1	3.10^{-3}-10^{-6}	0.5-0.001	0.4-0.04	10-0.03	8-4
Bsg	20-10	3-1.5	1-10^{-3}	2-1	2.10^{-3}-10^{-6}	0.3-0.001	0.04-	10-0.06	1-
Bd	10-5	1.5-1.	10^{-3}-10^{-6}	2-1	10^{-6}-10^{-9}	10^{-3}-10^{-6}	4.10^{-4}	3.10^{-2}-10^{-5}	4.10^{-2}
Be	10-5	1.5-1	10^{-2}-10^{-6}	2-0.5	10^{-5}-10^{-8}	10^{-2}-10^{-6}	10^{-3}-10^{-4}	3.10^{-1}-10^{-5}	6.10^{-2}-10^{-2}
Asg	25-5	4-1	10^{-2}-10^{-4}	0.3	10^{-7}	5.10^{-3}	10^{-2}	10^{-1}-10^{-3}	[2-0.4]10^{-1}
Ad	2	0.3	-	0.3	-	-	-	-	-
Sun	1	0.15	3.10^{-9}	0.8	10^{-12}	10^{-9}	4.10^{-7}	10^{-6}	3.10^{-4}
Msg	20-10	3-1.5	10-10^{-3}	0.3	10^{-4}-10^{-8}	5.10^{-4}	$0.4.10^{-3}$	10^{-2}-10^{-2}	10-10^{-1}
Novae	1	0.15	10^{-5}-10^{-6}	1-3	2.10^{5}-2.10^{3}	10^{7}-10^{6}	10^{5}-10^{4}	10^{-5}-10^{-6}	10^{-7}-10^{-8}
Recurrent Novae	1	0.15	10^{-6}-10^{-7}	1-3	2.10^{4}-2.10^{2}	10^{6}-10^{5}	10^{4}-10^{3}	10^{-6}-10^{-7}	10^{-8}-10^{-9}
Dwarf Novae	1	0.15	10^{-11}	-	-	10	10^{-3}	10^{-11}	10^{-15}

Symbols: M=stellar mass, ES = energy stored, $\dot{M}$ = mass-loss rate, V_{max} obsv. = maximum *observed* wind velocity, KE[M] = kinetic energy of mass overflow, E[M] = total energy of mass outflow, L = stellar luminosity.

speculation (I consider it elsewhere)—it is intended only as illustration that admitting mass flux in parallel with radiative flux has serious consequence. But I do not think the observations—especially of the variety of large-amplitude, long-time-scale variability exhibited by the CV class, *and its cousins* — permit other alternatives.

IV. PERSPECTIVE ON THE VOLUME'S APPROACH TO CV DATA DISCUSSION/ MODELING

In consequence of Section I—III, I have believed that the collecting, and discussing, of the CV observations should at least abstract observations of the widest possible range of even quasi-similar stars and modeling alternatives. By contrast, the editor/authors of the present volume have chosen to rest so strongly on their belief in the validity of the speculative-conceptual, pre-space formulated, mass-interchange model for *all* CV stars—indeed sometimes advocating that the CV class should be *defined* as those stars satisfying this Roche model—that they admit/discuss no other alternative. In consequence of their modeling outlook, they a priori exclude a possible capacity of CV—or other—stars to themselves produce an episodic increase of luminosity and mass-outflow.

So, my suggestion for such broad discussion of alternatives has been overuled by the combination of my NASA co-organizer/editor and the Volume editor/authors. I have however been granted this short Perspective to abstract my reasons for objecting to what I consider myopia, which I have done, in the preceeding pages of this Perspective Chapter.

Because this is the eighth, and final (we have exhausted our support), volume in this NASA-CNRS-sponsored monograph series on nonThermal phenomena in, and structure of, stellar atmospheres, I restate our initial objective in organizing the series. Possibly its orientation title should have been "nonLinearly-nonEquilibrium Thermodynamic" instead of "nonThermal", as being more explicit on its phenomenological/thermodynamic compass; but in stars, these alternative titles ultimately imply the same, which is particularly obvious in their atmospheric/outerboundary regions—and the latter title is shorter.

In planning, organizing, and editing the volumes, we focused on observation-guided/developed, not speculatively hypothesized, diagnostics and representation of these observations, and on translating such into atmospheric structure of real-world stars. That is, we urged those collecting, and discussing, observations to make no a priori judgement on quasiEquilibrium vs nonEquilibrium, or on thermal vs nonThermal, or on closed- vs open- system, thermodynamic character of the particular star being studied, but to adopt/construct, iteratively, a diagnostics that is thermodynamically consistent with that character of the star finally inferred from its application, not a priori assumed. Such inferred character, not that "classical-standard" one to which we contrast it, is the real-world star. Thus we hoped to produce—collaboratively with the stars —better atmospheric models, for themselves, and as a preliminary step toward revising interior-, then whole-star-, modeling on some better basis than simply speculative thermodynamics.

Such focus contrasts to the "classical-standard" one on simply applying quasi-Equilibrium diagnostics of only the radiative-energy flux to infer the differential chemical composition of various stars, under the assumption that each "normal" star's thermodynamic structure follows standard-classical models. This focus, and the standard-classical models, rest on trying to preserve Eddington's speculative picture of a "normal" star as being a quasiEquilibrium and closed thermodynamic system. Pre- and post- Eddington visual-spectral observations of "peculiar" stars, including the Sun, and current far-UV-spectral observations of both peculiar and "visual-spectral-normal" stars, show that speculative picture to be no longer applicable.

So a major objective of the monograph series was to clarify the possibility of stellar thermodynamic diversity in *basic* thermodynamic type via collaboration with the stars

themselves—they, to produce the variety of fluxes, we, to observe and diagnose them, to try to infer what such variety implied on such possible diversity in basic thermodynamic type among the stars studied—*without a priori judgement on what types exist*. We would proceed iteratively, to produce such a self-consistent, a priori unprejudiced, diagnostics and thermodynamics.

So, succinctly, we organized the monographs to collect all those data delineating: (a) the variety of stars to which Eddington-type thermodynamics/theory/modeling might be applicable—classically-"normal" stars; and (b) those "peculiar" varieties of stars to which it was definitely not applicable. Each volume was to focus on normal and peculiar stars of one (or one limited range of) visual-spectral class. We hoped that such empirical results would lead to at least empirical—maybe eventually axiomaticized—models based on a thermodynamics that sufficed to make the models real-star applicable. Possibly, the project might even lead to an interpretation of such empirically based axioms in terms of: *why* is such stellar structure, and *what* is its evolution under *all*, not just radiative-energy, fluxes. So, the approach of the monographs was to focus on observed-peculiar, vs speculative-normal, stellar atmospheres, to delineate the thermodynamics distinguishing them, and then to apply all this to atmospheric modeling. Eventually, somewhere, sometime, we hoped to apply these results to whole-star modeling.

At least that was *our* goal, as volume-organizers. Of course, once an author accepted to carry out the labour of data-collection, we could hardly dictate—only suggest—his diagnostic/modeling approach, and his communication of his efforts to his colleagues/readers. Occassionally, we could invite additional authors to contribute to a volume, to provide, via diversity, a missing balance. And we could write a Perspective Chapter, like this.

REFERENCES

Conti, P.S., Underhill, A.B. 1988, *O Stars and Wolf-Rayet Stars*, NASA/CNRS Series Volume 6, NASA SP-497.

Cram, L., Kuhi, L. 1989, *FGK Stars and T Tauri Stars*, NASA/CNRS Series Volume 7, NASA SP-502.

Eddington, A.S. 1930, *Internal Constitution of the Stars*, Cambridge University Press.

Emden, R. 1907, *Gaskugeln*, Teubner, Berlin.

Payne-Gaposchkin, C. 1925, *Stellar Atmospheres*, Harvard University Press.

Schwarzschild, M. 1958, *Structure and Evolution of the Stars*, Princeton University Press.

Thomas, R.N. 1983, *Stellar Atmospheric Structural Patterns*, NASA/CNRS Series Volume 4, NASA SP-471.

Underhill, A., Doazan, V. 1982, *B Stars with and without Emission Lines*, NASA/CNRS Series Volume 2, NASA SP-456.

Richard N. Thomas
Boulder, Paris 1990

RÉSUMÉ

Dans la définition originale, les caractéristiques qui définissent une étoile comme variable cataclysmique étaient les sursauts imprévisibles de son éclat. L'importance et l'échelle de temps de ces sursauts varient considérablement d'un membre à l'autre de cette classe d'objets. Aussi violents que ces sursauts puissent paraître, les observations photométriques et spectrographiques indiquent que la structure générale des novae naines et des novae n'en est pas affectée de facon significative.

Le système usuel de *classification des variables cataclysmiques* est basé sur les propriétés des courbes de lumière de ces sursauts. Bien que, dans la majorité des cas, il soit possible d'attribuer clairement à une étoile l'une ou l'autre de ces sous-classes, il y a de nombreux cas ambigus. Les "vieilles novae" apparaîssent comme essentiellement impossibles à distinguer des "novae naines" quiescentes. Si bien que la possibilité a été considérée que ces deux types désignent réellement la même espèce d'objets, vus seulement à différentes étapes d'une évolution peut-être cyclique. De plus, quelques unes des "novae récurrentes" (T CrB, RS Oph, V1017 Sgr) apparaîssent semblables aux "étoiles symbiotiques", sauf en ce qui concerne une amplitude plus grande des sursauts, alors que d'autres (U Sco, T Pyx) comportent plus de ressemblances avec les "novae classiques". En général, *les variables cataclysmiques manifestent toutes une individualité caractérisée* dans la plupart de tous leurs aspects observables, –si bien qu'on ne peut même pas dire qu'il existe pratiquement deux telles étoiles identiques.

Une donnée essentielle de l'observation, reconnue dès le milieu des années cinquante, c'est que *tous les objets bien observés* sont en fait des systèmes *binaires* composés d'une étoile de type tardif (une naine rouge dans le cas des novae naines, des novoïdes et des novae classiques, et probablement dans celui d'une ou deux novae récurrentes; une géante rouge dans les étoiles symbiotiques, et dans au moins deux novae récurrentes), et un compagnon chaud, mais sous-lumineux (généralement une naine blanche). Ceci conduit à l'hypothèse que *toutes* les variables cataclysmiques sont des binaires, ce qui conduit par conséquent à la formulation du *modèle de Roche* pour expliquer leur nature.

Les observations ultérieures (dans l'ultraviolet et dans le domaine des rayons X) ont confirmé les prévisions de ce modèle et ont renforcé l'idée que la binarité est d'une importance primordiale pour produire des événements cataclysmiques. Il faut dire aussi que l'hypothèse de la binarité fournit une explication facile à l'individualité marquée des systèmes, en raison des très nombreux degrés de liberté dans leur apparence physique, par rapport aux étoiles simples.

1. PROPRIÉTÉS GÉNÉRALES DES VARIABLES CATACLYSMIQUES

Ce volume commence par un chapitre d'introduction sur les *propriétés générales des variables cataclysmiques*. A l'exception des étoiles de type novoïde, elles sont caractérisées par des sursauts lumineux et soudains de plusieurs magnitudes, et par des variations corrélatives notables de leur spectre.

Les observations montrent une *perte de masse* occasionnelle,accompagnée ou non d'un *transfert de masse* entre les composantes de la binaire. La plupart des systèmes émettent une quantité substantielle de rayonnement dans la totalité du spectre électromagnétique, bien que dans les novae naines et dans les novoïdes il y ait seulement un flux marginal dans le domaine des ondes radio. Les régions responsables de l'émission dans les rayons X sont supposées être celles où l'interaction se produit entre le *disque d'accrétion* et l'étoile chaude. Les disques d'accrétion et les *enveloppes en expansion* des novae rayonnent plus dans l'ultraviolet. Les parties extérieures des disques, les *"pseudo-photosphères"* des novae soumises aux sursauts, les *nébulosités* entourant les vieilles novae, et les plus brillantes parmi les *étoiles secondaires* sont visibles dans le domaine optique. Les étoiles secondaires et la *poussière* formée dans les novae peuvent être

PRECEDING PAGE BLANK NOT FILMED

détectées aux longueurs d'ondes de l'infrarouge; et enfin, le flux radio des nova peut être attribué aux *couches extérieures* de gaz ionisé. De plus, dans deux étoiles symbiotiques, la formation et l'evolution de *jets* ont été détectés dans le domaine radio.

Les distributions spatiales et les paramètres systémiques, tels que masses, rapports de masse, périodes orbitales, et magnitudes absolues des vieilles novae, des novae naines et des novoïdes sont discutées. Les novae sont clairement plus concentrées au voisinage du plan galactique que les novae naines et les novoïdes. La distribution plus uniforme de ces deux dernières classes, en combinaison avec leur éclat intrinsèquement bas, prouve qu'ils sont de proches voisins du Soleil. Aucune différence statistique significative n'a été trouvée entre les masses et les rapports de masse dans les trois classes de variables cataclysmiques. Au contraire, les magnitudes absolues des novae quiescentes, des novae naines quiescentes et des novoïdes montrent de nettes différences. Les novae quiescentes sont concentrées autour de la valeur $M_v = 4$, les novoïdes autour de la valeur $M_v = 5$ et les novae naines autour de la valeur $M_v = 8$ à 9.

Une remarque assez importante concerne les périodes orbitales : La plupart des variables cataclysmiques ont des périodes comprises entre 1,3 et 5 heures, mais un *intervalle*, de 2 à 3 heures, existe, auquel correspondent très peu d'objets. Des différences existent entre les sous-classes en ce qui concerne les périodes orbitales, et, de plus, certains objets ont des périodes considérablement plus courtes ou plus longues que la vaste majorité des variables cataclysmiques.

2. LES NOVAE NAINES: OBSERVATIONS

Les chapitres 2 à 5 sont consacrés aux observations, et à l'interprétation des novae naines et des novoïdes.

Typiquement, on trouve les novae naines dans les états dit "quiescents", c'est-à-dire d'éclat faible; à des intervalles semi-réguliers de temps (de l'ordre typiquement de quelques dix à cent jours) l'éclat augmente environ de 2 à 5 magnitudes. Dans les classifications modernes, trois différents types de novae naines ont été distinguées : Les *étoiles de type U Geminorum*, les *étoiles Z Camelopardalis*, et les *étoiles SU Ursae Majoris*. Les étoiles Z Cam, après le déclin consécutif aux sursauts, restent occasionnellement à un niveau intermédiaire d'éclat pendant des semaines et des années (*"stagnation"*) avant de retourner à un éclat minimum. Les étoiles SU UMa, en plus des sursauts "normaux", comme ceux que l'on trouve dans toutes les autres novae naines, présentent des *"super-sursauts"* plus longs, et quelque peu plus brillants. Les novae naines, qui ne rentrent dans aucune de ces deux catégories sont classées comme des étoiles U Gem.

En ce qui concerne les propriétés statistiques, on discute simultanément le cas des novae naines et celui des novoïdes. En ce qui concerne les masses composantes stellaires, les rapports de masse, et les périodes orbitales, ces systèmes, lorsqu'on les considère comme des groupes, sont presque identiques. Cependant, quelques différences semblent associées avec le comportement des sursauts et les propriétés magnétiques.

Les propriétés photométriques des sursauts des novae naines les mieux étudiées sont décrites. Avec plus de 600 sursauts enregistrés pendant la presque totalité du siècle passé, SS Cyg, la plus brillante des novae naines connues, est l'objet le mieux étudié à cet égard; d'autres ont été également raisonnablement bien observées. En ce qui concerne les détails des changements photométriques pendant le sursaut, tel que le temps exigé pour atteindre l'éclat maximum, ou la durée totale de l'événement, pour n'importe quelle nova naine, différents types de sursauts peuvent d'habitude être distingués. On a pu également trouver des relations entre, par exemple, l'amplitude du sursaut, l'énergie totale libérée pendant un sursaut, et le temps de récurrence. D'autres relations positives semblent exister entre le taux du début du déclin après un sursaut et la période orbitale, et entre les périodes orbitales et la durée des sursauts larges et étroits respectivement. Et, finalement,

les caractéristiques des stagnations et des super-sursauts sont discutées.

Des changements appréciables de couleur se produisent pendant le cours d'un cycle de sursauts, lorsque des boucles caractéristiques sont décrites dans le diagramme à deux couleurs. La plupart de ces changements ont lieu pendant l'augmentation rapide vers le maximum, lorsque les étoiles deviennent considérablement plus bleues que la normale. Les changements pendant le cours du déclin sont beaucoup moins dramatiques.

Des changements photométriques, manifestes pendant la période de quiescence, souvent liés à la révolution orbitale, sont présents dans toutes les novae naines. Dans le domaine optique, il peut s'agir d'un accroissement temporaire de brillance, de quelques dizaines de magnitudes pour environ la moitié du cycle orbital : (c'est le *"hump"*), ou d'une éclipse pendant une petite fraction de la période orbitale, et d'une profondeur allant jusqu'à deux magnitudes. L'un ou l'autre, ou tous les deux, de ces phénomènes sont présents dans de nombreuses novae naines. Dans tous les systèmes, à tous les niveaux de la courbe de lumière du sursaut, superposés au niveau de la brillance générale, se produisent des changements irréguliers de brillance, qu'on appelle le *"papillotement"* (flickering, en anglais). Un très petit nombre de données seulement sont disponibles sur la variabilité des échelles de temps orbital dans le domaine ultraviolet, et pas beaucoup plus dans l'infrarouge. La variété des courbes de lumière infrarouge parmi les novae naines est apparemment assez grande. De nombreux systèmes sont connus pour présenter une éclipse secondaire à (environ) la phase 0.5 par rapport à l'éclipse primaire; cette éclipse secondaire n'est pas observée dans le domaine optique.

Une surveillance à long terme du niveau de lumière quiescent a été possible pour SS Cyg et U Gem. Pour la dernière de ces deux étoiles, le flux reste constant entre des limites très étroites, et aucune tendance systématique de changement n'a pu être détectée. D'un autre côté, SS Cyg conserve un niveau stable d'éclat pour plusieurs semaines, alors qu'à d'autres moments, le niveau de flux augmente systématiquement ou décroît, sur une période pouvant égaler celle de plusieurs phases quiescentes consécutives. Une telle surveillance à long terme a été faite pour CN Ori pendant un intervalle quiescent complet entre deux sursauts consécutifs. Les amplitudes du "hump" varient d'une facon cyclique avec une tendance superposée d'un niveau de lumière en augmentation au moment du maximum du "hump", alors que la brillance minimum aux phases intermédiaires entre les "humps" reste constante. Ces observations ont été suffisamment détaillées pour révéler également que la structure de la courbe de lumière orbitale ne se répète jamais exactement d'un cycle à l'autre ; mais cependant de nombreux aspects caractéristiques sont toujours présents.

Une section du chapitre 2 est consacrée à deux novae naines très spéciales, WZ Sge et BD Pav. Elles ont toutes les deux des périodes de sursauts extrêmement longues qui conduisent à leur ancienne classification en tant que novae récurrentes. Cependant, l'amplitude et les autres caractéristiques de ces sursauts sont typiques des novae naines, et c'est comme telles que l'on devrait plutôt les classer.

Une autre caractéristique de quelques novae naines, c'est la variation séculaire apparente de la période orbitale. Pour des raisons dynamiques, on peut exclure que cette variation soit le reflet de changements réels dans la période orbitale ; mais on ne sait pas encore clairement quelle est leur origine.

Il est étonnant de noter combien peu est connu en ce qui concerne les changements orbitaux pendant l'époque des sursauts. L'amplitude des "humps" est généralement plus nettement variable que pendant la période de quiescence, des éclipses simples tendent à disparaître, et des éclipses doubles à devenir simples à l'époque du maximum d'éclat. Les courbes de lumière orbitale des étoiles Z Cam, pendant les stagnations, ne peuvent être distinguées de celles observées à des états d'éclat comparable à

l'epoque du déclin après les sursauts normaux. Pendant les super-sursauts des étoiles SU U Ma, des *"super-humps"* sont observés, qui sont affectés de changements très caractéristiques pendant la durée du super-sursaut.

A une haute résolution temporelle, de l'ordre de quelques minutes ou secondes, des changements photométriques supplémentaires deviennent évidents dans les novae naines. Il y a un "papillotement", une variation au hasard de l'éclat, avec des amplitudes de quelques dizièmes de magnitudes et des temps caractéristiques de l'ordre de quelques secondes ou minutes ; et ceci est présent à toutes les phases de l'activité. Des *"oscillations cohérentes"* se produisent parfois dans les novae naines pendant les sursauts, ou dans les étoiles novoïdes dans leurs états brillants, et de plus dans WZ Sge pendant la phase de quiescence ; les périodes sont de quelque dix secondes, et des amplitudes de l'ordre de 0.002 mag. Et enfin, il y a des *"oscillations quasi-périodiques"*, avec des temps de cohérence extrêmement courts, sur des périodes de l'ordre d'une minute, avec des amplitudes un peu plus grandes que celles des oscillations cohérentes. Dans les trois novae naines les plus brillantes, SS Cyg, U Gem, et VW Hyi, des oscillations peuvent aussi être détectées dans le domaine des rayons X.

Toutes ces données photométriques montrent que les caractéristiques communes des novae naines sont les comportements de leurs sursauts, les courbes de lumière orbitales (qui présentent souvent un "hump" et/ou une éclipse), et les variations de flux à court terme sur plusieurs échelles de temps. Une considérable variété d'aspects peut être trouvée, non seulement dans les divers systèmes, mais aussi dans le même objet, à différents moments des sursauts. Les observations spectroscopiques indiquent que les novae naines émettent un flux appréciable, depuis le domaine des rayons X jusqu'à l'infrarouge, et dans quelques cas aussi dans le domaine radio. La plupart du flux est émis dans l'ultraviolet et, progressivement moins, à des longueurs d'ondes plus grandes. La distribution de flux est très différente de celle d'une étoile normale. Sur des intervalles de longueurs d'ondes de 1000 à 2000 A, un accord avec une distribution en *loi de puissance* est possible.

Pendant le sursaut, le spectre est plus raide que pendant la quiescence, et encore plus de flux est émis aux autres énergies. Dans quelques objets, le flux augmente encore dans l'infrarouge et décroît seulement à des longueurs d'ondes élevées après un maximum au voisinage de 1.5 à 2 μm. Bien que ce comportement général soit celui de toutes les novae naines, la distribution d'énergie diffère sensiblement d'un objet à l'autre, et à différents stades des sursauts. La croissance vers le maximum se produit simultanément aux longueurs d'ondes optiques et ultra-violettes ; au contraire le domaine optique peut commencer à manifester cette augmentation avant le domaine ultraviolet (jusqu'à un demi jour d'avance!). Il existe des indications selon lesquelles ce délai se prolonge dans le domaine des rayons X.

Le déclin après le sursaut se comporte toujours de façon simultanée à toutes les longueurs d'ondes. Aux énergies du domaine des rayons X, les novae naines quiescentes rayonnent de façon préférentielle dans le domaine des rayons X durs, cependant que pendant le sursaut on les voit plutôt dans le domaine des rayons X mous. Le flux dans les rayons X est très variable, à toutes les échelles de temps. On a trouvé une relation entre le rapport du flux des rayons X au flux visuel, et la largeur équivalente de Hβ. Un très petit nombre seulement de novae naines pourrait être détecté aux énergies radio.

Ces observations spectroscopiques du continu des novae naines suggèrent que le flux ultraviolet et la plus grande partie du flux optique proviennent du disque d'accrétion. L'infrarouge et probablement une portion du flux optique pendant la quiescence provient de la composante secondaire. Le rayonnement X est attribué à la couche de transition: supposée optiquement faible pendant la période de quiescence, par suite, elle émet alors des rayons X durs ; optiquement épaisse pendant le sursaut, du fait que par conséquent, le rayonnement est thermalisé avant de quitter les lieux, elle émet alors des rayons X mous.

Le spectre de raies pendant la quiescence est, dans la plupart des cas, caractérisé par des émissions fortes, bien que, dans quelques cas, les émissions dans le domaine optique soient faibles, voire même que les raies dans le domaine ultraviolet soient faiblement en absorption. Dans les systèmes à inclinaison forte, les raies d'émission de Balmer présentent des profils à deux pics. Dans de nombreux cas, le spectre d'absorption d'une étoile froide de la série principale est visible.

En général, dans le domaine optique, les raies subissent des changements de profils à des échelles de temps comparables à celles de l'orbite. En particulier, de nombreuses raies sont affaiblies pendant l'éclipse photométrique. Aucune observation de cette nature n'a été publiée dans le domaine ultraviolet. Dans de nombreux systèmes, ce qu'on appelle *l'onde S* est observée ; c'est une variation systématique de la force relative des pics rouges et bleus des raies de l'hydrogène pendant le cycle orbital. De même, les vitesses radiales se modifient en phase avec la courbe de lumière orbitale. Les spectres d'émission et d'absorption sont déphasés l'un par rapport à l'autre d'environ 180°.

Les caractéristiques spectrales observées montrent que les raies d'émission sont formées dans des régions du disque optiquement minces, alors que les raies d'absorption quelquefois observées dans l'ultraviolet suggèreraient plutôt que le disque intérieur est optiquement épais. Les modifications périodiques des vitesses radiales et des intensités de raies sont attribuées aux variations orbitales, cependant que des modifications au hasard sont attribuées aux inhomogénéités du disque d'accrétion. Les profils de raies à deux pics sont sans doute dus à la rotation des disques vus sous des angles correspondant à une inclinaison élevée. Le décalage de phase de 180° entre les raies d'absorption et d'émission est un effet de la binarité, les émissions étant produites dans le disque d'accrétion autour de la naine blanche, et l'absorption dans l'étoile froide secondaire. Les effets d'irradiation sont probablement responsables de la déviation d'un décalage de phase d'exactement la moitié d'une période orbitale.

Pendant le sursaut, le spectre de raies, aussi bien dans le domaine optique que dans le domaine ultraviolet, devient un spectre d'absorption. Le spectre d'absorption, à la fin des sursauts, est masqué par le flux continu en augmentation.

A peu près au moment du maximum, ou peu de temps après. les émissions commencent à augmenter dans le domaine des raies d'absorption larges ; et, pendant la période de déclin, le spectre quiescent est restauré.

Les vitesses radiales pendant le sursaut sont à peu près les mêmes que celles pendant la quiescence, mais les vitesses K et γ peuvent être différentes.
L'aspect du spectre dans les sursauts suggère que le disque est devenu opaque. Les profils, quelquefois observés comme déplacés vers le bleu, ou du type P Cygni, démontrent l'existence d'un vent à haute vitesse soufflé par le système pendant le sursaut. On soupçonne les variations dans les vitesses K et γ comme dues à des changements d'éclat du disque.

3. LES NOVOÏDES: OBSERVATIONS

Cinq classes d'étoiles novoïdes sont distinguées: les *UX Ursae Majoris*, les *novae anti-naines*, les *DQ Herculis*, les *AM Herculis* et les *AM Canum Venaticorum*.

Toutes les variables novoïdes ont la propriété commune de ne présenter en temps normal aucune activité importante sous forme de sursauts, bien qu'on puisse les observer dans des états "hauts" ou "bas".

L'aspect spectroscopique et l'aspect photométrique des étoiles UX UMa sont très semblables à ceux des novae naines, à certaines époques du cycle de l'activité.

Des novae anti-naines sont généralement trouvées dans un état d'éclat élevé. À des moments auxquels on ne peut les distinguer des étoiles UX UMa, elles subissent cependant des

chutes d'éclat de quelques magnitudes, et ressemblent alors à des novae naines pendant leur phase de minimum.

En en ce qui concerne leur comportement à long terme, les étoiles DQ Her (ou *polars intermédiaires*) comportent l'étendue complète des possibilités trouvées pour les variables cataclysmiques. Leur aspect caractéristique commun est la présence d'au moins une période photométrique hautement stable en sus de la pefiode orbitale. Sur la base de la longueur de la période de cette variabilité supplémentaire, entre deux ou trois sous-classes sont distinguées. Spectroscopiquement la plupart de ces étoiles n'apparaîssent pas différentes des étoiles UX UMa.

Comme les novae anti-naines, les étoiles AM Her (appelées aussi *polars*) sont normalement observées dans un état de brillance élevée, mais, de temps en temps, elles subissent des chutes d'éclat de plusieurs magnitudes. Toutes les étoiles AM Her sont caractérisées par un degré très élevé de polarisation qui varie en synchronisme parfait avec les changements orbitaux du niveau d'éclat général et de la vitesse radiale. Les courbes de lumière orbitale, aussi bien que les spectres, sont à bien des égards peu typiques pour des variables cataclysmiques.

Les étoiles AM CVn sont caractérisées par l'absence de toute trace d'hydrogène dans leur spectre, par des raies de l'hélium fortes, en absorption ou en émission, et par une activité de papillotement souvent prononcée.

Une interprétation de ces observations c'est que ces étoiles UX UMa et les étoiles anti-naines sont essentiellement les mêmes types d'objets. Cependant, dans les étoiles UX UMa le transfert de masse par le disque d'accrétion est toujours élevé ; par conséquent on pense que le disque est tout le temps stationnaire. Dans les novae anti-naines, d'un autre côté, le transfert de masse décroît de temps en temps. Dans les novae naines, le transfert de masse est si faible que le disque subit des changements semi-périodiques entre les événements de forte et de faible accrétion.

On pense que les étoiles DQ Her comportent une naine blanche magnétique faible. Cette étoile détruit le disque intérieur d'accrétion, mais le champ magnétique n'est pas assez fort pour maintenir l'étoile en synchronisme avec le mouvement orbital. La rotation de la naine blanche devient visible comme une période supplémentaire photométrique stable. Les étoiles AM Her sont supposées comporter une naine blanche fortement magnétique qui empêche entièrement la formation d'un disque d'accrétion, et assujettit la rotation de la naine blanche à l'orbite binaire.

4. MODÈLES DE NOVAE NAINES ET DE NOVOÏDES

Une histoire brève des modèles proposés pour expliquer les novae naines et les novoïdes est donnée. L'une des raisons de la difficulté de trouver jusqu'aux années 50 un modèle capable d'expliquer au moins la majorité des observations a été la resolution temporelle trop faible, qui a forcé les astronomes à se concentrer entièrement sur le comportement du sursaut, et de ce fait on n'a pas pu révéler les périodicités à des échelles de temps plus courtes. Ce fut Linnell (en 1950) qui a proposé, pour les UX UMa un modèle remarquablement semblable au modèle de Roche, maintenant communément accepté.

Quand il est devenu clair que toutes les variables cataclysmiques bien étudiées sont des systèmes binaires avec des périodes orbitales de quelques heures, que les étoiles secondaires, lorsqu'elles étaient observables, sont des étoiles froides de la série principale, et que les étoiles primaires sont des objets chauds dont la géométrie et la distribution du flux sont très différentes de celles d'étoiles normales, le modèle de Roche a été adopté comme une hypothèse de travail. Ce modèle est constitué d'une étoile de série principale froide qui remplit son lobe de Roche, et qui perd de la matière dans le lobe de Roche de la naine blanche. Le matériel transféré a un moment angulaire trop élevé pour pouvoir tomber directement sur la

surface de la naine blanche, mais construit plutôt un disque d'accrétion dans lequel il entre vers la naine blanche, suivant des mouvements en spirale, pour s'agglomérer ultérieurement à l'étoile.

Un nombre croissant d'observations, aussi bien photométriques que spectroscopiques, et pratiquement dans le domaine spectral entier, des rayons X durs à l'infrarouge, ont apporté de plus en plus de crédibilité à l'idée que le modèle de Roche est adéquat à décrire la physique de base des variables cataclysmiques. Cependant, de nombreux détails restent à expliquer, et la structure des systèmes est vraisemblablement plus compliquée que cela ne peut être théoriquement discuté à ce stade. L'un des paramètres qui décide de facon critique de l'apparence et des variations temporelles du disque d'accrétion est la *"viscosité"*, essentiellement inconnue. Cette viscosité est un moyen de décrire le mécanisme de transfert du moment angulaire dans le disque. On la représente d'une facon paramétrique comme une quantité α, définie comme le rapport de la vitesse turbulente à la vitesse du son, en y incluant les effets des champs magnétiques probablement à l'oeuvre. C'est, fondamentalement, un paramètre "libre", auquel on peut bien donner des valeurs différentes en différents points du disque.

Pour toute interprétation théorique, il est très important de connaître les valeurs absolues des paramètres d'un système, tels que les masses stellaires et les rayons, les angles d'inclinaison, les magnitudes absolues, les taux de transfert de masse. Pour cette raison, une discussion critique des méthodes de détermination de ces paramètres, et du degré de confiance que l'on peut avoir en elles, est donnée. Dans un systéme binaire normal détaché, les masses et les rayons, aussi bien que l'angle d'inclinaison peuvent être déduits des courbes de vitesses radiales et des courbes de lumière. Cependant, seulement deux binaires spectroscopiques à éclipses à raies dédoublées sont connues parmi les novae naines et les novoïdes. Si bien qu'en principe on ne peut déduire de masses que pour ces deux systèmes. De plus, la forme des courbes de lumière montre que la géométrie du système n'est pas celle d'un système détaché normal. Par conséquent, on peut se poser fortement la question de savoir si l'angle d'inclinaison et les rayons des étoiles peuvent être déterminés en utilisant le procédé usuel. Par exemple, un grand soin doit être pris pour la détermination des courbes de vitesse radiale, de telle sorte que les inhomogénéités du disque (comme par exemple la presence d'une *tache chaude*) et l'irradiation de l'étoile secondaire soit prise en compte d'une facon correcte. De plus, le spectre chaud est en général celui du disque d'accrétion, plutôt que celui de la naine blanche elle-même.

Les contraintes dues à l'hypothèse que l'on peut appliquer la géométrie de Roche sont fort utiles pour déterminer les paramètres du système. Par exemple, des relations existent entre le rayon de l'étoile secondaire et le rapport de masse des composantes stellaires. Une autre relation existe aussi entre l'amplitude des variations de la vitesse radiale de la composante primaire Kl, la vitesse de rotation projetée du disque et le rapport de masse. Cependant, des difficultés sévères sont rencontrées dans la détermination raisonnable de l'angle d'inclinaison et des vitesses radiales.

Les paramètres de l'étoile secondaire peuvent en principe être déterminés par exemple à partir des couleurs de l'infrarouge ; mais, là aussi, que de difficultés!

Des magnitudes absolues et des distances peuvent êtres tirées du spectre de l'étoile secondaire. De plus, des relations raisonnablement bien définies existent entre la magnitude absolue visuelle d'une nova naine au moment du sursaut, et la période orbitale, et également entre la magnitude visuelle et la largeur équivalente de l'émission en Hβ. La caractéristique d'absorption interstellaire à 2200 A, lorsqu'elle est présente, peut être également utilisée comme un indicateur de distance. Pour les étoiles U Gem and SS Cyg, des parallaxes trigonométriques ont été mesurées.

D'autres paramètres importants sont les taux de transfert de masse, -c'est-à-dire le taux de

transfert de masse depuis l'étoile secondaire jusqu'à l'intérieur du lobe de Roche de l'étoile primaire, la distribution de masse dans le disque d'accrétion, et le taux d'accrétion de masse sur la naine blanche. Toutes ces déterminations dépendent fortement du modèle. La méthode la plus sûre semble celle basée sur les techniques de modélisation des éclipses.

Bien que que les observations semblent indiquer que les changements d'éclat dans les novae naines soient directement dus aux changements dans le disque, il reste de nombreux problèmes non résolus.

Les hypothèses simplificatives généralement faites dans le travail théorique sont l'hypothèse que les effets relativistes sont négligeables, ainsi que ceux de l'autogravitation ; de plus le disque est supposé être géométriquement mince, reposant à plat dans le plan orbital du système. Il est supposé être en symétrie rotationnelle, et la seule source d'énergie est l'énergie gravitationnelle, convertie en énergie de rayonnement par les processus visqueux, ce qui rend compte de la séparation du moment angulaire et de la masse. Une certaine épaisseur verticale du disque est attribuée à une pression thermique due à l'énergie gravitationnelle et à la turbulence.

A partir de calculs de trajectoires de particules dans l'approximation à trois corps, la position approximative de la tache chaude peut être calculée. Des calculs hydrodynamiques fournissent une information sur les distributions d'éclat, sur les distributions des densités de surface, et sur les champs de vitesses dans le disque.

En supposant l'équilibre hydrostatique dans la direction verticale, et en utilisant les équations de base pour les atmosphères stellaires, on peut obtenir quelque idée des structures verticales du disque. Malheureusement, le paramètre le plus important et le moins bien connu de tous ces calculs est la viscosité.

Deux mécanismes possibles de sursauts ont été suggérés pour les novae naines, *l'instabilité visqueuse* dans le disque d'accrétion (*"instabilité du disque"*) ou un *transfert de masse* soudainement accru vers le disque à partir de l'étoile compagnon (*"instabilité de transfert"*). Le premier mécanisme suppose que la viscosité subit un cycle d'hystérésis, alors que l'état physique de la matière du disque passe d'un état convectif à un état radiatif. Des courbes de lumière très générales des sursauts, et même dans une certaine mesure assez détaillées, peuvent être reproduites thèoriquement.

L'autre mécanisme suggéré suppose que des instabilités de l'atmosphère de l'étoile secondaire conduisent à un accroissement temporaire du transfert de masse vers le disque, ce qui cause le sursaut. Dans ce cas également, un accord raisonnablement satisfaisant avec les observations peut être obtenu. Jusqu'à présent, aucune discrimination claire entre les deux modèles ne peut être proposée.

De même, aucun modèle largement accepté n'existe jusqu'à présent pour les "super-sursauts".

Les oscillations rapides, en raison de leurs fréquences élevées et de leurs temps de cohérence courts, sont attribuées soit à la région la plus superficielle de la naine blanche, soit aux régions les plus intérieures du disque d'accrétion.

Des variations séculaires de la période orbitale, comme on les observe dans de nombreuses novae et novoïdes, ne sont pas encore expliquées de facon satisfaisante.

Les modèles proposés pour expliquer les systèmes fortement magnétiques (étoiles AM Her) et les systèmes faiblement magnétiques (étoiles DQ Her) sont décrits. Pour les étoiles AM Her, on suppose qu'une naine blanche fortement magnétique, et en rotation synchrone, empêche la formation d'un disque d'accrétion, et contraint l'accrétion à se produire par des tubes magnétiques le long des lignes de force. Dans les étoiles DQ Her, la naine blanche possède seulement un champ magnétique modéré, capable de perturber le

disque à quelque distance de l'étoile, mais ce champ ne peut pas en empêcher entièrement la formation, pas plus qu'il ne peut maintenir l'étoile naine blanche en rotation synchrone avec le mouvement orbital. L'illumination des composantes du système du pôle chaud d'accrétion ou la radiation directe à partir de ces pôles produit les périodicités photométriques additionnelles que l'on observe.

5. INTERPRÉTATION DES SPECTRES DE NOVAE NAINES ET DE NOVOÏDES

Le *spectre* des novae naines et des novoïdes présente une variété d'apparences, spectre pur de raies d'émission, spectre pur de raies d'absorption, mélange des deux, profils de raie asymétriques, pentes très différentes des distributions du continu ; une même étoile peut présenter ces aspects à différentes époques. Pour simplifier le problème de la modélisation de ces spectres, on le divise généralement en trois problèmes séparés. Celui de la spécification du modèle physique qui sert de base aux calculs, celui du calcul du spectre continu, et celui du calcul du spectre de raies. Le modèle physique qui sert de base aux calculs est le modèle de Roche des variables cataclysmiques.

La distribution continue du flux ne ressemble pas à celle des étoiles variables, et une coïncidence approchée est possible si l'on suppose que seulement le disque contribue au rayonnement, et qu'à chaque distance de la naine blanche il rayonne comme un corps noir avec la distribution radiale de température telle qu'elle est calculée pour un disque d'accrétion stationnaire.

Le spectre de raies d'absorption est calculé de façon tout-à-fait analogue aux méthodes utilisées pour les atmosphères stellaires. La différence fondamentale entre une atmosphère stelaire et une atmosphère de disque est la *source d'énergie nucléaire* dans le premier cas, *gravitationnelle* dans le second. Mais ceci ne change rien en ce qui concerne le spectre émis, tant que le plan central du disque est optiquement épais. De plus, contrairement à ce qui se passe pour les atmosphères stellaires, les disques d'accrétion sont essentiellement des objets à deux dimensions, et, par conséquent, *l'angle d'inclinaison* est un paramètre important du rayonnement observé. La rotation képlérienne du disque conduit à un élargissement additionnel du profil de la raie, et à des profils d'absorption à deux pics. Des résultats essentiels obtenus à partir de spectres synthétiques sont ceux des principaux paramètres libres (c'est-à-dire la masse de la naine blanche, le taux de transfert de masse, les rayons intérieurs et extérieurs du disque, et l'angle d'inclinaison) ; la masse de la naine blanche et le rayon du disque extérieur n'ont pratiquement aucune importance. L'angle d'inclinaison a un effet dominant considérable sur le continu aussi bien que sur les raies. Le taux de transfert de masse intervient dans le profil radial de température, et par conséquent a une influence très importante sur l'aspect du spectre, et enfin le rayon intérieur du disque est d'une grande importance puisque sa variation signifie que l'on inclut ou que l'on néglige les parties les plus chaudes du disque, celles qui déterminent entièrement l'ultraviolet, et aussi une partie du rayonnement optique.

Les raies d'émission sont généralement observées pendant l'état quiescent ; on les attribue à des régions optiquement minces dans la portion intérieure et/ou extérieure du disque, ou même dans la totalité du disque. La modélisation est plus difficile que pour le spectre des sursauts, car, pendant la quiescence, le disque n'est probablement pas stationnaire (c'est-à-dire qu'aucune loi radiale de température n'est disponible à priori), et les effets non-ETL sont vraisemblablement importants.

Les observations optiques des novae naines et des étoiles novoïdes *pendant les sursauts* ne montrent *aucune trace de vent* : Les raies de Balmer sont vues en absorption, et ont des profils symétriques. Dans l'ultraviolet cependant, des forts profils de type P Cygni ou des absorptions déplacées vers les courtes longueurs d'onde du doublet de résonance du C IV, et, à l'occasion, du Si IV et de N V, sont

observés. Ces profils sont différents de ceux que l'on voit dans le spectre des étoiles chaudes normales. De plus, des systèmes avec des angles d'inclinaision très élevés montrent seulement des profils d'émission intenses, alors que toutes les autres raies sont vues, comme d'habitude, en absorption. Des calculs faisant l'hypothèse d'un disque d'accrétion optiquement épais, et d'un vent poussé à partir du centre du disque, et/ou de la couche de transition, peuvent reproduire les observations assez bien si les paramètres les plus importants (dans ce cas, le taux de perte de masse, le profil de vitesse du vent, la température et le profil de température du disque d'accrétion) sont choisis de façon convenable.

Grâce à des techniques de traitement d'image, la brillance de surface et la distribution de température des disques d'accrétion peuvent être reconstruits à partir des observations d'éclipses. Cette méthode permet en principe la détermination du profil radial de température et la localisation de l'origine géométrique des contributions diverses aux rayonnements dans les raies, la distinction entre les régions optiquement épaisses et optiquement minces du disque d'accrétion qui dépendent du type d'observation, et, selon le type d'observation, bien d'autres propriétés encore.

La détection de rayonnements X (mous et durs) dans le spectre de nombreuses novae naines et novoïdes est attribuée à une couche de transition entre le disque et la surface de la naine blanche, couche qui se forme là où se trouve la matière du disque, avec la vitesse képlérienne de rotation, et ralentit jusqu'à la vitesse de rotation de la naine blanche, afin de permettre l'accrétion. La structure détaillée de cette couche, aussi bien que les détails du spectre émis, ne sont pas encore compris.

L'état d'évolution des variables cataclysmiques est discuté. Leur distribution spatiale et les effets de sélection sont considérés. Les novae et les novae naines semblent avoir à peu près la même distribution spatiale, et les deux types d'étoiles sont généralement des objets de population I, bien que quelques novae naines soient connues pour appartenir aux amas globulaires. Les propriétés des composantes stellaires des systémes de variables cataclysmiques sont discutées. Selon certaines indications, les membres naines blanches des variables cataclysmiques sont, statistiquement, plus massives que les étoiles naines blanches simples. Ce désaccord peut être expliqué par des effets de sélection, dus principalement à la relation masse-rayon des naines blanches. Les étoiles secondaires apparaissent comme impossibles à distinguer des étoiles de la série principale normale. On s'attend à ce qu'il existe des secondaires naines noires dans ces systèmes, au dessous de l'intervalle vide des périodes, mais on n'a pas pu encore les détecter.

Une caractéristique tout-à-fait remarquable des variables cataclysmiques est l'existence d'un intervalle de périodes compris entre à peu près deux et trois heures, et la période orbitale minimum d'environ 80 minutes. L'extrémité supérieure de cet intervalle de période est due, on le comprend, à la cessation du freinage magnétique opérant sur l'étoile secondaire. Comme conséquence, l'étoile secondaire est détachée de son lobe de Roche, et le flux de masse d'un lobe à l'autre s'arrête. La radiation gravitationnelle joue dans le sens de la décroissance de la période orbitale, et au moment où la période a décrû jusqu'à une valeur d'environ 2 heures, elle raméne l'étoile en contact avec son lobe de Roche. La période continue à décroître en raison du rayonnement gravitationnel jusqu'à ce que, au moment du minimum orbital, l'étoile secondaire ait perdu une quantité de masse suffisante pour qu'elle ne soit plus capable de maintenir la production d'énergie nucléaire, et par conséquent devienne dégénérée. A des niveaux ultérieurs de l'évolution, la période orbitale augmente encore jusqu'à ce que l'étoile secondaire soit résolue.

C'este encore une question complètement ouverte de savoir quelles étoiles sont les progéniteurs des variables cataclysmiques. Bien que les étoiles W Ursae Majoris aient environ la même densité spatiale et la même distribution que les variables cataclysmiques, leur moment angulaire est trop petit pour qu'une naine blanche puisse être formée, et par conséquent

on peut les exclure comme des candidats possibles. Aucun autre groupe d'étoiles ne peut être identifié comme des progéniteurs possibles.

Des scénarios possibles de l'évolution d'un système binaire vers des étoiles cataclysmiques sont ensuite discutés.

Enfin, un scénario souvent décrit est présenté, selon lequel les novae, les novae naines et les novoïdes pourraient en réalité être les mêmes types d'objets, à différents stades de leur activité.

Le chapitre 5 résume les principaux arguments du débat concernant les novae naines, et les novoïdes, et discute la validité des systèmes de classification employés usuellement.

6. NOVAE CLASSIQUES ET RÉCURRENTS : OBSERVATIONS

Les chapitres 6 à 10 discutent les propriétés observées générales des novae classiques et récurrentes, les modèles théoriques, les caractéristiques et les modèles de quelques unes des novae classiques et des novae récurrentes bien observées.

Le chapitre 6 décrit les caractéristiques observables des novae classiques et des novae récurrentes obtenues par différentes techiques (photométrie, spectroscopie, et imagerie) dans tous les domaines spectraux disponibles, et à des phases variées de la vie de la nova. Ces phases sont schématisées comme suit : *quiescence* (*avant et après le sursaut*), *sursaut*, *déclin final*, et *phase nébulaire*.

L'examen de toutes les observations disponibles des vieilles novae, avant et après le sursaut, montre que l'éruption a eu un très petit effet sur la structure stellaire et sur le système binaire, quand les paramètres de ces derniers sont connus.

En fait, aussi bien les propriétés que photométriques et spectroscopiques restent les mêmes avant et après le sursaut, bien que dans quelques cas, des périodes de temps assez longues (plusieurs années) sont nécessaires pour que l'étoile revienne à la magnitude observée avant le sursaut. Par conséquent, il devrait être très important d'étudier les vieilles novae qui ont explosé il y a des siècles. Malheureusement, on ne connait que deux cas de tels objets, CK Vul 1670 et WY Sge 1783.

De nombreuses novae présentent, au minimum, des phénomènes de *papillotage*, et, très rarement, des *oscillations cohérentes* (DQ Her, V 533 Her), ou des *oscillations quasi-périodiques* (RR Pic, GK Per).

Le spectre de seulement trois novae quiescentes, avant le sursaut, c'est-à-dire avant qu'elles soient connues comme des novae, a été observé. Ces spectres, bien que limités à trois cas, et d'une qualité plutôt médiocre, suggèrent qu'ils ne diffèrent pas beaucoup de ceux pris après la fin du sursaut.

Les spectres des novae du passé sont caractérisés par un continu très bleu et des raies d'émission de HI, HeI, HeII ; il n'y a aucune évidence claire de la présence de raies d'absorption. La comparaison des spectres de nombreuses novae anciennes, novae naines et novoïdes ne fait pas apparaître de différences très nettes entre ces trois classes d'objets. Nous pouvons répéter encore que les caractéristiques photométriques aussi bien que spectroscopiques des novae sont impossibles à distinguer de celles des novae naines, bien que la luminosité et le taux d'accrétion ne soient pas les mêmes.

Des études statistiques des spectres de novae et de novae naines au minimum indiquent que la largeur des raies d'émission est étroitement liée à l'inclinaison du système : Plus les raies d'émission sont larges, plus l'inclinaison du disque d'accrétion est proche de 90°.

Bien que les caractéristiques photométriques des novae quiescentes soient assez semblables les unes aux autres, la courbe de lumière du sursaut peut différer fortement. Les novae sont par conséquent classées selon la rapidité du déclin après le maximum. Les classes sont : les *novae*

rapides (t_3 < 100 jours, où t_3 est le nombre de jours nécessaires pour que l'éclat diminue de 3 magnitudes), les *novae lentes* (t_3 > 150 jours) et les *novae très lentes* qui restent à leur maximum pendant plusieurs années. Une classification très détaillée proposée par Duerbeck (en 1987) prend en compte également la présence ou l'absence d'oscillations pendant la phase de transition, la présence ou l'absence d'un minimum profond dans la phase de transition et d'autres détails de la courbe de lumière des sursauts.

Une corrélation importante a été trouvée entre la magnitude absolue au maximum et la rapidité du déclin après le maximum, les novae les plus rapides étant les plus brillantes. Par conséquent, leur distance peut être estimée. Une autre méthode pour déterminer les distances, et utilisant les parallaxes d'expansion nébulaire, est discutée dans la section consacrée à la phase nébulaire des novae.

Le spectre de l'étoile pendant le sursaut, qui montre la présence de couches en expansion à de très hautes vitesses, passe par des phases variées.

a) Juste avant que le maximum d'éclat soit atteint, le *spectre pré-maximum* est très semblable au spectre d'une supergéante B ou A.

b) Le *spectre principal* remplace le spectre prémaximum dans un délai de quelques jours après le maximum, et persiste jusqu'à ce que l'éclat de la nova se soit atténué d'à peu près quatre magnitudes. Ce spectre est très semblable au spectre antérieur au maximum, mais généralement de type légèrement plus avancé et semblable à celui d'une supergéante A ou F. La vitesse radiale d'expansion est plus qrande que celle qui est indiquée par le spectre avant le maximum. Une corrélation existe entre le type du spectre principal et la vitesse d'expansion, qui va d'environ 2000 km/s pour les spectres les plus chauds (caractérisés par la présence de raie de N V), à 200 à 100 km/s pour les types F0-F8. C'est une indication très claire que c'est de l'énergie cinétique née pendant le sursaut qui est à l'origine du spectre observé.

c)Le *spectre diffus-renforcé* (diffuse-enhanced) apparaît plus tard que le spectre principal, et montre un taux de vitesse d'expansion plus élevé que celui-ci. Les raies d'absorption sont larges et fortes. Ce spectre atteint son intensité maximum lorsque l'étoile est à 2 magnitudes au-dessous de son maximum.

d) Le *spectre de type Orion* est semblable à ceux des étoiles de type B dans la nébuleuse d'Orion, et atteint son intensité maximum lorsque la nova est à 3 magnitudes au-dessous du maximum.

Ces quatre systèmes décrivent pratiquement toutes les caractéristiques d'absorption;à chaque système d'absorption correspond un système d'émission. Toutes les absorptions et les émissions correspondantes forment des profils caractéristiques du type P Cygni, typiques d'enveloppes en expansion.

e) Lorsque la nova s'est affaiblie de quatre magnitudes, un autre système d'émission apparaît, le *spectre nébulaire*, qui est complètement développé lorsque l'éclat de la nova a atteint 7 magnitudes au dessous du maximum. C'est d'abord un spectre nébulaire typique, caractérisé par les raies interdites de N I, O I, N II, O II, O III, et plus tard, dans quelques cas, par des raies coronales (c'est-à-dire avec des niveaux de ionisation plus élevés que celui du Fe VII, dont le potentiel d'ionisation est de 125 eV).

Les observations infrarouges de novae donnent des informations sur des régions beaucoup plus froides que celles à partir desquelles le rayonnement optique est produit. Elles ont révélé la formation de couches de poussière à des températures plus basses qu'environ 1000 K, et elles ont expliqué quelques caractéristiques des courbes de lumière à sursauts des novae lentes. Correspondant au minimum profond de la courbe de lumière, on observe une augmentation du flux infrarouge, ce qui indique qu'une couche de poussière se forme, qui absorbe le rayonnement optique. Quand le minimum profond est absent, l'excès infrarouge est également absent et aucune couche de poussière ne

se forme. Bien que peu de données soient disponibles pour permettre d'établir des statistiques fiables, les novae rapides ne forment pas de couche poussiéreuse optiquement épaisse, cependant que les novae lentes le font. Les novae intermédiaires forment seulement une couche de poussière mince. Cependant, les deux exemples connus de novae extrêmement lentes, HR Del et RR Pic, ne montrent pas ce minimum profond dans leur courbe de lumière qui devrait être un argument en faveur de la formation d'une couche de poussière.

Les observations menées à partir de satellites astronomiques ont permis l'observation des émissions ultraviolettes et dans le domaine des rayons-X, en provenance de novae. Quelques-unes de ces émissions sont issues de régions beaucoup plus chaudes que celles où le rayonnement optique est formé, et sont par conséquent complémentaires des observations faites à partir du sol.

L'importance des observations ultraviolettes peut être comprise si nous considérons que l'essentiel du rayonnement continu émis par les novae quiescentes se trouve, à très peu d'exceptions, dans l'ultraviolet. Des estimations de la température, de la luminosité et du taux d'accrétion de masse dans le disque et vers la surface de la naine blanche, qui sont d'une importance fondamentale pour la compréhension du phénomène de nova, ne peuvent être faites que grâce aux observations ultraviolettes.

Pour les novae à l'époque du sursaut, les observations du continu ultraviolet sont essentielles pour la détermination de la luminosité bolométrique. De plus, il est bien connu que presque toutes les raies fortes de résonance des ions abondants tombent dans l'ultraviolet. Ces raies fournissent une information sur les processus de l'excitation, sur les régions de formation des raies, sur la présence de phénomènes de perte de masse, et sur l'intensité du champ de rayonnement ionisant dans la région de l'extrême ultraviolet, difficile d'accès à cause de l'absorption interstellaire au dessous de 913 A.

Le comportement des novae dans l'ultraviolet est décrit dans deux sections différentes : *novae quiescentes*, et *novae en explosion*. Cette subdivision a une base physique. En fait, des observations de novae quiescentes fournissent une information importante sur les composantes chaudes, sur leur champ de rayonnement, et sur ceux des processus qui se produisent au voisinage de la composante compacte. En revanche, les observations faites pendant le sursaut et la phase de déclin qui le suit, donnent une information sur la structure physique de la pseudophotosphère étendue et sur sa composition chimique.

Le spectre continu ultraviolet des novae quiescentes peut généralement être reproduit raisonnablement bien par une distribution $F(\lambda) \propto \lambda^{-\alpha}$, où $\alpha \approx 2$, ce qui n'est pas très différent de la valeur "standard" $\alpha = 2.33$ trouvée pour un modèle théorique simple de disque d'accrétion calculé en 1969 par Lynden-Bell.

Le peu d'observations disponibles dans l'extrême ultraviolet (500-900 A) faites par la sonde Voyager indiquent que les modèles qui rendent compte de l'ultraviolet ne peuvent être extrapolés à la région de l'extrême ultraviolet.

Des exceptions au comportement général du continuum ultraviolet sont celles de GK Per dont le spectre continu est à son maximum vers 3600 A, au lieu de se trouver dans l'ultraviolet lointain comme pour les autres vieilles novae, telles que DQ Her, T Aur et BT Mon qui montrent un continu très plat, $\alpha \approx 0$.

Le paramètre très important $\dot{M}$ (taux de perte de masse) peut être estimé à partir de la luminosité d'accrétion du disque, $L(\text{disque}) = G \dot{M} M_1 / 2R_1$, où M_1 et R_1 sont la masse et le rayon de l'objet compact. Des valeurs de l'ordre de 10^{-8} $M_\odot$ par an ont été proposées, mais les méthodes impliquent de nombreuses incertitudes.

Le spectre de raies des vieilles novae est caractérisé par la présence de raies fortes d'émission d'atomes plusieurs fois ionisés comme NV, CIV, SiIV, HeII, NIV, NIII, CIII, SiIII. Des profils P Cygni ont été observés dans quelques cas, et mettent en évidence la perte de masse pendant un temps assez long après le

sursaut.

Comme dans le domaine optique, nous pouvons conclure que les spectres de novae en quiescence sont substantiellement semblables aussi dans l'ultraviolet. Le comportement optique et ultraviolet pendant le sursaut, au contraire, ne peut pas être décrit suivant un schéma commun, et chaque sursaut de nova a ses propres caractéristiques spécifiques.

Un résultat important obtenu à partir des observations ultraviolettes des sursauts de novae, c'est que la luminosité bolométrique reste pratiquement constante, ou décroît beaucoup plus lentement que l'éclat optique, jusqu'à ce que démarre le stade nébulaire. Le riche spectre de raies de l'ultraviolet a permis une détermination plus précise de la densité électronique et de la température des couches responsables des raies et par conséquent des déterminations de la composition chimique beaucoup plus fiables qu'il n'était possible de le faire par la seule observation du spectre optique. Un excès général de C, N, O, dans les novae classiques est confirmé. De plus, une nouvelle classe de novae, les *novae à néon*, a été découverte, caractérisées par la grande intensité des raies du néon. Certaines considérations suggèrent que l'enrichissement de la matière éjectée n'est pas une conséquence de réactions nucléaires dans l'enveloppe de la nova, mais reflète plutôt la composition de l'enveloppe au démarrage des TNR (réactions thermonucléaires). Des surabondances de C, N, O peuvent être expliquées par des TNR dans une couche déjà enrichie en ces éléments à partir de l'intérieur d'une naine blanche à C et O. L'enrichissement en Ne indiquerait que la matière éjectée a subi antérieurement des processus thermonucléaires conduisant au Ne dans ce qui est maintenant une naine blanche très massive à O-Ne-Mg. Des déterminations d'abondances, faites pour seulement quatre novae récurrentes, semblent indiquer que les abondances dans la matière éjectée, au contraire de ce qui se passe pour la matière éjectée par les novae classiques, sont essentiellement celles du Soleil.

L'accrétion est responsable également du rayonnement dans le domaine des rayons X, émis par les novae quiescentes. Il s'agit généralement de sources de rayons X de faible luminosité. Environ dix d'entre elles ont été détectées avec le satellite d'Einstein et l'on a : $L_x \approx 10^{31}$-10^{32} erg/s. Quelques autres étoiles de ce type ont été détectées avec EXOSAT, qui a fourni le premier enregistrement continu dans le domaine des rayons X d'une nova récurrente (RS Oph) pendant le sursaut.

Le déclin final des novae suit le creux de la courbe de lumière des novae lentes et précède l'apparition de l'enveloppe.

L'échelle de temps du retour à l'état de pré-nova est estimée être de l'ordre de grandeur de plusieurs dizaines d'années, bien que l'échelle de temps de consomption du noyau soit environ de l'ordre de 300 ans. Par conséquent, la raison physique de l'échelle de temps du retour à l'état de pré-nova n'est pas complètement comprise. Par exemple, l'analyse spectrophotométrique de la nova lente FH Ser montre que la transition se produit 200 jours après le sursaut. Or, la transition exige la consommation complète du carburant, soit par une combustion nucléaire, ce que n'est pas le cas en raison du temps nécessaire, beaucoup plus long que le temps observé, soit par quelque processus de ralentissement des réactions nucléaires, soit encore par quelque mécanisme de perte de masse.

Cette dernière peut se faire sous la forme d'un vent optiquement épais, c'est-à-dire la pseudo-photosphère en expansion de la nova en explosion; à moins que la perte de matière n'ait eu lieu à travers les points lagrangiens extérieurs du système, comme résultat de la friction dynamique pendant la phase de l'enveloppe commune.

Quand la nova a décliné, jusqu'à un état identique à ce qu'elle était avant le sursaut, la signature restante du sursaut est la nébulosité en expansion qui entoure l'étoile. Cette nébulosité semble un phénomène de vie relativement courte, parce qu'aucune nova ou novoïde, sans un sursaut enregistré, ne peut être identifiée comme une nova en raison de l'existence

d'une couche observable. Les enveloppes de nova ont été observées pour environ 20 objets. En général, elles sont ellipsoïdales, et présentent des condensations et des anneaux.

La dimension angulaire de la nébuleuse, la vitesse radiale d'expansion, et le temps qui s'est écoulé depuis l'explosion permettent de déterminer la *distance de la nova* à partir de l'hypothèse selon laquelle la vitesse de l'expansion est restée pratiquement constante. Cependant, des images de nébuleuses associées à des novae, et obtenues à différentes époques, montrent des décélérations notables avec le temps, de l'ordre de 10 à 2 km/s et par an. Ce freinage doit par conséquent être pris en compte pour une détermination correcte de la distance.

Les *masses des enveloppes de nova* sont de l'ordre de 10^{-5} à 10^{-4} masse solaire.

En dehors de la possibilité d'estimer les distances et de mesurer les masses, le spectre des enveloppes de nova permet aussi de déterminer la *composition chimique de la nébuleuse*, et, par conséquent, de vérifier si elle est affectée par les réactions nucléaires se produisant pendant le sursaut. Le spectre de raies d'émission de la nébuleuse permet une détermination plus précise des abondances que dans la phase de nova, où les raies d'absorption sont "blendées" par leurs composantes d'émission, à moins que les composantes des différentes couches en émission ne soient blendées les unes par les autres, et où les conditions sont très éloignées de celles d'une atmosphère stable. Au contraire, au moment où les couches deviennent séparées dans l'espace, la densité est si basse que la self-absorption et la désexcitation collisionnelle sont négligeables, si bien que la distance entre la couche d'une part et d'autre part l'objet stellaire complété par le disque d'accrétion, rend impossible toute confusion avec ces régions, qui subissent des conditions physiques très différentes. Les abondances de C, N, O peuvent être 10 à 100 fois égales à leur valeur solaire.

La possibilité d'étudier le résidu d'une très vieille nova a été offerte par une nébulosité entourant CK Vul 1670. Deux nébulosités faibles, à environ 5 secondes d'arc de l'objet central, plus quelques autres nébulosités encore plus faibles, ont des spectres semblables à ceux du matériel éjecté par la nova. L'intensité de la raie interdite [NII] 6548 est impressionnante, et celles de [SII], 6716 et 6730 sont également remarquables. La luminosité de l'objet central est beaucoup plus basse que celle des vieilles novae typiques, et comparable à celles des plus faibles novae naines. Cette luminosité peut être expliquée par une naine rouge normale et démontre l'absence de toute contribution de la naine blanche et du disque d'accrétion. Ceci peut indiquer que le transfert de masse s'est arrêté dans ce système.

Des observations radioastronomiques dans les longueurs d'ondes centimétriques ont mis en évidence des émissions radio à partir des étoiles HR Del 1967, V 1500 Cyg 1975, V368 Sct 1970 et FH Ser 1970. L'émission radioastronomique maximum a été atteinte entre 100 et 200 jours après le sursaut, pour la nova très rapide V 1500 Cyg, et environ 1000 jours après le sursaut, pour la nova très lente HR Del. En aucun cas, l'émission radio n'a été observable plus tôt que 50 jours après le sursaut. Les spectres sont cohérents avec celui de l'émission thermique d'une enveloppe de gaz ionisé en expansion.

Les observations de la vieille nova GK Per 1901, dans à peu près le même domaine de longueurs d'onde, ont permis de détecter une radio source étendue ressemblant à la nébulosité optique au voisinage de la nova. Le spectre indique que l'émission est de toute évidence non thermique.

La seule nova récurrente pour laquelle l'émission radio ait été détectée est RS Oph. Les observations ont commencées seulement 18 jours après le sursaut de 1985. La température de brillance est d'environ 10^7K (par contraste avec la valeur de seulement 10^4K observée pour les novae classiques) et elle indique une origine non-thermique du rayonnement.

7. MODÈLES DE NOVAE CLASSIQUES ET RÉCURRENTES

Le chapitre 7 discute les modèles des novae classiques et récurrentes. On remarque que le comportement des novae peut être divisé en deux étapes séparées : la quiescence et le sursaut. Cependant, ces deux étapes ne peuvent être complètement séparées, parce qu'il est possible que l'étoile compagnon et le disque d'accrétion qui déterminent le comportement de la nova à la quiescence puissent jouer un rôle pendant le sursaut, en raison de leur interaction avec la couche éjectée, ou avec la "naine gonflée" formée dans l'explosion. Le même modèle devrait être capable d'expliquer les caractéristiques observées pendant les deux phase typiques.

En dépit de la variété des formes de courbes de lumière et des détails spectroscopiques, il y a des ressemblances entre les différents objets. Des relations existent entre la magnitude absolue au maximum et le temps t_3, ou entre la vitesse de l'expansion et le type spectral du spectre principal, ou encore entre la vitesse d'expansion et le temps t_3. Ces relations indiquent qu'une unité systématique existe dans le groupe des novae. Sans doute des "paramètres cachés" déterminant la magnitude absolue au maximum, et la vitesse d'éjection, etc., sont-ils par exemple : la masse de la naine blanche et sa composition chimique, la masse du matériel accrété et le taux d'accrétion, le degré de mélange de la matière de la naine blanche vers la matière de la couche riche en hydrogène accrété, les éléments orbitaux. Malheureusement, les données déduites des observations au moment du minimum sont faibles.

Une histoire rapide des modèles anciens, leur recherche d'une cause sous-jacente et des possibles mécanismes d'éjection de masse sont décrits. Différents *mécanismes d'éjection de masse* sont étudiés : éjection par choc, éjection par pression, éjection par pression de radiation, et éjection par perte pulsationnelle de masse. On pense maintenant que les trois premiers mécanismes cités peuvent jouer un rôle pendant les stades variés du sursaut de la nova. L'éjection par choc semble prédominer dans les novae rapides et récurrentes, et un vent stellaire optiquement épais, poussé par la pression de radiation, semble important dans les novae lentes. On peut commenter ces processus comme suit:

a) *Ejection par choc* : Lorsque l'énergie est produite dans une certaine région en un intervalle de temps plus court que le temps de parcours de cette région par le son, une onde de choc est engendrée au bas de cette région et se propage vers l'extérieur. Après le passage du choc, le matériel éjecté a un gradient de vitesse très fort, avec la vitesse augmentant vers l'extérieur et décroissant avec le temps. Ceci est en général contraire à ce que l'on observe dans les novae classiques, sauf peut-être pour la matière des systèmes d'absorption du prémaximum.

b) *Ejection par pression* : Si l'énergie est stockée dans une région pendant un intervalle de temps plus grand que le temps que met le son à traverser cette région, mais plus court que l'intervalle de temps caractéristique de la diffusion du rayonnement, une onde de pression se développe, qui éjecte toute la matière au-dessus de la région, avec à peu près la même vitesse, qui croît avec le temps.

c) *La pression de radiation* due à la diffusion des électrons est importante dans les étoiles de haute luminosité.

d) *La perte de masse par pulsation*: En supposant une combustion thermique instable de l'hydrogène, une naine blanche chaude devient pulsationnellement instable. La dissipation des ondes de choc produites par la pulsation semble être un moyen plausible de chauffage de la surface, bien que les calculs ne montrent pas vraiment comment l'enveloppe de la nova a été éjectée.

Les observations montrent que la luminosité de toutes les post-novae, au moins peu de temps après le sursaut, sont égales à, ou plus grandes que, la luminosité critique d'Eddington

$$L_{crit} = 6.5 \times 10^4 \, (M/M_\odot) \, (L_\odot /(1+X))$$

où X est l'abondance (en pourcentage par masse) de l'hydrogène dans la couche extérieure de la nova. Ces observations ont joué un rôle important dans le développement des modèles modernes.

Les modèles simples permettant d'expliquer les courbes de lumière observées et le comportement spectral pendant l'activité ayant suivi le maximum ont été proposés. Cinq de ces modèles sont décrits. Il s'agit des modèles suivants:

Ejection instantanée I - La totalité (ou la presque totalité) de la matière est éjectée dans un temps *court* par rapport à la durée de l'activité postérieure au maximum optique. La matière éjectée est concentrée dans une *couche assez mince* dont l'épaisseur reste petite.

Ejection instantanée II - Une *enveloppe épaisse* est éjectée de facon instantanée. Cette enveloppe reste épaisse, alors que ses différentes portions peuvent avoir différentes vitesses.

Ejection continue A - Les modèles d'éjection continue soulignent l'importance de *vents* issus de la nova après le maximum optique. L'essentiel de l'émission du spectre continu dans les domaines optique et ultraviolet provient d'un *vent optiquement épais* (quasi-photosphère ou pseudo-photosphère).

Ejection continue B - Une forme d'éjection continue est possible, où la plupart de la luminosité vient de la matière antérieurement éjectée, éjectée à un temps où le taux de perte de masse était très élevé. Ce modèle est très semblable à celui de l'éjection instantanée de type I avec une enveloppe d'épaisseur constante.

Modèles avec étoile centrale dominante - L'éjection est supposée se produire à partir de l'une des composantes de la binaire centrale qui présente une augmentation générale, si bien que quelque chose ressemblant à une photosphère normale, presque stationnaire, une photosphère stellaire, est observée après le maximum optique. Dans ce cas, les couches en expansion à hautes vitesses (dont la présence est démontrée par le spectre) peuvent être optiquement épaisses dans le continu.

Chacun de ces modèles est limité par de fortes contraintes observationnelles. Une éjection instantanée de type II, et des modèles dominés par l'étoile centrale, exigent que les vitesses les plus basses soient rencontrées au voisinage du centre de l'enveloppe. Les distributions de vitesse prédites sont criticables dès que l'on se livre à une comparaison avec l'observation.

L'éjection instantanée de type I exige que le continu soit formé soit dans une couche mince, soit dans un résidu de nova ; les composantes d'absorption de type P Cygni déplacées vers le bleu doivent être très larges dans le premier cas et très minces dans le second. Des difficultés majeures s'opposent donc à ce modèle.

L'éjection continue de type A a aussi des contraintes très sévères. L'éclat continu est lié directement au taux de perte de masse.

On montre que la facon la plus productive de progresser est de combiner un modèle d'éjection continue de type A avec la présence d'une couche mince. Dans beaucoup de cas au moins, la majeure partie du rayonnement du spectre continu peut être compris facilement comme issu d'un vent optiquement épais, alors que la plupart du rayonnement dans les raies semble venir d'une couche mince.

Dans tous les cas, les modèles à symétrie sphérique sont probablement trop simples, et les déviations observées par rapport à la symétrie sphérique doivent être prises en ligne de compte.

Les caractéristiques observées des novae récurrentes, et tout particulièrement celles de T CrB et RS Oph sont assez différentes des novae classiques. Par exemple, la vitesse d'expansion des raies d'absorption de T CrB et RS Oph décroît avec le temps.

L'interaction entre la couche éjectée et une enveloppe circumstellaire pré-existante, formée

au cours de sursauts antérieurs, et/ou spécialement l'enveloppe due au vent stellaire à partir de la géante rouge présente dans le système de T CrB et RS Oph, peut être importante pour expliquer les caractéristiques spectrales pendant un sursaut. Les modèles proposés pour T CrB et RS Oph ne peuvent être appliqués aux novae récurrentes comme T Pyx ou U Sco qui, de toute évidence, n'ont pas de compagnon qui soit une géante rouge. Il n'est pas clair dans quelle mesure des modèles de novae classiques peuvent s'appliquer à ces novae récurrentes.
Une méthode empirique d'explication au moins partielle de la structure des novae est discutée. Les modèles ne prennent généralement pas en compte l'existence d'une stratification et les notions complexes suggérées par les observations. Par exemple, il est évident que la matière à plus haute vitesse se situe au dessous de la matière à plus basse vitesse, et que le système Orion a une ionisation plus élevée que les autres systèmes ; ceci suggère que son origine soit localisée dans les parties intérieures de l'enveloppe ; mais une étude quantitative des superposition de raies est encore absente. Des composantes d'absorption à très haute vitesse (jusqu'à 10^4 km/s) ont été détectées dans le spectre ultraviolet lointain de quelques novae. Les systèmes de vitesses les plus élevées de V 1370 Aql ont varié à une échelle de temps de quelques heures, suggérant que les raies se forment dans l'enveloppe intérieure.

Les composantes d'absorption du spectre principal sont toujours observées dans le spectre des novae classiques. Ceci veut dire que des déviations à partir de la symétrie sphérique n'apparaissent pas comme assez grandes pour empêcher la formation du système dans toutes les directions. Des systèmes à grandes vitesses sont aussi généralement observés. Par conséquent, des limites sont mises aux écarts possibles à la symétrie sphérique, également pour les systèmes à grandes vitesses.

Les observations montrent qu'une grande partie du continu doit être produite au dessous du niveau où toute raie d'absorption forte est formée. Par conséquent, lorsque les fortes raies d'absorption NIII du type Orion sont observées, une partie importante au moins du continu doit être produite dans des régions nettement plus intérieures. Ceci est compatible avec l'éjection continue de type A, ou avec des modèles à étoile centrale dominante. Dans ces modèles, la majeure partie du spectre continu est émise par une quasi-photosphère, formée par un vent optiquement épais, ou par une photosphère presque stationnaire, respectivement. Le rayonnement infrarouge cependant n'est pas inclus dans cette discussion, parce que l'on s'attend à ce que les parties extérieures de l'enveloppe soient beaucoup plus épaisses optiquement dans l'infrarouge que dans le domaine optique à cause de l'opacité de type libre-libre et celle due aux poussières. Les températures de couleur et les rayons peuvent être déterminés, ce qui permet, lorsque le modèle d'éjection continu est pris en considération, de les convertir en taux de pert de masse.

Les magnitudes continues, portées en fonction du logarithme du temps qui s'est écoulé après le maximum, ont souvent un comportement linéaire, c'est-à-dire que le flux de rayonnement varie alors comme une puissance du temps après le maximum. Le même comportement semble être celui du rayon, déduit des magnitudes du continu et de la température de Zanstra. Une importante donnée d'observation est que le déclin bolométrique est beaucoup plus lent que le déclin optique. Une autre c'est que les flux d'énergie totale, radiative et cinématique sont du même ordre de grandeur.

C'est encore une autre chose que la corrélation entre la vitesse du système d'Orion et l'éclat du continu.

La description la plus séduisante émergeant des observations semble être celle d'une accélération du vent par la pression de radiation à des grandes profondeurs optiques, où la luminosité totale est au-dessus de la limite d'Eddington. Une partie de cette luminosité totale est convertie en énergie cinétique. Un tel processus, s'il existe, ne peut pas être thermique.

Les méthodes de détermination de la composition chimique, à la fois à partir du spectre de

raies d'absorption antérieures au maximum, du spectre principal, et des émissions nébulaires formées dans la matière éjectée, sont discutées. Ces données sont très importantes pour vérifier les théories sur la cause des sursauts de novae. Cependant, elles sont très incertaines, et doivent être prises avec beaucoup de précaution. En dehors des excès de CNO, les rapports isotopiques ont été déterminés pour DQ Her par des méthodes de synthèse spectrale. Le rapport C^{12}/C^{13} est trouvé $\geq$ 1.5 et $N^{14}/N^{15} \geq 2$ (à comparer avec les valeurs trouvées dans le système solaire, respectivement 89 et 273).

Les observations infrarouges, malheureusement disponibles seulement pour un nombre d'objets relativement petit, mettent en évidence la formation d'une couche de poussière épaisse dans quelques novae lentes ; l'absence, ou en tout cas l'existence très faible d'un excès d'infrarouge dans une nova rapide, comme V1500 Cygni ; et l'évidence de l'existence d'une couche de poussière mince dans une nova modérément rapide comme V1668 Cyg.

Selon le modèle très ancien développé par Clayton et Wickramasinghe, les grains de poussière peuvent seulement se condenser à partir de la matière éjectée une fois que la température de condensation descend au dessous de 2000 °K, et les grains commencent alors à croître et à atteindre une taille maximum d'environ 2μm en quelques jours. Puisque la température photosphérique des novae augmente après le sursaut, la distance à laquelle les grains peuvent se former s'éloigne de la nova. La formation des grains dépend ainsi du fait que le matériel éjecté peut ou non dépasser la distance de condensation. Si c'est le cas, la formation des grains est possible, sinon l'environnement de la nova est toujours trop chaud. De plus, comme la matière éjectée se disperse, sa densité décroît, et à moins que la formation de grains ne démarre assez tôt, la quantité de grains finalement formée est négligeable.

Gallagher a développé un modèle idéalisé en supposant que la condensation des grains est contrôlée par le champ de radiation de la nova qui rayonne à luminosité constante. Il obtient une formule donnant le nombre de jours après le sursaut, t_d, nécessaire à la formation des grains, et l'échelle de temps d'ionisation t_i de la matière éjectée. Le rapport t_i/t_d est indépendant de la vitesse d'expansion, et dépend seulement de la luminosité qui est liée à la classe de vitesse des novae. Pour les novae rapides et très rapides, $t_i<t_d$, l'ionisation démarre avant que les grains ne peuvent se condenser, et par conséquent la couche poussiéreuse ne peut se former. Dans des novae modérément lentes et lentes, on a : $t_d>t_i$, et la formule donne des valeurs de t_d en accord raisonnable avec les observations de divers objets. Cependant, HR Del, R Pic et quelques autres novae très lentes ne peuvent êtres expliquées par ce schéma, parce qu'elles produisent trop peu de poussière pour leur petite vitesse.

Des recherches ultérieures ont impliqué une étude beaucoup plus détaillée des processus physiques, mais bien du travail reste à faire avant que la condensation à l'état de poussière ne soit correctement comprise.

Une raie très forte de l'infrarouge a été observée ; il s'agit de l'émission à 12,8 μm [NeII] dans QU Vul. A partir des raies de Ne III et de Ne IV qui sont présentes simultanément dans l'ultraviolet, une importante surabondance de Néon est déterminée. On croit maintenant qu'une nouvelle classe de novae, les novae Ne, existe. Elles seraient caractérisées par la présence dans le système d'une naine blanche O-Ne-Mg, avec une grande quantité de matière de la naine blanche mélangée à la couche.

Une description rapide des modèles de l'enveloppe radio est donnée. Les modèles de Hjellming et al. pour les novae plus lentes donnent des vitesses plus petites pour la matière éjectée, des masses plus faibles de la couche, et un temps plus important écoulé après le sursaut pour que la couche devienne optiquement mince dans le domaine radio.

Des déviations par rapport à la symétrie sphérique sont toujours rencontrées dans les quelques

couches de vieilles novae étudiées en détail. Ces enveloppes non sphériques peuvent être expliquées de différentes facons, telles qu'un guidage magnétique de la matière, des pulsations stellaires non radiales, une interaction de la nébuleuse en expansion avec les composantes secondaires (ceci pouvant résulter en nuages éjectés perpendiculairement au plan orbital), l'interaction de la nébuleuse en expansion avec le disque d'accrétion, les effets de la rotation stellaire, le freinage gravitationnel et l'accélération radiative, des instabilités au commencement de l'expansion, la rotation stellaire par elle-même, etc...

La cause des sursauts de novae admise actuellement est l'accrétion d'hydrogène par la composante naine blanche dégénérée du système binaire, à partir de son compagnon non dégénéré. Alors l'hydrogène est soumis à une destruction thermonucléaire. La description de cette théorie dépasse le propos de ce livre qui est consacré aux atmosphères. Par conséquent, on y souligne seulement l'impact de cette théorie sur les propriétés observées.

L'hydrogène accrété par la naine blanche tendra à être "brûlé". Le taux d'accrétion de masse, la composition chimique et la luminosité de la naine blanche influencent l'évolution du mécanisme qui donnera lieu à un sursaut. Les calculs suggèrent qu'une surabondance de CNO est nécessaire pour un sursaut de nova rapide, c'est-à-dire que le mélange de CNO dans l'enveloppe à partir de l'intérieur se produit.

Les surabondances de Ne et Mg observées dans quelques novae sont expliquées par le sursaut de nova lié aux étoiles naines blanches O-Ne-Mg. On s'attend à ce que ces naines blanches aient des masses proches de la limite de Chandrasekhar.

L'accrétion n'est pas sphériquement symétrique, et ce manque de symétrie sphérique devrait jouer un rôle important dans le développement de la pré-nova. Les conséquences de ce fait sont discutées, mais la situation est très compliquée et il reste beaucoup de travail à faire.

Certaines observations, et des arguments d'ordre statistique suggèrent que les novae entrent en *"hibernation"* ; c'est-à-dire que de très vieilles novae deviennent très faibles pendant des milliers d'années, et deviennent brillantes à nouveau avant l'accident thermonucléaire que nous avons évoqué. Les modèles d'hibernation supposent, comme il est suggéré dans le calcul, qu'après l'explosion d'une nova, la séparation des deux composantes augmente en général. Tout d'abord l'étoile secondaire continue à transférer la masse parce qu'elle est fortement irradiée, puis le transfert de masse décroît fortement parce que l'étoile secondaire ne remplit plus son lobe de Roche ; ceci permet à la matière antérieurement accrétée de se refroidir, de diffuser, et de devenir dégénérée, si bien qu'un fort événement thermonucléaire redevient possible à une époque ultérieure.

La séparation de la binaire est alors réduite par un freinage magnétique, et revient à sa valeur originelle dans un temps de l'ordre de quelques milliers d'années. Quand le transfert de masse est encore relativement faible, le sursaut de la nova naine pourrait être possible, si bien que les novae naines et les novae classiques appartiendraient alors à la même classe d'objets. En fait, quelques vieilles novae classiques sont connues pour présenter des éruptions, après le sursaut, semblables à celles des novae naines.

Les causes des sursauts des novae récurrentes sont discutées. Les novae récurrentes sont dans une certaine mesure intermédiaires entre les novae classiques et les novae naines, au moins celles (T Pyx et U Sco) qui n'ont pas de géantes rouges dans le système. Les trois autres novae récurrentes connues (T CrB, RS Oph et V1017 Sgr) ressemblent plutôt à des étoiles symbiotiques (en fait, V1017 Sgr est souvent classée comme une étoile symbiotique plutôt que comme une nova récurrente ; elle peut être aussi une nova classique, et avoir des sursauts du type de ceux des novae naines).

On peut voir, à partir de la théorie des novae classiques, que pour une naine blanche d'une

masse très proche de celle de la limite de Chandrasekhar, un retour d'activité thermonucléaire peut être produit pour une quantité relativement faible de matière accrétée. Par conséquent, si l'on suppose que le taux d'accrétion ne varie pas beaucoup, des temps de récurrence beaucoup plus courts que pour les novae classiques sont possibles.

Comme dans le cas des novae naines, les novae récurrentes peuvent en principe être également produites par des événements d'accrétion. Un mécanisme probablement plus efficace d'accrétion pour quelques novae récurrentes implique une instabilité soudaine de la composante froide, avec éjection de 10^{-3} à 10^{-4} masse solaire. Ce mécanisme peut être adéquat à la description de T CrB et RS Oph, cependant qu'un événement thermonucléaire dans une naine blanche massive pourrait expliquer T Pyx et U Sco. Malgré ces hypothèses, la situation est encore extrêmement incertaine.

8. COMPORTEMENT DE QUELQUES NOVAE CLASSIQUES ET BIEN ÉTUDIÉES

Le chapitre 8 décrit en détail le comportement de plusieurs objets bien étudiés appartenant à différentes classes de vitesse.

a) La nova très rapide V1500 Cyg 1975 a été étudiée à fond, dans les domaines optique et infrarouge ; quelques observations en ont été faites dans l'ultraviolet grâce au satellite photométrique ANS et avec COPERNICUS ; l'émission radio-thermique issue de l'enveloppe a été détectée environ 50 jours après le sursaut.

b) V603 Aql 1918 et CP Pup 1942 ont eu le même déclin rapide, t_3 = 8 jours. Cependant, leur courbe de lumière était différente parce que V603 Aql a présenté des oscillations dans la phase de transition, tandis que CP Pup a eu un déclin régulier, rapide, sans perturbation.

V603 Aql est l'une de ces vieilles novae qui a été étudiée de facon très détaillée dans l'ultraviolet à l'aide de OAO-2 et de IUE. L'enveloppe nébulaire a pratiquement disparu, comme cela est indiqué par l'absence de raie mince d'émission d'inter-combinaison dans l'ultraviolet. La variabilité dans les raies a été étudiée pendant pratiquement 2 cycles complets, et semble être liée au cycle orbital.

Des minimums ont été observés dans la courbe de lumière, mais ils ne sont pas périodiques, et par conséquent, on ne peut les expliquer comme dus à des éclipses. Des "humps" de la courbe de lumière ont été observés aussi se répétant avec une bonne régularité ; ils indiquent une période photométrique d'environ 10 minutes plus longue que la périod spectroscopique : 3 h 28.8 mn contre 3 h 18.9 mn. Les mesures de polarisation donnent une troisième période, plus courte, de 2 h 48 mn.

c) CP Pup est la seule parmi les vieilles novae connues à avoir une période orbitale d'une durée inférieure à l'intervalle de périodes de 2 à 3 heures.

Peu de temps après le maximum, le spectre a montré la présence de raies chromosphériques et coronales (jusqu'à celles du [FeX] et du [FeXI] et des raies de basse excitation comme OI, FeII, etc.

La magnitude apparente de CP Pup après le sursaut est environ de trois magnitudes plus brillante qu'elle n'était avant le sursaut. Il est de même pour V1500 Cyg. Ce comportement est exceptionnel, parce qu'en général la luminosité des novae est environ la même avant et après le sursaut.

CP Pup, en état de quiescence, est une source de rayons-X mous, forts et variables, avec le spectre le plus "mou" associé avec le flux le plus élevé.

d) GK Per est un objet exceptionnel. C'est la vieille nova qui a la période orbitale la plus longue connue, de presque 2 jours. Pendant le stade de transition qui a commencé à 3 magnitudes et demi en dessous du maximum, des fortes fluctuations de lumière ont apparu brusquement. L'amplitude en était de 1 à 1,5 magnitudes et la période de 3 à 5 jours. Ce phénomène a duré plus de trois mois. A chaque

minimum, le spectre était du type nébulaire ; à chaque maximum, les raies de haute excitation et les raies interdites étaient plus faibles, ce qui suggère une décroissance de température et un accroissement de densité dans la région responsable de l'émission des raies. Ces oscillations communes à plusieurs novae, étaient cependant exceptionnelles pour deux raisons. La première, c'est que l'intervalle de temps entre des maximums successifs de lumière a varié d'une façon sinusoïdale avec le temps, et que la période, l'amplitude et la valeur moyenne de cette sinusoïde ont augmenté avec le temps. La seconde particularité, c'est que les variations des vitesses radiales des composantes d'absorption déplacées vers le bleu du spectre d'Orion, n'étaient pas corrélées avec les oscillations de lumière comme pour les autres novae: Dans quelques autres novae, les vitesses négatives du spectre d'Orion, et les magnitudes pendant les oscillations sont en corrélation directe, la même relation peut être trouvée pour GK Per, mais les maxima des vitesses négatives du spectre d'Orion se produisent environ un minimum sur deux des fluctuations de lumière.

Après la phase de transition, GK Per s'est stabilisée à un taux très bas de déclin et n'a atteint son minimum de lumière que plusieurs années plus tard.

La nova quiescente GK Per présente aussi plusieurs particularités. En dehors de cette période exceptionnellement longue, la vieille nova présente une activité de sursauts similaire à celle de certaines novae naines. La durée d'un sursaut optique est de deux à trois mois, et les amplitudes varient de 1 à 3 magnitudes. Les temps observés des récurrences sont variables, mais toutes semblent être des sous-multiples de 2400 jours.

Une autre particularité de GK Per est que, contrairement à ce qui se passe pour d'autres vieilles novae, le spectre d'un compagnon de type K2 IV-V est observable au minimum. En dépit de la présence de raies d'émission de haute d'excitation, le continu ultraviolet est exceptionnellement plat et faible.

GK Per est une source transitoire de rayons-X durs. Une modulation cohérente et forte du flux de rayons-X durs a été observée grâce à EXOSAT pendant un sursaut important en 1983, montrant que GK Per est membre d'une sous-classe "intermédiaire polaire" des variables cata-clysmiques.

En raison de la disponibilité d'observations dans le domaine optique, s'étendant sur plusieurs décennies, et de beaucoup d'observations récentes dans l'infrarouge, dans l'ultraviolet et dans le domaine des rayons-X, des modèles sont discutés afin d'essayer d'expliquer le comportement complexe de la vieille nova.

e) V1668 Cyg a été la première nova dont le développement a été complètement suivi depuis la période antérieure au maximum jusqu'à la phase nébulaire, dans l'ultraviolet avec IUE et dans l'infrarouge à partir du sol.

Le spectre ultraviolet a permis de déterminer la température électronique et la densité de la matière éjectée ainsi que les abondances de C,N,O, renforcées par un facteur 30 par rapport à la valeur solaire.

f) FH Ser a été observée dans l'infrarouge et dans l'ultraviolet, avec OAO-2. Le résultat le plus important de ces observations, c'est que la luminosité totale apparaît constante jusqu'au jour 200, tandis que la luminosité optique a décru par un facteur d'environ dix, 53 jours après le maximum visuel. De nombreuses autres novae observées de l'ultraviolet à l'infrarouge ont montré un comportement similaire, la luminosité totale décroissant beaucoup plus lentement que la luminosité optique. Cependant, aucune d'elles n'est restée constante pendant une période de temps aussi longue que dans le cas de FH Ser.

g) DQ Her a été étudiée de facon trés détaillée pendant la totalité de son sursaut. Le grand nombre de composantes spectrales des raies dans son spectre est un exemple de la complexité que l'on peut trouver dans le spectre d'une nova. Il met clairement en évidence les interactions qui se produisent entre les différentes

couches, les plus rapides, intérieures aux autres, rejoignant les plus lentes (extérieures) de ces enveloppes. Une analyse chimique de la matière éjectée indique que le carbone est en excès d'un facteur 20 par rapport à la valeur solaire, et l'azote d'un facteur 100, alors que l'hélium est pratiquement normal.

Une particularité du spectre d'enveloppe de DQ Her, c'est que la température électronique, telle qu'indiquée par la discontinuité de Balmer très nette, est très basse, de l'ordre de 500°K environ, alors que, d'un autre côté, les raies d'émission du CII et de NII indiquent une température électronique d'environ 10^4. Ces données montrent bien que l'enveloppe contient une région chaude et une région froide. Une densité basse et une surabondance d'oxygène peuvent expliquer la température basse ; en fait, les raies de structure fine, dans l'infrarouge, du carbone, de l'azote et de l'oxygène, sont très efficaces pour refroidir les nébuleuses de faible densité.

La nova quiescente est caractérisée par la présence d'oscillations cohérentes avec une période de 71 sec. Son spectre montre que les raies permises de CII, CIII, NII, et HeII et le continu sont nettement affaiblis pendant l'éclipse primaire, cependant que les raies de Balmer et les raies interdites de OII et de OIII ne sont pas modifiées et sont par conséquent formées dans une enveloppe étendue non affectée par l'éclipse.

h) T Aur est la plus vieille nova galactique pour laquelle le sursaut a été suivi de façon complète. Elle est très similaire à DQ Her.
La nébuleuse qui entoure T Aur montre aussi des régions de basses températures, mais qui ne sont pas aussi basses que dans le cas de DQ Her, $T_e < 3000K$. Les abondances d'azote et d'oxygène sont en excès par des facteurs de 60 et 25 respectivement.

i) RR Pic, ainsi que HR Del, sont parmi les plus lentes novae observées. Le type spectral au maximum était de F8, ce qui est beaucoup plus tardif que celui des novae rapides (A0-A5) et les vitesses de perte de masse étaient relativement faibles, -100 jusqu'à -400 km/s pour le spectre principal. Dans la phase du spectre d'Orion, de nombreuses raies de [FeII], qui sont faibles ou absentes dans les novae rapides étaient présentes. La nébuleuse résiduelle a au contraire un spectre semblable à ceux des nébuleuses planétaires de haute excitation montrant des raies d'émission importantes du [FeV]. La source d'excitation est le champ de rayonnement ultraviolet de la composante chaude. L'azote est seulement modérément surabondant, par un facteur d'environ dix.

La nova quiescente a une période orbitale d'environ 3,5 jours et présente une large bosse de la courbe de lumière durant plus que la moitié de la période, et se terminant toujours par un affaiblissement soudain.

Le spectre ultraviolet de RR Pic peut être expliqué soit par la superposition de deux corps noirs, soit par une loi en puissance. Les températures de corps noir sont des couples de 28000K et 40000K, ou de 14000K et 90000K ou 20000K et 35000K, selon différents auteurs ; la valeur la plus basse est attribuée au disque, et la valeur la plus élevée à la couche de transition.

La variabilité dans le domaine de l'ultraviolet exclut toute possibilité d'une éclipse de la composante chaude, ce qui avait été suggéré par le creux observé ans la courbe de lumière optique.

j) La nova très lente HR Del a eu une courbe de lumière de sursaut caractérisée par la présence de deux maxima : le premier, le 12 décembre 1967, à une magnitude de 3,4 ; et un second maximum, en mai 1969, à une magnitude de 4,3. Les spectres à haute résolution ont été pris pendant la durée complète du développement de ce sursaut.

La nova quiescente a une période bien déterminée de 0,2141674 jours, soit légèrement plus grande que 5 heures. Aucune trace d'un corps secondaire n'est décelable. L'amplitude de la vitesse radiale de He II 4686 est de 104 km/s ; elle est seulement de 34 km/s pour Hβ.

Plusieurs déterminations de la composition chimique de la matière éjectée convergent vers la détermination d'un excès de CNO.

9. NOVA RÉCURRENTES

Le chapitre 9 décrit les caractéristiques des cinq novae récurrentes connues. Il s'agit de U Sco, T Pyx et RS Oph, toutes les trois ayant cinq sursauts observés, de V1017 Sgr, avec trois sursauts observés, et de T CrB, avec deux sursauts observés.

Ce petit groupe est très peu homogène. RS Oph, T CrB et V1017 Sgr, ont toutes une géante froide dans leur système. V1017 Sgr présente des caractéristiques semblables à celles d'une étoile symbiotique, et son appartenance au groupe des novae récurrentes est douteuse. U Sco semble avoir dans son système une étoile de la série principale de type solaire, tandis que T Pyx ne montre aucune évidence en faveur de l'existence d'un compagnon et présente plutôt un spectre ultraviolet très chaud.

a) Des observations de U Sco de l'infrarouge à l'ultraviolet faites pendant le sursaut de 1979, montrent que la distribution d'énergie reste constante. Ce comportement est différent de celui des novae classiques qui montrent un décalage vers l'ultraviolet variant avec le temps après le maximum. Le spectre de raies optique et ultraviolet montre un excès important d'hélium et un excès d'azote par rapport au carbone et à l'oxygène. Les novae classiques présentent un léger excès d'hélium, mais pas si important que dans le cas de U Sco. Aucune raie coronale interdite n'était présente dans son spectre.

b) T Pyx est la nova récurrente ayant au minimum le spectre le plus chaud que l'on connaisse. Le spectre nébulaire est caractérisé par la présence de raies d'émission de basse excitation, telle que OI, et de très haute excitation telle que [FeXIV]. Bien qu'une détermination exacte des abondances de la masse éjectée n'ait pas été faite, il n'y a aucun argument en faveur d'un excès de CNO.

c) RS Oph a été observée en grand détail. Tous ses sursauts, comme c'est le cas aussi pour T Pyx et T CrB, sont très semblables les uns aux autres. L'évolution spectrale très comparable suggère que les sursauts donnent lieu à un mécanisme soumis à une régulation efficace, capable de reproduire une série de plusieurs phénomènes complexes dans tous leurs détails et dans une même séquence chronologique. Le spectre nébulaire est caractérisé par la présence de plusieurs raies d'émission coronales fortes.

Les couleurs dans le proche infrarouge observées entre les sursauts situent RS Oph dans la région des variables de type Mira selon le diagramme à deux couleurs (J-K) - (H-K), alors que l'étoile est plus proche de la séquence normale géante-supergéante dans le diagramme à deux couleurs (J-K) - (K-L). Les observations IRAS mettent en évidence un excès d'infrarouge qui peut être expliqué par la présence de poussières à 350 K, poussières présentes aussi dans la période de quiescence. Une émission radio a été détectée 18 jours après le sursaut de 1985, la température de brillance étant plus grande que 10^7K. Il y a deux différences importantes par rapport aux novae classiques : Les émissions radio de ces dernières ne sont jamais observées avant 50 jours après le sursaut, et leur température est de l'ordre de 10^4K, typique de l'émission thermique d'un gaz ionisé.

La courbe de lumière bolométrique du sursaut de 1985 a été obtenue à partir d'observations de l'infrarouge à l'ultraviolet (les observations dans le domaine X, faites avec EXOSAT, indiquent que la contribution du domaine X au flux total émis le jour 51 se situait entre 0,5 et 10% ; et la contribution radio a toujours été inférieure à 1%). Cette courbe de lumière bolométrique est très semblable à celle que l'on obtient pour les novae classiques.

d) V 1017 Sgr est tout-à-fait atypique, puisque ses trois sursauts observés ont eu des amplitudes très différentes. Le second en 1919 a eu une amplitude de 8 magnitudes alors que le premier en 1901 et le troisième en 1973 ont eu une amplitude de 4 magnitudes, typique d'une

étoile symbiotique plutôt que d'une nova. Le spectre de raies quiescent indique un type G5 III, mais présente aussi un spectre continu violet fort. Aucune raie de haute excitation ou coronale n'est observable dans le spectre, après le maximum.

e) T CrB est une binaire spectroscopique à raies doubles avec une période de P = 227.5 jours, contenant une géante M3 et un compagnon plus chaud dont la nature (naine blanche ou étoile de la série principale ?) a paru jusqu'à présent plutôt bizarre. La courbe de lumière du sursaut est semblable à celle d'une nova classique, mais les caractéristiques du système binaire et le spectre pendant la période du sursaut nous permettent de classer T CrB comme étoile symbiotique.

Il est remarquable de noter que les deux sursauts observés sont arrivés à peu près à la même phase orbitale. Une caractéristique qui n'est pas observée dans les novae rapides classiques était la présence en 1946 de deux maxima, le premier à la magnitude 2 (le 9 février), et un large maximum secondaire à la magnitude 8 (entre juin et juillet) ; exactement le même comportement a été observé pendant le sursaut de 1866.

Les variations spectrales du sursaut de 1946 ont été observées de façon extensive. Elles sont notables, en raison de la vitesse d'expansion énorme du début : 4500 km/s. La première observation du sursaut de 1946 a été faite le 9 février ; le spectre continu a masqué les bandes de TiO de la composante géante M ; le 12 février, la présence de raies interdites du [FeX] et [FeXIV] était observée. Pendant le maximum secondaire le continu a augmenté encore, voilant les bandes de TiO et les raies fines d'absorption des métaux ionisés sont apparues. Ce comportement est semblable à celui observé dans quelques étoiles symbiotiques, plutôt que dans des novae rapides ou dans des novae lentes au moment du maximum secondaire.

Le spectre quiescent de T CrB a été observé très en détail pour en déduire les courbes de vitesses radiales de la géante et du compagnon chaud. Dans l'hypothèse selon laqnelle les raies d'émission de Balmer sont dues à la composante chaude, une masse de 1,9 masse solaire a été trouvée, qui est plus élevée que la limite de Chandrasekhar pour une naine blanche.

Les observations ultraviolettes faites avec IUE, et s'étendant sur 10 années, suggèrent au contraire que le compagnon chaud peut être une naine blanche.

Le continu ultraviolet peut être bien représenté par une loi simple en puissance $F(\lambda) \propto \lambda^{-\alpha}$, sur la totalité du domaine IUE. Cependant α est variable et varie de 0 à 1. Le spectre plat correspond à un minimum dans le flux ultraviolet, et plus le flux est élevé, plus le continu est "pentu". Le continu ultraviolet varie d'un facteur jusqu'à 10. Aucune variation significative dans le domaine optique n'est observée en corrélation avec celle de l'ultraviolet. De même, aucune corrélation n'a été trouvée avec la phase orbitale.

Les raies d'émission sont plus fortes que celles observées d'habitude dans les novae classiques quiescentes, et leur variabilité est corrélée avec les variations du continu.

Les raies d'absorption, principalement des métaux ionisés une fois, sont présentes généralement dans tous les spectres ultraviolets des T CrB. Cette caractéristique semble être une signature typique des étoiles symbiotiques pendant leur phase active. Par exemple un spectre de raies d'absorption similaire a été observé dans l'étoile symbiotique CH Cyg pendant les deux sursauts de 1967 et de 1977.

La densité électronique et la température électronique des régions responsables des raies d'émission ont été calculées en utilisant différentes raies permises et d'intercombinaisons ; des valeurs de 10^{10} à 10^{11} cm^{-3} et 13 000 °K ont été déterminées respectivement.

L'accrétion sur un objet compact est un mécanisme communément accepté pour expliquer la luminosité observée dans l'ultraviolet. La masse accrétée est : $\dot{M}$= 2RL/GM, où R et M se

réfèrent à l'objet accrétant. En supposant pour T CrB une distance de 1 300 pc, la luminosité moyenne intégrée dans le spectre IUE, corrigée pour le rougissement, est de 2.2 x 10^{35} ergs. L'énergie rayonnée dans le domaine optique est négligeable. Ceci est une importante indication en faveur d'un mécanisme d'accrétion par une naine blanche. En fait, une étoile de la série principale devrait émettre principalement dans la région optique. La présence d'une emission forte de HeII à 1640 exige aussi une température de 10^5 K, ce qui est à peine compatible avec une étoile de série principale. Par conséquent, les mesures de vitesses radiales des raies d'émission de Balmer, si on doit les attribuer au compagnon, indiqueraient une masse trop grande pour une naine blanche.

Les observations ultraviolettes suggèrent au contraire fortement que le compagnon est une naine blanche.

Le problème de la vitesse radiale est par conséquent d'une importance critique. Les raies d'émission de Balmer sont larges, et perturbées par des absorptions. De plus, les émissions ne sont pas nécessairement associées au mouvement orbital du compagnon. Il est clair qu'aucune conclusion définitive ne peut être tirée en ce qui concerne la nature du compagnon, sur la base seulement de ces mesures de vitesses radiales. Une série de spectres à haute résolution devrait être obtenue dans l'ultraviolet, afin d'en déduire une masse fiable du compagnon. C'est une tâche qu'il sera possible de mener seulement avec le Hubble Space Telescope.

10. *Le chapitre 10 résume* les résultats principaux, ci-dessus décrits, et les problèmes encore ouverts concernant les novae classiques et récurrentes à la fois du point de vue de l'observation et de la théorie.

11. ETOILES SYMBIOTIQUES : OBSERVATIONS

Les chapitres 11 à 14 sont consacrés à une vue d'ensemble des observations des étoiles symbiotiques, à une description des modèles différents proposés pour expliquer le phénomène symbiotique, et à la discussion de quelques objets choisis, respectivement.

Le terme *"étoile symbiotique"* désigne généralement des étoiles variables dont les spectres optiques présentent simultanément un spectre froid d'absorption, généralement d'une *étoile M géante, ainsi que des raies d'émission de haute ionisation*, telles que les raies He II 4686, [OIII] etc. *La courbe de lumière de variabilité varie d'objet à objet*, montrant que les mécanismes physiques responsables des phénomènes symbiotiques ont différents poids et différentes formes dans différents objets. En général la courbe de lumière des étoiles symbiotiques est caractérisée par une amplitude assez grande (une à quelques magnitudes), par des échelles de temps longues (des mois, des années, des décennies), quelquefois par de longues périodes de quiescence relative.

Les courbes de lumière de plusieurs étoiles symbiotiques sont décrites.

Un petit groupe d'objets montre une courbe de lumière différente de celle qui caractérise la majeure partie des étoiles symbiotiques ; on les appelle des "novae symbiotiques", parce qu'elles n'ont éprouvé qu'un seul sursaut, comme les novae classiques, mais avec une plus petite amplitude. De plus, elles restent à leur valeur maximum pour des périodes très longues.

En dehors des variations à long terme, les courbes de lumière des étoiles symbiotiques présentent des variations irrégulières, à des échelles de temps du jour et aussi de la minute.

Quelques-unes présentent une variabilité périodique et des éclipses, ce qui indique qu'il s'agit d'un système binaire, avec des périodes de plusieurs centaines de jours. Le spectre optique est caractérisé par trois composantes principales : le spectre stellaire froid, l'excès de continuum bleu, et le spectre de raies d'émission.

Le spectre infrarouge nous permet de distin-

guer deux classes d'étoiles symbiotiques: Celles qui ont un excès d'infrarouge fort par rapport à la distribution d'énergie à laquelle on s'attend pour une composante froide, excès qui est attribué à une émission thermique de poussière (en anglais, dust) (et pour cette raison, ce groupe est appelé *symbiotique-D*) et celles qui ont un spectre normal de type avancé (les *symbiotiques de type S*).

Le spectre continu bleu est hautement variable et tout particulièrement intense pendant les sursauts. Il reproduit un continu stellaire de type A ou B, et à quelques phases du sursaut, il est marqué par plusieurs raies d'absorption d'atomes métalliques ionisés une fois.

Les raies d'émission permises et interdites qui peuvent être produites par des éléments neutres et par des ions jusqu'au fer ionisé six fois sont observées. Dans quelques cas aussi, des raies coronales ont été observées. Les profils en sont souvent complexes, avec plusieurs composantes, et des absorptions de type P Cyg impliquant une vitesse radiale d'expansion de -100 à -300 km/s, par conséquent beaucoup plus faible que celle que l'on observe dans la majorité des novae, mais comparable en revanche avec celle des spectres pré-maximum et principal des novae lentes.

Des mesures de vitesses radiales indiquent que plusieurs symbiotiques sont des étoiles à grande vitesse. De plus, plusieurs objets présentent une variabilité de la vitesse radiale, qui peut être liée au mouvement orbital d'un système binaire. Des essais en vue de détecter des champs magnétiques, et de mesurer des polarisations intrinsèques dans les étoiles symbiotiques ont été faits par différents auteurs ; mais il reste beaucoup de travail à faire dans ce domaine, avant d'atteindre des résultats concluants.

Les observations IRAS ont mis en évidence 34 étoiles symbiotiques de type S et 28 de type D; quatre de ces dernières ont été détectées aussi à 100 µm. Les étoiles de type S sont placées dans une région limitée du diagramme IRAS à deux couleurs, proches de la région des géantes froides, alors que les étoiles de type D sont distribuées dans une région étendue, incluant les régions où se trouvent les étoiles variables de type Mira et les nébuleuses planétaires. Les étoiles de type D manifestent une variabilité infrarouge importante, ce qui apporte une argumentation directe pour la présence d'une variable de type Mira dans le système.

La majorité des observations infrarouges ont été faites pendant la phase quiescente. Cependant, aussi bien Z And que AG Dra ont été observées aussi pendant le sursaut. La photométrie infrarouge de ces objets a montré qu'aucun changement important ne se produit dans le spectre infrarouge.

Des observations simultanées dans l'ultraviolet et dans l'infrarouge ont montré cependant que le flux ultraviolet a décrû largement pendant le minimum, alors que le flux infrarouge est resté pratiquement le même. Il s'en déduit que la source de rayonnement infrarouge n'est pas affectée par le sursaut, et que la variabilité infrarouge est une particularité de la composante froide.

Une étude systématique étendue de 91 candidats dans le domaine radio a conduit à la découverte de seulement 9 sources. Une corrélation claire existe entre le flux à 14.5 GHz et l'émission de poussière à 10 μ.

Des images, dans le domaine radio, de quelques étoiles symbiotiques ont été obtenues, et elles ont révélé une variété de structures, comme des enveloppes, des halos, des jets et des nébuleuses bipolaires.

L'émission radio de V1016 Cyg a été résolue en deux lobes, séparés par 0.10 seconde d'arc, suggérant une éjection de matière, préférentiellement dans les directions polaires. HM Sge montre une émission diffuse et symétrique, ou un halo, d'une dimension d'environ 0,5 seconde d'arc, et une structure centrale bipolaire d'une extension d'environ 0,15 seconde d'arc. AG Peg présente trois structures séparées : une nébulosité sphérique, un noyau compact et une structure en forme de jet d'une

longueur de 0,8 seconde d'arc. CH Cyg a subi un sursaut radio (entre avril 1984 et mai 1985, le flux radio a augmenté d'un facteur 35) suivi par l'apparition de matière éjectée. Le 8 novembre 1984, deux nodosités radio ont été découvertes, séparées par 0.18 seconde d'arc ; 75 jours plus tard, l'image radio a évoluée en une structure à trois composantes, avec une séparation totale de 0,4 seconde d'arc. Ces quatre objets ont éprouvé récemment des sursauts optiques. De nombreux spectres ultraviolets d'étoiles symbiotiques ont été observés avec IUE ; en beaucoup de cas, il a été possible de disposer d'observations simultanées, ou presque simultanées, dans le domaine optique. Ces observations ont été très importantes pour permettre de décider de la réalité de l'existence supposée d'un compagnon chaud à la géante froide.

Le spectre dans l'ultraviolet proche a permis une détermination précise du rougissement interstellaire, grâce à l'exploitation de l'absorption à 2200 A. Puisque l'extinction interstellaire peut affecter fortement la distribution d'énergie dans l'ultraviolet lointain, ces mesures sont importantes pour permettre de déterminer une distribution de l'énergie corrigée, pour le compagnon le plus chaud, responsable du continu bleu et des raies de haute excitation qui caractérisent le spectre optique des étoiles symbiotiques.

Le continu, dans l'ultraviolet lointain, après correction pour l'extinction interstellaire, présente dans plusieurs cas un gradient rapide qui approche la queue de distribution de Rayleigh-Jeans d'un corps noir à une température de 40000K ou plus élevée; ceci implique la présence d'un objet chaud. Cependant, aucune raie d'absorption caractéristique d'une photosphère chaude n'a été jusqu'à présent décelée.

Le spectre de raies d'émission est caractérisé par un grand nombre de raies d'émission couvrant un domaine étendu d'ionisation de l'énergie. La longue durée de vie du satellite IUE a permis de suivre cette activité, et le développement des sursauts de plusieurs étoiles symbiotiques. Quelques-uns de ces phénomènes seront décrits en détail au chapitre 13.

Plusieurs étoiles symbiotiques présentent des raies d'émission appartenant à des groupes d'énergie de haute ionisation, jusqu'à 100 eV. Ce fait suggère l'existence d'un processus efficace d'ionisation que l'on pourrait associer à un plasma à haute température. Par conséquent, on s'est attendu à ce que ces objets soient aussi des sources de rayons X. En réalité, un petit nombre d'entre elles ont été observées avec les satellites EINSTEIN et EXOSAT, et leur flux et leur variabilité ont été mesurés. Des détections positives ont été obtenues pour RR Tel, V1016 Cyg, HM Sge, AG Dra, R Aqr et CH Cyg.

12. ETOILES SYMBIOTIQUES : LES MODELES

Une histoire brève des modèles proposés pour l'explication du phénomène symbiotique est donnée au chapitre 12. Des modèles doivent être capables d'expliquer le spectre composite et la variabilité de la brillance et du spectre.

Deux types de modèles d'étoiles simples ont été proposés : une étoile chaude avec une enveloppe dense, et une étoile froide avec une enveloppe chaude.

Les problèmes variés liés à ces modèles sont discutés. Les modèles binaires composés d'un objet compagnon chaud et d'une géante rouge expliquent très naturellement la présence d'un continu bleu ultraviolet et le spectre de type M ; et l'existence d'une éclipse est évidente pour certains de ces objets. L'accrétion peut jouer un rôle important en expliquant l'activité des étoiles symbiotiques. L'accrétion peut se produire : a) par le moyen d'un disque consécutif à un flux de matière à l'extérieur du lobe de Roche, par le même mécanisme que nous avons discuté pour les novae naines et pour les novae quiescentes ; b) par l'intermédiaire du vent de l'étoile compagnon. Ce dernier mécanisme est moins efficace ; cependant, il peut se produire dans de nombreux systèmes symbiotiques possédant une très longue période orbitale où la géante rouge ne remplit pas son lobe de Roche.

Un modèle a été étudié prenant en compte la possibilité que les deux composantes produisent des vents. Plusieurs caractéristiques spectrales observées peuvent être expliquées grâce à ce modèle.

Une autre possibilité envisagée, c'est que le phénomène symbiotique soit dû à une activité de type solaire particulièrement intense de la composante stellaire froide. Mais cette possibilité peut maintenant être rejetée.

En conclusion, de nombreux détails peuvent être expliqués en supposant la présence de l'accrétion dans des binaires en interaction, soit à partir d'un vent à travers le lobe de Roche, soit à partir d'un vent stellaire.

13. ETOILES SYMBIOTIQUES PARTICULIÈRES

La discussion détaillée de plusieurs objets bien observés est donnée au chapitre 13. Puisque l'échelle de temps typique des phénomènes symbiotiques va jusqua'à plusieurs années, peu d'objets ont été observés de façon étendue hors des domaines optiques accessibles du sol. Heureusement, quelques étoiles symbiotiques (Z And, AG Dra, CH Cyg, AX Per et PU Vul) ont éprouvé des sursauts récemment, et ont été observées avec IUE, et simultanément à l'aide de télescopes optiques et infrarouges, à partir du sol.

a) Z And a été considéré comme le prototype des symbiotiques. On a observé sa courbe de lumière depuis 1887 ; elle a montré quatre sursauts importants en 1895, 1914, 1939, 1959. Deux sursauts de moindre importance se sont produits en 1984 et 1985, et ont été observés avec IUE.

Les spectres optique et ultraviolet dans la période de quiescence sont riches en raies d'émission fortes et étroites, avec un domaine étendue d'énergie d'ionisation. Les raies d'émission et le continu ultraviolet varient de facon quasi périodique sur une échelle de temps de 760 jours, cependant que le spectre infrarouge ne montre pas de variation significative. La vitesse radiale de la géante M varie avec une période de 750 jours, ce qui est une indication de binarité ; mais les variations de l'éclat et la courbe de vitesse radiale n'ont pas les phases auxquelles on s'attendrait dans le cas d'une éclipse, ou s'il s'agissait d'effets de lumière réfléchie.

La phase active est caractérisée par une augmentation de la lumière de 1 à 2 magnitudes visuelles. Le sursaut est suivi par une séquence de maximums et de minimums, ressemblant au comportement d'un oscillateur amorti. Le spectre optique est soumis à des changements importants. Pendant l'activité, les bandes de TiO sont voilées par un continu bleu, et disparaissent presque complètement. Les raies de Balmer ont des émissions fortes et des centres d'absorption.

Le spectre d'émission riche de Z And (et d'autres variables cataclysmiques) est un moyen de diagnostiquer les conditions physiques (densité électronique et températures, densité de radiation ionisante, composition chimique) des régions émissives. Dans Z And, la densité électronique résultant de cette analyse est de l'ordre de 10^{10} cm^{-3} et la température électronique de l'ordre de 15 000 K. La composition chimique est semblable à celle des étoiles rouges.

La puissance du rayonnement émis dans l'ultraviolet n'est nullement une faible proportion de la puissance émise dans le domaine visible et infrarouge. Ceci exclut le modèle d'une étoile froide active. Le maximum double de la distribution d'énergie suggère fortement la binarité. Si la masse d'une composante froide est de quelques masses solaires, et en supposant pour le compagnon la masse d'une naine blanche, l'étoile froide est nettement à l'intérieur de son lobe de Roche. Si au contraire la composante froide de Z And est une géante brillante, comme cela est suggéré par les observations infrarouges, elle remplit probablement le lobe de Roche. Si c'est un système détaché, le vent stellaire jouera aussi un rôle important.

b) AG Dra est une étoile symbiotique à grande vitesse, et à grande latitude galactique, ce qui

implique son appartenance à la population II. Sa composante froide est une géante de type K plutôt qu'une géante de type M, comme pour la plupart des autres étoiles symbiotiques. La courbe de lumière a été observée depuis 1890 ; onze sursauts ayant été notés entre 1890 et 1966. En 1980, elle a présenté un autre sursaut et trois maximums de moindre importance en 1982, 1985 et 1986. De ce point de vue, AG Dra est semblable à Z And.

Au minimum, le spectre présente les raies d'absorption caractéristiques d'une étoile de type K et de classe luminosité III assez chaude. Pendant le sursaut, le spectre est voilé par le continu bleu. Le spectre de raies d'émission montre des raies fortes de HI, HeI, HeII, OIII, FeII jusqu'à [FeV] et [FeVI]. Dans l'ultraviolet, les raies de résonance de NV, CIV et la raie HeII 1640 sont également présentes.

Le continu ultraviolet proche est plat, cependant que le continu ultraviolet lointain augmente vers les longueurs d'ondes les plus courtes, et se rapproche de la distribution de Rayleigh-Jeans de la courbe d'énergie d'un objet très chaud.

Le sursaut important de novembre 1980 a été observé dans tous les domaines spectraux, de l'ultraviolet à l'infrarouge, et a été caractérisé par une amplitude croissante de la variation depuis l'infrarouge proche jusqu'aux longueurs d'ondes les plus courtes.

En avril 1980, lorsque l'étoile était à son minimum, un flux intense dans les rayons X a été détecté par HEAO-2. Les observations faites avec EXOSAT pendant les sursauts faibles de 1985 et 1986 ont également donné des résultats positifs. Des observations infrarouges faites avant et après le sursaut ont seulement mis en évidence de petites variations.

Les observations montrent clairement que AG Dra est un objet du halo qui est une binaire. La composante froide est une géante qui ne remplit pas son lobe de Roche. Son compagnon chaud n'est pas une étoile normale, puisqu'aucune raie d'absorption n'a été observée dans le continu chaud. Sa température est estimée être de l'ordre de 100 000 K ou plus.

c) *Novae symbiotiques*. Un petit groupe d'étoiles, qui n'ont eu qu'un seul sursaut observé, tant l'amplitude était plus faible que celle de la courbe de lumière d'une nova typique, mais qui par ailleurs se comportent tout-à-fait comme des novae très lentes, sont appelées des "novae symbiotiques". Il s'agit de AG Peg, RR Tel, V1016 Cyg, V1329 Cyg, HM Sge, PU Vul, RT Ser.

AG Peg se distingue dans ce groupe en raison de son type M tout-à-fait dominant ; les autres sont des symbiotiques de type D.

RR Tel a été observée en 1949, trois ans après le sursaut, lorsqu'elle a montré un continu fort, strié de nombreuses raies d'absorption de métaux ionisés une fois. A la fin de 1949, le continu est devenu plus faible, des ailes d'émission étaient importantes. Le niveau moyen d'ionisation augmentait régulièrement ; les observations en 1978 faites avec IUE ont montré un spectre marqué de raies d'émission très nombreuses et fortes, couvrant un large domaine d'ionisation des espèces atomiques neutres jusqu'au calcium cinq fois ionisé.

V1329 Cyg, RR Tel et V1016 Cyg ont montré des spectres antérieurs au sursaut du type M. PU Vul a aussi montré un spectre d'étoile géant de type M aprés le minimum profond de 1980, et AG Peg et RT Ser l'ont montré aprés le déclin consécutif au maximum. Dans V1016 Cyg et HM Sge qui n'ont pas encore décliné, le spectre M dans le visible est masqué par le continu fort et par les raies d'émission, mais le spectre, dans le proche infrarouge, est affecté par des variations de lumière du genre de celles qui affectent les étoiles de type Mira.

Le spectre au maximum de RT Ser, RR Tel et PU Vul présente un type spectral très semblable à celui des étoiles supergéantes de type A-F, tout comme les novae classiques, mais sans les absorptions fortement déplacées vers le violet. Ces spectres d'absorption n'ont pas été observés dans les autres novae symbiotiques.

Cependant, il est possible que la phase du spectre d'absorption ait été manquée. Des étoiles symbiotiques après le sursaut montrent un spectre d'émission très riche, tout comme les novae ; mais contrairement aux novae cependant, les raies d'émission ont des profils étroits, ce qui implique une faible vitesse d'expansion.

Les observations radio des étoiles symbiotiques ont été faites au cours de nombreuses années après le sursaut. En général, le spectre radio indique que la région émissive est optiquement épaisse, c'est-à-dire que l'enveloppe en expansion HII était encore dense plusieurs années après le sursaut. Les propriétés principales des novae symbiotiques suggèrent qu'elles puissent représenter un cas intermédiaire entre les symbiotiques typiques comme Z And, qui présentent plusieurs sursauts, et les novae classiques. Plusieurs mécanismes possibles de sursauts sont discutés.

e) Deux autres étoiles symbiotiques sont décrites, qui ont les caractéristiques communes d'avoir développé un jet optique et radio. Il s'agit de R Aqr et CH Cyg.

R Aqr a un spectre symbiotique typique, caractérisé dans le visible par de nombreuses raies d'émission, et une composante MIII tardive. C'est aussi une variable de type Mira typique, avec une période de 387 jours, et elle est au centre d'une nébuleuse planétaire. La nébuleuse est composée de deux couches séparées, en expansion à la vitesse de 30 à 50 km/s. Ces enveloppes devraient avoir été éjectées de l'objet central il y a 185 et 640 ans. Une structure ayant la forme d'un jet a été détectée en 1977 et réobservée à nouveau en 1980 et 1982, mais était absente en 1970. Des observations radio à très grandes résolutions spatiales ont identifié cinq radiosources ; le jet radio coïncide dans l'espace avec le jet optique.

Le spectre ultraviolet a été étudié depuis 1979 et a révélé la présence de raies d'émission d'excitation modérée. Les raies de NV et d'HeII sont faibles. Ces raies ont été grandement intensifiées dans le jet de 1982. Cette intensification pourrait être associée à la première détection de rayons X issus de R Aqr.

En dépit du grand nombre de données d'observation disponibles concernant R Aqr, il est difficile de trouver un modèle les décrivant de façon cohérente.

f) CH Cyg est une autre étoile symbiotique qui a présenté un jet optique et un jet radio à la fin de son dernier sursaut.

Pendant de nombreuses années, CH Cyg a été considérée comme une variable semi-régulière, normale M6III. Le premier sursaut, observé en 1963, a révélé les caractéristiques symbiotiques de l'étoile. Cependant, elle fut considérée comme une symbiotique assez anormale, en raison du fait que son spectre ne présentait pas un domaine étendu d'énergie d'ionisation, mais seulement des raies d'emission des ionisations basses. Un second sursaut s'est produit en 1967, et s'est terminé à la fin de 1970. Il a confirmé que CH Cyg est une étoile symbiotique de basse excitation. Un continuum bleu a voilé le spectre M6 pendant le sursaut, et plusieurs profils de type P Cyg, de métaux une fois ionisé, absorbaient le continuum bleu. Des vitesses d'expansion de -100 km/s ont été observées. Dans la période de quiescence, le spectre M6III a montré une émission Hα faible. Le troisième sursaut a commencé en 1977, et était presque fini en 1987. Il a été suivi à la fois à partir du sol dans le domaine optique, et avec IUE dans le domaine ultraviolet. Des observations infrarouges, à la fois à partir du sol et avec IRAS ont été faites à différentes époques, et sont en bon accord. Les observations dans les domaines X et radio ont été faites pendant la phase de déclin après le sursaut.

Pendant le sursaut de 1977, les raies d'absorption des métaux une fois ionisé ont présenté des profils P Cyg inverses, à l'opposé de ce qui a été observé en 1967. Seules les raies H et K du CaII ont présenté des profils P Cyg pendant les deux épisodes de sursaut.

Les vitesses radiales de la géante M6 montrent une variabilité d'une période d'environ 15 ans,

suggérant qu'elle puisse être due à un mouvement orbital. Cependant, la dispersion autour de la courbe moyenne est grande à cause des variations intrinsèques irrégulières dues aux mouvements atmosphériques dans l'atmosphère de la géante rouge. Il y a aussi quelques indications selon lesquelles les raies d'émission du FeII, et les noyaux d'absorption des raies d'ions métalliques une fois ionisés, toutes deux observables seulement pendant les sursauts, ont des vitesses radiales en déphasage de 180° avec les raies d'absorption de type M6.

Le spectre ultraviolet a été caractérisé par les raies d'absorption des métaux une fois ionisés et des raies de résonance CIV et SiIV et quelques émissions de très basse excitation et un continu plat. En janvier 1985, le spectre a changé complètement, devenant dominé par les émissions fortes de Lyα, NV, CIV, SiIV, FeIII, FeII. Le continu, à la fin du sursaut, est beaucoup plus faible, mais il y a eu quelque indication d'une augmentation du flux vers les longueurs d'ondes plus courtes que 1 300 A, ce qui suggère que nous sommes en train d'observer la portion Rayleigh-Jeans du spectre d'un corps faible et chaud.

Les observations radio à haute résolution spatiale ont été faites en avril 1984 et mai 1985 ; elles ont indiqué que CH Cyg a subi un sursaut radio important coïncidant avec l'apparition de jets à plusieurs composantes en expansion à un taux de 1,1 seconde d'arc/an. Le démarrage du sursaut radio a coïncidé avec une décroissance de la courbe de lumière observée en juillet 1984. La vitesse d'expansion était de l'ordre de 2 500 km/s, du même ordre que celle indiquée par la largeur de la raie d'émission Lyα et les raies de Balmer à la même époque, une vitesse en réalité tout-à-fait exceptionnellement élevée pour une étoile symbiotique, et comparable à celle que l'on observe dans le spectre des novae. Le jet a été observé aussi dans la raie de [OIII] à 5007 A en septembre 1986 et dans l'ultraviolet avec IUE en novembre 1987. Des essais pour l'observer de nouveau avec IUE en mai 1988 ont donné des résultats négatifs.

CH Cyg a été détecté avec EXOSAT en mai 1985. Des essais antérieurs pour mesurer son flux dans le domaine X, faits avec EINSTEIN, avaient été négatifs.

Cette longue série d'observations de CH Cyg suggère qu'il s'agit d'un système binaire composé d'une géante M6 et d'un compagnon faible et chaud. Si la période orbitale est celle que suggèrent les variations de vitesse radiale, d'environ 15 ans, la géante rouge ne doit pas remplir son lobe de Roche, et par conséquent l'accrétion doit se produire à partir du vent de la géante. Un disque d'accrétion optiquement épais doit se former pendant le sursaut, donnant lieu au continu bleu ultraviolet et aux raies d'absorption, simulant ainsi une supergéante chaude. A la fin du sursaut, le disque devient optiquement mince, le continu devient très fin et les raies d'émission dominent le spectre. Il est alors possible d'observer une émission dans le domaine X provenant de la couche de transition interne, et de détecter la portion Rayleigh-Jeans du spectre du flux émis par le compagnon faible et chaud.

14. LES PHÉNOMÈNES CATACLYSIMIQUES ET SYMBIOTIQUES : CONCLUSIONS

Le chapitre 14 résume les points importants concernant le phénomène symbiotique.

Il existe une forte évidence en faveur du fait que la plupart, des étoiles symbiotiques, sinon toutes, sont des systèmes binaires en interaction. L'étoile qui perd de la masse est une géante froide, l'étoile qui en gagne pourrait être une naine blanche, ou, dans quelques cas, une étoile de la série principale. L'accrétion peut se produire soit à partir de lobe de Roche rempli, soit à partir transport par le du vent de la composante la plus froide.

15. Le dernier chapitre : *Perspectives et problèmes non-résolus* examine rapidement les nombreux problèmes non-résolus, posés par les observations des classes différentes des variables cataclysmiques et d'étoiles symbiotiques. Des progrès importants ont été faits spécialement en exploitant la possibilité d'observer le même

objet, simultanément de l'espace et du sol, couvrant ainsi un très grand domaine spectral. Quelques contraintes imposées aux théories ont été ainsi définies. Cependant, de nouvelles questions se sont posées, exigeant de nouvelles observations et de nouvelles théories.

Notre conclusion est que pour une meilleure compréhension des classes diverses de variables cataclysmiques, nous avons besoin d'observations étendues sur de très longues périodes de temps, et dans un domaine spectral aussi large que possible, avec toutes les techniques disponibles (photométrie, spectroscopie, imagerie) *d'un petit nombre d'objets bien choisis*, plutôt que d'accumuler des morceaux dispersés d'observations d'un très grand nombre d'objets. C'est seulement de cette façon que l'on peut espérer préciser les contraintes nécessaires aux théories, et rendre les calculs théoriques plus réalistes.

SUMMARY

In the original definition, the characteristics that qualified a star as a cataclysmic variable were the occurrence of unpredictable outbursts. The strengths and time scales of outbursts vary greatly among individual members of this class of objects. Violent as these outbursts appear, photometric and spectroscopic observations indicate that the general structure of dwarf novae and novae is not significantly affected by them.

The current *classification system of cataclysmic variables* is based on properties of the outburst light curves. Although it is possible in the majority of cases to clearly assign a star to one of these sub-classes, there are several ambiguous cases. *Old novae* appear essentially indistinguishable from *quiescent dwarf novae*, so that the possibility has been considered that both types really comprise the same kind of object, and they are only seen at different stages of a possibly cyclic evolution. Furthermore, some of the *recurrent novae* (T CrB, RS Oph, V1017 Sgr) appear similar to *symbiotic stars* except for the larger amplitude of outbursts, while others (U Sco, T Pyx) bear more similarities to *classical novae*. In general, *cataclysmic variables all exhibit decided individuality* in almost all observable features so that not any two only nearly identical members are known.

The observational data suggest that *all the well observed objects are in fact binary systems*, a situation that was first recognized in the mid-fifties. These binary systems are composed of a late type star, which is a red dwarf in the case of dwarf novae, nova-like objects and classical novae, and probably in one or two recurrent novae, and is a red giant in symbiotics and at least two recurrent novae together with a hot underluminous companion, which is generally a white dwarf. This hypothesis that all cataclysmic variables are binaries, in turn, leads to the formulation of the *Roche model* for explaining the nature of all cataclysmic variables.

Later observations in the ultraviolet and X-ray ranges confirmed the predictions of this model and reinforced the notion that binarity is of primary importance for producing cataclysmic events. Also the assumption of binarity provides an easy explanation for the pronounced individuality of systems due to the many more degrees of freedom in physical appearance compared to single stars.

This volume begins with an introductory chapter on general properties of cataclysmic variables. With the exception of nova-like stars they are characterized by sudden light outbursts of several magnitudes and related appreciable spectral variations. The observations indicate occasional *mass loss* and / or *mass transfer* between the components of the binary. Most systems emit substantial amounts of radiation over the entire range of the electromagnetic spectrum, though in dwarf novae and nova-like stars there is only marginal flux at radio wavelengths. The X-ray emitting regions are thought to be those where interaction occurs between the *accretion disc* and the hot star. The accretion discs and the *expanding envelope* of novae are strongest in the ultraviolet. The outer parts of the discs, the *"pseudo-photospheres"* of outbursting novae, the *nebulae* surrounding old novae, and the brighter of the *secondary stars* are seen in the optical. The secondary stars and the *dust* formed in novae can be detected at infrared wavelengths. Finally, the radio flux as seen in novae is ascribed to the *outer shells* of ionized gas, and furthermore, in two symbiotic stars the formation and evolution of *jets* can be detected in the radio range.

Space distributions, and system parameters like masses, mass ratios, orbital periods and absolute magnitudes of old novae, dwarf novae and nova-like stars are discussed. Novae are clearly more concentrated toward the galactic plane than dwarf novae and nova-like stars. The more uniform distribution of the latter two classes, in combination with their intrinsically low brightness, indicates that they are close neighbors to the Sun. No clear statistical difference has been found between masses and mass ratios in the three classes of cataclysmic vari-

PRECEDING PAGE BLANK NOT FILMED

ables. Instead the absolute magnitudes of quiescent novae, quiescent dwarf novae and nova-like stars show distinct differences. Quiescent novae are concentrated around the value M_V = 4, nova-like stars around M_V = 5, and dwarf novae around M_V = 8-9.

A remarkable feature concerns the orbital periods. Most cataclysmic variables have periods included between 1.3 and 5 hours, but a *"period gap"* between some 2 and 3 hours exists which is strongly depleted of objects. Differences exist between sub-classes concerning the orbital periods, and in addition some objects have periods considerably shorter or longer than the vast majority of cataclysmic variables.

Chapters 2 through 5 are devoted to observations and interpretation of dwarf novae and nova-like stars.

Dwarf novae are typically found in the so-called quiescent, i.e., low brightness, state; and, at semi-regular intervals of time of typically some 10 to 100 days, the brightness rises by about two to five magnitudes. In the modern classification, three different types of dwarf novae are distinguished: the *U Geminorum stars*, the *Z Camelopardalis stars*, and the *SU Ursae Majoris stars*. The Z Camelopardalis stars, on decline from outbursts, occasionally stay at an intermediate brightness level for weeks or years (*"standstill"*) before returning to minimum light. SU Ursae Majoris stars, in addition to "normal" outbursts such as those found in all other dwarf novae, exhibit longer and somewhat brighter, so-called *"superoutbursts"*. Dwarf novae that do not fall into either of the former categories are classified as U Geminorum stars.

Concerning statistical properties, dwarf novae and nova-like stars are discussed together. In matters like masses of the stellar components, mass ratios, or orbital periods, these systems, when regarded as groups, are almost identical. However, some differences seem to be connected with the outburst behaviour and magnetic properties.

The photometric outburst properties of the best studied dwarf novae are described. With more than 600 recorded outbursts over the last almost 100 years, SS Cyg, the brightest known dwarf nova, is the best studied object in this respect, but others have been investigated reasonably well, too. Concerning details of photometric changes during outburst, such as the time required to reach maximum brightness or the total duration of the event, in any dwarf nova various types of outbursts can usually be distinguished. Also relations have been found between, for instance, the outburst amplitude, the total energy spent during an outburst, and the recurrence time. Another positive relation seems to exist between the rate of early decline from an outburst and the orbital period; between the absolute brightness reached during outburst and the orbital period; and between the orbital period and the widths of wide and narrow outbursts, respectively. And finally, characteristics of standstills and superoutbursts are discussed.

Appreciable colour changes occur during the course of an outburst cycle, when characteristic loops in the two-color-diagram are performed. Most of these changes take place during the fast rise to maximum when the stars become considerably bluer than normal; changes during decline are much less dramatic.

Pronounced photometric changes during quiescence, often related to the orbital revolution, are present in all dwarf novae. In the optical, these may be a temporary increase in brightness by some tenths of a magnitude for about half the orbital cycle (the *'hump'*) or an eclipse lasting for a small fraction of the orbital period and with a depth of up to two magnitudes, either or both of which are present in many dwarf novae. In all systems, at all levels of the outburst light curve, superimposed on the general brightness level are irregular brightness changes, the so-called *'flickering'*. Only very few data are available on the variability on orbital time scales in the ultraviolet range, and not much more in the infrared. The variety of infrared light curves among the dwarf novae apparently is rather large. Several

systems are known to exhibit a secondary eclipse at about phase 0.5 with respect to the primary eclipse, which is not seen in the optical.

Long-term monitoring of the quiescent light level has been possible for SS Cyg and U Gem. In the latter the flux remains constant within narrow limits and no systematic trend of changes could be detected. SS Cyg on the other hand maintains a stable light level for several weeks, at others the flux level is seen to systematically increase or decrease over as much as several consecutive quiescent phases. One such long-term monitoring was done for CN Ori during a full quiescent interval between two consecutive outbursts. The hump amplitudes varied in a cyclic manner with a superimposed trend of rising light level at hump maximum, while the minimum brightness at interhump phases stayed constant. These observations were detailed enough to also reveal that the structure of the orbital light curve never repeated exactly from one cycle to the other, but several characteristic features were still always present.

A section in this chapter is devoted to two very special dwarf novae, WZ Sge and BD Pav. They both have extremely long outburst periods which lead to their former classification as recurrent novae. However, the amplitude and other characteristics of their outbursts are more typical of dwarf novae, and thus they now commonly are classified as such.

Another further characteristics of some dwarf novae is an apparent secular variation of the orbital period. For dynamical reasons it can be excluded that these reflect actual changes in the orbital period, but what they really are due to is not clear yet.

Amazingly little is known about the orbital changes during the outburst state. The hump amplitude is generally more variable than in quiescence, single eclipses tend to disappear, and double eclipses tend to become single during light maximum. The orbital light curves of Z Camelopardalis stars during standstills are indistinguishable from those observed at comparable brightness stages at decline from normal outbursts. During superoutbursts in SU Ursae Majoris stars, '*superhumps*' are seen which undergo very characteristic changes during the course of a superoutburst.

At high time resolution of minutes or seconds, further photometric changes become apparent in dwarf novae. There is 'flickering', a random light variation with amplitudes of some tenths of a magnitude and characteristic time scales of between seconds and minutes, which is present at all stages of activity. '*Coherent oscillations*' occur at times in dwarf novae during outbursts, or in nova-like stars in the high state as well as in WZ Sge during quiescence. Periods are a couple of ten seconds, and amplitudes are on the order of 0.002 mag. Finally, there are '*quasi-periodic oscillations*' with very short coherence times, periods on the order of one minute, and amplitudes somewhat larger than those of coherent oscillations. In the three brightest dwarf novae, SS Cyg, U Gem, and VW Hyi, oscillations also could be detected in X-rays.

All these photometric data indicate that the common characteristics of dwarf novae are their outburst behaviour, the orbital light curves that often exhibit a hump and/or an eclipse, and short-term flux variations on several time scales. An enormous variety of features can be found not only in the various systems but also in the same object at different outburst stages.

Spectroscopic observation indicate that dwarf novae emit appreciable flux from the X-ray range to the infrared and, in a few cases, also in the radio range. The most flux is emitted in the ultraviolet and progressively less at longer wavelengths. The flux distribution is very different from that of a normal star. Over wavelengths ranges of 1000-2000 A a fit with a *power law distribution* is possible.

During outburst, the spectrum is steeper than during quiescence, and even more flux is emitted at high energies. In some objects, the

flux rises again in the infrared and only falls off longward of a maximum around 1.5-2μm. Although this general behavior is shared by all dwarf novae, the energy distributions are fairly different for different objects and at different outburst states. Rise to maximum either occurs simultaneous at optical and ultraviolet wavelengths, or the optical starts to rise up to half a day before the ultraviolet. There is indication that this delay continues in the X-ray range.

Decline from outburst always proceeds simultaneously at all wavelengths.

At X-ray energies, quiescent dwarf novae preferentially radiate in the hard X-ray range, while during outburst they are seen rather in the soft X-ray range.

The X-ray flux is highly variable on all timescales.

A relation was found between the ratio of the X-ray flux to the visual flux and the equivalent width of Hß.

Only very few dwarf novae could be detected at radio energies. These spectroscopic observations of the continuum of dwarf novae suggest that the ultraviolet flux and most of the optical flux originate from the accretion disk. The infrared and possibly some of the optical flux during quiescence comes from the secondary component. X-ray radiation is ascribed to the boundary layer, which is assumed to be optically thin in quiescence, and therefore emits hard X-rays, and optically thick in outburst and therefore, because the radiation is thermalized before escape, emits soft X-rays.

The line spectra during quiescence are, in most cases, characterized by strong emissions, although in some cases emissions in the optical are weak, or lines in the ultraviolet might even be weakly in absorption. High-inclination systems exhibit double-peaked profiles in the Balmer emission lines. In several cases, the absorption spectrum of a cool main-sequence star is visible.

In general, optical lines undergo profile changes on orbital time scales. In particular many lines are weakened during photometric eclipse. No such observations have been published for the ultraviolet range. In many systems the so-called *S - wave* is seen, a systematic variation of the relative strengths of the red and blue peaks of the hydrogen lines during the orbital cycle. Also the radial velocities change in phase with the orbital light curve. Emission and absorption spectra are out of phase by about 180°.

The observed spectral characteristics indicate that the emission lines are formed in optically thin disc areas, while the absorption lines sometimes observed in the ultraviolet rather suggest that the inner disk is optically thick. The periodic changes in radial velocities and line intensities are ascribed to orbital variations, while random changes are ascribed to inhomogeneities in the accretion disk. Double-peaked line profiles are believed to originate from rotation of disks seen at high-inclination angles. The phase shift of 180° between emission and absorption lines is an effect of binarity, the emissions being produced in the accretion disk around the white dwarf and the absorption in the cool secondary star. Irradiation effects are believed to be responsible for the deviation from a phase shift of exactly half an orbital period.

During outburst the line spectrum, both in the optical as well in the ultraviolet, turns into absorption. The late absorption spectrum is masked by the increased continuum flux.

Around or shortly after maximum, emissions start to grow in the broad absorption lines, and during the course of decline the quiescent spectrum is restored.

The radial velocities during outburst are roughly the same as those during quiescence, but K and Gamma velocities may be different.

The appearance of the absorption spectrum in outburst suggests that the disc has become opaque. The sometimes observed blue-shifted

or P Cygni profiles indicate a high-velocity wind blown off the system during outburst. The variation in K and Gamma velocities are suspected to be due to brightness changes in the disc.

Five classes of nova-like stars are distinguished: the *UX Ursae Majoris*, the *anti-dwarf novae*, the *DQ Herculis*, the *AM Herculis* and the *AM Canum Venaticorum* stars.

All nova-like variables have the common property of not normally showing large outburst activity, though they may be found in "high" or "low" states.

The spectroscopic and photometric appearance of UX Ursae Majoris stars are very similar to those of dwarf novae at some stage of the activity cycle.

Anti-dwarf novae are usually found in a bright state. At times in which they are undistinguishable from UX Ursae Majoris stars, however, they experience brightness drops by several magnitudes and then look mostly like dwarf novae during the minimum state. Concerning their long-term behavior, DQ Her stars (or *intermediate polars*) comprise the full range of possibilities found in cataclysmic variables. Their common characteristic feature is the presence of at least one highly stable photometric period besides the orbital variation. Between two and three subclasses are distinguished on the basis of the length of the period of this additional variability. Spectroscopically most of them do not appear any different from UX Ursae Majoris stars.

Like anti-dwarf novae, the AM Herculis stars (or *polars*) normally are found in a high-brightness state, but occasionally undergo drops by several magnitudes. All AM Herculis stars are characterized by a very high degree of polarization which varies in strict synchronism with (orbital) changes of the general light level and the radial velocity. Orbital light curves as well as spectra in many ways are atypical for cataclysmic variables. AM Canum Venaticorum are characterized by the absence of any trace of hydrogen in their spectra, strong absorption or emission lines of helium, and often pronounced flickering activity.

One interpretation of these observations is that UX Ursae Majoris stars and anti-dwarf novae basically are the same sort of objects. However in UX Ursae Majoris stars the mass transfer through the accretion disc is always high; therefore the disc is thought to be stationary all the time; in anti-dwarf novae, on the other hand, mass transfer occasionally drops. In dwarf novae, mass transfer is so low that the disc undergoes semi-periodical changes between high and low accretion events.

DQ Her stars are believed to have a weakly magnetic white dwarf in the system. This star disruptes the inner accretion disk, but the magnetic field is not strong enough to keep the star in synchronism with the orbital motion. The rotation of the white dwarf becomes visible as an additional stable photometric period. AM Her stars are believed to have a strongly magnetic white dwarf in the system, which entirely prevents the formation of an accretion disc and locks the rotation of the white dwarf to the binary orbit.

A brief history of the *models* proposed for explaining dwarf novae and nova-like stars is given. One of the reasons for the difficulty of finding a model capable of explaining at least the majority of observations until the 1950's was the low time resolution that focussed entirely on the outburst behavior, and thus could not reveal the periodicities at shorter time scales. It was Linnell in 1950 who proposed a model for UX UMa which was strikingly similar to the now commonly accepted Roche model.

When it became clear that all the well-studied cataclysmic variables turned out to be binary systems with orbital periods of a few hours, that the secondary stars, when observable, are cool main-sequence stars, and that the primary stars are hot objects with a geometry and flux distribution very different from that of normal stars, the Roche model was adopted as

a working hypothesis. This model consists of a cool main-sequence star which fills its Roche lobe and loses matter into the Roche lobe of the white dwarf. The transferred material has too much angular momentum to fall directly onto the surface of the white dwarf, but instead builds out an accretion disc in which it spirals toward the white dwarf to eventually be accreted.

An increasing number of observations, both photometric and spectroscopic, and in almost the entire spectral range from hard X-ray to infrared, have given more and more support to the notion that the Roche model is appropriate for describing the basic physics of cataclysmic variables. However many details remain to be explained, and the structure of the systems is presumably more complicated than can be theoretically handled at this stage. One of the parameters which critically determines the appearance and temporal variations of the accretion disc is the *"viscosity"*, which is largely unknown. This viscosity is a means for describing the mechanisms of angular momentum transport in the disc. It is usually parametrized as a quantity α, defined as the ratio of the turbulent velocity to the sound velocity including the actions of the probably present magnetic fields. It is basically a free parameter which well may have different values at different points in the disc.

For any theoretical interpretation it is very important to know absolute values of the parameters of a system such as stellar masses and radii, inclination angles, absolute magnitudes, and mass transfer rates. For this reason, a critical discussion of the methods for their determination and their reliability is given. In a normal detached binary system, masses and radii, as well as the inclination angle, can be derived from radial velocity curves and light curves. However, only two eclipsing double-lined spectroscopic binaries are known among dwarf novae and nova-like stars. So in principle one could derive masses only for these two systems. Moreover the shape of the light curves indicates that the geometry of the system is not that of a normal detached system. Hence it is highly questionable whether the inclination angle and radii of the stars could be determined using the standard procedure. For instance, great care must be taken in the determination of radial velocity curves, so that inhomogeneities in the disc (like the presence of the *hot spot*) and irradiation of the secondary star are properly taken into account. Furthermore, the hot spectrum generally is that of the accretion disk rather than that of the white dwarf itself.

Constraints due to the assumption of the applicability of Roche geometry are of great help in determining the parameters of the system. Relations exist, for instance, between the radius of the secondary star and the mass ratio of the stellar components, Or another relation exists between the radial velocity amplitude K_1 of the primary component, the projected rotational velocity of the disk, and the mass ratio. Still, severe difficulties are met in the reliable determination of the inclination angle and the radial velocities.

The parameters of the secondary star can, in principle, be determined from, for instance, the infrared colors; but difficulties are met here also.

Absolute magnitudes and distances can be derived from the spectrum of the secondary star. Moreover, relatively well defined relations exist between the absolute visual magnitude of a dwarf nova in outburst and the orbital period, and between the visual magnitude and the equivalent width of the Hß emission. Also the interstellar absorption feature at 2200 A, if present, can be used as a distance indicator. For U Gem and SS Cyg, trigonometric parallaxes were derived.

Other important parameters are the mass-transfer rates, i.e., the mass-transfer rate from the secondary into the Roche lobe of the primary, the mass throughput through the accretion disc, and the mass-accretion rate onto the white dwarf. All these determinations are strongly model dependent. The most reliable method seems to be that based on eclipse-mapping techniques.

Although observations seem to indicate that the brightness changes in dwarf novae are directly due to changes in the disc, still many unsolved theoretical problems remain.

The simplifying assumptions generally made in theoretical work are neglect of relativistic effects and self-gravity. Furthermore the disc is assumed to be geometrically thin, lying flat in the orbital plane of the system. It is assumed to be rotationally symmetric, and that the only energy source is gravitational energy, which is converted into radiation energy by viscous processes that also take care of the separation of angular momentum and mass. A certain vertical thickness structure of the disc is assumed to be due to thermal pressure originating from the transformed gravitational energy and turbulence.

From computations of particles trajectories in the restricted three-body approximation, the approximate position of the hot spot can be reproduced. Hydrodynamic computations provide information about brightness distributions, surface density distributions, and velocity fields in the disc.

Assuming hydrostatic equilibrium in the vertical direction and employing the basic equations for stellar atmospheres, some idea can be obtained about the vertical structure of the disc. Unfortunately, the most important and the weakest parameter in all these computations is the viscosity.

Two possible outburst mechanisms have been suggested for dwarf novae, *viscous instability* in the accretion disc (*"disc instability"*) or a suddenly enhanced *mass transfer* onto the disc from the companion star (*"transfer instability"*). The first mechanism assumes that the viscosity follows a hysteresis curve, as the physical state of the disc material changes between being convective or radiative. General and to some extent even detailed outburst light curves can be reproduced theoretically. The other suggested mechanism assumes that instabilities in the atmosphere of the secondary star lead to temporarily increased mass transfer onto the disc which causes the outburst. Also in this case a reasonably satisfactory agreement with the observations can be obtained. So far no definite discrimination between the two models can be made.

Also for superoutbursts no single generally accepted model exists so far.

The rapid oscillations, because of their high frequencies and short coherence times, are believed to originate either on the outermost surface of the white dwarf or in the innermost areas of the accretion disc.

The secular variations of the orbital period, as observed in several dwarf novae and nova-like stars, are not yet satisfactorily explained.

Models proposed for explaining the strongly magnetic systems (AM Herculis stars) and the weakly magnetic systems (DQ Herculis stars) are described. For AM Herculis stars it is assumed that a strongly magnetic, synchronously rotating white dwarf prevents the formation of an accretion disc, and forces accretion to occur through magnetic funnels along the field lines. In DQ Herculis stars, the white dwarf possesses only a moderately strong magnetic field, which is able to disrupt the disc at some distance from the star but cannot entirely prevent the formation of the disc, nor can it keep the white dwarf in synchronous rotation with the orbital motion. Illumination of system components by the hot accreting poles, or radiation directly from the poles, produces the observed additional photometric periodicities.

The spectra of dwarf novae and nova-like stars present a variety of appearances; pure emission line spectra, pure absorption line spectra, a mixture of both, asymmetric line profiles, very different slopes of the continuous flux distribution. The same star can present all these features at different times. To simplify the problem of modelling these spectra, it is usually split into three separate problems: that of specifying the physical model to serve as a background for the computations; that of computing the continuous spectrum; and that of

computing the line spectrum. The physical model underlying the computations is the Roche model for cataclysmic variables.

The continuous flux distribution does not resemble that of normal stars, and an approximate fit is possible if it is assumed that only the disc contributes to the radiation, and that at each distance from the white dwarf it radiates like a black body, with the radial temperature distribution as derived for a stationary accretion disc.

The absorption line spectrum is computed in close analogy to computations of stellar atmospheres. The basic difference between a stellar atmosphere and a disc atmosphere is the *energy source, nuclear* in the first case, *gravitational* in the second case. But this does not matter for the emitted spectrum, as long as the central plane of the disc is optically thick. Furthermore, in contrary to stellar atmospheres, accretion discs are essentially two-dimensional objects, and thus the *inclination angle* is an important parameter for the observed radiation. The Keplerian rotation of the disk leads to additional broadening of the line profile and to double-peaked absorption profiles. The major results obtained from spectrum synthesis calculations are the main free parameters (the mass of the white dwarf, the mass-transfer rate, the inner and outer radii of the disc, and the inclination angle). The mass of the white dwarf and the outer disc radius are of practically no importance. The inclination angle has a drastic effect on the continuum as well as on the lines. The mass transfer rate enters the radial temperature profile and therefore has a very important influence on the appearance of the spectrum. Finally, the inner disc radius is very important, since its variation means including or neglecting the very hottest parts of the disc, which entirely determine the ultraviolet, and also part of the optical, radiation.

The emission lines are generally observed during the quiescent state and are ascribed to optically thin areas in the inner and/or outer disc, or even the entire disc. Modelling is more difficult than for outburst spectra, because during quiescence the disc is probably not stationary (i.e., no radial temperature law is available a priori) and non-LTE effects are likely to be important.

Optical observations of dwarf novae in outburst and of nova-like stars give no evidence of winds. The Balmer lines are seen in absorption and with symmetric profiles. In the ultraviolet, however, strong P Cygni profiles or shortward shifted absorptions of C IV resonance doublet, and occasionally of Si IV and N V are observed. These profiles are different from those seen in normal hot stars. Furthermore, systems with very high inclination angles exhibit only strong emission profiles, while all the other lines are seen in absorption as usual. Computations assuming an optically thick accretion disk and a wind driven out from the disc center and/or boundary layer can reproduce the observations rather well, if the most important parameters - in this case the mass loss rate, the velocity profile of the wind, the temperature, and the temperature profile of the accretion disc - are chosen appropriately.

By means of image-processing techniques the surface brightness and temperature distribution of the accretion discs can be reconstructed from eclipse observations. This method, in principle, allows the derivation of the radial temperature profile, the localization of the geometrical origin of the various contributions to the line radiation, the distinction between optically thick and optically thin areas of the accretion disc, and, depending on the kinds of observations, many more system properties. Detection of soft and hard X-ray radiation from many dwarf novae and nova-like stars are ascribed to a boundary layer between the disc and the surface of the white dwarf, which is formed there where the Keplerian rotating disc material is braked down to the rotational velocity of the white dwarf, in order to be accreted. Its detailed structure as well as details of the emitted spectrum are not yet understood.

The evolutionary state of cataclysmic variables is discussed. Their space distribution and

selection effects are considered. Novae and dwarf novae seem to have about the same space distribution and both are generally population I objects, although some dwarf novae are known to belong to globular clusters.

The properties of the stellar components in cataclysmic variable systems are discussed. There is some indication that, statistically, the masses of white-dwarfs members of cataclysmic variables are more massive than single white dwarfs. This discrepancy can be accounted for by selection effects, mostly due to the mass-radius relation of white dwarfs. The secondary stars appear indistinguishable from normal main-sequence stars. Black-dwarf secondaries are expected to exist in systems below the period gap, but these could not yet be detected.

An outstanding characteristic feature of cataclysmic variables is the existence of a *period gap* between about two and three hours and the minimum orbital period of about 80 minutes. The upper end of the period gap is understood to be due to the cessation of magnetic braking as it is operating in the secondary star; as a consequence the secondary star is detached from its Roche lobe, and mass overflow stops. Gravitational radiation acts to decrease the orbital period, by which time the period has decreased to some 2 hours, and brings the star back into contact with its Roche lobe. The period keeps decreasing due to gravitational radiation until, at the minimum orbital period, the secondary star has lost a sufficient amount of mass to be unable to maintain nuclear energy generation, and thus becomes degenerate. At further evolution, the orbital period increases again until the secondary star will have resolved.

It is still an entirely open question what stars are the progenitors of cataclysmic variables. Although W Ursae Majoris stars have about the same space density and distribution as cataclysmic variables, their angular momentum is too small for a white dwarf to be formed, and, therefore, they can be excluded as possible candidates. No other group of stars can be identified as possible progenitors.

Possible scenarios for the evolution of a binary system to a cataclysmic variable are discussed.

Finally, the often discussed scenario is presented that novae, dwarf novae, and nova-like stars might actually be the same kinds of objects at different stages of activity.

The final Chapter in Part I, Chapter 5, summarizes the main issues on dwarf novae and nova-like stars and discusses the suitability of the currently employed classification systems.

Chapters 6 through 10 of Part II discuss the general observational properties of classical and recurrent novae, the theoretical models, and the characteristics and models for some well observed classical novae and recurrent novae.

Chapter 6 describes the observable characteristics of classical novae and recurrent novae obtained by different techniques (photometry, spectroscopy and imaging) in all the available spectral ranges, and at the various phases in the life of a nova. These phases are schematized as follows: *quiescence (pre- and post-outburst), outburst, final decline, and nebular phase.*

The examination of all the available observations of old novae before and after outburst indicates that the eruption has very little effect on the stellar structure and on the binary system, when the parameters of the latter are known.

In fact both photometric and spectroscopic properties remain the same before and after outburst, although in some cases long periods of time (several years) are necessary for the star to reach the observed pre-outburst magnitude. Hence it should be very important to study old novae, which erupted centuries ago. Unfortunately only two cases are known, CK Vul 1670 and WY Sge 1783.

Several novae at minimum present *flickering*, and, very rarely, *coherent oscillations* (DQ

Her, V 533 Her) or *quasi periodic oscillations* (RR Pic, GK Per).

The spectra of just three quiescent novae, before outburst, i.e., before they were known to be novae, have been observed. These spectra, although limited to three cases, and of rather poor quality, suggest that they do not differ very much from those taken after the end of the outburst.

The spectra of past novae are characterized by a very blue continuum and emission lines of H I, He I, He II and no definite evidence for the presence of absorption lines. Comparison of the spectra of several old novae, dwarf novae, and nova-like stars does not display any clear differences among the three classes of objects. We can repeat again that both photometric and spectroscopic characteristics of novae are indistinguishable from those of dwarf novae, although the luminosity and accretion rate are not the same.

Statistical studies of the spectra of novae and dwarf novae at minimum indicate that the emission line-width is related to the inclination of the system; the broader are the emission lines the closer to 90° is the *inclination of the accretion disc*.

Although the photometric characteristics of quiescent novae are rather similar to each other, their outburst light curves may differ strongly. Novae are therefore classified according to the rapidity of their decline from maximum. The classes are: *fast novae* ($t_3 < 100$ days, where t_3 is the number of days required to decline by 3 magnitudes), *slow novae* ($t_3 > 150$ days), and *very slow novae*, which stay at maximum for several years. A very detailed classification done by Duerbeck in 1987 takes into account also the presence or absence of oscillations during the transition stage, the presence or absence of a deep minimum in the transition stage, and other details of the outburst light curve.

An important correlation has been found between the absolute magnitude at maximum and the rapidity of decline from maximum, the fastest novae being the brightest (hence their distance can be estimated). Another method to derive the distance, the *nebular expansion parallaxes*, is discussed in the section devoted to the nebular phase of novae.

The spectra in outburst, which indicate the presence of layers expanding at high velocity, pass through various phases. Just before maximum brightness is attained, the *PRE-MAXIMUM spectrum* is very similar to the spectrum of a B or A supergiant. The *PRINCIPAL spectrum* replaces the pre-maximum spectrum within a few days after maximum, and persists until the nova has faded by about 4 magnitudes. It is very similar to the pre-maximum spectrum, but the type is generally slightly later, and is similar to the spectrum of an A or F supergiant. The expansion radial velocity is larger than that indicated by the pre-maximum spectrum. A correlation exists between the principal spectral type and the expansion velocity, which ranges from about 2000 km/s for the hotter spectral types (characterized by the presence of N V lines) to 200-100 km/s for types F0-F8. This is a clear indication that it is the kinematic energy originating in the outburst which produces the observed spectrum. The *DIFFUSE-ENHANCED spectrum* appears later than the principal one and presents an expansion velocity higher than the latter. The absorption lines are wide and strong. It reaches maximum intensity about two magnitudes below maximum. The *ORION spectrum* is similar to those of the B-type stars in the Orion nebula and reaches maximum intensity at three magnitudes below maximum. These four systems account for almost all the absorption features. To each absorption system corresponds an emission system. All absorptions and corresponding emissions form the characteristic P Cygni profiles typical of expanding envelopes. When the nova has weakened by four magnitudes another emission system appears, the *NEBULAR spectrum*, which is completely developed when the nova is seven magnitudes below maximum. At first, it is a typical nebular spectrum, characterized by forbidden lines of

N I, O I, N II, O II, O III and later on, in some cases, by coronal lines (i.e., with ionization states higher than Fe VII, IP = 125 eV).

Infrared observations of novae give information on regions much cooler than those from which optical radiation originates. They have revealed the formation of *dust shells* at temperatures lower than about 1000 K and explained some characteristics of the outburst light curves of slow novae. Corresponding to the deep minimum in the light curve, one observes a rise in the infrared flux, indicating that a dust shell is formed which absorbs the optical radiation. When the deep minimum is absent the infrared excess is also absent and no dust shell is formed. Although few data are known for a reliable statistics, fast novae do not form an optically thick dust shell, and slow novae do, while intermediate novae form just a thin dust shell. However, the two known examples of extremely slow novae, HR Del and RR Pic, do not show the deep minimum in their light curve, which should give evidence for the formation of a dust shell.

The observations from astronomical satellites have permitted the observation of ultraviolet and X-ray emissions from novae. Some of these emissions originate from regions which are much hotter than those where the optical radiation is formed and are therefore complementary to the ground based observations.

The importance of ultraviolet observations can be understood if we consider that the bulk of the continuum radiation emitted by quiescent novae is found, with very few exceptions, in the ultraviolet. Estimates of temperature, luminosity, and mass-accretion rate in the disc and onto the white dwarf's surface, which are of fundamental importance for understanding the nova phenomenon, can be made only by means of ultraviolet observations.

For novae in outburst, observations of the ultraviolet continuum are essential for the determination of the *bolometric luminosity*. Moreover, it is well known that almost all the strong resonance lines of abundant ions fall in the ultraviolet. These lines provide information on the excitation processes, the regions of line formation, the presence of outflow phenomena, and on the intensity of the ionizing radiation field in the extreme ultraviolet, which is scarcely accessible because of the hydrogen interstellar absorption below 913 A.

The behavior of novae in the ultraviolet is described in two separate sections: quiescent novae and novae in outburst. This subdivision has a physical basis. In fact, observations of quiescent novae provide important information on the hot components, on their radiation field, and on those processes which occur near the compact component. Instead, observations made during outburst and the following decline phase give information on the physical structure of the extended pseudophotosphere and its chemical composition.

The ultraviolet continuum of quiescent novae can generally be reproduced reasonably well by a distribution $F(\lambda) \propto \lambda^{-\alpha}$, with $\alpha \approx 2$, which is not very different from the "standard" value $\alpha = 2.33$ found for the simple theoretical accretion-disc model computed by Lynden-Bell in 1969.

The few observations in the extreme ultraviolet (500-900 A) made with the Voyager indicate that models fitting the ultraviolet cannot be extrapolated to the extreme ultraviolet wavelength region.

Exceptions to the general trend for the ultraviolet continuum are GK Per whose continuum peaks toward 3600 A, instead of in the far UV like the other old novae, DQ Her, T Aur, and BT Mon, which show a very flat continuum, $\alpha \approx 0$.

The very important parameter $\dot{M}$ can be estimated from the accretion luminosity of the disc, $L(\text{disc}) = G\dot{M}M_1/2R_1$ where M_1 and R_1 are the mass and radius of the compact object. Values of the order of 10^{-8} $M_\odot$ /yr have been estimated, but the methods involve many uncertainties.

The line spectra of old novae are characterized by the presence of strong emission lines of multiionized atoms like N V, C IV, Si IV, He II, N IV, N III, C III, Si III. P Cygni profiles have been observed in a few cases, giving evidence of material outflowing a long time after outburst.

As in the optical range, we can conclude that spectra of novae in quiescence are substantially similar in the ultraviolet. The optical and ultraviolet behavior in outburst, on the contrary, cannot be placed into a common scheme, and each nova outburst has its own specific characteristics.

One important result obtained from ultraviolet observations of the nova outbursts is that the bolometric luminosity remains practically constant or declines much slower than the optical one, until the nebular stage starts. The rich ultraviolet line spectra have enabled a more accurate determination of the electron density and temperature of layers producing the lines, and therefore a more reliable determination of the chemical composition than was possible by the sole observation of the optical spectrum. A general excess of CNO in classical novae is confirmed. Moreover a new class of novae, the *neon novae*, has been discovered, characterized by the great intensity of the neon lines. Several considerations suggest that the enrichments in the ejecta are not a consequence of nuclear reactions in the nova envelope, but rather reflect the composition of the envelope at the onset of the *TNR*. *CNO* overabundances can be explained by TNR in a shell already enriched by these elements from the interior of a *CO white dwarf*. The enrichment in *Ne* would indicate that the ejected material was previously processed to Ne in what is now a very massive *O-Ne-Mg white dwarf*. Abundance determinations made for only four recurrent novae seem to indicate that the abundances in their ejecta, unlike the ejecta of classical novae, are substantially solar.

Accretion is also responsible for the X-ray radiation emitted by quiescent novae. They are generally low-luminosity X-ray sources. About ten of them have been detected with the satellite EINSTEIN with $L_x \approx 10^{31}$ -10^{32} erg/s. A few others have been detected with EXOSAT, which provided the first X-ray recording of a recurrent nova - RS Oph - in outburst.

The final decline of novae follows the dip in the light curve of slow novae and precedes the appearance of the envelope.

The time scale for the return to the pre-nova state is estimated to be of the order of several tens of years, although the nuclear-burning time scale is approximately 300 years. Hence the physical reason for the time scale of the return to the pre-nova state is not yet understood. For instance the spectrophotometric analysis of the slow nova FH Ser indicates that the turn-off occurs 200 days after outburst. Now turn-off requires fuel exhaustion, either by nuclear burning (which is not the case because of the much longer time scale than the observed one) or some sort of quenching of the nuclear reactions, or some mechanism of mass loss. The latter can be an optically thick wind, that is the expanding pseudophotosphere of the outbursting novae, or the loss of matter through the outer Lagrangian points of the system, as a result of dynamical friction during the common envelope phase.

When the nova has declined to the pre-outburst state, the remaining sign of the outburst is the surrounding expanding nebulosity. This nebulosity seems to be a relatively short-lived phenomenon, because no dwarf nova or nova-like star without a recorded outburst can be identified as a nova because of an observable shell. Nova shells have been observed for about 20 objects. In general they are elliptical and present condensations and rings.

The angular size of the nebula, the expansion radial velocity, and the time elapsed from the explosion enable the derivation of the *distance of the nova*, using the hypothesis that the expansion velocity has remained practically constant. However, images of the nova nebulae obtained at different epochs indicate noticeable decelerations with time of the order of 10

to 2 km/s per year. This braking must therefore be taken into account for a correct determination of the distance.

The *masses of the nova shells* are of the order of 10^{-5} to 10^{-4} solar masses.

Besides the possibility of estimating the distance and of measuring the masses, the spectra of nova shells allow one to determine the *chemical composition of the nebulae*, and therefore to verify if it is affected by the nuclear reactions occurring during the outburst. The emission-line spectra of the nebulae permit a more accurate determination of the abundances than in nova spectra, where absorption lines are blended with their emission components, or where the components of the various expanding shells are blended together, and where the conditions are very far from those of a stable atmosphere. Instead, at the time when the shells become spatially resolved, the density is so low that self-absorption and collisional de-excitation are negligible, and the distance between the shell and the stellar object plus the accretion disc make impossible any confusion with these regions having very different physical conditions. CNO abundances can be 10 to 100 times the solar value.

The possibility of studying the remnant of a very old nova has been offered by a nebulosity surrounding CK Vul 1670. Two faint nebulosities at about 5 arcsec from the central object, plus other fainter nebulosities, display spectra similar to those of nova ejecta. The intensity of [N II] 6548 is impressive and also those of [S II] 6716 and 6730 are remarkable. The luminosity of the central object is much lower than that of typical old novae and comparable to those of the faintest dwarf novae. This luminosity can be explained by a normal red dwarf and indicates the absence of any contribution from the white dwarf and the accretion disc. This may indicate that mass transfer has stopped in the system.

Radio observations at centimetre wavelengths have indicated radioemissions from HR Del 1967, V 1500 Cyg 1975, V 368 Sct 1970 and FH Ser 1970. The maximum radioemission was reached between 100 and 200 days from outburst for the very fast nova V 1500 Cyg and about 1000 days after outburst for the very slow nova HR Del. In no case radioemission was observable earlier than 50 days from outburst. The spectra were consistent with thermal radiation of an expanding envelope of ionized gas.

Observations of the old nova GK Per 1901 in about the same range of wavelengths have detected an extended radio source resembling the optical nebulosity in the vicinity of the nova. The spectrum indicates that the emission is clearly non thermal.

The only recurrent nova for which radio emission was detected is RS Oph. The observations began only 18 days after the 1985 outburst. The brightness temperature of about 10^7 K (against the value of about 10^4 observed for classical novae) indicates a non-thermal origin for the radiation.

Chapter 7 discusses models for classical and recurrent novae. It is observed that the behavior of novae may be divided into two separate stages: quiescence and outburst. However the two stages cannot be completely separated, because it is possible that the companion star and the accretion disc, which determine the behavior of novae at quiescence, may play a role during outburst, due to their interaction with the ejected shell or the "bloated dwarf" formed in the explosion. The same model should be able to explain the features observed in both stages.

Despite the variety of light–curve shapes and spectroscopic developments, there are similarities between different objects. Relations exist between the absolute magnitude at maximum and the t_3 time, or between the expansion velocity and the spectral type of the principal spectrum, or between the expansion velocity and the t_3 time. These relations indicate that underlying systematics exist in novae. Possible "hidden parameters" determining the absolute magnitude at maximum, the ejection

velocity, etc., are, for instance: The mass of the white dwarf and its chemical composition; the mass of accreted material and the accretion rate; the degree of mixing of the white-dwarf material into the accreted hydrogen-rich shell material; the orbital elements. Unfortunately the data derived from minimum observations are poor.

A brief history of old models, their search for the underlying cause and the possible mechanisms of mass ejection are described. Different *mechanisms of mass ejection* were investigated: *shock ejection, pressure ejection, radiation pressure,* and *pulsational mass loss.* It is now believed that the first three can act during various stages of the nova outburst. Shock ejection seems to predominate in fast and recurrent novae, and an optically thick stellar wind driven by radiation pressure seems important in slow novae.

Shock ejection: When energy is generated in a region in a time interval shorter than the sound travel time across that region a shock wave is generated at the bottom of the region and propagates outward. After the passage of the shock, the ejected material has a steep velocity gradient with speed increasing outward and decreasing with time. This is generally contrary to what is observed in classical novae, except, perhaps, for material of the premaximum absorption system.

Pressure ejection: If the energy is deposited in a region during a time interval longer than the sound travel time across that region, but shorter than the time interval of radiation diffusion, a "pressure" wave develops, which ejects all the material above the region with about the same velocity, which increases with time.

Radiation pressure by electron scattering is important in high luminosity stars.

Pulsational mass loss: Assuming thermally unstable H burning, a hot white dwarf becomes pulsationally unstable. The dissipation of pulsationally produced shock waves appeared to be a plausible means of surface heating; however, the calculations do not show how the nova envelope is ejected.

The observations indicate that the luminosity of all post-novae, at least shortly after outburst, are equal or larger than the critical Eddington luminosity,

$$L_{crit}=6.5\times10^{4}\ (M/M_{\odot})(L_{\odot}/1+X),$$

where X is the percentage hydrogen abundance, by mass, in the external shell of the nova. These observations have played an important role in developing modern models.

Simple models for explaining the observed light curves and spectral behavior during post maximum activity have been proposed. Five of these models are described. They are:

Instantaneous ejection I - All or nearly all the material is ejected in a time short compared with the duration of post optical maximum activity. The ejected material is in a fairly thin shell, whose thickness remains small.

Instantaneous ejection II - A thick envelope is ejected instantaneously. This envelope remains thick as different parts of it have different velocities.

Continued ejection A - Continued ejection models emphasize the importance of winds from the nova after optical maximum. Most of the emission of the continuous spectrum in the optical and ultraviolet comes from an optically thick wind (the quasi-photosphere or pseudo-photosphere).

Continued ejection B - A form of continued ejection is possible, where most of the luminosity comes from previously ejected material, ejected at a time when the mass-loss rate was very high. This model is very similar to Instantaneous ejection, type I, with an envelope of constant thickness.

Central star dominant models - Ejection is supposed to occur from one of the components of the central binary, which presents a general swelling, so that something resembling a nor-

mal, almost stationary, stellar photosphere is observed after optical maximum. In this case, the high-velocity, expanding layers, whose presence is indicated from the spectrum, must be optically thin in the continuum.

Each of these models have strong observational constraints. Instantaneous ejection, type II, and central-star-dominant models require that the lowest velocities are near the centre of the envelope. The predicted velocity distributions encounter observational objections.

Instantaneous ejection, type I, requires the continuum either to be formed in a thin shell or in a nova remnant. Blueshifted P Cygni absorption components should be very wide in the first case, and very narrow in the second one. Major difficulties are encountered by this model.

Continued ejection A also has strong constraints. The continuum brightness is directly related to the mass-loss rate.

It is shown that the most fruitful way of making progress is to combine a continued ejection A model with the presence of a thin shell. In many cases, at least, most radiation of the continuous spectrum is easily understood to be coming from an optically thick wind, while most line radiation seems to come from a shell.

In any case, spherically symmetrical models are probably too simple, and the observed deviations from spherical symmetry need to be taken into account.

The observed characteristics of recurrent novae, and especially those of T CrB and RS Oph, are rather different from those of classical novae. For instance, the expansion velocity of the absorption lines of T CrB and RS Oph decrease with time.

Interaction between the ejected shell and a pre-existing circumstellar envelope, either one formed in previous outbursts, and/or especially one due to the stellar wind from the red giant present in the system of T CrB and RS Oph, may be important for explaining the spectral characteristcs in the course of an outburst. The models proposed for T CrB and RS Oph cannot be applied to recurrent novae like T Pyx or U Sco, which apparently do not have a red giant companion. It is not clear to what extent models for classical novae can be applied to these recurrent novae.

An empirical approach for explaining, at least partially, the structure of novae is discussed. Models generally do not take into account the existence of stratification and complex motions suggested from the observations. For instance there is definite evidence that higher velocity material lies below that of lower velocity, and that the Orion system has higher ionization than the others systems, suggesting its origin in the inner parts of the envelope; but a quantitative study of line superpositions is still missing. Very high velocity absorption components (up to 10^4 km/s) have been detected in the far-ultraviolet of some novae. The highest velocity system of V 1370 Aql varied on a time scale of a few hours, suggesting line formation in the inner envelope.

Absorption components of the principal spectrum are always seen in classical novae. This means that deviations from spherical symmetry do not appear to be large enough to prevent the formation of the system in any direction. High velocity systems are also generally seen. Therefore limits are also placed on possible deviations from spherical symmetry for the high velocity systems.

The observations indicate that a large part of the continuum must be produced below the level where any strong absorption line is formed. Hence, when strong Orion N III absorption components are observed, at least a large part of the continuum must be produced in more inner regions. This is compatible with the model continued ejection A, or with central star dominant models. In these models most of the continuum is emitted by a quasi-photosphere formed by an optically thick wind, or by a nearly stationary photosphere, respectively.

However infrared radiation is not included because the outer parts of the envelope are expected to be much more optically thick in the infrared than in the optical, due to free-free and dust opacity. Color temperatures and radii can be found, which, when the continuous ejection model is assumed, can be converted to mass-loss rates.

Continuum magnitudes plotted against logarithm of time from maximum often have a linear portion, i.e. the radiation flux varies as a power of the time from maximum. The same behavior seems to occur for the radii derived from continuum magnitudes and Zanstra temperatures. An important observational datum is that the bolometric decline is much slower than the optical one. One more is that the total radiative and kinetic energy fluxes are of the same order. Yet another one is the correlation between the velocity of the Orion system and the brightness of the continuum.

The most attractive picture emerging from the observations seems to be one of wind acceleration by radiation pressure at large optical depths, where the total luminosity is above the Eddington limit. Part of this total luminosity is converted to kinetic energy. Such a process, if it exists, cannot be thermal.

The methods for the determination of the chemical composition, both from the absorption lines of the pre-maximum spectrum and the principal spectra, as well as from the nebular emission lines formed in nova ejecta, are discussed. These data are very important for checking the theories on the causes of nova outbursts. However, they are very uncertain and must be viewed with caution. Besides the excess of CNO, isotopic ratios have been derived for DQ Her by spectral synthesis. $^{12}C/^{13}C$ was found ≥ 1.5 and $^{14}N/^{15}N \geq 2$ (to be compared with the solar–system values of 89 and 273 respectively).

The infrared observations, unfortunately available for a relatively small number of objects, show the formation of a thick dust shell in some slow novae, as well as the absence of, or a very small infrared excess in, a fast nova like V1500 Cyg, and also evidence for a thin dust shell in a moderately fast nova like V1668 Cyg.

According to the very early model developed by Clayton and Wickramasinghe, dust grains can only condense from ejecta once the temperature of condensation is below 2000 K, and grains begin to grow and reach a maximum size of about 2 μm in a few days. Since the photospheric temperature of novae increases after outburst, the distance at which grains can form recedes from the nova. Dust formation thus depends on whether the ejecta can overtake the condensation distance. If so, grain formation is possible, otherwise the nova environment is always too hot. Moreover, as the ejecta disperse, their density declines, and unless grain formation is initiated at an early stage the amount of dust eventually formed is negligible.

Gallagher developed an idealized model by assuming that the condensation of grains is controlled by the radiation field of the nova, which radiates at constant luminosity. He derives a formula giving the number of days from outburst, t_d, necessary for grain formation, and the ionization time scale t_i of the ejecta. The ratio t_i/t_d is independent of the expansion velocity and depends only on the luminosity (which is related to the speed class) of the novae. For fast and very fast novae $t_i < t_d$, ionization starts before grains can condense and, therefore, the dust shell cannot be formed. In moderately slow and slow novae $t_d > t_i$, and the formula gives values of t_d in reasonable agreement with the observations of several objects. However HR Del, R Pic, and other very slow novae are not explained by this picture, because they form too little dust for their slow speed.

Later work has involved a more detailed study of the physics, but much more remains to be done before dust condensation is properly understood.

A very strong line in the infrared has been observed. This is the 12.8 μm [Ne II] emission in QU Vul. From the Ne III and Ne IV lines

which are simultaneously present in the ultraviolet, a high overabundance of Neon is derived. It is now believed that a new class of novae, the *Ne novae*, exist. They would be characterized by the presence in the system of a *O-Ne-Mg white dwarf*, with a large amount of white dwarf material mixed into the shell.

A brief description of models for the radio envelope is given. Hjellming et al. models of slower novae give lower velocities of ejecta, lower masses of the shell, and greater time elapsed from outburst, for the shell to become optically thin in the radio range.

Deviations from spherical symmetry are always encountered in the few old nova shells studied in detail. These non-spherical envelopes can be explained in different ways, such as magnetic guiding of material, non-radial stellar pulsations, interaction of the expanding nebula with the secondary component (this may result in blobs ejected perpendicular to the orbital plane), interaction of the expanding nebula with the accretion disc, effects of stellar rotation, gravitational braking and radiative acceleration, instabilities at the beginning of the expansion, stellar rotation by itself, etc.

The cause of nova outbursts accepted at present is accretion of hydrogen by the degenerate white-dwarf component of the binary from its non-degenerate companion. Then the hydrogen undergoes a thermonuclear runaway. The description of this theory is beyond the purpose of this book, which is devoted to the atmospheres. Here what is emphasized is the impact of the theory on the observable properties.

Hydrogen accreted by the white dwarf will tend to be ignited. The mass-accretion rate, the chemical compostion, and the white-dwarf luminosity all influence the mechanism which will give rise to an outburst. The calculations suggest that an overabundance of CNO is necessary for a fast nova outburst, i.e., mixing of CNO into the envelope from the interior occurs.

The observed overabundances of Ne and Mg observed in some novae are explained by nova outburst of O-Ne-Mg white dwarfs. These white dwarfts are expected to have masses close to the Chandrasekhar limit.

Accretion is not spherically symmetric and this lack of spherical symmetry should play a role in the development of a pre-nova. The consequences of this fact are discussed, but the situation is very complicated and much work needs to be done.

A few observations and statistical evidence suggest that *novae "hibernate"*; i.e., very old novae become very faint for thousands of years, and brighten again before the following thermonuclear runaway. *Hibernation models* suppose, as suggested by calculation, that the separation of the two components usually increases following a nova explosion. At first the secondary continues to transfer mass because it is strongly irradiated. Then mass transfer strongly decreases because the secondary underfills its Roche lobe allowing the previously accreted material to cool, diffuse, and become degenerate, so that a strong thermonuclear runaway is possible at a later time.

The separation of the binary is then reduced by magnetic braking and returns to its original value on a time of the order of a few thousands years. When the mass transfer is still relatively low, a dwarf nova outburst should be possible, so classical and dwarf novae would then belong to the same class of objects. In fact several old classical novae are known, which present post-outburst eruptions similar to those of dwarf novae.

The causes of recurrent-nova outbursts are discussed. Recurrent novae are, to a certain extent, intermediate between classical novae and dwarf novae, at least those (T Pyx and U Sco) which do not have a red giant in the system. The other three known recurrent novae (T CrB, RS Oph and V1017 Sgr) are more similar to symbiotic stars (actually V1017 Sgr is often classified as a symbiotic star rather than as a recurrent nova; however, it may in fact be a classical

nova which can also have dwarf-nova-type outbursts). One can see from the theory for classical novae, that a runaway can be produced for a relatively small amount of accreted mass for a white dwarf with a mass very close to the Chandrasekhar limit. Hence if the accretion rate is not supposed to change very much, much shorter recurrence times are possible than for classical novae.

As in the case of dwarf novae, recurrent novae can in principle also be produced by accretion events. A more relevant accretion-event mechanism for some recurrent novae involves a sudden instability of the cool component, with ejection of 10^{-3} to 10^{-4} solar masses. This mechanism can be relevant for T CrB and RS Oph, while a thermonuclear runaway in a massive white dwarf may explain T Pyx and U Sco. However, the situation is still very uncertain.

Chapter 8 describes in detail the behavior of several well studied objects belonging to different speed classes.

The very fast nova V1500 Cyg 1975 has been extensively studied in the optical and infrared. A few observations have been made in the UV with the photometric satellite ANS and with COPERNICUS. Thermal radio emission from the shell was detected about 50 days after outburst.

V603 Aql 1918 and CP Pup 1942 had the same fast decline, t_3 = 8 days. However their light curves were different, because V603 Aql presented oscillations in the transition stage, while CP Pup had a smooth, fast decline without disturbances.

V603 Aql is one of the old novae that has been extensively studied in the ultraviolet with the OAO-2 satellite and with the IUE. The nebular shell has practically disappeared, as indicated by the absence of sharp UV intercombination emission lines. The line variability has been studied during almost two complete cycles, and seems to be related to the orbital cycle.

Minima were observed in the light curve, but they are not periodic, and therefore they cannot be explained as due to eclipses. Humps were also observed repeating rather regularly. They give a photometric period about 10 minutes longer that the spectroscopic one:3h 28.8m against 3h 18.9m. Polarization measurements give a third shorter period of 2h 48m. CP Pup is the only old nova known to have an orbital period below the 2-3 hour period gap.

Soon after maximum, the spectrum showed the presence of chromospheric and coronal lines up to [Fe X] and [Fe XI], and of low excitation lines like O I, Fe II, etc.

The post-outburst apparent magnitude of CP Pup is about three magnitudes brighter than it was before outburst. The same situation occurs also for V1500 Cyg. This behavior is exceptional, because the luminosity of novae is generally about the same before and after outburst.

CP Pup in quiescence is a strong, variable, soft X-ray source, with a softer spectrum associated with a higher flux.

GK Per is an exceptional object. It is the old nova with the longest known orbital period of almost 2 days. During the transition stage, which started at 3.5 mag below maximum, strong light fluctuations suddenly appeared. The amplitude was 1 to 1.5 mag and the period varied from 3 to 5 days. This phenomenon lasted for more than 3 months. At each minimum, the spectrum was of the nebular type. At each maximum, the high-excitation lines and the forbidden lines were weaker, indicating a decrease of temperature and an increase of density in the line-emitting region. These oscillations, which are common for several novae, were, however, exceptional for two reasons. The first is that the time interval between successive light maxima varied with time in a sinusoidal fashion in which the period, amplitude, and mean value of this sinusoid increased with time. The second peculiarity is that the radial-velocity variations of the blue-shifted absorption components of the Orion spectrum were not correlated with the light oscillations

in the same way as for other novae. In some other novae, the observed, negative Orion velocities and the magnitudes during the oscillations are directly correlated. The same relation can be found for GK Per, but the negative maxima of the Orion velocities occur every two minima of the light fluctuations.

After the transition stage, GK Per settled down to a very slow decline and reached its minimum light several years later. The quiescent nova GK Per also presents several peculiarities. Besides the exceptionally long period, this old nova presents an outburst activity similar to that of certain dwarf novae. The duration of an optical outburst is 2-3 months and the amplitudes range from 1 to 3 mag. The observed recurrence times are variable, but all of them seem to be submultiples of 2400 days.

Another peculiarity of GK Per is that, unlike for other old novae, the spectrum of a K2 IV-V companion is observable at minimum. In spite of the presence of high-excitation emission lines, the UV contimuum is unusually flat and weak.

GK Per is a hard X-ray transient. Strong coherent modulation of the hard X-ray flux was observed with EXOSAT during a strong outburst in 1983, indicating that GK Per is a member of the "intermediate polar" subclass of cataclysmic variables.

Because of the availability of observations in the optical, extending over several decades, and of many recent observations in the infrared, ultraviolet, and X-ray wavelength ranges, models are discussed that attempt to explain the complex behavior of this old nova.

V1668 Cyg was the first nova whose development was followed completely, from premaximum to the nebular phase, in the ultraviolet with the IUE and in the infrared from the ground.

The ultraviolet spectrum enabled the derivation of the electron temperature and density of the ejecta and the CNO abundances, which are enhanced by a factor 30 relative to the solar value.

FH Ser was observed in the infrared and in the ultraviolet with the OAO-2. The most important result of these observations is that the total luminosity appeared to remain constant until day 200, while the optical luminosity had decreased by a factor of ten 53 days after visual maximum. Several other novae observed from the UV to the IR have shown a similar behavior, the total luminosity decreasing much more slowly than the optical luminosity alone. However no nova remained constant for such a long period of time as FH Ser.

DQ Her has been extensively studied during its whole outburst. The large number of line components present in its spectrum is an example of the complexity which can be found in a nova spectrum. It gives clear evidence of the interactions occurring between different shells, the faster, inner ones overtaking the slower, outer envelope. Chemical analysis of the ejecta indicate that carbon has an excess abundance relative to the solar value by a factor of 20, and nitrogen by a factor of 100, while the helium abundance is practically normal.

A peculiarity of the shell spectrum of DQ Her is that its electron temperature, as indicated by the sharp Balmer emission jump, is very low, being about 500 K, while, on the other hand, emission lines of C II and N II indicate an electron temperature of about 10^4. These data indicate that the shell contains a cold region and a hot region. A low density and an enhanced oxygen abundance can explain the low temperature. In fact, infrared fine-structure lines of carbon, nitrogen, and oxygen are very efficient coolants for low-density nebulae.

The quiescent nova is characterized by the presence of coherent oscillations with a 71 sec period. Its spectrum shows that the permitted lines of C II, C III, N II and He II, and the continuum are greatly weakened during the primary eclipse, while the Balmer lines and the forbidden lines of O II and O III do not change,

and are therefore formed in an extended envelope not affected by the eclipse.

T Aur is the oldest galactic nova for which a complete record of the outburst is available. It is very similar to DQ Her.

The nebula surrounding T Aur also shows regions of low temperature, which are not as low as for DQ Her; in fact $T_e < 3000$ K. The abundances of nitrogen and oxygen are in excess by factors of 60 and 25, respectively.

RR Pic, together with HR Del, is one of the slowest observed novae. The spectral type at maximum was F8, which is much later than that of fast novae (A0-A5), and the outflow velocities were relatively low, -100 up to -400 km/s for the principal spectrum. In the Orion stage, numerous lines of [Fe II], which are weak or absent in fast novae, were present. The remnant nebula has instead a spectrum similar to those of high excitation planetary nebulae showing prominent [Fe V] emissions. The excitation source is the UV radiation field of the hot component. Nitrogen is only moderately overabundant, by a factor of about ten.

The quiescent nova has an orbital period of about 3.5 hour, and presents a broad hump lasting more than half the period, always ending in a sudden dip.

The UV spectrum of RR Pic can be explained either by the superpositon of two black bodies or by a power law. Black-body temperatures range between 28,000 and 40,000 K, or between 14,000 and 90,000 K, or between 20,000 and 35,000 K, according to different authors, the lower value being attributed to the disk and the higher value to the boundary layer.

The UV variability rules out the possibility of an eclipse of the hot component, which was suggested by the dip in the optical light curve.

The very slow nova HR Del had an outburst light curve characterized by the presence of two maxima. The first one on December 12, 1967 at mag 3.4, and a second one during May 1969 at mag 4.3. High resolution spectra were taken during the whole development of the outburst.

This quiescent nova has a well determined period of 0.2141674 days, or slightly longer than 5 hours. No trace of the secondary is detectable. The amplitude of the radial velocity of He II 4686 is 104 km/s, and is only 34 km/s for H β. Several determinations of the chemical composition of the ejecta agree in obtaining a CNO excess.

Chapter 9 describes the characteristics of the five known recurrent novae. They are U Sco, T Pyx, and RS Oph, all having five observed outbursts, V1017 Sgr with three observed outbursts and T CrB with two observed outbursts.

This small group is very inhomogeneous; RS Oph, T CrB, and V1017 Sgr all have a cool giant in their system. The object V1017 Sgr presents characteristics similar to a symbiotic star, and its membership in the group of recurrent novae is doubtful. U Sco seems to have a solar-type main-sequence star in its system, while T Pyx does not show any evidence of a companion, and instead presents a very hot ultraviolet spectrum.

Observations of U Sco from the infrared to the ultraviolet made during the 1979 outburst show that the energy distribution remains constant. This behavior is different from that of classical novae, which show a shift to the ultraviolet with time after maximum.

The optical and ultraviolet line spectra indicate a strong excess of helium and an excess of nitrogen relative to carbon and oxygen. Classical novae present a slight excess of helium, but not such a large one as U Sco. No forbidden and coronal lines were present in its spectrum.

T Pyx is the recurrent nova with the hottest spectrum at minimum. The nebular spectrum is characterized by the presence of emission lines of low excitation like OI and very high excitation like [Fe XIV]. Although an exact determi-

nation of the abundances of the ejecta has not been made, there is no evidence of an excess of CNO.

RS Oph has been extensively observed. All its outbursts, as is also the case for T Pyx and T CrB, are very similar to each other. The very similar spectral evolution suggests that the outbursts give rise to a well regulated mechanism able to reproduce a sequence of several complex phenomena in all their details, and in the same chronological sequence. The nebular spectrum is characterized by the presence of several strong coronal emission lines.

Near-infrared colors observed between outbursts place RS Oph in the region of Mira variables according to the (J-K)-(H-K) two-color diagram, while it lies closer to the normal giant-supergiant sequence in the (J-K)-(K-L) diagram. Observations made with the IRAS satellite indicate an infrared excess, which can be explained by the presence of dust at 350 K, which is present also in quiescence. Radio emission was detected 18 days after the outburst of 1985, the brightness temperature being larger than 10^7. These are two important differences from classical novae. Radio emissions from the latter have never been observed earlier than 50 days from outburst, and their temperature is of the order of 10^4 K, typical of thermal emission from an ionized gas.

The "bolometric" light curve of the 1985 outburst was derived using observations from the infrared to the ultraviolet (X-ray observations made with the EXOSAT indicate that the contribution of the X-ray radiation to the total flux emitted on day 51 was between 0.5% and 10%, and that the radio contribution was always less than 1%). The bolometric light curve is very similar to those obtained for classical novae.

V 1017 Sgr is atypical because its three observed outbursts had very different amplitudes. The second one in 1919 had an amplitude of 8 magnitudes, while the first in 1901, and the third in 1973, had an amplitude of 4 magnitudes, typical of a symbiotic star rather than a nova. The quiescent line spectrum indicates a type G5 III, but presents also a strong violet continuum. No high-excitation lines and coronal lines are observable in the post-maximum spectrum.

T CrB is a double-lined spectroscopic binary with a period P = 227.5 days, containing an M3 giant and a hotter companion whose nature (white dwarf or main sequence star ?) has so far been rather elusive. The outburst light curve is similar to that of a classical nova, but the characteristics of the binary system and of the spectrum in outburst enable us to classify T CrB as a symbiotic star.

It is remarkable that the two observed outbursts occurred at nearly the same orbital phase. A characteristic which is not observed in classical fast novae was the presence of two maxima, the first one being at mag 2 on February 9, 1946 and a broad secondary one being at mag 8 between June and July. Exactly the same behavior was observed during the outburst of 1866.

The spectral variations of the outburst of 1946 have been extensively observed. They are notable because of the enormous initial expansion velocity of -4500 km/s. The first observation of the 1946 outburst was made on February 9, when the continuum masked the TiO bands of the M giant component. On February 12 the presence of coronal forbidden lines of [Fe X] and [Fe XIV] was observed. During the secondary maximum, the continuum increased again, veiling the TiO bands, and sharp absorption lines of ionized metals appeared. This behavior is similar to that observed in some symbiotic stars, rather than in fast novae or in slow novae at the moment of secondary maximum.

The quiescent spectrum of T CrB has been observed extensively, in order to derive the radial velocity curves of the giant and of the hot companion. Assuming that the Balmer emission lines are due to the hot member, a mass of 1.9 solar masses is found, which is higher than the Chandrasekhar limit for a white dwarf. On

the contrary, ultraviolet observations made with the IUE and extending over 10 years suggest the hot companion may be a white dwarf.

The UV continuum can be represented by a single power law $F(\lambda) \propto \lambda^{-\alpha}$ over the entire IUE range. However, α is variable and ranges in value from zero to unity. The flat spectrum corresponds to a minimum in the UV flux. When the flux is higher, the continuum is steeper. The UV continuum varies by a factor up to 10. No significant optical variation is observed correlated with those in the ultraviolet. Similarly, no correlation with the orbital phase has been found.

The emission lines are stronger than those usually observed in quiescent classical novae, and their variability is correlated with the continuum variations.

Absorption lines, mainly of once-ionized metals, are generally present in all the UV spectra of T CrB. This characteristic seems to be a typical signature of symbiotic stars during active phase. For instance, a similar absorption-line spectrum has been observed in the symbiotic star CH Cyg during both outbursts of 1967 ad of 1977.

The electron density and electron temperature of the line–emitting regions have been derived, using several permitted and intercombination lines. Values of 10^{10} -10^{11} cm^{-3} and 13,000 K, respectively, have been derived.

Accretion onto a compact object is a commonly accepted mechanism for explaining the observed UV luminosity. The mass accreted $\dot{M}$= 2RL/GM, where R and M both refer to the accreting object. Assuming for T CrB a distance of 1300 pc, the average integrated IUE luminosity, corrected for reddening, is 2.2 x 10^{35} erg/s. The energy radiated in the optical is negligible. This is an important indication in favor of a white-dwarf accretor. In fact, a main-sequence star is expected to emit mostly in the optical region. The presence of a strong He II 1640 emission also requires a temperature of 10^5 K, which is hardly compatible with a main-sequence star. Hence, the radial velocity measurements of the Balmer emissions, if attributable to the companion, would indicate a mass too large for a white dwarf. The UV observations, on the contrary, strongly suggest that the companion is a white dwarf. The problem of the radial velocity is therefore of critical importance. Balmer emission lines are broad and distorted by absorptions; moreover emissions are not necessarily associated with the orbital motio, of the companion. It is clear that no definite conclusion can be drawn about the nature of the companion on the basis of these radial–velocity measurements. A series of high resolution UV spectra should be obtained for deriving a reliable mass of the companion, a task which can be achieved only with the HST.

Chapter 10 summarizes the main results and the open problems on classical and recurrent novae, both from the observational and theoretical aspects.

Chapters 11 through 14 of Part III are devoted to an overview of the observations of symbiotic stars, to a description of the various models proposed for explaining the symbiotic phenomenon, and to a discussion of a few selected objects, respectively.

The term *Symbiotic stars* commonly denotes variable stars whose optical spectra simultaneously present *a cool generally M-giant absorption spectrum and emission lines of high ionization energy* such as He II 4686, [O III] lines, etc. *The variability light curve varies from object to object*, indicating that the physical mechanisms responsible for the symbiotic phenomenon have different weights and forms in different objects. In general, the light curves of symbiotic stars are characterized by rather large amplitudes (one to a few magnitudes), long time-scale variations (months to years and decades), sometimes with long periods of relative quiescence. The light curves of several symbiotic stars are described.

A small group of objects shows a light curve different from those characterizing the majority of symbiotics. They are called symbiotic

novae, because they have shown a single outburst, like classical novae, but with a smaller amplitude. Moreover, they stay at maximum for very long periods.

Besides the long-term variations, the light curves of symbiotics present irregular variations on day, and also, minute, time scales.

Some of them present periodic variability, and eclipses indicating that they are binary systems with periods of several hundreds of days. The optical spectrum is characterized by three main components: the cool stellar spectrum, the blue continuum excess, and the emission-line spectrum.

The infrared spectrum enables one to distinguish two classes of symbiotics: those with a strong infrared excess with respect to the energy distribution expected for a cool component, which is attributed to thermal dust emission (and for this reason this group is called *D-symbiotics*); those with a normal late-type spectrum (the *S-type symbiotics*).

The blue continuum is highly variable and especially strong during the outbursts. It mimics an A- or B-type stellar continuum, and at some phases of the outburst is covered by several absorption lines of once-ionized metallic atoms.

Permitted and forbidden emission lines which can be produced by neutral elements, and ions up to six-times ionized iron are observed. In some cases coronal lines have also been seen. The profiles are often complex, with several components and P Cyg absorptions indicating an expansion radial velocity of -100 to -300 km/s, hence much lower than those observed in the majority of novae, but comparable with those of the pre-maximum and principal spectra of slow novae.

Radial-velocity measurements indicate that several symbiotics are high velocity stars. Moreover, several objects present periodic radial-velocity variability, which may be related to the orbital motion of a binary system.

Attempts to detect magnetic fields and to measure intrinsic polarization in symbiotic stars have been made by several authors, but much more work must be done in these fields before obtaining conclusive results.

Observations made with the IRAS satellite have detected 34 S-type and 28 D-type symbiotics, and four of the latter ones have been detected also at 100 μm.

S-type stars are placed in a limited locus in the IRAS two-color diagram, close to that of cool giants, while the D-type stars are distributed in a large region that includes the loci of the Mira variables and the planetary nebulae. D-type stars exhibit large infrared variability, providing direct evidence for the presence of a Mira variable in the system.

The majority of the infrared observations have been made in quiescent phase. However, both Z And and AG Dra were also observed during outburst. Infrared photometry of these objects has shown that no large changes occurred in the infrared spectrum.

Simultaneous ultraviolet and infrared observations have shown that, while the ultraviolet flux largely decreased during minimum, the infrared flux remained almost the same. Hence, the source of infrared radiation is not affected by the outburst, and the infrared variability is a peculiarity of the cool component.

An extensive radio survey of 91 targets led to the discovery of only 9 sources. A clear correlation exists between the flux at 14.5 GHz and the dust emission at 10 μm.

Radio images of a few symbiotics have been obtained, and they have revealed a variety of structures, such as shells, halos, jets, and bipolar nebulae.

Radio emission from V 1016 Cyg had been resolved into two lobes separated by 0.10 arcsec, suggesting ejection of matter preferentially in polar directions. HM Sge shows a diffuse symmetric emission, or halo, with a size of

about 0.5 arcsec and a central bipolar structure extended 0.15 arcsec. AG Peg presents three separate structures: a spherical nebulosity, a compact core, and a jet structure 0.8 arcsec long. CH Cyg underwent a radio outburst (between April 1984 and May 1985 the radio flux increased by a factor of 35) followed by the appearance of ejecta. On November 8, 1984 two radio knots were discovered separated by 0.18 arcsec, and 75 days later the radio image evolved into a three-component structure with a total separation of 0.4 arcsec. These four objects have all suffered recent optical outbursts.

Several ultraviolet spectra of symbiotics have been observed with the IUE, and in many cases it was possible to have simultaneous or almost simultaneous observations in the optical range. These obserations have been very important for deciding on the reality of the supposed existence of a hot companion to the cool giant.

The near-ultraviolet spectrum has enabled an accurate determination of the interstellar reddening, by means of the depression at 2200 Å. Since interstellar extinction can strongly affect the energy distribution in the far-ultraviolet, these measurements are important for deriving a corrected energy distribution of the hot companion, which is responsible for the blue continuum and the high-excitation features that characterize the optical spectrum of symbiotic stars.

The far-ultraviolet continuum, after correction for interstellar extinction, presents in several cases a steep gradient approaching the Rayleigh-Jeans tail of a black body at a temperature of 40,000 K or higher, implying the presence of a hot object. However, no absorption lines characteristic of a hot photosphere have been detected so far.

The emission-line spectrum is characterized by a great number of emission lines belonging to a wide range of ionization energies. The long life of the IUE satellite had allowed astronomers to follow the activity and the development of outbursts of several symbiotics. Some of these phenomena will be described in detail in Chapter 13.

Several symbiotics present emission lines belonging to species with high ionization energies up to 100 eV. This fact suggests the existence of an efficient ionization process which could be associated with a high-temperature plasma. Hence it was expected that these objects should also be X-ray sources. Actually a few of them have been observed with the satellites EINSTEIN and EXOSAT, and the flux and its variability have been measured. Positive detections were obtained for RR Tel, V1016 Cyg, HM Sge, AG Dra, R Aqr, and CH Cyg.

A brief history of the models proposed for explaining the symbiotic phenomenon is given in Chapter 12. Models must be able to explain the composite spectrum and the light and the spectrum variability.

Two kinds of single-star models have been proposed: a hot star with a dense envelope, and a cool star with a hot envelope. The various problems associated with these models are discussed.

Binary models composed of a hot, compact object and of a red giant explain very naturally the presence of the blue UV continuum and the M-type spectrum, and also the evidence for eclipse in some objects. Accretion can play an important role in explaining the activity of symbiotics. Accretion can occur a) via a disk, following Roche-lobe overflow, by the same mechanism discussed for dwarf novae and quiescent novae or b) from the wind of the companion star. The latter is a much less efficient mechanism. However, it must operate in several symbiotic systems with a very long orbital period, where the red giant does not fill its Roche lobe.

A model considering the possibility that both components produce winds has been examined. Several observed spectral characteristics can be explained with this model.

Another possibility that the symbiotic phenomenon is due to increased solar-type activity of the cool stellar component can now probably be rejected.

In conclusion, several details of the observations can now be explained, by assuming the occurrence of accretion in interacting binaries, either from Roche-lobe overflow or from a wind.

A detailed discussion of several well observed objects is given in Chapter 13. Since the typical time scale of the symbiotic phenomena is up to many years, few objects have been observed extensively outside the optical range accessible from the ground. Fortunately a few symbiotic stars (Z And, AG Dra, CH Cyg, AX Per, and PU Vul) have undergone outbursts recently and have been observed with the IUE and simultaneously with optical and IR telescopes from the ground.

Z And has been considered the prototype of symbiotics. Its light curve has been observed since 1887 and has shown four major outbursts in 1895, 1914, 1939, and 1959. Two minor outbursts which occurred in 1984 and 1985 have been observed with the IUE.

The optical and ultraviolet spectrum in quiescence is rich in strong, narrow emission lines with a large range of ionization energy. The emission lines and the UV continuum vary quasi-periodically on a time scale of 760 days, while the IR spectrum does not show significant variations. The radial velocity of the M giant varies with a period of 750 days, giving evidence of binarity, but the light variations and the radial-velocity curve do not have the relative phasing expected from eclipse or reflection effects.

The active phase is characterized by light increase of 1 - 2 visual magnitudes. The outburst is followed by a sequence of maxima and minima resembling a damped oscillator. The optical spectrum undergoes large changes. During activity the TiO bands are veiled by a blue continuum and almost disappear. The Balmer lines exhibit strong emission, and have absorption cores.

The rich line-emission spectrum of Z And (and of other cataclysmic variables) is a mean for diagnosing the physical conditions (electron density and temperature, ionizing radiation intensity, chemical composition) of the emitting regions. In Z And, the computed electron density is of order 10^{10} cm^{-3}, and the electron temperature of order 15,000 K. The chemical composition is similar to that of red giants.

The radiative power emitted in the ultraviolet is not a small proportion of the visual-infrared power. This rules out the model of an active cool star. The double maximum in the energy distribution strongly suggests binarity. If the mass of the cool component is a few solar masses, and one assumes for the companion the mass of a white dwarf, the cool star is well inside its Roche lobe. If, on the contrary, the cool component of Z And is a bright giant, as suggested by infrared observations, it will probably fill the Roche lobe. If it is a detached system, the stellar wind will then play an important role.

AG Dra is a high-velocity and high-galactic-latitude symbiotic, indicating its membership in population II objects. Its cool component is a K-type giant, instead of an M giant like in most other symbiotic stars. The light curve has been observed since 1890, eleven outbursts being observed between 1890 and 1966. In 1980, it presented another outburst, and three minor maxima were observed in 1982, 1985 and 1986. From this point of view, AG Dra is similar to Z And.

At minimum the spectrum presents the characteristic absorption lines of an early K-type star of luminosity class III. During outburst the spectrum is veiled by the blue continuum. The emission-line spectrum shows strong lines from H I, He I, He II, O III, and Fe II up to [Fe V] and [Fe VI]. In the UV, the resonance lines of N V, C IV and the He II 1640 line are present.

The near-UV continuum is flat, while the far-UV continuum rises toward short wavelengths, and is close to the Rayleigh-Jeans tail of the energy curve of a hot object.

The large outburst of November 1980 was observed in all the spectral regions from ultraviolet to infrared, and was characterized by an increasing amplitude of variation from the near-infrared to the shorter wavelengths.

In April 1980, when the star was at minimum, an intense X-ray flux was detected with the HEAO-2 satellite. Observations made with the EXOSAT during the minor outbursts of 1985 and 1986 also gave positive results. IR observations made before and after the outburst showed only small variations.

The observations clearly indicate that AG Dra is a halo object which is binary. The cool component is a giant that does not fill its Roche lobe. Its hot companion is not a normal star, since no absorption lines were observed in the hot continuum. Its temperature is estimated to be of the order of 100,000 K or more.

A small group of stars that have revealed just one observed outburst whose amplitude was lower than that of a typical nova, but which in other ways have behaved like very slow novae, are called symbiotic novae. They are AG Peg, RR Tel, V1016 Cyg, V1329 Cyg, HM Sge, PU Vul, RT Ser.

AG Peg is distinguished in this group, because of its prominent M-type spectrum. The other are D-type symbiotics.

RR Tel was observed in 1949, three years after outburst, when it showed a strong continuum with many absorption lines of singly ionized metals. By the end of 1949 the continuum became weaker and emission wings became important. The mean ionization level was increasing steadily. Observations made in 1978 with the IUE showed a spectrum with very numerous and strong emission lines with a wide range of ionization from neutral species to five-times ionized calcium.

V 1329 Cyg, RR Tel, and V1016 Cyg have shown pre-outburst spectra of type M. PU Vul also had shown an M-giant spectrum during the deep minimum of 1980, and AG Peg and RT Ser showed it after decline from maximum. In V1016 Cyg and HM Sge, which have not yet declined, the M-type spectrum in the visible is masked by the strong continuum and line emissions, but the near-infrared spectra present Mira-type light variations.

The spectra at maximum of RT Ser, RR Tel, and PU Vul displayed a spectral type very similar to that of A-F supergiants, like classical novae but without the highly violet-displaced absorptions. These absorption spectra have not been observed in the other symbiotic novae. However, it is possible that the absorption-spectrum phase was missed. Symbiotic novae after outburst exhibit a very rich emission-line spectrum like novae. Unlike novae, however, they have emission-line profiles that are narrow, indicating a low expansion velocity.

Radio observations of symbiotic novae have been made for several years after outburst. In general, the radio spectrum indicates that the emitting region is optically thick, i.e., that the H II expanding envelope was still dense several years after outburst. The main properties of the symbiotic novae suggest that they should represent an intermediate case between the typical symbiotics like Z And, which present several outbursts, and the classical novae. Several possible mechanisms of the outburst are discussed.

Two other symbiotic stars are decribed, which have the common characteristic of having developed an optical and a radio jet. They are R Aqr and CH Cyg.

R Aqr has a typical symbiotic spectrum characterized in the visual by many emission lines and a late M III component. It is also a typical Mira variable with a period of 387 days, and it is at the center of a planetary nebula. The nebula is composed of two separate shells expanding at a velocity of 30-50 km/s. These shells should have been ejected from the cen-

tral object 185 and 640 years ago. A jet-like feature was detected in 1977 and observed again in 1980 and 1982, but was absent in 1970. High-spatial-resolution radio observations have identified five radio sources. The radio jet is cospatial with the optical jet.

The ultraviolet spectrum, has been studied since 1979, and has revealed the presence of moderate-excitation emission lines. Lines of N V and He II are weak. These lines greatly increased in intensity in the jet in 1982. This intensification could be related to the first detection of X-ray from R Aqr.

In spite of the large amount of observational data available on R Aqr, it is difficult to find a model describing them consistently. CH Cyg is the other symbiotic star which has presented an optical and radio jet at the end of its last outburst.

For several years, CH Cyg was considered a normal M6 III semiregular variable. The first outburst observed in 1963 revealed the characteristics of symbiotic star. However, it was considered a rather anomalous symbiotic because its spectrum did not show a large range of ionization energies, but only low-ionization emission lines. A second outburst which commenced in 1967, was over at the end of 1970 and confirmed that CH Cyg was a low excitation symbiotic star. A blue continuum veiled the M6 spectrum during the outburst, and several P Cyg profiles of once-ionized metals were absorbing the blue continuum. Expansion velocities of -100 km/s were observed. In quiescence, the M6 III spectrum shows a weak Hα emission. The third outburst started in 1977 and was almost over in 1987. It was followed both from the ground in the optical range and in the ultraviolet with the IUE. Infrared observations, both from the ground and with the IRAS, were made at different epochs and agree very well. X-ray and radio observations were made during the decline phase of the outburst. During the outburst of 1977 the absorption lines of once-ionized metals presented inverse P Cygni profiles, the opposite of what was observed in 1967. Only the H and K lines of Ca II presented P Cygni profiles during both outburst episodes.

The radial velocities of the M6 giant show a variability with a period of about 15 years, suggesting that it may be due to orbital motion. However, the dispersion around the average curve is large because of intrinsic irregular variations due to atmospheric motions in the atmosphere of the red giant. There are also some indications that the Fe II emission lines and the absorption cores of the once ionized metallic ions, both observable only during the outbursts, have radial velocities 180° out of phase with the M6 absorption lines.

The ultraviolet spectrum was characterized by absorption lines of once-ionized metals, and of the C IV and Si IV resonance lines and a few low-excitation emissions, as well as a flat continuum. In January, 1985 the spectrum changed completely, becoming dominated by strong emissions of Lyα, N V, C IV, Si IV, Fe III, and Fe II. The continuum at the end of the outburst is much fainter, but there is some indication of an increase of the flux toward wavelengths shorter than 1300 Å, suggesting that we are observing the Rayleigh-Jeans tail of a faint hot body.

High-spatial-resolution radio observations made between April, 1984 and May, 1985 have indicated that CH Cyg underwent a strong radio outburst coincident with the appearance of a multi-component jet expanding at a rate of 1.1 arcsec/year. The onset of the radio outburst coincided with a drop in visual light observed in July, 1984. The expansion velocity was of the order of 2500 km/s, of the same order as that indicated by the full widths of the Lyα emission and the Balmer lines at the same epoch, a velocity exceptionally high for a symbiotic star and comparable to those observed in novae. The jet was observed also in the light of [O III] at 5007 Å in September, 1986 and in the ultraviolet with the IUE in November, 1987. Attempts to observe it again with IUE in May, 1988 gave negative results.

CH Cygni was detected with EXOSAT in May, 1985. Previous attempts to measure its X-

ray flux with EINSTEIN were negative.

This long series of observations of CH Cyg suggest that it is a binary system composed of an M6 giant and of a hot faint companion. If the orbital period is that suggested by the radial-velocity variations, of about 15 years, the red giant does not fill its Roche lobe, and hence accretion must occur from the wind of the giant. An optically thick accretion disk must be formed during the outburst, giving rise to the blue and ultraviolet continuum and to the absorption lines, simulating an early type supergiant. At the end of the outburst, the disk becomes optically thin, the continuum becomes very faint, and the emission lines dominate the spectrum. It is then possible to receive X-ray emission from the internal boundary layer and to detect the Rayleigh-Jeans tail of the flux emitted by the hot faint companion.

Chapter 14 summarizes the main points concerning the symbiotic phenomenon.

There is strong evidence that most, if not all, symbiotic stars are interacting binary systems. The mass loser is a cool giant; the mass gainer should be a white dwarf, or in some cases a main-sequence star. Accretion may occur either from Roche-lobe overflow or from the wind of the cool component.

The last chapter numbered Chapter 15 - Perspectives and Unsolved Problems - briefly examines the many unsolved problems posed by the observations of the different classes of cataclysmic variables and symbiotic stars. Great progress has been made, especially by exploiting the possibility of observing the same object simultaneously from space and from the ground, covering a very large spectral range. Some constraints to the theories for these objects have thus been obtained. However, new questions have been posed, requiring new observations and new theories.

Our main conclusion is that, for a better understanding of the various classes of cataclysmic variables, we need observations of a few selected objects, extending over very long periods of time and over as broad a spectral range as possible, using all available techniques (photometry, spectroscopy, imaging), rather than a further accumulation of scattered pieces of observations for a very large number of objects. Only in this way can we hope to set constraints on the theories and to make further theoretical computations feasible and relevant.

1

INTRODUCTION

M. Hack and C. la Dous

I. NOMENCLATURE AND CLASSIFICATION

Following the current astronomical terminology, in this book the term "Cataclysmic Variables" shall comprise classical novae, recurrent novae, dwarf novae, nova-like stars, and symbiotic stars. For most objects, their classification as a cataclysmic variable (or not) and as one of these subtypes is quite clear and well agreed upon. However there are other objects, such as, for instance, RR Tel and T CrB (novae or symbiotic stars?), WZ Sge (nova or dwarf nova?), and V1017 Sgr (recurrent nova or symbiotic star?), which are referred to as symbiotic stars by some authors, as recurrent novae by others, and as novae by still others. The reason for this confusing situation is that, as will be seen later, it is often very difficult, and to some extent arbitrary, to define classes in an unambiguous way and to clearly distinguish one from the other. For some objects even the "general agreement" about their classification has changed over the years. Although the classification scheme currently in common use clearly is not ideal (concerning the distinction between various sub-classes in particular), we have nevertheless decided to adopt it, lacking a better alternative. Our hope is, however, to provide suggestions and ideas for a new, more physical scheme by stressing similarities and differences between various objects and classes.

The term "cataclysmic variables" is derived from the Greek word kataklysmos (*καταχλυσμός* which means flood, storm), and has been chosen because all of these stars (with the exception of nova-like variables, which were introduced into the class of cataclysmic variables long after the term was adopted) are characterized by sudden increases in luminosity of several magnitudes and by simultaneous appreciable spectral variations. In most cases, these abrupt changes are recognized to be accompanied by mass flow, either mass leaving the objects or, if the object is a binary, possibly only mass transfer between the components. The term "symbiotic stars," by which we now refer to only a sub-class of cataclysmic variables, was introduced by Merrill (1941), originally as an equivalent alternative to "cataclysmic variables." The term symbiotic was adopted in analogy to its use in biology, since these stars show a "combination spectrum" with characteristics of different spectral classes. Now the name is used for objects which are characterized by a late giant spectrum which at some irregular epochs is associated with a blue continuum veiling the absorption lines of the giant and several permitted and forbidden emission lines, often of high excitation.

Since the members of all these classes of stars, symbiotic stars, novae and recurrent novae, dwarf novae and nova-like stars, bear

a wealth of similarities in their observational properties, they all shall be presented and discussed together in this volume.

We stress that there is one major difference between the objects discussed in this volume and the stars studied in the previous volumes of this series. In those earlier volumes, "peculiar stars" were compared to "normal stars" of the same spectral type. In this volume, on the contrary, all the stars considered have been recognized, since their discovery, to be "not normal," that is, to be out of the classical criteria of stellar classification. As already discussed in the previous volumes, especially when observations of *normal stars* from space (in the ultraviolet and X-ray spectral ranges) were added to observations made from the ground, it was clear that phenomena not predicted by the then existing theoretical models based on thermal, closed-system, linear thermodynamics, do occur in their atmospheres. The phenomena contradicting these theoretical models are, for instance, the P Cygni profiles of the UV resonance lines from highly ionized atoms, the X-ray fluxes detected in many stars belonging to different stellar classes, and large radio and IR fluxes. The nature of the physical processes causing these phenomena is still a matter of investigation, although many theoretical models have been so far proposed. The observed large difference in the UV and X-ray spectra among different stars should be ascribed to the variable amplitude and character of these nonthermal processes. It is therefore reasonable to assume that in the cataclysmic variables these processes are present with a much larger amplitude. Hence, instead of considering these objects as small classes of peculiar stars, we could use them as a basis for research on the physical processes of mass outflow, heating of the outer atmospheric layers, mass accretion, etc., for a much larger group of objects.

II. THE BIG PICTURE AND THE PLAN OF THIS BOOK

The purpose of this book is:

- To review what is known from observations about cataclysmic variables and related objects
- To look for similarities and differences in spectrum and light variability of the individual members of the various classes, with the aim to gain some insight into their physical properties
- To compare the observations with the predictions of the suggested models
- To determine observational constraints on the models

All cataclysmic variables and related objects are strongly variable both in the line as well as in the continuous spectrum in a very complicated way. Thus, in order to obtain a complete picture about them, ideally each object should be observed simultaneously both spectroscopically and photometrically in all spectral ranges for several years. But clearly this is practically impossible. Moreover the majority of these objects are faint. Hence the available data are very fragmentary, and reasonably complete patterns of activity are known only for a few relatively bright stars, while for the large majority the available material is very scanty. A valuable contribution comes from those amateur astronomers who have observed variable stars over long periods of time, hence providing information on long period phenomena.

Theoretically, even the "big picture" still is very controversial for symbiotic stars, while in the case of the other cataclysmic variables the gross physical properties seem to be fairly well understood. However, a lot of detailed work remains to be done. In brief, cataclysmic variables in a narrower sense (novae, recurrent novae, dwarf novae and nova-like stars) are now generally understood to be binary systems

in a very advanced stage of evolution; a Roche lobe-filling main sequence star or giant, via an accretion disc, transfers matter onto a white dwarf or, in a few cases onto a main sequence star (Roche model; this model will be described and discussed in further detail in Chapter 4). The evidence for binarity and mass exchange is not so clear for symbiotic stars but increases with the increasing number of observations, and especially ultraviolet observations give fairly good evidence for binarity for them, too.

Concerning the origin of outburst activity, it is now believed that the outbursts of classical novae are caused by a thermonuclear runaway of the material accreted onto the white dwarf, while those of dwarf novae are caused by a brightening of the disc as a whole due to an instability in the disc itself, or, alternatively, due to enhanced mass flow from the secondary star. It is not clear what is the origin of the outburst in symbiotic stars, in particular not in those where the red giant obviously does not fill its Roche lobe. It also is not clear whether the outbursts of recurrent novae have the same origin as those of classical novae or if they rather resemble symbiotic stars.

One major characteristic (and problem) of the objects we are dealing with is their individuality, in that the photometric and spectroscopic behavior of any single nova, symbiotic star, dwarf nova, etc. is substantially different from that of any other member of that same category. It is therefore very difficult, if not impossible, to give a comprehensive description of the behavior of each category as a whole. Alternatively, each individual object can be studied in great detail, investigating observations in all available wavelength ranges, and spanning as long a time interval as possible; then a synopsis of several such investigations of different objects will yield some idea of what might be typical characteristics of one class, and what physical mechanisms might underlie the observed differences between its members. Depending on what approach seemed most illuminating, and depending on the availability of information in the literature, we are going to pursue both approaches for various aspects of these stars.

The book is divided into three major sections dealing with dwarf novae and nova-like stars, with novae and recurrent novae, and with symbiotic stars, respectively. Each section will start out with a presentation of plain observational data, free from models and interpretations, with characteristics of various brightness stages and appearances well distinguished. In each of the cases this will be followed by an introduction of currently available theoretical models and their critical confrontation with the observations. In the sections on novae and recurrent novae and on symbiotic stars, a presentation and interpretation of some well studied systems will follow, something which seemed inappropriate for dwarf novae and nova-like stars, given the state of research in this field which tends to focus on the entire group rather than on individual objects. Each section will be concluded with a summary of the current knowledge in that area. A final part will discuss critically the existing models and their adequacy or inadequacy to describe the observations, and will try to indicate the directions of future work, necessary for a better understanding of the phenomenon of cataclysmic variables.

III. GENERAL PHYSICAL PROPERTIES OF CATACLYSMIC VARIABLES

Cataclysmic variables have spectra which show high excitation emission lines and a hot continuum dominating the blue and ultraviolet region, often in combination with a late-type absorption spectrum and a low-temperature continuum which dominates the red and infrared regions. Furthermore, the hot spectral components in particular, often exhibit irregular light variability. The similarity of the various classes is restricted to just these very general properties; when seen in more detail, the objects contained in each class are physically very different.

Different ranges of the electromagnetic spectrum give information on different regions of the object. The X-ray observations are thought to reflect the hot regions where interaction occurs between the accretion disc and the primary star; ultraviolet radiation is emitted mostly by the accretion disc; the optical range gives information about the outer cool disc and about the "photosphere" of the nova envelope and on the secondary star; the infrared spectrum provides information again on the secondary companion and on a possibly present envelope of dust and ionized gas; and finally the radio radiation is due to the outer ionized gas and/or jets (if present).

In all cataclysmic variables, except possibly the symbiotic stars, the primaries are white dwarfs. For novae there is evidence that the secondary star is a red dwarf or subgiant. Among recurrent novae, the best known, T CrB, contains a red giant and has an orbital period of 227.6 days. In two other cases of recurrent novae, RS Oph and V1017 Sgr, the companion is probably a giant too, while in the case of U Sco it seems more probable that the companion is a dwarf. Too few recurrent novae are known to decide whether they represent a class which is significantly different from classical novae, or whether all novae undergo outbursts on time scales longer than historical time scales. In almost all known dwarf nova and nova-like systems the secondary is a red dwarf.

The absolute magnitude of dwarf nova systems at minimum, on the order of 8 mag, is much brighter than that of a white dwarf (M>10mag). The current picture is that in dwarf novae and nova-like stars, as well as in novae and recurrent novae during the quiescent state, the accretion disc is probably the main source of radiation. By definition, nova-like variables are objects which display photometric and spectroscopic characteristics similar to some outburst states of dwarf novae. Their absolute magnitude is of the same order as that of dwarf novae during outburst, M $\simeq$4-5.

Statistically the system parameters (like masses of the components, orbital periods, etc.) all are of about the same value for novae, dwarf novae and nova-like stars (see below, Section V). Furthermore, several quiescent novae exhibit characteristics very similar to those of quiescent dwarf novae. Hence it might be possible that dwarf novae evolve into nova-like stars (or vice-versa) and eventually may undergo nova explosions, and thus we actually may be observing the same systems at various stages of evolution (see also Chapter 4.V.F).

The group of symbiotic systems consists of stars whose spectra present characteristics of a late-type giant, generally TiO absorption bands plus a red and infrared continuum, and permitted and forbidden emission lines from various excitation levels, ranging from H I, O I, He I, He II to forbidden lines of [Fe VII], or in some cases even [Fe X]. The spectra of several symbiotic stars and those of the recurrent nova T CrB and of the very slow nova RR Tel show similar characteristics, and it appears somewhat arbitrary to include them in different groups. Thus, these novae, like T CrB and RR Tel and others with similar characteristics, are sometimes referred to as "symbiotic novae."

Often the group of BQ [ ] stars is included in symbiotic stars. The term BQ was introduced by Wackerling (1970) and indicates B-type stars which exhibit a shell spectrum. When also forbidden lines are present, the symbol [ ] is added to the name. We will not consider here this class of stars which is rather related to Be stars. However objects like, for instance, Z And, classified as symbiotic star, have many similarities with Be stars.

The main properties justifying the division of stars into the mentioned groups are summarized in Table 1-1 which distinguishes between characteristics of quiescent and outbursting objects. Under quiescent properties are considered the absolute magnitude at minimum light, the quiescent spectrum before and after

Table 1-1.

a) Intrinsic Stellar Characteristics

	N	RN	DN	NL	SS
M_v at min. light	~ 4	~ 0–1	$\sim$7–10	~ 5	~ 0
Spectrum in quiescence (*)	Hot Sd	M	dM+emissions	dM+emissions	M III
Percentage of proven binaries (**)	$\sim$10%	$\sim$100%	$\sim$ 20%	$\sim$100%	$\sim$ 50%
Masses ($M_\odot$ = 1) M_1 (WD)	~ 1		$\sim$ 0.5–1.4	$\sim$ 1–1.4	
M_2	~ 1		~ 1	$\lesssim 1$	

*) No appreciable differences between the spectra observed long time before and after outburst. For more details see chs 2,6,11.

**) The orbital period is known or in the case of SS – the RV curve or the light curve or both, strongly suggest binarity. However the general characteristics and similarity with the "proven binaries" suggest that $\sim$100% of these objects are binaries.

b) Characteristics of the outburst

	N	RN	DN	NL	SS
Ejecta	Multiple	Multiple or single	–	–	Single (sometimes multiple)
Expansion Velocity (Km s^{-1})	$\sim 10^3$	$\sim 10^3$	small (visual) up to 6×10^3 (UV)	–	$\sim 10^2$
Mass lost from the system per outburst ($M_\odot$ = 1)	$10^{-5} - 10^{-6}$	$10^{-6} - 10^{-7}$	$10^{-11} - 10^{-12}$		10^{-8}
Mass transferred from the secondary to the hot companion ($M_\odot$ =1)	It is estimated to range between 10^{-7} and 10^{-11} being positively correlated with the length of the orbital period (Patterson, 1984).				
Radiative energy emitted during an outburst (erg)	$10^{44} - 10^{45}$	$10^{43} - 10^{44}$	$10^{38} - 10^{39}$	–	$\sim 10^{43} - 10^{44}$
Mechanical energy per outburst (erg)	$10^{43} - 10^{44}$	$10^{42} - 10^{43}$	10^{37}	–	$10^{39} - 10^{40}$
Δm	8 – 18	5 – 9	3 – 5	–	? – 4
Time interval between outbursts	?	20 – 50 years	10 – 100 d	–	500 – 1000 d
Duration of an outburst	months	months	days	–	months or years

outburst, the percentage of proven binaries, and the masses of the stellar components; outburst properties consider the number of shells formed during an explosion, their typical expansional velocity, the mass lost during the explosion, the radiative and mechanical energy emitted during the outburst, the typical amplitude of light variation, the typical time interval between outbursts and the duration of an outburst. Pre-outburst and post-outburst spectra are an efficient tool for deciding if an outburst has affected deeply the structure of the objects. Actually pre- and post-outburst spectra are generally undistinguishable.

These data are often incomplete and/or based on only a small number of individuals, and invariably their determination is very difficult (see Chapter 4.II.C). It is often claimed in the literature that all, or almost all, cataclysmic variables are binaries. Although the percentage of proven binaries is much lower than 100%, we shall see in the following chapters that actually there is strong evidence in favor of this statement, and that all the objects studied in sufficient detail so far have turned out to be binaries.

IV. SELECTION EFFECTS

It is estimated that our Galaxy contains something like 10^{11} stars; on any plate of, for instance, the *Palomar Sky Survey* some hundred thousand or more of them can be seen as tiny spots. Yet, only a tiny fraction of them have been "identified," i.e., recognized as being remarkable for one reason or another. Any sort of obvious variability clearly provokes interest, in particular, if it is either very violent or very frequent, because historically stars have been assumed to be invariable objects. Indeed in most of them relevant changes in appearance only occur on time-scales which are much longer than humanity's historical memory. So cataclysmic variables by their very nature are scientifically very interesting objects. But there are more selection effects at work.

Classical novae, having a large outburst amplitude of some 8 to 18 magnitudes, have for a given minimum brightness a much higher probability for detection than other cataclysmic variables of lesser amplitude variability. This advantage is somewhat compensated for by their flaring up only once during the recorded history of astronomical observations. Nevertheless, a bright state lasts for at least a couple of weeks. With the many amateur astronomers of the *American Association of Variable Star Observers*, the *Variable Star Section of the Royal Astronomical Society of New Zealand*, and similar organizations elsewhere in the world scanning the sky at almost every minute, we have reason to believe that at least for the past couple of decades our sample of novae reaching an apparent brightness of some 10 or 12 mag could be approximately complete. Only very few of them can be observed in detail later on when they are back to their minimum state; when a star is fainter than some 17 mag, its observation requires considerable effort. So, although of the order of 250 novae have actually been seen at outburst, only a few dozen of them can be observed comfortably in their quiescent state.

Dwarf nova outbursts are much less spectacular and the absolute brightness of dwarf novae at quiescence is even several magnitudes less than that of novae; but since dwarf novae seem to be more common cosmical objects, and thus on the average can be found closer to the Sun than novae, on the average they appear brighter. The *General Catalogue of Variable Stars* (Kukarkin et al, 1970-71; Kholopov et al, 1985-87) contains more than twice as many objects classified as dwarf novae than objects classified as novae (although some caution must be applied concerning the correctness of these classifications, the tendency seems significant). The short duration of a maximum might be made up for by its frequent occurrence. Those systems which in addition to being eruptive exhibit also other photometric variabilities like eclipses or humps (to be explained later) have an extra chance of being detected.

The brighter a system is the easier it can and will be observed extensively. In the Roche model, objects with long periods, high mass transfer rates, and large masses of the white dwarf, by having large, luminous accretion discs, have a higher detection probability than others; and they are particularly favored the more the system is seen pole-on, i.e., the better the entire disc is visible. Duerbeck (1984) determines a space density of known novae and dwarf novae apparently brighter than 11.5 mag of some 1-2 10^{-6} pc^{-3} in a sphere of 250 pc around the Sun. Assuming this value and the above selection effects due to system properties, and adopting what seem reasonable statistical system parameters, Ritter and Burkert (1986) derive an intrinsic space density of these systems of 2 10^{-4} pc^{-3} (for further details see Chapter 4.V.A). This means that only one out of 200 cataclysmic variables in the solar neighborhood has actually been identified as such.

Most of the nova-like variables are not strongly variable intrinsically. Many of them have been detected because they exhibit emission lines which a priori identify them as valuable objects for further scientific study. A dramatic increase in their number, though, occurred during the past decade when X-ray observations became possible, because some of the nova-like stars are strong X-ray sources.

There is another selection effect which must not be forgotten-that of fashion- which selects out of the almost infinite number of possible astronomical targets those actually observed. While this does not bear directly on the detection of objects, indirectly it does, since certain features, like certain kinds of variability, are looked for in a systematic way, thus increasing selectively the number of certain kinds of objects. And, last but not least, these fashionable aspects are related to the general tendency of allocation committees for telescope time to selectively favor certain kinds of research.

V. A STATISTICAL VIEW OF NOVAE, DWARF NOVAE AND NOVA-LIKE STARS

At first glance novae, dwarf novae, and nova-like stars all seem to be fairly different types of stars; at closer inspection they are surprisingly similar in a surprisingly large number of properties; and when looked at from a statistical point of view they turn out to be almost indistinguishable from each other. This latter view shall be taken for a moment before the emphasis will shift more towards differences between classes for the reminder of this book.

In Figure 1-1 the position in galactic coordinates of several novae, dwarf novae, and nova-like stars is displayed. Novae are obviously concentrated toward the galactic plane as well as toward the galactic center; but while dwarf novae also show a tendency to concentrate toward the galactic plane, they are frequently found at higher galactic latitudes, and their number only slightly increases toward the galactic center. Nova-like objects clearly follow the distribution of dwarf novae rather than that of novae. The implication is that on the average novae are to be found at much larger distances from the Sun than dwarf novae and nova-like stars. The fact that they only rarely can be found in the direction of the galactic anti-center and at high latitudes points to their lower space density than that of dwarf novae and nova-like stars at least in the solar neighborhood. Dwarf novae and nova-like stars, on the other hand, seem to be fairly immediate and frequent neighbors of ours, since only in that case is it to be expected that they are found essentially all over the sky, as they are, and, given their low apparent brightness, they must be intrinsically faint. Determinations of distances and absolute magnitudes of cataclysmic variables (e.g., Patterson, 1984; Warner 1986, 1987) confirm these findings. Actual galactic distributions and space densities of various sub-types of cataclysmic variables, however, are very

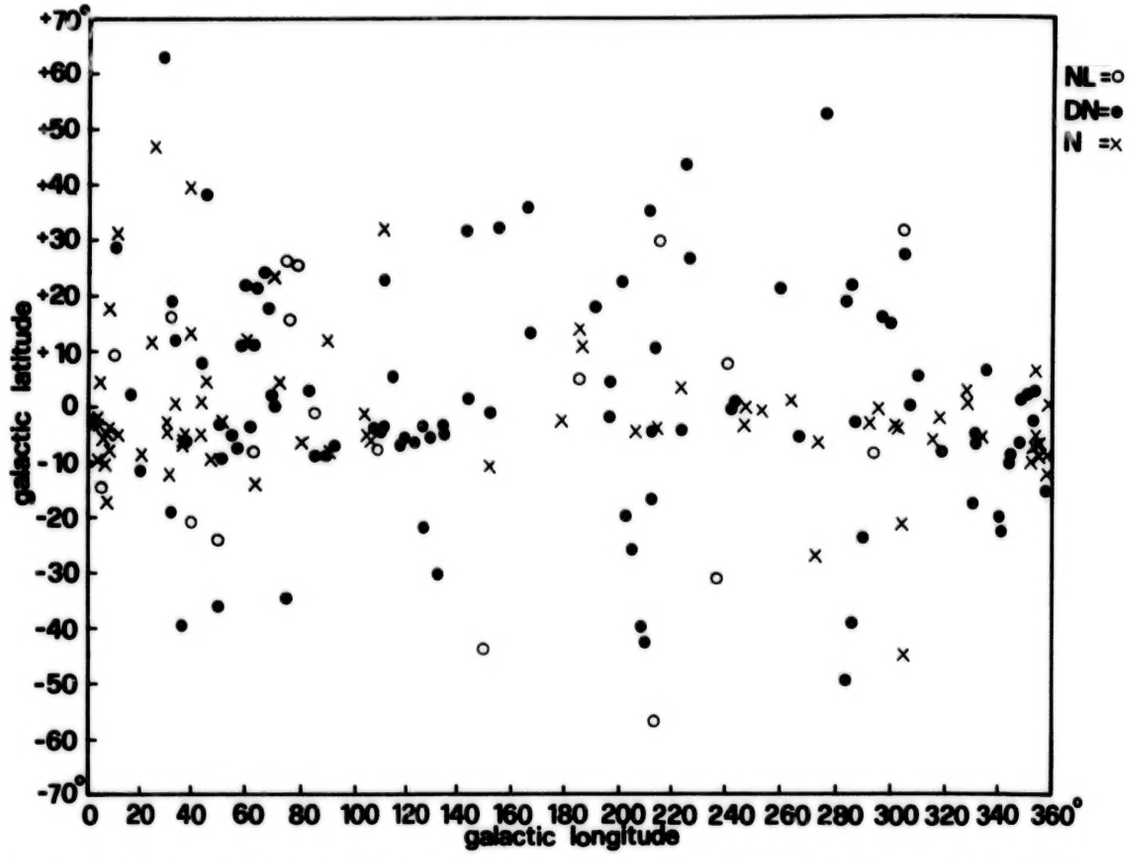


Figure 1-1. The positions in galactic coordinates, of novae (crosses), dwarf novae (full dots) and nova-like objects (open circles).

controversial issues, which will be discussed in further detail in Chapter 4.V.A.

Soon after the detection that some cataclysmic variables are spectroscopic binaries it was suggested that all of them may be binaries (e.g. Walker, 1954; Joy, 1954, 1956; Kraft, 1958). Since then it has turned out that almost all cataclysmic variables that have been subject to a thorough investigation did prove to actually be binaries. The only two exceptions, for which, in spite of distinct efforts, the binarity has not yet been proven, are EY Cyg and V1017 Sgr, both of which, however, have composite spectra consisting of a hot emission component and a cool absorption component*. Assuming the validity of the Roche model, it is to be expected that a small fraction of stars will be seen pole-on, in which case the binary motion would not be detected. Since all the brightest and thus the most easily observable cataclysmic variables have so far proved to be binaries, there is no contradiction to the assumption that all cataclysmic variables are binaries.

The orbital periods of all novae, dwarf novae, and nova-like stars contained in the *Catalogue of Cataclysmic Variables, Low Mass X-Ray Binaries, and Related Objects* (Ritter, 1987) are displayed in Figure 1-2. Some remarkable features become obvious. The most prominent one is the so-called period gap between roughly some 2 and 3 hours which is almost devoid of systems, whereas many objects can be found with both longer and shorter periods. Furthermore, all these cataclysmic

*There are many other cataclysmic variables for which no orbital period is yet known, but so far, once spectra or photometric data of a reasonable quality have been obtained, invariably they have turned out to be binaries except for those two just mentioned.

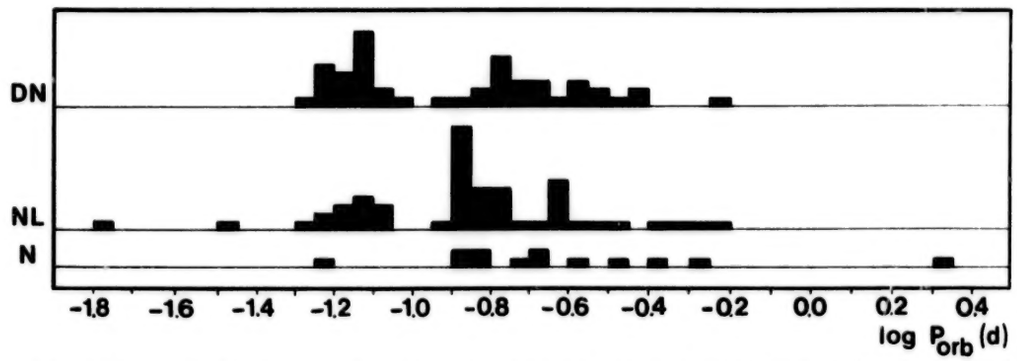


Figure 1-2. Orbital periods of novae, dwarf novae and nova-like stars (from Ritter, 1987). Note the "period gap" between about 2 and 3 hours.

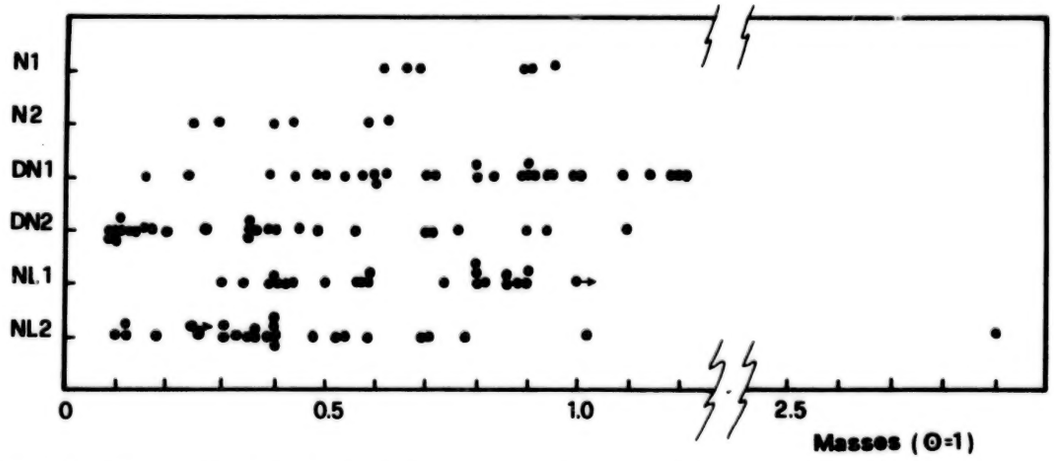


Figure 1-3. Masses of the white dwarfs (index 1) and secondary stars (index 2) of novae, dwarf novae and nova-like systems (from Ritter 1987).

variables, except for four systems which are also peculiar in other respects, have orbital periods in excess of 80 minutes, and, again with two peculiar exceptions, shorter than 15 hours; by far most systems have periods between 1.3 and 5 hours. When the same data are considered by object classes (without taking into account further differentiation of sub-classes; these will be dealt with in Chapter 2.I.C), statistically novae, dwarf novae and nova-like stars appear to have the same orbital periods. However, among novae, just one, CP Pup, has a period below the gap, and just one nova among all the cataclysmic variables, GK Per, has a period longer than 1 day.

When masses of the white dwarfs (primary components) are considered (Figure 1-3), the situation is approximately the same for dwarf novae and nova-like stars: most masses are found between 0.5 and 1.0 $M_\odot$ with masses between 0.3 and 1.5 $M_\odot$ well possible*. The white dwarf masses of all known novae are less than 1.0 $M_\odot$; however, given the small number of novae for which system parameters are available, and considering the inaccuracies in determining them, the significance of this result is rather low, i.e., the white dwarf masses of all these types of cataclysmic variables may be statistically identical.

Mass ratios between masses of the white dwarfs and the mass losing companions typically are found to be between 1 and 6 for all these three classes of cataclysmic variables (Figure

*As to the problem of determining reliable masses of cataclysmic variables, see Chapter 4.II.C.

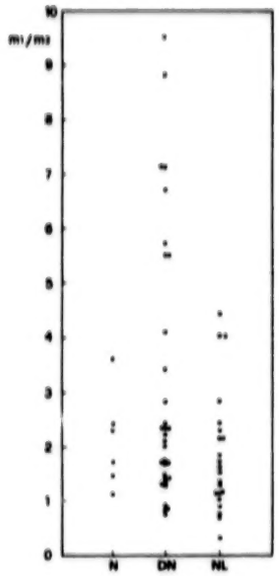


Figure 1-4. (Left) mass ratios of white dwarf (m_1) and secondary (m_2) components in novae, dwarf novae and nova-like systems (from Ritter, 1987).

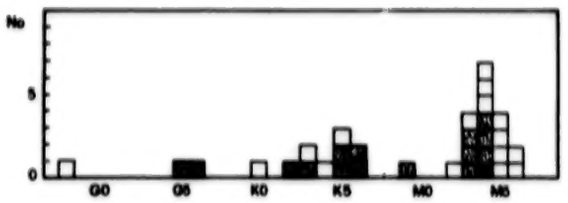


Figure 1-5. Spectral types of the secondary stars in novae (black squares), dwarf novae (dotted squares) and nova-like systems (white squares), from Ritter (1987).

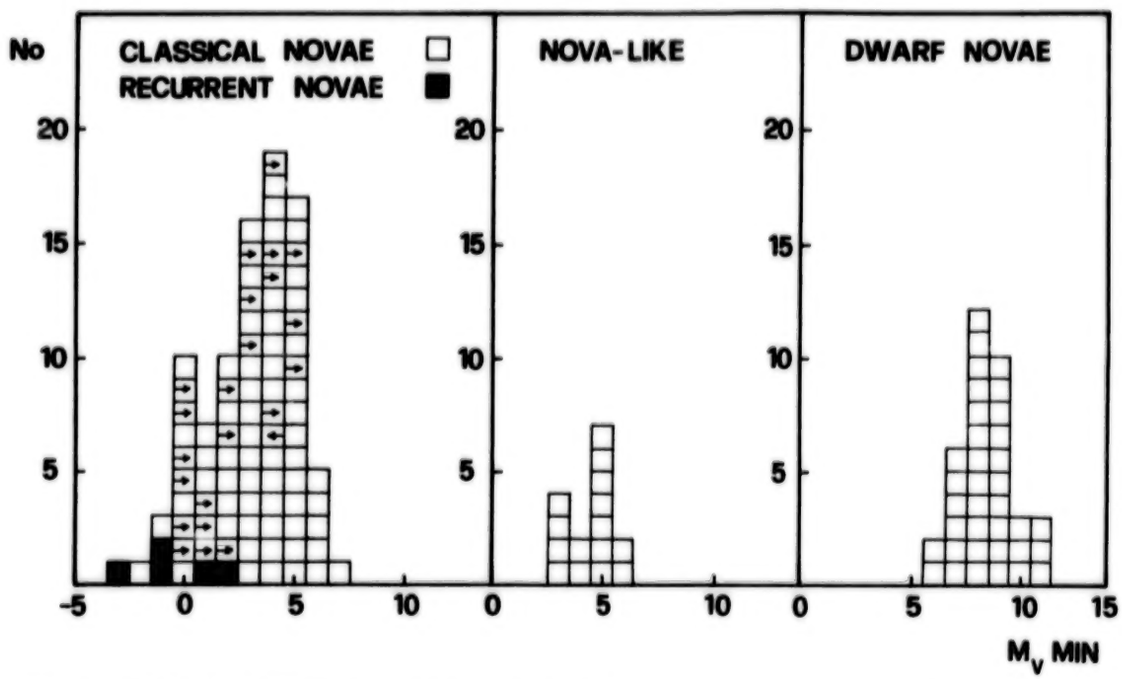


Figure 1-6. Absolute visual magnitude at minimum for classical novae, recurrent novae, nova-like stars and dwarf novae. The arrows indicate upper (←) or lower (→) limits (from Warner, 1987).

1-4), whereby the distribution of mass ratios between sub-classes seem to bear some relevance for the physical appearance of the system (for further details see Chapter 2.I.C). In a few longer-period systems, mass ratios of slightly less than one (i.e., the secondary star is more massive than the white dwarf) have been found; whether or not it is significant that none of these systems is a classical nova is not clear, due to the small number of systems. Corresponding to these low masses, the spectral types of cataclysmic variable secondaries all are G0 or later, with a typical spectral type of K or M (Figure 1-5).

C-2

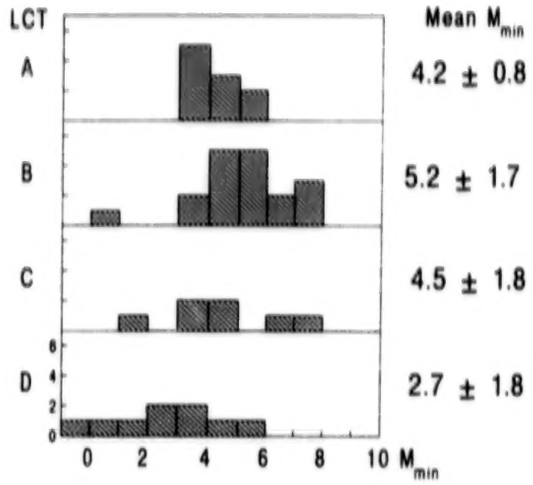


Figure 1-7. Absolute magnitudes of old novae sorted according to outburst light curve types, from Duerbeck (1981, 1986). A refers to very fast, D to very slow novae. For details see Chapter 6.II.B.

The masses and orbital periods of cataclysmic variable systems yield typical system dimensions on the order of one solar diameter. Furthermore, it is clear, as will be discussed in more detail later, that the companion stars must be almost filling their Roche volume, which of course is a necessary condition for Roche-lobe overflow, and thus the formation of an accretion disc, to occur.

And finally, when absolute magnitudes of quiescent novae and dwarf novae and of nova-like stars in their normal (bright) state are compared (Figure 1-6), there are very distinct differences. Brightnesses of novae are concentrated around the value of M_V of about 4 (the few known recurrent novae are considerably brighter), nova-like stars are a little fainter (M_V around 5), and dwarf novae have absolute magnitudes on the order of M_V about 8 or 9.

Duerbeck (1986) gives the absolute magnitudes of old novae sorted according his classification of outburst light curve types (see Chapter 6). Although the number of objects is rather small, there is some indication that slow old novae are brighter at minimum than fast old novae (Figure 1-7).

REFERENCES

Duerbeck, H. W. 1981, *Publ. Astr. Soc. Pac.*, **93**, 165.

Duerbeck, H. W. 1984, *Astr. Space Sci.*, **99**, 363.

Duerbeck, H. W. 1986, *Mitteilungen Astron. Ges.*, **67**, 309.

Joy, A. H. 1954, *Astrophys. J.*, **120**, 377.

Joy, A. H. 1956, *Astrophys. J.*, **124**, 317.

Kholopov, P. N. 1985, Vol. I, Vol. II, 1987, Vol. III., *General Catalogue of Variable Stars*, (Moscow, 4th. ed.)

Kraft, R. P. 1958, *Astrophys. J.*, **127**, 625.

Kukarkin, B. F., Kholopov, P. N., Efremov, Yu. N., Kukarkina, N. P., Kurochkin, N. E., Medvedeva, G. I., Perova, N. P., Feorovich, V. P., and Frolov, M. S. 1969, Vol. I., 1970, Vol. II., 1971, Vol. III., *General Catalogue of Variable Stars*, (Moscow, 3d. ed.).

Merrill, J. E. 1941, (in P. Swings, *Symbiotic Stars and Related Peculiar Objects, in Spectroscopic Astrophysics*, ed. G. H. Herbig, University of California Press 1970, p. 189)

Patterson, J. 1984, *Astrophys. J. Suppl.*, **54**, 443.

Ritter, H. 1987, *Astr. Astroph. Suppl.*, **70**, 335.

Ritter, H., and Burkert, A. 1986, *Astr. Astroph.*, **158**, 161.

Wackerling, L. R. 1970, *Mem. R. Astr. Soc.*, **73**, 153.

Walker, M. F. 1954, *Publ. Astr. Soc. Pac.*, **66**, 230.

Warner, B. 1986, *Mon. Not. R. Astr. Soc.*, **222**, 11.

Warner, B. 1987, *Mon. Not. R. Astr. Soc.*, **227**, 23.

PART I

DWARF NOVAE AND NOVA-LIKE STARS

Written by

Constanze la Dous

PRECEDING PAGE BLANK NOT FILMED

N95
27069
UNCLAS

N95- 27069

2

DWARF NOVAE

I. CLASSIFICATION

I.A. HISTORICAL OVERVIEW

ABSTRACT: Dwarf novae are defined on grounds of their semi-regular brightness variations of some two to five magnitudes on time scales of typically 10 to 100 days. Historically several different classification schemes have been used.

see also: 145

nova-like stars: 95

Novae, or "new stars," have been known for some centuries. Stars given this name had never been seen before; then they suddenly appeared in the sky for some duration and disappeared again. Many of these old novae seen in historic times are now referred to as supernovae, describing a very powerful event which profoundly affects the mass and structure of the entire star; these are not dealt with in this book. The much less violent events of what we now call novae, recurrent novae, or symbiotic stars, and also nova-like stars are subjects of later chapters of this book. In this chapter, dwarf novae, which undergo comparatively less violent outbursts, are introduced. They became known only in the last century.

In December 1855, a star which behaved like a nova (later named U Geminorum), was detected by Hind (1856); it suddenly became visible and soon thereafter disappeared. However, in March 1856, and recurrently since then in semi-regular intervals of time, it brightened and disappeared abruptly again (Pogson, 1906). By definition, it could not be a nova. Eventually more and more stars were detected which behaved similarly, so they were regarded as a new class of stars, and referred to as *dwarf novae*.

For a long time, the outburst light curve was the only observable feature of these stars, and so it was (and still is) the basis for their classification. That the temporal brightness changes were only approximately, and not strictly, periodic was confusing. A physical similarity between the two brightest of these stars, SS Cyg and U Gem was conjectured, but also doubted, since the time between successive brightness maxima and the shape of different maxima was confusingly different for each single star, and even more different from one star to another.

Müller and Hartwig (1918) gave a complete list of the then known variable stars. Stars which now are known as dwarf novae are described in this catalogue in terms of their similarity or dissimilarity to SS Cyg (for frequent, irregular maxima) or U Gem (for less frequent, but more regular, maxima). However, for a brief period, SS Cyg itself posed a problem and its relation to U Gem and other dwarf novae was questioned when it stopped exhibiting its normal outburst activity for a while during 1907 and 1908, and only exhibited irregular brightness fluctuations (see Figure 2-1c). Nevertheless, this anomalous event was soon forgotten, and SS Cyg returned to its place as a proto-type of dwarf novae.

PRECEDING PAGE BLANK NOT FILMED

The 1918 catalogue by Müller and Hartwig was followed by an updated version by Prager in 1934. In the introduction he gives a brief classification of types of variable stars. Under "physical variables," subtype "expanding stars," there appears a class "U Geminorum stars." The description reads: "The brightness changes of these stars are characterized by the appearance of short-lasting, moderately sharp maxima, clearly not unlike those of novae; their recurrence time ranges from 10 to 100 days for different stars and is not strictly aperiodic. The normal light is slightly variable." Furthermore he distinguishes four sub-classes of U Geminorum stars: SS Cygni stars ("variables with weak, almost constant normal light and quick brightening of large amplitude (up to 6 mag) in not entirely irregular time intervals"); flickering stars ("stars of low apparent brightness which suffer very short-lasting brightenings like SS Cygni stars. Amplitude 3 mag, duration of brightening about 30 minutes, ..." -nowadays these objects are not regarded to be dwarf novae); CN Orionis stars ("U Geminorum-like stars for which the constant minimum is very short or missing entirely so that an almost steady change of light by 2 to 3 mag originates"); and Z Camelopardalis stars ("similar to SS Cygni stars, but with shorter intervals up to the disappearance of a constant minimum and inclination for larger disturbances of the light curve; at times there are long standstills at a mean light level (declining shoulder) or degeneration of the light curve to a sequence of irregular low amplitude waves"). Neither of the terms dwarf nova or nova-like star are mentioned.

Parenago and Kukarkin (1934) and Kukarkin and Parenago (1934) refer to U Geminorum variables as a sub-type of nova-like variables. And Voronstsov-Velyaminov (1934) refers to stars like SS Cyg, RS Oph, and V Sge (which today would be classified as dwarf novae, recurrent novae, and nova-like stars, respectively) all as "nova-like" stars. Gerasimovič (1934) and Miczaika (1934) use the term SS Cygni stars for what Prager defined as U Geminorum stars. For the next 30 to 40 years both terms became almost equivalents of the term dwarf novae, with a tendency for U Geminorum stars to be preferred.

In 1952 another attempt was made by Brun and Petit to establish definitions of sub-classes of U Geminorum variables. They distinguish seven sub-types, named after the best-known representatives: Z Camelopardalis stars (exhibiting standstills at a mean light level), CN Orionis stars (with very frequent relatively regular maxima), SU Ursae Majoris stars (exhibiting infrequent supermaxima of somewhat larger amplitude and much longer duration than the more frequent normal maxima), X Leonis stars (having frequent long and even more frequent short maxima), SS Cygni stars (with about the same number of long and short maxima alternating irregularly), U Geminorum stars* (high amplitude, quick rise, longer and shorter maxima, long minimum phase), and finally, UV Persei stars (with long minimum phases, large amplitudes, and either very long or very short maxima). This classification was subsequently used only by the authors, but otherwise it was not accepted in this form. For instance Kraft (1962b) defines the terms "U Geminorum star" and "dwarf nova" as equivalent names of the class of stars which consists of the two sub-classes of SS Cygni stars and Z Camelopardalis stars. The same definition was adopted by Mumford (1967b). Smak (1971) defines only one sub-class of Z Camelopardalis stars to the main class of U Geminorum stars.

Vogt (1974) and Warner (1975) independently detected that the dwarf nova VW Hyi exhibited periodic light variations, so-called "superhumps," during a supermaximum (see e.g., Figure 2-49); the remarkable feature of this superhump was that its strict periodicity

*The term "U Geminorum star," in their scheme, thus denotes both the entire class as well as one particular sub-class.

was a few percent longer than the binary period of VW Hyi. Soon other stars were detected to show superhumps during supermaxima (and - almost - only then). They all belonged to the class of SU Ursae Majoris stars as defined by Brun and Petit (1952). Having become a favorite subject of astronomical research, the name *SU Ursae Majoris stars* was quickly established generally for this sub-class of dwarf novae. Ironically, with the introduction of a superhump as a defining characteristic of SU Ursae Majoris stars, its former proto-type, SU UMa, was excluded from the class which carried its name until, finally, in 1982 superhumps were detected during one of its superoutbursts (Wade and Oke, 1982), too.

During the outburst of WZ Sge in 1978 it turned out that this star, which so far had been classified as a recurrent nova, rather behaved like a (somewhat atypical) dwarf nova; mostly the very long outburst period of 33 years was disturbing. Thus another class, *WZ Sagittae stars*, containing just this one object, was introduced intermediate between recurrent novae and dwarf novae. Later it was discovered that during this same outburst WZ Sge displayed superhumps, which qualified it as an SU Ursae Majoris star. Currently all three classifications of WZ Sge are used. (In this book it will be referred to as a peculiar SU Ursae Majoris star.)

I.B. MODERN CLASSIFICATION

ABSTRACT: According to their outburst characteristics, three types of dwarf novae are distinguished: U Geminorum stars, Z Camelopardalis stars, and SU Ursae Majoris stars.

see also: 1

nova-like stars: 95, 96, 102, 112, 125, 140

In the modern classification scheme which was discussed in the Introduction, dwarf novae are regarded to be a sub-class of cataclysmic variables. *The defining characteristic of dwarf novae* is that they undergo outbursts, which are brightness increases of typically 3 to 5 magnitudes, in semi-periodic intervals of time. For most of them, the faint state, i.e., the *quiescent state* or *minimum*, is their normal state. Most of them can be found in outburst for only a relatively small fraction of the time. The time interval between outburst maxima, which is also somewhat misleadingly called the *outburst period*, usually is on the order of 10 to 100 days. Extreme cases do occur, like WZ Sge with an outburst period of about 33 years, or AH Her, the quiescent state of which can be as short as one day, or even not be reached at all before, after the decline from one maximum, rise to the next occurs. Possibly there is a continuous transition to nova-like stars. These latter in general do not exhibit any outburst activity, but can, on the contrary, sometimes drop in brightness by several magnitudes (see Chapter 3). For any given object, the outburst period is only a statistical average, which, however, usually is followed reasonably well within certain limits. The duration of an outburst* is of some 1 to 10 days, depending on the object. The rise to an outburst usually is fast, while the decline to minimum is slower. The shape of the outburst light curve, its period, and the quickness of rise and decline are characteristic features of every object, though an object can have more than one such typical shape. Also any particular outburst shape is not strictly repeated in all details, but only approximately.

Today, dwarf novae are divided into three sub-classes: the U Geminorum stars, the SU Ursae Majoris stars, and the Z Camelopardalis stars. The definition of *Z Camelopardalis stars* is that they occasionally, on decline from an outburst, stay at an intermediate brightness level, a so-called *standstill*, for weeks or years, exhibiting only minor brightness fluctuations before they return to minimum light (Figure

* Superoutbursts are special types of outbursts and will not be distinguished from ordinary outbursts in this general section. For further details see Chapter 2.II.A.4.

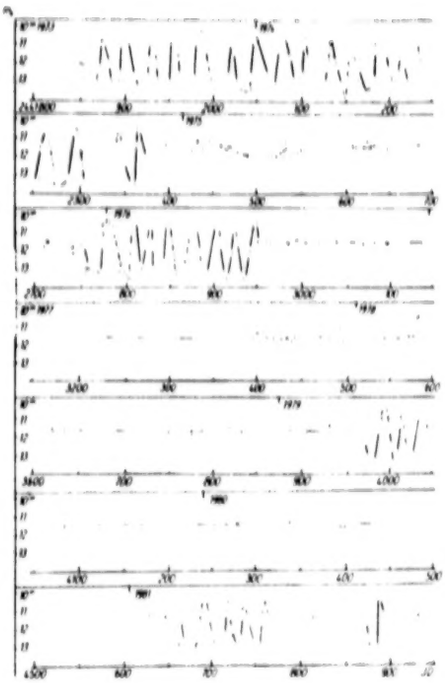


Figure 2-1a. Outburst light curve of the dwarf nova Z Cam (Gunther, Schweitzer, 1982; reproduced from Hoffmeister et al, 1984). Occasionally the star remains at some intermediate brightness for several months to several years.

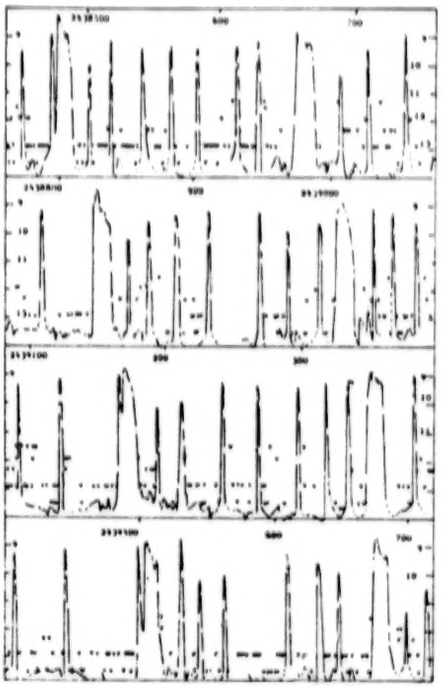


Figure 2-1b. Outburst light curve of the SU Ursae Majoris type dwarf nova VW Hyi (Bateson, 1977). Normally the system undergoes short outbursts; at rather regular intervals of time so-called superoutbursts occur which are brighter and last for much longer than normal outbursts.

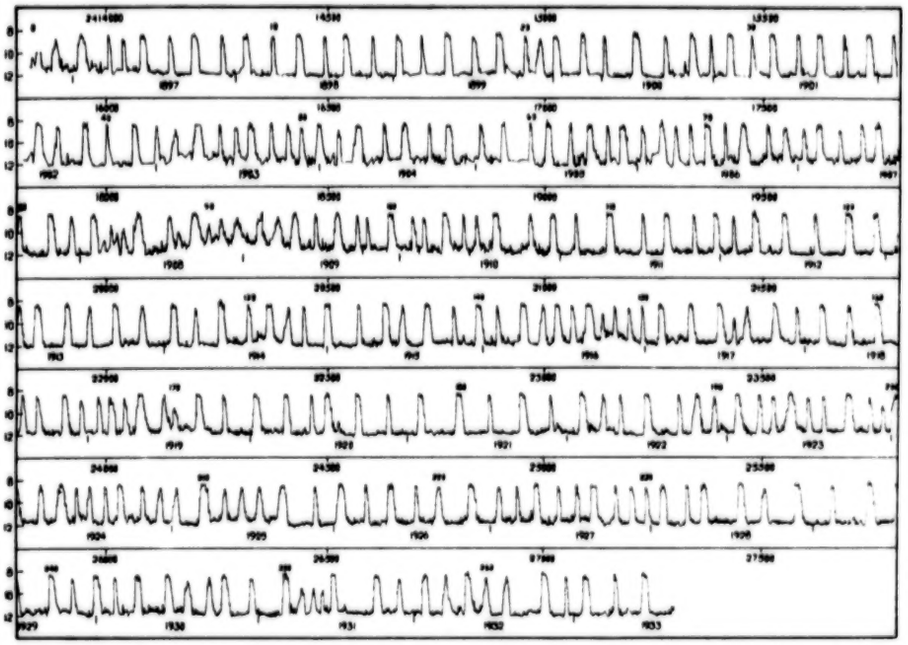


Figure 2-1c. Outburst light curve of the U Geminorum type dwarf nova SS Cyg in 1896 - 1933 (Campbell, 1934). Shorter and longer outbursts follow each other in an irregular sequence.

2-1a). *SU Ursae Majoris stars* exhibit two types of outbursts, so-called *normal outbursts* and the noticeably longer and brighter *superoutbursts* (Figure 2-1b). And the third sub-class is the *U Geminorum stars*, to which all those dwarf novae belong which are neither SU Ursae Majoris stars nor Z Camelopardalis stars (Figure 2-1c). The membership of a star in the class of SU Ursae Majoris stars or of Z Camelopardalis stars seems to be exclusive; the membership in the U Geminorum class is exclusive by definition. Since quite detailed observations are required in order to identify a star as belonging to the SU Ursae Majoris sub-class in particular, some as yet unrecognized SU Ursae Majoris stars may well be hidden in the U Geminorum stars.

Several lists of dwarf novae and their classification compiled under various aspects, have been published in the literature. One such list is contained in the *General Catalogue of Variable Stars* (Khopolov, 1985). The disadvantage of this list is that it contains variable stars of all kinds which makes it a tedious task to select the dwarf novae. Also by no means all stars which are classified therein as dwarf novae would be referred to as such by those who work in the field, and, vice versa, objects that are conventionally classified as dwarf novae are assigned some other type. *The AAVSO Variable Star Atlas* contains names, coordinates, classifications, and ranges of brightness variability of all those stars that are possibly observable with the telescopes of amateur astronomers. Again, since all kinds of variable stars are included, it is time-consuming to select just the dwarf novae. Since, however, practically all dwarf novae have been detected by amateurs, and thus are observable by them, this is likely to be the most reliable and complete source for dwarf novae. Lists of classifications and system parameters of cataclysmic variables (dwarf novae and other types) for which orbital periods are known, are given by Patterson (1984) and by Ritter (1984, 1987). The shortcoming of these catalogues is that, due to the adopted limitation, they are rather incomplete with respect to the full sample of known dwarf novae.

I.C. SOME STATISTICS

ABSTRACT: Dwarf novae and nova-like stars are treated together here. Both the observed orbital periods and, to some extent, the ratios between the masses of the two stars seem to be related to the outburst behavior.

see also: 7

interpretation: 217, 219, 222

As was pointed out earlier, the first dwarf nova, U Gem, was detected in 1855, and the number of these systems increased only slowly thereafter. By the beginning of this century only one more dwarf nova, SS Cyg (detected in 1896), was known. Müller and Hartwig (1918) report that eight members of this class were known; by 1934 their number had doubled (Gerasimovič, 1934); and Petit (1958) states that, out of the 149 variable stars which by that time were classified as dwarf novae in the *General Catalogue of Variable Stars* and its supplements, only 56 were certain to be dwarf novae, a further 47 of them were probable dwarf novae, and the rest were doubtful. This same catalogue in the version of 1983 classifies 254 stars as dwarf novae; assuming that again some 30% are doubtful, this still means that currently some 200 dwarf novae are known.

In the Introduction (Chapter 1.V), statistical properties of dwarf novae and nova-like stars were discussed in the context of other cataclysmic variables, without, however, dealing with them in detail. As stated in the previous section, dwarf novae are divided into sub-classes, the U Geminorum stars, the SU Ursae Majoris stars, and the Z Camelopardalis stars. Similarly, as will be discussed in more detail in Chapter 3.I nova-like stars are also divided into sub-classes, namely the UX Ursae Majoris stars, the anti-dwarf novae, the DQ Herculis stars, the AM Herculis stars, and the AM Canum Venaticorum stars. Although

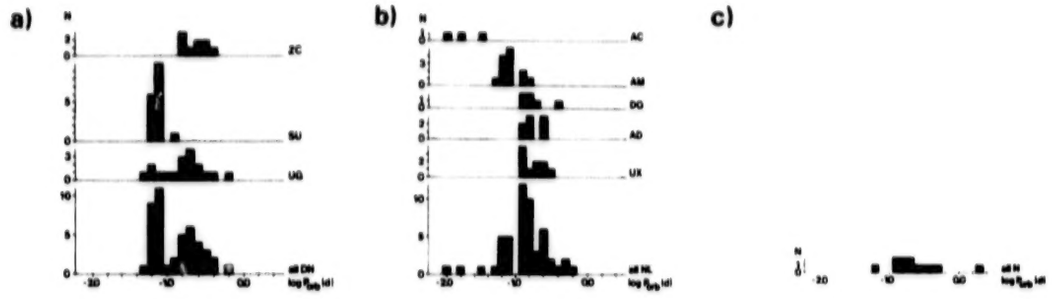


Figure 2-2. Distribution of orbital periods among sub-classes of dwarf novae (a) and nova-like stars (b); for comparison the distribution of novae is given as well (c). No objects are found with periods between about two and three hours; only three peculiar systems have periods shorter than some 80 minutes; only very few objects have periods that are longer than some ten hours.

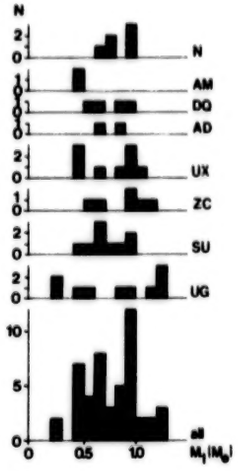


Figure 2-3a. Distribution of the masses of the white dwarfs among sub-classes of dwarf novae and nova-like stars; for comparison the distribution of novae is given as well. No very obvious relation to sub-classes seems to exist.

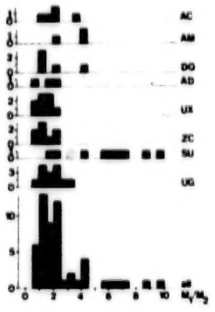


Figure 2-3b. Distribution of mass ratios among sub-classes of dwarf novae and nova-like stars with distribution of nova masses for comparison. Mass ratios mostly are very high for SU Ursae Majoris stars; they tend to be higher than normal for AM Herculis stars (i.e, for those nova-like stars which are believed to possess strongly magnetic white dwarf(s); otherwise typically the secondary star is half as massive as the white dwarf.

nova-like stars are not the issue of this chapter, they are still so similar to dwarf novae in almost all of their properties that it would seem all too artificial to formally separate them entirely. In particular, a statistical consideration of both groups together, the dwarf novae and the nova-like stars, can be rather illuminating. This is the course which will be pursued in this particular section; for the remainder of this chapter, however, only dwarf novae will be considered, and observations of nova-like stars will be the issue of Chapter 3.

Figure 1-2 gives all the known orbital periods of cataclysmic variables separated by object classes. In Figure 2-2 these same data are presented in another way: the sub-classes of dwarf novae and nova-like stars are separated, and, for comparison, the orbital periods of novae are shown as well. Z Camelopardalis stars, and the UX Ursae Majoris stars, closely related in appearance, and anti-dwarf novae can all be found exclusively above the period gap; SU Ursae Majoris stars, on the other hand, with only one exception all have orbital periods below the gap, the one exception, TU Men, being very close to the upper edge of the gap; the AM Canum Venaticorum stars also fall below the period gap, below even the short period cut-off of all the other cataclysmic variables; all DQ Herculis stars can be found above the gap, except for EX Hya; the AM

Herculis stars tend to be found below it, although some objects lie above it; and finally, dwarf novae with no particular characteristics, the U Geminorum stars, can have any value of the orbital period.

White dwarf masses seem to be statistically identical for dwarf novae and nova-like stars as well as for their various sub-classes (Figure 2-3a). When, however, mass ratios are considered there is a tendency for SU Ursae Majoris stars and AM Herculis stars to have distinctly higher than average values, which might bear on the observable idiosyncrasies of these classes of objects (Figure 2-3b). Objects belonging to other classes tend to cluster around values of M_1/M_2 of 1 or 2, but much higher values are possible. For the entire sample, the white dwarf is the more massive of the components for the majority of systems; if mass ratios of less than one occur, they almost always are found to be close to one.

GENERAL INTERPRETATION: All cataclysmic variables are believed to be binary stars. Dwarf novae and nova-like stars are regarded to be essentially the same kind of objects. Due to a higher mass transfer rate from the secondary star into the Roche lobe of the white dwarf, nova-like stars normally can be found in the outburst state. The distribution of mass ratios and orbital periods is suspected to be due at least partly to evolutionary effects.

OBSERVATIONAL CONSTRAINTS TO MODELS:

- *The physical difference between dwarf novae, nova-like stars, novae, and recurrent novae is not clear. (See 176, 229)**
- *Is binarity a necessary condition for an object to be a cataclysmic variable? (See 151, 179, 188, 190, 214)*
- *A vague relation between orbital periods and outbursts behavior has been observed. (See 177, 181)*
- *A minimum orbital period, a period gap, and some evidence for a maximum orbital period have been observed. (See 222)*
- *Most SU Ursae Majoris stars and AM Herculis stars seem to have higher mass ratios than other cataclysmic variables.*
- *Almost all known secondaries in cataclysmic variables seem to be cool main sequence stars. (See 219)*

*The raised points are dealt with theoretically in the indicated pages.

II. PHOTOMETRIC OBSERVATIONS

II.A. OUTBURST BEHAVIOR

ABSTRACT: Outbursts of dwarf novae occur at semi-periodic intervals of time, typically every 10 to 100 days; amplitudes range from typically 2 to 5 mag. Within certain limits values are characteristic for each object.

related spectroscopic changes: 61, 81

nova-like stars: 102, 113, 125

interpretation: 171

The outburst behavior of dwarf novae is the one phenomenon which has been studied for the longest time about these objects. In fact, until the discovery of the binary nature of cataclysmic variables, essentially all research involved attempts to understand what physical processes could produce the semi-periodic, but not strictly periodic, recurrence times of the outbursts and the observed shapes of the light curves. As soon as some strictly periodic behavior was found as evidence for the binary motion, almost all research turned away from explaining the long-term variability. A limited interest in this field was reawakened with the detection of the peculiarities observed during superoutbursts in SU Ursae Majoris stars (see below), and again with the recent opportunity to perform observations in the UV and X-ray spectral ranges. Overall, a number of very valuable investigations have been undertaken, and these have revealed many interesting

features which are still far from being understood.

No strictly periodic pattern is obvious in the outburst behavior of dwarf novae (see Figures 2-1 a-c). There is some average time interval between successive outbursts; the individual scatter, however, can be considerable. Also the outburst amplitude for any individual object can only be given within wide limits, the minimum as well as the maximum brightness levels being variable.

In spite of this apparently random behavior, attempts have been made since the beginning of this century to find some underlying systematics or periodicity in the behavior of both single objects and the entire class of dwarf novae. The highlights of these investigations shall be presented in the following section.

II.A.1. SS CYGNI — A WELL-STUDIED CASE

ABSTRACT: More than 600 outbursts of SS Cyg have been observed. Their investigation reveals a number of statistically characteristic features and repetitive properties.

see also 24

SS Cyg is by far the best-studied dwarf nova due to its large apparent brightness (m_v = 12.7 - 8.2 mag) and its outstanding position as a circumpolar star for many of the northern hemisphere observatories. Almost certainly not one single outburst has passed unobserved since the detection of SS Cyg in 1896, yielding well over 600 observed outbursts to date. In addition, the shapes of the outbursts as well as the brightness during minimum state have subsequently been recorded extremely well. Figure 2-1c displays the complete light curve between 1896 and 1933. Very extensive statistical studies have been carried out by Krytbosch (1928), Campbell (1934), Sterne and Campbell (1934), Martel (1961), Howarth (1978), and Bath and van Paradijs (1983). A summary of some of their results follows.

Inspection of Figure 2-1c reveals that the shapes of the outbursts are by no means always the same, but still some characteristic features are repeated. Campbell derived a classification scheme (Figure 2-4) based on the times needed for rise (light increase) from minimum level to maximum: class A is a very rapid rise, class B is somewhat slower, class C moderately slow, and class D extremely slow; further sub-division of each class was undertaken in order to account for different widths of maxima. Class A is by far the prevailing type with 64% of all 267 maxima investigated by Campbell, class B has 9%, class C 18%, and class D again 9%. Classes C and D together also are referred to as *anomalous*, a term that has since been used for other dwarf novae to describe all outbursts with slow rises, in spite of the fact that they have proved to be a rather normal feature of dwarf nova outbursts in general. There is an obvious distinction within classes A and B into long and short (wide or narrow) outbursts. This is seen even more clearly in the histogram of widths of 437 maxima of SS Cyg (Martel, 1961) in Figure 2-5; this can be approximated by two normal distributions centered at 7.5 and 15 days, respectively, with a gap at about 11 days. It appears that the width of class A outbursts lies close to the statistical averages of 7.5 and 15 days, whereas outbursts of class B, C, and D are more randomly distributed in duration. The rate of rise and decline (light decrease) in classes A and B is essentially the same for both long and short eruptions, the rise being about twice as fast as the decline. The main differences between both types are that during long eruptions the star remains at almost constant brightness for about a week, and statistically the maximum brightness of long eruptions is somewhat larger than that of short ones (8.4 mag vs. 8.6 mag). Almost all faint maxima which reach only a brightness of 8.8 mag or less have long rise times (Campbell's classes B, C, and D). There is a clear tendency for long and short outbursts to alternate and a less than random probability for sequences of long-long or short-short eruptions to occur.

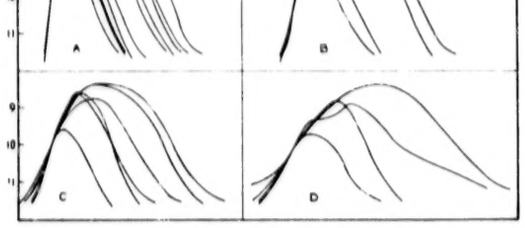


Figure 2-4. Classification of outburst light curves of SS Cyg (Campbell, 1934).

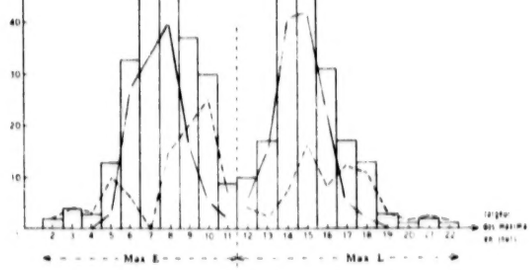


Figure 2-5. Distribution of widths of maxima of SS Cyg. The histogram shows the total distribution, the solid line gives the frequency of type A outbursts, the dashed line that of types B, C, and D together (Martel, 1961; his figures 4 and 14 combined). In all cases a clear bi-modal distribution appears.

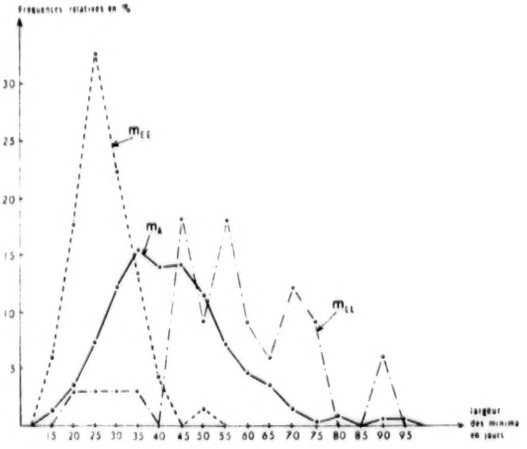


Figure 2-6. Duration of minima of SS Cygni in relation to the duration of both the preceding and the following outbursts (m_{EE} : between two short outbursts; m_{LL}: between two long outbursts; m_A: between either a long and a short, or a short and long outburst) (Martel, 1961). Minima between two short outbursts of SS Cyg tend to be short, minima between two long outbursts tend to be long.

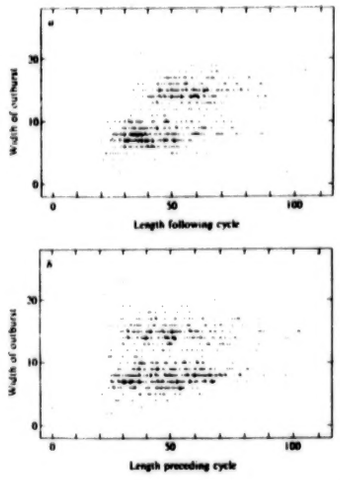


Figure 2-7. Width of maxima in SS Cyg versus the duration of the preceding and the following minimum time (Bath and van Paradijs, 1983). A vague correlation exists with the length of the following cycle, clearly not with the preceding cycle.

The maximum brightness of an outburst is uncorrelated with the brightness of both the preceding and the following outburst.

Investigation of the length of minima between successive outbursts leads to the result displayed in Figure 2-6: the average duration of minima between long-short and short-long pairs is almost identical, peaked at some 35 days, while durations of only 10 days and up to 100 days are possible; minima between two successive short eruptions last for only some 25 days on the average, and hardly ever are longer than 50 days; and minima between successive long outbursts can last for almost any length of time between some 40 and some 95 days. Looking at all kinds of outbursts together, a loose correlation exists between the duration of an outburst and the duration of the following cycle, while there is no such relation with the preceding minimum period (Figure 2-7); class D outbursts, however, tend to be preceded by minima of considerably shorter duration than average (Bath and van Paradijs, 1983).

One final statistical feature of outbursts of SS Cyg is that type A outbursts usually start from a quiescent brightness of 11.9 ± 0.12 mag, whereas all slower rises (classes B, C, D) start from brighter quiescent states of 11.64 ± 0.30 mag (Bath and van Paradijs, 1983).

II.A.2. OTHER DWARF NOVAE

ABSTRACT: Although samples are not as statistically significant as for SS Cyg, similar characteristic features seem to exist in other dwarf novae as well.

see also: 22

interpretation: 171

Equally extensive studies are not available for other dwarf novae, mostly because their lesser brightness makes it difficult for them to be observed by amateurs (who are the main source of information on dwarf nova outburst behavior). Besides SS Cyg, probably the best investigated dwarf novae concerning their outburst activity are U Gem (with comprehensive studies by van der Bilt (1908), Greep (1942) and Saw (1982 a)) and VW Hyi, which has mostly been analyzed with respect to its superoutbursts, the discussion of which will be deferred to a latter section in this chapter.

Like the SS Cyg, the occurrence of two types of outburst, long (or wide) and usually more luminous ones, and short (or narrow) and often less luminous ones, is a very common, if not universal, feature of dwarf novae (some examples are given in Figure 2-8). We could not find one single conclusive case of a uni-modal distribution with the possible exception of WZ Sge for which, however, only a total of three outbursts were observed. But while most dwarf novae exhibit wide and narrow outbursts, and the SU Ursae Majoris stars exhibit normal as well as considerably wider (by a factor of five to ten) superoutbursts, TU Men (the only known SU Ursae Majoris star with an orbital period above the period gap between two and three hours) is the only known system which undergoes narrow, wide, and superoutbursts (Bateson, 1979, 1981; Warner, 1985a). Normally, within extreme ranges, all durations are possible, but some are still rare enough to leave the general distribution with two clear maxima. Szkody and Mattei (1984) claim that such bi-modal distributions occur only in SU Ursae Majoris stars and very few others, while most stars in their sample show uni-modal distributions. It must be noted, however, that their data base is very short compared to that of most other investigations, and that statistics based on more data show clear evidence for a general bi-modal distribution of outbursts for the objects in their sample. A more convincing conclusion to be drawn from their investigation is that the overall outburst behavior of a dwarf nova may well undergo changes in the course of years. Histograms of the outburst activity of EM Cyg, probably a very radical example, illustrate the point (Figure 2-9): if the distributions of outburst widths for only a short interval of time are regarded (one and three years in this example), the resulting distributions may come out considerably different from each other, as well as from averages over long intervals of time. Furthermore, there are objects in which long and short maxima keep strictly alternating for many years. The most famous example of such outburst activity is U Gem, which was never seen to deviate from this regular alternation during the first 50 years of its surveillance (van der Bilt, 1908).

In general, provided both types of maxima occur about equally frequently, there is a tendency for them to alternate. When more short maxima than long ones occur, most of the long maxima are both followed and preceded by a short one, while a short one may well be followed by another short one; in other words, pairs of two short outbursts are not unlikely, while pairs of two long outbursts are extremely rare. When anomalous outbursts (i.e., outbursts with an unusually long rise time) occur in an object, these are likely to come in groups; i.e., they are the only kind of outburst to be observed for some duration, or at least then they occur considerably more frequently than any other type (Petit, 1961).

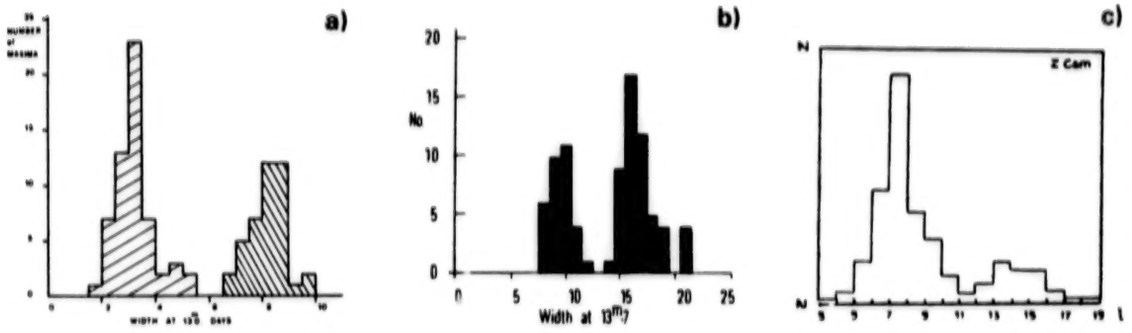


Figure 2-8. Bi-modal distributions of the lengths of dwarf nova outbursts: a:X Leo (Saw, 1982b), b:U Gem (Isles, 1976), c:Z Cam (Petit, 1961). Possibly all dwarf novae show distributions like this.

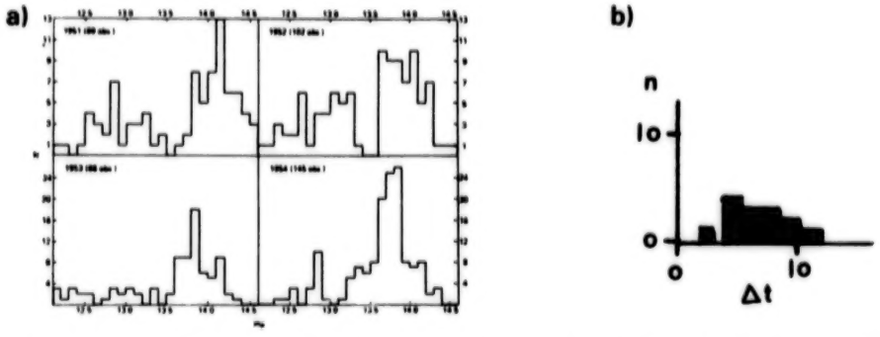


Figure 2-9. Distributions of durations of outbursts of EM Cyg for (a) the years 1951 through 1954 each (Brody and Herczec, 1977), and for (b) approximately 1974 - 1976 (JD 2442300 - 2443300) (Szkody and Mattei, 1984). The bi-modal distribution only becomes obvious when observations over a very long interval of time are considered.

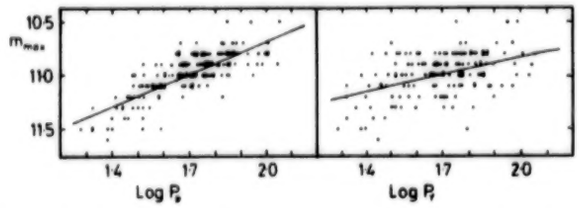


Figure 2-10. Maximum outburst magnitude versus the duration of the preceding (left) and the following (right) quiescent period in SS Aur (Howarth, 1977). In contrast to SS Cyg, in VW Hyi the maximum brightness of an outburst is dependent on both the durations of the preceding as well as the following minimum.

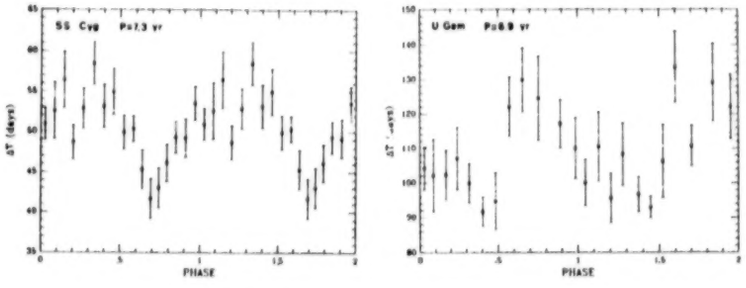


Figure 2-11. Semi-regular variations of the duration of quiescent intervals between two consecutive outbursts of SS Cyg and U Gem (Bianchini, 1988).

In this same investigation Petit found that the average ratio of the number of long per short maxima increases as the outburst period of a system increases: SU UMa and AY Lyr (with outburst periods of some 13.4 and 24 days, respectively) exhibit about one long outburst per 7 or 8 short ones; Z Cam (21 days), X Leo (20 days), and UZ Ser (31 days) have typically 1 long outburst per 2 or 3 short ones; in SS Cyg (50.7 days) and SS Aur (53.3 days) about 2 long outbursts can be observed per 3 short ones; and finally in U Gem (103.4 days) and UV Per (360 days) this ratio increases to approximately 5 long outbursts for every 4 short ones.

Several investigations have been carried out to look for a possible correlation between the length of quiescent (low brightness) intervals and the kind of outbursts a system undergoes. The emerging picture is clearly not consistent: In the case of SS Cyg, CN Ori, and CZ Ori the width of an outburst, and in the case of FQ Sco, BI Ori, and U Gem its maximum brightness (which normally is higher for long outbursts than for short ones) are correlated with the length of the following quiescent interval but not with the preceding one* (Bath and van Paradijs, 1983; Isles, 1976; Gicger, 1987); in the case of VW Hyi both the total width and the maximum brightness, in UZ Ser and TU Men the width, and in WW Cet the maximum brightness are correlated with the preceding minimum, but not with the duration of the following one* (Gicger, 1987; Smak, 1985; van der Woerd and van Paradijs, 1987); in the case of SS Aur the maximum brightness, and in the case of UY Pup the width correlate with both the preceding and the following quiescent state (Gicger, 1987; Howarth, 1977) (see Figures 2-7 and 2-10).

As to the length of quiescent periods between long and/or short outbursts, from investigating large amounts of data of many dwarf novae, Petit (1961) concluded that the durations of minima, irrespective of kinds of outburst between which they occur, tend to be almost normally distributed about some mean value which is characteristic for each object. Minima occurring between two short outbursts have a tendency to be shorter than average. This is in agreement with results of detailed investigations of SS Cyg (Figure 2-6) and X Leo (Saw, 1982b). For several systems, there is some indication for them to be the fainter the longer the quiescent state lasts. Furthermore, in several objects, like in SS Cyg, U Gem, and RU Peg, there is evidence for cyclic secular changes in the duration of the quiescent period of dwarf novae (Campbell, 1934, Petit, 1961, Saw, 1983, Bianchini, 1988) (Figure 2-11).

*Results for other correlations are not given.

II.A.3. NUMERICAL RELATIONS

ABSTRACT: Relations between the outburst amplitude, or the total energy released during outburst, and the recurrence time have been found, as well as relations between the orbital period and the outburst decay time, the absolute magnitude during outburst maximum, and the widths of long and short outbursts, respectively.

interpretation: 177, 181

All dwarf novae are highly individualistic objects; no two systems have been found which can be regarded as approximately identical, and certainly there is nothing like a "typical" dwarf nova. This applies to their outburst behavior, but it proves valid for other aspects of their nature just as well. Still, it clearly would be wrong to say that they are all totally different from each other.

For more than half a century attempts have been made to find some relations that all dwarf novae, if possible even all cataclysmic variables, would obey. The first such relation was found by Kukarkin and Parenago (1934) who suggested a relation

$$A = 0.63 + 1.66 \log P \qquad (2.1)$$

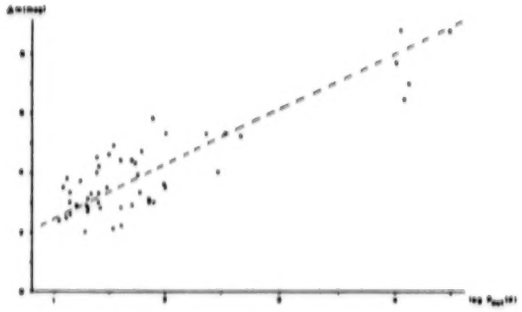


Figure 2-12a. Kukarkin-Parenago relation between outburst amplitude Δm and recurrence time P_{out} of dwarf novae and recurrent novae (data from Petit, 1958). The original relation as given by Kukarkin and Parenago (1934) is indicated as a solid line; its physical significance is not clear.

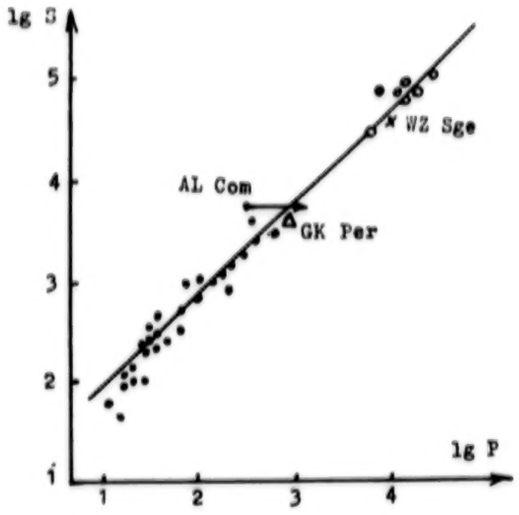


Figure 2-12b. Revised Kukarkin-Parenago relation between the energy spent during an outburst and the recurrence time (Antipova, 1987).

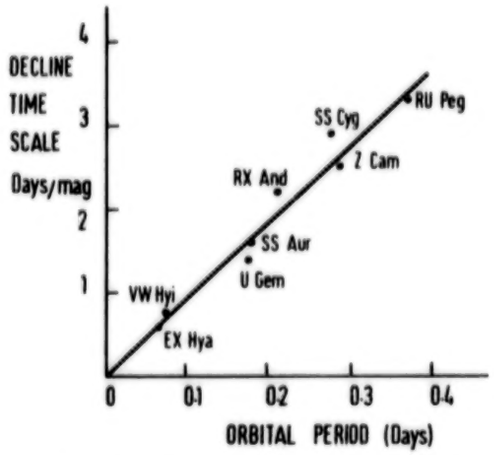


Figure 2-13. Bailey relation between the time for early decline from a dwarf nova outburst and the orbital period (Bailey, 1975).

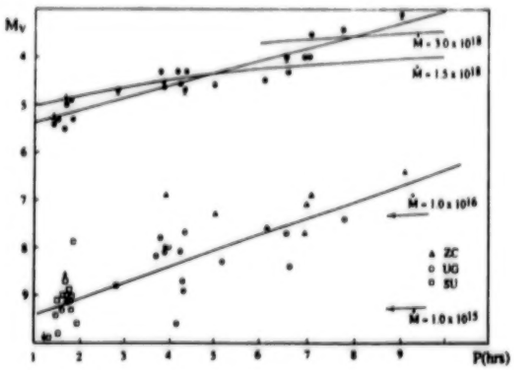


Figure 2-14. Relation between absolute brightness during outburst maximum and the orbital period (Warner, 1987).

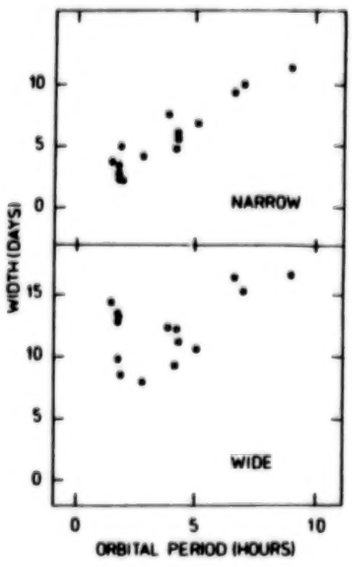


Figure 2-15. Relation between width of an outburst and orbital period (van Paradijs, 1983).

between the outburst amplitude A of dwarf novae and recurrent novae (which fit into the same relation) and their recurrence time (outburst period) P (*Kukarkin-Parenago relation*). Since then this numerical relation has been somewhat modified by others (Petit, 1958; Khopolov and Efremov, 1976; Greep, 1942; Payne-Gaposchkin, 1957; van Paradijs, 1985), but the differences in effect are small (Figure 2-12a). Extrapolation to outburst amplitudes to novae would predict recurrence times of several thousand years, so the relation appears not unreasonable. It is not known, however, whether there is a common physical process underlying this relation or whether it is a mere product of chance: the scatter for dwarf novae is large enough for the relation to not be very meaningful for any single object; the inclusion of recurrent novae gives it a convincing appearance, but this often has been ascribed to pure chance because of the presumed very different outburst mechanisms for dwarf novae and recurrent novae*; and whether or not this relation holds for novae cannot be tested due to the very definition of novae.

A revised version of this relation recently has been suggested by Antipova (1987) who correlates the total outburst energy (instead of the amplitude) with the outburst period. Assuming that all quiescent dwarf novae have the same absolute brightness (which is a very questionable assumption - see Chapter 4.II.C.2), and after applying some (largely arbitrary) correction for the contribution of the secondary star, dwarf novae (normal outbursts as well as superoutbursts), recurrent novae, and even GK Per (which exhibits dwarf nova-like outbursts during its quiescent state as a nova - see Chapter 8), all seem to fall on a nearly straight line (Figure 2-12b). Due to the assumptions Antipova made, however, it is questionable whether this relation actually reflects a common underlying physical process, as it seems to suggest.

*The outburst mechanism for recurrent novae is not known with certainty; it may or may not be the same as for novae; it clearly is not, however, the same as for dwarf novae, i.e., a collapse of the accretion disc.

Another relation, between the orbital period, P_{orb} and the rate of early decline of dwarf novae from their outburst, T (which always seems to occur in about the same way in each system, irrespective of the type of outburst), was first suggested by Bailey (1975) (*Bailey relation*, Figure 2-13):

$$T = 9.2\ P_{orb} \qquad (2.2)$$

Warner (1987) found a remarkably tight relation, namely that the absolute brightness of a dwarf nova during outburst increases approximately linearly as the orbital period of the system increases (Figure 2-14):

$$M_{V,max} = (5.64 \pm 0.13) - (0.259 \pm 0.024)\ P\ [hr] \qquad (2.3)$$

From inspection of published data in the literature, van Paradijs (1983) found a relation between the orbital period of a dwarf nova system and the width of wide and narrow outbursts, respectively (Figure 2-15):

$$W_{wide}\ [d] = (1.2 \pm 0.5) + (28.6 \pm 2.9)\ P_{orb}\ [d] \qquad (2.4a)$$

$$W_{narrow}\ [d] = (9.89 \pm 1.2) + (15.3 \pm 9.7)\ P_{orb}\ [d] \qquad (2.4b)$$

And finally, Szkody and Mattei (1984) suggest that three relations exist between the duration of the entire outburst of a dwarf nova (including rise and decline), the rise time and the time needed for decline, on one hand, and the orbital period on the other. None of these, however, looks in any way convincing.

II.A.4. STANDSTILLS AND SUPEROUTBURSTS

ABSTRACT: Z Camelopardalis stars at times discontinue their normal outburst activity for a while and remain at an intermediate brightness level. - Besides normal (short) outbursts, SU Ursae Majoris stars also show superoutbursts; these occur at more predictable intervals of time than normal outbursts, they last 5 to 10 times longer, and are slightly brighter.

see also: 96, 102

interpretation: 172, 178, 184

There are two special groups of dwarf novae, the Z Camelopardalis stars and the SU Ursae Majoris stars, both of which are classified on the basis of peculiarities in their outburst behavior.

The Z Camelopardalis stars behave like normal dwarf novae (U Geminorum stars) with short outburst periods most of the time, exhibiting all the normal features. Occasionally, however, at unpredictable times on decline from an otherwise seemingly normal outburst, they remain at a brightness level about midway to minimum brightness (Figure 2-16). This hold may last for a couple of days up to many months or years. Usually, after the end of such a *standstill,* the star returns to minimum brightness and resumes its normal outburst activity, which, however, may be ended by another standstill as soon as the next decline. However, at least one case is known (Mumford, 1962) in which a standstill of Z Cam ended in a rise to maximum. As can be seen in the example of Z Cam in Figure 2-16, before a period of standstill, the minimum brightness level reached between consecutive maxima may or may not increase continuously; and also a progressive decrease in the intervals between maxima before eruptions is observed occasionally. During standstills, brightness fluctuations of some tenths of a magnitude may occur which are reminiscent of the regular outburst behavior exhibited at other times.

The other special group of dwarf novae are the SU Ursae Majoris stars, for which the long outbursts (*superoutbursts*) are longer by about a factor of 5 to 10 than the short ones, and in all but one system (WZ Sge) occur much more seldom than the short (normal) ones. Extensive investigations of the outburst light curves of one of the best-known SU Ursae Majoris stars, VW Hyi, have been undertaken by Bateson (1977), Smak (1985), and van der Woerd and van Paradijs (1987). A part of the outburst light curve is presented in Figure 2-1b. All of these studies are based on the same compilation of data from almost 22 years of observations covering a total of 292 consecutive maxima, out of which 44 were supermaxima. The average time interval between normal (short) outbursts is 27.3 days; for superoutbursts it is 179 days; they last on the average for 1.4 and 12.6 days, respectively. The brightness at maximum is approximately 9.5 mag for normal and 8.5 mag for superoutbursts.

Normal outbursts of VW Hyi are like short outbursts of any other dwarf nova. Often a marked dip of up to 0.5 mag in a minimum brightness is seen immediately before the onset of an outburst, irrespective of whether it is a short or a long outburst, and often there is also an increase in brightness by about 0.5 mag as soon as the bottom of the decline has been reached.

Between three and eight normal outbursts can occur in VW Hyi between two consecutive superoutbursts (i.e., during a so-called '*supercycle*); the total length of the supercycle hardly is affected by this, but always has an average length of about 179 $\pm$12 days. The last normal outburst before a superoutburst always occurs less than 167 days after the last superoutburst. As for normal outbursts, immediately after a superoutburst they are narrower and fainter than usual, and they then become increasingly more energetic later in the supercycle (Figure 2-17). The length of normal cycles decreases with increasing supercycle phase. Irrespective of the total number of short outbursts within a supercycle, the first outburst in each cycle always starts within 17 to 29 days after the last supermaximum, while in general the time elapsing between two consecutive normal outbursts can vary between 10.9 and 70.7 days, with an average of 36.0 days. The last two normal outbursts before a superoutburst tend to have about equal length, which is either short (both cycles together last for less than 45 days: type S superoutburst) or long (both together last for more than 60 days: type

L superoutburst); no values in the gap between 45 and 60 days seem to exist (Figure 2-18). After about half of a supercycle has elapsed, it can be distinguished whether the last two cycles are going to be long or short: the lengths of normal outburst cycles for type S superoutbursts decrease, while those in type L superoutbursts increase. When they are long (type L), the maximum visual brightness of the following superoutburst tends to be larger, the longer these last quiescent intervals last; no such relation seems to exist for S-type cycles. There also is no difference between the total length of type L and type S supercycles.

According to their shape, Bateson (1977) divided the optical light curves of supermaxima into eight classes, S1 to S8 (Figure 2-19). The rise always is indistinguishable from the rise to short outbursts. For somewhat less than half of the observed superoutbursts of VW Hyi, a more or less pronounced decline (dip) of up to two magnitudes occurs in the optical after the typical maximum brightness of short outbursts has been reached, after which the superoutburst starts as if triggered by a normal outburst (classes S6 to S8). A number of investigators (Pringle et al, 1987; Verbunt et al, 1987; van Amerongen et al, 1987; Polidan et al, 1987; Heise et al, 1987) carried out simultaneous observations of VW Hyi in many wavelengths and found that, although there was no trace in their data of a precursor in the optical, it was clearly seen in the UV and at X-rays. The time elapsed since the last superoutburst tends to be shorter than the average (151 $\pm$12 days vs. an average of 163 $\pm$12 days) if the last normal cycle was short, and it is followed sooner by a normal outburst than by other supermaxima. Furthermore, the larger the pre-supermaximum dip, the more normal outbursts follow before the next supermaximum occurs, and the maximum brightness is the larger and the maximum the broader, the deeper the dip is.

Vogt (1980) undertook an extensive study of the outburst properties of those SU Ursae Majoris stars known at that time. One very striking feature of superoutbursts is their fairly strict periodicity which is kept within rather narrow limits, very unlike the short outbursts which, clustered about some mean value, occur at almost random intervals of time. The scatter of cycle lengths in SU Ursae Majoris stars amounts to roughly half the mean cycle length of normal outbursts, suggesting that superoutbursts may be triggered by normal outbursts. An even closer inspection of individual cycle lengths reveals that superoutbursts follow a very neatly defined linear ephemeris for typically 10 to 20 cycles, then they switch to another equally well defined ephemeris which is slightly different from the former one. For each star, a small number (typically two to three) of such superoutburst periods can be determined between which the star switches at random (Figure 2-20). The ratios between different cycle lengths of one star typically are on the order of 1.1 to 1.3. It remains to be seen whether similarly tight relations also hold for the more recently detected SU Ursae Majoris stars. An investigation of long outbursts of SS Cyg and U Gem did not yield any comparable results.

Vogt (1981) suggested a relation between the periods of normal outbursts and superoutbursts in SU Ursae Majoris stars. This relation looked quite convincing at the time he proposed it. Taking into account, however, the more recently detected SU Ursae Majoris stars and more modern values of outburst periods, there is no evidence for such relation any longer.

Based on the indication that probably all dwarf novae exhibit long as well as short outbursts, van Paradijs (1983) suggested that superoutbursts may be a general phenomenon in dwarf novae. Support for this comes from the observation that the duration of short outbursts seems to increase appreciably with the orbital period of the system, while the duration of long outbursts hardly does so (see above). The striking contrast between long and short outbursts in SU Ursae Majoris stars (all of which have very short orbital periods) appears to be a consequence of the increasing contrast

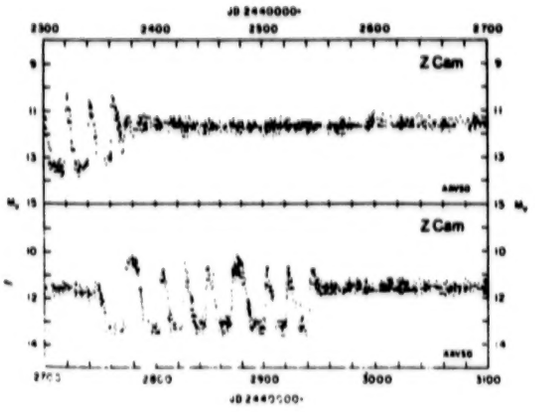


Figure 2-16. Outburst light curve of Z Cam (Lin et al, 1985 and see also Figure 2-1a). A standstill can be entered from either the bright state (the more frequent case) or from the quiescent state; in the particular example given the quiescent brightness level increased systematically before standstill was entered.

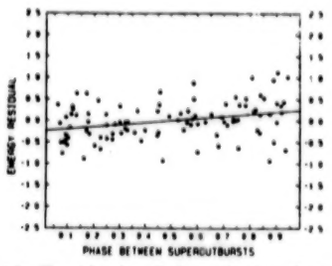


Figure 2-17. Residuals of the relation between outburst energy of VW Hyi and the duration of the preceding minimum versus supercycle (van der Woerd and van Paradijs, 1987). Before a superoutburst the short maxima become increasingly more energetic.

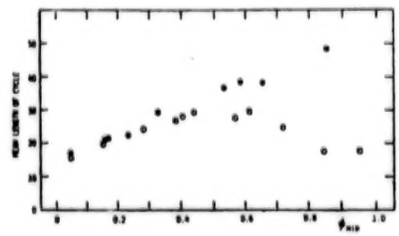
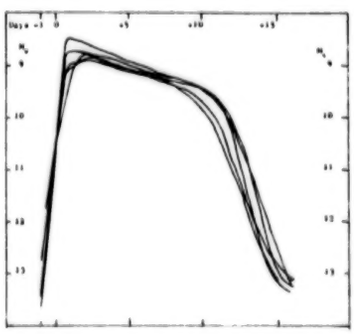


Figure 2-18. Mean length of normal cycles of VW Hyi as a function of the supercycle phase. Filled circles refer to L-type supercycles, open circles to S-type supercycles (see text for further explanation) (Smak, 1985).

a)



b)

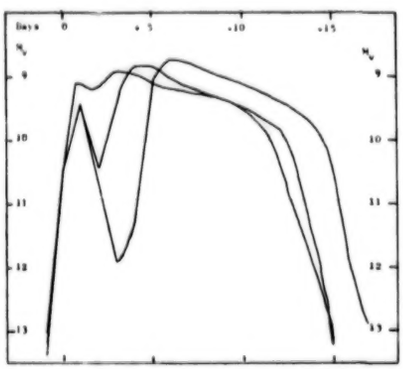
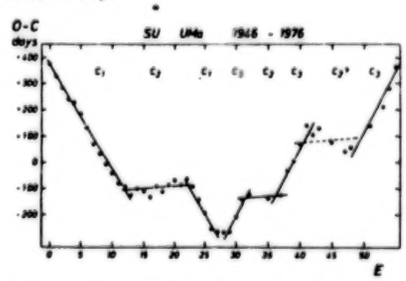


Figure 2-19. Classes of superoutburst light curves of VW Hyi with classes S1-S5 in 2-19a and S6-S8 in 2-19b (Bateson, 1977).

a)



b)

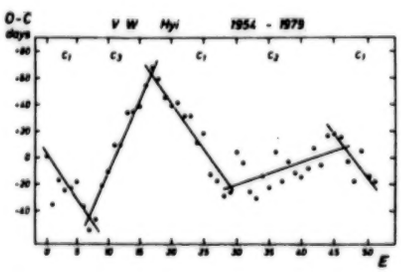


Figure 2-20. O-C residuals from a linear ephemeris versus supercycle number of superoutbursts of a) SU UMA and b) VW Hyi. The solid lines are fits to periods of constant cycle length (Vogt, 1980). Systems appear to switch between several possible intervals between successive superoutbursts; each period is followed for a certain time before the system switches to another one.

between wide and narrow outbursts with decreasing orbital period; with increasing orbital period, wide and narrow outbursts become more and more similar.

The definition of the term *superoutburst* implies the occurrence of other features, in particular small-scale variations with a period slightly in excess of the orbital period, the so-called superhumps (see Chapter 2.II.C.2). The fact that superhumps are not observed during long outbursts of long-period (i.e., non-SU Ursae Majoris) systems, van Paradijs (1983) ascribes to an observational selection effect which makes it very difficult (but certainly not impossible) to observe such periodicities. Observational tests of this hypothesis clearly are called for.

II.A.5. TEMPORARY SUSPENSION OF ACTIVITY

ABSTRACT: Some dwarf novae are known to have suspended their normal outburst activity altogether for a while. They later resumed it without having undergone any observable changes.

nova-like stars: 102, 113, 125

interpretation: 177

Some cases are known in which dwarf novae interrupted their normal outburst activity altogether for some months or years and only fluctuated close to minimum brightness. Later they resumed their normal activity without any apparent trace that any irregularities had happened. The transition from very low-brightness anomalous outburst activity to what appears to be an almost total cessation of it, seems to largely be a question of taste.

The earliest recorded event of this sort happened to SS Cyg in 1907/8 (see Figure 2-1c). At that time this was so confusing that it was questioned whether SS Cyg could reasonably be regarded as a dwarf nova any longer. Inspection of the light curve over very long intervals of time reveals, however, that, strange as such behavior may seem, SS Cyg is often seen to be on the verge of it.

Another similar example is SU UMa, which stopped virtually all relevant activity for over three years (AAVSO Circulars) before it returned to normal behavior. Mattei (1983, in discussion of Robinson, (1983)) hints at something similar having happened to HT Cas. Bateson (1985; see also Zhang et al, 1986) gives some evidence that the cycle length for superoutbursts in TU Men may have changed from values ranging between 123 and 162 days (for May 1963 to December 1981) to 164 to 517 days (in 1982 to 1984); it is not clear if this is merely a switch in cycle length as has been found for other dwarf novae (Vogt, 1980, see above) or if some major physical changes took place in the system.

II.A.6. COLOR VARIATIONS DURING OUTBURST CYCLE

ABSTRACT: The optical colors of dwarf novae all are quite similar during outburst, considerably bluer than during the quiescent state. During the outburst cycle, characteristic loops in the two-color diagram are performed.

interpretation: 173, 181, 193

Compilations of optical colors of cataclysmic variables can be found in Vogt (1983b), Bruch (1984), and Echevarria (1984). In Figure 2-21 the optical colors of dwarf novae during quiescence and during the outburst state are displayed in the two-color diagram. A few features become obvious: Dwarf novae are considerably bluer during outburst than during quiescence, and all dwarf novae have approximately the same optical colors during outbursts. SU Ursae Majoris stars statistically tend to be slightly bluer than other dwarf novae during quiescence in both (U-B) and (B-V), and they are bluer only in (B-V) during superoutbursts. In the two color diagram, all cataclysmic variables, in the faint as well as in the bright state, consistently appear above (i.e., are bluer than) the main sequence and often even above the black-body line.

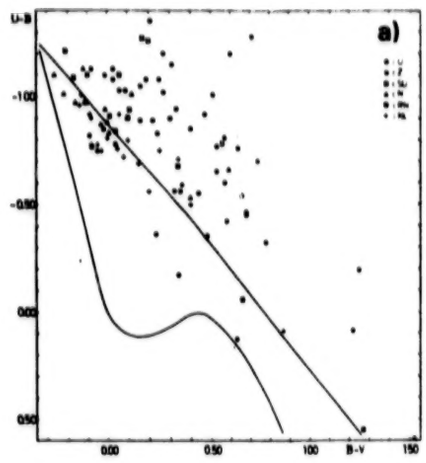


Figure 2-21a. Two-color diagram of cataclysmic variables during quiescence (corrections for interstellar reddening were applied wherever necessary); the solid lines represent the main sequence and black bodies, respectively (Bruch, 1984).

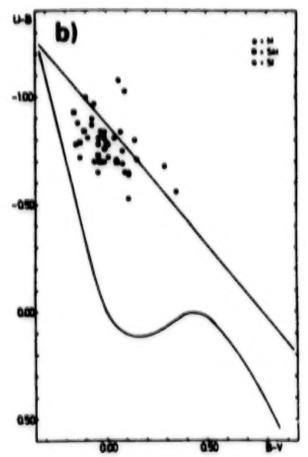


Figure 2-21b. Two-color diagram for dwarf novae during outburst. Presentation as in Figure 2-21a (Bruch, 1984). During outburst the optical colors of dwarf novae are remarkably similar.

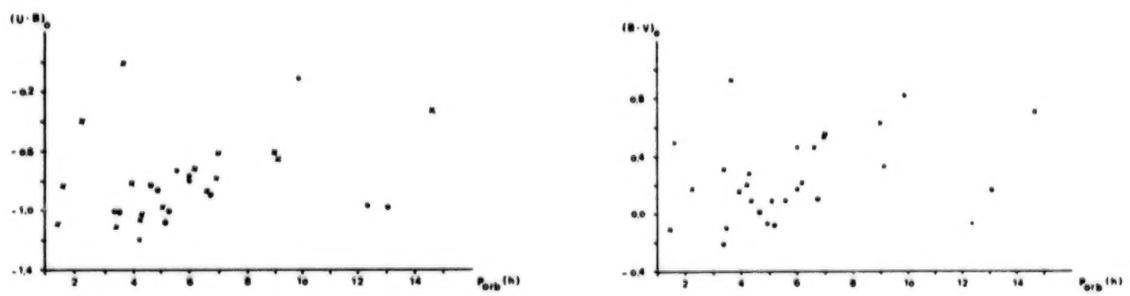


Figure 2-22. Relation between intrinsic optical colors of dwarf novae (x) and novae (o) during quiescence and nova-like stars (·) during the bright state versus the orbital period (values from Vogt, 1983b, Ritter, 1987). The longer the period the redder the systems appear.

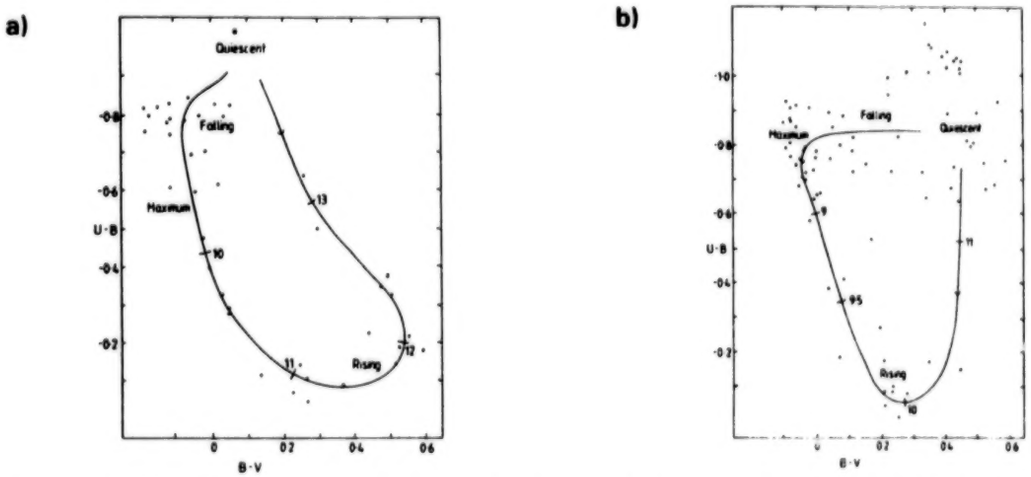


Figure 2-23. Loops of dwarf novae in the two-color diagram during the outburst cycle: VW Hyi (a) and SS Cyg (b) (Bailey, 1980). Color changes of dwarf novae during the outburst cycle seem to be rather characteristic for each object; the most pronounced changes occur during the rise phase.

A gap in the two-color diagram with a width of almost 0.2 mag in which no cataclysmic variables could be found was discussed by Vogt (1981); this gap was thought to be highly significant at that time, although it has since completely disappeared as more data have become available.

For cataclysmic variables with orbital periods in excess of some 3 hours, there may be a tendency for the colors to be loosely correlated with the orbital period of the system (Figure 2-22), although some otherwise not obviously peculiar systems do not follow this relation, and in the set of intrinsic colors as determined by Bruch (1984) this tendency is even less pronounced. It is remarkable that, again, cataclysmic variables of all different kinds follow the same relation. Systems with orbital periods shorter than 2 hours have about the same colors as other cataclysmic variables, but do not follow the above relation.

Only very few investigations of color changes in dwarf novae during the full outburst cycle have been carried out. It is obvious, however, that all dwarf novae perform a loop in the two-color diagram during such a cycle. Complete loops have been published for VW Hyi and SS Cyg (Figure 2-23). The data presented cover eight normal outbursts of VW Hyi and seven normal outbursts of SS Cyg. Single data points available for other objects (Z Cam, V436 Cen, WW Cet, U Gem, AH Her) follow the same trends. In all cases very large color changes take place during the fast rise to maximum. Color changes during the decline to quiescence are not very dramatic and take place slowly.

Single observations of VW Hyi during rise to supermaximum follow the same trends as observed for rises to normal outbursts. During rises to anomalous outbursts in SS Cyg, however, color variations are restricted almost entirely to changes in (B-V). Whether the same behavior can be observed during anomalous outbursts of other objects is as yet unknown.

GENERAL INTERPRETATION: The outbursts of dwarf novae are understood to be due to enhanced mass transfer through the accretion disc, a picture which can be reconciled with the observed color changes. The two possible scenarios which are currently discussed are: either temporarily enhanced mass transfer from the secondary star into the accretion disc, or a spontaneous release of material which was stored in the outer disc areas during quiescence. Standstills are believed to be semi-permanent outbursts, i.e., large mass transfers through the accretion disc which last for long times.

OBSERVATIONAL CONSTRAINTS TO MODELS:

- *Some dwarf novae not only undergo normal outbursts, but in addition also undergo superoutbursts or standstills. (See 184)*
- *Outburst durations (in all systems?) exhibit a bi-modal distribution.*
- *Long and short outbursts tend to alternate.*
- *It is not quite clear whether superoutbursts are merely a particular case of long outbursts, or whether they have a different physical cause. (See 184)*
- *TU Men, the SU Ursae Majoris star with the longest orbital period, is the only known system to undergo narrow and wide outbursts, as well as superoutbursts.*
- *There is some regularity, but no strictly repeated pattern, in the shapes of outbursts. (See 174)*
- *Outbursts occur semi-periodically rather than periodically. (See 174, 179)*
- *Superoutbursts follow a much stricter periodicity than other outbursts. (See 184)*
- *There are several superoutburst periods for each SU Ursae Majoris object, each of which is maintained for a while, until an abrupt change to a slightly different period occurs.*
- *Some objects occasionally stop all relevant outburst activity for a while. (See 177)*
- *Relations have been proposed between outburst amplitude and outburst period, between decay time and orbital period, and between absolute brightness during outburst maximum and orbital period. (See 177, 181)*

- *During the course of an outburst, color changes follow a certain characteristic pattern, which seems to be different for normal and for anomalous outbursts. (See 173, 181, 193)*

- *Dramatic color changes only seem to occur during the rise phase. (See 173, 181, 193)*

- *All dwarf novae have about the same optical colors during outburst, but not during quiescence. (See 193)*

- *For systems with orbital periods in excess of three hours, the optical colors in quiescence are related to the orbital period. (See 193)*

II.B. ORBITAL CHANGES DURING THE QUIESCENT STATE

ABSTRACT: At a time resolution on the order of minutes, strictly periodic photometric changes due to orbital motion become visible in the light curves of dwarf novae. These are characteristic for each system.

related spectroscopic changes: 73

nova-like stars: 96, 103, 114, 117, 123, 125, 140

interpretation: 151, 153

As the time resolution of photometric observations is enhanced from days or hours to minutes or seconds, many more structures in the light curves of dwarf novae become apparent. At first, features seen during the quiescent state of dwarf novae shall be described.

Three different features imposed on a generally flat light curve can be distinguished in the light curves of dwarf novae: a temporary increase in brightness by some tenths of a magnitude for about half of the orbital cycle, which is referred to as a *hump*; an *eclipse* lasting for a couple of minutes, the depth of which in some objects can reach some two magnitudes; and rapid, irregular brightness changes of some 0.5 mag, the so-called *flickering*, superimposed on the orbital light curve. In addition, brightness variations on time-scales of minutes or seconds with amplitudes of typically some 0.02 mag are seen in some objects. However, these usually are not apparent in the raw light curves (these will be discussed in Chapter 2.II.D.2). Eclipses and humps are variable from one object to another as well as to some extent in the same object, so that in general an orbital light curve never is strictly repeated. If these features occur, however, they appear with a very strict periodicity which in almost all objects (exceptions are, e.g., CN Ori and TT Ari, see Chapters 2.II.B.3 and 3.III.A.2) is identical with the periodicity in the radial velocity curve; neither outbursts of dwarf novae nor changes in the brightness state of nova-like stars change this phase relation.

II.B.1. ORBITAL LIGHT VARIATIONS IN THE OPTICAL

ABSTRACT: The appearance of the light curve is characteristic for each dwarf nova, but a wide range of appearances is possible for the whole class: some objects exhibit no periodic features at all, others show humps (occasionally, or in each cycle), intermediate humps, eclipses, or double eclipses, or even several of these features, and they all repeat with a strict periodicity. For most of the time the optical colors remain constant, conspicuous changes occur during eclipses.

see also: 46, 75

nova-like stars: 96, 103, 114, 117, 119, 122

interpretation: 151, 153, 166

Many of the known dwarf novae exhibit neither a hump nor an eclipse. An example is given in Figure 2-24. These objects still show appreciable brightness variability due to flickering activity, but no features can be detected which repeat strictly periodically.

Many others, however, possess more elaborate light curves. An example of an object exhibiting a very clear hump in the light curve is VW Hyi (Figure 2-25). The relative and absolute amplitudes of humps are variable from cycle to cycle, with a tendency for them to be brighter when the entire system is brighter (in

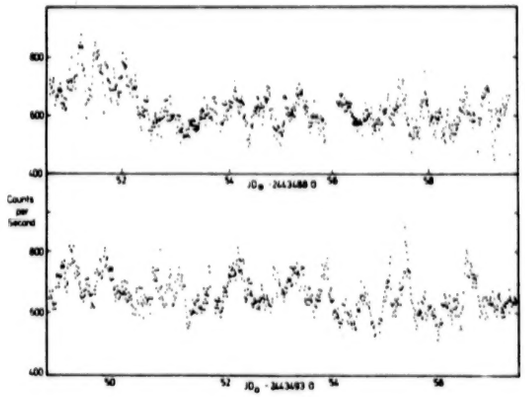


Figure 2-24. Optical light curve of V436 Cen (Bailey, 1979b). The light curves of some dwarf novae are entirely governed by irregular variations and show no periodically repeating patterns.

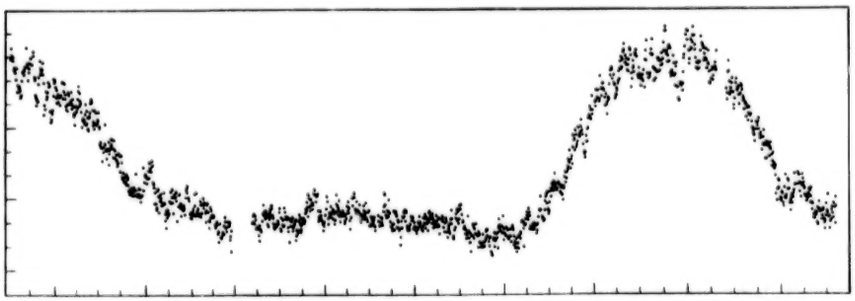


Figure 2-25. Optical light curve of VW Hyi (Warner, 1975). In other dwarf novae the hump repeats with a strict periodicity which turns out to be the orbital period.

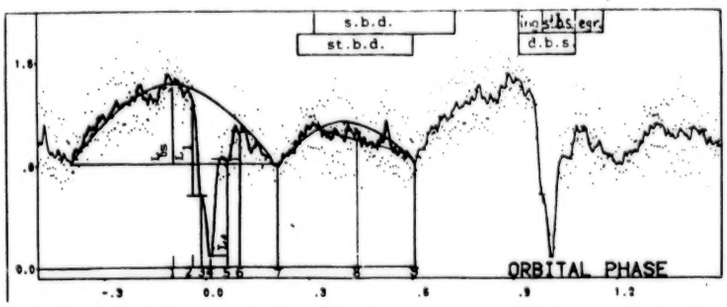


Figure 2-26. Optical light curve of OY Car (Schoembs and Hartmann, 1983). In some systems, in addition to the orbital hump, a so-called intermediate hump occurs which lasts approximately from the end of one main hump until the beginning of the next. OY Car possesses a so-called double eclipse (see text and Figures 2-29, 2-30, and 2-31).

many systems the brightness during quiescence varies by some tenths of a magnitude or more). If a hump is present, it normally lasts for about half of the orbital period, with beginning and end always occurring at approximately, though not precisely, the same orbital phases.

In addition to the main hump, other objects like BV Cen or OY Car (Figure 2-26) at times or always (depending on the system) exhibit an additional *intermediate hump* lasting from approximately the end of one main hump until the beginning of the next. The intermediate hump normally is considerably less pronounced in brightness than the main hump, and it is more variable in shape and brightness. As can be seen from the little scatter at the respective points in Figure 2-26 (which is the average light curve of 14 orbits), the beginnings and the ends of the main and intermediate humps are remarkably well defined.

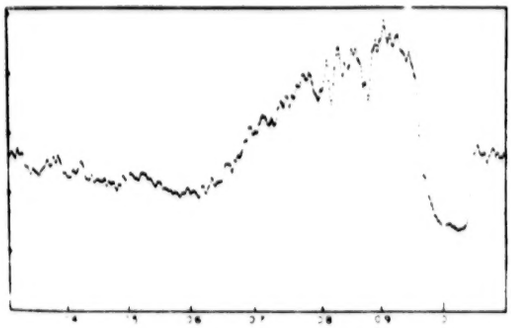


Figure 2-27. Optical light curve of U Gem (Warner and Nather, 1971). In several dwarf novae an eclipse occurs at the declining part of the orbital hump. It is mostly eclipsing systems which also exhibit an orbital hump.

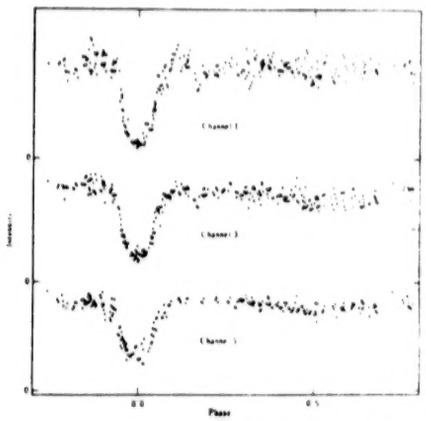


Figure 2-28. Orbital light curve of AC Cnc at 3330-3700 Å (Channel 1), 4300-4670 Å (Channel 3), and 5265-6005 Å (Channel 5), from Yamasaki et al (1983). There are some dwarf novae which have an eclipse but no hump at all.

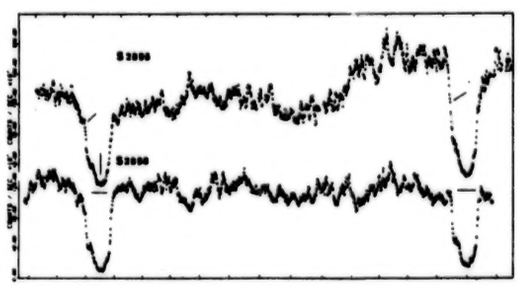


Figure 2-29. Orbital light curves of V2051 Oph (Warner and Cropper, 1983). In still other systems the orbital hump is present at times but absent at others.

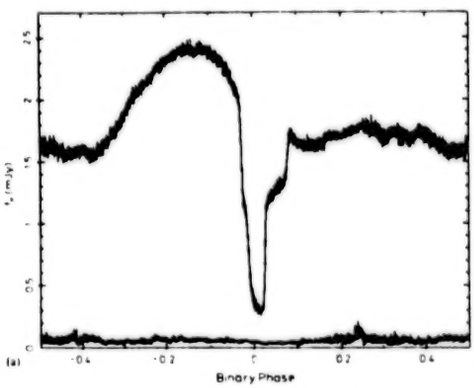


Figure 2-30. Optical light curve of Z Cha (Wood et al, 1986). In five known dwarf novae two eclipses occur, one during the other; this phenomenon is called a double eclipse.

In many objects, a fast considerable drop in brightness, the *eclipse*, occurs shortly after hump maximum (Figure 2-27). Its total duration usually is on the order of 0.1 of the orbital period. The exact shape of the eclipse also is subject to some variability if different minima of one object are compared. The general shape of the eclipse is approximately the same for all eclipsing objects with the exception of systems which show a so-called double eclipse (see below). No case of a dwarf nova is known in which the eclipse occurs at or before hump maximum (though in some nova-like stars this happens occasionally, see Chapters 3.II.C and 3.III.B), nor is there any case in which it occurs entirely outside the hump. Some objects are known, however, which do not have a hump but which do show an eclipse (Figure 2-28), or which, although they are eclipsing, show a hump at some times, though usually they don't (Figure 2-29).

Five dwarf novae (Z Cha, OY Car, V2051 Oph, HT Cas, IP Peg) are known to exhibit a very special kind of eclipse, the so-called *double eclipse* as shown in Figure 2-30: the ingress into eclipse, as it occurs in many other dwarf novae, holds for a short while at a brightness level somewhat below the normal brightness outside the hump, before ingress into even another eclipse occurs. The depth of these double eclipses can reach up to 2.5 mag. The egress also occurs in two steps, with the hold

between both parts of the rising branch being considerably longer than on the declining branch. Since these double eclipses potentially reveal a lot of information about the physical properties of the different components of the systems, they have been subject to extensive investigations (e.g., Warner, 1974a; Bailey, 1979; Patterson et al, 1981b; Warner and Cropper, 1983; Berriman, 1984; Cook and Warner, 1984; Cook, 1985a; Schoembs et al, 1986; Wood, 1986; Wood et al, 1986; Zhang et al, 1986). Inspection of examples of many different eclipses of every one of these objects (e.g., Figure 2-31) demonstrates how variable the eclipse shapes can be even from one orbital cycle to the next. It is clear from these observations that two light sources are eclipsed, and that the first sharp drop is the eclipse of the primary (or white dwarf, supposing the applicability of the Roche model), followed by the eclipse of the hot spot after a brief hold; after a more or less flat-bottomed minimum there is the egress of the white dwarf, followed after a longer hold, by the egress of the hot spot. This latter phase in the light cur e, the egress of the hot spot, is particularly variable from one cycle to the next. Also the ingress phases of the hot spot are variable, but much less so than the egress, and there seems to be no correlation between the durations of one and the other. The primary eclipse in all objects proved to be a highly stable feature.

The eclipse light curve of Z Cha has been investigated in detail by Warner (1974a), Bailey (1979a), and Cook and Warner (1984). In all these sets of observations the primary eclipse appears to be highly stable in its occurrence in orbital phases, with ingress and egress lasting for about 40 sec each. The eclipse of the hot spot, in contrast, is subject to appreciable variability. Warner noted holds before ingress and egress of 20 sec and 340 sec, respectively, whereas Bailey reported that the standstill before ingress lasts for 80 sec, and the standstill before egress often is not apparent at all. In Cook and Warner's data the standstill before egress of the hot spot lasts for some 300 sec. Furthermore, not only the orbital phases of the onset of ingress and egress of the hot spot are variable; the times for which both last are variable as well: times for the ingress have been observed to last between 84 and 207 sec, for egress between 42 and 203 sec (Cook and Warner, their Table 3). The brightness of the primary was constant within 20% for all the measurements by Bailey; the hot spot varies by nearly a factor of two in brightness; variations can be very strong at times, or approximately stable for a couple of orbital cycles. The flux level at the bottom of the eclipse is low and possibly variable, but essentially unaffected by minor brightness fluctuations of the system outside eclipse (see also Patterson et al, 1981b; Warner and Cropper, 1983).

If all these findings are regarded together, it is obvious that a dwarf nova consists of at least three sources of luminosity: one (the primary star) which is geometrically relatively sharply confined and has approximately constant brightness, a second (the hot spot, which in the Roche model is supposed to be located at the outer edge of the accretion disc) which is highly variable in geometrical position and dimensions as well as in brightness, and is much more extended than the primary and not spherically symmetric; and a third source (the secondary star) which is eclipsing the others and which is supposed to be responsible for at least part of the brightness remaining during eclipse minimum; another brightness contribution may originate from uneclipsed parts of the accretion disc.

At phases outside a hump or an eclipse, the optical colors of dwarf novae in quiescence are essentially featureless, subject to only irregular fluctuations of at most 0.05 mag. When a hump appears in the light curve, (U-B) becomes slightly redder during hump maximum and slightly bluer during hump minimum, and the total amplitude of the change is on the order of 0.1 mag (Figure 2-32). (B-V) usually is not variable at all with hump phase; if so, it is somewhat bluer at hump maximum and

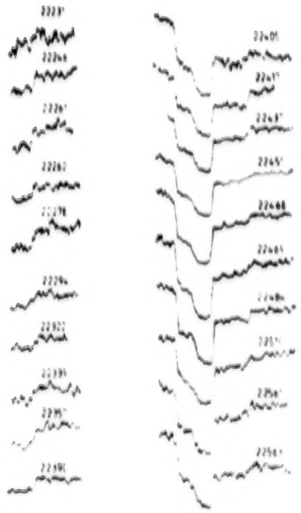


Figure 2-31. Double eclipses of OY Car (Cook, 1985a). The exact shape and duration of the double eclipse is variable from one orbital cycle to the next; the first ingress and egress are rather stable features.

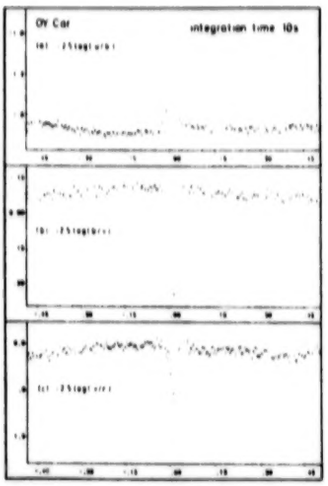


Figure 2-33. Orbital light and color curves of OY Car (Schoembs et al, 1986). During eclipse the system becomes bluer in (U-B) and redder in (B-V).

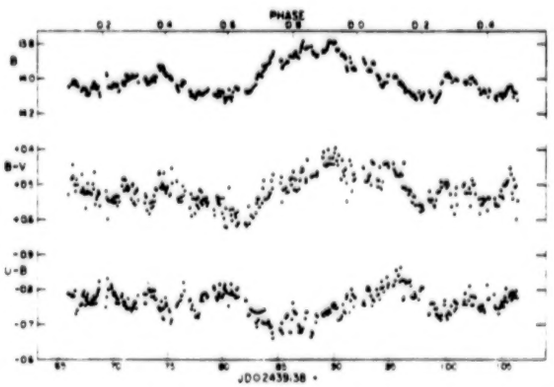


Figure 2-32. Orbital light and color curves of Z Cam (Kraft et al, 1969). Outside the hump the optical colors do not change; during times when the hump is visible the system becomes slightly redder in (U-B) and bluer in (B-V); in many systems (B-B) is hardly variable at all.

somewhat redder at hump minimum (e.g., Kraft et al, 1969). Truly conspicuous changes in the colors only occur during eclipse: (U-B) becomes considerably bluer, (B-V) equally considerably redder than during normal light (Figure 2-33). The same trend as in (B-V) (reddening during eclipse) can be seen in (B-R) and (B-I) light curves of OY Car (Schoembs et al, 1986). Observations of V2051 Oph by Cook and Brunt (1983), in addition to the blue peak during the very eclipse, show a short reddening in (U-B) at ingress and egress of the eclipse.

In general not much is known in detail about the color behavior of quiescent dwarf novae. Since the results which are available in the literature all show the same tendency, these probably are common to all dwarf novae.

II.B.2. ULTRAVIOLET AND INFRARED PHOTOMETRY

ABSTRACT: Hardly any information about photometric variability in the UV on orbital time scales is available. The contribution of the hump decreases with decreasing wavelengths. - At IR wavelengths in some dwarf novae, in addition to the

primary minimum a secondary minimum appears half an orbital period later; only in two (peculiar) dwarf novae is this minimum seen in the optical.

related spectroscopic changes: 74, 78, 80

nova-like stars: 99, 108, 115, 118, 121, 123, 135, 139, 142

interpretation: 151, 193

Due to the lack of powerful UV photometers, hardly anything is known about light variations of cataclysmic variables at UV wavelengths on time scales shorter than some dozens of minutes (i.e., shorter than the time resolution obtainable for cataclysmic variables with the IUE satellite). Phase resolved photometry of dwarf novae in the UV has been carried out by Wu and Panek (1982) with the ANS satellite (Figure 2-34). They observed U Gem and VW Hyi during their quiescent states with a time resolution of some 10 min. In VW Hyi there is a slight indication for the hump to be present at UV wavelengths, although with decreasing amplitude at shorter wavelengths. In U Gem, a system which shows a very pronounced hump at optical wavelengths, a comparable effect is not seen, neither in Wu and Panek's data, nor in the IUE. Clearly better time resolution and observations of more objects are desirable.

The situation is considerably better concerning the infrared wavelength range. Some dwarf novae have been observed at high time resolution during their quiescent states; no such observations during the outburst states have been published. Figure 2-35 shows a typical example of an IR light curve of a quiescent dwarf nova.

The depth of the primary eclipse and amplitude of the hump increase with increasing wavelength. OY Car so far is the only case where a sufficiently high time resolution has been achieved in the infrared to resolve fine structures of the primary eclipse (Figure 2-36 — compare with Figure 2-31). It appears that, although the general shape is changed appreciably at 12500 Å (J-band), the character of a double eclipse still is there.

In many systems at about phase 0.5 (with respect to the center of the primary eclipse), a secondary eclipse becomes visible which is not seen in the optical (the only two exceptions are the peculiar dwarf novae WZ Sge and BD Pav, see Chapter 2.II.B.4). The general character of all the light curves in the infrared changes from one cycle to the next, but the shape of the secondary eclipse is particularly severely affected by this.

The variety of infrared light curves among dwarf novae is huge, as far as one can tell from the still very limited number of available observations. In some objects, like EM Cyg (Jameson et al, 1981), the light curves in the IR still closely resemble the appearance in the V-band, with only the addition of the secondary eclipse (if the systems are eclipsing at all). U Gem and TW Vir, on the other hand, exhibit sinusoidally-shaped light curves in the IR, which are totally different in appearance from the optical light curves (Figure 2-37a, see also Mateo et al, 1985). In Figure 2-37b, observations are shown which were taken shortly before an outburst, and at the end of decline from the same outburst; both minima have been affected by the outburst, the secondary minimum to a much larger degree than the primary minimum.

II.B.3. CONTINUOUS LONG-TERM MONITORING

ABSTRACT: In some dwarf novae the quiescent brightness between consecutive outbursts undergoes systematic changes. Two dwarf novae were observed in a high speed photometric mode more or less continuously for many days during quiescent state each. The light curves show semi-periodic, in one case clearly transient, events.

interpretation: 174

SS Cyg and U Gem probably are those two dwarf novae which have been monitored best in their optical appearance over very long intervals of time (Mattei et al, 1985; 1987). In particular, a very good coverage of the quiescent light is available. Inspection of this reveals that

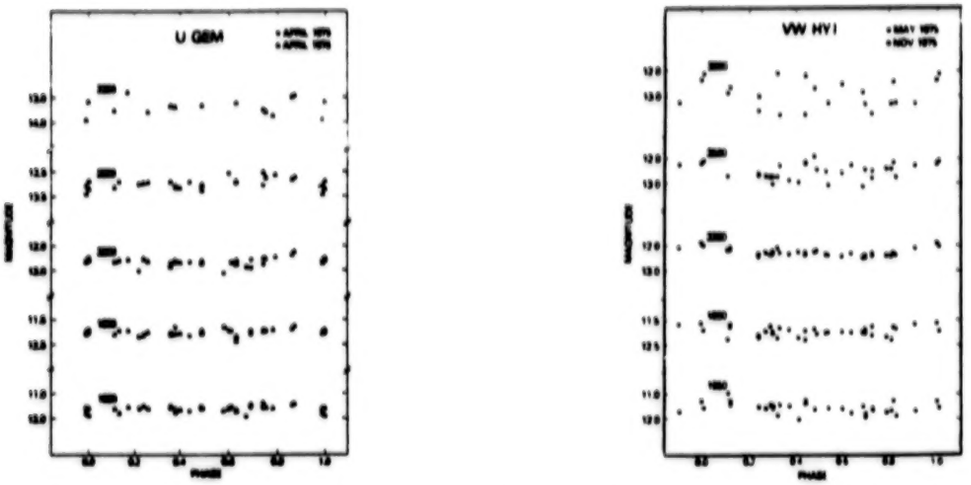


Figure 2-34. UV photometry of U Gem (a) and VW Hyi (b) (Wu and Panek, 1982). Possibly the orbital hump is seen in VW Hyi.

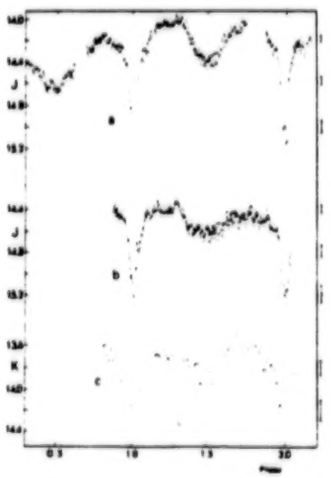


Figure 2-35. IR photometry of OY Car (Sherrington et al, 1982). The shape of the light curve varies appreciably with wavelength. A secondary eclipse is seen in the infrared.

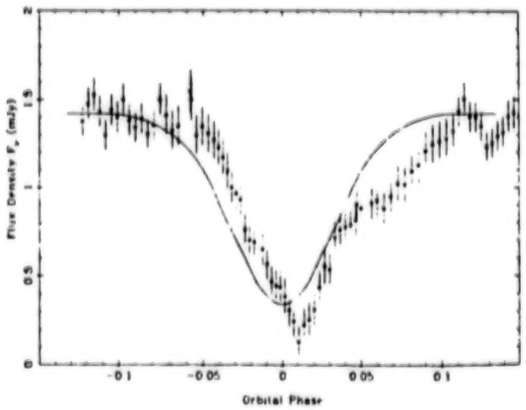


Figure 2-36. IR light curve of OY Car (Berriman, 1987). The double eclipse is still visible at IR wavelengths. (The solid line corresponds to a model discussed in Berriman's text.)

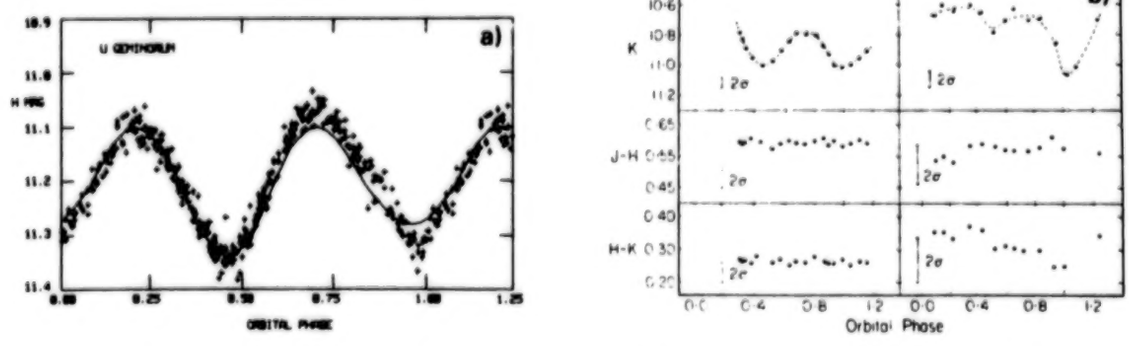


Figure 2-37. IR light curve of U Gem. a) During quiescence the light curve is approximately sinusoidally shaped (Oke and Wade, 1982, and optical light curve in Figure 2-27). b) It is highly distorted just after the end of an outburst (Berriman et al, 1983).

in U Gem the minimum flux level stays constant within fairly narrow limits between consecutive outbursts, and clearly no systematic trend of any kind can be detected. SS Cyg, on the other hand, while normally it has stable quiescent levels like U Gem (Figure 2-38a), exhibits at other times a systematic increase in flux level over several consecutive quiescent phases (Figure 2-38b); and at even other epochs, a very considerable decrease in the flux level can be observed between two consecutive outbursts (Figure 2-38c).

Semi-continuous monitoring of one star in a photometric high-speed mode over a time-interval of many days has been carried out in only one case: CN Ori was observed during quiescence from the end of decline from an outburst until the end of the next outburst (Figure 2-39), with only some short gaps in the light curve during quiesceuce. The hump amplitudes vary in a beat-like manner between the eruptions, with an additional superimposed general trend of increasing maximum light of successive humps; at the same time the minimum brightness of the inter-hump regions stays practically constant. A display of the entire minimum light curve on a larger time scale (Figure 2-40) reveals a large variability of the hump structure from one orbital cycle to the next, while the overall shape is approximately maintained. The times of minimum light between the humps are variable in duration, and the structure of the light curve is never exactly repeated from one cycle to the next.

The dwarf nova OY Car also has been monitored for a long time during quiescence, but this was done from only one observing site, so the gaps between runs of uninterrupted monitoring are longer than in the case of CN Ori (Figure 2-41). In this object additional minor "flares" of some 0.1 m lasting for 0.2 or less of the orbital period are superimposed on the otherwise very smooth and regular light curve (some of them are marked with "0" in Figure 2-41). A further investigation of the temporal repetition of these flares revealed that they repeated with a good periodicity, different from the orbital period, for about 6 days, and then they dissolved into irregularity. On one occasion a flare coincided with a double eclipse and became partly eclipsed itself.

II.B.4. WZ SGE AND BD PAV — TWO VERY UNUSUAL DWARF NOVAE

ABSTRACT: While WZ Sge displays two kinds of orbital light curves during its quiescent state, only one resembles that of a cataclysmic variable. Color variations are atypical for a dwarf nova. WZ Sge and the similar dwarf nova BD Pav have extremely long outburst periods.

comparison with "normal" dwarf novae: *see above*

One object is quite unique among the dwarf novae in almost all its characteristics, so occasionally it will have to be discussed separately. This object is WZ Sge. Originally it was classified as a recurrent nova because of its outburst period of about 33 years, because of its outburst light curve, and because of its large outburst amplitude of about 8 mag, which make its light curve look rather like that of an ordinary nova than like that of a dwarf nova (Figure 2-42). However, during the last outburst, in 1978, it was detected that WZ Sge exhibited superhumps which, by definition, qualify it as a SU Ursae Majoris star. Still, its optical light curve during the quiescent state was much different from that of a "normal" dwarf nova (Figure 2-43). At times the light curve closely resembled that of a W Ursae Majoris star (Krzeminski and Smak, 1971), i.e., it showed a sinusoidal light variation with two symmetric minima of comparable depth; at other times the behavior became more erratic, resembling the light curve of a cataclysmic variable with an eclipse placed on the declining branch of a hump. The appearance of the light curve changed back and forth, transitions from one to another occurring as quickly as within one orbital cycle. Shapes, and in particular, depths of minima were only approximately repeated. No extended photometry of

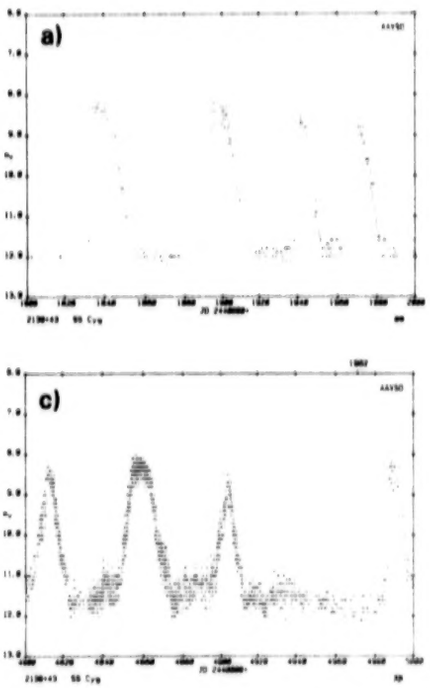


Figure 2-38. Outburst light curves of SS Cyg (Mattei et al, 1985). The quiescent light level between outbursts can be flat (a), it can rise systematically until the next outburst starts (b), or it can decline systematically (c).

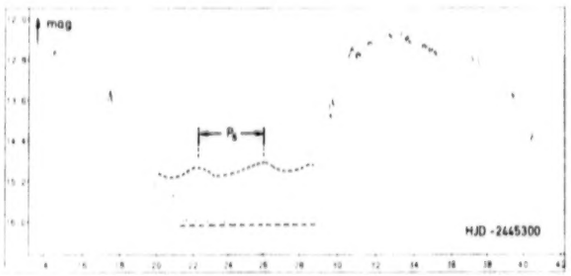


Figure 2-39. Light curve of CN Ori between two successive outbursts (Mantel et al, 1988). The minimum light level at interhump phases stays practically constant, while the hump amplitude undergoes cyclic variations.

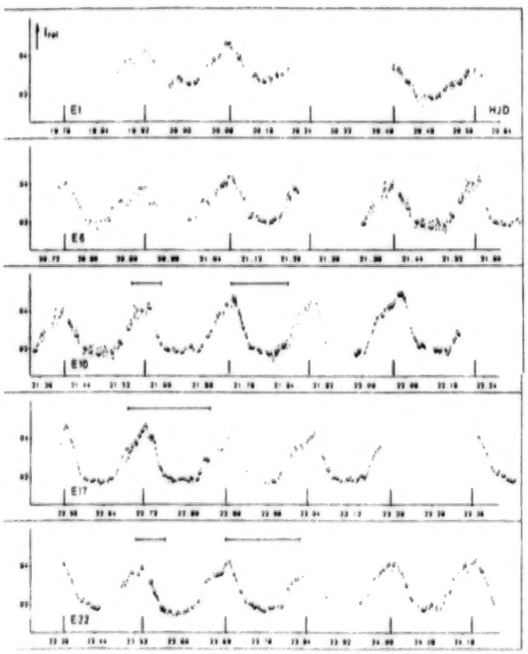


Figure 2-40. Same data as in Figure 2-39, at higher resolution (Mantel et al, 1988). The hump structure appears to be highly variable from one orbital cycle to the next.

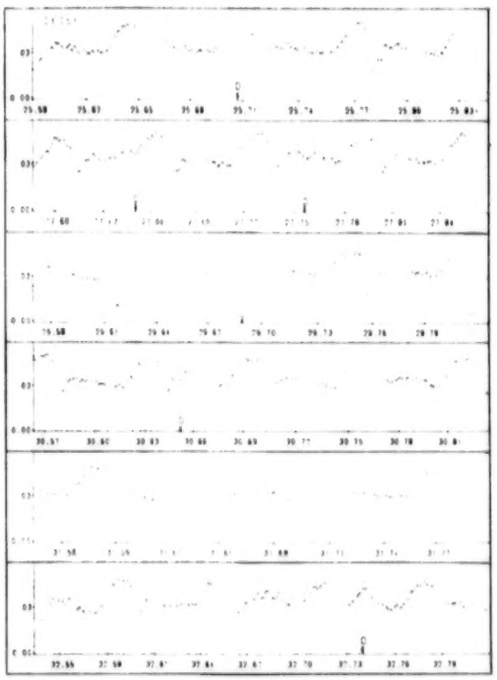


Figure 2-41. Optical light curve of OY Car in quiescence (Schoembs et al, 1986). For a while flares repeat with a good periodicity and then resolve.

ORIGINAL PAGE IS
OF POOR QUALITY

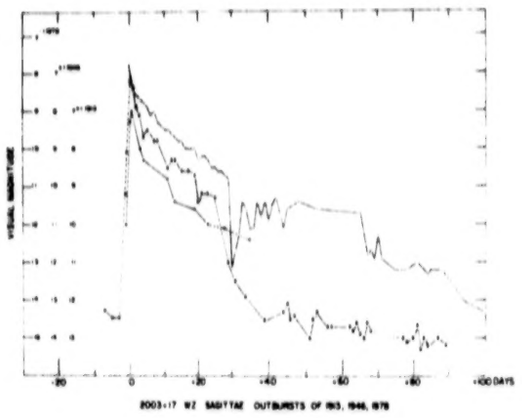


Figure 2-42. Outburst light curves of WZ Sge (Patterson et al, 1981b). The light curve resembles more that of a nova than that of a dwarf nova.

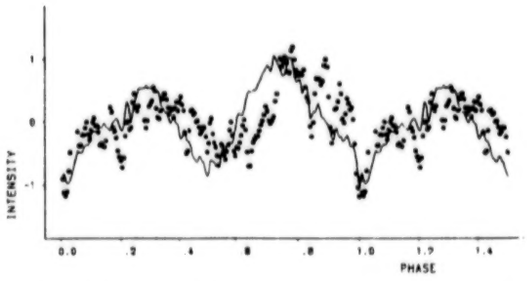


Figure 2-44. Orbital light curve of BD Pav, asterisks are observations in U light, the solid line corresponds to V (Barwig and Schoembs, 1983). In many ways BD Pav is similar to WZ Sge.

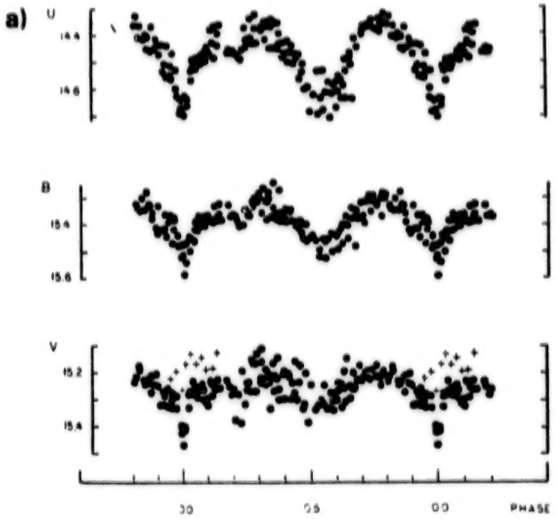


Figure 2-43. Orbital light curves of WZ Sge (a: Krzeminski and Smak, 1971; b: Warner and Nather, 1972). The character of the light curves is entirely different; changes can occur as quickly as within one orbital cycle.

WZ Sge after the 1978 outburst has been published.

One feature all the light curves of WZ Sge have in common is a "dip," a sort of additional eclipse-like feature at about phase 0.25. Its depth, exact phase (the minimum occurring between phase 0.2 and 0.4), width (ranging from 0.06 to 0.1 of the orbital period), and shape are very variable from one cycle to another. The depth, however, was never observed to drop below that of the primary minimum.

The primary minimum recurs with a stable period of 0.056688 days, irrespective of the shape of the light curve; its depth amounts to some 0.3 m in V but is variable, as are its shape and width (between some 200 and 300 sec). It usually, but not always, is flat-bottomed. When the light curve is of cataclysmic variable-type, the ingress and egress of primary eclipse are fairly steep and well defined. In the case of the W Ursae Majoris-type light curve, a secondary eclipse is clearly visible. Its exact shape and depth, however, are highly variable, and, in particular, it occurs somewhere between phase 0.50 and 0.59 with respect to the primary eclipse (Krzeminski and Smak, 1971) and not, as expected for an eclipse of a stellar object, always at the same phase; or it even can disappear completely. In the cataclysmic variable-type light curve, an eclipse-like feature occurs around phases 0.4 to 0.5, but neither its shape nor its position is repeated even approximately.

There is a very strong color dependence of the light curves; in particular, the secondary

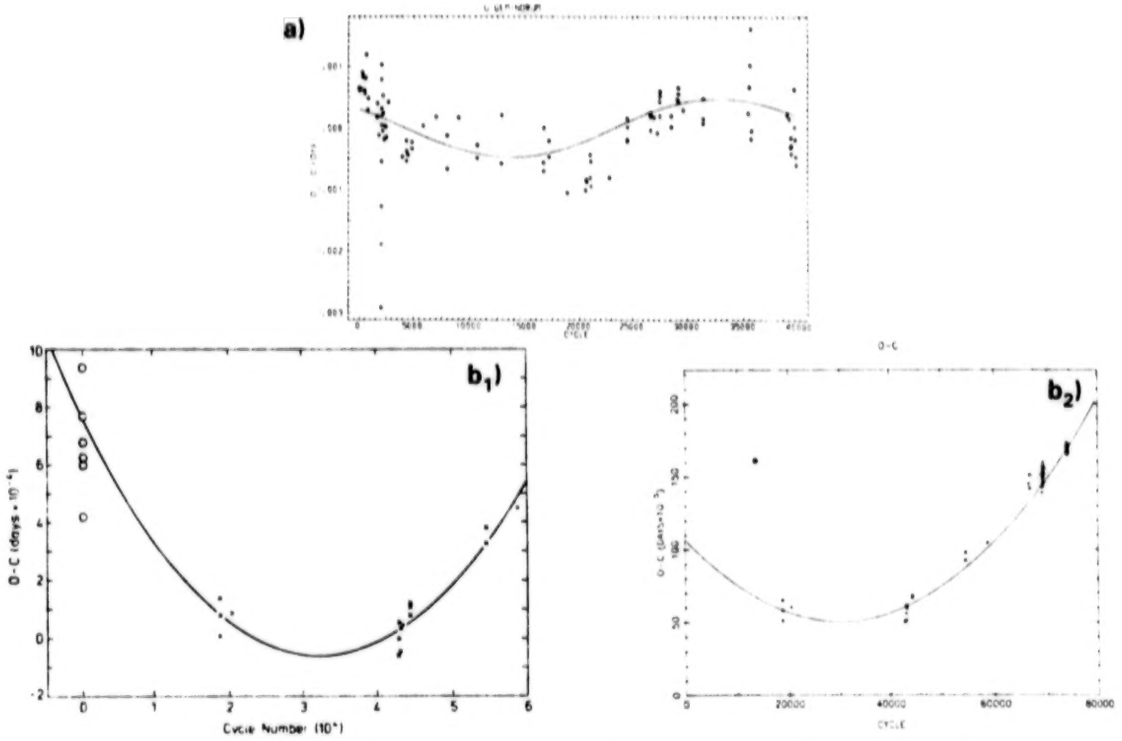


Figure 2-45. Secular variations of the orbital period were observed in several dwarf novae. In U Gem (a) the variation appears to be cyclic (Eason et al, 1983); in Z Cha (b1 and b2) it appears to be steadily increasing (Wood et al, 1986).

eclipse can at times completely disappear in V while it is well visible at shorter wavelengths (U and B). In both sorts of light curves, the W Ursae Majoris-type and the cataclysmic variable-type, color variations in WZ Sge are opposite to what normally is observed in dwarf novae (see Chapter 2.II.B.1 and Figure 2-33): during primary eclipse the system becomes slightly bluer in (B-V) or does not change at all, but in (U-B) it becomes strongly redder; during secondary minimum the system becomes redder in both colors.

BD Pav is a system reminiscent of WZ Sge. Originally it also was classified as a nova (outbursts were observed in 1934 and 1985 — Duerbeck, 1987), but new observations rather let it appear as a dwarf nova with very long outburst periods (Barwig and Schoembs, 1983). The quiescent light curve looks similar to the cataclysmic variable-type light curve of WZ Sge (Figure 2-44). Strong flickering is present at all orbital phases, possibly slightly diminished during a periodically recurring narrow eclipse. The brightness variations in the U and V filters coincide during eclipse but are out of phase by up to 0.1 of the orbital period 180° away from eclipse. Colors are remarkably red for a cataclysmic variable of as short a period as BD Pav has.

II.B.5. SECULAR VARIATIONS OF THE ORBITAL PERIOD

ABSTRACT: Secular changes of the orbital period have been measured in several dwarf novae. In some objects, changes seem to be semi-periodic with time-scales on the order of 10 years.

nova-like stars: 98, 111, 115

interpretation: 186

As discussed above, the detailed shape of the orbital light curve of a dwarf nova usually is somewhat variable. The period with which humps or eclipses occur, however, is very stable, and phase relations seen during minimum are not disturbed by the eruptions. Nevertheless, in a couple of systems, very slow systematic period changes seem to occur.

The two best studied cases are U Gem in which the orbital period appears to cyclically decrease and increase (Figure 2-45a), and Z Cha in which the observations suggest that the period increases on a time-scale of $P/\dot{P} = 2.46\ 10^7$ years (Wood et al, 1986, and Figure 2-45b). Similar general trends might be contained in the data from other systems (e.g., Beuermann and Pakull, 1984). Clearly more observations are needed in order to determine whether these changes are significant, whether this behaviour is universal in dwarf novae or even in cataclysmic variables in general, and whether these all rather are cyclic variations as seen in U Gem.

A different sort of period changes was observed in CN Ori. From data taken during the decline from one outburst and the rise to the following one, which occurred after only a very short stay of the star at quiescent brightness, Schoembs (1982) determined two photometric periods of some 234.9 and 229.6 min, respectively, from the times at which hump maxima occurred, and when the entire run was analyzed together; on the other hand when decline, minimum, and rise were analyzed separately, hump periods of 233.6, 234.8, and 235.7 min, respectively, were obtained (Mantel et al, 1988). Observations taken one year later confirm none of these periods (for the data base, see Figure 2-39): derivation of a period from hump maxima yielded a period of some 236.0 min.

For dynamical reasons it can be excluded that these photometric periods reflect actual changes of the orbital period of the system. Instead, it seems that hump maxima do not repeat at exactly the same orbital phase in all objects. This result probably needs to be taken into account when evaluating the reliability of orbital changes in cataclysmic variables.

GENERAL INTERPRETATION: Orbital changes in cataclysmic variables are ascribed to periodically varying aspects under which the binary system is seen. Systems which are seen almost pole-on display hardly any photometric changes; while the larger the angle of inclination becomes, i.e., the more the system is seen edge-on, the more pronounced become light contributions from the hot spot, which are visible as a hump in the light curve. At very high inclinations the hot spot, and at even higher inclinations also the central object, are eclipsed by the secondary star, thus causing a single or a double eclipse, respectively. Due to the varying shape, temperature, and position of the hot spot, its eclipse as well as its spectral distribution are variable, while the eclipse of the central white dwarf/boundary layer is a stable feature. At IR wavelengths, light contributions from the secondary star become prominent; under certain conditions this star can be eclipsed by the disc around orbital phase 0.5, or the IR variation, if sinusoidal, can be due to rotational variations of the non-spherical secondary star.

OBSERVATIONAL CONSTRAINTS TO MODELS:

- *In several objects there occurs an intermediate hump.*
- *CN Ori, at various times exhibits different photometric periods; it is not clear which, if any, is the orbital period.*
- *The hump amplitude in CN Ori during quiescence was observed to undergo quasi-periodic variations, while the brightness of the inter-hump regions did not change.*
- *The orbital period of some dwarf novae seems to be variable. (See 186)*
- *WZ Sge and BD Pav, in several respects, are very unusual dwarf novae.*

II.C. ORBITAL CHANGES DURING THE OUTBURST STATE

ABSTRACT: Remarkably little is known about orbital variations during the course of an outburst.

Given the importance of outbursts in the life of a dwarf nova and the many observations of them that have been carried out, remarkably little is known about the orbital light curves during the outbursts. Due to its intrinsic unpredictability, it is difficult to observe the very start of a rise. Still, such observations are of particular importance for investigations of the outburst behavior since they can put constraints

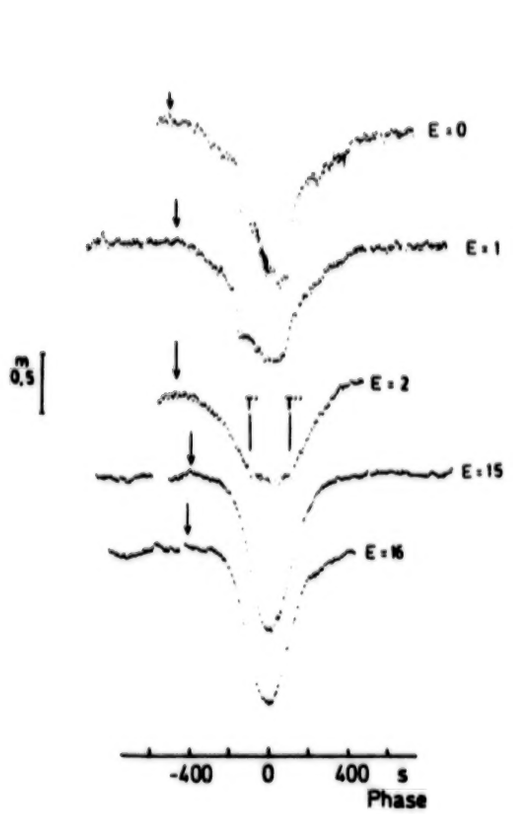


Figure 2-46. Development of the eclipse shape in OY Car during rise to an outburst, epochs (E) are counted from onset of rise (Vogt, 1983a). Gradually the double eclipse evolves into a single one.

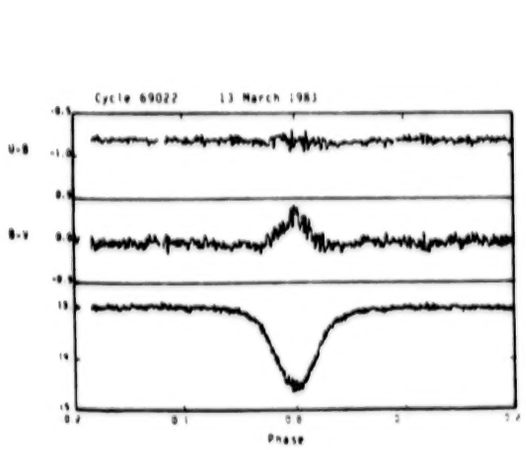


Figure 2-47. Orbital color changes in Z Cha during a normal outburst (Cook, 1985b). Changes are comparable to what is seen during quiescence.

on possible theoretical models (Chapter 4.III). In spite of considerable effort, so far it has not been possible to fully monitor the transition from quiescent state to outburst in any dwarf nova. Nevertheless, some very valuable information is available, about the rise phase as well as about the further development of a dwarf nova outburst.

II.C.1. NORMAL OUTBURSTS

ABSTRACT: Observations seem to indicate that an outburst starts without any previous notice. Hump light curves can be traced all through the outburst, and the hump amplitude is more variable than during quiescence, though mostly of about the same intensity. Single eclipses largely disappear, and double eclipses become single during light maximum.

related spectral changes: 65, 81

nova-like stars: 96, 103, 113, 114, 117, 119, 122, 125, 140

interpretation: 151, 153, 194

All available observations of different dwarf novae indicate that the onset of an outburst occurs rather suddenly without a conspicuous precursor. Figure 2-39 shows an observation of CN Ori in which this critical phase was almost covered (similar observations are reported in Schoembs, 1982). In the quiescent light curves immediately preceding the rise, no indication like, for instance, increased hump intensity, can be detected for the outburst to come. In CN Ori the hump intensity remains constant during rise until an optical brightness of about 13.5 m is reached. Then the hump shape becomes rather irregular for the greater part of the outburst with occasional, brief flare-like, appreciable brightness increases. The hump only gains back its quiescent shape at the optical brightness of, again, some 13.5 m on decline (Mantel et al, 1988).

Several observations of the rise to an outburst of VW Hyi are available (Vogt, 1974; Warner, 1975; Haefner et al, 1979). Normally the hump amplitude remains constant within a factor of two during rise; it becomes almost invisible for some two days around maximum light (when the disc is very bright), probably due mostly to contrast in intensity, and recovers at decline, resuming the old orbital phase relation. Rather dramatic changes of the hump in-

tensity from one cycle to the next, reminiscent of the observations of CN Ori reported above, were seen during one outburst of VW Hyi (Warner and Brickhill, 1978). On one occasion the hump amplitude was seen to be enhanced by a factor of up to 8.7 on the rising branch, at a phase in the outburst cycle when normally it is not appreciably changed with respect to its quiescent brightness. On one other occasion, for a few days during minimum light immediately after outburst, the hump shape and amplitude, were seen to be more intense and less stable than later during the quiescent state.

At times VW Hyi, like some other dwarf novae, in addition to the normal hump, exhibits a highly variable intermediate hump about half a period out of phase with the normal hump (Figure 2-25). This *intermediate hump* usually is much less intense than the orbital hump. It disappears during rise and only occasionally is visible during outburst maximum. In one of the observed outbursts it grew quickly in intensity as outburst maximum was approached, and exceeded the intensity of the main hump by a factor of three; during the next night it was very faint (Haefner et al, 1979). No relation could be detected between the amplitude of the hump, or that of the intermediate hump during the course of the outburst and any other characteristics of the outburst. Similar observations of other dwarf novae mostly indicate that the intensity of the hump remains mostly unaffected by an outburst.

The double eclipsing dwarf nova OY Car was observed photometrically by Vogt (1983a) during the rise to an outburst (Figure 2-46). At early rise the double eclipse is fully present, like it is in quiescence; as the rise proceeds the eclipse becomes single and flat-bottomed, while the depth and the phases of ingress and egress remain unaffected. At maximum light the ingress occurs later and the egress earlier than during quiescence, the eclipse becomes very deep, partial, and symmetric. Similar conclusions can be drawn from less complete observations of Z Cha (Vogt, 1982a).

On the declining branch the development of the eclipse shape is approximately reverse from what is seen during rise: during maximum light it is deep and partial; at a somewhat later stage it first becomes flat-bottomed, but still is single; slowly then, during the course of a couple of days, the double eclipse in its original shape is restored step by step (Figure 2-52). Other eclipsing dwarf novae were observed to show very similar behavior. Although the shape of the eclipse and times of ingress and egress change during the outburst, the post-outburst light curves follow the same phase relations as before outbursts. In addition, in some objects the eclipse appears wider right after an outburst than just before rise, but times of mid-eclipse don't change (Krzeminski, 1965; Cook, 1985b).

Cook (1985b) carried out color measurements of Z Cha during a normal outburst and found that, like during the quiescent state, the system becomes significantly redder in (B-V) during the eclipse, whereas, unlike in quiescence where the more pronounced reddening is in (U-B), during outburst maximum there is no change in this color (Figure 2-47).

II.C.2. STANDSTILLS AND SUPEROUTBURSTS

ABSTRACT: Orbital light curves during standstills cannot be distinguished from those at comparable brightness levels during normal outbursts. During superoutbursts very characteristic superhumps can be observed. Their recurrence period is slightly larger than the orbital period and survives in the form of the late superhump for some time after the end of the superoutburst. Only once were superhumps seen during an ordinary outburst of an SU Ursae Majoris star.

related spectral changes: 48

interpretation: 178, 184

No peculiarities have been observed during times of standstill in Z Camelopardalis stars. The light curves do not look any different from those of comparable brightness stages during normal declines from outburst.

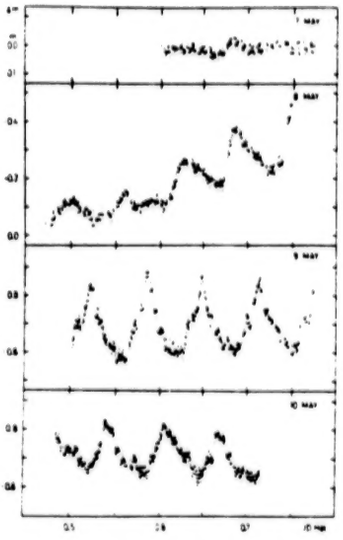


Figure 2-48. Formation and development of superhumps in V436 Cen (Semeniuk, 1980). It starts to develop at late rise just before outburst maximum; at maximum (May 9) the amplitude is largest, during the slow decline on the plateau it gradually decreases.

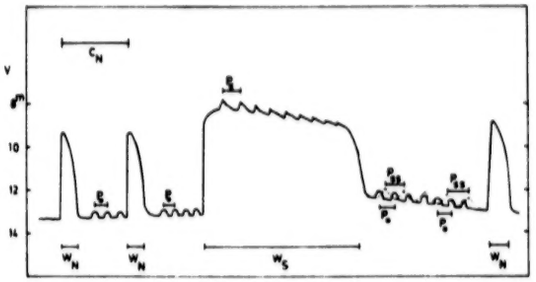


Figure 2-49. Main features of a superoutburst (Vogt, 1983c). At about superoutburst maximum the superhumps originate and very quickly reach their maximum amplitude; superhumps recur with a period P_s that is slightly longer than the orbital period P_o; during the course of the outburst, on the plateau of the superoutburst, the superhump amplitude gradually disappears while the superhump period decreases slightly; after the fast decline from superoutburst the remains of the superhump and the orbital hump interfere with each other to form the late superhump with a period P_{ss}.

Superoutbursts of SU Ursae Majoris stars, however, do present several peculiarities, all of which were seen in all observed superoutbursts. In fact, normal outbursts of SU Ursae Majoris stars in general cannot be distinguished from outbursts of other dwarf novae, nor do they exhibit any of the typical SU Ursae Majoris features (as discussed below). Also there is no intermediate type of outburst. One single exception to this is known of one short outburst of VW Hyi exhibiting superhumps (Marino and Walker, 1979). This outburst occurred shortly before the expected time for a superoutburst; the next outburst was the then somewhat delayed superoutburst.

Originally the class of SU Ursae Majoris stars was defined by their occasionally exhibiting *superoutbursts*, i.e., outbursts of exceptionally long duration which also are slightly brighter than normal outbursts (Brun and Petit, 1952 and also Chapter 2.1). Observing the same superoutburst of the SU Ursae Majoris star VW Hyi with high time resolution in December 1972, Vogt (1974) and Warner (1975) independently detected the presence of strong hump-like features during light maximum, whereas most dwarf novae show only weak, if any, humps during the bright state, as does VW Hyi during normal (short) eruptions. More striking than their presence was the fact that these *superhumps* repeated with a period that was some 3% longer than the orbital period as determined from the quiescent hump. Since then the presence of superhumps in addition to, or almost rather than, long outbursts has become the defining characteristic of SU Ursae Majoris stars. The most recent edition of Ritter's catalogue (1987) lists 18 SU Ursae Majoris stars, and their number probably will keep increasing, as it did during the last decade, since the search for superhumps and investigation of the SU Ursae Majoris stars has become fashionable, and, correspondingly, a lot of detailed information about their properties has become available.

Superhumps have been observed during all superoutbursts in all stars which ever have been observed to exhibit them. The rise to a superoutburst cannot be distinguished from the rise to a normal outburst. Superhumps

normally do not develop until some time after maximum brightness of a normal outburst has been reached. Their appearance usually is accompanied by a further brightness increase by some tenths of a magnitude. Figure 2-48 gives an example of the light curve of V 436 Cen during a superoutburst. In VW Hyi, there often occurs a drop in brightness before the final rise to a superoutburst (Figure 2-1b); the superhump normally does not develop until rise to the very supermaximum (Marino and Walker, 1979).

During the first one or two days after its appearance, the superhump develops to reach an intensity of some 30% to 40% of the total system intensity, then the amplitude decreases as the superhump proceeds. Unlike the minimum hump, its shape is well-defined and repeats with some flickering superimposed. The shape usually is slightly asymmetric with the rise to maximum light being faster than the decline. A decline from superhump maximum usually is immediately followed by the next rise without a longer interhump phase of constant brightness. Warner (1985a) points out that there is some indication for the superhump amplitude to be modulated by the orbital hump, indicating that the latter still might be present at the appropriate phase also during superoutbursts.

The main features of a superoutburst are given schematically in Figure 2-49: the superhump develops around maximum brightness, and quickly reaches its maximum amplitude and period. Both decrease gradually during the course of the outburst, and the superhump becomes almost undetectable at the end of the *plateau*, i.e., before the steep decline to quiescence. Already at about the middle of the plateau, the original superhump structure resolves into many distinct features of comparable strength, all of which still repeat with the superhump period (Figure 2-50), while the original superhump disappears. After, in a steep drop of intensity, the star has returned to almost minimum brightness the so-called *beat phenomenon* occurs: one of the features, the *late superhump*, which is about 180° out of phase with the original superhump, for some time modulates the amplitude of the orbital hump with the beat period of the orbital motion and the superhump period (Figure 2-50).

Superimposed on the general shape of the superoutburst and the decay of the superhump amplitude, Schoembs (1986) found in OY Car a semi-periodic brightness variation with a periodicity of some 3 days persisting well into the quiescent level (Figure 2-51).

Superhumps occur in all SU Ursae Majoris stars irrespective of the angle of inclination of the system with respect to the observer on Earth. It is observed with comparable strength for instance in OY Car (which exhibits a double eclipse in quiescence, indicating an inclination on the order of 90°), in VW Hyi (which shows only a hump) and in WX Hyi (which has neither a hump nor an eclipse at minimum light, thus probably having a very low inclination angle of some 30° or 40°). In all cases the superhump period is a few percent longer than the orbital period (extremes are between 0.8% for WZ Sge and 12.7% for TY Psc; the average is some 3% or 4%). During the course of a superoutburst in most objects the superhump period decreases slightly, though never reaching the length of the orbital period; however, in V436 Cen and OY Car there is indication for an increase of the superhump period with time. For any object the superhump period and its rate of temporal change are constant within the error limits for all outbursts (e.g., van Amerongen et al, 1987b).

In OY Car, Z Cha, and WZ Sge pronounced "dips" (of some 5% to 10% of the intensity) in the light curve have been observed (Figure 2-52, marked with "D") which are too strong to be attributed to flickering; they also cannot be eclipse features since their orbital as well as their superhump phases are variable. Closer inspection reveals that in all three objects the dips cluster about times when the orbital and superhump phases coincide (Schoembs, 1986).

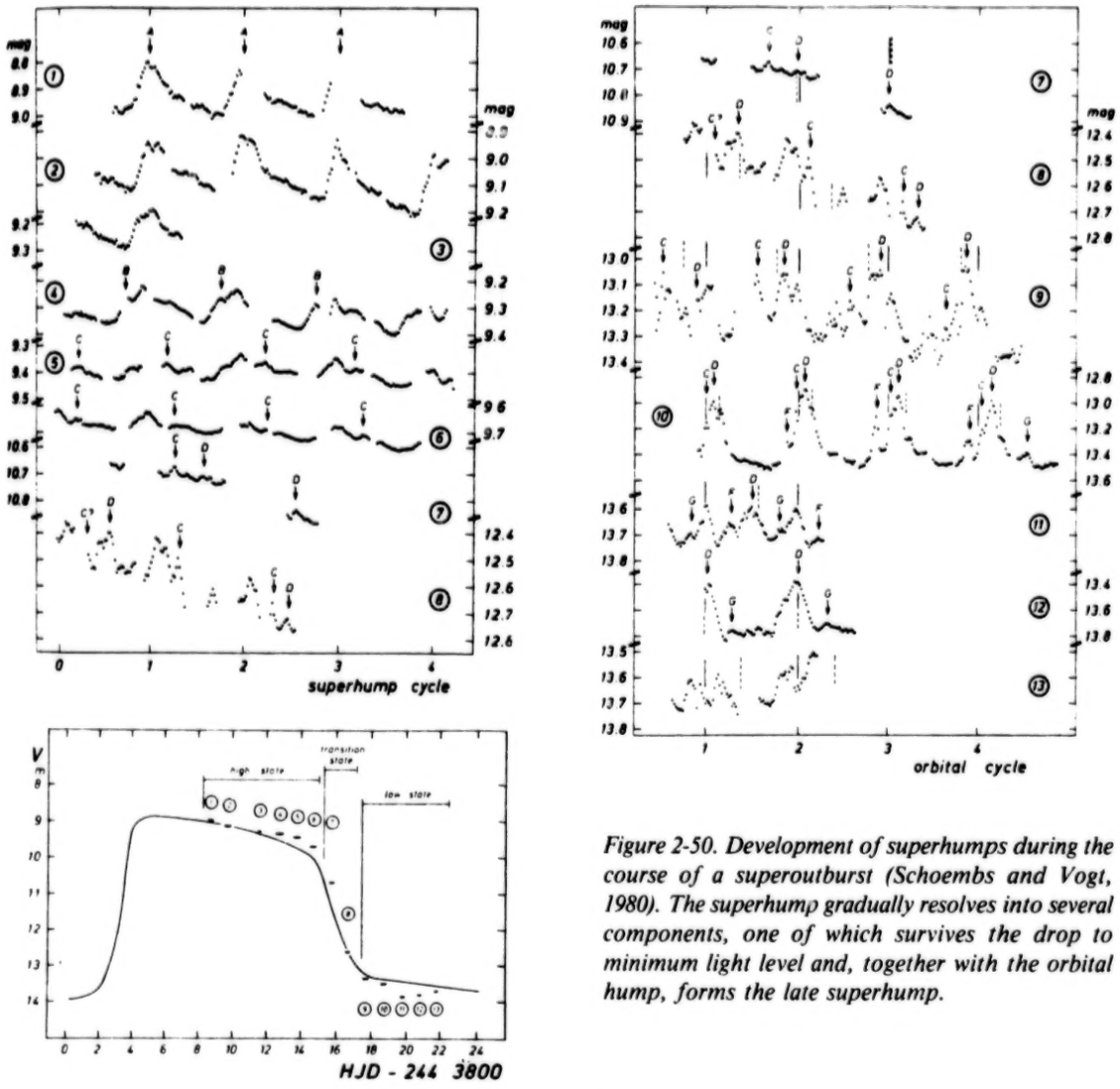


Figure 2-50. Development of superhumps during the course of a superoutburst (Schoembs and Vogt, 1980). The superhump gradually resolves into several components, one of which survives the drop to minimum light level and, together with the orbital hump, forms the late superhump.

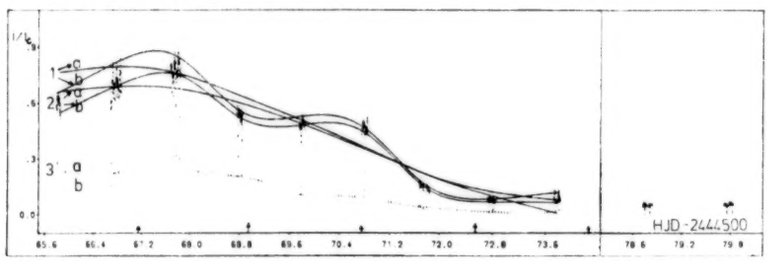


Figure 2-51. Semi-periodic brightness variations of OY Car on decline from a superoutburst (Schoembs, 1986).

Two SU Ursae Majoris stars, OY Car and Z Cha, show double eclipses during the quiescent state. Those eclipses can be used as a probe for the origin and location of the superhumps, which in turn seem closely related to the phenomenon of superoutbursts. The eclipses of OY Car have been observed by Krzeminski and Vogt (1985) and Schoembs (1986) for the early and later parts of two different superoutbursts, respectively. During the first half of the superoutburst (including times when the superhump had not yet developed), Vogt found the depth of the eclipse (in magnitudes) to increase with time, with a superimposed periodic

variation with superhump period. The width of the eclipse, on the other hand, decreases with also a superimposed variation of superhump period, but 180° out of phase with respect to the changes in depth of the eclipse. The amplitude of the variation increases with increasing wavelength.

As to the second half of the outburst, from inspection of Figure 2-52a and the sketches given at the right side of each panel, it can be seen that the ingress is flattened when the superhump phase zero (labeled "C") occurs close to the eclipse (runs 4 and 5), and egress is flattened when it occurs far away from this (runs 2, 3, and 6). The situation becomes more complicated for later stages of the outburst when the minimum shape of eclipse is slowly restored. At the plateau of the outburst the eclipse is round-bottomed and approximately symmetric, without any indication for a second eclipse within this eclipse, like it is detectable at minimum. Also no variation of the slight asymmetry with the beat period can be detected, as was found during earlier stages of the different outburst which was observed by Vogt (see above). Immediately after the fast drop in brightness at the end of the superoutburst plateau, the eclipse bottom becomes flatter and shows irregular features with indication of a second eclipse; gradually the total width of the eclipse becomes narrower, regaining its normal quiescent appearance. This process of restoring the quiescent light curve is not a well-defined one, but when quiescent features evolve, they well may experience setbacks, become more like what they were during outburst, and later develop anew (Figure 2-52b).

Warner (1985a) observed Z Cha during different superoutbursts and finds that, not taking into account the superhump, the shape of the light curve and in particular the shape of the eclipse are well repeated from one outburst to another. Eclipse depths correlate with the superhump phase, being deepest when the superhump occurs at about orbital phase 0.5 (i.e., 180° away from eclipse), somewhat unlike what has been observed in the case of OY Car where there is no clear relation between depth of eclipse and superhump phase, though a modulation is present. Furthermore, in Z Cha the eclipse occurs at a later time than predicted ($\Delta\varphi$ some 0.005) whenever it coincides with the superhump.

The color variations of superhumps have been investigated by Vogt (1974), Schoembs and Vogt (1980), and van Amerongen et al (1987a) in the case of VW Hyi. Very extensive five-color measurements by the latter authors reveal several remarkable features: the shape of the superhump is qualitatively the same in all five (Walraven) colors they observed, but with decreasing amplitude toward shorter wavelengths; all amplitudes decrease as the superoutburst proceeds and the superhump becomes progressively redder. And while one period fits times of the superhump maxima in all colors, there is a phase shift between the times of superhump maximum in that it occurs increasingly later towards shorter wavelength (Figure 2-53); the total phase shift amounts to about 0.06 of the orbital period between the V and the W filters. Qualitatively similar results were obtained by the other groups. TU Men is reported to become bluer in (B-R) and (B-I) at times of rise to superhump maximum (Stolz and Schoembs, 1984).

WZ Sge already has been introduced as a slightly extravagant system (see Chapter 2.II.B.4). In 1978 it underwent an outburst which in its overall shape resembled a nova outburst (outburst light curve, see Figure 2-42) rather than that of a dwarf nova. Its photometric appearance on orbital time scales strongly resembles superoutburst light curves of SU Ursae Majoris stars, in particular in exhibiting a very strong periodic hump feature (Figure 2-54). The periodicity of this feature turns out to be some 0.8% longer than the quiescent orbital period, which by definition qualifies WZ Sge to be a member of the SU Ursae Majoris class of dwarf novae. The eclipse feature seen during quiescence could not be detected during outburst.

ORIGINAL PAGE IS
OF POOR QUALITY

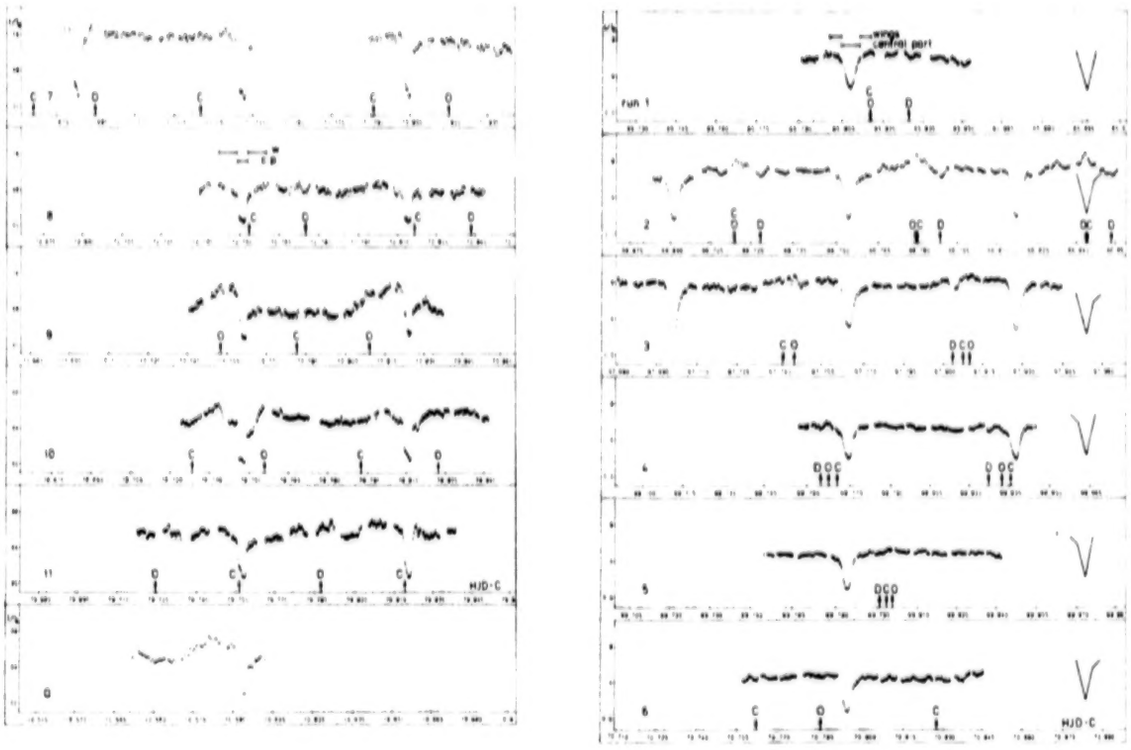


Figure 2-52. In OY Car the eclipse shape during superoutburst is seen to vary with the superhump phase (Schoembs, 1986). Also shown is the gradual restoration of the double eclipse at the end of the superoutburst.

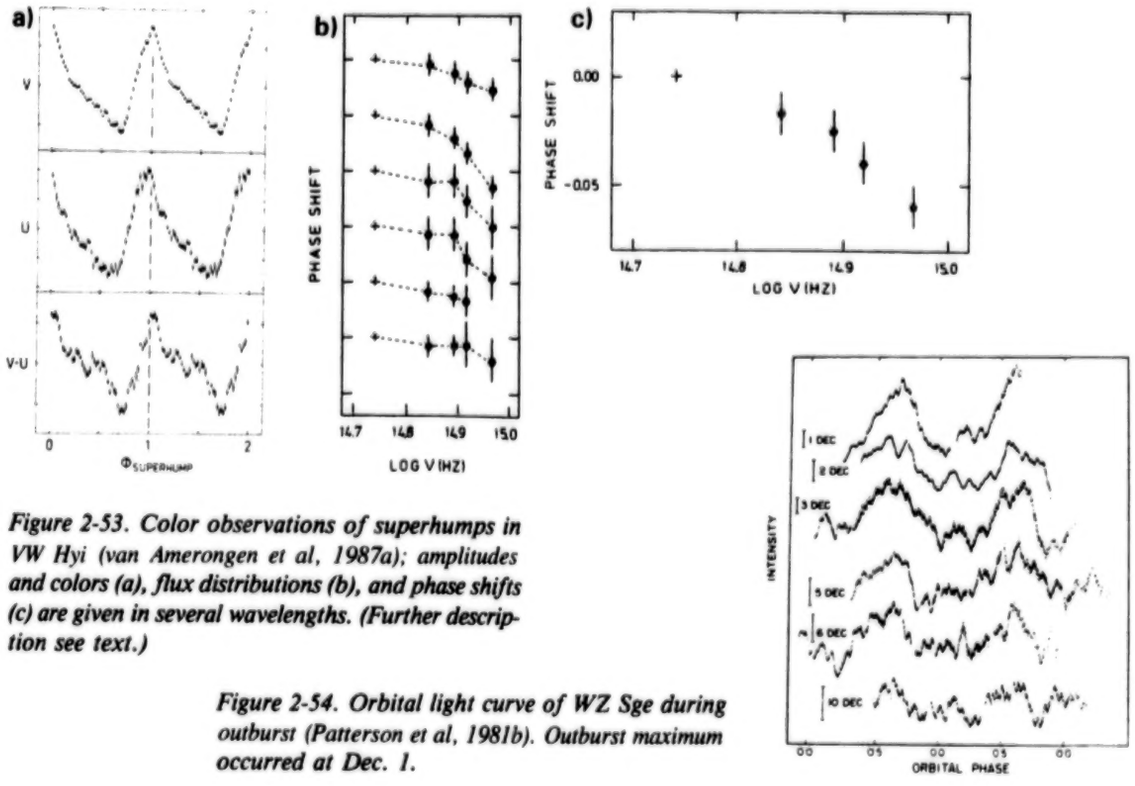


Figure 2-53. Color observations of superhumps in VW Hyi (van Amerongen et al, 1987a); amplitudes and colors (a), flux distributions (b), and phase shifts (c) are given in several wavelengths. (Further description see text.)

Figure 2-54. Orbital light curve of WZ Sge during outburst (Patterson et al, 1981b). Outburst maximum occurred at Dec. 1.

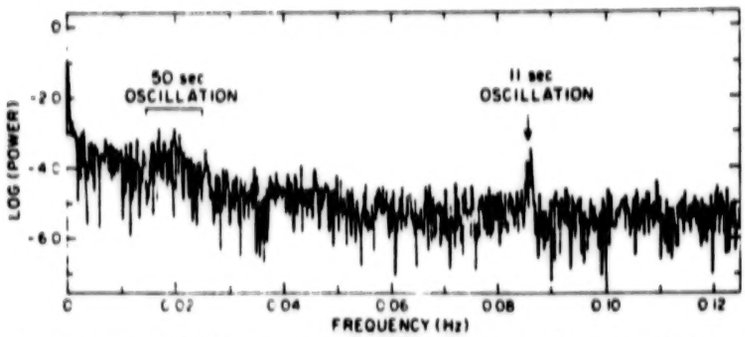


Figure 2-55. Power spectrum of RU Peg (Patterson, 1981) showing coherent oscillations at 11 s, quasi-periodic oscillations at 50 sec, and flickering at even lower frequencies.

GENERAL INTERPRETATION: Most photometric variations on orbital time scales during outburst or standstill are ascribed to aspect variations due to orbital revolution. Double eclipses become single because the brightness distribution in the disc changes considerably. Outbursts are believed to be due to an instability either in the disc or in the secondary star; standstills are understood to be prolonged outbursts. The mechanism of superoutburst and superhumps is not well understood.

OBSERVATIONAL CONSTRAINTS TO MODELS:

- *Why do outbursts occur? (See 171)*
- *Why do standstills occur? (See 178)*
- *What are superoutbursts and superhumps? (See 184)*
- *The amplitude of superhumps seems to be rather independent of the angle of inclination. (See 184)*

II.D. SHORT-TERM VARIATIONS

ABSTRACT: On time-scales of minutes and seconds, further more or less periodic types of variability are seen in dwarf novae.

In dwarf novae there occur three different types of short-term variations: the *flickering*, a random light variation which is present to some degree at all stages of activity with amplitudes of some tenths of a magnitude and time-scales of seconds or minutes; the *coherent oscillations* (which are also referred to as *dwarf nova oscillations, dwarf nova pulsations,* or, possibly somewhat misleadingly, as *white dwarf pulsations*) with periods of a few tens of seconds and amplitudes on the order of 0.002 mag, occurring in dwarf nova outbursts, in nova-like stars during their bright state, and in WZ Sge during quiescence; and finally, also seen during dwarf nova outbursts, there is an intermediate class of variations, the so-called *quasi-periodic oscillations* with periods on the order of one minute and somewhat larger amplitudes than the coherent oscillations, in which periods change stochastically. Figure 2-55 is a power spectrum of the dwarf nova RU Peg showing all three types of variability.

II.D.1. FLICKERING

ABSTRACT: Flickering is a random, aperiodic brightness variability on time-scales between some 20 sec and many minutes. Amplitudes can reach up to 0.5 mag and generally are highly variable. Flickering is present to some degree in all dwarf novae (as well as nova-like stars and old novae), and in all brightness stages. During eclipse minimum it is either strongly reduced or disappears altogether. The amplitude is largest in U and slightly decreases toward longer wavelengths.

nova-like stars: 98, 103, 106, 114, 117, 119, 122, 128, 140

interpretation: 151, 181

As can be seen in many of the previous figures in this section, the light curves of dwarf novae — and other cataclysmic variables as well — besides exhibiting humps, eclipses and light variations due to outbursts, are by no means smooth. Superimposed on the orbital light

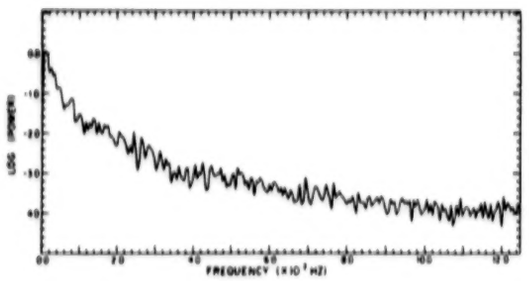


Figure 2-56. Power spectrum of RX And showing only flickering (Robinson, 1973b).

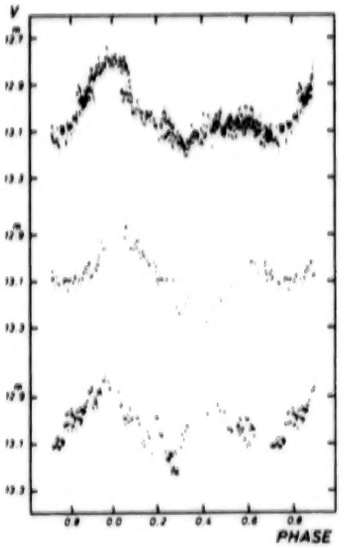


Figure 2-57. Optical light curve of BV Cen (Vogt and Breysacher, 1980b). Variable flickering activity can give the light curves rather different appearances.

variations, brightness changes occur at random with amplitudes of typically some 0.1 to 0.5 mag on time scales of some 10 minutes. This phenomenon is called *flickering* (for a collection of flickering amplitudes see Moffet and Barnes, 1974). Power spectra clearly indicate that flickering time-scales can well be as short as 20 sec, and with a continuous distribution of frequency, there is practically no limit to longer time scales.

To some degree flickering is present in all dwarf novae and nova-like stars in all stages of activity, as well as in novae during the quiescent state. No periodicities or general patterns of amplitude changes can be found in the flickering of these stars.* A typical power spectrum of the flickering is shown in Figure 2-56: the power is large at low frequencies and falls off toward higher frequencies; no peaks indicating prevailing periods are present. In general, however, even during comparable brightness levels in a given object, very different degrees of flickering activity have been observed in many systems (e.g., Figure 2-57). Usually there is a tendency for the flickering amplitude to be largest at times of hump maximum and to be strongly reduced during eclipse. Detailed observations of eclipses of the dwarf novae HT Cas, V2051 Oph, and the nova-like system RW Tri (which is very similar to dwarf novae) indicate that the main source of the flickering is the hot inner disc close to the white dwarf, rather than the hot spot, as often has been claimed (Patterson, 1981; Warner and Cropper, 1983; Horne and Stiening, 1985). In general, flickering is present during outburst, but then it can be stronger as well as weaker than during quiescence, varying from object to object and also during the course of an outburst (e.g., Robinson, 1973a, b).

No significant differences have been found between the pattern of flickering in different colors, only normally the amplitude is larger at shorter wavelengths. There is no information about flickering activity in the UV.

A systematic investigation of flickering in dwarf novae was carried out by Elsworth and James (1986) on YZ Cnc. They find that the frequency distribution is not that expected from a point-like source but rather that from some kind of extended optically thick source. The geometrical extent of this source appears to increase as the system's brightness increases.

*This is due mainly to terminology: there are periodic variations hidden in this seemingly random behavior which are referred to as *oscillations*, as will be discussed later.

II.D.2. OSCILLATIONS

Application of fast-fourier-transformation techniques to cataclysmic variables revealed that hidden in the random flickering there are periodic light variations with periods of some dozens of seconds. These were called *oscillations*.

II.D.2.a. COHERENT OSCILLATIONS

ABSTRACT: During outburst of dwarf novae, strictly monochromatic oscillations with time scales of typically 10 to 30 sec, amplitudes of 5 10^{-3} to 5 10^{-4} mag, and coherence times of several minutes can sometimes be seen. They were only found during certain observing runs in some dwarf novae. Periods always lie in a certain characteristic range for any given object. During the course of an outburst, characteristic shifts in frequency can be seen; at any moment only one frequency contains considerable power.

see also: 59, 61, 63

nova-like stars: 98, 106, 112, 116, 117, 119, 122, 129, 141

interpretation: 185, 213

The so-called *coherent oscillations* (or *dwarf nova oscillations, dwarf nova pulsations*, or *white dwarf pulsations*) are observed mostly in dwarf novae during outburst, though they were seen to occur in some nova-like stars in their bright state as well. These are purely monochromatic oscillations with periods of typically between 10 and 30 sec, coherence times of typically 10^3 cycles, and amplitudes of 0.0005 to 0.005 mag. Because of these characteristics they usually are invisible in the raw observational data, and only very special representation of data makes them appear. In the power spectra these oscillations appear as single sharp peaks with power up to 100 times as much as the neighboring frequencies, and no power in excess of noise in any of the harmonics (Figure 2-58). When a signal appears to be wider than the numerical resolution it can always be resolved, at closer inspection, into several independent spikes; they never seem to form a continuum. As ever smaller segments of one observing run are analyzed, the power can be seen to slowly migrate from one frequency to another with usually only one frequency being strongly excited at any one time, and no continuum of frequencies being present (e.g., Figure 2-61 and Warner and Bickhill, 1974). It is not obvious that, as has been claimed by several authors, more than one frequency can be present at a time with appreciable power; this multi-frequency appearance well might be an artifact of too coarse a time resolution. It never has been observed that excited frequencies which apparently coexisted were more than a fraction of a second separated from each other.

Coherent oscillations cannot always be seen in all dwarf novae. Despite considerable searching they have so far never been detected during the quiescent state of any dwarf nova. They have been observed in all types of dwarf novae during normal outbursts and superoutbursts; however, they have never been seen during the standstill phase of any Z Camelopardalis star. Reported detections of coherent oscillations in dwarf novae have been summarized by Warner (1986b). The period of the oscillation is variable in all stars, but for different outbursts they always cluster around some characteristic value. During the course of an outburst the oscillation period is subject to very characteristic changes in the log period — log intensity plane of the spectrum, called the "banana diagram" by Patterson (1981, and also Figures 2-59 - 2-62): at some stage of the rising branch the oscillations appear with an identifiable period, the period shifts towards shorter periods as the system brightens, when it approaches maximum visual brightness the oscillations fade or even become undetectable, and at the declining branch they reappear first with quickly increasing, then with slowly decreasing amplitude. As the system fades the period shifts to ever longer periods; this happens not quite monotonically but with no evidence for sudden changes, almost displaying a mirror image of the light curve (Figure 2-60). Any period typically is strong for some 20 min and stable for about one hour. The rate at which the period changes

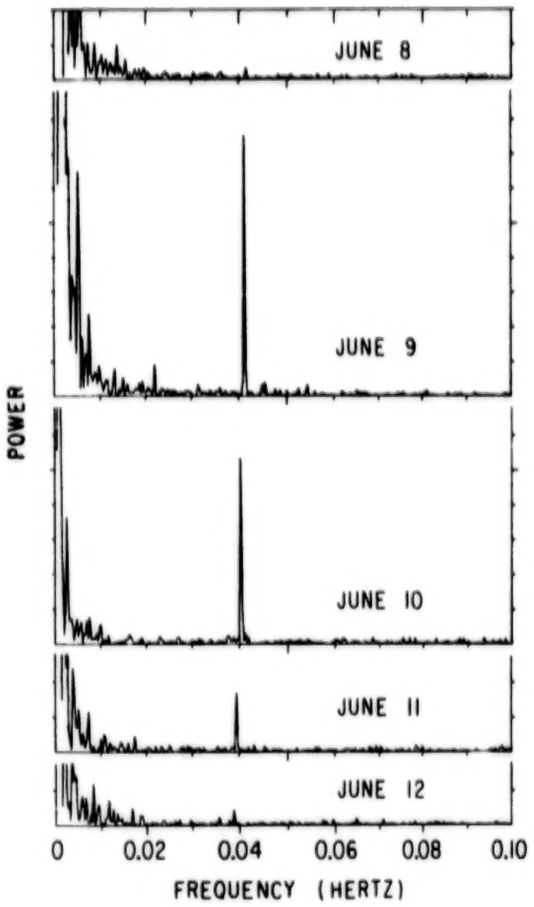


Figure 2-58. Power spectra of AH Her (Stiening et al, 1979) showing strictly monochromatic coherent oscillations and their development during the course of an outburst.

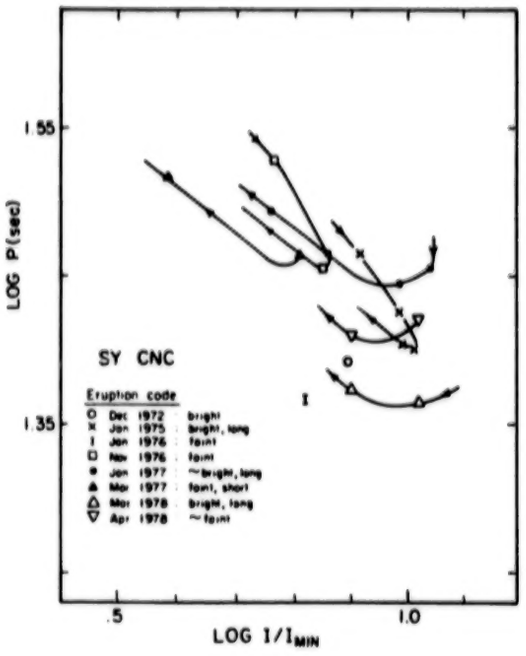


Figure 2-59. The "banana diagram:" the periods of coherent oscillations undergo characteristic frequency changes as the system's brightness changes during the course of an outburst (Patterson, 1981).

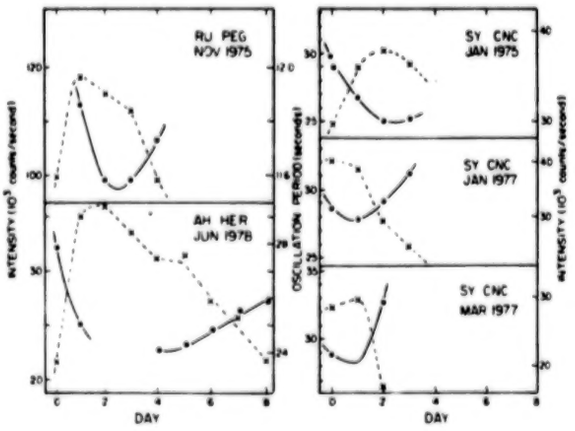


Figure 2-60. Similarly the intensity of the oscillation varies with the general brightness level (Patterson 1981). The full curves represent variations of the oscillation periods, the broken lines give the brightness variations for comparison.

as the system brightness changes is roughly constant for different outbursts in each object on the declining branch, while it is fairly variable on the rising branch. The actual values of the period at a given system brightness vary from one outburst to another in every object (Figure 2-59).

Oscillations have not been detected in outbursts of all dwarf novae, and in no object can they be seen in all outbursts. The result of a systematic search for oscillations by Nevo and Sadeh (1978) might be representative: they detected oscillation in 11 out of 90 runs, and in 4 out of 11 objects. It is not clear if there are outbursts in which oscillations are really not present, or, since they are a somewhat transient phenomenon, if they have only remained unobserved.

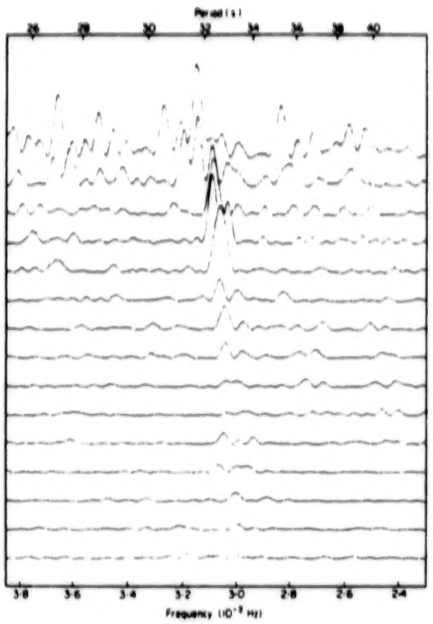


Figure 2-61. Development of oscillations in CN Ori during rise; time increases toward the top (Warner and Brickhill, 1978). It is not quite clear whether the oscillations are really polychromatic or monochromatic but then survive only for a short while.

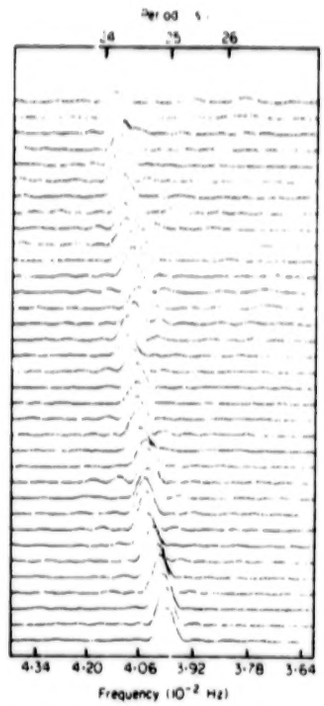


Figure 2-62. Period shifts of the coherent oscillations in CN Ori during the course of an outburst (Warner and Brickhill, 1978). A cyclical variation is superimposed on a general period drift.

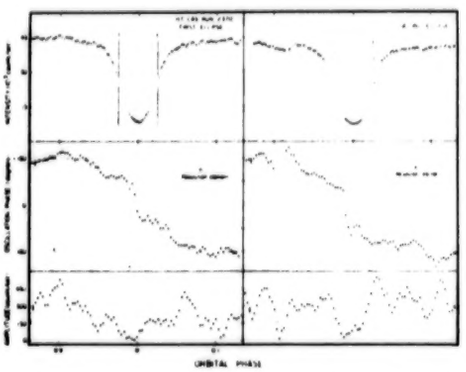


Figure 2-63. During eclipse in HT Cas the oscillations undergo a phase shift of −360° and amplitudes are strongly reduced just before mid-eclipse (Patterson, 1981).

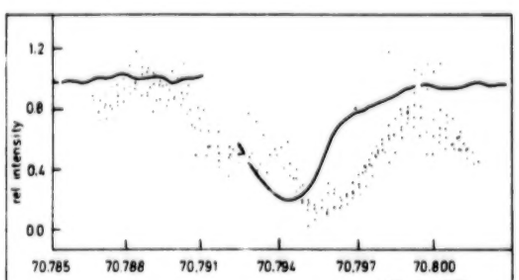


Figure 2-64. In OY Car the oscillations are almost totally eclipsed, but only after photometric mid-eclipse (Schoembs, 1986). Dots represent the relative oscillation amplitude, the full line is the light curve, both in relative units.

In several systems (Warner and Brickhill, 1978; Patterson, 1981; Schoembs, 1986), coherent oscillations have been observed during photometric eclipses. In HT Cas (Patterson, 1981) the oscillations undergo a steady phase shift of -360° during eclipse. The amplitudes of the oscillations were observed to be strongly reduced shortly before mid-eclipse, and the eclipse of the oscillation preceded that of the optical light by 0.01 of the orbital period (Figure 2-63). The oscillations in OY Car (Schoembs, 1986) are practically completely eclipsed; this eclipse, however, followed that of the visual light by a short time (Figure 2-64). In OY Car no phase variations of the oscillations during the eclipses were found.

The colors of the oscillations were investigated by Hildebrand et al (1981) in AH

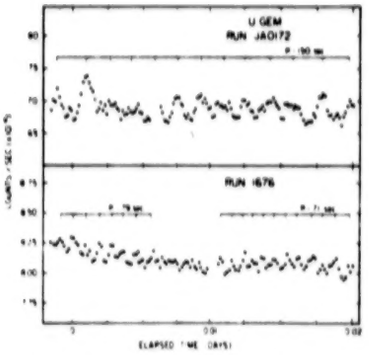


Figure 2-65. Quasi-periodic oscillations in U Gem (Robinson and Nather, 1979); sometimes they are easily visible already in the raw data.

Her and by Middleditch and Córdova (1982) in SY Cnc. AH Her was measured in two colors and the authors found the flux ratios to be in agreement with a black body temperature of 28000 K < T < 73000 K. SY Cnc was measured in three colors and it was found that no kind of black body nor a power law could be fitted to the data. No change of the colors was evident during three nights of observations.

II.D.2.b. QUASI-PERIODIC OSCILLATIONS

ABSTRACT: Besides, or instead of, flickering and coherent oscillations, polychromatic oscillations of some 0.001 mag amplitude are displayed in some dwarf novae during outburst. Usually they consist of a wide range of periodicities which are considerably longer than those of the coherent oscillations. Very different values of periods are possible in one object during different outbursts.

see also: 51, 61, 63

nova-like stars: 98, 106, 112, 116, 117, 119, 122, 129, 141

interpretation: 185, 213

There is still a second kind of short-term variability present in some dwarf novae: the so-called *quasi-periodic oscillations* (Figure 2-55). They are characterized by a broad hump in the power spectrum indicating a (quasi-) continuum of frequencies with amplitudes of up to 0.01 mag. Because of these relatively large amplitudes, quasi-periodic oscillations are often already visible in the raw data without any help of data analysis (Figure 2-65). Often, however, the autocorrelation function lets the periodicity appear more clearly. The periods of the quasi-periodic oscillations normally are several times as long as those of the sharply defined coherent oscillations, so usually no confusion is possible. But, there are exceptions to this, as will be seen.

Quasi-periodic oscillations have been detected in many dwarf novae, and, like coherent oscillations, they are seen only during outburst; they also can be found in some nova-like systems (Ritter, 1987, see also Chapter 3). Periods typically range from some 20 sec to several hundred sec, and, like the coherent oscillations, they are confined to a fairly narrow period range which is just a few seconds wide. During different outbursts of one object, however, fairly different period values seem possible. In addition, sometimes several such ranges of frequencies occur simultaneously, each with somewhat different characteristics: usually one is a quasi-periodic oscillation in the conventional sense, while another more resembles coherent oscillations. Like the coherent oscillations, quasi-periodic oscillations do not seem to occur in all outbursts of a dwarf nova, and in many dwarf novae they have never been detected at all. When seen during different outbursts of a system, they can have significantly different periods (e.g., Robinson and Nather (1979) found a period of 150 sec in one outburst of U Gem, while during another outburst, Patterson (1981) found quasi-periodic oscillations with a period of only 24 sec). Quasi-periodic oscillations may or may not appear simultaneously with coherent oscillations: in objects like RU Peg and SS Cyg they do; in other objects, either only coherent oscillations or only quasi-periodic oscillations, or in some cases none at all, were detected. It is not clear whether quasi-periodic oscillations can occur on the rising branch of an outburst.

As the name suggests, the quasi-periodic oscillations are not strictly periodic. For a short interval of time, a mean period can be defined, which however is not usually kept strictly. The decay times of these mean periods are on the

order of just a few cycles, and within that short a time, new periods emerge (Figure 2-65) which usually are not strongly different from the former. The change of periods occurs at random and does not follow any monotonic trend as in the case of coherent oscillations. At times the amplitudes are strong, while at other times they die out completely for some minutes, and during such times, phase and/or period changes are very likely to occur. There are entire nights without any detectable quasi-periodic oscillations, while during both the preceding and the following night they might be strong (Robinson and Nather, 1975).

In U Gem quasi-periodic oscillations have been observed to be present throughout the eclipse, whereas flickering in this object largely is eclipsed (Robinson and Nather, 1975).

II.D.2.c. X-RAY PULSATIONS

ABSTRACT: In U Gem, SS Cyg, and VW Hyi, pulsations were detected at soft X-rays during outbursts. In SS Cyg the periods were on the same order as optical coherent oscillations, but with much shorter coherence times; in VW Hyi they were of a considerably different length than optical oscillations; in U Gem they have been observed simultaneously with optical quasi-periodic oscillations.

see also: 61

nova-like stars: 121

interpretation: 185, 213

In all three dwarf novae which so far could be observed extensively in the soft X-rays (SS Cyg, U Gem, and VW Hyi), oscillations, or *pulsations* as they are called in the x-ray regime, were observed during decline from outburst (Figure 2-66).

SS Cyg was observed twice, once during maximum of a long outburst and once on the declining branch of a short one. Both times the pulsation period was in the same range as the optical coherent oscillations: 8.8 sec and 10.7 sec, respectively. U Gem was observed at three outbursts, during one of which pulsations with a period of some 25 sec were detected — and observed simultaneously in the optical (Córdova, 1979). In another outburst there was marginal evidence for 21 sec pulsations, and the third outburst did not show any pulsations at all. In the optical, no coherent oscillations were found in U Gem so far, but only quasi-coherent oscillations with periods of some 75 sec and 150 sec, respectively.

VW Hyi was monitored with EXOSAT during several normal outbursts and superoutbursts during the years 1983 through 1985 (van der Woerd et al, 1987). Only during two superoutbursts could pulsations be detected in soft X-rays (> 5Å). In November 1983, there appeared coherent oscillations with a period of 14.06 ± 0.02 sec. During another superoutburst in October 1984, rather unstable pulsations were seen, which were variable in frequency between 14.2 and 14.4 sec and also variable in amplitude; in addition these seem to have had a somewhat harder spectrum than those seen the year before. No simultaneous optical observations are available, but oscillations in VW Hyi which are at times seen in the optical (see below) normally are variable with periods of some 30 sec.

The X-ray pulsations are remarkably incoherent and rather resemble the optical quasi-periodic oscillations than the coherent oscillations, although in the case of SS Cyg they have the same periodicity as the optical coherent oscillations. In SS Cyg they showed coherence times of about 20 cycles and 2 cycles, respectively, for the two sets of observations, as opposed to typically some 1000 cycles in the optical. Like the optical coherent oscillations, however, they also perform slow shifts in frequency in X-rays as time goes by (Córdova et al, 1984).

The pulsed fraction of the soft X-ray radiation varies between zero and 100%, with typical values of 30% and 17%, respectively, in the two observations of SS Cyg, and some 15% in U Gem (Córdova et al, 1980) — as opposed to

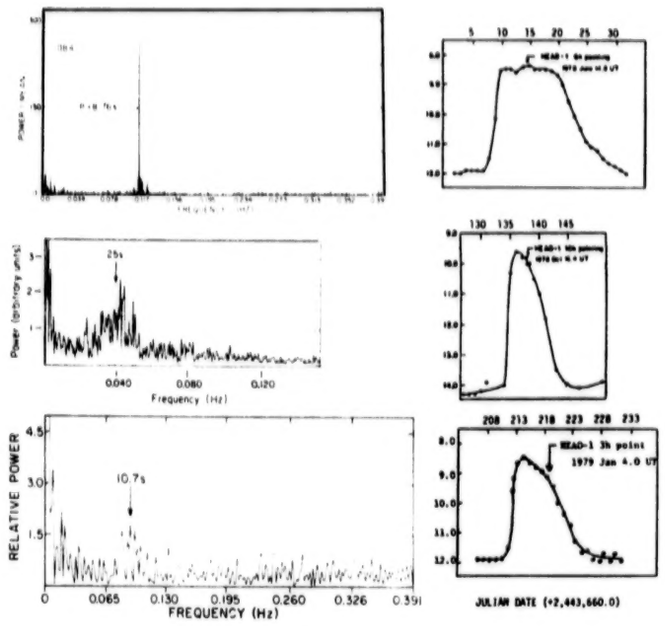


Figure 2-66. X-ray pulsations in SS Cyg and U Gem (Córdova and Mason, 1980); they have approximately the same periods as the optical coherent oscillations.

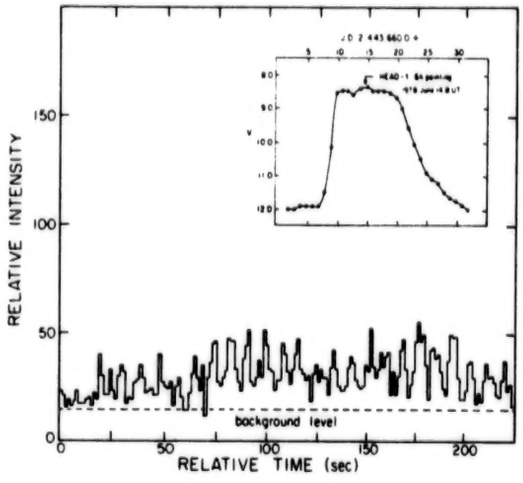


Figure 2-67. X-ray pulsations in SS Cyg (Córdova et al, 1980). Because they involve a considerable fraction of the X-ray flux, the pulsations are readily seen in the raw data.

some 2% in the optical. The range of variability was seen to be much narrower (about 15 to 20%) in the case of VW Hyi. Because of this great strength, the pulsations are already easily seen in the raw X-ray light curves (Figure 2-67). Frequent and sudden amplitude and phase changes were seen in all cases.

II.D.2.d. VW HYI — A VERY CONFUSING CASE

ABSTRACT: Many different kinds of oscillations have been observed in VW Hyi, which cannot be classified as any of the conventional types.

For oscillations in dwarf novae, the *normal* case seems to be that coherent oscillations have periods on the order of typically 10 to 30 sec, while quasi-periodic oscillations rather have periods on the order of 50 to 100 sec. However, it has been mentioned already that in U Gem quasi-periodic oscillations with periods as short as some 24 sec have been detected in X-rays, casting some doubt on the physical significance of the strict distinction between coherent and quasi-periodic oscillations. The case of VW Hyi makes this even more questionable.

In various independent observations, the oscillations in VW Hyi (all with periods on the order of 30 sec) appear to be changing periods in a much more erratic way than do oscillations in other dwarf novae, in which the multiple peaks probably reflect quick changes (or insufficient time resolution), rather than several frequencies being present simultaneously (Figure

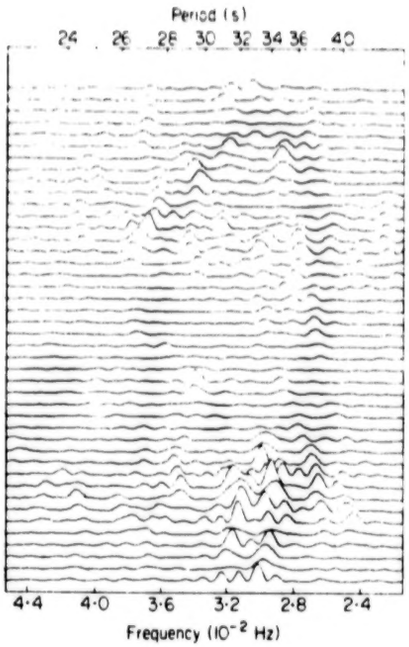


Figure 2-68. Quasi-periodic oscillations in VW Hyi (Warner and Brickhill, 1978). Unlike in other dwarf novae, in VW Hyi periods rather change at random.

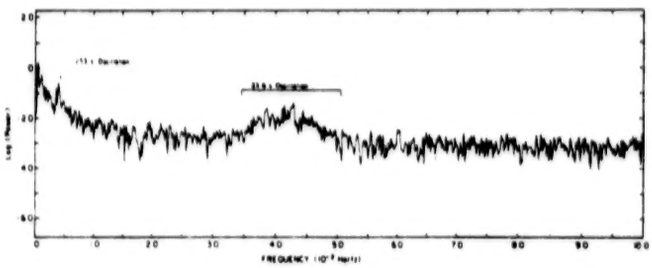


Figure 2-69. Observation of two sets of quasi-periodic oscillations in VW Hyi, no coherent oscillations are visible (Robinson and Warner, 1984).

2-68). The first time any oscillations were observed in VW Hyi, in December 1972 (Warner and Brickhill, 1974), there was no doubt that the oscillations were coherent: drifting slowly (though not altogether monotonically, a feature which is not common in other dwarf novae) from 28 sec toward longer periods. During a normal outburst of VW Hyi in November 1974, oscillations were seen to be modulated in amplitude with a period of 413 ± 1 sec. In observations of a superoutburst in December 1974, Haefner et al (1977) found a coherent oscillation with 192.3 sec at very early rise which could only be observed again two nights later (with a period of 193.7 sec). During the following night close to maximum light, there appeared a strictly coherent oscillation of 266.0 sec which never appeared again. At the end of another superoutburst in 1975, one could see a couple of clearly distinct sinusoidal periods between 85 and 90 sec for seven consecutive nights, which appeared at random with no obvious trend of development, and it seems that several of these were present simultaneously. Their coherence times, however, seem to have been on the order of several hours (Schoembs, 1977; Haefner et al, 1977). So, from their lengths and erratic changes, these variations should be classified as quasi-periodic oscillations; according to their stability and their being distinct from each other, they qualify as coherent oscillations. For these oscillations, there are indications that their amplitudes are larger at times of orbital hump maximum than at other times, as in the case of flickering. This did not appear to be the case in any oscillations in any other dwarf nova. In addition, in two of the above mentioned observations, there also appeared coherent oscillations with periods of 28.8 and 35.7 sec, respectively, in close agreement with observations during another outburst of VW Hyi by Warner and Brickhill (1974). Finally, somewhat more erratic processes, possibly quasi-periodic oscillations, were observed to develop at late decline, with a general tendency to drift from a mean value of some 130 sec to some 150 sec as the decline proceeds.

In 1978 Robinson and Warner (1984) observed two simultaneous sets of quasi-periodic oscillations, but no coherent oscillations, during a normal outburst of VW Hyi. In the power spectrum (Figure 2-69), an oscillation near 23.6 sec is clearly visible, having all the characteristics of a quasi-periodic oscillation except for the unusually short period. An

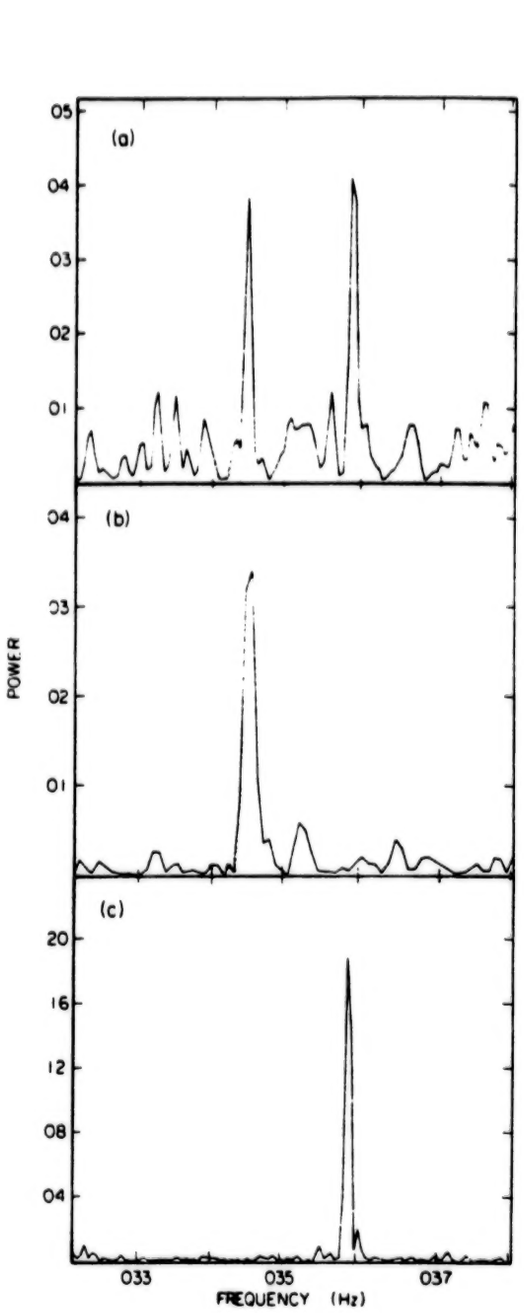


Figure 2-70. Power spectra of WZ Sge during quiescence (Robinson et al, 1978). The 28.87 sec period was seen to be almost always present for several years, other periods were seen occasionally.

oscillation at 253 sec appears to be almost monochromatic, thus being rather similar to coherent oscillations. Inspection of the light curve, however, reveals that this latter period is subject to frequent erratic changes and at times dies out altogether, a behavior very characteristic of quasi-periodic oscillations.

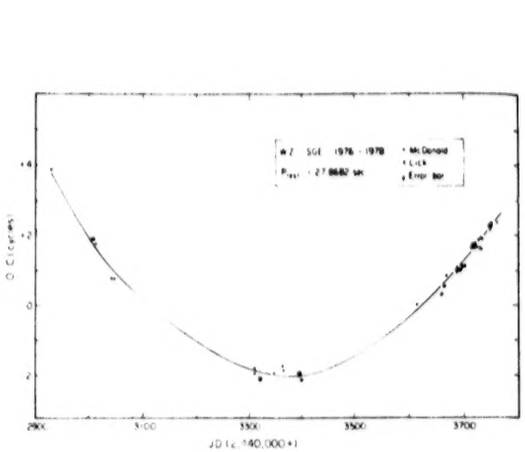


Figure 2-71. Secular variations in the 29 sec period in WZ Sge in 1976 through 1978 (Patterson, 1980).

II.D.2.e. WZ SGE — AS USUAL, AN UNUSUAL CASE

ABSTRACT: In WZ Sge coherent oscillations have been observed in quiescent state; they proved to be very stable over a couple of years.

related spectroscopic observations: 91

nova-like stars: 98, 106, 112, 116, 117, 119, 122, 129, 141

interpretation: 185

In photometric observations of WZ Sge, Robinson et al (1978) detected coherent oscillations during the quiescent (!) state with a period of either 27.87 ± 0.02 sec or 28.98 ± 0.04 sec. Either or both of those periods were present every time they observed the system, and no other periods containing significant power could be detected (Figure 2-70). Either the amplitudes were about 0.0043 and 0.0034 mag, respectively, or the periods were undetectable altogether. No shift in the periods could be detected during any observing run.

Patterson (1980) added new observations to these until the time of outburst in December, 1978, and carried out a more extensive investigation of the periods. He found that the period of 28.87 sec was very stable and was always present during the years 1976 through 1978, though with irregularly varying amplitude. Besides this, there were four other

peaks at lower frequencies, usually with much less power. The period of 28.97 sec seems to be real, the others can be explained as orbital sidebands of the principal frequency, though their relatively high power makes this hard to believe. Investigation of the principal period revealed it to be like a highly stable clock, though with a continuously increasing period between 1976 and 1978 (Figure 2-71).

The amplitudes of all the observed periods were variable, but no systematic variations, in particular none in connection with the orbital period, could be detected. There also was no indication for the oscillations to be in any way influenced by the eclipse. No similar investigations have been carried out so far, after the 1978 outburst.

GENERAL INTERPRETATION: Flickering is ascribed mainly to slight variations of the mass stream hitting the disc at the hot spot, thus causing slight temperature variations. However, other observations rather would suggest that its origin is in the vicinity of the white dwarf. — There is practically no understanding of what physical process causes the oscillations, and whether coherent and quasi-coherent oscillations have different causes, or whether they rather are different aspects of the same phenomenon. The short periods place their origin in, or in the vicinity of, the white dwarf.

OBSERVATIONAL CONSTRAINTS TO MODELS:

- *In dwarf novae and nova-like stars, short-period oscillations are occasionally observed. (See 185)*
- *They cannot be observed at all times. (See 185)*
- *When they occur, this is always only during the high brightness state. (See 185)*
- *The frequencies undergo characteristic changes which are related to the general brightness level of the system ("banana diagram").*
- *Oscillations in the optical and at X-rays seem to be correlated with each other.*
- *The systems VW Hyi and WZ Sge behave in very atypical ways.*

II.E. POLARIMETRIC OBSERVATIONS OF DWARF NOVAE

ABSTRACT: Only very few dwarf novae have been detected polarimetrically. The fraction of polarized radiation typically is some tenths of a percent or less. Variations in the fraction of polarized light were seen in VW Hyi during decline from a superoutburst.

nova-like stars: 98, 106, 113, 131

As a consequence of the small apparent magnitude of dwarf novae, polarimetric data of dwarf novae are extremely scarce. SS Cyg has been observed by Kraft (1956), U Gem by Krzeminski (1965), and Z Cam by Belakov and Shulov (1974), all with negative results.

Schoembs and Vogt (1980) carried out polarimetric observations of VW Hyi during maximum and decline from superoutburst. They found a significant but small linear polarization between 0.02% and 0.1%, which increases as the source becomes fainter during decline. During outburst the radiation is clearly less polarized than during quiescence. No clear evidence for periodic variability on time scales between 120 sec and twice the orbital period could be detected.

Szkody et al (1982a) carried out a systematic search for polarized radiation in dwarf novae and nova-like stars. They observed four dwarf novae, out of which three, SS Cyg, AH Her, and RX And, did show polarization on also the 0.3% level; but no polarization could be detected in U Gem. There is no significant change evidently related to the outburst cycle. RX And was observed well enough for investigations on orbital time scales (Figure 2-72); a variability is clearly present, but whether or not this is related to the orbital period cannot be decided with certainty.

The wavelength dependence of the polarization could be investigated in three nova-like systems (AE Agr, V426 Oph, CI Cyg (Szkody et al, 1982a)) and in the dwarf nova SS Cyg. In all of them it was found to be decidedly different from the wavelength dependence of the interstellar polarization, suggesting an origin in the systems themselves.

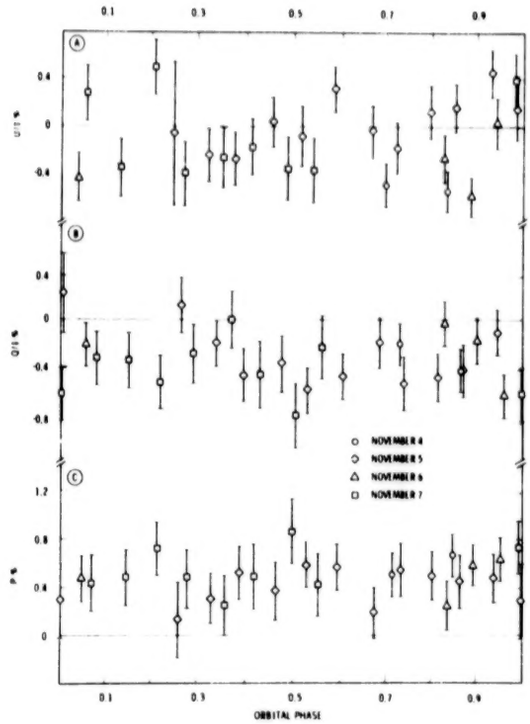


Figure 2-72. Polarimetric observations of RX And (Szkody et al, 1982a).

GENERAL INTERPRETATION: The polarized fraction of the light is believed to be due to scattering in a non-spherical corona above the disc. As this corona changes its shape during the course of an outburst, also the fraction and position angle of the polarized light change.

GENERAL CONSTRAINTS TO MODELS:

- *It is still not clear whether the above scenario is theoretically feasible.*

III. SPECTROSCOPIC OBSERVATIONS

III.A. GENERAL FLUX DISTRIBUTION

Appreciable flux is emitted by dwarf novae at all wavelengths from the X-rays to the longest IR wavelengths, and in some cases even in the radio. The general flux distribution of dwarf novae and its characteristic changes during the outburst cycle shall be presented in what follows. We shall first deal with the UV through IR emission, which can be observed over the entire range. The X-rays are separated from this by a gap between 912 Å and some 300 Å due to interstellar absorption. The flux and its changes in X-rays will then be considered. Finally some brief remarks will be made about attempts to detect dwarf novae at radio wavelengths.

III.A.1. ULTRAVIOLET, OPTICAL, AND INFRARED EMISSION

ABSTRACT: The strongest flux is usually emitted in the UV, falling monotonically towards longer wavelengths. During outburst, the spectrum is steeper than during quiescence with even more flux at high energies. The flux distribution is very different from that of single stars. It roughly can be fitted by a power law distribution over, typically, wavelength ranges of 1000 to 2000 Å; an even approximate fit with just one black body clearly is not possible. In some objects the flux rises again in the IR and only falls off longward of a maximum around 15000 to 20000 Å. — Rise to an outburst either occurs simultaneously at all wavelengths, or it starts at long wavelengths and then is seen at progressively shorter wavelengths. The decline is simultaneous at all wavelengths. In any one object, no differences seem to exist between the continuous flux distributions at the same optical brightness between different outbursts; this does not hold for the line radiation.

photometric changes during outburst cycle: 21, 47

nova-like stars: 99, 107, 116, 119, 122, 124, 134, 141

interpretation: 151, 192

In general terms, the continuum flux is falling monotonically from the Lyman edge to the infrared. During outburst, in addition to a general increase in flux, the distribution steepens markedly toward the blue, indicating that much higher temperatures prevail then. Though in general this appearance is shared by all dwarf novae, in detail the distributions are fairly different for different objects and for different outburst states. Figure 2-73 gives examples of observed flux distributions of dwarf novae in various outburst states. In Figure 2-73, an attempt has also been made to ascribe some

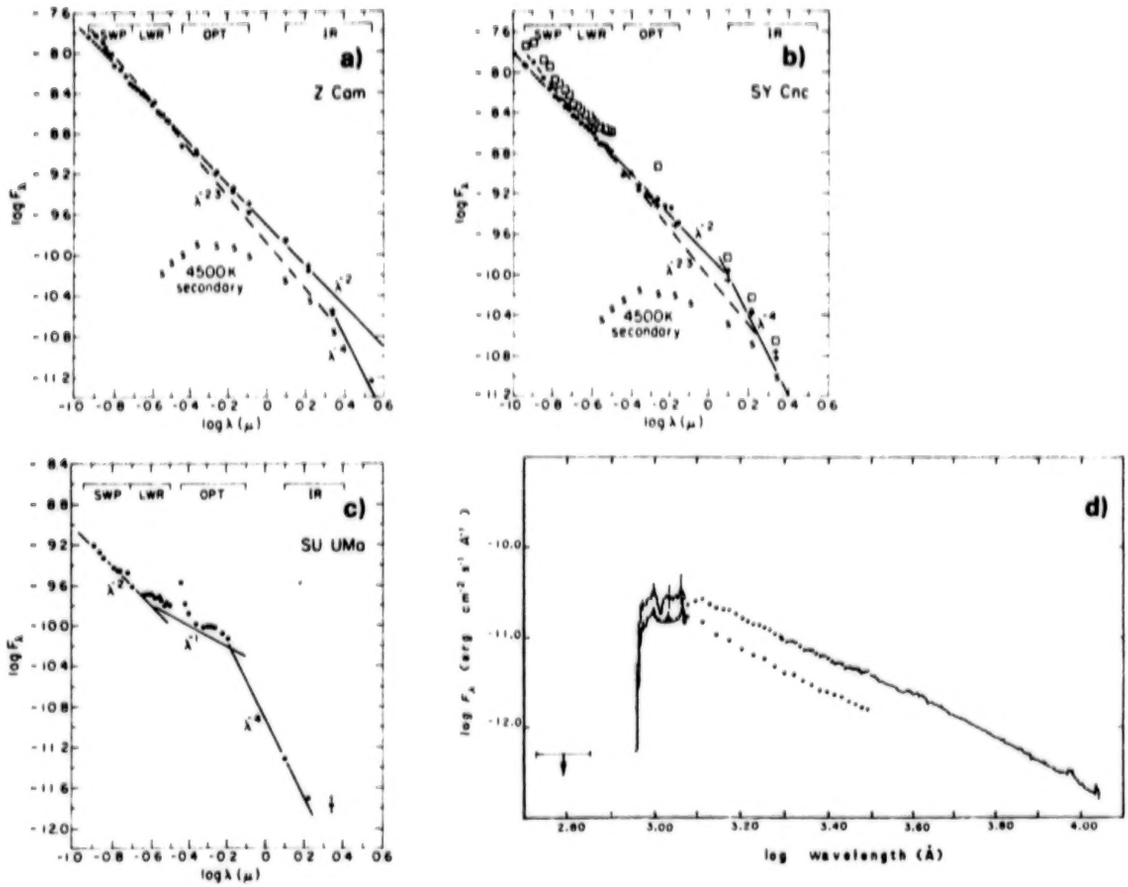


Figure 2-73. Typical flux distributions of dwarf novae: (a) Z Cam at standstill, (b) SY Cnc at maximum and decline, and (c) SU UMa at minimum (Szkody, 1981 — dots and squares represent the observed continuum flux at various brightness stages, the solid lines are fitted power laws, the symbol "S" indicates the flux distribution of the secondary component), and (d) SS Cyg (upper) and U Gem (lower) at outburst (Polidan and Holberg, 1984).

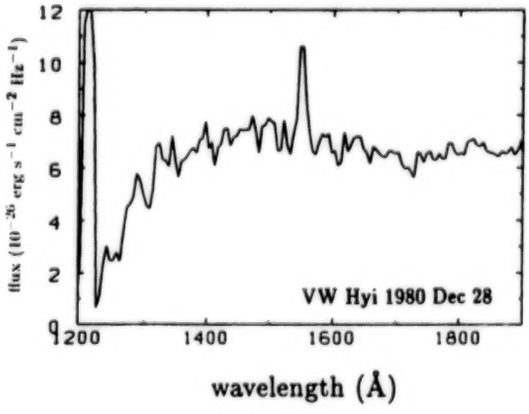


Figure 2-74. UV flux distribution of VW Hyi during quiescence (Verbunt, 1987). In some dwarf novae (and nova-like stars in the low state) the UV flux is seen to steeply decline at short wavelengths.

power law fits to the flux distributions. Typically slopes of α_λ (with $F_\lambda \sim \lambda^{\alpha_\lambda}$) between 0.0 and -4.0 apply locally to the spectra of dwarf novae (as well as to nova-like stars), but usually at least two such fits are needed in order to represent reasonably accurately the entire range from the Lyman limit to the IR; and clearly no black body fit is in any way satisfactory.

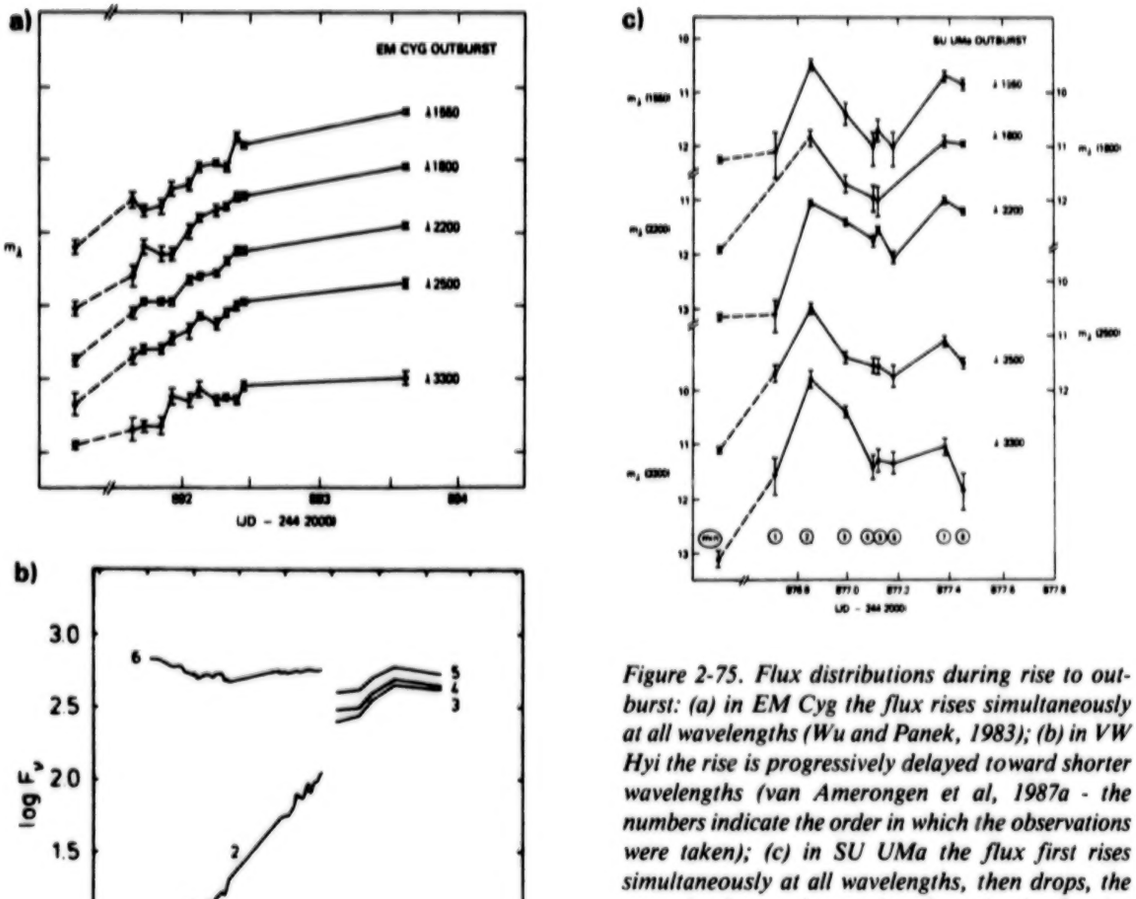


Figure 2-75. Flux distributions during rise to outburst: (a) in EM Cyg the flux rises simultaneously at all wavelengths (Wu and Panek, 1983); (b) in VW Hyi the rise is progressively delayed toward shorter wavelengths (van Amerongen et al, 1987a - the numbers indicate the order in which the observations were taken); (c) in SU UMa the flux first rises simultaneously at all wavelengths, then drops, the more the shorter the wavelength, and only after this rises to outburst (Wu and Panek, 1983).

In several objects during quiescence the flux increases in the IR between roughly 6000 and 12000 Å, due to the contribution of the cool companion (Figure 2-73). Contrary to what at times has been claimed in the literature, from inspection of published flux distributions (e.g., Oke and Wade, 1982; Sherrington and Jameson, 1983) there is no evidence for an additional red component to be present preferably in just those dwarf nova systems with long orbital periods; for any period a red component may or may not be visible*. At the short wavelength end of the spectrum, in four dwarf novae (WZ Sge, EK TrA, Z Cha, and VW Hyi; see Verbunt, 1987) during quiescence the flux is seen to decrease considerably shortward of some 1400 Å (Figure 2-74). In the Roche model this can be ascribed to either the wings of the Lyα line of the white dwarf (when the disc is cool enough to not contribute much flux at these wavelengths), or to a generally cool disc. During outburst, both the short wavelength turn-over as well as the infrared excess disappear when the contrast to the generally increased flux level becomes too small.

At rise to an outburst in most objects the flux distribution changes entirely. In several cases

*Still it holds that in the optical lines of the secondary component are visible only in long period systems (see Chapter 2.III.B.1.a).

this phase in outburst cycle has been observed simultaneously in the optical and in the UV. Three principally different modes of behavior were observed. In CN Ori, EM Cyg and SS Cyg (Pringle et al, 1986; Wu and Panek, 1983; Verbunt, 1987) the flux rose simultaneously in the optical and in the IR with a steady steepening of the spectral slope (Figure 2-75a). In VW Hyi, WX Hyi, SU UMa, RX And, SS Cyg (for which both types of rise were seen to occur) and possibly also in SS Aur (Hassall et al, 1983; Wu and Panek, 1983; Pringle and Verbunt, 1984; Polidan and Holberg, 1984; Schwarzenberg-Czerny et al, 1985; Verbunt, 1987), the rise to an outburst in the optical precedes that in the UV by typically several hours to half a day (Figure 2-75b); furthermore in VW Hyi there is indication for this delay to continue into X-rays (see below). Two such events were observed in VW Hyi, but at comparable optical brightness the slopes of the UV continuum were different (Verbunt et al, 1987). Van Amerongen et al (1987c) performed mulit-wavelength photometric measurements of VW Hyi in the optical during two rises to outburst and found that the delay in rise toward shorter wavelengths also holds for just the optical range (Figure 2-75b). From photometric observations of RX And at infrared wavelengths, Szkody (1976) finds some evidence that this delay might extend into the infrared as well; attempts to carry out similar observations of other dwarf novae so far did not lead to any conclusive results (Szkody, 1985a; 1985b). A third kind of change during rise in the UV has been observed in SU UMa during rise to a normal outburst (Wu and Panek, 1983) and in VW Hyi during rise to a superoutburst (Polidan and Holberg, 1986): in both cases the UV first rose up to the level of a normal outburst, delayed with respect to the optical, and then the flux dropped to some intermediate level (the drop was considerably deeper at shorter wavelengths than at longer ones), after which another rise led to the outburst or superoutburst, respectively (Figure 2-75c). In the case of SU UMa the corresponding optical changes are not quite clear. In VW Hyi, where occasionally such precursors to superoutbursts are observed in the optical (see Chapter 2.II.A.4, Figure 2-19), no drop in optical brightness was observed in this particular outburst; it clearly was seen, however, at soft X-rays (van der Woerd et al, 1986).

During outburst maximum the flux in all dwarf novae is markedly bluer than during all other times. Decline from outburst always proceeds simultaneously at all wavelengths. As the typical example of Figure 2-76a shows, the spectral index stays roughly constant throughout outburst longward of some 15000 Å, and just the flux level as a whole changes. In the optical and UV, after an initial decline at constant flux distribution, the flux level decreases ever more rapidly with decreasing wavelength. Only at the very last phase of decline is the quiescent flux distribution restored (Figure 2-76b). During quiescence, between outbursts, the flux of VW Hyi and WX Hyi in the UV has been seen to keep falling until onset of the following outburst (Figure 2-77), while no such trend could be detected in U Gem (Hassall et al, 1985; Verbunt et al, 1987); appropriate observations of other dwarf novae in the UV are not available. VW Hyi also was monitored in the optical for this purpose. After the end of an outburst — as defined from the general outburst light curve — the system brightness kept declining slightly for another couple of days; but after this, besides erratic variations, the flux level stayed constant (van Amerongen et al, 1987c). Similarly, extensive monitoring of CN Ori during quiescence demonstrated that the brightness of the interhump times from the very end of one outburst until the onset of the next stayed constant (Figure 2-40).

The UV-optical flux distribution of all dwarf novae, nova-like stars, and quiescent novae can be described to a very first approximation by a power law fit during all stages of activity; when looked at in more detail, however, there are clearly differences in the continuum flux

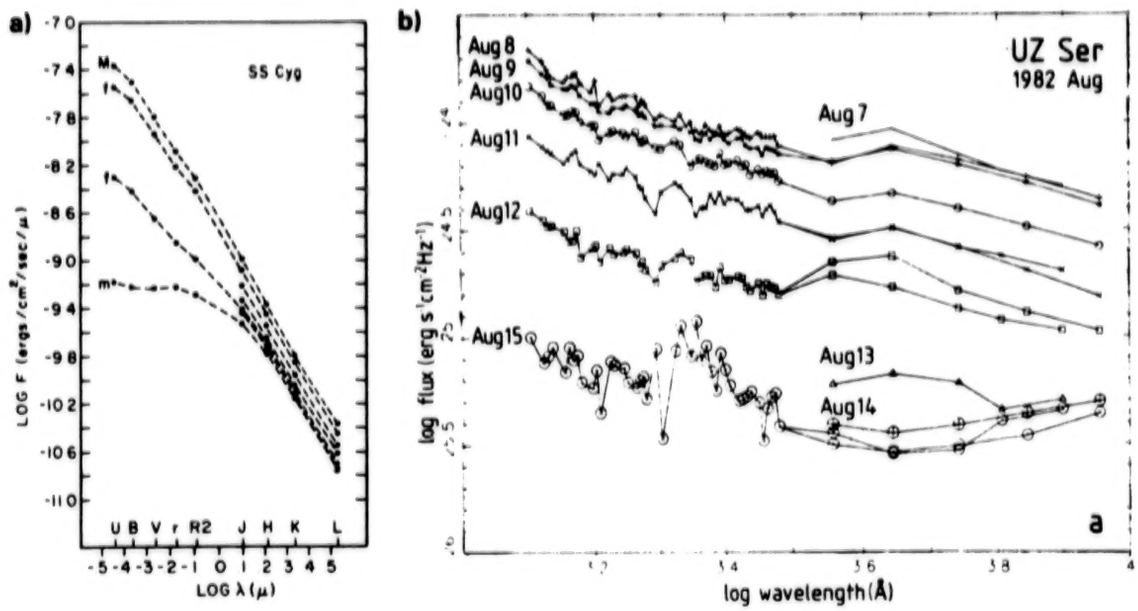


Figure 2-76. Flux changes during decline. (a) SS Cyg no color changes occur at long wavelengths, while they are appreciable at short ones (Szkody, 1977); (b) in UZ Ser the flux declines simultaneously at all optical and UV wavelengths except for very late stages (Verbunt et al, 1984).

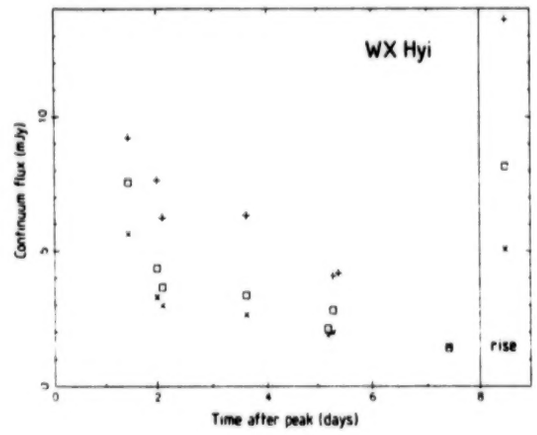


Figure 2-77. In this observation WX Hyi the UV flux keeps declining after an outburst until the following rise (Hassall et al, 1985).

distributions. Verbunt (1987) carried out an extensive survey, in particular of UV observations, at all stages of outburst activity with — besides others — the aim of deciding whether or not relations can be found between the continuous flux distribution and some other properties of cataclysmic variables. He could not find any correlation with the orbital period, with the angle of inclination, or with the average length of the outburst cycle. He did find, however, that, no matter when during an outburst of a dwarf nova a spectrum was taken, the continuous UV flux distribution is the same at the same optical brightness level; the only exceptions, of course, are spectra taken during the rise.

III.A.2. X-RAY EMISSION

ABSTRACT: During quiescence dwarf novae emit mostly hard X-rays; during outburst, soft X-rays. A relation seems to exist between the amount of hard X-rays emitted and the equivalent width of Hβ. The X-ray flux is highly variable on all time-scales.

nova-like stars: 108, 119, 122, 134

interpretation: 212, 153, 193

The X-ray radiation of stars only became accessible to astronomers when technical developments permitted observations to be

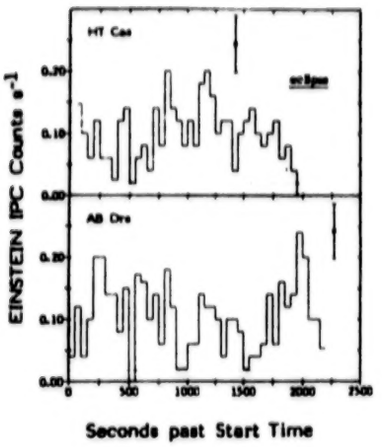


Figure 2-78. In quiescent dwarf novae the flux level at hard X-rays is highly irregularly variable (Córdova and Mason, 1984).

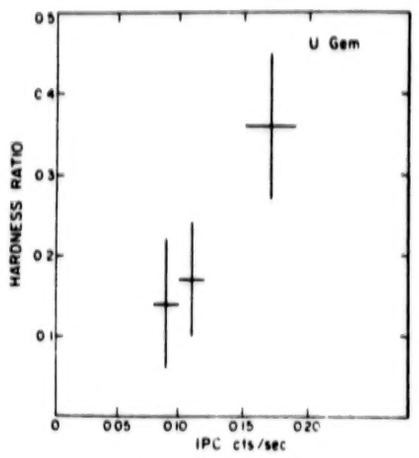


Figure 2-79. In U Gem the X-ray spectrum during quiescence becomes harder as the source becomes more intense (Fabbiano et al, 1981).

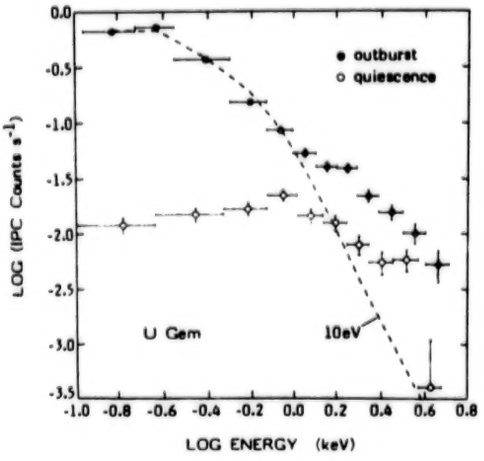


Figure 2-80. X-ray flux in U Gem in outburst and quiescence (Córdova and Mason, 1984). There are hardly any changes at hard X-rays while the soft X-ray flux strongly increases.

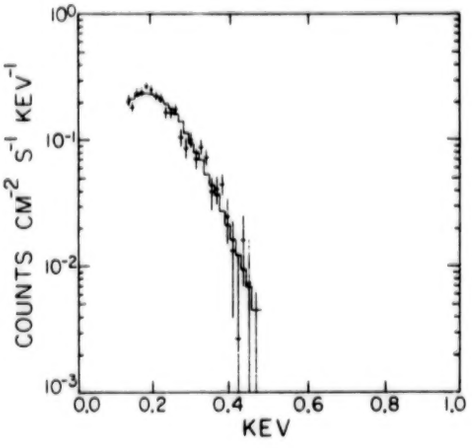


Figure 2-81. Soft X-ray flux distribution of SS Cyg in outburst (crosses); the flux can well be fitted with a 30 keV black body (solid line) (Córdova et al, 1980).

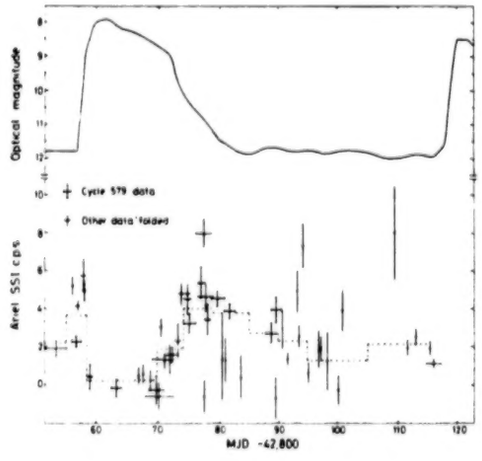


Figure 2-82. Optical and X-ray light curve of SS Cyg during the outburst cycle (Ricketts et al, 1979). For discussion see text.

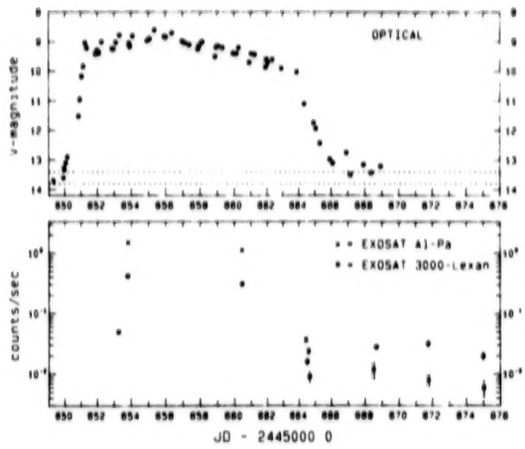


Figure 2-83. Superoutburst light curve of VW Hyi in the optical and X-rays (van der Woerd et al, 1986). For discussion see text.

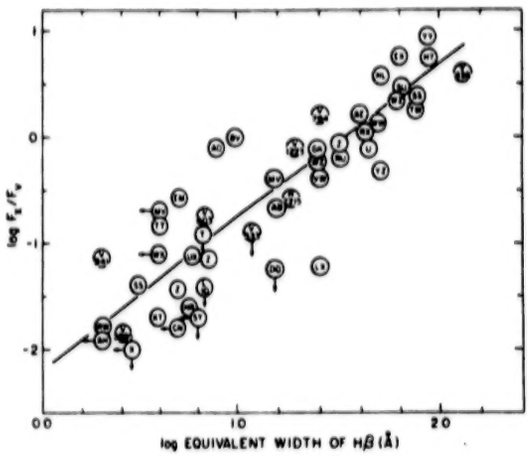


Figure 2-84. Relation between the Hβ equivalent width and the ratio between optical and X-ray flux (Patterson and Raymond, 1985a).

made from space. The first dwarf nova detected in X-rays was SS Cyg, which was seen during an optical outburst in soft X-rays (0.15 - 0.28 keV) in a rocket experiment (Rappaport et al, 1974). Further detections of, again, SS Cyg, and eventually also other cataclysmic variables in different outburst states and in different energy bands, soon followed by the HEAO 1, Apollo-Soyuz, Ariel V, Einstein, and EXOSAT satellites. In spite of considerable effort, before Einstein, SS Cyg and U Gem were the only dwarf novae which were positively detected in X-rays, although some nova-like stars had been seen as well. Altogether, Einstein was pointed at 66 cataclysmic variables, out of which 45 (of all sub-classes) could be detected in X-rays at a level of about 10^{29} $(d/100pc)^2$ erg/s (Córdova and Mason, 1983; Patterson and Raymond, 1985a).

During the quiescent state, cataclysmic variables can only be detected in hard X-rays ($\sim$0.1 - 4.5 kev). The flux distribution in this range follows approximately a thermal bremsstrahlung spectrum of $kT_{brems} \approx 10keV$ (Córdova and Mason, 1983; Patterson and Raymond, 1985a). In some systems, like SS Cyg or some nova-like stars, two flux components can be fitted to the observations (see SS Cyg, below). The flux level is highly irregularly variable on time-scales of minutes, hours, and days by a factor of two or more (Figure 2-78).

Investigation of the variations in SS Cyg during quiescence revealed that hard (2-20 keV) and soft (0.04 - 2 keV) X-rays vary together in similar ways, with a maximum correlation for a time lag of $+60 \pm 15$ sec between the hard and soft signals (King et al, 1985). The fast intensity changes are accompanied by changes in the flux distribution. The hardness ratio (color) as a function of count rate has been investigated for U Gem and SS Cyg during quiescent state: in both cases, though "hardness" refers to slightly different energy regimes, since the data were acquired with different satellites, the spectrum becomes harder as the source becomes more intense (Figure 2-79).

For dwarf novae during outburst, the ratio of X-ray flux to optical flux, F_x (0.1-4 keV)/F_v (5000-6000 Å), is found to be on the order of

1 to < 0.06%(Córdova and Mason, 1984); only the brightest dwarf novae were detected marginally in soft X-rays. During outburst there is hardly any increase, or in some objects there is even a decrease in the hard X-ray flux (van der Woerd et al, 1986: Córdova and Mason, 1984) (Figure 2-80); while in those systems which have so far been detected in soft X-rays, the soft X-ray flux (0.18 - 0.5 keV) rises by a factor of 100 or more, even though most of the radiation is hidden in the EUV range (Córdova and Mason, 1984). The soft X-ray spectra can be fitted with either black bodies of kT ≈ 25 eV - 30 eV or, alternatively, with bremsstrahlung spectra of 30 or 40 eV (Figure 2-81). Rather extensive studies of X-ray changes during the outburst cycle are available only for U Gem, SS Cyg, and VW Hyi, but considering the detection limits of X-ray satellites, there is no contradiction to the assumption that all dwarf novae follow more or less the same pattern of behavior.

The dwarf nova studied most extensively during the outburst cycle at X-rays is VW Hyi (van der Woerd et al, 1986); less extensive coverage is available for SS Cyg (Ricketts et al, 1979; Watson et al, 1985) and U Gem (Mason et al, 1978; Swank, 1979). The behavior is slightly different in all three systems; but in each system it seems to be rather accurately repeated from cycle to cycle.

In SS Cyg, both during early rise and also during late decline of the optical outburst, the hard X-ray flux increases appreciably; during the outburst, however, it drops to practically zero intensity, and then recovers slowly during the optical decline (Figure 2-82). A similar hard X-ray flare during rise was seen in U Gem (Mason et al, 1978; Swank, 1979), but never in VW Hyi. On the other hand, as in SS Cyg, the hard X-ray flux in VW Hyi disappears altogether during outburst maximum, recovers to somewhat above normal during optical decline, and is highly, erratically, variable during the optical quiescent level (van der Woerd et al, 1986).

Three normal outbursts and two superoutbursts of VW Hyi were observed with EXOSAT. In one of the superoutbursts (November 1983) the rise in X-rays was delayed with respect to the optical by about 2.5 days — i.e., the delay is even much larger than the typical delay of some 12 hours between the optical and the UV in VW Hyi (Figure 2-83); while in the case of all other outbursts which were observed in X-rays, the delay was shorter than 12 hours (van der Woerd et al, 1986). As to decline, no matter what kind of optical outburst occurs, the soft X-ray flux seems to start declining immediately after the flux maximum in X-rays has been reached; at superoutburst the rate during first decline is smaller than normal (Figure 2-83). After the optical decline has ended, the soft X-ray flux keeps falling down to well below the quiescent level, then rises gradually to slightly above the normal level and goes on falling at a small rate untii onset of the next outburst. Only when the minimum soft X-ray flux is reached after the end of the outburst does the generally soft spectrum seen during outburst change into the hard quiescent spectrum.

No significant difference in X-ray characteristics seems to exist between members of sub-classes of dwarf novae and nova-like objects, respectively, but Córdova and Mason (1983) found some indication that in general the X-ray flux might be higher in dwarf novae than in nova-like stars. Furthermore, Patterson and Raymond (1985b) found that eclipsing systems emit significantly less X-ray flux than others. From inspecting the relation between hard X-rays and optical flux from cataclysmic variables, they found that those objects for which both fluxes are of comparable strength exhibit optical spectra with strong hydrogen emission lines, while the lines become less pronounced, the stronger the visual flux is compared to the X-rays. Relating the ratio of the X-ray flux to the visual flux with the equivalent width of Hβ, an amazingly tight relation emerges (Figure 2-84) which contains only observational data.

III.A.3. RADIO EMISSION

nova-like stars: 119, 134

Searches for radio emission from dwarf novae have been conducted with the 100 m telescope in Effelsberg as well as with the VLA (Córdova et al, 1983; Benz et al, 1985). Córdova et al checked six dwarf novae and nova-like stars and could detect none. Benz et al detected SU UMa during an optical outburst at 4.75 GHz; during quiescence SU UMa was too weak to be observable; it also could not be detected at 4.9 GHz by later observers (Chanmugam, 1987). In addition, the dwarf novae TZ Per and UZ Boo both were detected at 2.5 GHz (Turner, 1985).

GENERAL INTERPRETATION: The UV flux and most of the optical flux of dwarf novae and nova-like stars is believed to originate in the accretion disc. The IR flux seen during quiescence, and possibly some of the optical flux, come from the secondary star and, if strong, cause a rise of the flux at IR wavelengths. The rise to an outburst either occurs simultaneously at all wavelengths when the rise is slow, or, when it is fast, starts progressively later with decreasing wavelengths as ever more central (hotter) parts of the disc become involved. During decline, all of the disc cools simultaneously. In a small or cool disc, contributions from the boundary layer between the disc and the white dwarf might be seen in the UV. X-ray radiation is ascribed to the boundary layer which is optically thin during quiescence (thus emitting hard X-rays) and optically thick during outburst (emitting soft X-rays because the radiation is thermalized before escape).

OBSERVATIONAL CONSTRAINTS TO MODELS:

- *The UV through optical flux distribution of dwarf novae is clearly not that of a normal star. (See 192, 194.)*
- *Very characteristic flux changes at all wavelengths occur during the outburst cycle. (See 192, 194.)*
- *There exists some relation between short-term changes in the optical and the X-ray flux. (See 212.)*
- *There is no obvious relation between the spectral index and any of the system parameters.*

III.B. LINE RADIATION

III.B.1. SPECTRA DURING QUIESCENCE

III.B.1.a. GROSS APPEARANCE

ABSTRACT: Most dwarf novae exhibit strong emission line spectra in the optical and UV during quiescence, although some have only very weak emissions in the optical and/or weak absorptions at UV wavelengths. Many exhibit double-peaked profiles in the Balmer emission lines. In several objects, the absorption spectrum of a cool main sequence star is visible.

photometric appearance: 35

nova-like stars: 99, 107, 117, 119, 122, 124, 134, 141

interpretation: 192, 200

In the quiescent state, the optical spectra of dwarf novae usually are characterized by more or less strong emission lines of the Balmer series of hydrogen and He I, and occasionally of He II and/or Ca II; and sometimes even lines of Fe II, C III-N III, etc., can be seen (exceptions will be discussed below). Corresponding to the emission line strength, the Balmer jump is normally seen in emission during quiescence. The Balmer decrement generally is very flat, with Hβ or even Hγ often stronger than Hα. In many objects the Balmer lines appear to have two peaks, shortward and longward of the rest wavelength. All dwarf novae which show an eclipse also show such double-peaked emission lines, but many others do as well. Most of these dwarf novae exhibit a strong hump in their light curve, but there is, for example, V436 Cen which has neither a hump nor an eclipse but clearly shows double-peaked emission lines (Gilliland, 1982a). A representative collection of quiescent optical spectra of dwarf novae is given in Figure 2-85.

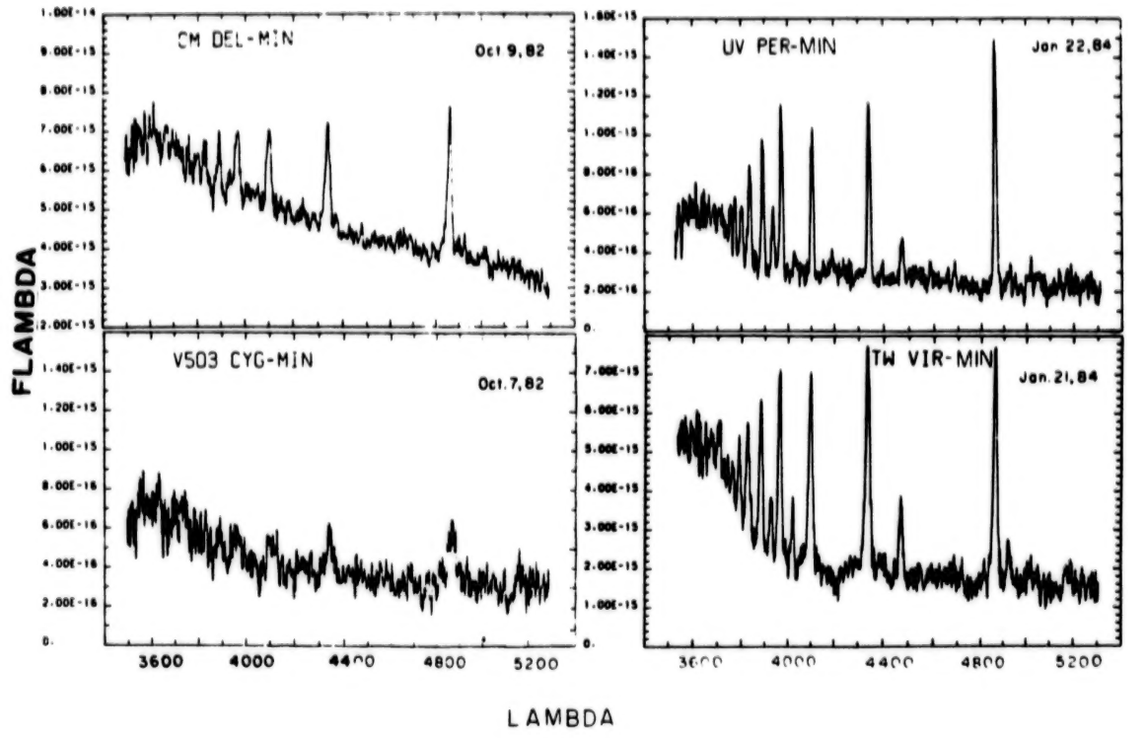


Figure 2-85. Typical quiescent spectra of dwarf novae in the optical (Szkody, 1985a). Almost all the spectra show the Balmer lines and the Balmer jump strongly in emission.

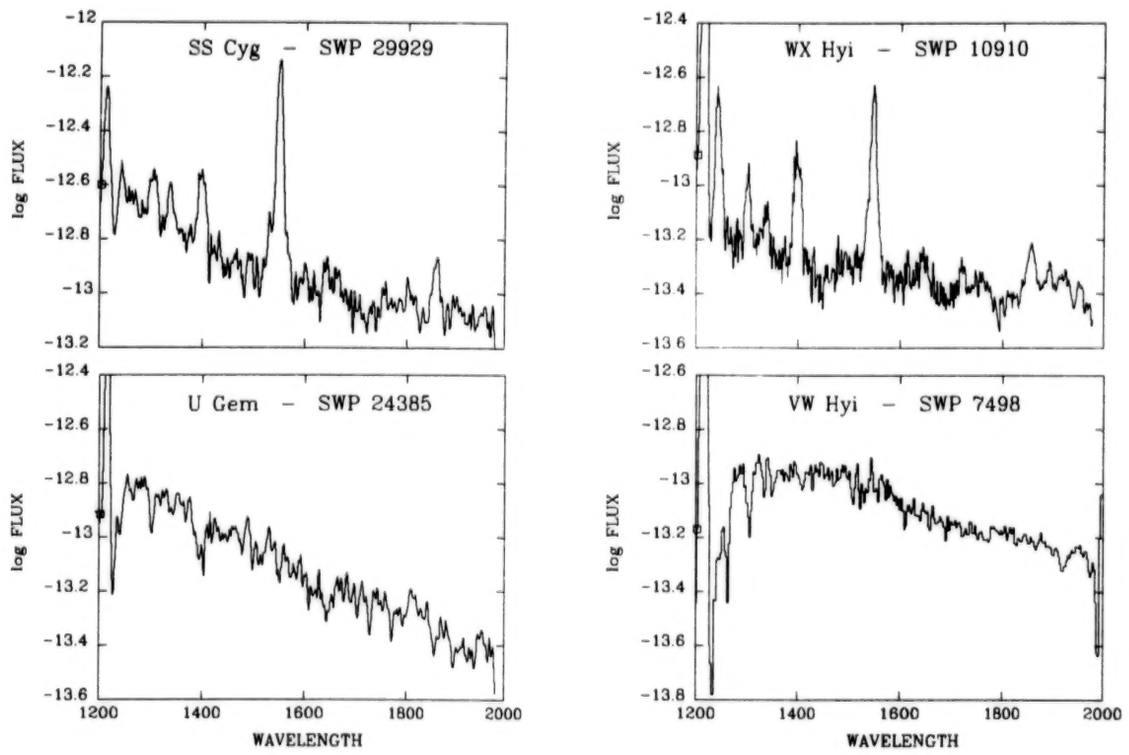


Figure 2-86. Typical quiescent spectra of dwarf novae in the UV. Flux is in erg cm^{-2} sec^{-1} $Å^{-1}$.

Williams (1983) published equivalent widths and line widths of all measurable lines for a sample of 153 spectra of novae, dwarf novae, recurrent novae, and nova-like stars. Comparing values for various types of cataclysmic variables, it turns out that the equivalent widths of the Balmer lines are statistically significantly larger for dwarf novae and nova-like stars than for novae. On the average, they are also larger for dwarf novae than for nova-like stars, but the difference is small enough to not be a distinguishing characteristic. No significant difference appears to exist between the equivalent widths and line widths of the various sub-classes of dwarf novae and nova-like stars. While the ratios of the equivalent widths of $H\beta/H\gamma$ are approximately the same for all dwarf novae and nova-like stars, $H\beta$ often is of comparable strength to, or even stronger than $H\alpha$ in dwarf novae, whereas $H\alpha$ is generally the stronger line in nova-like stars. The Ratio of $H\alpha$/HeII (4686 Å) is on the order of one for novae, and is very much larger than this for dwarf novae and nova-like stars. The line wings in all cataclysmic variables can extend to as much as 2000 km/s away from the line center. In novae, the full line widths at half intensity are statistically smaller than in dwarf novae and nova-like objects, being some 500 to 600 km/sec and some 700 to 800 km/sec, respectively. In all cases, however, the scatter between different objects of the same class is very large (see also chapter 6.III.A, Table 6.6, and Figures 6.14a, b, c, d).

In addition to the emission line spectrum, a cool absorption spectrum, normally of spectral type G5V or later, is visible in some objects. Provided the systems are bright enough at minimum light level, this cool spectrum normally is seen in the optical in objects with orbital periods in excess of some 6 hours, but at close inspection, and in the infrared, it also is seen at much shorter periods.

Quiescent dwarf novae usually also exhibit a strong emission line spectrum of all the resonance lines in the UV which can be seen by IUE, frequently with the exception of N V 1240 Å; moreover, He II 1640 Å is usually also seen. As in the optical, normally the line width is on the order of several hundred km/sec Doppler velocity. Only few objects, like U Gem, Z Cha, CN Ori, and TY Psc, instead show a weak absorption spectrum consisting of also mainly the resonance lines. A sample of representative UV spectra of dwarf novae during the minimum state is given in Figure 2-86. There is no apparent relation between the appearance of the UV spectrum (emission or absorption lines) and the optical spectrum, nor is there any relation to any sub-classes of dwarf novae. Also, independent of what the UV spectrum at shorter wavelengths looks like, strong emission in the Mg II doublet (2800 Å) is present in many objects.

In general, the quiescent spectrum of each dwarf nova is very characteristic for each system and is repeated in fair detail after each outburst.

III.B.1.b. THE HOT SPECTRUM

ABSTRACT: No conclusive information about orbital spectral changes in the UV is available. In the optical, usually all lines undergo profile changes on orbital time scales; in particular many of these lines are weakened during photometric eclipse. In some objects the changes seem to be unrelated to orbital changes.

related photometric changes: 35

nova-like stars: 99, 107, 117, 119, 122, 124, 134, 141

interpretation: 192, 200

No general changes in the appearance of the quiescence spectra of any dwarf nova could be found in the UV during all the time IUE has been working. The only long-term changes that have been detected so far are slight decreases in the UV line fluxes from VW Hyi and WX Hyi (sufficiently accurate data are not available for other systems) between successive outbursts (Hassall et al, 1985; Verbunt et al, 1986).

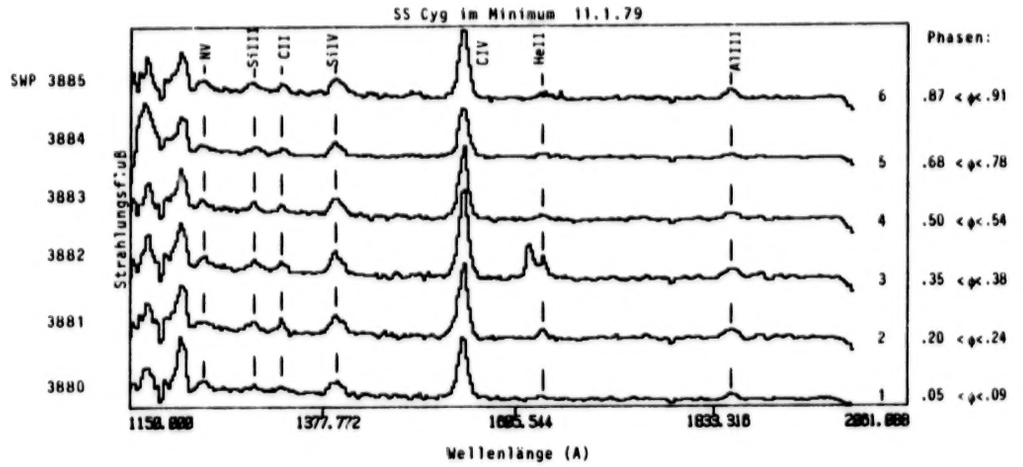


Figure 2-87. Changes of the UV flux on orbital time-scales in SS Cyg during quiescence. It is not clear whether the changes are related to the orbital revolution or not (la Dous, 1982).

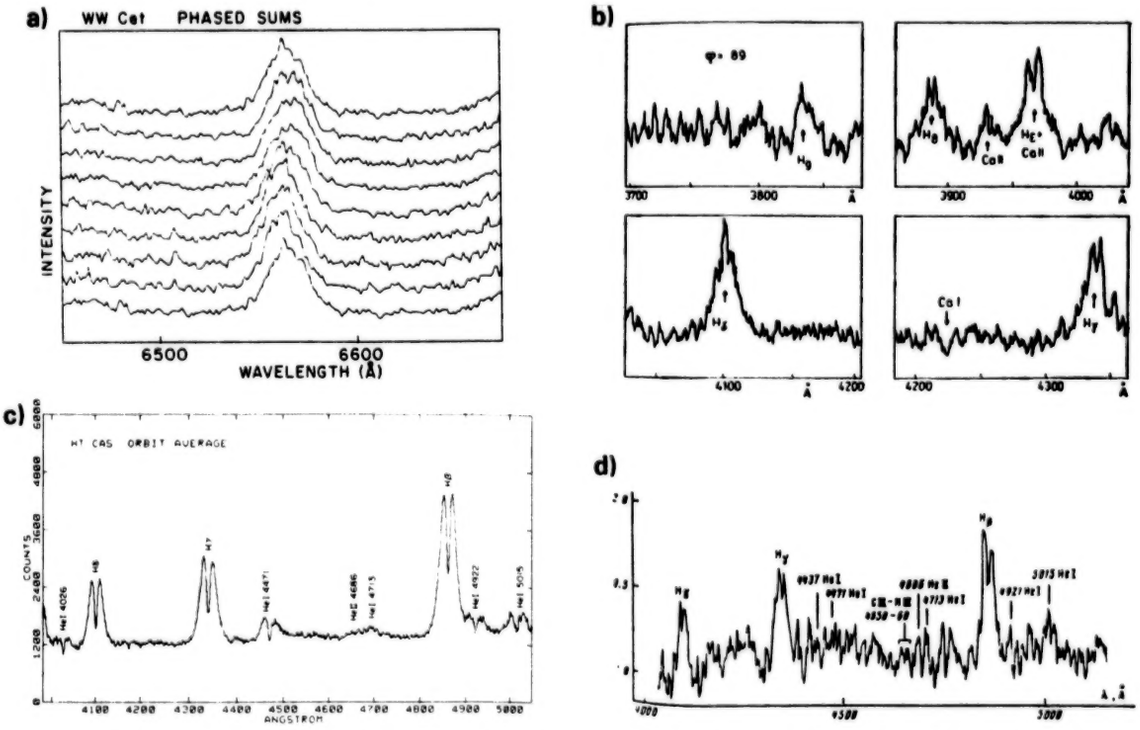


Figure 2-88. Optical emission line profiles in dwarf novae: (a) WW Cet: Thorstensen and Freed, 1985, (b) SS Cyg: Giovannelli et al, 1983, (c) HT Cas: Young et al, 1981b, (d) RZ Sge: Voikhanskaya and Nazarenko, 1984, (e) Z Cha, Marsh et al, 1987. (See text for discussion.)

Most dwarf novae are too faint in quiescence for any orbital phase-resolved spectroscopy in the UV to be possible, not even in the low resolution mode of IUE, since exposure times are still typically on the order of the orbital period. Two exceptions are SS Cyg and U Gem. In both cases some marginal variability of the line profiles and strengths is visible, but it is not clearly related to orbital variations (Figure 2-87). No radial velocity measurements are possible with IUE in the low dispersion mode, nor is the wavelength resolution good enough for line profiles to be investigated in detail.

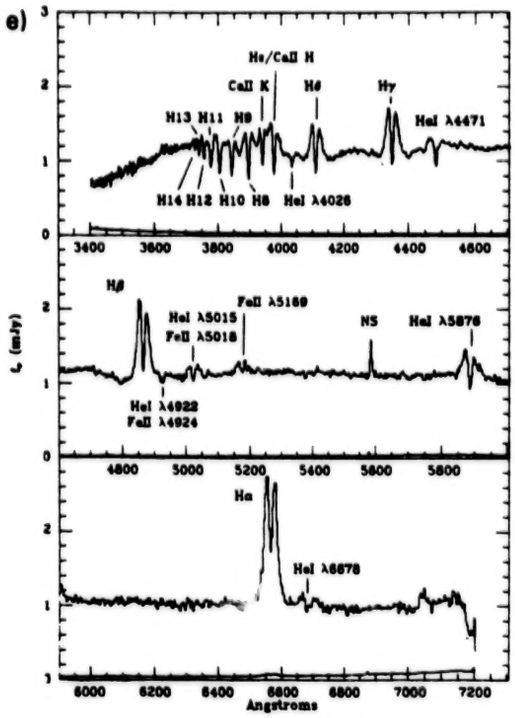


Figure 2-88e.

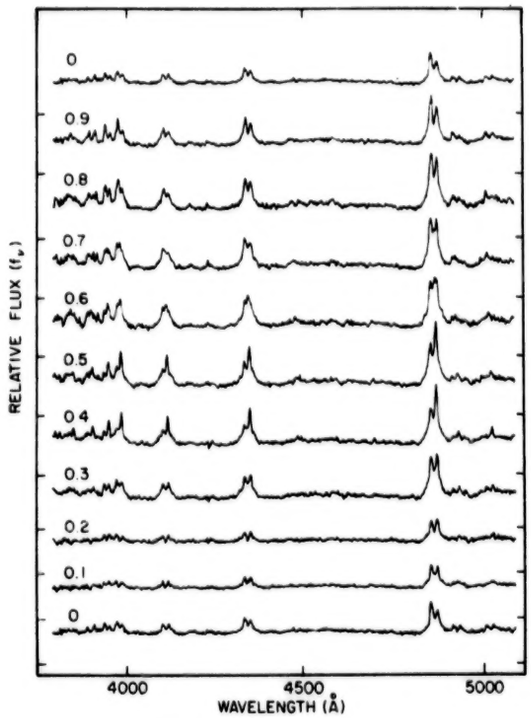


Figure 2-89. Orbital line profile variations in U Gem (Stover, 1981a). Phase zero is at mid-eclipse.

As mentioned already, the optical emission lines (Balmer lines and He II) often exhibit a double-peaked structure when observed at sufficiently high spectral resolution. Many objects* also have single-peaked lines when observed at high resolution (Figure 2-88a), but still the structure of the profiles is extremely complicated and by no means smooth. In other cases (Figure 2-88b), some of the Balmer lines are clearly double peaked; others are not, or are so only at certain orbital phases. There is a general tendency for the higher members of the Balmer series to have more complex profiles than the lower ones. When a clear double-peaked structure is present, the relative depth of the central dip in most objects increases with increasing quantum number (Figure 2-88c); in some, like RZ Sge or V436 Cen it decreases (Figure 2-88d). In many objects, the separation between the two emission peaks of the hydrogen lines, measured in Doppler velocities, increases with increasing quantum number (e.g., Schoembs and Hartmann, 1983). In OY Car and Z Cha the absorption is seen to clearly drop below the continuum level in the higher Balmer lines, from $H\gamma$ on (Figure 2-88e). In Z Cha the emission peaks even completely disappear for $H\epsilon$ and higher members of the series, so that this object emits a combination of an emission and an absorption spectrum in quiescence in the optical. In Z Cha, OY Car, and possibly also in HL CMa during the quiescent state, the strong hydrogen emission lines from $H\beta$ on are placed in very wide, shallow absorption features (Figure 2-88e).

All the lines usually are subject to profile changes with the orbital cycle. Whether, or to what extent, these variations are a stable pattern over long time-scales, and whether the source of the emissions undergoes changes are unknown; all investigations so far only covered, at best, just a few orbital cycles which were not

*That most objects are discussed extensively in the literature have doubl-peaked profiles must be regarded as a selection effect, namely which objects astronomers choose to observe. Objects with a double-peaked structure tend to have high inclination angles which allow for a relatively easy determination of the system parameters; consequently they are observed with high priority.

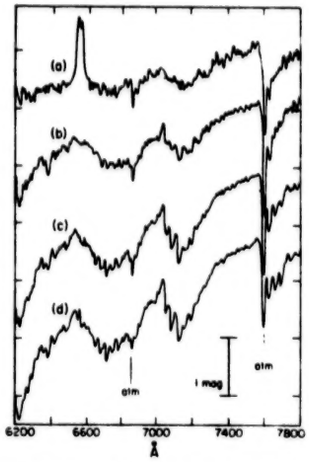


Figure 2-90b. IR spectrum of U Gem (distribution a; distributions b - d are of M dwarfs for comparison) (Wade, 1979). In this system the secondary spectrum is clearly visible at IR wavelengths.

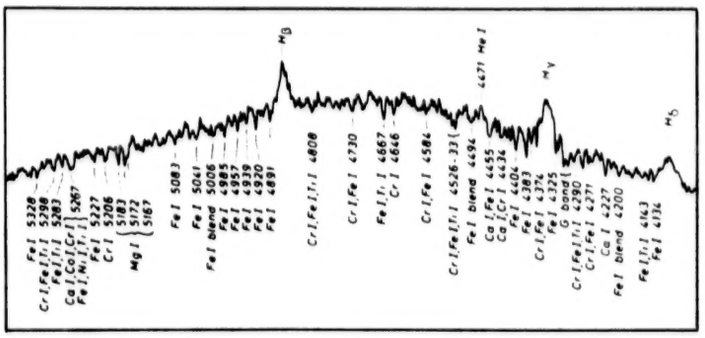


Figure 2-90a. Optical spectrum of BV Cen during quiescence (Vogt, 1980b). The absorption spectrum of the cool companion is well visible at optical wavelengths.

separated by longer time intervals. However, the strength and nature of these changes seems to become more pronounced with increasing inclination angle; i.e., changes become stronger when a hump or even an eclipse is present. In eclipsing dwarf novae there normally are no dramatic orbital changes in the appearance of the line profiles outside eclipse, but emission line fluxes are appreciably reduced only at times when a strong orbital hump is seen. During eclipse, however, the continuum flux as well as the lines are strongly reduced; the line profiles undergo dramatic changes showing clearly how first the blue and then the red wings of the lines are being eclipsed (Figure 2-89). During all these kinds of changes the width of the line wings is hardly affected. Photometrically, EM Cyg is an extremely variable, quickly, erratically changing object, showing rapid flickering and a shallow eclipse which is highly variable in both shape and depth (Stover et al, 1981). The behavior of the emission lines seems to follow this general characteristic, line profiles and strengths are extremely variable on time-scales at least as short as the orbital period (some 7 hours), being single-peaked, double peaked, or even more complex; but no correlation with the orbital phase can be detected. A similarly chaotic behavior is reported for the also photometrically very active star BV Cen (Vogt and Breysacher, 1980b).

III.B.1.c. THE LATE ABSORPTION SPECTRUM

ABSTRACT: At IR wavelengths and in systems with long orbital periods at wavelengths longward of some 6000 Å, the absorption spectrum of a cool main sequence star becomes visible.

related photometric observations: 39

nova-like stars: 102, 109, 115, 122, 139

interpretation: 153, 194

In many of the dwarf novae with long orbital periods, the absorption spectrum of a cool star has been detected, in addition to the emission spectrum, in the optical and, more often, in the IR (Figure 2-90a). The spectral type usually is G5 or later, approximately that of a cool main sequence star (Figure 2-90b). The visibility of the secondary spectrum varies inversely with the continuum flux: it is easily visible during quiescence when the continuous flux of the hot component is low, and it essentially disappears during outburst. No variation could be detected in these secondary spectra except for that due to orbital changes. The orbital changes usually only consist of changes in the radial velocity. In RU Peg does the luminosity class of the secondary change from spectral type III at upper conjunction (red star behind) to spectral type V at right angles to this (Kraft, 1962b),

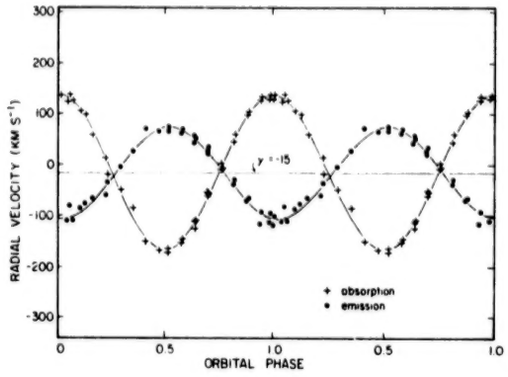


Figure 2-91. Radial velocity changes of SS Cyg during quiescence (Stover et al, 1980). The velocities of the Balmer emissions and the cool absorptions are out of phase by not quite 180°.

suggesting that the side of the secondary star facing the white dwarf is less dense due to reduced gravity around L_1.

III.B.1.d. RADIAL VELOCITY CHANGES

ABSTRACT: The radial velocity curves of both emission and (cool) absorption lines have the same periods as the hump/eclipse light curves. Emission and absorption spectra are out of phase by about 180°.

related photometric changes: 35

nova-like stars: 101, 107, 115, 119, 122, 134, 142

interpretation: 151, 156

The emission lines and, to the extent measureable, the absorption lines undergo periodic changes in their radial velocities.* In almost all dwarf novae, the spectroscopic periods are identical with the photometric periods**, determined from eclipse features or humps, within the limits of accuracy. Emission and absorption lines are out of phase by almost

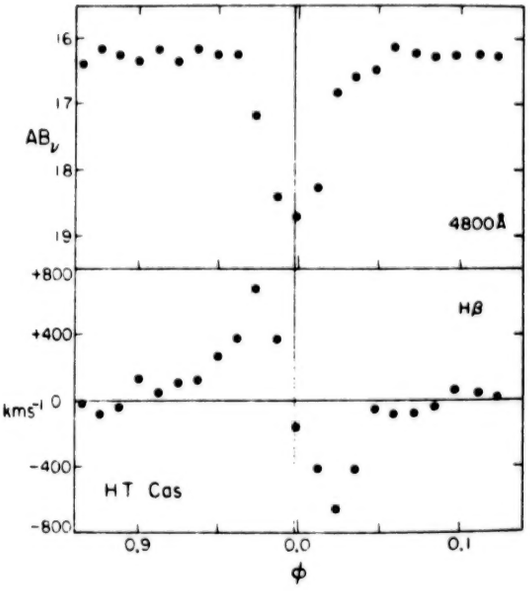


Figure 2-92. Radial velocity changes in HT Cas through eclipse (Young et al, 1981b).

(not quite!) 180° (Figure 2-91): there is a phase lag of typically 5° to 10° of the emission with respect to the absorption in all objects that have been investigated in sufficient detail so far; the exact angle varies from one object to another but seems to be stable for any given system (e.g., Kraft et al, 1969). The K-amplitude is typically on the order of 50 to 200 km/sec. The phase of maximum emission-line velocity is on the rising branch of the hump, so eclipses have phases of 0.2 to 0.3 with respect to this.

As mentioned earlier, very dramatic changes in the emission line profiles occur during eclipse (Figure 2-89). The radial velocity changes of Hβ through eclipse of HT Cas are shown in Figure 2-92: within only five minutes the line velocity changes from +700 km/sec to -700 km/sec, centered at phase 0.998. Young et al, (1981b) call this the *Z-wave* for its resemblance to this symbol.

*There are considerable difficulties connected with measuring radial velocities in cataclysmic variables, which will be discussed in chapter 4.II.C.1. There is no very basic difference, however, between radial velocities derived from either of the emission peaks, the central absorption, or the line wings, even though it is not clear exactly what physical property is being measured.

**In CN Ori several different photometric periods have been measured at different times, of which it is not clear which is the orbital period. No reliable spectroscopic period is available as yet (Mantel et al, 1988).

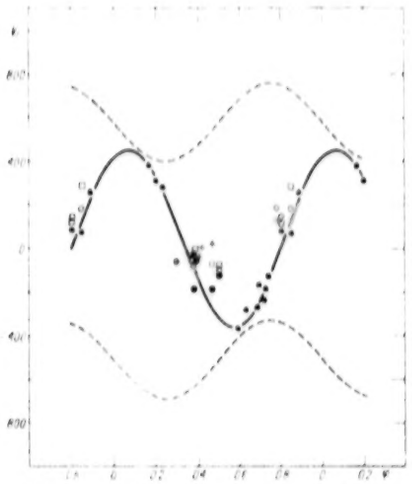


Figure 2-93. Radial velocity changes of the S-wave in U Gem (Smak, 1976). The various symbols represent radial velocity measurements in different lines; the solid line is the solution for He I 4471 Å; the dotted line represents radial velocity measurements for the red and blue wings of Hγ, respectively.

III.B.1.e. THE S-WAVE

ABSTRACT: The particular orbital changes connected with profiles of double-peaked emission lines often are referred to as "S-wave."

nova-like stars: 102, 110, 122, 124, 135, 142

Inspecting Figure 2-89, one realizes that the relative strength of the red and blue peaks of the hydrogen lines varies systematically over the orbital cycle, irrespective of whether or not the system is being eclipsed. Similar effects are seen in other lines (He I, Ca II), and in other objects. There are still other objects, however, like OY Car, Z Cha, and others, in which no such effects could be found despite an intensive search. This effect of changing profiles is usually referred to as *S-wave*. This often is understood to be an additional third emission component which wanders independently between the two wings of the line. Smak (1976) determined its radial velocity from the hydrogen lines of U Gem, but also from He I 4471 Å and Ca II K, both of which seem to originate entirely in the source of the S-wave emission in U Gem (Figure 2-93). It should be noted that the velocity amplitude of the S-wave is more than twice that of the wings, and that there is a phase shift of about 100° in U Gem, slightly different for different lines, between the S-wave and the main emission of the hydrogen lines. A phase shift of about -80° is seen in HT Cas (Young et al, 1981b); and the radial velocity curve of the main component and the S-wave in T Leo are almost anti-correlated (Shafter and Szkody, 1984). There is no way to explain the almost random behavior of the profiles in EM Cyg with some kind of S-wave.

III.B.1.f. UV FLARES

nova-like stars: 117

Walker and Chincarini (1968) and Walker (1981) report the appearance of "UV-flares" in the spectra of SS Cyg during quiescence. These are temporarily (on the order of some tens of minutes) increased fluxes in mostly the Balmer lines, but He I and Ca II can also be affected at times, and to a small degree the continuum flux. Similar flares have been detected in the nova-like stars RW Tri and AE Aqr (sometimes also classified as dwarf novae), however, with a much lower frequency than in SS Cyg (Walker, 1981).

GENERAL INTERPRETATION: The generally observable emission line spectra in quiescent dwarf novae are ascribed to optically thin disc areas; absorption spectra in the UV, as seen in a few systems, may indicate that the inner accretion disc is basically optically thick. The cool absorption spectrum in the (optical and) infrared is ascribed to the secondary star. — Periodic changes in radial velocities and line profiles are ascribed to orbital changes, and periodic random profile changes to inhomogeneities in the brightness distribution of the accretion disc. The double-peaked line profiles in high-inclination systems are believed to be due to disc rotation. In those cases where the dip between both peaks reaches below the continuum level, the white dwarf absorptions are believed to influence the line flux significantly. The phase shift between the radial velocities determined from emission and absorption is an effect of binarity, as the emission lines originate in the disc and the absorption spectrum in the secondary star.

OBSERVATIONAL CONSTRAINTS TO MODELS

- *The high-inclination systems in particular exhibit double-peaked emission line profiles. (See 202.)*
- *In many systems, the emission line profiles undergo characteristic changes during the orbital cycle.*
- *In many systems, an "S-wave" is seen to move between the two peaks of the emission lines in phase with the orbital cycle.*
- *A relation is observed to exist between the line width and the equivalent width of the hydrogen lines and the sub-types of cataclysmic variables.*
- *In some objects, the Balmer emission lines are placed in broad absorption shells. (See 151, 194.)*

III.B.2. SPECTRA DURING THE OUTBURST STATE

III.B.2.a. GROSS APPEARANCE

During outburst, there appears an absorption spectrum of the resonance lines and of He II 1640 Å in the UV and of mostly the Balmer lines in the optical (Figure 2-94, 2-95), where He II, and C III-N III may be present as well. At maximum and during decline, the optical lines sometimes have emission cores. The UV resonance lines often display strong asymmetric blue-shifted line profiles or P Cygni profiles. The late absorption spectrum, which might have been seen in quiescence, disappears due to the increased hot continuum flux during outburst. In both the appearance and the variability of their spectra, there is no difference between the sub-classes of dwarf novae (which were defined on grounds of photometric behavior).

III.B.2.b. THE RISE PHASE

ABSTRACT: During rise the emission lines gradually sink into broad absorption shells. The cool absorption spectrum can hardly be detected any longer.

related photometric observations: 46

nova-like stars: 99, 107, 117, 119, 122, 124, 134, 141

interpretation: 192, 194, 200

Until the very onset of an outburst, no changes of the line profiles in excess of normal variations could be observed in SS Cyg during the quiescent state (Clarke et al, 1984, and Figure 2-96). During the very early rise in SS Cyg, the flux in the Balmer emission lines remained constant, an observation confirmed by Walker and Chincarini (1968) for a different outburst of SS Cyg. As the continuum level increased, however, the equivalent widths decreased slightly, and for a while the spectrum appeared almost featureless. When the steep rise to maximum began, the emission line flux decreased rapidly and became undetectable; at the same time strong Balmer absorption lines appeared. Also, at late rise to an outburst in SS Cyg as well as in many other systems, the Balmer jump as well as the Balmer absorption lines can, for a short while, become much stronger than during the remainder of the outburst. Also during the rise in SS Cyg (Walker and Chincarini, 1968), the Ca II K line, which is clearly in emission during quiescence, was seen to go into absorption and to split into two peak components which are separated from each other by about 800 km/sec Doppler velocity, in contrast to some 300 km/sec separation of the tiny emission peaks in quiescence. The He I emission lines largely followed the early hydrogen emissions in their development during the rise and were undetectable during most of the bright state. The He II emission line at 4686 Å and the C III - N III blend at 4650 Å (which are only marginally visible, if at all, in quiescent dwarf novae) basically followed the development of the continuum flux during outbursts: they became strongly visible at late rise, faded during decline, and disappeared again at some late stage of decline. No extensive coverage is available for any other dwarf nova; but the information that is available does not contradict the assumption that this kind of

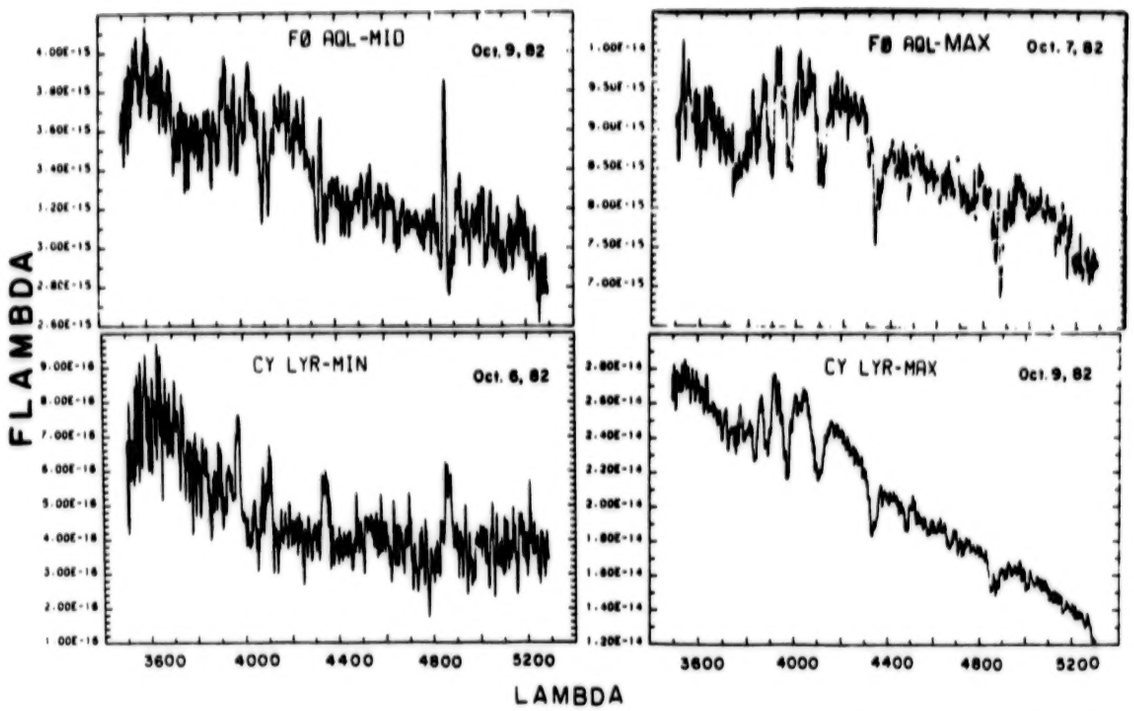


Figure 2-94. Typical spectra of dwarf novae during outburst: FO Aql at maximum and decline; CY Lyr at maximum and quiescence (Szkody, 1985a). During outburst the spectra are dominated by strong Balmer absorption lines.

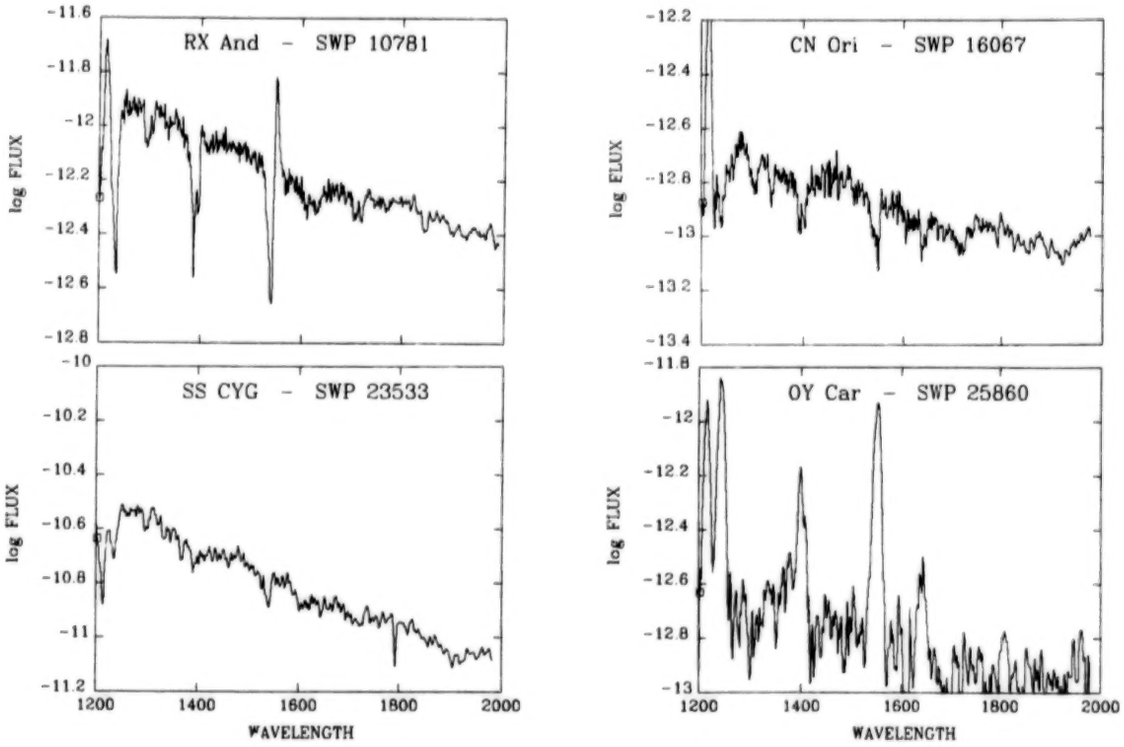


Figure 2-95. Typical UV spectra of dwarf novae during outburst. Flux is in erg cm^{-2} sec^{-1} $Å^{-1}$. The spectra are dominated by absorption lines, possibly P Cygni profiles; only double-eclipsing systems show pure emission spectra.

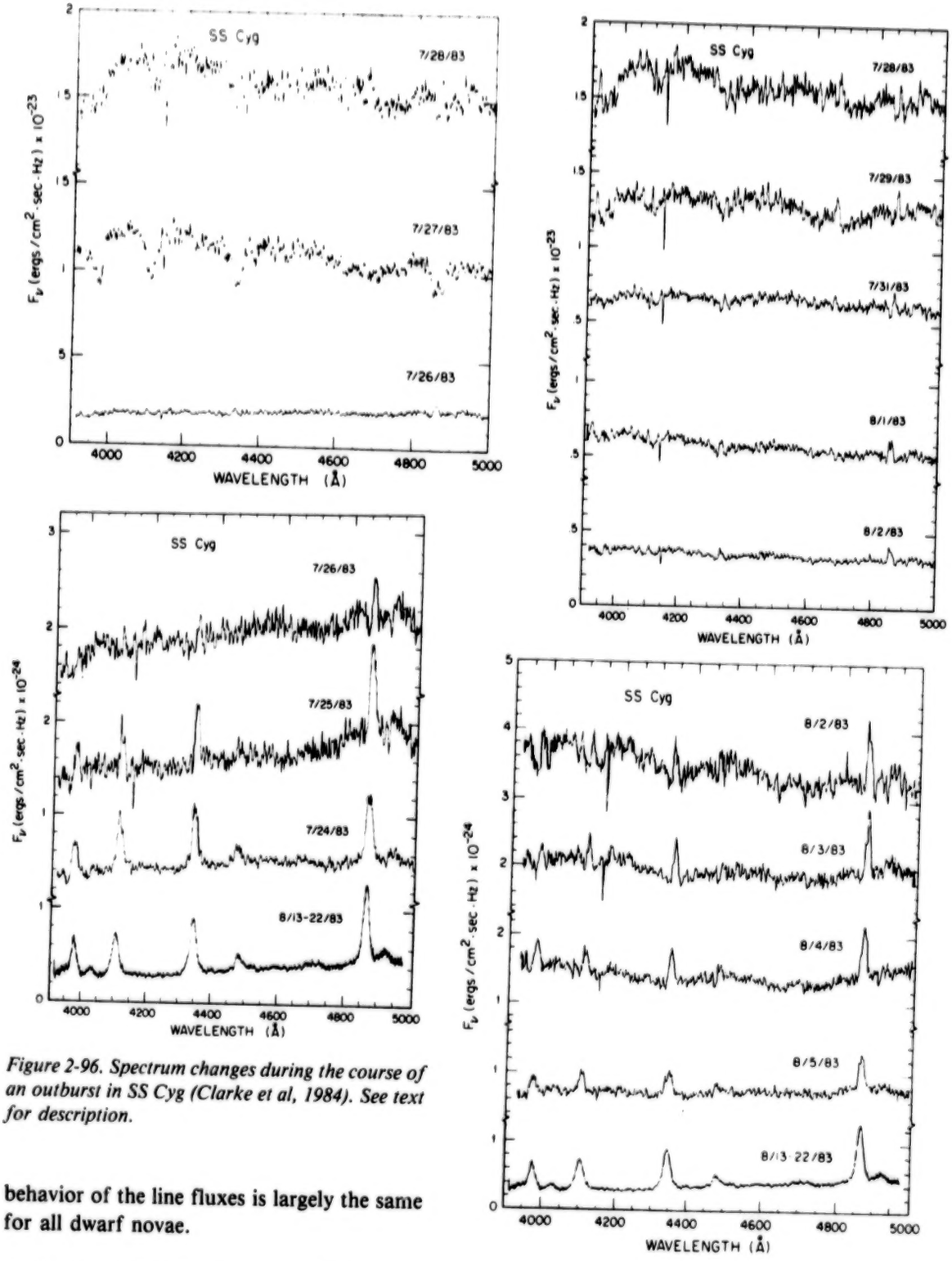


Figure 2-96. Spectrum changes during the course of an outburst in SS Cyg (Clarke et al, 1984). See text for description.

behavior of the line fluxes is largely the same for all dwarf novae.

The absorption line spectrum of the cool component soon disappeared almost completely in the rising continuum flux and could only be reliably detected again just before the minimum brightness had been reached at the end of the decline. Hessman et al (1984), however, did succeed in observing the secondary spectrum in SS Cyg during outburst.

III.B.2.c. OUTBURST MAXIMUM AND DECLINE

ABSTRACT: At or shortly after maximum light emission cores begin to grow in the absorption lines; during the course of decline gradually the quiescent spectrum is restored.

related photometric observations: 46

interpretation: 192, 194, 200

The usual appearance of the line spectra of dwarf novae in the optical during outburst is that of hydrogen absorption lines the wings of which extend several thousand km/sec Doppler width away from the line center. Relatively narrow emission components of different strength can be present at times, superimposed on these absorptions. Besides these lines, there are usually emissions of the He II and C III-N III, and probably a few other lines. Thus either a pure absorption spectrum (the less common case), or a mixed absorption and emission spectrum can develop (Figure 2-97). The Balmer jump is generally very weak, on the order of 0.1 mag at maximum; it decreases during the course of decline and eventually goes into emission around the time when the quiescent state is reached again. No P Cygni profiles or asymmetric line profiles, which are common in the UV, have been detected in the optical. In one case, in Z Cha during a superoutburst (there are no observations of a normal outburst), there are no broad absorption lines of hydrogen, but rather the Balmer lines of Hα through Hγ appear as pure, double-peaked emission lines (the peak-to-peak separation is clearly less than during quiescence), while the higher series members appear as pure single-peaked absorption lines (Figure 2-98), so the spectrum looks very similar to the quiescence spectrum (Figure 2-88e). Also during superoutburst, OY Car and Z Cha exhibit pure emission spectra in the UV (see below) — both stars show double eclipses during the quiescent state and thus have an inclination angle close to 90°. No basic difference (at any rate, no more difference than is normal between different outbursts) seems to exist between the spectra of outbursts and superoutbursts and of standstills in dwarf novae.

The development of the lines during decline in dwarf novae can be seen from the typical example of SS Cyg in Figure 2-99 (see also Figure 2-96): as the continuum flux fades, the, in the beginning small, Balmer emission cores grow inside the absorption lines while the absorption gradually fades. At all phases the emission is the weaker the higher the quantum number of the Balmer lines. At the brighter stages of the outburst, the hydrogen lines are considerably narrower than those seen during quiescence; they become progressively broader as the decline proceeds. Comparison between the two sets of decline spectra of SS Cyg demonstrates that, though the gross behavior is repeated, the line profiles, as well as the sort of lines visible besides the hydrogen lines, vary from outburst to outburst. Hessman (1986) investigated the profiles of the absorption components of the Hβ and Hγ lines during decline in the SS Cyg, and found that they are practically constant throughout decline.

Schoembs and Vogt (1980) observed VW Hyi spectroscopically during decline from a superoutburst. First there was a pure absorption spectrum near maximum brightness. Around the end of this outburst a faint emission spectrum exhibiting lines of H, He I, and Fe II was observed, which, however, was replaced by an essentially continuous spectrum during the following two nights. The spectra during these two nights stayed featureless, while photometrically large changes of up to 0.5 mag were observed, due to a coincidence of the orbital hump and the superhump. At the very end of decline of VW Hyi from a normal outburst, Schwarzenberg-Czerny et al (1985) observed very dramatic changes in Hα and Hβ on time scales of hours, which, however, were not related to the orbital phase (Figure 2-100).

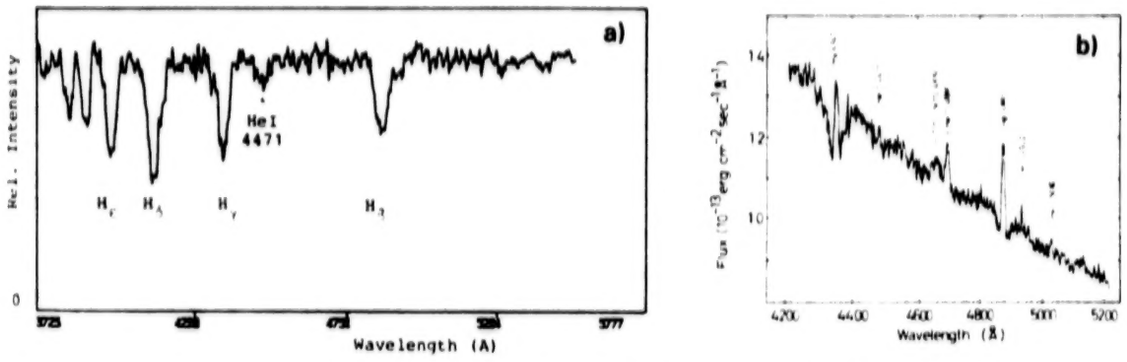


Figure 2-97. Outburst spectra of dwarf novae: a) TU Men (Stolz and Schoembs, 1984) shows pure absorption profiles; b) the more normal case is that emissions are placed in the cores of the absorptions, as e.g., in HL CMa (Wargau et al, 1983a).

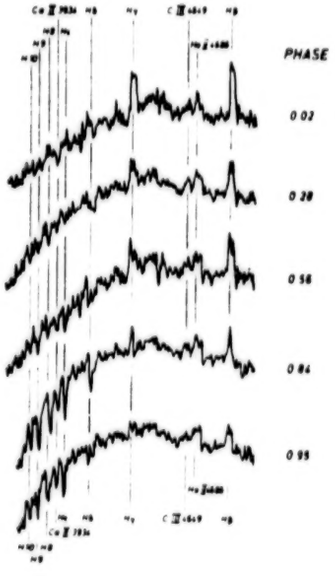
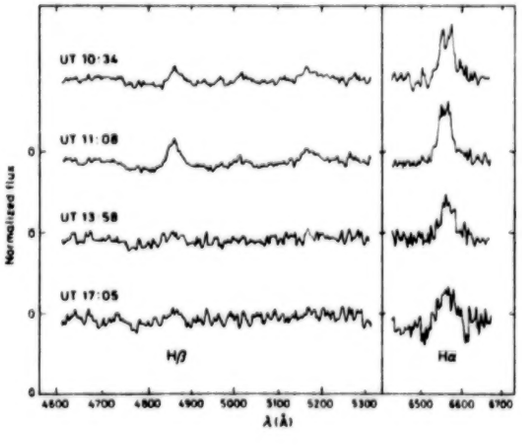


Figure 2-98. Optical spectrum of Z Cha during superoutburst (Vogt, 1982a). The spectrum is hardly any different from the quiescent spectrum (See Figure 2-88e).



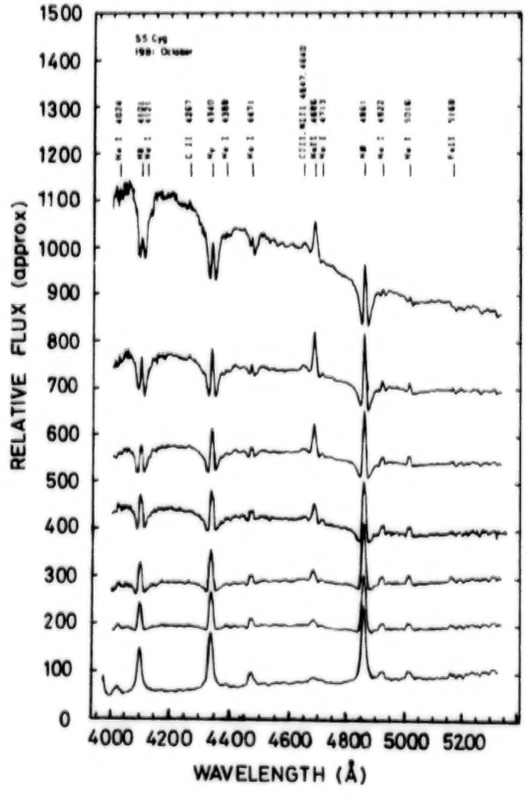


Figure 2-99. Development of optical lines in SS Cyg during decline from outburst (Hessman et al, 1984). Emission cores gradually grow in the centers of the absorption lines.

Figure 2-100. Line profile changes in VW Hyi at late decline (Schwarzenberg-Czerny et al, 1985).

For a few objects, phase resolved spectra during outburst or superoutburst have been taken. In TU Men (Stolz and Schoembs, 1984), which shows a pure absorption spectrum without emission cores of the Balmer lines during the plateau of superoutburst, variability of the line profiles during the orbital cycle can be seen. However, only for the absorption of He I 4471 Å might there be a correlation with the orbital phase, in that the absorption is enhanced near the upper conjunction of the secondary (near phase 0.5). In HL CMa (Wargau et al, 1983), the emission cores of the hydrogen lines are very variable on time scales of a fraction of an orbital period, but no relation with the orbital phase can be detected. In Z Cha, on the plateau of the superoutburst during eclipse, the emission lines of H are significantly stronger and the absorption lines significantly weaker than outside eclipse, unlike in quiescence where there were no strong variations of the line profiles with orbital phase; and during the remainder of the orbital cycle line fluxes decrease or increase, respectively (Vogt, 1982a, and Figure 2-98). In SS Cyg, on the other hand, during an outburst in October 1981 the narrow Balmer emission components showed a clear S-wave that normally only is seen in quiescent spectra of dwarf novae. In EK TrA it was possible to separate the contribution of the superhump from the radiation emitted by the rest of the system (Hassall, 1985): this revealed an almost featureless continuous spectrum which contains significant flux only shortward of some 4200 Å in the optical.

III.B.2.d. RADIAL VELOCITIES DURING OUTBURST

ABSTRACT: Radial velocities during outburst are roughly the same as during quiescence, K- and γ-velocities can be different. In TU Men and Z Cha, the γ-velocity seems to be a function of both the orbital and the superhump phase.

see also: 91

nova-like stars: 101, 107, 115, 119, 122, 134, 142

Radial velocity measurements of outburst spectra and of quiescence spectra yield roughly the same orbital elements, within the limits of error. The most extensive study in this respect was carried out on SS Cyg (Hessman et al, 1984; Hessman, 1986). Radial velocity changes of the wings of the Balmer absorption lines in outburst yield the same K-velocity (K_{out} = 97 ± 6 km/sec, K_{min} = 96 ± 3 km/sec), and also the same shape of the curve, as the wings of the Balmer emission lines seen during quiescence. The wings of the emission cores in outburst, however, have a K-velocity (107 ± 3 km/sec) some 10 km/sec larger than the quiescent emission lines. The only remarkable difference is that the γ-velocity, which was found to be 0 ± 4 km/sec at outburst for the absorption components, was -23 ± 2 km/sec at quiescence. Also the phase shift between Balmer emissions and the absorption spectrum of the secondary star was 190° ± 2° in quiescence, while during outburst it was seen to be 174° ± 4° for the hydrogen absorption wings. The wings of the emission cores, however, were shifted by 199° ± 2° with respect to the late component. The γ-velocities agree within the indicated limits. At different nights during decline from the outburst no substantial changes in the radial velocities could be found.

Again in the well-studied system SS Cyg, the radial velocities of the He II line at 4688 Å are different when measured from the base of the line at continuum level or from the peak (Figure 2-101): The K-velocity and the γ-velocity are 118 ± 6 and −60 ± 4 km/sec, respectively, for the line base, and 52 ± 7 and −47 ± 5 km/sec for the peak, i.e., considerably different for both components of the Balmer lines and, as will be seen immediately, also from the secondary spectrum. The phase shift with respect to the latter is +216° ± 3° and 217° ± 9°, respectively, for line base and peak — again different from anything else that has been measured.

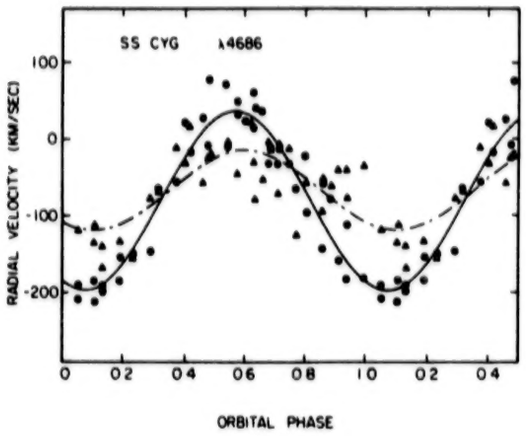


Figure 2-101. Radial velocities of the He II 4686 Å line as measured from the line base (circles) and from the peak (triangles) (Hessman, 1986). See text for discussion.

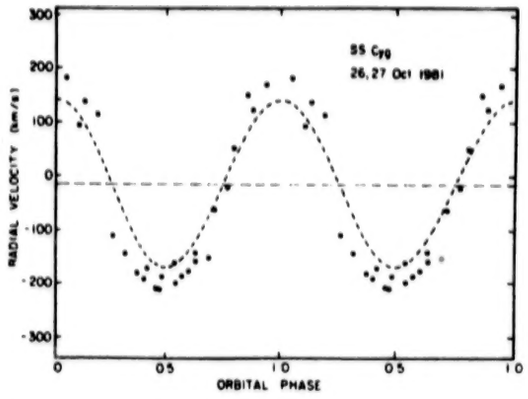


Figure 2-102a. Radial velocity curve of the secondary absorption spectrum in SS Cyg during outburst (dots); the curve as determined during quiescence is indicated as a dashed line (Hessman et al, 1984).

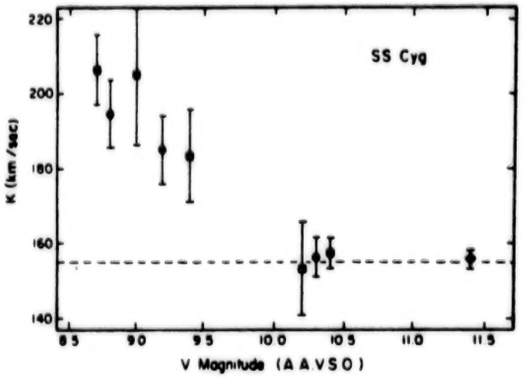


Figure 2-102b. The K-amplitude of the secondary absorption spectrum gradually decreases as the optical flux declines (Hessman et al, 1984). See text for discussion.

While detailed interpretations of these results certainly will involve a good deal of modeling, it is clear from the above results that many different light sources contribute to the integrated flux of the system, and to various degrees of importance at different brightness levels. It also is clear that neither the K-velocity nor the γ-velocity should reasonably be ascribed exclusively to dynamic properties of the system (systemic motion, orbital motion), but that changes in temperature and luminosity distribution are involved as well, and that this effect can be quite different for different lines, as they obviously originate in different parts of the system (several aspects of this will be discussed in Chapters 4.II and 4.IV).

In SS Cyg the absorption spectrum of the late component has been measured during outburst, and radial velocity curves could be derived (Hessman et al, 1984). On all nights of the decline, the phase shift with respect to the late absorption spectrum seen in quiescence was zero within the error limits, but the K-velocity showed a systematic development (Figure 2-102): it was considerably larger than during quiescence at the peak of the outburst, and the difference gradually decreased to zero as the system faded. The γ-velocity was somewhat lower at outburst maximum than during quiescence (-21 ± 2 km/sec vs. -15 ± 2 km/sec), and was more than twice the quiescent value (-35 ± 4 km/sec) at late decline.

In Z Cha and TU Men, both observed spectroscopically at the plateau of a superoutburst, the γ-velocity of the hydrogen absorption lines, (not those of the hydrogen emission lines in Z Cha!) were seen to vary from night to night (Vogt, 1982a; Stolz and Schoembs, 1984). The values measured in TU Men are compatible

with the assumption that the γ-velocity varies with the beat period between orbital hump and superhump.

III.B.2.e. DEVELOPMENT OF LINES IN THE ULTRAVIOLET

ABSTRACT: In slow gradual changes from quiescent to outburst spectrum and back, the UV follows the same general pattern as the optical. Unlike the continuous flux distribution, the appearance of the line spectrum of one object varies slightly from one outburst to another. While most systems exhibit absorption spectra during the outburst, possibly with P Cygni emission components in C IV, double eclipsing systems show pure emission spectra.

interpretation: 194, 206

In some dwarf novae the rise phase has been observed in the UV. WX Hyi has a spectrum exhibiting strong emission lines in quiescence. At early rise the line fluxes increase slightly as the continuum level rises (Figure 2-103). At some time during rise the whole character changes considerably, since at late rise the spectrum resembles very much that of seen at maximum light (Hassall et al, 1983): strong P Cygni profiles are visible in the C IV and Si IV lines. Two nights later, at the peak of the supermaximum (normal outburst and superoutburst exhibit similar spectra), the emission component of C IV had strongly decreased, that of Si IV had disappeared altogether, and the absorption components of both lines had increased strongly in strength, while the terminal velocities had remained approximately the same. Early rise has also been observed in VW Hyi (Verbunt et al, 1986). In quiescence the only lines seen are C IV in emission and Si III in absorption. At early rise Si III becomes stronger, while C IV turns into absorption, and He II appears as a very strong absorption line. A late rise spectrum of AH Her (Verbunt et al, 1984), as in the case of WX Hyi, looks like a maximum spectrum with the lines absorbing just a little less flux than at maximum.

Aside from rise, the outburst spectra of dwarf novae in the UV are all characterized by very strong absorption lines of the resonance lines visible in the UV range, and in the EUV by the Lyman series (Polidan and Holberg, 1984, and Figure 2-73b). Normally C IV has a strong asymmetric absorption profile with the blue wings extending some 4000 to 6000 km/sec Doppler velocity (depending on the object and the particular outburst observed) away from the line center; and often this line even has a P Cygni profile, but the emission component typically only extends some 2000 km/sec redward. In some spectra, Si IV and N V also show marginal P Cygni emission components in addition to asymmetric absorptions (Figure 2-95). Whenever P Cygni profiles are observed in some outbursting dwarf novae, the strength of the absorption component in absolute terms is considerably larger than that of the emission component except for the rise. There are objects like VW Hyi, however, in which all lines are usually symmetric, and only very rarely does C IV show an indication of an asymmetric profile. Only a high resolution spectrum of VW Hyi during a superoutburst revealed that the line centers of the six strong symmetric resonance lines, the doublets of N V, Si IV and C IV, all are shifted shortward by 400 $\pm$ 100 km/sec with respect to the rest wavelengths (Verbunt et al, 1984).

The development of the UV lines during late rise and during decline of an outburst is shown in Figure 2-104. Different, but in principle the same, behavior is seen in detail in all other dwarf novae. During the course of decline the lines gradually fade as the continuum fades, without dramatically changing their appearance. The characteristic minimum spectrum only appears at the very end of decline in a smooth transition. It has been found ever again that, although the continuous flux distribution of different outbursts and also of standstills (these spectra are not basically different from those observed during normal outbursts) show the same wavelength dependence at the same optical brightness in the continuum, the line profiles do by no means follow this pattern: at the same brightness level in different outbursts absorption as well as emission line

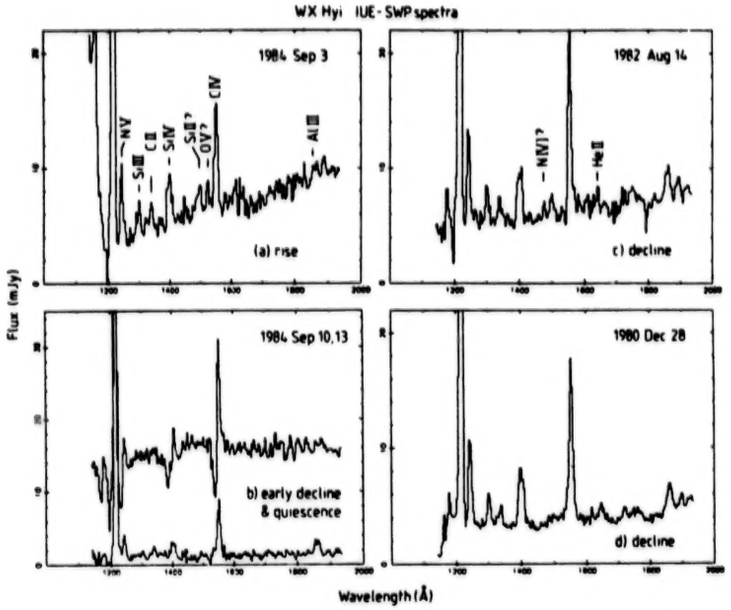


Figure 2-103. Development of the UV spectrum of VW Hyi during the course of an outburst (Hassall et al, 1985).

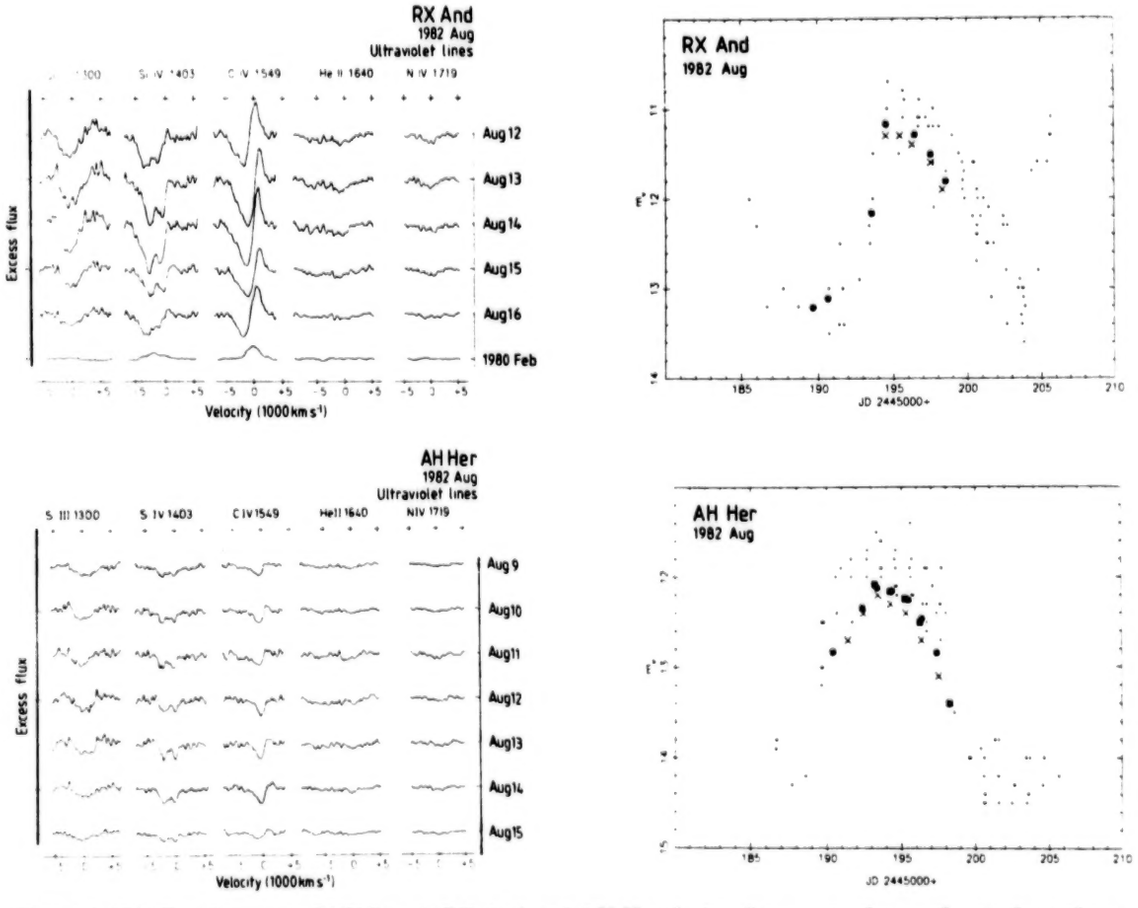


Figure 2-104. Development of UV lines in RX And and AH Her during the course of an outburst; the outburst light curves are given for comparison (Verbunt et al, 1984). Small dots are optical observations by the AAVSO, large dots are SAAO observations in the Johnson V filter, and crosses are IUE-FES observations.

ORIGINAL PAGE IS
OF POOR QUALITY

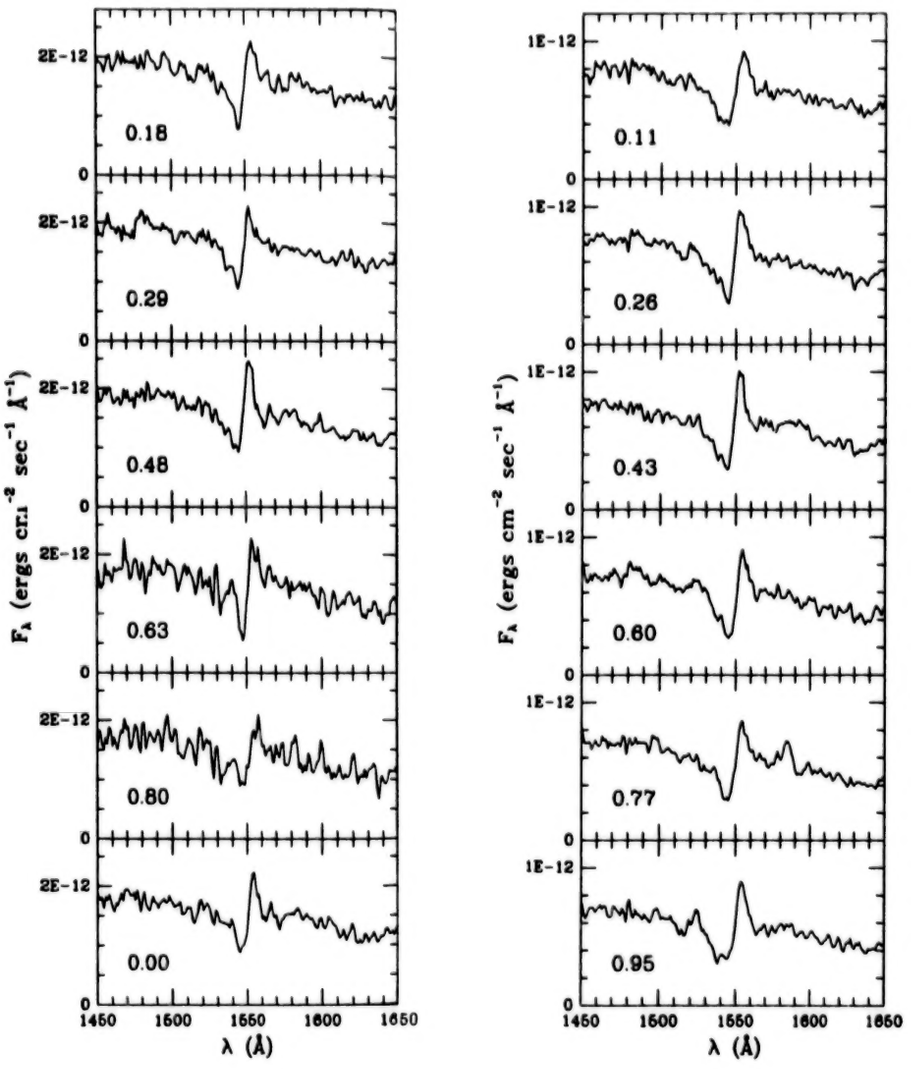


Figure 2-105. Phase-resolved C IV line profiles in Z Cam during outburst (Szkody and Mateo, 1986). The two series were taken two days apart. It appears that although profile changes occur on orbital time-scales, the variations are not directly related to the orbital revolution.

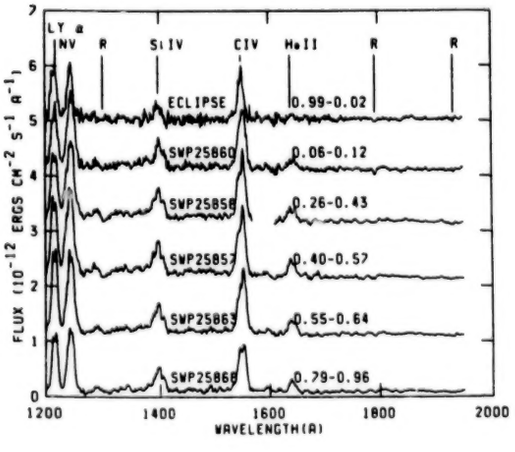


Figure 2-106. Phase-resolved UV spectra of OY Car during a superoutburst (Naylor et al, 1987). For discussion see text.

profiles can look entirely different. Thus for any system the physical state of the continuum source at outburst obviously is characteristic, and the same conditions and their temporal development are found in every outburst. The observed absorption lines thus do not seem to originate together with most of the continuum, reflecting that their source is not as well determined in its physical state. Finally, the emission lines probably originate from an extended region, the exact shape and/or physical state of which is not reproduced in detail from one outburst to another.

Phase-resolved UV spectra of Z Cam on decline from outburst were acquired by Szkody and Mateo (1986). In the C IV profile (Figure 2-105), considerable changes are seen on time-scales on the order of one hour, but no obvious relation to the orbital phase can be detected. The equivalent widths of the resonance lines, however, seem to suggest some vague phase dependence of the absorption components on the maximum absorption coinciding with the optical hump maximum. Appreciable variations of the C IV P Cygni profile with the orbital phase was observed in YZ Cnc (Drew and Verbunt, 1988).

During a superoutburst of the high-inclination (double eclipsing) system OY Car, Naylor et al (1987) got phase-resolved UV spectra of this object (Figure 2-106); in particular they got spectra during the eclipse phase. Unlike most dwarf novae, OY Car exhibits a pure emission line spectrum during (super-)outburst, with the resonance lines of C IV, Si IV, N V, Lyα, and He II being visible. Compared to a "normal" minimum spectrum of a dwarf nova (OY Car itself is too faint at quiescence to be observed with IUE) the lines are unusually broad. The strength of N V 1240 Å is comparable to that of C IV 1550 Å, which is very unusual for a dwarf nova. The C IV line is strongly asymmetric, with a steep strong blue and a somewhat fainter red component. At some phases, there appear two separate emission peaks which are separated by some 10 Å (the separation of the doublet components is 2.5 Å). All the line profiles are variable during the orbital cycle, but no clear phase relation is evident. Except for Lyα, which is not eclipsed, all other lines are considerably eclipsed at the same time no eclipse is visible at soft X-rays.

III.B.2.f. THE SPECTRAL BEHAVIOR OF WZ SGE

ABSTRACT: Appreciable changes in the appearance of the line spectrum occurred as a consequence of the outburst in 1978, and lasted until very long after the end of the outburst.

related photometric observations: 42, 63

Except for the last outburst in 1978, spectra of WZ Sge have been published for only a few occasions before and after the outburst: Krzeminski and Kraft (1964) describe the spectrum as it appeared several years before the outburst; Voikhanskaya (1983a) obtained spectra both half a year before and two and a half years after the outburst; Gilliland et al (1986) observed WZ Sge six months after the outburst when it had not yet quite returned to its quiescent state. In fact, ten years after the outburst it still keeps declining in brightness at a very small rate (Hassall, private communication). Finally, Brunt (1982) observed the star half a year before and half a year after the outburst.

The emerging picture concerning the spectral appearance of WZ Sge is confusing. All authors agree that WZ Sge exhibits a blue continuum with superimposed double-peaked hydrogen emission lines which are placed in wide absorption troughs (Figure 2-107); but this is about as far as the agreement reaches. The strength of the emission lines is clearly highly variable when spectra taken before and after the outburst are compared. There was no emission in Hα half a year before outburst, while half a year afterward it was very strong. The depth of the minimum between the two line peaks clearly reached far below continuum level for Hβ on towards higher series members half a year after outburst; but at least in Hβ, the minimum was clearly much less deep before as

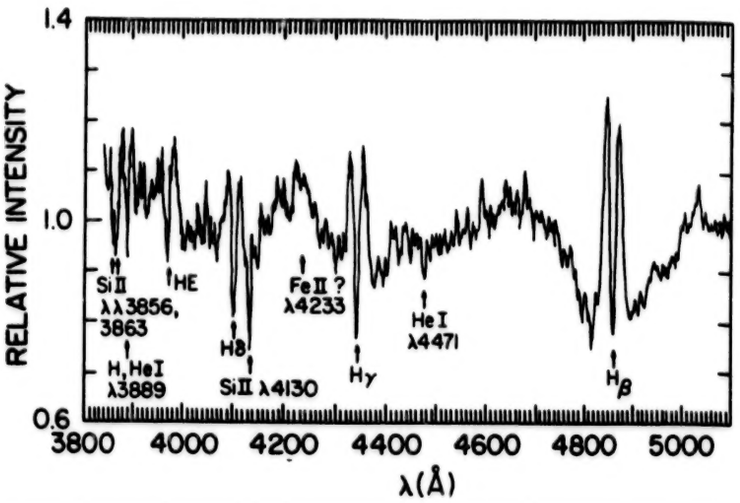


Figure 2-107. Near-quiescence optical spectrum of WZ Sge (Gilliland et al, 1986). See text for discussion.

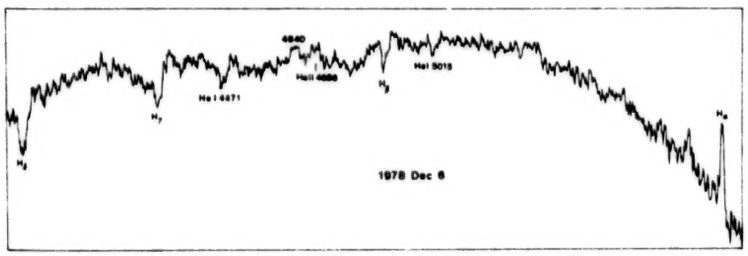


Figure 2-108. Optical spectrum of WZ Sge shortly after outburst maximum (Ortolani et al, 1980).

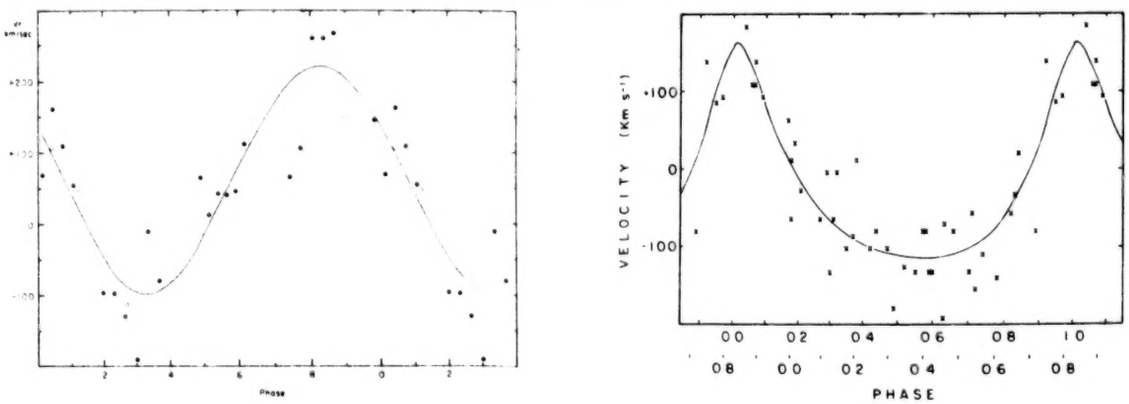


Figure 2-109. Radial velocity curves of WZ Sge on decline from outburst: a:Walker and Bell, 1980: b:z Gilliland and and Kemper, 1980. See text for discussion.

well as long after outburst. A strong S-wave is reported to have been present at times long before outburst, while at other times it was seen to be weak; after outburst it has not been seen to be of any major importance. The separation of the peaks of the Balmer lines decreased from some 1450 km/sec before outburst to some 1370 km/sec afterwards. The radial velocity before the outburst was rather smooth and well in phase with the orbital motion, while after outburst radial velocity variations of both the emission and the absorption components were rather erratic in shape and amplitude, implying that phase shifts were occurring with respect to the pre-outburst radial velocity curve. Furthermore, a considerably different γ-velocity was determined from the spectra for each of the considered epochs, different even for different lines (Hα, Hβ) and different parts of the same line (emissions, absorptions). It is not clear how the observations can be accommodated within the framework of the Roche model, which also applies to the rather dwarf nova-unlike photometric changes in WZ Sge.

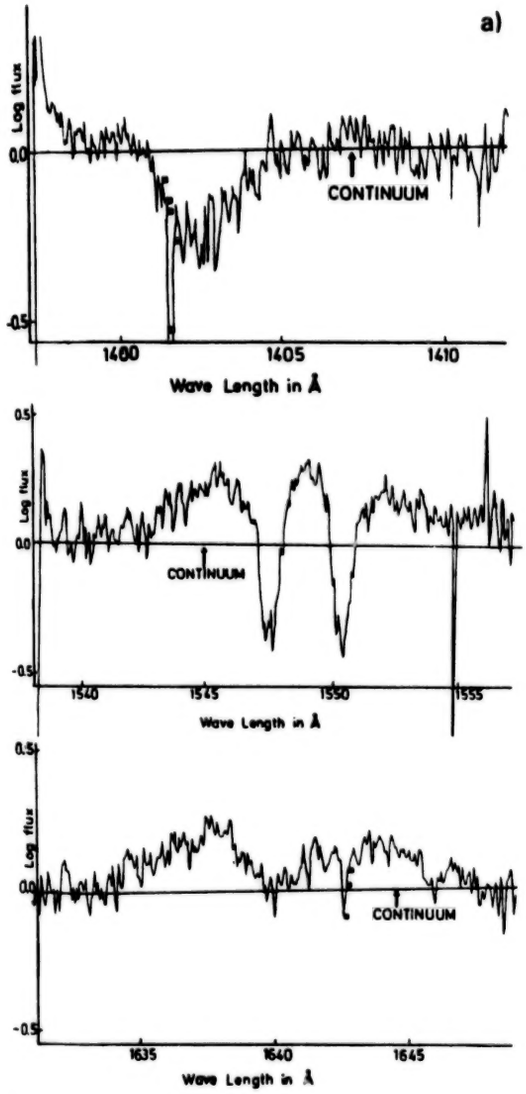
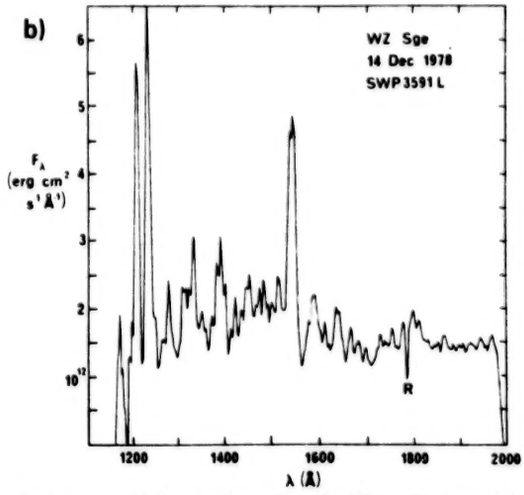


Figure 2-110. UV spectra of WZ Sge during outburst: a: Friedjung, 1981; b: Fabian et al, 1980. See text for discussion.

The first spectrograms of the outbursts were taken by Brosch et al (1980) at the very maximum of the outburst on December 1, 1978. They report Hα and Hβ to have been in emission together with He II 4686 Å and C III - N III 4640 Å, while the higher Balmer lines were in absorption. At maximum light, on December 1.7, Hα could hardly be detected above the continuum, while 24 hours later it was strongly in emission with a clear double-peak structure and a peak separation of about 10 Å, one third of the separation seen at quiescence. The structure of Hβ was similar.



For most of the outburst only Hα (along with He II, C III - N III) was seen in emission, while the other Balmer lines and He I were in absorption (Figure 2-108). The peak separation of Hα was still seen to be 10 Å on December 8. When the next spectrum was taken, on December 20, the double-peaked emission had disappeared, only to return on December 22, but then with a peak separation of some 30 Å, the value observed during quiescent state. One night before this (and only then), Hβ, which for most of the outburst was seen in absorption, showed clear inverse P Cygni profiles, the emission component of which varied with the orbital phase (Gilliland and Kemper, 1980).

On some occasions during the outburst, radial velocity measurements were undertaken. For December 9 and 10 a sine curve gives an acceptable fit to the data points when they are plotted on the pre-outburst phasing (Figure 2-109a); the shape of the curve for December 14 has changed considerably (Figure 2.109b), so these data points were fit assuming an eccentric orbit with e = 0.4(+.05,-2). Observations taken by Walker and Bell (1980) on December 21 agree in shape and phasing with the December 14 data. Gilliland and Kemper note that there was no change in the shape of the radial velocity curve between December 14 and 23, although the γ-velocity did change considerably from night to night, which also is consistent with the measurements by Walker and Bell (a phenomenon also observed in TU Men and Z Cha during superoutburst).

Four days after outburst maximum high resolution IUE observations of WZ Sge were acquired. They show wide absorption profiles of C II and Si IV, much narrower deep absorptions which are superimposed on broad emissions of C IV and N V, and a possibly double-peaked profile of He II (Figure 2-110a). On December 14 the UV spectrum is characterized by emission lines of C IV, N V, Si IV and He II, and by absorption lines of the lower ionization lines, on a steep blue continuum; not unlike, but also not quite like, a dwarf nova in outburst (Figure 2-110b). The spectrum is highly variable on time-scales of a few tens of minutes, in the continuum as well as in the line flux. C IV shows a pronounced variable double-peak structure which is reminiscent of the optical S-wave phenomenon as seen in many dwarf novae. On December 24 the continuous spectrum has somewhat flattened, the line strengths have decreased, and the spectrum as a whole is only a little variable.

GENERAL INTERPRETATION: During outburst all the disc is assumed to be opaque, thus only absorption spectra can be seen. Blue-shifted absorption profiles are believed to be caused by a high-velocity wind which is blown off the system during outburst. The general pattern of profile changes is understood to be due to opacity changes in the accretion disc: the disc is (partly) optically thin during quiescence and turns optically thick during outburst; changes take place gradually. Variations in K- and γ-velocities with respect to quiescent values, and variations in the phase relations between the disc spectrum and the secondary spectrum are suspected to be caused by brightness changes in the disc. Profile changes are likely to be brightness inhomogeneities in the disc.

OBSERVATIONAL CONSTRAINTS TO MODELS:

- *In most dwarf novae, in the optical as well as in the UV, emission spectra are seen during quiescence, and absorption spectra are seen during outburst. (See 151, 192.)*
- *Profile changes during the course of an outburst follow a very characteristic pattern.*
- *The Balmer decrement is very small during outburst. (See 194.)*
- *The faint cool absorption spectrum seen in several systems in the optical during quiescence disappears during outburst. (See 151, 194.)*
- *There is a good relation between the continuous flux distribution and the optical brightness changes during the course of an outburst: this does not hold for the line spectra.*
- *Line wings and line cores follow different radial velocities.*
- *There is a different phase shift between the primary and secondary spectra during quiescences as compared to outburst. (See 156.)*
- *K- and γ-velocities can have different values during outburst then during quiescence.*
- *Double-eclipsing systems display pure emission spectra in the UV during outburst. (See 206.)*
- *Spectrum changes in WZ Sge are very atypical for a dwarf nova.*

N95
27070
UNCLAS

N95- 27070

3

NOVA-LIKE VARIABLES

I. DEFINITIONS AND GENERAL CHARACTERISTICS*

ABSTRACT: On grounds of different observable characteristics five classes of nova-like objects are distinguished: the UX Ursae Majoris stars, the anti-dwarf novae, the DQ Herculis stars, the AM Herculis stars, and the AM Canum Venaticorum stars. Some objects have not been classified specifically. Nova-like stars share most observable features with dwarf novae, except for the outburst behavior.

There has always been a common understanding of what constitutes a dwarf nova, even though the terminology was subject to many changes. A corresponding agreement cannot be found for the nova-like stars. Many objects which are now classified as "nova-like," were in earlier times simply regarded as irregular variables. For some of them, like V Sge (Ryves, 1932; Payne, 1934), AE Agr (Schneller, 1954; Crawford and Kraft, 1956), or MV Lyr (Walker, 1954a; Greenstein, 1954, similarity to novae or dwarf novae was noted. Others like AM Her (Schneller, 1957) were classified as Mira variables, RW Aurigae stars, flare stars, or other types of stars. Similarly, since for a long time the name "nova-like" was taken literally, this term was used for objects which in the modern use of the word clearly must not be classified under this name; P Cygni stars and symbiotic stars were included particularly often (e.g., Vorontsov-Veljaminov, 1934; Glasby, 1968). In his review on cataclysmic variables, Warner (1976) equates the terms "nova-like variable" and "UX Ursae Majoris star," which, in contrast to the literal meaning of the word, already comes close to the modern definition.

Many more observations, more refined observing techniques, and in particular the availability of UV and X-ray data brought about an enormous increase in the number of detected nova-like stars during the last 10 to 15 years, but the need also became obvious for a more diversified classification scheme. The definition of what constitutes a nova-like variable was a very controversial issue until the use of this expression was restricted to cataclysmic variables (understood in the modern sense).

All *nova-like variables* have some properties in common: they do not show large outburst activity (though they may be found in "high" or "low," "on" or "off" states), so they are neither novae nor dwarf novae, but in one way or another they look like a dwarf nova in some stage of activity. The bulk of their observable features is in agreement with the assumption of the Roche model for the explanation of the underlying physical nature. The range of variability they display is considerable.

Five classes of nova-like stars are distinguished: the UX Ursae Majoris stars, the anti-dwarf novae, the DQ Herculis stars, the AM Herculis stars, and the AM Canum Venaticorum stars; and some systems are just classified as nova-like when they cannot be attributed to either of the former classes.

*In the following, whenever they exist, variable star names will be used according to Kukarkin's catalogue, rather than the names of objects involving their coordinates; cross-correlations between names are given in the index list.

ORIGINAL PAGE IS
OF POOR QUALITY

The spectra of UX Ursae Majoris stars look very similar to those of dwarf novae at some stage of the outburst cycle. They may show emission or absorption lines, or both, often with wide absorption shells underlying strong emission lines. The appearance of a spectrum can be variable. Photometric variations are within narrow limits, of typically 1 mag or less, and do not follow any regular patterns.

The anti-dwarf novae got their name from the appearance of their light curves: usually they are found in a bright state, indistinguishable from UX Ursae Majoris stars; at times, however, their brightness drops by several magnitudes for extensive periods of time, rendering them similar to dwarf novae in the minimum state. The drop in brightness seems to happen at random. Thus it is quite possible that more stars of this subclass are hidden among the UX Ursae Majoris stars. An alternative name for these stars is VY Sculptoris stars, after the name of one of its members.

DQ Herculis stars, or "intermediate polars," cannot be readily distinguished from the UX Ursae Majoris stars, either spectroscopically or in their long-term behavior. When observed photometrically with high time resolution, however, they are found to show extremely stable pulsations of high coherence and with periods of many minutes; and even more than one such periodicity can be exhibited at a time.

AM Herculis stars, or "polars," are characterized by a very high optical polarization synchronous with the binary period. In addition, they exhibit strong high-amplitude flickering. The spectrum is dominated by strong narrow emission lines.

AM Canum Venaticorum stars are characterized by the absence of any hydrogen lines, but they show strong lines of helium, the strengths and profiles of which are quite unlike those of single He white dwarfs. In addition they show flickering activity.

GENERAL INTERPRETATION: The understanding is that dwarf novae, UX Ursae Majoris stars, and anti-dwarf novae are basically the same sort of objects. The difference between them is that in UX Ursae Majoris stars the mass transfer through the accretion disc always is high so the disc is stationary all the time; in anti-dwarf novae for some (unknown) reason the mass transfer occasionally drops considerably for some time, and in dwarf novae it is low enough for the disc to undergo semi-periodic changes between high and low accretion events. DQ Herculis stars are believed to possess weakly magnetic white dwarfs which disrupt the inner disc at some distance from the central star; the rotation of the white dwarf can be seen as an additional photometric period. In AM Herculis stars, a strongly magnetic white dwarf entirely prevents the formation of an accretion disc, and at the same time locks the rotation of the white dwarf to the binary orbit. Finally, AM Canum Venaticorum stars are believed to be cataclysmic variables that consist of two white dwarf components.

II. UX URSAE MAJORIS STARS

II.A. PHOTOMETRIC OBSERVATIONS

II.A.1. PHOTOMETRIC CHANGES ON ORBITAL TIME SCALES

ABSTRACT: The photometric appearance is very similar to that of dwarf novae in exhibiting flickering, humps, and eclipses, and in the related color dependences. The eclipsing systems are remarkably similar to each other in appearance. Unlike in dwarf novae, the hump maximum can occur before as well as after the eclipse.

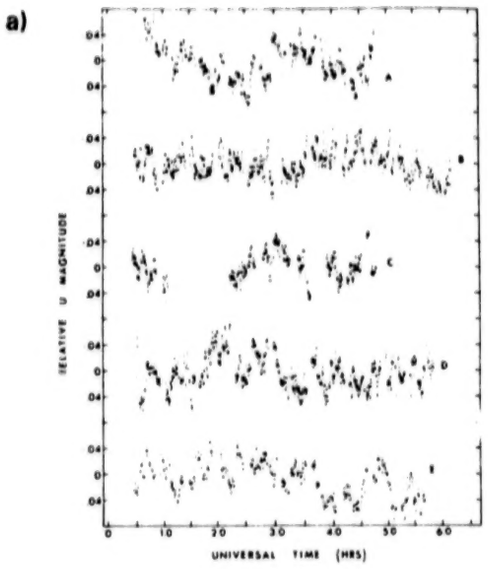
other nova-like stars: *103, 113, 114, 117, 119, 122, 125, 140*

dwarf novae: *35, 46*

interpretation: *172, 177, 190, 194*

UX Ursae Majoris stars are distinct from dwarf novae only in that they do not show any semi-regular outburst activity. However, in some systems the brightness can increase or decrease irregularly on time-scales of years, by about one magnitude (Figure 3-1), but the star's photometric or spectroscopic appearance is not significantly affected by this.

ORIGINAL PAGE IS
OF POOR QUALITY



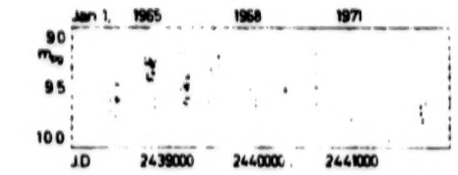


Figure 3-1. Long-term variations of IX Vel (Wargau et al, 1984).

b)

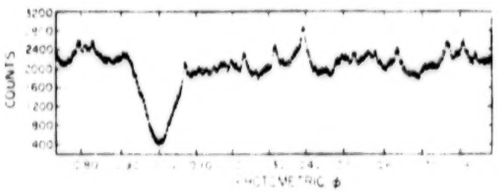


Figure 3-2. Typical orbital light curves of UX Ursae Majoris stars: a) SW Sex (Penning et al, 1984); b) IX Vel (Williams and Hiltner, 1984).

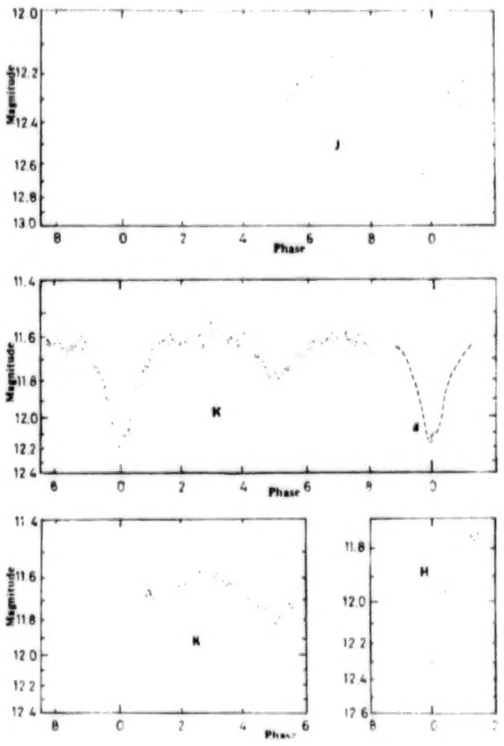


Figure 3-3. (left) IR light curves of RW Tri (Longmore et al, 1981).

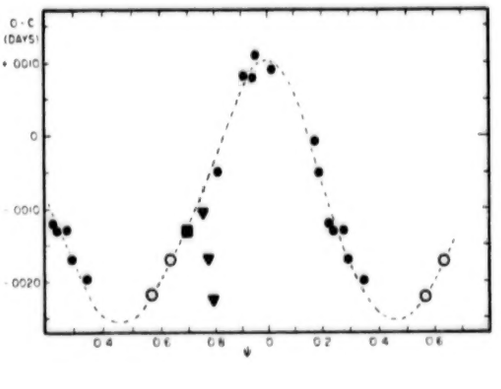


Figure 3-4. Secular period variations in UX UMa (Quigley and Africano, 1978).

The orbital light curves are indistinguishable from those of dwarf novae in showing more or less pronounced flickering and, possibly, humps (Figure 3-2a). There can be appreciable changes in the appearance of the light curve from cycle to cycle, even, in the case of SW Sex, including occasional irregular flare activity (Penning et al, 1984).

Some of the objects (like UX UMa, RW Tri, SW Sex, LX Ser, V363 Aur) show eclipses in their light curves (see Figure 3-2b; see also, e.g., Figure 4-1 and Johnson et al, 1954 for UX UMa; Africano et al, 1978 and Horne and Stiening, 1985 for RW Tri; and Horne et al, 1982 for V363 Aur). All these eclipse light curves look surprisingly similar to each other and also to the light curves of dwarf novae in outburst (see e.g., Figures 2-28, 2-16, 2-52) in being noticeably asymmetric, in changing the slope of ingress shortly after the first contact, and most notably, in normally having a pronounced, though highly variable, hold at egress; the bottom usually is rounded. In all objects a hump is at times visible, at other times it is absent. In RW Tri and UX UMa the hump maximum can occur before as well as after the eclipse. When UX UMa exhibits a hump, the system's brightness decreases steadily after hump maximum until the next hump starts; there is no phase of constant light (see Figure 4-1); this effect is the more pronounced the shorter the wavelength. From an extensive investigation of RW Tri, Walker (1963) found that the eclipse is the deeper and starts the later the fainter is the system's brightness. Color changes during eclipse in RW Tri are the same as in dwarf novae in the sense that the system becomes bluer in (U-B) and redder in (B-V). V363 Aur on the other hand becomes redder in both colors during eclipse (Horne et al, 1982). RW Tri has been observed photometrically at IR wavelengths. A secondary eclipse of 0.4 mag in K centered about phase 0.5 is clearly visible in J and K (Figure 3-3). The widths of primary and secondary eclipses are the same, both lasting for some 80 minutes. In UX UMa no secondary minimum can be detected in J and K (Frank et al, 1981).

The eclipse timings are very strictly periodic, although for RW Tri and UX UMa (like in several other cataclysmic variables — see e.g., Chapter 2.II.B.5) a small cyclic secular variation of this timing has been found (e.g., Figure 3-4); whether or not these are periodic is still controversial (Mandel, 1965; Africano and Wilson, 1976; Kukarkin, 1977; Africano et al, 1978; Quigley and Africano, 1978).

Polarimetric observations were carried out for UX UMa (Szkody et al, 1982a). They revealed an insignificant polarization of 0.30 ± 0.10%, which lies in the range observed for dwarf novae. For SW Sex an upper limit of 0.15% in circular polarization was obtained (Penning et al, 1984).

II.A.2. FLICKERING AND OSCILLATIONS

ABSTRACT: Rapid monochromatic coherent oscillations are occasionally present. The periods are slightly variable but no simultaneous, overall brightness changes occur in the system.

other nova-like stars: ***106, 113, 117, 121, 122, 128, 141***

dwarf novae: ***54, 56***

interpretation: ***151, 181, 185, 213***

On time-scales of minutes all UX Ursae Majoris stars show pronounced flickering with amplitudes between several hundredths and some tenths of a magnitude, with a tendency for the amplitude to be larger at shorter wavelengths, as it is observed in dwarf novae. Observations of RW Tri show that the flickering disappears entirely in all colors between phases −0.04 and +0.04 with respect to central eclipse (the photometric eclipse itself lasts from phase −0.07 to +0.07), showing that (1) whatever the source of flickering may be, it is centered on the main eclipsed source, and, (2) flickering obviously is not directly related to the source of the hump, since in these particular observations the hump followed the eclipse, (Horne and Stiening, 1985).

Rapid coherent oscillations with periods on the order of 30 sec have been detected in UX UMa (Nather and Robinson, 1974) and V3885 Sgr (Warner, 1973). Their characteristics are very similar to those of coherent oscillations seen at times in dwarf novae during outburst.

They are not always present; they have been seen twice in UX UMa for some nights, while several weeks later they had disappeared. When they are present, the power spectra show one single sharp spike and no harmonics, but slowly, on time-scales of days, the period drifts to either longer or shorter values; whether this is a cyclic behavior or not is not clear (Nather and Robinson, 1974). No conspicuous brightness changes of the system comparable to changes of dwarf novae in outburst are reported to have occurred along with the period changes. In UX UMa, a phase shift of $-360°$ was seen to occur during primary eclipse, just as in dwarf novae (Nather and Robinson, 1974).

II.B. SPECTROSCOPIC OBSERVATIONS

ABSTRACT: In the optical as well as in the UV, this class of stars exhibits the full range of appearances known from dwarf novae at all stages of activity, i.e., ranging from pure emission to almost pure absorption spectra. Pronounced changes in the appearance of one object over longer times are known to occur. Appreciable changes can also be connected with the orbital motion.

other nova-like stars: 107, 116, 119, 122, 124, 134, 141

dwarf novae: 65

interpretation: 151, 192

Considering the UX Ursae Majoris stars as a group, they exhibit a remarkably wide range of appearance in their optical and UV spectra. In the optical they range from pure emission line spectra of hydrogen (sometimes also He I and He II) — but emissions are normally not as pronounced as in dwarf novae — to almost pure absorption spectra. Absorption lines can exhibit either weak or strong emission cores (e.g., Figure 3-5). In the UV the resonance lines of highly ionized elements are often found in absorption, but they just as well can be in emission, as the example of UX UMa demonstrates; even for a single object the appearance of the UV spectrum can be highly variable with time (Figure 3-6). C IV and N V often, though by no means always, show P Cygni profiles with or without an emission component. Not much is known about temporal changes of the spectra on time-scales longer than a few orbital cycles. But as published spectra of RW Tri demonstrate (Williams and Ferguson, 1982; Williams, 1983), considerable changes in the line flux do occur over longer intervals of time (Figure 3-7).

Considering the strengths and profiles of the UV lines, observations show that they are subject to many kinds of strong changes in every single object, changing from being strongly present to entirely absent within weeks — a matter which, however, has so far not been investigated sufficiently. In the case of IX Vel, Sion (1985) investigated the C IV P Cygni profile in particular and found that it is variable within fractions of hours in all its characteristics: the strengths of both absorption and emission components, the position of emission and absorption peaks, and the blueward extension of the absorption wings.

In some systems changes are known to be conspicuous on orbital time scales. For example the observations of RW Tri in Figure 3-7a show pronounced changes in the optical lines as well as in the optical continuum radiation which are related to the eclipse: the continuum becomes considerably redder than it is outside eclipse and, correspondingly, the equivalent widths of the lines increase; some lines are clearly being eclipsed, while others become visible or go into emission only during eclipse. Similar changes have been observed in other UX Ursae Majoris systems (e.g., Williams and Ferguson, 1982; Drew and Verbunt, 1985).

For several objects spectra with a time resolution on the order of 200 sec were obtained (e.g., Kaitshuk et al, 1983; Schlegel et al, 1983; Honeycut et al, 1986), so it was possible to construct light curves for single spectral lines (Figures 3-8). In all these cases the He II light

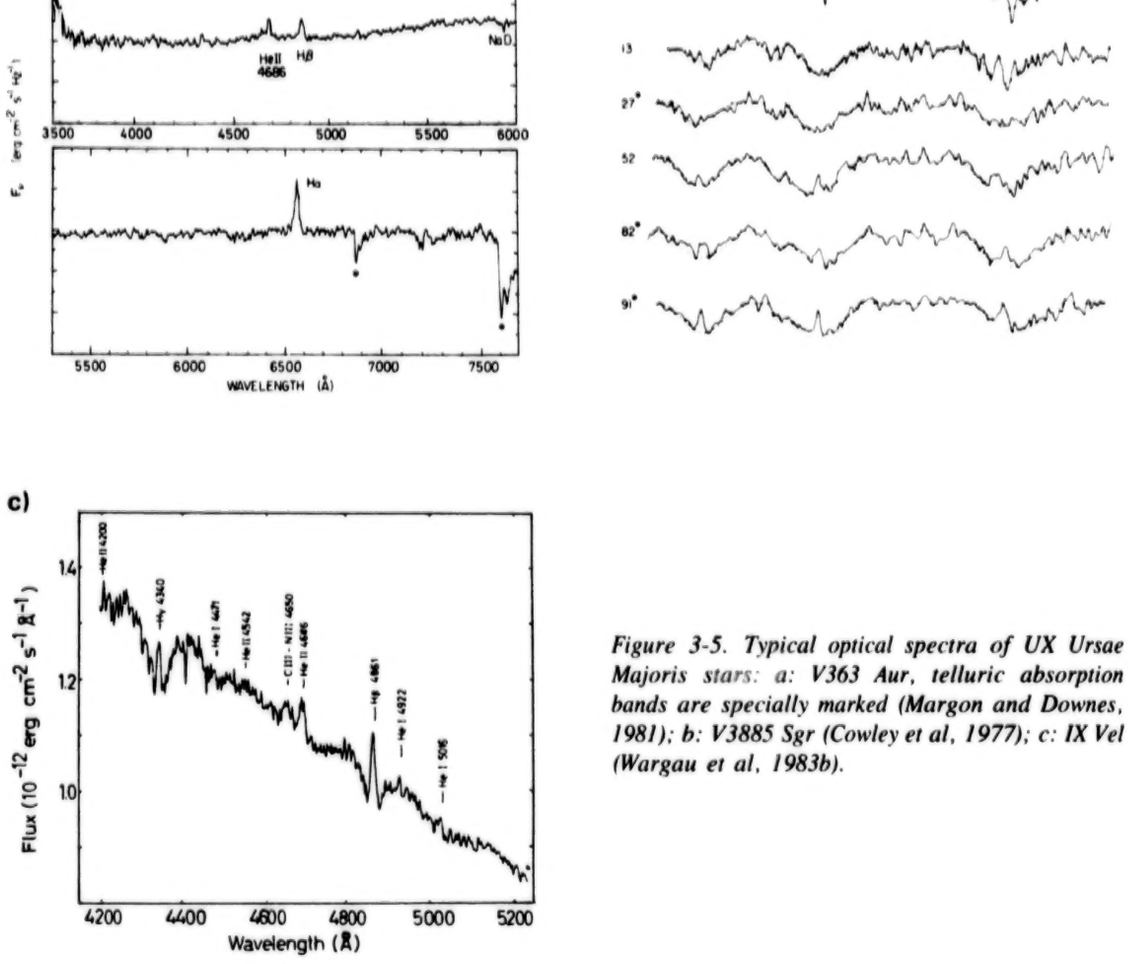


Figure 3-5. Typical optical spectra of UX Ursae Majoris stars: a: V363 Aur, telluric absorption bands are specially marked (Margon and Downes, 1981); b: V3885 Sgr (Cowley et al, 1977); c: IX Vel (Wargau et al, 1983b).

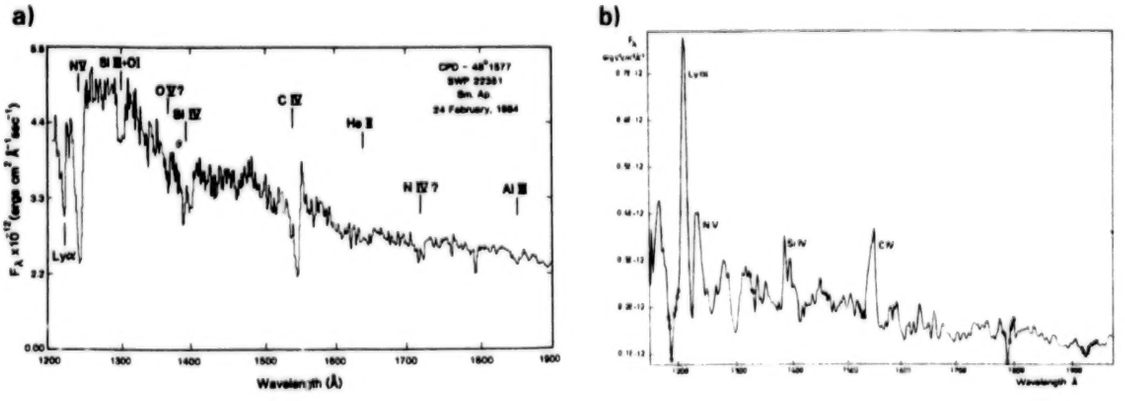
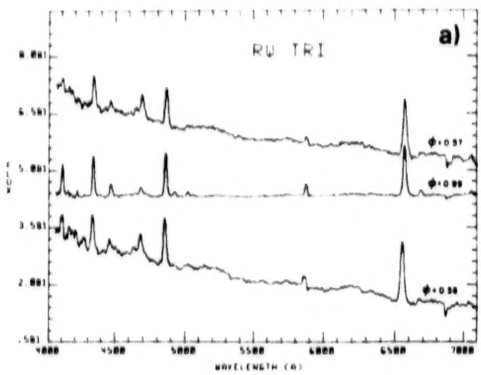


Figure 3-6. Typical UV spectra of UX Ursae Majoris stars: a: IX Vel (Sion, 1985); b: UX UMa (King et al, 1983).



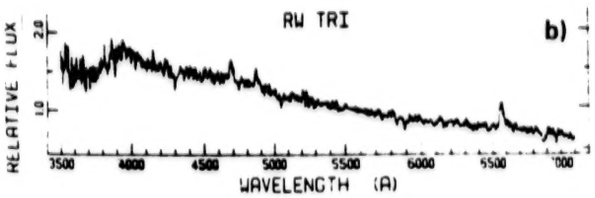
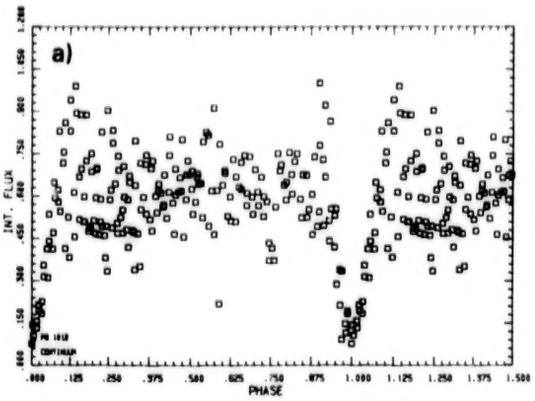
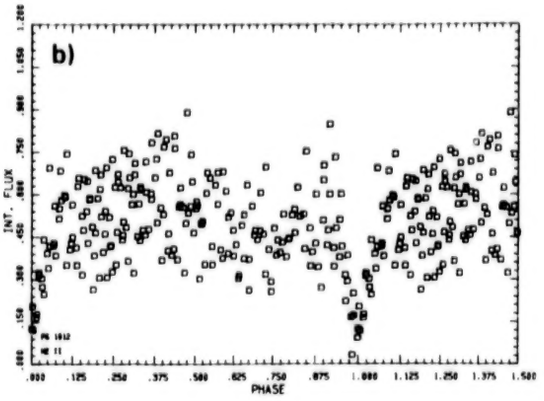


Figure 3-7. Spectral changes in RW Tri: a: changes during eclipse (Williams and Ferguson, 1982); b: long-term changes; the spectrum was taken at a different time than that displayed in Figure 3-7a (Williams, 1983).





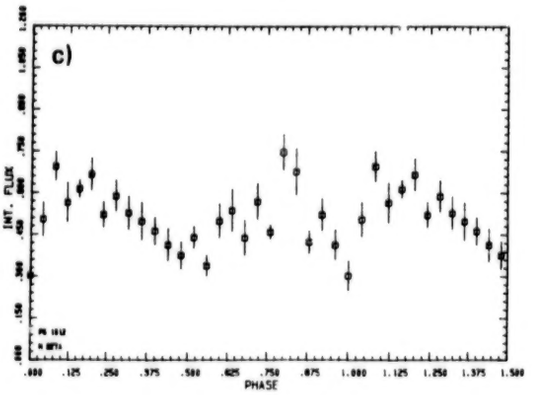
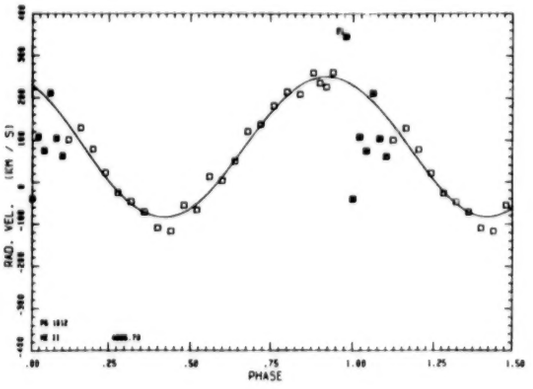
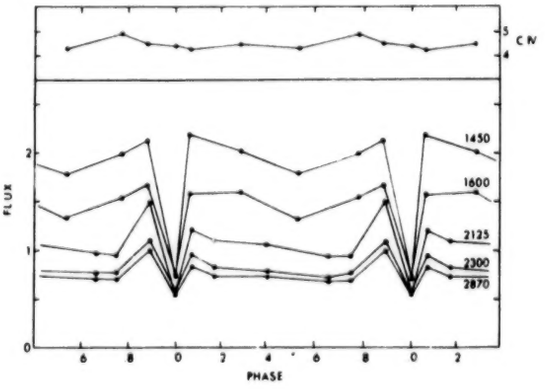


Figure 3-8. (above and left) Orbital light curves of RW Tri: a: continuum flux; b: He II 4686 Å emission line; c: Hβ emission (Honeycutt et al, 1986).

Figure 3-9. (below, left) Rotational disturbance in the radial velocity curve of He II of SW Sex during optical eclipse (Honeycutt et al, 1986).

Figure 3-10. (below) UV eclipse light curves of UX UMa (Holm et al, 1982).





curve is a rough image of the continuum light curve, but the duration of the primary eclipse is decidedly shorter and less deep (in the case of SW Sex, for instance, 0.06 orbits for He II, compared to 0.08 for the continuum). Both Hβ and He I in SW Sex show a secondary eclipse which is not visible in the continuous light curve; in RW Tri there also is some indication for a secondary eclipse. Outside eclipse the line profiles do change around the orbit, but it is not clear whether these changes are related to the aspect the observer has of the system or to what extent the light source is intrinsically variable (e.g., Wargau et al, 1984).

In UX UMa and RW Tri Hβ and Hγ exhibit a double-peaked structure, with the radial velocity of the red and the blue components having the normal sine shape and the period of the orbital motion (Kaitchuk et al, 1983; Schlegel et al, 1983). In addition there is a third S-wave component moving between the two line peaks, with the same period but with a phase shift of 150° in UX UMa and of 180° in RW Tri — as is seen in dwarf novae. In SW Sex, and to a lesser degree in RW Tri, the radial velocity curves of He II 4686 Å and of C III — N III 4645 Å, but not of Hβ, show a clear rotational disturbance at primary eclipse (Figure 3-9).

Extensive studies of the UV radiation have been carried out by Holm et al (1982) and King et al (1983), on UX UMa, and by Sion (1985) on IX Vel. In UX UMa, the continuous radiation was found to be strongly eclipsed at the time of primary optical eclipse (Figure 3-10). The eclipse is the deeper the shorter the wavelengths. The presence of the hump prior to and also somewhat after eclipse is clearly visible at longer UV wavelengths, but it is not entirely absent at short wavelengths where it even seems to last for an entire orbital cycle (in dwarf novae the hump shows up in the UV very infrequently, and then only weakly). As to the strong UV lines, N V, Si IV, and He II are clearly eclipsed, whereas C IV is not eclipsed (King et al, 1983).

GENERAL INTERPRETATION: Photometrically and spectroscopically UX Ursae Majoris stars exhibit all characteristics of dwarf novae, with the single exception of outburst activity. Thus the understanding is that these stars can be regarded as dwarf novae with an essentially constant (high) mass transfer rate through the accretion disc.

OBSERVATIONAL CONSTRAINTS TO MODELS:

- *Dwarf novae, UX Ursae Majoris stars, and anti-dwarf novae share most of their characteristics except for their outburst behavior. (See 229)*
- *In some objects, optical color changes during eclipse are the reverse of what is seen in dwarf novae.*
- *Also unlike the case of dwarf novae, the hump in some objects is strong in UV wavelengths.*
- *Unlike in dwarf novae, hump maximum can occur before as well as after eclipse.*

III. ANTI-DWARF NOVAE

III.A. PHOTOMETRIC OBSERVATIONS

III.A.1. LONG-TERM VARIATIONS

ABSTRACT: The normal photometric appearance of anti-dwarf novae is indistinguishable from that of UX Ursae Majoris stars. Occasional drops in brightness by several magnitudes occur. During these times the objects resemble quiescent dwarf novae.

other nova-like stars: 113, 125

dwarf novae: 21

interpretation: 172

Stars which are classified as *anti-dwarf novae* or *VY Sculptoris stars* (just two names for the same thing) cannot be distinguished from the UX Ursae Majoris stars most of the time: they show orbital light curves like those expected for cataclysmic variables; the spectra consist of H emission lines, which may or may not be superimposed on broad shallow absorp-

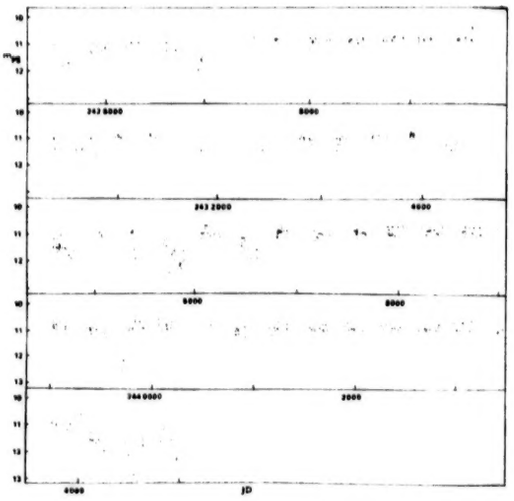


Figure 3-11. Long-term variations of TT Ari (Hudec et al, 1984).

tion features; and the brightness fluctuates about some mean value, deviating up and down irregularly by no more than about 1 magnitude. From time to time, however, the general brightness drops by a very considerable amount (some 2 - 3 mag, but see below) for as much as a few hundred days, after which the star again returns to the high level. Times for both decline and rise seem to be on the order of 100 days (Figure 3-11 — see also, e.g., Liller, 1980). In some objects the upper and the lower states have reasonably well defined brightness levels to which the star returns; in others there is no evidence for this. In contrast to dwarf novae, the high state for anti-dwarf novae is the normal state of the star. No periodicities comparable to outburst periods in dwarf novae could be found in anti-dwarf novae, as the drop in brightness occurs at random and unpredictably. In the best studied case, TT Ari, a couple of such drops often follow each other, after which the brightness remains essentially constant at high level for several years. No secular brightness changes could be detected for any star. Some objects (TT Ari, MV Lyr, and possibly others as well, except most anti-dwarf novae have not been adequately studied over longer times) drop to an unusually faint state at times, another 2 mag below the "normal" low (= intermediate) state.

III.A.2. CHANGES ON ORBITAL TIMESCALES IN THE HIGH AND LOW STATES

ABSTRACT: The photometric appearance of an object can vary considerably from night to night. In TT Ari during the high state the hump is very pronounced in the UV. During high state this system also occasionally exhibits quasi-periodic oscillations, which never were seen during low state.

other nova-like stars: 96, 113, 114, 117, 119, 122, 125, 140

dwarf novae: 35, 46

interpretation: 177, 194

The orbital light curves of anti-dwarf novae during high state look like light curves of UX Ursae Majoris stars: for instance the light curve of MV Lyr is characterized by strong flickering up to 0.3 mag in which, however, no variability with the orbital period, like a hump, can be detected. TT Ari possesses a very pronounced hump in the light curve, on which flickering is superimposed (Figure 3-12a); and LX Ser and VZ Scl have eclipse light curves, which look very similar to those of UX Ursae Majoris stars, and also suffer appreciable flickering which mostly disappears during eclipse. A hump is visible in VZ Scl which can either precede or follow the eclipse (as is the case in some UX Ursae Majoris stars) (Warner and Thackeray, 1975; Horne, 1980). LX Ser usually does not possess a hump, though at some times it can be present. In the IR a secondary eclipse at about phase 0.5 is visible in VZ Scl (Sherrington et al, 1984). For LX Ser in the high state, there exist optical color measurements during an eclipse which look just like those in quiescent dwarf novae (Figure 3-13, compare with Figures 2-32, 2-33).

Photometric observations have been carried out for TT Ari during the intermediate state (V $\approx$ 14 mag; V $\approx$ 10.2 Mag at high state) and during the very low state (V $\approx$ 16.5 mag). The

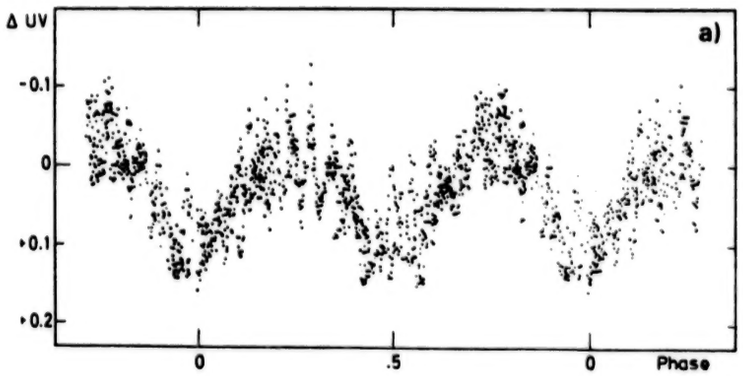
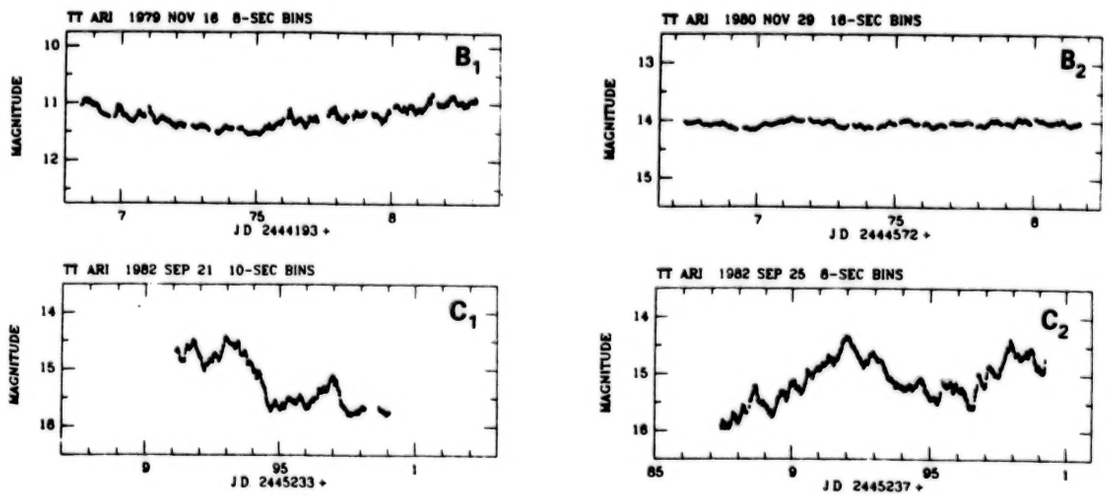


Figure 3-12. Orbital light curves of TT Ari: a: during high state (Smak, and Stepien, 1968); b: during intermediate level (Shafter et al, 1985); c: during low level (Shafter et al, 1985).



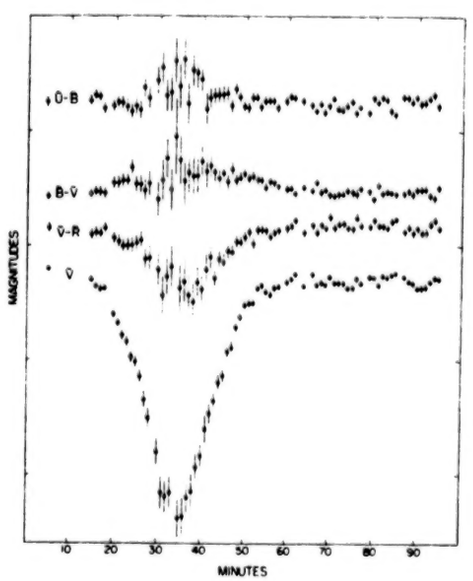


Figure 3-13. Color changes in LX Ser during eclipse (Horne, 1980).

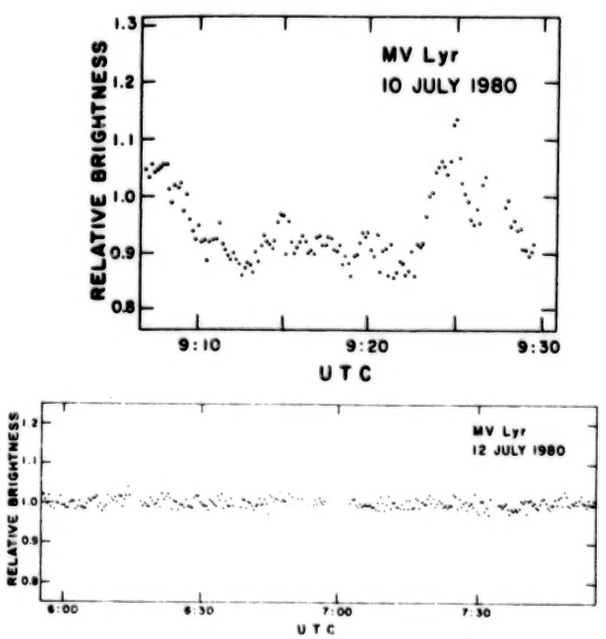


Figure 3-14. Optical light curves of MV Lyr in the low state, taken two days apart (Robinson et al, 1981).

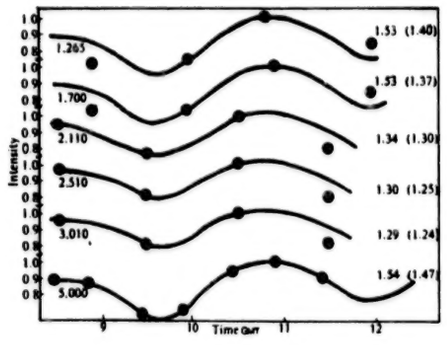


Figure 3-15. Wavelength dependence of the UV hump light curve of TT Ari in the high state (Jameson et al, 1982b), on the left the effective wavelengths for the light curves are indicated, since in this figure all amplitudes are normalized, on the right their actual amplitudes are given.

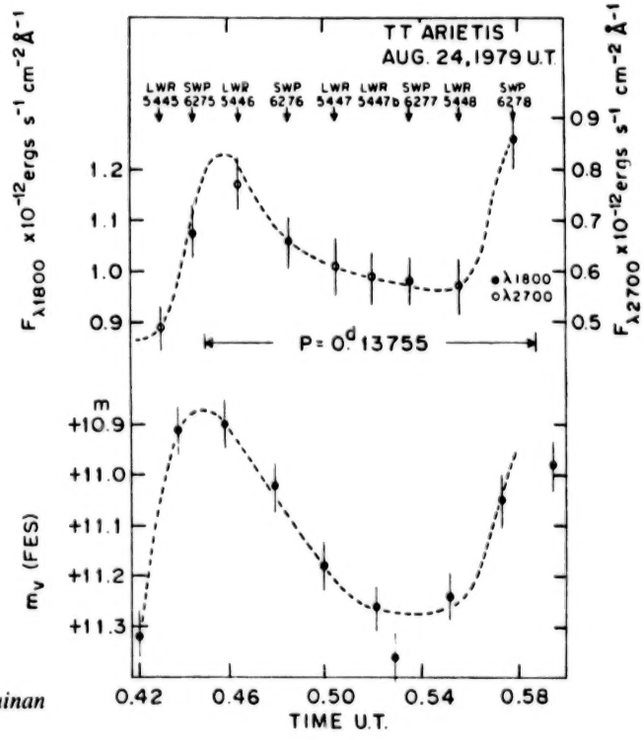


Figure 3-16. (right) UV light curve of TT Ari (Guinan and Sion, 1981).

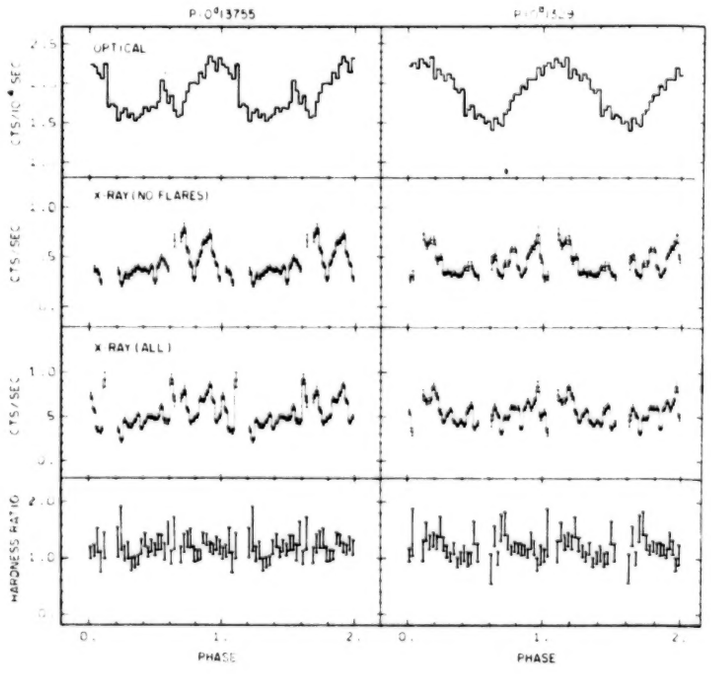


Figure 3-17. (left) X-ray photometry of TT Ari (Jensen et al, 1983).

hump and most of the flickering activity disappeared at intermediate state, leaving an essentiallv constant light curve (Figure 3-12b). In the very low state the flickering is present again (Figure 3-12c), and its absolute intensity is fainter than at higher state; whether or not an orbital hump is present cannot be decided from the data available, but clearly the light curve is not as smooth and straight as during the intermediate brightness. Measurements of MV

Lyr during faint state show strong activity during one night (Figure 3-14a); two nights later, no photometric changes in excess of slight random variations can be detected at the same optical brightness (Figure 3-14b).

TT Ari has been observed photometrically at IR wavelengths during the high state (Jameson et al, 1982b). The light curve is highly variable on times-scales of hours, though no relation to orbital variations is evident; simultaneous light curves in the optical and at different IR wavebands are only vaguely similar and strongly change from one night to the next.

At UV wavelengths, brightness changes in connection with the orbital motion can clearly be seen. In TT Ari the hump amplitude is seen to decrease between 5000 and 3000 Å, but then increases again with decreasing wavelength, to be at least as pronounced at 1500 Å as in the optical (Figure 3-15), much unlike in dwarf novae, in which the hump amplitude strongly decreases with decreasing wavelength and is only marginally (if at all) detectable in the UV. From phase-resolved spectroscopy, a UV light curve has been derived for TT Ari in the high state (Figure 3-16) which, like the optical light curve, clearly reflects the orbital motion of the system.

TT Ari has been observed with the EINSTEIN satellite in X-rays and simultaneously in the optical (Jensen et al, 1983b). The X-ray flux is strongly variable on most time-scales. There is some evidence for orbital variation in the X-rays, mostly in that the X-ray flickering amplitude increases around times of the optical hump (Figures 3-17). The hardness ratio, i.e., the color of the X-ray radiation, remains unchanged during the orbital cycle.

Polarization of the radiation from TT Ari and KR Aur of some 0.3% has been measured (Popova and Vitrichenko, 1979; Szkody et al, 1982a), in full agreement with observations of dwarf novae.

III.A.3. FLICKERING AND OSCILLATIONS

ABSTRACT: Just as in dwarf novae, flickering is also observed in anti-dwarf novae at high as well as low states. Only during the high state in some objects oscillations occasionally can be seen.

other nova-like objects: 98, 113, 117, 121, 122, 128, 141

dwarf novae: 54, 56

interpretation: 151, 181, 185, 213

In all systems, rapid flickering is observed with amplitudes of some hundredths to some tenths of a magnitude on time-scales of seconds to minutes. It is usually strongly diminished in amplitude or disappears altogether during eclipses in the high state. No other relation with the orbital phase than this could be detected. Simultaneous X-ray and optical observations of TT Ari during the bright state revealed a strong relation between flickering observed in both wavelength ranges: The power spectra look very similar, the flickering in X-rays is delayed by some 58 seconds with respect to flickering in the optical (Jensen et al, 1983). The flickering amplitude amounts to some 15% to 20% in the optical and to some 70% to 100% of the flux in the X-rays. High-speed photometric observations of TT Ari and MV Lyr in different brightness stages showed that flickering can also be present in low states. Two observations of MV Lyr at low state were obtained two days apart (Robinson et al, 1981): very pronounced flickering similar to that seen during the bright state was present during one observing run, while brightness fluctuations did not exceed photon noise during the next run; the overall optical brightness had not changed during this time. In similar observations of TT Ari, no flickering could be seen at an intermediate brightness level, whereas it was even more conspicuous at low state than during high state; the absolute amplitude was somewhat lower at low state (Figure 3-12). In none of these observations could a relation with orbital phases be detected. Flickering in the IR is about as strong as in the optical (Jameson et al, 1982b).

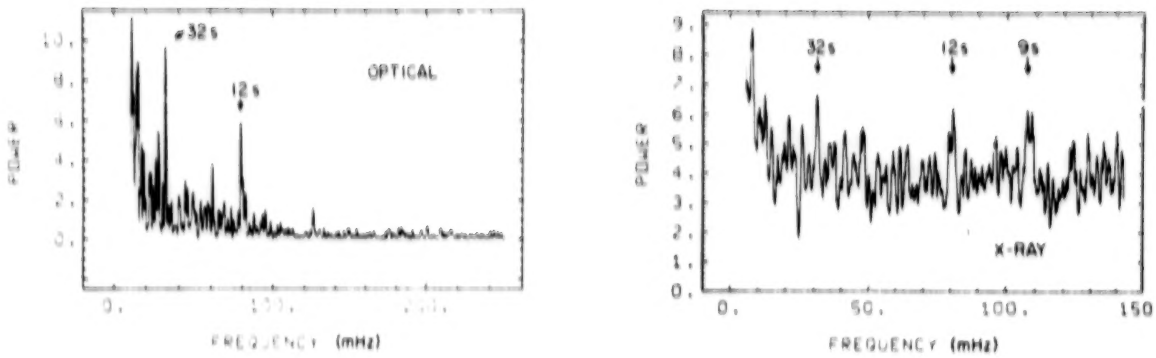


Figure 3-18. Optical and X-ray power spectra of TT Ari from simultaneous observations (Jensen et al, 1983).

Besides the flickering, there is occasionally also a component of quasi-periodic oscillations with periods on the order of seconds or minutes during high states. No detection during low states has ever been reported. The most extensive investigations have been carried out for TT Ari (Mardirossian et al, 1980; Jensen et al, 1983). The oscillations here are not always present. Periods vary erratically between 32 and 43 sec. In the power spectra which were extended over a lengthy run the peaks of the oscillation frequencies are not strictly monochromatic, but rather have a narrow bandwidth which is again variable from one run to another. It is not clear whether the oscillations in TT Ari are intrinsically polychromatic (which would distinguish it from other cataclysmic variables in which the peaks are either monochromatic or much broader than those in TT Ari), or whether this is merely due to the coarse time resolution. Periods and life times are on roughly the same order as in other cataclysmic variables.

Simultaneous optical and X-ray observations of TT Ari have revealed oscillations at different frequencies. A monochromatic 32 sec oscillation and a non-monochromatic oscillation around 12 sec were seen in both energy regimes; in addition, a narrow frequency band was present around 9 sec only in X-rays (Mitrofanov, 1980; Jensen et al, 1983; Figure 3-18). The pulsed fractions are 15 - 25% in the X-rays, and some 1.5% in the optical — in close analogy to observations of dwarf novae. No time relation between optical and X-ray oscillations has been reported, but the identical frequencies at both wavelengths lead one to suspect a physical connection between the observed phenomena.

III.B. SPECTROSCOPIC OBSERVATIONS

ABSTRACT: During the high state the spectra exhibit characteristics of outbursting dwarf novae, during low state those of quiescent dwarf novae. Contrary to dwarf novae, in which the UV is more affected by the outburst activity, in anti-dwarf novae the optical changes most. The spectrum of MV Lyr is highly variable during high state. The spectroscopic period of TT Ari is distinctly different from the photometric.

other nova-like stars: 99, 116, 119, 122, 124, 134, 141

dwarf novae: 45, 65, 80

interpretation: 151, 192

The general flux distribution of anti-dwarf novae during the high state is not any different from that of other cataclysmic variables. During the high state, characteristics of outbursting dwarf novae can be seen. In some of the anti-dwarf nova systems, variations of the line profiles with orbital phase have been observed. The two systems LX Ser and VZ Scl show changes in their spectra during eclipses which affect the

C-3.

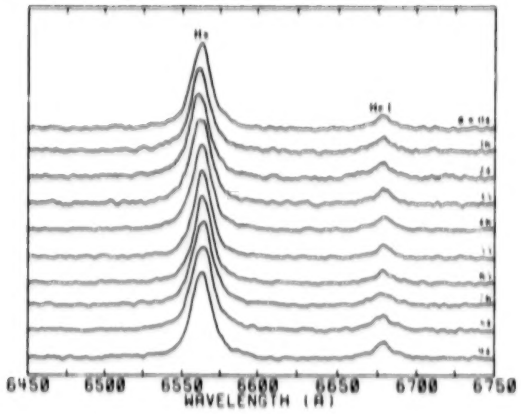


Figure 3-19. Phase-resolved spectroscopy of KR Aur during the high state (Shafter, 1983).

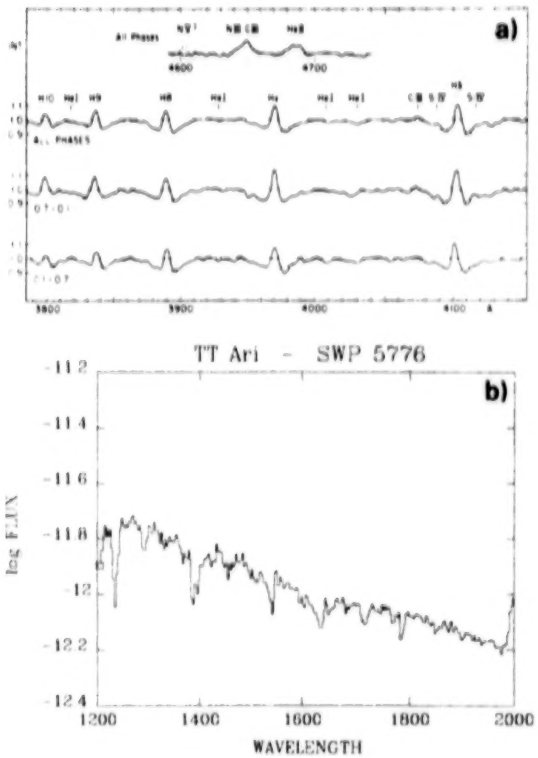


Figure 3-21. Spectral appearance of TT Ari: a: optical spectrum in the high state (Cowley et al, 1975); b: UV spectrum in the high state; c: optical and UV spectra in the high state between two successive low states (Jameson et al, 1982b); d: optical spectra at (a) high state and (b) intermediate brightness (Voikhanskaya, 1983b); e: UV spectrum at intermediate brightness (Krautter et al, 1981b); f: Optical spectrum at low brightness level (Shafter et al, 1985); g: UV spectrum at low brightness level (Shafter et al, 1985).

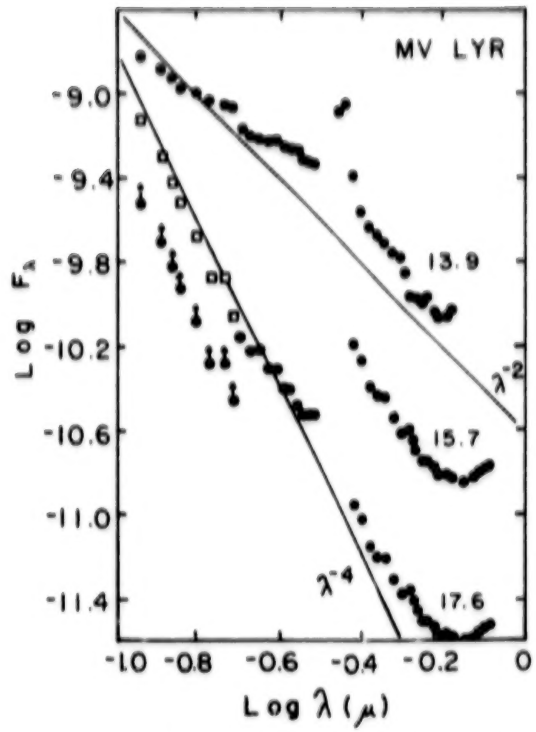
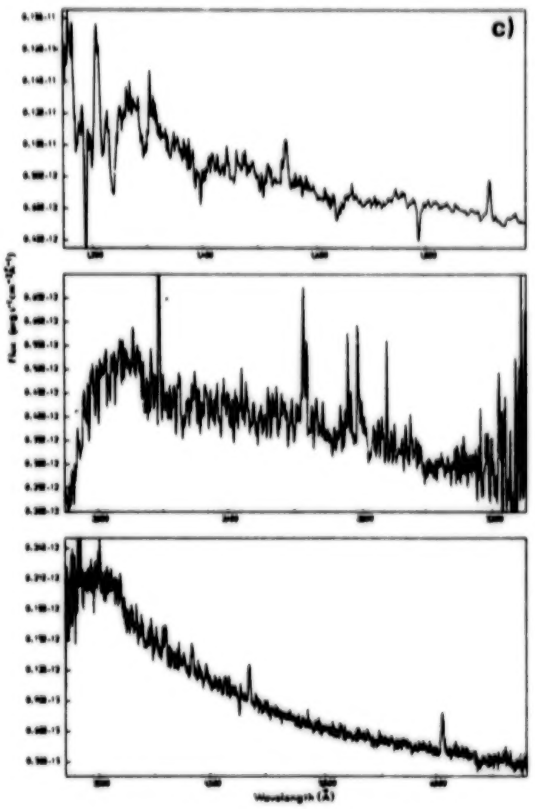


Figure 3-20. Flux distribution of MV Lyr during high, intermediate, and low states (Szkody and Downes, 1982).



ORIGINAL PAGE IS
OF POOR QUALITY

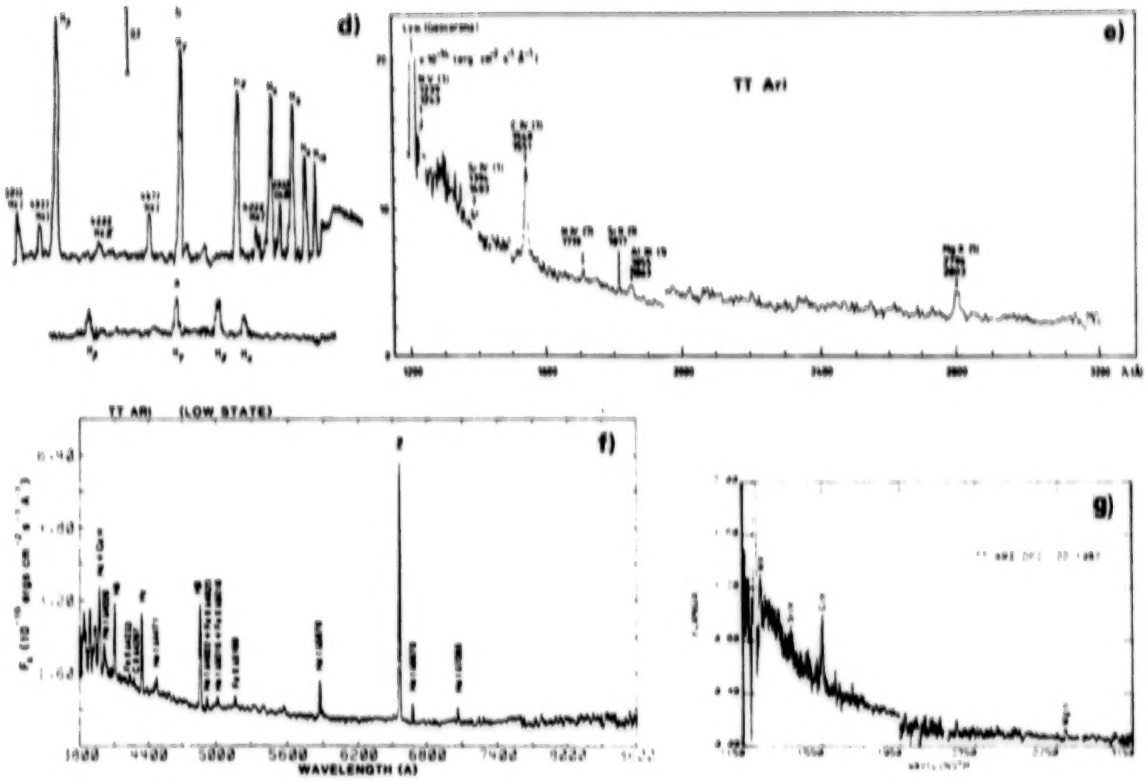
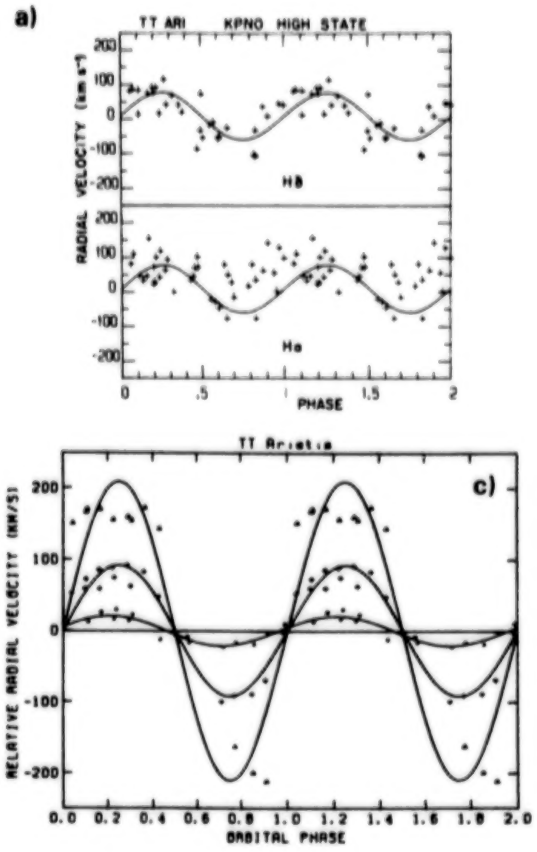


Figure 3-21. (Continued)



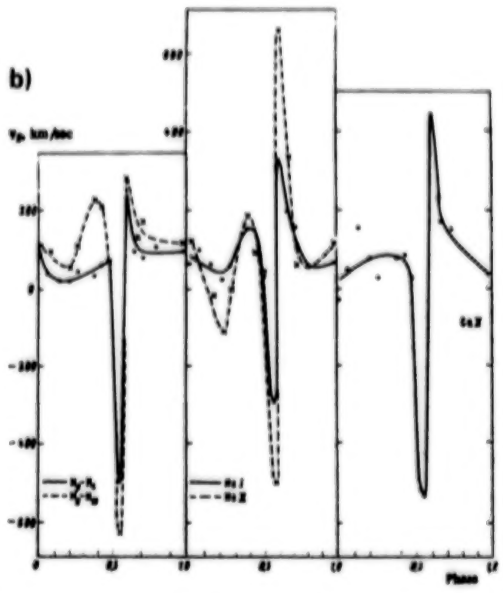


Figure 3-22. Radial velocity curves of TT Ari: a: Hα and Hβ curves during high state (Thorstensen et al, 1985 — the least square sinusoidal fit to Hδ is plotted in both panels); b: at intermediate state (Voikhanskaya, 1983b — the solid and dashed lines are fits to observations of different lines as indicated in the figures); c: at low state, measured from different parts of the line profiles (peak component: dots; broad base: crosses; narrow base: triangles).

continuum shape as well as the strengths and profiles of the lines, much like UX Ursae Majoris systems. S-wave variations in the H emission profiles are seen in LX Ser, TT Ari, and KR Aur, although in no system, not even in the eclipsing* system LX Ser, are the lines double-peaked (Young et al, 1981a; Shafter, 1983; Shafter et al, 1985; and Figure 3-19). In the lower states, spectroscopically, the systems resemble more quiescent dwarf novae. Changes in the continuous flux distribution between high and low state, however, are of a different quality than in dwarf novae: while in dwarf novae most of the flux changes during an outburst cycle occur at UV wavelengths, in anti-dwarf novae it is the optical which is more strongly affected, although clearly the changes occur at all wavelengths. Changes in the overall distribution between high, intermediate, and low state in MV Lyr are shown in Figure 3-20 (compare with, e.g., Figure 2-76): the drop in brightness affects more the optical wavelengths than the UV. During the low state in MV Lyr, as well as TT Ari, the secondary component becomes prominent at low energies (Chiapetti et al, 1982; Shafter et al, 1985).

The different brightness stages not only show effects on the continuum shape, but even more conspicuous effects in the line spectra. Changes in the two best-studied systems, TT Ari and MV Lyr, are described in the following. During the high state, before the first recorded spectacular low state in fall 1980, the spectrum of TT Ari exhibited moderately strong H emission lines in the optical, which were placed in wide shallow absorptions — strongly reminiscent of a dwarf nova during decline from outburst (Figure 3-21a). The UV was dominated by the usual strong resonance lines in absorption, with C IV exhibiting a P Cygni profile (Figure 3-21b). Between the two minimum states in fall 1980 ($m_v \approx 14.5$), and fall 1982 ($m_v \approx 16.5$), there was a time when TT Ari returned to its normal brightness around 12.0 mag. In spectra taken during this period, no pronounced absorption shells around the H emissions are visible. In the UV, C IV and Mg II were entirely in emission, and the other resonance lines were in absorption (Figure 3-21c).

During the intermediate state at $m_v \approx 14.5$, the UV lines all went into emission, and the continuum was bluer than in the bright state; the optical lines became narrower and much stronger in emission, correspondingly the Balmer jump was seen strongly in emission (Figures 3-21d, 3-21e). Comparing the flux at intermediate and low (≈ 16.5 mag) states, there is hardly any change in the UV shortward of 1500 Å; at 3000 Å, however, the flux decreased by a factor of 5, and in the optical by a factor of nearly 100, by which, in total, the spectrum has steepened considerably toward shorter wavelengths. In line radiation in the UV no major changes can be seen; the optical lines become even much narrower than during intermediate state, with the H lines, as at high state, again placed in absorption shells (Figure 3-21f).

MV Lyr exhibits a highly variable line spectrum during its bright state. MacRae (1952) reports the star to show weak H lines and strong He II 4686 Å (it is not clear from his description whether these lines are in absorption or in emission) at a brightness of 12.18 mag. Diffuse shallow absorptions were also seen in 1952; in 1954 MV Lyr exhibited strong H emissions; and in 1963 narrow emission lines and rapid radial velocity variations were reported (Voikhanskaya, 1980). All this seems to have happened at roughly the same optical brightness. In 1977 through early 1979 Voikhanskaya observed MV Lyr several times spectroscopically; all throughout this time the AAVSO reports the apparent magnitude to fluctuate around 12.5 mag. In July 1977, a plain continuum without any appreciable lines was observed, which persisted for at least 8 months. In summer 1978, H emission lines were seen which briefly dis-

*Normally eclipsing systems show double-peaked lines.

appeared shortly afterwards around mid-July; they reappeared and stayed until late October when they gradually vanished and left only a continuous spectrum. This then seems to have lasted at least until mid-January 1979. When emissions were present, the line profiles of Hβ, Hγ, and Hδ were subjected to extremely rapid variations in strength and position on time-scales of minutes, while Hα stayed roughly constant. And over longer time-scales of weeks, as it seems, the strength of all these lines, including Hα, changed considerably but differently for different members of the Balmer series. Continuous spectra at times exhibited wide shallow absorption shells of H with some weak emission cores. No He could be detected.

All published spectra of fainter brightness states of MV Lyr show strong emission lines of mostly H and He which become the narrower the lower is the overall brightness level (Robinson et al, 1981; Schneider et al, 1981; Szkody and Downes, 1982); and the lower the level is, the flatter (cooler) become the optical flux distribution, much like the spectra of TT Ari. Whether or not spectra at fainter states are generally more stable in appearance than at high state is not known. Some variability is clearly present: in spectra of the very faint state absorption shells can be seen at times around the H emission lines which are not visible at other times when the system has roughly the same optical brightness (Schneider et al, 1981; Szkody and Downes, 1982). MV Lyr has been observed on two occasions at $m_v \approx 17.3$ mag and 16.5 mag, when the continuum slopes were almost identical but the line strengths were very different (Robinson et al, 1981).

In TT Ari the spectroscopic period, as determined from the radial velocity, is clearly different from the photometric period, as determined from the repeating hump. Furthermore, when all radial velocity data from different epochs and brightness stages are taken together, no period can be found which fits all the data. If, however, observations from high, intermediate, and low states are analyzed separately, they all lead to a spectroscopic period of $0.^d1375511$, implying phase shifts of the radial velocity of 0.28 and 0.58 orbital periods, respectively, between the high and low states (Shafter et al, 1985; Thorstensen et al, 1985). The photometric period was found to decrease from $0.^d1329$ in 1961/2, to $0.^d1327$ in 1966, and to $0.^d1324$ in 1978 (Thorstensen et al, 1985). It is not clear what these findings mean in terms of a physical model of TT Ari; it only is clear that more than just orbital rotation causes the observed changes. A case of similar confusion seems to be the dwarf nova CN Ori, for which several photometric periods have been determined from various observations which may or may not be identical with the spectroscopic period (see Chapter 2.II.B.3).

For TT Ari radial velocities have been obtained at all brightness stages (Figure 3-22). In the high state, the radial velocity curve of Hα can be seen to be considerably more distorted than that of Hδ; furthermore, the γ-velocity is systematically lower for higher-order Balmer lines. At intermediate brightness, the radial velocity curve is highly distorted and asymmetric with a sharp short-lasting drop in the velocity at about phase 0.5 of the spectroscopic period, while the equivalent width of the line stays constant. This is probably not a rotational disturbance since, first, TT Ari is not known to have an eclipse; second, if the change in radial velocity were caused by eclipse effects, one would expect to see first a rise in the radial velocity followed by a drop, and not vice versa, unless the white dwarf in TT Ari would be rotating retrogradely; and third, the disturbation lasts far too long to be related to the white dwarf. At the very low state, the curve determined from the broad base of the lines again has a more sinusoidal shape and is in fairly good agreement with the radial velocity determined from the high state (as is also the case in many other cataclysmic variables, for which different radial velocities are determined from different parts of the line profile; this effect is very pronounced in TT Ari during the low state).

GENERAL INTERPRETATION: Like the UX Ursae Majoris stars, anti-dwarf novae can be distinguished neither spectroscopically nor photometrically from dwarf novae (at some activity stage), except for their outburst behavior. Thus anti-dwarf novae are also considered to be essentially identical to dwarf novae in their physical nature. The mass transfer rate is assumed to be fairly high and stable for most of the time; only at (unpredictable) times is it considerably reduced.

OBSERVATIONAL CONSTRAINTS TO MODELS:

- *Dwarf novae, UX Ursae Majoris stars, and anti-dwarf novae share most of their characteristics except for their outburst behavior.*
- *Unlike in dwarf novae, the changes between high and low state in anti-dwarf novae have a considerable effect on the flux at long wavelengths.*
- *Optical color changes during eclipse in some anti-dwarf novae are the reverse of what is seen in dwarf novae.*
- *Also unlike in dwarf novae, the hump is strong at UV wavelengths in some anti-dwarf novae.*

IV. DQ HERCULIS STARS

Observationally the criterion for a cataclysmic variable to be classified as a *DQ Herculis star (intermediate polar)** is the existence of more than one photometric period, one of which is identical with the spectroscopic period (and this is the orbital period), and at least one other which is appreciably different from this. In addition, all these periods must be strongly coherent over all times the system has been observed.

This definition is vague enough to actually render the class of DQ Herculis stars highly inhomogeneous, comprising objects which are also classified as members of, or bear strong similarities to, other sub-classes of cataclysmic variables (incidentally, the prototype DQ Her is an old nova; see Chapters 6 and 8). Two main groups within this class can be distinguished.

The first group consists of stars with one additional photometric period which is some two orders of magnitude smaller than the orbital period (the systems DQ Her and AE Aqr belong to this group; for several years also V533 Her had to be regarded as one); originally only these stars were called "DQ Herculis stars."

The second group consists of stars with additional photometric periods that are only about one order of magnitude smaller than the photometric period (like TV Col, FO Aqr, V1223 Sgr, BG CMi, and EX Hya, although the latter system is different from all the others); for most of these objects two or more, usually fairly similar, additional periods have been detected in the optical, one of which often also shows up strongly in the X-rays. Originally these objects were referred to as "intermediate polars," because their additional periods are intermediate between the very short periods of the DQ Herculis stars (which are understood to be the rotational periods of the white dwarfs, see Chapter 4.III.F.2) and the synchronous rotation of the polars (Chapter 3.V).

Then there is one additional group of "related objects:" their photometric period is different from the spectroscopic period, but other than "real" DQ Herculis stars they do not have one photometric period which is identical with the spectroscopic period, e.g., the systems HR Del, V603 Aql, TT Ari, are regarded as "related" (see Ritter, 1987). These will not be regarded here, but rather these objects have been dealt with in the context of the other sub-classes of cataclysmic variables (see index).

The classification of the systems AE Aqr and WZ Sge is controversial: both are at times referred to as peculiar dwarf novae or, alter-

*There is no general agreement as to how these terms shall be used: some authors use them as equivalents, others distinguish between them according to the definitions given below.

natively, as some kind of nova-like stars. Since the detection of superhumps during the last outburst of WZ Sge, this object is usually classified now as a dwarf nova of sub-type SU Ursae Majoris, and has been dealt with as such in Chapter 2, although the 28 sec pulsation also would justify a classification as a DQ Herculis star. As for AE Aqr, one striking feature is a highly stable pulsation with a period of some 33 sec, while its dwarf nova activity is restricted to mere irregular fluctuations; it will be dealt with in this section on DQ Herculis stars.

Concerning their general appearance and behavior, DQ Herculis stars exhibit all characteristics common to cataclysmic variables, including even nova outbursts in some cases. However, they are fairly individualistic as single objects, and except for the photometric periods they do not have much in common concerning details.

Polarization in the emitted radiation is undetectable or just barely present.

IV.A. LONG-TERM VARIATIONS AND GENERAL ORBITAL CHANGES

ABSTRACT: The long-term behavior of all members of this class, when considered together, comprises the full range of possibilities found in cataclysmic variables from nova outbursts to dwarf novae and nova-like activity. Respective variations are found in orbital photometric variability.

other nova-like stars: 102, 125

dwarf novae: 21

interpretation: 171

Long-term variabilities of DQ Herculis stars span the entire range of possibilities exhibited by cataclysmic variables. Two objects, DQ Her and V533 Her* are old novae. DQ Her had a 12.8 mag outburst in 1934, V533 Her had a 11.3 mag outburst in 1963; when these outbursts are compared to those of other novae, there seems to have been nothing unusual about them (Chapters 6 and 8). EX Hya more resembles dwarf novae in its outburst activity. Normally it fluctuates about a brightness of 13 mag with occasional flares of some 0.5 to 1.0 mag amplitude; in intervals of 450 to 500 days it has dwarf nova-like eruptions of some 2 mag amplitude which only last for some 4 days (Córdova and Riegler, 1979). AE Aqr fluctuates irregularly between some 10 mag and 11 mag, without any detectable periodicity in this behavior (AAVSO Report 29). AO Psc fluctuates about 13.3 mag with amplitudes of some 0.4 mag (Patterson, 1985); inspection of some old photographic plates revealed only one excursion to a brightness well below normal (Belserene, 1981). TV Col, on the other hand, has remained close to 14 mag ever since detection, except for one occasion in November 1982, when it rose by some 2 mag for about 2 days. And finally for V1223 Sgr, which normally can be found near 12.3 mag, a total of five drops by 2 - 3 magnitudes have been reported (Belserene, 1981).

Light curves on orbital time scales are highly reminiscent of other cataclysmic variables: they may or may not show humps and eclipses, and suffer substantial flickering. Different from what normally can be found in cataclysmic variables, the coexistence of several photometric periodicities often gives the light curves a very irregular appearance. Since the systems are fairly different from each other photometrically, DQ Herculis stars and intermediate polars, in the stricter sense, will be dealt with separately.

*As will be seen, this object cannot really be regarded as a DQ Herculis star, but since it bears many features characteristic of DQ Herculis stars, it will be dealt with briefly in this chapter.

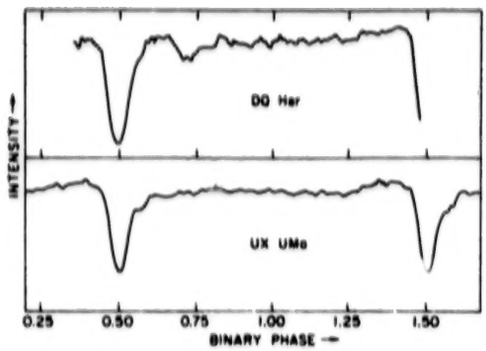


Figure 3-23. Orbital light curve of DQ Her, as compared to the light curve of UX UMa (Petterson, 1980).

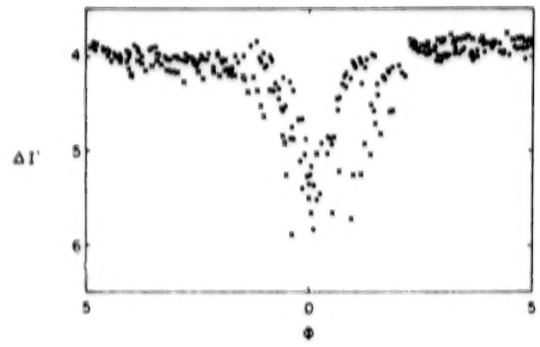


Figure 3-24. IR eclipses of DQ Her, measured at different times (Nelson and Olson, 1976).

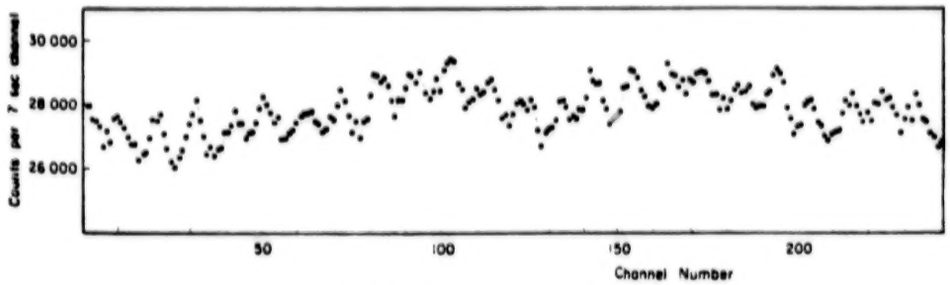


Figure 3-25. 71 sec oscillation in DQ Her (Warner et al, 1972).

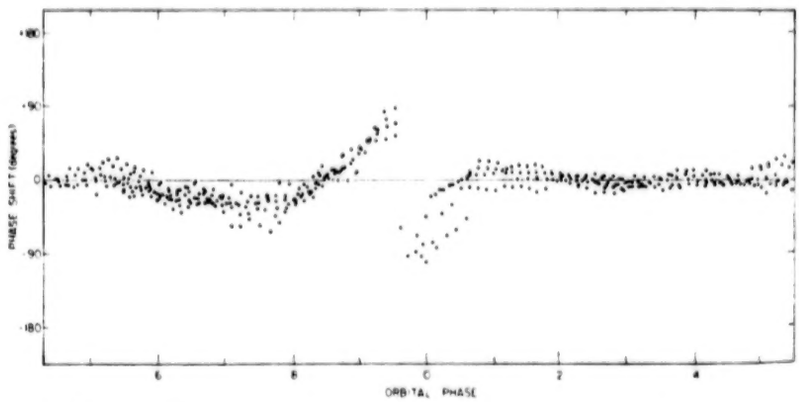


Figure 3-26. Phase shift of the oscillations in DQ Her during eclipse (Patterson et al, 1978b).

IV.B. DQ HERCULIS STARS
(in the narrow sense)

IV.B.1. DQ HERCULIS

ABSTRACT: The orbital light curve of the prototype DQ Her is almost identical to that of UX UMa; the color dependence is somewhat different. A 71 sec pulsation has been seen in all photometric observations. The spectrum is in no ways exceptional for a nova-like star.

other nova-like stars: 96, 102, 117, 119, 122, 125, 140

dwarf novae: 35, 46, 65

interpretation: 190

The orbital light curve of DQ Her is almost identical to that of UX UMa (Figure 3-23), the orbital periods are different by only 4.4 minutes: there is a primary eclipse of about one magnitude depth, the exact shape and

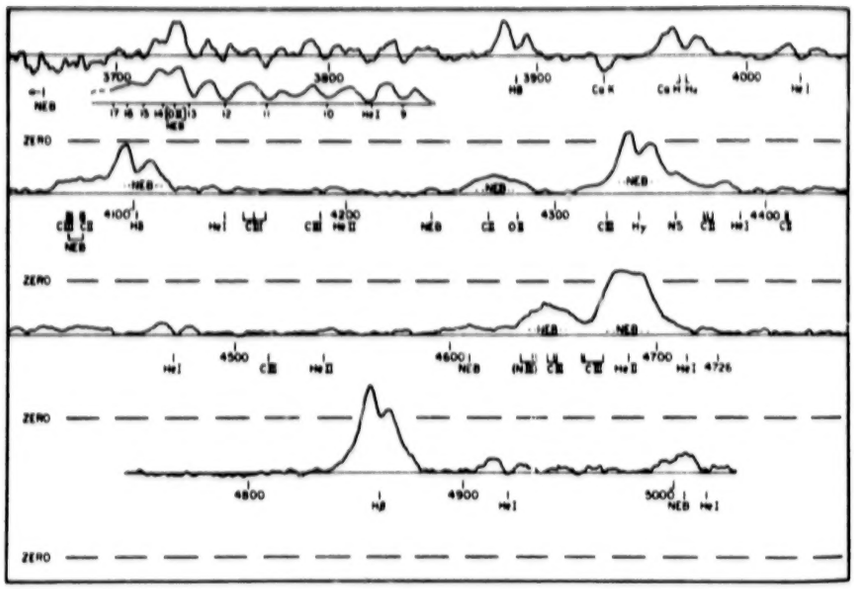


Figure 3-27. Optical spectrum of DQ Her (Hutchings et al, 1979).

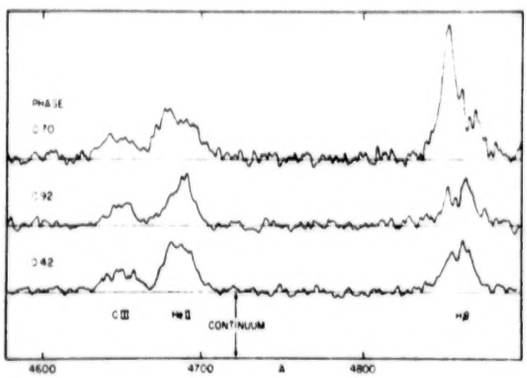


Figure 3-28. Optical spectrum of DQ Her through eclipse (Hutchings et al, 1979).

width of which are variable from cycle to cycle; the ingress is substantially more stable in appearance than the egress; the egress is asymmetric and most of the time, as in UX UMa, has a halt lasting for a couple of minutes shortly before reaching normal brightness; shortly after egress between phases 0.110 and 0.325 (with respect to central eclipse) there is a phase of extremely-large-amplitude irregular variability, the particular character of which again varies from cycle to cycle; after that, like in UX UMa, the light level decreases until about phase 0.7, when it starts rising again and a hump-like feature which will be interrupted by the eclipse becomes visible; the hump maximum can occur before as well as after the eclipse, and the amplitude varies strongly with time (e.g., Walker, 1957; 1958). Unlike in UX UMa, where the eclipse is deeper in U and V than in B, in DQ Her in 1978 it was observed to become deeper with decreasing wavelength, whereas in 1954 it became shallower (Walker, 1957; Schneider and Greenstein, 1979); this change in behavior probably can be ascribed to the influence of the surrounding nebulosity which had been ejected during the nova outburst. At IR wavelengths the effect is partially reversed: in I the depth of the eclipse is about the same as in U (Mumford, 1976). Furthermore, features are considerably more distorted in the IR eclipse than in the optical, and they are subject to even stronger temporal changes (Figure 3-24). No hump can be seen in the IR when it is clearly visible in the optical (Nelson and Olson, 1976); nor can a secondary eclipse be detected.

The times of eclipse, which are a pure effect of binary motion, show a sine-like modulation with a period of about 14 years; due to the relatively short time during which this star has been observed, it is not clear whether these changes are strictly periodic or merely cyclical (Patterson et al, 1978b).

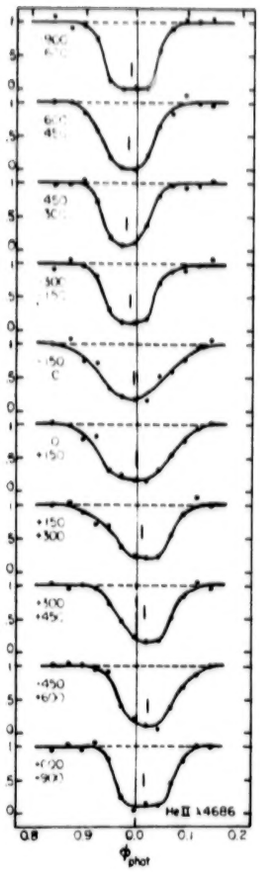


Figure 3-29. Eclipse profiles of He II 4686 Å as measured at various distances from the line center (Young and Schneider, 1980).

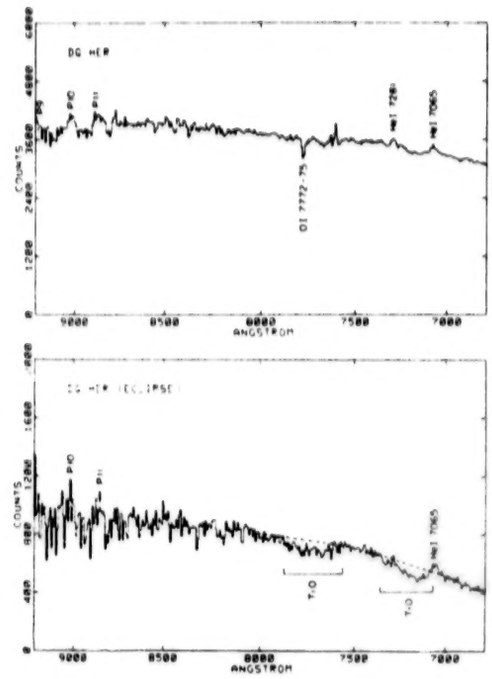


Figure 3-30. IR spectrum of DQ Her outside and during eclipse (Young and Schneider, 1981).

The strong, seemingly irregular brightness changes near phase 0.2 in DQ Her encouraged closer inspection, which eventually revealed a monochromatic periodicity of 71 sec. This can be found in all observations in the optical with sufficiently high time resolution up to wavelengths of at least 8600 Å (Figure 3-25) — superimposed is an irregular flickering with lower frequencies (Chanan and Nelson, 1979). The amplitude of this pulsation varies over the orbital cycle: it has an amplitude of 0.3 to 0.5 mag near phase 0.1, and gradually decreases until phase 0.6 when it is barely detectable; it increases again as the hump becomes visible; during eclipse it is again strongly diminished, is entirely absent for two short moments around mid-eclipse, and then recovers rapidly and is again most pronounced near phase 0.1 (Warner et al, 1972; Patterson et al, 1978). In addition, the pulsed fraction of the flux seems to vary over longer time-scales (Chanan and Nelson, 1979). Regarding pulse times during the orbital cycle with respect to the average ephemeris, a change of 360° in phase shortly before mid-eclipse can be seen (Figure 3-26). When all observations of the 71 sec pulsations since 1959 are regarded together, a secular decrease in the period becomes apparent (Patterson et al, 1978b).

No dependence of the pulse times on wavelengths could be detected, while the amplitude in U is almost 70% of that in V. Only the He II 4686 Å and C III — N III 4640 Å emission lines are much more strongly modulated than the underlying continuum. In addition, in He II, there is a phase shift in pulse arrival times with respect to the continuum pulsations, which increases over the width of the line with increasing wavelength: the line

center pulsates in phase with the continuum, the blue wing lags behind, and the red wing leads it; the largest amplitude of the pulsation is shifted to wavelengths slightly longward of the line center (Chanan and Nelson, 1979).

In the optical spectrum of DQ Her, all lines except Ca II K are seen in emission (Figure 3-27). Carbon lines are unusually strong. There are large differences in profiles between H, He I, and He II and C lines: H, and He I, and, weakly, He II show double-peaked profiles, whereas all C lines are single peaked. There are pronounced profile changes over the orbital cycle, in particular during eclipse when all lines are considerably weakened (Figure 3-28). The eclipse shape is dependent on the wavelength in the line profile and is in general fairly asymmetric (Figure 3-29): the curve is roughly symmetric and centered about the continuum eclipse for the line center; it becomes asymmetric and the center is shifted away from the center of the continuum eclipse for higher Doppler velocities, and ingress and egress occur more rapidly at higher velocities; the total width of the eclipse is approximately 0.11 of the orbital cycle for all velocities except for the line center, where it increases to 0.15 of the total rotational period. The blue wings of the Balmer lines are eclipsed before the respective parts of He II 4686 Å, and similarly the eclipse ends later for the red wing of the H lines. During eclipse in He II 4686 Å and in the Balmer lines there appears a pronounced rotational disturbance (Young and Schneider, 1980). During mid-eclipse the spectrum of the secondary companion becomes visible (Figure 3-30).

IV.B.2. OTHER DQ HERCULIS STARS

ABSTRACT: For some years the old novae V533 Her exhibited a stable pulsation like a DQ Herculis variable. In AE Aqr, a 33 sec variability could be observed ever since its detection. In most other properties AE Aqr appears to be a normal cataclysmic variable.

other nova-like stars: 96, 102, 114, 119, 125, 140

dwarf novae: 35, 46, 65

interpretation: 190

Rapid coherent oscillations of some 63 sec have been discovered in the old nova V533 Her in 1978 (Patterson, 1979a). They had a mean amplitude of 1%, were purely monochromatic, and were visible all through the orbital cycle. Observations were extended over a period of 64 days during which time the pulsations stayed strictly coherent. They also seem to have been detected in 1982 (Robinson and Nather, 1983). — When the system was observed again in 1982, there was strong flickering, but the 63 sec pulsation had entirely disappeared (Robinson and Nather, 1983).

The photometric variability of AE Aqr on time-scales of hours has been investigated extensively by Chincarini and Walker (1981). A photometric period of 9h53m is apparent in both the light curve as well as in the radial velocity curve. AE Aqr is often found in a state of pronounced flaring activity, which also seems to be responsible for the observed long-term variations (Figure 3-31). Flares occur mostly around orbital phases 0.25 and 0.8, the times of maximum and minimum radial velocity, which are also times of photometric maxima; the continuum light level remains much less affected by the flares than are the lines (Figure 3-32). Inspection of optical light curves taken at different wavelengths demonstrates that most of the activity occurs in the U-band, less in the B-band, and by far the least in V.

Investigation of the variability of the spectrum during flares revealed three types of flares: those which occur exclusively in the (mainly blue) continuum, those which occur in the wide components of the H emission lines, and those which occur in both together (Chincarini and Walker, 1981).

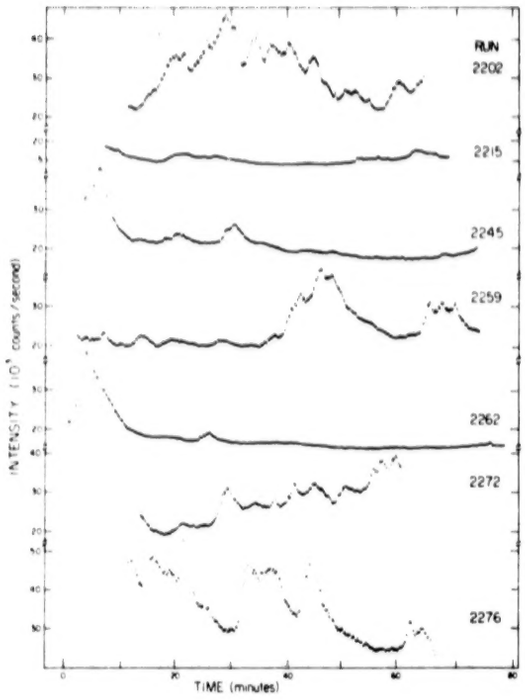
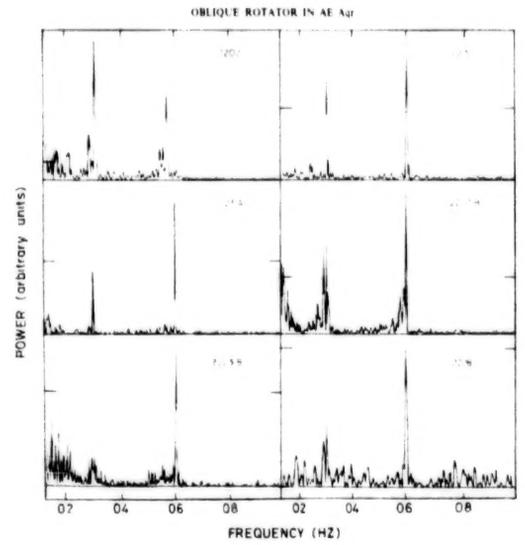


Figure 3-31 (left) Light curves of AE Aqr taken at various epochs (Patterson, 1979b).



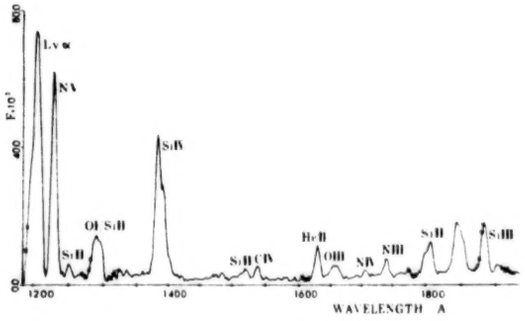


Figure 3-32. Orbital light curves of AE Aqr, measurements from different epochs (Chincarini and Walker, 1981).

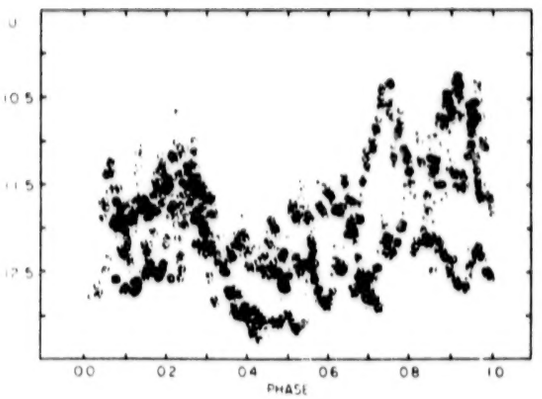


Figure 3-34. Relation between flickering amplitude and mean intensity in AE Aqr (Patterson, 1979b).

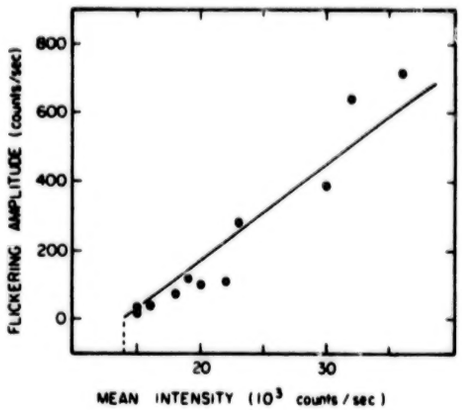


Figure 3-33. (left) Power spectra of AE Aqr (Patterson, 1979b).

Figure 3-35. UV spectrum of AE Aqr (Jameson et al, 1980).

Power spectrum analysis of different photometric brightness levels exhibits the presence of a highly coherent oscillation with 33.08 sec period over many years, as well as a comparable, often more powerful, oscillation in the first harmonic at 16.04 sec (Figure 3-33). In addition, far less coherent quasi-periodic oscillations containing much less power can be present together with, or even instead of, the coherent oscillations — although at those times when only quasi-periodic oscillations can be detected, the latter are so strong that the simultaneous presence of the coherent oscillations cannot be excluded. Quasi-periodic oscillations only could be detected at times of enhanced flaring activity, never during minimum normal light. The amplitudes of both coherent and quasi-periodic oscillations usually are on the order of 0.1 – 0.2 % of the general flux level, though during times of strong flares they can increase to up to 2% within only some two minutes. X-ray observations in the range of 0.1 – 4.0 keV revealed the 33 sec periodicity to be present also there, agreeing in phase with the optical pulsation. Besides these more or less coherent variabilities, normal flickering can also be observed at much lower frequencies. The amplitude is well correlated with the general brightness of the system (Figure 3-34).

The optical spectrum of AE Aqr consists of a dK0 absorption spectrum as well as H, He I, and Ca II emission lines (Chincarini and Walker, 1981). In particular, the H lines show a very complex structure consisting of a wide and a narrow component. Radial velocity curves of the narrow component almost agree in phase and K-amplitude with those of the absorption spectrum, thus suggesting a common origin, whereas the wide emission component is out of phase by roughly 180°. In addition, rapid changes in radial velocity are reported which are not related to the orbital motion.

The UV spectrum of AE Aqr is very atypical for a cataclysmic variable (Figure 3-35). The continuum rises slightly towards the red from Lyα on. The line spectrum consists exclusively of emissions. N V (1240 Å), and Si IV (1400 Å) are strong, whereas C IV (1550 Å) is remarkably weak; Mg II (2800 Å) is unusually strong; emissions of Si II, Si III, N II, N IV, and He II are strongly present. There is indication for the line flux to be anti-correlated with the optical brightness of the system (Jameson et al, 1980).

AE Aqr has been detected at radio wavelengths at 15 mJy by Bookbinder and Lamb (1985, see also Chanmugam, 1987).

IV.C. INTERMEDIATE POLARS

IV.C.1. EX HYDRAE

ABSTRACT: EX Hya is a very unique object. The binary period is given by a recurring eclipse; in addition there is another period which is shorter by ⅓, most pronounced in the appearance of a recurring hump. X-rays and the line spectrum vary with both periods. Optical color variations connected with the shorter period are different from what is seen in other cataclysmic variables.

other nova-like stars: 96, 102, 114, 117, 122, 125, 140

dwarf novae: 35, 46, 65

interpretation: 190

EX Hya is a very unique object in many respects. It is closely related to dwarf novae in its outburst activity. As a DQ Herculis star, it is the only known object in which the second photometric period is close to 2/3 of the orbital period. For all other objects this parameter is either some one or some two orders of magnitude shorter than the binary period.

Power spectrum analysis of the optical data reveals two other periodicities besides the 98 and 67 min periods, one at 49.1 min which is one-half of the orbital period, and one at 46.4 min which does not have any other correspondence.

As in many other cataclysmic variables, the orbital period shows cyclic secular variations on time-scales of 10 – 14 years. The 67 min

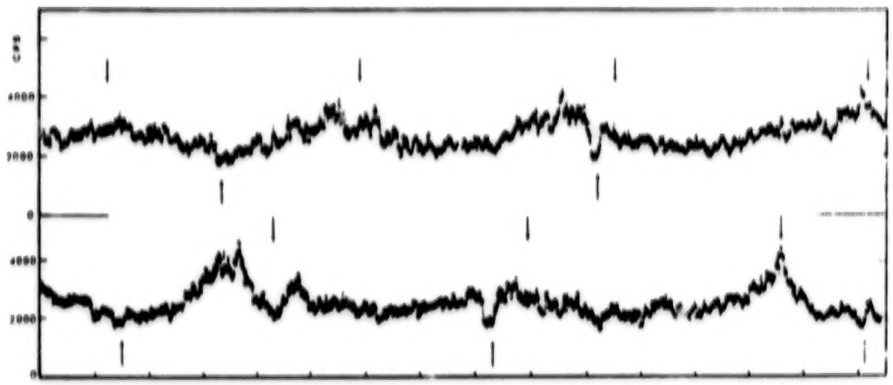


Figure 3-36. Optical light curve EX Hya (Warner and McGraw, 1981).

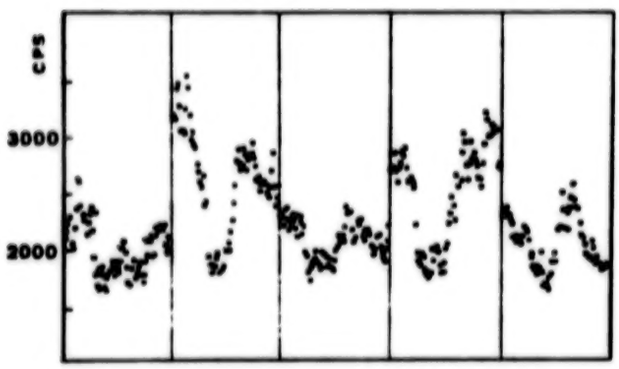


Figure 3-37. Eclipse depths of EX Hya at various epochs (Warner and McGraw, 1981).

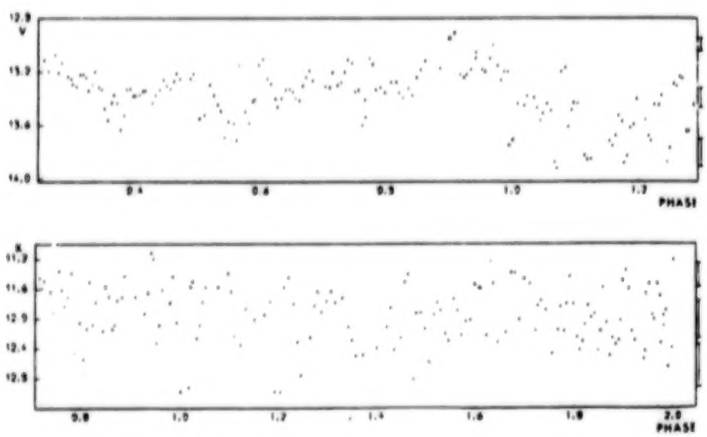


Figure 3-38. V and K light curves of EX Hya (Sherrington et al, 1980).

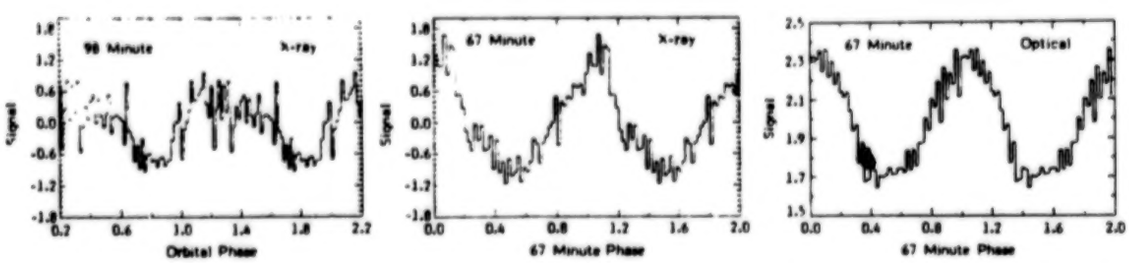


Figure 3-39. X-ray light curves of EX Hya folded with the orbital period and the 67 min period (Córdova et al, 1985).

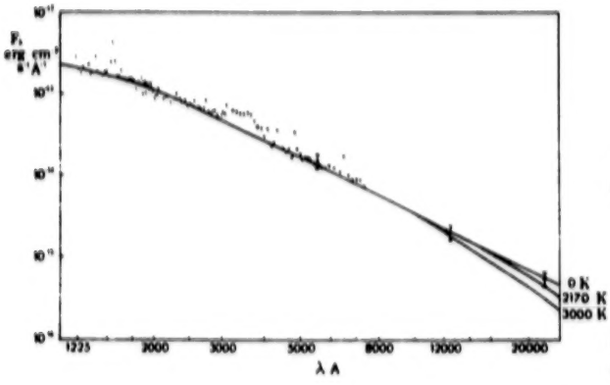
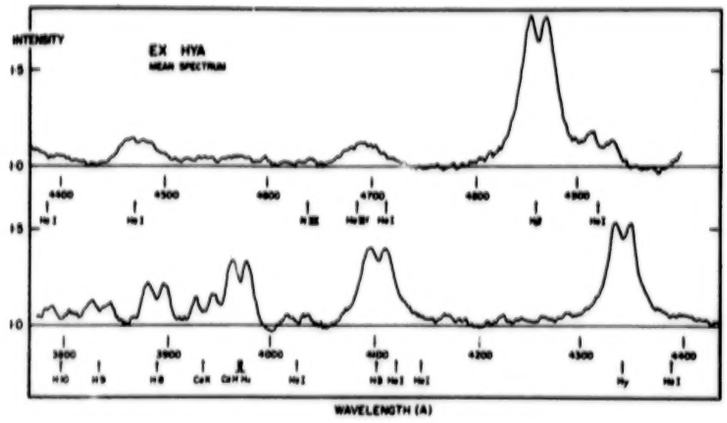


Figure 3-40. General flux distribution of EX Hya (Sherrington et al, 1980).

Figure 3-41. (below) Optical spectrum of EX Hya (Cowley et al, 1981).



period, however, clearly decreases on time-scales of 10^6 years (Jablonski and Busko, 1985).

The most pronounced photometric changes in the light curve occur in connection with the 67 minute period, which appears with a hump-like feature; the brightness at hump minimum stays almost constant, although the amplitude can vary (Vogt et al, 1980). Superimposed is an eclipse phenomenon which recurs with the orbital period of some 98 minutes; furthermore, there is strong flickering and flaring activity throughout the orbital cycle (Figure 3-36; see also Vogt et al, 1980).

The eclipse has a fairly variable depth (Figure 3-37) which turns out to be related to the phase of the eclipse in the 67 min cycle: the bottom of the eclipse always reaches approximately the same brightness level, thus being shallow or almost absent at times of minimum of the 67 min cycle, and deep (up to 0.8 mag) at its maximum. Furthermore, eclipses tend to occur systematically late by up to 35 sec with respect to a mean ephemeris when they occur between phases 0.0 to 0.5 of the 67 min cycle, and systematically early by the same amount of time during the second half of the 67 min period (Jablonski and Busko, 1985).

Color changes during the 67 min hump are opposite to what is observed in dwarf novae during hump maximum: it becomes bluer during hump maximum and redder during minimum. Similar to dwarf novae, the amplitude of the hump is largest ($\sim$0.4 mag) in U and slightly smaller at longer wavelengths. Light changes in the IR do not have any obvious relation to changes in the optical, although there might be a slight dip present at orbital phase zero. No real trace of the 67 min period can be found in the IR (Figure 3-38).

The 67 min optical period is strongly visible in soft X-rays in the range of 0.1 - 2 keV with

a pulsed fraction of some 30%. The orbital period of 98 min is visible too, but with a lower amplitude of only some 15% (Figure 3-39). A narrow dip corresponding to phase and duration of the optical eclipse is apparent, and there is also a broad dip around phase 0.7 which has no correspondence in the optical. The profiles of both light curves are asymmetric. At 1-4 keV the 67 min period is still visible with an amplitude of some 36%, and some 24% in 4-9 keV (Beuermann and Osborne, 1985); the only X-ray flux modulation which can be seen with the orbital period at these high energies is a 30% to 60% deep narrow eclipse at the time of optical minimum and with approximately the duration of the optical eclipse; again, individual eclipses are reported to show pronounced difference, in particular in depth, as a function of their phase in the 67 min cycle as well as the orbital period (Beuermann and Osborne, 1985; 1988). At even higher energies (kT ≈ 8 keV) a constant low level flux can be observed (Heise et al, 1987).

The flux distribution of EX Hya decreases monotonically from 1200 Å to 20000 Å (Figure 3-40); then however, it turns up again. The corresponding temperature between 550 and 750 K responsible for this rise is far too low to be ascribable to the secondary star (Frank et al, 1981b).

While EX Hya can by no means be closely compared with WZ Sge photometrically, both systems are fairly similar spectroscopically. EX Hya shows very strong and extremely broad (~ 7000 km/sec at the base) emission lines of H, He I, He II, and some other species (Figures 3-41). All H lines are double-peaked with a separation of 1000 - 1400 km/sec, He II 4686 Å is single peaked. The line profiles show a pronounced S-wave variation with the orbital period (Gilliland, 1982b). While there is no correlation between the equivalent widths and the orbital cycle, they vary with the 57 min period (Vogt and Breysacher, 1980a, Hellier et al, 1987). The maximum of the equivalent width closely coincides with the maximum continuum flux and the maximum X-ray flux, so the variation is not merely due to variable continuum level. Gilliland (1982b) found that the line profiles vary one half of the 67 min period as well as on the orbital period, while Hellier et al (1987) found no evidence for this from later observations. Hβ shows a pronounced rotational disturbance (Cowley et al, 1981).

IV.C.2. OTHER INTERMEDIATE POLARS

ABSTRACT: Usually more than one photometric period in addition to the orbital period can be detected in the optical. These periods are all on the order of 10 to 20 min and in every object they are remarkably similar to each other. Usually the longer period turns out to be the beat period between the shorter period and the orbital period. In most objects, one of the short periods is visible in X-rays. The spectra do not look any different from those of other nova-like stars.

other nova-like stars: 96, 102, 114, 117, 119, 125, 140

dwarf novae: 35, 46, 65

interpretation: 190

The pulsation periods of the remaining DQ Herculis stars are short enough to merely appear as photometric disturbations of the orbital light curves. None of those known so far possesses an eclipse, but all do show a hump to some extent. The recurrence times of the hump correspond to the spectroscopic periods. The short-term variability is visible in all optical wavelengths of all objects. The pulsations are monochromatic, although there might be some power in the first harmonics (e.g., Patterson and Steiner, 1983; Agrawal et al, 1984). The two pulsation periods of AO Psc occur with appreciably different power at different optical energies: at shorter wavelengths the shorter period is stronger than at longer wavelengths (Figure 3-42). When photometric observations of AO Psc are folded with all three photometric periods, i.e., 805 sec, 859 sec, and the orbital period of 3h 35.5 m, it becomes apparent that the spectral distribution of the shorter pulsational variations has about the

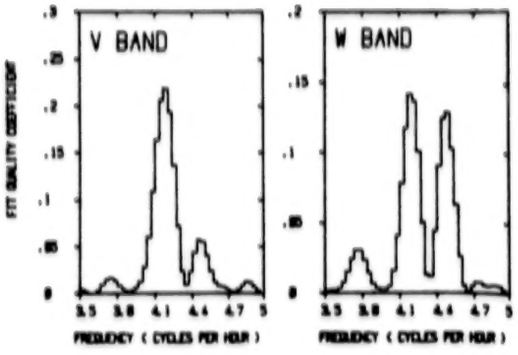


Figure 3-42. Power spectra of AO Psc in Walraven W and V bands (Motch and Pakull, 1981).

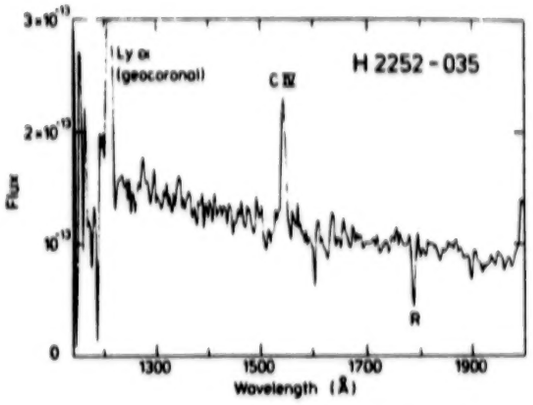


Figure 3-43. UV spectrum of AO Psc (Hassall et al, 1981).

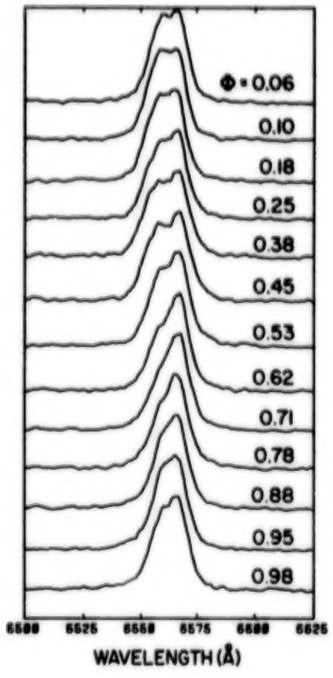


Figure 3-44. Phase-resolved optical spectroscopy of FO Aqr (Shafter and Targan, 1982).

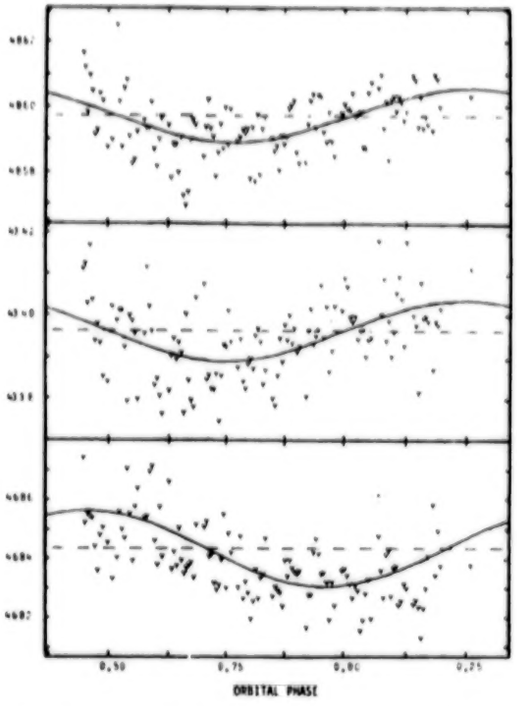


Figure 3-45. V1223 Sgr: radial velocity curves of Hβ, Hγ, He II (from top to bottom) plotted against the orbital phase (Penning, 1985).

same flux distribution as the orbital variation, while that of the longer pulsational period is different (van der Woerd et al, 1984).

In almost all of the systems, two photometric periods of comparable length have been detected besides the photometric period, and usually the longer of those two turns out to be equal to the beat period of the shorter pulsation period and the orbital period. In AO Psc, the two are in phase just after minimum of the orbital light variation and out of phase by 180% at maximum orbital light (Motch and Pakull, 1981); in V1223 Sgr the situation is just the opposite (Warner and Cropper, 1984). Also in AO Psc there are some indications that the 805 sec period is rather a transient phenomenon, which seems to be absent at

times, whereas the 859 sec period is always present (van der Woerd et al, 1984). In V1223 Sgr the 745 sec period is detectable at IR wavelengths, not so the 746 sec variation (Watts et al, 1985). In V1223 Sgr and FO Aqr a secular decrease of the short photometric periods was detected with $\dot{P}$ on the order of several times 10^{-11} years (van Amerongen et al 1987a; Jablonski and Steiner, 1987; Shafter and Macry, 1987).

While usually the spectroscopic and one of the photometric periods are identical, in TV Col there is no photometric period equal to the orbital period of the system (Hutchings et al, 1981). In this respect it is similar to the anti-dwarf nova TT Ari and, possibly, to the dwarf nova CN Ori (see Chapters 2.II.B.3, 3.III.A.2).

In TV Col, FO Aqr, AO Psc, and V1223 Sgr, a pulsation period has been detected in hard X-rays. In V1223 Sgr this is a period which is not seen in the optical: the optical shows pulsations of 14.61 and 13.24 min, in the X-rays only a period of 12.4 min can be seen (Osborne et al, 1985). In the other three systems the X-ray pulsation period is equal to the shorter of the optical pulsation periods (e.g., Lamb, 1983; Cook et al, 1984; Schrijver et al, 1985). The X-ray pulsation and the respective optical one are in phase in all systems within the limits of observations. Amplitudes of the X-ray pulsation vary between some 20% and some 90%. In none of the systems has an appreciable flux been found in soft X-rays.

The optical and UV spectra of the intermediate polars do not look any different from "normal" spectra of cataclysmic variables, with all lines in emission, and a normal continuous flux distribution (e.g., Hutchings et al, 1981; Hassall et al, 1981; Kitamura et al, 1983; Warner, 1983; Mateo and Szkody, 1985; Watts et al, 1985). The UV spectrum of AO Psc is remarkable only in that there are no strong lines besides C IV (Figure 3-43). On one occasion when TV Col showed a brief outburst in both optical and UV, C IV and Si IV developed P Cygni profiles (Szkody and Mateo, 1984). In all systems, there are line profile changes in phase with the orbital revolution. FO Aqr shows line profile variations in Hα which are reminiscent of an S-wave, but they are restricted to only the blue wing of the line (Figure 3-44). The line flux in AO Psc is reported to be variable also on the 859 sec period (Motch and Pakull, 1981).

Radial velocities in BG CMi and V1223 Sgr show different phasings within the orbital period for the H, and He II lines, respectively (Figure 3-45); indications for this to be the case are also given in AO Psc and FO Aqr (Hutchings et al, 1981; Penning, 1985). The line fluxes in FO Aqr vary with the orbital period, while there is indication for the line profiles to vary on the 21 min pulsation period (Shafter and Targan, 1982). The C IV 1550 Å line flux in TV Col varies with the orbital phase (Mateo and Szkody, 1985).

GENERAL INTERPRETATION: The white dwarf in DQ Herculis stars is believed to possess an appreciable magnetic field. It is not strong enough, however, to keep the star in synchronism with the orbital revolution. The star accrets preferentially onto its magnetic poles which then become X-ray radiators. As they sweep around due to the white dwarf's rotation they produce a hot area on the inner side of the accretion disc and/or on the surface of the secondary star, which photometrically are seen as further periodicities in the light curves.

OBSERVATIONAL CONSTRAINTS TO MODELS:

- *Possible additional photometric periods seem to be constrained to values either about one or about two orders of magnitude smaller than the orbital period.*
- *EX Hya is an exception to this.*
- *The shorter photometric period, which is not the orbital period, has been seen to decrease secularly in some objects.*
- *Two or possibly three, systems are known in which none of the photometric periods is identical to the spectroscopic period.*

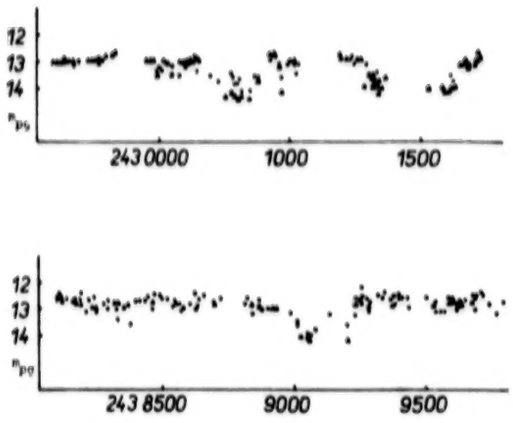


Figure 3-46. Long-term variations of AM Her (Hudec and Meinunger, 1976).

V. AM HERCULIS STARS

AM Herculis stars (polars) are distinguished from other cataclysmic variables by exhibiting very strong optical polarization (up to 30% or more has been observed) which is variable in strength with the same period as the flux at all observable wavelengths, as the radial velocity, and as the line intensities.

V.A. PHOTOMETRIC APPEARANCE

V.A.1. LONG-TERM VARIATIONS

ABSTRACT: The long-term variability is very similar to that of anti-dwarf novae in showing mostly high (in the case of AM Herculis stars they often are called "on") and low (called "off") states.

other nova-like stars: *96, 102, 114, 117, 119, 122, 140*

dwarf novae: *35, 46, 65*

interpretation: *188*

The long-term variability of AM Herculis stars is similar to that of DQ Herculis stars or anti-dwarf novae: most of the time they can be found close to some "high" (or "on") brightness level; at irregular intervals of time, typically on the order of months or years, the brightness drops by about 2 to 3 mag to the "low" (or "off") state, where it will stay for typically a hundred to a few hundred days, possibly exhibiting some brightness variation as well before returning to the bright state (Figure 3-46). In addition VV Pup was once observed at a high state that was even brighter by some 0.3 mag than the normal high state; and AN UMa and DP Leo were found in unusually low states, which in the case of AN UMa was some 2 mag fainter than the normal low. DP Leo, which is extremely faint in any case, became almost undetectable below some 20 mag (Liebert et al, 1982a; Biermann et al, 1985). Furthermore, VV Pup did not brighten above 15 mag since 1960, although the "normal" bright state until then had been around 14.4 mag (Liebert et al, 1978). The transition between high and low states is not abrupt like in dwarf novae, but is instead very gradual, taking at least a few tens of days. No periodicity in this movement between states could be detected in any AM Herculis star. Dexter et al, (1976) claim to have found a tendency for drops in brightness in AM Her to occur about every 670 days; however, investigations by means of periodogram analysis carried out by Feigelson et al, (1978) and based on observations from 1890 to 1976 did not reveal any significant periodicity in the range between 2 and 10^4 days.

V.A.2 PHOTOMETRIC CHANGES IN THE HIGH AND LOW STATES

ABSTRACT: Orbital variations are very dissimilar to those observed in other cataclysmic variables, consisting mostly of continuous variation, with no clear

distinction between hump and interhump phases possible. The appearance of the light curve is highly color dependent. So far only one object is known to show a brief total eclipse, the shape of which again is atypical for a cataclysmic variable. Flickering and flaring are very pronounced. Quasi-periodic oscillations occur. — During off states the appearance of an object can vary strongly from one night to the next. The strong X-ray radiation varies synchronously with the optical light.

other nova-like stars: 96, 102, 114, 117, 119, 122, 140

dwarf novae: 35, 46, 65

interpretation: 188

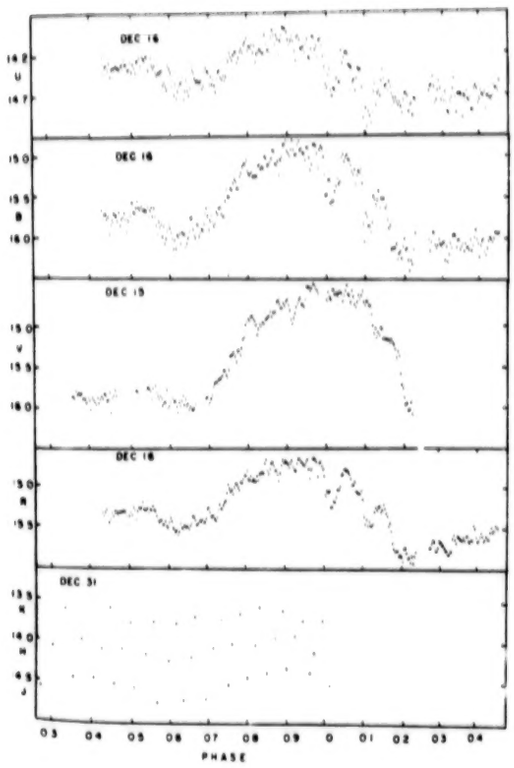
The stable photometric periods of AM Herculis stars — which turn out to be the orbital periods of the systems — are typically on the order of one to two hours, although the periods of some AM Herculis stars (AM Her, H0538 + 608, QQ Vul) lie above the period gap of cataclysmic variables. The light curves, although they are quite different from one object to another, are mostly very dissimilar from those of other cataclysmic variables: a distinction between hump and interhump phase is hardly possible, since the light keeps changing all the time; between one and three minima (or maxima) per cycle can be distinguished in different objects; and, also much unlike in other objects, the shape of the light curves is highly dependent on the wavelength. Typical optical and IR light curves of an AM Herculis system, VV Pup, are given in Figure 3-47a (more examples can be found in Gilmozzi et al, 1978; Raymond et al, 1978; Szkody and Capps, 1980; Frank et al, 1981a; Miller, 1982), and a schematic set of curves of EF Eri is given in Figure 3-47b. As for instance in the examples of Figure 3-47, the phases of the minima of the light curves in some objects are strongly dependent on wavelength, which indicates that these are probably not eclipses as observed in many other nova-like stars and dwarf novae; in others, like MR Ser or QQ Vul, they all occur at roughly the same phase at all energies. In BL Hyi the brightness variability in U seems to be anticorrelated to that in V (Thorstensen et al, 1983).

Corresponding to the wavelength dependence of the light curves, and again much unlike other cataclysmic variables in which the optical colors hardly vary outside the times of eclipse, the color curves are highly variable with phase, and reasonably well-defined loops in the color-color diagram are performed. All systems seem to become redder consistently during the brighter orbital phases, which merely is a reflection of the amplitude increase with increasing wavelength.

The exact shapes of the light curves of all these objects are variable from one cycle to the next and even more so on time-scales of months or years (only referring to the "normal" high state so far); an example is shown in Figure 3-48 (see also Cropper et al, 1986). Mostly the shape and amplitude of the maxima is affected, while the minimum light level is much less variable. Phase shifts of the minimum in U light by 0.3 in phase have been reported for AM Her (Szkody, 1978; Visvanathan and Wickramasinghe, 1979).

The amplitudes of the brightness changes with orbital phase in all AM Herculis stars are smallest in U and increase considerably toward longer wavelengths, and the variability in U is often only poorly correlated with the more synchronized behavior at lower energies and is the most sinusoidally shaped (Figure 3-47). At very low energies the light variation again becomes largely independent of that in the optical and near IR: The K-light curves (2.2 μ) in VV Pup and EF Eri are again almost sine-like. One exception to this is the system QQ Vul, in which the light curves are very similar in shape and amplitude in all wavelengths from U to I (Figure 3-49), with the exception of the variations around the minimum at about phase 0.4 which become increasingly ill-defined at longer wavelengths.

The only AM Herculis star which really is an eclipsing variable is DP Leo (Figure 3-50): for about 4 minutes around phase 0.71 the flux in the optical as well as the X-rays drops to zero.



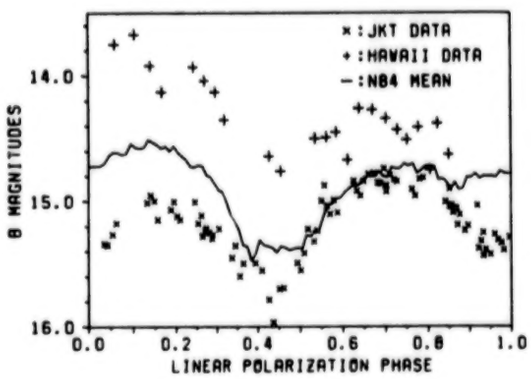


Figure 3-48. Variability of the optical appearance of QQ Vul on long time-scales (Mukai et al, 1986).

Unlike eclipses known in other cataclysmic variables, this one is very symmetric, ingress and egress both last for equally long times (somewhat less than 40 seconds), and there is no preceding hump, nor is there any detectable hold during ingress or egress, as always occurs for total eclipses in other cataclysmic variables. The optical light and the polarization are strictly locked to each other in phase.

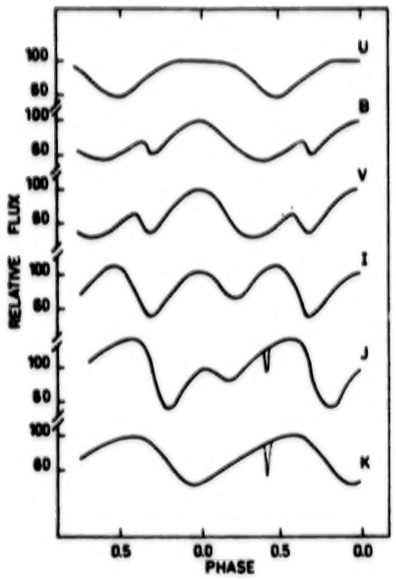


Figure 3-47b. (above) Schematic optical light curve of EF Eri in different colors (Motch et al, 1982).

Figure 3-47a. (left) Optical light curve of VV Pup in U, B, V, R, K, H, and J light (top and bottom) (Szkody et al, 1983).

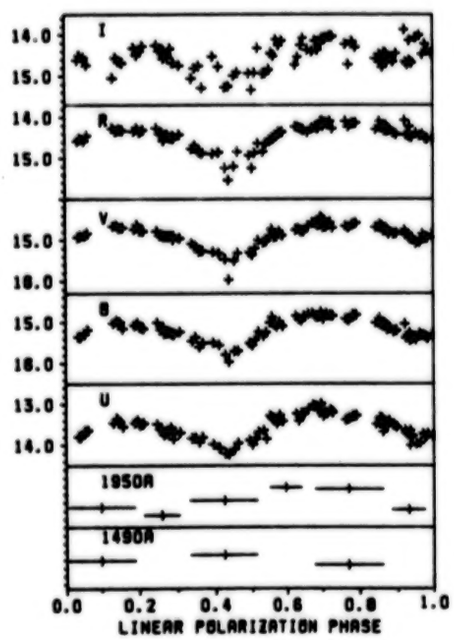


Figure 3-49. Optical light curve of QQ Vul in various colors (Mukai et al, 1986).

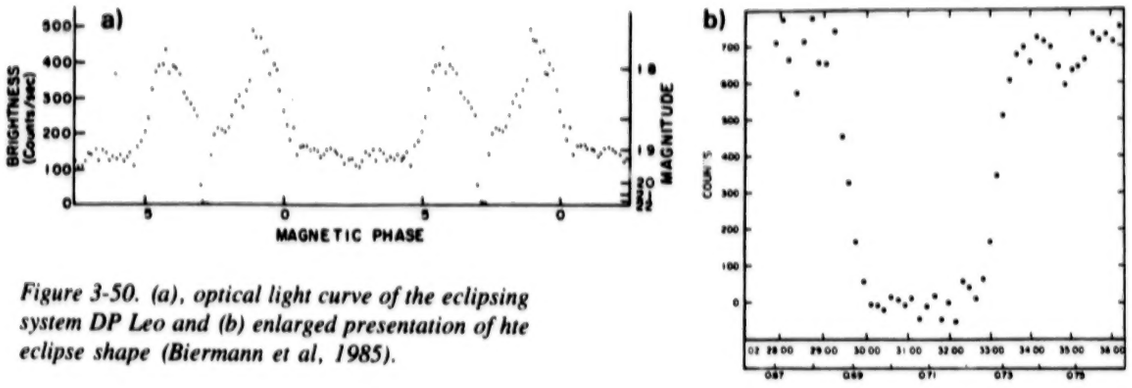


Figure 3-50. (a), optical light curve of the eclipsing system DP Leo and (b) enlarged presentation of hte eclipse shape (Biermann et al, 1985).

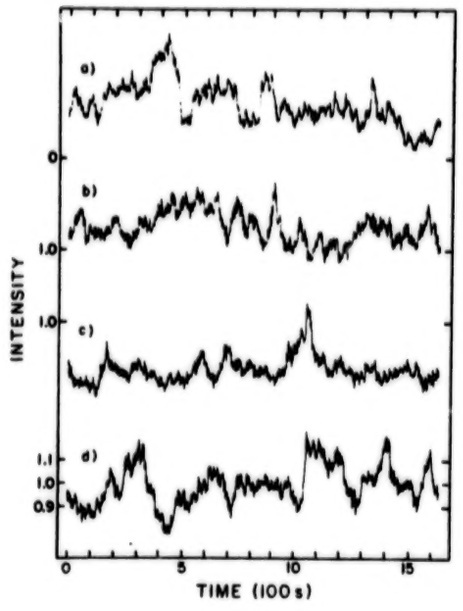


Figure 3-51. Optical flaring activity in AM Her (Panek, 1980).

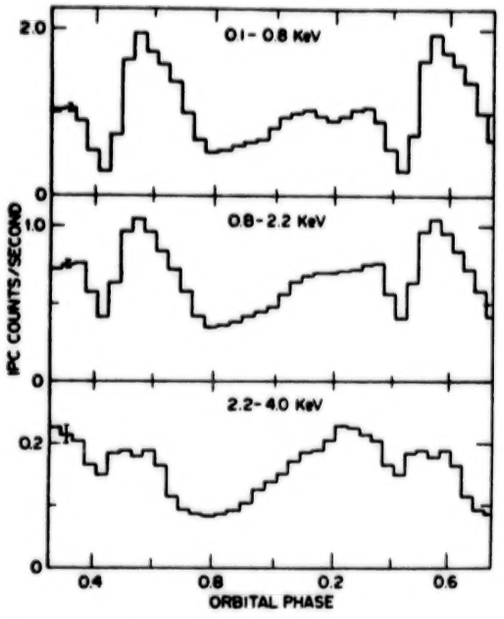


Figure 3-52. X-ray light curves of EF Eri in different energy bands (Patterson et al, 1981a).

In addition to orbital variations, flickering activity is observed in all systems. It is present with equal strength at all orbital phases. Similar to other cataclysmic variables, amplitudes range from just 0.1 to 0.3 mag in AM Her to 0.8 to 1.0 mag in VV Pup, and time-scales are on the order of a couple of minutes. In AM Her the flickering at different optical and infrared wavelengths has been found to be correlated: the main peaks seem to occur simultaneously at all wavelengths with U slightly leading the lower energies (Bailey et al, 1977; Olson, 1977; Szkody and Margon, 1980).

Another sort of irregular activity in AM Herculis stars is the so-called "flaring," which occasionally can also be observed in some other cataclysmic variables, but then with a higher amplitude (e.g., SS Cyg and RW Tri, chapters 2.II.D.1, 3.II.A.2). This term refers to rapid irregular brightness increases by some tenths of a magnitude every couple of hundred seconds, lasting for about one minute (Figure 3-51). It seems to occur simultaneously at all wavelengths. The amplitude increases toward longer wavelengths. No periodic behavior in this phenomenon could be detected over longer

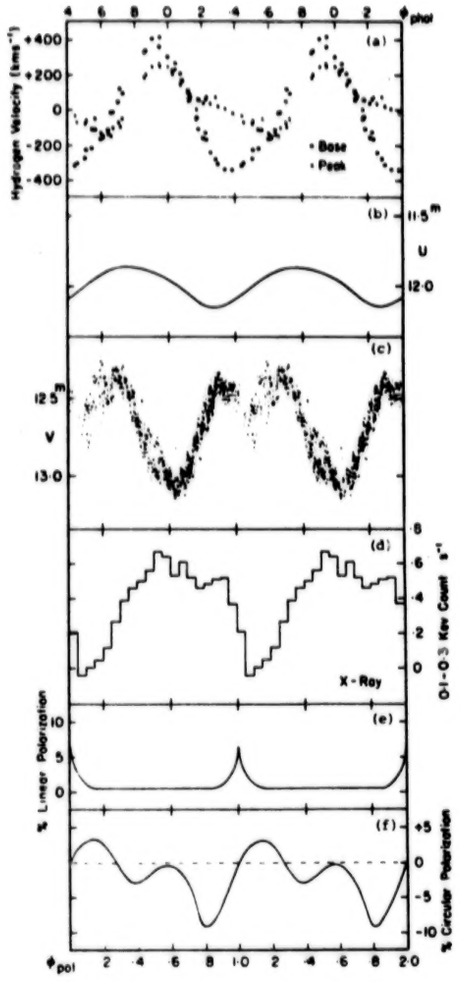


Figure 3-53. Phase relations between photometric and polarimetric variations of AM Her (Crampton and Cowley, 1977).

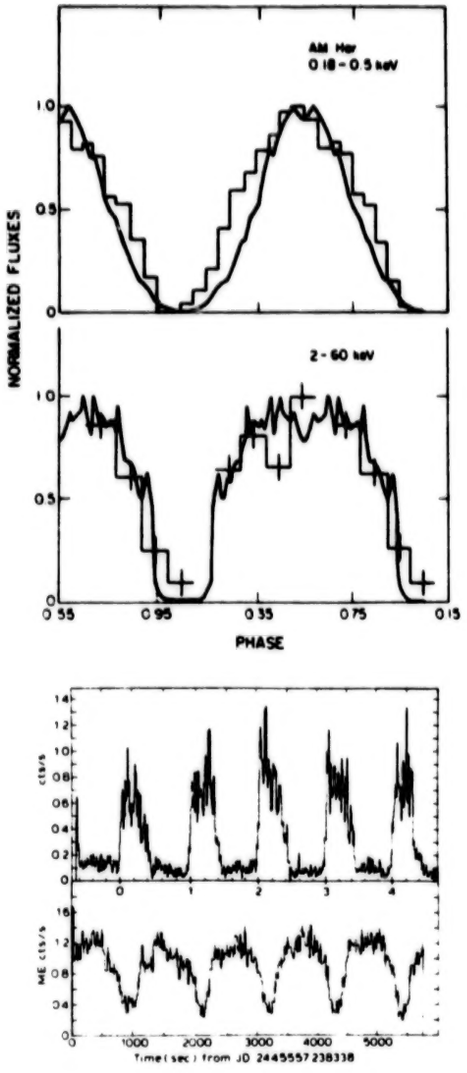


Figure 3-54. X-ray light curves of AM Her in (a) normal high and (b) reversed high modes (a: Imamura, 1984; b: Heise et al, 1985).

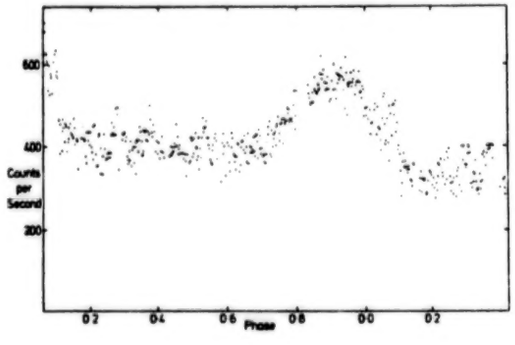


Figure 3-55. Optical light curve of VV Pup in the low state (Bailey, 1978).

time-scales. The distinction between flickering and flaring is one of amplitude and frequency. In one object the distinct flares have somewhat higher amplitudes than the flickering which is always present; their amplitude may, however, well be of the same order as the flickering in some other object.

Periodic variabilities on time-scales of seconds, which are very strong and common in many dwarf novae, occur only rarely in AM Herculis stars. Quasi-periodic oscillations in the range of 1.25 to 2.5 sec once were found in

V834 Cen, in AN UMa, and in EF Eri with powers of a few percent, respectively; whereas no trace of this could be detected in AM Her (Middleditch, 1982; Larsson, 1987; Cropper et al, 1986). Other observations of AM Her revealed the simultaneous presence of many, though not very strong, monochromatic spikes in the power spectra with periods between 62 and 450 sec, reminiscent of the coherent oscillations in dwarf novae; these did not repeat from night to night (Berg and Duthie, 1977). Szkody (1978) reports oscillations of 197 sec and 512 sec to have been present during four consecutive nights, while an oscillation of 426 sec only could be found around phase 0.3; in addition, she also found many highly transient monochromatic spikes in the power spectra for periods between 27 and 1280 sec. On different occasions, a quasi-periodic oscillation near 6 minutes was found in EF Eri which was also seen in X-rays and circular polarization (Williams and Hiltner, 1980; Crampton et al, 1981; Patterson et al, 1981a; Williams and Hiltner, 1982). At other times, however, no oscillation whatsoever could be seen, or oscillations appeared with very different periods, similar to what occasionally is observed in AM Her. Furthermore, different oscillations were seen in different wavebands (Bond et al, 1979; Motch et al, 1982).

All AM Herculis stars are strong, and variable sources of both hard and soft X-rays. The variability at all X-ray energies is strictly synchronous with the variability in the UV, optical, and IR, as well as with spectrum and polarization changes. The shape of the light curve varies with the energy band, as in the optical (Figure 3-52). Except for relatively minor changes, the shape of the light curve at any energy seems to be rather stable for a longer time; in particular, the phase relation between individual features in the optical light curves and the X-ray light curves remains constant over many years (Swank et al, 1977). The X-ray light curves of different objects are remarkably dissimilar, often resembling the respective optical light curves.

As an example, the phase relations between different, periodically variable properties of AM Her are shown in Figure 3-53; similar relations exist in all other AM Herculis stars as well. In the particular case of AM Her, the X-ray eclipse, which is total, almost coincides with the partial optical secondary eclipse, whereas no X-ray minimum occurs at the time of the optical primary minimum. Similarly, it can be seen that at the time of the X-ray eclipse there is a hold in circular polarization and ingress which coincides with the strong pulse in linear polarization (see also below). In the eclipsing system DP Leo, the X-rays are eclipsed at exactly the same time as the optical flux. In DP Leo, ST LMi, and VV Pup, the X-ray flux is zero for almost half of the orbital period, exhibiting just one hump for the rest of the time (Patterson et al, 1984; Beuermann and Stella, 1985; Biermann et al, 1985). A dip in the X-ray flux occurs in VV Pup around phase 0.94, at the same time when a small dip is also seen in the optical. In EF Eri, a narrow eclipse feature can be seen in J and K around phase 0.42, which is not present at optical wavelengths (Figure 3.47b); during this same phase, as will be shown later, the emission lines longward of 5500 Å all go into absorption; and at X-rays, centered at around phase 0.43, a narrow eclipse feature can be seen which is total for energies between 0.1 and 0.8 keV, and not visible at all for energies above 3 keV (Patterson et al, 1981a).

Some flickering does occur at X-rays as well. In most cases there seems to be no correlation, however, with times and amplitudes of flickering in the optical. In EF Eri, however, it was found that the correlation between flickering in hard X-rays and the optical is very strong, while it is much weaker between soft X-rays and the optical (Crosa et al, 1981; Crampton et al, 1981; Patterson et al, 1981a; Singh et al, 1984; Beuermann and Stella, 1985; Watson et al, 1987).

Two very unusual events have been reported for the X-rays of AM Her. In 1976 the optical

secondary minimum had disappeared. The X-ray flux was variable by about a factor of 2, but any pattern occurred at random and at other times strict periodicity was lost; optical and hard X-ray flux were at their average high level, whereas the soft X-ray flux had decreased by a factor of 3 (Priedhorski, 1986).

In 1983 and 1984, on different occasions, the system was observed to display a previously unknown kind of X-ray light curve, shown in Figure 3-54: The hard X-rays reached a minimum periodically at the same orbital phase as was seen in previous observations for energies above 1 keV, and the shape of this light curve also remained roughly the same. However, in former observations of the soft X-rays the flux variation had been almost sinusoidal with the minimum coinciding with that observed in hard X-rays, in this so-called "reversed mode" it showed very distinct high and low levels, each lasting for about half a period, with very short transition times of only 2 to 3 minutes. The center of the highly variable high phase was seen to coincide with the minimum of the hard X-ray flux. Rise to the high level occurred at phase 0.95, i.e., before maximum of the linear polarization pulse (see below).

Between different events of the reversed mode the system briefly returned to the normal mode (still at high level of the optical flux) and then to optically low level. During both the reversed and the normal high mode, optical photometric observations were carried out which in no way appeared peculiar when compared with each other or former observations (Mazeh et al, 1986).

Osborne et al (1987) report remarkably similar dramatic changes to have occurred in the systems QQ Vul in 1985. Here the relative fluxes in X-rays, UV, and optical changed appreciably, together with the shape of all the light curves: the x-ray light curve in 1985 looked strikingly similar to that of AM Her in reversed mode.

During the rare faint states the optical light curves of AM Herculis stars become very irregular or smoothed out while the IR is much less affected (Figure 3-55; see also e.g., Szkody, 1978; Allen et al, 1982; Szkody et al, 1982b; Tuohy et al, 1985). The minima and maxima which are easily seen during high state practically disappear in the optical, in particular since the flickering usually remains strong. In BL Hyi, narrow minima appear around phase zero, which, however, are not separated by one orbital period and thus have no geometric origin (Tuohy et al, 1985). In VV Pup in low state, no significant hump in the light curve could be seen during observations of one night, whereas it was clearly present on the following night (Bailey, 1978). Similar behavior has been reported for other AM Herculis stars (e.g., Szkody et al, 1983).

During the optically low state the flux in both hard and soft X-rays drops as well. The synchronous variations of the X-rays with the optical variations remains. In AM Her, the eclipse in soft X-rays is reported to disappear (Priedhorski and Marshall, 1982); otherwise, no dramatic changes are reported for any other object other than a decrease in flux level (this may be due to lack of data since, even for otherwise bright objects, the x-ray flux is too low to be measured accurately during the low state).

V.B. POLARIZATION

ABSTRACT: The systems exhibit up to 30% circularly and linearly polarized radiation. Strong variations in the degree of polarization occur synchronously with spectroscopic and photometric variations.

other nova-like stars: 98, 106, 113

dwarf novae: 64

interpretation: 188

AM Herculis stars emit very strong and strictly periodically variable circularly and linearly polarized radiation, very much unlike

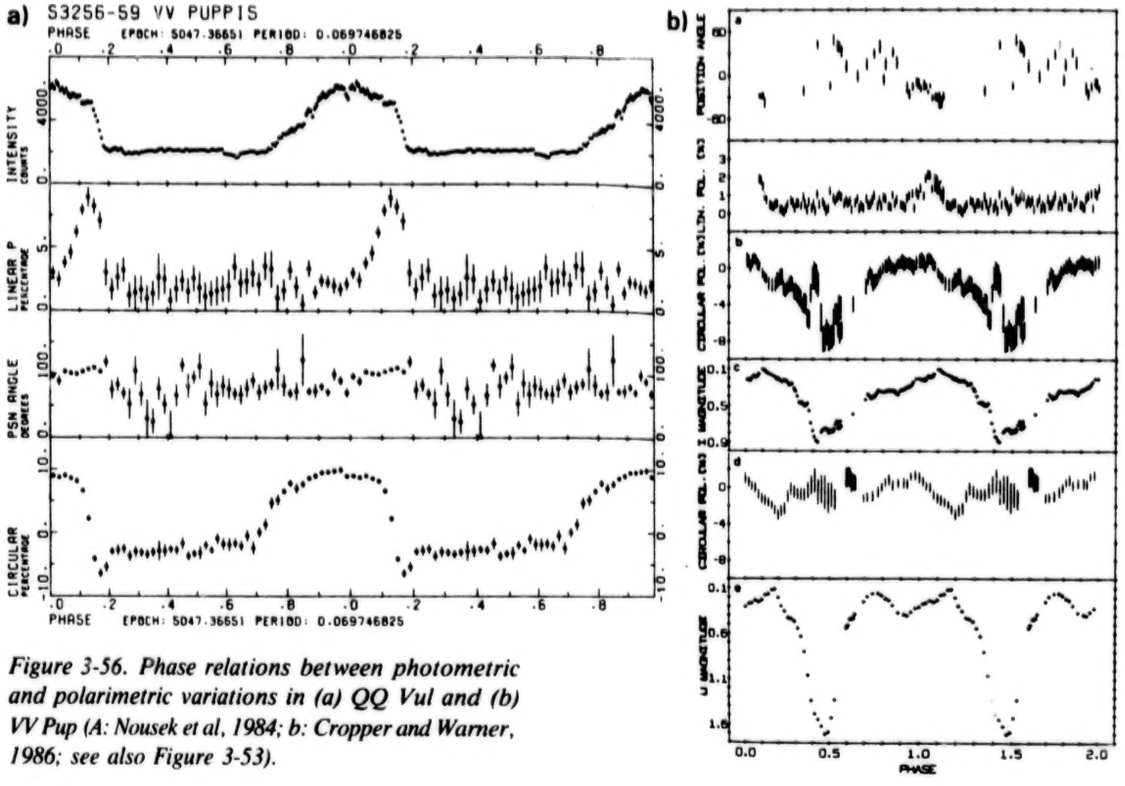


Figure 3-56. Phase relations between photometric and polarimetric variations in (a) QQ Vul and (b) VV Pup (A: Nousek et al, 1984; b: Cropper and Warner, 1986; see also Figure 3-53).

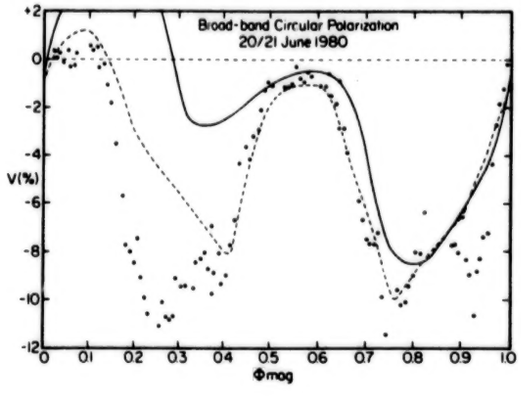


Figure 3-57. Circular polarization of AM Her in the low state (filled circles), and the high state (dashed line: Bailey and Axon, 1981; solid line: Young and Schneider, 1979) (Latham et al, 1981).

other nova-like stars or dwarf novae for which the level of polarized flux is typically on the order of 0.3% if detected at all. The variability follows the same periodicity as any other orbital variabilities in AM Herculis stars, wherein the polarization curve usually exhibits a fairly intricate but stable pattern. Examples of polarization curves and their phase relations to other variable properties are shown in Figure 3-56 (other examples can be found in, for instance, Allen et al, 1981; Liebert et al, 1982b; Biermann et al, 1985; Cropper, 1986). The circular polarization typically varies with an amplitude of up to 10 - 30% of the flux, the linear polarization by about half this value. With the exception of ST LMi, which exhibits two spikes in linear polarization, usually only one sharp spike in linear polarization is observed per orbital cycle in AM Herculis stars. By convention, normally the maximum of this for all orbital variability is defined as phase zero.

The linear polarization pulse lasts for about one to two tenths of the orbital cycle, depending on the object. Between two consecutive

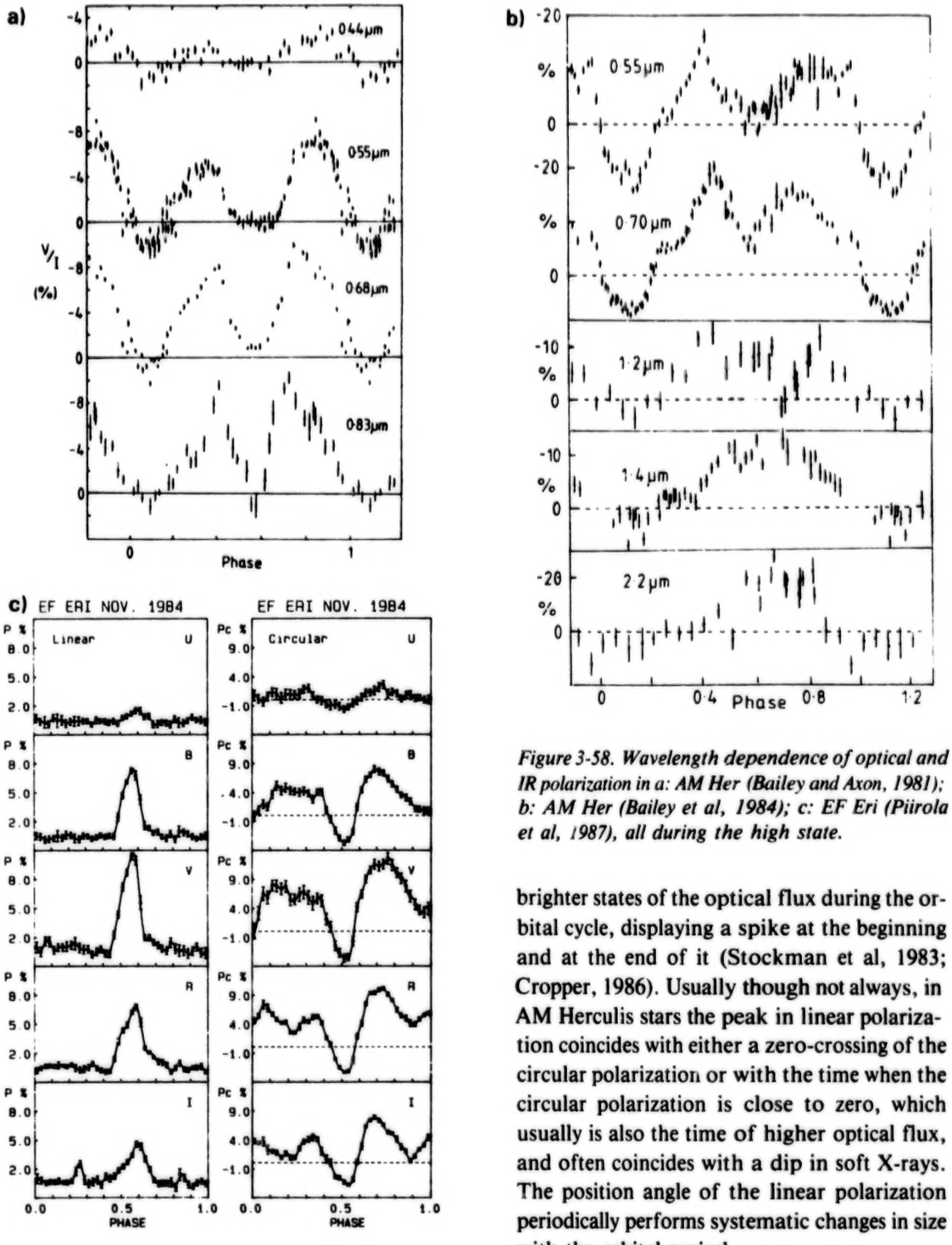


Figure 3-58. Wavelength dependence of optical and IR polarization in a: AM Her (Bailey and Axon, 1981); b: AM Her (Bailey et al, 1984); c: EF Eri (Piirola et al, 1987), all during the high state.

pulses the linear polarization usually is zero or close to this. In EF Eri, Allen et al (1981) report an occasionally present secondary peak in linear polarization around phase 0.4. In ST LMi, the linear polarization is strong throughout the brighter states of the optical flux during the orbital cycle, displaying a spike at the beginning and at the end of it (Stockman et al, 1983; Cropper, 1986). Usually though not always, in AM Herculis stars the peak in linear polarization coincides with either a zero-crossing of the circular polarization or with the time when the circular polarization is close to zero, which usually is also the time of higher optical flux, and often coincides with a dip in soft X-rays. The position angle of the linear polarization periodically performs systematic changes in size with the orbital period.

The shape of the circular polarization curve usually is fairly complex, exhibiting several relative minima and maxima during one cycle. For most objects it is either mostly or entirely

either negative or positive, showing polarization of the other sign for only a short time and with a distinctly lesser degree of polarization. Though its shape is characteristic for each object, it is variable over longer time-scales, in particular when dropping to low optical flux, as has been shown in the case of AM Her by Latham et al (1981) and (Figure 3-57). The linear pulse is also subject to changes in amplitude on longer time-scales.

Like the optical flux, both the linear and circular polarization are strongly color dependent (Figure 3-58; see also Figure 3-56, Krzeminski and Serkovski, 1977; Bailey et al, 1982; Szkody, 1985; Piirola et al, 1987). The variability usually is small in U, increasing in amplitude toward longer wavelengths up to 6000 to 8000 Å (depending on the object), then slowly decreasing again, but it still is readily measurable at 20000 Å. In the course of years the shape of the polarization curve changes significantly, like the light curve (e.g., Figure 3-57; Cropper et al, 1986, Remillard et al, 1986).

V.C. SPECTROSCOPIC OBSERVATIONS IN THE HIGH AND LOW STATES

ABSTRACT: The general appearance of AM Herculis stars is not very different from that of other cataclysmic variables. Almost pure emission line spectra are observed. The hydrogen lines mostly consist of a broad base and a narrow peak component which vary independently of each other. The narrow component still can be seen during the low state. Also during low state absorption features become visible which are identified with Zeeman lines. The absorption spectrum of a cool companion is seen in some objects. Radial velocity variations (in high and low states) are synchronous with photometric and polarimetric variations.

other nova-like stars: 99, 107, 116, 119, 122, 124, 141

dwarf novae: 65

interpretation: 151, 192

The overall flux distributions of three typical AM Herculis stars are shown in Figure 3-59. Statistically the flux distribution is not dramatically different from that of other cataclysmic variables. Clearly no fit of the entire spectrum with one black body or a power law is possible, even when restricted to only optical and UV wavelengths; several different components contribute to the observable flux. With regard to the transition from high to low state, the effect is different in different objects: in VV Pup for instance, strong changes occur in the optical, while changes are rather small at IR wavelengths; in ST LMi on the other hand, changes are most appreciable in the IR, while they are a lot smaller in the optical.

A positive detection at radio energies has so far only been possible for AM Her, although several other AM Herculis stars have been looked at (Dulk et al, 1983). AM Her was detected at 4.9 GHz with no obvious flux variation correlated with the orbital phase being present (Chanmugam and Dulk, 1982; Bastian et al, 1985). At no time could AM Her be detected at either 1.4 or 16 GHz, not even during the 4.9 GHz outburst.

The X-ray spectrum of AM Her obviously consists of two components: a strong soft component with maximum flux around 0.2 keV, and a much weaker hard component which fades toward higher energies and becomes undetectable below 100 keV (Figure 3-60). Similar tendencies, though not measured that accurately, are seen in other AM Herculis stars. In AM Her and EF Eri, an emission feature at 6.5 ± 1.5 keV is easily visible. Both spectra were observed during optical high state.

Optical and UV spectra of AM Herculis stars are shown in Figure 3-61. In the optical as well as in the UV, the spectra are characterized by either a flat continuum or one which rises toward the IR. Superimposed are very strong emission lines of the usually visible resonance lines, of H, He I, and He II, as well as of C II, C III, C IV, Si IV, N III, N V, Fe II, etc.; i.e., the average ionization potential is somewhat higher than for other nova-like stars or dwarf novae. In particular it is noteworthy

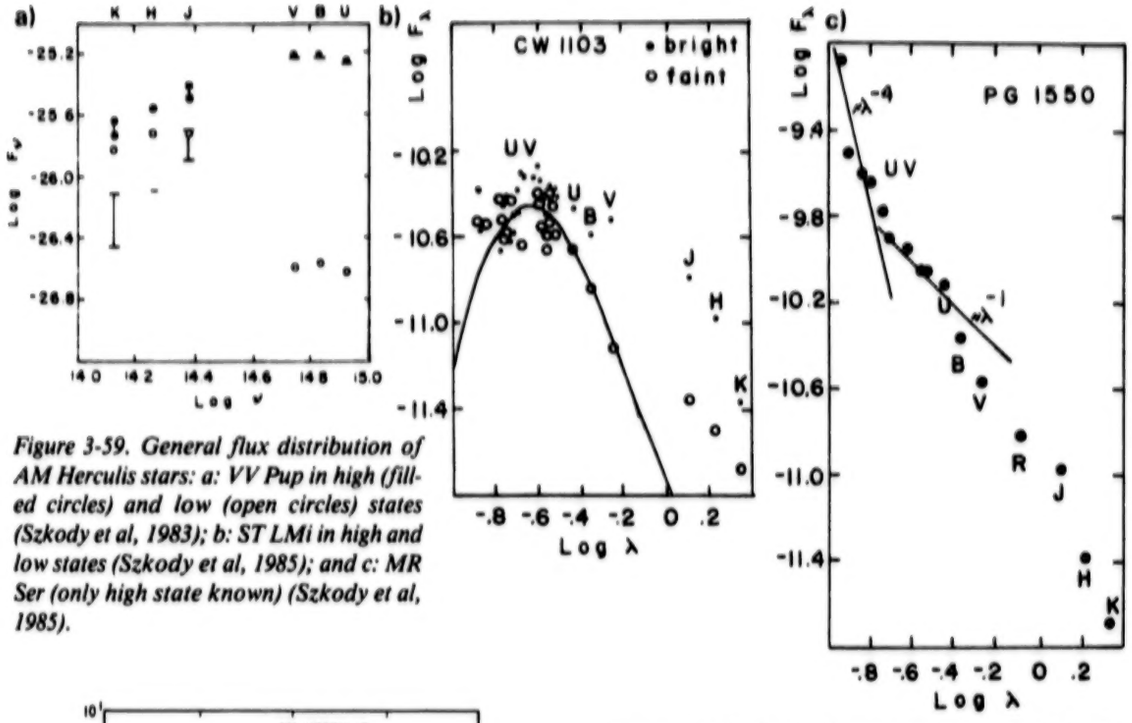


Figure 3-59. General flux distribution of AM Herculis stars: a: VV Pup in high (filled circles) and low (open circles) states (Szkody et al, 1983); b: ST LMi in high and low states (Szkody et al, 1985); and c: MR Ser (only high state known) (Szkody et al, 1985).

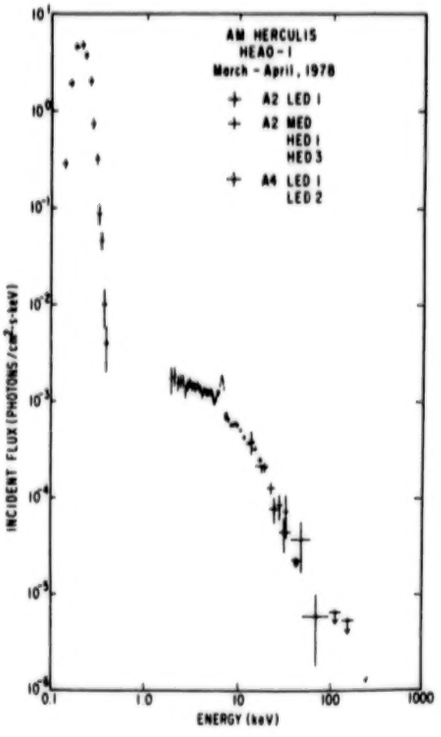


Figure 3-60. (left) X-ray spectrum of AM Her (Rothschild et al, 1981).

that the Balmer decrement for Hα and Hβ usually is either very flat or even reversed, and the flux in He II 4686 Å is often on the order of, or even larger than, that in Hβ. No forbidden lines are detectable. The UV spectrum of H0538+608 was found to have changed significantly within one year (Bonnet-Bidaud and Mouchet, 1987).

When traced over a full orbital cycle, the spectra show marked variability synchronous with the orbital period (Figure 3-62). The line flux is strong for about half the orbital period, centered at the time of the linear polarization pulse, and then it drops considerably, often very quickly, around phase 0.4 for some time, although ratios of line intensities hardly seem to be affected; recovering toward higher intensities takes longer than the drop (Figure 3-63). In EF Eri, lines longward of 5500 Å (including Hα) even go into absorption for a while around phase 0.45 (Biermann et al, 1985). In many objects these changes are accompanied by changes in the continuum flux (e.g., Visvanathan and Wickramasinghe, 1981), as is also reflected in the photometric light curves. No pronounced intensity changes are observed for faint lines. Temporal changes in the behavior of the line fluxes have been observed on occasions (e.g., Bailey and Ward, 1981; Visvanathan and

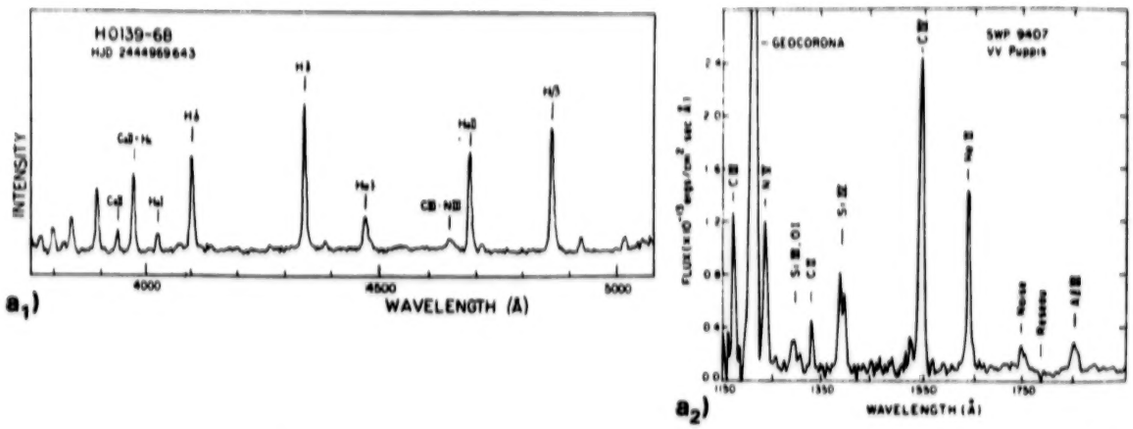


Figure 3-61. (a) Optical (Thorstensen et al, 1983) and (b) UV spectra of AM Her stars (Patterson et al, 1984).

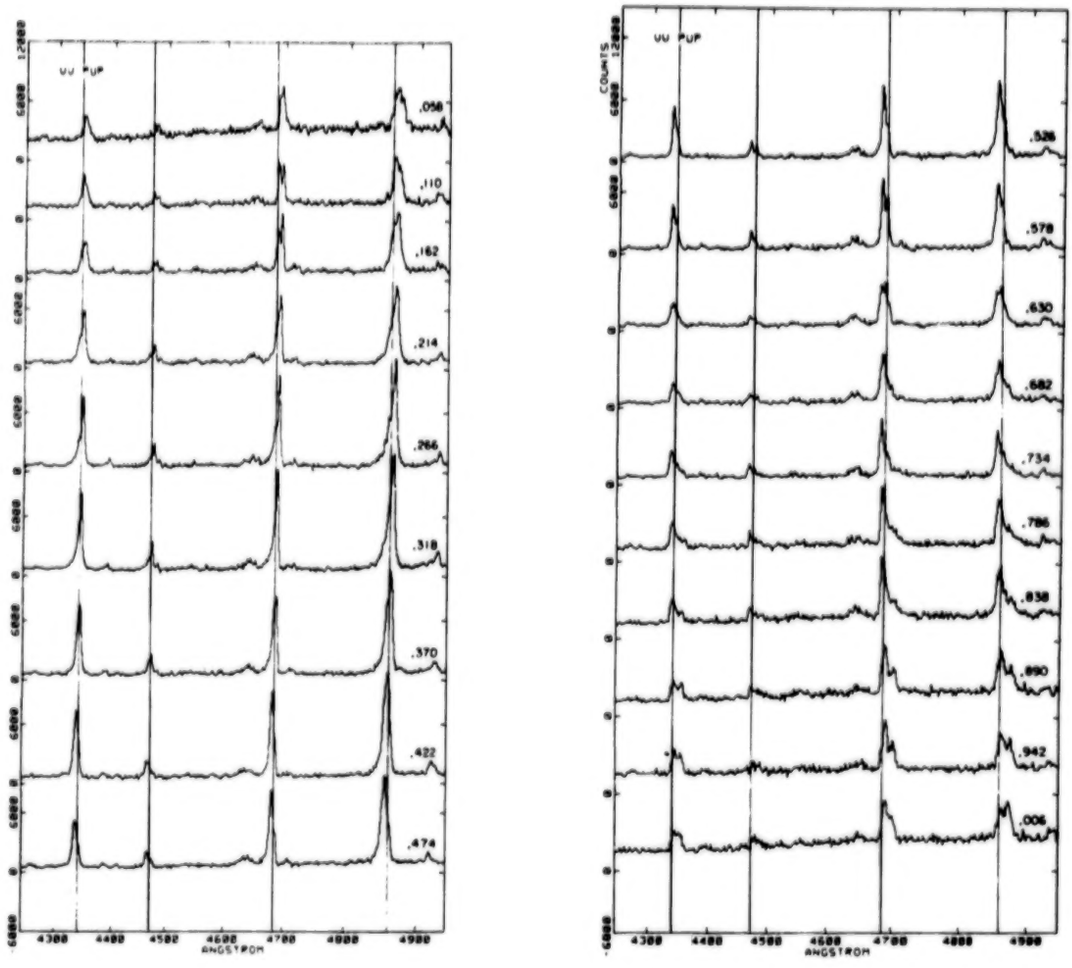


Figure 3-62a. Orbital spectrum changes in VV Pup (Schneider and Greenstein, 1980).

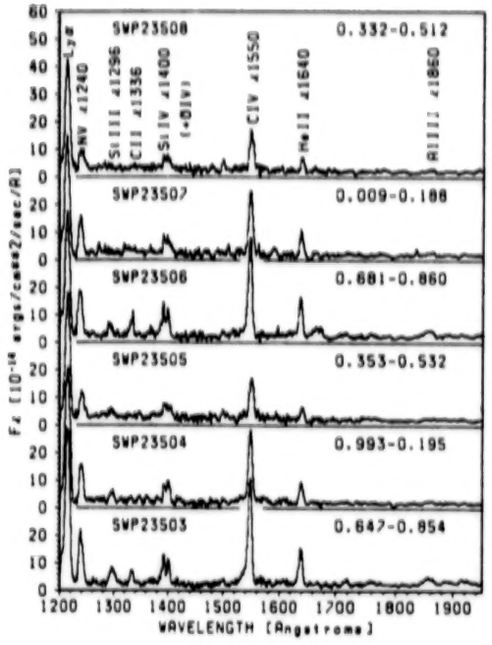


Figure 3-62b. Orbital Spectrum changes in QQ Vul (Mukai et al, 1986).

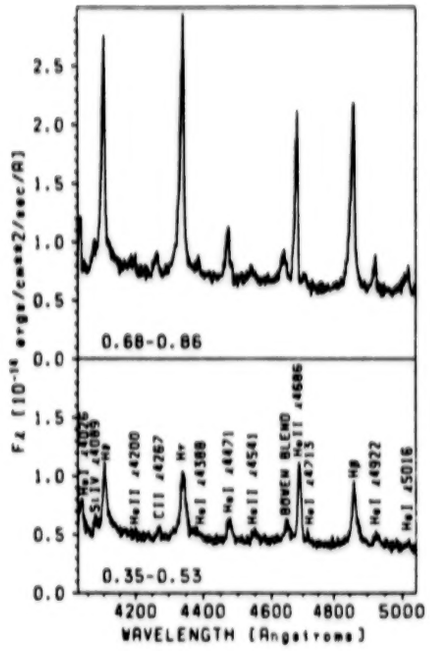


Figure 3-63. Changes in the line flux between high and low states in QQ Vul (Mukai et al, 1986).

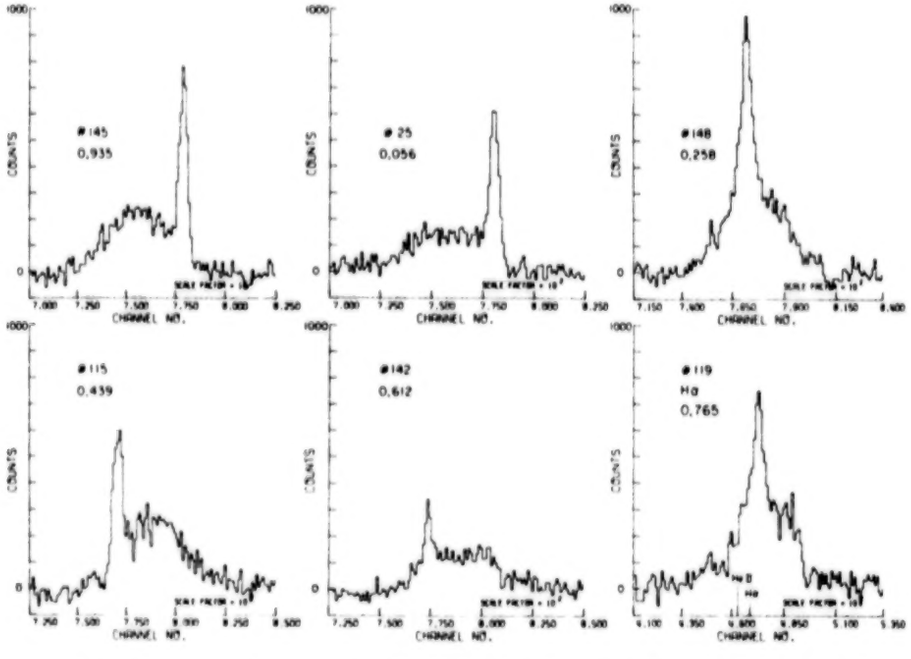


Figure 3-64. Broad and narrow line components in AM Her (Greenstein et al, 1977).

Wickramasinghe, 1981; Cowley et al, 1982; Mukai et al, 1986), indicating that the drop in intensity probably is not due to an eclipse by a stellar object, the confinements of which should be stable over long times.

Not only the line intensities, but even more the line profiles undergo marked complex, S-wave-like changes synchronous with the orbital cycle (Liebert et al, 1982a). In most, though not all, AM Herculis stars, both the

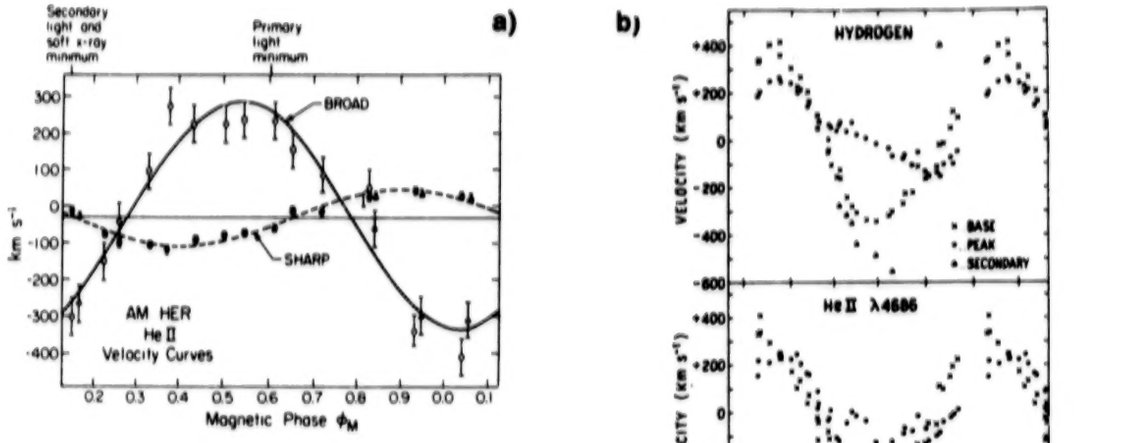


Figure 3-65. Radial velocities of AM Her at various epochs (a: Greenstein et al, 1977, b: Cowley and Crampton, 1977).

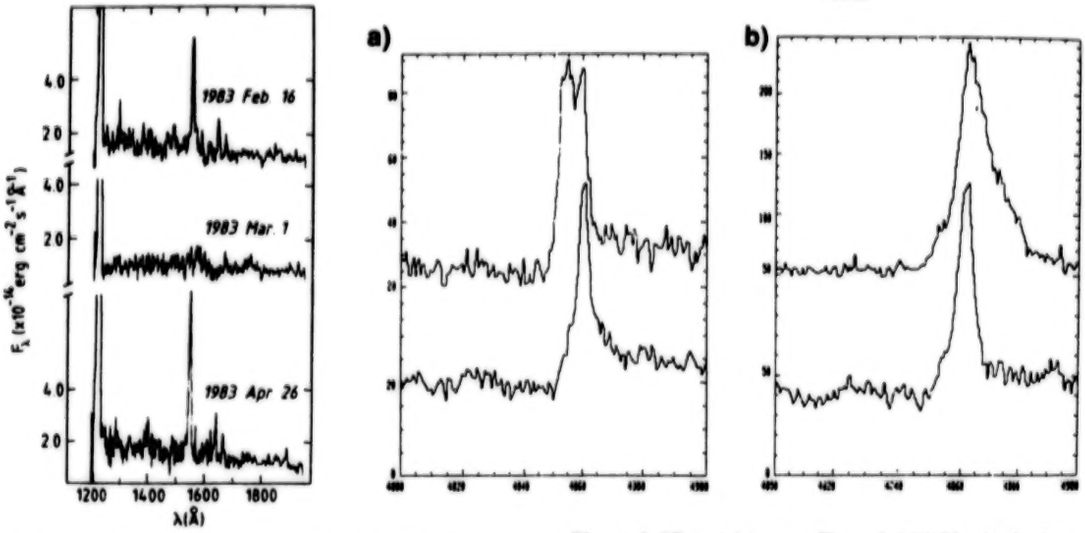


Figure 3-66. Spectral changes between high and low states in V834 Cen (Maraschi et al, 1984).

Figure 3-67. (a) Line profiles of AM Her in the low state at magnetic phases 0.58 and 0.60. (b) Spectra taken 0.09 orbital phases apart during a strong flare event (Latham et al, 1981).

Balmer lines and He II 4686 Å in particular consist of two components: a broad base component, stretching out to almost ± 1000 km/sec Doppler velocity, and a narrow sharp peak component (Figure 3-64) - often even more components can be distinguished (e.g., Rosen et al, 1987). In addition, the peak component can appear with a double-peaked structure at some orbital phases, but a single peak at other times, as the example of VV Pup in Figure 3-62a shows. The radial velocities of both peak and narrow components are different in K and γ-velocity as well as in orbital phasing (Figure 3-65). Usually the broad base has the larger velocity amplitude. The degree of phase lag is different for each object; for instance, it is almost zero for BL Hyi, 25% for EF Eri, 53% for VV Pup, and 133% for AM Her (Schneider and Greenstein, 1980; Thorstensen et al, 1983. As the example of AM Her in Figure 3-65 shows, however, this also seems to be subject to long-term changes. Similarly, as shown in Figure 3-65, velocity phases and amplitudes are different for different sorts of emission lines.

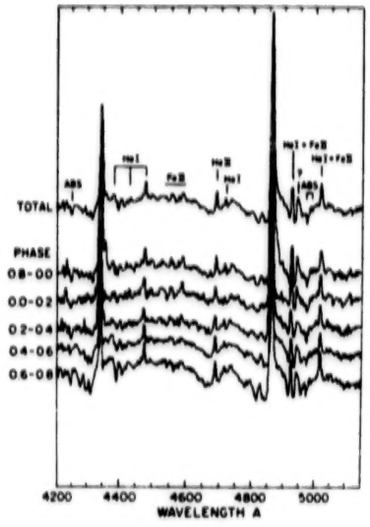


Figure 3-68. Cyclotron absorption features in AM Her (Latham et al, 1981).

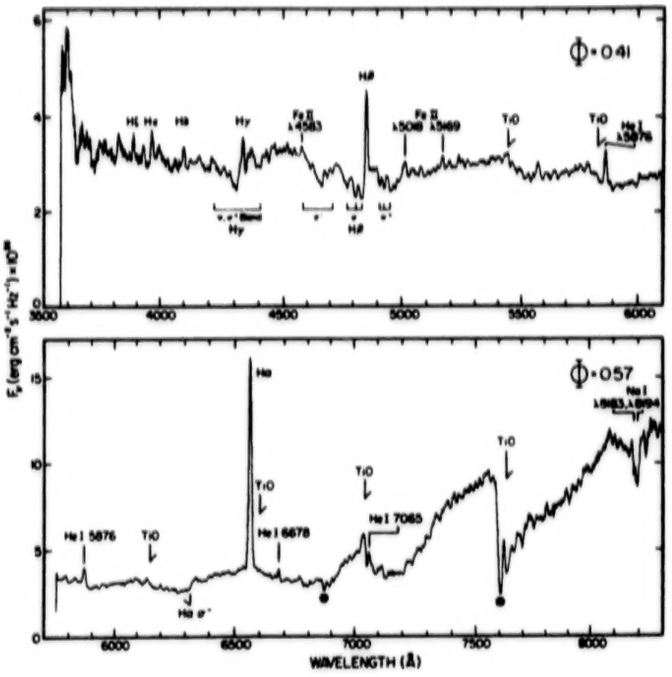


Figure 3-69. Secondary spectrum in AM Her in the low state (Schmidt et al, 1981).

During the optically high state, no stellar absorption features, as ascribed to the secondary star and often visible in other cataclysmic variables, can be detected with certainty.

Changes in the line spectra are related to changes in the systems between high and low states. The continuous flux distribution becomes even flatter, and emission lines are either weakened or disappear altogether. In ST LMi the UV radiation is hardly affected, whereas all emission lines disappear in V834 Cen (Figure 3-66). The broad base components which are visible during optically high states disappear. The He and metal lines usually are not visible any longer.

The radial velocities of the narrow H emissions follow almost the same pattern as those of the narrow components seen during high state, though they can be slightly out of phase. During one night an additional emission component of the H lines was visible in AM Her; this was much broader than the emission, reminiscent of the broad base during high state, though the radial velocities did not correspond to those seen during the brighter phase (Figure 3-67).

In all AM Herculis stars that have been observed during an optically faint state, complex absorption features are visible at the short and long wavelength sides of the H emission lines. Those features are only slightly variable with the orbital phase (Figure 3-68). In all cases they have been identified with Zeeman absorption features originating from magnetic fields with a strength of some 10 - 20 MG.

In some objects, the continuum flux increases considerably longward of about 5000 Å — like in other cataclysmic variables — and absorption bands of TiO and the Na I resonance lines at 8183 and 8194 Å become visible, indicating the presence of an M dwarf secondary (Figure 3-69; see also Mukai and Charles, 1986; 1987).

GENERAL INTERPRETATION: The white dwarfs in AM Herculis systems have strong magnetic fields, strong enough to entirely prevent the formation of

an accretion disc in the systems. Material spilled over from the secondary star is funneled directly onto the magnetic poles of the primary star; the gravitational energy is liberated in standing shocks right above the poles, which are the source of most of the observable photometric, polarimetric, and spectroscopic phenomena. Photometric and polarimetric light curves change in appearance when for some reason the position of the accretion poles on the surface of the white dwarf changes. A temporary decrease of mass overflow from the secondary star leads to low brightness states.

OBSERVATIONAL CONSTRAINTS TO MODELS:

- *AM Herculis stars exhibit very strong linearly and circularly polarized radiation. (See 188)*
- *Temporal variations of the photometric, polarimetric, and spectroscopic appearance occur in phase at all wavelengths. (See 188)*
- *Occasionally the systems' flux can drop by several magnitudes. (See 188)*
- *In two systems (AM Her and QQ Vul) the total flux distribution was observed to change appreciably; in this "reversed mode" the X-ray light curves of both objects looked rather similar.*
- *The optical line profiles have a very complex structure in which several independently varying components can be identified.*
- *In the low states, Zeeman absorption features appear next to the emission lines. (See 188)*

VI. AM CANUM VENATICORUM STARS

The class of *AM Canum Venaticorum stars* so far consists of four members only: AM CVn (= HZ29), GP Com (= G61-29), PG 1346 + 082, and V803 Cen. Their most characteristic features are the total absence of hydrogen in their spectra, colors which are typical of cataclysmic variables, and extremely short photometric and/or spectroscopic periods.

VI.A. PHOTOMETRIC OBSERVATIONS

ABSTRACT: Photometric light curves are highly variable, displaying a sine-shaped appearance with two almost equal parts in the high brightness states and a more irregular appearance in the lower states. Strong flickering and at times quasi-periodic oscillations are present.

other nova-like stars: 96, 98, 102, 103, 106, 113, 114, 117, 119, 122, 125

dwarf novae: 35, 46

interpretation: 178

Photometrically, the most extensively observed AM Canum Venaticorum star is AM CVn itself. A part of its light curve is shown in Figure 3-70a. At approximately regular intervals of some nine minutes, photometric minima with a depth of typically 0.2 to 0.4 mag repeat; occasionally every other minimum is absent, or for a while no minimum can even be detected at all (Smak, 1975; Patterson et al, 1979; Solheim et al, 1984). Strong flickering on time scales of 20 sec to 5 min, which in amplitude can exceed the periodic photometric variations, is superimposed on the light curve.

There have been arguments over what the photometric period of this system would be. The occasional disappearance of every other minimum, and at the same time the usually relatively strong appearance of the remaining ones led to the conclusion that the 18 minute periodicity might be the orbital period. Assuming this to be the case, the secondary minimum would be placed at phase 0.54. Still, the periods change slightly at random about some mean value which is referred to as "phase jitter" (Patterson et al, 1979). However, it is not entirely clear that it is always the same minimum (eclipse) which is seen strongly, which then leads to aliases in period counting (Patterson, 1979; Solheim, 1984). Extensive analysis of all available photometric observations of AM CVn lead to the conclusion that the main photometric period is 0.0121648423 d — or half of it — and a period decrease of (-1.6 ± 0.03)

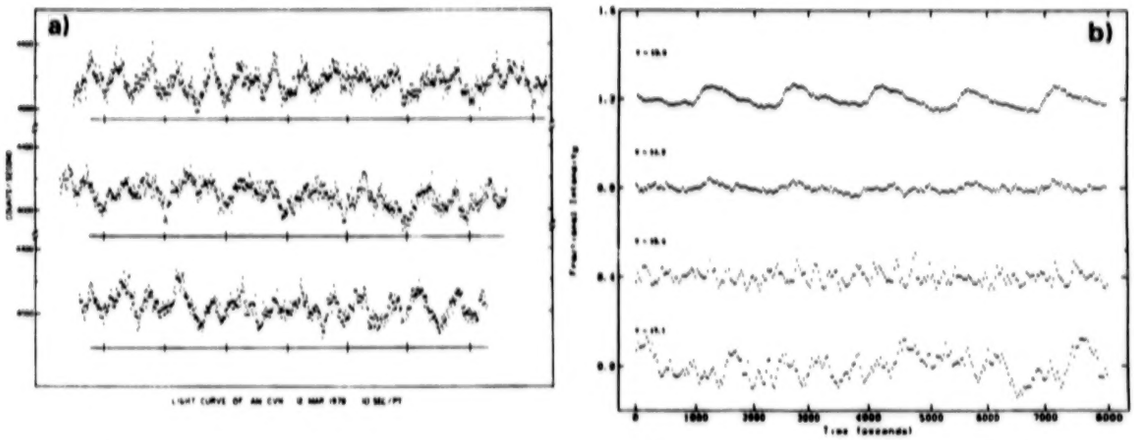


Figure 3-70. Optical light curves on orbital time scales of (a) AM CVn (Patterson et al, 1979) and (b) PG 1346 + 082 (Wood et al, 1987) at various brightness levels.

10^{-12} sec^{-1}. Superimposed on this development is a cyclical, but not strictly periodic, increase and decrease of the photometric period (Solheim, 1984).

Periodogram analysis of AM CVn at higher frequencies carried out by Warner and Robinson (1972) revealed the existence of photometric variations reminiscent of transient quasi-periodic oscillations with periods of 121, 118.9, 112.8, and 115.5 sec on three different occasions. The oscillations do not seem to be monochromatic, and during one night two periods were present simultaneously in one run both, however, might be an artifact due to too coarse a time resolution, similar to results in dwarf novae, where quickly shifting monochromatic oscillations are observed which could not be resolved in a coarse time resolution.

AM CVn so far only was seen at brightness levels around 14^m, and GP Com around 16^m. The other two Canum Venaticorum stars, V803 Cen and PG1346 + 082, are known to undergo brightness changes of some 4 mag amplitude (Wood et al, 1987; O'Donoghue et al, 1987). In PG1346 + 082, appreciable changes in the appearance of the light curve are connected with the overall brightness changes (Figure 3-70b): during the high state the light curve is reminiscent of that seen in AM CVn; as the light level decreases it becomes more and more irregular. Rather stable, though not totally coherent, oscillations with periods of several hundred seconds and some 25 minutes were found in all objects except for GP Com.

GP Com has been reported by Warner (1972) to show rapid irregular photometric variability. Nather et al (1981) observed the star on several occasions, but found hardly any photometric changes at all.

VI.B. SPECTROSCOPIC OBSERVATIONS

ABSTRACT: No trace of H can be detected in the spectra of AM Canum Venaticorum stars.

other nova-like stars: 99, 107, 114, 117, 119, 122, 134

dwarf novae: 65

The spectra of all AM Canum Venaticorum stars are similar in that none of them shows any trace of hydrogen. In the optical, very strong broad helium lines dominate; no hydrogen and hardly any lines of other elements can be found. In AM CVn, and in PG 1346 + 082 and V803 Cen during the high states, all lines are in absorption, in the latter two during low states; and in GP Com they are in emission (Figure 3-71; see also Robinson and Nather, 1975; Westin,

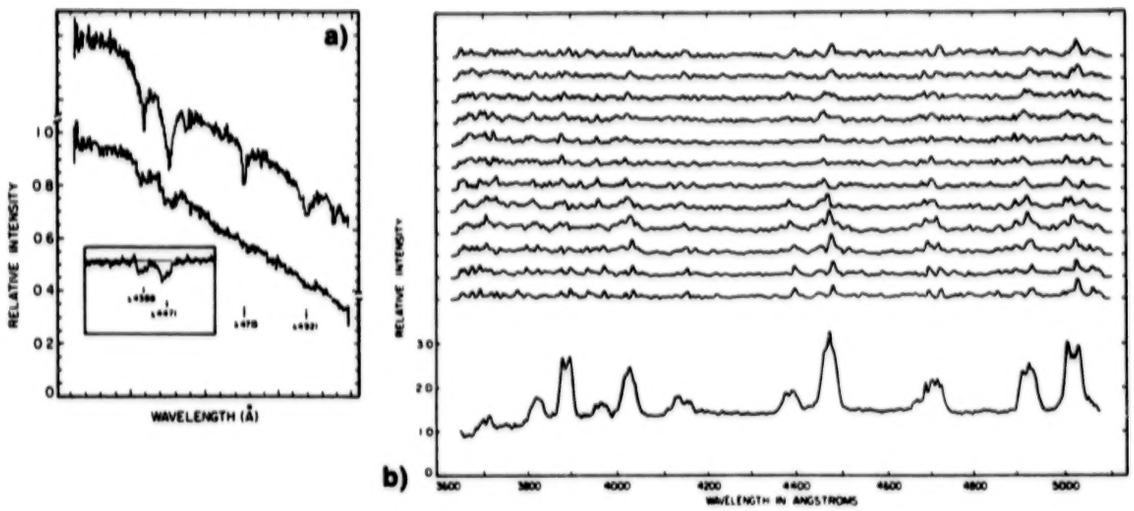


Figure 3-71. Optical spectra of (a) PG 1346 + 082 (lower spectrum) and AM CVn (insert); in the top panel the spectrum of a He white dwarf is displayed for comparison (Nather, 1985); (b) GP Com (Nather et al, 1981).

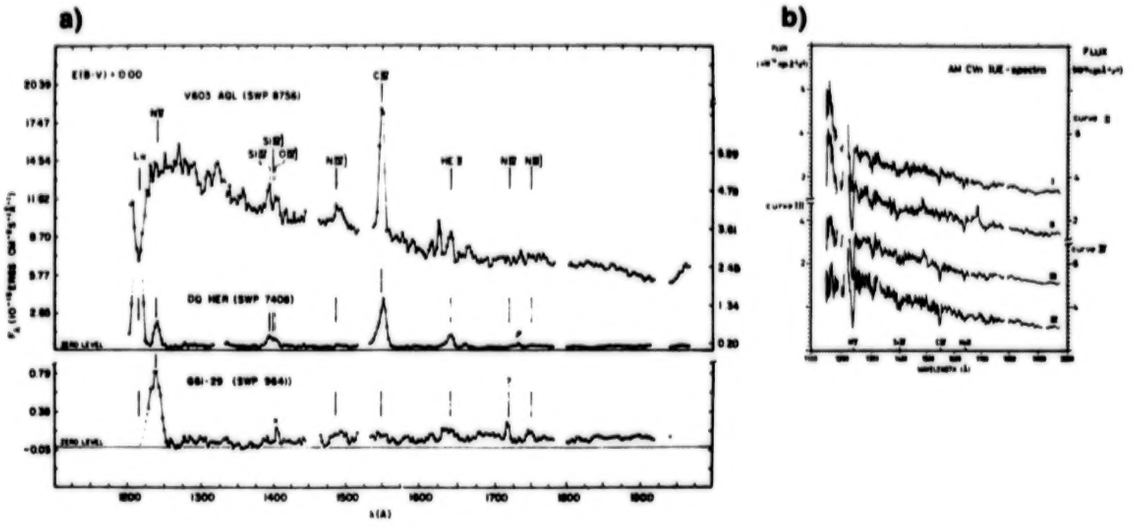


Figure 3-72. UV spectrum of (a) GP Com (=G61-29) (Lambert and Slovak, 1981) and (b) AM CVn (Solheim and Kjeldseth-Moe, 1987).

1980; Wood et al, 1987; O'Donoghue et al, 1987). In no case do the spectra resemble those of He white dwarfs (see Figure 3-71a) and, as Robinson and Nather point out, the ratios of He line strengths in AM CVn (and thus also in PG1346 + 082) and the remarkably asymmetric profiles are rather abnormal, not at all like what is expected in "normal" stars.

Time-resolved spectroscopic observations were carried out on GP Com (Nather et al, 1981). They find that the radial velocities measured from the wings of the emission lines lead to an orbital period of 46.52 min. Between the blue and red peaks a third narrow S-wave component clearly can be seen to migrate back and forth with the orbital period (Nather et al, 1981).

In the UV spectrum of GP Com (Figure 3-72a), NV 1240 Å is strongly in emission, He II 1640 Å is clearly present, N IV 1790 Å, N

IV] 1486 Å, and N III] 1750 Å are probably present. There is no trace of C IV 1550 Å, which in all other cataclysmic variables is the strongest or at least one of the strongest lines in the UV. The UV spectrum of AM CVn (Figure 3-72b), on the other hand, does not look abnormal for a cataclysmic variable: the normally strong lines like C IV, Si IV, and He II are all seen strongly in absorption; the lines are symmetric with no traces of mass out-flow.

GENERAL INTERPRETATION: These systems are currently understood to be cataclysmic variables consisting of a pair of white dwarfs.

OBSERVATIONAL CONSTRAINTS TO MODELS:

- *The orbital periods of AM Canum Venaticorum stars are decidedly shorter than those of all other cataclysmic variables.*
- *No hydrogen can be found in the spectra.*
- *These stars are not known to show any outburst activity. (See 178)*

N95
27071
UNCLAS

N95-27071

4

MODELS FOR VARIOUS ASPECTS OF DWARF NOVAE AND NOVA-LIKE STARS

I. HISTORY OF MODELING

A. HISTORICAL OVERVIEW

RELEVANT OBSERVATIONS: For about the first 100 years of research in dwarf novae, almost only outburst light curves were known. Neither photometric nor spectroscopic variabilities on time scales shorter than a couple of hours were resolved. Practically no nova-like systems (in the modern sense of the word) were known.

see: 15, 21, 95

ABSTRACT: The first attempts to explain the nature of dwarf novae were based on the assumption of single-star phenomena, in which emission lines were assumed to be caused by circumstellar gas shells. The outburst behavior was tentatively ascribed to the kind of (also not understood) mechanism leading to nova outbursts. The realization that some, and possibly all, dwarf novae and nova-like stars (and novae) are binaries eventually led to models which bore more and more similarities to the modern interpretation on the basis of the Roche model.

The first dwarf nova, U Gem, was detected in 1855; SS Cyg followed in 1896; and soon afterwards they were joined by ever more similar objects. Along with these detections, from the beginning of this century on, ever new attempts were undertaken to develop conceptual models of what a dwarf nova may consist of physically. The major problem, and the reason for the failure of all attempts to arrive at a suitable explanation until the 1950's, was that no strictly periodic pattern could be found in any of the dwarf nova light curves. Only the availability of ever larger telescopes and ever more sophisticated technology, finally, in 1955, revealed the searched-for periodicity in the nova-like star AE Aqr and in the old nova DQ Her and thus their binary nature (the strong similarity between novae, dwarf novae, and nova-like stars meanwhile had well been established). This quickly led to the formulation of the Roche model (Chapter 4.II.A) which is still today the only serious model for these objects and, in fact, in an ever more sophisticated form, seems to be able to account for at least the majority of the observed features.

A brief survey is given below of the development from initial tentative interpretations to the modern understanding. As we approach the present era in the historical summary, more and more features in the successive attempts to explain these stars emerge which resemble the modern explanation, and, in retrospect, the development towards the Roche model appears to have been rather direct, until, at one point, this model must have seemed an obvious next step.

For about the first century of observations of dwarf novae, photometric observations were mostly restricted to visual brightness estimates; spectroscopic measurements were, when possible, of very low wavelength and temporal resolution. Thus, attention was focused on the outburst behavior alone, while the existing periodicities, on the order of hours and less, remained undetected. This led to some immensely

PRECEDING PAGE BLANK NOT FILMED

valuable statistical investigations of the outburst behavior of the two brightest objects, SS Cyg and U Gem, which are discussed in Chapter 2.II.A. However, detailed and extensive as these studies were in revealing some obvious correlations, they provided but little aid for constructing models. Certain observational features were particularly puzzling, like the occasional standstills of Z Camelopardalis stars or the temporary suspension of activity in SS Cyg (the only known example at that time); but in first attempts at interpretation these were ignored.

Eventually the first observations of U Gem were almost entirely forgotten. Prejudices due to our modern ideas about its nature make it hard to believe that there is any basis at all to what was historically reported: Hind (1856), on December 15, 1855, was the first person to detect U Gem as a 9th mag star in the sky, in a field which, he claims, he had been familiar with for five years (the outburst period of U Gem has been between 60 and 150 days ever since, and the maximum brightness always has been on the order of 9 mag). Did it only in 1855 start its outburst activity? Some support is given to this conjecture by reports of very unusual behavior at somewhat later times (van der Bilt, 1908): Pogson, who was reputed to have been a very careful observer, reports having seen "the variable subject to strange fluctuations of intervals of 6 to 15 seconds, and quite to the extent of 4 mgs. The neighboring small stars were steady, not at all twitching like the variable. The phenomenon.... was watched for about half-an-hour...."; and according to van der Bilt, other observers also described the star as being very variable at that time; no similar reports can be found for later times. Similar behavior has never been reported for any other dwarf nova or nova-like star.

Van der Bilt (1908) seems to have been one of the first persons to attempt to gain some hints for a model from inspection of the then already huge data base of outburst records of U Gem, but he ends his article with a discouraging statement: "All attempts to detect some law in the changes of the period have failed.... As the material now lies before us, only useless speculations can result from it." But he also expresses his hope that, with further careful extended observations, "the day may come, when Mr. J. A. Parkhurst's statement of some ten years ago 'predictions in regard to it [U Gem], can be better made after the fact' will be left wholly to oblivion."

Van der Bilt (1908) reports a first interpretation by Nijland, who tentatively assumes that long and short eruptions are essentially identical, with only short outbursts due to a superposition of an eclipse at the end of the outburst. In fact, a subtraction of a short outburst from a long one (for SS Cyg and U Gem) leaves a curve like that known from Algol variables. It is not explained, however, how an eclipse, i.e., a geometrical phenomenon, can account for the clearly not constant time intervals between successive short maxima, and for the irregular sequence of short and long maxima.

More usual attempts at explanation were based on the appreciation of the features common to novae and dwarf novae: a quick and sudden rise to maximum, and a slower decline. In some cases, similarities in the spectra can be noted as well. Common, or at least similar, underlying causes for the brightness changes were suspected, supported by the realization that dwarf novae and recurrent novae seem, statistically, to follow the same relation between time spent in minimum state and amplitude of the outburst (Chapter 2.II.A.3). This relation would predict recurrence times of several thousand years for novae, in full agreement with their having been observed only once in historical times. And it also is in agreement with Gordeladse's (1938) finding that the mass ejected by dwarf novae (supposing the same mechanism is at work as in novae), integrated over outbursts during some 5000 years, amounts to approximately the same mass (he derives some 10^{29} g) as ejected by a typical nova during one outburst.

A suggestion by Vorontsov-Velyaminow (1934) was based on the apparent similarities of the spectra of several types of stars, all of which he classifies as "nova-like:" in modern terms, these are recurrent novae, dwarf novae, nova-like stars, and also R CrB stars, P Cyg and others. He supposes that they all are related to novae in some way: when a nova undergoes an outburst, he assumes, its atmosphere expands considerably; this, however, is not a stable state because the star collapses again, and at some state of collapse it reaches a new equilibrium; according to the resemblance of their spectra to those of the outbursting novae, the "nova-like" stars are regarded as different final states of this collapse — recurrent novae, for instance, and symbiotic stars (using modern terms) did not collapse very far; since this state is not quite stable in the long run, one day these stars will undergo an outburst. Dwarf novae and modern nova-like stars have collapsed much further and thus are moderately stable. That this is no satisfactory explanation, in fact no explanation at all, for the photometric behavior of dwarf novae is obvious, since practically none of the then already known observational features are explained. No further work along this line has been pursued.

Gerasimovič and Payne (1932) investigated color changes in U Gem and SS Cyg as they changed from minimum to maximum state, respectively. Since they could find changes in the color index by only 0.3 mag, they concluded that almost all of the brightness changes must be ascribed to changes of the radii of the stars, and that temperature changes play only a subordinate part.

This opinion is strongly contradicted by Hinderer (1948), who gained extensive photometric and spectroscopic observations of SS Cyg during various stages of activity. He concluded that most of the changes in brightness are due to mere changes in temperature (from some 5650 to 9600 K), except during the brightest phases of an outburst when the star's radius increases by a small amount. From the strong hydrogen emission lines during maximum a Zanstra temperature of some 20000 to 50000 K (or in some modified version of 10000 to 15000 K) would have to be derived, values which to Hinderer seemed unacceptably high; so he concluded that the conditions for the application of this method are not met and that the star's shell may be more highly excited than what corresponds to the equilibrium value. He also mentioned the additional difficulty that He II 4686 Å was seen in emission during quiescence, which also required an ionization temperature of at least some 20000 K. During maximum state, only absorption lines were observed, with no trace of emissions, which led him to conclude that the shell producing the emission lines had largely disappeared or had at least become fainter with respect to the photospheric region. During intermediate stages of decline, a superposition of broad symmetric absorption lines and narrower, but also symmetric, emission lines was observed. Since the line centers of both components coincided within the accuracy of these measurements and no changes in radial velocity could be determined, Hinderer concluded that the whole outburst was mostly an effect of variable opacity in the atmosphere, not connected with any relevant motions of material. The very broad absorption lines which were observed (corresponding to Doppler velocities of up to almost ± 3000 km/s) do provide a problem: if they would result from rotational motions of the star, this star would be torn apart. Elvey and Babcock (1943) argued that such rotational velocities may still be possible for a short time when the star goes through a period of instability during rise. However, this would not explain how these velocities could be maintained for many days almost all the way down the decline. Hinderer rejected this possibility altogether. He also discarded the possibility of the widening originating from the Stark effect, since this would require high pressures and thus high densities which cannot be reconciled with the existence of emission lines. Why there could not be two independent regions of line emission from which the two

sorts of lines could be emitted, he did not comment on. So he concluded with only the assumption that the lines were broadened by turbulent motions in the outer layers of the star, without considering any further what turbulent motions of the required strength might do to the atmosphere, and what might cause them.

On the basis of these conclusions, Hinderer devised a model for the physical processes occurring in dwarf novae during their outburst cycle. He emphasized that the observations he made of SS Cyg and the conclusions based on them were in excellent agreement with the spectroscopic observations of many other dwarf novae by Elvey and Babcock (1943), so he conjectured that his model might be applicable to the entire class. Noting that there was no conclusive evidence for dwarf novae to be white dwarfs (as was suggested by Elvey and Babcock and also by Miczaika and Becker (1948)), Hinderer, in accordance with Joy (1948), assumed that dwarf novae were main sequence stars of type G3 to G4 corresponding to a color temperature of about 5000 K. In his picture, they are surrounded by a shell of thin gas extending outward to some 1.8 stellar radii; this shell produces the observed emission lines; the cause of the outburst is believed to be the liberation of some inner energy of the star, as for novae, which leads to an increase in temperature and a moderate increase of the visible radius out to about the outer limit of the emission line region. The importance of this region to the emitted radiation is thus largely reduced, leaving only the absorption spectrum; only slowly, when the star's radius shrinks during decline, does it gain back its old importance. The different shapes of the outburst light curves are due to the energy not always being liberated in exactly the same way; the similarity of the brightness changes in all the decline phases results from the system properties during relaxation, after the energy supply is turned off. During the time between outbursts new energy is accumulated. The Z Camelopardalis stars are regarded as a transition state to "normal" stars.

The dwarf nova SW UMa was observed spectroscopically by Wellmann (1952) during a maximum. Here also very broad absorption lines are visible, and Wellmann is concerned with their interpretation. He immediately discards rotational broadening as a likely possibility for the same reason as Hinderer, namely, that a stellar rotation of 1600 km/s (in the case of a system such as SW UMa) simply would not be stable. Turbulent motions as supposed by Hinderer also do not seem reasonable, since, in order to be strong enough to account for the observed line width, the turbulent pressure would inflate the atmosphere up to 10 to 50 stellar radii, in which case the emission line spectrum would have a distinctly different appearance. As another possibility, Wellmann suggests that very broad absorption lines which already possess the full observed line width, may partly be filled in by emission originating in an extended shell of optically thin material surrounding the star. No explanation is provided for the questions as to what process may produce such strong absorption lines and why the emissions almost always just fill in the line center and appear as emission profiles of their own only in less luminous stages.

From radial velocity measurements in 1954, AE Aqr, classified in modern astronomy as a dwarf nova or a nova-like star (Joy, 1954), and DQ Her, a nova (Walker, 1954b), were detected to be binary stars; and they were soon followed by others. This led to the speculation that possibly all cataclysmic variables are binaries. In fact, the subsequent detection of the binary nature of eventually almost all well investigated cataclysmic variables finally led to a quite promising model for these stars and represented to many astronomers (at least until the present time, and there is no real indication for this period to be about to end) an end to a long search. This new "Roche Model," first outlined by Crawford and Kraft (1955; 1956), is practically unchallenged and forms the basis for all modern interpretation of all the members of the class of cataclysmic variable stars. It will be

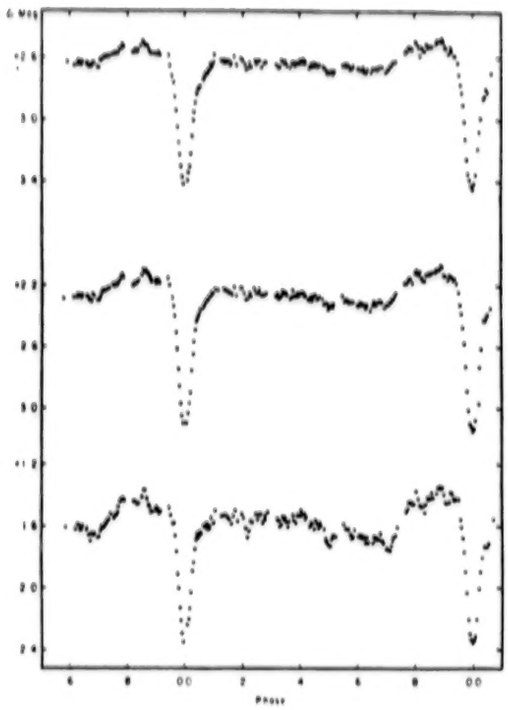


Figure 4-1. Orbital light curve of the nova-like variable UX UMa in V, B, and U — from top to bottom (Johnson et al, 1954). The light curve clearly is not that of a normal eclipsing binary system.

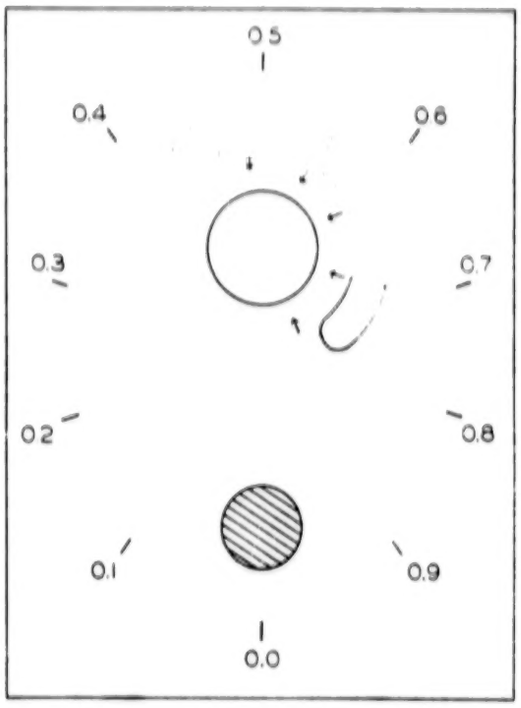


Figure 4-2. The first model for UX UMa (Walker and Herbig, 1954). An inhomogeneous gas cloud is surrounding one of the binary components.

presented and discussed in detail in Chapter 4.II. For its derivation, observations of the few known nova-like stars, in particular of UX UMa, were of great importance. This star and early explanations of its nature shall now be presented briefly.

UX UMa has been known since 1933 to be an eclipsing variable star (Beljawsky, 1933). It is not just an ordinary eclipsing star, but a very remarkable one (Figure 4-1): for a long time it was the one system with the shortest known orbital period, of only 0.1967 days, but it does not show the W UMa-type light curve which would be expected if normal stellar components are very close together; its light curve looks similar to that of an Algol star. Any attempts to derive orbital elements failed, however, since a hump appears shortly before and extends until shortly after eclipse, and the exact shape of both the hump and the eclipse are available from one cycle to the next. Thus it was clear that this system was not just two normal stars eclipsing each other. Linnell (1950) proposed prominences or gaseous streams at some distance from the eclipsed star, to account for both the hump before and after eclipse as well as for a hold seen at rise from minimum light; the additional gas was assumed to be hidden by one of the stars at times of normal brightness, and the most active region on one of the stars was supposed to be eclipsed at times of the hold; the observed variability of the hump might be a sign of either variable prominence activity or variable activity in the steam-like region. The fact that the hump was decidedly more pronounced before than after eclipse could be understood as either different cross sections of the stream being seen or rather as some persistent hot spot which was connected with the advancing hemisphere of the bright star. (Essentially this same scenario was later adopted by Walker and Herbig (1954) and further refined on the basis of more observational

material.) A gaseous cloud was proposed with inhomogeneous temperature distribution having a hot "head" and a cool "tail" to circulate around the bright component (Figure 4-2). As will be seen in the next chapter, this interpretation of UX UMa bares a striking similarity to the modern explanation via the Roche model: the gas cloud will be replaced by a gaseous disc, the bright "head" by a "hot spot," but otherwise it remains about the same.

Before turning entirely to the Roche Model, one final, though unsuccessful, attempt to explain the outburst behavior of dwarf novae should be mentioned. Also inspired by the discovery that possibly all cataclysmic variables are binary stars and by his own new theory of nova outbursts, Schatzmann (1959) tried to explain the outbursts of the dwarf nova SS Cyg in terms of a resonance phenomenon between binary motion and non-radial oscillations of the surface of one of the stars, leading to ignition of He burning in locally constrained areas of the star's surface. Based on this theory, Zuckermann (1961) deduced a more elaborate model of SS Cyg. She assumes that the system consists of a G5 main-sequence star and a blue subdwarf — the explosive star — which is embedded in a spherical envelope of ionized gas; all the system may be surrounded by a cloud of circumstellar material. By this explanation the colors of the minimum spectra can be accounted for. During an outburst, she supposes, the outer layers of the shell which surrounds the blue dwarf are accelerated outward by the hot events underneath, but in the course of the process of expansion the shell cools appreciably.

Neither of these concepts on the cause of a dwarf nova outburst or on how the system is structured and evolves otherwise could stand up to further confrontation with observations. The light curves of eclipsing dwarf novae during the outburst clearly demonstrate that the seat of the outburst cannot be a restricted area on the surface of one of the stars; and an outburst is accompanied by a very appreciable heating in the system and clearly not by any sort of cooling.

Eventually the Roche model became the currently only widely accepted model for a cataclysmic variable. This is not to say that it provides the complete solution, and it cannot be excluded that one day new discoveries will force us to give up this model and to replace it with another one; but so far it mostly works. Thus a gross model seems to apply to all cataclysmic objects (with the possible exception of symbiotic stars), subject to refinements and modifications which may account for characteristics of sub-classes and peculiarities of single objects. At the same time, it cannot be denied that there are observations which either cannot be explained at all within the framework of this model, or which can only be explained by introducing additional, questionable assumptions.

II. MODERN INTERPRETATION

The history of the first 100 years of observations of dwarf novae and nova-like stars was reviewed in the previous chapter. Attempts to understand the physical nature of these systems invariably failed until it was determined that all of these objects, including novae, are probably binary stars. Now, more than 30 years later, there is no observational evidence to contradict this hypothesis, and for theoretical modeling it has proven to be extremely useful.

Not all cataclysmic variables are known binaries. In fact, with respect to the entire number of known objects, the proven binaries are still the minority, but all the brightest variables are in fact known to be binaries. Not a single system is known which exhibits the usual characteristics of a cataclysmic variable and at the same time can be declared with certainty to be a single star. Two systems are known, the dwarf nova EY Cyg and the recurrent nova V1017 Sgr, in which, in spite of intensive search, no radial velocity variations

have been found; but they still exhibit composite spectra consisting of a bright continuum, an emission spectrum, and a cool absorption spectrum. If the Roche model is correct, it is to be expected that a small percentage of objects is viewed pole-on, so orbital motions do not make themselves felt as Doppler shifts of spectral lines. So even these two systems support the hypothesis that all cataclysmic variables (with the possible exception of symbiotic stars) are binaries.

II.A. THE ROCHE MODEL

RELEVANT OBSERVATIONS: All well-studied cataclysmic variables turn out to be binary systems with orbital periods of typically 90 minutes to four hours. One component usually is a cool main sequence star (if the orbital period is not larger than some 10 hours), and the other is usually a hot object with a geometry and flux distribution much unlike normal stars.

see Chapters 2 and 3

ABSTRACT: The canonical model of a cataclysmic variable is a Roche lobe-filling cool main sequence star which loses matter into the Roche lobe of the white dwarf. The transferred material has too much angular momentum to fall onto the surface of the white dwarf, but builds out an accretion disc in which it slowly spirals towards the white dwarf to eventually be accreted.

Observational evidence for the various components has been given in the theoretical abstracts following major sections in Chapters 2 and 3. Here, a more detailed description of the basic Roche model is given. For every binary system it applies that from the combined effect of the gravitational potentials of the two stars and their motion around each other, for each component there is a maximum geometrical volume, the *Roche volume* (or, in a two-dimensional picture, the *Roche lobe*), matter contained in which is bound gravitationally to the respective star; outside of this, matter either is bound to the system as a whole or, even further outside, it is hardly affected by the system at all (Figure 4-3). If it is further assumed that, for the special case of a cataclysmic variable binary system, one component is a white dwarf and the two components are close enough to each other so that one component (normally, but not necessarily, a main sequence star) fills its Roche lobe, then the model follows immediately.

Based on the evidence that all cataclysmic variables are binaries (as was first expressed by Struve, 1955), and making use of promising aspects of former models, the Roche model for cataclysmic variables was first developed by Crawford and Kraft (1955; 1956) and was quickly established, mainly due to extensive research by Kraft, Krzeminski, Mumford, Walker and co-workers (Kraft, 1962b; Krzeminski, Kraft, 1964; Mumford, 1964; Kraft, 1965; Mumford, 1966; Mumford, 1967; Mumford, 1971). The model became more refined and sophisticated in order to be able to explain ever more observational details and properties of cataclysmic systems, but in essence it never was changed. In particular, the hypothesis gained increasing support that the binary nature is a necessary condition for a system to become a cataclysmic variable.

THE ROCHE MODEL FOR CATACLYSMIC VARIABLES:

One component of the system, the *primary star*, is a white dwarf much smaller than its Roche lobe, the other, the *secondary star*, fills its Roche lobe (Figure 4-4). At the inner Lagrangian point L_1 the secondary star slightly overfills this volume, and thus matter is spilled over into the Roche Lobe of the white dwarf. Since angular momentum has to be conserved, and because of the tiny dimensions of the primary, this material flying along its trajectory inside the white dwarf's Roche volume would not hit the star's surface, but rather would meet again the stream of injected matter, thus forming a ring around the central object. As viscous forces are at work, the matter gradually loses angular momentum, and this

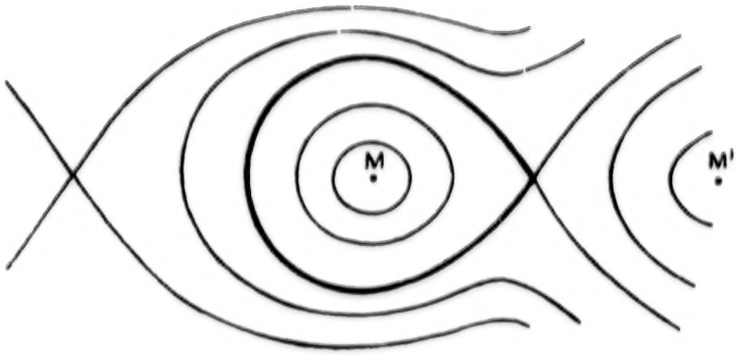


Figure 4-3. Roche surfaces. Material contained in one of the critical surfaces clearly belongs to the respective star; the two volumes touch each other at the inner Lagrangian point L_1 (Kopal, 1978).

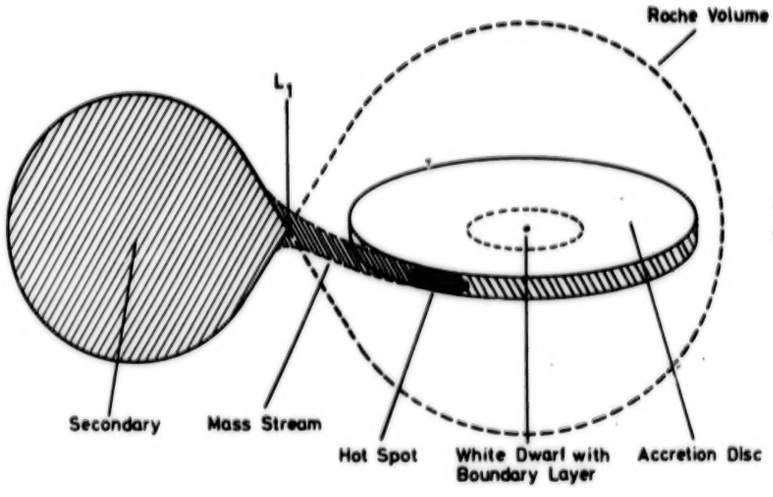


Figure 4-4. The Roche model for cataclysmic variables.

ring eventually spreads out to form a disc which lies in the rotational plane of the system, eventually extending down to the white dwarf. At its outer rim, where newly incoming material hits the disc, the so-called *hot spot*, or *bright spot*, is formed. When matter is approaching the white dwarf it has to get rid of excess gravitational energy, half of which — according to the Virial Theorem — is converted into kinetic energy of the disc material, while the other half is transformed into radiative energy, causing the disc to shine as a luminous object. The white dwarf need not rotate at Keplerian velocity; thus, at the interface between the innermost disc area and the white dwarf, the disc material will have to be braked down to the velocity of the white dwarf, in the process of which additional radiative energy will be liberated and the *boundary layer* will be formed.

In this picture, a dwarf nova outburst is attributed to a sudden collapse of much of the accretion disc, induced either by some process intrinsic to the disc itself, or by a sudden mass outburst from the secondary star. A nova-like star is thought to be a dwarf nova in permanent outburst; and a nova-explosion itself is thought to be due to a thermonuclear runaway on the surface of the white dwarf. A special sort

of cataclysmic variable originates if the primary's magnetic field is strong enough to entirely prevent the formation of an accretion disc (as postulated in the AM Herculis-type nova-like variables). In this case, the matter which falls in from the secondary star is funneled directly onto the white dwarf.

II.B. CONCEPTUAL PROBLEMS AND BASIC EQUATIONS

ABSTRACT: The Roche model appears to determine the basic physics of cataclysmic variable systems. Concerning details, however, the situation is not yet clear, but it is probably far more complicated than can reasonably be handled theoretically at this stage.

It is one thing to devise a conceptual model of a cataclysmic variables system and to develop plausible explanations for certain observed features. It is quite another matter to try to reproduce theoretically observed light curves or spectra. Allowing the Roche model to become "alive" and to consist of physically reasonable objects rather than two neatly defined balls of gas (the stars) and a smooth disc, it is obvious that the physical processes in a cataclysmic system are very likely to be rather intricate. This somehow has to be accounted for if computations of the emitted spectrum and the outburst light curves are to have any relevance. It will turn out, however, that most of the physical effects one can imagine likely to be present cannot now be dealt with theoretically in a satisfactory way, either for lack of adequate physical understanding or numerical skills, or due to limited computer capacity.

Observations indicate that the secondary stars are main sequence stars or at least lie close to the main sequence. In some cases their temperature and radius can be determined. From observations the spectral types are determined to be approximately G to M. In analogy to what is known about such stars (when they are single), magnetic activity brings about spots on the surface, surges, prominences, magnetic loops, and coronae and mass outflow, all of which probably does have some effect on other parts of the system and in turn is influenced by them. It is not known what effect it has on the structure and evolution of the star to be confined to the non-spherical shape of the Roche volume and what influence the dramatic lowering of the gravitational acceleration in the vicinity of the Lagrangian point L_1 may have on the outer layers of the star, and what the enforced co-rotation (at a speed much higher than normal for this kind of stars) may do to the secondary.

The masses, and thus the radii, of the white dwarfs in cataclysmic variables are known only with large uncertainty, which probably is of only little importance for the dynamics of the system, in particular the disc; but this is of great importance for the emitted spectrum (Chapter 4.IV). Furthermore, the white dwarf may possess a magnetic field, like many single white dwarfs do. Fields with a strength of up to some 10^6 G normally cannot be measured directly in these stars, but such fields are able to push the inner disc radius far away from the surface of the white dwarf because, at the distance of the Alfvén radius, the influence of the stellar magnetic field on the matter circulating in the disc becomes strong enough to force the matter to co-rotate with the star's field lines rather than follow the motion of the disc, thus disrupting the disc at this distance from the stellar surface. For a strongly magnetic white dwarf which creates a bi-polar field, the distance of the Alfvén radius from the stellar surface and the gross structure of the magnetic field can be calculated easily (Lamb et al, 1973). If, however, the magnetic field is weak enough so that the disc is disrupted relatively close to the surface of the white dwarf, the field is no longer bi-polar and conditions become rather complicated.

Problems are also severe in the seemingly simpler case of a non-magnetic white dwarf. For the disc to be stable, matter in the disc is

expected to rotate at Keplerian velocity. It is fairly unlikely, however, that the white dwarf also rotates with this velocity, which for it would be at the limit of disruption; indeed, it may not be rotating at all. The probable case is somewhere between these two extremes. If the white dwarf is rotating at a velocity slower than its Keplerian velocity, the matter arriving from the disc must be slowed down in the boundary layer before accretion onto the white dwarf is possible. According to the Virial Theorem the kinetic energy of material close to the white dwarf is of the same order as the total energy radiated away by the entire disc. Thus in the case of a non-rotating white dwarf all this energy is liberated in the boundary layer. The faster the white dwarf is rotating, the less kinetic energy has to be converted into radiative energy, and the less spectacular the boundary layer and its radiation will be.

If no frictional forces were at work, the material transferred into the accretion disc from the secondary would circulate infinitely around the white dwarf without ever being accreted. It is only the viscosity which causes the particles to lose energy and thus to slowly spiral onto the white dwarf while the remaining angular momentum, carried by a small fraction of the material, is being carried away from the white dwarf. Thus, the physical parameter which very critically determines the appearance and temporal behavior of the accretion disc is the viscosity, which, however, is largely unknown.* The viscosity determines how much energy is liberated at any point in the disc (i.e., the temperature); it governs the geometrical and, together with the temperature, the optical thickness at any distance from the white dwarf; and it also probably governs the cause and development, the presence or absence, of any outburst behavior. Whatever computations involving the viscosity are carried out, some essential, but still somewhat arbitrary, assumptions are needed; and the constraints imposed by available observations are not as tight as one would like.

There is one particular assumption — although it is certainly somewhat arbitrary — which has proved very useful for spectrum computations in particular (Chapter 4.IV), since it provides a simple analytical formula for the radiation emitted by the accretion disc. The assumption is that the whole disc is stationary, i.e., matter transferred from the secondary star is transported at a constant rate all the way down onto the white dwarf — in other words, the mass transfer rate $\dot{M}$ is constant throughout the disc. In this case the entire energy emitted by the disc is

$$L_d = \frac{G\, M_{WD} \dot{M}}{2 R_{WD}} \qquad (4.1)$$

and if a non-rotating white dwarf is assumed, that same amount is emitted once more in the boundary layer (see Chapter 4.IV.F). Equally, under this assumption the effective temperature $T_{eff}(r)$ at each distance r from the white dwarf can be shown to be

$$T_{eff}^4(r) = \frac{3\, G\, M_{WD}\, \dot{M}}{8\pi\sigma\, r^3}\left(1 - \sqrt{\frac{R_{WD}}{r}}\right) \qquad (4.2)$$

(all symbols have their usual meaning; for details of the derivation see Verbunt, 1982). The term in brackets accounts for the transfer of

*It should be realized that "viscosity" is just a different word to describe the mechanisms of probably turbulent angular momentum transport in the disc which are suspected to be present. Its parameterization by, for instance, a quantity α, defined as the ratio of the turbulent velocity to the sound velocity, including the actions of probably present magnetic fields (Shakura and Sunyaev, 1973), at any point in the disc (thus the often used expression "α-disc" which refers to just this way of parameterization) has no real physical meaning other than that of a basically free parameter which is likely to have different values at different points in the disc. As for its size, considerations about disk stability require it to be on the order of 10^{16} cm/sec (e.g., Hensler, 1982b), which is decidedly larger than molecular viscosity.

angular momentum between the disc and the white dwarf and imposes a certain, though in practice probably unimportant, uncertainty on the value of the effective temperature. It needs to be stressed, however, that the radial temperature distribution is not known theoretically if accretion occurs in some non-stationary fashion: besides irradiation which is not considered here, the only energy source in the disc is gravitational energy, set free by viscous interaction; if material circulates in the disc at a constant orbit, no energy is gained. In Chapter 4.IV.E, ways will be discussed how temperature distributions can possibly be derived in an empirical way. No matter what the viscosity is (unless it is unreasonably large), the material in the disc is rotating at Keplerian velocity v_φ, corresponding to its distances from the white dwarf:

$$v_\varphi^2 = \frac{G\, M_{WD}}{r} \qquad (4.3)$$

The approximate size of the disc can be estimated by, on one hand, the observational as well as theoretical result that is smaller than some 2/3 of the entire Roche radius and, on the other hand, by the total size of the Roche radius which is estimated from the orbital period and the masses of the two stars as approximately

$$R_2/R_\odot = 0.959\ M_2/M_\odot \qquad (4.4)$$

(for details and inherent assumptions see Chapter 4.II.C.1). The inner disc radius is set by the white dwarf's radius in the case of a non-magnetic, or weakly magnetic, star; and in the case of a magnetic white dwarf, the exact value of it at some distance from the surface depends on the mass of the star, the field strength, and the mass accretion rate.

The hot spot is the place at which the stream of infalling matter from the secondary star hits the accretion disc. From observations, its azimuthal angle with respect to the line connecting the centers of the two stars is approximately known; not so, however, its radial distance from the white dwarf, nor its exact shape. Depending on how wide the stream is with respect to the geometrical thickness of the outer disc, the stream can be imagined to either swamp this part of the disc or, if it is much narrower, to deeply penetrate into it. Clearly both the radiation (through the radiation characteristics of the spot) and possibly the outburst behavior (through the place and amount of energy deposited in the disc — see Chapter 4.III.C.2) of a cataclysmic system depend on the nature of the hot spot.

One final point is that in a cataclysmic system radiation emitted by different components and, to the extent they are present, magnetic fields will interact with each other and with other parts of the system changing conditions there. One can imagine that irradiation is particularly important if strong X-rays are emitted from the boundary layer and illuminate, and thus heat, the inner disc close to the white dwarf. A sort of corona may be formed, which probably accounts for the very strong emission lines of heavy elements seen in dwarf novae during quiescence, as well as strong P Cygni profiles seen during outburst in dwarf novae and in many nova-like stars.

II.C SYSTEM PARAMETERS

Absolute values of parameters of many systems have been quoted in the literature (e.g., Córdova and Mason, 1983; Smak, 1983, Patterson, 1984; Patterson and Raymond, 1985a; Ritter, 1984, 1987; Warner, 1987). Since it is important to have as reliable values of physical quanities as possible, and since it is even more important to know how reliable these are, different methods for determining various of these quantities will be described and discussed in the following sections. This discussion is not intended to be totally comprehensive; its aim is mainly to caution, and to point out where in the determination of these parameters problems are likely to occur.

II.C.1 STELLAR MASSES, STELLAR RADII, AND INCLINATION ANGLES

ABSTRACT: Great care must be taken in the determination of radial velocity curves that inhomogeneities in the disc and irradiation of the secondary star are properly taken into account. Constraints due to the Roche geometry have proved to be important in determining system parameters.

In a normal detached binary system, absolute masses and radii as well as the inclination angle can be derived from radial velocity curves and light curves, applying well-established standard procedures. Prejudice-free (i.e., model independent) application of this procedure to cataclysmic variables caused much confusion in the past before the Roche model was applied to cataclysmic variables; and it led to practically no useful results. Only two eclipsing double-lined spectroscopic binaries are known among these systems, so strictly speaking it should only be possible to determine masses for these two systems. Furthermore, from the shape of the light curves it is clear that the system geometry is not really that of two detached stellar components, so it is highly questionable whether the inclination angles — and radii — of the stars could be determined in a meaningful way using the standard procedure for binary stars.

The establishment of the Roche model brought about a considerable improvement in this situation. Geometrical considerations and the assumption that the secondary star fills its Roche lobe impose enough constraints so that system parameters can now be derived for a large number of cataclysmic variable systems. At the same time, however, new problems arise.

The function $M \sin^3 i$ can be derived from the radial velocity curve of each component, as in other binary systems. There are, however, major problems in the determination of the radial velocity curve itself. In the case of the primary component (white dwarf), the spectrum emitted by the star itself is only very rarely visible, and if so, it is still heavily contaminated by radiative contributions from the disc. In most cases the lines which are observable (in dwarf novae during the quiescent state these are mostly emission lines) are those originating in the accretion disc surrounding the white dwarf. If the disc were perfectly rotationally symmetric in its radiation pattern, its presence should not pose a problem, and the orbital motion of, in effect, the white dwarf would still be measurable. But it is not. Certainly the hot spot brings a decidedly inhomogeneous element to the radiation pattern (which clearly is visible in the line profiles). However, since neither its temperature nor its radiation characteristics nor its position in the disc are known for sure, it is not clear what part of the line profile is due to the hot spot and what is due to the disc in any single case. So clearly the normal way of fitting a Gaussian profile to the wings of a line (at least in systems which exhibit a hump) is bound to include all the distortions caused by the hot spot, and thus will not yield reliable results. (Incidentally, Stover (1981b) suggests that the phase shift of some 5-10° between emission and absorption components in double-lined spectroscopic binaries (Chapter 2.III.B.1.d) is due to just the effect). The often found result that the line centers move with different velocities than the (extreme) line wings is merely a result of inhomogeneities like the hot spot. In many, in particular high-inclination, systems, the Balmer lines exhibit a double-peaked profile which is explained as being due to the rotation of the disc; the peaks are ascribed to the outer edges of the disc and often radial velocities are derived from them. It is not clear, however, what this outer edge is, physically, or whether it is circular — thanks to the hot spot it probably is not — so the same problem will be encountered as described above.

The most reliable parts of a line profile for deriving the radial velocity curve are the extreme wings. Radiation producing them in a Keplerian rotating disc originates in the innermost disc close to the white dwarf, in an area

where at least the influence of the hot spot should be negligible, even though it cannot be excluded that inhomogeneities exist also there. At any rate, this seems to be the safest way to measure the radial velocity of the primary star. Shafter (1985) compared radial velocity curves of T Leo derived from different portions of the line wings (Figure 4-5) and found that the results depend dramatically on how the measurement was carried out. He suggests that the most reliable results can be obtained when several radial velocity curves are derived from different points in the line wings, so the point can be determined where the line wings just begin to merge into the continuum, believing that this then probably reflects most closely the motion of the white dwarf.

As for the secondary star, at first glance there should not be any problems; as long as the cool absorption spectrum is measurable it probably represents the cool star. That things are not that simple was first pointed out by Robinson et al (1986) who realized that the seven (!) measurements of the radial velocity amplitudes K_1 and K_2 for SS Cyg (which really should be the best measured radial velocity curve of all) all yield largely discordant results which do not even agree within the indicated errors (Table 4-1). A closer investigation of this case revealed that heating of the secondary star (of that half facing the disc) by the accretion disc changed the amplitude of the radial velocity curve (K_2) and also distorted it into a non-sinusoidal shape (Figure 4-6).

If both radial velocity curves, that of the emission spectrum (disc/white dwarf) and that of the absorption spectrum (secondary star) can be measured with some confidence, the orbital period P and the ephemeris T_o can be determined; furthermore, it is possible to obtain the "system velocity" γ *, the mass ratio q, the distance between the centers of gravity, and the individual masses, all as some function of the angle of inclination.

In a double-eclipsing system the angle of inclination can be derived with fairly high accuracy from geometrical considerations, using contact times and system dimensions (Figure 4-7a), if the eclipses are identified as those of the white dwarf in first ingress and first egress and of the hot spot in second ingress and second egress (Smak, 1979; Ritter, 1980; Patterson, 1981; Vogt et al, 1981; Berriman, 1984; Priedhorski et al, 1987). In the case of a single eclipse the system geometry can be invoked only in combination with the mass ratio to derive some upper and lower limits for the inclination angle (Figure 4-7b). If no eclipse can be observed, guesses of the inclination angle i are much more complicated and mostly rely on the presence or absence of a hump in the optical light curve.

As already noted, the constraints imposed by the Roche geometry have proved to be a big advantage in determining system parameters. The radiation of a spherical star filling the same volume as a Roche lobe-filling star has been computed by Paczynski (1971) to be

$$R_2/a = 0.38 + 0.20 \log q \qquad (4.5a)$$

$$\text{for } 0.3 < q < 20$$

$$R_2/a = 0.462 \left(\frac{q}{1+q}\right)^{1/3} \qquad (4.5b)$$

$$\text{for } 0 < q < 0.8$$

with

$$q = {}^{M_2}/_{M_1} \ ,$$

i.e., R_2 only depends on the mass ratio and the distance between the two stars. Furthermore, there is plenty of evidence that the secondary

*Observations of several dwarf novae during outburst (e.g., SS Cyg, SU Ursae Majoris stars — see Chapter 2.III.B.2) demonstrate, however, that γ can be a convolution of the system velocity and something else, since it is observed to be variable.

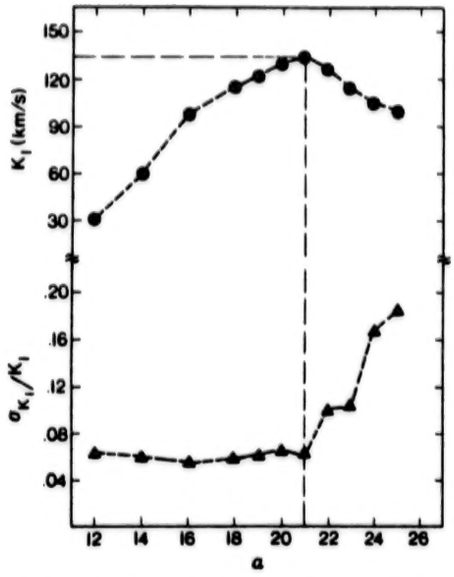


Figure 4-5a. Depending at what distance (a, in Å) from the center of an emission line the radial velocity of a cataclysmic variable system is measured (here: T Leo), different amplitudes K_1 are obtained; σ/K_1 is a measure for the noise which increases strongly where the line wings merge into the continuum. The amplitude variation is attributed to inhomogeneities in the accretion disc (Shafter, 1985).

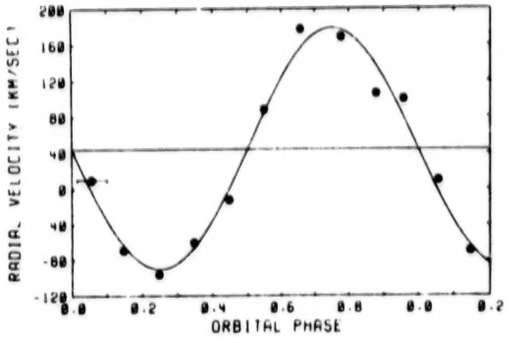


Figure 4-5b. The radial velocity curve of T Leo, measured from the outermost wings of the emission lines (Shafter, 1985).

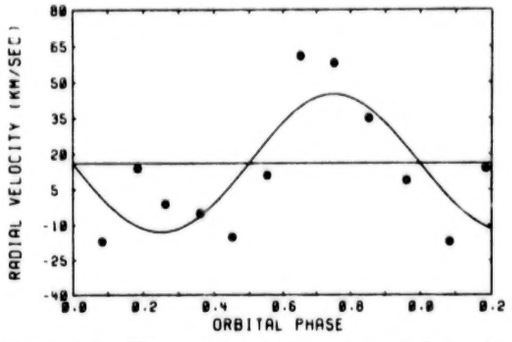


Figure 4-5c. The radial velocity measured from the centroid of the Hα emission line (same spectra as for Figure 4-5b). A satisfactory fit is clearly not possible (Shafter, 1985).

stars in systems with orbital periods below some 6 hours are indistinguishable from main sequence stars; for the latter there exists a relation between mass and radius which, to a fairly good approximation, is given by

$$R_2/R_\odot = 0.959\ M_2/M_\odot \qquad (4.6)$$

(Warner, 1972; 1976) for the range of interest for cataclysmic variables. Combining this with equation 4.4 and Kepler's third law yields

$$M_2/M_\odot = 3.18 \times 10^{-5}\ P[s] \qquad (4.7)$$

(Warner, 1976). So the knowledge of M_1, M_2, $\sin^3 i$, q, and the orbital period immediately provides a reasonably reliable inclination and thus individual masses.

The spectrum of the secondary star normally can only be measured in longer period cataclysmic variable systems, the more normal case being that only the emission spectrum, originating in the accretion disc, is visible. However, in this case too the Roche geometry helps to determine more system parameters than one normally would expect, although results become less reliable as more assumptions about system components and dimensions have to be introduced. Warner (1973) shows that the ratio between the radial velocity amplitude K_1 and v sin i for the equilibrium radius for a particle which is newly spilled into the Roche lobe is a function of only the mass ratio:

$$\frac{K_1}{v(r_d)\sin i} = \frac{f^2(q)\ q}{(1+q)^2} \qquad (4.8a)$$

with

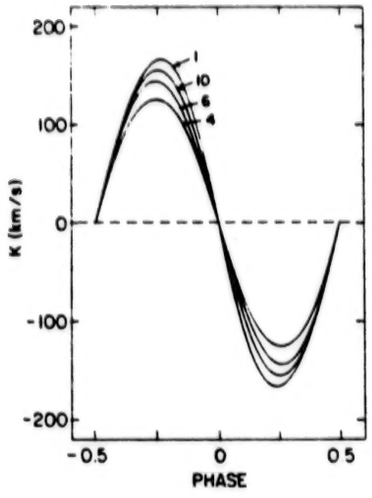


Figure 4-6. Theoretical radial velocity curves for a K5V star in SS Cyg for different mass-transfer rates. The distortions of the shape and amplitude are due to heating of the secondary star by the disc and the white dwarf (Robinson et al, 1986).

MEASUREMENTS OF THE AMPLITUDES OF THE RADIAL VELOCITY CURVES OF SS CYGNI

K Velocity (km s^{-1})		
K5 V Star	White Dwarf	Reference
115	122	Joy 1956
115[a]	122[a]	Walker and Chincarini 1968
165[b]	85 ± 4	Kiplinger 1979
153 ± 2	90 ± 2	Stover *et al.* 1980
120 ± 6	118 ± 8	Cowley *et al.* 1980
123 ± 2	107 ± 2	Walker 1981
156 ± 3	96 ± 3	Hessman *et al.* 1984

[a] Walker and Chincarini adopted Joy's K velocities.
[b] Kiplinger rejected this velocity because it disagreed with Joy's and because the absorption lines in his spectra were sometimes doubled.

Table 4-1. Determinations of amplitudes of the radial velocities, K_1 and K_2 in SS Cyg (Robinson et al, 1986).

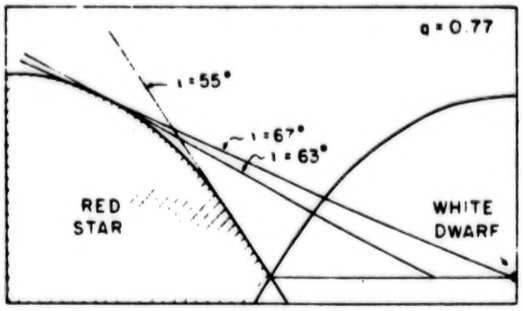


Figure 4-7b. In the case of a single eclipse, only upper and lower limits of the inclination angle can be obtained, from considerations about the system geometry (Robinson, 1974).

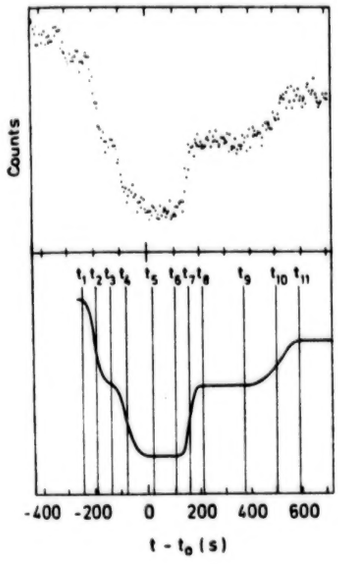


Figure 4-7a. In a double eclipsing system, the angle of inclination can be derived with high accuracy from the contact times of the eclipses of the white dwarf and hot spot, respectively (Ritter, 1980).

$$f(q) = 0.500 - 0.227 \log q \,, \quad (4.8b)$$

$$\text{for } 0.1 \leqslant q \leqslant 10$$

where (f is the distance between the center of the white dwarf and L_1 (Warner, 1976). Furthermore, he shows that

$$\frac{R_2}{M_2^{1/3}} = \left(\frac{G}{4\pi}\right)^{1/3}\left(\frac{1+q}{q}\right)^{1/3} \times \quad (4.9)$$

$$\times P^{2/3}\,(0.38 + 0.20 \log q),$$

which is only weakly dependent on q provided $0.1 < q < 1$ (Warner, 1973). So in combination with the mass-radius relation (equation 4.4), the

mass of a cataclysmic variable system can be determined for every system for which the radial velocity curve of the emission lines can be measured.

Difficulties with this method are obvious: how can $v(r_d)$ sin i be measured, and what part of the line profile represents radiation emitted from this hypothetical equilibrium radium in the disc? Warner (1976) tentatively identifies the half-width of the emission profiles with this value, but the physical significance of this is not at all clear. Schoembs and Vogt (1980) suggest a modification of this method of mass determination which is based on measurements of the far line wings, which originate in an area adjacent to the white dwarf. Their method probably yields much more reliable results since it is based on more reliable measurements. Further complications arise, of course, from measurements of K_1, as discussed above, and from the not very well determined mass-radius relation.

Robinson (1976) suggests an alternative to determine the masses if either the mass ratio q is known (for all double-lined systems) or, in the case of single-lined systems, if the inclination angle is known. In the first case, use is made of the relation between the secondary's mass and the orbital period, similar to equation 4.5:

$$M_2^2 = [0.996 \quad 10^{-8} P^2 (1+q) \times (0.38 - 0.2 \log q)^3]/0.804 \qquad (4.10a)$$

with $$q = M_1/M_2 \qquad (!) \qquad (4.10b)$$

(Robinson, 1976). In the second case, the above equation is solved simultaneously with the equation for the mass function for cataclysmic variables:

$$\frac{M_2 \sin^3 i}{(1+q)^2} = \frac{P K_1^3}{2\pi G}, \qquad (4.11)$$

the right-hand side of which only contains known values (in the case of a single-lined system). The advantage of this method over the method suggested by Warner (1976, see above) is that all the necessary input values can be determined reliably (while the basic assumption about the nature of the system and in particular about the secondary are the same). The disadvantage is that the difficulty of measuring the radial velocity curve of some ill-defined radius at the outer edge of the disc is replaced by the not necessarily easier task of guessing the inclination angle.

Another procedure for determining the parameters of the secondary star relies on considerations of, in particular, IR colors (Wade, 1982). If the contribution of the disc to the IR flux can be estimated — e.g., from the assumption of a stationary disc with some outer radius (a maximum of course is the radius of the Roche lobe), or from the optical and IR flux distribution, which in some objects shows a distinct rise to the IR that can be ascribed to the secondary star — then any excess flux in the IR is ascribed to the secondary and thus its spectral type can be determined. Assuming that it is a main sequence star, the mass and radius follow immediately. The obvious shortcoming of this method is that the IR flux of the disc is extremely poorly known. A more reasonable estimate would go the other way, namely, if from the size of the secondary's Roche lobe (i.e., from the orbital period — see equation 4.5) its IR flux is estimated, the contribution of the disc at IR wavelengths can be determined.

An unconventional method of determining the inclination angle was devised by Horne et al (1986). They made use of the constraints that the mass of the white dwarf must not exceed the Chandrasekhar limit and that the secondary is a main sequence star, and then used Monte Carlo techniques to determine that value of i

which with the highest probability produced the observed values of K_1 and K_2.

II.C.2 ABSOLUTE MAGNITUDES AND DISTANCES

ABSTRACT: In principle the spectral type of the secondary star can be used to determine absolute magnitudes. Relatively well-defined observational relations exist between the V-magnitude of a dwarf nova in outburst and the orbital period, and between the V-magnitude and the equivalent width of the Hβ emission line, the UV absorption feature at 2200 Å, if present, should be indicative of the distance.

A search in the literature for distances and absolute magnitudes of dwarf novae and nova-like stars yields a wealth of values for each system which, even within the error limits, disagree. Since these values were derived under various assumptions, this very clearly reflects the serious difficulties which are encountered in this task, and leads one to suspect the large errors reflect a strong model dependence.

The first determinations of absolute magnitudes and/or distances of dwarf novae were based on parallax determinations. For U Gem and SS Cyg, trigonometric parallaxes were derived (Strand 1948; van Maanen, 1938; Becker and Mczaika 1948). A mean absolute brightness during minimum was derived for U Gem, SS Cyg, RU Peg, and EM Cyg from radial velocities and proper motions (Kraft, 1962b). This latter method is particularly dubious since, as has been discussed above, measurements as well as interpretations of the radial velocity curves are very difficult, and it is not at all clear what is being measured.

In many systems, in particular in those with longer orbital periods, the spectrum of the secondary component is visible in the optical, or at least in the IR. Under the (justified — see Chapter 4.IV.C) assumption that it is a main sequence star, it is in principle possible to determine its absolute magnitude — thus that of the entire system — from estimating its spectral type. This method has been applied to many systems (e.g., Wade, 1979, 1982; Berriman et al, 1985). If radial velocity measurements of the late spectrum are available, a determination of the spectral type should be straightforward and fairly accurate. If only low-resolution spectra or colors are available, however, it is usually not clear what contribution to the observed flux can be ascribed to the outer cool areas of the accretion disc. The constraint that the secondary fills its Roche lobe helps to provide a fairly reliable guess in cases where the mass ratio and the orbital period are known.

Bailey (1981, see also Warner, 1987) calibrated the surface brightness of the cataclysmic variable secondaries in the K-band, arriving at the relation

$$S_K = K + 5 \log d + 5 \log ({}^{R}/_{R_\odot}) \qquad (4.12a)$$

with

$$S_K = 2.56 + 0.508\,(V-K) \qquad (4.12b)$$

$$\text{for } (V-K) < 3.5$$

$$S_K = 4.26 + 0.58\,(V-K)$$

$$\text{for } (V-K) > 3.5$$

(Figure 4-8). He points out that the interstellar absorption is no problem at these wavelengths, and that the K magnitude is relatively insensitive to the temperature of the cool star. If the period and mass ratio of a system are known, the secondary's radius can be derived (see Chapter II.C). So the main difficulty again is to estimate the contribution of the star in the V band — which is a very serious problem for most systems, since here the flux from the star is probably weak while that from the disc can be fairly strong. Unless other information about the secondary is also available to constrain possible values, the errors in distances derived by this method are expected to be considerable.

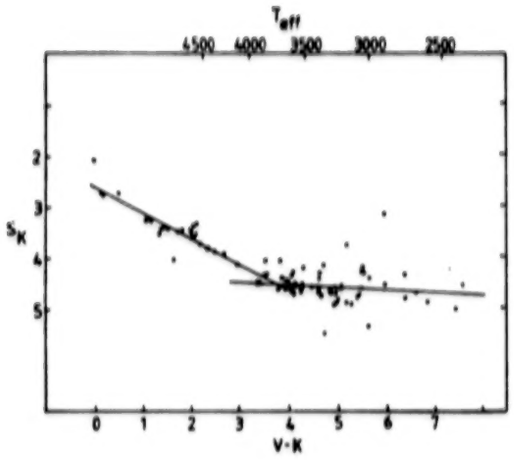


Figure 4-8. The surface brightness of the secondary stars in the K band (22000 Å) is a good measure of their effective temperature (Bailey, 1981).

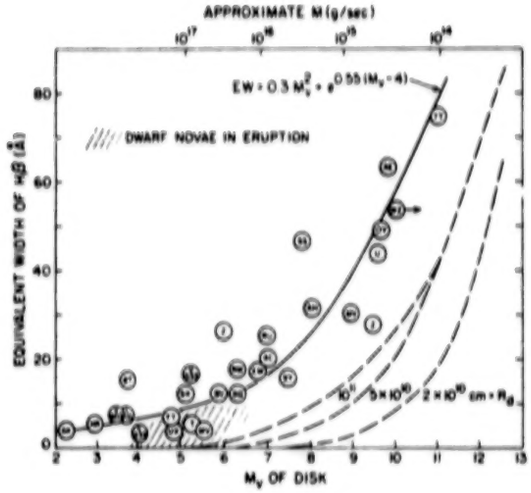


Figure 4-9. An empirical relation has been derived between the equivalent widths of the Hβ emission line and the absolute visual brightness of the accretion disc of cataclysmic variables (Patterson, 1984).

Warner (1987) found that there exists a relatively well defined relation between the absolute V magnitude of dwarf novae, in particular during outburst, and the orbital period (Figure 2-14; the theoretically inferred relation between the absolute magnitudes and mass transfer rates in cataclysmic variables is indicated as well)

$$M_v\,(\max) = \underset{\pm 0.13}{5.64} - \underset{\pm 0.024}{0.259}\,P[hr], \tag{4.13}$$

which then provides absolute magnitudes for all dwarf novae for which the orbital period has been determined with an accuracy of ± 0.23 mag.

Finally, the interstellar absorption feature at 2200 Å has been used frequently to derive distances since the availability of UV spectra. Reddening curves have been published by, e.g., Nandy et al (1975) and Seaton (1979). In order to derive the amount of reddening, the observed spectra are corrected for interstellar absorption by using successively different values for E(B-V) until the absorption feature disappears from the spectrum. Normally results derived by this method are not in striking disagreement with values determined by other means, although error limits are fairly large — since the "best fit" is to some degree a question of taste. Furthermore, it is not certain that one single absorption law is applicable equally reliably to all directions in the Galaxy. Also experience has shown that great care must be taken to use well-exposed spectra for this procedure, since otherwise results are unreliable. Only an upper limit can be derived for most dwarf novae and many nova-like stars, however, since due to their proximity to the Earth no dip in the interstellar absorption is visible in the spectrum.

Patterson (1984) finds an empirical relation between the equivalent width of Hβ and the visual magnitude of cataclysmic variables (Figure 4-9):

$$EW(H\beta) = 0.3\,M_V^2 + e^{0.55\,(M_v - 4)}, \tag{4.14}$$

which allows an estimate of the absolute visual magnitude within some ± 1.5 mag for systems with strong emission lines ($W_\lambda > 15$Å).

II.C.3 MASS TRANSFER RATES

ABSTRACT: It is necessary to distinguish between the mass transfer rate from the secondary star into the Roche lobe of the primary, the mass throughput through the disc, and the mass accretion rate onto the white dwarf. All determinations are strongly model dependent. Determinations based on eclipse-mapping techniques seem to be the most reliable.

A distinction must be made between the mass transfer rate from the secondary star into the Roche lobe of the white dwarf, the mass throughput through the accretion disc — which need not be uniform throughout the disc but well may depend on the distance from the white dwarf, and, as observations show, is clearly variable with time — and the mass accretion rate onto the white dwarf, although this is often not done carefully in the literature on cataclysmic variables. Only in the special (though theoretically most often considered) case of a stationary accretion disc are all these values by definition identical. In all other cases they are more likely to be different from each other, while relative relations can easily change with time: e.g., assuming that the mass transfer rate from the secondary into the primary's Roche lobe is not significantly changed during an outburst, then this mass transfer rate is probably the largest of the three during their quiescent state of dwarf novae, when material is preferentially stored in the outer disc rather than transported on towards the white dwarf and thus the two other rates will be close to zero; during outburst, on the other hand, when the matter which was stored in the outer ring during quiescence is suddenly transferred through the disc to be accreted by the white dwarf, the mass throughput is probably largest, closely followed by the mass accretion rate*, while the mass transfer rate might temporarily be smallest. Although one can imagine that differences can be fairly large, normally no distinction is made when values for $\dot{M}$ are determined, and implicitly either the mass transfer rate or the mass throughput are determined.

All known methods for determining the mass transfer rate are strongly model dependent, though all give results which agree within surprisingly narrow limits — as long as systems are considered which probably are close to the steady state (i.e., nova-like stars in the high state and dwarf novae during outburst). Fairly extensive discussions of various methods are given by (Patterson, 1984; Verbunt and Wade, 1984).

The theory of evolution of cataclysmic variables (Chapter 4.V.D) assumes that mass transfer in the ultra-short period systems, with periods shorter than 2 hours, is driven solely by gravitational radiation, while above the period gap magnetic braking (which results in strong mass loss) is at work. Computations for the amount of mass loss in short period systems yield qualitative agreement with mass transfer rates derived from observations (Patterson, 1984 — see also Figure 4-54), demonstrating that these mass transfer rates should be on the order of 10^{-10} to 10^{-11} $M_\odot$/yr. For long period systems above the period gap, larger mass transfer rates are expected. Thus, in general, mass transfer rates significantly lower than 10^{-11} $M_\odot$/yr can be excluded for cataclysmic variables. For an upper limit, values of $\dot{M}$ both from observations and from computations (Figure 4-54), as well as values by other authors, suggest that mass transfer rates significantly in excess of 10^{-7} $M_\odot$/yr are quite unlikely to occur in cataclysmic variables, since then these systems would be dynamically unstable.

There are several ways to derive a mass throughput rate for the accretion disc, most of which, however, implicitly assume that the disc is stationary.

If somehow the radiation flux from the disc can be estimated, the mass throughput rate can be obtained from

*Some mass is lost in stellar wind, observable in the P Cygni profiles, and some is carried outward in the disc, taking care of the excess angular momentum.

$$L_d = \frac{G\, M_{WD}\, \dot{M}}{2\, R_{WD}} \quad . \qquad (4.15)$$

A determination of the disc luminosity is difficult, since the bulk of the radiation is probably emitted at unobservable EUV wavelengths. So even if the disc is really stationary (which often is rather questionable), and even if the entire accessible wavelength range from the IR to the Lyman edge is covered observationally, some (largely arbitrary) bolometric correction has to be adopted in order to determine the luminosity. Correspondingly worse is the situation if either no UV data are available for the system, or if the disc is obviously not in a stationary state, as is the case for quiescent dwarf novae, for instance.

Another way of estimating the mass throughput rate is to compare the observed continuous flux distribution in the optical and UV with theoretical models and then derive values for $\dot{M}$ from this. However, as will be discussed in more detail in Chapter 4.IV, the difficulty here is that the currently available models for stationary, and even less for non-stationary, discs are far too unreliable and far too dependent on details of the assumptions and of the program codes with which they were constructed to inspire any confidence, other than they might be crude estimates at best.

In some cases attempts have been made to determine average mass transfer rates from observed changes in the orbital periods of cataclysmic variable systems (e.g., Smak, 1971; Warner and Nather, 1971). These authors assume conservation of mass and angular momentum in the system, which, as Patterson (1984) points out, is inconsistent with evolutionary theories about these systems (Chapters 4.V.C and 4.V.D). Furthermore, since observations show that period changes do change their signs occasionally, it is clear that they cannot be due to mass transfer in the system.

In other cases attempts have been made to determine the mass transfer rate from the luminosity of the hot spot (Krzeminski and Smak, 1971; Paczynski and Schwarzenberg-Czerny, 1980). The obvious difficulties with this approach are that neither the shape nor the geometrical radiative characteristics of the hot spot are known, nor is its flux distribution (from which some kind of sensible bolometric correction could be derived), nor is the location of the hot spot in the disc which determines the amount of energy that is liberated.

A possibly reliable method to determine the mass throughput was derived by Horne and coworkers (Horne and Cook, 1985; Horne and Stiening, 1985; Wood et al, 1986) using the eclipse mapping method (Chapter 4.IV.E): the image of the accretion disc is reconstructed from photometric observations during the eclipse of a cataclysmic variable, preferentially in several colors; and from the colors at each point the temperature distribution and thus the local (!) values of $\dot{M}$ can be determined.

III. THE ACCRETION DISC

Accretion discs have become very fashionable in astrophysics for explaining a wealth of phenomena which cannot be understood in terms of processes occurring, for instance, in normal stellar atmospheres. They have been applied to quasars, to active galactic nuclei, to X-ray and cataclysmic binaries, to symbiotic stars, to protostars, and to many more areas. Only in cataclysmic variables, however, does it seem that most astronomers are reasonably confident that the brightness changes observed in dwarf novae and nova-like stars in the optical and the UV are due directly to changes in the discs. Thus, the study and understanding of accretion discs in these systems can, and hopefully will, bear potentially valuable consequences for many other fields in astronomy.

It should be noted, however, that the unsolved or poorly understood theoretical problems concerning accretion discs are many and

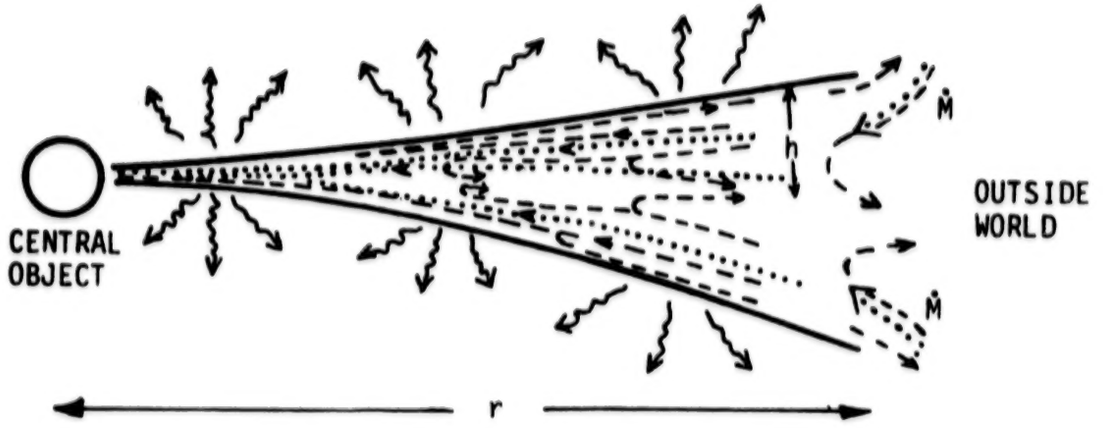


Figure 4-10. Qualitative model of an accretion disc. Indicated are the flow of mass (dotted lines) and angular momentum (dashed lines) in the disc; energy is generated by viscous heating which is the reason for the finite thickness of, and the radiation from, the disc (Katz, 1985).

difficult. A single particle added inside the Roche lobe of the white dwarf revolves around the central start in a circular orbit at a distance which is determined by the equilibrium between its own angular momentum and the gravitational attraction it experiences. When many such particles circulate in this way at the same distance from the star, they also interact with each other, and the distance-dependent Keplerian velocity ensures that shear stresses will develop between neighboring regions, probably causing many kinds of turbulence, while magnetic fields might also be present to further complicate the situation. The net effect is that mass and angular momentum become separated, with the bulk of the mass moving in orbits ever closer to the center of gravity as this material is deprived of ever more of its angular momentum, while most of the angular momentum, tied to very little mass, is transported outwards in the disc. (At the outer edge it either leaves the system, or, more likely, through interaction with the secondary star, is fed back into orbit as angular momentum.) Thus the mass which originally all circulated at roughly the same distance spreads out into a disc, both increasing the outer radius and decreasing the inner radius. Details of the strength and nature of the particle interaction are not known, but commonly they are covered conveniently under the term "viscosity." To understand the nature and the role of the viscosity is the harder part, since complex processes of plasma kinetics, (magneto-) hydrodynamics, and poorly known radiative interactions, and other system parameters are involved. Notwithstanding, the study of the outburst behavior of dwarf novae and the brightness changes occurring during times between outbursts, might still provide some useful constraints on various concepts about, and models of, accretion discs. At all outburst stages the viscosity determines the size and geometrical shape of the disc, its radial and vertical temperature and pressure stratification, the spectrum emitted, and — since the gravitational potential is the only available energy source, made available exclusively by the viscosity — all observable (and unobservable) temporal changes. The theoretical study of these quantities shall be the concern of this section.

The general assumptions in theoretical work in the area of cataclysmic variables are: the neglect of relativistic effects and of self-gravity (i.e., the mass contained in the disc is negligible compared to the mass of the white dwarf); a disc which is assumed to be geometrically thin, lying flat in the orbital plane of the system and rotationally symmetrical with gravitational energy as the only energy source, which is converted into radiation energy by viscous processes which also cause the separation of

angular momentum and mass. A certain vertical thickness structure of the disc is due to thermal pressure originating from the transformed gravitational energy (Figure 4-10.)

III.A. 2 DIMENSIONAL HYDRODYNAMICS

RELEVANT OBSERVATIONS: Photometric observations point to the disc being an essentially flat object.

ABSTRACT: The approximate position of the hot spot can be reproduced from computations of particle trajectories in the restricted three-body approximation. Hydrodynamic computations provide information about brightness distributions, surface density distributions, and velocity fields in the disc.

The incentive to introduce accretion discs for the explanation of cataclysmic variables came from observations. The first attempts to justify this hypothesis by means of computations were undertaken in the early 1960's (for a bibliographic overview see Flannery (1975a) and Hensler (1982a)), and in the course of the following decades the theories became ever more elaborate. Still, many properties of the disc can be derived from basic physical principles without extensive use of computers.

The secondary star can safely be assumed to co-rotate with the binary orbit (the synchronization time is very short, see Chapter 4.V.C), and matter leaving its surface at the inner Lagrangian point L_1 is likely to have a velocity on the order of the local sound speed (e.g., Lin and Pringle, 1976), which is about an order of magnitude less than the orbital velocity of the secondary star around the primary. When material is spilled into the Roche lobe of the white dwarf, it thus has an angular momentum with respect to the central star which is high enough so that it will pass by the star's surface on its trajectory in the white dwarf's gravitational field. The velocity is not high enough, however, for the particles to leave the field altogether, so they are deflected into an orbit around the white dwarf. A "hot spot" is formed where the orbit and stream of newly infalling matter collide. Each single particle, were it left alone, would settle down into an orbit around the white dwarf corresponding to the equilibrium between its centrifugal force keeping it away from the star's surface and the gravitational force attracting it. All velocity components perpendicular to the orbital plane of the binary system (which may well be present as the particle enters the Roche lobe) are quickly smoothed out by the primary's gravitational attraction, which increases away from the plane, and thus the orbit will lie entirely in the orbital plane (see equation 4.17). Eventually many particles will orbit around the white dwarf all at (about) the same distance, making collisions and other interactions unavoidable. Thus some viscous mechanism has to be at work which is then able to separate mass from angular momentum: most of the material moves closer to the white dwarf (having less angular momentum), and comparatively little mass — ever less as the distance from the white dwarf increases — carrying most of the angular momentum is transported outward. The original torus spreads out (Figure 4-11).

First attempts to verify these considerations numerically followed the motion of individual particles in the restricted three-body approximation (e.g., Flannery, 1975a). The predicted position of the hot spot was in reasonable agreement with the observations, but more precise predictions were hardly possible. As more powerful computers became available, two-dimensional hydrodynamic computations were carried out to various degrees of sophistication (e.g., Novick and Woltjer, 1975; Lin and Pringle, 1976; Hensler, 1982a; and references therein). Basically, the motion of many individual particles is followed through a geometrical grid which covers the entire Roche lobe; at consecutive time steps each cell is checked for the number and dynamical states of particles in it, some adopted numerical "viscosity" allows for momentum exchange as particles pass close by to each other, and, as ever more mass is fed into the initially empty

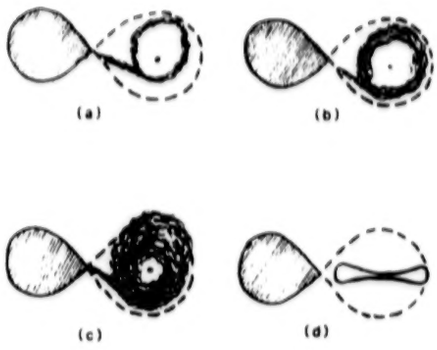


Figure 4-11. Formation of an accretion disc due to mass overflow from the secondary star: initially only a ring is formed, which eventually spreads out and forms an accretion disc; (d) is a side-view of the system (Petterson, 1983).

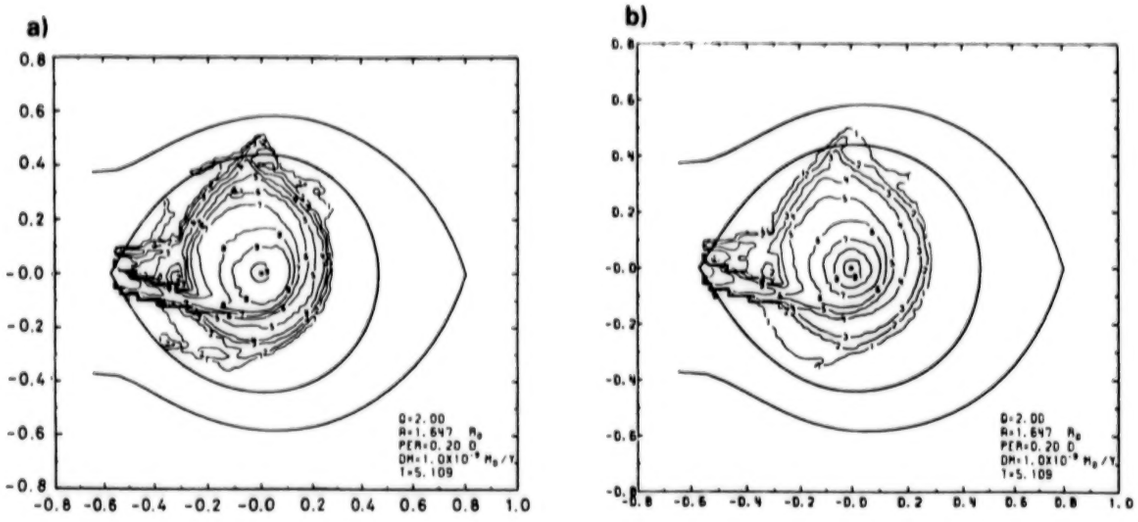


Figure 4-12. Two-dimensional hydrodynamic computations provide information about (a) the column density and (b) the radiation intensity of the accretion disc (Hensler, 1982a).

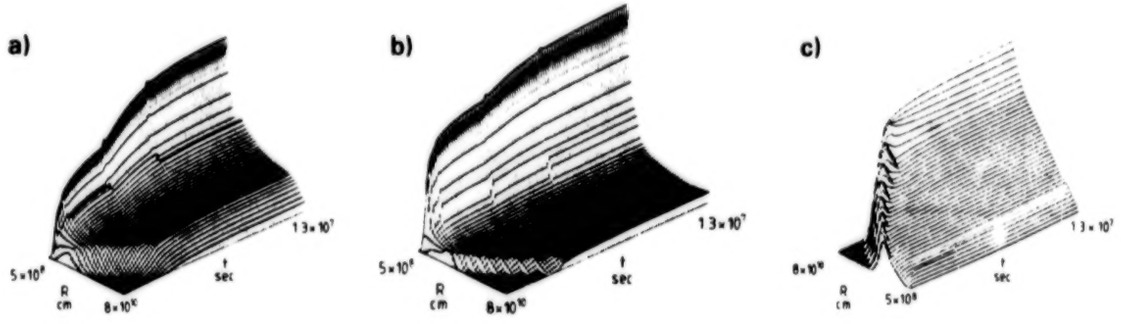


Figure 4-13. Temporal evolution of an accretion disc from first formation to a stationary state at constant mass transfer; displayed are the radius of the disc, the time, and (a) the surface density, (b) the temperature, and (c) the semi-thickness (Bath and Pringle, 1981).

Roche lobe, the process is followed until a stationary state builds up. In this way information about the mass density, the velocity field, and the radiation intensity* are obtained at the same time. Examples of such computations are given in Figure 4-12 for the column density and the radiation field. Similarly, Bath and Pringle (1981) computed the development of the temperature and surface density ($\Sigma = \int \varrho \, dz$) and the geometrical (semi-)thickness of the disc (Figure 4-13). Details about these results strongly depend on the assumptions about the viscosity, but the gross features are represented as expected from the observations.

It is also possible to obtain some approximate information on how much of the mass in the disc is accreted by the white dwarf, and on what happens to the mass that is carrying outward angular momentum. In principle, the alternative for material in the outermost disc areas is to either leave the system carrying away all the angular momentum or, exposed to ever stronger tidal forces by the secondary stars as it moves away from the white dwarf, to feed the angular momentum back into the orbital motion (Lin and Pringle, 1976; Papaloizou and Lin, 1979; Hensler, 1982a). The action of tidal forces on the outer parts of the disc is to try to slow down the rotation and to thus feed angular momentum back into the orbit. Viscosity, on the other hand, tends to counteract this and to make the material leave the Roche lobe, or even the system. With vanishingly little viscosity all angular momentum would be given back to the system, with no tidal forces acting, and 30% to 50% of the originally transferred mass would be lost from the system (Papaloizou and Pringle, 1977). What really will happen depends on the balance of the two, and thus also on the mass ratio between the components, which determines the strength of the tidal forces. Papaloizou and Pringle guess that the amount of mass lost from a typical cataclysmic variable system is on the order of a few percent*.

A hot spot originates where the stream hits the disc and strong velocity gradients occur. This feature is clearly present in all two-dimensional hydrodynamic computations, and it is considered responsible for the hump structure present in the light curves of many cataclysmic variables. More controversial is the geometrical shape and structure of the hot spot and its position in the disc. If a hump is seen at all in a cataclysmic variable light curve, it normally is visible only for about half of the orbital period, i.e., when the system is viewed from behind the hot spot it must be veiled by some material; at any rate the characteristic emerging radiation pattern is highly anisotropic. Furthermore, it is not clear from observations at what distance from the white dwarf the hot spot is located. For clarification of the structure and location of the hot spot, it is essential to know the vertical structure of the accretion disc (perpendicular to the rotational plane), and theoretical details about the hot spot depend very crucially on assumptions made about this structure or, what is almost identical, about the viscosity in the disc.

It is quite possible that the incoming stream penetrates the outer areas of the disc and only is stopped comparatively close to the white dwarf, where the density of the disc material is high enough to stop further penetration. Thus it follows that the actual shock may occur well within the disc far below optical depth one, hidden from direct observations, and that only gradually will the excess radiation find its way to the surface (e.g., Bath et al, 1983a, and Chapter 4.III.C.2).

*At this level of numerical treatment there was still no vertical component included in the computations, and thus no information about the vertical structure could be obtained, but only about the integrated values.

*Observations also lead to the conclusion that not much matter can be lost from the system, since no traces of gas shells have been observed around any system except for novae, which represent a different situation.

Clearly, in any further investigation of the disc structure, and in particular of dwarf nova outburst behavior, it will be necessary to take into account the third dimension of the problem, the vertical stratification of the accretion disc — which will be the issue of the next section.

The viscosity in the disc usually is assumed to be due to shear forces between the differentially (Keplerian) rotating particles in the disc, producing turbulent and/or magnetic interaction. Both are likely to be present in an ionized, rapidly rotating medium — but although this viscosity determines practically everything happening in the disc, no clear concept about its physical nature exists so far.

A kind of "effective viscosity" — the only physical function of which is to allow matter to be accreted by the white dwarf — has been suggested by Sawada et al (1986a; 1986b; 1987), whose hydrodynamic computations show that, under the action of tidal forces, shock waves are formed in the outer areas of an inviscid disc and then travel inwards toward the white dwarf. The gas in the disc loses enough angular momentum in these shocks for accretion to take place without any viscosity due to particle interactions being at work in the disc. Since these ideas are currently quite new, this alternative has not yet been pursued more deeply, so it will not be considered any further in what follows. All other computations of dwarf nova outburst behavior, etc., are based on the assumption of a turbulent viscosity.

III.B THE THIRD DIMENSION

RELEVANT OBSERVATIONS: Common sense says that the disc must be extended to some degree in the vertical direction.

ABSTRACT: Some idea can be obtained about the vertical structure of an accretion disc, assuming hydrostatic equilibrium in the vertical direction and employing the basic equations for stellar atmospheres and interiors. The least understood and at the same time the most important, parameter in the computations is the viscosity.

The hydrodynamic computations of accretion discs described above can provide averaged information about the vertical structure, which is the assumption underlying the computations. In order to obtain a clearer picture about disc properties, it is essential to consider the vertical stratifications. Certain properties of flux densities and surface densities are known from two-dimensional considerations. If prescriptions for the vertical pressure and density stratifications and some viscosity (energy source) are assumed, the normal equations for the computation of stellar atmospheres and interiors provide a vertical structure for each point in the disc when, as a good approximation, a locally plane-parallel approximation is assumed, and the gravitational acceleration is the vertical component of the force exerted by the white dwarf (equation 4.17). The weakest point in this procedure is again the poorly understood viscosity, which is generally assumed to be due to turbulence or small-scale magnetic fields. At present almost any assumption on the viscosity's temperature and pressure dependence, from a simple relation with, say, the pressure ("α-disc") to a very intricate dependence, is equally conceivable and justifiable.

Meyer and Meyer-Hofmeister (1982) carried out detailed computations of this sort. They assumed hydrostatic equilibrium in the vertical direction and the diffusion approximation to obtain the vertical temperature dependence; energy transport in the vertical direction was allowed to occur by means of radiation and convection, whichever was required. In the first models, they adopted a constant α throughout the disc, which was assumed to be proportional to the local pressure (α-disc); alternatively, allowance is made for "magnetic viscosity."

For different values of the mass transfer rate they construct model discs with a constant value of $M_{WD} = 1\ M_{\odot}$. The geometrical shape of the disc surface ($\tau = 1$) is displayed in Figure 4-14. At some radius at the outside of the disc these models become convective, which leads to a flattening of the disc surface; at smaller

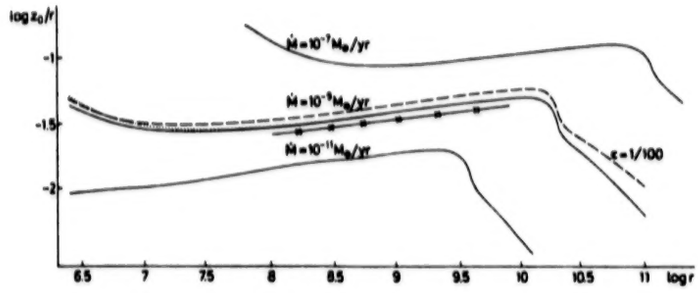


Figure 4-14. Thickness of an accretion disc at the height of the photosphere for various accretion rates as a function of the distance from the central object. The solid and dashed line give results for different viscosities; the crossed line represents computations for the same viscosity as the dotted line, but for a higher central mass (Meyer and Meyer-Hofmeister, 1982).

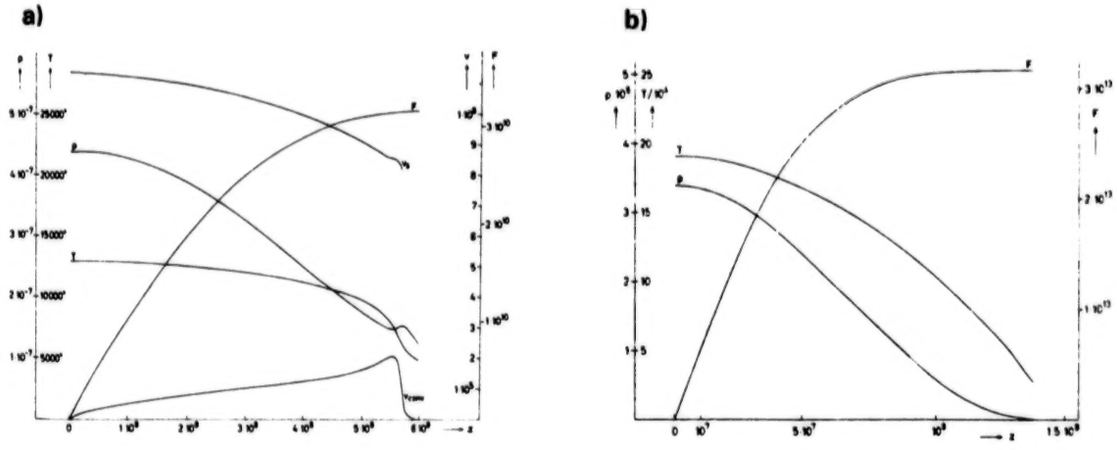


Figure 4-15. Vertical structure of one of the discs in Figure 4-14 i.e., for $\dot{M} = 10^{-9}\ M_\odot$ /yr; solid line, (a) at a distance log r = 10.5 cm, in the outer convective region, (b) at a distance log r = 9.5 cm in the inner radiative region. The course of the temperature, density, radiation flux, and, only in (b), the sound speed and the convective velocity are given as a function of the vertical height in the disc (Meyer and Meyer-Hofmeister, 1982).

radii the disc becomes exponentially thicker with increasing distance from the white dwarf. Figure 4-15 shows the vertical structures for one point in the radiative regime and for one point in the convective regime, respectively.

It turns out from these computations that neither the exact value of the viscosity (keeping the general prescription of the dependence on only the local pressure) nor the mass of the white dwarf have a significant influence on the results (Figure 4-14). The viscosity law however, (in another paper: Meyer and Meyer-Hofmeister, 1983b) turns out to be of decisive influence. In Figure 4-16 the surface density vs. the effective temperature (the so-called *S-curve*) is displayed for essentially identical models (approximately the same as in Figures 4-14 and 4-15), but computed with either constant alpha or with alpha dependent on the ratio of the pressure scale height to the radial distance from the star, demonstrating that the choice of viscosity is a very important factor in the computations. A similar investigation was carried out by Pojmanski (1986), who demonstrates that the chemical abundance and the opacities used have no dramatic influence on the shape of the S-curve — and thus the vertical struc-

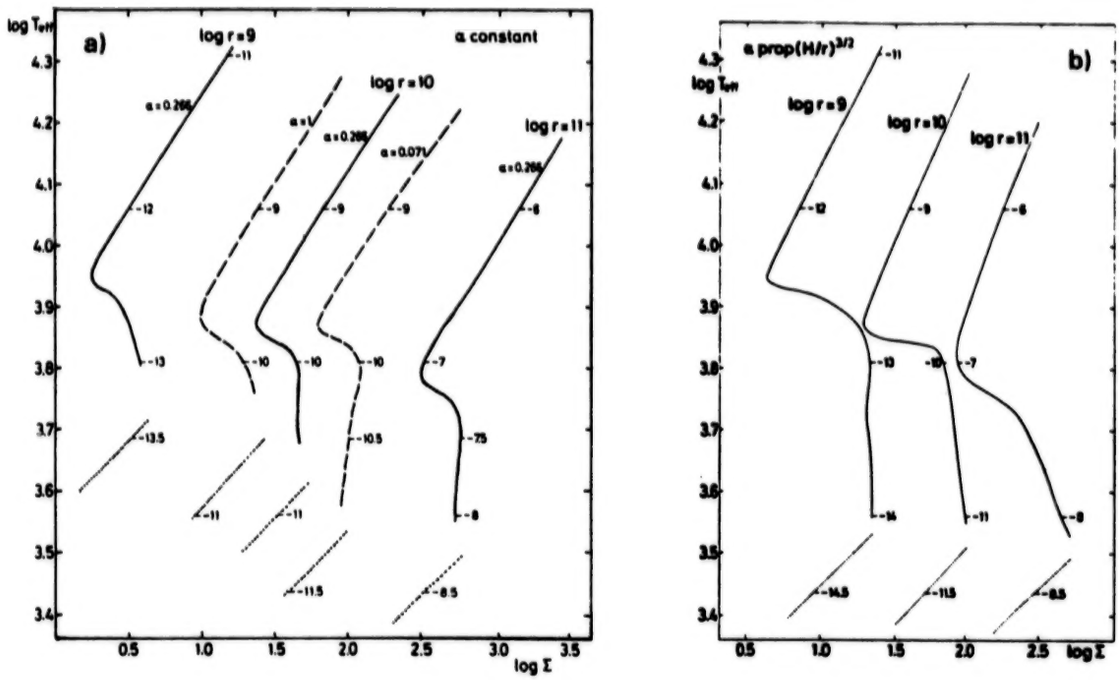


Figure 4-16. Viscosity — surface density relations (S-curves) at different distances from the central object, where models are very similar to those in Figures 4-14 and 4-15. (a): the viscosity parameter alpha is constant throughout the disc; (b): alpha is assumed to be variable as a function of the ratio between the pressure scale height and the distance from the central star (Meyer and Meyer-Hofmeister, 1983b).

ture of the accretion disc — while the choice of the mixing length does.

Observations have led to a general concept of dwarf nova outbursts in which, during the quiescence state, matter is stored in the outer areas of the disc and then released by some mechanism towards the white dwarf during outburst; the sudden liberation of gravitational energy leads to the observed brightening. For a long time no suitable physical mechanism for this behavior could be identified. Then Meyer and Meyer-Hofmeister (1981) pointed out that the double-valued function of the surface density in the log T_{eff} — Σ diagram (the S-curve in Figure 4-16) might be a promising candidate: due to the interplay of viscous heating and radiative or convective cooling the viscosity might jump from being low during quiescence to being high during outburst, regulated through the surface density. This so-called limit-cycle instability is the subject of the next section.

One way to obtain more constraints on possible values and dependencies of α is to compare the predictions of theoretical models with observations. The observations to which the value of α is most sensitive are the outburst light curves of dwarf novae, in particular their timescales, including the duration of the quiescent state and the outburst, respectively, and brightness changes during rise, decline, and quiescence.

III.C. MODELING THE OUTBURSTS BEHAVIOR

RELEVANT OBSERVATIONS: Dwarf novae increase in brightness by two to five magnitudes, in semi-regular intervals of time. Characteristic color changes occur; the rise at optical wavelengths in some objects precedes the rise in the UV by several hours, while in other objects both rise simultaneously. The much slower decline occurs simultaneously in all wavelengths.

see chapter: 21

Two possible outburst mechanisms have been suggested: viscous instability, or disc instability, in the accretion disc itself (Bath et al, 1974b; Osaki, 1974), and a suddenly enhanced mass transfer onto the disc from the companion star, called transfer instability (Bath, 1973; Bath et al, 1974b). Both are discussed in this order in the following sections.

III.C.1. THE DISC INSTABILITY MODEL

ABSTRACT: The general, and to some degree even the detailed outburst light curves can be reproduced, with the assumption that the viscosity follows a hysteresis curve as the disc material changes between the convective and the radiative state.

Bath et al, (1974b) and Osaki (1974) suggested that dwarf nova outbursts might be due to "intermittent accretion," in which times of comparatively low accretion onto the white dwarf, during which matter infalling from the secondary star is stored in the outer disc, alternate with times of enhanced accretion, triggered by some instability in the disc itself. Following this, Bath and Pringle (1982) then suggested that it might be the viscosity which, under certain physical conditions, might have two stable equilibrium values between which the state of the disc can alternate if conditions are right. Because the viscosity ν is responsible for the efficiency of material transport through the disc, this implies that the major changes really are of the surface density (Figure 4-17). For a disc to be stable, the condition $d\nu/d\Sigma \geqslant 0$ must be met (Lightman and Eardley, 1974); if a condition like the one in Figure 4-17 exists, there is a range of viscosity values for which no corresponding stable value of the surface density exists; the consequence is a limit-cycle behavior. Suppose the hypothetical equilibrium value of the viscosity (which would lead to a steady state) were ν_0. An originally low surface density increases up to a value Σ_1 (in Figure 4-17). A further increase in Σ_1 implies a jump in viscosity; since the viscosity ν_1 (this is the condition for the limit-cycle to occur) is higher than ν_0, more material is transported out of this particular region in the disc than is fed in, and thus the surface density decreases until it reaches a value Σ_2. Now a further decrease implies another jump in viscosity, this time, however, to a value ν_2, lower than the equilibrium value ν_0. As a consequence the surface density increases again and the cycle continues, always trying to establish, unsuccessfully, an equilibrium state. Since in accretion discs a higher throughput of mass through a particular area implies a higher temperature, the semi-regular brightness changes in dwarf novae can be understood if somehow this limit-cycle activity would involve the entire disc, or at least a considerable portion of it. If, on the other hand, the mass input into the disc always is high enough to ensure a surface density for which there exists an accessible value of the viscosity to maintain an equilibrium between mass input and mass output, no "outbursts" would have to occur. This case is assumed to apply to UX Ursae Majoris stars and possibly to quiescent novae, while Z Camelopardalis stars and anti-dwarf novae are believed to be boundary cases in which the mass input is mostly just below or just above, respectively, the lower limit for equilibrium, and slight changes in the mass transfer rate from the secondary star have a dramatic effect, by either leading to temporary attainment of an equilibrium or by temporarily pushing the disc out of it.

Meyer and Meyer-Hofmeister (1981) point out that the change in surface density due to ionization of hydrogen (Figure 4-16), i.e., due to the change from a convective to a radiative state of the disc, is a likely candidate for providing the physical background for the limit-cycle activity. Thanks to the opposite temperature dependence of the hydrogen absorption coefficient for neutral and (partly) ionized hydrogen of

$$\varkappa_1 \approx 10^{-36}\, \varrho^{1/3}\, T^{10} \qquad (4.16a)$$

$$\text{for } T \lesssim T_0$$

$$\varkappa_2 \approx 1.5 \times 10^{20}\ \varrho\ T^{-2.5}$$

$$\text{for } T \gtrsim T_0$$

with

$$T_0 \approx 1.2 \times (10^8\ \varrho)^{0.53} \times 10^4, \qquad (4.16b)$$

$$(\approx 10^4 K)$$

(Faulkner et al, 1983) either heating or cooling prevails in the area.

More recently, several groups have carried out computations of the behavior of accretion discs under the assumption that hydrogen ionization is the driving mechanism for the disc instability, and thus for dwarf nova outburst behavior (e.g., Cannizzo et al, 1982; Faulkner et al, 1983; Meyer and Meyer-Hofmeister, 1983b; Mineshige and Osaki, 1983; Papaloizou et al, 1983; Meyer, 1984; Meyer and Meyer-Hofmeister, 1984; Cannizzo et al, 1985; Lin et al, 1985; Mineshige and Osaki, 1985; Cannizzo et al, 1986; Mineshige, 1986; 1988; Meyer-Hofmeister, 1987; Meyer-Hofmeister and Meyer, 1987). Mostly these differ in their assumptions about the viscosity — whether it is assumed to be single-valued all over the disc, whether there are two different but constant values for the radiative and the convective state, respectively, or whether the viscosity is radially or vertically variable in some way — and whether, and how, radial interactions between adjacent parts of the disc are taken into account in the computations. The reader is referred to the original articles for details. It should be stressed, however, that all of these efforts succeeded to some degree in reproducing the general features of the outburst light curves of dwarf novae, in some cases in remarkable detail. Some of these results are presented in what follows.

In general the disc is found to be optically thin in its convective (cool) part, which for "typical" dwarf novae comprises most of the disc. Depending on adopted numerical methods and assumed particular values of the viscosity, the temperature of the outer disc is found to be between 5000 and 6000K (e.g., Papaloizou et al, 1983) or between 2000 and 3000 K (e.g., Cannizzo et al, 1986) over large areas. During the quiescent state the outer disc slowly becomes optically thick, and the temperature rises until an outburst occurs (Figure 4-18).

A very detailed discussion of the physics of dwarf nova outburst cycles based on the disc instability is given in Papaloizou et al (1983). It is found that, depending on details of the physical conditions, the outburst can start in different regions of the disc. A change to the ionized state can start from the innermost disc (called "type 1" by Papaloizou et al, and "type B" by Smak (1984)) if during quiescence all the disc is optically thin and cool, and if the viscosity is large enough for the inner regions to become optically thick first. In this case, the increased temperature heats up neighboring areas to produce a wave of ionization which travels outwards through the disc until the whole disc is in "outburst." If on the other hand α is very small, the material piles up in outer disc areas and cannot be transported inwards efficiently, in which case the outburst starts at intermediate regions, causing two ionizing waves, one traveling outwards (like in the example above) and the other inwards (this is called a "type 2" outburst by Papaloizou et al, and "type A" by Smak). A third type of outburst originates if a sizable fraction of the central disc is permanently fully ionized and transitions are constrained to occur in the outer part only; the outburst is then triggered at the interface between the temporarily cool and the permanently hot region with the transition wave traveling outwards from there on ("type 3").

Corresponding to these three possibilities for initiating an outburst, there are also three ways of stopping it. In "type 1," all of the disc is depleted during the outburst since the mass throughput is higher than the mass input, the outer areas will be depleted first, the

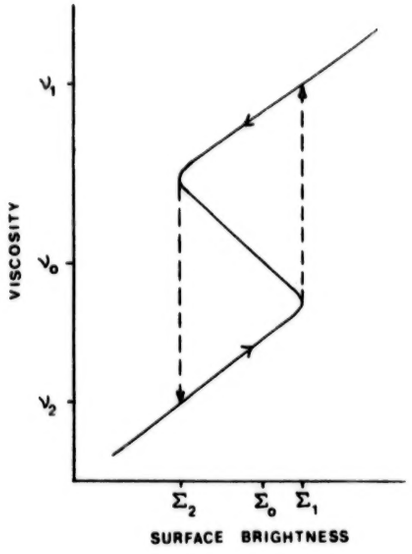


Figure 4-17. Conditions for occurrence of a limit-cycle activity: for the viscosity (ν_0, Σ_0) which would lead to a steady state, there exists no corresponding accessible value of the surface density; conditions in the disc will oscillate about the equilibrium value between (ν_1, Σ_1) and (ν_2, Σ_2) which leads to the observed outburst activity (Bath and Pringle, 1982).

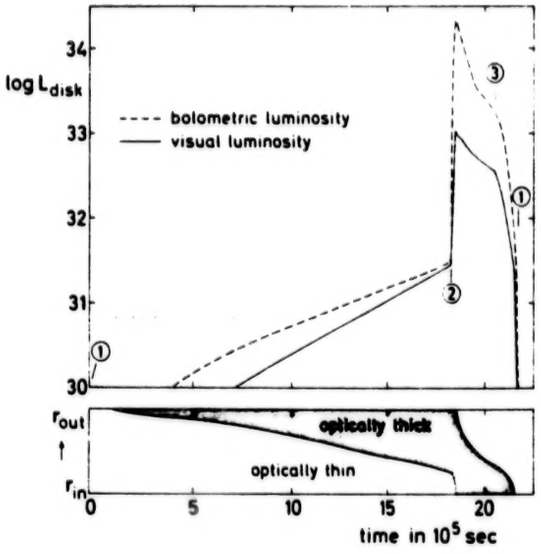


Figure 4-18. Development of the luminosity of the accretion disc and the optical thickness of the disc during the outburst cycle: at the end of an outburst the disc is depleted; in the outer areas it is refilled by material coming from the secondary star and ever larger parts become optically thick, until at some point in the disc conditions for a jump in viscosity are given, which triggers the next outburst (see also Figure 4-23) (Meyer-Hofmeister and Meyer, 1987).

temperature falls below the critical temperature, and the material becomes neutral again. Ongoing depletion in more central areas as well as contact with neighboring cool areas causes a "downward transition" front to travel inwards. If, on the other hand, initially during the rise phase, not all of the outer disc was fully ionized, this cooling front originates at the outer interface between hot and cool areas and travels inward from there ("type 2"). Finally, a "type 3" decay is one during which the cooling wave can travel through only part of the disc, until it meets areas which stay fully ionized during quiescence, because the mass input rate and the viscosity are high enough.

Lin et al, (1985) constructed series of outburst light curves and investigated the influence of various parameters on the appearance of the light curves. They found that the amount of energy which is deposited in the disc at the hot spot, rather than being dissipated into radiation, influences the brightness level during quiescence by changing the general temperature distribution in the disc, but that it has practically no effect on the outburst light curve. Likewise the precise radial location and extent of the region into which matter is fed by the incoming stream (supposing the stream does penetrate the disc for some distance before it is stopped and forced to deposit its mass and energy) has no appreciable effect, unless a part of the disc happens to be very close to the transition to the fully ionized state during quiescence (Figure 4-19a). It is obvious that the outburst light curve is determined to a large extent by the condition in which the disc was left after the previous outburst, so that outbursts of considerably different shape may follow each other, and only sequences of two or more

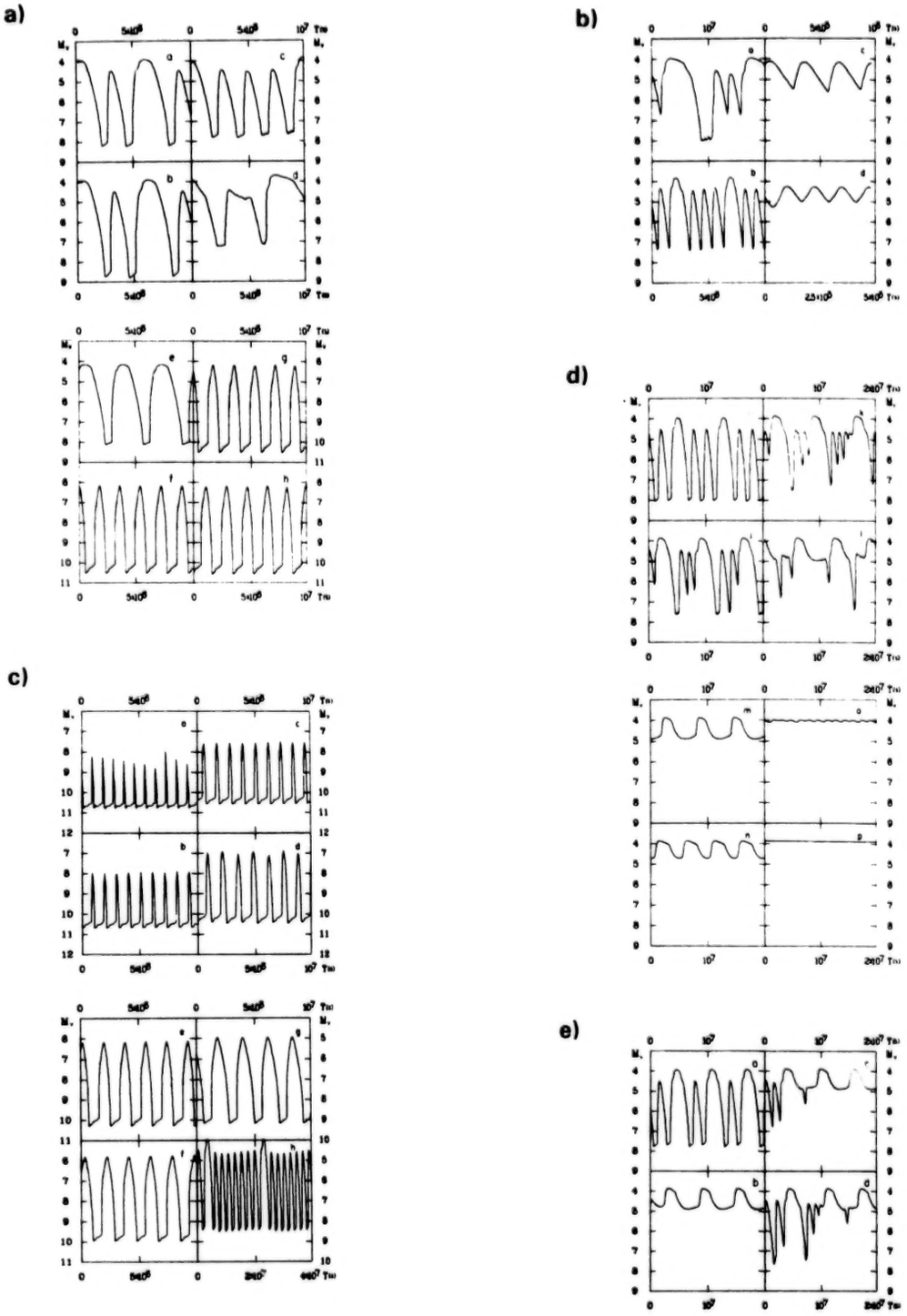


Figure 4-19. Synthetic dwarf nova outburst light curves on the basis of the disc instability model. (a) a-b: Various amounts of energy are inferred into the disc by the hot spot; c-e: effect of location and physical characteristics of the mass stream; f-h: varying the mass input rate from 2.8 100 to 100. (b): Effect of varying the viscosity. (c),(d): Effect of varying the mass input rate (in $M_\odot$/yr): a: $\dot{M} = 9\ 10^{-12}$; b: $1.8\ 10^{-11}$; c: $3.6\ 10^{-11}$; d: $7.2\ 10^{-11}$; e: $1.8\ 10^{-10}$; f: $3.6\ 10^{-10}$; g: $7.2\ 10^{-10}$; h: $1.44\ 10^{-9}$; i: $2.16\ 10^{-9}$; j: $3.24\ 10^{-9}$; k: $3.60\ 10^{-9}$; l: $3.96\ 10^{-9}$; m: $4.36\ 10^{-9}$; n: $5.76\ 10^{-9}$; o: $7.2\ 10^{-9}$; p: $8.64\ 29^{-9}$. (See text for description.) (d): Effect of increasing the mass input during decline from outburst (Lin et al, 1985).

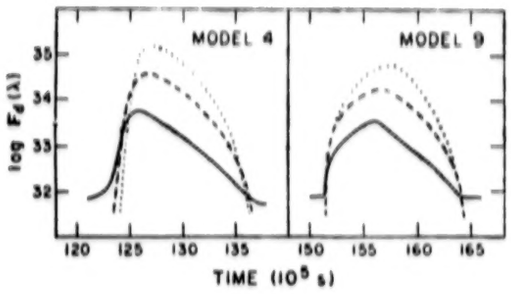


Figure 4-20. If the outburst starts in the outer disc, the rise is fast and it starts later at shorter wavelengths than at longer; if the outburst starts in the inner disc the rise is slow and simultaneous at all wavelengths (Smak, 1984).

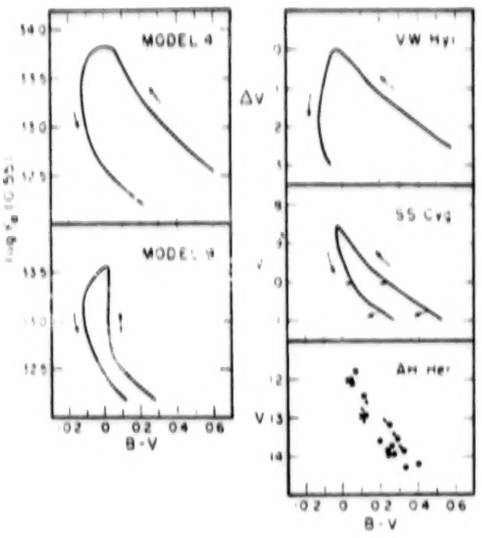


Figure 4-21. Observed and computed color changes during the outburst cycle in the disc instability model (Smak, 1984).

repeat. The shape of the outburst light curve depends very critically on both the adopted value of the viscosity and the mass input rate. In Figure 4-19b, the effect of increasing (each time-constant) viscosity is demonstrated. Very low values of the viscosity result in occasional large, long-lasting outbursts which affect all the disc, followed by a long quiescent time during which the disc has to be refilled; the next large outburst is preceded by a sequence of short low-amplitude bursts, between which the disc does not return entirely to its quiescent brightness level but during which the central area of the disc remains fully ionized. At increased values of the viscosity parameter α the long outbursts become shorter, the short ones become longer and more evenly distributed between the long ones, and the central disc area remains ionized all the time. If the viscosity becomes even larger all proper outburst behavior disappears, first leaving small amplitude brightness oscillations of the outer disc areas, until, at a further increase in viscosity, they disappear altogether.

The effect of increasing the mass input rate, but keeping it constant in each single case, is illustrated in Figure 4-19c. The characteristics of the light curve remain essentially unchanged, for larger ranges of the mass transfer rate while only the amplitude and duration increase, and the frequency decreases, with increasing mass transfer rate. Then suddenly the whole character changes at a certain critical value, as more areas of the disc become only marginally unstable or, finally, remain fully ionized all the time. It is to be emphasized that the appearance of the light curve can change from being very simple and regular to having the most complicated appearance, simply by varying the rate of mass input. Eventually, if all the disc becomes permanently ionized, all activity ceases.

Lin et al, suggest that the basic difference between old novae and dwarf novae may be a different mass transfer rate, a view which is supported by observationally deduced mass transfer rates and absolute magnitudes — see Chapter 4.II.C.3. In their picture, the mass transfer rate in novae is high enough to permanently prevent outburst activity and thus gives the system a larger intrinsic brightness than dwarf novae have Some other old novae like GK Per might then be border cases, being at just the lower end of stability, so that they can undergo small-scale outburst activity at slight variations of the mass transfer rate.

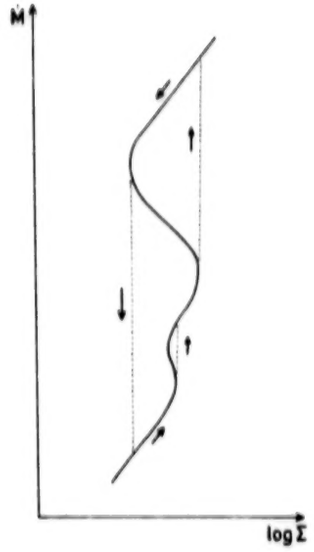


Figure 4-22. Use of molecular opacities mainly changes the appearance of the S-curve in the cool areas of the accretion disc (compare with Figure 4-17) (Meyer-Hofmeister and Meyer, 1987).

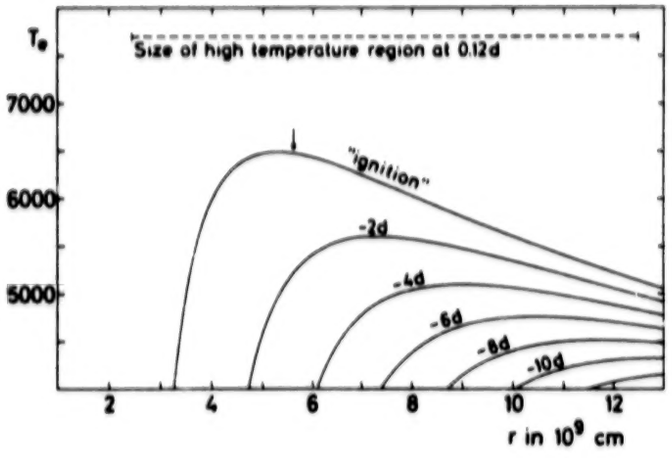


Figure 4-23. Development of the temperature in the outer disc before outburst, corresponding to Figure 4-18. The temperature in the disc rises continuously in ever larger areas of the disc until conditions for an outburst are met at some distance from the white dwarf (Meyer-Hofmeister and Meyer, 1987).

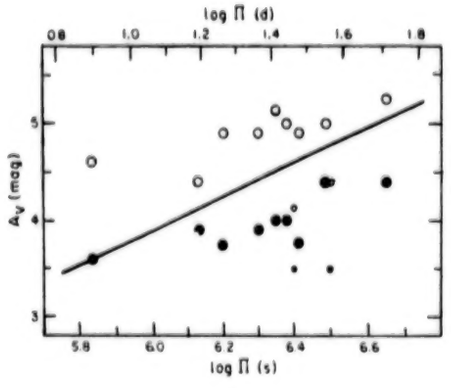


Figure 4-24. The observed vague relation (solid line) between the outburst period and amplitude can be reproduced with the disc instability model; open circles denote models which take into account only radiation from the accretion disc, filled circles take into account contributions from the hot spot as well (Smak, 1984).

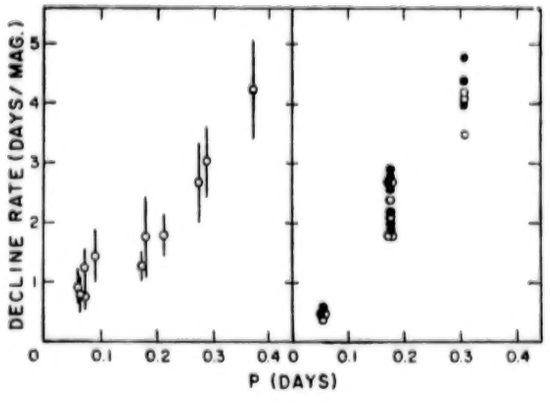


Figure 4-25. The observed relation between the orbital period and the rate of decline from an outburst can be reproduced with the disc instability model; the left panel shows the observed relation, while the right panel gives the results from models (Smak, 1984).

Similarly, nova-like variables can be assumed to lie just above the critical mass transfer rate for outburst activity to occur.

If certain values of the viscosity parameter α or of the mass transfer rate alone can bring about very complicated patterns of the light

curve, it is clear that changes of the mass transfer rate at some stage during the outburst cycle can also produce patterns of any degree of intricacy (Figure 4-19e). Temporary standstills entered from either a high or a low brightness state, as observed in Z Camelopardalis variables, can also easily be produced.

In all the above examples, α was kept constant throughout the activity cycle. In fact the calculated light curves only resemble the observed light curves in their general appearance. The observed feature of a much steeper rise than decline cannot be fitted in this way. Most other authors assumed a small value of α during quiescence and a much larger one during outburst (ionization). Under this assumption it is possible to fit either a fast or a slow rise (as compared to decline), if the outburst starts either at the outer (type A or 2) or at the inner (type B or 1) disc (Figure 4-20). Even the observed delayed rise at shorter wavelengths in the case of fast rises and the simultaneous rise at slow rises are reproduced with the correct time scales (see also Cannizzo et al, 1986). Similarly, optical color curves derived for the outburst behavior clearly do resemble the observations (Figure 4-21).

From the above results it appears that the observations probably best suited for distinguishing between different α prescriptions is the early rise phase. Meyer-Hofmeister (1987) and Mineshige (1988) carried out investigations of this phase, particularly with respect to the influence of molecular opacities on the surface density. Meyer-Hofmeister (1987) found that the characteristic curve at very low temperatures might indeed be more complicated than assumed so far (Figure 4-22) in exhibiting an additional halt in the limit-cycle $T_{eff} - \Sigma$ curve. The effect is that shortly before the actual rise to outburst the transition to the intermediate point occurs, resulting in a slow brightness increase during which a considerable area of the disc will be heated up to some 6000 - 7000 K. Only after this (Meyer-Hofmeister's results show a steady rise for some 5 to 10 days, Mineshige's results show a halt for about 1 day) does the actual rise occur (Figure 4-23, see also Figure 4-18) — in the case of the outburst starting from the outer disc.

Smak (1984) compared two observed relations concerning dwarf nova outburst behavior with his models: a vague relation between outburst period and amplitude (Figure 4-24), and the relation between the orbital period and the rate of decline from an outburst (Figure 4-25 — see Chapter 2.II.A.3. Both theoretical relations are in reasonably satisfactory agreement with the observations.

Similar disc-instability computations have been carried out for the hydrogen-deficient AM Canum Venaticorum variables as for "normal" hydrogen rich cataclysmic variables (Cannizzo, 1984; Smak, 1984). They find that dwarf nova-like outburst behavior due to He-ionization instability is quite possible in these objects as well. The disc temperature during quiescence is found to be of the order of 10000 K, and the disc is marginally optically thin. At outburst, Cannizzo (1984) found temperatures between 20000 and 50000 K in the disc. The system brightness rises by about 2 - 3 mag with an outburst period between 16 hours and some 10 days (in his computations), a value which is very critically dependent on the assumed mass transfer rate.

III.C.2. THE TRANSFER INSTABILITY MODEL

ABSTRACT: This alternative model assumes that instabilities in the atmosphere of the secondary star lead to temporarily increased mass transfer into the disc, which then causes the outburst. Modeling the observed brightness changes also yields satisfactory results.

In the above section, the cause of a dwarf nova outburst was assumed to be variable conditions in the disc itself, while the mass transfer rate was usually assumed to be constant with time. At any rate it influenced the outburst

behavior only rather indirectly. Alternatively, it has been suggested (Bath, 1973; Bath et al, 1974b) that the outburst might be due to an instability in the Roche lobe-filling companion star which leads to a temporarily increased mass transfer into the disc. This latter possibility has been pursued by Bath and co-workers (Bath, 1975; Papaloizou and Bath, 1975; Bath, 1976; 1977; Bath and Pringle, 1981; Bath et al, 1983b; Mantle and Bath, 1983; Bath, 1984; Bath et al, 1986).

The basis of this theory is the realization that the dynamic equilibrium of a star which is confined to a Roche lobe is quite different from that of a single isolated star, once the star's surface comes close to the confinement of the critical Roche surface (Bath, 1975; Papaloizou and Bath, 1975). The important difference is that the energy required for material to escape the surface of a single star must be sufficient for the material to reach infinity, while in the case of a Roche lobe it is sufficient to lift it only above the critical Roche surface, which requires a lot less energy. Papaloizou and Bath point out that there are two possible destabilizing effects in the confined atmospheres of a cool star: convection in the envelopes, and ionization zones in the vicinity of L_1 at which point the net gravitational acceleration is zero.

The general idea of the transfer instability is that once the atmosphere of the secondary star becomes unstable in the vicinity of the Lagrangian point L_1, enhanced mass overflow into (mainly) the Roche lobe of the white dwarf occurs, leading to an outburst and at the same time depleting the atmosphere. It stops when the energy provided by the instability is no longer sufficient to lift further material into the neighboring Roche lobe (Bath, 1976). Since this process has brought the star out of thermal equilibrium, the star contracts and detaches from the Roche surface, while during its "quiescent" state mass overflow is maintained only on a low level through normal stellar wind. Eventually, with the support of energy supplied from deeper stellar layers, thermal equilibrium is gained again, and the star expands and is ready for the next instability to occur.

Computed outburst periods (i.e., relaxation times of the destabilized atmospheres) are in the range of 10 to 200 days, mass transfer rates during outburst maximum are on the order of 10^{17} to 10^{19} g/sec and amplitudes are of several magnitudes — all in accordance with observed values.

Since a lot of material with low angular momentum is transferred into the disc, during the initial phases of an outburst the disc radius is expected to shrink as this new material mixes with material that is already contained in the disc, and only later does it expand again as angular momentum from the inner disc is transferred outward (e.g., Bath and Pringle, 1981). This prediction is quite in contrast to what the disc instability model predicts, namely, an increase in the disc's radius from the very beginning of an outburst if the outburst starts at the outer disc, or no change at all if it starts at the inner disc. Thus, in principle, it should be possible to decide between the two models from investigation of the outer disc radius, but since the outermost disc may be optically thin, determinations of the disk radii are not reliable.

Equally, an increase in the intensity of the orbital hump would be expected from enhanced mass transfer, while no effect should occur in the case of the disc instability. Here again the problem arises that neither the shape and position nor the geometrical radiation pattern of the hot spot are known. It is possible that the enhanced mass flux disappears entirely in the disc at the beginning of an outburst, while the excess radiation only eventually diffuses outward; and if the radiation pattern which originates then is rather isotropic, no enhanced hump would be seen at all — or, if this radiation is anisotropic, the enhanced hump may become visible with considerable delay (Bath et al, 1983b).

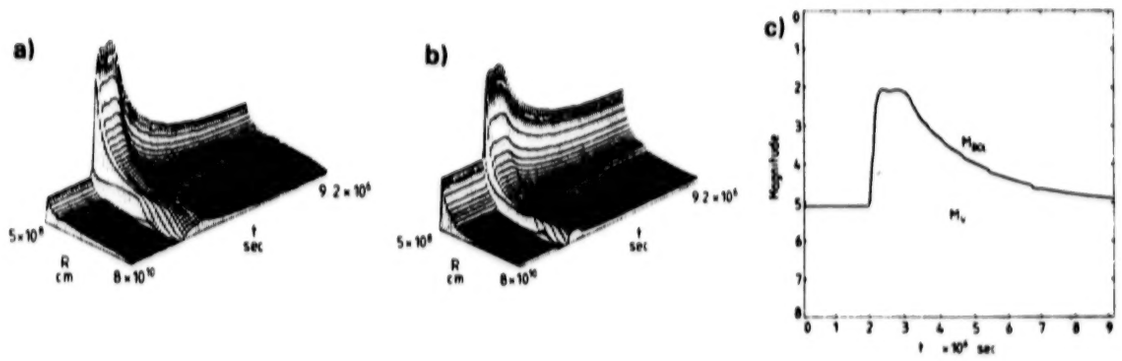


Figure 4-26. Temporal evolution of the accretion disc in response to a mass pulse: (a): evolution of the surface density; (b): evolution of the central disc temperature (at z = 0); (c): corresponding synthetic light curve (Bath and Pringle, 1981).

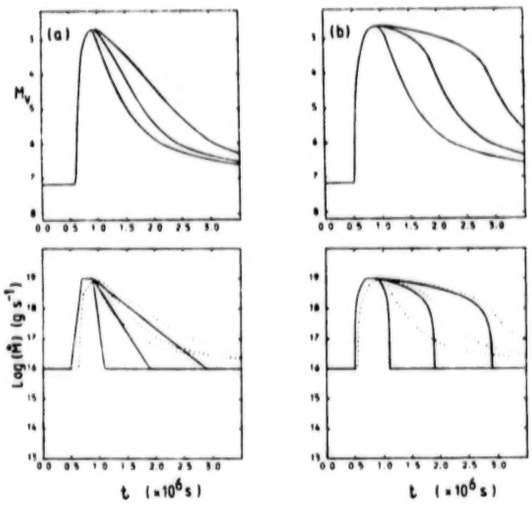


Figure 4-27. The typical shapes of dwarf nova outburst profiles (solid lines) can roughly be reproduced with the transfer instability model; different profiles can be obtained when the strength and duration of the mass pulse are changed. Dotted lines represent the accretion rates on the white dwarf. Occurrence of disc instabilities is numerically prevented (Bath et al, 1986).

The general course of an outburst induced by a transfer instability is shown in Figure 4-26: The mass pulse leads to a brief contraction of the radius, then the disc spreads out while its temperature increases, and the disc slowly relaxes to its equilibrium state; the corresponding outburst light curve is shown in Figure 4-26c.

A systematic investigation of theoretical outburst light curves has been carried out by Bath et al (1986). In their computations the mass burst profile is a free parameter, since knowledge of the atmospheres of the cool companions is not sufficiently detailed to make meaningful predictions. By appropriate choices of the pulse profiles they are able to reproduce gross features of the outburst light curves (Figure 4-27). In general they find that the rise is fast, following essentially the rise time of the mass flux, if the time-scale for the rise in mass transfer is shorter than the viscous time scale of the disc, while the whole behavior follows only the mass flux variation if the variations are slower than the viscous time scale of the disc. In particular, very long-lasting outbursts can be produced if the mass transfer goes on for a long time. For all these computations a viscosity parameter of $\alpha = 2$ was assumed and numerically any ionization instability was

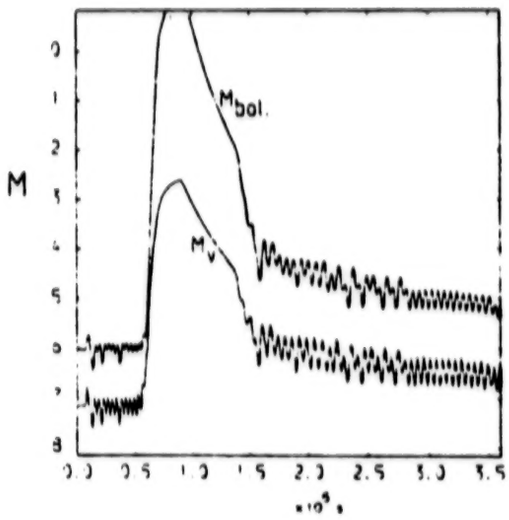


Figure 4-28. When disc instabilities are allowed for, they lead to a flickering-like activity during quiescence but not during outburst (Bath et al, 1986). When compared with Figure 4-19, this might be due to the large alpha used in these models.

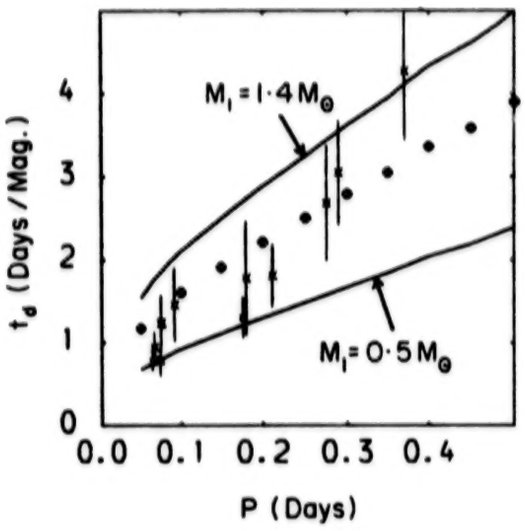


Figure 4-29. As in the case of the disc instability model, the observed relation between decay time and orbital period can be reproduced with the transfer instability model (Mantle and Bath, 1983).

prevented from occurring, so the effects of the transfer instability alone would be visible.

Suppression of the disc instability was abandoned in a further step of the investigation (Bath, 1986). Given the high value of alpha and the mass transfer rate of 10^{16} g/sec ($=1.6\ 10^{-10}\ M_\odot$/yr), not surprisingly*, during quiescence, minor instability fluctuations were found to occur, which tentatively were interpreted as the origin of the flickering, while during outburst all this activity was totally damped out (Figure 4-28).

In the case of the transfer instability model, the explanation for the vague relation between outburst amplitude and time for the next outburst to occur (Kukarkin-Parenago relation, Chapter 2.II.A.3) finds a natural explanation, since the more depleted the secondary's atmosphere is during the outburst, the more time it is likely to take to recover. As in the case of the disc instability model, the observed relation between outburst decay time and orbital period (Bailey relation, Chapter 2.II.A.3) is reproduced in a fairly satisfactory way (Figure 4-29), due to the longer relaxation time of larger accretion discs in longer-period systems.

III.C.3. CONCLUSIONS FROM OBSERVATIONS

ABSTRACT: From comparison with observations no clear distinction between the two proposed outburst models is possible so far.

Since the disc instability model and the transfer instability model do not produce the same light curves, it should be possible to distinguish between them by comparing theoretical results with observations. Pringle et al (1986), Verbunt (1986), and Cannizzo and Kenyon (1987) tried to do this in a systematic way. In particular, Pringle et al compare observed optical and UV flux changes which occurred during rise to an outburst in VW Hyi and CN Ori with predictions by various models

*This is in view of results described in the previous section where such a high value of the viscosity reduced all outburst activity to mere small-scale brightness fluctuations

(Figure 4-30). In VW Hyi, a delay of the rise in UV with respect to the optical of about half a day is observed, while in CN Ori the rise proceeds simultaneously in all wavelengths. The decline in both systems is simultaneous in the optical and in the UV.

Adopting parameters suited for these two systems, Pringle et al find that the rise phase of VW Hyi cannot be modeled satisfactorily with a disc instability, whether it is starting from the inner or from the outer disc. In light of results presented in Chapter III.C.1, it would be expected that an instability in the outer disc would produce such a delay, but in their computations the temperature in the outer areas rises far too quickly to produce a delay of the order required. In the case of CN Ori, an instability in the inner disc can produce reasonably acceptable agreement with the observations. For both systems, the observed flux development can be reproduced by suitable choice of the mass flux profile which, given the uncertainties in that theory, is no surprise. In any case the decline depends only on the relaxation of the disc, so it is fitted about equally well by all three models, though the decline proceeds somewhat too fast in the transfer instability computations.

Cannizzo and Kenyon, on a more general basis, arrive at similar conclusions. All authors note, however, that these results do not imply a failure of the disc instability model, given the large uncertainties in the prescription of the viscosity and its dependence on other physical parameters. The only reliable conclusion one can arrive at, then, as Pringle et al point out, is that the dependence of α on local physical conditions certainly is neither simple nor universal if the disc instability is the mechanism for driving dwarf nova outbursts.

Since the decline process is more or less the same for all possible types of outburst, the rise phase to the outburst, if anything, should provide distinctive evidence for one model or the other.

The outer disc radius is predicted to shrink slightly at the very beginning of an outburst in the case of a transfer instability, while in the case of a disc instability it either increases (if the outburst starts in the outer disc) or remains unchanged (if it starts in the inner disc). In all cases it is expected to increase around the phase of outburst maximum and slowly shrinks as decline proceeds, so excess angular momentum can be carried away efficiently. It is questionable whether this predicted shrinking is observable. It may not occur at all if the stream material penetrates deeply into the disc, or it may occur only for a very short time and not be very pronounced, so it clearly could escape the observations. If shrinking could be observed without any doubt in a system, it would exclude the disc instability as the cause of the outburst, at least for this particular (hypothetical) system.

An indication in favor of the disc instability would probably be the observation of the predicted halt in brightness at about 6000 K for up to half a day at a level slightly above the quiescent brightness level before the real rise to the outburst occurs, as predicted by Meyer-Hofmeister (1987) and Mineshige (1988).

As discussed above, the behavior of the orbital hump cannot currently provide the basis for distinguishing between models, since it is not known how deeply the mass stream penetrates into the disc and how isotropic or anisotropic the characteristics of the outgoing radiation are. In particular, the hump size is not a useful discriminant, since it is quite possible that, as soon as the outburst starts, triggered by a disc instability, the secondary star is heated by irradiation and itself reacts with increased mass transfer, leading to a delayed increased hump (as is also expected from the deeply penetrating original mass transfer pulse). Conversely, it also is perceivable that a transfer instability triggers a disc instability, so again both effects become interwoven. The fact that in some objects all kinds of different shapes of outburst light curves are observed certainly indicates that the underlying physics is not trivial or straightforward.

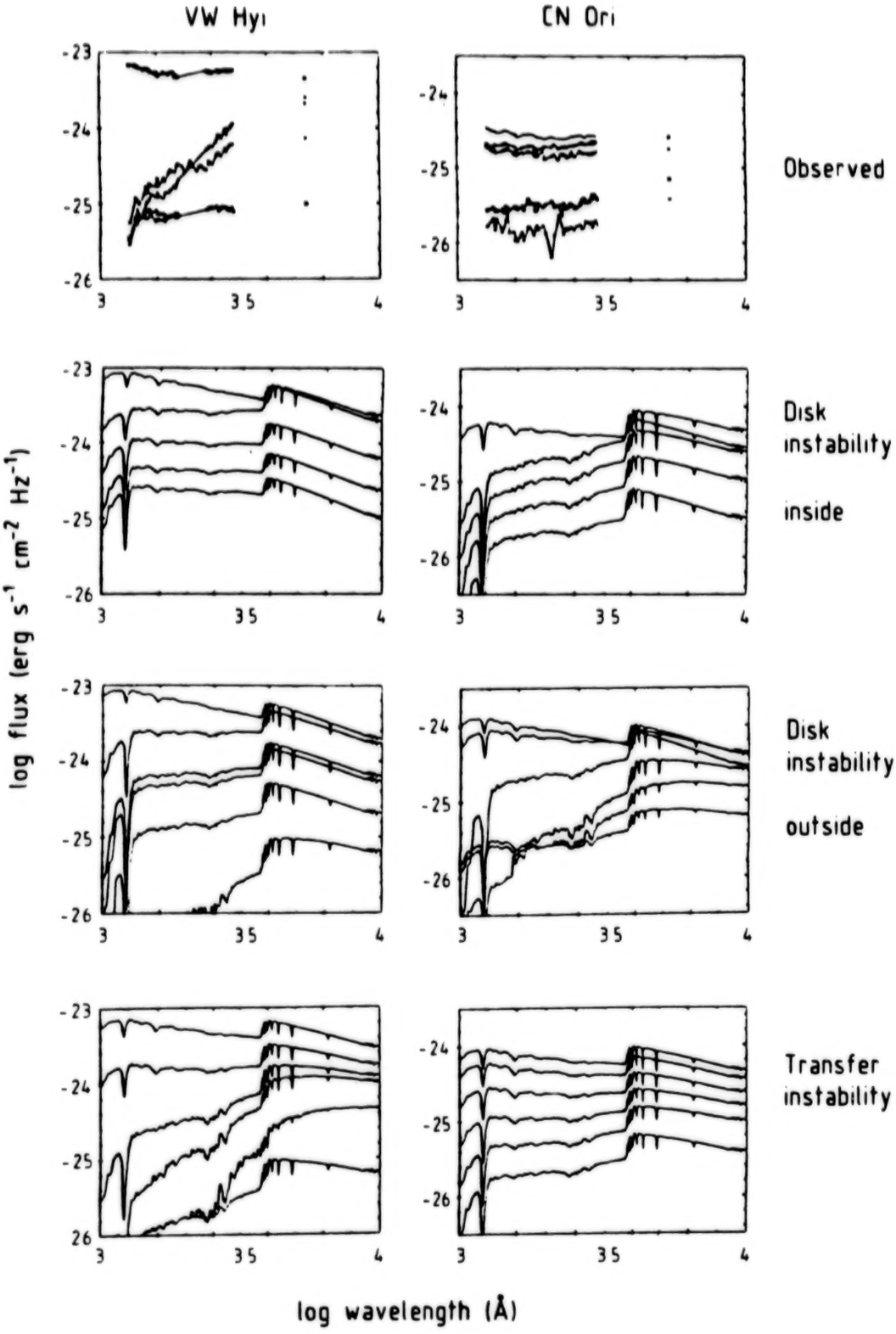


Figure 4-30. Comparison between observed and various computed spectral changes during rise to an outburst (see text for discussion) (Verbunt, 1986).

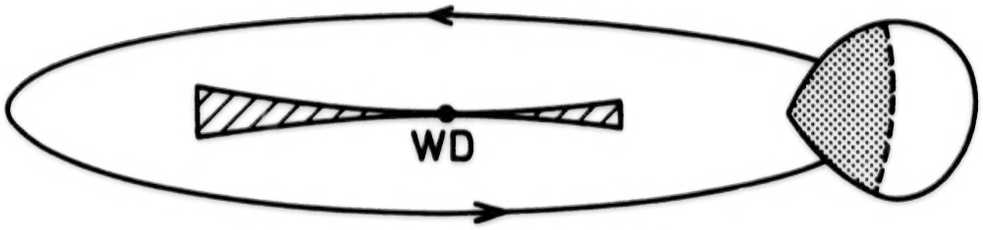


Figure 4-31. Schematic model for a precessing elliptic disc. This model for a superoutburst combines characteristics of both the disc instability and the transfer instability model; a precessing eccentric disc can explain the photometric phenomena observed during superoutburst (Osaki, 1985).

III.C.4. SUPEROUTBURST MODELS

RELEVANT OBSERVATIONS: In some short-period dwarf novae, besides the normal outbursts, so-called superoutbursts are observed which are about one magnitude brighter and last considerably longer than normal outbursts. A number of characteristic phenomena are observed only during superoutbursts.

see 28

ABSTRACT: No single generally accepted model exists so far. The most promising of the current models combines features of the disc instability and the transfer instability which lead to a temporary deformation of the accretion disc.

Since the detection of superhumps occurring during superoutbursts in certain dwarf novae, the SU Ursae Majoris stars (Vogt, 1974; Warner, 1975), almost a dozen models have been developed to explain this phenomenon and other related phenomena, ranging from strongly magnetic rotating white dwarfs (Papaloizou and Pringle, 1979; Patterson, 1979b; Vogt, 1979) to flux tubes emerging from the surface of the secondary star and then connecting with the disc (Meyer, 1979), spots on the surface of the cool star (Vogt, 1977; Haefner et al, 1979), eccentric discs surrounding an inner concentric disc (Vogt, 1982b), outer eccentric discs (Gilliland and Kemper, 1980) and the response of a moderately strong magnetic white dwarf to a variable mass transfer rate (Warner, 1985). Vogt (1982b) and Warner (1985) present and discuss most of these models and show why almost all of them are unable to account for all, or even the most important, of the observed phenomena. There is no need to repeat this here. We will concentrate on only those few models which have survived to date.

Currently there are only two such models which seem plausible. The first was proposed by Papaloizou and Pringle (1979). They suggest that the orbits of SU Ursae Majoris stars are slightly eccentric ($e \approx 10^{-4}$). Due to the then variable distance between the two stars, the size of the secondary's Roche lobe is also slightly variable, which leads to a variable mass transfer rate with the precession period of the line of absides. If dwarf nova outbursts are caused by a disc instability, the mass transfer rate normally should not be influenced by this, so no major effects are expected on the hump amplitude either. Only if an outburst induces an increase in the mass transfer rate as well (e.g., due to a periodic instability of the secondary's atmosphere), do the mass transfer rate, and thus the hump amplitude, strongly vary with the precession period. Papaloizou and Pringle show that such an eccentricity is expected to be driven and maintained by tidal forces, particularly in systems with a large mass ratio (which is the case for all SU Ursae Majoris stars). The difficulties with this model are that neither the variable γ-velocity nor the late superhump find a satisfactory explanation.

A somewhat related model has since been suggested by Osaki (1985). He assumes a circular orbit and an accretion disc which undergoes outbursts due to a disc instability. The secondary star normally transfers material at a relatively low rate into the Roche lobe of the white dwarf. If the secondary is very cool (as is the case in the ultra-short period systems with periods less than 2 hours, since the Roche lobe is too small to accommodate a larger star), the star's atmosphere reaches a certain degree of instability semi-periodically. When a normal outburst occurs at about the same time this instability is reached, then during the outburst the hot disc and boundary layer bring the cool atmosphere out of equilibrium by irradiation, and for some time mass transfer proceeds at an enhanced rate. The first sudden pulse of mass causes a non-axisymmetric perturbation of the disc which deforms it into an eccentric shape (Figure 4-31). For some time, the stream impact and energy release always are much stronger when the stream hits the disc near periastron (closer to the white dwarf), thus maintaining the elliptical shape and producing a stronger hump as long as the enhanced mass transfer lasts. Since the disc precesses with some period, the observed superhump period is slightly longer than the orbital period, and the observed decrease in superhump period can be explained as due to a slight continuous contraction of the disc which leads to a somewhat enhanced precession period. Once the mass reservoir of the secondary is exhausted, the mass transfer rate returns to normal (causing the fast decline from superoutburst) and the disc relaxes to a circular shape, during which the late superhump (with the correct phase shift or about 180° in Osaki's computations) is visible.

III.D. RAPID OSCILLATIONS

RELEVANT OBSERVATIONS: During the optically high state (outburst) of some dwarf novae and some nova-like stars, low-amplitude brightness fluctuations with periods of typically some seconds to some minutes and coherence times between a few cycles and several hundred cycles can at times be observed.

see 56, 98, 106

ABSTRACT: Due to the short periods and low stability, the origin of the oscillations has to be placed either on the outermost surface of the white dwarf or in the innermost areas of the accretion disc. No satisfactory model is available as yet.

Rapid brightness variations on time scales of some 10 to 100 seconds have occasionally been observed in many dwarf novae during outburst, as well as in several nova-like systems during the high brightness state (Chapters 2.II.D.2., 3). The emerging picture is very confusing. Conventionally, a distinction is made between coherent and quasi-periodic oscillations, but it is by no means clear whether this reflects any real physical differences underlying the observed phenomena.

Likewise, the theoretical understanding is not very advanced. Patterson (1981) summarizes and comments on most of the suggested scenarios. The very short observed periods place the origin somewhere on, or in the vicinity of, the white dwarf (i.e., clearly the secondary star can be discarded as a possible source). Furthermore, the short coherence times and the period changes point to only very little mass being involved in the process.

The latter constraint excludes rotation of the white dwarf as the source, since there is no way to change its period on time scales of hours, and the oscillations clearly cannot be due to a spotty surface of the white dwarf due to magnetic fields. If the surface were rotationally decoupled from the white dwarf's interior (Paczynski, 1978) the hypothesis could possibly be saved from a dynamical point of view, but the question remains why no pulsations are seen during quiescence in those systems (e.g., HT Cas, Z Cha) which during quiescence seem to be dominated by the radiation from the white dwarf.

Non-radial pulsations (g-modes) of the white dwarf have been suggested as a possible source by several authors (e.g., Faulkner et al, 1972;

Osaki and Hausen, 1974). The problem with these pulsations is, as Papaloizou and Pringle (1978b) point out, that the observed changes in period and amplitude require energies and time-scales that are far too high for a cataclysmic system. Papaloizou and Pringle conclude, however, that when the rotation of the star is properly taken into account, another kind of non-radial oscillations, which they call r-mode oscillations, are confined to only the outermost surface layers of the star and could be responsible for the observed oscillations. Even so, the resulting phase coherence may still be orders of magnitude larger than observed (Córdova et al, 1980).

The latter authors tentatively place the origin of radial pulsations in the boundary layer between the disc and the white dwarf. Variations of the thickness and structure of the boundary layer would lead to changes in the period and amplitude of the pulsations.

Bath (1973) suggests inhomogeneities in the inner accretion disc as they might originate during outburst as possible source of the observed oscillations. They are periodically eclipsed by the white dwarf as they rotate; after a while they would dissolve and others would originate at slightly different radii. Radius changes would bring about period changes, as the inhomogeneities presumably rotate with Keplerian velocity. The large amplitudes and the long time scales of some of the observed oscillations seem problematic, as well as why always only one such blob should be visible.

Similarly, Sparks and Kutter (1980) invoke waves of turbulent condensed material produced in the process of accretion onto the white dwarf as the source for oscillations in dwarf novae. Again the question arises why only one such wave should be present at a time, and how its (often) long lifetime can be explained, and why these waves are not observable during all outbursts of all dwarf novae and in all nova-like systems with high mass transfer rates.

The most recent model by Tajima and Gilden (1987) supposes the reconnection of small-scale magnetic fields generated in the inner disc to be the physical cause of the oscillations. The problems here are identical with Sparks' and Kutter's model.

In general it seems safe to conclude that the radiation source of the observed short-period oscillations and pulsations is to be sought somewhere in the area of the inner disc, boundary layer, and/or white dwarf. Since this probably is the very region in a cataclysmic system where the physics and structure are least understood, there seems to be no real hope of improving our knowledge of the oscillations in dwarf novae until a better physical understanding of that part of the system is gained. The hope that observations of the oscillations might set limits on possible models of, in particular, the boundary is clearly greatly diminished by the totally confused picture the observations currently present.

III.E. SECULAR VARIATIONS OF THE ORBITAL PERIOD

RELEVANT OBSERVATIONS: Secular changes of the orbital period have been measured in several dwarf novae and nova-like stars. In some objects these changes seem to be semi-periodic with time scales on the order of 10 years or more.

see 45, 98, 111, 115

ABSTRACT: Several possible explanations have been suggested. None of these provide a satisfactory explanation of the observed phenomena. It is possible that a good deal of the changes are artifacts of numerical manipulation.

Observed secular changes in the orbital period of some cataclysmic variable systems have been reported. In principle, several mechanisms can be imagined to cause a change in the observed orbital period: the presence of a third (unseen) body in the system, rotation of the line of absides, loss of angular momentum and/or mass from the system, redistribu-

tion of mass and/or angular momentum within the system, motion of the relative position of the hot spot with respect to the other system components, or any combination of these mechanisms. In addition, it ought to be kept in mind that the determination of the orbital period is by no means trivial, and results must be scrutinized very carefully before it can be concluded that the period is variable at all. As the example of the photometric observations of CN Ori (Chapter 2.II.B.3) demonstrates, it is not necessarily possible to derive a reliable orbital period from the light curve of a non-eclipsing system; and if an eclipse is present, it is not obvious what is being measured, say, at the deepest point or at mid-eclipse, since the shapes of eclipses are known to be variable, and slight changes can be misinterpreted as period changes. Only the moment half-way between white dwarf/boundary layer ingress and egress of double eclipsing systems seems to give a stable reference point; the radius of the white dwarf is a stable feature, and, if a boundary layer is present, it is likely to be both thin (compared to the dimensions of the white dwarf) and symmetric in the rotational plane, which is what is observed in double-eclipsing variables. Finally, care must be taken of light travel times and leap seconds. Spectroscopically determined orbital periods (from radial velocities) which are sufficiently accurate have been available only for some 15 years and thus do not provide a sufficiently long time basis. Also some care must be taken in combining photometric and spectroscopic data, since for some objects (e.g., TT Ari, possibly CN Ori) these are different, for as yet unknown reasons. In view of all this, none of the published results of orbital period changes seem particularly reliable, for one reason or another. However, for the sake of theoretical considerations, published values are taken at face value in what follows.

To most of the published O-C data a parabolic as well as a higher order function, or even a part of a sine curve, can all be fitted about equally well, because too few points are known. In cases where observations are clustered about few epochs with no single observations in between, occasional occurrences of sudden changes rather than continuous changes cannot be excluded.

In three of those objects which have been observed for a long time (U Gem, UX UMa, DQ Her), the change in the orbital period has been seen to invert its direction; time scales are on the order of 15 years for U Gem and DQ Her, and 29 years for UX UMa. Time bases are still too short to allow for a decision on whether the changes are really periodic or merely semi-periodic. The data in the O-C diagram of U Gem (Figure 2-45) significantly deviate from a tentatively fitted sine curve. In the case of UX UMa there is no longer any support for a 29-year periodicity to be present in O-C. So far, no such conclusions can be drawn for any other object for lack of observational data.

Several mechanisms have been suggested to explain period changes in cataclysmic variables. To date, however, not a single one can be identified that seems likely to work. Among those mechanisms suggested is a third body circulating the cataclysmic system (Nather and Robinson, 1974; Patterson et al, 1978b) by means of which strictly periodic period changes could be explained in principle. However, besides the fact that this kind of change is not what is observed, constraints on the mass of this hypothetical third body are unreasonably high for it to be a likely explanation for many systems. Rotation of the line of apsides (Patterson et al, 1978b) again would produce strictly periodic period changes, and, in addition, the predicted time scales are on the order of months rather than decades. Redistribution of mass within the system, or loss of mass and/or angular momentum from the system (Pringle, 1975) all lead to only either a period increase or a period decrease, but clearly not to any kind of cyclic or even periodic changes. The only mechanism considered so far which might be able to explain non-monotonic changes of the

orbital periods is changes of the relative position of the hot spot in the system, though no explanation has been offered why this should happen on time scales of tens of years.

III.F. MAGNETIC ACCRETION

III.F.1. STRONGLY MAGNETIC SYSTEMS — AM HERCULIS STARS

RELEVANT OBSERVATIONS: In this class of objects photometric (at all observable wavelengths), spectroscopic, and polarimetric changes all occur with the same period.

see 125

ABSTRACT: The current model envisions a strongly magnetic, synchronously rotating white dwarf which prevents the formation of an accretion disc, so accretion occurs through magnetic funnels along the field lines.

There is a class of cataclysmic variables which exhibits very strong linearly and circularly polarized, Zeeman splitted lines during its photometrically low state, and in which all temporal variations occur with exactly the same period that is typical for the orbital period of catclysmic variable systems.

The general interpretation which has been suggested for these AM Herculis stars is that the rotation of a very strongly magnetic white dwarf (field strengths of several times 10^7 G have been determined from both polarization observations and Zeeman splitting) is phase-locked with the binary motion, and the strong field and correspondingly large Alfvén radius prevent the formation of an accretion disc in these systems. (For a recent review see Liebert and Stockman (1985).)

The gross picture is that material leaves the companion star at the Lagrangian point L_1 and enters the white dwarf's Roche lobe. For the first part of its journey to the white dwarf the trajectory of the material is hardly different from that in other cataclysmic variables, but eventually the magnetic field increasingly governs the flow and channels the matter onto one or both of its poles where it is braked and then accreted in a strong standing shock (Figure 4-32). The usual case is that one pole, the one closer to the secondary star (the white dwarf's rotational and magnetic axis can have any orientation with respect to each other) accretes most of the material, while the second, depending again on its position, in the extreme case may receive no material at all.

The observed hard and soft X-ray radiation, roughly having the shape of a bremsstrahlungs spectrum and a black body, respectively, are thought to be emitted from the accreting pole, whereby soft X-rays result from hard X-rays which have been degraded in the white dwarf's photosphere (e.g., Chanmugam, 1986). The third continuum component, a cyclotron spectrum which dominates the optical and the IR, is conjectured to originate higher up in the shock front (Figure 4-33). The observable photometric variations are brought about by aspect variations and/or temporary eclipses of the accreting pole(s), and differences between various systems are mostly due to differences in the inclination angle, the different orientation of the white dwarf's magnetic axis, and — related to this — whether and how strongly one or both poles accrete material. The observed sharp strong emission lines are believed to originate from the heated surface of the secondary star (e.g., Mukai et al, 1986), while the board bases of these lines seem to be emitted by the gas stream close to the shock front as it approaches the white dwarf. The very broad emission features in the optical and IR continuum (Figure 4-34a) are understood to be cyclotron emission lines (e.g., Wickramasinghe and Meggitt, 1982).

At irregular intervals of time, some AM Herculis systems are seen to drop in brightness by three to five magnitudes, an effect which is ascribed to temporary cessation of the mass overflow like that in other nova-like stars. At

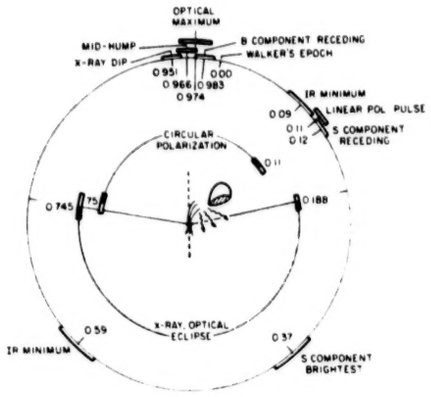


Figure 4-32a. Phase diagram of events around the orbit of the AM Herculis object VV Pup (Patterson et al, 1984).

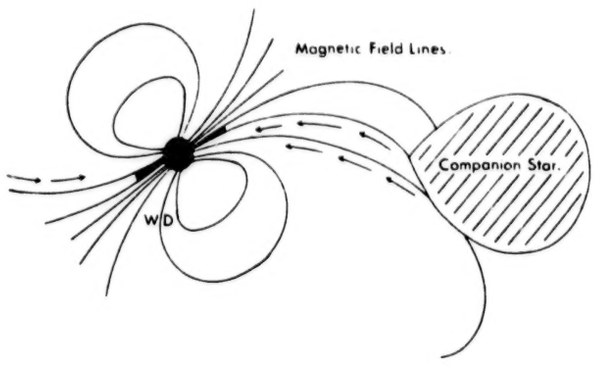


Figure 4-32b. Schematic model of an AM Herculis system (for description see text) (King, 1983).

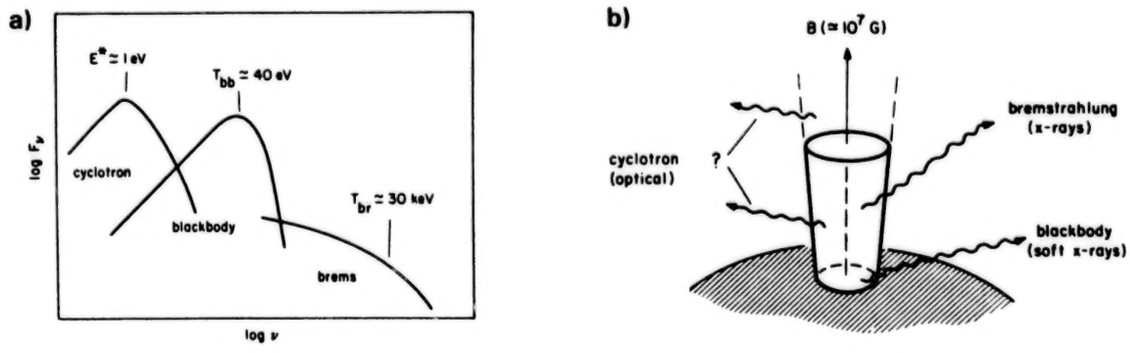


Figure 4-33. (a) Components of radiation from an AM Herculis system and (b) loci of origin above the accretion pole (Lamb, 1985).

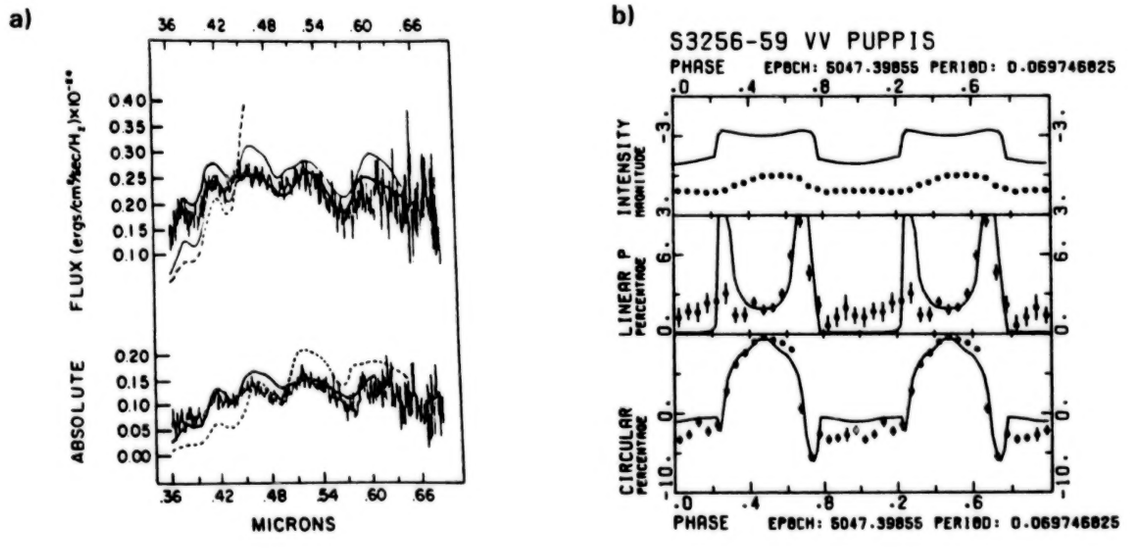


Figure 4-34. Model fits to observed spectra (a) and photometric and polarimetric variations (b) of the AM Herculis system VV Pup (Chanmugam, 1986; Osborne et al, 1986).

these states the X-ray influx is reduced, the strong narrow emission lines are strongly reduced or disappear altogether (the secondary star is not heated any longer), their broad bases disappear (since the accretion column is more or less non-existent), and in some systems the spectrum of the secondary component becomes visible in the IR (e.g., Bailey et al, 1985). At this stage several lines in the optical appear to exhibit Zeeman absorption components corresponding to the strength of the white dwarf's magnetic field as derived from polarization measurements (e.g., Mitrofanov, 1980; Schmidt et al, 1983; Bailey et al, 1985). The polarization stays unaltered during low states — supporting the view that it originates from the white dwarf and that mass transfer from the secondary star is the cause for the observed changes.

Theoretically a very difficult and controversial point about AM Herculis stars is the actual physical structure and the geometrical size and shape of the accretion shock. A wealth of literature has been published on this subject during recent years, but many points have yet to be clarified (e.g., King, 1983; Langer et al, 1983; Frank and King, 1984; Meggitt and Wickramasinghe, 1984; Wickramasinghe and Meggitt, 1985a; 1985b; Chanmugam, 1986). An extensive review of the current state of the theory of AM Herculis stars, discussing the difficulties and prospects, has been given by Lamb (1985).

For conditions found in these systems, the main cooling process is optically thin cyclotron emission. Model computations based on this assumption fit the observed flux and polarization fairly well, in spite of the obviously still serious theoretical problems (Figure 4-34). From such fits the strength of the magnetic field, the geometrical size and shape of the accretion column, the various inclination angles, temperatures of the emitting region, and accretion rates can be obtained. The still obvious disagreements with the observations seem to become smaller if a reasonable temperature structure for the shock region, other than a single temperature, and other cooling effects than just cyclotron radiation are considered.

III.F.2. WEAKLY MAGNETIC SYSTEMS — DQ HERCULIS STARS

RELEVANT OBSERVATIONS: These systems exhibit more than one highly stable photometric period. Otherwise their appearance is like that of other (non-magnetic) nova-like stars.

see 112

ABSTRACT: The magnetic field of the white dwarf is of intermediate strength and disrupts the disc at some distance from the star; final accretion occurs along the field lines onto the magnetic poles. The white dwarf rotates asynchronously with the binary orbit. Illumination of system components by the hot accreting poles, or radiation from the poles themselves, produces the additional photometric periodicities.

The appearance and temporal variability of most cataclysmic variables can be understood satisfactorily without invoking magnetic fields; but, as was discussed in the previous section, there are others in which strong magnetic fields are directly measurable, and these fields determine the nature of these systems to a very considerable extent. If very weakly magnetic, or non-magnetic, systems and very strongly magnetic systems exist, it seems reasonable to assume the existence of systems with moderately strong magnetic fields.

A couple of systems have been observed, the DQ Herculis stars, which exhibit two or more extremely stable photometric periods. These have been tentatively identified with moderately strong magnetic systems (Bath et al, 1974a; Lamb, 1974; Patterson et al, 1978a; Chester, 1979; Patterson, 1979b; Patterson, 1980; Hassall et al, 1981; Patterson and Prince, 1981; Warner, 1983; 1985a; Cordova et al, 1985; Warner, 1985b; 1986a. For recent reviews see Warner, 1983; 1985a.) Neither polarization nor

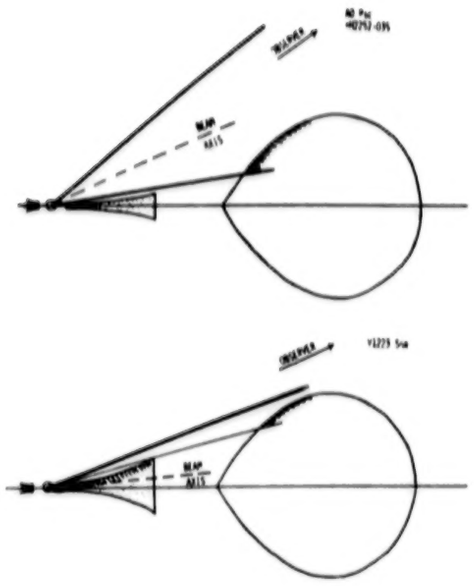


Figure 4-35. Schematic model of DQ Herculis systems (Warner, 1985b). Variation of the angle of inclination can explain the observed differences between different systems.

Zeeman splitting in the lines is observable in DQ Herculis systems, but if magnetic fields are assumed to be one to two orders of magnitude smaller than those observed in AM Herculis stars, one would not expect to observe any direct evidence for these fields with current techniques.

The basic physics of these systems is identical to that of non-magnetic cataclysmic variables: a white dwarf accretes material from a Roche lobe filling secondary star through an accretion disc. However, here the magnetic field of the white dwarf is strong enough (estimates — mostly based on observed spin-up rates of the white dwarfs — predict field strengths on the order of 10^5 to 10^6 G, i.e., 1-2 orders of magnitude weaker than fields in AM Herculis stars (Lamb, 1985)) to disrupt the inner edge of the disc at some distance from the white dwarf. Interior to this Alfvén radius all material is forced to co-rotate with the field lines (i.e., with the white dwarf), thus accretion in this area occurs through accretion funnels which end in two hot regions around the magnetic poles on the surface of the white dwarf. Since the white dwarf does not rotate synchronously with the binary orbit, and since its magnetic axis is not in general aligned with the rotational axis, a beam of light from each magnetic pole sweeps over the system with the rotational period of the white dwarf. Thus, what is observable from these systems first of all are the normal brightness variations of a cataclysmic variable system, like humps, eclipses, etc. In addition, beams from one or both magnetic poles might be seen. Furthermore, the secondary star and the inner edge and/or the surface of the accretions disc or the hot spot are irradiated by the magnetic poles which produces radiation that is modulated with the rotational period of the white dwarf and/or some beat period with the orbital motion. Which part contributes how much to the observed radiation strongly depends on the system geometry, the orientation of the magnetic axis, and the position relative to the observer. Furthermore, changes in the disc geometry in particular, as for instance due to changes in the mass transfer rate, can account for more or less irregular brightness (amplitude) variations, or even time delays, of the degraded radiation. X-ray radiation is expected to be emitted from the accretion poles, which may or may not be directly observable depending again on the inclination angle; but certainly the X-rays are a powerful heat source in the system.

Warner (1986) carried out a systematic investigation of theoretically predicted and observed Fourier spectra of photometric variabilities in DQ Herculis variables, and was able to explain in a consistent way the optical and X-ray idiosynchrasies of as different systems as V1223 Sgr, FO Aqr, and AO Psc, and several others by simply assuming different inclination angles of the magnetic axis (Figure 4-35).

Phase shifts of the oscillations (71 sec period) of about 180° have been observed in DQ Her during the eclipse (Patterson et al, 1978a, see

Figure 3-26). Assuming the reflection of a rotating beam at the inner edge of the disrupted disc, a progradely rotating white dwarf with a rotational period of 71 sec, and a system inclination of about 90°, Patterson (1980) was able to theoretically reproduce the observed behavior. A similar shift seen in the occasionally present short-period oscillations in the very similar, but probably not magnetic, system UX UMa can be explained in the same way, if a somewhat larger inclination angle is assumed, and if bright blobs circulating in the inner disc are assumed to be the source for the brightness variations.

IV. MODELING THE OBSERVED SPECTRA

The observed spectra of dwarf novae and nova-like stars have been presented in the previous chapters. They comprise a fairly large range: pure emission spectra, pure absorption spectra, a mixture of both, asymmetric line profiles, very different slopes of the continuous flux distribution — and one single system may exhibit all of these features at different times. Changes from one sort of spectrum to another have been observed to occur as quickly as within one hour or less. Usually, however, they occur within a couple of hours or days.

From considering many of the observed properties, a conceptual model has been developed of what a cataclysmic variable may look like, the so-called Roche model, or a canonical model (see Chapter 4.II.A). This model makes predictions as to what parts of the system emit what kind of radiation. So in principle it should be possible to synthesize a theoretical spectrum of a cataclysmic variable by means of — probably slightly modified — conventional spectrum computations. Agreement and disagreement between computed and observed spectra should show whether or not the Roche model is applicable and where it probably will have to be modified and improved.

During the past ten years a couple of such attempts have been undertaken which are discussed in this section. It will be seen immediately that a reasonably comprehensive approach which accounts for all the observed features is currently well beyond our physical understanding of these systems, not to mention the numerical problems to be encountered along the way. The problem of computing spectra for cataclysmic variables is split into basically three separate problems: that of specifying the physical model to serve as a basis for the equations and the computations; that of computing the continuous spectrum; and that of computing the line spectrum.

IV.A. THE BLACK BODY APPROACH

RELEVANT OBSERVATIONS: The observed flux distribution of the continuous radiation does not resemble that of normal stars.

see 65

ABSTRACT: An approximate fit of the observed flux distribution is possible if it is assumed that only the accretion disc contributes to the radiation, and that at each distance from the white dwarf it radiates like a black body with a radial temperature distribution derived for a stationary disc.

No attempts have ever been made to compute spectra of cataclysmic variables based on a conceptual model other than the Roche model, since, in spite of some obvious shortcomings, no reasonable alternative exists. In fact, computations based on the Roche model do yield results which bear definite similarities to many of the observed features.

The assumption that the Roche model is valid grossly determines which parts and properties of the system — i.e., the masses of the stars, the orbital period, the inner and outer disc radius, and the angle of inclination of the system with respect to the line of sight of the observer — primarily determine the spectrum. Observations impose some further limitations

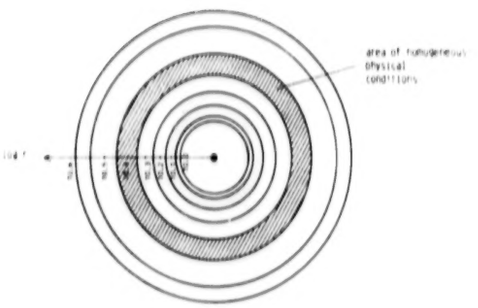


Figure 4-36. For purposes of spectrum computations the accretion disc is divided into concentric rings of homogeneous physical properties (la Dous, 1989).

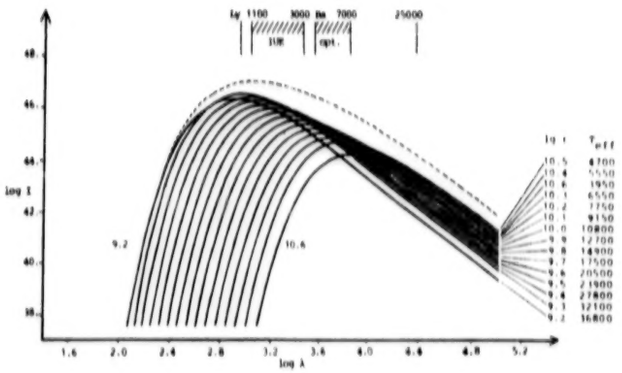


Figure 4-37. Contribution functions of a black body disc. The log r values correspond to the areas given in Figure 4-36 (la Dous, 1989). The UV radiation is dominated entirely by radiation from the central disc; the central and middle disc contribute to the optical; the IR radiation comes from the middle and outer disc. The dashed line is the integrated spectrum.

on possible parameter combinations, such as minimum and maximum orbital periods of some 80 minutes and some 10 to 15 hours, respectively, and also the observation that the secondary stars are usually close to the main sequence. Furthermore, from observed energies and velocities it is certainly justifiable to neglect all relativistic effects.

The easiest way to test the suitability of the Roche model from the spectroscopic point of view, and also to gain some experience and understanding of the radiation emitted by an accretion disc, is to assume that every point of its surface radiates like a black body. This first has been done by Tylenda (1977). He assumes a stationary accretion disc and thus can make use of the theoretical radial temperature distribution given by equation 4.2. For numerical purposes, the disc is divided into concentric "rings" of homogeneous physical conditions (Figure 4-36). The radiation of the entire disc is obtained from integrating over the contributions of all these "rings." He demonstrates that it is possible to qualitatively reproduce the observed spectra of the dwarf nova SS Cyg in outburst and of the old novae RR Pic and V603 Aql in a rather satisfactorily way.

This kind of computation proved to be a very valuable and straightforward tool for investigating the major influences of various parts of the system on the integrated radiation (la Dous, 1986; 1989). In Figure 4-37, the contribution functions of the "rings" of which the synthetic disc consists are displayed together with the resulting integrated spectrum. It is evident that in the example given, the UV radiation is entirely due to the very innermost 1 - 5% of the disc area, whereas the optical radiation is produced by both the inner and the middle areas, and the IR comes from the middle and the outer areas. It is particularly important to realize that very dramatic changes of the size of the cool outer disc hardly affect the optical radiation and do not at all affect the UV radiation. Furthermore, the radius of the white dwarf (which is critically dependent on the mass (Nauenberg, 1972)) has a very determining influence on the UV radiation. Likewise, the rate of mass throughput through the disc is by definition identical to the mass transfer rate from the secondary star (in a stationary accretion disc) is of crucial importance to the radiation emitted by the disc.

The influence of the boundary layer between the disc and the white dwarf on the spectrum,

is hard to estimate, since the amount and wavelength distribution of that radiation depends critically on the rotational velocity of the white dwarf as well as on the geometrical size and physical structure of the boundary layer, none of which are known. Computations demonstrate that this radiating component may or may not be of any importance in the UV, depending on local conditions. Clearly, however, it can always be neglected at optical and IR wavelengths.

Considering the contribution the secondary star provides to the integrated radiation from the system, its immediate influence is restricted to long wavelengths in the red and IR regions, since temperatures typically are on the order of 4000 K or less, and the projected surface area is comparable to the size of the disc. The secondary's contribution can become important, however, if the angle of inclination of the system is such that the disc is seen almost edge-on, so that its hot central parts do not contribute to the observed radiation.

For a very large accretion disc which comprises a very large temperature range, a spectral index of $\alpha_\nu = 1/3$ ($\alpha_\lambda = -7/3$, respectively) is predicted analytically by just integrating the radiation of a black body disc (Lynden-Bell, 1969). It has often been claimed in the literature that the observation of such a continuum slope is an indication that the radiation is emitted by a stationary disc. From adopting maximum reasonable system parameters for the computations, however, it becomes immediately clear that accretion discs in cataclysmic variables are both too small and too cool for the spectral index to be around $\alpha_\nu = 1/3$ for more than a very small spectral range. Thus, the fact that such an index has been observed on occasions has to be taken as an indication that the disc emitting that spectrum is not stationary but rather possesses some different radial temperature distribution.

IV.B. CONTINUOUS AND ABSORPTION LINE SPECTRA

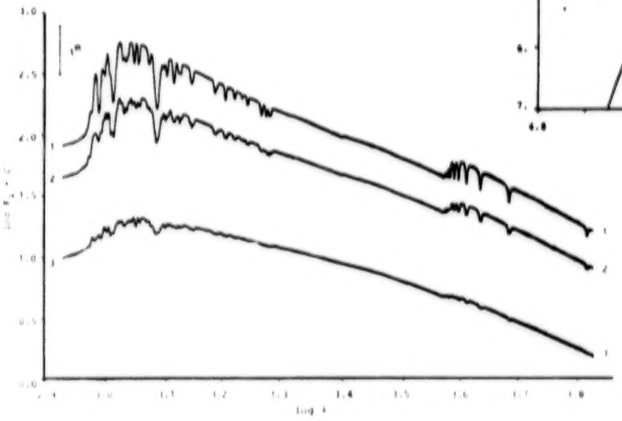
RELEVANT OBSERVATIONS: In dwarf novae during outburst, one observes mainly broad absorption lines in the optical and UV.

ABSTRACT: A reasonable first-order fit of the spectra of dwarf novae during outburst is possible, adopting current methods of spectrum computations.

When optical and UV continuous and absorption line spectra of cataclysmic variables are computed, to a rather good approximation it is sufficient to concentrate just on the radiation emitted by the disc and to ignore contributions from all other components of the system. Furthermore, as in the case of black body discs (see above), it is quite reasonable to numerically divide the disc into concentric rings of homogeneous physical conditions and compute the spectrum emitted by each such ring, in close analogy to stellar (absorption) spectra. The basic difference between a star and a disc is the energy source, nuclear in one case, gravitational energy in the other, but as long as the central plane of the disc is optically thick, so that it is safe to assume that all the energy has been set free well below the photosphere, it does not matter for the emitted spectrum what the nature of the energy source is.

Spectrum computation requires the knowledge of the chemical abundance, the effective temperature, and the gravitational acceleration in the atmosphere. As to the chemical abundance, to adopt solar composition seems reasonable and in agreement with considerations about the evolutionary status of cataclysmic variables. Furthermore, slight changes in the chemical abundances show hardly any effect on the emitted spectra of discs. Again, under the assumption that the disc is stationary (which has been assumed so far in all published computations), equation 4.2 provides the radial temperature distribution. The gravitational acceleration in the vertical direction is determined by the geometrical thickness

Figure 4-38. (below) Spectrum emitted by the same system, seen under inclinations of 23°, 60°, and 83° (la Dous, 1989). The inclination angle is of great importance for the received radiation.



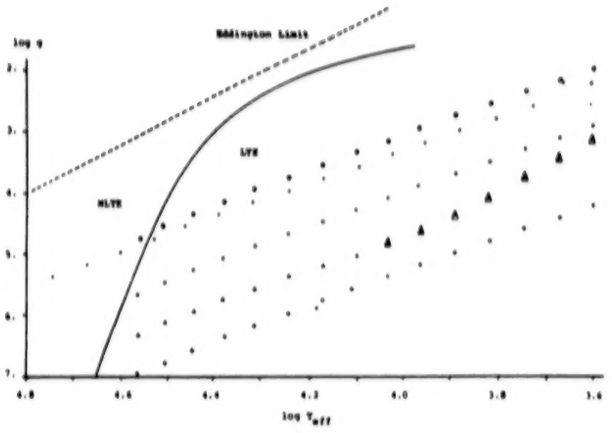


Figure 4-39. Log g and T_{eff} values of various disc models. The solid line divides the regions in the atmospheres where non-LTE conditions are important from that where they are not. Non-LTE effects can be neglected in accretion discs in cataclysmic variables (la Dous, 1989).

z of the disc, and increases with increasing distance from the central plane:

$$g(z,r) = \frac{G M_{WD}}{\sqrt{r^2 + z^2}} \frac{z}{\sqrt{r^2 + z^2}} \approx \frac{G M_{WD}\, z}{r^3} \quad \text{for } z \ll r \tag{4.17}$$

(all the symbols have their usual meaning). The disc's photosphere is defined to be at the geometrical height z_0. From observations it can be concluded that z_0 is small compared with the distance from the white dwarf, but its actual value is unknown. Slightly different assumptions were made by different authors about the value of z_0, but any of these is essentially as arbitrary as any other. A comparison of synthetic disc spectra with various values for z_0 in the range between $0.05° \leqslant \vartheta \leqslant 15°$ ($\vartheta = \tan^{-1} z_0/r$), as well as values which resulted from hydrodynamic computations of optically thick discs by Meyer and Meyer-Hofmeister (1982), revealed that differences in the computed spectra are too small to be seen in actually observed spectra unless the inclination becomes very large and the limb darkening law makes itself felt, in particular since effects of other theoretical parameters on the spectrum are much more serious (la Dous, 1986). Thus it can be concluded that for geometrically thin, optically thick accretion discs any value of $z_0(r)$ is reasonable as long as $z_0(r) << r$ or $\vartheta \leqslant 10°$.

Also, in many of the published spectrum computations it is assumed that the gravitational acceleration does not vary within the atmosphere. Whether or not this is a justified assumption depends on the relative thickness of the atmosphere with respect to the underlying optically thick disc. Again, test computations revealed that as long as the disc is really (and not just marginally) optically thick in the central plane, the assumption that g(z) = constant is quite justified (la Dous, 1986; 1989). The situation of course changes entirely either if energy production in the disc atmosphere is taken into account, by means of which the atmosphere can become very extended with its outer parts then called a "corona," or if the disc is optically thin in the central plane.

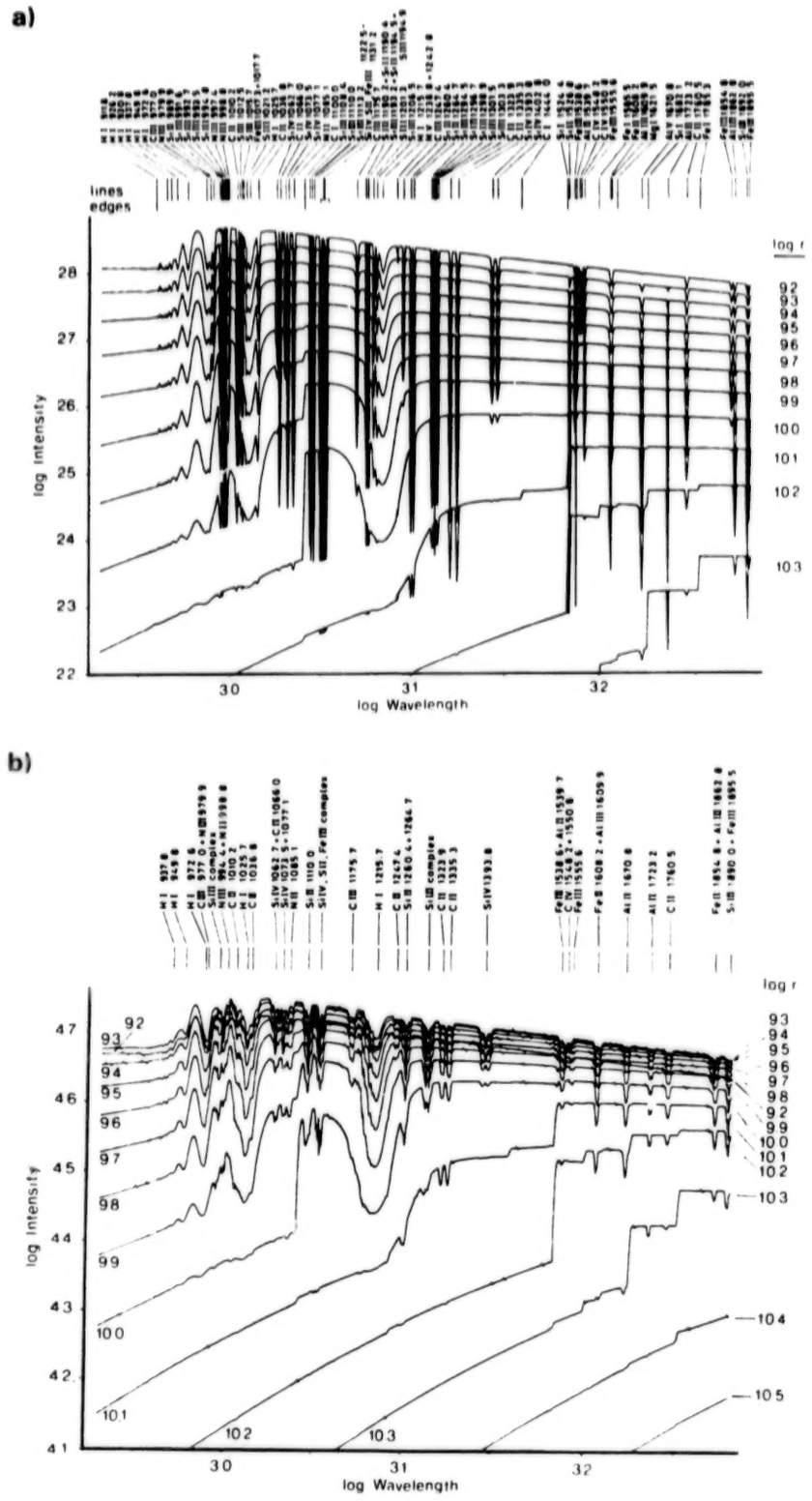


Figure 4-40. Contribution functions from an accretion disc model: (a) lines have not yet been broadened by the disc rotation; (b) lines broadened by the Doppler velocity.

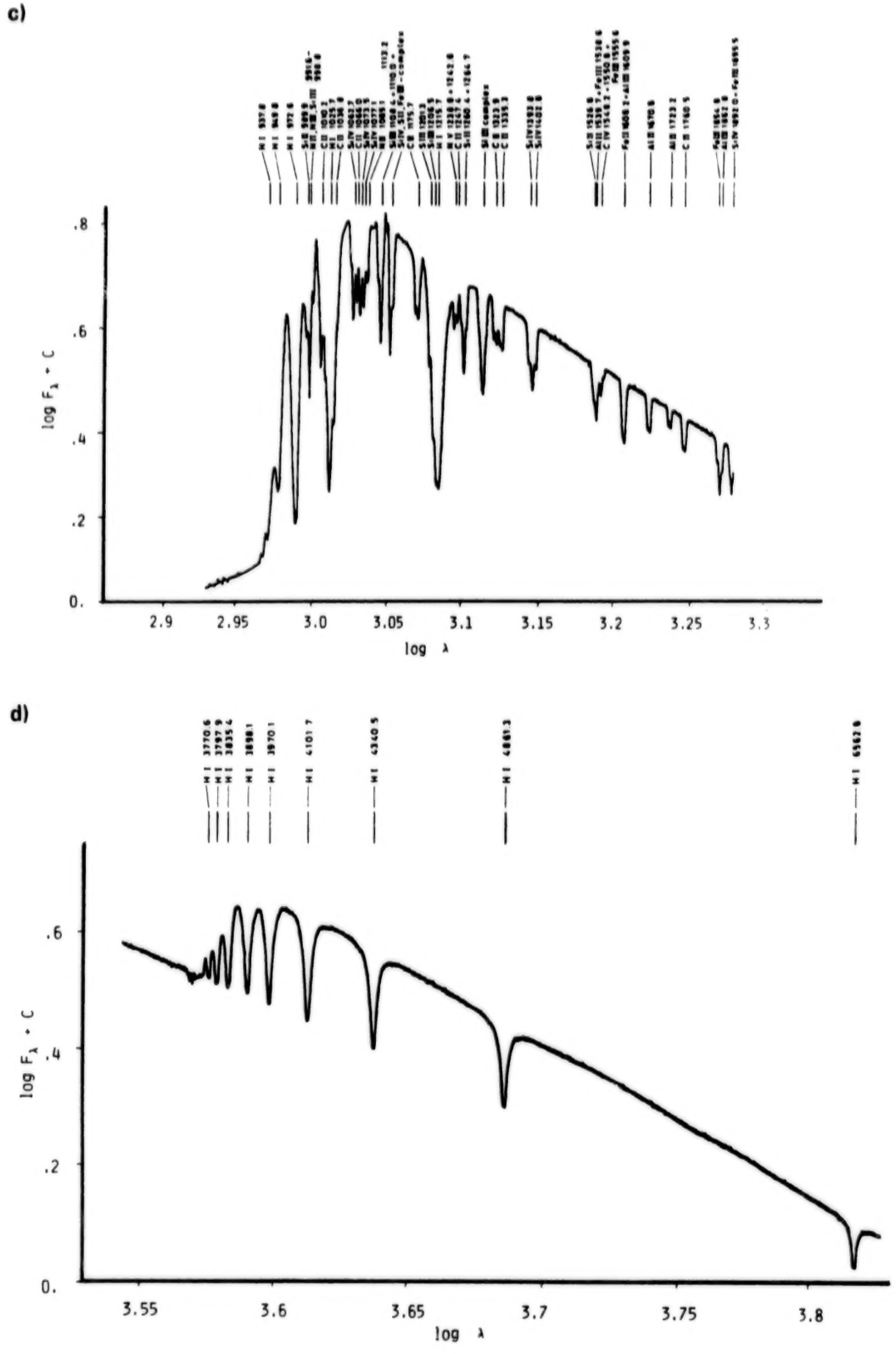


Figure 4-40. (Continued) Integrated disc radiation (c) in the UV and (d) in the optical (la Dous, 1989).

ORIGINAL PAGE IS
OF POOR QUALITY

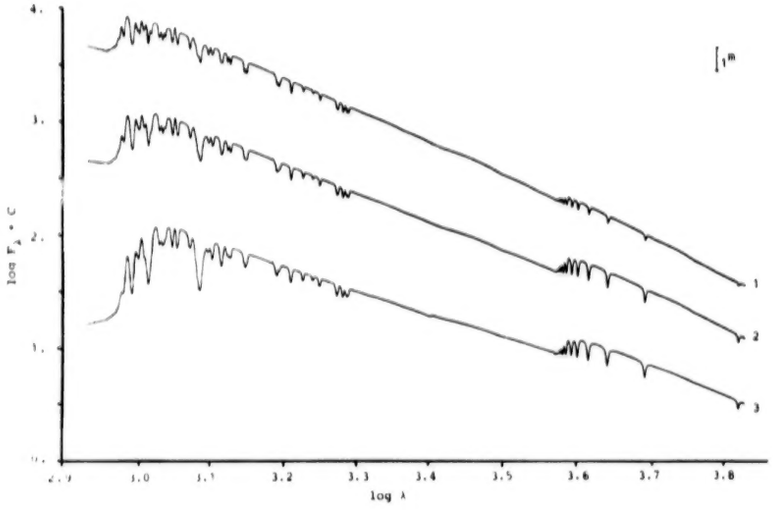


Figure 4-41. Influence of the mass-transfer rate on the disc radiation: (1) 10^{-7} $M_\odot$/yr; (2) 10^{-8} $M_\odot$/yr; (3) 10^{-9} $M_\odot$/yr, with otherwise identical model parameters. The greatest effect is clearly on the UV radiation, while optical colors are hardly changed (la Dous, 1989).

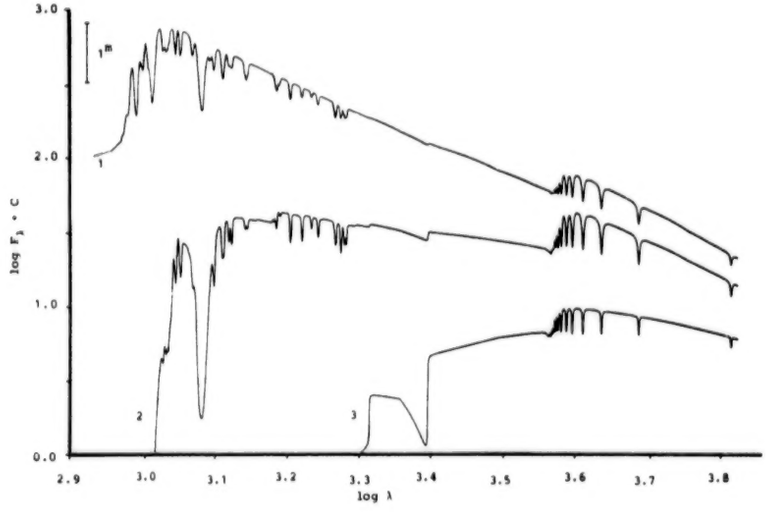


Figure 4-42. Influence of variation of the inner disc radius on the disc radiation: (1) $r_i = 10^{9.2}$ cm; (2) $r_i = 10^{9.9}$ cm; (3) $r_i = 10^{10.3}$ cm (la Dous, 1989). Such effects could result from a varying size of the Alfvén radius due to a magnetic field of the white dwarf. While dramatic changes occur in the UV, the optical colors remain unchanged.

One further principle difference between atmospheres of stars and atmospheres of discs is that, unlike stars, discs are essentially two-dimensional objects and thus the angle of inclination i between the normal on the rotational plane and the line of sight of the observer is important for the observed radiation. This mostly affects the limb-darkening in that mainly the radiation emitted by the cooler layers of the atmosphere is received at the higher inclinations (Figure 4-38). With respect to computing a spectrum this means that, in a disc, it is the angle-dependent flux emerging from each part of the atmosphere which has to be integrated over all the disc rather than the angle-averaged flux. Since published stellar spectra (computed or observed) all yield only the angle-averaged flux, this implies serious limitations to comparing computed stellar spectra with observations when used as a basis for synthesizing relevant disc spectra.

The parameter ranges covered by accretion discs in cataclysmic variables suggest that, with the possible exception of the very central parts close to the white dwarf (where the boundary layer probably has a large influence), LTE is a good approximation for atmosphere computations (Figure 4-39). Radiation pressure can well be neglected. Electron scattering, however,

can become very important in some areas of the disc. Convection does become important at larger distances from the central object. However, irrespective of their large geometrical size, the contribution of these cool parts to the total radiation of a stationary, optically thick accretion disc is negligible in the optical and UV, so proper treatment of convection is not of crucial importance.

When line radiation is included, the effect of the Keplerian rotation of the disc must be taken into account, which leads to both additional line broadening as well as to double-peaked absorption profiles (in analogy to emission profiles, see Figure 4-45, Chapter 4.IV.C). The main effect on the Balmer lines is that they appear double-peaked, particularly at high inclination angles, while the UV lines of heavy elements can be broadened by many times their pressure-broadened value, and a lot of detailed information can be washed out.... an effect which is strongly enhanced by the integration of radiation from all parts of the disc (Figure 4-40).

Spectrum synthesis for stationary, geometrically thin, optically thick accretion discs has been performed by several authors (Herter et al, 1979; Kiplinger, 1979; 1980; Mayo et al, 1980; Pacharintanakul and Katz, 1980; Tylenda, 1981a; Wade, 1984; la Dous, 1986, 1989), using either published sets of, or program codes for, stellar atmospheres and including, or in some cases not including, absorption lines in the computations. The effects of parameter changes on the theoretical spectra have been investigated (quoted references should be checked for details). The major results which emerged are that, of the possible free parameters investigated which might influence the character of the computed spectrum (the mass M_{WD} of the white dwarf, the mass transfer rate $\dot{M}$, the inner and outer disc radii r_i and r_o, respectively, and the angle of inclination i), the mass of the white dwarf — not considering its influence on the star's radius — and the outer disc radius are of practically no importance. The drastic effect of the inclination angle i on lines as well as on the continuum flux already has been shown in Figure 4-38. The mass transfer rate $\dot{M}$ enters the radial temperature profile and thus is a very determining factor for the appearance of the disc spectrum (Figure 4-41), and variations of r_i strongly alter the temperature range. If due to a magnetic field which the white dwarf may possess, the inner disc radius r_i also is a variable parameter, this is even more important for the disc spectrum than $\dot{M}$ (Figure 4-42), since its variation means including or neglecting the very hottest areas of the disc which entirely determine the UV and also partly the optical radiation.

In general, almost any parameter variations have much more pronounced effects on the UV than on the optical radiation, so that no useful information about the system as a whole can generally be obtained from the optical colors of cataclysmic variables alone. Including also UV colors is of limited use. Meaningful system parameters may possibly be derivable from high-quality, high-resolution spectroscopic data of the optical plus UV range or from continuum observations alone, if the mass of the white dwarf is known with some confidence (la Dous, 1989), but this has not been tried yet.

Irradiation of the disc by hot central areas and/or the boundary layer, or generation of energy in the atmosphere, lead to the formation of extended chromospheres and coronae above the accretion disc which change considerably the nature of the emitted radiation, even if the accretion disc itself is optically thick (Schwarzenberg-Czerny, 1981; Kříž and Hubený, 1986; Shaviv and Wehrse, 1986). Results so far have not led to more than the demonstration that such thin extended regions are present.

IV.C. EMISSION LINE SPECTRA

RELEVANT OBSERVATIONS: During the quiescent state, most dwarf novae are dominated by strong emission lines of hydrogen in the optical and by strong metal resonance emission lines in the UV.

see 73

ABSTRACT: The line emission is attributed to optically thin areas in the inner and/or outer accretion disc, or even to the entire disc. Modeling is considerably more difficult than for outburst spectra since there is evidence that the disc is not stationary (i.e., no radial temperature law is available à priori), and non-LTE effects might become important, in particular in the presence of energy generation in the atmosphere.

The spectra of quiescent dwarf novae, some nova-like systems, and old novae, usually exhibit strong emission lines of H, HeI, HeII, and, particularly in the UV, of highly ionized elements such as C IV, Si IV, N V. Different lines in one spectrum can, and usually do, exhibit vastly different profiles; in particular, the Balmer and He lines often are double-peaked if the system is seen under a large inclination angle, while normally all other lines exhibit single-peaked profiles. The shapes of the radial velocity curves are different for different lines and species, normally lines are eclipsed if the continuum undergoes an eclipse, but different lines are eclipsed in different ways, and all are affected differently than the continuous radiation. In general, it can be concluded that emission lines originate from the Roche lobe of the primary stars (white dwarf); that most emission lines originate near the orbital plane, i.e., in or near the accretion disc; that not all lines are formed in the same region of the disc; and that some lines, in particular those with the highest ionization potential, are formed far away from the orbital plane.

From lines and line ratios seen in the spectrum of the old nova V603 Aql, Ferland et al (1982a) conclude that the line emission probably originates in an extended corona filling most of the white dwarf's Roche lobe which is heated by irradiation from the disc. Similarly, Jameson et al (1980) conclude from the UV spectra of the somewhat peculiar cataclysmic variable AE Aqr that the cool emission lines, Mg II, Ca II, and about half of Ly α are likely to originate in optically thin parts of the accretion disc itself, while the lines of the highly ionized elements, in particular N V, Si IV, C IV, and He II are likely to originate in a chromospheric region outside the disc, which again is heated by the hot central parts of the disc.

In general, emission lines in cataclysmic variables can originate either in a corona above or below the accretion disc, or in optically thin parts of the disc itself. Williams (1980) included the possibility for the disc to be optically thin in the continuum in the outer cool disc areas (far away from the white dwarf), while it is still optically thick in the lines. The particular features of his results are highly dependent on the choice of the viscosity and on the assumption that the entire disc is stationary, but the general features are of wider significance. He finds that larger areas of the outer disc become optically thin in the continuum with decreasing mass transfer rate while the inner disc is still optically thick (Figure 4-43a); at very small transfer rates (of the order of $\dot{M} \lesssim 10^{-12}$ $M_\odot$/yr in his models) the entire disc becomes optically thin in the continuum. The Balmer lines remain optically thick throughout almost all of his model discs. The intensity ratio he obtains for the emissions of Hα, Hβ, and Hγ are in reasonable agreement with observed ratios; however, he does not take into account contributions from absorption lines produced by the optically thick parts of the disc. None of his models produce any He lines of appreciable strength, from which Williams concludes that — for discs of the kind investigated — the lines, which are observed to be fairly strong at times, originate in some other, hotter, optically thin regions of the system. The disc in Bailey and Axon (1981) is assumed to be stationary, thus the optically thin outer disc has to heat up considerably over the respective black body

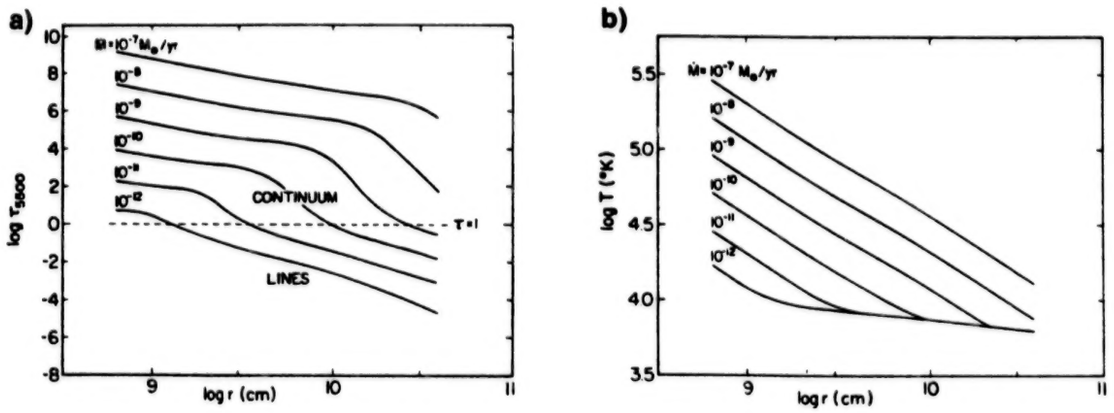


Figure 4-43. Continuum optical thickness and temperature of the accretion disc as a function of the mass transfer rate and distance from the white dwarf (Williams, 1980). At low mass transfer rates (during quiescent state) large parts of the outer accretion disc can be optically thin and at approximately constant temperature.

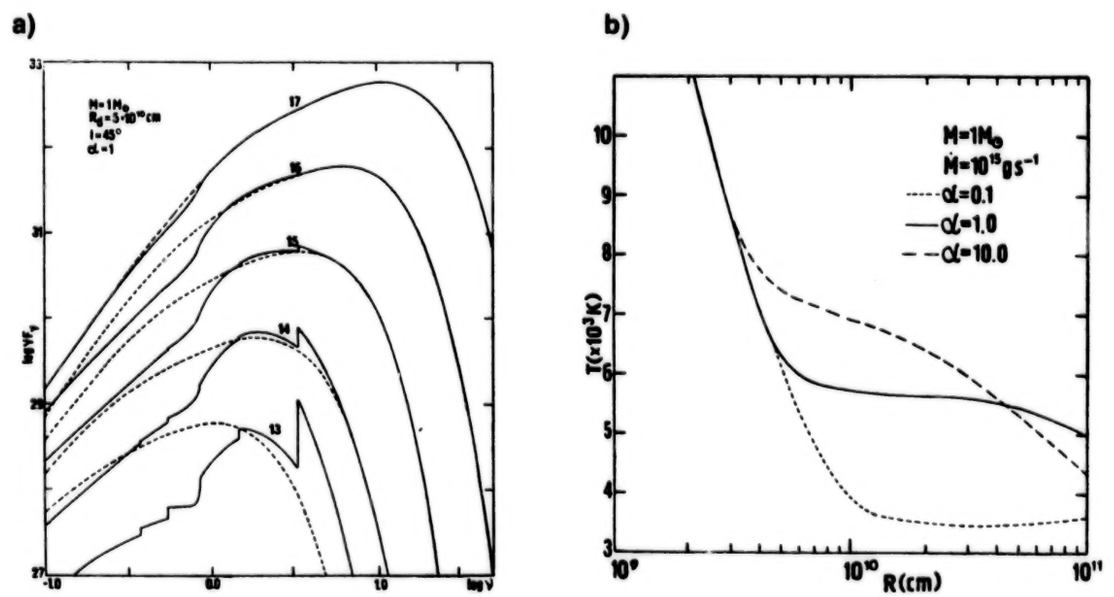


Figure 4-44. When accretion discs become optically thin with decreasing mass-transfer rate, the emitted flux is represented ever more poorly by black body radiators (Tylenda, 1981a).

temperature in order to radiate away all of the locally created energy. This results in the temperature in these outer regions staying more or less constant (at about 6500 K for the viscosity chosen in William's example) over geometrically large areas (Figure 4-43b).

Tylenda (1981a) arrives at very similar results from only slightly different computations. He stresses the point how increasingly poorly, particularly at optical and UV wavelengths, black bodies represent the continuous radiation emitted by accretion discs as ever larger optically thin areas are involved, increasing in size with decreasing $\dot{M}$ and increasing outer disc radius (Figure 4-44a), but also how sensitive the actual temperature reached in the outer disc is to the particular choice of the viscosity (Figure 4-44b). He also finds that the emission line profiles are critically dependent on $\dot{M}$ and viscosity, and also on the inclination angle, as one would expect.

When it comes to modeling actually observed emission line profiles, it is known that they depend on a wealth of parameters in addition to the influences already discussed above in the case of absorption lines; on the radial and azimuthal brightness distribution in the accretion disc, on the inner and outer radius of the region where the particular line under investigation originates, on gas densities in the region, on the amount of turbulent motions present, on the rotational velocities in the discs and their relative size in different regions, on the shape and geometrical origin of the continuous spectrum as well as of the absorption lines, and on even more parameters, depending on the degree of sophistication of the computations. Several increasingly promising attempts to model emission line profiles have been undertaken so far, in particular of the Balmer lines of hydrogen; but clearly a lot of research remains to be done. The double-peaked lines of high-inclination systems are particularly well suited for testing of models, since these profiles have sufficient structure to impose considerable constraints on model parameters.

Double-peaked profiles are believed to be due to the combined effects of the disc being a two-dimensional object and Keplerian rotation, in the same way double-peaked absorption profiles arise in the computations of optically thick accretion discs (Chapter 4.IV.B). In principle, the peak separation should be indicative of the rotational velocity of the outermost radius in the disc, where a considerable contribution to the line under investigation originates (Figure 4-45). Computations indicate that such a peak separation should already be visible at inclinations as low as 15°. There are objects on the other hand, like BT Mon, LX Ser, and SW Sex, which exhibit clear single-peaked hydrogen emission profiles, yet they show eclipses of the continuous as well as of the line radiation which point to fairly high inclinations (Williams et al, 1988). One suggestion for solving this problem was to assume the presence of an additional component in the core of the emission lines, the geometrical origin of which was not specified further (Smak, 1981). Recently however, Marsh (1987) and Williams et al (1988) pointed at the importance of Stark broadening in smoothing out the peaks of theoretical emission line profiles in accretion discs, an effect which is also able to explain the presence of very broad wings of the Balmer emission lines in some systems which are seen nearly pole-on. The actual importance of the Stark effect depends largely on the surface density of electrons and thus on the temperature. Due to different ways in which the Stark effect acts on H and He, a situation is conceivable wherein double-peaked H lines coexist with single-peaked He lines (Williams et al, 1987) — a situation which is actually observed at times (see Chapter 2.II.B.1, Figure 2-93). Marsh (1987) stresses the point that while Stark broadening certainly has a very important influence on line profiles in the inner disc, it may not be very important for the formation of double-peaked profiles of the H lines if the bulk of emission originates in the outer cool disc areas where the electron density is low. Furthermore, there is an observational indication against Stark broadening to be the cause of the single-peaked profiles, at least in the nova-like system LX Ser, since the Paschen lines should still have double structure if Balmer lines appear single-peaked due to Start effect, which in LX Ser they do not, when observed at sufficiently high wavelength resolution (Young et al 1981a).

A Keplerian rotating accretion disc implies the presence of significant velocity gradients in the atmosphere. This does not pose a problem for the continuum radiation, nor does it probably pose one for absorption lines according to Rybicki and Hummer (1983). They elaborate on the importance of this additional asymmetry when dealing with accretion discs which are optically thin in the continuum. They discuss in particular conditions in the outer cool parts of the discs where the strong H emission lines are formed. They try to apply the Sobolev theory (a simplified version of the general escape probability method, applicable in the presence of high velocity gradients), but conclude that

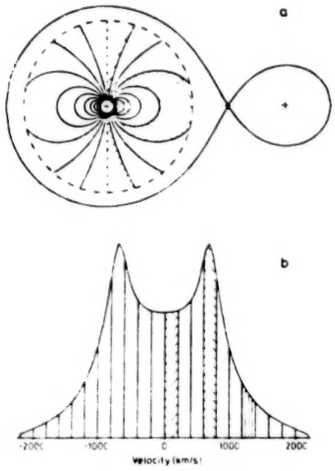


Figure 4-45. Geometrical origin of double-peaked line profiles in accretion discs (Horne and Marsh, 1986).

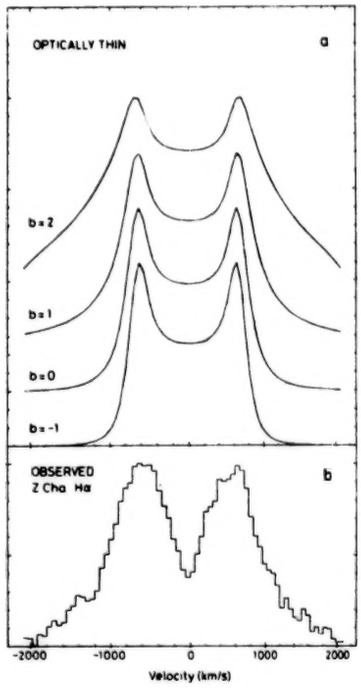


Figure 4-46b. Profiles of optically thin lines for different emissivities in the disc: mostly the line wings are affected (Horne and Marsh, 1986).

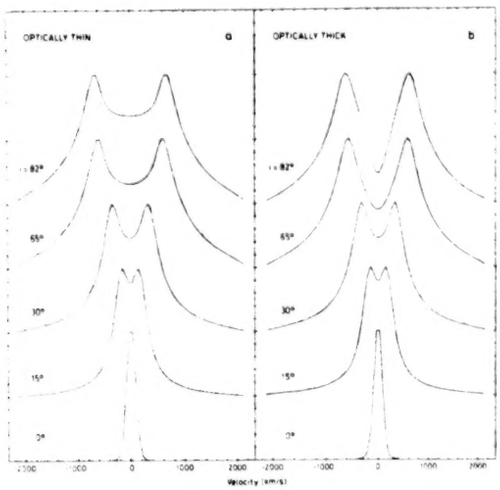


Figure 4-46a. (left) Synthetic line profiles of optically thin and optically thick lines at various angles of inclination (Horne and Marsh, 1986). Optically thick lines yield profiles which resemble more those mostly seen in dwarf novae (e.g., Figure 4-47b).

physical conditions in accretion discs in cataclysmic variables at best marginally allow for applicability of this particular method.

Horne and Marsh (1986) deal further with this problem, again assuming a condition where the disc area investigated is optically thin in the continuum and either optically thin or optically thick in the lines. In order to show the general influence of some physical effects on the emission line profiles they still adopt the Sobolev approximation for sake of simplicity, fully aware, however, of its limitations. They find that the local anisotropy can become a very important factor for the profiles of optically thick emission lines, particularly when the disc is seen under large inclination angles, while it is of only minor importance for optically thin lines, which by definition radiate isotropically. The effect on optically thick lines is illustrated in Figure 4-46a: for inclination angles larger than about 60° the minimum between the two peaks of the emission lines becomes considerably deeper if shear broadening is taken into account, compared to the case when it is not. Comparison of these computed profiles with an observed profile (Figure 4-46b) of Hα in Z Cha demonstrates that the fit is decidedly better

ORIGINAL PAGE IS
OF POOR QUALITY

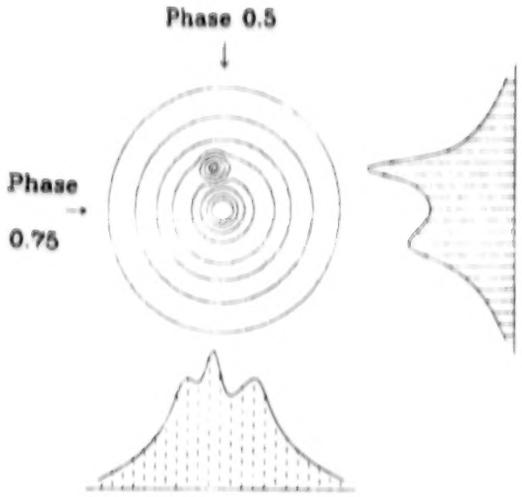


Figure 4-47. The principle of the line deconvolution: when a disc with asymmetric brightness distribution is seen under different angles, different line profiles result; the deconvolution method tries to reconstruct the information contained in the line profiles (Marsh, 1986).

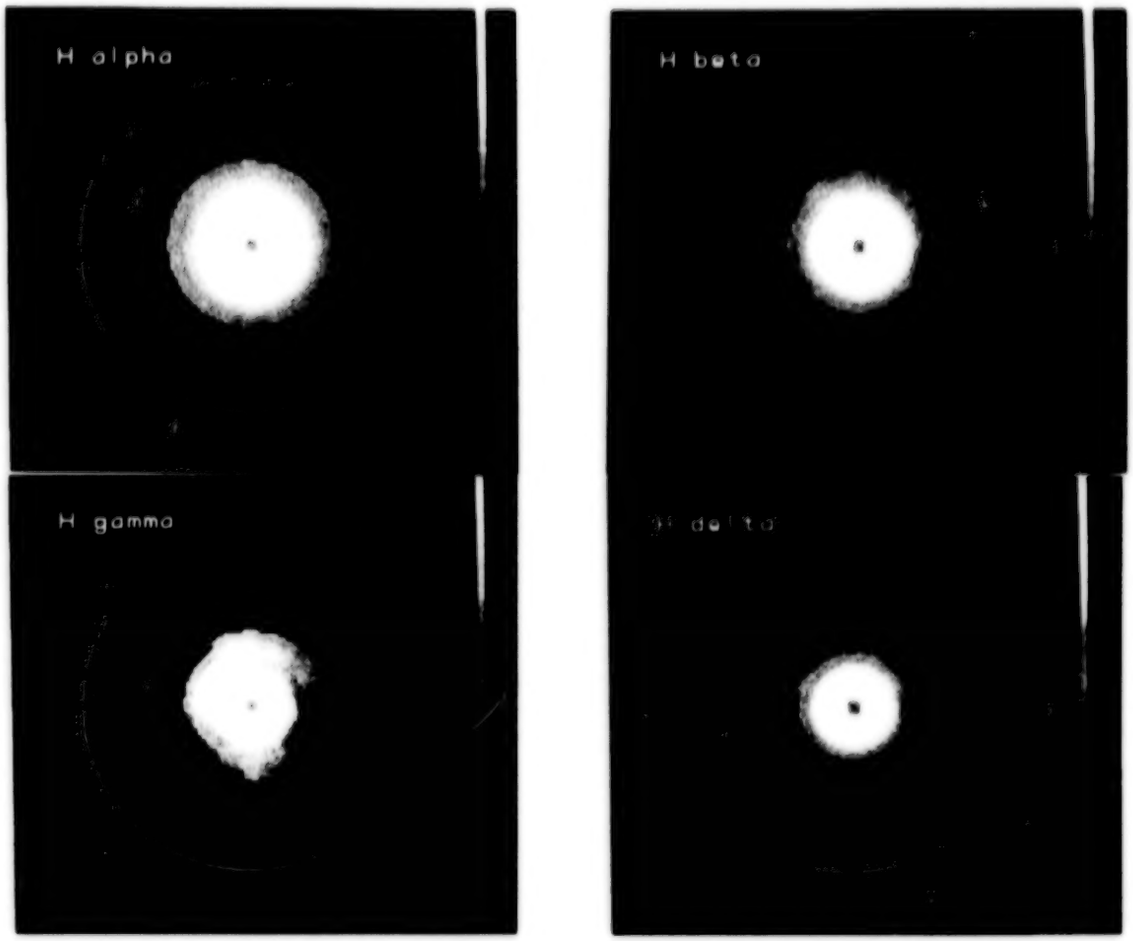


Figure 4-48. Reconstructed emission of Z Cha during quiescence in four Balmer lines: (a) total emissivity.

c-4.

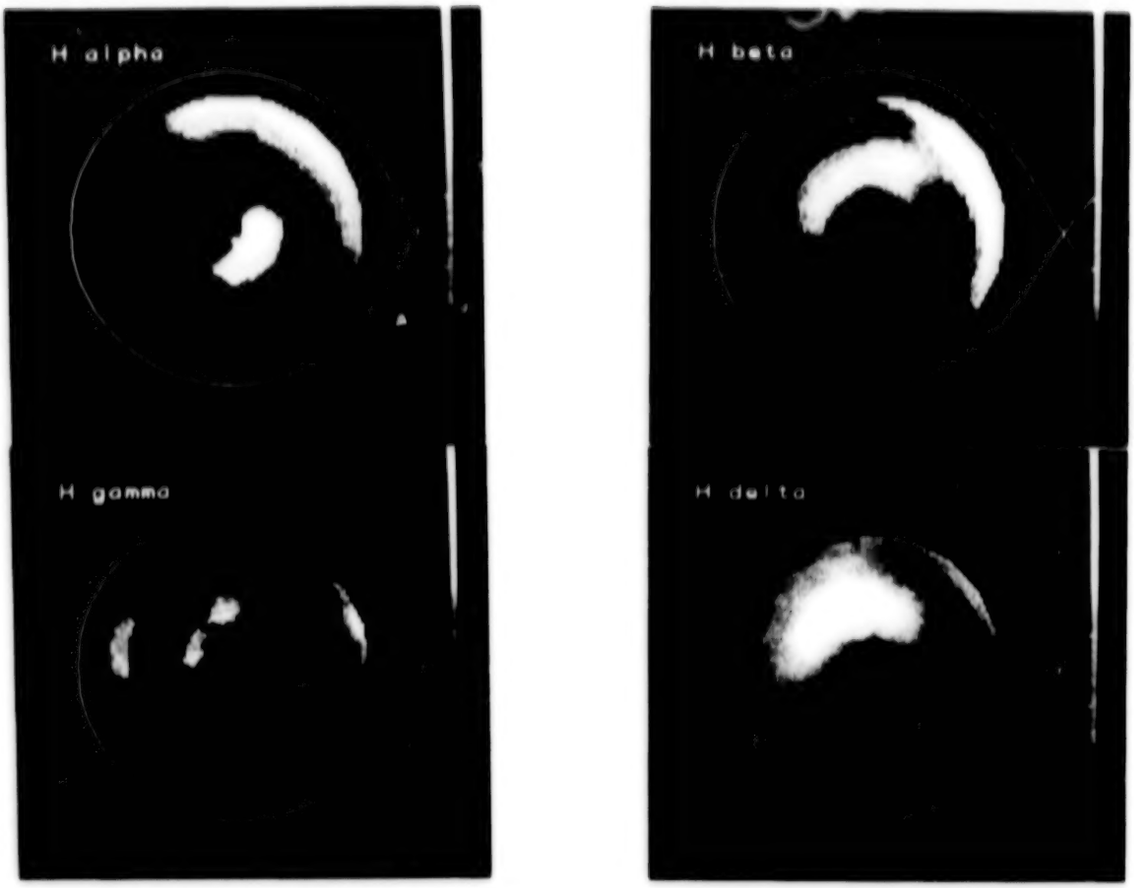


Figure 4-48(b) Fractional deviations from symmetry.

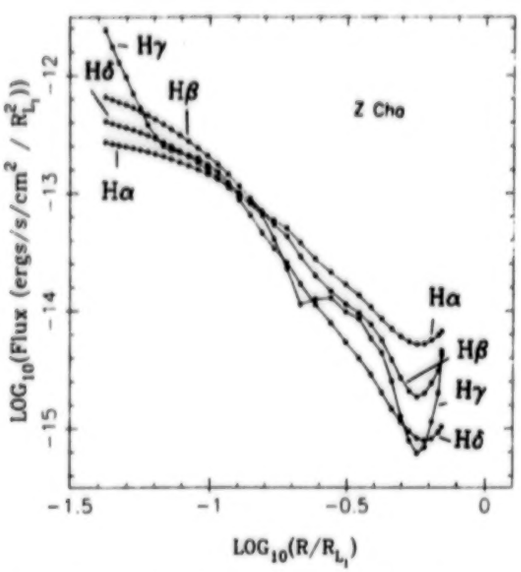


Figure 4-48(c) Radial dependence of the emission line flux in the Balmer lines. The disc is decidedly asymmetric in radial as well as azimuthal directions in its physical properties (Marsh, 1986).

when the effect of this velocity gradient is taken into account; a similar situation accounts for observed profiles of U Gem (Stover, 1981a).

In order to compute the profile of a line emitted by an entire accretion disc some radial dependence of the line emissivity has to be adopted (like assuming the disc is rotationally symmetric). The assumption of a power-law dependence:

$$f(r) \sim r^{-b} \qquad (4.18)$$

for the radial variation of the emissivity proved successful for modeling observed eclipses of H and He lines in DQ Her, with b=0 for the

Balmer lines and b = 2 for He II 4686 Å. Applying the same hypothesis and analyzing observed line profiles of different cataclysmic variables, values in the range $1 \leq b \leq 2.2$ provided the best fit (Smak, 1981, and references therein). Horne and Marsh demonstrate how various choices of b mostly affect the wings of the theoretical profiles (Figure 4-46b).

In basically the same way in which Horne et al (Horne, 1985; Horne and Cook, 1985; Horne and Stiening, 1985; Wood et al, 1986 see also Chapter V.IV.E) tried to reconstruct the continuum brightness distribution of accretion discs from UBV observations during eclipses, Marsh (1986) attempted to reconstruct the brightness distribution within the discs for line emission, by relating profiles observed at different orbital phases (Figure 4-47). The basic assumptions for this computation were Roche geometry and that the line radiation be emitted by the stationary, Keplerian rotating accretion disc. As a first approximation an azimuthally homogeneous disc was assumed. The resulting radial and azimuthal distribution of the emissivity in Hα, Hβ, Hγ, and Hδ in the eclipsing dwarf nova Z Cha during quiescent state (as reconstructed from phase-resolved echelle spectra) is displayed in Figure 4-48. Approximately the expected pattern is obtained: the emissivity basically is azimuthally (rotationally) symmetric, with the single exception of Hγ which for unknown reasons departs considerably from symmetry; fractional deviations from symmetry indicate the presence of the hot spot at about the place where it is expected according to theoretical considerations, which, since it only becomes visible when deviations from rotational symmetry are considered in turn indicates that the contribution of the hot spot to the integrated radiation cannot be more than a few percent; and, finally, the radial distribution of the emissivity clearly does not follow a simple power law (which would be a straight line in Figure 4-48c) but a more complicated pattern which is unique for each of the investigated lines.

Marsh attempts to reconstruct theoretically the observed spectrum with this probably reasonable distribution of the line emissivity, taking into account Stark broadening and shear broadening and using both a fairly accurate brightness temperature distribution derived from eclipse mapping methods and also a fairly reliable angle of inclination of the system (derived in Wood et al, 1986). He concludes that the disc is probably not in a steady state, since the mass transfer rate estimated from the luminosity of the hot spot is much larger than permissible for an optically thin accretion disc; an optically thick disc, on the other hand, matches the observations decidedly worse than an optically thin one; secondly, non-LTE conditions have to be assumed in order to match the high Balmer emissivity observed from the center of the disc.

4.IV.D. P CYGNI PROFILES, WINDS, AND CORONAE

RELEVANT OBSERVATIONS: Strong P Cygni profiles or blue-shifted absorptions are seen in C IV, and occasionally also in Si IV and N V, during the outburst of dwarf novae and in many nova-like stars. These profiles are considerably different from those of normal hot stars. Systems with very high inclination angles exhibit only strong emission profiles in these lines. All other lines are seen in absorption as usual.

see 84, 99, 107

ABSTRACT: The observations can be reproduced rather well assuming an optically thick accretion disc and a wind driven out from the disc center and/or boundary layer.

In many nova-like stars and in dwarf novae during the outburst state the Balmer lines of H in the optical are seen in absorption, with profiles that are symmetric about the line center. In the UV, however, many systems exhibit absorptions in C IV (1549 Å), N V (1240 Å), and in Si IV (1400 Å), which are asymmetrically blue shifted by 3000 - 5000 km/sec or more. In addition, the C IV line also has an appreciable red-shifted emission component

which is often seen at the same time, making it a classical P Cygni profile; while no more than a slight indication of an emission can be detected in the Si IV and N V lines. Other systems exhibit spectra with C IV in emission during the photometrically bright state, while the other lines are either in absorption or in emission; but all lines are roughly symmetric about line center (Chapters 2.II.B.2.3). When compared with system parameters it turns out that P Cygni profiles seem to appear exclusively in low-inclination systems, while very high-inclination systems show at least C IV in emission during the outburst state. Eclipse observations of RW Tri and UX UMa show that Si IV and N V are decidedly less affected than the continuum at the time of strong attenuation of the continuous flux, while C IV is hardly eclipsed at all (Drew and Verbunt, 1985). From these observations in these two stars, it can be concluded that all of these lines are formed in an extended region centered about the white dwarf, and that C IV also originates in a much larger volume which thus is practically insensitive to the eclipse. Furthermore, from the observation that C IV does exhibit P Cygni profiles while Si IV and N V do not, it can be concluded that the abundance of the latter two ions is much less than that of C IV.

In analogy to P Cygni profiles observed in O, B, and Wolf-Rayet stars, it was inferred from their mere presence that mass loss occurs from dwarf novae and nova-like stars. Several authors (Krautter et al, 1981b; Cordova and Mason, 1982; Greenstein and Oke, 1982; Klare et al, 1982) tried to derive mass-loss rates for cataclysmic systems from comparing synthetic P Cygni profiles for O-stars by Olson (1978) or Castor and Lamers (1979) with the observed profiles. They arrived at some computed values, but most of their computed profiles can hardly be matched by any of the observed ones, and also, as pointed out by Drew and Verbunt (1984; 1985), it is by no means obvious that their inherent assumption that the physics underlying mass outflow from hot single stars is basically identical to that working in cataclysmic variables applies. In other words, is the geometry of stars and discs different enough to be likely to have effect on observable line profiles? Drew and Verbunt attempted to gain more insight into the problem of mass loss from cataclysmic variables by actual modeling of line profiles and comparing them with observations (Drew and Verbunt, 1984; 1985; Drew, 1986; 1987). Their findings are reported in what follows.

They start by investigating the properties of a wind which is driven away from the vicinity of the white dwarf. Such a wind cannot be driven thermally by conditions in the inner disc or boundary layer, since temperatures of around 10^8 K would be required to produce a wind in that way.* Such temperatures could not, however, drop down sufficiently on relevant time-scales to account for the observed ionization states. Consequently, the authors assume that the wind is probably driven by radiation pressure due to radiation from the boundary layer, i.e., by conversion of (E)UV photons into kinetic energy of the ions, which requires a much lower temperature in the vicinity of the white dwarf.

Assuming that the wind is radiatively driven, and assuming that the ions were to escape from near the surface of the white dwarf to infinity — which requires an escape velocity of order 5000 km/sec, a velocity of the order observed in the blue-shifted absorptions of the UV resonance lines — an estimate of the mass-loss rate from the system can be obtained:

$$\frac{\dot{M}_w}{\dot{M}} < \frac{v_{esc}^2}{v_\infty c} \approx \frac{v_{esc}}{c} , \qquad (4.19)$$

where $\dot{M}_w$ is the mass loss rate, $\dot{M}$ is the mass accretion rate, v_{esc} and v_∞ are the escape

*In the boundary layer of a non-rotating white dwarf, a considerable amount of energy, equal to the luminosity of the entire disc, could be released in principle but there is no evidence for 10^8 K temperatures there — see Chapter 4.B.2.

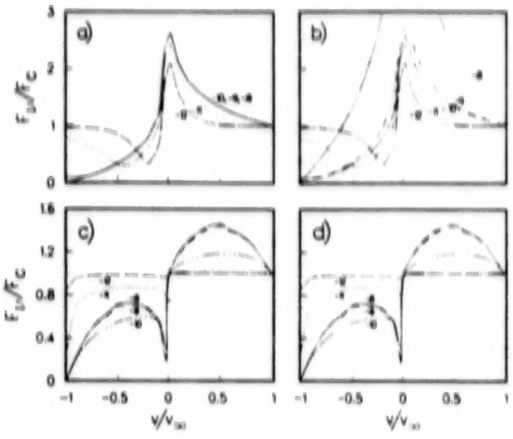


Figure 4-49a. P Cygni profiles from winds above accretion discs. (a) profiles for various mass-loss rates for an underlying stellar source (a and b) and an extended disc source (c and d); models in a and c were computed assuming coherent scattering in the lines, models b and d with collisional excitation (Drew, 1986).

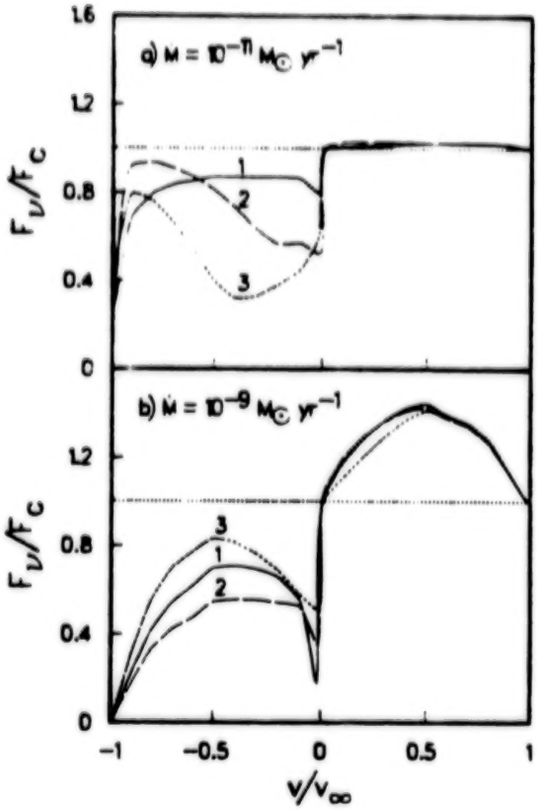


Figure 4-49b. P Cygni profiles in discs for different mass loss rates and wind accelerations: profiles shown in panel a result from acceleration closer to the white dwarf than those shown in panel b (Drew, 1986).

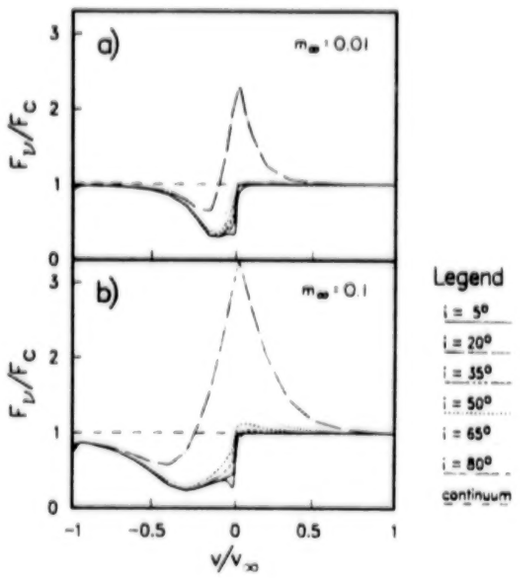


Figure 4-49c. P Cygni profiles in discs for various angles of inclination of the system for a) an essentially optically thin and b) more opaque line forming regions (Drew, 1987).

velocity and the terminal velocity in the wind, respectively, and c denotes the speed of light. This result implies that the mass-loss rate should not amount to more than a few percent of the mass accretion rate.

Based on these findings and considerations of the physical structure of winds in cataclysmic variables, Drew (1986; 1987) carried out a systematic investigation of theoretically expected resonance line profiles (C IV). She

assumed an optically thick, geometrically thin accretion disc in which the temperature is assumed to decrease with increasing distance from the white dwarf, according to equation 4.2 — i.e., no hot boundary layer is required for the production of these profiles. In this case the wind originates preferably from the disc center and/or boundary layer. The outflow was assumed to be spherically symmetric, unless mentioned otherwise below. Computations were carried out in the Sobolev approximation, which as Drew points out, will yield results which may not be accurate in detail, but will show gross properties in a reliable way.

As shown in Figure 4-49, there is a very marked difference in P Cygni profiles originating from single stars and from extended discs, respectively. Due to the much larger extension of the geometrical size of the continuum source, a mass loss rate higher by an order of magnitude is needed in cataclysmic variables in order to produce any observable effect in the line profiles. The shapes of both the absorption and the emission components in P Cygni profiles originating from discs look totally different from those of stars: the emission component is much shallower and the absorption component much weaker than for a comparable situation in stars. One consequence of this is that, somewhat dependent on the radial velocity law in the wind, conditions could exist under which the absorption minimum does not reach below half of the continuum intensity even in totally optically thick lines. It is in accordance with the observations that the absorption minimum lies close to the central wavelength in the case of a disc, whereas it can be blue-shifted by a considerable amount in the case of stars. Furthermore, the amount of scattering in the winds from discs is found to be fairly unimportant for the appearance of the line profiles, much unlike the case in stars, where it is very important. The effect of the radial velocity of the wind on the line profiles is demonstrated in Figure 4-49b, which shows that at high $\dot{M}$ slow wind acceleration causes the absorption to develop a sharper, deeper minimum, while the emission is strongly enhanced. Comparison with observations thus leads to the conclusion that acceleration in discs is likely to occur much more slowly than in single stars. The dependence of the profile on the inclination angle is considerable (Figure 4-49c), as expected from observations where, as pointed out above, P Cygni profiles are seen only in systems where the inclinations are not too high; for a small angle in the computations, when the disc is seen more or less face-on, only blue-shifted absorption components can be seen, and only for discs which are seen almost edge-on (i.e., at inclination angles which most likely would produce eclipses of the continuous radiation) does the emission become very strong. If some limb-darkening of the disc continuum is assumed (the exact characteristics of which are unknown), or when a bi-polar wind outflow is assumed rather than a spherically symmetric one, the absorption disappears completely for high inclinations, while the profiles for low inclinations are hardly affected. Mauche and Raymond (1987) arrive at very similar results from similar investigations.

In conclusion, of greatest importance for determining the actual shape of the resulting line profile according to these calculations are the mass loss rate, the velocity profile of the wind, and the temperature and the temperature profile of the accretion disc.

4.IV.E. ECLIPSE MAPPING

RELEVANT OBSERVATIONS: Photometric eclipses observed in dwarf novae and nova-like stars contain a lot of information about which parts of the system are being eclipsed.

see 35, 96, 103

ABSTRACT: The surface brightness and temperature distribution of the accretion discs can be reconstructed from eclipse observations by means of image processing techniques. The results agree well with the concepts of the Roche model.

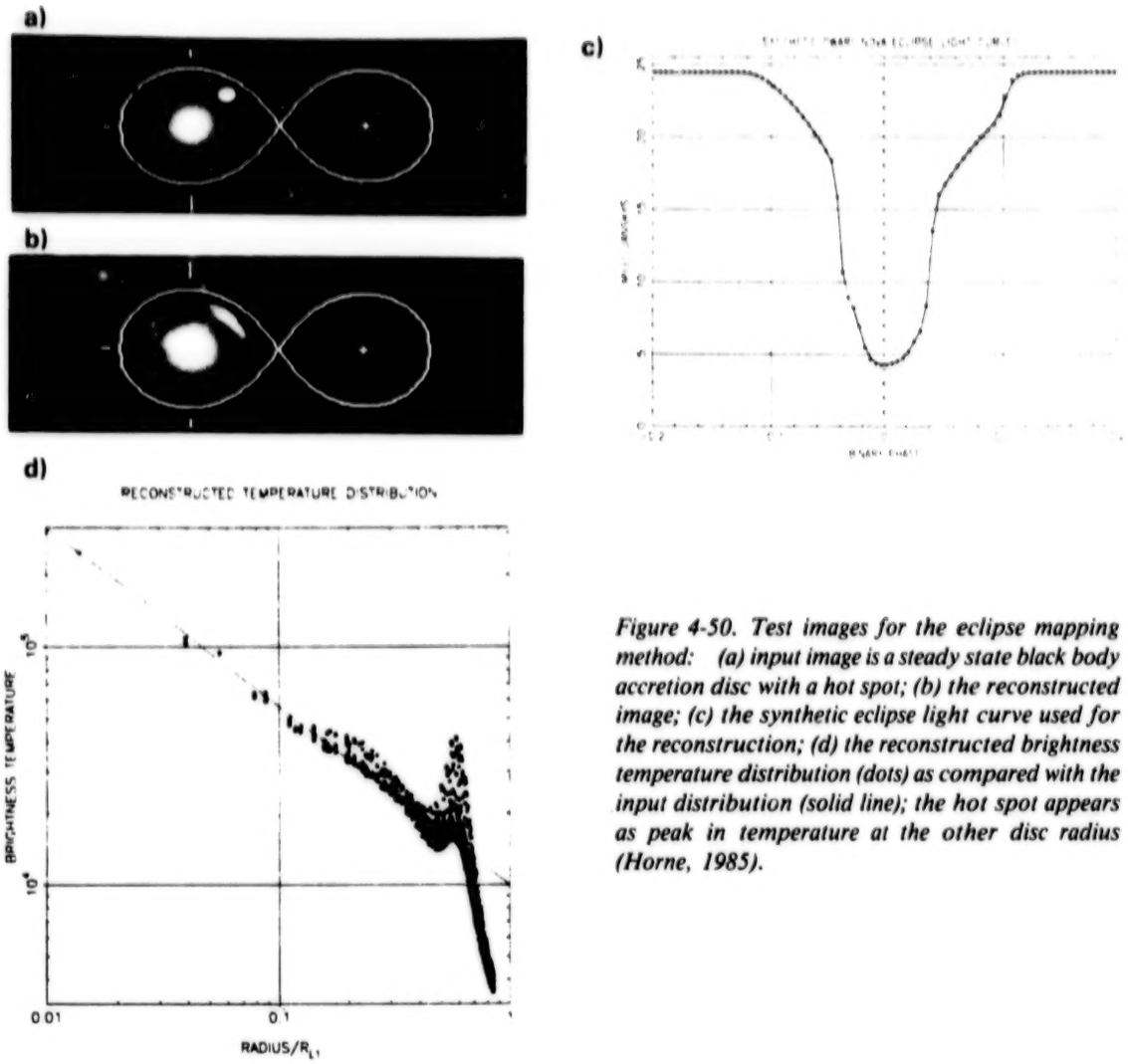


Figure 4-50. Test images for the eclipse mapping method: (a) input image is a steady state black body accretion disc with a hot spot; (b) the reconstructed image; (c) the synthetic eclipse light curve used for the reconstruction; (d) the reconstructed brightness temperature distribution (dots) as compared with the input distribution (solid line); the hot spot appears as peak in temperature at the other disc radius (Horne, 1985).

When trying to compute the spectra of accretion discs, the most serious problem encountered is that the temperature distribution in the disc is in general not known. However, a useful method for the empirical determination of the surface-brightness distribution in accretion discs has been developed by Horne (1985). He applies methods of image-processing to light curves of eclipsing cataclysmic variables. The general idea is that an eclipse light curve is determined by, and thus contains information on, the brightness distribution in the accretion disc. Being a one-dimensional set of data, it does not contain all the information of an essentially two-dimensional object, but, provided some additional information is given about the system investigated, the range of possible solutions and parameters can be narrowed considerably. The assumptions made are that the eclipse is one of an axi-symmetric two-dimensional object and that a default image ensures an optimum reconstruction of the radial brightness distribution on the expense of azimuthal information (i.e., the hot spot will cause a bright ring at the outer radius of the reconstructed image, and it will appear as a hot peak in the derived radial temperature law — see Figure 4-50b, d). Out of the several solutions still possible for image deconvolution, that image is chosen which maximizes the entropy for each element (Horne, 1985, equation 5). The data shown in Figure 4-50 demonstrate that the reconstruction (Figure 4-50b) of the input disc image (Figure 4-50a) from the "ob-

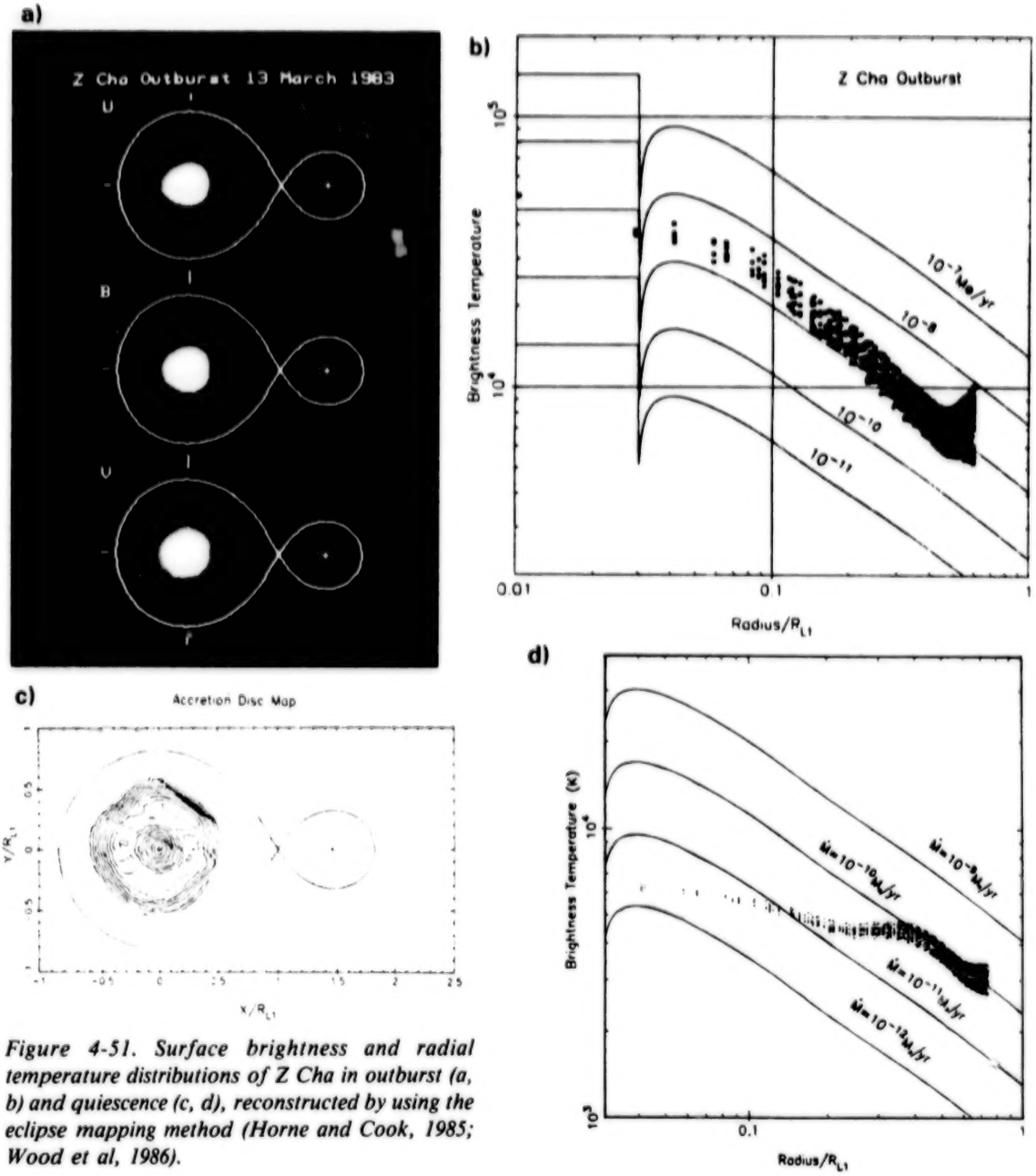


Figure 4-51. Surface brightness and radial temperature distributions of Z Cha in outburst (a, b) and quiescence (c, d), reconstructed by using the eclipse mapping method (Horne and Cook, 1985; Wood et al, 1986).

served'' light curve (Figure 4-50c) is convincing. One other input into this test image was a radial temperature law as it is assumed to hold for stationary accretion discs, $T(r) \sim r^{-3/4}$, which is reconstructed with 20% accuracy (Figure 4-50d). In terms of mass transfer rates for stationary accretion discs this translates into an accuracy of within a factor of two.

Possible applications of this method are obvious for the derivation of any radial temperature profile — thus also allowing for the localization of geometrical origin of the various line radiations, for the distinction between optically thick and optically thin disc areas from the analysis of light curves obtained in different colors, for tracing the development of the disc through the outburst cycle, and, as already mentioned, for the determination of the mass transfer rates, and finally of distances.

Some of these possibilities have not been exploited yet, but this eclipse mapping method has been applied to two objects already, to

UBV observations of the dwarf nova Z Cha during outburst (Horne and Cook, 1985) and in white light during quiescence (Wood et al, 1986), and to the nova-like system RW Tri. The reconstructed images and radial temperature profiles of Z Cha are shown in Figure 4-51. From these it is clear that during outburst the radial temperature distribution agrees with that of a stationary accretion disc, while this is not at all the case during quiescence. Furthermore, all the disc is probably optically thick during the bright state, while in the low state the inner disc is probably optically thin (no conclusive results can be obtained from measurements in merely white light) and the outer disc is optically thick, having a much higher mass transfer rate than the inner disc. Both results are in agreement with the concept that during quiescence matter is accreted only in the outer disc, while it is accreted onto the white dwarf during outburst. Inferred mass transfer rates are $10^{8.9\pm0.3}$ $M_\odot$/yr during the observed outburst, and somewhere between $10^{-10.23}$ and $10^{-10.08}$ $M_\odot$/yr for the outer parts of the quiescent disc, down to some $10^{-11.7}$ $M_\odot$/yr at disc center. During the quiescent state the disc temperature increases only very slowly from some 4000 K at the outer rim to some 7000 K in the center; during outburst it ranges from some 7000 K at the outer edge to some 35000 K in the center (it should be kept in mind here that optical colors are quite insensitive to UV flux, so that the temperature of 35000 K should be regarded as somewhat approximate). The radial colors for the disc in outburst all fall between the theoretical lines for black bodies and for main sequence stars for the hot central parts of the disc ($r \gtrsim 0.3$ of the radius of the Roche lobe), indicating that the vertical temperature gradient in the disc is flatter than that of main sequence stars. Finally, a distance of 105 ± 20 pc is derived from the angular diameter of the disc, assuming a radial velocity amplitude of the red companion star of 400 km/sec.

A similar analysis was carried out for U, B, R observations of RW Tri (Horne and Stiening, 1985). This disc is obviously optically thick*, and it follows roughly a radial temperature dependence as expected for a stationary disc. The temperature ranges from 10000 K to 40000 K, and a mass transfer rate of $\dot{M} = 10^{-7.9\pm0.4}$ $M_\odot$/yr and a distance of some 500 pc are derived.

4.IV.F. THE BOUNDARY LAYER

RELEVANT OBSERVATIONS: Hard and soft X-ray radiation which cannot be ascribed to the accretion disc is observed from many dwarf novae and nova-like stars.

see 60, 69

ABSTRACT: A boundary layer between the disc and the white dwarf is assumed to form where the Keplerian rotating disc material is braked down to the rotational velocity of the white dwarf in order to be accreted. The detailed structure of this layer is not yet clear.

A final weak point in current spectrum computations is that only very little is known about the physical structure of the radiation emitted from the boundary layer. The current state of knowledge is summarized in this section. For other recent reviews see e.g., Shaviv (1987) and Stanley and Papaloizou (1987).

Material in the accretion discs of cataclysmic variables is assumed to circulate with Keplerian velocity at any distance from the white dwarf. The white dwarfs, on the other hand, are not likely to rotate at the Keplerian velocity corresponding to their surface (which would mean just short of brake-up). So, at the boundary where the inner disc meets the surface of the star, a velocity gradient is likely to be present. By some mechanism the excess kinetic energy of the disc material has to be converted into some other form of energy so that at least a significant fraction of this material can eventually settle onto the surface of the white dwarf. This region is referred to as the boundary layer.

*This combination of colors permits a clear distinction to be made between optically thick and optically thin areas.

The amount of energy liberated depends on the velocity gradient. An upper limit can be obtained from assuming a non-rotating star in which case no boundary layer would be formed. In general the luminosity of the boundary layer is

$$L_{BL} \lesssim \frac{G\, M_{WD}\, \dot{M}}{R_{WD}} \quad , \qquad (4.20)$$

where all the symbols have their usual meaning; i.e., once again about as much energy as that radiated away by the entire disc can be liberated in the boundary layer, an energy of the order of 10^{33} erg/sec. Given the small geometrical size of the boundary layer,* it is the probable place of origin of the observed X-ray radiation from cataclysmic variables. While other places of origin have been suggested, like the coronae of the secondary stars or the hot spot, these other sites lead to severe theoretical problems concerning the amounts of energy liberated (Patterson and Raymond, 1985a); thus the boundary layer seems the most likely site. Observations indicate that during the quiescent state the hard X-ray flux obtained from dwarf novae can be as high as the optical plus the UV flux from the disc, while no soft X-ray flux can be seen. During outburst the hard X-ray flux increases only slightly, if at all, while the soft X-ray radiation increases by one to two orders of magnitude (Chapter 2.III.A.2). The sample of observations in the latter case is not really statistically significant (three objects: U Gem, SS Cyg, VW Hyi), but negative observations of other sources do not contradict a generalization of this kind.

Theoretically, the physical structure and luminosity of the boundary layer are not yet known reliably. For making estimates, it is almost always assumed that the white dwarf is non-rotating (consistent with high observed X-ray luminosities), in which case hard X-rays are likely to be due to an optically thin boundary layer which has to heat up considerably in order to radiate away all of the energy produced. Soft X-rays occurring at high accretion rates, on the other hand, are attributed to optically thick boundary layers where the radiation is thermalized before being able to escape the system (Pringle, 1977; Pringle and Savonije, 1979; Tylenda, 1981b; Frank et al, 1985; Patterson and Raymond, 1985a; 1985b). Energy is assumed to be liberated either by very efficient viscous interaction (Tylenda, 1981b) or by shocks, as the fast-rotating material approaches the surface of the white dwarf (Pringle, 1977; Pringle and Savonije, 1979). One problem with this latter approach is the necessity to produce radial shocks in a basically azimuthally moving material, where shear flows and consequent turbulence reduce the efficiency of the shocks (Frank et al, 1985). King and co-workers (King and Shaviv, 1984; Frank et al, 1985) propose that during quiescence, when the turbulence is expected to occur, the boundary layer heats the gas to temperatures up to 10^8 K and also causes it to expand out of the boundary layer, thus forming a hard X-ray emitting corona around the central object. At high accretion rates — a value typically considered, in agreement with the observations, is $\dot{M} \gtrsim 10^{16}$ g/sec — the expansion is suppressed, thus reducing the hard X-ray flux and at the same time increasing the soft X-ray radiation. Elaborating on an idea suggested by Icke (1976) that shocks created by turbulent activity in the disc form a corona above the accretion disc, Jensen et al (1983) suggest that a dynamo coupling differential rotation and convection generates a magnetic field, which leads to the formation of a hard X-ray emitting corona, in analogy to models suggested for the formation of the solar corona. By this concept the authors are able to explain qualitatively the observed relation between oscillations seen in hard X-rays and in optical wavelengths in particular. Such a corona could also be responsible, at least partly, for the UV resonance lines observed in emission in most quiescent dwarf novae; it cannot be responsible, however, for the P Cygni pro-

*Whatever the assumptions or computations are, it cannot be considerably larger than the dimensions of the white dwarf.

files seen during outburst, since then the observed X-ray radiation is softer. Any of the scenarios proposed above can be reconciled with the tentatively established relationship between the angle of inclination and the observable X-ray flux (Patterson and Raymond, 1985a) which suggests an obscuration of the source of hard X-rays, thus implying that the emitting region must be confined to an area fairly close to the white dwarf.

How much radiation in X-ray energies is to be expected from cataclysmic variables is subject to a wealth of assumptions and hypotheses. A so-called "mystery of the missing boundary layer" has been mentioned a couple of times in the literature (Ferland et al, 1982a; Burkert and Hensler, 1985; Kallman and Jensen, 1985). What is meant by this term is that the observed soft X-ray flux from many cataclysmic variables is lower by a factor of 10 to 100 than what has been predicted from theoretical considerations. A careful examination reveals that all the quoted estimates of expected X-ray flux are upper limits based on the assumptions of a non-rotating white dwarf plus a couple of other somewhat arbitrarily chosen parameters which will be considered below. The "mystery" seems to consist of still questionable assumptions, not paradoxical results. The amount of observable radiation depends on: the geometrical size of the boundary layer, which is normally assumed to be small, on the order of the thickness of the disc near the white dwarf, the rotational velocity of the white dwarf, which gives a range to the flux of anything between zero and the flux of the entire disc; the mass and thus the radius of the white dwarf which can make a difference of up to one order of magnitude in the predicted flux; the mass accretion rate, which is not known at all for quiescent dwarf novae in particular, only that it clearly is different from the mass transfer rate from the secondary star, and the distance of the object from the observer, which usually also only is known within fairly wide limits.

Considering that observations, in particular of X-rays, are only carried out in certain energy bands and do not cover the entire spectrum, the wavelength dependence of the emitted spectrum also has to be considered when discussing expected fluxes. Qualitative considerations clearly seem to support the view that a) the boundary layer is the origin of the observed X-rays, b) the boundary layer is optically thin for low accretion rates, i.e., for quiescent dwarf novae, and c) it becomes optically thick for high accretion rates (Patterson and Raymond, 1985a; 1985b). In no case, however, have self-consistent computations of the physical structure of the boundary layer been carried out predicting any spectrum. Program codes for two-dimensional hydrodynamic boundary layer computations are being developed by Robertson and Frank (1986), Kley and Hensler (1986), and Kley (1989). The first results from these do not contradict the qualitative concepts reported above, but they do indicate that the boundary layer seems to be much more extended and expansive than assumed so far. Papaloizou and Stanley (1986) carried out computations of the temporal development of the boundary layer and found that quasi-periodic oscillations can originate due to small-scale viscosity instabilities in there — as observed occasionally in nova-like stars and in dwarf novae during outburst (Chapters 2.II.D.2, III.D).

4.V. THE EVOLUTIONARY STATE OF CATACLYSMIC VARIABLES*

4.V.A. SPACE DISTRIBUTION AND SELECTION EFFECTS

ABSTRACT: Various determinations of the space densities of sub-classes of cataclysmic variables depend critically on assumptions about outburst time scales (for novae and recurrent novae) and about observational selection effects.

In order to understand the context of cataclysmic variables in the evolutionary big picture of all stars, it is of great importance to

*Cataclysmic variables in this section are restricted to novae, nova-like stars, dwarf novae, and possibly recurrent novae; symbiotic stars are not included in the discussion.

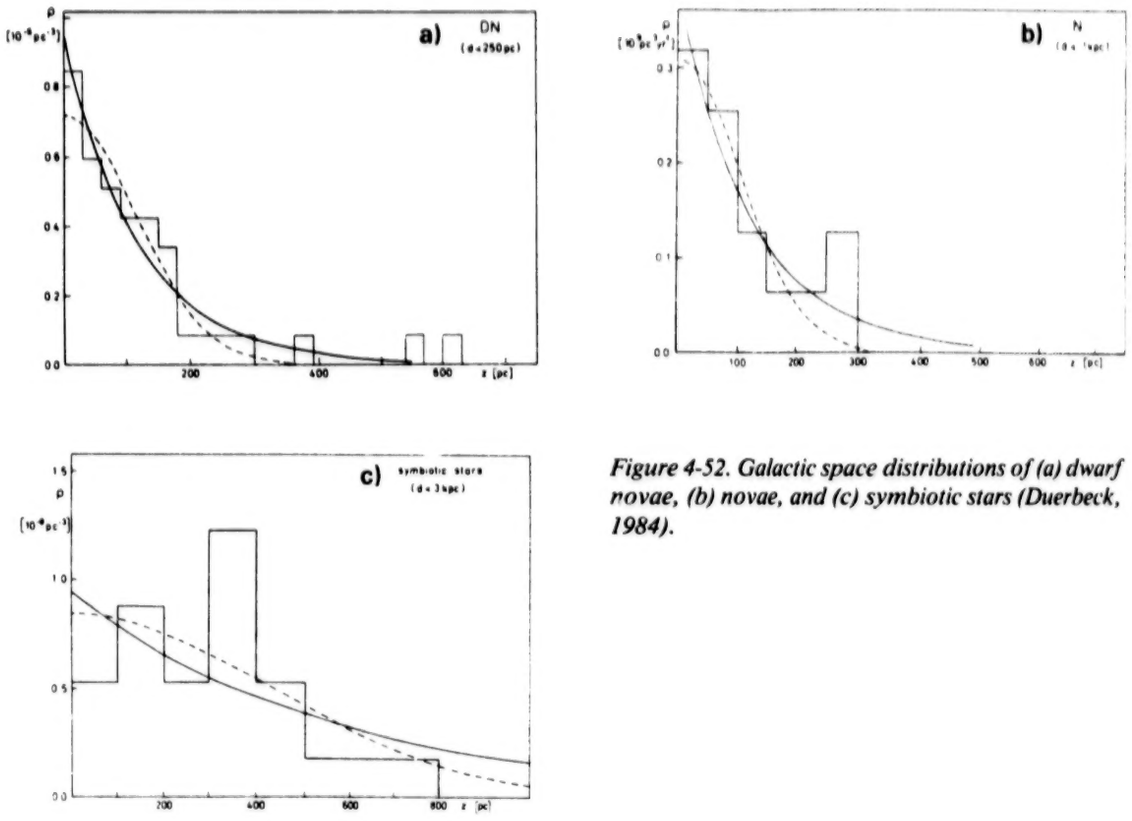


Figure 4-52. Galactic space distributions of (a) dwarf novae, (b) novae, and (c) symbiotic stars (Duerbeck, 1984).

THE SPACE DENSITY ($\times 10^{-7}$ pc^{-3}) OF CATACLYSMIC VARIABLES

Class	This Work	Previous	Reference
Dwarf novae	2.4	3	Patterson 1984
		4	Warner 1974
Novalike ..... (confirmed only)	1.5	5	Warner 1974
Novalike ..... (with candidates)	4.4	...	
Novae	1.4	4	Patterson 1984
		13	Duerbeck 1984
		1000	Bath and Shaviv 1978
		1	Warner 1974

Table 4-2. Determinations of space densities of cataclysmic variables (Downes, 1986).

know the space distribution and space density of these objects. Whatever the evolutionary model for cataclysmic variables, their space density and distribution must be compatible with those of supposed progenitors and descendants.

Several attempts have been undertaken to derive the space density of cataclysmic variables (e.g., Kraft, 1965; Warner, 1974b; Bath and Shaviv, 1978; Duerbeck, 1984; Patterson, 1984; Downes, 1986; Ritter and Burkert, 1986) with different results, depending on what assump-

tions were made about the absolute magnitudes of cataclysmic variables and about the completeness of observed samples. An extensive investigation of the space distribution of different sorts of cataclysmic variables and possible progenitors has been carried out by Duerbeck (1984). Some of the resulting distributions are displayed in Figure 4-52. One of the conclusions from this study is that novae, dwarf novae, and possibly supernovae of type I have very similar galactic distributions, which in turn are fairly similar to those of W Ursae Majoris stars and Algol systems. Recurrent novae and symbiotic stars have similar galactic distributions, but these are distinctly different from the former ones. Thus there is support for the view that either W Ursae Majoris stars or Algol systems, or both, might be progenitors of most cataclysmic variables on the basis of their space densities; however, since the angular momentum of W Ursae Majoris stars is too small for the formation of a white dwarf, they can be discarded (Ritter, 1976). Space distributions of dwarf novae are consistent with the hypothesis that they might develop into type I supernovae (see also Chapter 4.V.E).

The shape of the galactic distribution of dwarf novae and novae (see also Figure 1-1) points at their being population I objects. Some novae (T Sco, N Oph 1938) and possibly some dwarf novae are members of globular clusters, however, so they are population II objects (Webbink, 1980).

According to Duerbeck's study, novae and dwarf novae seem to have almost equal space distributions, but dwarf novae are some 10 times as abundant as novae. On the other hand, Bath and Shaviv (1978) determined the space density of dwarf novae to be 200 times less than that of classical novae; Patterson (1984) derived the density of dwarf novae and nova-like stars together (without AM Herculis stars) to be about as high as that of novae; Warner (1974b) derived about equal densities for both novae and dwarf novae; and Downes (1986) arrived at approximately the same distributions for novae, dwarf novae, and nova-like stars from a survey of UV-excess objects! (Table 4-2). The point of disagreement is the completeness of the observed sample. On one hand this is a reflection of the problem of accurate distance determination (see Chapter 4.II.C.2), which, however, for statistical purposes is probably not too severe in the case of dwarf novae, since all those which are observable are relatively close by. A much more important question is the assumed outburst period of classical novae about which nothing is known at all.

For dwarf novae and nova-like stars alone, Ritter and co-workers (Ritter, 1986a; Ritter and Burkert, 1986; Ritter and Özkan, 1986) investigated the influence of various system parameters on the observable, magnitude-limited, sample. They found that the selection is rather insensitive to assumptions about the assumed galactic distribution function and the interstellar absorption, as well as to the bolometric correction. By far the strongest selection effect was due to the mass-radius relation of white dwarfs, according to which the star's radius decreases considerably with increasing mass, yielding a larger gravitational potential and thus a brighter disc. The consequence is a strong statistical overrepresentation of the brighter systems containing massive white dwarfs. Finally they found that, since different effects act in different ways on the system's brightness, selection effects become less severe as the limiting apparent brightness decreases. Owing to these selection effects, they concluded that only a very minor fraction, about 1 out of 200, of the existing cataclysmic variables are actually observed.

4.V.B. THE WHITE DWARFS

White dwarfs in cataclysmic variables seem to have statistically higher masses than single white dwarfs. This difference can be fully accounted for by selection effects.

The determination of the masses of the two stellar components in a cataclysmic system is very difficult and not particularly reliable (Chapter 4.II.C.1). In particular, there are only two relatively highly reliable determinations for the masses of the white dwarfs, based on the analysis of double-lined spectroscopic eclipsing systems: EM Cyg and U Gem. The masses obtained are 0.57 ± 0.08 $M_\odot$ for EM Cyg (Stover et al, 1981) and 1.13 ± 0.15 $M_\odot$ for U Gem (Stover, 1981a). Less reliable masses have been obtained for several other cataclysmic systems (Ritter, 1987). With the necessary caution, however, this sample may be regarded as statistically representative of the white dwarf masses in cataclysmic variable systems. For the mass distribution of the white dwarfs in sub-classes of cataclysmic variables, see Figure 1-5. There is no evidence for any striking systematic difference in the masses of different sub-classes of cataclysmic variables. The mean white dwarf mass in cataclysmic variables is 0.90 ± 0.06 $M_\odot$, whereas that of single white dwarfs is only 0.62 ± 0.08 $M_\odot$ (Ritter, 1987). Even if the masses derived for white dwarfs in cataclysmic variables are not very reliable, it seems fairly unlikely that such a severe distortion can be due to poor data, particularly since the two reliable values, for EM Cyg and U Gem, fit into the general pattern.

The white dwarfs in cataclysmic variables, as white dwarfs in general, are believed to be formed from red giants or supergiants which are eventually stripped off their envelopes as will be discussed later. The white dwarf is simply the He or CO core of the evolved star. Since the core mass keeps increasing as long as the star still possesses its shell, the mass of the remaining white dwarf depends on the time when the surrounding shell is lost. Thus, in the geometrically constrained case of the evolution taking place within the Roche lobe, statistically, the masses of the white dwarfs in cataclysmic variables are expected to be even smaller than those of single white dwarfs, since the shell was lost when it exceeded the Roche limit, no matter how little advanced the giant's evolution was at that stage.

Another possible explanation for this large discrepancy is to assume that it is in the nature of cataclysmic variables, or rather their progenitors, that they are formed preferentially with massive white dwarfs. Computations have been carried out by, e.g., Law and Ritter (1983; see also Ritter, 1983) and Livio and Soker (1984a) in order to investigate this question. Both these computations must be seen in the context of the general concept of binary evolution leading to the formation of cataclysmic variables which will be discussed in a later Chapter 4.V.E. Here only the basics, relevant to the present question, will be outlined. Law and Ritter suggest that white dwarfs in close binaries cannot only be formed through what they call case B,* leading to low-mass white dwarfs, and case C,* leading to massive white dwarfs, events but also through what they call case BB. In their case B mass transfer event and common envelope evolution, the primary of an initially wide binary system loses the binary period and thus the size of the Roche lobe has decreased considerably. If conditions are then right, i.e., if the mass of the helium star is not too high ($M_{He} < 3.4\ M_\odot$, as a larger mass would eventually lead to a supernova explosion) and the Roche lobe is not too large, a case B mass transfer event may occur, leaving a white dwarf near the Chandrasekhar limit of 1.4 $M_\odot$. However, estimates of the abundances of possible progenitors for this sort of white dwarf leads to the conclusion that, while they probably do exist, their probability of occurrence is much too small to provide an explanation for the observed discrepancies in the mass spectra of white dwarfs.

*Catastrophic mass transfer in a binary system is referred to as case B when it sets in before, and is referred to as case C when it sets in after, core helium burning in the more massive component.

Livio and Soker (1984a) investigate the question whether details of the common envelope phase of binary evolution favor massive white dwarfs in some way. They show that the two stellar components are much more likely to survive the spiralling-in process during common envelope evolution if the envelope is a relatively less dense supergiant envelope — and thus the core is a massive white dwarf — rather than a denser giant envelope. However, Ritter and Burkert (1986) hold against this hypothesis observations of detached post-common-envelope systems whose mean white dwarf mass ($0.62 \pm 0.08\ M_\odot$) is not any higher than that of single white dwarfs.

Another possibility that has been suggested is that the mass of the white dwarf might grow secularly due to continued accretion of material from the disc. Ritter (1985; see also Ritter and Burkert, 1986) discusses this possibility in more detail. He rejects it with two arguments: first, a much larger number of type I supernovae would be expected if the accumulation of a significant amount of mass were possible whenever the Chandrasekhar limit for the white dwarf mass was exceeded (see also Nomoto and Sugimoto, 1977); second, analysis of nova ejecta* suggests that the white dwarf loses mass during the course of a nova outburst.

Yet another possibility to explain the two different mass spectra of the white dwarfs is the action of selection effects on the observed sample. This aspect has been dealt with by Livio and Soker (1984b) and Ritter and co-workers (Ritter 1986a; Ritter and Burkert, 1986; Ritter and Özkan, 1986). Livio and Soker estimate that there are $6.86\ 10^3$ more outbursts for a $1.3\ M_\odot$ white dwarf than for a $0.6\ M_\odot$ white dwarf with otherwise identical conditions. Considering this theoretical dependence of outburst time-scales of novae on the white dwarf masses (on which no observational data are available) they conclude that these relatively frequent outbursts in novae containing a massive white dwarf could account for the excess average mass in novae. A little discouraging in this respect are the derived masses of novae which, while mostly higher than the average of $0.6\ M_\odot$ for single white dwarfs, are somewhat at the lower end of the distribution in cataclysmic variables (see Figure 2-3a).

A selection effect favoring dwarf novae with high-mass white dwarfs is the mass-radius relation for white dwarfs according to which, as the material a white dwarf consists of is degenerate, the radius shrinks considerably as the mass increases, thus making the respective accretion discs much brighter due to the higher gravitational potential in the hot inner disc. Ritter and co-workers (see above) carried out extensive computations in order to find out the strength of this selection effect, and found that this mass-radius relation for white dwarfs can fully account for the observed mass spectrum of white dwarfs in cataclysmic variables as compared to that of single white dwarfs. Ritter (1986b) investigated a sample of pre-cataclysmic objects which is probably not strongly biased observationally and found that the mean white dwarf mass for these systems is $0.6 \pm 0.08\ M_\odot$, in perfect agreement with the results for single white dwarfs.*

*Nova ejects are overabundant in CNO by up to a factor of 100 compared with the solar composition, while the matter transferred onto the disc from the secondary star can reasonably be assumed to have solar abundance.

*One cautioning remark about white dwarf masses in cataclysmic variables should be added. A lot of the discrepancy between single white dwarf masses and those of white dwarfs in cataclysmic variables seems to be due to difficulties in deriving the masses from observations, akin to the problem of determining the radial velocity curve (see Chapter 4.II.C.1). When masses given in the catalogues by Ritter from 1984 and 1987 are compared, the average has shifted down from $1.04 \pm 0.3\ M_\odot$ (1984) to $0.90 \pm 0.06\ M_\odot$ (1987), largely as a result of a redetermination of white dwarf masses using more elaborate techniques.

4.V.C. THE SECONDARY STARS

RELEVANT OBSERVATIONS: The secondary components are seen in the optical range in systems with orbital periods in excess of some 6 hours; often they are also seen in shorter period systems at infrared wavelengths.

see 78

ABSTRACT: Observationally, the secondary stars cannot be distinguished from main sequence stars. On theoretical grounds, they must originally have been considerably more massive, but lost most of their mass during the common envelope phase and later evolution. After the common envelope phase the stars are drawn together by magnetic braking of the secondary component until this star comes into contact with its Roche lobe. Thereafter, mass transfer is driven primarily by magnetic braking above the period gap, and by gravitational radiation below it. Black dwarf secondaries are expected to exist below the period gap but have not been detected so far; selection effects can account for this.

As in the case of white dwarfs, masses of the secondary stars can only be determined reliably for the two eclipsing double-lined spectroscopic binaries, U Gem and EM Cyg (numerical values for these and other systems are given in Chapter 4.II.C.1). Furthermore, in all those systems which have a known orbital period, the radius of the secondary can be derived from the assumption that the star just fills its critical Roche volume. In this case the mass and the radius of the star are linked only by an almost constant factor the value of which depends mainly on the orbital period and only very weakly on the mass ratio (Faulkner et al, 1972; Patterson, 1984). Furthermore, the spectral types of the secondary stars are known for a couple of systems. The assumption that the radius and spectral type of the secondary ought to correspond to each other puts further limits on the possible mass of the companion star. Finally, dynamical stability of the system requires that the mass of the secondary star must not exceed significantly that of the white dwarf (although at least the case of EM Cyg, with q = 0.77, demonstrates that nature is not quite as restrictive as our theories). From this constraint it immediately follows — and is observationally confirmed — that the secondaries in systems with $P_{orb} \gtrsim 10$ h must be evolved stars.

Ritter (1983b; 1985; 1986a) derived physical parameters for 13 secondary components using just the above criteria, in order to test the frequently made assumption that the secondary stars in cataclysmic variables are main sequence stars. He compares these results with theoretical and observed (from detached visual and spectroscopic main sequence binaries) mass-radius relations, as well as with the spectral types and mean densities of main sequence stars (Figure 4-53). From these investigations it becomes apparent that, observationally, the secondaries in cataclysmic variables with orbital periods smaller than about 10 hours are very close to the main sequence and may not even be distinguishable from main sequence stars, which in turn implies that they are essentially unevolved. As Ritter (1983b) stresses, it cannot be concluded from this that they are zero-age-main-sequence stars, a point which will be considered more closely in a moment. It might be useful to emphasize, however, that for cataclysmic variables with orbital periods smaller than 10 hours the assumption that the secondaries look like main sequence stars provides an easy, though not highly reliable, method to obtain the masses of both stars. (See Chapter 4.II.B.1).

If the masses of the secondary stars, which are typically smaller and may be much smaller than 1 $M_\odot$, are taken at face value, it is not likely that they have evolved significantly during their lifetimes. On the other hand, the progenitors of cataclysmic variables are not yet known with certainty, so not much is known about the initial mass of these stars. It probably can be taken for granted from general evolutionary theory that the mass of the primary star was originally the larger one of the two, and that it evolved faster than its companion and

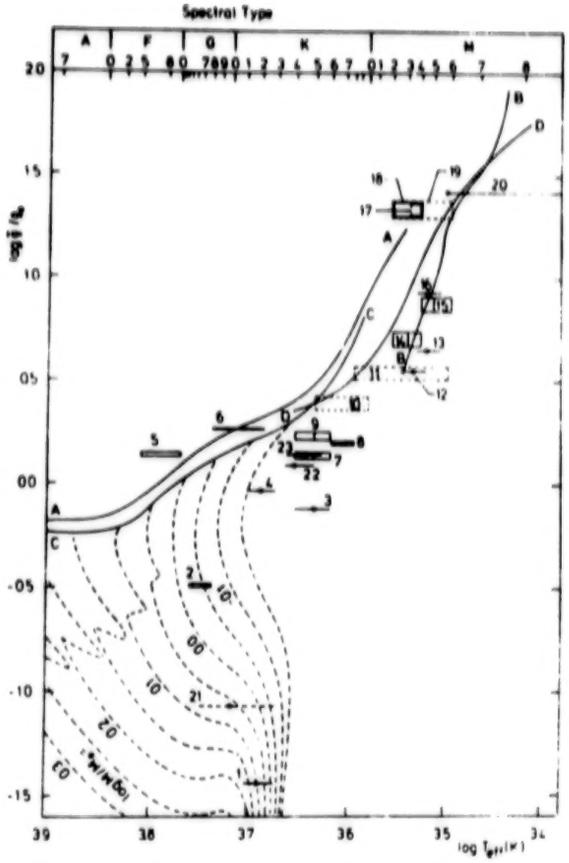


Figure 4-53. Effective temperature vs. mean density relation for secondaries in cataclysmic variables (numbers 1-20; numbers 21-23 represent low-mass X-ray binaries) together with several theoretical computations of the zero-age main sequence (A-D) (Ritter 1986c). Observationally the stars i.e., approximately on the main sequence.

eventually became a white dwarf. If the secondary star originally was only slightly less massive than the white dwarf, it also should have evolved significantly by the time the common envelope phase of the evolution was initiated by the primary (see below). The mass of the white dwarf primary after this stage has to be less than the Chandrasekhar limit of 1.4 $M_\odot$, so, if stability against mass transfer* is to be attained, the secondary star also has to lose a certain possibly large fraction of its initial mass. If this happens after the star has had a chance to evolve, the remaining secondary is expected to exhibit decided traces of its evolution. The effect is expected to be the stronger the closer to unity the initial mass ratio is. In fact most secondaries, in particular those in systems with orbital periods smaller than 10 hours, do not seem to be significantly evolved, since, if they resembled normally evolved stars they should be found above the main sequence, and if they were the chemically homogeneous cores of formerly fairly massive stars they should lie below the main sequence (Ritter, 1983b). This situation can only be understood. in terms of the typical critical mass ratios having originally been larger than two, in which case, theoretically, no significant trace of evolution is expected to be present in the remaining secondary star.

The secondary star obviously loses mass continuously to the primary at a rate on the order of 10^{-8} to 10^{-11} $M_\odot$/yr (see Chapter 4.II.C.4). If the star has a comparatively large mass, or the system a long orbital period, it hardly is affected by this. As the star loses mass, its radius shrinks due to magnetic braking or gravitational radiation (Chapter 4.V.D), and the Roche lobe shrinks as well, so the star loses

*Mass loss from the secondary star results in a shrinking of the star's radius, rather than an expansion. The latter would lead to an uncontrolled increase of mass transfer.

still more mass. Mass transfer continues without dramatic consequences, since the thermal time scale for the secondary to adjust to mass loss is much smaller than the time-scale at which gravitational radiation proceeds. If this process continues for long enough, however, eventually the star is driven out of thermal equilibrium and becomes a degenerate black dwarf. As will be discussed in the next section, at the time when the star is out of thermal equilibrium the system reaches a minimum orbital period, which at later stages of the evolution increases again as the secondary continues losing mass.

Rappaport et al (1982) point out that close to the minimum orbital period the secondaries cannot be assumed to follow the mass-radius relation of main-sequence stars any longer, but they are expected to have systematically smaller masses by eventually as much as 20%, after they are driven out of thermal equilibrium. No such effect is apparent in observations (Figure 4-53). However, this might be due to the still relatively long orbital periods of the systems for which the secondaries have been investigated.

For systems containing a degenerate black dwarf secondary, i.e., systems which have evolved through the minimum period, a secular increase of the orbital period is predicted. Such an increase has been observed in Z Cha (Cook and Warner, 1981; for observations see Chapters 2.II.B.5, 3.II.A, 3.III.A, 3.IV.A, and also Chapter 4.III.E). Faulkner and Ritter (1982) investigate whether the assumption of a black dwarf secondary is in agreement with observational properties of Z Cha and find that it is in clear contradiction: the predicted amplitude of the radial velocity is smaller than observed; the radii of both the accretion disc and the white dwarf are smaller than observed (Z Cha is a double-eclipsing system which allows for fairly accurate determination of these parameters); the mass transfer rate of 10^{-13} $M_\odot$/yr inferred from the system's apparent brightness, would bring it close enough to the Sun for it to show a large parallax and a high proper motion, neither of which are observed; and, finally, although the sign of the observed period change is what is to be expected in the case of a black dwarf, the predicted period change on a time-scale of some 10 years is in strict contradiction to the value of 9.6 ± 10^6 years claimed by Warner and Cook. By analogous arguments Faulkner and Ritter also exclude the presence of black dwarf secondaries in two other ultra-short-period systems, HT Cas and OY Car.

Rappaport et al (1982) estimated that up to 20% of the ultra-short-period cataclysmic variables (systems with orbital periods shorter than 2 hours) could contain a black dwarf secondary. With such a high postulated percentage it is surprising that not a single such system could be found so far, although selection effects may act strongly against them. When the secondary component is a normal undegenerate main sequence star, the hot spot is eclipsed during the eclipse of the white dwarf at very high inclination angles, rendering the system with a double eclipse. Since the time interval between the two parts of a double eclipse depends on the geometrical size of the secondary star, becoming larger as the secondary becomes smaller, the two parts of the double eclipse should occur with a much larger time interval between them in the case of a black dwarf secondary, or even be separated into two independent eclipses, one immediately following the other (unpublished computations on this matter are reported in Ritter (1983a)). This means that in principle one should be able to identify black dwarf systems from observations of eclipse light curves. Nevertheless, the expected fraction of double eclipsing systems is very low, even among cataclysmic variables with main sequence secondaries. It is even lower by a factor of up to three in systems with a black dwarf, since the probability of occurrence of such an eclipse decreases with increasing mass ratio between the primary and secondary

star. Furthermore, it is the mass transfer rate which determines the luminosity of an accretion disc; just this, however, is lower by one or two orders of magnitude from a degenerate secondary than from a main sequence star, which renders black dwarf systems intrinsically a lot fainter than others. Taking all these effects into account, only between 0.1 and 3.0 percent of the observed systems in a magnitude-limited sample are expected to contain a black dwarf. Finally, it is possible that the outer disc as well as the hot spot are optically thin, if the low predicted accretion rates are correct. In this case, even if the geometry were right for a double eclipse, only the eclipse of the white dwarf would appear in the light curve, and thus the system would be indistinguishable from other cataclysmic variables.

4.V.D. THE PERIOD GAP, THE MINIMUM PERIOD, AND THE SECULAR EVOLUTION OF CATACLYSMIC VARIABLES

RELEVANT OBSERVATIONS: In the distribution of orbital periods of cataclysmic variable systems, the period gap between some two and three hours and the minimum orbital period of about 80 minutes are outstanding features.

see 9

ABSTRACT: The upper end of the period gap is understood to be due to the cessation of magnetic braking which detaches the secondary star from its Roche lobe so that mass overflow stops. Gravitational radiation then brings the star and its Roche lobe back into contact, by which time the period has decreased to some 2 hours. The period keeps decreasing due to gravitational radiation until, at the minimum orbital period, the secondary mass has decreased enough so the star cannot maintain nuclear energy generation any longer. At this point, the star rapidly becomes degenerate (a black dwarf) and with further mass loss the orbital period increases.

Figures 1-2 and 2-2, featuring the distribution of orbital periods of cataclysmic variables, reveal a couple of interesting properties of the systems. The orbital period is the physical property of a cataclysmic system which, if measurable at all, usually is by far the most accurately known of all.

There are mavericks at both ends of the distribution: at the short period end they are the AM Canum Venaticorum stars. They all fail to show any trace of hydrogen in their spectra, and thus are assumed to be degenerate. They will not be dealt with for the moment, but only later in this section.

At the other end there is GK Per, a somewhat peculiar old nova which, in its quiescent state as a nova, exhibits brightness fluctuations reminiscent of dwarf nova outburst behavior. This system is dealt with in detail in Chapter 8. Since the secondary in this system certainly is an evolved star, GK Per also will not be included in the following discussion.

The bulk of cataclysmic variables have orbital periods shorter than 10 hours, and their number rises appreciably toward shorter periods. There is a very characteristic gap between about 2 hours 50 minutes (TU Men) and 2 hours 15 minutes (AR And) in which no object has been found, although at both ends many objects are known. There is also a very sharp cut-off at about 1 hour 16 minutes (AF Cam) below which only objects have been found which do not possess any hydrogen.

The sharpness of the two cut-offs, the period gap and its width, and the minimum orbital period, suggest that they are of real physical significance. Furthermore, the tendency for certain sub-types of cataclysmic variables to appear preferentially at one or another side of the gap (see Chapters 1, 2.I.C) suggests an evolutionary cause of the observed distribution*.

*No distinction will be made in the following discussion between the different sub-types of cataclysmic variables.

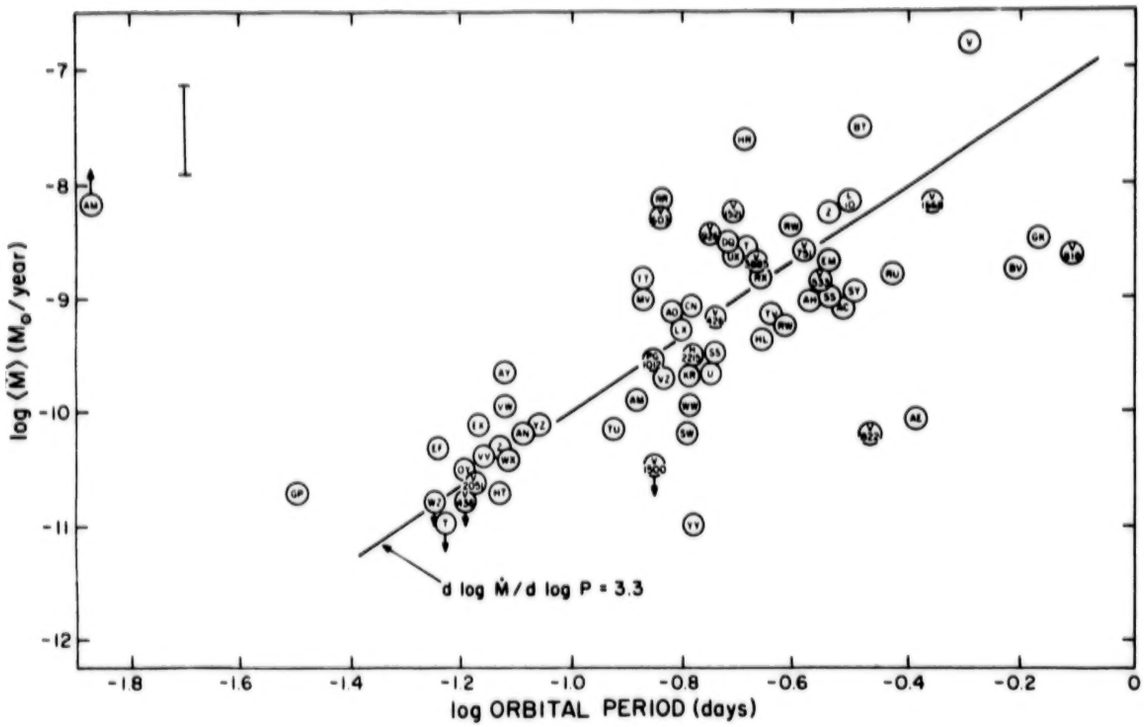


Figure 4-54. Dependence of the orbital period on the mass transfer rate in cataclysmic variables (Patterson, 1984).

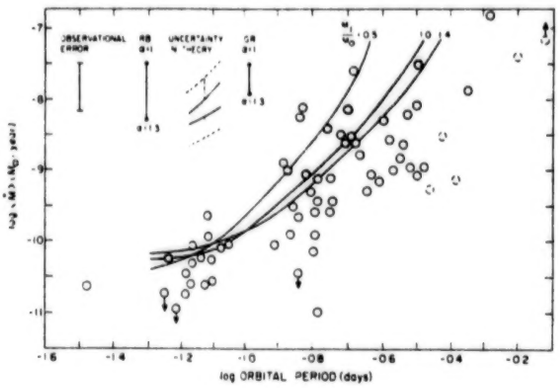


Figure 4-55. Same observational data as in Figure 4-54, with superimposed theoretical relation (solid lines), assuming magnetic braking plus gravitational acceleration to be at work above the period gap and only gravitational radiation below (Patterson, 1984).

The most obvious agent of secular evolution in cataclysmic variables is the mass loss from the secondary star, which is bound to cause secular changes in the orbital periods of these systems. An extensive literature has been published on computations and general theoretical aspects of this issue (e.g., Faulkner, 1971; 1976; Taam et al, 1980; Paczynski, 1981; Paczynski and Sienkiewicz, 1981; Verbunt and Zwaan, 1981; D'Antona and Mazzitelli, 1982; Rappaport et al, 1982; Joss and Rappaport, 1983; Paczynski and Sienkiewicz, 1983; Ritter, 1983b; Spruit and Ritter, 1983; Taam, 1983; Patterson, 1984; Verbunt, 1984; Nelson et al, 1985). The main results shall be reviewed briefly in the following.

For Roche-lobe overflow to occur, either the secondary has to expand beyond its Roche lobe or the Roche lobe has to shrink. Expansion of the secondary can occur either through nuclear evolution or through dynamical instabilities in the star's outer layers. For stars on the main

sequence, mass transfer rates due to nuclear evolution are less than 10^{-12} $M_\odot$/yr and are thus smaller by at least an order of magnitude than the mass transfer rates inferred from observations (see Figure 4-54 and Patterson, 1948)*. Dynamical instabilities, on the other hand, produce pulse-like events which might explain the outburst behavior of dwarf novae (Chapter 4.III.C), but not the continuous mass transfer at rates of 10^{-11} to 10^{-8} $M_\odot$/yr occurring at quiescent state.

Thus, the more likely cause for Roche-lobe overflow is shrinking of the volume available to the secondary star, which also implies a secular period decrease of the system. Simple conservative mass transfer from the (lower mass) secondary to the (higher mass) primary as well as mass loss from the system both result in a period increase, and thus a growth of the secondary's Roche lobe. The only known mechanism to counteract the above tendency for the period to increase, even leading to a period decrease (i.e., shrinkage of the primary's Roche lobe), is loss of angular momentum from the system (Patterson, 1984). Here again two possible mechanisms are known: gravitational radiation and magnetic braking.

The concept of gravitational radiation is based on the field equations for gravitational forces in general relativity which predict the existence of gravitational waves and corresponding energy loss from every object. It was not clear for a long time whether this radiation could be of any astrophysical importance; estimates for single star evolution suggested that it was not. The situation is different for stars whose geometrical size is determined by factors external to the star itself, like the Roche volume in close binary systems. In this case gravitational radiation can become important enough to control the evolution of the system.

Energy loss from a binary system depends on the entire mass of the stars involved as well as on the orbital period of the system (Faulkner, 1976). The time scale τ for significant changes in the system due to this form of energy loss is on the order of

$$\tau \approx 3 \times 10^8 \, P^{8/3} , \qquad (4.21)$$

if the two masses are of roughly comparable size. This means that the typical time scale for changes due to gravitational radiation is shorter than 10^{10} years for cataclysmic systems with orbital periods smaller than 8 hours, it becomes considerably shorter than this for very short period systems, and eventually it becomes even shorter than nuclear time scales (Faulkner, 1976). When the secondary's Roche lobe shrinks due to gravitational radiation, the star must lose the excess mass which lies outside the critical Roche surface, preferentially through the zero-gravity point L_1, which means into the Roche lobe of the white dwarf. The theoretically inferred mass-loss rate is of the order of 10^{-10} to 10^{-11} $M_\odot$/yr for low-mass main sequence stars, and is nearly independent of the orbital period (Rappaport et al, 1982; Patterson, 1984; see also Faulkner, 1976). If this value is compared with observationally inferred mass-transfer rates, it is clear that for systems with orbital periods in excess of 3 hours, i.e., for systems above the period gap, this mechanism, though probably present, is not strong enough to explain the mass-transfer rates which are one to two orders of magnitude higher. For systems with periods below the gap on the other hand, it provides just about the correct mass-loss rate (see Figure 4-54).

Another mechanism which has been suggested for causing a secular period decrease is magnetic braking. This mechanism is at work in cool main sequence stars ($M \lesssim 1.5$ $M_\odot$) which possess a convective envelope and a

*For numerical values of mass transfer rates, possibilities or their determination, and their reliability, see Chapter 4.II.C. In the context of this chapter it should be kept in mind that the numerical values are not very accurate, but they are not likely to be seriously in error either.

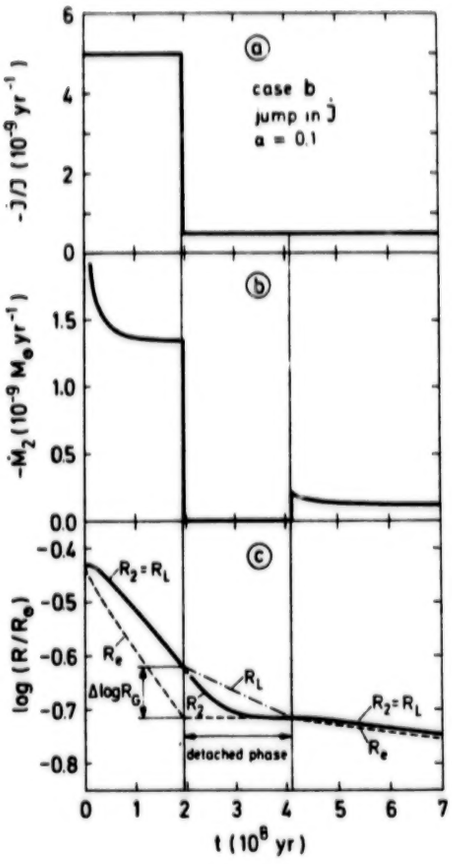


Figure 4-56. Evolution of a cataclysmic variable into and out of the period gap: (a) the relative angular momentum loss drops as soon as magnetic braking ceases to be at work; (b) the mass transfer rate is high above the gap, drops to zero in the gap as the secondary becomes detached from the Roche surface, and is resumed at a small rate below that when gravitational radiation has brought the star into contact with the Roche surface again; (c) corresponding changes in the star's radius (solid line), its equilibrium radius (dashed lines, and the size of the Roche surface (dash-dotted line) (Spruit, Ritter, 1983).

radiative core; due to solar-like activity these stars lose considerable amounts of angular momentum in their stellar winds which decreases the stars' rotational velocity. In a close binary system, time scales of tidal forces working to synchronize the rotation of the secondary star are significantly shorter than any other time scale of evolutionary significance; and thus, in practice, the secondary always rotates synchronously with the orbital motion no matter how much angular momentum is carried away by stellar wind. This in turn leads to an increase of the stellar wind and drains even more angular momentum from the system, thus forcing the two stars closer together and the Roche lobe of the secondary to shrink (Huang, 1966; Mestel, 1968; Eggleton, 1976; Verbunt and Zwaan, 1981; Patterson, 1984; see also Paczynski, 1985). To estimate mass-loss rates to the primary's Roche lobe from this scenario is very difficult since the secondaries in cataclysmic variables are rotating much faster (at an almost constant velocity of some 130 km/sec for all systems according to Patterson (1984)) than any known single stars of similar spectral type due to forced synchronism. Assuming that gravitational radiation plus magnetic braking are at work above the period gap and that only gravitational radiation is at work below, sine these stars are fully convective, Patterson tries to derive mass transfer rates and arrives at values well in agreement with the observationally derived values (Figure 4-55).

A different approach has been undertaken by Spruit and Ritter (1983). They point out that just at the stage when the stars are assumed to become fully convective, a strong decrease in indicators of magnetic activity (Ca II and H α emission, and X-rays) is observed, pointing to break down of the magnetic field — which also is expected on theoretical grounds when the interface between the radiative core and the convective envelope no longer exists as the star becomes fully convective at an orbital period of about three hours. Since the star is significantly out of thermal equilibrium due to former excessive loss of angular momentum (see above), it detaches from its Roche lobe and shrinks until it reaches its equilibrium radius. Even if no magnetic braking is acting any longer, the Roche lobe keeps decreasing due to gravitational radiation until, eventually, it again meets the star's surface (Figure 4-56). After this, mass transfer starts again, proceeding at the rate of some 10^{-10} to 10^{-11} $M_\odot$/yr due to gravitational radiation. Choosing appropriate parameters, Spruit and Ritter are able to

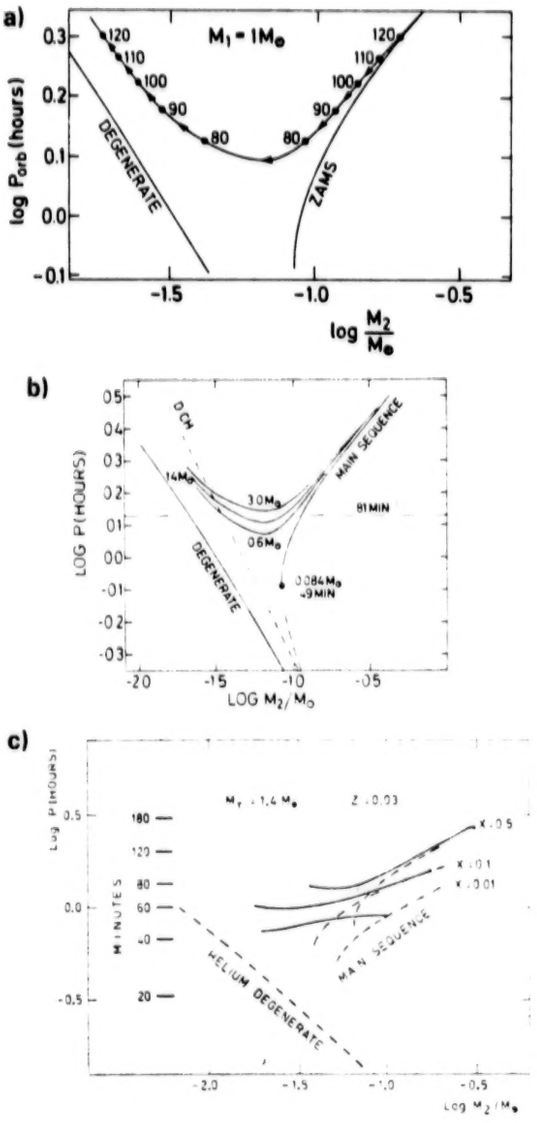


Figure 4-57. Evolution of the secondary star below the period gap under the influence of gravitational radiation: (a) A minimum orbital period of the system is reached as the star becomes degenerate (Ritter, 1983 after Paczynski and Sienkiewicz, 1981). The exact value of the minimum orbital period depends on the total mass of the system (as indicated in the figure); (b) for solar composition it always is on the order of 80 minutes (Paczynski and Sienkiewicz, 1981); (c) when the chemical abundance is changed, the minimum orbital period changes as well (Sienkiewicz, 1985).

theoretically reproduce the observed period gap of the right position and size. Furthermore, in analogy to the Sun, it is assumed that magnetically active stars possess many star spots which disappear together with the magnetic activity; this alone can produce a gap like the one observed, even if the star remains in thermal equilibrium all the time.

Whichever of these above two scenarios is applied to explain the period gap, results still depend strongly on the assumed initial conditions and parameter values, and clearly considerable theoretical work remains to be done.

For systems below the period gap there is theoretical agreement that mass transfer is driven by gravitational radiation alone. The orbital period keeps decreasing as the secondary loses ever more mass. When the star's mass approaches some 0.1 $M_\odot$, corresponding to an orbital period of some 120 min, the thermal time-scale becomes comparable to the time-scale of gravitational radiation. The star cannot adjust to the permanent mass loss any longer and is driven out of thermal equilibrium. This occurs when its radius becomes distinctly larger than the radius of a main sequence star having the same mass (see above). The continued mass loss causes the nuclear burning in the core to be extinguished. Since there is no longer any support by nuclear generated thermal pressure against gravitation contracting the star, the star cools off and collapses. As a consequence it becomes degenerate (Rappaport et al, 1982).

Both the period gap and the strong cut-off at a minimum orbital period still need to be explained. In principle there are three possible ways for producing a period gap: either, a) for some reason systems are not formed in the gap and also do not eventually evolve into it, or b) they move through the gap very quickly so the detection probability decreases strongly, or c) for a while the system is a detached binary, mass transfer stops, and thus they are not recognizable as cataclysmic variables. Patterson (1984) and Verbunt (1984) summarize and discuss previous, unsuccessful, attempts to explain the gap; these are not reviewed here.

Currently, two possible additional scenarios are under consideration. The basic idea of one of these concepts is (D'Antona and Mazzitelli, 1982; Joss and Rappaport, 1983) that, as the secondary star loses matter and its internal structure tries to adjust to the ever new conditions (staying close to the main sequence, nevertheless), the convection zone penetrates deeper and deeper into the star's interior while the star's central temperature decreases. Since new He 3 is mixed into the core from the outer, chemically unconsumed layers of the star, the energy production increases conspicuously just as the star becomes fully convective at an orbital period of some three hours. The increased energy production leads to a temporarily enhanced mass transfer, hence stronger mass loss from the star and also a fall of its internal temperature which in turn means nuclear energy generation becomes less effective. The system becomes detached, as nuclear energy generation becomes too inefficient and the stellar radius shrinks below the Roche radius. Only when gravitational radiation has reduced the Roche lobe strongly enough for it to reach once more the surface of the secondary star does mass transfer begin anew.

The orbital period of a binary system depends to first order only on the radius and thus on the mass of the secondary star. For a non-degenerate star the radius shrinks as it loses mass, whereas the situation is opposite in the case of degenerate material. Due to this the binary period reaches a minimum — the exact value of which depends on the total mass of the system and its chemical composition — just at the time when the secondary star becomes degenerate, after which it increases as the secondary loses even more mass (Figure 4-57a). Paczynski and Sienkiewicz (1981) and Sienkiewicz (1985) investigated the theoretical value of the minimum orbital period as a function of the total mass of the system ($M_1 + M_2$) as well as of the chemical composition. They find that, quite independent of the entire mass, the minimum orbital period for hydrogen-rich systems for which they assume X = 0.70, Y = 0.27, Z = 0.03 is 81 ± 6 minutes (Figure 4-57b), while for hydrogen-poor systems with mass fractions down to 0.01 the minimum period can be as short as 40 minutes (Figure 4-57c). Thus the period of GP Com, 46.5 minutes, can be explained in this way, while the periods of PG1346+182 (24.8 min) and AM CVn (17.5 min, but somewhat questionable) require another, as yet unknown, mechanism. Eventually the mass will become too low for the star to be degenerate. From this moment on the period will decrease again as the star loses mass, and only gravitational radiation will be at work until the mass of the star will be almost entirely lost. What little mass will be left is probably just a rapidly spinning white dwarf (Nather, 1985).

4.V.E. PROGENITORS AND DESCENDANTS

ABSTRACT: In general, the progenitors of cataclysmic variables must be wide binaries with orbital periods of months or years. No known class of stars has been identified with them so far. Alternatively, a small fraction may be formed by extensive mass accretion onto a planet from a star during a common envelope phase. At the end of the lifetime of a cataclysmic variable, mass overflow from the secondary star continues until this mass is entirely transferred. A single white dwarf then remains.

All cataclysmic variables contain a white dwarf primary which can only have evolved from the core of a red giant or supergiant, thus from a progenitor whose radius was much larger than the dimensions of a cataclysmic system. Since most observed white dwarfs in cataclysmic variables are rather massive ($M_{WD} \gtrsim 0.45\ M_\odot$), they must have originated through case C mass transfer which implies a large angular momentum of the original system, most of which (up to 95%) must have been lost during the evolution toward a cataclysmic variable (Ritter, 1976).

This is about all that can be concluded about the progenitors from inspection of existing

observed systems. Several attempts have been made to at least qualitatively model stellar evolution before cataclysmic systems emerge (e.g., Paczynski, 1976; Ritter, 1976; Webbink, 1979; Law and Ritter, 1983; Paczynski, 1985). Although the details are by no means well understood theoretically, there is general agreement about the following overall scenario:

The progenitors must be fairly wide binaries with orbital periods of many months or years, in order to later be able to accommodate a red giant or supergiant in the primary's Roche lobe, which in turn is needed in order to eventually produce a white dwarf. W Ursae Majoris stars can be excluded as possible candidates, even though their space density and distribution well match those of cataclysmic variables (Duerbeck, 1984, and see Chapter 4.V.A), since their angular momentum is so small that no white dwarf could be formed (Ritter, 1976). No other group of stars has been identified as a possible class of progenitors.

Whatever the progenitors are, the two stars must evolve independently for most of their lives on time-scales dictated by their masses. The more massive star eventually becomes a red giant, harboring a future white dwarf in its core. It will expand and fill its critical volume as either a giant or a supergiant, depending on the size of the Roche lobe, and, correspondingly, case B or case C Roche lobe overflow will take place onto the still rather unevolved secondary star, unless $q \approx 1$ (Kippenhahn and Weigert, 1967). Initially, the mass transfer onto the secondary star is very violent with a mass-loss rate as high as 0.1 $M_\odot$/yr (Webbink, 1979). The secondary star clearly is not able to adjust to this flood of material and possibly as soon as within a few orbital periods (Paczynski, 1976), blows up to become a red giant-like object. Thus both stars together find themselves wrapped in a common envelope. Angular momentum is transferred to the envelope, and the two cores are drawn ever closer together while the envelope expands. It is not clear theoretically how this binary system and the envelope finally become detached from each other. If this scenario is qualitatively correct, one would expect to observe a close binary system consisting of a white dwarf and a main sequence star with an orbital period of less than 2 days to occur inside a planetary nebula.

Observational support for this scenario came from the detection of several close binary systems consisting of a white dwarf and a main sequence star, ten of which are central stars of planetary nebulae (Ritter, 1986b). In particular the planetary nebulae must be very young since they become invisible some 10^4 years after their ejection. These so-called pre-cataclysmic binaries (or V471 Tauri stars) are considered the immediate progenitors of cataclysmic variables (Patterson, 1984; Bond, 1985; Ritter, 1986b).

They are not quite cataclysmic systems yet, however, since the orbital periods are still too long for the secondary components to fill their Roche lobes. Again, the known mechanisms for angular momentum loss which are efficient enough to act on relevant time-scales are gravitational radiation and magnetic braking or expansion of the secondary on nuclear time-scales. Gravitational radiation is at work in all binary systems. It has been mentioned above, however, that contraction of these systems due to gravitational radiation takes a very long time for long orbital periods, so that systems for which only this mechanism applies are not likely to become cataclysmic variables within the lifetime of the Galaxy. Magnetic braking, on the other hand, only works within fairly narrow limits of physical conditions, namely, a differentially rotating secondary which possesses a convective envelope, implying that it must be a main-sequence star with a mass between roughly 0.3 and 1.3 solar masses in a sufficiently close binary system which ensures tidal interactions to be able to force the stars to co-rotate. Bond (1985) points out that, given all these constraints, cataclysmic variables may well be only a tiny fraction of possible end-products of common envelope evolution.

Evolution toward and through the life of a cataclysmic variable was already outlined above (Chapter 4.V.D): magnetic braking eventually brings the period down to some three hours; when this mechanism brakes down, the secondary detaches from its Roche lobe and mass transfer stops. All further evolution is dominated by gravitational radiation bringing the stars ever closer together until mass overflow resumes again. The orbital period keeps decreasing until a minimum value is reached when the secondary becomes degenerate. After this it increases again until so much of the secondary's mass is transferred that it is not even degenerate any longer. The period then decreases again as further mass is lost, until all of this star has finally been cannibalized by its white dwarf neighbor.

On the way to this stage, however, further obstacles can be met. If the white dwarf should succeed in crossing the Chandrasekhar limit by accreting enough mass (that this can happen theoretically is by no means obvious — see Chapter 4.V.B), the white dwarf will undergo a supernova explosion of type I which may or may not destroy the secondary; at any rate such an event would seriously influence the further fate of the system. Also, it is not clear theoretically what repeated nova explosions, if they occur at all, might do to a system in terms of angular momentum balance and white dwarf masses.

As mentioned earlier (Chapter 4.V.D), AM Canum Venaticorum stars, i.e., systems containing two degenerate stars orbiting around each other with periods of less than 40 minutes, cannot be explained by the above scenario, since the minimum orbital period from gravitational radiation is larger than the orbital period of two of these systems. A possible explanation for the existence of such objects was given by Livio and Soker (1983, 1984b; Livio, 1983 — see also Rappaport et al, 1982). They start out from a star-planet system. The star evolves and becomes a red giant. The planet is exposed first to a strong stellar wind, later it is embedded in the envelope and accretes matter, and may, if conditions are right, finally become a low-mass star of order 0.14 $M_\odot$. Spiralling-in diminishes the distance between the planet/star and the white dwarf core of the giant. It depends on the initial conditions what the end product of this evolution will be. If the initial separation is too small (smaller than some 500 $R_\odot$), the planet will spiral into the star before the star had lost its envelope and only the star is left, if it is too large (larger than some 2000 $R_\odot$) the planet will not be able to accrete a significant amount of mass and the separation between the two cores will not be reduced. Concerning masses, if the initial mass was too small (smaller than 0.01 $M_\odot$) the planet will evaporate during the spiralling-in phase; only if the mass is larger than some 0.0125 $M_\odot$ will a low-mass star result, of some 0.14 $M_\odot$, whose mass will be determined almost entirely by the mass contained in the giant's envelope.

4.V.F. NOVAE — DWARF NOVAE — AND NOVA-LIKE STARS

RELEVANT OBSERVATIONS: Except for their outburst behavior and its immediate consequences, novae, dwarf novae, and nova-like stars cannot be physically distinguished from each other.

see 19

ABSTRACT: It is suggested that all systems cyclically pass through all these stages of activity.

In all of the above discussion no reference was made to the type of cataclysmic variable (novae, dwarf novae, or nova-like star) considered. In fact, observationally, no striking statistical differences can be found between the members of the various sub-classes of cataclysmic variables except, it seems, for the outburst activity. This may be due partly to difficulties in determining system parameters reasonably accurately (see Chapter 4.II.C). It is certainly still an open question why some objects appear as novae, others as dwarf novae, and even others as different types of nova-like

systems. Probably the only clear cases are AM Canum Venaticorum systems which contain two degenerate stars, and AM Herculis stars which are governed by the magnetic field of the white dwarfs (these two kinds of systems are not considered here).

Since system parameters of essentially all cataclysmic variables seem to be approximately identical, the general feeling is that all these systems may really be effectively identical, and just be seen at different stages of a cyclic evolution. A nova explosion is expected to occur as soon as a sufficient amount of hydrogen-rich material has accumulated on the surface of the degenerate white dwarf. The necessary material is assumed to come from the secondary star via the accretion disc. Furthermore, novae by definition only have been observed to erupt once, and so far there has been no observationally imposed reason to change this definition.* Of course this does not mean that all novae erupt only once, but only that the outburst interval is in excess of a couple of hundred years. Since a nova outburst obviously is not very traumatic for a cataclysmic system, such an event well may happen to the system many times.

There are a few old novae which occasionally exhibit small-scale brightness fluctuations fairly reminiscent of dwarf nova outbursts (see, e.g., Livio, 1987): The most prominent example is GK Per, discussed extensively elsewhere in this book. In a tentative scenario, U Geminorum variables, Z Camelopardalis stars, anti-dwarf novae, and finally UX Ursae Majoris stars all can be linked comfortably to stages in an evolutionary sequence with an increasing fraction of time spent in the high/outburst state.

Following this general idea, Vogt (1982b, see also, e.g., Shara et al, 1986) tentatively suggested a cyclic behavior in which a nova explosion blows away the entire accretion disc which then eventually is built up again: first the system starts to exhibit dwarf nova-like behavior of an old nova; then it becomes a U Geminorum star; then, as the torus/disc mass increases it will be a Z Camelopardalis star, and later an UX Ursae Majoris star, until enough hydrogen-rich material has accumulated on the surface of the white dwarf for it to undergo another nova explosion. There are observational as well as theoretical problems with this scenario. Observationally, there is no evidence for quiescent novae to be physically significantly different from other cataclysmic variables at least for the first couple of decades after eruption. In particular there is every indication that they all possess accretion discs. Theoretically, the mass-transfer rates of typically some 10^{-9} $M_\odot$/yr in UX Ursae Majoris stars are about an order of magnitude too high for thermonuclear reactions to occur on the surface of the white dwarfs (Paczynski, 1985).

The mass-transfer rates derived for quiescent novae are of about the same order, some 10^{-9} $M_\odot$/yr or even higher than those derived for UX Ursae Majoris stars. This poses the problem that in novae new nova outbursts are not expected to occur. On the other hand the general feeling is that the nova phenomenon is likely to be a recurrent one. To propose a way out, Shara et al (1986) and Livio (1987) suggested that after the nova outburst high mass-transfer rates are maintained for some 50 to 300 years by irradiation of the secondary by the still hot white dwarf. The two stars are driven somewhat apart by the outburst. (A period decrease after, as compared to before, the outburst has been claimed for the old nova BT Mon, observed in 1939 (Shaefer and Patterson, 1983; Livio, 1987). Thus as the white dwarf cools and is ever less able to heat the secondary,

*Some recurrent novae have been observed. There is plenty of support, however, for the assumption that they all contain evolved secondaries which might have played a part in their evolution. At any rate, they can comfortably be excluded from considerations concerning the bulk of cataclysmic variables by stating that they are not typical representatives of this class, and in fact some of them, like T CrB, seem almost indistinguishable from symbiotic systems — see Chapters 9 and 11.

this star will shrink to its normal dimensions which, due to the now somewhat enlarged Roche lobe, will underfill its critical volume and thus mass transfer will either be strongly reduced or be stopped altogether (Livio calls this state "hibernation"), until, by magnetic braking or by gravitational radiation, the system is brought into contact again and dwarf nova activity is resumed until the next nova outburst occurs. Observational support for this is an observed decrease in luminosity in the old nova RR Pic (Nova Pic 1925) as well as very low mass-transfer rates for the two very old novae CK Vul (1670) and WY Sge (1783).

At any rate, concerning this aspect of understanding cataclysmic variables, considerable theoretical work remains to be done.

5

SUMMARY

In the preceding chapters an attempt has been made to convey a picture of the current state of research in dwarf novae and nova-like stars. Chapters 2 and 3 summarize the observational appearance of dwarf novae and nova-like stars, respectively. The aim in these chapters was to present the data independent of any interpretation, while at the same time to point out implications these observations have for any model. In order to facilitate understanding, in particular for newcomers to the field, a "general interpretation" of the main observed features within the framework of the Roche model was given at the end of each major section. Finally in Chapter 4 the Roche model for cataclysmic variables and the main streams of current theoretical work in dwarf novae and nova-like stars were presented with abstracts of the relevant observations for the models preceding major theoretical sections. In addition, a system of cross-references should enable easy comparison between similar features in different sub-classes of dwarf novae and nova-like stars.

The emerging picture is that, in gross features and in most respects, dwarf novae and nova-like stars, as well as quiescent novae are almost indistinguishable. Nevertheless, in addition to their different outburst behaviors, there appear to be some further differences between dwarf novae and nova-like stars such as:

- a tendency for the Balmer emission lines of hydrogen to have larger equivalent widths in dwarf novae than in nova-like stars (see Chapter 2.III.B.1.a);
- in dwarf novae Hβ is often of comparable strength to, or stronger than, Hα, while in nova-like stars Hα is normally the stronger line (see Chapter 2.III.B.1.a);
- in some nova-like systems the changes between high and low brightness states are considerably more pronounced at optical wavelengths and in the IR than in the UV, while in dwarf novae it always is the UV that is most strongly affected; other nova-like-stars behave in the same way as dwarf novae (see Chapters 2.III.A, 3.III.B, 3.V.C);
- in several eclipsing nova-like stars the orbital hump appears at some times before, at others after eclipse, while in dwarf novae it always appears before eclipse (see Chapters 2.II.B, 3.II.A.1, 3.IV.B);
- in dwarf novae the hump amplitude always seems to be strongest in the optical, decreases in intensity toward shorter wavelengths, and is practically absent in the UV; in some nova-like stars, however, it was seen to be strong in the optical, decreases around the U filter, and increases again shortward of this (see Chapters 2.II.B, 3.II.B, 3.III.A.2).

The reasons for these differences are not yet understood. In fact, hardly any attention has been paid to them so far. Commonly the understanding is that nova-like stars can be regarded as dwarf novae in a permanent state of outburst. There is evidence, though, that the differences between these two classes of stars go beyond this view.

PRECEDING PAGE BLANK NOT FILMED

In general it is difficult to make statements about "the" behavior of nova-like stars since this class is far from being a homogeneous one. The definition of a nova-like star is that, except for the outburst behavior, it exhibits all the photometric and spectroscopic characteristics of a dwarf nova; and then, as was discussed in Chapter 3, the whole class is divided again into various sub-classes according to certain observed properties.

Some comments about this classification should be made. As was pointed out in earlier chapters, the distinction between dwarf novae, novae, and nova-like stars is by no means as clear as it may seem at first glance. As examples of this, systems like EX Hya and AE Aqr, which are classified primarily as nova-like stars of sub-type DQ Herculis, occasionally are regarded instead as dwarf novae; and the system WZ Sge clearly is to be placed somewhere intermediate between dwarf novae of sub-type SU Ursae Majoris and recurrent novae. Furthermore WZ Sge clearly exhibits (or rather exhibited, since no investigations of this have been published for times after the last outburst in 1978) strictly coherent, highly stable oscillations which would qualify it as a DQ Herculis stars, and thus a nova-like variable. Finally, DQ Her itself is regarded as both an old nova as well as a nova-like system. This list can be extended, and for many objects, it turns out, classification is a matter of taste.

It also becomes apparent that problems of classification are encountered most often with the nova-like stars of sub-type DQ Herculis. This group literally comprises objects of all other classes of cataclysmic variables (see also Ritter, 1987). The defining characteristic of DQ Herculis variables is the occurrence of oscillations which, in any object, are present with the same periods at all times. From the problems over classification, it seems likely that these highly coherent oscillations are a rather common property of cataclysmic variables as a whole, quite independent of outburst properties; consequently their observation is probably a very unfortunate basis for classification.... as long as the classification scheme is based primarily on the properties of the long-term light curves.

Another difficulty with the currently used classification scheme exists in the distinction between UX Ursae Majoris stars and anti-dwarf novae, since this requires a long and complete record of observations. Most of the time the objects in both classes cannot be distinguished from each other. However, at unpredictable times, anti-dwarf novae suffer a drop in brightness by 2 to 5 magnitudes, from which, after weeks or months, they recover to the normal "high" state. The first indication for such behavior was found in 1980 in the object TT Ari (Krautter et al, 1981a). Since then, a considerable number of (former) UX Ursae Majoris variables were reclassified into anti-dwarf novae, based on either direct observations or from inspection of old photographic plates. It may well be that all UX Ursae Majoris stars suffer the fate of an anti-dwarf nova from time to time, and thus both classes are really identical. The observational proof of this might be merely a matter of time.

Finally there exists a problem in the classification of dwarf novae in that the distinction between U Geminorum stars, on one hand, and SU Ursae Majoris and Z Camelopardalis stars, on the other, also requires rather extended, and in the case of SU Ursae Majoris stars also rather thorough, observations. By definition, all systems that are not clearly SU Ursae Majoris or Z Camelopardalis stars are referred to as U Geminorum stars. Z Camelopardalis stars are defined by occasionally undergoing more or less extended standstills, a behavior which can be detected simply from long-term monitoring. The occurrence of standstills seems to be restricted to systems with short outburst periods, so it becomes clear which U Geminorum stars are candidates for being thus far unrecognized Z Camelopardalis stars, and these can be monitored more closely. Certainly the classification should be clear by now for the

long-known systems. Amazingly the exact classification of the dwarf nova CN Ori, which first was detected in 1906 (Wolf and Wolf, 1906), is still a matter of debate: it is commonly referred to as a Z Camelopardalis star, although except for one hand-drawn light-curve in a notoriously unreliable source (Glasby, 1968, see also Pringle and Verbunt, 1986) there is no evidence that CN Ori was ever observed to undergo a standstill.

The occurrence of superoutbursts seems to be restricted primarily to dwarf novae with orbital periods below 2 hours (i.e., below the period gap), although TU Men is proof that SU Ursae Majoris systems can also be found at least just above the gap. In any event, short period dwarf novae are clearly candidates for being SU Ursae Majoris systems, and, again, the extensive migration from being classified as U Geminorum to SU Ursae Majoris stars indicates that possibly all short-period dwarf novae are SU Ursae Majoris stars. Accordingly, thorough investigation of the (so far) U Geminorum stars below the period gap eventually might be able to tell whether or not this is really the case.

In light of all these problems with classification, clearly the question arises whether the outburst behavior, which currently is the basis of almost all classification, is really a suitable criterion for sorting cataclysmic variable into physically related groups. The two remaining classes of nova-like systems, the definitions of which are based on something other than outburst activity, are the AM Herculis stars with their strong polarization, and the AM Canum Venaticorum stars in the spectra of which no hydrogen can be found. These two classes are clearly and unambiguously defined. Possibly, from a physical point of view, DQ Herculis stars are a well-defined class. . . . or maybe the occurrence of stable oscillation is such a common property that again it is not suitable. Nevertheless, it seems that, as more detailed observations of cataclysmic variables become available, the more pressing becomes the need to revise their classification scheme, a scheme which, after all, was designed when nothing but the outbursts of cataclysmic variables could be observed.

In spite of all these difficulties, dwarf novae and nova-like systems are statistically almost identical in most of their properties, and theoretically they can be, and have been treated together, without — at least at the current level of theoretical understanding — the need for a more sophisticated distinction arising. To a large extent this also applies to the modeling of novae in the quiescent state (i.e., a long time after outburst).

All dwarf novae, novae, and nova-like stars that were investigated thoroughly turned out to be short-period binary systems, and there is no contradiction to the hypothesis that all of these objects are indeed binaries. The theoretical foundation of all modeling these days is the Roche model (Chapter 4.II.A), and indeed, within this framework, a surprising large fraction of the observations can be explained. In particular, all of the gross features can be accounted for. Thus clearly it makes sense to retain this general model for the time being. However, agreement between theory and observations is so far still restricted to these gross features, and our current level of understanding is far from inspiring hope that we will soon understand the nature of cataclysmic variables in detail.

REFERENCES

Africano, J., and Wilson, J. 1976, *Publ. Astr. Soc. Pac.*, **88**, 8

Africano, J.L., Nather, R.E., Patterson, J., Robinson, E.L., and Warner, B. 1978, *Publ. Astr. Soc. Pac.*, **90**, 568

Agrawal, P.C., Apparao, K.M.V., Singh, K.P., Vivekananda Rao, P., and Sarma, M.B.K. 1984, *Astron. Astrophys.*, **131**, 192

Allen, D.A., and Cherepashchuk, A.M. 1982, *Mon. Not. Roy. Astr. Soc.*, **201**, 521

Allen, D.A., Ward, M.J., and Wright, A.E. 1981, *Mon. Not. Roy. Astr. Soc.*, **195**, 155

Antipova, L.I. 1987, *Astrophys. Space Sci.*, **131**, 453

Bailey, J. 1975, *Journ. Brit. Astr. Ass.*, **86**, 30

Bailey, J. 1978, *Mon. Not. Roy. Astr. Soc.*, **185**, 73p

Bailey, J. 1979a, *Mon. Not. Roy. Astr. Soc.*, **187**, 645

Bailey, J. 1979b, *Mon. Not. Roy. Astr. Soc.*, **188**, 681

Bailey, J. 1980, *Mon. Not. Roy. Astr. Soc.*, **190**, 119

Bailey, J. 1981, *Mon. Not. Roy. Astr. Soc.*, **197**, 31

Bailey, J., and Axon, D.J. 1981, *Mon. Not. Roy. Astr. Soc.*, **194**, 187

Bailey, J., Hough, J.H., Axon, D.J., Gatley, I., Lee, T.J., Szkody, P., Stokes, G., and Berriman, G. 1982, *Mon. Not. Roy. Astr. Soc.*, **199**, 801

Bailey, J., Hough, J.H., Gilmozzi, R., and Axon, D.J. 1984, *Mon. Not. Roy. Astr. Soc.*, **207**, 777

Bailey, J., and Ward, M. 1981, *Mon. Not. Roy. Astr. Soc.*, **196**, 425

Bailey, J., Watts, D.J., Sherrington, M.R., Axon, D.J., Giles, A.B., Hanes, D.A., Heathcote, S.R., Hough, J.H., Hughes, S., Jameson, R.F., and McLean, I. 1985, *Mon. Not. Roy. Astr. Soc.*, **215**, 179

Barwig, H., and Schoembs, R. 1983, *Astron. Astrophys.*, **124**, 287

Bastian, T.S., Dulk, G.A., and Chanmugam, G. in *Radio Stars*, R. Hjellming and D.M. Gibson (eds.), 1985, p. 225

Bateson, F.M. 1977, *New Zealand J. Sci.*, **20**, 73

PRECEDING PAGE BLANK NOT FILMED

Bateson, F.M. 1979, *Publ. Var. Star Sect. Roy. Astr. Soc. New Zealand, No. 7*, **5**

Bateson, F.M. 1981, *Publ. Var. Star Sect. Roy. Astr. Soc. New Zealand, No. 9*, **2**

Bateson, F.M. 1985, in Proc. ESA Workshop: *Recent Results on Cataclysmic Variables*, Bamberg, IRG, 17–19 April, 1985, ESA SP-236, p. 287

Bath, G.T. 1973, *Nature Phys. Sci.*, **246**, 84

Bath, G.T. 1975, *Mon. Not. Roy. Astr. Soc.*, **171**, 311

Bath, G.T. 1976, in IAU Symp. 73, *Structure and Evolution of Close Binary Systems*, P. Eggleton, S. Mitton, J. Whelan (eds.), 28 July – 1 Aug., 1975, Cambridge, England, Reidel Publ., p. 173

Bath, G.T. 1977, in *Novae and Related Stars*, Proc. of an international conference held by the Institute d'Astrophysique, Paris, France, 7 to 9 Sept., 1976, M. Friedjung (ed.), Reidel Publ., p. 41

Bath, G.T. 1984, *Astrophys. Space Sci.*, **99**, 127

Bath, G.T., Clarke, C.J., and Mantle, V.J. 1986, *Mon. Not. Roy. Astr. Soc.*, **221**, 269

Bath, G.T., Edwards, A.C., and Mantle, V.T. 1983a, *Mon. Not. Roy. Astr. Soc.*, **205**, 171

Bath, G.T., Edwards, A.C., and Mantle, V.T. 1983b, in IAU Coll. 72, *Cataclysmic Variables and Related Objects*, Aug. 9–13, 1982, Haifa, Israel, M. Livio, G. Shaviv (eds.), Reidel Publ., p. 55

Bath, G.T., Evans, W.D., and Pringle, J.E. 1974a, *Mon. Not. Roy. Astr. Soc.*, **166**, 113

Bath, G.T., Evans, W.D., Papaloizou, J., and Pringle, J.E. 1974b, *Mon. Not. Roy. Astr. Soc.*, **169**, 447

Bath, G.T., and Herczeg, T.J. 1977, *Publ. Astr. Soc. Pac.*, **89**, 71

Bath, G.T., and Pringle, J.E. 1981, *Mon. Not. Roy. Astr. Soc.*, **194**, 967

Bath, G.T., and Pringle, J.E. 1982, *Mon. Not. Roy. Astr. Soc.*, **199**, 267

Bath, G.T., and Shaviv, G. 1978, *Mon. Not. Roy. Astr. Soc.*, **183**, 515

Bath, G.T., and van Paradijs, J. 1983, *Nature*, **305**, 33

Belakov, E.T., and Shulov, O.S. 1974, *Trud. Astr. Obs. Len.*, **30**, 103

Beljawsky, S. 1933, *Pulk. Circ.* **9**, 34

Belserene, E.P. 1981, *Bull. Am. Astr. Soc.*, **13**, 524

Benz, A.O., Fuerst, E., and Kiplinger, A.L. 1983, *Nature*, **302**, 45

Benz, A.O., Fuerst, E., and Kiplinger, A.L. 1985, in *Cataclysmic Variables and Low-Mass X-ray Binaries*, Proc. of the 7th North American Workshop held in Cambridge, Mass., Jan. 12–15, D.Q. Lamb, J. Patterson (eds.), Reidel Publ., p. 331

Berg, R.A., and Duthie, J.G. 1977, *Astrophys. J.*, **211**, 859

Berriman, G. 1984, *Mon. Not. Roy. Astr. Soc.*, **207**, 783

Berriman, G. 1987, *Mon. Not. Roy. Astr. Soc.*, **228**, 729

Berriman, G., Beattie, D.H., Gatley, I., Lee, T.J., Mochnacki, S.W., and Szkody, P. 1983, *Mon. Not. Roy. Astr. Soc.*, **204**, 1105

Berriman G., Szkody, P., and Capps, R.W. 1985, *Mon. Not. Roy. Astr. Soc.*, **217**, 327

Beuerman, K., and Osborne, J. 1985, *Space Sci. Rev.*, **40**, 117

Beuerman, K., and Osborne, J. 1988 *Astron. Astrophys.*, **189**, 128

Beuerman, K., and Pakull, M.W. 1984, *Astron. Astrophys.*, **136**, 250

Beuermann, K., and Stella, L. 1985, *Space Sci. Rev.*, **40**, 139

Beuermann, K., Thomas, H.-C., Giommi, P., and Tagliaferri, G. 1987, *Astron. Astrophys.*, **175**, L 9

Bianchini, A. 1988, *Inf. Bull. Var. Stars*, **3136**

Biermann, P., Schmidt, G.D., Liebert, J., Stockman, H.S., Tapia, S., Kuehr, H., Strittmatter, P.A., West, S., and Lamb, D.Q. 1985, *Astrophys. J.*, **293**, 303

Bond, H.E. 1985, in *Cataclysmic Variables and Low-Mass X-ray Binaries*, Proc. of the 7th North American Workshop held in Cambridge, Mass., Jan 12–15, 1983, D.Q. Lamb, J. Patterson (eds.), Reidel Publ., p. 15

Bond, H.E., Chanmugam, G., and Grauer, A.D. 1979, *Astrophys. J. Lett.*, **234**, L 113

Bookbinder, J., and Lamb, D.Q. 1985, *Bull. Am. Astr. Soc.*, **17**, 589

Bonnet-Bidaud, J.M., and Mouchet, M. 1987, *Astron. Astrophys.*, **188**, 89

Brady, R.A., and Herczeg, T.Y. 1977, *Publ. Astr. Soc. Pac.*, **89**, 17

Brosch, N., Leibowitz, E.M., and Mazeh, Z. 1980, *Astrophys. J. Lett.*, **236**, L 29

Bruch, A. 1984 *Astron. Astrophys. Suppl.*, **56**, 441

Brun, A., and Petit, M. 1952, *Bull. de l'Assoc. Franc. d'Obs. d'Etoiles Var.*, **12**

Brunt, C. C. 1982, Ph.D. thes., Cambridge

Burkert, A., and Hensler, G. 1985, in Proc. ESA Workshop: *Recent Results on Cataclysmic Variables*, Bamberg, FRG, 17–19 April, 1985, ESA SP-236, p. 67

Campbell, L. 1934, *Harv. Ann.*, **90**, 93

Cannizzo, J.K. 1984, *Nature*, **311**, 443

Cannizzo, J.K., Ghosh, P., and Wheeler, J.C. 1982, *Astrophys. J. Lett.*, **260**, L 83

Cannizzo, J.K., Ghosh, P., and Wheeler, J.C. 1985, in *Cataclysmic Variables and Low-Mass X-ray Binaries*, Proc. of the 7th North American Workshop held in Cambridge, Mass., Jan 12–15, 1983, D.Q. Lamb, J. Patterson (eds.), Reidel Publ., p. 307

Cannizzo, J.K., and Kenyon, S.F. 1987, *Astrophys. J.*, **320**, 319

Cannizzo, J.K., and Wheeler, J.C. 1984, *Astrophys. J. Suppl.*, **55**, 367

Cannizzo, J.K., Wheeler, J.C., and Polidan, R.S. 1986, *Astrophys. J.*, **301**, 634

Castor, J.I., and Lamers, H.J.G.L.M. 1979, *Astrophys. J. Suppl.*, **39**, 481

Chanan, G.A., Nelson, J.E., and Margon, B. 1979, *Astrophys. J.*, **226**, 963

Chanmugam, G. 1986, in *Plasma Penetration into Magnetospheres*, N. Viylatis, J. Papamastorakis, J. Ventura (eds), Crete Univ. Press, P. 153

Chanmugam, G. 1987, *Astrophys. Space Sci.*, **130**, 53

Chanmugam, G., and Dulk, G.A. 1981, *Astrophys. J.*, **244**, 569

Chanmugam, G., and Dulk, G.A. 1982, *Astrophys. J. Lett.*, **255**, L 107

Chester, T.J. 1979, *Astrophys. J.*, **230**, 167

Chiapetti, L., Maraschi, L., Tanzi, E.G., and Treves, A. 1982, *Astrophys. J.*, **258**, 236

Chincarini, G., and Walker, M.F. 1981, *Astron. Astrophys.*, **104**, 24

Clarke, J.T., Capel, D., and Bowyer, S. 1984, *Astrophys. J.*, **287**, 845

Cook, M.C. 1985a, *Mon. Not. Roy. Astr. Soc.*, **215**, 211

Cook, M.C. 1985b, *Mon. Not. Roy. Astr. Soc.*, **216**, 219

Cook, M.C., and Brunt, C.C. 1983, *Mon. Not. Roy. Astr. Soc.*, **205**, 465

Cook, M.C., and Warner, B. 1981, *Mon. Not. Roy. Astr. Soc.*, **196**, 55p

Cook, M.C., and Warner, B. 1984, *Mon. Not. Roy. Astr. Soc.*, **207**, 705

Cook, M.C., Watson, M.G., and McHardy, I.M. 1984, *Mon. Not. Roy, Astr. Soc.*, **210**, 7p

Córdova, F.A. 1979, in IAU Coll. 53, *White Dwarfs and Variable Degenerate Stars*, Rochester, N.Y., 30 July - 2 Aug., 1979, H.M. van Horne, V. Weidemann (eds.), Univ. of Rochester, p. 398

Córdova, F.A., Chester, T.J., Mason, K.O., Kahn, S.M., and Garmire, G.P. 1984, *Astrophys. J.*, **278**, 739

Córdova, F.A., Chester, T.J., Tuohy, I.R., and Garmire, G.P. 1980, *Astrophys. J.*, **235**, 163

Córdova, F.A., and Mason, K.O. 1982, *Astrophys. J.*, **260**, 716

Córdova, F.A., and Mason, K.O. 1983, in *Accretion Driven Stellar X-Ray Sources*, W.H.G. Lewin, E.P.J. van den Heuvel (eds.), Cambridge Univ. Press, p. 147

Córdova, F.A., and Mason, K.O. 1984, *Mon. Not. Roy. Astr. Soc.*, **206**, 879

Córdova, F.A., Mason, K.O., and Hjellming, R.M. 1983, *Publ. Astr. Soc. Pac.*, **95**, 69

Córdova, F.A., Mason, K.O., and Kahn, S.M. 1985, *Mon. Not. Roy. Astr. Soc.*, **212**, 447

Córdova, F.A., and Riegler, G.R. 1979, *Mon. Not. Roy. Astr. Soc.*, **188**, 103

Cowley, A.P., and Crampton, D. 1977, *Astrophys. J.*, **212**, L 121

Cowley, A.P., Crampton, D., and Hesser, J.E. 1977, *Astrophys. J.*, **214**, 471

Cowley, A.P., Crampton, D., and Hutchings, J.B. 1982, *Astrophys. J.*, **259**, 730

Cowley, A.P., Crampton, D., Hutchings, J.B., and Marlborough, J.M. 1975, *Astrophys. J.*, **195**, 413

Cowley, A.P., Hutchings, J.B., and Crampton, D. 1981, *Astrophys. J.*, **246**, 489

Crampton, D., and Cowley, A.P. 1977, *Publ. Astr. Soc. Pac.*, **89**, 374

Crampton, D., Hutchings, J.B., and Cowley, A.P. 1981, *Astrophys. J.*, **243**, 567

Crawford, J.A., and Kraft, R.P. 1955, *Publ. Astr. Soc. Pac.*, **67**, 337

Crawford, J.A., and Kraft, R.P. 1956, *Astrophys. J.*, **123**, 44

Cropper, M. 1986, *Mon. Not. Roy. Astr. Soc.*, **222**, 853

Cropper, M., Menzies, J.W., and Tapia, S. 1986, *Mon. Not, Roy. Astr. Soc.*, **218**, 201

Cropper, M., and Warner, B. 1986, *Mon. Not. Roy. Astr. Soc.*, **220**, 633

Crosa, L., Szkody, P., Stokes, G., Swank, J., and Wallerstein, G. 1981, *Astrophys. J.*, **247**, 984

D'Antona, F., and Mazzitelli, I. 1982, *Astrophys. J.*, **260**, 722

Dexter, L.H., Gottlieb, E.W., and Liller, W. 1976, *Bull. Am. Astr. Soc.*, **8**, 511

Downes, R.A. 1986, *Astrophys. J.*, **307**, 170

Drew, J.E. 1986, *Mon. Not. Roy. Astr. Soc.*, **218**, 41 p

Drew, J.E. 1987, *Mon. Not. Roy. Astr. Soc.*, **224**, 595

Drew, J.E., and Verbunt, F. 1984, in Proc. of the Fourth European IUE Conference, Rome, Italy, 15–18 May, 1984, E. Rolfe, B. Battrick (eds.), ESA SP-218, p. 387

Drew, J.E., and Verbunt, F. 1985, *Mon. Not. Roy. Astr. Soc.*, **213**, 191

Drew, J.E., and Verbunt, F. 1988, *Mon. Not. Roy. Astr. Soc.*, **234**, 341

Duerbeck, H.W. 1984, *Astrophys. Space Sci.*, **99**, 363

Duerbeck, H.W. 1987, *Space Sci. Rev.*, **45**

Dulk, G.A., Bastian, T.S., and Chanmugam, G. 1983, *Astrophys. J.*, **273**, 249

Eason, E.L.E., Africano, J.L, Klimke, A., Quigley, R.J., Rogers, W., and Worden, S.P. 1983, *Publ. Astr. Soc. Pac.*, **95**, 58

Echevarría, J. 1984, *Rev. Mex. Astr.*, **9**, 99

Eggleton, P.P. 1976, in IAU Symp. 73, *Structure and Evolution of Close Binary Systems*, Cambridge, England, 28 July - 1 Aug., 1975, P. Eggleton, S. Mitton, J. Whelan (eds.), Reidel Publ., p. 209

Elsworth, Y.P., and James, J.F. 1982, *Mon. Not. Roy. Astr. Soc.*, **198**, 889

Elsworth, Y.P., and James, J.F. 1986, *Mon. Not. Roy. Astr. Soc.*, **220**, 895

Elvey, G.T., and Babcock, H.W. 1943, *Astrophys. J.*, **97**, 412

Fabbiano, G., Hartmann, L., Raymond, J., Steiner, J., Branduardi-Raymond, G., and Matilski, T., *Astrophys. J.*, **243**, 911

Fabian, A.C., Pringle, J.E., Strickland, D.J., and Whelan, J.A.J. 1980, *Mon. Not. Roy. Astr. Soc.*, **191**, 457

Faulkner, J. 1971, *Astrophys. J. Lett.*, **170**, L 99

Faulkner, J. 1976, in IAU Symp. 73, *Structure and Evolution of Close Binary Systems*, Cambridge, England, 28 July - 1 Aug., 1975, P. Eggleton, S. Mitton, J. Whelan (eds.), Reidel Publ., p. 193

Faulkner, J., Flannery, B.P., and Warner, B. 1972, *Astrophys. J. Lett.*, **175**, L 79

Faulkner, J., Lin, D.N.C., and Papaloizou, J. 1983, *Mon. Not. Roy. Astr. Soc.*, **205**, 359

Faulkner, J., and Ritter, H. 1982, in *Binary and Multiple Stars as Tracers of Stellar Evolution*, Z. Kopal, J. Rahe (eds.), Reidel Publ., p. 483

Feigelson, E., Dexter, L., and Liller, W. 1978, *Astrophys. J.*, **222**, 263

Ferland, G.J., Lambert, D.L., McCall, M.L., Shields, G.A., and Slovak, M.H. 1982a, *Astrophys. J.*, **260**, 794

Ferland, G.J., Langer, S.H., MacDonald, J., Pepper, G.H., Shaviv, G., and Truran, J.W. 1982b, *Astrophys. J. Lett.*, **262**, L 53

Flannery, B.P. 1975a, *Astrophys. J.*, **201**, 661

Flannery, B.P. 1975b, *Mon. Not. Roy. Astr. Soc.*, **170**, 325

Frank, J., and King, A.R. 1981, *Mon. Not. Roy. Astr. Soc.*, **195**, 227

Frank, J., and King, A.R. 1984, *Astron. Astrophys.*, **134**, 328

Frank, J., King, A.R., and Raine, D.J. 1985, *Accretion Power in Astrophysics*

Frank, J., King, A.R., Scherrington, M.R., Jameson, R.F., and Axon, D.J. 1981a, *Mon. Not. Roy. Astr. Soc.*, **195**, 505

Frank, J., King, A.R., Sherrington, M.R., Giles, A.B., and Jamesen, R.F. 1981b, *Mon. Not. Roy. Astr. Soc.*, **196**, 921

Friedjung, M. 1981, *Astron. Astrophys.*, **99**, 226

Gerasimovič, B.P. 1934, *Astr. Nachr.*, **251**, 255

Gerasimovič, B.P., and Payne, C.H. 1932, *Harv. Bull.*, **889**, 3

Gieger, A. 1987, *Acta Astr.*, **37**, 29

Gilliland, R.L. 1982a, *Astrophys. J.*, **254**, 653

Gilliland, R.L. 1982b, *Astrophys. J.*, **258**, 576

Gilliland, R.L., and Kemper, E. 1980, *Astrophys. J.*, **236**, 854

Gilliland, R.L., Kemper, E., and Suntzeff, N. 1986, *Astrophys. J.*, **301**, 252

Gilmozzi, R., Messi, R., and Natali, G. 1978, *Astron. Astrophys.*, **68**, L 1

Giovannelli, F., Gaudenzi, S., Rossi, C., and Piccioni, A. 1983, *Acta Astr.*, **33**, 319

Glasby, J.S. 1968, *Variable Stars*, Constable & Co. Ltd., London and Cambridge Mass. Univ. Press

Gordeladse, S.G. 1938, *Bull. Abastumani Astr. Obs.*, **3**, 91

Greenstein, J.L. 1954, *Publ. Astr. Soc. Pac.*, **66**, 79

Greenstein, J.L., and Oke, J.B. 1982, *Astrophys. J.*, **258**, 209

Greenstein, J.L., Sargent, W.L.W., Boroson, T.A., and Boksenberg, A. 1977, *Astrophys. J. Lett.*, **218**, L 121

Greep, P. 1942, *Diss. Utrecht*

Gribbin, J. 1971, *Astrophys. Lett.*, **8**, 175

Guinan, E.F., and Sion, E.M. 1981, in *The Universe at Ultraviolet Wavelengths, The First Two Years of International Ultraviolet Explorer*, Proc. of a Symposium held at the NASA Goddard Space Flight Center, Greenbelt, MD, May 7–9, 1980, NASA Conf. Publ., **2171**, p. 477

Haefner, R., Schoembs, R., and Vogt, N. 1977, *Astron. Astrophys.*, **61**, L 37

Haefner, R., Schoembs, R., and Vogt, N. 1979, *Astron. Astrophys.*, **77**, 7

Hassall, B.J.M. 1985, *Mon. Not. Roy. Astr. Soc.*, **216**, 335

Hassall, B.J.M., Pringle, J.E., Schwarzenberg-Czerny, A., Wade, R.A., Whelan. J.A.J., and Hill, P.W. 1983, *Mon. Not. Roy. Astr. Soc.*, **203**, 865

Hassall, B.J.M., Pringle, J.E., and Verbunt, F. 1985, *Mon. Not. Roy. Astr. Soc.*, **216**, 353

Hassall, B.J.M., Pringle, J.E., Ward, M.J., Whelan, J.A.J., Mayo, S.K., Echevarría, J., Jones, D.HP., Wallis, R.E., Allen, D.A., and Hyland, A.R. 1981, *Mon. Not. Roy. Astr. Soc.*, **197**, 275

Heise, J., Brinkmann, A.C., Groneschild, E., Watson, M., King, A.R., Stella, L., and Kienboom, K. 1985, *Astron. Astrophys.*, **148**, L 14

Heise, J., Mewe, R., Kruszewski, A., and Chlebowski, T. 1987, *Astron. Astrophys.*, **183**, 73

Hellier, C., Mason, K.O., Rosen, S.R., and Córdova, F.A. 1987, *Mon. Not. Roy. Astr. Soc.*, **228**, 463

Hendry, E.M. 1983, *Inf. Bull. Var. Stars*, **2381**

Hensler, G. 1982a, *Astron. Astrophys.*, **114**, 309

Hensler, G. 1982b, *Astron. Astrophys.*, **114**, 319

Herter, M.G., Lacasse, M.G., Wesemael, F., and Winget, D.E. 1979, *Astrophys. J. Suppl.*, **39**, 513

Hessman, F.V. 1986, *Astrophys. J.*, **300**, 794

Hessman, F.V., Robinson, E.L., Nather, R.E., and Zhang, E.-H. 1984, *Astrophys. J.*, **286**, 747

Hildebrand, R.H., Spillar, E.J., and Stiening, R.F. 1981, *Astrophys. J.*, **248**, 268

Hind, J.R. 1856, *Mon. Not. Roy. Astr. Soc.*, **16**, 56

Hinderer, F. 1949, *Astr. Nachr.*, **227**, 193

Hoffmeister, C., Richter, G., and Wenzel, W. 1985, *Variable Stars*, Springer Verlag

Holm, V.A., Panek, R.J., and Schiffer, F.H. III 1982, *Astrophys. J. Lett.*, **252**, L 35

Honeycutt, R.K., Schlegel, E.M., and Kaitchuk, R.H. 1986, *Astrophys. J.*, **302**, 388

Horne, K. 1980, *Astrophys. J. Lett.*, **242**, L 167

Horne, K. 1985, *Mon. Not. Roy. Astr. Soc.*, **213**, 129

Horne, K., and Cook, M.C. 1985, *Mon. Not. Roy. Astr. Soc.*, **214**, 307

Horne, K., Lanning, H.H., and Gomer, R.H. 1982, *Astrophys. J.*, **252**, 681

Horne, K., and Marsh, T.R. 1986, *Mon. Not. Roy. Astr. Soc.*, **218**, 761

Horne, K., and Stiening, R.F. 1985, *Mon. Not. Roy. Astr. Soc.*, **216**, 933

Horne, K., Wade, R.A., and Szkody, P. 1986, *Mon. Not. Roy. Astr. Soc.*, **219**, 791

Howarth, I.D. 1977, *Journ. Brit. Astr. Ass.*, **87**, 176

Howarth, I.D. 1978, *Journ. Brit. Astr. Ass.*, **88**, 458

Huang, S.S. 1966, *Ann. d'Astr.*, **29**, 331

Hudec, R., Huth, H., and Fuhrmann, B. 1984, *Observatory*, **104**, 1

Hudec, R., and Meinunger, L. 1976, *Inf. Bull. Var. Stars*, **1184**

Hutchings, J.B., and Cote, T.J. 1985, *Publ. Astr. Soc. Pac.*, **97**, 847

Hutchings, J.B., Cowley, A.P., and Crampton, D. 1979, *Astrophys. J.*, **232**, 500

Hutchings, J.B., Crampton, D., Cowley, A.P., Thorstensen, J.R., and Charles, P.P. 1981, *Astrophys. J.*, **249**, 680

Icke, V. 1976, in IAU Symp. 73, *Structure and Evolution of Close Binary Systems*, Cambridge, England, 28 July - 1 Aug., 1975, P. Eggleton, S. Mitton, J. Whelan (eds.), Reidel Publ., p. 267

Imamura, J.N. 1984, *Astrophys. J.*, **285**, 223

Isles J.E. 1976, *Journ. Brit. Astr. Ass.*, **86**, 327

Jablonski, F., and Busko, I.C. 1985, *Mon. Not. Roy. Astr. Soc.*, **214**, 219

Jablonski, F., and Steiner, J.E. 1987, *Astrophys. J.*, **323**, 672

Jameson, R.F., King, A.R., and Sherrington, M.R. 1980, *Mon. Not. Roy. Astr. Soc.*, **191**, 559

Jameson, R.F., King, A.R., and Sherrington, M.R. 1981 , *Mon. Not. Roy. Astr. Soc.*, **195**, 235

Jameson, R.F., King, A.R., and Sherrington, M.R. 1982a, *Mon. Not. Roy. Astr. Soc.*, **200**, 455

Jameson, R.F., Sherrington, M.R., King, A.R., and Frank J. 1982b, *Nature*, **300**, 152

Jenson, K.A., Córdova, F.A., Middleditch, J., Mason, K.O., Horne, K., and Gomer, R. 1983, *Astrophys. J.*, **270**, 211

Johnson, H.L., Perkins, B., and Hiltner, W.A. 1954 *Astrophys. J. Suppl.*, **1**, 91

Joss, P.C., and Rappaport, S. 1983, *Astrophys. J. Lett.*, **270**, L 73

Joss, P.C., and Rappaport, S. 1984, *Publ. Astr. Soc. Pac.*, **52**, 324

Joy, A.U. 1954, *Astrophys. J.*, **120**, 377

Kaitchuck, R.H., Honeycutt, R.K., and Schlegel, E.M. 1983, *Astrophys. J.*, **267**, 239

Kallman, T.R., and Jensen, K.A. 1985, *Astrophys. J.*, **299**, 277

Katz, J.I. 1985, in *Cataclysmic Variables and Low-Mass X-ray Binaries*, Proc. of the 7th North American Workshop held in Cambridge, Mass., Jan 12–15, 1983, D.Q. Lamb, J. Patterson (ed.), Reidel Publ., p. 359

Khopolov, N.P. 1985, *General Catalogue of Variable Stars*, 4th edition, Moscow

Khopolov, P.N., and Efremov, Y.N. 1976, *Var. Stars*, **20**, 277

King, A.R. 1983, in IAU Coll. 72, *Cataclysmic Variables and Related Objects*, Haifa, Israel, Aug. 9–13, 1982, M. Livio, G. Shaviv (eds.), Reidel Publ., p. 181

King, A.R., Frank, J., Jameson, R.F., and Sherrington, M.R. 1983, *Mon. Not. Roy. Astr. Soc.*, **203**, 677

King, A.R., and Lasota, J.P. 1979, *Mon. Not. Roy. Astr. Soc.*, **188**, 653

King, A.R., and Shaviv, G. 1984, *Nature*, **308**, 519

King, A.R., Watson, M.G., and Heise, J. 1985, *Nature*, **313**, 290

Kiplinger, A.L. 1979, *Astrophys. J.*, **234**, 997

Kiplinger, A.L. 1980, *Astrophys. J.*, **236**, 839

Kippenhahn, R., and Weigert, V. 1967, *Zeitschr. f. Astr.*, **66**, 58

Kitamura, M., Okazaki, A., and Yamasaki, A. 1983, in IAU Coll. 72, *Cataclysmic Variables and Related Objects*, Haifa, Israel, Aug. 9–13, 1982, M. Livio, G. Shaviv (eds.), Reidel Publ., p. 17

Klare, G., Krautter, J., Wolf, B., Stahl, O., Vogt, N., Wargau, W., and Rahe, J. 1982, *Astron. Astrophys.*, **113**, 76

Kley, W. 1989, *Astron. Astrophys.*, **208**, 98

Kley, W., and Hensler G. 1987, *Astron. Astrophys.*, **172**, 124

Kopal, Z. 1978, *Dynamics of Close Binary Systems*, Reidel Publ.

Kraft, R.P. 1956, *Carnegy Yearbook*

Kraft, R.P. 1962a, *Adv. in Astr. and Astroph.*, **2**, 43

Kraft, R.P. 1962b, *Astrophys. J.*, **135**, 408

Kraft, R.P. 1965, *Astrophys. J.*, **142**, 1588

Kraft, R.P., Krzeminski, W., and Mumford, G.S. 1969, *Astrophys. J.*, **158**, 589

Kraft, R.P., Matheus, J., and Greenstein, J.L. 1962, *Astrophys. J.*, **136**, 312

Krautter, J., Klare, G., Wolf, B., Duerbeck, H, Rahe, J., Vogt, N., and Wargau, W. 1981b, *Astron. Astrophys.*, **102**, 337

Krautter, J., Klare, G., Wolf, B., Wargau, W., Drechsel, H., Rahe, J., and Vogt, N. 1981a, *Astron. Astrophys.*, **98**, 27

Kříž, S. and Hubený, I. 1986, *Bull. Astr. Inst. Czech.*, **37**, 129

Krytbosch, W.E. 1928, *Bull. of the Astr. Inst. of the Netherlands*, **144**, 145

Krzeminski, W. 1965, *Astrophys. J.*, **142**, 1051

Krzeminski, W., and Kraft, R.P. 1964, *Astrophys. J.*, **140**, 921

Krzeminski, W., and Serkowski, K. 1977, *Astrophys. J. Lett.*, **216**, L 45

Krzeminski, W., and Smak, J. 1971, *Acta Astr.*, **21**, 133

Krzeminski, B.V., and Vogt, N. 1985, *Astron. Astrophys.*, **144**, 124

Kukarkin, B.V. 1977, *Mon. Not. Roy. Astr. Soc.*, **180**, 5p

Kukarkin, B.V., and Parenago, P.P. 1934, *Var. Stars*, **4**, 251

Kukarkin, B.V., and Parenago, P.P. 1948, *General Catalogue of Variable Stars*, first ed., Leningrad

la Dous, C. 1982, *Diploma Thesis*, Univ. Muenchen

la Dous, C. 1986, *Ph.D. Thesis*, Univ. Muenchen

la Dous, C. 1989, *Astron. Astrophys.*, **211**, 131

Lamb, D.Q. 1974, *Astrophys. J. Lett.*, **192**, L 129

Lamb, D.Q. 1983, in IAU Coll. 72, *Cataclysmic Variables and Related Objects*, Haifa, Israel, Aug. 9-13, 1982, M. Livio, G. Shaviv (eds.), Reidel Publ., p. 299

Lamb, D.Q. 1985, in *Cataclysmic Variables and Low-Mass X-ray Binaries*, Proc. of the 7th North American Workshop held in Cambridge, Mass., Jan. 12–15, 1983, D.Q. Lamb, J. Patterson (eds.), Reidel Publ., p. 179

Lamb, D.Q., and Patterson, J. 1983, in IAU Coll. 72, *Cataclysmic Variables and Related Objects*, Haifa, Israel, Aug. 9-13, 1982, M. Livio, G. Shaviv (eds.), Reidel Publ., p. 229

Lamb, F.K., Pethick, C.J., and Pines, D. 1973, *Astrophys. J.*, **184**, 271

Lambert, D.L., and Slovak, M.H. 1981, *Publ. Astr. Soc. Pac.*, **93**, 477

Langer, S.H., Chanmugam, G., and Shaviv, G. 1983, in IAU Coll. 72, *Cataclysmic Variables and Related Objects*, Haifa, Israel, Aug. 9-13, 1982, M. Livio, G. Shaviv (eds.), Reidel Publ., p. 199

Larsson, S. 1987, *Astron. Astrophys.*, **181**, L 15

Latham, D.W., Liebert, J., and Steiner, J.E. 1981, *Astrophys. J.*, **246**, 919

Law, W.Y., and Ritter, H. 1983, *Astron. Astrophys.*, **123**, 33

Liebert, J., and Stockman, H.S. 1985, in *Cataclysmic Variables and Low-Mass X-ray Binaries*, Proc. of the 7th North American

Workshop held in Cambridge, Mass., Jan 12–15, 1983, D.Q. Lamb, J. Patterson (eds.), Reidel Publ., p. 151

Liebert, J., Stockman, H.S., Angel, J.R.P., Woolf, N.J., Hege, K., and Margon, B. 1978, *Astrophys. J.*, **225**, 201

Liebert, J., Stockman, H.S., Williams, R.E., Tapia, S., Green, R.F., Rosenkranz, D., and Ferguson, D.H. 1982b, *Astrophys. J.*, **256**, 594

Liebert, J., Tapia, S., Bond, H.E., and Grauer, A.D. 1982a, *Astrophys. J.*, **254**, 232

Lightman, A.P., and Eardley, D.M. 1974, *Astrophys. J. Lett.*, **187**, L 1

Liller, M.H. 1980, *Astronom. J.*, **85**, 1092

Lin, D.N.C., Papaloizou, J., and Faulkner, J. 1985, *Mon. Not. Roy. Astr. Soc.*, **212**, 105

Lin, D.N.C., and Pringle, J.E. 1976, in IAU Symp. 73. *Structure and Evolution of Close Binary Systems*, Cambridge, England, 28 July - 1 Aug., 1975, P. Eggleton, S. Mitton, J. Whelan (eds.), Reidel Publ., p. 237

Linnell, A.P. 1950, *Harv. Circ.*, **455**, 13

Livio, M. 1983, in IAU Coll. 72, *Cataclysmic Variables and Related Objects*, Haifa, Israel, Aug. 9–13, 1982, M. Livio, G. Shaviv (eds.), Reidel Publ., p. 269

Livio, M. 1987, *Comments in Astrophys.*, **12**, 87

Livio, M., and Soker, N. 1983, *Astron. Astrophys.*, **125**, L 12

Livio, M., and Soker, N. 1984a, *Mon. Not. Roy. Astr. Soc.*, **208**, 763

Livio, M., and Soker. N. 1984b, *Mon. Not. Roy. Astr. Soc.*, **208**, 783

Longmore, A.J., Lee, T.J., Alleu, D.A., and Adams, D.J. 1981, *Mon. Not. Roy. Astr. Soc.*, **195**, 825

Lynden-Bell, D. 1969, *Nature*, **223**, 690

Mandel, O.E. 1965, *Variable Stars*, **15**, 480

Mantel, K.-H. 1986, *Diplomarbeit*, Univ. Muenchen

Mantel, K.-H., Marschhaeuser, H., Schoembs, R., Haefner, R., and la Dous, C. 1988, *Astron. Astrophys.*, **193**, 101

Mantle, V.J., and Bath, G.T. 1983, *Mon. Not. Roy. Astr. Soc.*, **202**, 151

Maraschi, L., Treves, A., Tanzi, E.G., Mouchet, M., Lamberts, A., Motch, C., Bonnet-Bidaud, J.M., and Phillips, M.M. 1984, *Astrophys. J.*, **285**, 214

Mardirossian, F., Mezzetti, M., Pucillo, M., Santin, P., Sedmak, G., and Guiricin, G. 1980, *Astron. Astrophys.*, **85**, 29

Margon, B., and Downes, R.A. 1981, *Astron. J.*, **86**, 747

Marino, B.F., and Walker, W.S.G. 1979, *Changing Trends in Variable Star Research*, F.M. Bateson, J. Smak, I.H. Urch (eds.), Univ. of Waikato, p. 29

Marsh, T. 1986, *Ph.D. Thesis*, Univ. Cambridge

Marsh, T.R. 1987, *Mon. Not. Roy. Astr. Soc.*, **228**, 779

Marsh, T.R., Horne, K., and Shipman, H.L. 1987, *Mon. Not. Roy. Astr. Soc.*, **225**, 551

Martel, L. 1961, *Ann. d'Astr.*, **24**, 267

Mason, K.O., Lampton, M., Charles, P., and Bowyer, S. 1978, *Astrophys. J. Lett.*, **226**, L 129

Mateo, M., and Szkody, P. 1985, *Astrophys. J.*, **288**, 292

Mateo, M., Szkody, P., and Bolte, M. 1985, *Publ. Astr. Soc. Pac.*, **97**, 45

Mattei, J.A., Saladyga, M., Waagen, E.O., and Jones, C.M. 1985, *AAVSO Monograph I*

Mattei, J.A., Saladyga, M., Waagen, E.O., and Jones, C.M. 1987, *AAVSO Monograph II*

Mauche, C.W., and Raymond, J.C. 1987, *Astrophys. J.*, **323**, 690

Mayall, M.W. 1972, *AAVSO Report*, **29**

Mayo, S.K., Wickramasinghe, D.T., and Whelan, J.A.J. 1980, *Mon. Not. Roy. Astr. Soc.*, **193**, 793

Mazeh, T., Kienboom, K., and Heise, J. 1986, *Mon. Not. Roy. Astr. Soc.*, **221**, 513

McRae, D.A. 1952, *Astrophys. J.*, **116**, 592

Meggitt, S.M.A., and Wickramasinghe, D.T. 1984, *Mon. Not. Roy. Astr. Soc.*, **207**, 1

Mestel, L. 1968, *Mon. Not. Roy. Astr. Soc.*, **138**, 359

Meyer, F., 1979, in IAU Coll. 53, *White Dwarfs and Variable Degenerate Stars*, Rochester, N.Y., 30 July - 2 Aug., 1979, H.M. van Horne, V. Weidemann (eds.), Univ. Of Rochester, p. 528

Meyer, F. 1984, *Astron. Astrophys.*, **131**, 303

Meyer, F., and Meyer-Hofmeister, E. 1981, *Astron. Astrophys.*, **104**, L 10

Meyer, F., and Meyer-Hofmeister, E. 1982, *Astron. Astrophys.*, **106**, 34

Meyer, F., and Meyer-Hofmeister, E. 1983a, *Astron. Astrophys.*, **121**, 29

Meyer, F., and Meyer-Hofmeister, E. 1983b, *Astron. Astrophys.*, **128**, 420

Meyer, F., and Meyer-Hofmeister, E. 1984, *Astron. Astrophys.*, **132**, 143

Meyer-Hofmeister, E. 1987, *Astron. Astrophys.*, **175**, 113

Meyer-Hofmeister, E., and Meyer, F. 1987, *Astron. Astrophys.*, **194**, 135

Miczaika, G.R. 1934, *Zeitschr. f. Astr.*, **8**, 292

Miczaika, G.R., and Becker, U. 1948, Veroeff. Heidelberg, **15**, 8, 79

Middleditch, J. 1982, *Astrophys. J. Lett.*, **257**, L 71

Middleditch, J., and Córdova, F.A. 1982, *Astrophys. J.*, **255**, 585

Miller, H.R. 1982, *Mon. Not. Roy. Astr. Soc.*, **201**, 21 p

Mineshige, S. 1986, *Publ. Astr. Soc. Jap.*, **38**, 831

Mineshige, S. 1988, *Astron. Astrophys.*, **190**, 72

Mineshige, S., and Osaki, Y. 1983, *Publ. Astr. Soc. Jap.*, **35**, 377

Mineshige, S., and Osaki, Y. 1985, *Publ. Astr. Soc. Jap.*, **37**, 1

Mitrofanov, I.G. 1980, *Nature*, **283**, 176

Moffet, T.J., and Barnes, T. III 1974, *Astrophys, J.*, **194**, 141

Motch, C., and Pakull, M.W. 1981, *Astron. Astrophys.*, **101**, L 9

Motch, C., van Paradijs, J., Pedersen, H., Iovaisky, S.A., and Chevalier, C. 1982, *Astron. Astrophys.*, **110**, 316

Müller, G., and Hartwig, E. 1918, *Geschichte und Literatur des Lichtwechsels der bis Ende 1915 als sicher veraenderlich erkannten Sterne nebst einem Katalog der Elemente ihres Lichtwechsels*, Poeschel and Trepte, Leipzig

Mukai, K., Bonnet-Bidaud, J.-M., Charles, P., Corbet, R.H.D., Maraschi, L., Osborne, J.P., Smale, A.P., Treves, A., van der Klis, M., and van Paradijs, J. 1986, *Mon. Not. Roy. Astr. Soc.*, **221**, 839

Mukai, K. and Charles, P.A. 1986, *Mon. Not. Roy. Astr. Soc.*, **222**, 1 p

Mukai, K., and Charles, P.A. 1987, *Mon. Not. Roy. Astr. Soc.*, **226**, 209

Mumford, G.S. 1962, *Sky and Tel.*, **23**, 71

Mumford, G.S. 1964, *Astrophys. J.*, **139**, 476

Mumford, G.S. 1966, *Astrophys. J.*, **146**, 411

Mumford, G.S. 1967a, *Astrophys. J. Suppl.*, **15**, 1

Mumford, G.S. 1967b, *Publ. Astr. Soc. Pac.*, **79**, 283

Mumford, G.S. 1971, *Astrophys. J.*, **165**, 369

Mumford, G.S. 1976, *Inf. Bull. Var. Stars*, **1128**

Nandy, K., Thompson, G.I., and Wilson, R. 1975, *Astron. Astrophys.*, **44**, 195

Nather, R.E. 1985, in *Interacting Binaries*, P.P. Eggleton (ed.), Reidel Publ., p. 349

Nather, R.E., and Robinson, E.L. 1974, *Astrophys. J.*, **190**, 637

Nather, R.E., Robinson, E.L., and Stover, R.J. 1979, in IAU Coll. 53, *White Dwarfs and Variable Degenerate Stars*, Rochester, N.Y., 30 July - 2 Aug., 1979, H.M. van Horne, V. Weidemann (eds.), Univ. of Rochester, p. 453

Nather, R.E., Robinson, E.L., and Stover, R.J. 1981, *Astrophys. J.*, **244**, 269

Nauenberg, M. 1972, *Astrophys. J.*, **175**, 417

Naylor, T. Bath, G.T., Charles, P.A., Hassall, B.J.M., Sonneborn, G., van der Woerd, H., and van Paradijs, J. 1987, *Mon. Not. Roy. Astr. Soc.*, **231**, 237

Nelson, L.A., Chau, W.Y., and Rosenblum, A. 1978, *Mon. Not. Roy. Astr. Soc.*, **182**, 595

Nelson, L.A., Chau, W.Y., and Rosenblum, A. 1985, *Astrophys. J.*, **299**, 658

Nelson, M.R., and Olson, E.C. 1976, *Astrophys. J.*, **207**, 195

Nero, I., and Sadeh, D. 1978, *Mon. Not. Roy, Astr. Soc.*, **182**, 595

Nomoto, K., and Sugimoto, D. 1977, *Publ. Astr. Soc. Jap.*, **29**, 765

Nousek, J.A., Takalo, L.O., Schmidt, G.D., Tapia, S., Hill, G.J., Bond, H.E., Grauer, A.D., and Agrawal, P.C. 1984, *Astrophys. J.*, **277**, 682

Novick, R. and Woltjer, L. 1975, *Astrophys. Lett.*, **16**, 67

O'Donoghue, D., Menzies, J.W., and Hill, P.W. 1987, *Mon. Not. Roy. Astr. Soc.*, **227**, 347

Oke, J.W., and Wade, R.A. 1982, *Astronom. J.*, **87**, 670

Olson, E.C. 1977, *Astrophys. J.*, **215**, 166

Olson, E.C. 1978, *Astrophys. J.*, **226**, 124

Ortolani, S., Rafanelli, P., Rosino, L., and Vittone, A. 1980, *Astron. Astrophys.*, **87**, 31

Osaki, Y. 1974, *Publ. Astr. Soc. Jap.*, **26**, 429

Osaki, Y. 1985, *Astron. Astrophys.*, **144**, 369

Osaki, Y., and Hausen, C.J. 1974, *Astrophys. J.*, **185**, 277

Osborne, J.P., Beuermann, K., Charles, P., Maraschi, L., Mukai, K., and Treves, A. 1987, *Astrophys. J. Lett.*, **315**, L 123

Osborne, J.P., Rosen, R., Mason, K.O., and Beuermann, K. 1985, *Space Sci. Rev.*, **40**, 143

Pacharintanakul, P. and Katz, J.I. 1980, *Astrophys. J.*, **238**, 985

Paczynski, B. 1971, *Ann. Rev. Astr. Atroph.*, **9**, 183

Paczynski, B. 1976, in IAU Symp. 73, *Structure and Evolution of Close Binary Systems*, Cambridge, England, 28 July - 1 Aug., 1975, P. Eggleton, S. Mitton, J. Whelan (eds.), Reidel Publ., p. 75

Paczynski, B. 1978, in *Nonstationary Evolution in Close Binaries*, Second Symposium of the Problem Commission Physics and Evolution of Stars, Warsaw, Poland, June 20–25, 1977, A.N. Zytkow (ed.), Polish Scientific Publ., p. 89

Paczynski, B. 1981, *Acta Astr.*, **31**, 1

Paczynski, B. 1985, in *Cataclysmic Variables and Low-Mass X-ray Binaries*, Proc. of the 7th North American Workshop held in Cambridge, Mass., Jan. 12–15, 1983, D.Q. Lamb, J. Patterson (eds.), Reidel Publ., p. 1

Paczynski, B., and Schwarzenberg-Czerny, A. 1980, *Acta Astr.*, **30**, 126

Paczynski, B., and Sienkiewicz, R. 1981, *Astrophys. J. Lett.*, **248**, L 27

Paczynski, B., and Sienkiewicz, R. 1983, *Astrophys. J.*, **268**, 825

Panek, R.J. 1980, *Astrophys. J.*, **241**, 1077

Panek, R.J., and Eaton, J.A. 1982, *Astrophys. J.*, **258**, 572

Papaloizou, J.C.B., and Bath, G.T. 1975, *Mon. Not. Roy. Astr. Soc.*, **172**, 339

Papaloizou, J., Faulkner, J, and Lin, D.N.C. 1983, *Mon. Not. Roy. Astr. Soc.*, **205**, 487

Papaloizou, J.C.B., and Lin, D.N.C 1979, *Mon. Not. Roy. Astr. Soc.*, **186**, 799

Papaloizou, J., and Pringle, J.E. 1977, *Mon. Not. Roy. Astr. Soc.*, **181**, 441

Papaloizou, J., and Pringle, J.E. 1978a, *Astron. Astrophys.*, **70**, L 65

Papaloizou, J., and Pringle, J.E. 1978b, *Mon. Not. Roy. Astr. Soc.*, **182**, 423

Papaloizou, J., and Pringle, J.E. 1979, *Mon. Not. Roy. Astr. Soc.*, **189**, 293

Papaloizou, J.C.B., and Stanley, D.Q.G. 1986, *Mon. Not. Roy. Astr. Soc.*, **220**, 593

Parenago, P., and Kukarkin, B. 1934, *Variable Stars*, **4**, 249

Patterson, J. 1979a, *Astrophys. J.*, **233**, L 13

Patterson, J. 1979b, *Astrophys. J.*, **234**, 978

Patterson, J. 1980, *Astrophys. J.*, **241**, 235

Patterson, J. 1981, *Astrophys. J. Suppl.*, **45**, 517

Patterson, J. 1984, *Astrophys. J. Suppl.*, **54**, 443

Patterson, J. 1985, in *Cataclysmic Variables and Low-Mass X-ray Binaries*, Proc. of the 7th North American Workshop held in Cambridge, Mass., Jan. 12–15, 1983, D.Q. Lamb, J. Patterson (eds.), Reidel Publ., p. 435

Patterson, J., Beuermann, K., Lamb, D.Q., Fabbiano, G., White, J.C., Raymond, J.C., and Swank, J. 1984, *Astrophys. J.*, **279**, 785

Patterson, J., Brauch, D., Chincarini, G., and Robinson, E.L. 1980, *Astrophys. J. Lett.*, **240**, L 133

Patterson, J., McGraw, J.T., Coleman, L, and Africano, J.L. 1981b, *Astrophys. J.*, **248**, 1067

Patterson, J., Nather, R.E., Robinson, E.L., and Handler, F. 1979, *Astrophys. J.*, **232**, 819

Patterson, J., and Price, C.M. 1981, *Astrophys. J.*, **243**, L 83

Patterson, J., and Raymond, J.C. 1985a, *Astrophys. J.*, **292**, 535

Patterson, J., and Raymond, J.C. 1985b, *Astrophys. J.*, **292**, 550

Patterson, J., Robinson, E.L., and Kiplinger, A.L. 1978a, *Astrophys. J. Lett.*, **226**, L 137

Patterson, J., Robinson, E.L. and Nather, R.E. 1978b, *Astrophys. J.*, **224**, 535

Patterson, J., and Steiner, J.E. 1978, *Astrophys. J.*, **224**, 570

Patterson, J., and Steiner, J.E. 1983, *Astrophys. J. Lett.*, **264**, L 61

Patterson, J., Williams, G., and Hiltner, W.A. 1981a, *Astrophys. J.*, **245**, 618

Payne, C.H. 1934, *Harv. Bull.*, **894**, 18

Payne-Gaposchkin, C. 1957, *The Galactic Novae*

Payne-Gaposchkin, C., and Gaposchkin, S. 1938, *Variable Stars*, Cambridge

Penning, W.R. 1985, *Astrophys. J.*, **289**, 300

Penning, W.R., Ferguson, D.H., McGraw, J.T., Liebert, J., and Green, R.F. 1984, *Astrophys. J.*, **276**, 233

Petit, M. 1958, *Ciel et Terre*, **74**, 195

Petit, M. 1961, *Asiago Contr*, **119**, 31

Petterson, J.A. 1980, *Astrophys. J.*, **241**, 247

Petterson, J.A. 1983, in *Accretion Driven Stellar X-Ray Sources*, W.H.G. Lewin, E.P.J. van den Heuvel (eds.), Cambridge Univ. Press, p. 367

Piirola, V., Reiz, A., and Coyne, G.V. 1987, *Astron. Astrophys.*, **186**, 120

Pogson 1906, *Mon. Not. Roy. Astr. Soc.*, **67**, 119 (edited by H.H. Turner and F.R.S. Savilian)

Pojmanski, G. 1986, *Acta Astr.*, **36**, 69

Polidan, R.S., and Holberg, J.B. 1984, *Nature*, **309**, 528

Polidan, R.S., and Holberg, J.B. 1986, *Mon. Not. Roy. Astr. Soc.*, **225**, 131

Popova, M.D., and Vitrichenko, E.A. 1979, *Sov. Astr.*, **22**, 438

Prager, R., 1934, *Geschichte und Lichtwechsel der Veraenderlichen Sterne*, Veroeff. Univ. Sternwarte Berlin Babelesberg

Priedhorski, W. 1986, *Astrophys. J. Lett.*, **306**, L 97

Priedhorski, W., and Marshall, F. 1982, *Bull. Am. Astr. Soc.*, **14**, 980

Priedhorski, W., Marshall, F.J., and Hearn, D.R. 1987, *Astron, Astrophys.*, **173**, 95

Pringle, J.E. 1975, *Mon. Not. Roy. Astr. Soc.*, **170**, 633

Pringle, J.E. 1977, *Mon. Not. Roy. Astr. Soc.*, **178**, 195

Pringle, J.E., Bateson, F.M., Hassall, B.J.M., Heise, J., van der Woerd, H., Holberg, J.B., Polidan, R.S., van Amerongen, S., van Paradijs, J., and Verbunt, F. 1987, *Mon. Not. Roy. Astr. Soc.*, **225**, 73

Pringle, J.E., and Savonije, G.J. 1979, *Mon. Not. Roy. Astr. Soc.*, **187**, 777

Pringle, J.E., and Verbunt, F. 1984, in Proc. of the Fourth European IUE Conference, Rome, Italy, 15–18 May, 1984, E. Rolfe, R. Battrick (eds.), ESA SP-218, p. 377

Pringle, J.E., Verbunt, F., and Wade, R.A. 1986, *Mon. Not. Roy. Astr. Soc.*, **221**, 169

Quigley, R., and Africano, J., 1978, *Publ. Astr. Soc. Pac.*, **90**, 445

Rappaport, S., Cash, W., Doxsey, R., McClintock, J., and Moore, G. 1974, *Astrophys. J.*, **187**, L 5

Rappaport, S., Joss, P.C., and Webbink, R.F. 1982, *Astrophys. J.*, **254**, 616

Raymond, J.C., Black, J.H., Davis, R.J., Dupree, A.K., Gursky, H., Hartmann, L., and Matilsky, T.A. 1978, *Astrophys. J. Lett.*, **230**, L 95

Remillard, R.A., Bradt, H.V., McClintock, J.E., Patterson, J., Roberts, W., Schwartz, D.A., and Tapia, S. 1986, *Astrophys. J. Lett.*, **302**, L 11

Ricketts, M.J., King, A.R., and Raine, D.J. 1979, *Mon. Not. Roy. Astr. Soc.*, **186**, 233

Ritter, H. 1976, *Mon. Not. Roy. Astr. Soc.*, **175**, 279

Ritter, H. 1980, *Astron. Astrophys.*, **86**, 204

Ritter, H. 1983a, in *High Energy Astrophysics and Cosmology*, Y. Jian, and Z. Cisheng (eds.), Nagking, Gordon and Breach, p. 207

Ritter, H. 1983b, in IAU Coll. 72, *Cataclysmic Variables and Related Objects*, Haifa, Israel, Aug. 9–13, 1982, M. Livio, G. Shaviv (eds.), Reidel Publ., p. 257

Ritter, H. 1984, *Astron. Astrophys. Suppl.*, **57**, 385

Ritter, H. 1986a, *Astron. Astrophys.*, **168**, 105

Ritter, H. 1986b, *Astron. Astrophys.*, **169**, 139

Ritter, H. 1986c, in *The Evolution of Galactic X-Ray Binaries*, Truemper J., W.H.G. Lewin, W. Brinkman (eds.), Rottach-Egern, FRG, June 17-21, 1985, Reidel Publ. p. 217

Ritter, H. 1987, *Astron. Astrophys. Suppl.*, **70**, 335

Ritter, H., and Burkert, A. 1986, *Astron. Astrophys.*, **158**, 161

Ritter, H., and Oezkan, M.T. 1986, *Astron. Astrophys.*, **167**, 260

Robertson, J.A., and Frank, J. 1986, *Mon. Not. Roy. Astr. Soc.*, **221**, 279

Robinson, E.L. 1973a, *Astrophys. J.*, **180**, 121

Robinson, E.L. 1973b, *Astrophys. J.*, **183**, 193

Robinson, E.L. 1974, *Astrophys. J.*, **193**, 191

Robinson, E.L. 1976, *Astrophys. J.*, **203**, 485

Robinson, E.L. 1978, *Astrophys. J.*, **219**, 168

Robinson, E.L. 1983, in IAU Coll. 72, *Cataclysmic Variables and Related Objects*, Haifa, Israel, Aug. 9–13, 1982, M. Livio, G. Shaviv (eds.), Reidel Publ., p. 1

Robinson, E.L., Barker, E.S., Cochran, A.L., Cochran, W.D., and Nather, R.E. 1981, *Astrophys. J.*, **251**, 611

Robinson, E.L., and Nather, R.E. 1975, *Astrophys. J. Lett.*, **200**, L 23

Robinson, E.L., and Nather, R.E. 1979, *Astrophys. J. Suppl.*, **39**, 461

Robinson, E.L., and Nather, R.E. 1983, *Astrophys. J.*, **273**, 255

Robinson, E.L., Nather, R.E., and Patterson, J. 1978, *Astrophys. J.*, **219**, 168

Robinson, E.L., and Warner, B. 1984, *Astrophys. J.*, **277**, 250

Robinson, E.L., Zhang, E.-H., and Stover, R.J. 1986, *Astrophys. J.*, **305**, 732

Rosen, S.R., Mason, K.O., and Córdova, F.A. 1987, *Mon. Not. Roy. Astr. Soc.*, **224**, 987

Rothschild, R.E., Gruber, D.E., Knight, F.K., Matteson, J.L., Nolan, P.L., Swank, J.H., Holt, S.S., Serlemitos, P.J., Mason, K.O., and Tuohy, I.R. 1981, *Astrophys. J.*, **250**, 723

Rybicki, G.B., and Hummer, D.G. 1983, *Astrophys. J.*, **274**, 380

Ryves, P.M. 1932, *Mon. Not. Roy. Astr. Soc.*, **92**, 715

Saw, D.R.B. 1982a, *Journ. Brit. Astr. Ass.*, **92**, 127

Saw, D.R.B. 1982b, *Journ. Brit. Astr. Ass.*, **92**, 220

Saw, D.R.B. 1983, *Journ. Brit. Astr. Ass.*, **93**, 70

Sawada, K., Matsuda, T., and Hachisu, I. 1986a, *Mon. Not. Roy. Astr. Soc.*, **219**, 75

Sawada, K., Matsuda, T., and Hachisu, I. 1986b, *Mon. Not. Roy. Astr. Soc.*, **221**, 679

Sawada, K., Matsuda, T., Inone, M., and Hachisu, I. 1987, *Mon. Not. Roy. Astr. Soc.*, **224**, 307

Schatzmann, E. 1959, *Ann. d'Astr.*, **22**, 436

Schlegel, E.M., Honeycutt, R.K., and Kaitchuck, R.H. 1983, *Astrophys. J. Suppl.*, **53**, 397

Schmidt, G.D., Stockman, H.S., and Grandi, S.A. 1983, *Astrophys. J.*, **271**, 725

Schmidt, G.D., Stockman, H.S., and Margon, B. 1981, *Astrophys. J. Lett.*, **243**, L 157

Schneider, D.P., and Greenstein, J.L. 1979, *Astrophys. J.*, **233**, 935

Schneider, D.P., and Greenstein, J.L. 1980, *Astrophys. J.*, **240**, 871

Schneider, D.P., Young, P., and Shectman, S.A. 1981, *Astrophys. J.*, **245**, 644

Schneller, H. 1954, *Geschichte und Lichtwechsel der Veraenderlichen Sterne*, Akademie Verlag, Berlin

Schoembs, R. 1977, in IAU Coll. 42, *The Interaction of Variable Stars with their Environment*, Bamberg, Sept. 6-9, 1977, R. Kippenhahn, J. Rahe, W. Strohmeier (eds.), = Veroeff. Sternwarte Bamberg Bd. XI, Nr. **121**, p. 218

Schoembs, R. 1982, *Astron. Astrophys.*, **115**, 190

Schoembs, R. 1986, *Astron. Astrophys.*, **158**, 233

Schoembs, R., Dreier, H., and Barwig, H. 1986, *Astron. Astrophys.*, **181**, 50

Schoembs, R., and Hartmann, K. 1983, *Astron. Astrophys.*, **128**, 37

Schoembs, R., and Vogt, N. 1980, *Astron. Astrophys.*, **91**, 25

Schoembs, R., and Vogt, N. 1981, *Astron. Astrophys.*, **97**, 185

Schrijver, J., Brinkman, A.C., van der Woerd, H., Watson, M.G., King, A.R., van Paradijs, J., and van der Klis, M. 1985, *Space Sci Rev.*, **40**, 121

Schwarzenberg-Czerny, A. 1981, *Acta Astr.*, **31**, 241

Schwarzenberg-Czerny, A. A., Ward, M., Hanes, D.A., Jones, D.H.P., Pringle, J.E., Verbunt, F., and Wade, R.A. 1985, *Mon. Not. Roy. Astr. Soc.*, **212**, 645

Seaton, M.J. 1979, *Mon. Not. Roy. Astr. Soc.*, **187**, 73 p

Semeniuk, I. 1980, *Astron. Astrophys. Suppl.*, **39**, 29

Shaefer, B.E., and Patterson, J. 1983, *Astrophys. J.*, **268**, 710

Shafter, A.W. 1983, *Astrophys. J.*, **267**, 222

Shafter, A.W. 1985, *Cataclysmic Variables and Low-Mass X-Ray Binaries*, Proc. of the 7th North American Workshop held in Cambridge, Mass., Jan. 12-15, 1983, D.Q. Lamb, J. Patterson (eds.), Reidel Publ., p. 355

Shafter, A.W. Macry, J.D. 1987, *Mon. Not. Roy. Astr. Soc.*, **228**, 193

Shafter, A.W., and Szkody, P. 1984, *Astrophys. J.*, **276**, 305

Shafter, A.W., Szkody, P., Liebert, J., Penning, W.R., Bond, H.E., and Grauer, A.D. 1985, *Astrophys. J.*, **290**, 707

Shafter, A.W., Targan, D.M. 1982, *Astronom. J.*, **87**, 655

Shakura, N.I., and Sunyaev, R.A. 1973, *Astron. Astrophys.*, **24**, 337

Shara, M.M., Livio, M., Moffat, A.F.J., and Orio, M. 1986, *Astrophys. J.*, **311**, 163

Shaviv, G. 1987, *Astrophys. Space Sci.*, **130**, 303

Shaviv, G., and Wherse, R., 1986, *Astron. Astrophys.*, **159**, L 5

Sherrington, M.R., Bailey, J., and Jameson, R.F. 1984, *Mon. Not. Roy. Astr. Soc.*, **206**, 859

Sherrington, M.R., and Jameson, R.F. 1983, *Mon, Not. Roy. Astr. Soc.*, **205**, 265

Sherrington, M.R., Jameson, R.F., Bailey, J., and Giles, A.B. 1982, *Mon. Not. Roy. Astr. Soc.*, **200**, 861

Sherrington, M.R., Kawson, P.A., King, A.R., and Jameson, R.F. 1980, *Mon. Not. Roy. Astr. Soc.*, **191**, 185

Sienkiewicz, R. 1984, *Acta Astr.*, **34**, 325

Singh, K.P., Agrawal, P.C., and Riegler, G.R. 1984, *Bull. Astr. Soc. Ind.*, **11**, 66

Sion, E. 1985, *Astrophys. J.*, **292**, 601

Smak, J. 1971, *Acta Astr.*, **21**, 15

Smak, J. 1973, in IAU Coll. 15, *New Directions and Frontiers in Variable Star Research*, W. Strohmeier (ed.), Bamberg = Veroeff. Sternwarte Bamberg **9**, p. 248

Smak, J. 1975, *Acta Astr.*, **25**, 371

Smak, J. 1976, in IAU Symp. 73, *Structure and Evolution of Close Binary Systems*, Cambridge, England, 28 July - 1 Aug., 1975, P. Eggleton, S. Mitton, J. Whelan (eds.), Reidel Publ., p. 149

Smak, J. 1979, *Acta Astr.*, **29**, 325

Smak, J. 1981, *Acta Astr.*, **31**, 395

Smak, J. 1983, *Acta Astr.*, **33**, 333

Smak, J. 1984, *Acta Astr.*, **34**, 161

Smak, J. 1985, *Acta Astr.*, **35**, 357

Smak, J., and Stepień, K. 1968, in IAU Coll. 4, *Non-Periodic Phenomena in Variable Stars*, Held in Budapest, Hungary, L. Detre (ed.), Sept. 5-9, 1968, Academic Press Budapest, p. 335

Solheim, J.E., and Kjeldseth-Moe, O. 1987, *Astrophys. Space Sci.*, **131**, 785

Solheim, J.E., Robinson, E.L., Nather, R.E., and Kepler, S.O. 1984, *Astron. Astrophys.*, **135**, 1

Sparks, W.M., and Kutter, G.S. 1980, *Space Sci. Rev.*, **27**, 643

Spruit, H.C., and Ritter, H. 1983, *Astron. Astrophys.*, **124**, 267

Stanley, G.Q.G., and Papaloizou, J.C.B. 1987, *Astrophys. Space Sci.*, **130**, 315

Sterne, T.E., and Campbell, L. 1934, *Harv. Ann.*, **90**, 201

Stiening, R.f., Hildebrand, R.H., and Spillar, E.J. 1979, *Publ. Astr. Soc. Pac.*, **91**, 384

Stockman, H.D., Foltz, C.B., Schmidt, G.D., and Tapia, S. 1983, *Astrophys. J.*, **271**, 725

Stolz, B., and Schoembs, R. 1984, *Astron. Astrophys.*, **132**, 187

Stover, R.J. 1981a, *Astrophys. J.*, **248**, 684

Stover, R.J. 1981b, *Astrophys. J.*, **249**, 673

Stover, R.J., Robinson, E.L., Nather, R.E., and Montemayor, T.J. 1980, *Astrophys. J.*, **240**, 597

Stover, R.J., Robinson, E.L., and Nather, R.E. 1981, *Astrophys. J.*, **248**, 696

Strand, K.A. 1948, *Astrophys. J.*, **107**, 106

Struve, O. 1955, *Sky and Tel.*, **14**, 275

Swank, J.H. 1979, in IAU Coll. 53, *White Dwarfs and Variable Degenerate Stars*, Rochester, N.Y., 30 July - 2 Aug., 1979, H.M. van Horne, V. Weidemann (eds.), Univ. of Rochester, p. 135

Swank, J., Lampton, M., Boldt, E., Holt, S., and Serlemitsos, P. 1977, *Astrophys. J. Lett.*, **216**, L 71

Szkody, P. 1976, *Astrophys. J.*, **210**, 168

Szkody, P. 1977, *Astrophys. J.*, **217**, 140

Szkody, P. 1978, *Publ. Astr. Soc. Pac.*, **90**, 61

Szkody, P. 1981, *Astrophys. J.*, **247**, 577

Szkody, P. 1985a, *Astronom. J.*, **90**, 1837

Szkody, P. 1985b, in Proc. ESA Workshop: *Recent Results on Cataclysmic Variables*, Bamberg, FRG, 17-19 April, 1985, ESA SP-236, p. 39

Szkody, P., Bailey, J.A., and Hough, J.H. 1983, *Mon. Not. Roy. Astr. Soc.*, **203**, 749

Szkody, P., and Capps, R.W. 1980, *Astronom. J.*, **85**, 882

Szkody, P., and Downes, R.A. 1982, *Publ. Astr. Soc. Pac.*, **94**, 328

Szkody, P., Liebert, J., and Panek, R.J. 1985, *Astrophys. J.*, **293**, 321

Szkody, P., Margon, B. 1980, *Astrophys. J.*, **236**, 862

Szkody, P., and Mateo, M. 1984, *Astrophys. J.*, **280**, 729

Szkody, P., and Mateo, M. 1986, *Astrophys. J.*, **301**, 286

Szkody, P., Mattei, J. 1984, *Publ. Astr. Soc. Pac.*, **96**, 988

Szkody, P., Michalsky, J.J., and Stokes, G.M. 1982a, *Publ. Astr. Soc. Pac.*, **94**, 137

Szkody, P., Raymond, J.C., and Capps, R.W. 1982b, *Astrophys. J.*, **257**, 686

Taam, R.E., 1983, *Astrophys. J.*, **268**, 361

Taam, R.E., Flannery, B.P., and Faulkner, J. 1980, *Astrophys. J.*, **239**, 1017

Tajima, T., and Gilden, D. 1987, *Astrophys. J.*, **320**, 741

Thorstensen, J.R., and Freed, I.W. 1985, *Astronom. J.*, **90**, 2082

Thorstensen, J.R., Schommer, R.A., and Charles, P.A. 1983, *Publ. Astr. Soc. Pac.*, **95**, 140

Thorstensen, J.R., Smak, J., and Hessman, F.V. 1985, *Publ. Astr. Soc. Pac.*, **97**, 437

Tuohy, I.R., Visvanathan, N., and Wickramasinghe, D.T. 1985, *Astrophys. Space Sci.*, **118**, 291

Turner, K.C., 1985, in *Radio Stars*, R.M. Hjelming and D.M. Gibson (eds.), p. 283

Tylenda, R. 1977, *Acta Astr.*, **27**, 235

Tylenda, R. 1981a, *Acta Astr.*, **31**, 127

Tylenda, R. 1981b, *Acta, Astr.*, **31**, 267

van Amerongen, S., Bovenschen, H., and van Paradijs, J. 1987a, *Mon. Not. Roy. Astr. Soc.*, **229**, 245

van Amerongen, S., Damen, E., Groot, M., Kraakman, H., and van Paradijs, J. 1987b, *Mon. Not. Roy. Astr. Soc.*, **225**, 93

van Amerongen, S., and van Paradijs, J. 1987c, *Astrophys. Space Sci.*, **130**, 127

van der Bilt, J. 1908, *Recherches Astronomiques de l'Observatoire d'Utrecht III*

van der Woerd, H., Heise, J., and Bateson, F. 1986, *Astron. Astrophys.*, **156**, 252

van der Woerd, H., Heise, J., Paerels, F., Beuermann, K., van der Klis, M., Motch, C., and van Paradijs, J. 1987, *Astron. Astrophys.*, **182**, 219

van der Woerd, H., de Kool, M., and van Paradijs, J. 1984, *Astron. Astrophys.*, **131**, 137

van der Woerd, H., and van Paradijs, J. 1987, *Mon. Not. Roy. Astr. Soc.*, **224**, 271

van Maanen, A. 1938, *Astrophys. J.*, **87**, 424

van Paradijs, J. 1983, *Astron. Astrophys.*, **125**, L 16

van Paradijs, J. 1985, *Astron. Astrophys.*, **144**, 199

Verbunt, F. 1982, *Space Sci. Rev.*, **32**, 379

Verbunt, F. 1984, *Mon. Not. Roy. Astr. Soc.*, **209**, 227

Verbunt, F. 1986, in Lecture Notes in Physics **266**, *The Physics of Accretion onto Compact Objects*, Proc. of a Workshop held in Tenerife, Spain, April 21–25, 1986, K.O. Mason, M.G. Watson, N.E. White (eds.), Springer Verlag, p. 59

Verbunt, F. 1987, *Astron. Astrophys. Suppl.*, **71**, 339

Verbunt, F., Hassall, B.J.M., Pringle, J.E., Warner, B., and Marang, F. 1987, *Mon. Not. Roy. Astr. Soc.*, **225**, 113

Verbunt, F., Pringle, J.E., Wade, R.A., Echevarria, J., Jones, D.H.P., Argue, R.W., Schwarzengerg-Czerny, A., la Dous, C., and Schoembs, R. 1984, *Mon. Not. Roy. Astr. Soc.*, **210**, 197

Verbunt, F., and Wade, R. 1984, *Astron. Astrophys. Suppl.*, **57**, 193

Verbunt, F., and Zwaan, C. 1981, *Astron. Astrophys.*, **100**, L 7

Visvanathan, N., and Wickramasinghe, D.T. 1979, *Nature*, **281**, 47

Visvanathan, N., and Wickramasinghe, D.T. 1981, *Mon. Not. Roy. Astr. Soc.*, **196**, 175

Vogt, N. 1974, *Astron. Astrophys.*, **36**, 369

Vogt, N. 1977, in IAU, Coll. 42, *The Interaction of Variable Stars with their Environment*, Bamberg, FRG, Sept. 6–9, 1977, R. Kippenhahn, J. Rahe, W. Strohmeier (eds.) = Veroeff. Sternwarte Bamberg Bd. XI, Nr. **121**, p. 227

Vogt, N. 1979, *Mitt. Astr. Ges.*, **45**, 158

Vogt, N. 1980, *Astron. Astrophys.*, **88**, 66

Vogt, N. 1981, *Habilitationsschrift, Univ. Bochum*

Vogt, N. 1982a, *Astrophys. J.*, **252**, 653

Vogt, N. 1982b, *Mitt. Astr. Ges.*, **57**, 79

Vogt, N. 1983a, *Astron. Astrophys.*, **128**, 29

Vogt, N. 1983b, *Astron. Astrophys. Suppl.*, **53**, 21

Vogt, N. 1983c, *Sterne und Weltraum*, **22**, 588

Vogt, N., and Breysacher, J. 1980a, *Astron. Astrophys.*, **87**, 349

Vogt, N., and Breysacher, J. 1980b, *Astrophys. J.*, **235**, 945

Vogt, N., Krzeminski, W., and Sterken, C. 1980, *Astron. Astrophys.*, **85**, 106

Vogt, N, Schoembs, R., Krzeminski, W., and Pedersen, H. 1981, *Astron. Astrophys.*, **94**, L 29

Voikhanskaya, N.F. 1980, *Sov. Astr.*, **24**, 300

Voikhanskaya, N.F. 1983a, *Sov. Astr.*, **27**, 5

Voikhanskaya, N.F. 1983b, *Sov. Astr.*, **27**, 670

Voikhanskaya, N.F., and Nazarenko, I.I. 1984, *Sov. Astr. Lett.*, **10**, 439

Vorontsov-Veljaminov, W. 1934, *Astr. Journal of the Sov. Union 11*, **294**

Wade, R.A. 1979, *Astronom. J.*, **84**, 562

Wade, R.A. 1981, *Astrophys. J.*, **246**, 215

Wade, R.A. 1982, *Astronom. J.*, **87**, 1558

Wade, R.A. 1984, *Mon. Not. Roy. Astr. Soc.*, **208**, 381

Wade, R.A., and Oke, J.B. 1982, *Bull. Am. Astr. Soc.*, **14**, 880

Walker, M.F. 1954a, *Publ. Astr. Soc. Pac.*, **66**, 71

Walker, M.F. 1954b, *Publ. Astr. Soc. Pac.*, **66**, 230

Walker, M.F. 1956, *Astrophys. J.*, **123**, 68

Walker, M.F. 1957, in IAU Symp. 3, *Non-Stable Stars*, held in Dublin, Ireland, 1 Sept., 1955, G.H. Herbig (ed.), Cambridge Univ. Press, p. 46

Walker, M.F. 1958, *Astrophys, J.*, **127**, 319

Walker, M.F. 1963, *Astrophys. J.*, **137**, 485

Walker, M.F. 1981, *Astrophys. J.*, **248**, 256

Walker, M.F., and Bell, M. 1980, *Astrophys. J.*, **237**, 89

Walker, M.F., and Chincarini, G. 1968, *Astrophys. J.*, **154**, 157

Walker, M.F., and Herbig, G.H. 1954, *Astrophys. J.*, **120**, 278

Wargau, W., Bruch, A., Drechsel, H., and Rahe, J. 1983a, *Astron. Astrophys.*, **125**, L 1

Wargau, W., Bruch, A., Drechsel, H., Rahe, J., and Schoembs, R. 1984, *Astrophys. Space Sci.*, **99**, 145

Wargau, W., Drechsel, H., Rahe, J., and Bruch, A. 1983b, *Mon. Not. Roy. Astr. Soc.*, **204**, 35 p

Warner, B. 1972, *Mon. Not. Roy. Astr. Soc.*, **159**, 315

Warner, B. 1973, *Mon. Not. Roy. Astr. Soc.*, **162**, 189

Warner, B. 1974a, *Mon. Not. Roy. Astr. Soc.*, **168**, 235

Warner, B. 1974b, *Mon. Not. Roy. Astr. Soc. South Afr.*, **33**, 21

Warner, B. 1975, *Mon. Not. Roy. Astr. Soc.*, **170**, 219

Warner, B. 1976, in IAU Symp. 73, *Structure and Evolution of Close Binary Systems*, Cambridge, England, 28 July - 1 Aug., 1975, P. Eggleton, S. Mitton, J. Whelan (eds.), Reidel Publ., p. 85

Warner, B. 1983, in IAU Coll. 72, *Cataclysmic Variables and Related Objects*, Haifa, Israel, Aug. 9–13, 1982, M. Livio, G. Shaviv (eds.), Reidel Publ., p. 155

Warner, B. 1985a, in *Interacting Binaries*, P.P. Eggleton, J.E. Pringle (eds.), Reidel Publ., p. 367

Warner, B. 1985b, in *Cataclysmic Variables and Low-Mass X-Ray Binaries*, Proc. of the 7th North American Workshop held in Cambridge, Mass., Jan. 12–15, 1983, D.Q. Lamb, J. Patterson (eds.), Reidel Publ., p. 269

Warner, B. 1986a, *Mon. Not. Roy. Astr. Soc*, **219**, 347

Warner, B. 1986b, *Astrophys. Space Sci.*, **118**, 271

Warner, B. 1987, *Mon. Not. Roy. Astr. Soc.*, **227**, 23

Warner, B., and Brickhill, A.J., 1974, *Mon. Not. Roy. Astr. Soc.*, **166**, 673

Warner, B., and Brickhill, A.J. 1978, *Mon. Not. Roy. Astr. Soc.*, **182**, 777

Warner, B., and Cropper, M. 1983, *Mon. Not. Roy. Astr. Soc.*, **203**, 909

Warner, B., and Cropper, M. 1984, *Mon. Not. Roy. Astr. Soc.*, **206**, 261

Warner, B., and McGraw, J.T. 1981, *Mon. Not. Roy. Astr. Soc.*, **196**, 59 p

Warner, B., and Nather, R.E. 1971, *Mon. Not. Roy. Astr. Soc.*, **152**, 219

Warner, B., and Nather, R.E. 1972, *Mon. Not. Roy. Astr. Soc.*, **156**, 297

Warner, B., Peters, W.L., Hubbard, W.B., and Nather, R.E. 1972, *Mon. Not. Roy. Astr. Soc.*, **159**, 321

Warner, B., and Robinson, E.L. 1972, *Mon. Not. Roy. Astr. Soc.*, **159**, 101

Warner, B., and Thackeray, A.D. 1975, *Mon. Not. Roy. Astr. Soc.*, **172**, 433

Warner, B., and van Citters, G.W. 1974, Obs, **94**, 116

Watson, M.G., King, A.R., and Heise, J. 1985, in Proc. ESA Workshop: *Recent Results on Cataclysmic Variables*, Bamberg, FRG, 17–19 April, 1985, ESA SP-236, p. 217

Watson, M.G., King, A.R., and Williams, G. 1987, *Mon. Not. Roy. Astr. Soc.*, **226**, 867

Watts, D.J., Giles, A.B., Greenhill, J.G., Hill, K., and Bailey, J. 1985, *Mon. Not. Roy. Astr. Soc.*, **215**, 83

Webbink, R.F. 1979, in IAU Coll. 53, *White Dwarfs and Degenerate Variable Stars*, Rochester, N.Y., 30 July - 2 Aug., 1972, H.M. van Horne, V. Weidemann (eds.), Univ. of Rochester, p. 426

Webbink, R.F. 1980, in IAU Symp. 88, *Close Binary Stars: Observations and Interpretation*, held in Toronto, Canada, Aug. 7–10, 1979, M.J. Plavec, D.M. Popper, R.K. Ulrich (eds.), Reidel Publ., p. 561

Wellmann, P. 1952, *Zeitschr. f. Astr.*, **31**, 123

Westin, B.A.M. 1980, *Astron. Astrophys.*, **81**, 743

White, N.E. 1981, *Astrophys. J.*, **244**, L 85

Wickramasinghe, D.T., and Meggitt, S.M.A. 1982, *Mon. Not. Roy. Astr. Soc.*, **198**, 975

Wickramasinghe, D.T., and Meggitt, S.M.A. 1985a, *Mon. Not. Roy. Astr. Soc.*, **214**, 605

Wickramasinghe, D.T., and Meggitt, S.M.A. 1985b, *Mon. Not. Roy. Astr. Soc.*, **216**, 857

Wickramasinghe, D.T., Visvanathan, N., and Tuohy, I.R. 1984, *Astrophys. J.*, **286**, 328

Williams, G. 1983, *Astrophys. J. Suppl.*, **53**, 523

Williams, R.E. 1980, *Astrophys. J.*, **235**, 939

Williams, R.E., and Ferguson, D.H. 1982, *Astrophys. J.*, **257**, 672

Williams, R.E., and Hiltner, W.A. 1980, *Publ. Astr. Soc. Pac.*, **92**, 178

Williams, R.E., and Hiltner, W.A. 1982, *Astrophys. J.*, **252**, 277

Williams, R.E., and Hiltner, W.A. 1984, *Mon. Not. Roy. Astr. Soc.*, **211**, 629

Williams, R.E., Lin, D.N.C., and Stover, R.J. 1988, *Astrophys. J.*, **327**, 234

Wolf, M., and Wolf, G. 1906, *Astron. Nachr.*, **171**, 77

Wood, J., and Crawford, C.S. 1986, *Mon. Not. Roy. Astr. Soc.*, **222**, 645

Wood, J., Horne, K., Berriman, G., Wade, R., O'Donoghue, D., and Warner, B. 1986, *Mon. Not. Roy. Astr. Soc.*, **219**, 629

Wood, M.A., Winget, D.E., Nather, R.E., Hessman, F.V., Liebert, J., Kurtz, D.W., Wesemael, F., and Wegner, G. 1987, *Astrophys. J.*, **313**, 757

Wu, C.-C., and Panek, R.J. 1982, *Astrophys. J.*, **262**, 244

Wu, C.-C., and Panek, R.J. 1983, *Astrophys. J.*, **271**, 754

Yamasaki, A., Okazaki, A., and Kitamura, M. 1983, *Publ. Astr. Soc. Jap.*, **35**, 423

Young, P., and Schneider, D.P. 1979, *Astrophys. J.*, **230**, 502

Young, P., and Schneider, D.P. 1980, *Astrophys. J.*, **238**, 955

Young, P., and Schneider, D.P. 1981, *Astrophys. J.*, **247**, 960

Young, P., Schneider, D.P., and Shectman, S.A. 1981a, *Astrophys. J.*, **244**, 259

Young, P., Schneider, D.P., and Shectman, S.A. 1981b, *Astrophys. J.*, **245**, 1035

Zhang, E.H., Robinson, E.L., and Nather, R.E. 1986, *Astrophys. J.*, **305**, 740

Zuckermann, M.-C. 1961, *Ann.d' Astr.*, **24**, 431

PART II

CLASSICAL NOVAE AND RECURRENT NOVAE

Written by

Antonio Bianchini

Hilmar Duerbeck

Michael Friedjung

Margherita Hack

Pierluigi Selvelli

N95
27072
UNCLAS

N95- 27072

6

CLASSICAL NOVAE AND RECURRENT NOVAE - GENERAL PROPERTIES

M. Hack, P.L. Selvelli, and H. Duerbeck

I. INTRODUCTION.

In this chapter, we will describe the observable characteristics of classical novae and recurrent novae obtained by different techniques (photometry, spectroscopy, and imaging) in all the available spectral ranges. We will consider the three stages in the life of a nova: quiescence (pre- and post-outburst), outburst, final decline and nebular phase.

Since the majority of these objects has been observed only—or much more extensively—in the optical range, we will start discussing these observations. In section 6.II.A we will describe the photometric properties during the quiescent phase. Quiescent novae, as a rule, present light variability; in several cases, this variability can be interpreted as characteristic of an eclipsing binary, with period shorter than 1 day (only known exception—GK Per with a period of about 2 days). These curves are, however, variable from one period to the other; in several cases rapid (minutes), irregular, small amplitude (few tenths of magnitude) variations are observed. We will describe some characteristic examples since each object is a special case. Many of them—in quiescence—are indistinguishable from dwarf novae and nova-like stars and, in fact, are classified as such and have been extensively discussed in Chapters 2 and 3. In 6.II.B we describe the photometric properties during outburst, the classification according the rate of decline (magnitudes per day), which permits us to define very fast, fast, intermediate, slow, and very slow novae and the correlation between luminosity and speed class.

In 6.III.A, we report the scanty data on the spectra of the few known prenovae and those on the spectra of old novae and those of dwarf novae and nova-like, which, however, are almost undistinguishable (see also Chapters 2 and 3).

In 6.III.B, 6.III.C, and 6.III.D, we describe the typical spectra appearing from the beginning of the outburst—just before maximum—up to the nebular phase and the correlation between spectral type at maximum, expansional velocity, and speed class of the nova.

In 6.IV.A, we report the existing infrared observations, which permit us to explain some of the characteristics of the outburst light curve, and give evidence of the formation of a dust shell in slow and intermediate novae (with the important exception of the very slow nova HR Del 1967) and its absence or quasi-absence in fast novae. In 6.V and 6.VI, the ultraviolet and X-ray observations are described. The far ultraviolet spectra of several old novae have been provided by the International Ultraviolet Explorer (IUE). Some of them can be fitted by the Rayleigh-Jeans tail of hot black bodies, indicating the presence of a hot companion. In other cases, the spectrum is flat, as due to free-free transitions of ionized gas, or can be fitted by a power law. In 6.VI, the X-ray observations of novae—mainly from the two satellites EINSTEIN and EXOSAT—are reported. Several novae are soft X-ray sources, indicating the presence of regions in the nova system having temperatures as high as 10^6 K or more. Correlations between X-ray flux and speed class seem to exist.

PRECEDING PAGE BLANK NOT FILMED

In 6.VII, observations of the final decline and of the envelopes appearing several months after outburst are reported. Spectra, images and radioastronomical observations are the tools for studying the envelopes.

II. PHOTOMETRIC PROPERTIES

About 170 novae have been observed up to now, and 55 of them have been observed at minimum light. The known recurrent novae are five only. A catalogue of all known novae has been published by Duerbeck (1987c) giving designations, positions and finding charts, magnitude at minimum and maximum, light-curve type according the classification scheme by Duerbeck (1981) and references.

II.A. NORMAL (OR QUIESCENT) PHASE

A study of all the existent observations has been made by Robinson (1975). He observes that the ejected material gives little insight into the nature of the underlying star. It is important to compare pre-eruption and post-eruption stages, in order to see if differences exist between the two stages, and therefore what has been the effect of the explosion on the stellar structure or on the stellar atmosphere, or on the system as a whole, in case of binary systems.

Old novae (that we consider as the "normal state," or non-eruptive state of novae) are variable, and several of them present non-periodical short time-scale variability (Mumford, 1966a, 1966b). Flickering with an amplitude of 0.1 - 0.2 mag over a time scale of minutes is a common feature among old novae, as well as among dwarf novae and nova-like stars. Walker (1957) noted it first in DQ Her. However DQ Her is peculiar in having also periodic variations, with P = 71 sec, amplitude of 0.04 mag (Walker, 1956), which are rarely observed in other novae (Robinson and Nather, 1977). Another nova, V 533 Her, has presented the same phenomenon (Patterson, 1979a) with a period of 63 sec. These oscillations disappeared in 1982 (Robinson and Nather, 1983). The properties of the oscillations were very similar in both stars, although the outburst properties were very different. In 1981, Warner has observed another nova, RR Pic, presenting very short-lived, rapid oscillations with periods of 20 - 40 seconds. Rapid coherent oscillations (where for coherent oscillations we mean that they stay in phase for time long compared to the period, that is for several hours, Robinson, 1976) with periods of few seconds are also observed sometimes in dwarf novae and nova-like. They are not common and seem to appear with about the same frequency in all classes of cataclysmic variables (old novae, dwarf novae, and nova-like).

Most prenovae, as well as pastnovae, are low-amplitude (few tenths of magnitude) variables. Robinson (1975) found that the preeruption and posteruption magnitudes are the same for all the 18 stars for which both magnitudes are known. The only exception was BT Mon, for which m (prenova) was recorded as fainter than 16.8 because it was not observable on about 150 Harvard patrol plates taken between 1898 and 1939 (with limiting magnitude of about 17), while m (post-nova) is equal to 15.8. However, a recent photometric study of BT Mon (Robinson et al., 1982) shows that there is no compelling reason to believe that the preeruption magnitude was different from its posteruption magnitude. In fact, BT Mon is an eclipsing binary with period 8h.01 or 1.0014d/3. Now the eclipse lasts about 1.6 h and is 2.7 mag deep. The Harvard plates were exposed at about the same hour every night, so BT Mon was always in eclipse at the epoch of these observations.

Also the light curves for pre and posteruption, when known, are the same, with one exception, V446 Her. In the latter case, the pre-eruption light curve has an amplitude of almost 4 mag, while the post-eruption light curve presents variation of no more than 0.4 mag. Hence in general, a nova eruption has very little effect either on the erupting star or on the binary system as a whole.

Of over 12 stars for which pre-eruption light curves were well known, 6 present probable or

conclusive changes in the light curves as early as 1 to 15 years before the eruption.

Several old novae have been extensively observed and their photometric characteristics present many similarities with dwarf novae and nova-like stars. In the following sections, we will give some examples of the photometric behavior of some old novae.

The binary character of the old nova V603 Aql (1918) was discovered by Kraft (1964), who derived an orbital period of 3h19m.5 from Palomar coudé spectrograms. There is evidence of 3 minima observed with IUE(*) by Rahe et al. (1980) and by Slovak (1980) at the McDonald Observatory during more than two complete cycles. These measurements, as well as those made by Slovak, show a period compatible with that derived by the RV curve determined by Kraft. The shape of the light curve varies from cycle to cycle. The observed minimum was interpreted by the authors as a partial eclipse of the accretion disk around the compact companion by the late component or as an occultation of a hot spot by the disk itself. The absence of any secondary minimum may probably be due to the fact that the major fraction of light is emitted by the disk, in case an eclipse really occurs. However, the low value of v sin i obtained by Kraft (38 km/sec) and a detailed study of the nova ejecta made by Weaver (1974) suggest a rather low inclination and hence make improbable the occurence of an eclipse.

Actually, Cook (1981) brings arguments against the possibility of eclipse, because the values of the orbital period and RV amplitude of the primary (sdBe according to Kraft) suggest $i<20°$. In this case, the light variations could be explained by orientation effects, due to asymmetric distribution of light in the disk. Such alternative explanation of the light variation was already suggested by Rahe et al. They suggest that the surface of the secondary facing the primary is heated by a strong, optically unseen (UV and/or X) flux, hence, the light variations are explained by varying orientation of the secondary. Ultraviolet observations of V603 Aql made with OAO 2 (Gallagher and Holm, 1974) and by Lambert et al. with IUE (1980) confirm the presence of a large ultraviolet flux.

Because the IUE FES observations give a rather coarse temporal resolution, Slovak (1981) has made a series of high-speed photometric observations of V 603 Aql. He does not find any evidence for eclipse or other periodic features, therefore making it difficult to accept the alternative explanation of the varying aspect of the surface of the secondary facing the primary and heated by its UV flux. It is suggested that transient phenomena lasting for a few cycles can occur in the accretion disk and produce the irregular minima. Random flickering of large amplitude (0.20 - 0.30 mag) has been observed by all the quoted authors. Search for coherent oscillations was made by Slovak with negative result.

Extensive photometric and polarimetric observations were made by Haefner and Metz (1985). Contrarily to what Slovak found, they observe a light curve characterized by the appearance of a hump structure repeating with a period of 3h 18m.9. Moreover, linear and circular polarization are modulated with a period of 2h48m.0. We will come back in chapter 7 on the model proposed to explain these observations (see also Chapter 4.III.F.2). Let us say here that they are able to explain the observations by assuming an intermediate polar (i.e., a magnetic degenerate component whose rotation is not synchronized to the orbit) combined with a temporarily existing eccentric disk.

A field of 10^6 gauss in indicated by the measured circular polarization.

The very fast nova V 1500 Cyg presented a periodic 3.3-hour variation within one week of the outburst, a characteristic never observed before for any other nova from broad-band photometry, (Tempesti, 1975) and from the H

(*) The Fine Error Sensor (FES) aboard the satellite gives a measure of the stellar flux related to the stellar visual magnitude (Holm and Crabb, 1979, NASA–IUE Letter 7).

Alpha profile (Campbell, 1975, 1976). The period was changing, decreasing by about 2% in 10 months in 1976 (Patterson 1978 and references therein). In 1977, the period increased again by 1%. Figure 6.1 by Kleine and Kohoutek (1979) gives the period length vs. time. Photometry through October 1978 establishes that the period has stabilized at 0.139617 +/- 0.000002 days in early 1977 (Patterson, 1979b). The amplitude of the light variation is changing from cycle to cycle, being around 0.64 - 0.72 mag. Later observations extending to 1981 confirm the stabilization of the period (Kruszewski et al., 1983). These authors suggest that the change $\Delta P/P = -3.5 \times 10^{-5}$ occurred between 1977 and 1978 can be caused by the slow outflow of matter through the outer Lagrangian point of the binary system (little more than 10^{-6} solar masses should be sufficient to explain the period change).

A series of observations made by Pavlenko (1983) covering 19 cycles of 3.3 h between July 25 and October 5, 1981 indicate night to night changes in the form of the light curve, its amplitude (from a minimum of 0.4 to a maximum of 1 mag), and the mean brightness. It seems therefore very probable that the 3.3 h period represents the orbital period of the system. In addition, as in the majority of cataclysmic variables, small amplitude rapid flickering (time scale 1 to 10 minutes) is present in the light curve of this old nova.

It is interesting to compare the light curves of the two old novae V1500 Cyg 1975 and CP Pup 1942. They share the common property of having been very fast novae with exceptionally large outburst amplitude—larger than 19 mag and more than 17 mag respectively—more typical of a supernova rather than a nova; however, the radial velocities observed during the eruption indicate in both cases that they are classical novae (V exp.<2200 km/s for V 1500 Cyg, and < 1400 km/s for CP Pup, while SNs have radial velocities larger than 10,000 km/s). High speed photometric observations of CP Pup were made by Warner (1985b) (Figure 6.2). The photometric period is 0.06614 d (or 1.58736 hours) and differs from the spectroscopic one, as shown in Figure 6.2. The light curve is variable in shape, amplitude and mean brightness and low amplitude flickering with time scale of 1 - 10 min in superposed. CP Pup is the classical nova with the shortest known period and the only one below the gap in the periods shown by the CVs between 2.1 and 2.82 hours.

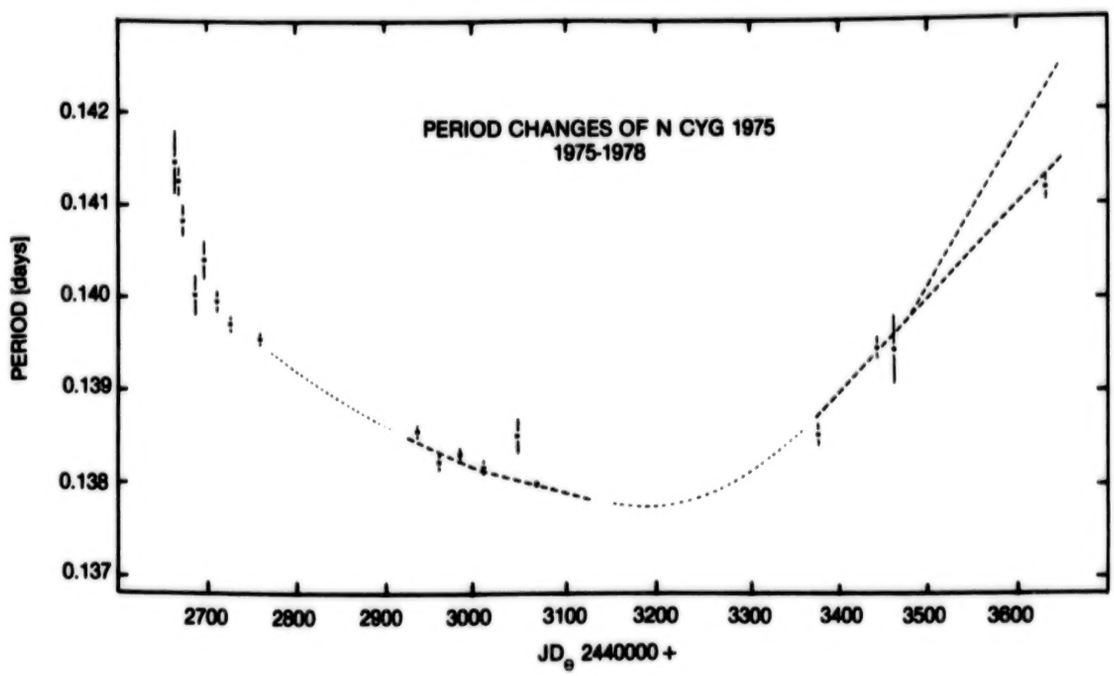


Figure 6-1. Photometric period variations for V 1500 Cyg (1975). (from Kleine and Kohoutek, 1979)

V1668 Cyg 1978 has been observed near its maximum light in the attempt to detect short-period variations like those observed in old novae (Giuricin et al., 1979). The time resolution was 0.01 sec. Rapid flickering (down to 0.2 sec was observed. No stable periodic brightness variations were detected, although there is strong evidence of the existence of short-lived oscillations during the nights of September 14 and 15, 1978. Precisely during the first night (J.D.2443766.5), oscillations with periodicity of about 0.067 sec and 0.01 sec, lasting 100 - 200 sec were seen. During the second night (J.D.2443767.4), a different phenomenon was observed: the presence of oscillations with a period of 5.26 sec monotonically decreasing in amplitude and lasting 500 sec (Figure 6.3a, 3b).

Photoelectric observations with a lower time resolution (10 sec) were made by Campolonghi et al. (1980) during several nights in September and October 1978. Superposed on the decline following the outburst, they found a periodic variation of brightness with a period of 10.54 hours and amplitude of 0.15 mag. This behavior is very similar to that shown by V

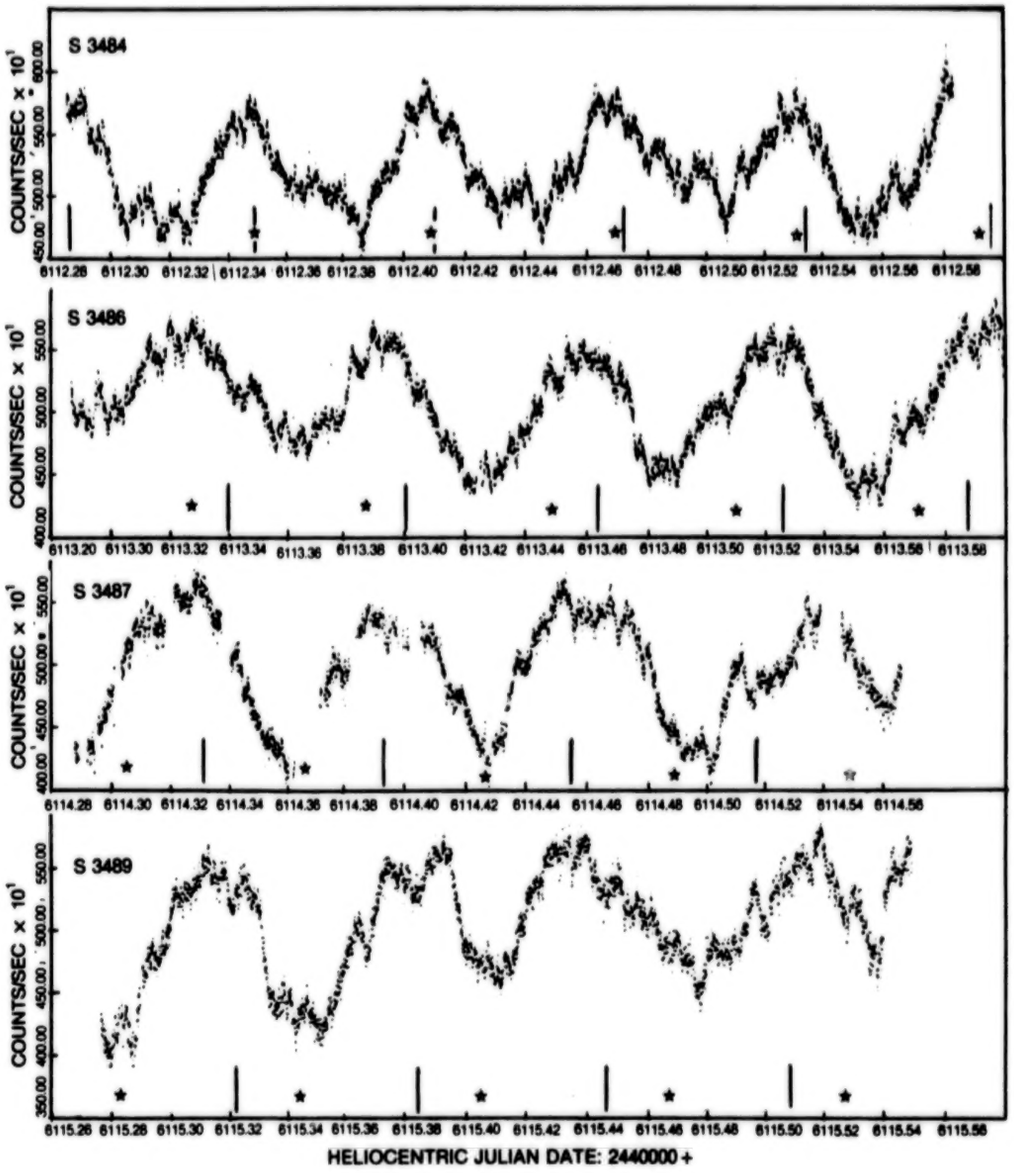


Figure 6-2. Light curves of CP Pup: Vertical arrows indicate predicted times of maxima according to the photometric ephemeris. Stars indicate times of maxima according to the spectroscopic period. (from Warner, 1985b)

1500 Cyg 1975. The authors suggest that this behavior is probably common to all novae and is not due to any eclipse in the system but rather to pulsation of the envelope produced by periodic perturbation of it caused by the binary system orbiting inside it. The light curve of the almost pole-on old nova system of V603 Aql 1918 could be explained by this mechanism.

The slow nova HR Del 1967 was also found to present a short period light variability with P = 0.1775 d and amplitude 0.16 mag in 1977 and 0.10 mag in 1979 (Kohoutek and Pauls, 1980). The photometric period seemed to be identical with the spectroscopic one according to Hutchings (1979a). However the scatter of the photometric data is large and the spectroscopic radial velocities were obtained from different cycles with a gap of almost one year. More recent data by Bruch (1982) give a spectroscopic period (which represents the orbital motion of the binary) P = 0.2141674. Kohoutek and Pauls also observed that the U, B, V, colors suggest a tendency for the system to be redder at maximum light, although the presence of the nebular emission lines can severely affect the colors. From these data, it seems more probable that the light curve features are due to the presence of an accretion disk of nonuniform brightness rather than to eclipse (see also Chapter 8).

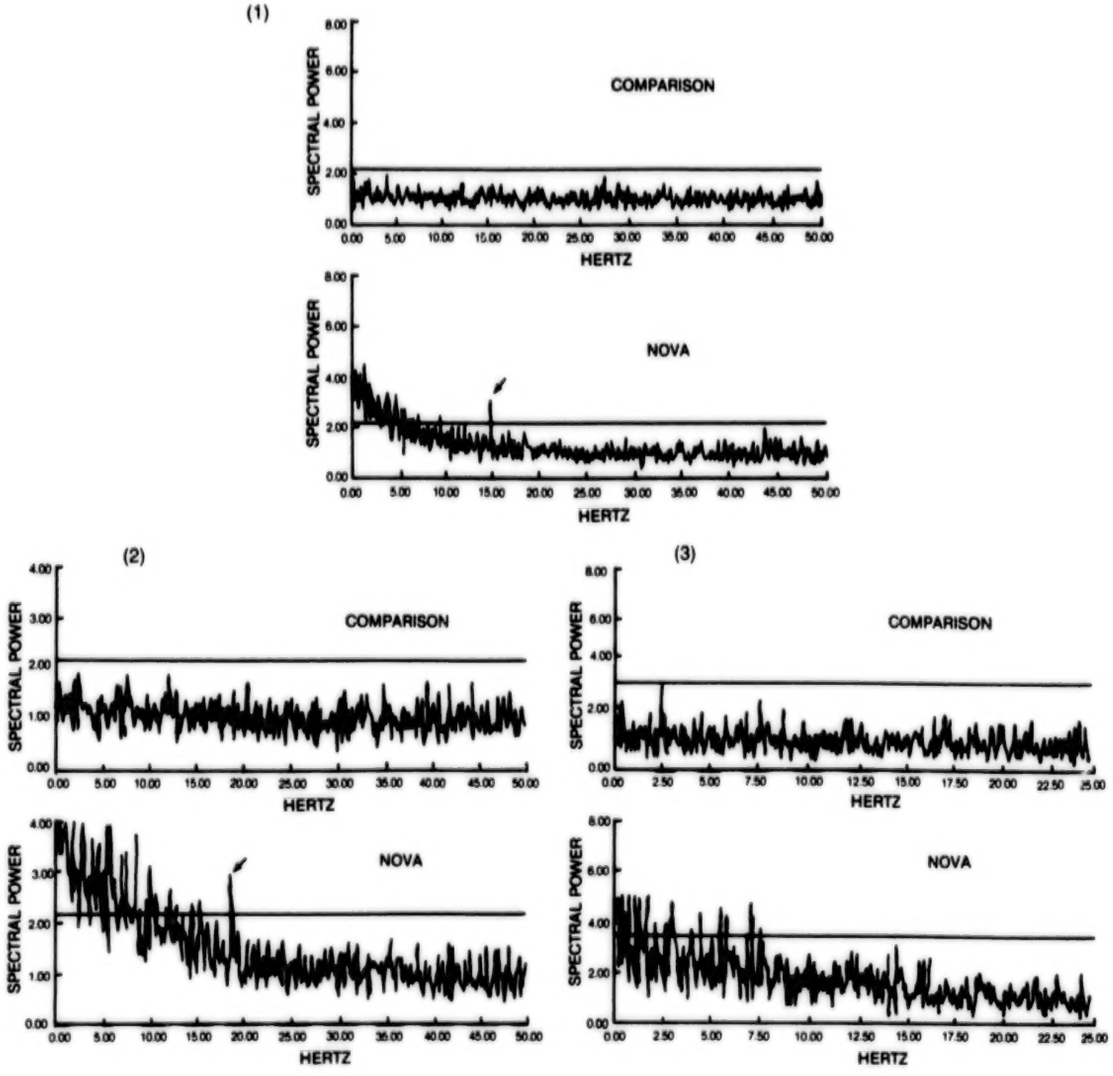


Figure 6-3a. Rapid photometry of V 1668 Cyg (1978). Observations of Sep. 14, 1978: Simultaneous power spectra of the nova and the comparison star. The peak at 15 Hz is evident in the upper graph (1) started at U.T. = JD 2443766.45555; time interval 154 s. The same peak is disappeared in the power spectra obtained with 50 Hz (graph 2) and 25 Hz (graph 3) upper frequency limits, started 2648 seconds later for the same time interval of 154 s.

DQ Her 1934 has been extensively observed since the epoch of the outburst. We will discuss it in larger detail in the chapter devoted to single objects. However, it is interesting to briefly discuss it here for comparison with the photometric behavior of the other old novae. DQ Her shows a light curve indicating clearly the presence of eclipse of a hot companion. The phase interval $0 < \phi < 0.06$ is repeating with slight variation from cycle to cycle, while the phase interval $0.06 < \phi < 0.3$ shows strong deviation from one cycle to the other. Less strong but still remarkable variations from cycle to cycle are observed at phases included between 0.3 and 0.9. The light curve is very similar to those of typical dwarf novae (see Chapters 2.II.B.1 and 3.IV.B.1). Dmitrienko and Cherepashchuk (1980) discuss this curve. They con-

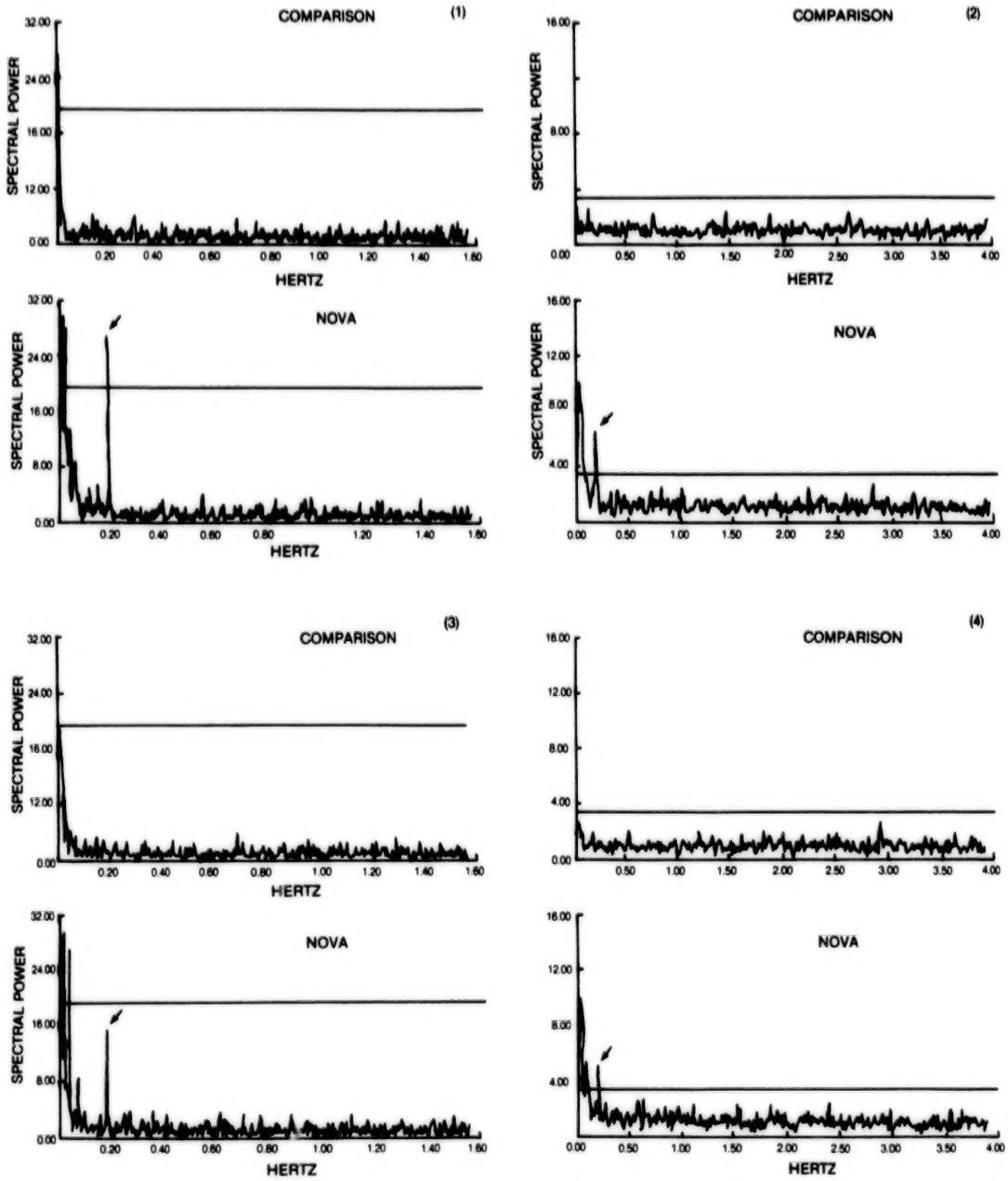


Figure 6-3b. Observations of Sep. 15, 1978. Same as a) The sequence of power spectra shows evidence of a transient peak at 0.19 Hz whose amplitude decreases with time: starting times: 1)JD 2443767.37265, time interval 655 s;2) 2443767.37325, time interval 655 s;3) 2443767.38794, time interval 655 s;4) 2443767.38888, time interval 573s. (from Giuricin et al. 1979)

clude that the hot companion is a white dwarf of abnormally high luminosity (20-200 $L_\odot$) and temperature of about 1.0-1.7 x 10^5 K, practically unchanged for some 20 years. Such prolongated persistence of this anomalous brightness and temperature may imply continuous accretion of material from the accretion disk. Unlike other old novae, DQ Her presents the coherent oscillations with a period of 71.066 sec and a mean amplitude of 0.04 mag. One explanation that has been discussed in Chapter 4.III.F.2 is that the white dwarf in DQ Her is magnetized and that the gas accreting into the white dwarf funnels down the magnetic field lines, creating bright regions at the poles. The 71-sec periodicity is thought to be produced by rotation of the white dwarf with a period of 71 sec or possibly of 142 sec. (see Patterson, 1980). The other nova showing a similar behavior, according to observations made in 1978 and 1980, was V533 Her 1963, which had a periodicity of 63.6 sec, (Patterson, 1979a, and Middleditch and Nelson, 1980) very similar to that presented by DQ Her and was therefore explained by the same mechanism. However, observations by Robinson and Nather made in 1982 (1983) indicate that the 63-sec periodicity has disappeared. Hence, it cannot be related to rotation of a magnetic white dwarf. A similar behavior was shown by WZ Sge—an object whose belonging to the class of recurrent novae or of dwarf novae is a matter of discussion. Although the mechanism explaining the periodicities in WZ Sge is not known with certainty, the most probable explanation is pulsation of the white dwarf (Robinson et al., 1978 and Middleditch and Nelson, 1979). Hence, it seems probable that V533 Her and WZ Sge obey to the same mechanism, different from that active in DQ Her. We will discuss other evidences in favor or against the presence of a magnetic field in Chapter 7.

The old nova GK Per 1901 is exceptional among old novae for several reasons:

a) The orbital period derived by radial velocity measurements (Kraft, 1964; Bianchini et al., 1981) is about 1.9 days, much longer than those of the other old novae. These authors derived an eccentricity of 0.4, which was also exceptional. However, a more recent analysis by Crampton et al. (1983) reveals a period of 1.99679 d with a circular orbit.

b) Almost all old novae have an optical spectrum dominated by the light of the hot primary (white dwarf or accretion disk); GK Per, on the contrary, shows the presence of a K2IV component (Kraft, 1964; Gallagher and Oinas, 1974).

c) GK Per shows strong fluctuations in luminosity together with spectral variations.

d) GK Per is a transient hard X-ray source (King et al., 1979).

e) GK Per is a nonthermal radiosource (Reynolds and Chevalier, 1984).

All these characteristics will be discussed extensively in Chapter 8. Sabbadin and Bianchini (1983) have collected all the existing photometric observations of this old nova since the 1901 outburst (February 22, V=0.2 mag.). The light curve from February 1901 to 1904 is the typical light curve of a fast nova. During the period March through June 1901, a series of semiperiodic oscillations are superposed over the secular decrease of brightness. The historical preoutburst minimum of 15 mag was reached again in 1916. The observations at minimum show a gradual passage from continuous, irregular fluctuations (from 1916 to 1947) to the present epoch, when the old nova is generally quiescent, and at intervals of several hundreds of days, endures outbursts of 2-2.5 mag that we will call minor outbursts, for distinguishing them from the 1901 typical nova outburst. The minor outbursts became evident in July 1948 for the first time.

Details of the behavior of GK Per during these quasi-periodical outbursts are given by Bianchini and Sabbadin (1982), Bianchini et al. (1982, 1986) and by Szkody et al. (1985). The outburst that occurred in February through April 1981 was particularly large, with an

amplitude of 3 mag (Bianchini et al., 1982). Spectra obtained at different moments of the outburst vary and will be discussed in the relative Section 6.III.

High-speed optical photometry of GK Per made during the minor outburst occurred in 1983 (Mazeh et al., 1985b) shows the presence of a small amplitude (4%) periodic modulation of 360 +/- 7 sec on September 12, while on August 11 and 18, a 400-sec modulation was observed, together with a long-term (0.8 hours) variation. Similar periodic modulations were observed also in the X-ray range (E >2 keV) with EXOSAT with a periodicity of 351 sec during the same outburst (Watson et al., 1984).

Another well-studied old nova is RR Pic 1925. The prenova was observed on several occasions since 1889, and it always was at constant brightness of 12.75 visual magnitude. Its present magnitude, 60 years after outburst, is 12.3 and is still becoming fainter.

Van Houten (1966), Mumford (1971) and Vogt (1975) have made photometric observations and found a light curve with a broad irregular maximum repeating with a period of 0.1450255 d, and interpreted this behavior as due to orbital motion. The binary nature of RR Pic was confirmed by spectroscopic observations of Wyckoff and Wehinger (1977). Further photometric observations were made by Marino and Walker (1982), Haefner and Metz (1982), and Kubiak (1984). High-speed photometry on 23 nights from December 1972 to December 1984 has been made by Warner (1986a). These data show that in the 1970s there was a strong orbital modulation of brightness, which has been replaced in the 1980s by an irregular, shallow eclipse superimposed on a flickering background. The disappearance of the orbital modulation coincided with decline in mean brightness of the system. The figure 6.4, taken from Warner, indicates that the curves in the 1970s have a double-humped shape with one large broad maximum and a second lower one, a principal minimum (No. 1) at the end of the principal maximum, at phase near 0.43 P, and a second minimum (No. 2) at phase near 0.74 P. In the 1980s, the first minimum has become very little, whereas the second minimum is now the dominant recurrent feature. The flickering on time scales of 5-10 min is stronger in the 1980s than in the 1970s.

Classical novae are often observed to be brighter than their prenova magnitude for several tens of years after outburst, sometimes for more than 100 years. Hence, to know the true state of "old nova," it should be desirable to observe novae that erupted centuries ago. Unfortunately, very few accurate positions of old novae erupted before Nova Oph 1848 exist. However, two very old novae have been firmly identified recently: they are WY Sge 1783 and CK Vul 1670. Nova CK Vul was discovered by Père Dom Anthelme, monk in Dijon, on June 20, 1670, and a month later, by Hevelius on July 25 in Poland. By collecting all the existing records, Shara et al. (1985) have reconstructed the light curve of this object, which reached two maxima of visual magnitude 3 in June 1670 and of magnitude 2.6 in April 1671.

To present two maxima is an unusual behavior, which has been observed in some very slow novae, as , for instance, in HR Del. Now at the position of CK Vul they have found a central star of magnitude R=20.7 surrounded by a nebulosity with a morphology suggestive of equatorial ejection and several bright subcondensations very similar to those observed in more recent and well-studied old novae. We will come back to CK Vul in section 6.III, devoted to the spectra of old novae, and in Section 6.VII, on nova shells. No photometric measurements of this star have yet been made.

WY Sge 1783 was discovered by the French astronomer D'Agelet when it was of magnitude 5.4 +/- 0.4. On the basis of the position, the brightness, rapidly and irregularly fluctuating between 18.6 and 19.5 photographic magnitude, the blue color, and the absence of any measurable proper motion (which, if measurable would indicate that the star is nearby and the observed fifth magnitude at maximum would not be consistent with the brightness expected from a nova explosion), Weaver

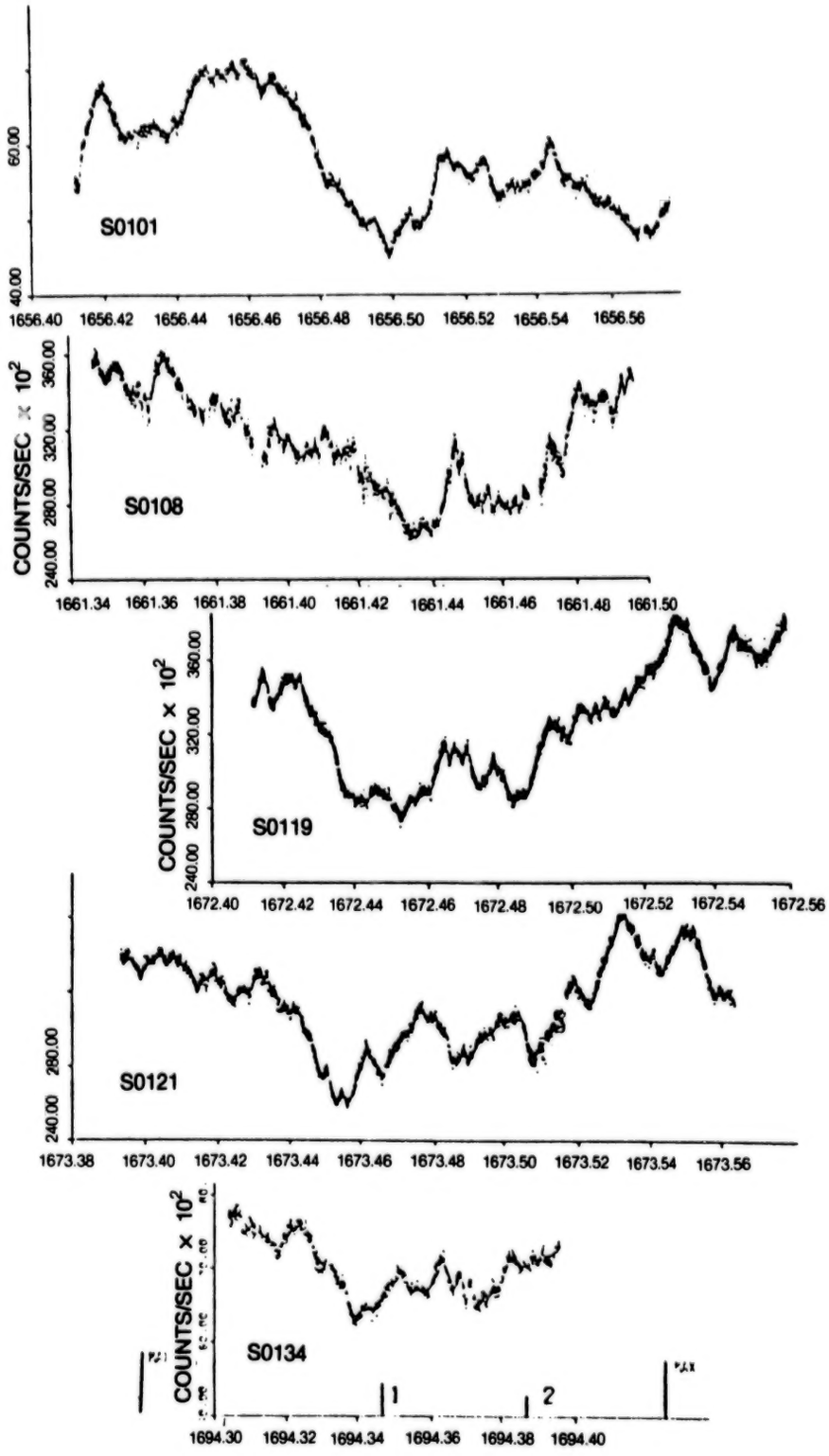


Figure 6-4. Light curves of RR Pic: a) Dec. 1972-Jan. 1973 aligned in orbital phase (Abscissa JD+2444000). Positions of the broad maximum and two minima calculated from Vogt's (1975) ephemeris are indicated.b) same as a), period Dec. 1973-Nov. 1975.c) same as a), period Feb. 1980-Dec. 1981.d) same as a), period Dec. 1981-Dec. 1984. e) Decline portion of the outburst light curve. (from Warner, 1986a)

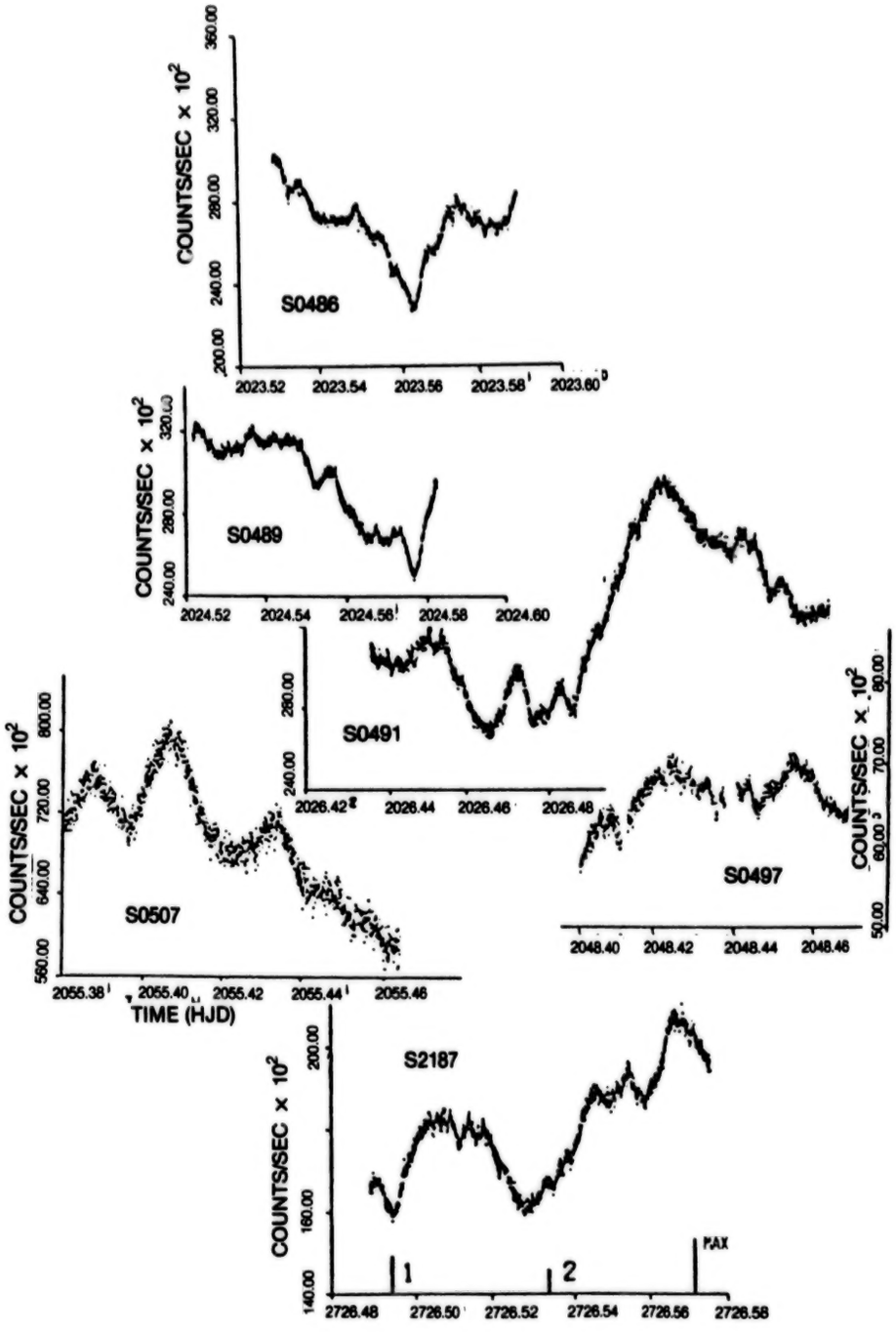

COUNTS/SEC × 10²
S0486
2023.52
2023.54
2023.56
2023.58
2023.60
S0489
2024.52
2024.54
2024.56
2024.58
2024.60
S0491
2026.42
2026.44
2026.46
2026.48
S0507
2055.38
2055.40
2055.42
2055.44
2055.46
TIME (HJD)
S0497
2048.40
2048.42
2048.44
2048.46
S2187
1
2
MAX
2726.48
2726.50
2726.52
2726.54
2726.56
2726.58

Figure 6.4b

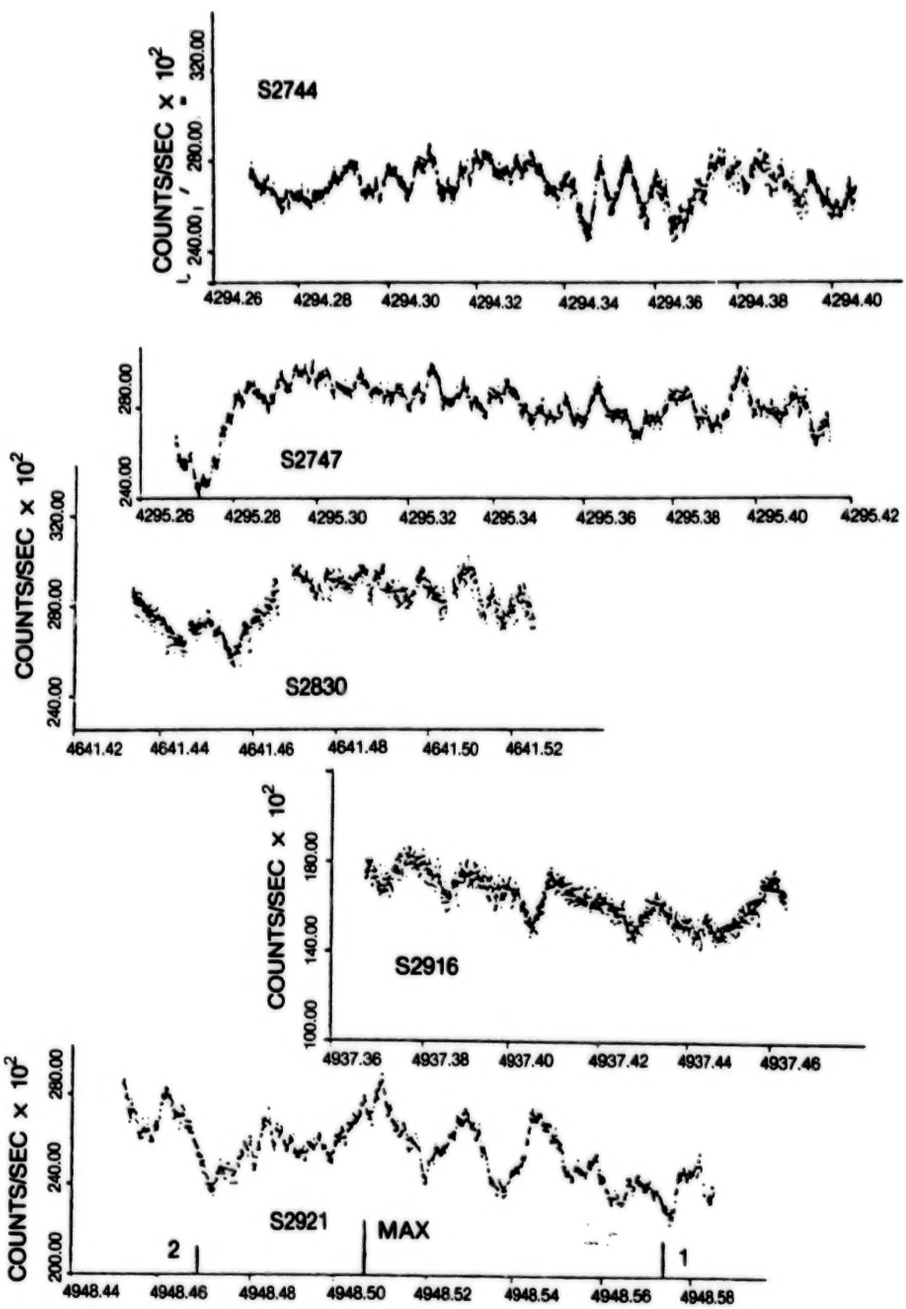

COUNTS/SEC x 10²
320.00
280.00
240.00
S2744
4294.26
4294.28
4294.30
4294.32
4294.34
4294.36
4294.38
4294.40
280.00
240.00
S2747
4295.26
4295.28
4295.30
4295.32
4295.34
4295.36
4295.38
4295.40
4295.42
COUNTS/SEC x 10²
320.00
280.00
240.00
S2830
4641.42
4641.44
4641.46
4641.48
4641.50
4641.52
COUNTS/SEC x 10²
180.00
140.00
100.00
S2916
4937.36
4937.38
4937.40
4937.42
4937.44
4937.46
COUNTS/SEC x 10²
280.00
240.00
200.00
S2921
MAX
2
1
4948.44
4948.46
4948.48
4948.50
4948.52
4948.54
4948.56
4948.58

Figure 6.4c

(1951) identified the old nova with a faint blue star less than 6 arc sec from the position given by D'Agelet. Warner (1971) has observed this star photometrically with time resolution of 5 sec. It presents rapid flickering with time scales of 5-15 min and amplitude of 0.1-0.2 mag. This kind of rapid variation, which is ubiquitous in nova remnants, is a strong indication that the Weaver identification with the Nova Sge 1783 is correct. Shara and Moffat (1983) and Shara et al. (1984) have observed it again both photometrically and spectroscopically. The spectrum shows the characteristics expected for old novae. We will come back to this in Section 6.III.A.

Photoelectric photometry has permitted to derive a light curve with a deep minimum (1.5-2 mag) lasting about 30 min, rapid egresses (5 min) and slightly slower ingresses and a period of 3h41m14s. On one night (June 17, 1982), it was 1.6 mag brighter than normal, and the

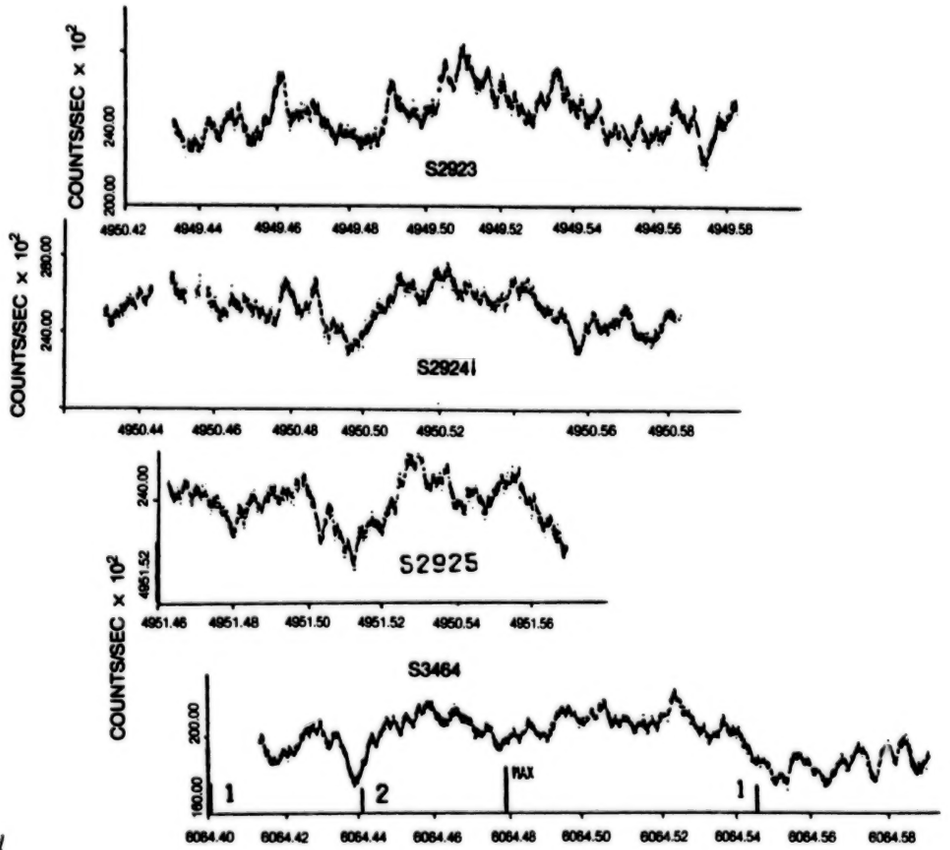


Figure 6.4d

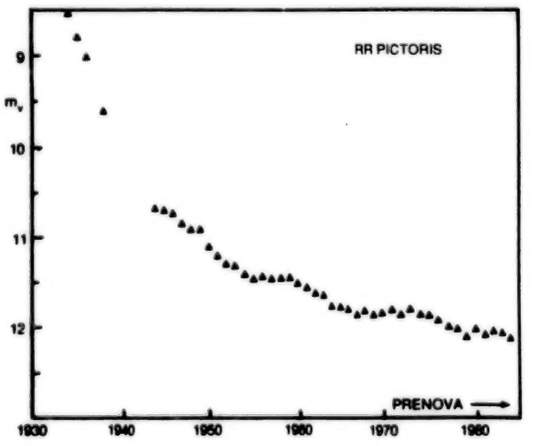


Figure 6.4e

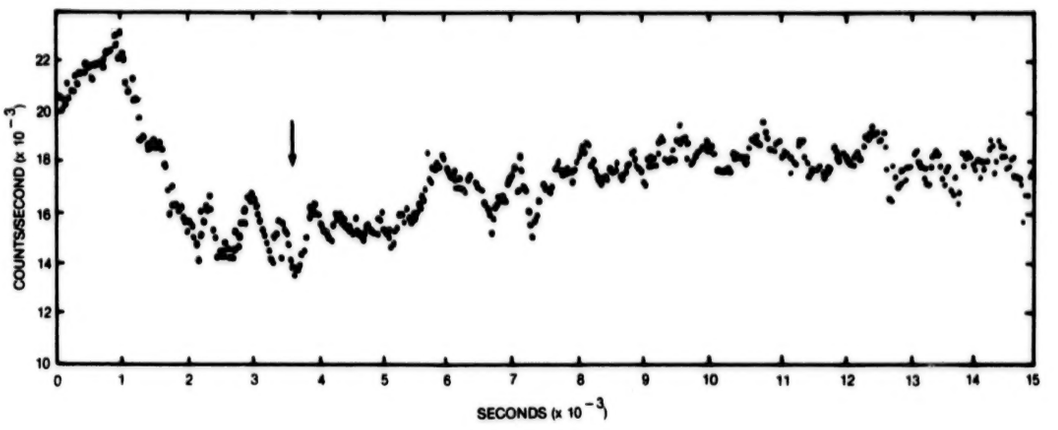


Figure 6-5. High speed photometry of the old nova WY Sge observed on June 16-17, 1982. An expected eclipse centered at the position indicated by the arrow is not seen. The flickering is about half its usual amplitude, while the nova is about four times brighter than usual.
(from Shara et al., 1984)

Table 6.1a (*)
Optical oscillations in cataclysmic variables

Object	Type	Orbital period(hr)	Coherent periods(s)	Quasi periods (s)	Additional references
SS Cyg	DN	6.60	7.5-9.7	32-36	
RU Peg	DN	8.99	11.6-11.8	~51	
TT Ari	NL	3.2		~12, ~32, ~40, 50-1100	Jensen *et al.* (1983) Mardirossian et al.(1980) Sztajno (1979)
EM Cyg	DN	6.98	14.6-21.2		Steining et al. (1982)
Z Cam	DN(Z)	6.96	16.0-18.8		
V436 Cen	DN(SU)	1.50	19.5-20.1		
VW Hyi	DN(SU)	1.78	20-32	23,88,253,413	Robinson and Warner (1984) Warner (unpublished)
HT Cas	DN	1.77	20.2-20.4	~100	
RR Pic	N	3.48		20-40	Schoembs and Stolz (1981)
KT Per	DN	-	22.0-29.2	82-147	
SY Cnc	DN	-	23.3-33.0		
AH Her	DN	5.93	24.0-38.8	~100	
CN Ori	DN	3.91	24.3-25.0		Schoembs (1982)
CDP -48° 1577	NL	4.5:	24.6-29.1		Warner et al. (1984)
PS74	DN(SU)	2.0:	27-29	248	Warner (unpublished)
Z Cha	DN(SU)	1.79	24.8, 27.7		Warner (unpublished)
WZ Sge	DN	1.36	27.87, 28.97		
UX UMa	NL	4.72	28.5-30.0		
V3885 Sgr	NL	4.94	29.32		Warner (unpublished)
AE Aqr	NL	9.88	33.08	~36	
RX And	DN	5.08		36	
V2051 Oph	DN(SU)	1.50	40		O'Donoghue and Warner (unpublished)
V533 Her	N	-	63.63		Robinson and Nather (1979)
DQ Her	N	4.65	71.07		
U Gem	DN	4.25		73-146	
YZ Cnc	DN (su)	2.21		75-95	
X Leo	DN	-	~160		
GK Per	N, DN	1.99d		360-390	Watson *et al.* (1984)
RW Sex	NL	5.93		620,1280	
V442 Cen	DN	11:		925	Marino and Walker (1984)

(*) from Warner (1986b)

ORIGINAL PAGE IS
OF POOR QUALITY

Table 6.1b

X-ray oscillations in cataclysmic variables

Object	Type	Orbital period(hrs)	Coherent period (s)	Quasi periods (s)	References
SS Cyg	DN	6.60		9-12	Cordova *et al.* (1984)
TT An	NL	3.2		9,12,32	Jensen *et al.* (1983)
VW Hyi	DN (SU)	1.78	14.06		Heise *et al.* (1984)
U Gem	DN	4.25		20-30	Cordove *et al.* (1984)
AE Aqr	NL	9.88	33		Patterson (1980)
YZ Cnc	DN (SU)	2.21		227	Cordova and Mason (1984)
GK Per	N, DN	1.99 d	351		Watson *et al.* (1984)

expected eclipse minimum was not seen (Figure 6.5). One and three nights later, it was back at its quiescent brightness. This behavior is very similar to that observed in dwarf novae. Warner (1986b) gives a list of the cataclysmic variables for which rapid coherent or quasi-periodic oscillation have been observed (Table 6.1). He defines quasi-periodic oscillations as those in which the coherence length may be as short as a few cycles, while coherent oscillations last at least for hundreds of cycles. Of the over 30 cataclysmic variables exhibiting, or which have exhibited, one or both of these kinds of oscillations, only four are classical novae: DQ Her and V533 Her (coherent oscillations) and RR Pic and GK Per (quasi-periodic oscillations). The latter has presented a coherent oscillation with period of 351 sec in the X-ray range.

II.B. ACTIVE PHASE

Many cataclysmic variables exhibit unpredicted and abrupt changes in their luminosity. We have two aspects of such changes: their rise and their fall. On completely unpredictable objects like classical novae, we cannot anticipate the epoch of outburst, and therefore we have very scanty data on the characteristics of their rise to maximum, and these are always due to chance. Thus we can classify the light curves of novae only on the basis of their fall. Dwarf novae, on the other hand, are classified on grounds of repetitive features in the outburst light curves.

Both classical and recurrent novae are therefore classified according to the rapidity of their decline from maximum in Na: fast novae, t(3) < 100 days, rate of decline > 0.2 mag/d; Nb: slow novae, t(3) > 150 days, rate of decline < 0.02 mag/d; Nc: very slow novae: they stay at maximum for several years; t(3) is the time employed for a brightness decrease of 3 magnitudes.

A more detailed classification is given by Duerbeck (1981) and reported in his catalogue of novae (1987c).

The number of novae in class Na is much larger than that on Nb in our Galaxy, while in M 31 there is evidence of the reverse (Arp, 1956). Arp excludes the possibility of any observational bias. This result suggests that this property of novae is related to an overall characteristic of the galaxy, like, for instance, the chemical composition. Unfortunately, the large majority of the observational data for extragalactic novae consist of light curves; no spectra are available to check this hypothesis.

Maximum brightness and rate of decline are correlated, in the sense that the larger is the absolute brightness of a nova at maximum, the faster is its decline (Arp, 1956, from observations of novae in M 31; McLaughlin, 1945, from observations of novae in our Galaxy). The empirical relation found by these authors has been recalibrated by Pfau (1976), and more recently by Shara (1981) who used 47 well-observed novae: 11 in our Galaxy, 26 in M 31, 7 in the LMC, and 3 in the SMC. The importance to know such relation is evident, since it permits us to derive the luminosity at maximum from relatively easily observable characteristics like the light curve, and because the determination of the energy emitted and mass ejected depend on our knowledge of the distances.

The recent calibrations give the following relations:

- M phot = -10.5 + 1.82 log t(2) (Schmidt-Kaler, 1965, based on galactic novae only)

- M(B) = -11.5 + 1.8 log t(2) (Pfau, 1976)

- M phot = -11.3 + 2.4 log t(3) (de Vaucouleur, 1978)

- M(B) = -11.3 + 2.4 log t(3) (Shara, 1981)

A still more recent relation has been found by Cohen (1985) who used a large number of observations of nova shells and used the expansion parallax method(*):

Mv(max) = -10.70 (+/- 0.30) + 2.41 (+/- 0.25) log t(2).

Payne-Gaposchkin (1957), by an examination of the light curves observed at that time (about 40 cases), is able to describe a certain number of typical light curves, which are correlated with the decline rate. Fast and very fast novae generally present a smooth early decline, and a generally smooth transition, while slow novae present oscillations during the early decline (and often more than one maximum) and they oscillate and dip during the transition phase (Figure 6.6). The oscillations in magnitude have periodicities of the order of few days and amplitudes < 1 mag. Insight into the nature of the dip has been given by infrared observations, which show that a maximum IR luminosity is reached just when the visual dip occurs. This can be explained by the formation

(*) The observed expansion velocity and the time elapsed from the outburst permit us to derive the true dimension, in kms of the nebula. By comparing it with the observed angular size, the distance is derived.

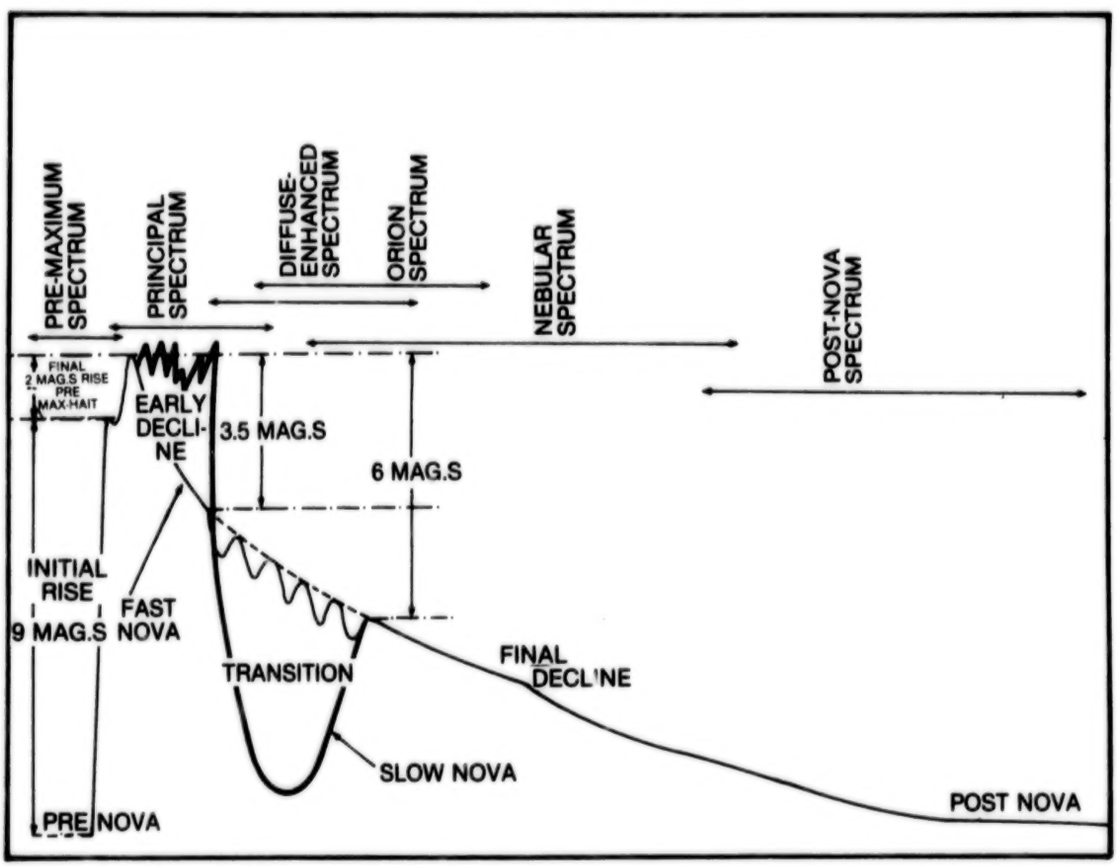


Figure 6-6. Schematic light curve for fast and slow novae. Three typical behaviors are observed during the transition stage: oscillations can be present or absent both in fast and slow novae. The deep minimum is typically found in slow novae. The position on the light curve when the various spectra are present, is indicated.
(adapted from Payne-Gaposchkin, 1957)

of a dust shell or by the heating of a preexistent envelope of dust.

The more detailed classification of nova light curves given by Duerbeck (1981) is based on about 100 galactic novae.

Table 6.2 from Duerbeck gives his classification scheme, and Table 6.3 applies this scheme to the galactic novae with sufficiently known light curves. Figures 6.7-6.11 from Duerbeck give some examples of light and color curves of the various classes.

Of the novae with well observed light curves, about 3/4 (73 objects) are type Na-fast-novae- (t_3 < 100 d), and about 1/4 (27 objects) are type Nb-slow novae- (t_3 > 100 d).

The distribution among the light curve types (Duerbeck, 1981) is as follows:

A. 39%, among them 2% Ar, 29% A, 8% Ao.

B. 29%, among them 10% Ba and 11% Bd, the rest is unclear.

C. 18%, among them 6% Ca, 11% Cb, the rest is unclear.

D. 12%, among them 1% DR.

E. 2%, this low percentage is also due to the fact that some type E novae are counted among the symbiotic stars.

Note that 18% of all novae are novae with noticeable dust formation (type C).

Duerbeck gives the following relations:

$M_V = -12.25 + 2.66 \log t_3$ (valid only for light curves of type A)

$M_V = -6.4 +/- 0.5$ (light curves of type B, C, D,)

Table 6-2(*)
A Classification Scheme for Nova Light Curves

type	description	examples	classification of Woronzow-Weljaminow (1953)
A	smooth, fast decline without major disturbances	CP Pup, V1500 Cyg	Rs - rapid, smooth star (CP Pup)
Ao	smooth, fast decline without major disturbances, oscillations in the transition stage	GK Per, V603 Aql	Ro - rapid, oscillating star (GK Per)
Ar	smooth, fast decline, recurrent nova	T CrB, RS Oph	Rd - fast star with a drop in the light curve (T CrB)
B	decline with minor or major irregularities		
Ba	decline with standstills or other minor irregular fluctuations during decline	V533 Her, LV Vul	Sss - slow, smooth star (V841 Oph)
Bb	decline with major fluctuations (e.g. double or multiple maxima)	DN Gem, NQ Vul	
C	extended maximum, deep minimum in transition phase, with		Sd - slow star with a drop in the light curve (DQ Her)
Ca	small variation of visual brightness at maximum (< 2^m)	T Aur, DQ Her	
Cb	stronger brightness decline during maximum	FH Ser	
D	slow evolution, extended premaximum, delayed maximum, often with several brightness peaks	HR Del, RR Pic	So - slow, fluctuating star (RR Pic)
DR	recurrent nova with slow evolution and delayed maximum	T Pyx	
E	extremely slow nova with irregular light curve	V99 Sgr, V711 Sco	Sss - extremely slow star (RT Ser)

(*) from Duerbeck (1981)

Although it is impossible to say at the first recorded outburst if a nova will be recurrent or not, a few distinct points of difference in the light curve were identified by McLaughlin (1960). The recurrent novae return to minimum in less than one year, while classical novae remain usually brighter than their preoutburst magnitude for several years. Of the four recurrent novae classified by Duerbeck, three belong to his class A, i.e., show a smooth, fast decline, while only one—T Pyx—belongs to his class D, i.e., shows a slow evolution and a delayed maximum, like the very slow classical novae HR Del or RR Pic. The number of known recurrent novae is too small for this 3 to 1 ratio of fast to slow novae to have statistical significance.

Duerbeck derives the absolute magnitudes for 31 classical galactic novae (Table 6.4) by means of different methods: 1) nebular expansion parallaxes; 2) differential galactic rotation (the stellar radial velocity, based on the hypothesis that it is mainly due to the motion in a circular galactic orbit, and the galactic longitude, permit us to derive the distance; 3) the interstellar line strengths; and 4) the interstellar reddening. Figure 6.12 gives the relation M(V) at maximum vs log t(3). The existence of two well-separated groups is evident: the higher luminosity group includes only fast novae and the other slow and very slow novae. We will come back to this result in Chapter 7. Duerbeck shows that Group I can be interpreted by a quasi-instantaneous mass-loss at a lumi-

Table 6-3(*)
Classification of Light Curves of Galactic Novae

type A:	X Cir	(6.6)	Q Cyg	(22)	V476 Cyg	(16)	V1500 Cyg	(3.6)
	V446 Her	(16)	CP Lac	(10)	CP Pup	(8)	V630 Sgr	(6)
	V909 Sgr	(7.6)	V1059 Sgr	(<24)	T Sco	(21)	V697 Sco	(<15)
	V723 Sco	(17)						
type Ao:	V528 Aql	(35)	V603 Aql	(8)	DK Lac*	(32)	GK Per	(13)
	LU Vul	(21)						
type Ar:	T CrB	(6.8)	RS Oph	(18)	U Sco	(5.2)		
poss.A:	V368 Aql	(30)	V604 Aql	(24)	QZ Aur	(<34)	DM Gem	(22)
	HR Lyr	(80)	GI Mon	(37)	FL Sgr	(32)	KP Sco	(42)
type Ba:	EL Aql	(25)	V500 Aql	(42)	OY Ara	(83)	IV Cep	(37)
	V465 Cyg	(104)	V1668 Cyg	(23)	DM Gem*	(22)	V533 Her	(44)
	DK Lac*	(32)	V400 Per	(43)	V441 Sgr	(106)	V787 Sgr	(45)
	RU UMi	(140)	LV Vul	(37)				
type Bb:	DN Gem	(37)	DI Lac	(43)	V840 Oph*	(36)	V849 Oph	(175)
	V1016 Sgr	(176)	V1017 Sgr	(160)	FS Sct	(86)	V373 Sct	(85)
	NQ Vul	(65)						
poss.B:	V1229 Aql	(38)	V1301 Aql	(78)	RS Car	(?)	RR Cha	(?)
	IL Nor	(108)	V841 Oph	(112)	HS Pup	(65)	FM Sgr	(30)
	V363 Sgr	(80)	V1275 Sgr	(30)	V4021 Sgr	(100)	V368 Sct	(31)
type Ca:	T Aur	(100)	V450 Cyg	(100)	DQ Her	(94)	HZ Pup*	(70)
	V732 Sgr	(64)	V720 Sco	(17)				
type Cb:	V606 Aql	(34)	V726 Sgr*	(90)	V707 Sco	(49)	V719 Sco	(24)
	EU Sct	(42)	FH Ser	(62)	Ser 1978	(50)	XX Tau	(42)
	CQ Vel	(53)						
type D:	DO Aql	(900?)	EL Aql	(?)	V356 Aql	(~170)	HR Del	(230)
	RR Pic	(150)	X Ser	(?)	CN Vel	(800)		
type Dr:	T Pyx	(88)						
type E:	n Car	(?)	AR Cir	(415)	V794 Oph	(?)	HS Sgr	(?)
	V999 Sgr	(?)	V711 Sco	(?)	RR Ser	(?)	RR Tel	(?)

Note: the t_3 time is given in parentheses. Novae with uncertain light curve classification are marked with an asterisk.

(*) from Duerbeck (1981)

nosity far above the Eddington limit and Group II by continued radiation at the Eddington limit from a bloated white dwarf.

This finding is based only on galactic novae, because too few data are available for the Magellanic Clouds. Actually, the large extent of the Magellanic Clouds requires very long programs of surveys with "time resolution" sufficient to record the maxima and the time of decline. The surveys made by Arp (1956) and by Rosino (1964, 1973) would be suitable for a comparison with the galactic relation. However, novae of Duerbeck Group II can be classified only by a small fraction of their light curves, which is not sufficient for an accurate determination of t(3). Moreover, no very bright novae have been found in M 31, and the maxi-

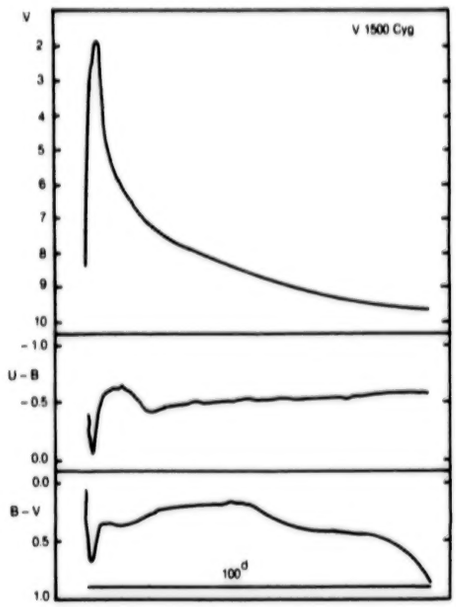


Figure 6-7. Light and color curves of V1500 Cyg (type A, Duerbeck classification)
(from Duerbeck, 1981)

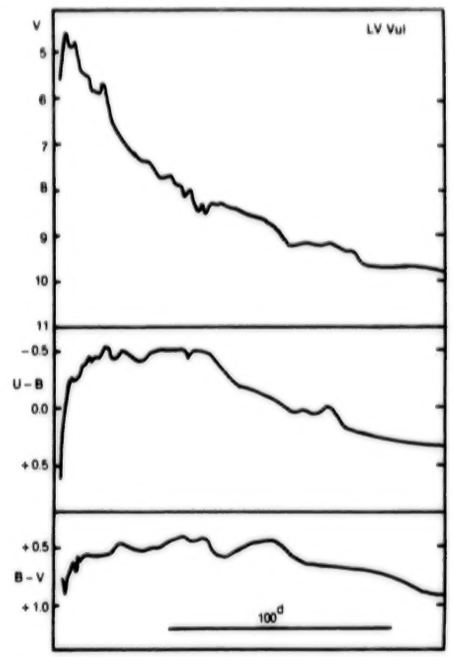


Figure 6-8. Light and color curves of LV Vul (type B)
(from Duerbeck, 1981)

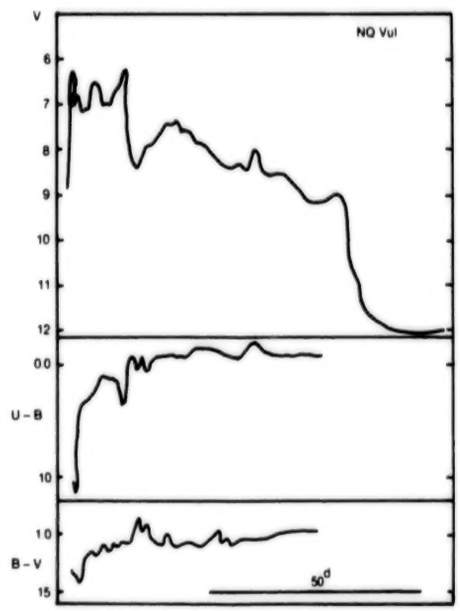


Figure 6-9. Light and color curves of NQ Vul (type Bb)
(from Duerbeck, 1981)

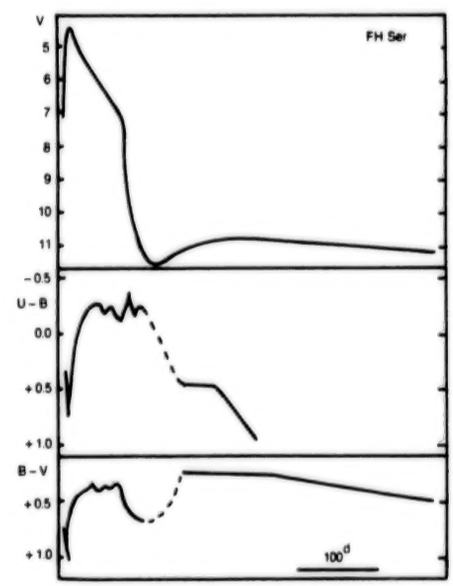


Figure 6-10. Light and color curves of FH Ser (type Cb)
(from Duerbeck, 1981)

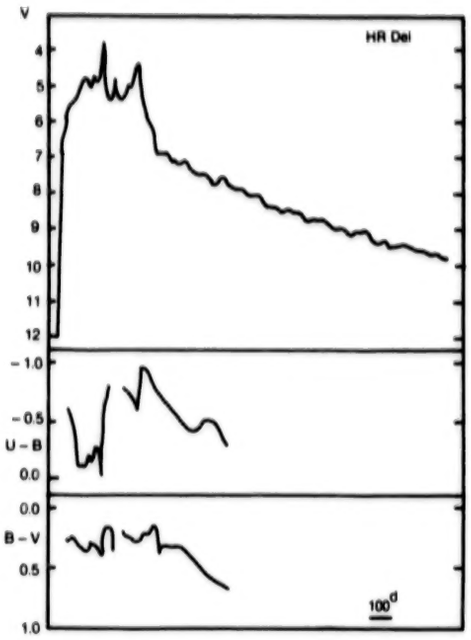


Figure 6-11. Light and color curves of HR Del (type D) (from Duerbeck, 1981)

mum brightness of novae of Duerbeck Group I is generally fainter than for galactic novae of Group I. A recent work by Van den Bergh and Pritchet (1986) discusses the observations of 73 novae in M 31 and the possibility of using novae as extragalactic distance indicators, if novae in all galaxies should turn out to have the same luminosity function at maximum light.

From a study of the nucleus of M 31 in the light of H Alpha, Ciardullo et al. (1983) have detected four novae and observed that the decay time of H Alpha emission was much longer than the decay time in the continuum. Hence, H Alpha emission of novae might represent a standard candle for extragalactic measurements. To be applicable, all these methods need disponibility of a very large number of observations of novae in nearby galaxies.

Van den Berg and Youngh (1987) have collected all the published UBV photometric data

Table 6-4(*)
Distances, Absorption Values, and Absolute Magnitudes of 35 Novae

object	a	b	m_{max}	m_{min}	M_{max}	M_{min}	type	t_3	d(pc)	A_v	source
V356 Aql	037°.42	-04°.94	7.0p	17.7p	-6.5	+4.0p	D	212	1700	2.04	N
V528 Aql	036.68	-05.90	7.2p	18.1p	-7.6	+3.3p	Ao:	35	2400 - 600	2.6-0.6	N
V603 Aql	033.46	+00.84	-1.1p	11.6v	-9.6	+3.5v	Ao	8	330	0.5	UV
V1229 Aql	040.54	-05.44	6.5p	19p	-6.8	+5.7p	Ba?	38?	1730	1.6+0.4	D,N
T Aur	177.14	-01.71	4.1p	14.9v	-6.7	+4.4v	Ca	100	600	1.25+0.25	D,N
IV Cep	099.61	-01.64	7.5v	17.5v	-5.8	+4.3v	Ba	37	2050 + 150	1.65+0.1	D,N
T CrB	042.38	+48.17	2.0v	9.9v	-8.5	-0.6v	Ar	6.8	1250 + 600	0.08	N
V450 Cyg	079.12	-06.46	7.0p	|17p	-5.9	|+4.1p	Ca	100	1800 + 400	1.4+0.1	D
V476 Cyg	087.37	+12.42	2.0v	17.1v	-9.5	+5.2v	A	16	1650 + 50	0.85+0.4	D,N
V1500 Cyg	089.82	-00.07	1.85v	|21B	-10.1	|+10.1B	A	3.6	1350	1.25+0.25	App.
V1668 Cyg	090.84	+06.76	6.1v	20B	-6.2	+7.9B	Ba	23	2300 + 500	1.10	D,N
HR Del	063.43	-13.97	3.8v	11.9v	-6.5	+1.6v	D	230	880	0.56	D,N
DN Gem	184.01	+14.70	3.6p	15.6v	-5.3	+7.0v	Bb	37	450 + 70	0.27+0.1	D,N
DQ Her	073.16	+26.44	1.3v	14.7v	-5.9	+7.5v	Ca	94	260	0.16	N
V446 Her	045.41	+04.71	3.0p	18.8p	-8.5	+6.8p	A	16	790 + 170	1.7+0.5	D,N
V533 Her	069.19	+24.27	3.0p	15.6v	-6.7	+6.2v	Ba	44	680 + 250	0.25	N
CP Lac	102.14	-00.84	2.1p	15.6p	-9.6	+3.9p	A	10	1000 + 100	1.5+0.1	D,N
DK Lac	105.23	-05.35	5.0p	15.5p	-7.2	+3.3p	B?Ao?	32	1500 + 200	1.2+0.2	D,N
BT Mon	213.86	-02.63	4.5:p	16p	-6.3:	+5.2p	?	42	1000 + 200	0.63	D
RS Oph	019.80	+10.38	5.0v	11.4v	-8.7	-2.3v	Ar	18	1800:	2.4:	App.
V849 Oph	039.23	+13.49	7.3:p	|15p	-5.9:	|+1.8p	Bb	175	3100	0.72	N
GK Per	150.95	-10.11	0.2v	13.0v	-9.2	+3.7v	Ao	13	5250.7 +	0.15	D,N
RR Pic	272.36	-25.67	1.2p	12.0v	-6.9	+3.9v	D	150	400	0.04	N
CP Pup	252.92	-00.84	0.5p	14.3p	-11.5	+2.3p	A	8	1500	0.8+0.2	D,N
T Pyx	257.20	+09.70	7.0p	14.9v	-7.4?	+1.4v	Dr	88	3000 + 2000	0.35+0.05	N
V630 Sgr	357.77	-06.06	4.0p	14.4p	-9.3	+1.1p	A	9	2000	1.6+0.8	D,N
V1275 Sgr	355.07	-06.17	7.5p	|13p	-6.2	?	B??	30?	3200 300	1.0+0.5	D,N
T Sco	352.67	+19.47	6.8v	|12v	-9.2	?	A	21	12000	0.6	
U Sco	357.67	+21.88	8.5p	19.2p	-8.7	+2.0p?	Ar	5.2	17000?	0.95?	N
EU Sco	029.72	-02.97	8.0p	17.0p	-7.0:	+0.9:p	Cb	42	5060 + 1700	2.6+0.6	N
V368 Sel	026.67	-02.63	6.9v	18.6v	-5.8	+5.9p	B?	31	1750 + 350	1.6	N
FH Ser	033.91	+05.78	4.5v	15.1v	-6.9	+3.7v	Cb	62	650	2.3	N
Ser 1978	012.86	+06.04	8.3p	?	-7.0	?	Cb	50	4800	1.2	N
LV Vul	063.30	+00.85	9.5v	16.9B	-6.3	+5.4B	Ba	37	820 + 50	1.2:	D,N
NQ Vul	055.35	+01.28	6.1v	18.3p	-6.6	+4.6p	Bb	65	1200:	2.5+0.6	N

source of the extinction data: d=Deutschman, Davis and Schild (1976), N = Necket (1967)

(*) from Duerbeck (1981)

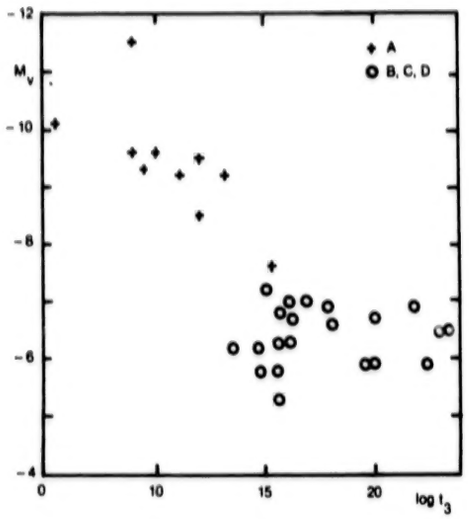


Figure 6-12. Absolute magnitude M_V vs. log t(3) for classical galactic novae.
(from Duerbeck, 1981)

on novae up to November 1, 1986. They have obtained two main results from this study:

1) The intrinsic color of novae two magnitudes below maximum is found to be $(B-V)_0$ = -0.02 +/- 0.04 with an internal dispersion σ (B-V) < 0.12 mag. At maximum $(B-V)_0$ = + 0.23 +/- 0.06. The $(U-B)_0$ colors at maximum, on the contrary, present a large intrinsic scatter.

2) Novae with smooth light curves become redder both in B-V and U-B centered within one day of maximum light. This reddening lasts about 5 days for fast novae to 14 days for slow novae. That novae are reddest at maximum can be understood because at maximum they have maximum photospheric radius (and therefore minimum surface temperature).

III. SPECTROSCOPIC PROPERTIES

III.A. QUIESCENT PHASE.

For understanding the reason of the outburst, it would be extremely important to know the physical state of the star before and after the eruption. Unfortunately, very few data are available, especially for the phase preceeding the outburst. Low-resolution spectra obtained with objective prism in the photographic region from before outburst are available only for V 603 Aql 1918 (Cannon, 1920), V 533 Her 1963 (Stephenson and Herr, 1963) and HR Del 1967 (Stephenson, 1967).

V 603 Aql: all the spectra were underexposed. The best pre-eruption spectrum was obtained on July 1, 1899. The spectrum appears to be nearly continuous, but the Balmer series is detectable in absorption. The energy distribution resembles that of Class B or A, and Class G can be clearly excluded.

V 533 Her: the spectrum was recorded nearly two years before outburst, on June 16, 1961. The image is underexposed, and only a faint continuum is observable, with no detectable spectral lines, either in emission or in absorption. However, since the image is so weak, the only positive indication about the absorption lines is that there can be neither hydrogen lines as strong as those of an A-type star, nor H and K lines of Ca II as strong as in a normal G-type star, nor any of the several absorption features that would be seen in a spectral type later than G. The energy distribution between 4800 and 3300 A is very similar to that of a little reddened O star or early B.

HR Del: two well-exposed spectra were recorded on objective prism plates seven years before outburst, on July 16, 1960. The spectrum is continuous without any definite absorption or emission feature (at dispersion 580 A/mm at H Gamma), and the energy distribution is clearly that of an unreddened O or very early B-type star.

Like photometric observations, also the spectroscopic ones, although limited to these three cases, suggest that pre and post-outburst characteristics remain almost the same. However, for V 603 Aql, no absorption lines are observed—at the dispersion of 18 A/mm—in the postnova spectrum (Greenstein, 1960) while the prenova spectrum, according to Cannon, showed H I absorption lines observable at the much lower dispersion of her spectrograms.

Spectroscopic observations of old novae generally indicate that they present very blue continuous spectra with some weak emission lines. A complete review of data on postnova spectra was given by Greenstein (1960); see Table 6.5 from his paper. In addition to broad H I emissions, He I and He II emissions are observable in several cases, and , when relatively close to the epoch of the explosion, nebular lines are still observable; in all cases the excitation decreases with time after outburst. For instance, in the spectrum of Nova Her 1963 in 1967 when the nova was 1.5 mag above its minimum, the nebular lines of [O III] were strong, while in 1969 they were barely visible; in 1976 He II 4686 was fainter than the H I lines, and there was no trace of the nebular lines.

No definite evidence for the presence of absorption lines has been found in the spectra of past novae. The spectra of all novae at minimum are sensibly alike and do not appear to be correlated with the characteristics of the explosion. The emission line intensity and width are often variable, as indicated, for instance, by the extended series of observations made by Williams (1983). The lines are generally broad with widths of several hundreds of km/s, sometimes more than 1,000 km/s (Williams, 1983).

The spectra of five old novae (two slow and three fast novae) and one quiescent recurrent nova are shown by Wyckoff and Wehinger (1977). They present some differences that one can imagine to be related to their type: the two slow novae have Balmer lines much weaker than the three fast novae; the slow recurrent nova also has weak Balmer emissions and, moreover, does not present the 4640 emission, which is a blend of C III and N III (Figure 6.13). It is not clear if these differences are imputable to different physical conditions (temperature and density), or to a different chemical composition (i.e., a different evolutionary stage) or consequence of different conditions of the thermonuclear runaway, see chapter 7. By adding to these observations the data given by Greenstein (Table 6.5) we observe that generally the spectra of past novae of class Na have hydrogen lines stronger than helium lines, while the reverse is true for past novae of class Nb. The only exception is CP Pup 1942, which was an exceptionally fast nova and one of the brighter ones. This star showed also [O III] lines whose Doppler shift indicated that the original ejection velocities were still present. However, an extended series of spectroscopic observations of past novae, quiescent recurrent novae, dwarf novae and nova-like stars made by Oke and Wade (1982) and by Williams (1983) do not give evidence of systematic differences in the spectra of different classes of novae. The differences between spectra of single objects seem rather due to different physical conditions in the region where the spectrum is produced at the moment of the observations, and not to the characteristics of the outburst.

Panek (1979) has compared the energy distribution of the old nova V 603 Aql with that of one nova-like star and two dwarf novae at both quiescent and active phase. All spectra are similar, except that the old nova shows a very small Balmer discontinuity and stronger emission lines, especially 4686 He II. Panek shows the position of these objects (the old nova V 603 Aql, the dwarf novae VW Hydri, and UZ Ser just after outburst and in quiescence, and the nova-like star V 3885 Sgr) in a two-color diagram u-b, b-v (where u, b, and v were formed by averaging the linear fluxes measured at 3448 and 3636 A (u), 4210 and 4566 A (b), and 4990, 5556, 6055 A (v) and compares them with the position of black bodies at temperatures included between 50,000 K and 10,000 K and of model atmospheres with log g = 8 and effective temperatures between 50,000 K and 8,000 K. The four objects fall either on the black body line or between the black body and the model atmosphere curve. But we cannot generalize these results based on very few objects. A more extended sample of spectra of CV's has been collected by Williams (1983). He studies the spectra of 69 CV's including 13 old novae, (8 fast and 5 slow novae) and 4 quiescent recurrent novae, 29 dwarf novae, and 23 nova-like stars. This study indicates important differences in the spectra of the various old novae both in energy distribution and emission

line strength (Table 6.6 and Figure 6.14 a, b, c, and d), but no correlation with the subclass is apparent. Using his data, we have compared the line intensities of H alpha, H beta, 6678 and 5876 He I and 4640 C III+ N III, and their widths (in km/s) for the different classes of CV's. The line widths in general, (but there are exceptions) are an indication of the inclination of the system: all CV's show a loose correlation between *i* and the line width (Figure 6.15 a, b): the broader the emission lines are the closer to 90° the inclination of the accretion disk is. Warner (1986c) also found a correlation between the equivalent widths of H alpha, H beta, and 4686 He II and the orbital inclination (Figure 6.16). It is interesting to add that by using this correlation, Warner was able to estimate the effect of the orbital inclination on the magnitude of old novae, confirming the expectation given from the spectral characteristics that their main source of brightness at minimum is the disk. In fact, from the best available determinations of $M_{v(max)}$ and from the range $m_{v(max)}$-$m_{v(min)}$, he derives $M_{v(min)}$ and finds the correlation $M_{V(min)}$ vs cos i (Figure 6.17). The frequency distribution of the observed $M_{V(min)}$

Table 6-5

Characteristics of the Spectra of Old Novae

Nova	Spectrum and Other Data	Type
V603 Aql 1918	H>He II (Hu 1938; Mc 1950; and G 1957); He I, λ 4650 A present; Δλ=7A; no absortion lines at 18 A/mm	Na
T Aur 1891	Weak He II>H (Hu 1933, 1937)	Nb
T Crb 1866, 1946	Symbiotic, red companion, spec. binary; dwarf blue object is nova; recurrent U?	RN
Q Cyg 1876	Em. weak (Hu 1936); sharp and weak (G 1957)	Na
V476 Cyg 1920	H=He II (Hu 1936, Mc 1938); H>He II, broad > H (G 1958)	Na
EM Cyg	H>He II, broad (Burbidge); never seen at bright max; U?	—
DM Gem 1903.....	Continuous? (Hu 1933)	Na
DN Gem 1912	H weak (Hu 1933); He II=H (Mc 1933); He II broad > H (G 1958)	Nb
DQ Her 1934	He II>H, broad, Δλ=20 A, double em. lines (G 1956); variable in 4^{hr} period (Kraft); ratio of high-low series members changes at quadratures; eclipsing binary; shell still contributes	Nb
DI Lac 1910.....	Continuous (Hu 1936); broad absorption lines, like white dwarf, emission H>He II, sharp (G 1959)	Na
HR Lyr 1919	Continuous (Hu 1936); weak He II (G 1959)	Na
MacRae + 43 1	H>He I, variable ratio to continuum; Δλ=7 A(G 1953); never seen at bright maximim	—
V841 Oph 1848	Continuous (Hu 1936); He II>>H, He I weak (G 1956); lines sharp	Nb
RS Oph 1898, 1933, 1958	Symbiotic red star; complex em.; atypical; recurrent	RN
GK Per 1901	He II>H, He I, Δλ=16 A (Hu 1937); H>He II, He II = He I; Δλ=17 A (G 1953)	Na
CP Pup 1942	He II>>H, He I weak; [O III] persists in shell and shows original ejection velocities still present (G 1956); velocity structure absent in H and He II	Na
T Pyx 1890, 1902, 1920, 1944	He II>H, [O III] (Hu 1934); He II>>H, sharp (G 1956, 1958)	RN
V Sge	He II>H, *V/R* variable; Δλ=40 A; shortward-displaced core (Elvey and Babcock); never seen at bright maximum; (U?)	—
WZ Sge 1913, 1946	Continuous (Hu 1934); white dwarf absorption lines; Be type, H emission (G 1956)	RN
V1017 Sgr 1901, 1919	Continuous (Hu 1936)	RN

* G = Greenstein; Hu = Humason; Mc = McLaughlin. Dates given are those of observations of spectra. U? = Object may be related to U Gem stars or other nova like stars; Δλ = width of emission at half-intensity.

agrees with the theoretical distribution expected for randomly orientated disks (Figure 6.18).

The Figures 6.14 a, b, and c, give the equivalent widths for H alpha, H beta, 6678 and 5876 He I, 4686 He II and 4640 C III+ N III for all classes of CVs. When several measurements for a same star have been made, we have plotted the average values. The values are generally dependent from the state of the object (quiescent or in outburst for dwarf novae, while several old novae and nova-like stars may present line variability). In order to judge the degree of variability, we have given in the Table 6.6 the mean value and, in parenthesis, the standard deviation s, both for the line intensities and the line widths. We also report the intensity ratios H alpha/6678 He I, H beta/4686 He II, H alpha/H beta, and 4686 He II/5876 He I, in order to ascertain if the spectra of the members of the different classes present some systematic characteristics permitting us to distinguish one class from the other. As shown from the Figures 6.14, no clear systematic difference is evident. The comparison may be biased by the fact that the number of individuals among novae is much lower than among dwarf novae and nova-like. Hence the samples are not comparable. Anyway, we can say that 6678 and 5876 He I are generally stronger in dwarf novae and nova-like than in novae and recurrent novae. The intensities of H alpha and H beta are in large part included in the same interval of values for all classes, although very high values (W > 80 A) are found only among dwarf novae and nova-like stars. The same can be said for 4686 and 4640, although very high values for 4686 (W > 30 A) are found only among the nova-like stars. The 4640 line is

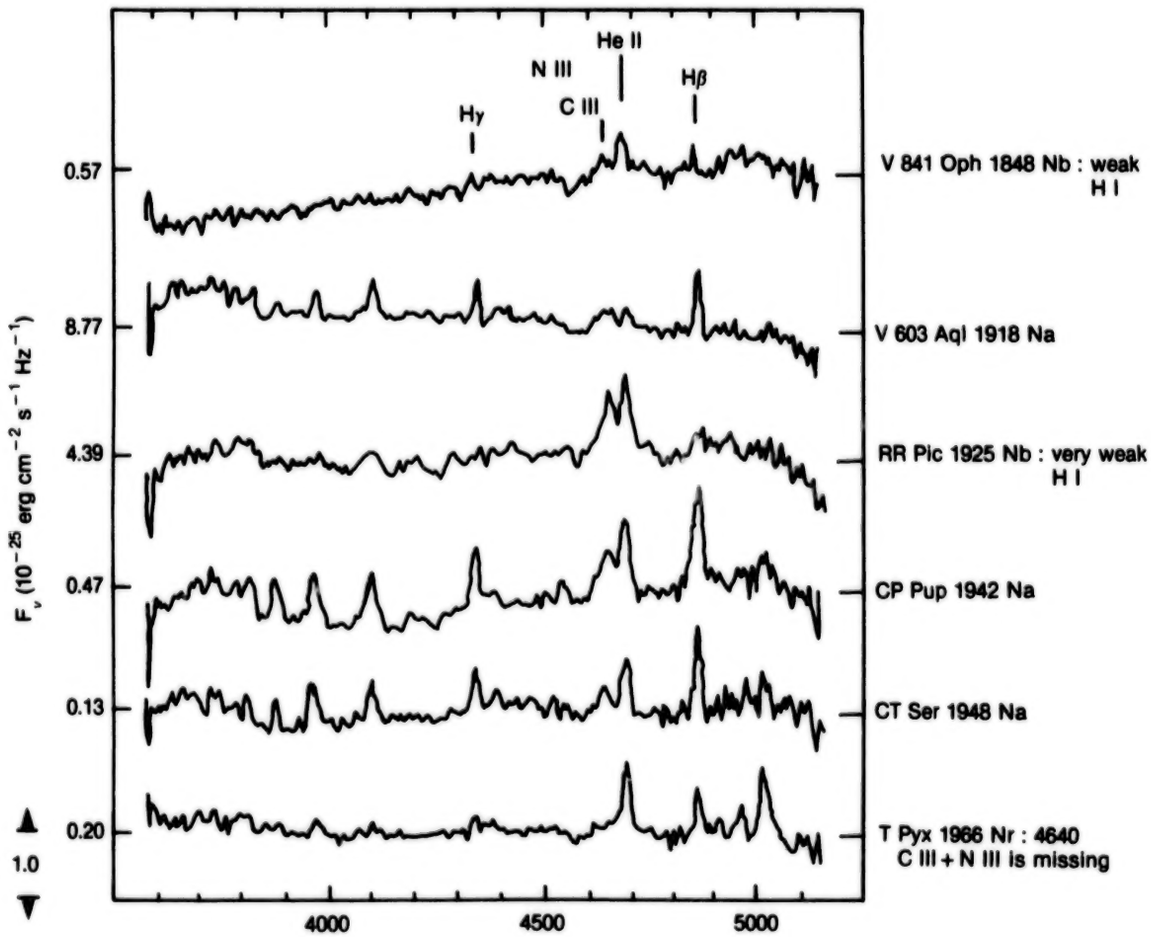


Figure 6-13a. Spectra of old novae (from Wyckoff and Wehinger, 1977)

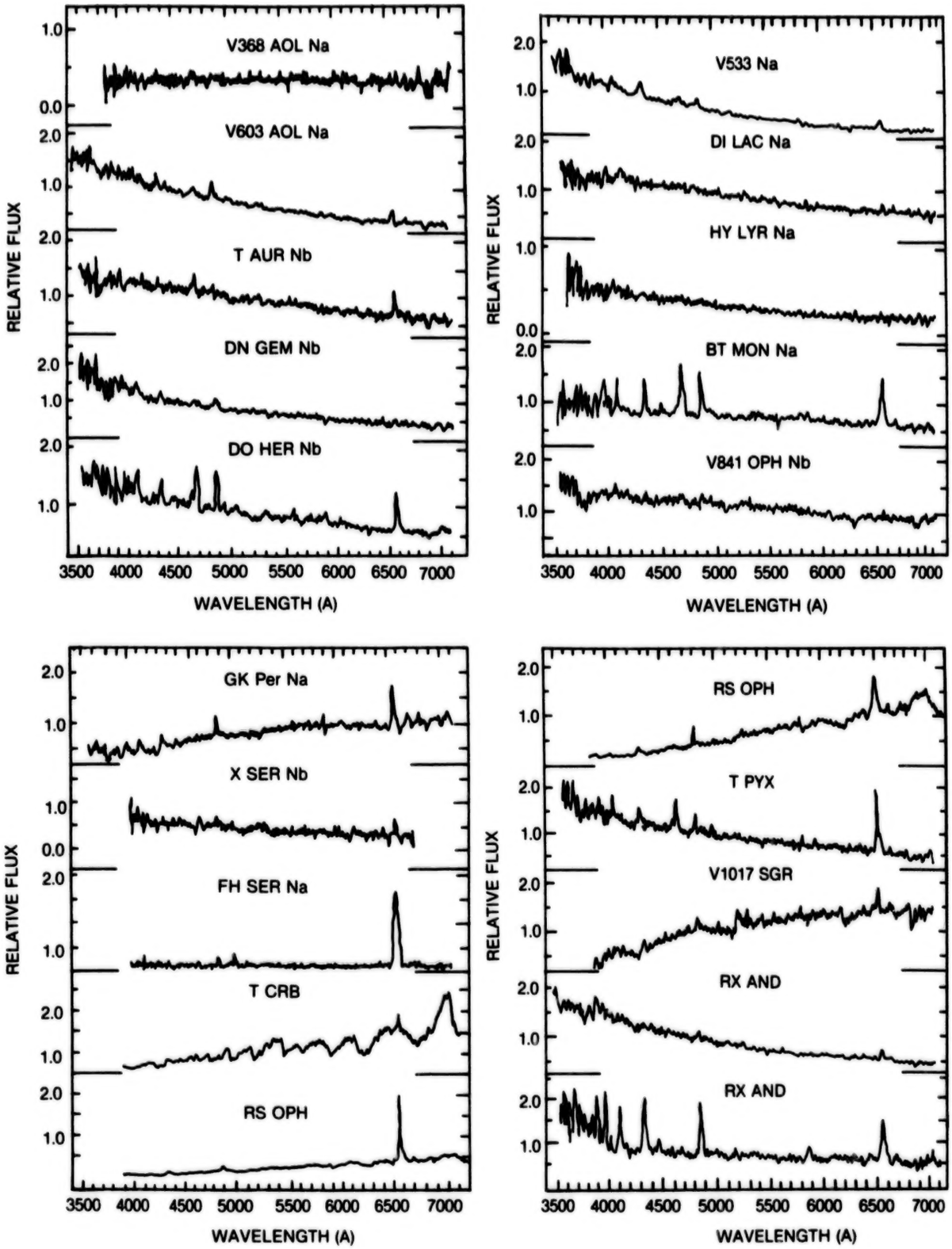


Figure 6-13b. Spectra of old novae (from Williams, 1983)

Table 6-6

Mean Equivalent Widths, Line Widths and Line Ratios for Novae, Recurrent Novae, Dwarf Novae and Nova-Like Stars. (Data from Williams, 1983).

Name	Class		Hα	Hβ	6678	5876	4686	4640	Hα/Hβ	Hα/6678	Hβ/4686	4686/5876 or (4686/6678)
V 603 Aql	N	Wλ(A)	13.3	6.9	2.7	2.4	4.4	3.3	1.9	4.9	1.6	1.8
i = 16		s	3.3	1.1	1.1	1.25	0.7					
		Δλ(Km/s)	210									
		s	87									
T Aur	N	"	24.1	6.7	5.7		10.1		3.6	4.2	0.7	(1.8)
i = 68°			5.4	1.8	-		-					
			467	583	474		1066					
			26	255	-		-					
DN Gem	N	"	9.3	8.4			4.4		1.1		1.9	
i = 30°		-	-			-						
			329	562			619					
			-	-								
DQ Her	N	"	70	23	3.4	4.8	15.3	5.9	3	20	1.5	3.2
i = 89°			40	8.7		1.9	2.4	1.3				
			547	495	366	290	513	425				
			50	31		170	63	47				
V533 Her	N	"	22.2	4.9	4.3				4.5	5		
i = 62°			-	-								
			653	396	600							
			-	-	-							
DI Lac	N	"	3.6		2.0	3.5				1.8		
i = 30°			-			-						
			81			282						
BT Mon	N	Wλ(A)	47	28	5.3	5.6	25	9	1.7	8.9	1.1	4.5
i = 84°		s	7.5	6		1.3	4.5	3				
		Δλ(Km/s)	438	545	312	235	424	495				
		s	158	136		49	32	85				
V 841 Oph	N	Wλ	2.6									
i = 0												
GK Per	N	Wλ	19	10.8	5.2	3.9	2.4		1.8	3.7	4.5	0.6
i = 75°		s	1.3		1.8	0.25						
		Δλ	323	309	344	149						
		s	57		40	110						

Table 6-6 (continued)

Mean Equivalent Widths, Line Widths and Line Ratios for Novae, Recurrent Novae, Dwarf Novae and Nova-Like Stars. (Data from Williams, 1983).

Name	Class		Hα	Hβ	6678	5876	4686	4640	Hα/Hβ	Hα/6678	Hβ/4686	4686/5876 or (4686/6678)
X Ser	N	Wλ	23.4	7.1	6.2		9.3		3.3	3.8	0.76	(1.5)
		Δλ	317	259	70		609					
FH Ser	N	"						9.4	1.5		3	
i = 40°		54.2	37.3			12.5						
		749	378			289						
T CrB	RN	"	5.35	3.5					1.4			
			1.2	0.4								
RS Oph	RN	Wλ	53.2	12.7	3.9	2.1			4.2	13.6		
T Pyx	RN	Wλ	74.6	9.7	5.5	3.4	13.7	3.5	7.7	13.6	0.71	4
		Δλ	687	554								
RX And	DN	Wλ	23.3	17.3	7.1	7.75			1.35	3.3		
i = 65°		s	24.3	27	8.3	8.4						
		Δλ	304	353	283	350						
		s	204	215	191	284						
AR And	DN		56	38.8					1.4			
		"	22	0.4								
			581	540								
			1	228								
UU Aql	DN		60	65.6	4.2	8.0			0.9	14.3		
		"	9.4	21		2.5						
			401	562		272						
			35	153		-						
Z Cam	DN	"	11.3	4.5	0.9				2.5	12.5		
			4.2	0.7								
i = 60°			421	359								
			-	-								
SS Aur	DN	Wλ(A)	109	108	10.2	26.2	13		1.0	10.7	8.3	0.5
i = 32°		s	6.5	13.5	1.3	4.5						
		Δλ(Km/s)	444	639	396	435	767					
		s	41	114	111	113						
FS Aur	DN	"	30.9	48	5.3	5.7	8.2		0.64	5.8	5.8	1.4
		"	4.7	18	-	-	4.4					
			358	737	230	125	907					
			30	235	-		-					

Table 6-6 (continued)

Mean Equivalent Widths, Line Widths and Line Ratios for Novae, Recurrent Novae, Dwarf Novae and Nova-Like Stars. (Data from Williams, 1983).

Name	Class		Ha	Hb	6678	5876	4686	4640	H_α/H_β	H_α/6678	H_β/4686	4686/5876 or (4686/6678)
HT Cas	DN	"	204	107	33	38.6	12.1	16.8	1.9	6.2	8.9	0.3
i = 76°			4	13.6	15	14	-	-				
			831	987	935	1206	1437	1407				
			18	63	354		-	-				
WW Cet	DN	"	32.6	34	2.7	6.0			0.96	12		
i = 40°			6.3	12.2	-	0.7						
			538	761	247	412						
			155	124	-	81						
1E 0643.0	DN	"	47.4	46.9	6.15	15.5	18.6	4.3	1.01	7.7	2.5	1.2
			19.6	30	3.5	6.2	9.0	0.7				
			478	594	351	425	1142	310				
			65	207	179	107	474	26				
SY Cnc	DN		13.2	13.7	9.5	5.1			0.96	1.4		
i = 50°		"	13	-	-							
			327	498	671							
			172	-	-							
YZ Cnc	DN		65.5	54.5	15.9	28.5			1.2	4.4		
			74.5	62.4	10.5	14.2						
		"	449	737	485	612						
			243	360	4	18						
SS Cyg	DN	Wλ(A)	48.9	55.6	6.3	9.0	6.9		0.88	7.8	8.0	0.77
i = 30°		s	12.5	22	1.1	2.3	1.6					
		Δλ(Km/s)	456	592	394	134	995					
		s	151	169	71	61	531					
EM Cyg	DN	Wλ	5.0	2.6			4.8		1.9		0.5	
i = 63°												
AB Dra	DN	Wλ	31.3	19.6	3.7	3.6	3.2		1.6	8.4	6.1	0.9
		Δλ	564	973		370	947					
U Gem	DN		58.3	15.4		12.8			3.8	(4.4)		
i = 67°		"	626	579		648						
IR Gem	DN	"	117	80.6	18.7	29	15.2		1.5	6.2	5.3	0.5
i = 50°			478	554	392	332	1209					

Table 6-6 (continued)

Mean Equivalent Widths, Line Widths and Line Ratios for Novae, Recurrent Novae, Dwarf Novae and Nova-Like Stars. (Data from Williams, 1983).

Name	Class		Hα	Hβ	6678	5876	4686	4640	H_α/H_β	H_α/6678 (H_α/5876)	H_β/4686	4686/5876 or (4686/6678)
AH Her	DN	Wλ	26.4	26.5		3.2			1.0	(8.2)		
i = 46°		Δλ	427	682								
EX Hya	DN	Wλ	98.4	70	10.4	19.6	14		1.4	9.0	5.0	0.7
i = 75°		s	0.3	14	3.1	1.9	3.9					
		Δλ	860	1192	570	770	1282					
		s	48	279	219	52	165					
T Leo	DN	Wλ	203	115	22.7	38.7			1.76	8.9		
i < 50°		Δλ	500	457	321	472						
X Leo	DN	"	30.8	22.3	2.5				1.4	(12.3)		
i=45°			564	919								
CN Ori	DN	"	14									
i = 50°			550									
CZ Ori	DN	"	87.7	43.5						2.0		
			758	503								
RU Peg	DN	Wλ	10.9	4.5	3.1	2.2	2.9		2.4	3.5	1.6	1.3
i = 32°		s	3.9	0.3								
		Δλ	175	516	201							
		s	156									
KT Per	DN	Wλ	14.5	18.6					0.8			
i = 65°		s	-	-								
		Δλ	544	871								
		s	-	-								
WZ Sge	DN	Wλ	123	27.8	8.5	4.1			4.4	14.4		
		Δλ	893	725	404	325						
SW UMa	DN	Wλ	129	67.9	12.6	19.8			1.9	10.2		
i = 50°		s	17	5.2		1.9						
		Δλ	506	741	249	583						
		s	8	119		8						
TW Vir	DN	"	72.5	80	14	20	13.7		0.9	5.2	5.8	0.7
i = 43°			16	14	9	5	5					
			497	695	529	447	1044					
			63	103	139	85	163					

Table 6-6 (continued)

Mean Equivalent Widths, Line Widths and Line Ratios for Novae, Recurrent Novae, Dwarf Novae and Nova-Like Stars. (Data from Williams, 1983).

Name	Class		H_α	H_β	6678	5876	4686	4640	H_α/H_β	H_α/6678 (H_α/5876)	H_β/4686	4686/5876 or (4686/6678)
Z And	NL	Wλ	174	43					4.0			
		Δλ	187									
AE Aqr	NL	Wλ	34	21.6	1.5				1.6	23		
i = 64°		s	14									
		Δλ	369	369	264							
		s	35									
TT Ari	NL	"	26	13	4	5.8			2.0	6.5		
i = 23°			17	9	1	5.9						
			248	118	115	166						
			32	145	76	80						
KR Aur	NL	Wλ	12.1	5.3					2.3			
		Δλ	254	400								
G 61-29	NL	"			50.5	73	35.1					0.5
					808	852	1845					
YY Dra	NL	"	124	129	9.8	24.9	12.7		0.96	12.7	10.1	0.5
			596	739	424	389	1059					
2A 0311-227	NL	"	20.8	43.9	1.9	5.9	33.7		0.5	10.9	1.3	5.7
			686	901		457	1192					
VV Pup	NL	"	123	93.9	18.6	19.4	69.2	15.9	1.3	6.6	1.4	3.6
			661	513	478	311	435	551				
AM Her	NL	W_λ(A)	55	34	7.7	7.5	15.6		1.6	7.1	2.2	2.1
		s	24	20	2	6.4	2.3					
		Δλ(Km/s)	307	333	266	297	298					
		s	126	135	68	202	49					
V 426 Oph	NL	Wλ	31.3	14.9	2.8	1.6			2.1	11		
i = 60°		Δλ	659	813	184							
V 442 Oph	NL	"	12.5	4.8	4.3		3.9		2.6	2.9	1.2	(0.9)
			322	469	269		354					
V 2051 Oph	NL	"	193	124	24.8	35.3	9.9		1.6	7.8	12.5	0.3
			787	853	532	517	999					

Table 6-6 (continued)

Mean Equivalent Widths, Line Widths and Line Ratios for Novae, Recurrent Novae, Dwarf Novae and Nova-Like Stars. (Data from Williams, 1983).

Name	Class		H_γ	H_α	6678	5876	4686	4640	H_γ/H_β	H_γ/6678 (H_γ/5876)	H_β/5686	4686/5876 or (4686/6678)
HK Sco	NL	Wλ	334	113	7.6	12.7	47.1		2.95	44	2.4	3.7
		s	173	65								
CL Sco	NL	Wλ	427	58	9	12.5	7.5	7.6	7.4	47	7.7	0.6
		s	194	11	2	2	1	2.7				
		Δλ	305	150	110	23	186	280				
		s	178	183	27			80				
V Sge	NL	"	166	59			111	7.6	2.8		0.5	
			2	5			6	3.2				
			785	724			720	342				
			55	73			83	136				
V 3890 Sgr	N or NL	Wλ	379	59.6	14.1	35.5	16.7	18.0	6.35	27	3.6	0.5
		Δλ	514	208	81	171	227	462				
RW Tri	NL	Wλ	16.6	6.0	1.3		5.0		2.8	12.8	1.2	(3.8)
i = 72°		s	6	2.8	0.6		0.8					
		Δλ	636	442			555					
		s	215	145			201					
UX UMa	NL	"	16	6.5		3.2	4.5		2.5	(5)	1.4	1.4
i = 72°				4.9			0.8					
			384	516			559					
			71	180			280					
AN UMa	NL	W_λ(A)	33	26	11.4	3.4	12.3	3.3	1.3	2.9	2.1	3.6
		s	3	2.8		0.9	0.5					
		Δλ(Km/s)	366	722	266		321					
		s	114	86			103					
2H 2215-086	NL	"	68.6	23.5	6.6	5.8	17.2	4.2	2.9	10.4	1.3	3
			17	5	1.3	2.7	1.5	1.9				
			442	469	351	418	396	381				
			43	205	212	148	129	222				
2H 2252-0.35	NL	"	20.2	9.2	3.5	2.7	4.7	3.0	2.2	5.8	2.0	1.7
			5	1.2	1.3		0.6					
			398	449	204	327	311	631				
			78	119	93		89					
0623+71	NL	Wλ	6.5									

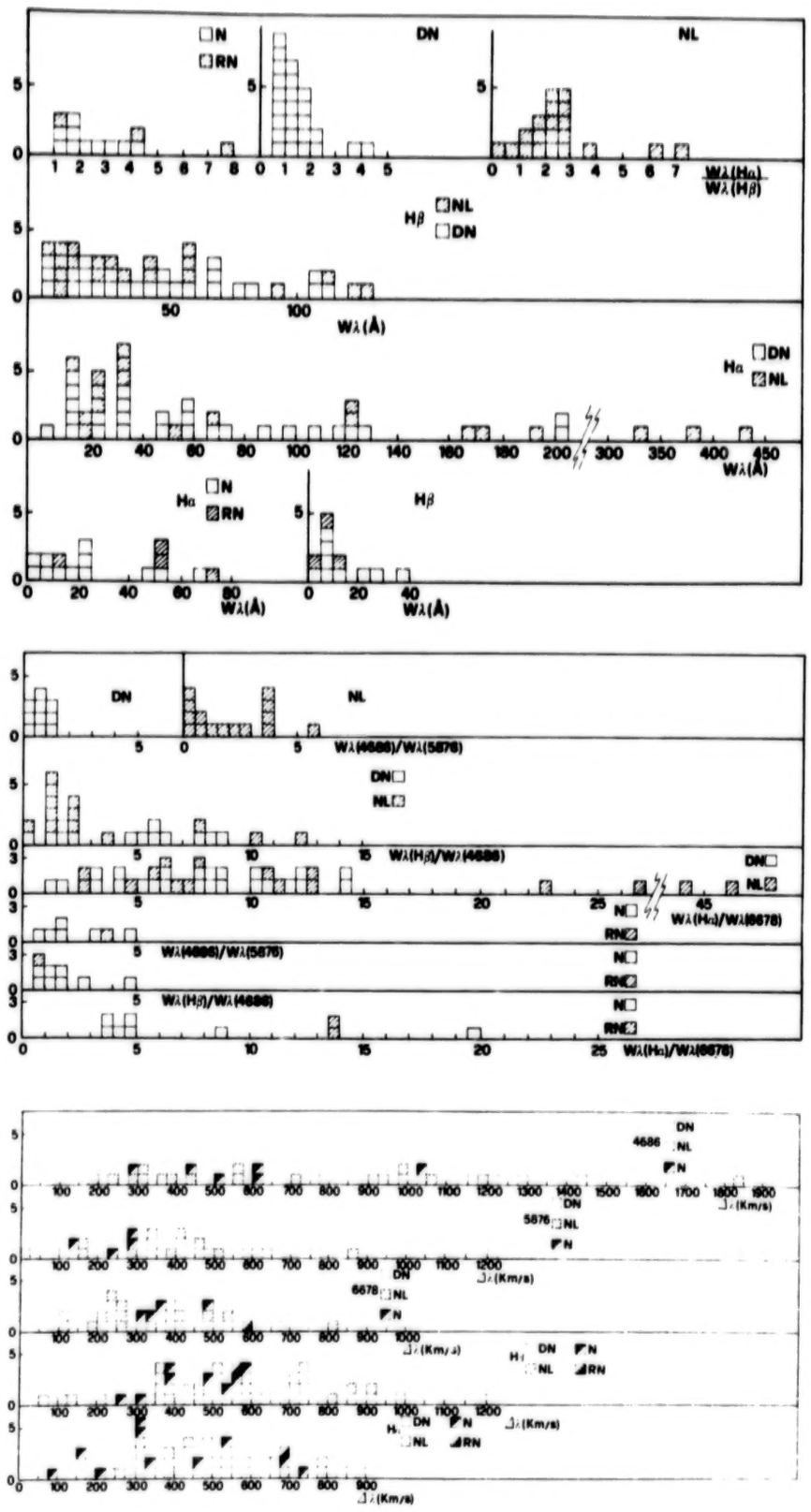


Figure 6-14 -a) The equivalent widths of Hα, Hβ and the ratio Hα/Hβ for classical and recurrent novae, dwarf novae and nova-like stars. b) Ratios of the equivalent widths Hα/6678, Hβ/4686, 4686/5876. c) Widths (km/s) of Hα, Hβ, 6678, 5876, and 4686 for classical and recurrent novae, dwarf novae and nova-like stars.
(data from Williams, 1983)

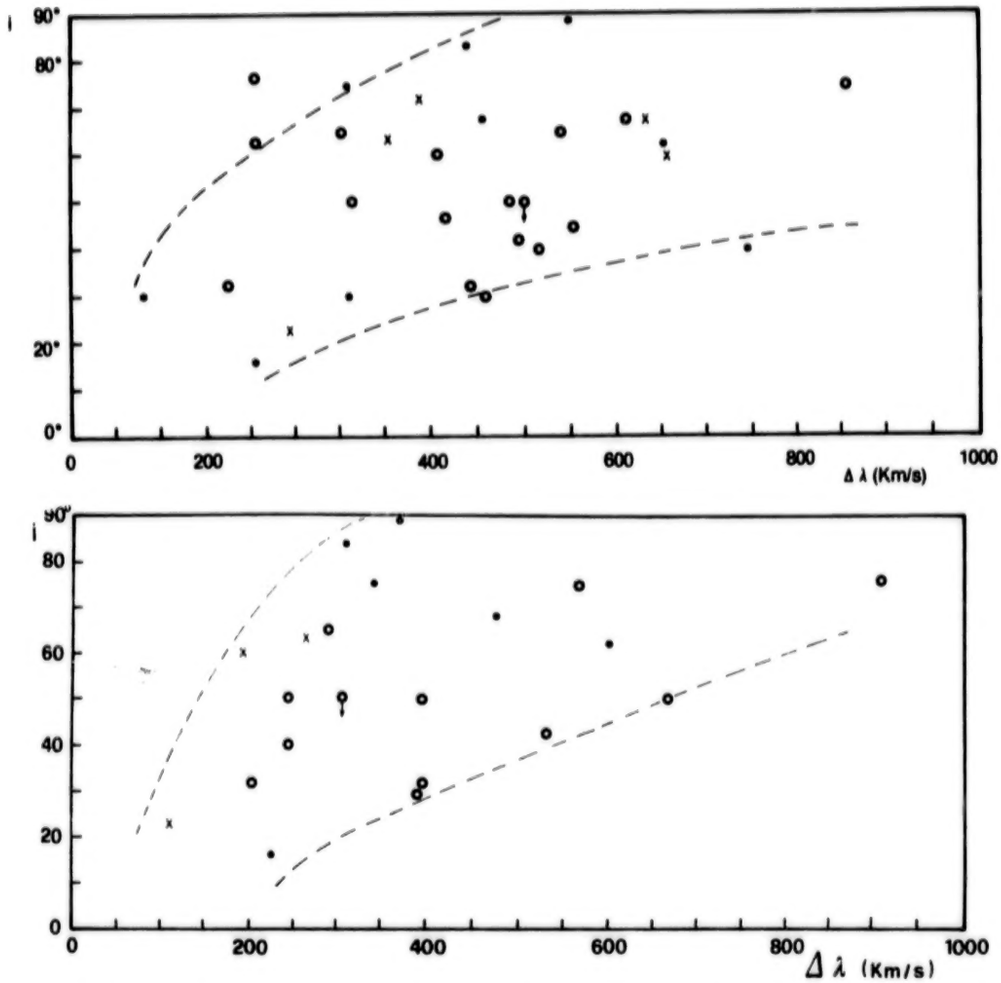


Figure 6-15 -a) Orbital inclination of the system versus the line width (km/s) of H α for classical novae (black dots), dwarf novae (circles) and nova-like systems (crosses). b) same as a) for 6678 He I.
(data from Williams, 1983)

generally absent or not measurable in dwarf novae. The ratio H alpha/H beta for the majority of novae and dwarf novae is included between 1 and 2, and few have values between 2 and 5. About 50% of nova-like stars on the contrary, have values between 2 and 3. This value is a measure of the Balmer decrement, which is a well-known indication of the physical mechanisms at work in the gas, depending on the physical conditions of it (optical thickness and temperature).

The line widths for novae are included in the same range of values as those for dwarf novae and nova-like (but the highest values—ΔV > 1000 km/s—are found among dwarf novae and nova-like stars.

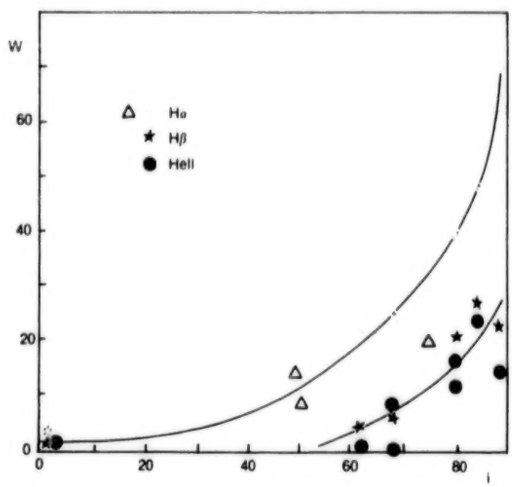


Figure 6-16. Correlations between emission-line equivalent width and orbital inclination. The triangles are data from Williams (1983), the others from Warner (1986).
(adapted from Warner, 1986)

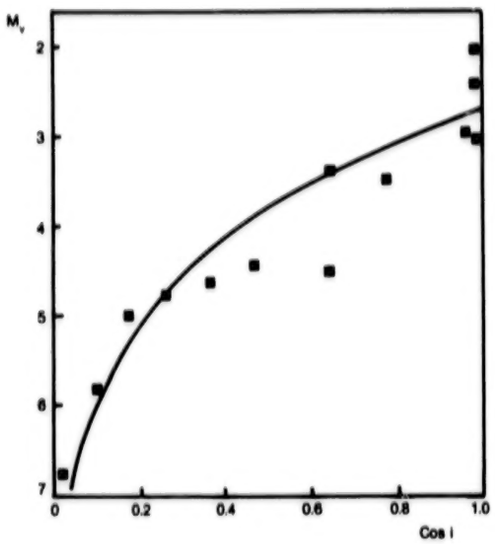


Figure 6-17. Correlation between absolute magnitude M_v and orbital (or disc) inclination for old novae. (from Warner, 1986 c)

WY Sge 1783 also shows a typical old nova spectrum with a faint blue continuum and strong emission of H I, He I and He II, C III+ N III, variable with the orbital phase (Shara and Moffat, 1983; Shara et al. 1984) (Figure 6.19 a, b). The central object of the very old nova CK Vul 1670, on the contrary, is too faint to be detectable. Only the nebulosities ejected from the nova are observable, and they present a spectrum characterized by a strong H alpha emission (Shara et al., 1985).

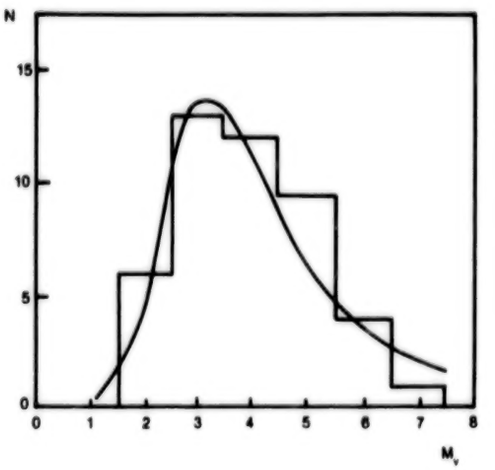


Figure 6-18. Frequency distribution of absolute magnitudes (histogram) compared with theoretical distribution (continuous curve) for randomly orientated discs broadened by a Gaussian with 1 mag dispersion. (from Warner, 1986 c)

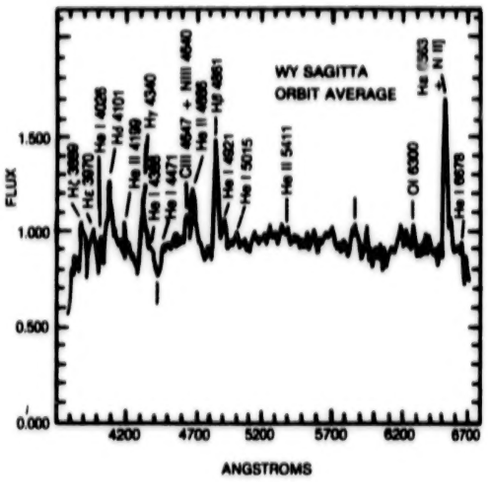


Figure 6-19a. The spectrum of the old nova WY Sge (1783), orbit averaged. (from Shara and Moffat, 1983)

No trace of absorption lines and in particular of lines of a late-type companion is generally found in classical post-novae spectra, even in the case of GK Per, whose color is that of a K-type star and whose orbital period is exceptionally long among novae, 1.99 days.

Among dwarf novae, on the contrary, the spectrum of the late companion is generally visible when the orbital period is longer than about 6 hours, because then the orbital size is large enough to house a sufficiently bright red star. This rule is apparently not valid among old novae; beside GK Per, also the cool component of BT Mon - orbital period 8.01 hours - contributes only about 6% to the total luminosity of the system (Robinson et al. 1982). The other past novae with known orbital period larger than 6 h are V 1668 Cyg (P = 10.54 h) and Nova Lac 1910 (P = 13.05 h). No evidence of a late-type companion is found in the spectrum of the former, while no data are available for the latter.

Although the spectrum of GK Per in quiescent phase does not show the strong blue continuum and the strong flux at 4686 He II and at 4267 C II generally present in old nova spectra, during its minor recurrent outbursts the spectrum becomes more similar to those of the majority of old novae. Spectra obtained at different moments of the minor outbursts (Figure

6.20, Bianchini et al., 1982) indicate that the ratio 4686 He II/H beta increases regularly with increasing brightness. Hence, during these outbursts, the spectrum of GK Per becomes more similar to those of the other old novae. The line width measured at zero intensity in outburst and in quiescence has about the same value—40 A (Szkody et al., 1985).

In the case of DQ Her, which is a well-ascertained binary, as indicated by the occurrence of eclipses, Kraft (1959) was able to show that

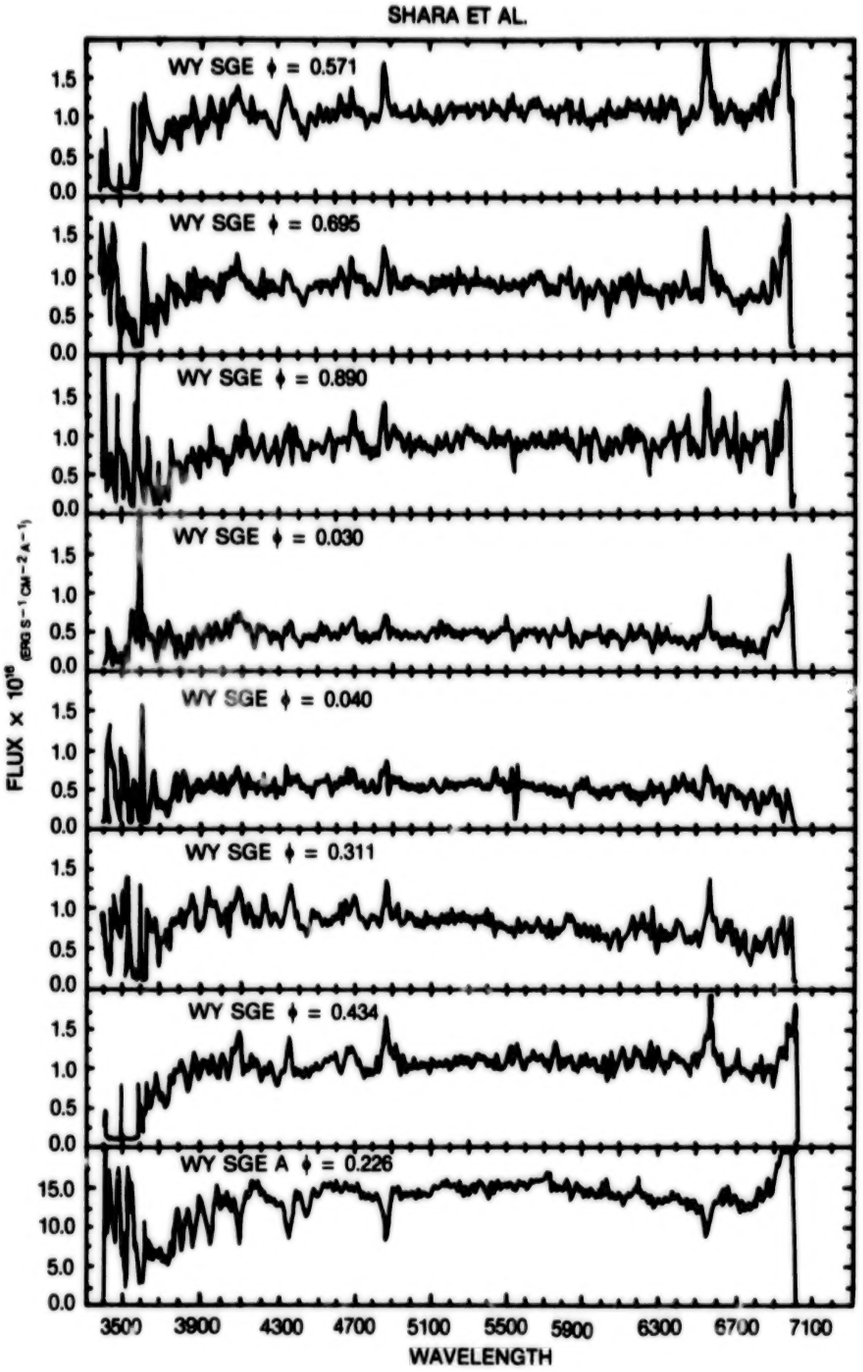


Figure 6-19b. The spectra of WY Sge at different phases. (from Shara et al., 1984)

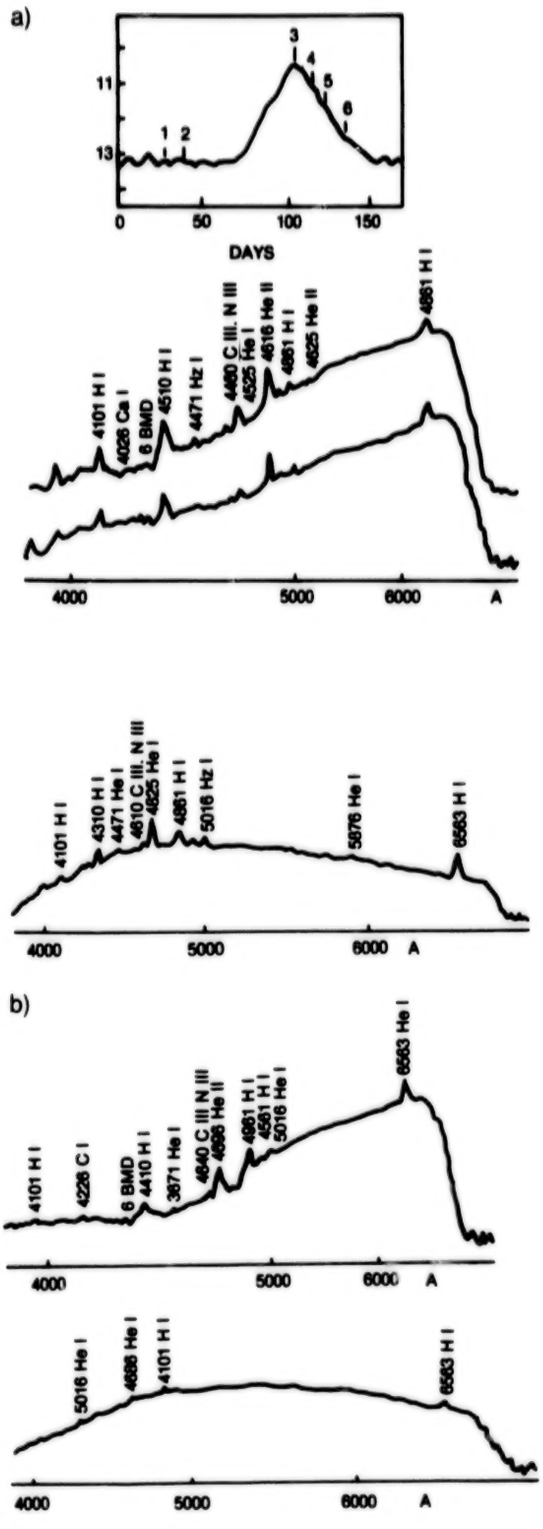


Figure 6-20c. Mean light curve of GH Per of the 1975 and 1981 outbursts. The positions when the spectra shown in b) have been taken is indicated. b) Density tracings of spectra obtained in vicinity and during the 1975 and 1981 outbursts.
(from Bianchini et al., 1982)

both the line and continuum emission arise mainly from a region near the compact component. In fact, the rotational disturbance(*) in the radial velocity curve of λ 4686 (Kraft, 1958) and the onset of the eclipse begin at the same moment, indicating that the He II emission and the continuum originate in the same region. From the Balmer jump, the He II intensity, and the observed colors, an electron density $N_e = 3 \times 10^{13}$ cm^{-3} and a T_{color} 40,000 K are derived. These values support the picture that much of the light comes from a rather dense disk or ring surrounding the nova.

The very slow nova RT Ser (1909) is probably an exception among classical novae. Spectra taken in the red region in 1975 and 1978, in addition to the nebular emission lines, show TiO absorption bands. Spectra taken in the blue region in 1964 show only nebular emissions, but probably this is not due to a real variation of the spectrum but rather to the fact that the cool companion becomes more easily detectable in the red region (Fried, 1980). Another very slow nova—RR Tel—shows the presence of a red giant component as indicated by its spectral characteristics. The two recurrent novae T CrB and RS Oph also show a symbiotic spectrum with evidence of a red giant companion. Hence, it seems that the visibility of the two spectra and the luminosity of the red companion - class III - are characteristics common to symbiotics and to some recurrent novae and some very slow novae, which are often also called symbiotic novae.

III.B. SPECTRA DURING THE OUTBURST AND DECLINING PHASES OF NOVAE

Several indicators of nonthermal phenomena are observed in the spectra of the majority of novae during their explosive phases:

(*) We remind that the rotational disturbance consists in a deviation of the orbital radial velocity curve occurring just at the beginning and at the end of the eclipse. The radial velocity of the eclipsed star shows an excess of positive velocity at the beginning of the eclipse (when the part of the stellar disk, rotating toward us, is eclipsed; the reverse occurs at the end of eclipse (in the hypothesis that, for mechanical reasons, rotation and revolution occur in the same directions).

1) Anomalously high ionization, which probably requires nonradiative heating (e.g., presence of coronal lines).
2) Nonthermal widths of spectral lines (up to 3000-4000 km/s).
3) Nonthermal atmospheric extent (from less than 1 solar radius up to several hundreds solar radii as derived by the product of the expansion velocity by the time elapsed from outburst).
4) Mass-flow, as indicated by the line-shifts and the asymmetric line-cores and wings.
5) Simultaneous presence of high and low excitation + ionization features.

Hence, we have macroscopic evidence of mass-flux and mechanical heating of the atmosphere.

III.C. DEVELOPMENT OF THE SPECTRUM DURING THE OUTBURST

The spectra at maximum are generally similar to those of an A- or F-type supergiant. V 1500 Cyg 1975 had one of the earliest type, B2 Ia and V1148 Sgr 1943 the latest (K-type).

Although the absorption spectra of novae at maximum are similar to those of supergiants of Classes B, A, or F, they are not identical to them. However, if we consider the violence of the outburst, it is rather surprising that they are so similar.

The spectra are characterized by absorption and emission lines (P Cygni profiles).

Several typical absorption systems have been identified. Figure 6.6 shows schematically the shape of the light curves for fast and slow novae and indicates when the various spectral systems are present.

The PREMAXIMUM spectrum is observed during the light increase until just after maximum. It generally resembles a spectral type of a B or A supergiant. The PRINCIPAL spectrum replaces the premaximum within a few days after maximum and persists until the nova has faded by about 4 mag. The principal spectrum closely resembles the premaximum spectrum and it is often difficult to distinguish the one from the other. However, in general, the premaximum spectrum tends to be hotter than the principal spectrum. Generally, the latter is similar to that of an A or F supergiant with Ca II lines stronger than normal and strong lines of O I and C I. The Mg II line at 4481 A weakens rapidly, while the lines of Fe II, Ti II, and Mg I, with lower levels in a metastable state, persist along with the H I lines. Hence, there is evidence of increasing dilution of the radiation incident on the expanding principal shell. The expansional radial velocity is larger than that indicated by the premaximum spectrum. The DIFFUSE-ENHANCED spectrum appears later than the principal one; it reaches maximum strength at about two magnitudes below maximum. It presents strong and wide lines of H I, Ca II and usually Fe II, O I, and Na I. Slow novae have richer diffuse-enhanced spectra, with lines of Ti II and Cr II. In the later stages, the hydrogen lines can present several components. The expansional radial velocity is about two times larger than that indicated by the principal spectrum, and it is often variable with time. The ORION spectrum (so called because it is similar to the spectra of the B-type stars in the Orion nebula) appears when the diffuse-enhanced is strongest and reaches its maximum intensity at three magnitudes below maximum. It resembles that of an early-type star with O II and N II relatively strenghtened. Hydrogen lines can be either present or absent. The radial velocity is variable and equal or higher than that of the diffuse-enhanced spectrum.

These four systems account for all but a few absorption features. To each absorption system, a corresponding emission system is correlated. In fact, all the absorption and corresponding emission features form the characteristic P Cyg profiles, which are typical of the expanding envelopes. Moreover, another emission system—the NEBULAR system—appears when the nova has weakened by four magnitudes and is completely developed when the nova is still three magnitudes weaker; i.e., seven magnitudes below maximum. At first it

consists of lines typical of nebulae, like [NI], [OI], [NII], [OII], [OIII] and later on of coronal lines. We define "coronal lines" those with upper potential higher than 125 eV, corresponding to the ionization potential of Fe VII.

The nebular emission lines have the same width as the emissions associated with the principal spectrum: this means that when the shell is diluted enough to become optically thin in the continuum (and therefore when the absorption lines disappear), it is still optically thick in the lines and produces the nebular spectrum. In this sense, one says that the nebular spectrum "replaces" the principal spectrum.

The postnova system is observable when the nova envelope is dissipating in the interstellar medium. Nebular and coronal lines are present. The nebular spectrum is characterized by the permitted emissions of H I, He I, He II, N II, N III, N IV, O II, O III, O IV, C II, Si IV, and by the forbidden emissions of O I, O II, O III, N II, Fe II, Fe V, Fe VI, Fe VII, Fe XIV, Ne III, Ne IV, Ne V, A X, Ca V, S II, K V, Ni VIII, Ni XIII, Ni XVI, and Na IV, with ionization potentials ranging between 13 and 500 eV. Hence, the regions where the coronal lines are formed are similar to those observed in the solar corona. The temperature of these regions is much higher than that of the stellar photosphere (required electron temperature Te > 10^6) and still much higher than that of the dusty envelope surrounding the majority of past novae, and which is indicated by their infrared spectrum. Several mechanisms of heating of the "corona" have been proposed and will be discussed in Chapter 7.

The coronal lines become observable a few months after outburst and remain observable sometimes for years. A few examples are given by Malakpour (1980). Very slow nova HR Del 1967: the outburst occurred on June 6, 1967; the coronal lines were observed in November 1972, 4 years after the onset of the nebular phase. Fast nova V 433 Her 1960: the outburst occurred on February 26, 1960; the coronal lines became observable already on March 20, 1960, but became almost invisible in August 1960. Fast Nova Her 1963: the outburst occurred between the 19th and the 28th of January 1963. The coronal lines became visible on February 11, 1963, and were observed until July 1963. Slow Nova FH Ser 1970: the outburst occurred on February 11, 1970; only one coronal line, 5534.6 [A X], was observed in August 1970 and was not present on May 25, 1970. Slow nova V373 Sct 1975: the outburst occurred on April 4, 1975. The coronal lines were observable from July 14 to the end of August. Very fast nova V 1500 Cyg 1975: the outburst occurred on August 25; the coronal lines were not present on September 12, but they were present on September 29, and were still present in January 1976.

The mechanical energy liberated by mass-loss during the explosion is comparable to the radiative energy produced: both are of the order of 10^{44} ergs.

III.D. EXPANSION VELOCITIES

The expansion velocities are correlated with the speed class and with the spectral type at maximum. Moreover, the expansional velocities of the various absorption systems generally increase from premaximum to orion system. Figure 6.21 gives the relation between speed class and expansional velocity of the principal spectrum. The two recurrent novae for which these data are known are T CrB, which obeys to the general relation, and T Pyx, which deviates strongly. Too few data are available to say if recurrent novae do obey or do not to the same relation of classical novae. Typical expansional radial velocities of the various spectral systems are indicated in the following Table 6.7, based on novae representing various speed classes.

C. Payne-Gaposchkin (1957) has observed that spectral type and expansional radial velocity of the principal spectrum are correlated: the earlier the spectral type, the higher the radial velocity. Since we are dealing with a shock front, it is plausible that it is "the velocity which determines the spectrum" (C. Payne-Gaposchkin, 1957, in *The Galactic Novae*, p. 82).

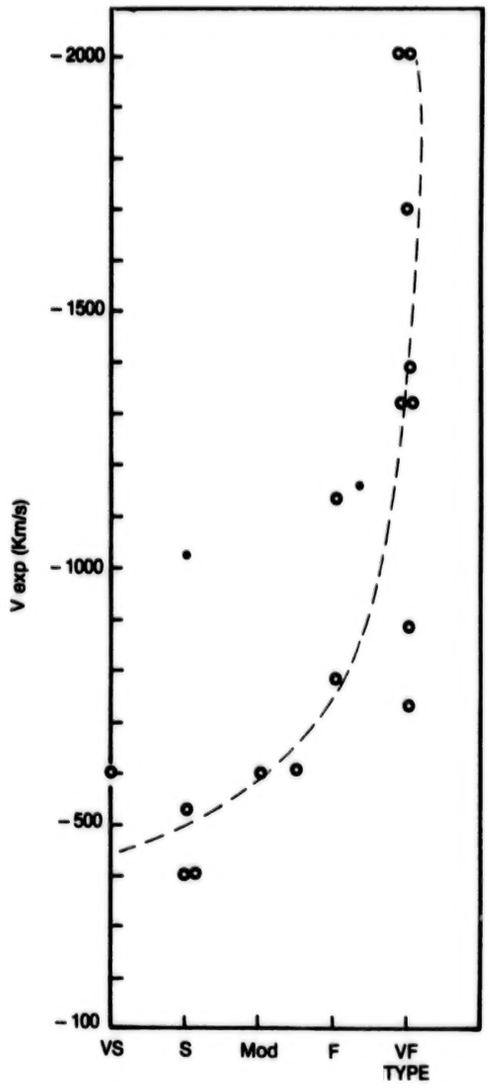


Figure 6-21. Relation between the speed class and the expansion velocity of the principal spectrum. VS=very slow; S=slow; Mod=moderately fast; F=fast; VF=very fast. Open circles: classical novae; black dots: recurrent novae (T Pyx and T CrB).

Similar relations exist also between spectral type at maximum and the radial velocity difference between the diffuse-enhanced and the principal spectrum.

The data by C. Payne-Gaposchkin are given in Table 6.8.

A loose relation also exists between the expansion velocity and the absolute visual magnitude at maximum (Figure 6.22). Data from Mustel (1978) shows that the expansion velocity of the "photosphere" (i.e., the layers where the continuum and absorption spectrum are formed, or where $\tau \approx 1$) grows with time, and the growth is particularly rapid in the latest periods of expansion, just before light maximum. For instance, in V 603 Aql, the expansion velocity during the day before t_{max} was twice that of the previous day; the same picture was shown by DQ Her. V 1500 Cyg 1975 had V exp of -1300 km/s on August 29, -1700 on August 30 (epoch of maximum) and -2200 on August 31. The slow nova RR Pic had the first maximum on June 7, 1925. From June 6 to June 7, the expansional velocity came up to 250 km/s, while between June 4 and 5 it was only 40 km/s. Hence, the rate of energy generation in the inner subphotospheric layers increases just before light maximum; the velocity of the gas on the photospheric level records a sharp increase due to a second shock wave that hits the first expanding layer. It is the accelerated matter that forms the principal envelope.

The spectra of recurrent novae seem to show a different behavior than that of classical no-

TABLE 6.7

EXAMPLES OF EXPANSIONAL RADIAL VELOCITIES.

Object	Type	Expansional velocity (km/s)			
		Premax.	Princ.	D-E	Orion
N Aql 1918	Fast	-1300	-1500	-2200	-2700
N Gem 1912	Average	- 400	- 800	-1400	-1600
N Her 1934	Slow	- 180	- 300	- 800	- 500
					-1000
N Cyg 1975	Very fast	-1300	-1700	-3000	
				-4000	

TABLE 6.8

CORRELATION BETWEEN SPECTRAL TYPE AT MAXIMUM AND EXPANSIONAL VELOCITY OF THE PRINCIPAL SPECTRUM.

Spectral Type	Corresponding Temperature	Average RV (km/s)	Number of Objects
F8	6,000 K	142	2
F5	7,000	- 168	2
F0-F2	8,000	- 268	4
A5	8,500	- 618	4
A2	9,000	- 560	3
A0	10,000	- 600	2
B9	11,000	- 600	2
B5	15,000	-1000	1
B1	25,000	-1210	1
N III lines	50,000	-1378	7
N V lines	200,000	-1950	3

These are mean values. We add here a few examples for some individual objects, which may deviate from the average values:

The very slow nova HR Del 1967: Sp. A, V = -625 km/s

The fast nova V1668 Cyg 1978: Sp. F, V = -600 km/s

The very fast nova V1500 Cyg 1975: Sp. B2 Ia, V = - 1,700 km/s

vae. We remind the reader however that only four of them have been observed spectroscopically, and among them T Pyx (the only known slow recurrent nova, which has been observed fragmentarily) behaves like classical novae. T Cr B and RS Oph do not show systems corresponding to the diffuse-enhanced and the orion spectrum, and during the light decrease present strong coronal lines of [Fe X], [Fe XIV]; U Sco, on the contrary, does not show highly ionized forbidden lines.

Details on the spectral behavior of single objects will be given in Chapters 8 and 9.

IV. INFRARED OBSERVATIONS OF NOVAE

A dozen novae have been observed from the ground in the infrared (from about 1 μm to 20 μm). Moreover, the infrared satellite IRAS has observed some recent, old and very old novae. Infrared observations are important because many novae are known to produce dust shell few weeks after outburst.

The first evidence for the formation of a dust cloud around a nova was given by Geisel et al. (1970) who observed the decline of FH Ser 1970 between 1 and 22 μm. They observed that when the visual light curve showed the dip typical of slow novae, infrared emission started to increase (see Figure 6.23 and 6.24). The infrared emission was very similar to that of a black body at temperatures varying between 1,300 to 900 K. Circumstellar dust was the natural candidate for interpreting this emission. The lack of any spectral feature at 10 μm suggested that silicate grains are absent and that the dust may be formed of graphite. McLaughlin (1935, 1937) was the first to suggest that the diminution of about 9 mag observed in the visual light curve of DQ Her was due to a cloud of dust formed from the ejecta. Now the recent infrared observations of novae confirm his prediction.

Bode and Evans (1983) review the evidence for the presence of dust in novae and classify them, according to their infrared development, in three classes, as follows:

"Class X: novae for which the infrared luminosity = luminosity of the underlying object. These novae invariably have a pronounced discontinuity in the visual light curve, which coincides with infrared flux rise. The temperature of the dust shell attains a minimum before rising to a plateau - the so-called isothermal phase. Typical member, NQ Vul" (see figure 6.25).

"Class Y: novae for which the infrared luminosity < 10 per cent that of the underlying object. The visual light curve is smooth and the dust shell temperature decreases

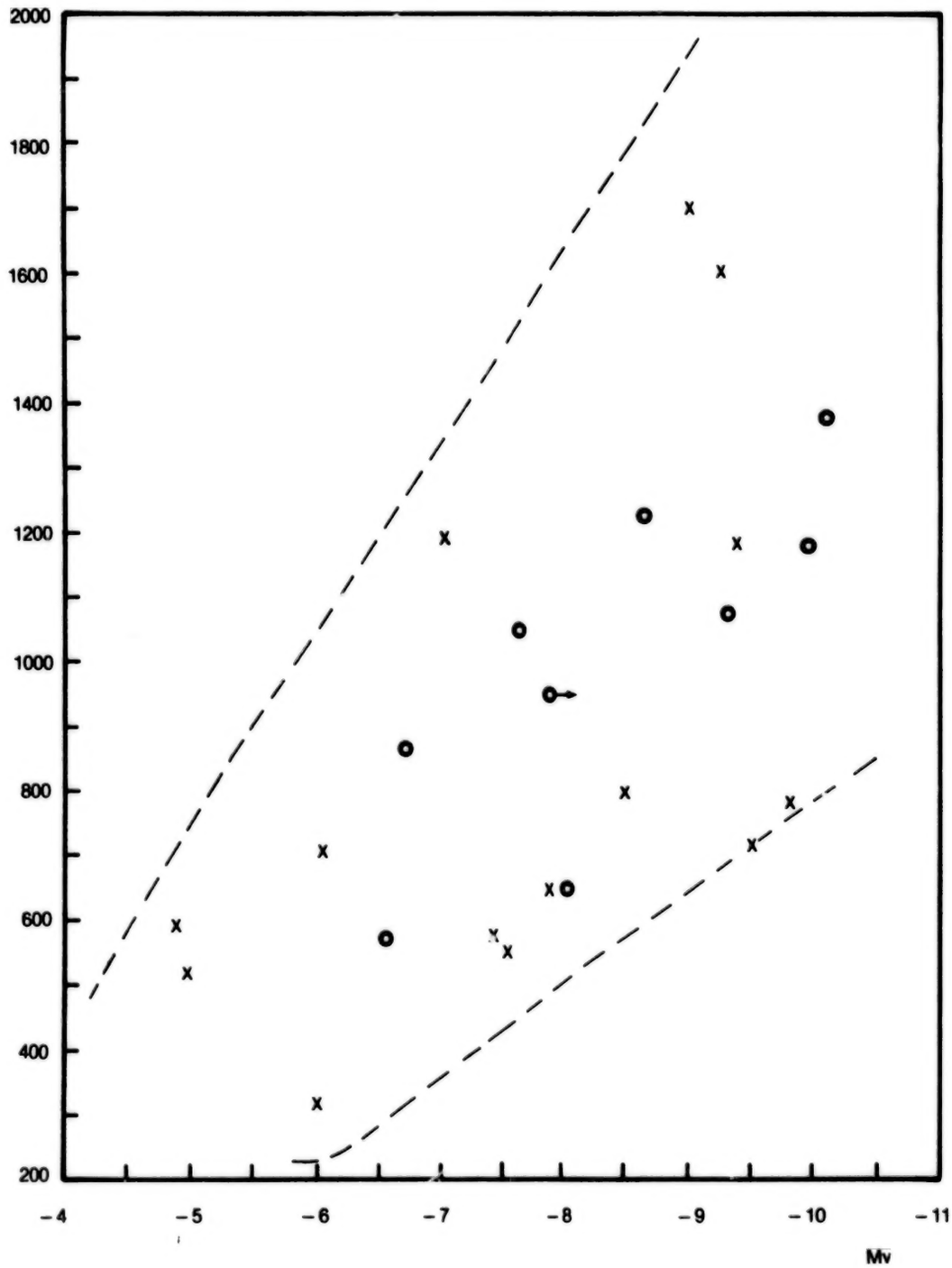


Figure 6-22. Relation between the expansion velocity of the principal spectrum and the absolute visual magnitude. Crosses: data from Cohen and Rosenthal, 1983; circles: data from Cohen, 1985.

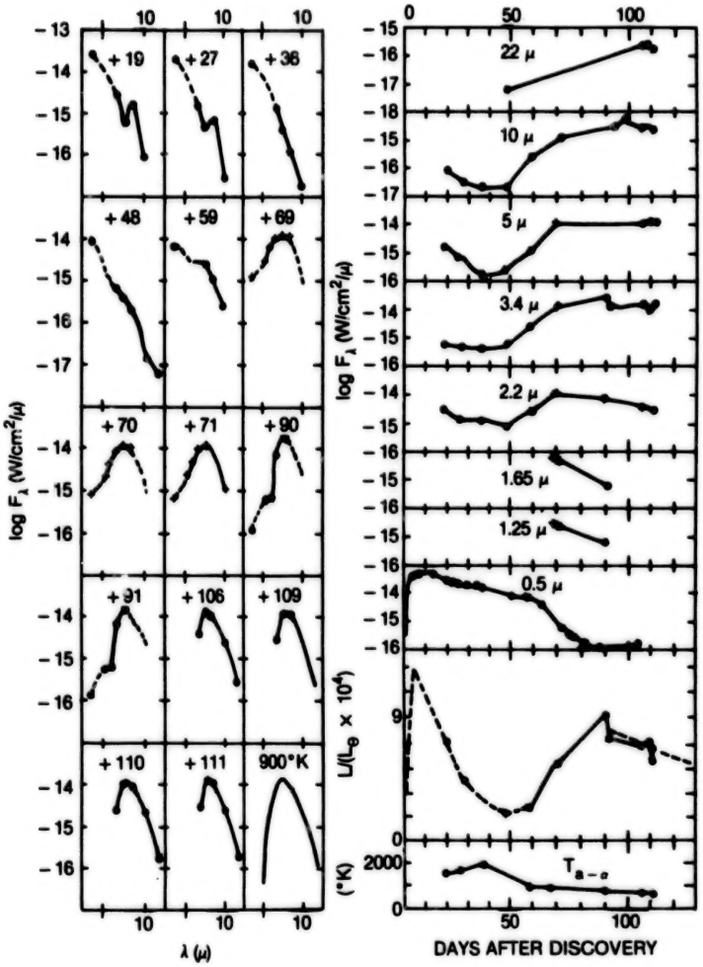


Figure 6-23. FH Ser 1970: left, Fλ vs λ on successive days after its discovery. A 900 K black body distribution is given for comparison. Right, light curves for different wavelengths, and total luminosity (at optical and IR wavelengths) in solar units. The color temperature T(K-N) is plotted to show the cooling of the dust as the luminosity of the system changes.
(from Geisel et al., 1970)

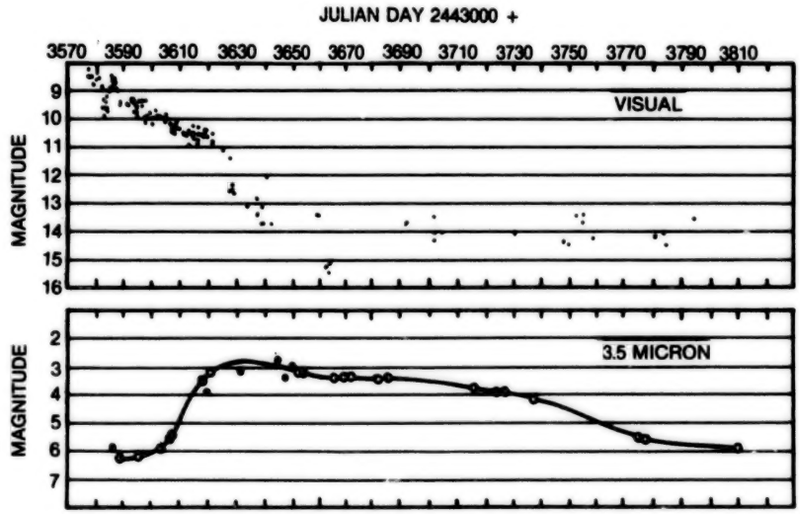


Figure 6-24-LW Ser 1978: visual light curve and 3.5 μm light curves. (from Gehrz et al. 1980 a)

monotonically. Typical member, V 1668 Cyg" (Figure 6.26).

"Class Z: novae with little or no infrared excess, i.e. little or no dust. The visual light curve is usually smooth. The only member known with certainty to date is V 1500 Cyg" (Figure 6.27).

It is important to note that these different infrared behaviors are correlated with the speed class: slow novae generally belong to

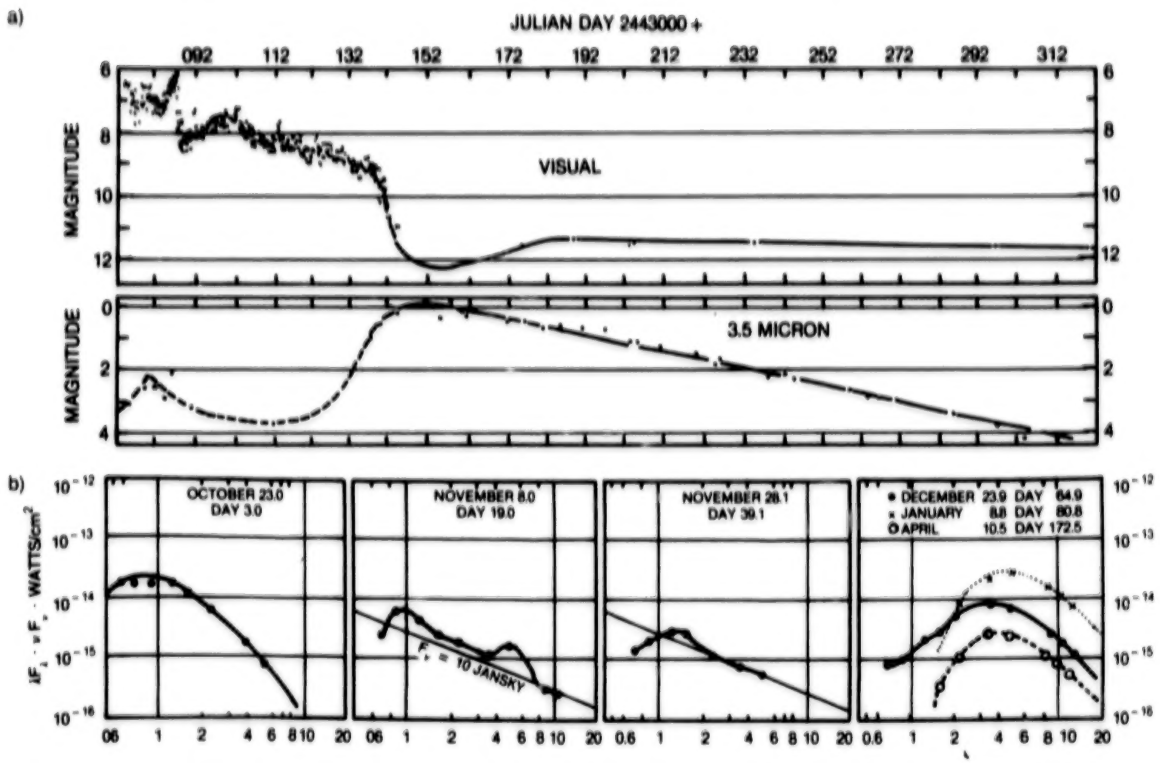


Figure 6-25a. NQ Vul: visual and 3.5 μm light curves. The visual magnitude dims as the 3.5 μm magnitude brightens, as the dust condenses. b) Distinct phases of the nova development: day 3.0 shows the initial pseudophotosphere; day 19.0 the free-free phase with an unidentified feature at 5 μm superposed; day 39.1 the free-free prior to dust condensation; days 64.9 to 172.5 the thermal reradiation by the condensed dust.
(from Ney and Hatfield, 1978)

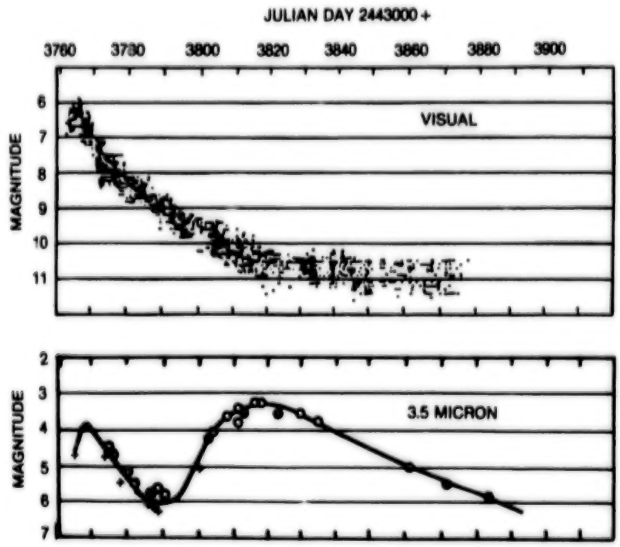


Figure 6-26. V1668 Cyg 1978: visual and 3.5 μm light curves. The visual light curve shows no transition phase as condensing dust causes the IR flux to rise. (from Gehrz et al., 1980 b)

C-5.

Class X, intermediate novae, to Class Y, and very fast novae, to Class Z. Of course these conclusions are based on a relatively small number of observations, and exceptions could be revealed when a larger sample will be available.

More detailed description of the infrared behavior of some typical novae is given in the following.

The best studied novae are FH Ser 1970, V1301 Aql 1975, V 1500 Cyg 1975, NQ Vul 1976, V1668 Cyg, LW Ser 1978, Nova Aql 1982.

Slow novae of the DQ Her type, which exhibit a deep minimum in the visual light curve and then recover before starting their smooth decline (the visual transition stage), form a

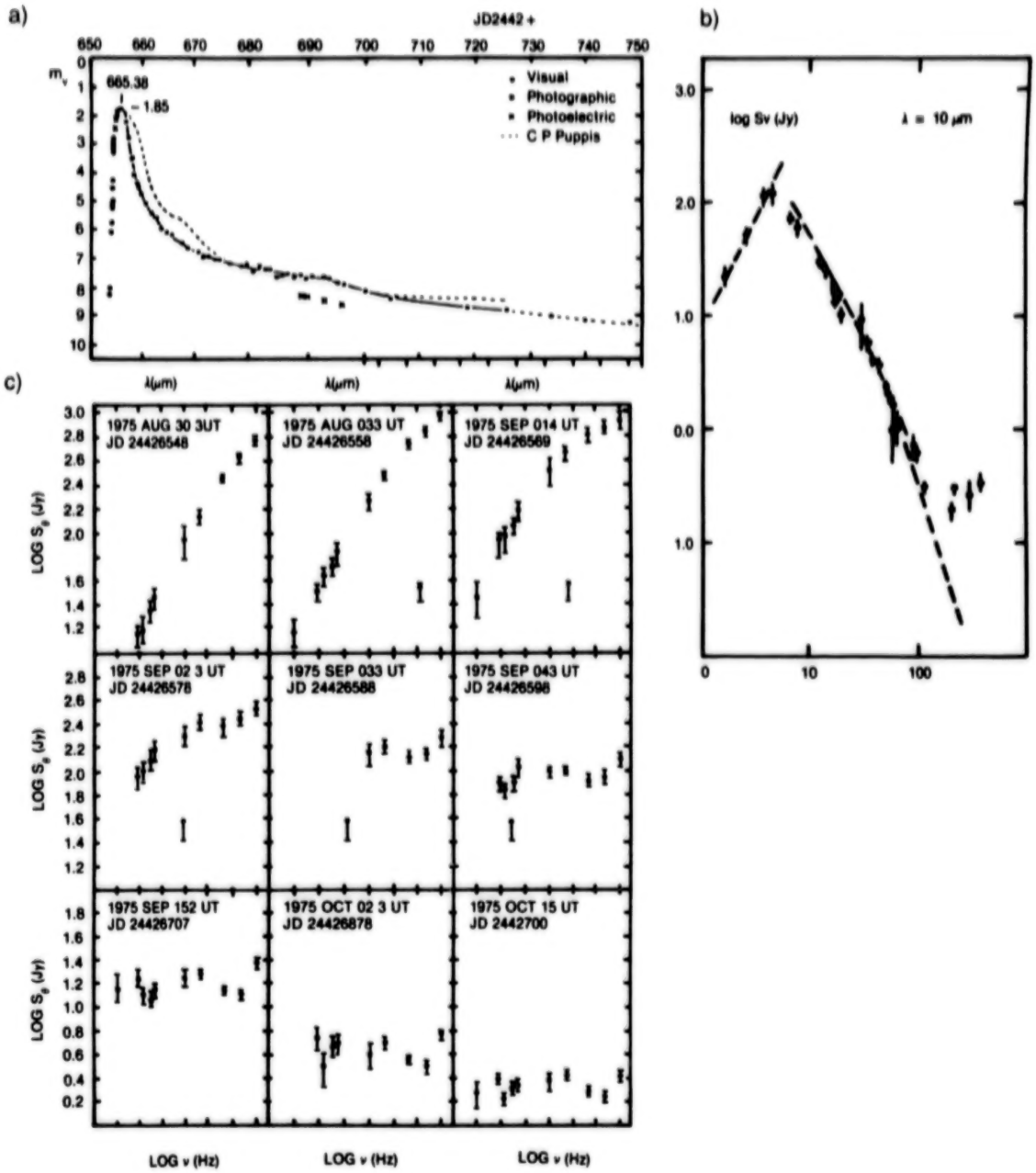


Figure 6-27a. Optical light curve for V1500 Cyg (1975) (from Wolf, 1977) b) IR (10 μm) light curve for V1500 Cyg 1975 (from Ennis et al. 1977) c) Energy distribution from 1.2 μm to 20 μm at various epochs of the outburst. The transition from black body to thermal bremstrahlung emission occurred on Sep. 2, 1975. (from Ennis et al., 1977)

thick circumstellar dust shell. They belong to the Class X. FH Ser, LW Ser, NQ Vul belong to this type. The very fast nova V 1500 Cyg, representative of Class Z, on the contrary, radiated like an optically thin expanding plasma for nearly one year; there is some weak evidence that a small amount of dust was formed after one year from outburst.

V 1668 Cyg, representative of Class Y, is a moderately fast nova. After an initial expansion of the hot gas shell, an optically thin dust shell was formed, and it reached its maximum visual optical depth of 0.1 about 60 days after outburst.

The very slow nova HR Del 1967 represents an exception to the correlation between speed class and infrared behavior. In fact, it has not formed a thick shell. When the dust shell remains optically thin or does not form at all, no deep minimum is observed. This is the case of HR Del, whose light curve presents a slow, smooth decline and no dip.

IV.A. COMPARISON OF INFRARED AND VISUAL LIGHT CURVES OF SOME TYPICAL NOVAE

The visual and infrared light curves of several novae are plotted in Figures 6.25, 6.26, and 6.27.

The visual and infrared (1.2 to 10 μm) light curves of the extremely fast nova V 1500 Cyg (Figures 6.27a, b) exhibit about the same behavior: all reach a maximum and then decrease smoothly. However, the maximum brightness is reached at progressively later epochs with increasing wavelength; e.g., the visual maximum was reached on August 30, 1975, and that at 10 μm on September 2, 1975. The energy distribution is typical of a black body with temperatures varying from 10,000 K to 5,000 K until day 3.2 after outburst; then the energy distribution changes gradually to that typical of free-free radiation (Figure 6.27 c). Only 300 days after outburst, a slight infrared excess, which can be attributed to the formation of dust, is observable at wavelengths equal to or larger than 3.6 μm. These data show the nova to present a thick "pseudophotosphere" until day 3.2 and then to consist of an expanding mass of ionized gas.

The visual and infrared light curves of FH Ser, LW Ser, and NQ Vul (Figures 6.23, 6.24, and 6.25) all have the common property that they are almost the mirror image of one another; when the visual brightness starts to decrease, the infrared curves show increasing brightness. The energy distribution in infrared is that of a black body at temperatures of the order of 1,000 K and decreases with time from the outburst (Figure 6.23) Hence, we have a clear example of the different behavior of V 1500 Cyg with its thin electron shell and FH Ser, LW Ser, and NQ Vul with their thick dust shell.

In the case of FH Ser, Hyland and Neugebauer (1970) and Geisel et al. (1970) observed the commencement of infrared emission about 60 days after discovery, coincident with the rapid decline in visual light. Ultraviolet observations up to day 57 and infrared observations by day 90 indicated that the total luminosity remained equal to that observed at outburst (see section 6.V on ultraviolet observations for more details).

Infrared observations were continued by Mitchell et al. (1985) and continued until day 529 after discovery. Figure 6.28 from Mitchell et al. shows the infrared light curves at 1.25, 1.65, 2.2, 3.5, 4.8, and 10 μm. It must be noted that the discontinuity in the light curves, occurred between day 111 and day 129; after that event, fading occurred in all bands (except at J=1.25 μm, where, however, the observations are very uncertain and data are lacking). The energy distribution at various epochs is shown in Figure 6.29, together with approximate black body fits. The temperature decreases from 960 K on day 70 to 760 K on day 91. The discontinuity in the light curves is reflected by the slight increase to 800 K on day 154. Later on, it is difficult to represent the observations by a single black body only. Instead, there is evidence for a cool black body component, responsible for the major part of the infrared luminosity, and an excess in the 1-3 μm region.

The cool component decreases in temperature from 700 K on day 210 to 400-500 K after day 400, while the short wave excess increases in relative strength and temperature.

The interpretation of these data will be discused in Chapters 7 and 8. We anticipate here that to explain these observations and especially the discontinuity in the light curves, we must assume that the dust grains grow from day 60 to day 111 and undergo a significant reduction in size between day 111 and day 129. The excess flux at the shorter infrared wavelengths may probably be due to increasing line emissions as the shell expands.

V 1668 Cyg differs from V 1500 Cyg, as well as from the three class X novae, because it shows two distinct phases in its infrared light curves: a first phase with a thin electron shell, when the infrared light curves decrease smoothly, as does the visual one, thus resem-

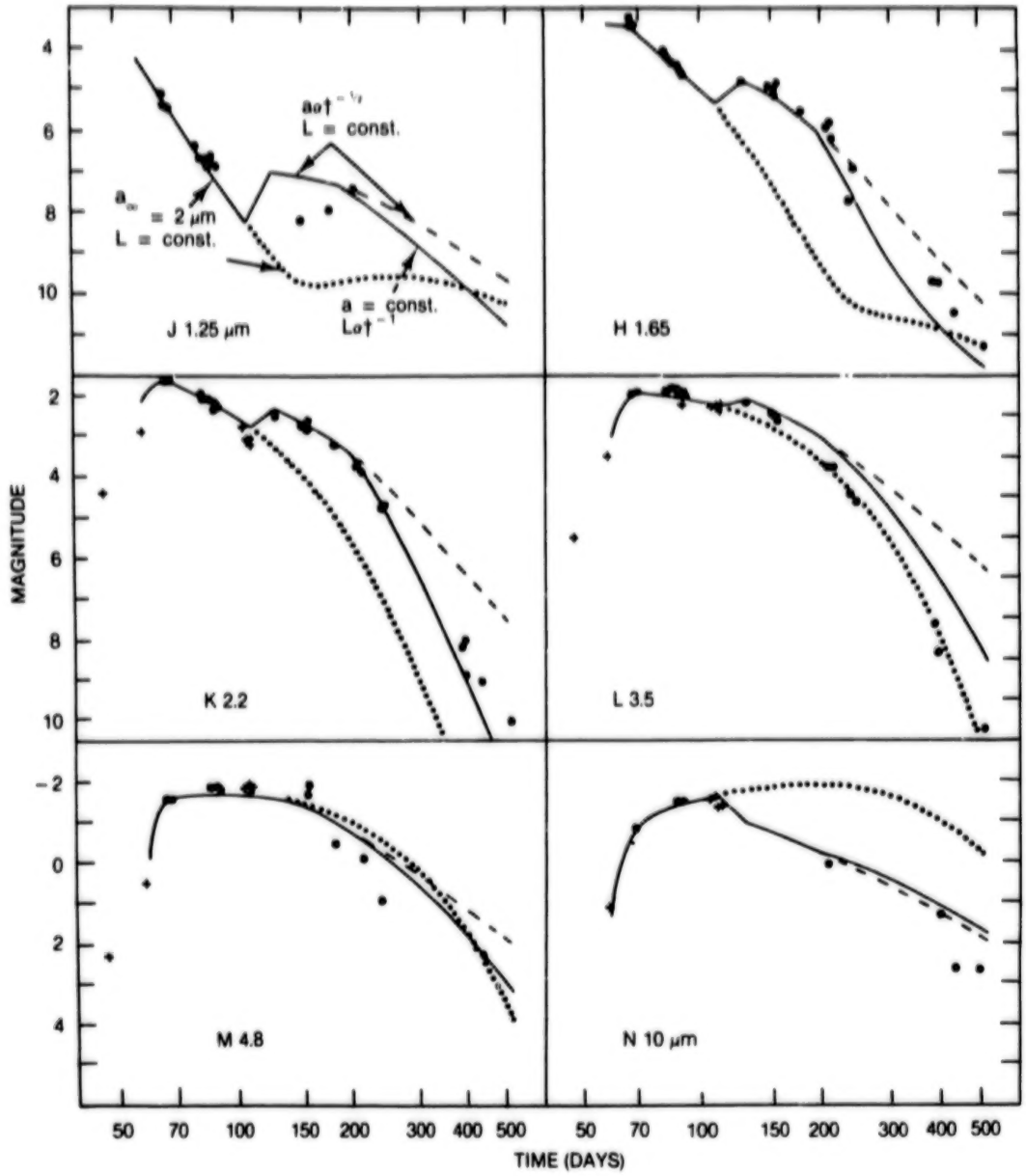


Figure 6-28. Infrared light curves of FH Ser. Dotted and dashed lines correspond to the predicted light curves for continuing grain growth beyond day 111, and for constant bolometric luminosity and continued grain size reduction beyond day 200 respectively.
(from Mitchell et al., 1985)

bling V 1500 Cyg (Figure 6.26) and a second phase with an optically thick dust shell, as indicated by the infrared increasing brightness reached when the visual brightness is almost gone back to the preoutburst magnitude.

A different case is represented by the fast Nova Aql 1982 (Bode et al., 1984). It was discovered by Honda (1982) on January 27, 1982. The initial decay was of 0.3 mag/day, typical for a fast nova, as well as the relatively smooth early light curve. On day 37, it had developed an infrared excess characteristic of a dust shell at T = 1100 K.

Figure 6.30 by Bode et al. shows the visual

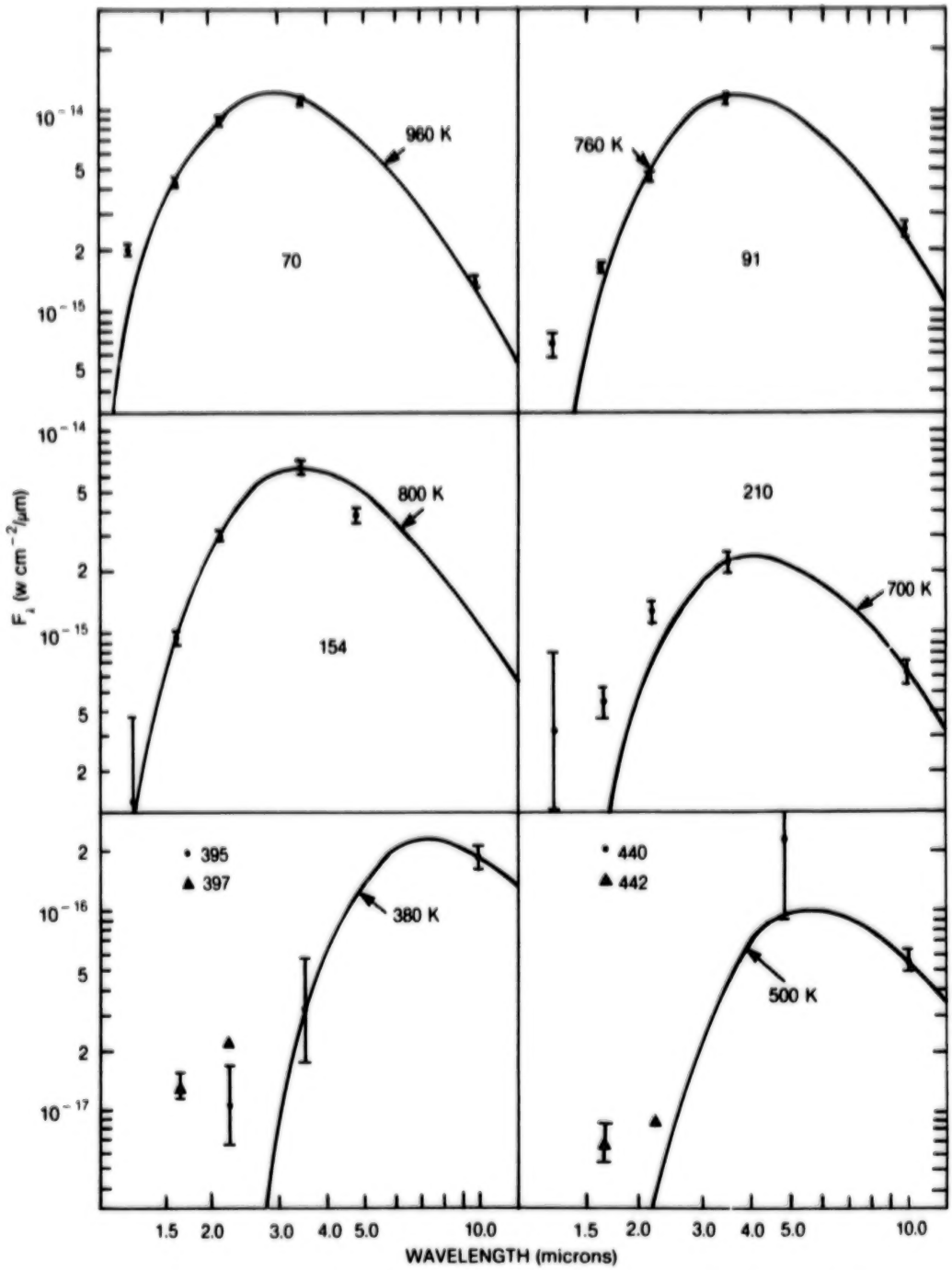


Figure 6-29. Energy distribution of FH Ser and approximate black body fits. Beyond day 210 the energy distribution broadens due to excess emission in the 1-3 μm region appearing above the cool dust emission component. (from Mitchell et al., 1985)

and infrared light curves: no dip in the visual light curve, a smooth brightness decrease in the infrared curve. Figure 6.31 shows the fit of the infrared flux to the black body curves. Ultraviolet observations suggest that the bolometric luminosity was not maintained (differently from FH Ser; see Section 6.V). A very interesting observation made on July 3-4, 1982, 156 days after discovery shows the presence of an emission feature peaking near 10 μm (Figure

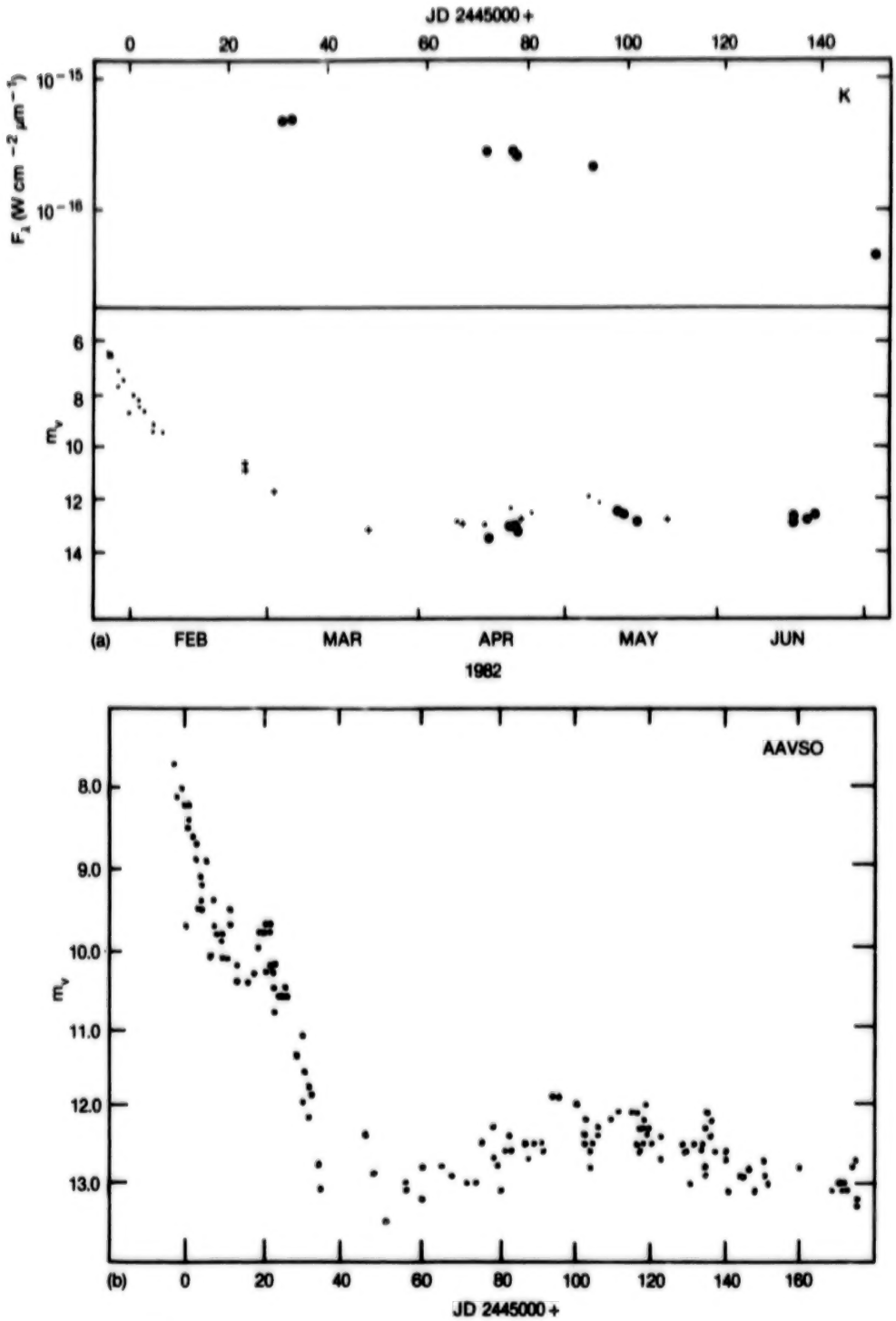


Figure 6-30. Nova Aql 1982: 1) infrared light curve from K band photometry; 2) Visual light curve obtained collecting visual estimated (dots), IUE FES measurements (plus) and V band photometric observations (circles); 3) Visual light curves from AAVSO observations.
(from Bode et al., 1984)

6.32), which can be attributed to SiC grains, and which has never been detected before in the other novae observed in infrared. It was the absence of this silicate feature that suggested that generally dust is formed of graphite grains.

Beside the emission feature, one spectrum observed on April 18, 1982, in the range 1 to 4 μm (Figure 6.33) shows one broad and shallow absorption at 3.9 μm, which is also often seen in the spectra of oxygen-rich stars (Rinsland

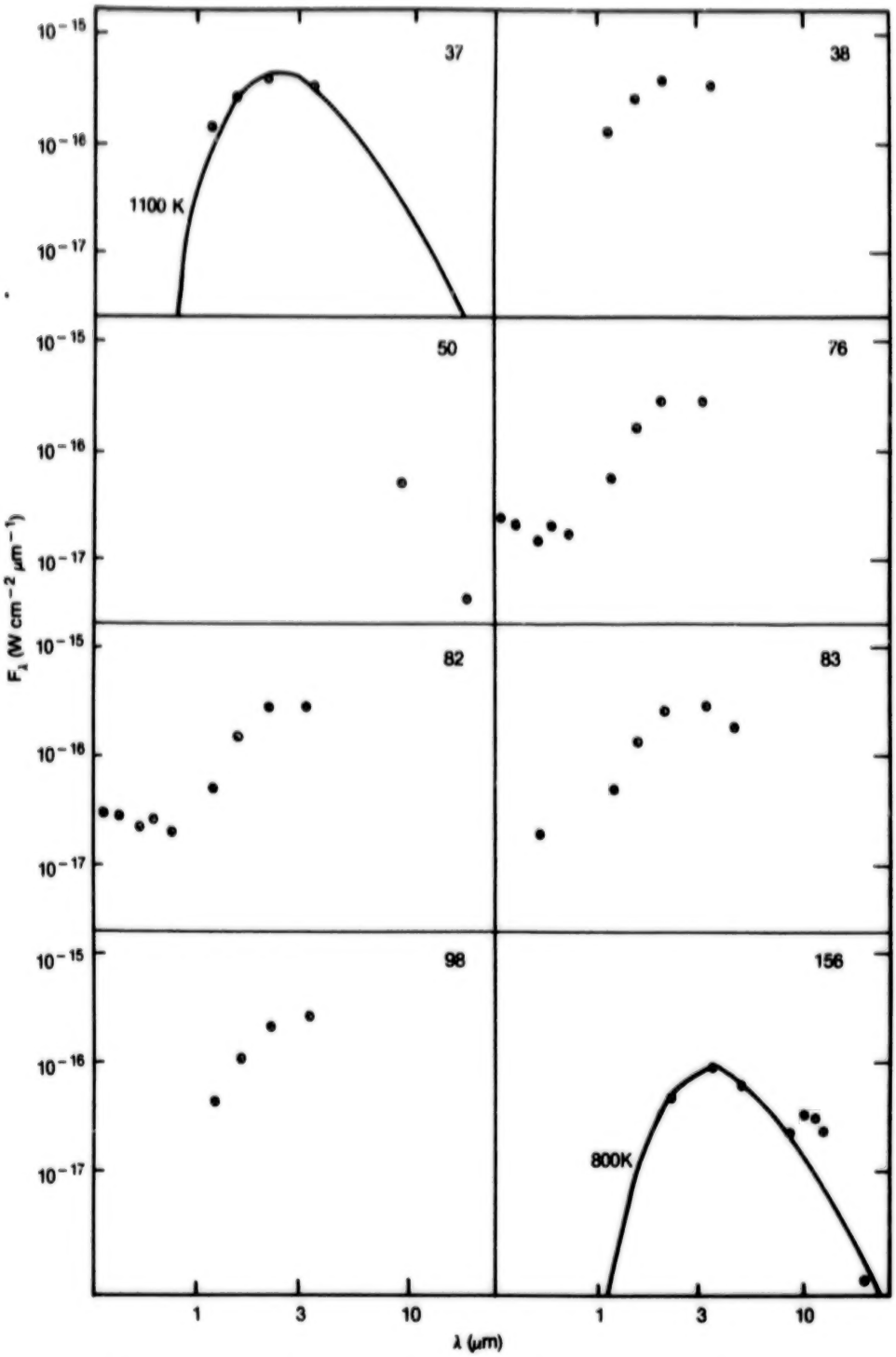


Figure 6-31. Energy distribution of Nova Aql 1982 and comparison with black body curves. The time in days after outburst is indicated.
(from Bode et al., 1984)

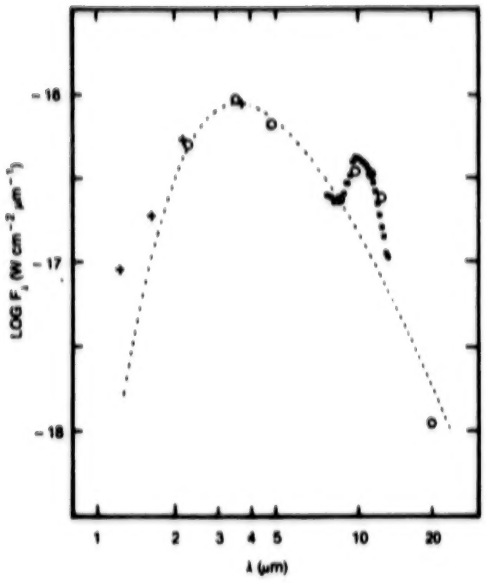


Figure 6-32. Near infrared flux distribution of Nova Aql 1982 on July 3-4. The broken line is an 800 K black body curve. A strong broad emission is present at about 10 μm.
(from Bode et al., 1984)

and Wing, 1982). It is identified with SiO in the gaseous phase. These emission and absorption features suggest that in this case, grains are formed in an oxygen-rich environment. Hence, the formation of graphite grains is improbable. It is more probable that dust grains are formed of iron composites. In fact, if carbon is slightly less abundant than oxygen, oxygen makes composites with the other elements and leaves no free atoms to combine with carbon. The composition of the dust grains in the shell of Nova Aql 1982 is unique among novae studied in the infrared. The sample, however, is still very small. Thermonuclear runaway models suggest that CNO are overabundant in nova ejecta and that C > O (Starrfield et al., 1978). In the case of Nova Aql 1982 it appears, on the contrary that O > C.

These kinds of observations are important because they can give a clue for deciding which is the origin of grains. Two main theories have been proposed. They are a), Grain growth in nova ejecta .d b) Pre existing grains. In case a), we expect that grains reflect the composition of the interstellar medium.

Another emission line was observed in the infrared spectrum of nova Vul 1984 No 2, 140 days after outburst. A very strong emission was observed at 12.8 μm, which is identified with [Ne II].* It is the strongest 12.8 μm line ever observed in an astrophysical source (Gehrz et al., 1985, their Figures 1 and 2). A suggestion for the presence of the same line in the infrared spectrum of V1500 Cyg one year after outburst was made by Ferland and Shields (1978b) in order to explain the excess observed in the 10 μm band.

The Infrared Astronomical Satellite (IRAS) has observed the field of several novae (Table 6.9). The IRAS point source catalogue gives the opportunity to 1) search for emission from novae of different speed classes at various phases of their evolution, and 2) to search at longer wavelengths (12, 25, 60, and 100 μm) than is possible from the ground for finding evidence of very cool dust.

Search for infrared emission from CK Vul 1672, V 1370 Aql 1982 and MU Ser 1983 was negative (Callus et al., 1986).

The spectra of several novae, obtained by plotting the fluxes given in the IRAS Point Source Catalogue versus the wavelength are given in Figures 6.34a and 6.34b. The symbiotic nova RR Tel and the very slow nova V 605 Aql present a flux that is an order of magnitude higher than that from the other observed novae. The flux for V 605 Aql fits the black body curve for T=50 K, while that RR Tel fits the black body curve for T=290 K. The measurements at 60 and 100 μm for the other novae are not reliable. Their maximum flux falls at wavelengths shorter than 12μm indicating color temperature higher than 300 K. Dinerstein (1986) has performed a more detailed study of four classical novae (two relatively young—V 4077 Sgr 1982 and GQ Mus 1983—and two relatively old—FH Ser 1970 and HR Del 1967) with well-determined optical positions, which seem to have true infrared counterparts (Table 6.10 a and b). The criterion adopted for positive identifica-

* Ultraviolet observations have identified a few novae which are Ne-rich. They could belong to a subclass of novae where the white dwarf is a O-Ne-Mg star instead of a CO star.

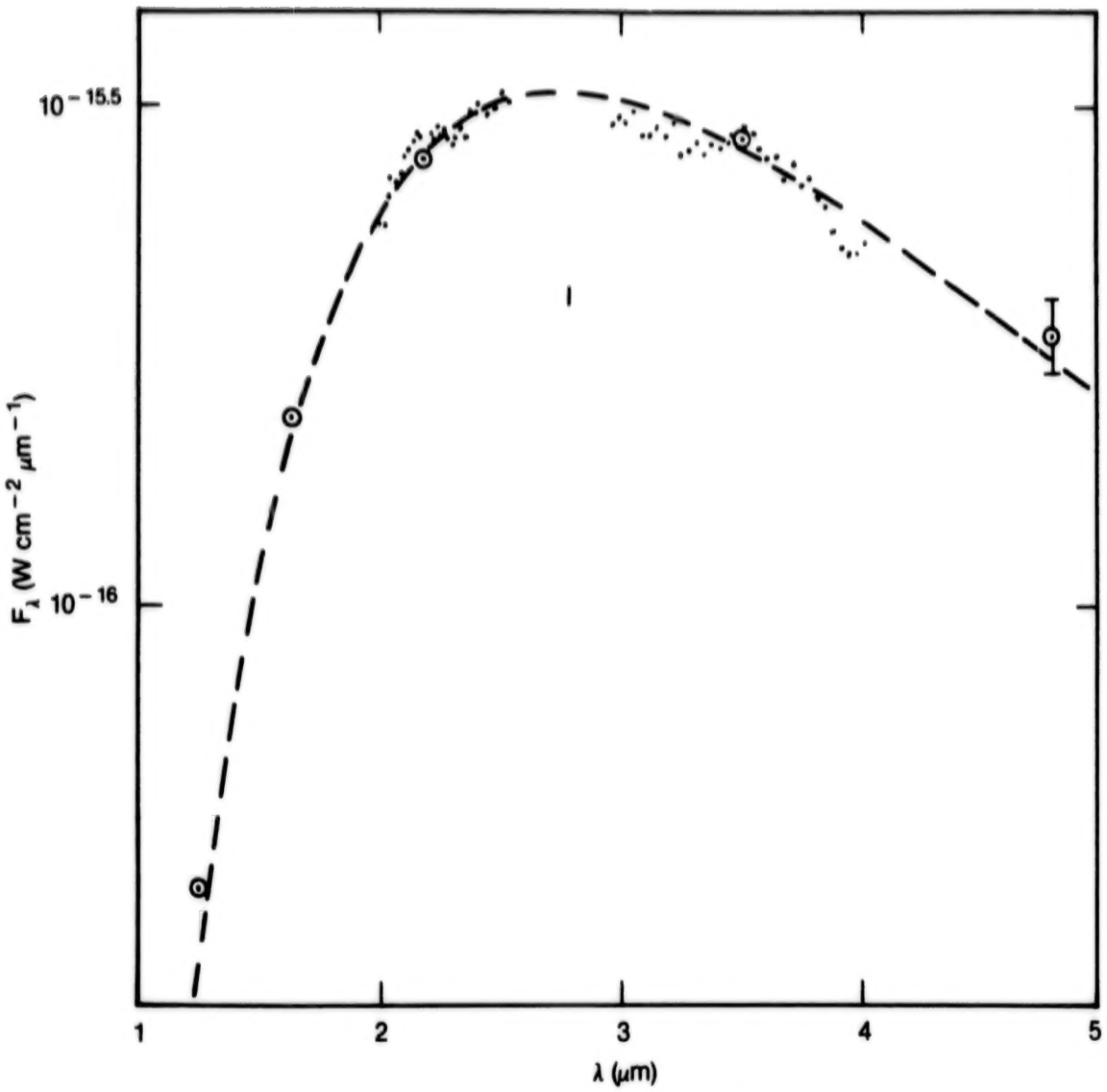


Figure 6-33. Near infrared flux distribution of Nova Aql 1982 on April 18.1, 1982. A broad shallow absorption is present at 3.9 μm.
(from Bode et al., 1984)

tion is that the difference between optical and infrared position is smaller than the quoted error ellipses for IRAS measurements. Search for infrared emissions from other novae was made by coadding the data from the original IRAS survey in order to increase the sensitivity. By this method, positive detection was obtained for DQ Her and for the recurrent nova T CrB. V 4077 Sgr was observed with IRAS 161, 169, and 357 days after maximum. Its spectrum fits the black body curves for T = 1000 K, except at 60 μm when the observed flux is lower (Figure 6.35 from Dinerstein, 1986). It is interesting to remark that the dust temperature apparently does not vary from 6 to 12 months after maximum. From the temperature and the observed flux, and the absolute luminosity derived from the speed class-luminosity relation (Duerbeck, 1981) a rough estimate of the mass of the emitting dust can be made: this one is found of the order of 10^{-16} solar masses.

The fast nova GQ Mus has a flux lower by two orders of magnitude than V 4077 Sgr. By using the technique of coadding fluxes, it is possible to see that its IR spectrum is flat, characteristic of free-free emission, in agreement with previous data obtained from the ground at 5 and 10 μm (Krautter et al., 1984;

TABLE 6.9

Novae observed by the Infrared Astronomical Satellite (IRAS).

NOVA	Outburst	Type of light curve (Duerbeck).	
CQ Vel	1940	Cb	
EU Sct	1949	Cb	
FH Ser	1970	Cb	(1986, Dinerstein)
HR Del	1967	D	(1986, Dinerstein)
KP Sco	1928	A	
LQ Sgr	1897	?	
RR Tel	1948	E	
RS Oph	Rec. N	Ar	
T Cr B	Rec. N	Ar	(1986, Dinerstein)
V 1016 Sgr	1899	?	
V 605 Aql	1919	D	
V 949 Sgr	1914	?	
NQ Vul	1976	Bb	(1985, Evans)
DQ Her	1934	Ca	(1986, Dinerstein)
V 4077 Nova Sgr	1982	Bb	(1986, Dinerstein)
GQ Nova Mus	1983	A	

Whitelock et al., 1984). There is no evidence for a dust component.

This result is a confirmation of the correlation between the speed class of a nova and the efficiency for the formation of a dust shell during its early phases of expansion: slow novae have generally dust shell, while fast novae do not. We remind that HR Del, however, is an important exception to this rule.

FH Ser was detected in the Point Source Catalogue at 12 μm only. Coaddition of the data permits detection at 25 μm too. The resulting color temperature is 500 K. However the dust appears much hotter than expected for an optically thin expanding dust shell of constant thickness. In fact, if the central luminosity source remains constant, the IR flux should decline with time as t^{-2} and the dust temperature as $t^{-1/3}$ (Gehrz et al , 1980a). Hence, for log t = 3.8, T dust should be one order of magnitude lower. It is suggested a contribution from IR fine structure lines.

HR Del was detected in the 25 μm band but not at 12 and 60 μm. This result suggests that we are not observing the thermal continuous spectrum, but rather line emission. We remind that [Ne II] emission at 12.8 μm was observed in Nova Vul 1984 N. 2 and probably also in Nova Cyg 1975. In the case of HR Del, candidate lines falling in the 25-μm band are [SIII] 19 and 34 μm, [NeV] 24 μm, [OIV] 26 μm, and [SiII] 35 μm.

DQ Her was detected at 60 and 100 μm by coaddition of data. A color temperature of 60 K was found consistent with the upper limit at 25 μm. Evans (1985) reports that non survey mode observations give a lower temperature, 34 K.

T CrB is detected in the Point Source Catalogue. However, coaddition of data gives more precise results (Table 6.10 c). The flux at 12 and 25 μm gives a dust temperature of 900 K.

The detection of such hot dust in a recurrent nova is interesting, because it cannot be the remnant of the last outburst that occurred in 1946, but rather an indication of continuous dust-rich mass loss. This is a plausible possibility, because T CrB is a well-known binary system where the M giant member is almost

Table 6.10

TABLE a) Data for nova Sgr 1982.

HCON	Date (1983)	Days after maximum	Uncorrected flux density (Jy) *Color-corrected flux density (Jy)* *IRAS* band [12 μm]	[25μm]	[60μm]	[100μm]	Mass of hot dust ($M_\odot$)
1	25 Mar	161	24.0±2.1 *18.9±1.6*	9.2±1.1 *6.9±0.2*	1.3±0.2 *1.0±0.2*	<2.8 <2.6	4.2 X 10^{-6}
2	1 Apr	169	21.8±1.6 *17.2±1.3*	7.5±0.7 *5.6±0.5*	0.94±0.13 *0.7±0.1*	<2.8 <2.6	3.4 X 10^{-6}
3	7 Oct	357	2.5±0.2 *2.0±0.2*	0.84±0.14 *0.63±0.10*	<0.4 *< 0.3*	<4.0 *< 3.7*	3.8 X 10^{-7}

* Assuming d = 2.5 kpc (see the text).

TABLE b) Catalog and coadded fluxes for detected novae.

Object	λ(μm)	Flux density (Jy) Catalog[a]	Coadded[b]	Corrected[c]
GQ Mus	12	0.24 ± 0.06	0.26 ± 0.03	—
	25	0.31 ± 0.97	0.26 ± 0.03	—
	60	<0.30	0.30 ± 0.04	—
	100	<3.0	<0.72	—
FH Ser	12	0.32 ± 0.04	0.32 ± 0.03	0.29 ± 0.03
	25	<0.30	0.18 ± 0.03	0.14 ± 0.03
	60	<0.60	<0.29	<0.23
	100	<3.7	<1.2	<1.1
HR Del	12	<0.30	<0.08	—
	25	0.36 ± 0.06	0.34 ± 0.03	—
	60	<0.40	<0.11	—
	100	<1.0	<0.32	—

[a] Catalog values corrected for detection rate.
[b] Uncorrected coadded values.
[c] Coadded values corrected for color effects.

TABLE c). Additional coadded novae.

Object	Date	Optical position α(1950)	δ(1950)	Uncorrected flux density (Jy) *IRAS* band [12 μm]	[25 μm]	[60 μm]	[100 μm]
T Aur	1891	$5^h28^m46^s$	+30°24'36"	<0.10	<0.14	<0.16	<0.88
RR Pic*	1925	$6^h33^m32^s$	-62°47'17"	1.22 ± 0.05	0.29 ± 0.02	<0.40	<1.0
T Cor	recurrent	$15^h57^m25^s$	+26°02'32"	0.72 ± 0.03	0.26 ± 0.03	<0.12	<0.34
DQ Her	1934	$18^h06^m05^s$	+45°51'01"	<0.06	<0.05	0.58 ± 0.08	0.61 ± 0.07
V1370 Aql	1982	$19^h20^m50^s$	+02°23'35"	<0.10	<0.10	<0.15	<0.87
CK Vul	1670	$19^h45^m32^s$	+27°11'22"	<0.11	<0.10	<0.37	<3.7
E2000 + 223	?	$20^h00^m39^s$	+22°20'00"	<0.09	<0.09	<0.14	<0.77

* Source at nominal position of RR Pic as given by Wyckoff and Wehinger (1978); appears to correspond not to the nova, but rater to a field SAO star (see the text).

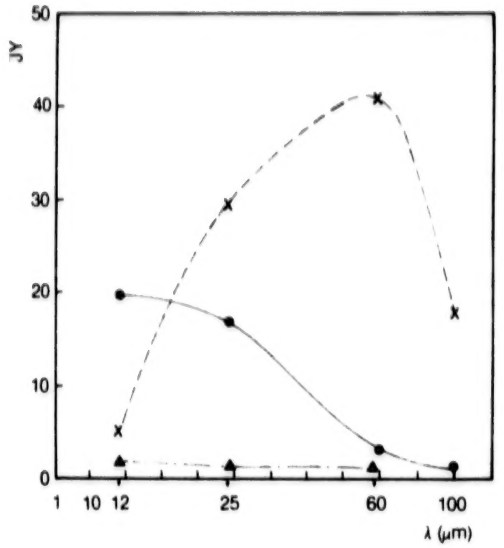


Figure 6-34a) Energy distribution curve for RR Tel (dots), V 605 Aql (crosses) and V1016 Sgr (triangles) from data of the IRAS Point Source Catalogue, 1984. b) the same as a) for CQ Vel (▲), T Cr B (•), T CrB (o, coadded data from Dinerstein, 1986), KP Sco (x). RS Oph (Δ), LQ Sgr (■), FH Ser (●), V 949 Sgr (♦). EU Sct (◊), HR Del( ). The data are from the IRAS Point Source Catalogue.

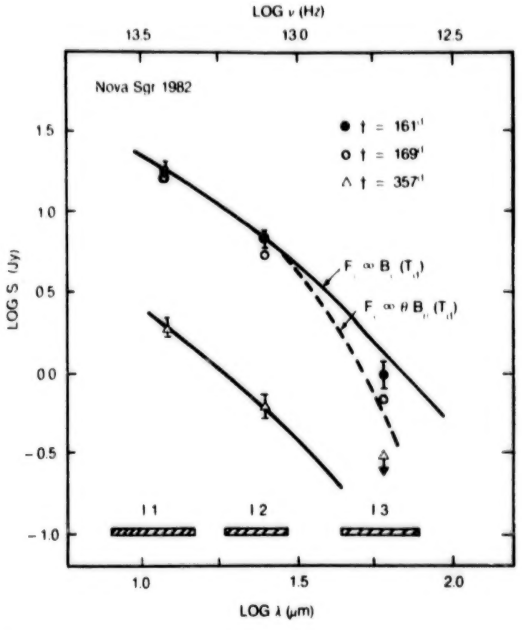
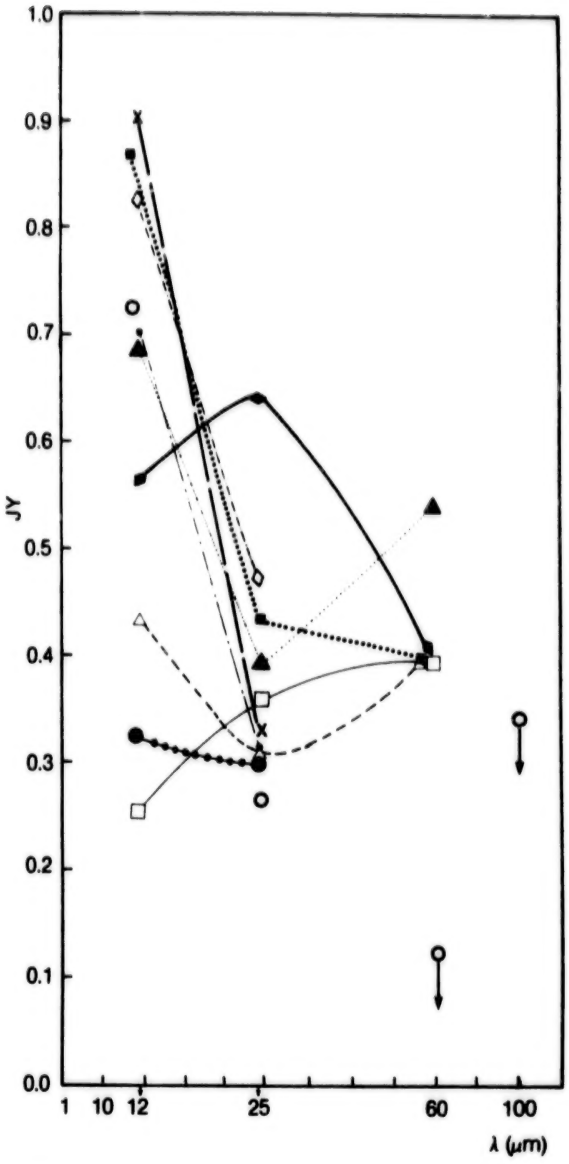


Figure 6-35. Energy distribution curve for Nova Sgr 1982 at three epochs. Black body curve for 1000 K (full line) are drawn through the IRAS data for days 161 and 357 from outburst. The dotted line shows the extrapolated curve for a grain emissivity varying as the frequency between 25 and 60 μm. The hatched horizontal bars indicted the passbands of the IRAS data. (from Dinerstein, 1986)



filling its Roche lobe. We can expect that dust will condense in the envelope produced by the M giant wind.

Evans (1985) reports the results of the observtions of NQ Vul 1976. This nova produced an optically thick dust shell 60 days after outburst. The expected temperature of the shell, derived by assuming that it decreases as $t^{-1/2}$ (case of free expansion, and constant luminosity of the remnant), is 240 K. The observed dust temperature, on the contrary, is 72 +/- 5 K. This result can be understood if we assume that the bolometric luminosity in 1983 was 7.6 x 10^{-3} times that of the constant bolometric luminosity, which was maintained during the first year after outburst.

V. ULTRAVIOLET OBSERVATIONS OF NOVAE AND RECURRENT NOVAE

(written by Selvelli)

V.A. INTRODUCTION

The far UV and X-ray radiation of novae originates from regions that are much hotter than those where the optical and infrared radiation is formed.

Thus, space observations of novae are complementary to the ground-based optical ones, and have given and are still giving a new, fundamental contribution to our knowledge on the nature of these objects.

The importance of UV observations of the continuum and line emission of CVs is manifold:

The bulk of the continuum radiation emitted by *quiescent novae* (QN) falls, with very few exceptions, in the satellite UV spectral region. The study of this radiation provides fundamental information about the physical processes that take place in the hot regions of the system, generally associated with the innermost disk part and the white dwarf surface. Estimates of T, L and of the mass accretion rate $\dot{M}$ in QN, a parameter of basic importance for the understanding of the nova phenomenon, are crucially dependent on the observations in this wavelength range.

For *novae in outburst*, observations of the UV continuum are essential for the determination of the bolometric luminosity and of its variations with time from the first outburst (OB) phases until the nebular stage.

In the satellite UV region of the spectrum, several important, strong resonance lines belonging to abundant elements (such as CIV λ 1550, SiIV λ 1400, NV λ 1240) are observed. Most of these ions lack strong lines in the optical region. High excitation lines produced by recombination such as He II λ 1640 or by fluorescence such as the OIII Bowen nebular lines near λ 3000 are also observed in CVs. Moreover, nebular lines (such as SiIII λ 1892, CIII λ 1909, OIII λ 1666, NIV λ 1486, etc.) are observed in novae during the nebular stage, in recurrent novae, and in a few old novae. The study of all these classes of lines provides valuable information on the excitation processes, the region(s) of line formation, the presence of outflow phenomena, and the intensity of the radiation field in the scarcely accessible EUV spectral range.

If semiforbidden or forbidden lines are present, they provide a useful tool for the diagnosis of the physical conditions (Ne, Te) in the low density regions of the system. In addition, in several cases, especially in novae in the nebular stage, the presence of lines of different ionization states of a given element has also allowed a careful determination of the chemical abundances in the ejecta, a parameter of paramount importance for testing the various theories on the processes that lead to the nova phenomenon and for understanding the evolutionary state of the system.

An accurate determination of the parameters above mentioned, together with the knowledge of their variations with time, can be used to set severe constraints on the various physical models of nova, both for the quiescent phase (Q), in which especially T and L are important, and for the eruptive one, where the dynamic, density, and chemical composition of the ejecta are concerned.

In the present section the behavior of novae in the UV is subdivided in two parts: 1) novae (classical and recurrent) in quiescence, and 2) novae (classical and recurrent) during outburst and post-OB phases. This subdivision might seem somehow artificial but it has a physical ground: UV observations of novae in Q provide important clues on the hot components of their radiation field and, therefore, on those processes that take place near the compact component. Little information is gained about the physical conditions in the outer regions since, with a few exceptions, the envelope ejected at the time of the outburst is no more detectable. On the other hand, observations made during the various OB and post-OB phases are related to the physical structure of the extended pseudophotospere formed in early OB phases,

and to the physical conditions (n_e, T_e, chemical composition, and velocity fields) in the ejected envelope.

V.B. ULTRAVIOLET OBSERVATIONS OF POST NOVAE

The launch of the IUE satellite (Boggess et al., 1978) has opened a new era in the UV observations of post novae, allowing the acquisition of about 200 UV spectra for a dozen objects with m_v up to 15.

Table 6.11 lists the postnovae observed with IUE until November 3, 1987.

Two comprehensive reviews on the UV observations of classical novae by Starrfield and Snijders (1987) and by Friedjung (1988) have recenly appeared. The reader is referred to them for a detailed description of the OB phenomenology and for specific considerations on the abundances of the ejecta.

V.B.1. THE UV CONTINUUM

After correction for the interstellar reddening, which is usually determined from the λ 2200 absorption feature, a general characteristic of most objects is the presence of a hot continuum as indicated by the flux increase toward shorter wavelengths. The origin of this continuum is commonly attributed to the dissipation, through viscous processes in the accretion disk formed around the compact companion, of the gravitational energy released when mass is transferred from the companion onto the surface of the white dwarf.

A possible contribution from the white dwarf itself, still active and hot a long time after the OB, cannot be ruled out, and this possibility must be kept in mind when comparing data with the theoretical models.

The interpretation and modeling of the UV continuum is not a well established operation like, for example, that of fitting a stellar continuum with a model atmosphere. While a steeper slope toward shorter wavelengths is commonly interpreted as an indication of higher temperature, the actual value depends a lot on the details of the model chosen. The accretion disk spectrum is calculated as the sum of the contributions of the individual surface elements (annuli), each one emitting with a different temperature. Generally these models are based on sums of emissions of Kurucz's models or on sums of black bodies. A deeper criticism on the

TABLE 6.11

NOVAE and RECURRENT NOVAE Observed with IUE during Optical Quiescence.

OBJECT	R.A. (1950)			DECL (1950)		
GK Per	03	27	47	+43	44	05
T Aur	05	28	46	+30	24	36
RR Pic	06	35	10	-62	35	49
BT Mon	06	41	16	-01	58	09
CP Pup	08	09	52	-35	12	04
T Pyx	09	02	37	-32	10	47
T Cr B	15	57	25	+26	03	37
V 841 Oph	16	56	42	-12	48	59
RS Oph	17	47	32	-06	41	39
DQ Her	18	06	05	+45	51	02
V 533 Her	18	12	46	+41	50	22
V 603 Aql	18	46	21	+00	31	36
HR Del	20	40	04	+18	58	52

assumptions and limitations of the models and on the advantages and disadvantages of the various methods can be found in Wade (1984) and in Chapter 4.IV.B.

Generally, the power-law UV continua can be better reproduced using sums of contributions of stellar atmospheres. It is rather difficult, however, to produce a good agreement of the models with data that include both the UV and the optical continuum.

Wade (1984) has pointed out that a disk model with a range of temperatures has the same slope, for a given wavelength range, as a model with a single temperature. In other words, it is possible to associate with the flux ratio at, say, 2880 Å and 1460 Å, a corresponding temperature of a model atmosphere. The slope of the classical Lynden-Bell (1969) distribution ($F(\lambda) \propto \lambda^{-2.33}$) is the same as that of a Kurucz model with T=17.000° K, while that of a power-law distribution with α=2.0, quite common for cataclysmic variables (CVs), corresponds to a model with T=14.000° K.

In practice, in several cases, the observed continuum has been fitted equally well by a single component (i.e., a power law or a black body) or by two components (i.e., two black bodies or a black body and a power law). As a consequence, it is not surprising that different authors have proposed for the same objects fits with quite different temperature components; compare, for example, the determination of the temperature in HR Del made by Hutchings (1979a), Krautter et al. (1981), Rosino et al. (1982), Dultzin-Hacyan et al. (1980), and Wargau et al. (1983) (Table 6.12).

It is remarkable that with few exceptions (Verbunt, 1987) the slope of the continua of the different classes of CV s (dwarf novae, novae, nova-like) is rather similar. In the more luminous and best studied old novae (i.e., V 603 Aql, RR Pic, HR Del), the continuum slope in the UV (after correction for reddening) is very close to the slope of an $F(\lambda) \propto \lambda^{-2}$ distribution, in fair agreement with the "standard" $\lambda^{-2.33}$ distribution. (Figure 6.36)

It is not clear, on the basis of the IUE observations alone, how correct it is to extrapolate toward shorter wavelengths the continuum slope found from the IUE observations. Voyager data on V 603 Aql (Figure 6.37) led Carone et al. (1985) to conclude that for this object (but its trend is common to all other CVs observed with Voyager), the rising IUE flux distribution does not continue into the EUV.

It is remarkable that the EUV region (900-1200 Å) is rather flat (flattening begins near λ 1300 Å) for almost all CV s observed, while the EUV continuum (500-900 Å) is extremely weak ($< 5 \times 10^{-13}$). Carone et al. (1985), on the basis of these data, conclude that models that fit the IUE UV fail to fit the EUV region. Exceptions to the general trend $F(\lambda) \propto \lambda^{-\alpha}$ with $\alpha \sim 2$ are GK Per, DQ Her, BT Mon and T Aur.

GK Per (Rosino et al., 1982) is quite peculiar, since its UV continuum, unlike that of other old novae, shows an energy distribution curve that is not peaked toward the extreme ultraviolet but around λ 3600 (figure 6.38), an indication of a lower temperature. However, high excitation and ionization lines are present. Even from the IUE low-resolution spectra, a larger line width than in other old novae can be appreciated. Moreover, unlike in other old novae, there is some contribution in the UV from the K2 IV-V companion. GK Per is also a copious hard-x-ray emitter, and this emission shows a strong coherent modulation with a period of 351 s (Watson et al., 1984). This is a signature of the "intermediate polars" or DQ Her class of CVs, characterized by the presence of a rather strong magnetic field, of the order of 10^5 - 10^6 gauss. Probably, the magnetic field causes the disruption of the innermost disk part, where the missing UV continuum would otherwise be produced. (See Chapters 4.III.F.2.) Another intermediate polar is DQ Her, a system seen at quite high inclination, which shows periodic eclipse phenomena. Its far UV continuum is nearly flat and can be represented by a power law with spectral index α close to zero over the whole UV spectral range.

TABLE 6.12

Temperature Estimates in HR Delphini

		E(B-V)	
Rosino et al	(1982)	0.1	35000+20000 BB'S
Duerbeck et al.	(1980a)	0.19	28000°K BB
Andrillat et al.	(1982)	0.17	$\lambda^{-2.33}$ and BB with T=47000°K.
Friedjung et al.	(1982)	0.17	$F(\lambda) \propto \lambda^{-2.33}$
Hutchings	(1980)	0.10-0.15	16000°K model atmosphere.
Dultzin-Hacyan et al.	(1980)	(0.18)	40000°K BB plus power-law (far UV)
Krautter et al.	(1981)	0.15	45000°K+25000°K BB or power law with α=-2.09
Hutchings	(1979a)	0.23	15000°K or 50000°K BB plus power-law at λ 1500 A.
Wargau et al.	(1982)	0.15	80000°K plus 15000°K BB's.
<u>The same for V 603 Aql.</u>			
Dultzin-Hacyan et al.	(1980)	0.07	50000°K plus 8000°K BB's.
Duerbeck et al.	(1980a)		30000°K BB
Krautter et al.	(1981)	0.07	45000°K plus 25000°K BB or power-law with α=-1.99.
Wargau et al.	(1982)	0.00	200000°K plus 11000°K BB's.
Lambert et al.	(1980)	0.07	Thick disk
Ferland et al.	(1982a)	0.07	Power-law: $\nu^0 + \nu^{0.5}$.
<u>The Same for RR Pic</u>			
Krautter et al.	(1981)	0.01	Power-law with α=1.81 or 40000°K plus 28000°K BB's.
Wargau et al.	(1982)	0.03	90000°K plus 14000°K BB
Rosino et al.	(1982)		33000°K plus 22000°K BB's.
Duerbeck et al.	(1980a)		27500°K BB.

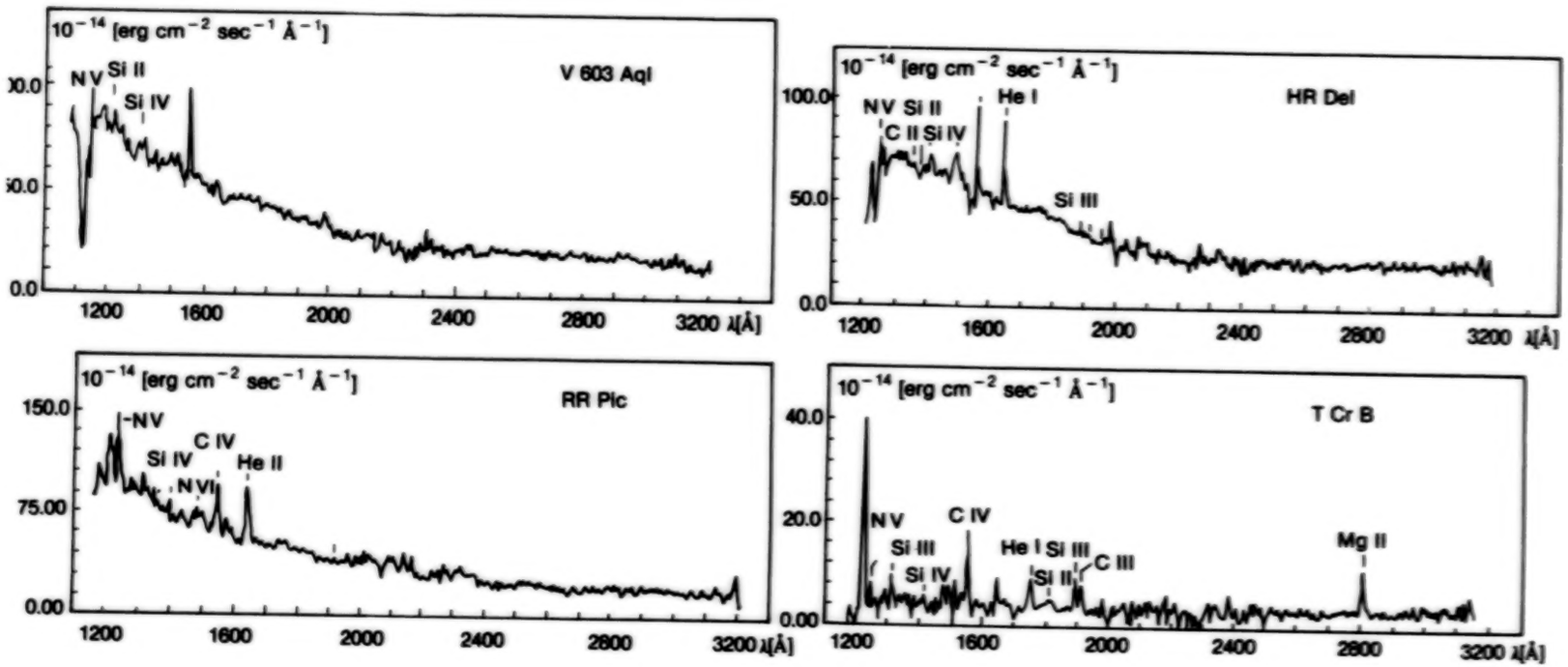


Figure 6-36. The UV continua of the brightest old novae V 603 Aql, HR Del, RR Pic, and of recurrent nova T Cr B. (from Krautter et al., 1981)

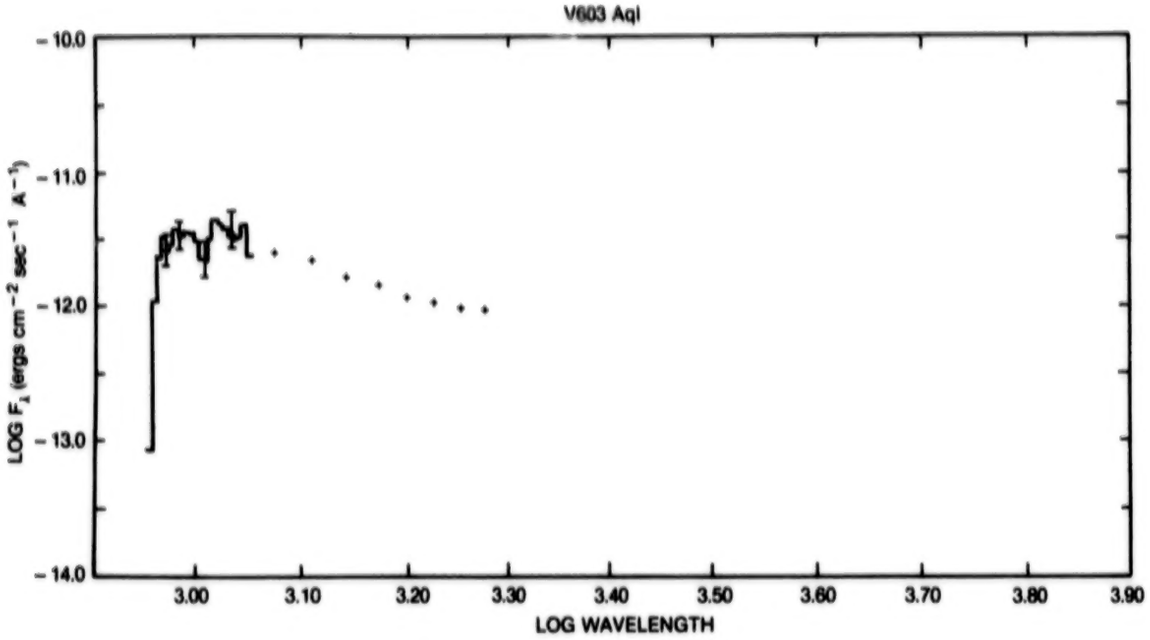


Figure 6-37. Voyager observations of V 603 Aql, dereddened by 0.07.
(from Carone et al., 1985)

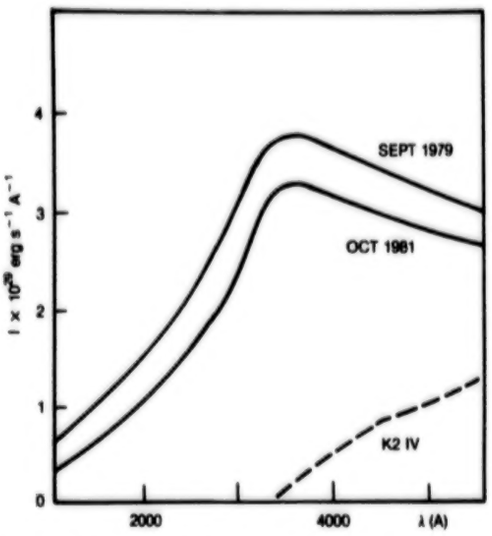


Figure 6-38. The continuum distribution of GK Per at quiescence.
(from Rosino et al., 1982)

It is tempting to ascribe this peculiarity in the continuum slope in DQ Her to an inclination effect that causes the disk to be seen in its outermost coolest components. This suggestion is supported by the nearly flat continua of BT Mon (i~84°) (Figure 6.39) and T Aur (i~68°), and is in agreement with an optical study of Warner (1986c) who has found a strong correlation between the absolute visual magnitude and the inclination of the system. Warner has interpreted this result in terms of darkening of the disk limb when viewed at different inclination angles. Verbunt (1987), however, from a statistical study of the UV spectra of several CVs has concluded that the continuum slope does not show a definite dependence on the system inclination; his disk models show instead that the slope of the continuum depends strongly on the white dwarf mass.

V.C. THE MASS ACCRETION RATE AND LUMINOSITY OF OLD NOVAE

The disk luminosity is linked to the mass accretion rate $\dot{M}$, a quantity whose knowledge is essential for understanding the evolution of the system and physics of the outburst. In principle, $\dot{M}$ can be determined after a comparison of the slope of the continuum with theoretical models: a steeper UV slope indicates an higher $\dot{M}$. Unfortunately, as pointed out by Verbunt (1987), theoretical disk models show that the slope of the continuum depends also, and critically, on the white dwarf mass. Because of this, the $\dot{M}$ values reported in the literature might be affected by this uncertainty if the white dwarf mass was not previously well determined.

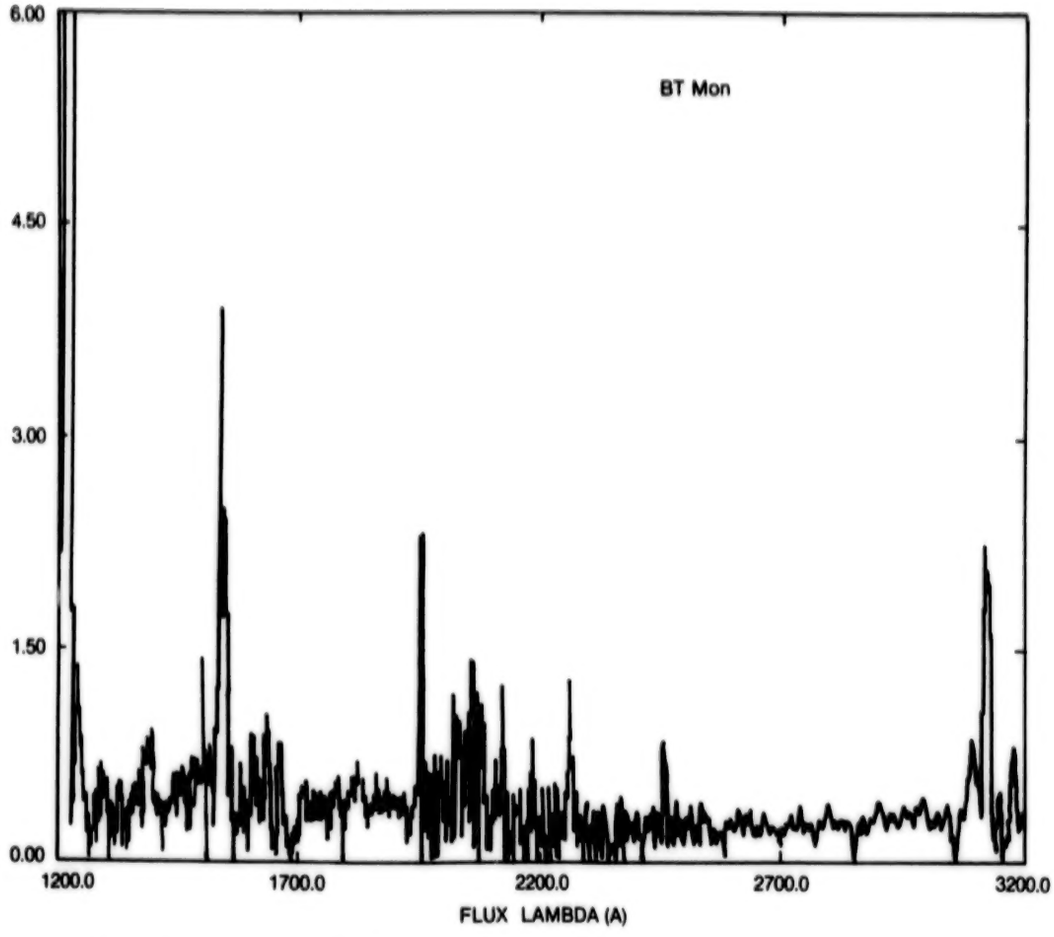


Figure 6-39. The flat continuum of BT Mon (i=90°).

An alternative, less model-dependent method for the determination of $\dot{M}$ is simply based on an estimate of the accretion luminosity from the observed UV (mainly) and optical fluxes. Once the luminosity is known, a lower limit for $\dot{M}$ can be assigned from the relation $L(disk)=1/2\ G\dot{M}M\ R^{-1}$ where $M \sim M_{\odot}$. (See also Chapter 4.II.C.2.)

The considerable differences in the L(UV) estimates for the same object by different authors are due to two main reasons: 1) uncertainties with the distances, and 2) uncertainties in the fitting of the observed continua with models. Wade (1984) has shown that luminosities deduced from fits with stellar atmosphere models are much lower (by factors from 10 to 100) than those obtained from blackbody fits to the same data.

The uncertainties in L are reflected in the uncertainties in $\dot{M}$, and quite serious discrepancies between the $\dot{M}$ values proposed in the literature for the same objects are present. Thus, for HR Del, Friedjung et al. (1982) derived $\dot{M} \sim 10^{-8}\ M_{\odot}\ yr^{-1}$, while Krautter et al. (1981) found $\dot{M} \sim 4.6\ 10^{-8}\ M_{\odot}\ yr^{-1}$, and Hutchings (1979a) gave indication of a value in excess of 10^{-8}. Kenyon and Webbink (1984) have suggested determining $\dot{M}$ by fitting the observed flux at different wavelengths to models of disks seen at different inclinations and emitting like the sums of blackbodies. With this method, they obtained for HR Del a $\dot{M}$ of the order of $4 \times 10^{-8}\ M_{\odot}\ yr^{-1}$ in fair agreement with Krautter's et al. (1981) value, which is a lower limit based on the "observed" UV luminosity only.

A compilation of mass accretion rates can be found in Verbunt and Wade (1984).

V.D. THE LINE SPECTRUM OF OLD NOVAE

A common characteristic of the line spectrum of cataclysmic variables in quiescence is the presence of strong emission lines of high excitation character like NV 1240, SiIV 1400, CIV 1550, and HeII 1640.

Intercombination lines like NIV 1486, NIII 1750, SiIII 1892 and CIII 1908; or lines of low excitation like OI 1303, CII 1335, and resonance lines of SiII are generally much weaker or absent except in the case of the recurrent novae T Cr B and RS Oph and in the case of those few old novae who still show evidence of the shell ejected at the time of the outburst. Table 6.13 lists the most common emission lines usually found in old novae.

TABLE 6-13

List of common UV Lines in Post-Novae.

λ	ION		λ	ION	
1240	N	V	1640	He	II
1260	Si	II	1750	N	III
1300	Si	III	1815	Si	II
1335	C	II	1860	Al	III
1400	Si	IV	1892	Si	III
1486	N	IV	1909	C	III
1550	C	IV	2800	Mg	II
1575	Ne	V			

V.D.1. P CYG PROFILES IN OLD NOVAE

Krautter et al. (1981) have reported the presence of P Cyg profiles in the spectra of the old novae HR Del, RR Pic, and V 603 Aql. Although the presence of some of the P Cyg profiles is questionable (e.g., λ 1640 in HR Del, CIV in RR Pic, etc.), they are clearly present in HR Del at CIV (Figure 6.40). The presence of such profiles indicates that material is still outflowing a long time after the outburst, and this poses several questions about the nature of the mechanism that originates the wind and the duration of the processes related to the outburst. Hutchings (1979a) has reported marked differences in the P Cyg profiles in the several spectra available. He suggested the presence of two absorption components of varying strength that could be consistent with mass loss in the form of a spiralling wind.

A more complete set of observations was obtained by Friedjung et al. (1982) who related the variations to the orbital phase of the observations. (See also the next section.)

Krautter et al. (1981) estimated the mass loss rate in HR Del by fitting the absorption component of the CIV doublet with the grid of theoretical profiles of Castor and Lamers (1979). Assuming a spherically symmetric wind and all carbon=CIV and taking V edge = 4,000 km s^{-1}, they derived $\dot{M} \sim 2.6\ 10^{-11}\ M_{\odot}\ yr^{-1}$. The uncertainty in this value is due to the rather crude assumptions that have been made. The

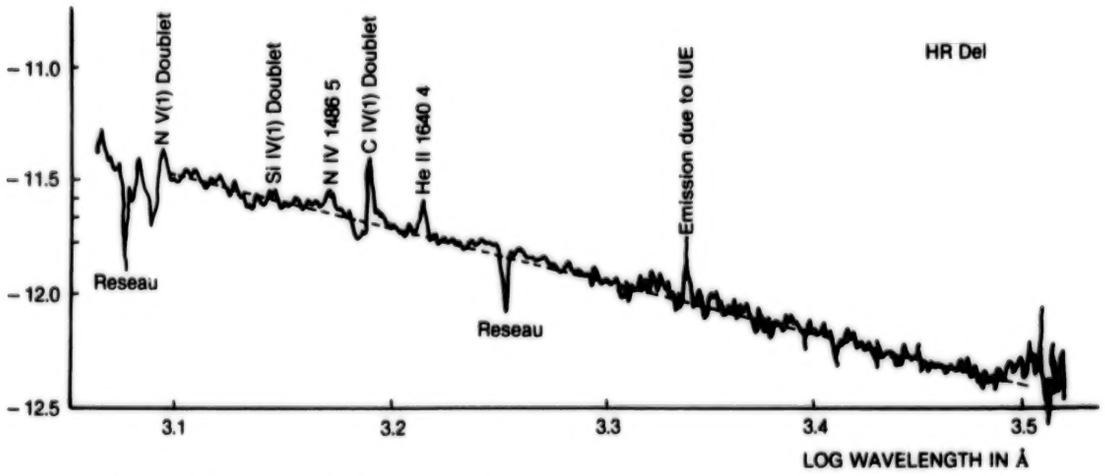


Figure 6-40. The P Cyg profiles in the spectrum of HR Del.

terminal velocities in the HR Del wind are of the order of 3 x 10^3 kms^{-1} for CIV. Hutchings (1979) and Rosino et al. (1982) give 2320 km s^{-1}, while Dultzin-Hacyan et al. (1980) give 2,900 and 3,500 km s^{-1} and Krautter et al. (1981) give 4,000 km s^{-1}. For NV Hutchings gives 2,800 km s^{-1} and Rosino gives 2,900 km s^{-1}. It must be pointed out, however, that in the low resolution IUE mode, a wide Ly α absorption of circumstellar or interstellar origin, which can extend up to λ1230, could mimic a shortward displaced absorption for the NV doublet, thus contaminating the true one.

In a study of dwarf novae, Cordova and Mason (1982) have suggested the presence of a conical outflow, perpendicular to the disk plane. They have also suggested that the mechanism responsible for the wind is radiation pressure in the resonance lines, as in hot-star winds. It is not clear, however, if this model might be applied to HR Del and why among old novae such P Cyg profiles have been clearly detected only in HR Del. (See also Chapter 4.IV.D.)

A marginal wind detection has been claimed by Cordova and Mason (1985) in the CIV doublet of DQ Her also. A comparison of the eclipse profile of CIV with the out of eclipse one showed that the latter is fairly symmetric, while the former appears to be skewed to the red. They suggest that a wind may be present but contributes only part of the total line emission.

If the wind geometry in old novae is similar to that of dwarf novae in OB, this result seems to contradict the indication by Cordova and Mason (1985) that P Cyg profiles in dwarf novae are more common in objects with low inclination (unlike DQ Her).

Recent observations of V 841 Oph (Cassatella et al., 1988), indicate the presence of P Cyg profiles in its UV spectrum also (Figure 6.41).

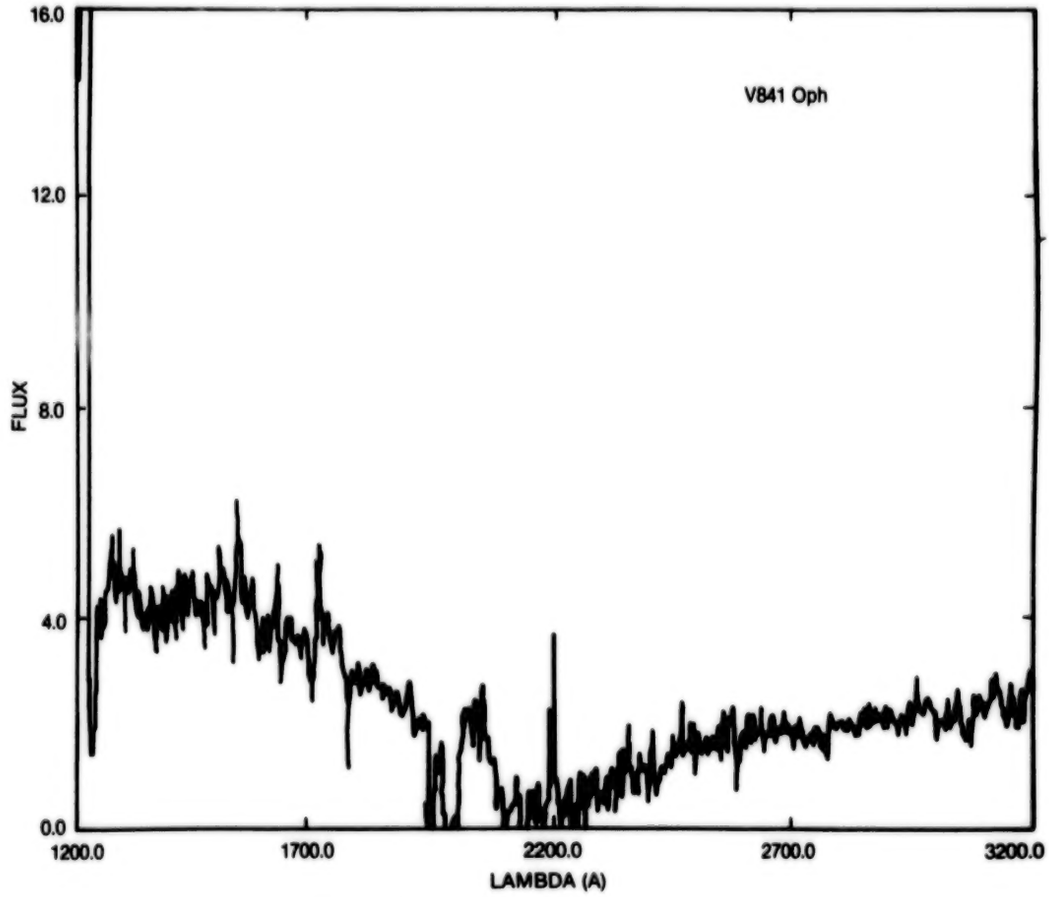


Figure 6-41. The UV spectrum of the post-nova V 841 Oph.

V.D.2. HIGH-RESOLUTION LINE PROFILES

Observations of emission line profiles in the UV spectra of old novae in quiescence are limited by the IUE performance. These objects are fainter than m_v 11.5, and although very hot, their far UV flux does not permit IUE observation in the high-resolution mode. Such observations would be of invaluable importance for the acquisition of high-resolution profiles, which would allow a deeper study of the region where the lines are formed and of their dynamical structure. V 603 Aql, the brightest nova remnant, is the sole object in this class that has been just barely observed in the high-resolution mode (Selvelli and Cassatella, 1981). The two spectra, (SWP + LWR) although at about 50% of the optimal exposure, clearly show emission lines of Si IV, CIV, and He II. These emissions are wide and shallow and centered on the nominal wavelength (Fig. 6.42). There is no trace of any P Cyg absorption. Their FWHM indicates v~1,800 km s^{-1} and FWZI give, v ~ 4,000 km s^{-1}. These profiles and velocities are those expected by lines formed in the innermost region of an accretion disk orbiting a white dwarf.

It is notable that over the whole spectrum, there is no evidence of sharp (and more easily detectable) nebular lines. This indicates that the envelope ejected at the time of the outburst has by now vanished.

V. E. THE UV SPECTRAL VARIATIONS

The time resolution between successive IUE spectra has an intrinsic lower limit of about 20 minutes also if the exposure time is much shorter, because of the cameras read-preparation times. However, even when the proper exposure time (typically 20 minutes for the brightest old novae) is added, still a rather satisfactory time resolution as compared with the orbital period can be achieved.

V603 Aql. Rahe et al. (1980) and Drechsel et al. (1981) have detected variations of the emission intensities and of the continuum both in the optical and in the UV range. These variations seem to be related to the orbital period. The intensity of the CIV, SiIV, and HeII emissions is

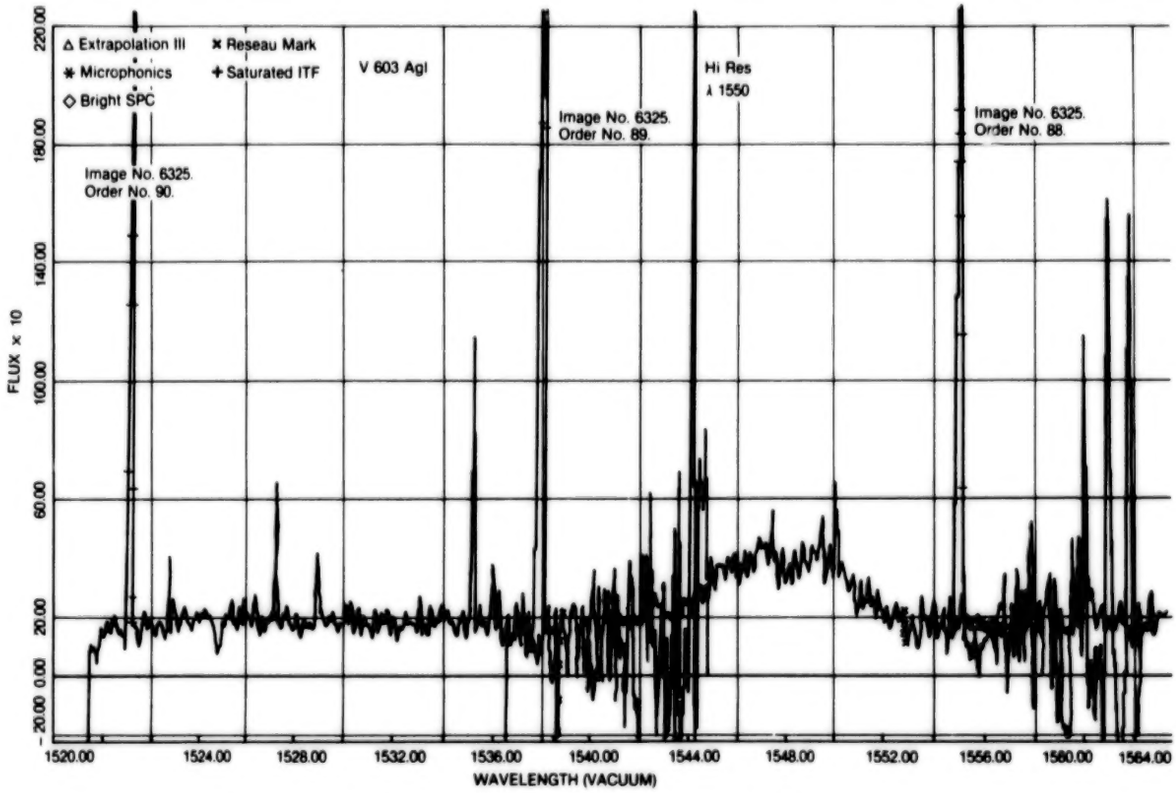


Figure 6-42. The high–resolution profile of the C IV 1550 dublet in V 603 Aql.

highest during maximum light at phase 0.5, and lowest near orbital phase 0.0. Similar results were found by Selvelli and Cassatella (1981) on less homogeneous material. Both Drechsel et al., and Selvelli and Cassatella have resorted to occultation or partial eclipse effects to explain the variations, but the small inclination of the system sheds serious doubts on this hypothesis.

Selvelli and Cassatella (1982) have also studied the variations in the λ 2000 – 3200 region. Maxima in the line emission and continua occur near phase 0.0, in disagreement with the previous results. This all suggests that the variations might be due to transients, and not to phase-related phenomena.

The results of Hutchings (1979a) suggested UV spectral variations in *HR Del*, although a quite large scatter is shown in his graphs. Andrillat et al. (1982) have considered these effects as phase-related. They found minima near phase 0.0 both in the 1200 - 2000 and in the 2000 - 3200 regions. In a study based on more homogeneous material, Friedjung et al., (1982) detected clearly phase-related variations both in the continuum and in emission and absorption lines. Fig. 6.43 (from Friedjung et al.) gives the observed variations. Inspection of this figure shows a periodic variation in the NV emission with a minimum around phase 0.9. The CIV emission seems to vary in antiphase with respect to NV, but possibly, its variations are more complex. A minimum seems to be present in all cases, except for CIV, around phase 0.9 both for lines and continuum. Note that phase 1.0 is that of maximum radial velocity.

The authors interpret the minimum as due to an occultation of the central part of the disk by a splash where the stream of accreted gas reaches the disk. The wind, which is responsible for the P Cyg profile variations, has evidently more complex variations.

A behavior similar to that of V603 Aql and HR Del is also present in *RR Pic*. Significant variations, both in the lines (by a factor up to six) and in the continuum (by a factor 1.5) are clearly

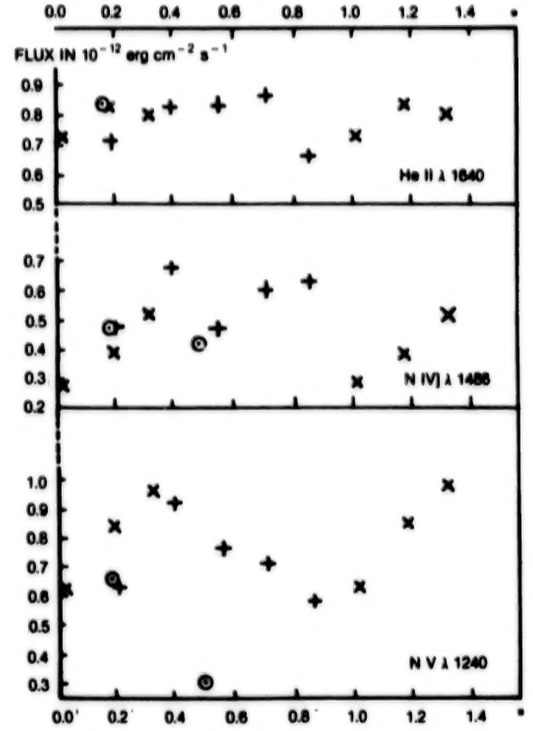


Figure 6-43. The variations with phase of the emission line intensities in a series of successive IUE spectra of HR Del.
(from Friedjung et al., 1982)

evident in spectra taken by Selvelli (1982) in a close sequence of alternate exposures with the SWP and LWR cameras during a 6-hour monitoring. The observed variations are in disagreement with the photometric behavior in the optical, reported by Vogt (1975) and by Haefner and Metz (1982). In addition, UV spectra taken at nearly the same phase in two different cycles show very different characteristics, thus confirming the reality of transient phenomena. It seems reasonable to suppose that both phase-related and transient phenomena contribute to the observed spectral variability, and that the transient phenomena are more evident in the UV region since the three best studied objects present this behavior. These results are in agreement with the conclusion of Verbunt (1987) that all systems for which time-separated observations are available show UV variability with time scale of the order of hours. He also suggests that these variations are probably not of orbital origin, since observations at different periods but at the same orbital phase show significant spectral changes.

V.F. CONCLUDING REMARKS

To conclude this section on classical old novae, it is important to emphasize that of the dozen old novae that are accessible to IUE, only a few have been studied in some detail. Selection effects could be very serious, considering the scarceness of the sample, and thus we might risk drawing general conclusions (for example, on L , T, $\dot{M}$, etc.) based on the behavior of the more luminous members of the class. It is therefore mandatory to improve these rather poor statistics by observing carefully all objects that are accessible to IUE.

V.G. THE UV SPECTRUM OF RECURRENT NOVAE IN QUIESCENCE

Recurrent novae represent a small class of objects whose recurrence time between outbursts is intermediate between classical novae and dwarf novae.

The major problem for the understanding of recurrent novae is the nature of their outbursts and the nature of the accreting objects. Recently, Webbink et al. (1987) have reviewed the properties of the rather different members of the "class" and have suggested the existence of two subclasses on the basis of their OB mechanisms:

1)Those powered by TNR on a white dwarf (T Pyx and U Sco) as in classical novae. In this case theoretical consideration (Starrfield et al.,1985) show that in order to produce outbursts with recurrence time scales compatible with those of T Pyx , the white dwarf must be very massive (M_{wd}~1.38 $M_{\odot}$) and the accretion rate must exceed $2x10^{-8} M_{\odot}$ yr^{-1}, that is, much higher than accepted for classical novae.

2) Those powered by the transfer of a burst of matter from the red giant onto a main sequence companion (T Cr B and RS Oph). In this case, the inter outburst accretion rate is expected to be rather low.

T Pyx. This regularly recurrent nova (P_r 20 ±1 years) has been observed by Bruch et al. (1981). Because of its faintness and of the severe reddening (0.35), the IUE spectrum was underexposed. However, a hot continuum is clearly evident, together with emission lines of CII, CIV 1550, HeII 1640, and NIII 1750. It is notable that, unlike in other recurrent novae (T Cr B and RS Oph), the MgII doublet is absent. This is interpreted as indication of the absence of the red giant in the system.

The three existing sets of IUE data of T Pyx in 1980, 1986, and 1987, show that the UV continuum is very hot (Fig. 6.44) and practically constant, an indication of a very high accretion rate, which seems to support the thermonuclear powered model. The suggestion by Webbink et al. (1987) that the OB of T Pyx is nuclear powered is based mainly on the difficulty encountered by the accretion-powered model in explaining the behavior of T Pyx during the OB phases and the dominance of a hot continuum source during quiescence, although some unresolved problems remain with the luminosity and the unusually blue color at minimum.

The recurrent nova *T Cr B* has been observed from the early phases of IUE's life until very recently (Cassatella et al., 1986). The UV continuum distribution can be represented, at the various epochs by a single power-law spectrum $F(\lambda) \propto \lambda^{-\alpha}$ over the entire IUE range, α ranges from 0.7 to 2.2 with a mean value of about 1.3.

In general, when the flux is higher, the continuum is steeper. A distinctive peculiarity of T Cr B is that significant UV variations correspond to very small changes in the visible light. The UV emission line spectrum shows wide range of ionization and excitation with the presence of ions from OI to NV and HeII. Radial velocity studies of Kraft (1958), Paczinski (1965), and more recently by Kenyon and Garcia (1986) have indicated that the companion of the red giant is a main sequence star, since its mass is about 1.8 $M_{\odot}$. However, the UV and X-ray observations seem to suggest a white dwarf companion. In fact:

1) The disk luminosity is radiated mostly in the UV, with a negligible contribution to the optical, contrary to what is expected from a

main sequence accretor.

2) A quite strong HeII λ 1640 emission generally present, with an average luminosity of 1.3 x 10^{33} erg s^{-1}. This emission is an indicator of temperatures of the order of 10^5 °K

3) The x-ray luminosity in the range 0.16 to 4.5 Kev is of 5 x 10^{31} erg s^{-1}, with the same order of magnitude of the few other detections of "classical" novae in quiescence. (Cordova et al. 1981b).

4) A recent high-resolution spectrum (Selvelli et al. 1988) has shown that the CIV λ 1550 emission is wide and shallow. The half-width at zero intensity (HWZI) indicates a velocity larger than 1500 km s^{-1}, and the shape resembles that observed in the CIV λ 1550 emission in a high-resolution spectrum of V 603 Aql. See Chapter 9 for a more expanded discussion.

RS Oph. In the UV, it is quite faint because of the strong reddening E(B - V) = 0.73, and only underexposed spectra were obtained (Rosino et al., 1982). The continuum is quite flat (Fig. 6.45), and the only spectral feature that is clearly evident is the NIII λ 1750 semi-forbidden line. CIV, HeII, and the other common emissions are not detectable. (See next section for the UV spectrum in outburst).

V.H. UV OBSERVATIONS OF NOVAE AND RECURRENT NOVAE IN OUBURST

Unlike old novae, for which there is a substantial similarity in the UV spectroscopic signatures (a hot continuum and high excitation lines), the UV behavior of novae during the outburst phases can hardly be reconducted into a common scheme. In this respect, each nova outburst represents a unique phenomenon with its own specific characteristics.

Since the launch of IUE, a dozen novae have been observed in the UV during their decline after the visual maximum. Only in a few cases was the nova monitored in the various post maximum phases until the detection limit.

Table 6.14 lists all novae and recurrent novae in OB observed with IUE. The studies of these observations were generally aimed to obtain information on the physical and chemical parameters of the ejecta (from spectra in the nebular phase) and on the dynamic and energetic of the outflow

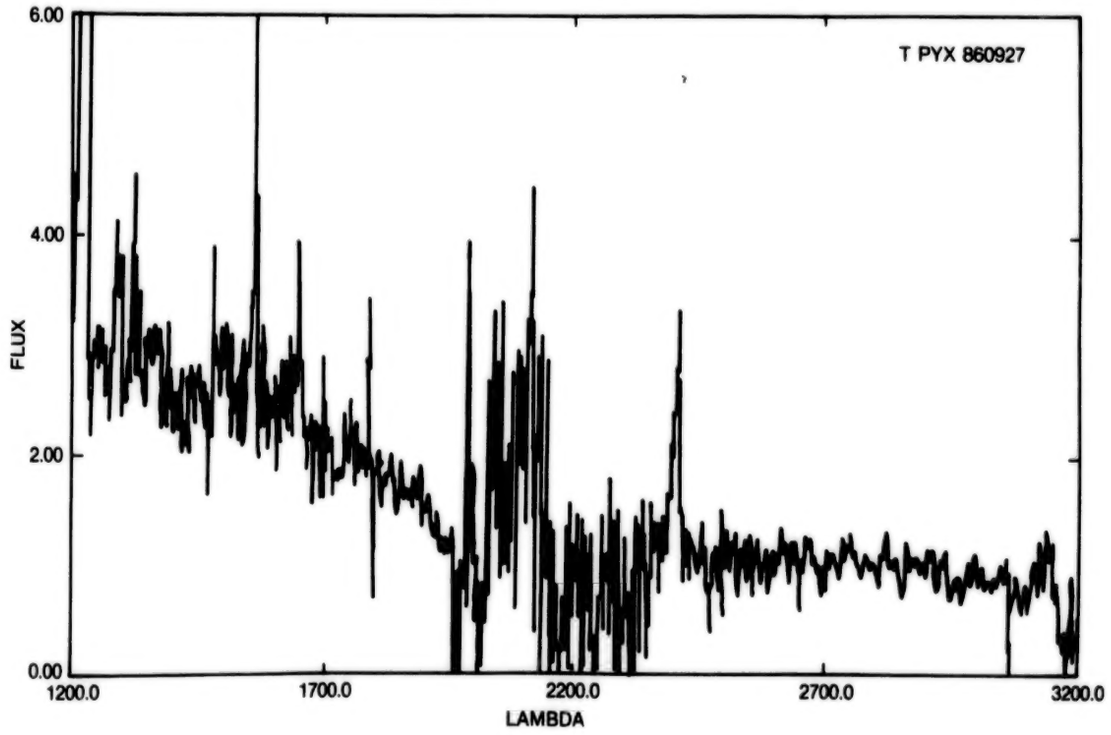


Figure 6-44. The UV spectrum of the recurrent nova T Pyx.

phenomenon.

For some of these objects enough IUE data have been available to permit an adequate study of their spectroscopic changes in the various phases following the OB. In particular, these data have made it possible to obtain reliable estimates of the bolometric luminosity and an accurate determination of the outflow velocities in the ejected envelope.

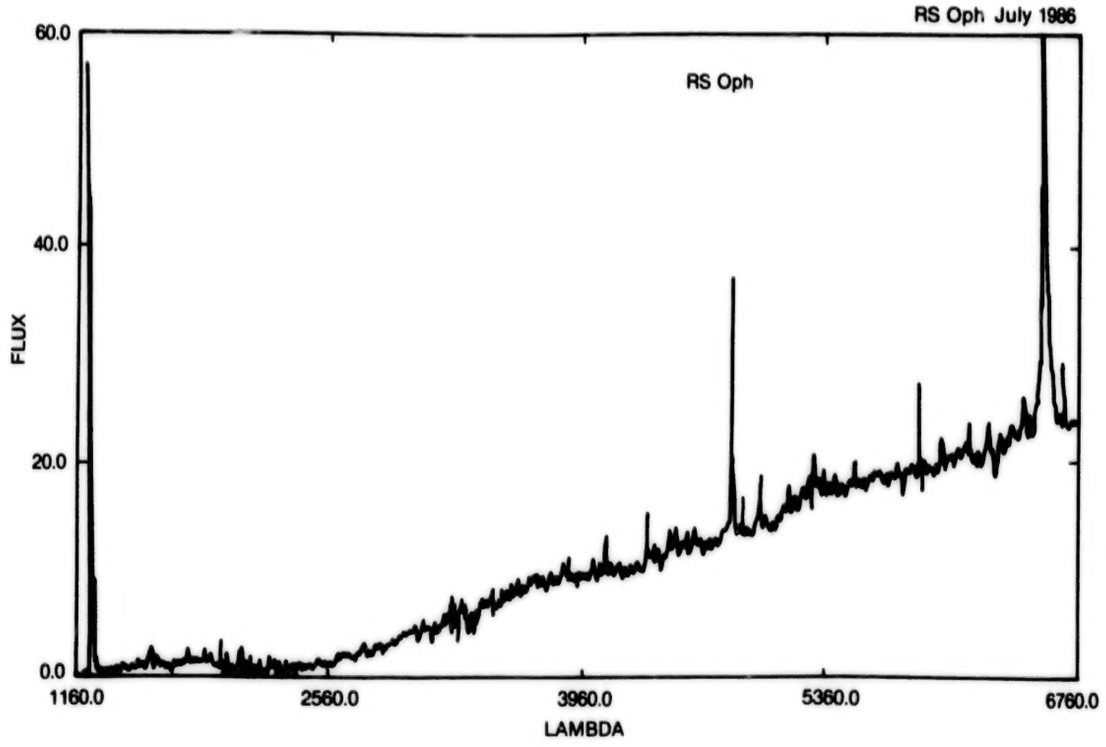


Figure 6-45. The spectrum of the recurrent nova RS Oph from 1200 to 6800 A. (from Cassatella et al., 1988)

TABLE 6.14

NOVAE and RECURRENT NOVAE in Outburst Observed with IUE until 1987.

OBJECT			R.A. (1950)			DECL (1950)		
NOVA	Mus	1983	11	49	35	-66	55	39
NOVA	Cen	1986	13	17	42	-55	34	30
U	Sco		16	19	37	-17	45	43
RS	Oph		17	47	32	-06	41	39
NOVA	Ser	1983	17	53	02	-14	00	56
V 394	Cr A		17	56	58	-39	00	27
NOVA	Cr A	1981	18	38	33.6	-37	34	09
V 4077	Sgr	1982	18	31	33	-26	28	27
NOVA	Her	1987	18	41	26.6	15	16	15
V 1370	Aql	1982	19	20	50.1	+02	23	35
PW	Vul	1984-1	19	24	03.5	+27	15	55
NOVA	Vul	1984-2	20	24	40.5	+27	40	48
NOVA	Cyg	1978	21	40	38	+43	48	10
NOVA	And	1986	23	09	47.5	+47	12	00

Moreover, observations made during the nebular stage have made possible a reliable determination of the chemical abundances in the ejecta. This parameter is of paramount importance for testing theories on the nova phenomenon and for understanding the evolutionary state of the system.

The physics of the nebular state is relatively simple and quite well understood. The methods and principles of the studies of gaseous nebulae have been successfully applied also to the study of the symbiotic stars, whose emission spectra are nebular-like; see the recent review by Nussbaumer and Stencel (1987) for details and the Section VII on the envelopes in this chapter.

The most important features of novae in outburst in the UV are reported here.

FH Ser, the first nova to be detected in the UV, was observed with OAO-2 over an interval of 53 days, starting about the time of visual maximum, and another observation was made about a year and a half later. (Code, 1971).

During the observed period, the spectrum changed from an absorption-like, spectrum, similar to that of an F star, to a strong emission-like spectrum. While the star in the optical was steadily fading in luminosity, both the UV continuum and the UV emission lines continued to brighten.

During the first 60 days after the OB, the energy distribution from 1000 to 6000 Å indicated an approximately constant integrated luminosity, where the decline in the optical was compensated by a progressive shift toward the UV. These results supported a model of nearly constant bolometric luminosity in novae after outburst.

V 1500 Cyg 1975 was observed with Copernicus just after maximum and was too cool to be detected at λ 2700 A (Jenkins et al, 1977). It became unobservable for Copernicus about 100 days after maximum. Measurements made after that date with ANS made it possible to derive that the bolometric luminosity at maximum and 100 days after outburst varied by a factor of 20, while the visual luminosity (measured in the y band) decreased by a factor of 6600, and the effective temperature increased from about 10,000 to 65,000 °K.

NOVA Cyg 1978 was the first nova observed with IUE: thanks to the capability of the IUE Observatory of a prompt reaction to any event considered worthy of observation, it was monitored from the first phases immediately following the outburst. The first IUE image was taken on September 14, 1978, by Cassatella et al. (1979) one day after visual maximum. The continuum looks like that of an F-type supergiant.

The main line features are FeII absorptions and emission of FeII, CrII, MnII and OIII (Bowen fluorescence mechanism). The MgII doublet consists of a P - Cyg profile with a strong emission component. A high-resolution spectrum taken two weeks later shows the same emission features with widths indicating expansion velocities of about 400 Km s^{-1} .

The OIII lines show larger (525 Km s^{-1}) expansion velocities, while the two components of the MgII 2800 doublet appear blended due to their broadness (FWHM 815 km s^{-1}). The narrow FeII and MnII absorptions of this high-resolution spectrum were studied also by Friedjung (1981b). He concluded that most of the absorption was circumstellar rather than interstellar and estimated the column densities.

A significant redistribution of energy toward the UV and IR is observed both in the continuum and in the lines during the phases of the decline in the optical. The maximum brightness at λ 2740 is reached about 20 days after OB and at λ 1450 about 45 days after OB. The total bolometric luminosity, obtained from UV + opt. + IR observations, reached its maximum about six days after the visual maximum with a value of about 3 times the Eddington luminosity for a 1 $M_\odot$ star (Stickland et al 1981). Between days 13 and 27 the total luminosity remained approximately constant at about 1 $L^{Edd} \sim 1.7 \times 10^4 L_\odot$ and then started to decline (Figure 6.46).

The behavior of Nova Cyg 1978 from the early OB phases until the nebular stage was monitored by Stickland et al. (1981) who provided the first

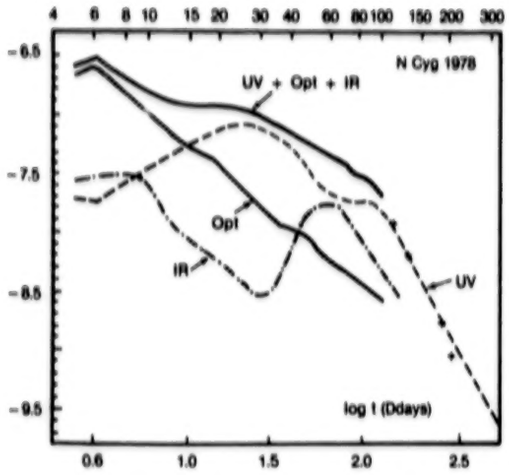


Figure 6-46. Light curves (UV, optical, IR and bolometric) of Nova Cyg 1978.
(from Stickland et al., 1981)

complete coverage of the UV outburst of a nova.

They performed a very detailed quantitative study of the physical conditions in the ejecta during the nebular phase by applying standard and original methods for the analysis of nebular spectra. The nebular spectrum in the UV shows emission lines of OV], NV, OI, OII, OIV, CII, OIV], NIV], CIV, HeII, OIII], NIII], CIII], and MgII. The nebular continuum is due to contribution of recombination and free-free processes of H and He mainly, plus a hot photosphere with T ~ 1.5 x 10^5 °K and R ~ 0.13 $R_\odot$.

The expansion velocity of the nebular shell, estimated by the widths of the nebular lines is 1270 Km s^{-1}, when deduced from the extreme widths, and 760 Km s^{-1}, when estimated from the widths of the flat-topped plateau regions in the centers of the line profiles.

Stickland et al. (1981) derived the electron temperature T_e in the nebula from the emission lines ratios CII 1335/CIII] 1908, CIII 2297/CIV 1550, and NIV 1718/NV 1240, where the first line in each pair is produced by dielectronic recombination via low-lying autoionizing states and the second line is produced by the more usual mechanism of collisional excitation. T_e values are around 9000 °K in the CII] region, around 11,500 °K in the CIV region and around 14,500 °K in the NV region.

The electron density N_e was determined from the ratios NII] 2140/[NII] 5755, and OIII] 1663/[O III] 5007, which yielded $N_e \sim 8 \times 10^7$ el. cm^{-3}. Abundances were then determined relative to H. The CNO abundances are enhanced, with respect to the solar ones, by a factor of 20 for total CNO and by 200 for N.

This indicates a TNR origin of the outburst. The value of the ionized ejected mass is of the order of 10^{29} g, and the corresponding kinetic energy is 6 x 10^{44} ergs, in agreement with the estimates for other classical novae.

Cassatella and Gonzalez-Riestra (1988) have included N Cyg 1978 in a study of the behavior of the FeII UV lines in novae in the early post maximum phases, using the extensive IUE material available.

During about one month after the maximum (near September 12, 1978), the object showed strong FeII lines, especially from multiplet UV 1, which appeared with a P Cygni structure particularly prominent in the low-resolution spectra of September 11. In the subsequent days, the violet shifted absorption components of FeII UV 1 progressively fainted, while the emission components became stronger, reaching a maximum probably near September 23. Finally, in the spectra of middle October, the emission component also disappeared, and FeII UV 1 was only visible in absorption, probably produced by the zero voltage lines 2599.4 and 2585.9 A. These changes were accompanied by the appearance, at the later date, of nebular lines and by a dramatic change of the UV energy distribution, as shown in (Figure 6.47.)

Nova Cr A 1981. IUE spectra of Nova Cr A have been obtained during 6 months on 11 dates beginning from the outburst in April 1981 up to mid-November 1981, when it entered the sun constraints of IUE (Sparks et al; 1982). These spectra cover the whole IUE range and are mostly at low resolution. It is noteworthy that the initial spectral evolution, immediately after the OB, is quite similar to that of Nova Cyg 1978. The strongest line in the first spectrum is OI 1303. The emission lines cover a range in ionization potential from

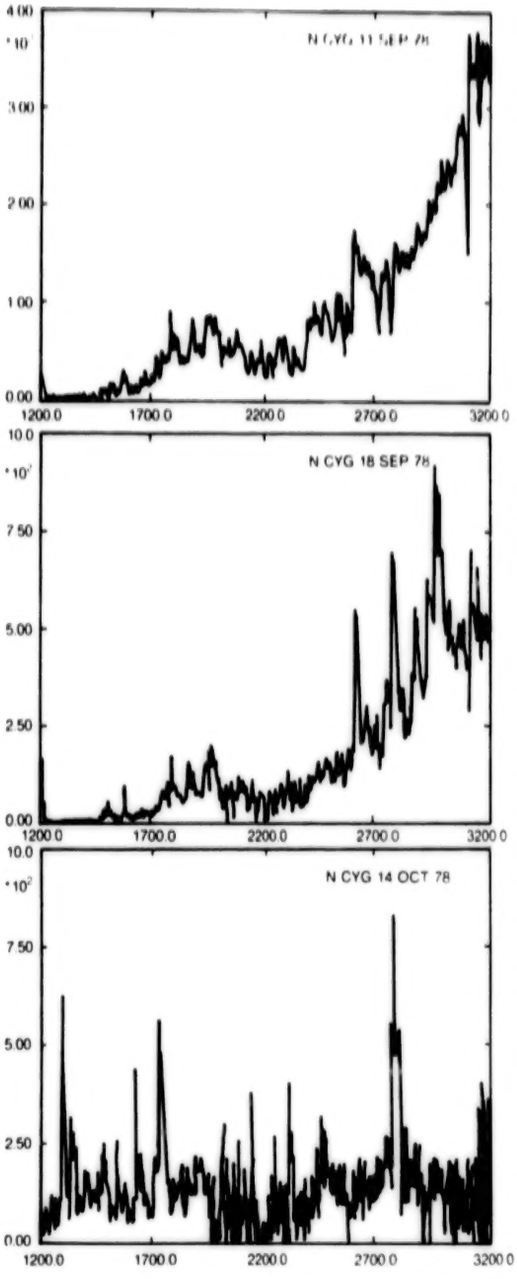


Figure 6-47. Observed UV spectra of N Cyg 1978 in outburst. In the spectrum of Oct. 14, 1978 the nebular lines have become strong and a hot continuum emerges in the short wavelength region.
(from Cassatella and Gonzales Riestra, 1988)

8 eV (MgII) to 80 eV (NV). Forbidden emission lines of high ionization character such as [MgVII] and [AlVI] were present for short periods in May and June 1981. (Figure 6.48) These lines seem to be produced by photoionization and not in a high temperature coronal region because of the absence of high excitation "auroral" emissions, which would be expected under coronal conditions.

On May 25, the FWHM of CIV emissions was 4500 km s^{-1}, a value quite uncommon for a moderately fast nova. At 200 days after maximum the nebular stage was not yet reached.

Williams et al. (1985) have made a quantitative study of the emission lines present in the spectra, with the purpose of determining accurately the physical conditions and the chemical composition in the gas ejected during the outburst. The ratio NIV 1719/NV 1240 yielded T_e~11,000 °K. Abundances relative to He have been determined for several elements by applying a quite elaborate method. (Figure 6.49) illustrates their results, which indicate that CNO elements are enhanced relative to He and, presumably, relative to H also. What is noteworthy is the very high enrichment of neon, together with that of Mg and Al. The study suggests N/C~20 and Ne more overabundant than CNO (!).

(The overabundance of neon is indicated by the strength of the [NeIV] 1602, [NeIV] 2422, and [NeIII] 1815 lines).

Nova Aql 1982 has been observed with IUE for the first time on February 24 and then on several dates up to June 30, 1982 (Snijders et al., 1984, 1987b).

Figure 6.50 (from Snijders et al., 1987) shows the estimated fluxes in the UV, optical, and IR. The total flux declined rather slowly with time, with a dominant contribution from the IR region. It is remarkable that the combined UV plus optical continuum [after correction for reddening: E(B-V)~0.55-0.60] varies at various epochs as $F(\lambda) \propto \lambda^{-2}$ from at least 1,400 to 6,000 A and that these fluxes vary approximately in *phase*, unlike in other novae. A dip in the UV flux was observed near d=77, probably because of absorption by dust internal to the nova shell, while the IR contribution becomes dominant.

Figure 6.51 shows IUE spectra at various epochs after the outburst.

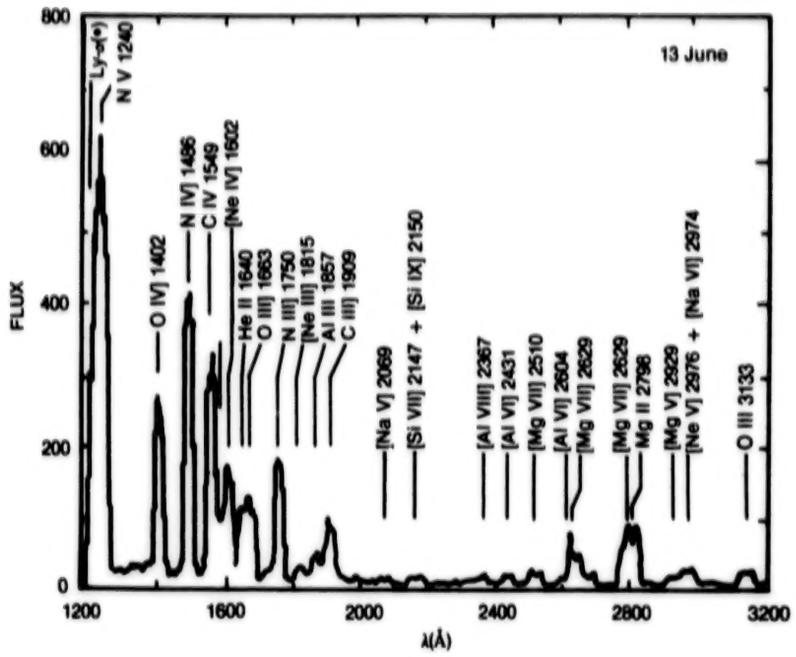


Figure 6-48. Low dispersion UV spectrum of Nova CrA on June 13, 1981. Units of flux are 10^{-14} erg cm^{-2} s^{-1} A^{-1}.
(from Williams et al., 1985)

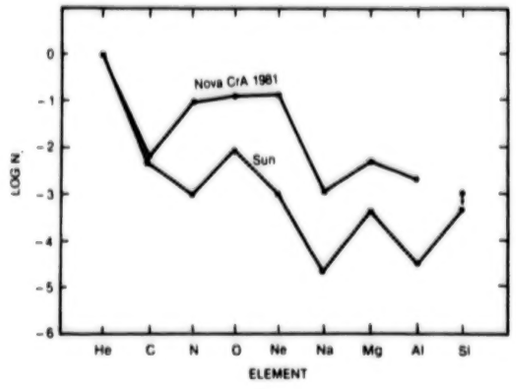


Figure 6-49. The logarithm of the abundances, by number, of the elements that it was possible to analyze for both Nova CrA 1981 and the Sun.
(from Williams et al., 1985)

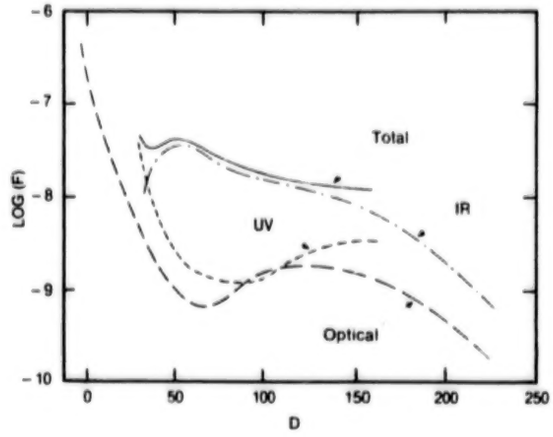


Figure 6-50. Nova Aql 1982: Smoothed curves showing the time-variation of total fluxes (corrected for IS extinction) in the UV (912 A-3200 A), optical (3200-10000 A) and IR (>10000 A).
(adapted from Snijders et al., 1984)

The first IUE observation (d=29) showed the presence of dramatic P Cyg features with velocities of up to 10^4 km s^{-1}. If this edge velocity is interpreted as a terminal velocity, it is very high; only supernovae show such values, while the highest velocity observed in the Orion system of novae is –3800 km s^{-1} (Payne Gaposchkin, 1957).

N Aql 1982 was characterized by a remarkably composite structure in the UV lines which show:

1) Quite "narrow" emissions of semiforbidden and permitted lines (FWHM 2000 km s^{-1}).
2) Broad absorptions up to -4000 km s^{-1} in the common resonance lines like NV and CIV.
3) An unusually high-velocity component with edge velocity at -10,000 km s^{-1} (system b); this high-velocity gas has been detected *only in the UV* and was evident on February 24 and March 2 (days 29 and 36 after OB).

It is notable that systems *a* and *b* are observed in the resonance lines of CIV and SiIV, while only system *a* is observed in the resonance doublet of Al III and only system *b* is observed in an excited line of NIV, which has high excitation. This might suggest that system *b* is formed closer to the pseudophotosphere, and the slower system *a* consists of material ejected earlier and swept up by system *b*.

The electron density of the medium velocity gas has been determined using the ratio SiIII 1892/ CIII 1908 yielding $N_e \sim 1 \times 10^{10}$ el. cm^{-3}. Another set of emission line ratios provided a separate determination of T_e and N_e that resulted in these ranges: $9600 \leq T_e \leq 11{,}000$, and $1.6 \times 10^8 \leq N_e \leq 5 \times 10^8$ with a best estimate for the diagnostic, in which $T_e = 10^4$ K and $N_e = 2.5\ 10^8$ cm^{-3}.

Using the above parameters, abundances of several elements have been calculated by Snijders et al. (1987b) for the medium velocity gas

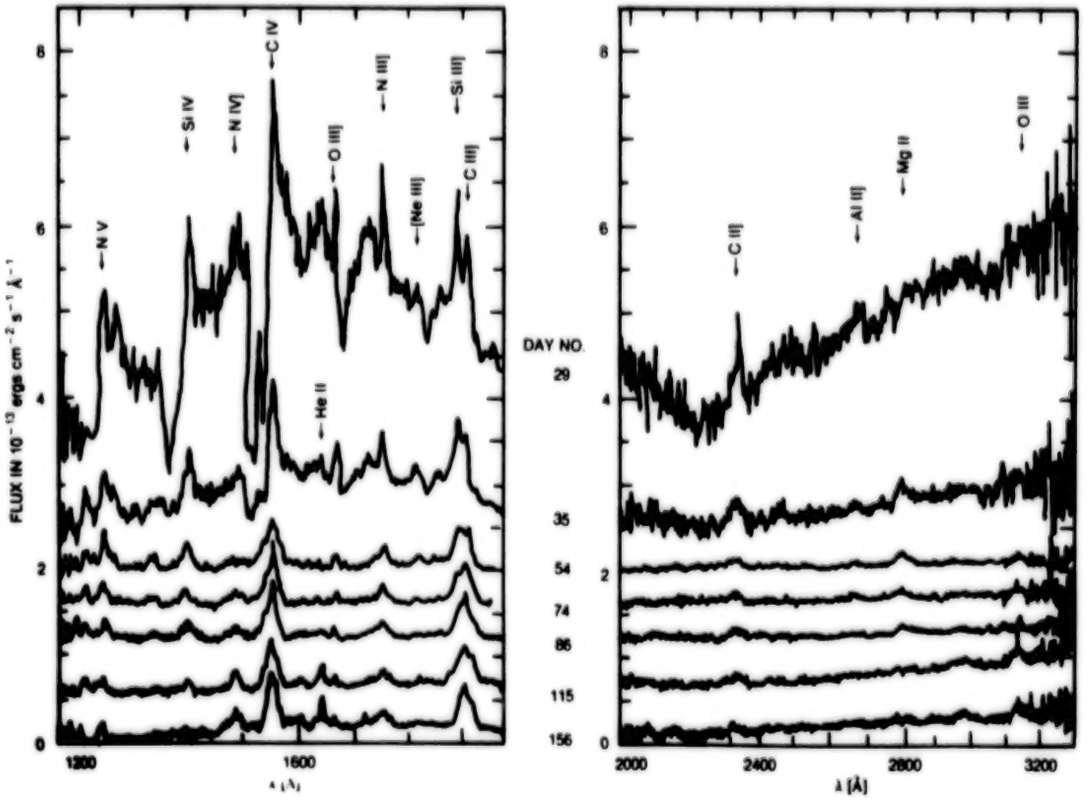


Figure 6-51. Nova Aql 1982: Fluxes observed with IUE (uncorrected for extinction). The fluxes shown are shifted upwards by constant amounts for each day number, by 3.2 on d=29; by 2.4 on d=35; by 2.0 on d=54; by 1.6 on d=86; by 0.6 on d=115 and by 0.0 on d=156.
(from Snijders et al., 1987 b)

on d=156. The high overabundances of sulphur, nitrogen, and neon are remarkable: (N/H=0.21, Ne/H=0.73, S/H=0.064).

These overabundances resemble those found in the shell ejected by Nova Cr A 1981.

The mass of the medium velocity gas was estimated as 7×10^{-6} $M_{\odot}$ indicating that the total mass ejected was about 10^{-2} less than in other novae.

Due to the great intensity of the neon lines in its spectrum, N Aql 1982 has been labelled as a "neon nova." However, as pointed out by Friedjung (1988), the gas-phase abundance of neon was larger than that for other abundant elements only because neon is a noble gas and does not condense into grains.

U Sco. The outburst of this recurrent nova was first recorded on June 24, 1979. This OB was much faster than either the OB of N Cyg 1978 or N Cr A 1981; it was an extremely rapid, burst-like event. The IUE observations started on June 24 and continued until 11. The spectrum (Williams et al., 1981; Sparks et al., 1980) was initially a mixture of both high-ionization and low-ionization lines. NV 1240 was strong, HeII, CIV, SiIV, N IV] 1486 were present, with PCyg profiles in CIV and Si IV lines. Unlike in other recurrent novae in outburst, no forbidden coronal lines have been observed. (Figure 6.52). After June 30, the absorptions disappeared and the general level of ionization increased.

The emission and absorption features were all very broad, characteristic of expansion velocities up to -7500 Km s^{-1}.

It is noteworthy that there was no change in the color temperature over the period covered by the observations of Williams et al. The observed ratio F_{vis}/F1300 remained nearly constant around the value of 0.5.

According to Barlow et al. (1981), over a large part of the dereddened optical and UV ranges, the continuum of July 6 could be fitted by a power-law $F(\lambda) \sim \lambda^{-2.4}$. However, this index should be

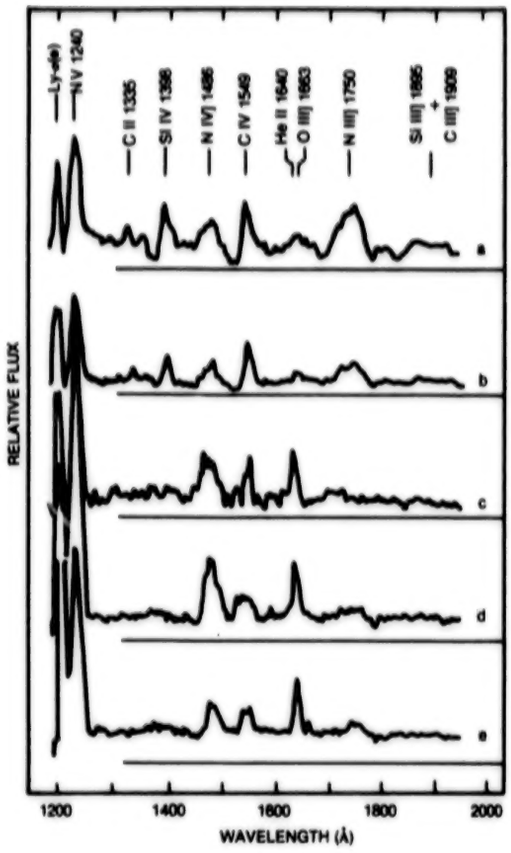


Figure 6-52. UV spectra of U Sco in the period following outburst. The dates for the IUE scans, together with the visual magnitude as determined from the Fine Error Sensor, are as follows: a) June 28, V=11.4; b) June 30, V=11.9; c) July 2, V=13.1; d) July 4, V=13.8; e) July 11, V=14.3.
(from Williams et al., 1981)

taken with caution because of the uncertainties in the reddening correction.

A detailed analysis of the emission lines shows that the ejecta are very rich in N, although the combined CNO abundance seems essentially solar, because carbon is very underabundant with respect to nitrogen. A depletion of H is indicated by the optical spectra which suggest that He/H is about 2 (in number density).

The amount of ejected mass was only 10^{-7} $M_{\odot}$, about 10^{3} smaller than that usually ejected in a classical nova outburst.

It is noteworthy that both U Sco and N Aql 1982 have shown an unusual spectral evolution during outbursts: no color changes (no flux redis-

tribution toward the IR and UV), similar spectral indexes (λ^{-2} in N Aql 82, $\lambda^{-2.4}$ in U Sco), ejection of a less massive envelope than the other novae ($\sim 10^{-6} \div 10^{-7}$ $M_\odot$ instead of $\sim 10^{-4} \div 10^{-5}$ $M_\odot$).

The fifth recorded OB of U Sco occurred in 1987, only 8 years after the previous one. Such a short recurrence time cannot be easily explained in terms of the present TNR theories for the OB of recurrent novae.

N Sgr 82. The OB was discovered on October 4, 1982, and the visual maximum was reached on October 15. The IUE observations of this fast nova started on October 18, when the object was in the early decline. The continuum was that of an early F-type object with T around 9000°K (Mazeh et al., 1985a). It was similar to that of N Cyg 1978 in the corresponding stage (Figure 6.53). The UV continuum of October 18 was very weak and started increasing at the end of October as a consequence of the commonly observed flux redistribution toward UV (and IR) after the visual maximum. The line spectrum was initially characterized by emissions and absorptions of low ionization like FeII, OI, and other neutrals. The MgII doublet showed a P Cyg profile with v edge = -1700 Km/s.

In the following stages, the evolution was quite similar to that of N Cyg 1978, and the nebular stage was reached about 210 days after outburst.

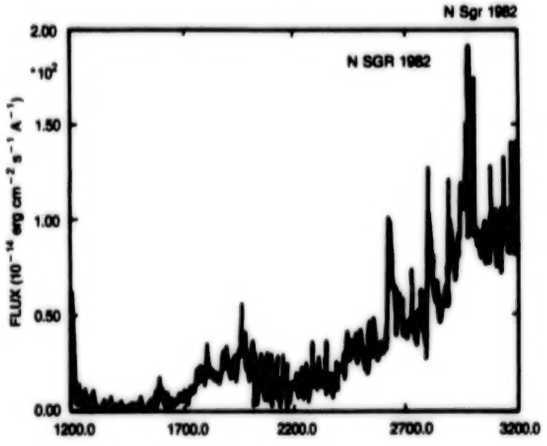


Figure 6-53. Observed UV energy distribution of N Sgr 1982 on Oct. 14, 1982 (about four days after maximum). The spectrum is very similar to that of N Cyg 1978 shortly after maximum.
(from Cassatella and Gonzales Riestra, 1988)

N Ser 1983. This is a very fast nova with $t_3 \sim 5$. The first IUE observations were made 11 days after maximum. A peculiarity of its UV spectral behavior is the wide ionization range with the presence of ions ranging from FeI to NV. CIII] 1908 is also present. (Drechsel et al., 1984) (Figure 6.54).

The emissions are strong and broad and the P Cyg profiles in the CIV and MgII doublets indicate extremely high outflow velocities of -9000 km s^{-1} and -1000 km s^{-1} respectively. These velocities are comparable with those reported by Snijders et al. (1987b) for N Aql 1982.

N Mus 1983. The outburst of this moderately fast nova was reported on January 18, 1983. IUE observations started on February 19, 1983, (Krautter et al. 1984, Krautter, 1986) and continued for several months, covering the Orion to nebular phases. The first spectra showed a wide excitation range and the presence of several semiforbidden lines also (Krautter et al., 1984). The overall evolution was quite similar to that of N Cyg 1978, and ionization increased while the spectral evolution was approaching the nebular phase (Figure 6.55). From August 1985 to June 1986, the [OIII] line fluxes decreased substantially, while high ionization species like [Fe VII] showed an increase of the line intensities.

In the early spectra, the structure of the MgII lines is complex with components at -320 and +540 Km/s. The HeII, SiIII] and C III] emissions shows also a composite structure and have FWZI of about 1500 Km s^{-1} (Figure 6.56).

The total luminosity near maximum (January 21) was estimated at about 1.5 L_{Edd} (for a $1 M_\odot$ white dwarf), assuming that the UV flux distribution decreased in the UV as it did for N Sgr 1982 early in the decline. For March 4, 1983, a SWP IUE spectrum and m_v permit a rough estimate of 0.5 L_{Edd}, with the assumption that the $F \propto \lambda^{-2}$ distribution still holds for the optical and IR range.

An abundance analysis has led to the determination of considerable nitrogen enrichment with respect to carbon and oxygen [N (N) = 80 times the solar value]. From the strength of CNO lines, an overabundance of all these elements seems indicated. It is noteworthy that more than one year after OB (on April 20, 1984), soft x-ray emission was detected by EXOSAT (Ogelman, et al., 1984).

At that epoch also FeX 6374 was detected in the optical. The values of temperature (3.5 10^5 K) and L (10^{37} erg s^{-1}) derived from this emission suggest its origin from the surface of a very hot white dwarf.

Nova Vul 1984 I (PW Vul)

High resolution spectra of PW Vul (Visual magnitude at maximum 6.4) have been obtained two months after maximum. The spectra are crowded with absorption and emission lines from Si II, N II and Fe II. The absorption lines have at least three separate components at different expansion velocities: at about 0 km/s, -750 km/s and -1550 kms. Figure 6.57 shows the profiles of multiplet 191 of Fe II and multiplet 1 of Si II in the region 1780-1820. A, and the region 1710-1770

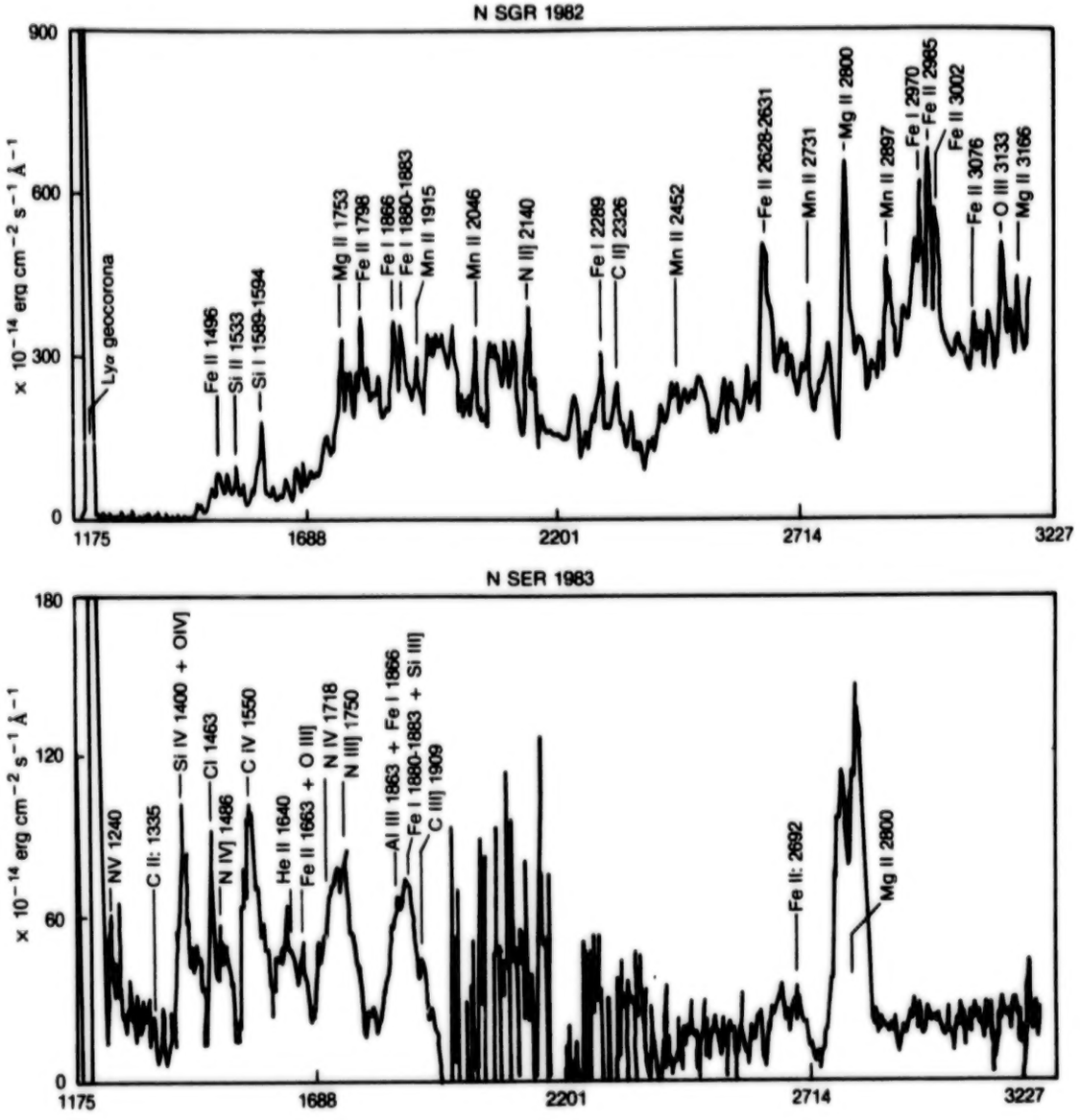


Figure 6-54. Dereddened IUE spectra of the classical novae N Sgr 1982 and N Ser 1983. (from Drechsel et al., 1984)

where several lines of Fe II and Ni II are present. The three absorption components are clearly detectable in the lines of multiplet 191 of Fe II and in the ground multiplets of Si II and Ni II.
6-75

RS Oph 1985 An outburst of this recurrent nova was announced on January 26, 1985, and IUE osbservations started on February 8 and continued for about two months (Cassatella et al. 1985). The UV spectral evolution after OB has collowed the trend of increasing ionization level with time. In a graph emission intensity versus time, the emission intensity from highly ionized species peaks at a much later stage in the decline than emissions from low-ionization species. A decrease of N_e with time was deduced by using the N_e sensitive ratio SiIII] 1892 /CIII] 1908.

The UV FeII emission lines of RS Oph have been studied by Cassatella and Gonzalez-Riestra (1988).

Figure 6.58 shows how the fluxes of the FeII emission lines from multiplet UV 1 (around 2600 A) vary with time during the 1985 outburst of RS Oph, compared with other strong emission lines of different ionization level such as OI 1300 A, N IV] 1487 A, NV 1240 A, and [FeXI] 2648.7 A. The figure shows clearly that the FeII lines peak in intensity very soon after the outburst, like the low-ionization line OI 1300 A (and MgII 2800 A, not shown in the figure). Emission lines from higher ionization species, on the contrary, reach a maximum at later stages: NIV], for example, is maximum around day 35; NV, around day 43; while the [FeXI] line is maximum in a plateau between days 42 and 62. The time of maximum is then correlated with ionization potential of the line considered.

Apart from the UV 1 multiplet, other FeII lines are present, although fainter, in the postmaximum spectra of RS Oph: the ones which could be identified with more confidence are those from multiplet UV 191 around 1786 A and those from UV 62 and 63.

In the later decline stages, forbidden emissions from [FeXI] 1467 and 2649 and from [FeXII] at 1350, 2406, and 2568 (Figure 6.59) were detected. The time evolution of the profile of the

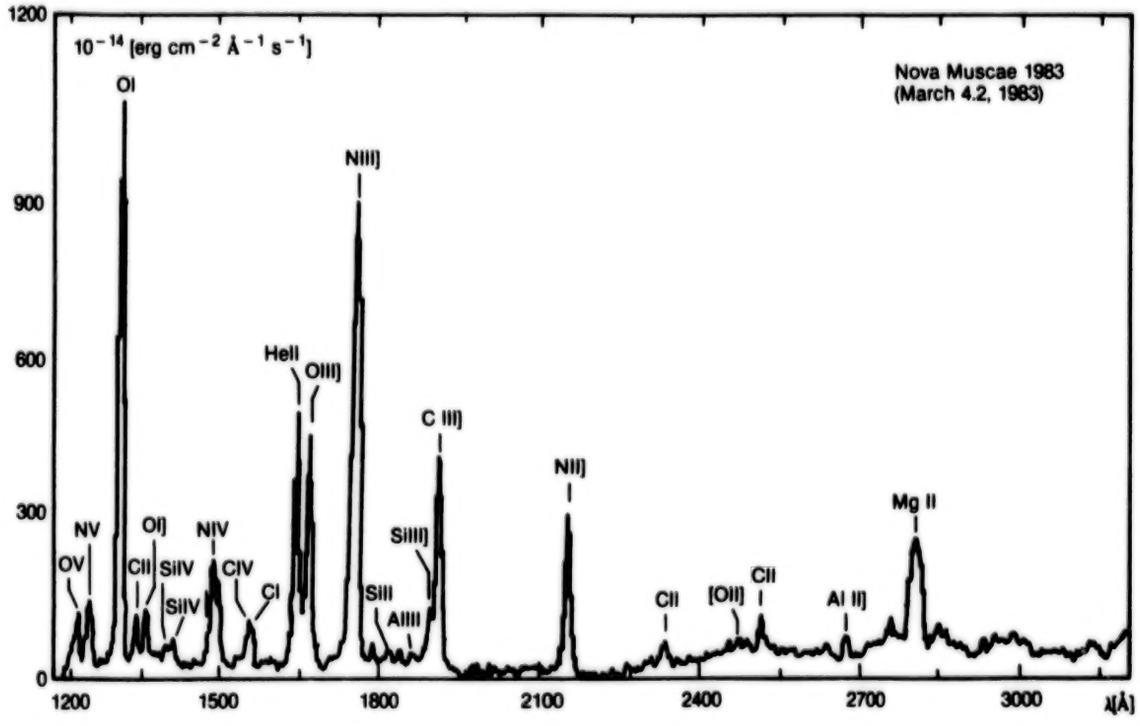


Figure 6-55. The UV spectrum of N Mus 1983. (from Krautter et al., 1984)

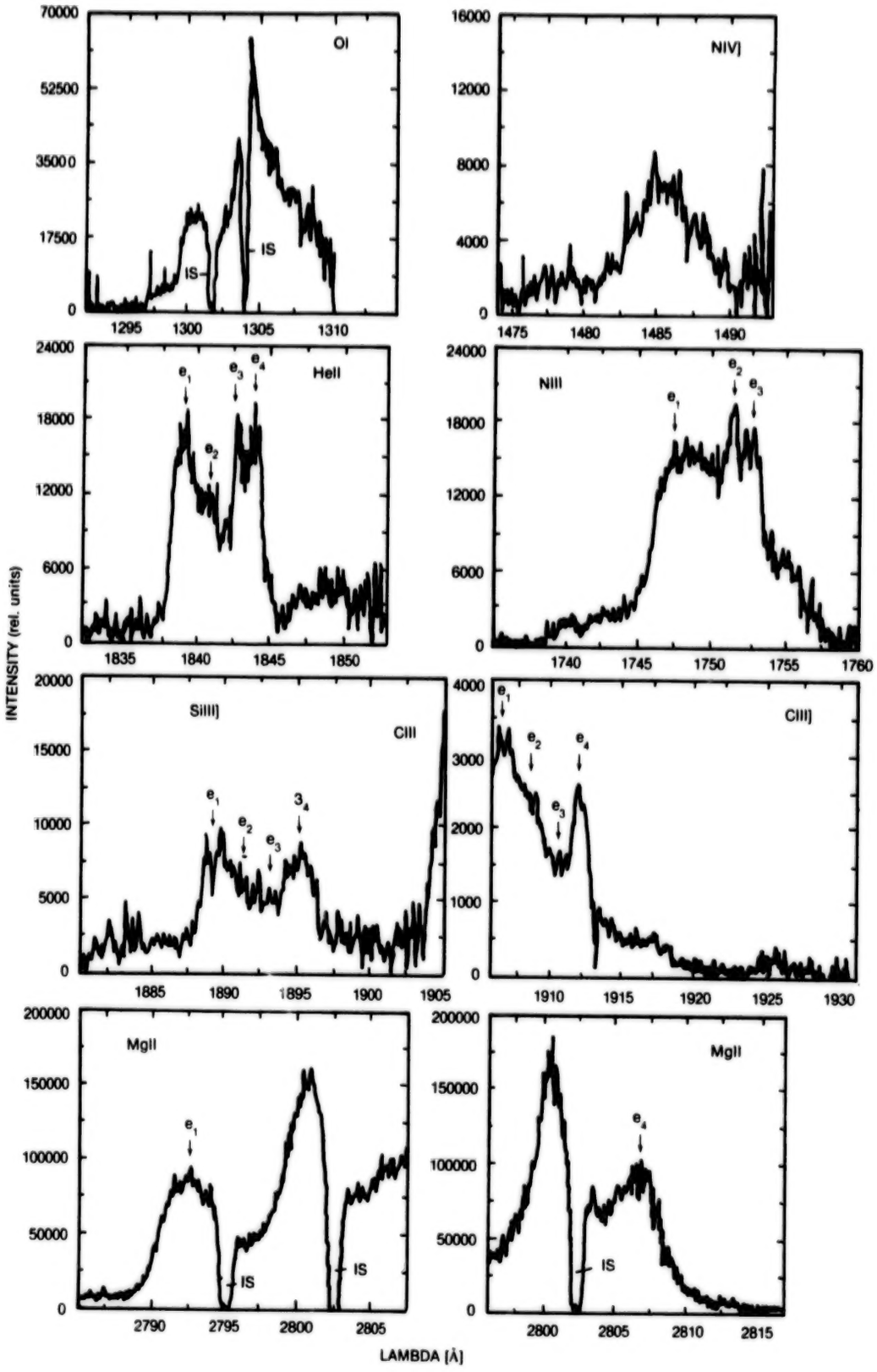


Figure 6-56. High-resolution profiles of the most prominent emission lines of N Mus 1983. (from Krautter et al., 1984)

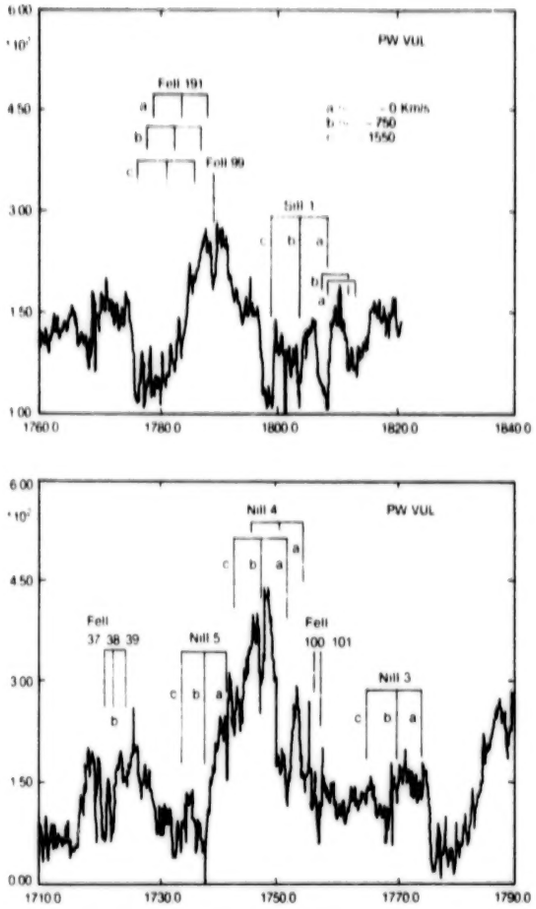


Figure 6-57. High-resolution spectra of N Vul 1984 a in two wavelength regions. The spectra are crowded with absorption and emission lines from Si II, N II and Fe II. The absorption lines have at least three separate components at different expansion velocities: at about 0 km/s,-750 km/s and -1550 km/s. Particularly strong is the emission-absorption structure from Fe II UV multiplet 191 and N II UV multiplets 4 and 5.

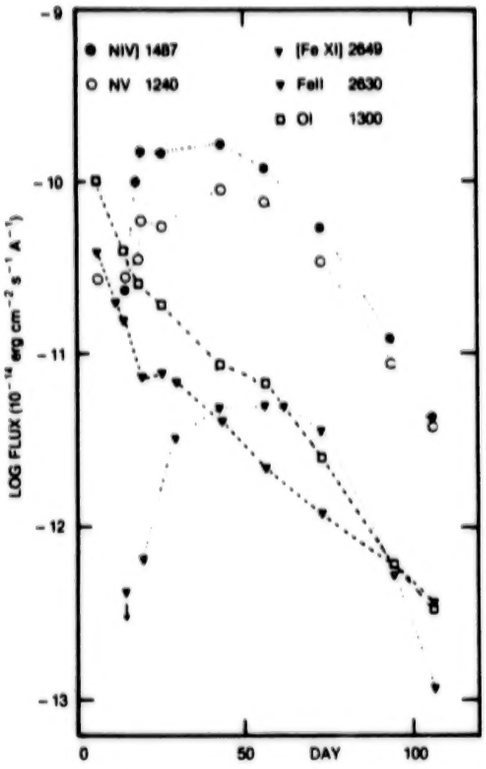


Figure 6-58. Time variability of the emission lines in RS Oph during its outburst of 1985. Abscissae represent the time after maximum, assumed on Jan. 28, 1985. The figure shows that the lines of lower ionization level peak very soon after maximum while [Fe XI] 2648.7 is maximum in a plateau between day 42 and 62.
(from Cassatella and Gonzales Riestra, 1988)

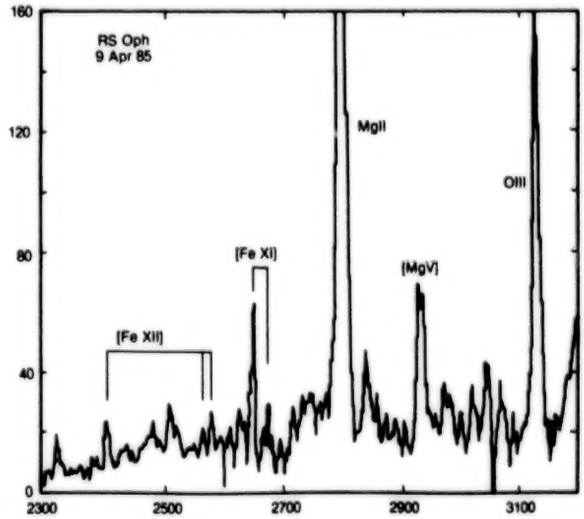


Figure 6-59. The spectrum of RS Oph in the interval 2300-3200 A. High excitation lines are clearly present.

[FeXI] 2648.7 A line is shown in (Figure 6.60). Such data can provide important clues to the understanding of the dynamics and geometry of the ejection. The complex profile of [FeXI] is probably indicative of a non-spherically symmetric and, perhaps, discrete ejection process. It is worth recalling that RS Oph is the first astrophysical source in which so strong high-ionization lines were detected in the ultraviolet, apart from the solar corona.

Snijders (1987a) made an estimate of the mass of the ejected shell and, using the method developed by Pottash (1959), obtained M(eject)~ 5 x 10^{-7} $M_{\odot}$.

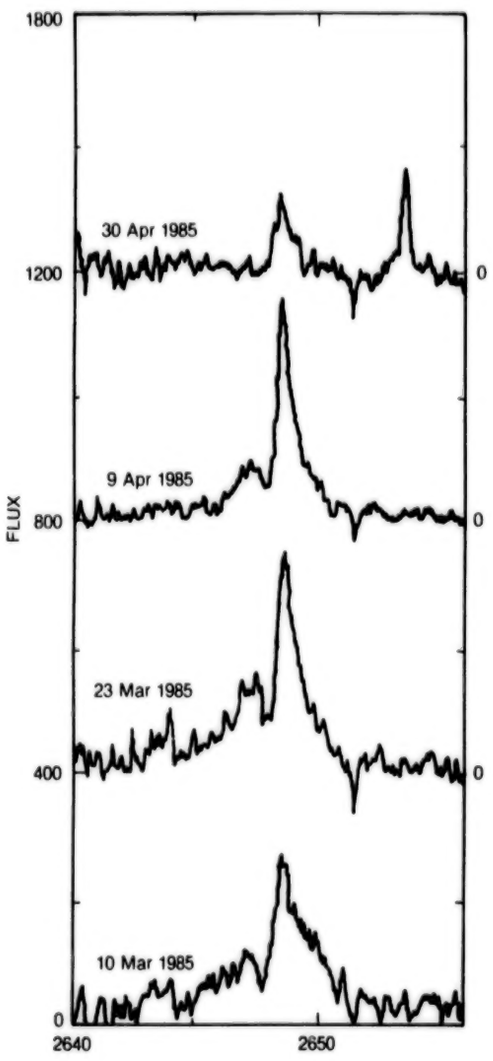


Figure 6-60. High-resolution data of the recurrent nova RS Oph (outburst of 1985) showing the time evolution of the profile of [Fe XI] 2649 A.

This quite low value is in agreement with previous estimates and theoretical expectations (Starrfield et al., 1985) from a recurrent nova outburst. Snijders also made an estimate of the luminosity after OB and found a peak value of about 4 L_{Edd} and a plateau value $L = L_{Edd}$ for a massive white dwarf.

A considerable enrichment of nitrogen seems to be present in the ejecta, as was found in other novae. The ratio N(He) / N(N) is in the range 3-40.

The cause for the recurrent outbursts of RS Oph (every 9 to 35 years since the first event was discovered in 1898) may be different from the thermonuclear runaway invoked for classical Novae (Livio, Truran, and Webbink, 1986). Also, it is possible that important differences exist, for example, in the total mass ejected and in the ejection velocity, compared to classical novae. In any case, *RS Oph* offers a unique opportunity to study one important phenomenon: the interaction of ejected matter with the stellar wind from the cool giant companion and with the surrounding circumsystem material, not yet dissipated at the time of the new outburst.

The appearance of strong emission lines from very high-ionization species observed shortly after the outburst both in the optical (Joy and Swings 1945; Rosino, Taffara, and Pinto, 1960) and in the ultraviolet (Cassatella et al. 1985), as well as the detection of a strong x-ray flux (Mason et al. 1987) is a demostration of the effectiveness of such an interaction.

Intense soft x-ray emission (1 - 6 keV) has been detected with EXOSAT in March 22, 1985. The characteristic temperature (Mason et al. 1987) is of the order of a few million degrees, and the total flux, after correction for the interstellar medium (ISM) absorption is of the order of 10^{-9} erg cm^{-2} s^{-1}.

It is noteworthy that this strong emission is seen a long time after OB and that there is no short-time variation associated with it.

Moreover, a weak, but significant, residual x-ray emission was still detected in October 1985.

This much weaker emission is consistent with temperatures of the order of 3 - 5 x 10^5 K as found for Nova Mus 1983 (Ogelman et al., 1984).

V. I. CONCLUDING REMARKS

6-79

As it has emerged from the description of individual objects, each nova in OB has shown some peculiar characteristics that have made it different from the other novae; however, in spite of these individualities, the study of the UV data, both in the continuum and in the emission lines, has been of fundamental importance for the determination of some basic common properties in the behavior of novae in OB. The studies of the UV observations have led to two important results:

1)-Accurate determinations of chemical composition of the ejecta

No one object has ejected material of solar-like composition. Large enrichments of CNO have been found in practically all ejecta, while, in a substantial fraction, a large over-abundance of Ne has been found. Several considerations (see, for example, Truran, 1985), have led to the conclusion that the enrichments in the ejecta are not a direct consequence of nuclear reactions in the nova envelope, but rather reflect the composition of the envelope at the onset of the TNR. The most likely mechanism responsible for this enrichment is outward mixing of core matter from the interior to the surface of the white dwarf, a consequence of the shear-induced turbulence produced by the accreted material when it strikes the dwarf surface layers. Thus, CNO over-abundances can be explained in terms of TNR in a shell already enriched of these elements in a CO white dwarf. The enrichment of Ne (as detected from the anomalously high intensity of the λ 1602 Å line four novae) has been an important and unexpected result, indicating that the ejected material was processed to Ne during the previous evolution in a very massive O-Ne-Mg white dwarf (Law and Ritter, 1983). Iben and Tutukov (1984), from theoretical considerations, estimated a ratio of approximately 35 for systems containing a CO white dwarf to systems with an (O-Ne-Mg) white dwarf. The reason for the observed higher percentage of (O-Ne-Mg) white dwarfs in novae is not clear and could be explained on the basis of selection effects, since nova OBs are expected to be more frequent in the more massive (O-Ne-Mg) white dwarfs. The implications of the presence of this kind of white dwarf on our understanding of the nova phenomenon and the evolutionary state of the system are still to be investigated.

2)-Reliable estimates of the bolometric luminosity and of its variations with time.

IUE observations of the continuum of novae in outburst have confirmed the general trend of the redistribution of the flux toward the UV (and the IR) as the outburst progresses, and shown that the bolometric luminosity in the early postmaximum phases remains nearly constant or declines more slowly than the visual one.

The total luminosity is generally closed to the Eddington limit for a $1M_\odot$ star(~$1.55.10^{38}$ erg s^{-1}), but the exact value depends critically on the distance that has been assumed.

The possibility that L exceeds L_{Edd} would have as a consequence the formation of a supercritical wind, accelerated by the high radiation pressure corresponding to that super-Eddington Luminosity.

Before the launch of IUE, it was not clear whether the ejection of mass from the "nova" was instantaneous (i.e., occurring in a short time interval as compared with the typical time scale of the "nova" phenomenon) or continuous. Friedjung (1977a) suggested that even using only ground-based observations, there was a good evidence for continued ejection decreasing with time, although most mass was probably ejected near visual maximum. The smallness of the decline in L_{bol} after visual maximum, as found using UV (and IR) observations, has been interpreted as a suggestion that nuclear burning continues on the white dwarf surface after the initial explosion,

thus producing a continuous ejection of mass (after the sudden ejection of the first shell). The presence of very high-velocity components (up to 10^4 km s^{-1}) in the UV spectrum of Nova Aql 1982 and in other novae in OB has been interpreted by Friedjung as an evidence of the presence of super-critical winds accelerated by radiation with super-Eddington luminosity.

6-80

There are, however, several problems related with the continuous ejection model that are still unclear, as, for instance, the interpretation of all the absorption systems. Collisions between envelopes at different velocities are expected, leading to x-ray emission observable in the late outburst stages. The x-ray emission detected in N Muscae (Ogelman at al., 1984) could be due to this mechanism.

VI. THE X-RAY EMISSION OF NOVAE AND RECURRENT NOVAE

(Written by Selvelli)

Accretion, which is the main source of the UV radiation emitted by novae in quiescence, is also responsible for the x-ray radiation emitted by these objects. In the standard picture (a geometrically thin, optically thick accretion disk) a rough estimate of the energy dissipation indicates that about one half (that is $\frac{1}{2} G \frac{M \dot{M}}{R}$) of the accretion luminosity is released in the disk as optical and (mainly) UV radiation, while the other half is released as soft/hard x-ray radiation in the boundary layer, the region at the interface between the innermost disk part and the surface of the white dwarf.

Generally, the keplerian or nearly keplerian velocity of the material in the inner disk is much greater than the velocity at the surface of the white dwarf but, as it approaches the white dwarf, it must become slower, and the excess of mechanical energy will be dissipated. Simple calculations (see, for example, Kylafis and Lamb (1982), Ferland et al (1982b) show that if the boundary layer is assumed to be optically thick, for parameters typical of a CV ($\dot{M} \sim 10^{18}$ gr s^{-1}, $M_1 \sim 1 M_\odot$, $R_1 \sim 10^{-2} R_\odot$), it will have temperatures of the order of 2-5 $\times$ 10^5 °K and, therefore, will emit most of its radiation in the EUV-soft-x-ray range). The boundary layer can be defined as the region between the point where the angular velocity deviates from the keplerian one and the surface of the white dwarf. (See Chapter 4. IV. F.) The presence of a hard x-ray component (E~a few keV) with a much lower luminosity than that expected for the EUV-soft-x-ray component, and the lack of detection of the soft component (this absence, however, can find a natural explanation in terms of interstellar absorption) indicates that the real picture is more complex and that a more detailed modelling of the boundary layer is required. See, for example, Ferland et al. (1982a,b), Patterson and Raymond (1985a,b), and Jensen 1984. It must also be pointed out that the presence of the boundary layer as described above, depends critically on the absence (or weakness) of the magnetic field in the white dwarf.

If a strong magnetic field ($\geq 10^7$ gauss) is present, the accreting material will flow along the lines of the magnetic field and the accretion disk will be disrupted at a radius of the order of the Alfven radius. In this case, the accretion material will form accretion columns at the magnetic poles of the white dwarf. In this chapter, only the x-ray behavior of classical and recurrent novae, in which the magnetic field intensity is less than 10^6 gauss and therefore not so high as to affect seriously the disk structure, will be described, leaving out the magnetic CVs (polars or AM Her stars, magnetic field ~ 10^8 gauss).

VI.A. X-RAY OBSERVATIONS OF POST-NOVAE

The HEAO-1 X-ray survey of cataclysmic variable stars (Cordova at al, 1981a) revealed that quiescent novae were, at best, low luminosity sources with fluxes, in the 0.18 - 2.8 keV range, below the HEAO -1 A2 detector thereshold (of the order of 2 -3x 10^{-11} erg cm^{-2} s^{-1}). Thanks to the higher sensitivity of the instruments onboard HEAO-B (EINSTEIN), a positive detection of about ten sources and the assignment of upper limits for a few other ones has been possible.

Several old novae are indeed X-ray sources but at a quite lower level (L ~ 10^{31} -10^{32} erg s^{-1}) with

respect to the UV and optical fluxes. Table 6.15 is a compilation of data from the observations made mainly by Becker and Marshall (1981), Cordova et al (1981a,b) and Cordova and Mason (1984). A description of the EINSTEIN imaging proportional counter (IPC) detector used to make the observations is reported in Giacconi et al (1979). The data of table 6.15 refer to the energy interval 0.16 - 4.5 keV. The conversion from counts s^{-1} to intensity is a critical point, since it depends on the adoption of a spectral distribution. Generally, since most data are indicative of a quite hard thermal component, a nominal 10-KeV thermal bremsstrahlung spectrum, and $N_H \sim 10^{20}$ cm^{-2} have been assumed. With these assumptions, one IPC count s^{-1} from a source with such spectrum corresponds to a flux at the Earth of 3.6 x 10^{-11} erg cm^{-2} s^{-1} in the 0.15 - 4.5 keV range (Patterson and Raymond, 1985). This conversion factor is not very sensitive to kT and N_H, however. In most studies a conversion factor of 2.7 was assumed, but in the last processing of the IPC date the conversion factor 3.6 was suggested (Patterson and Raymond 1985), and, in the compilation of Table 6.15, this last value has been used. It is evident from Table 6.15 that the mean 0.1 - 4.0 keV luminosity of old novae is of the order of 6 x 10^{31} erg s^{-1}. We recall that their UV luminosity is instead much higher, of the order of 10^{34} -10^{35} erg s^{-1}. Old novae are generally "hard" x-ray emitters with hardness ratio H/S (counts above 0.55 keV to counts below 0.55 keV) larger than one (from 2.2 ± 0.9 for RR Pic to 37.6 for GK Per). The "hardness" of GK Per has been confirmed by Cordova and Mason (1984) who found a distribution with kT > 8keV. The recurrent nova T CrB is the weakest source detected. A very soft component (kT ~ 50 e V), such as that observed in U Gem and SS Cyg during optical outburst, is not present in quiescent novae. It is also remarkable that a weak "hard" X-ray emission is a common characteristic of all classes of cataclysmic variables. This fact is an indication that the same mechanism is responsible for the X-ray emission in all these systems.

TABLE 6.15

X-Ray Fluxes and Luminosities of the Post-Novae Detected with EINSTEIN

Object	Data of Observation	IPC counts/s	FLUX (0.16–4.5 KeV) in 10^{-13} erg s^{-1} cm^{-2}	Lx (0.16–4.5 KeV) in 10^{32} erg s^{-1}
	56/1979	0.310	111.60	3.06
GK Per	239/1979	0.174	64.08	1.73
RR Pic	298/1979	0.031	11.20	0.31
CP Pup	328/1979	0.060	21.60	1.27
T CrB	57/1979	0.0083	2.99	0.60
V 841 Oph	265/1979	0.019	6.84	0.61
V 1017 Sgr	98/1980	0.022	7.92	-
V 603 Aql	265/1979	0.279	100.00	1.70
		0.71	220.00	4.50
V 1059 Sgr	295/1979	0.014	5.04	1.13
HR Del	311/1979	0.0084	7.00	0.20

The brightest sources of Table 6.15 are GK Per and V 603 Aql, which have also provided enough photons for time variability studies. Becker and Marshall (1981) reported a short-lived flare in V 603 Aql during which the x-ray intensity doubled. GK Per was found to be variable (during optical quiescence) by Cordova and Mason (1984) in data taken during three consecutive days. They detected variations by a factor of 2 on a time scale of hours and, in addition, significant variations on time scales of about 100 s.

No evidence was found for extended X-ray emission corresponding to the 60-arcsecond size of the optical remnant. GK Per was detected as a transient x-ray source by the Ariel V SSI (2-18 KeV) at a time (June 19 to July 31, 1978) of an optical brightening by about 1 magnitude (King et al., 1979). After the launch of EXOSAT, Watson et al. (1984) reported observations of GK Per during an optical brightening on August 9, 1983. During these activity phases, GK Per is the brightest x-ray source among CVs, with a quite hard spectrum and a 2 - 20 KeV luminosity of about 10^{34} erg s^{-1} (Figure 6.61).

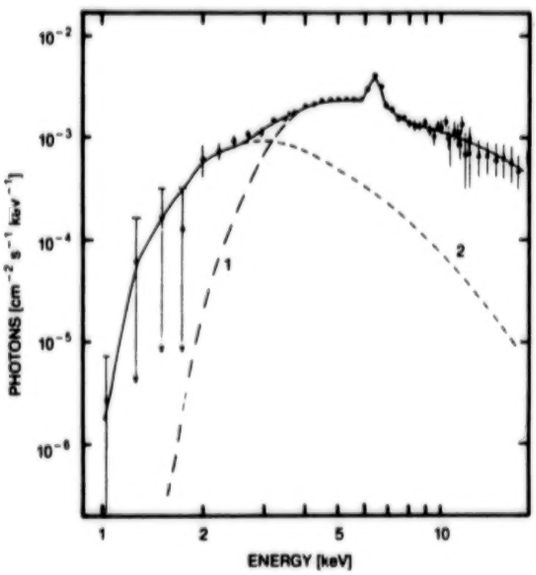


Figure 6-61. The spectrum of GK Per for the range 1 to 20 keV.
(from Watson et al., 1984)

Interestingly, this hard X-ray emission shows a strong coherent modulation with a period of 351 s. The pulse wave form is nearly sinusoidal (Figure 6.62).

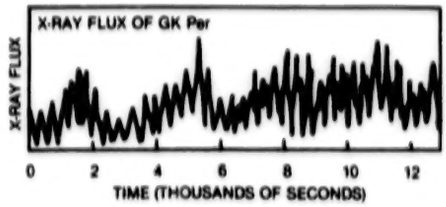


Figure 6-62. The X-ray flux curve of GK Per observed by EXOSAT (2-10 keV) during an optical brightening. The curve is a modulated sinusoidal with a pulsation period of 351 s.
(from Watson et al., 1985)

It is still unclear how bright GK Per becomes bolometrically during these activity phases, because the X-ray spectrum is complex with evidence for two hard components above 2 KeV and a soft component below 0.1 keV. Thus a substantial part of the X-ray luminosity lies outside the spectral range accessible to EXOSAT.

V 603 Aql was reobserved in 1981 (by Drechsel et al., 1983a, b) with the IPC and MPC instruments on board the EINSTEIN observatory. Periodic phase-related flux-variations were detected. The maximum X-ray luminosity in the 0.15 -20 keV range was of about 3 x 10^{33} erg s^{-1} with indication of a hard spectrum.

Although the sample of old novae observed with EINSTEIN was small and liable to selection effects, it has been possible to look for correlations between L_x and other parameters. Becker (1981) suggested a possible correlation of the X-ray luminosity with the inclination of the system, in the sense that in highly inclined systems (e. g. , DQ Her, T Aur) there was a substantial lack of X-ray emission, while the low-inclination system V603 Aql was one of the most luminous. RR Pic, which probably has a high-inclination angle, as derived from the presence of photometric eclipse-like effects (Vogt, 1975), is, however, an X-ray emitter and shows a hot UV continuum. Becker, alternatively, suggested that the speed class of the nova outburst was correlated with L_x in the sense that the four most luminous old novae were all "fast" novae with $L_x \sim 10^{32}$ erg s^{-1}, while those old novae with the most severe upper limits were all "slow" novae with $L < 5 \times 10^{31}$ erg s^{-1}.

At variance, Cordova and Mason (1984) noted that the two old novae which pulse optically (DQ Her and V 533 Her) both lack X-ray emission ($F_x < 1x10^{-13}$ erg cm^{-2} s^{-1} in the 0.16 - 4.5 keV range), and the orbital inclination of V 533 Her is not high, since no evidence of eclipses has been found (Patterson, 1979a).

It is notable that fast old novae, with $L_x \sim 10^{32}$ erg s^{-1}, had a high probability of being accidentally detected by EINSTEIN. However, the EINSTEIN observatory has not been successful in locating previously unidentified cataclysmic variables (Becker, 1981), thus leading to a discrepancy between the assumed space density of classical novae systems (10^{-4} pc^{-3}), (Bath and Shaviv, 1978), and the accidental detection rate of CVs by the IPC. The scarceness of X-ray emitting old novae could be attributed either to a much lower actual space density, of the order of 10^{-7} pc^{-3}, or to a large decrease in L_x occurring many years after the nova outburst.

VI.B. X-RAY OBSERVATIONS OF NOVAE IN OUTBURST

Nova Mus 1983 has been the first classical nova to be detected in the X-ray range during outburst phases (Ogelman et al., 1984). A few previous attempts with earlier X-ray satellites gave negative results, e.g., Nova Cyg 1975 (Hoffmann et al., 1976) using Ariel (2 - 18 keV, threshold limit ~ 3.5 10^{-11} erg cm^{-2} s^{-1}). The lack of detection was probably due to the fact that X-ray observations were made soon after outburst, when the high-density envelope absorbed the soft X-ray emission. The initial discovery of soft X-rays from Nova Mus 1983 was made using the EXOSAT satellite, on April 20, 1984, about 460 days after optical maximum. Other observations were made on July 15, 1984, and December 22, 1984 (Krautter et al., 1985). The spectrum was quite soft and was observed with the LE telescope in the 0.040 - 2 keV range. No flux was detected with the ME detector (1 -50 keV).

The X-ray flux was roughly constant from April to December 1984, while the optical magnitude decreased significantly. The measured low-energy count rates resulted in fluxes on the detector of blackbody-type input spectra in the 0.01 - 0.40 keV temperatures range, or thermal bremstrahlung spectra in the 0.30 - 3 keV temperatures range. Column densities $N_H \sim 3 \times 10^{21}$ [cm^{-2}] were assumed.

A further observation (July 17, 1985) showed a decline by a factor larger then two in the X-ray flux (Ogelman et al., 1987).

The data reported above were interpreted as compatible either with a shocked shell of circumstellar gas emitting 10^7 °K thermal bremsstrahlung at luminosity of about 10^{35} erg s^{-1}, or with a hot white dwarf remnant emitting 3.5 x 10^5 °K blackbody radiation at about 10^{37} erg s^{-1}.

Considerations on the cooling time for a circumstellar plasma at 10^7 K lead to values of the order of 30 - 60 years, a time scale which contrasts with the drop in the X-ray flux in the 1985 observation.

One additional indication in favor of the origin of the X-ray emission from the central star (which became very hot after outburst) and not from the shell is the fact that Nova Vul 1984 became observable with EXOSAT only a few months after the outburst. (Ogelman et al 1984). However, optical spectra of Nova Mus showed the strong coronal line of FeXIV 5303, which requires temperatures of the order of 2 x 10^6 °K.

The discovery of soft X-rays from Nova Mus 1983 stimulated EXOSAT observations of other novae during outburst phases. (Ogelman et al., 1987).

Nova Vul 1984-1 and Nova Vul 1984-2 were observed in various epochs, from the onset of the outburst until the first year after the outburst.

The data indicated intensity values and rise time values that are consistent with those expected from a constant bolometric luminosity model of a hot white dwarf remnant.

With the assumption that Nova Mus 1983 and Nova Vul 1984-1 and -2 had similar X-ray light curves, Ogelman et al. (1987) suggested that the X-ray emission from novae increases from zero at outburst to a plateau in a time scale of about 400 days; it remains constant for approximately 400 days and then decays with approximately the same time scale. The X-ray life time of the remnant is thus of the order of 2 - 3 years.

The EXOSAT observations of RS Oph in 1985 have provided the first X-ray recording of a recurrent nova in OB. RS Oph was one of the brightest sources recorded by EXOSAT LE telescope.

Mason et al. (1987) reported intense soft X-ray emission with a characteristic temperature of a few million degrees approximately 2 months (March 22, 1985) after the January 1985 optical outburst. The intensity steeply decreased between 60 and 90 days after the OB (April and May 1985). A lower limit for the total flux between, 1 -6 keV in March 22, 1985, was estimated at about 1.5×10^{-10} erg cm^{-2} s^{-1}. Bode and Kahn (1985) have interpreted this X-ray emission in terms of the interaction of the ejecta with the envelope produced by the wind of the red giant. A weak residual X-ray emission was detected with the LE telescope about 250 days after OB, in October 1985. This flux is indicative of a temperature of ~ 300.000 °K and is consistent with the presence of a hot white dwarf of $L \sim 10^{37}$ erg s^{-1}, $R \sim 10^{9}$ cm at a distance of ~1.6 Kpc ($N_H \sim 3 \times 10^{21}$ cm^{-2}).

It is remarkable that these values for L and T are in agreement with those proposed by Ogelman et al. (1987) for the soft X-ray emission from Nova Mus 1983.

VII. FINAL DECLINE AND NOVA ENVELOPES.

(written by Duerbeck and Hack)

VII.A. THE FINAL DECLINE OF NOVAE

From the theorist's side, who wants to check predictions of current nova models, the final decline of novae is interesting because it presumably encompasses several decisive moments in the development of a nova outburst:

1) The shell should be depleted, either by a strong wind or by dynamical friction in the shell by the secondary star, to such an extent that nuclear burning is halted in the shell. The remaining material should then settle down on the surface of the white dwarf.

2) The accretion disk should be reestablished, possibly only for a short time (hibernation model, see Chapter 7).

From the observer's side, in the past, spectroscopic investigations were, in most cases, restricted to the emission lines, leaving the continuum underexposed. The use of linear receivers has improved the situation recently.

The situation is somewhat better for photometric observations. Light curves that cover the late decline for some bright objects are available. The interpretation of such light curves is complicated by the fact that the flux of the nova is composed of several components: the light of the central object (a continuous spectrum, in first approximation a blackbody spectrum), the nebula (emission line spectrum plus free-free and bound-free continua), and, in some cases, wavelength-dependent obscuration represents modulation of the continuum by circumstellar dust.

Most available light curves have the disadvantage that they are broadband (e.g., visual, photographic, Johnson filters) and thus include both the continuum and strong nebular lines. More useful data are obtained in spectral regions isolated by medium-or narrow-band filters (e.g., Stromgren *y*). Absolute spectrophotometry from objective prism spectra or with digital receivers calibrated by spectrophotometric standards is, of course, ideal, because it gives both information on emission line strengths and the continuum energy distribution.

The decline of a nova becomes more difficult to interpret if excessive dust formation occurs in the shell. A good example is FH Ser, which remained at a constant bolometric luminosity

until about 200 days after maximum; in the beginning, the visual decline was caused by a shift of the maximum of radiation to the ultraviolet. In later stages, dust formation shifted the peak of radiation to the middle infrared (3 - 6 μm). In such a case, spectrophotometry in the optical does not at all give an indication of the total energy output of the nova and its variation.

This example shows that the sum of the contributions of all radiation sources in the visual band is not very helpful in describing the development of the outburst in its late stages. Even if all contributing sources in the optical region can be clearly disentangled, the problem is still there that the overall energy distribution is only incompletely known. Observations in the infrared and ultraviolet, as well as in the x-ray region, have in recent years improved the situation quite a lot; how scarce they might be for some objects or at some phases of the outburst. Indeed, the late decline is covered least by such multifrequency observations, and more or less regular observations of a future (bright) nova might remedy the situation somewhat.

As mass loss is decreasing with time, the photospheric radius decreases and, since the energy source has not yet turned off completely, the photospheric temperature rises. The associated hardening of the radiation causes the nova to become a UV, an EUV, and ultimately a soft x-ray source (detectable with EXOSAT or equivalent X-ray facilities). Infrared emission of x-ray heated grains should also be detectable during the soft X-ray phase.

In the past, a description of the (broadband) decline of light curves in the optical region was introduced by Vorontsov-Velyaminov (1940, 1948, 1953). He approximated a nova light curve by

$$m(t) = m_o + b_1 \log (t - t_o), \qquad (6.1)$$

where t is measured in days, and, if a discontinuity occurs in a later stage, by

$$m(t) = m_1 + b_2 \log (t - t_o) \quad (\text{for } b_2 > b_1). \qquad (6.2)$$

For the average nova, b_1 has the value 2.5, and thus the luminosity in the visual region can be described as L = A/t. Discontinuities occur mostly at $\Delta m = 3.8$ (counted from maximum), and at $\Delta m = 6.3$. They indicate the onset and end of the transition stage.

A large collection of m / log t curves has been compiled by Vorontsov Velyaminov (1948, 1953) (see Figure 6.63) and by Gershberg (1964).

Most of the better observed objects, where continuum and line intensities are available, are discussed below.

V1500 Cyg. The data used are those of Lockwood and Millis (1976), based on Strömgren y photometry. Another illustration of the usefulness of well - defined spectral regions is the plot of continuum and line fluxes (continuum at 0.479 μm and 2 μm, as well as Hβ and [O III] fluxes). While the continuum fluxes and Hβ decline at a more or less equal rate, the [O III] flux decreases more slowly. Also, the visual flux decreases more slowly in late phases, when it vanishes as does also the IR flux, which originates from optically thin free-free emission, but comes from the remnant (Figure 6.64, Ferland et al., 1986). In the first phase, the slope in the relation m(t) = a log t is 4.5. Here, as usual, the zero-point of the time is the moment of maximum light.

Similar data are available for V1668 Cyg. Kaler (1986) used Strömgren and Hß wide filters to study the decline in late phases. The continuum slope is first 3.5, then 6.5, possibly even steeper in the very late phases. The Hß flux (which also includes some contribution of [O III]) declines much more slowly.

The light curve of V446 Her, also studied with a narrow-band filter in a relatively line free spectral region by Gyldenkerne, Meydahl, and West (1969), gives a slope of 4.11. Pioneering spectrophotometry by Meinel (1963) is also available for this object. The light curve of V533 Her, from spectra calibrated by broad band photometry, and derived continuum fluxes by Friedjung and Smith (1966) yields a slope of 3.57.

Spectrophotometry of "historical" novae by means of objective prism plates was carried out by Payne-Gaposchkin and collaborators: DQ Her (Whipple and Payne-Gaposchkin, 1936, 1937, Payne-Gaposchkin and Whipple, 1939); RR Pic (Payne-Gaposchkin, and Menzel, 1938), and GK Per, V603 Aql, and others (Payne-Gaposchkin and Gaposchkin, 1942).

The spectrophotometry of HR Del by Drechsel et al. (1977) is also based on objective prism spectra. The continuum magnitude yields, after an unusually long plateau with a practically negligible slope, an extremely rapid and nonlinear decline of about 8.3, which is faster than that of a fast nova, because it occurs at a much later time as counted from maximum. (see Figure 6.65).

The physical reason for the time scale of the return to the prenova state is not yet understood. A $M_{\odot}$ is required to trigger a runaway. Nuclear burning proceeds at a luminosity of approximately $3 \times 10^4 L_{\odot}$, thus the nuclear burning time scale is approximately 300 years. MacDonald, Fujimoto, and Truran (1985) think that the time scale of classical nova systems is of the order 10 - 30 years. The spectrophotometric analyses (especially the study of FH Ser over a wide wavelength band) indicates that turnoff for this fairly slow nova occurs 200 days after outburst.

Turnoff requires fuel exhaustion either by nuclear burning (which appears not to be the case, in view of the quoted time scales), some sort of quenching of the nuclear reactions, or some mechanism of mass loss. This can be the "thick wind" of outbursting novae (Bath, 1978; Ruggles and Bath, 1979), or the loss of the shell through the outer Lagrangian points of the binary system as a result of dynamical friction during the common envelope phase (MacDonald, Fujimoto and Truran, 1985; MacDonald, 1986).

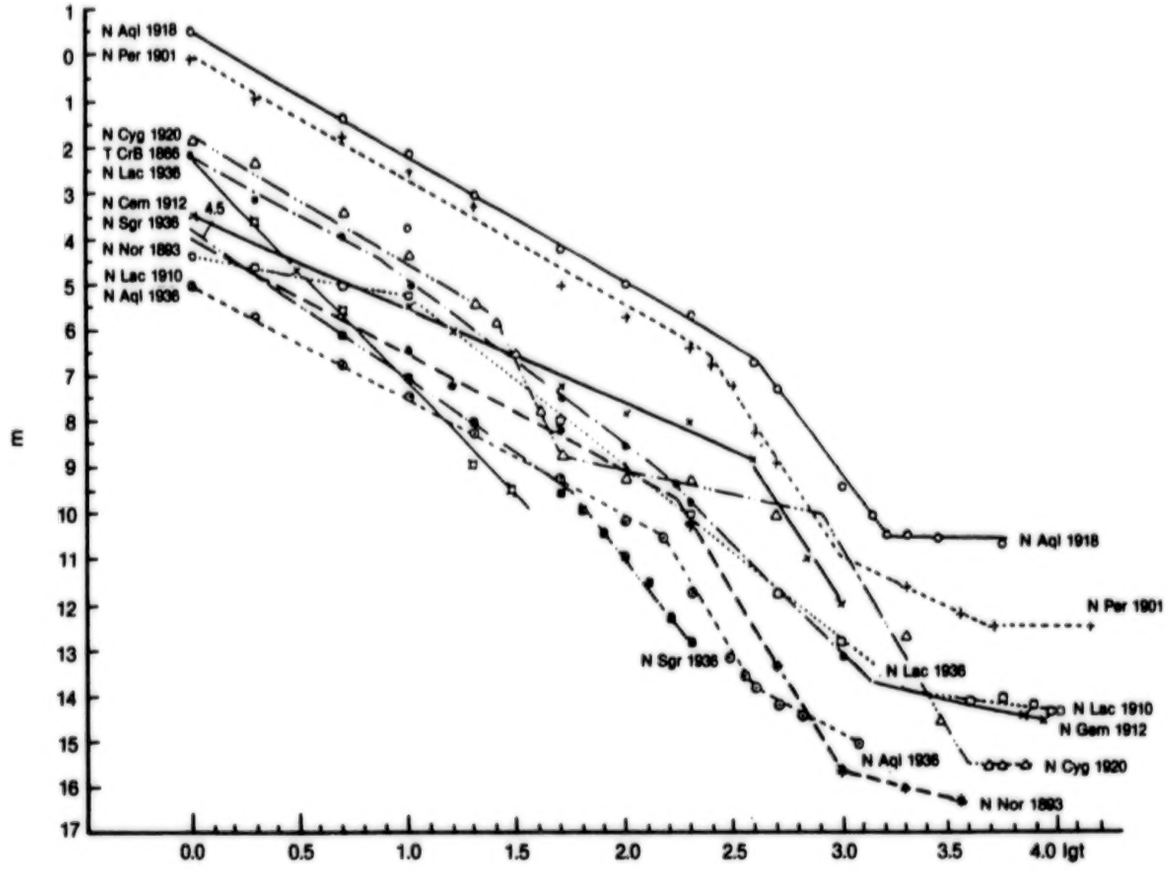


Figure 6-63. An m-log t diagram of visual nova light curves (from Vorontsov-Velyaminov, 1953)

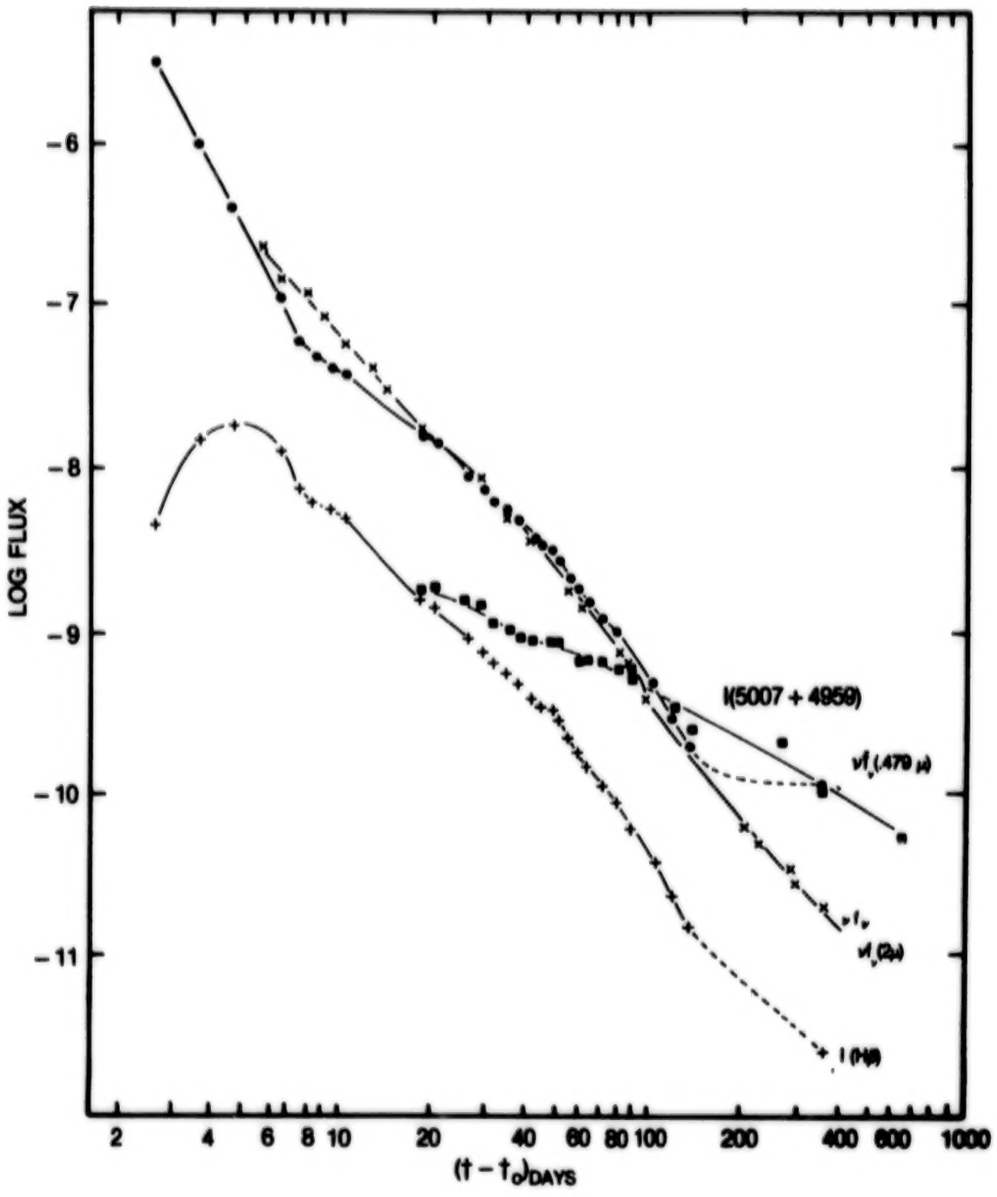


Figure 6-64. The development of line and continuum strengths in Nova V 1500 Cyg during its decline. The plotted quantities have not been corrected for interstellar reddening and are either the integrated strength of the emission line in erg s^{-1} cm^{-2} or νf, a continuum measure with similar units. The continua at 2 μm and 0.479 μm are shown by x and • respectively. These nearly coincide during the interval over which the optical and infrared continua are optically thin free-free emission (t=10....150 days) and sharply diverge when the underlying remnant becomes visible, about one year after outburst. The Hβ line follows the continuum strength closely, while [O III] 5007 and 4957 line declines much more slowly.
(from Ferland et al., 1986)

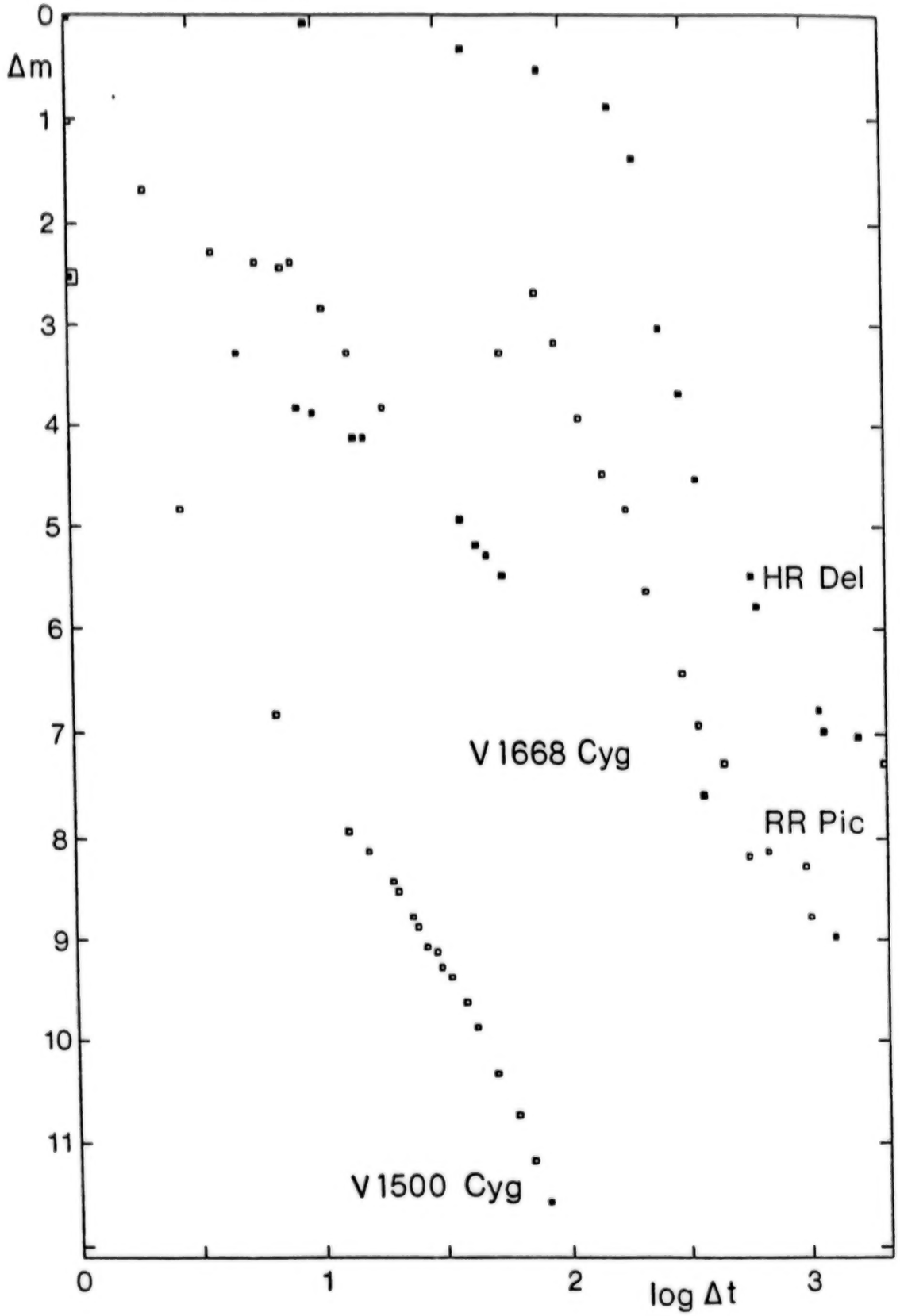


Figure 6-65. Δm(continuum)-log Δt diagram for several novae (for references, see text).

VII.B. THE POSTNOVA PHASE WITH SURROUNDING NEBULOSITY

When the nova has declined to its preoutburst state, the only remaining sign of the outburst is the surrounding expanding nebulosity. This seems to be a comparatively short-lived phenomenon, since no "past nova" or "nova-like object" without recorded outburst could be identified as a nova because of an observable shell. A few counter examples, e.g., E2000+223 (Takalo and Nousek, 1985) and 623+71 (Krautter et al. 1987), are extremely dubious. This can be explained by the fact that nova shell masses are fairly small and are easily lost several decades after outburst when their surface brightness becomes very small. This has to do with the fact that the "central stars" are not very powerful in exciting the surrounding nebulosities, and most energy is drawn from the interaction with the interstellar material. Thus, in the course of time, nova shells are decelerated, interaction becomes less powerful, and the shells are less excited and fade in optical light.

Combined spectroscopic and direct observations can give information on their distance, on the mass lost in the outburst, and on their chemical composition and physical structure.

One of the best methods for deriving the distance of a nova is to measure the angular size of the nebula formed around it as the result of the explosion. By knowing the expansion velocity and the time elapsed since the explosion, we can compute the real dimension of the nebula and derive its distance. The distance determined by this method can be used for calibrating the relationship between absolute magnitude at maximum and rate of decline.

McLaughlin (1960) and Cohen and Rosenthal (1983) have studied twelve old novae in order to measure the surrounding nebula. Cohen (1985) added eight new spatially resolved nova shells. The data relevant for the determination of the size of the envelope, and therefore for the the distance, are given in Table 6.16 (adapted from Cohen and Rosenthal, 1983, and Cohen, 1985, while Table 6.17 (from Cohen and Rosenthal, 1983) gives the observed and expected radii of the shells. The majority of these shells have nonspherical shape. The expansion velocities from McLaughlin, from Cohen and Rosenthal, and from Cohen (1985) are in rather good agreement, with the exception of V603 Aql and CP Lac. For these objects, the radial velocities are supposedly those of the accretion disk. The shells are too faint to be discovered by those authors.

Cohen (1985) has observed all classical novae that exploded before 1976, which were at maximum brighter than V = 6.6 mag, and are observable from Mt. Palomar. Of the 18 objects, 9 showed no detectable shell. Since the shells emit especially in the light of Hα + [N II], interference filters centered at Hα, having a full width at half maximum (FWHM) of 16 and 30 Å were used.

Like supernova shells, the expanding nova shells interact with the surrounding interstellar material. The kinetic energy of a nova shell shortly after outburst is, however, already much smaller; it lies between $2\ 10^{45}$ and $1\ 10^{44}$ erg (e.g., Chevalier, 1977). The snowplow model, put forward by Oort (1946, 1951), has been applied to old supernova remnants and nova remnants with satisfactory results (see Chapter 7).

Recently, by comparing outburst photographs and CCD frames of nova shells taken at different times, Duerbeck (1987a) found noticeable decelerations with time, as postulated by the snowplow model.

The temporal variation of the shell radius r (in arc seconds) is approximated by

$$r(t) = c_0 + c_1\, t + 0.5\, c_2\, t^2 \qquad (6.3)$$

where c_0, the size of the shell at the time of outburst, is assumed to be zero. c_1 is the initial expansion rate, measured in arc sec yr^{-1}. c_2 is the deceleration parameter (in arc sec yr^{-2}), which can be converted into the braking b (in km s^{-1} yr^{-1}):

$$b = \frac{c_2}{c_1} V_{exp}. \qquad (6.4)$$

TABLE 6-16a NOVA CHARACTERISTICS

Nova	Exp.rate "/y	Expansional velocity (1) km/s	(2)	Distance pcs	m_{max}	m_{min}	absorption (1)	(2)	M_{vis} Max (1)	(2)	Min
V 603 Aql	.956	1700	255	376	-1.1	10.8	.2	.2	-9.2	-9.15	+2.7
T Aur	.117	460	655	830	+4.2	15.4	.7	1.5	-6.2	-7.9	+5.0
V476 Cyg	.093	700	790:	1590	+2.0	16.1	.6	.6	-9.6	-9.85	+4.5
DQ Her	.27	290	315	230	+1.4	15.1	.2	.2	-5.6	-6.2	+8.1
CP Lac	.25	1600	295:	1340	+2.1	15.3	.8	.8	-9.3	-9.35	+3.9
GK Per	.54	1200	1200	470	+0.2	13.5	.3	.3	-8.5	-8.55	+4.8
RR Pic	.18	410	475	480	+1.2	13.3	.2	.2	-7.4	-7.3	+4.7
CP Pup	.21	700	710	700	+0.4	17.5	.3	.3	-9.1	-9.55	+8:
HR Del			520		+4.8			.2		-5.05	
V533 Her			580		+3.5			.2		-7.45	
BT Mon*			800								
FH Ser			560		+4.4			2.8		-7.55	

*) BT Mon was discovered only in its late decline stage.
(1) Data by McLaughlin (1960).
(2) Data by Cohen and Rosenthal (1983).

TABLE 6-16b. NOVA LUMINOSITIES AND LIGHT CURVES (from Cohen, 1985)

Object	V_{erp} (km s^{-1})	Source of V_{erp}	A_v (mag)	m_v(max)[a] (mag)	t_2 (days)	Light Curve Source	M_v(max) (mag)	M_v(15) (mag)
Novae of Paper II (Cohen, 1985)								
v1229 Aql 1970	575	1	1.2 ± 0.5	6.5	18	7	-6.6	-4.8
v500 Aql 1943	1380	2	3.0 ± 1.5	6.5:	20:	8	-10.35	-8.85
*v1500 Cyg 1975.....	1180	1	1.2	1.85	2.4	9	-9.95	-5.1
*v446 Her 1960	1235	3	0.8	2.75	5	7	-8.7	-5.55
*v533 Her 1963	1050	4	0.6	3.5	26	10	-7.7	-6.6
DK Lac 1950	1075	5	1.4	5.0	19	5	-9.35	-7.35
XX Tau 1927	650:	1	$1.3^{+0.2}_{0.7}$	6.0	24	11	-8.05	-6.75
RW UMi 1956	950:	1	0.1	≤6.0	200:	12	≤-7.85	...
*LV Vul 1968	860	6	1.2	4.5	21	6	-6.75	-5.25
Novae Discussed in Paper I (Cohen and Rosenthal,1983)								
*603 Aql 1918	....	....	....	..	4	....	-9.15	-5.35
T Aur 1891	....	....	1.2 ± 0.5	..	80	....	-7.4	-7.0
v476 Cyg 1920	....	....	....	..	7	....	-9.95	-6.85
HR Del 1967	....	....	....	4.6	> 150	....	-5.25	-5.25
*DQ Her 1934	....	....	....	..	67	....	-6.2	-5.2
*CP Lac 1936.....	....	....	....	..	5	....	-9.35	-5.95
BT Mon 1939	....	....	....					
*GK Per 1901	....	....	....	..	6	....	-8.55	-5.75
*RR Pic 1925	....	....	....	..	80	....	-7.3	-6.0
*CP Pup 1942	....	....	....	..	5	....	-9.55	-5.55
T Sco 1860	....	....	0.6	7.0	9	13	-8.9	-6.5
FH Ser 1970	....	....	....	..	42	....	-7.55	-6.55

NOTE--Sources of data in cols (3) and (7) are as follows: (1) V_{erp} from double spectrograph observations at current epoch; (2) Sanford 1943; (3)V_{erp} from Cohen's measurements of spectra from plate vault of Mount Wilson and Las Campanas Observatories; (4) Baschek 1964; (5) Larsson-Leander 1953, 1954; (6) Hutchings 1970; (7) AAVSO (Mattei 1984); (8) Gaposchkin 1943; (9) Young et al. 1976; (10) Chincarini 1964; (11) Cannon 1928; (12) (Kukarkin 1963, Ahnert 1963; (13) Sawyer 1938.

The half-lifetime is determined by

$$t_{1/2} = \frac{V_{exp}}{2b} = \frac{1}{2}\frac{c_1}{c_2} \qquad (6.5)$$

The observational results of four shells are listed in Table 6-18.

The deceleration is larger for higher expansion velocities, the mean half-time, after which the expansion velocity has dropped to half its initial value, is 75 years. The expansion of a pronounced feature of the shell of GK Per, the "bar," is illustrated in Figure 6-66. The results are in accordance with expectations from the snowplow model put forward by Oort (1946, 1951).

This braking must be taken into account in the determination of nebular expansion parallaxes. Errors can be as large as 20 to 30%, which is about as large as the uncertainty of choosing the "true" expansion velocity of the shell, derived from the Doppler displacement of absorption lines at maximum. Usually, it is assumed that the "true" velocity is that of the principal spectrum, which is lower than that of the diffuse-enhanced and of the

TABLE 6-16c. SHELLS NOT DETECTED (from Cohen, 1985)

Object	Seeing (FWHM) (arcsec)	Central Pixel (DN)	m_v(max)[a] (mag)	r (mag)	Hα (mag)
IV Cep 1971	1.3	13,200	7.5	16.08	16.14
Q Cyg 1876.....	1.0	30,700	3.0	14.93	14.94
v450 Cyg 1942	1.0	5,600[b]	7.8	16.48	16.58
DI Lac 1910	1.0	58,675[c]	4.6	14.58	14.90
HR Lyr 1919.....	1.0	18,300	6.5	15.95	15.99
v841 Oph 1848	2.5	11,700	5.0:	....	....
v368 Sct 1970.....	1.0	9,070	7.0	....	12.71
v373 Sct 1975.....	1.0	3,600[b]	6.0	18.07	16.98
WY Sge 1783	1.0	4,120	6:	18.10	17.89

[a] From Payne-Gaposchkin 1957, 1977.
[b] Faint star(s) closer than 4" to postnova star.
[c] Cental pixel saturated. Its value was extrapolated using the point-source image profile.

TABLE 6-17. SIZES OF NOVA SHELLS

NAME	RADIUS (arcsec) Observed (1981)	Expected	NOTES
V603 Aql ..	not detected	60	
T Aur	9.5	10.5	1
V476 Cyg ..	5.7	5.7	
DQ Her	10.5	12.7	1
CP Lac	not detected	11.3	
GK Per	41.5	43.2	1
CP Pup	7	8.2	2
RR Pic	11.5	9.7	1,3
HR Del	1.8	....	1,4
FH Ser	2.0		
V533 Her ..	1.6		
BT Mon	3.8		

NOTES—(1) Shell non-spherical. (2) Radius from Williams 1982. (3) Radius from Williams and Gallagher 1979. (4) Radius from Kohoutek 1981.

(From Cohen and Rosenthal, 1983)

TABLE 6-18. EXPANSION AND DECELERATION OF NOVA SHELLS

nova	V_{exp} (km s^{-1})	c_1 ("yr^{-1})	b (km s^{-1} yr^{-1})	$t_{1/2}$ (yr)	d (pc)
V603 Aql	1700	1.09	13.2	65	330
GK Per	1200	0.65	10.3	58	390
V476 Cyg	725	0.10	3.1	117	1500
DQ Her	335	0.26	2.4	67	265

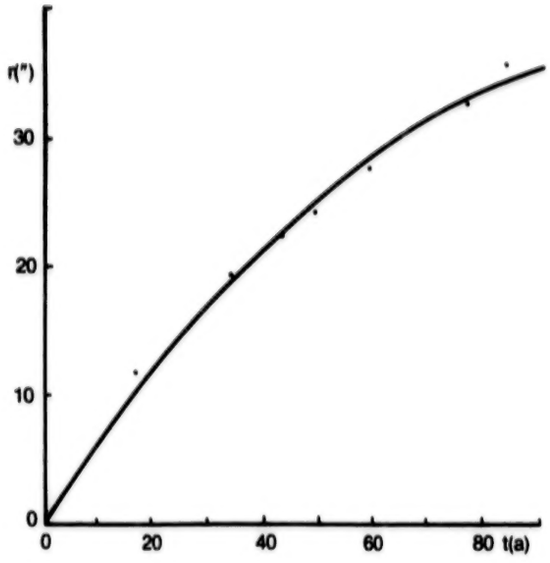


Figure 6-66. Deceleration of the bar in the shell of GK Per, using data of Duerbeck (1987a).

Orion spectra. At visual maximum, when the principal spectrum is dominating, the mass loss rate also reaches a maximum, and the main portion of the shell is formed.

An estimate of the masses of the shells is made by Cohen and Rosenthal (1983) by using several assumptions. The absolute flux of Hβ, corrected for interstellar absorption, gives the electron density. The electron temperature is assumed to be 10^4 K. It is also assumed that the shell thickness *a* is 10% of the shell radius, and that the filling factor *b* of this shell is 10%. With these assumptions, the masses of the shells are computed and the values are found to range between 1.9×10^{-5} $M_\odot$ for V1500 Cyg and 1.3×10^{-4} $M_\odot$ for V476 Cyg. These data are given in Table 6-19, together with other values for the same and different objects, determined by different methods. The uncertainty in mass determinations is clearly seen. Masses of the shells of classical novae cluster between $1 - 10 \times 10^{-5}$ $M_\odot$.

TABLE 6-19. DETERMINATIONS OF NOVA SHELL MASSES (in 10^{-5} $M_\odot$)

Type	Object	Mass	Reference	Method
F	V603 Aql	10	Gordeladse (1937)	wind model
		14	Pottasch (1959d)	Hα flux
F	V1301 Aql	1	Snijders et al. (1984)	UV spectrum
F	T Crb	10	Gordeladse (1937)	wind model
F	V478 Cyg	0.2	Gordeladse (1937)	wind model
		13	Cohen, Rosenthal (1983)	Hβ flux
F	V1500 Cyg	4.5	Neff et al. (1978)	opt. spectrophotometry
		24	Hjellming et al. (1979)	Radio
		14	Seaquist et al. (1980)	Radio
		6.1	Duerbeck (1980)	wind model
		1.9	Cohen, Rosenthal (1983)	Hβ flux
F	V1668 Cyg	1.7	Duerbeck (1980)	wind model
		0.9	Peimbert and Sarmiento (1984)	UV spectrum
S	HR Del	25	Malakpur (1973a)	Hβ flux
		9	Anderson, Gallagher (1977)	Hβ flux
		1000	Antipova (1977)	optical spectroscopy
		≤145	Robbins, Sanyal (1978)	
		8.6	Hjellming et al. (1979)	Radio
		11	Duerbeck (1980)	wind model
		2.2	Cohen, Rosenthal (1983)	Hβ flux
		0.2	Solf (1983)	
	DN Gem	0.4	Gordeladse (1937)	wind model

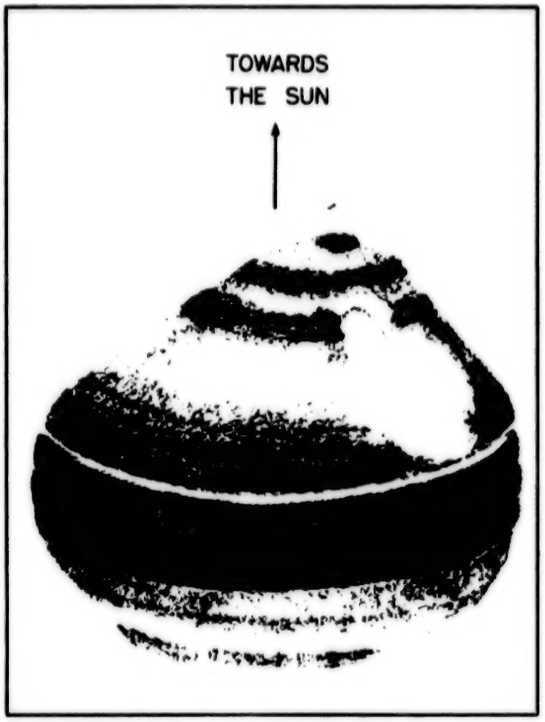
S	DQ Her	9	Gordeladse (1937)	wind model
		0.7	Pottasch (1959)	Hα flux
		4.6	Mustel, Boyarchuk (1970)	optical line flux
		4.8	Ferland et al. (1984)	UV, optical spectrum
F	V533 Her	2.0	Cohen, Rosenthal (1983)	Hβ flux
F	CP Lac	3.6	Pottasch (1959)	Hα flux
F	RS Oph	0.5	Sayer (1937)	
		0.02	Folkart et al. (1964)	
		0.05	Pottasch (1967)	
			Snijders et al. (1987)	
F	GK Per	0.3	Gordeladse (1937)	wind model
		3.8	Pottasch (1959)	Hα flux
S	RR Pic	14	Gordeladse (1937)	wind model
		10	Pottasch (1959)	Hα flux
S	T Pyx	8	Seitter (1987)	Hα flux
S	FH Ser	4.3	Seaquist, Palimaka (1977)	Radio (spherical)
		3.1	Seaquist, Palimaka (1977)	Radio (polar)
		4.5	Hjellming et al. (1979)	Radio
		6.1	Duerbeck (1980)	wind model
		2.0	Cohen, Rosenthal (1983)	Hβ flux
F	LV Vul	7.8	Duerbeck (1980)	wind model
F	NQ Vul	13	Duerbeck (1980)	wind model

VII.B.1. MORPHOLOGY OF NOVA SHELLS

A general overview of nova shell morphology is given by Mustel and Boyarchuk (1970). They found, from a study of a handful of objects, that most shells have an oval shape, exhibit "polar blobs" at the end of the major axis, and an "equatorial belt", which coincides with the plane of the minor axis.

DQ Her: The system is seen perpendicular to the major axis; the shell is oval. "Polar condensations" are situated at the very ends of the large axis, and an equatorial belt is visible.

V603 Aql: The system is seen nearly parallel to the major axis; the shell appears nearly circular. An approaching polar condensation is seen in spectra and on direct images of 1933 and 1940. A system of several (two to three) rings seems to exist in the equatorial region. A thorough study of spatially resolved spectra in the nebular phase by Weaver (1974) confirmed largely the findings of Mustel and Boyarchuk (1970). Weaver's model is shown in Figure 6.67.



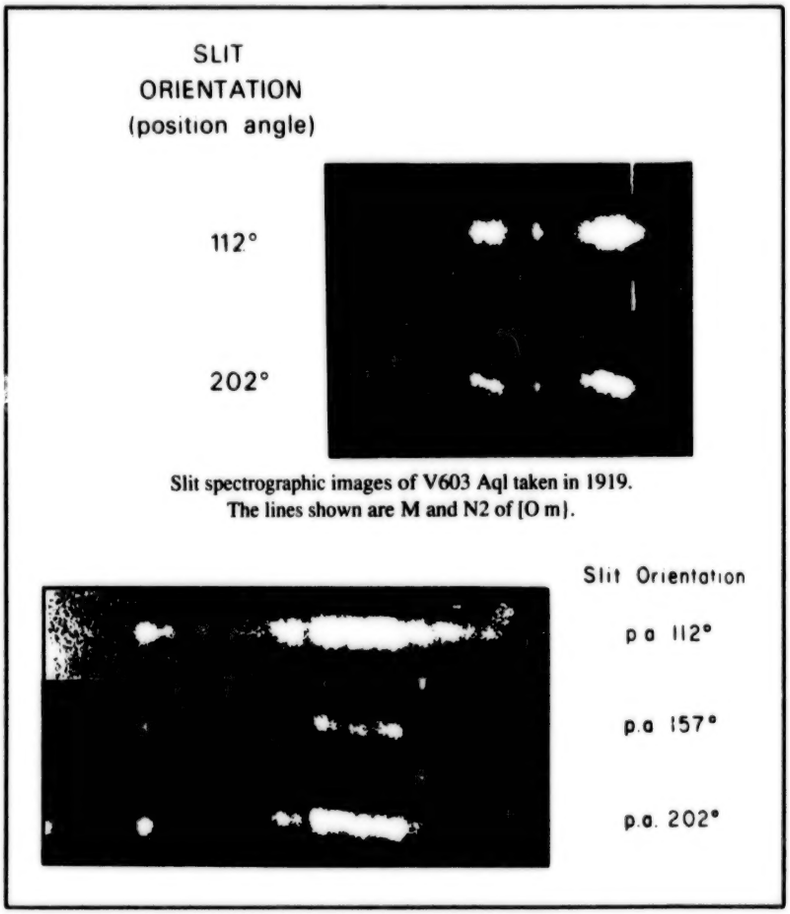


Figure 6-67. a) Drawing of a three-dimensional model of the shell of V 603 Aql, derived from b) space-resolved spectrograms taken at Lick Observatory in 1919. (from Weaver, 1974)

T Aur (See Figure 6.68): The system may have the same orientation as DQ Her, because eclipses of the central object also occur. The shell appears oval. Polar condensations and the equatorial belt seem to be missing, possibly due to the old age of the remnant. Generally, the authors argue that the equatorial belt is in the equatorial plane of the binary and polar blobs perpendicular to that plane (see also Chapter 7).

RR Pic (See Figure 6.69): The shell appears nearly circular, but this may be due to an inclination effect: it is oval when looked at in the plane of the binary. The absence of eclipses and the presence of periodic features in the light curve are in agreement with this assumption. A double-ring blob system is obvious, which can be explained by precessional motion of the erupting object in the course of the extended outburst. Deep CCD frames indicate the presence of high-velocity clouds surrounding the brighter parts of the shell, which could be material from the diffuse-enhanced mass outflow (Duerbeck, 1987b). However, a spectroscopic investigation of this faint halo is necessary to prove whether it is outflowing nova material or shocked interstellar material.

CP Pup (See Figure 8.30): The shell appears circular, but may be inclined by an angle of 30°

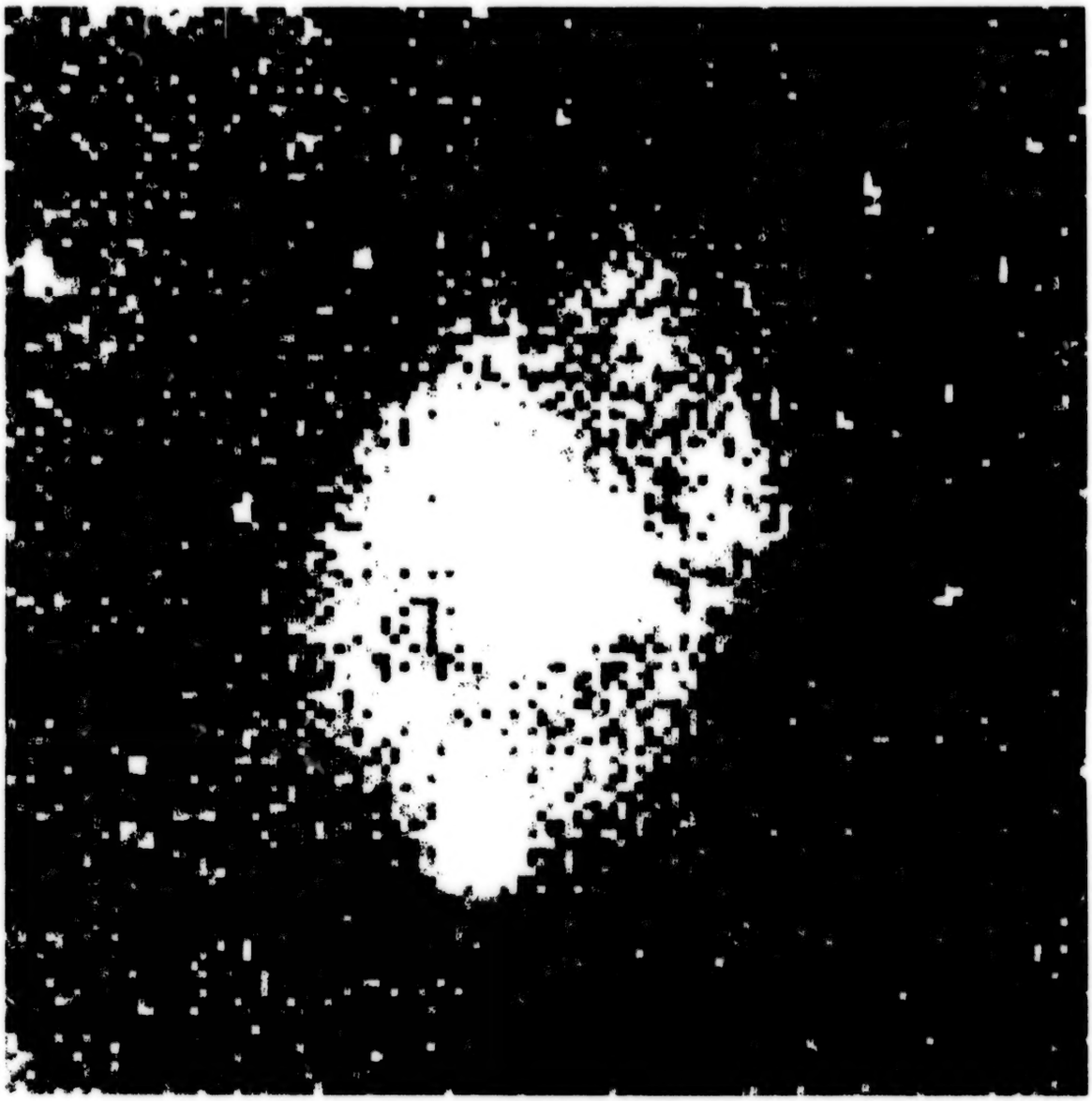


Figure 6-68. CCD frame of the shell of T Aur, taken through an Hα filter with the Calar Alto 2.2 m telescope.

with respect to the celestial plane, as revealed by radial velocity determinations. The circular belt is fragmented into at least 11 condensations, which apparently were already present a few months after outburst, as noted in high-dispersion spectral studies of CP Pup in the nebular stage.

Seitter (1971), Hutchings (1972), and Malakpur (1973a) have modelled nova shells from the nebular spectra of HR Del, FH Ser, and LV Vul, respectively. They also yield a ring/shell-type structure, which was confirmed for the objects Hr Del and FH Ser by direct imaging in later phases.

Hutchings (1972) discussed this nonspherical distribution of the matter in the nebula as a consequence of the binary nature of the nova system. He observes that the time scale of the mass loss during the outburst is longer than the orbital period (days or months as compared with hours). The interaction will occur in a ring around the equatorial region of the expanding nova photosphere. The interaction with the companion by purely gravitational forces will have the effect to reduce the original spherical symmetry to two polar cones and to give rise to a) a faster-moving ejecta that move out initially in all directions from the outer parts of the equatorial band and later either disappear or are more concentrated to the

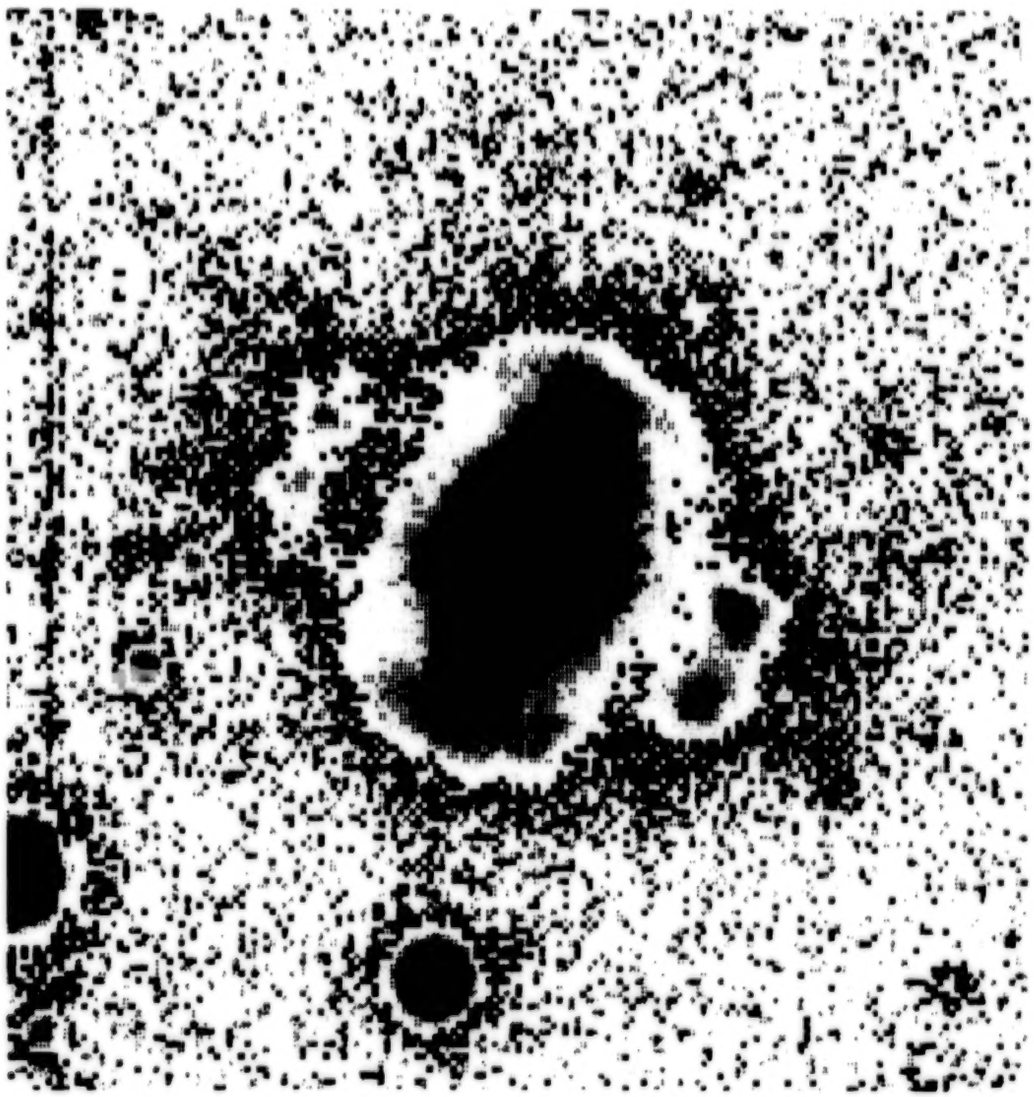


Figure 6-69. The shell surrounding RR Pic, taken through an H α filter, with a CCD camera at the ESO 2.2 m telescope. For this composite, the central section of the highly amplified picture was set to zero, and a low magnification image of the central nebula was inserted.

equatorial plane, and b) some slower-moving equatorial remnants (Figure 4 from the paper by Hutchings). The comparison of the observed emission line profiles with those computed for different geometry and inclination to the line of sight of the nova envelope will be discussed in Chapter 7.

In recent years, direct imaging and spatially resolved spectroscopy of nova shells has progressed quite much, due to the advance in detector technology. The following Table 6-20 summarizes such work.

It should be noted that the morphological description given in the table is extremely scarce. More detailed discussions of the shape of V603 Aql is given by Weaver (1974); that of GK Per is described in Duerbeck and Seitter (1987); those of RR Pic, CP Pup, and T Pyx by Duerbeck and Seitter (1979) and Duerbeck (1987b). A detailed discussion of several envelopes will be found in Chapters 8 and 9.

nuclear reactions occurring during the explosion, and hence to check the theories of the outburst. According to the theory proposed by Starrfield et al. (1977; see also Chapter 7), a fraction of the accretion disk material reaches the surface of the degenerate star (assumed to be a carbon-oxygen white dwarf) building up a layer of H-rich material on the surface. Eventually, compression of the accreting gas causes heating up to temperatures at which nuclear burning sets in. According to their calculations, if the CNO nuclei are enhanced in the envelope (as a consequence of the previous history of the material), a thermonuclear runaway occurs, producing a fast nova. Otherwise, a slow nova outburst occurs. A knowledge of the element abundance in novae is fundamental to understand the nature of the outburst and to check the theories.

A discussion of various methods for deriving the chemical composition of novae is given by Williams (1977). He shows that many causes of uncertainty affect the abundances derived from

TABLE 6.20 NEBULAR SHAPES, TEMPERATURES, AND ABUNDANCES

nova	T (K)	abundances	morphology
T Aur (1892)	low	CNO high	elliptical
DQ Her (1934)	500	[CNO/H]=100	elliptical,pol.blobs
GK Per (1901)	$\geqq$20000	N enh.	single blobs; complicated structure
RR Pic (1925)	16500	He,N,Ne? enh.	ring + blobs
CP Pup (1942)	800	[N/H]=1000	many blobs
T Pyx (recurr)	$\geqslant$20000	solar?	several shells

VII.B.2. SPECTRA AND ABUNDANCES IN NOVA SHELLS

Besides the possibility to derive their distances and to measure their masses, nova shells are important because their spectra offer more precise methods to measure their chemical composition and therefore to verify if this is affected by the absorption spectrum around maximum light. Such a rapidly changing spectrum is very far from the usual conditions in a stable atmosphere; the abundance of CNO depends upon an assumed temperature distribution in the pseudophotosphere, which is highly uncertain. Emission line spectra in early decline give also uncertain results, because emission and ab-

sorption components are blended together, making uncertain the measure of the emission line intensity, and because of the uncertainties of the parameters of the emitting gas. One can hope that more reliable abundance determinations can be obtained by the study of the spectra of old extended shells that behave in a similar way to young planetary nebulae. At the time when the shells become spatially resolved, the density is so low that self-absorption and collisional de-excitation should be negligible. The distance between the shell and the stellar object plus accretion disk make impossible any confusion with these regions having very different physical conditions.

Table 6-21 (Tylenda, 1979) compares the average abundances of novae with those of planetary nebulae and the solar values.

Anyway, the physical and chemical properties of nova shells are difficult to determine and subject to controversy. We will quote the results of several investigations of the shells of DQ Her, RR Pic, and CP Pup. A more detailed discussion is given in Chapter 8.

Several models of the shell of DQ Her have been presented in the last decade, and every time, the previous results (or predictions) have been partially discarded. Williams et al. (1978) carried out spectroscopy in the visible region, and obtained the following results:

The electron temperature, T_e, of the shell must be low because of the narrow Balmer continuum emission at 3644. Most of the hydrogen emission and the C II, N II, and O II recombination lines originate in the cold, ionized gas. The line strengths of CNO are much greater, as compared with the Balmer lines, than in ordinary H II regions or planetary nebulae, indicating a high abundance. Lines of [N II] indicate a hot ($T_e > 5000$ K) component of gas.

Spectra at the ends of the major axis differ from those at the ends of the minor axis. While the line strengths of H, [O II] and [N II] are similar, C II, N II and O II are weaker or absent along the minor axis. Williams et al. estimate that the CNO abundances might be 100 times solar at the polar blobs and still 10 times solar in the equatorial (minor axis) region.

The source of excitation of the nebula remains a controversial topic. Williams et al. had postulated a "frozen-in ionization," but this could not explain a lower C- abundance in an earlier nebular phase, because C^{++} recombines Z^2 times faster than H^+ in a time-dependent model, thus C^{++}/H^+ should decrease with time.

A model of the nebula which is photoionized by the X-ray radiation from the central object was proposed by Ferland and Truran (1981), which showed better consistency with the observed lines in the optical regions. It predicted line strengths in the UV, which could not be verified in a subsequent study of the UV spectrum of the nebula (Ferland et al. 1984). A careful analysis of the energy distribution of the central

TABLE 6.21. CHEMICAL COMPOSITION (IN NUMBER OF ATOMS) OF NOVA DEL 1967 AND OTHER OBJECTS*

Element	Novae [1]	Planetary nebulae [2]	Sun [3]	Cosmic [4]
He/H	0.25	0.10	0.085	0.085
10^4×N/H	30	1.0	0.98	0.91
10^4×O/H	50	4.9	8.3	6.6
10^4×Ne/H	1	1.3	1.3	0.83

References: [1] Collin-Souffrin (1977); [2] Aller (1978); [3] N and O from Lambert (1978); He/O and Ne/O from Bertsch *et al.* (1972); [4] Allen (1973). *from Tylenda (1979)

object was made (which contradicted many previous models because of its deficient far UV and X-ray flux). Using the deduced continuum flux, photoionization models of the nebula are calculated and showed that the low observed electron temperature is the result of the very high metal abundances which are characteristic for nova shells. Infrared fine-structure lines are efficient coolants, and low temperatures are achieved for a wide variety of radiation fields.

The authors find that the 88-μm and 52-μm lines of [OIII] are extremely efficient coolants, provided that the gas density is below the critical density for the J = 1,2 sublevels of the $O^{+2/3p}$ ground state (N = 670 and 4900 cm^{-3}, respectively, see Osterbrock 1974). At high densities, only UV resonance lines are efficient coolants, and the gas equilibrates at T around 10^4 K. When the optical [O III] lines begin to cool the gas (at N < 10^6 cm^{-3}), the temperature falls to about 6000 K. Finally, the temperature falls to below 1000 K when the infrared fine-structure lines are no longer collisionally deactivated (N < 10^3 cm^{-3}). They postulate that these cold nova shells should be powerful radiators of IR lines. Together, the [OIII] fine-structure lines should have an observed flux of 2.7 x 10^{-12} erg cm^{-2} s^{-1}. Indeed, Dinerstein (1986) found for the 60-μm and 100-μm bands of the IRAS satellite the following fluxes:

F(lambda, 60 μm) = 4.8 x 10^{-13} erg cm^{-2} s^{-1}

F(lambda, 100 μm) = 1.8 x 10^{-13} erg cm^{-2} s^{-1}

Dinerstein states that Ferland postulates several 10^{-19} W m^{-2}, while IRAS measured 10^{-18} W m^{-2} in the 60 μm band. Emission in the 88-μm line is similar to that in the 52-μm for densities lower than about 10^3 cm^{-3}.

Spectroscopy of the blobs in the shell of RR Pic was carried out by Williams and Gallagher (1979), and by Duerbeck (1987b). They noted that the spectra are similar to those of high-excitation planetary nebulae, such as NGC 2022. The spectra show strong [Fe V], [Fe VI], and [Fe VII] lines, which were also prominent in the first years after outburst (Spencer Jones, 1931). An ionization model with $T_* = 2.5 \times 10^5$ K and $L_* = 2.2 \times 10^{34}$ erq s^{-1} was applied. The electron temperature was determined to be 16,500 K. A comparison with the observed line strengths leads to an enhancement of the elements He, N, and Ne. Helium is at least twice as abundant as in the sun, oxygen seems to be normal, N is enhanced by at least a factor of 10, and Ne possibly also by a factor of 10.

The large value of N/O in RR Pic is unusual, but could possibly be accounted for if equilibrium CNO burning has occurred and converted most of the C and O into N. This is predicted for slow novae by current models. However, spectroscopy of the ring yields strong [O III] lines.

The shell around CP Pup was also studied by R.E. Williams (1982). He noted similarities with the shell of DQ Her, a similar low temperature (800 K), and a high N abundance (N/H = 0.1).

Seitter (1985) pointed out that the [O III] lines are much stronger in the polar blobs than in the equatorial ring of RR Pic. Such inhomogeneities were studied in the following years by comparing CCD frames of nova shells taken through interference filters isolating the [O III] and the [N II = Hα]

1)A bipolar structure is seen in the shell of RR Pic; the blobs radiate more in [O III].

2)A bipolar structure is seen in DQ Her; the polar regions radiate in the [O III] filter region, while no [O III] has been found spectroscopically.

3)A bipolar structure is visible in the recurrent nova T Pyx (Duerbeck 1987b).

4)A bipolar structure is visible in the shell of GK Per. This shell has often been classified as irregular, but the chemical inhomogeneities show a regular pattern. IUE spectroscopy of different parts of the shell gave good arguments for the reality of chemical inhomogeneities (Bode, Duerbeck, and Seitter, 1988).

Thus, chemical (or excitation) inhomogeneities are well established in nova shells.

Spectra of RR Pic taken with the Cassegrain spectrograph and a CCD receiver at the ESO 2.2 m telescope are shown in Figure 6-70.

In addition to several classical novae, Cohen (1985) discusses the spectrum and the image of the nebula around CK Vul 1670, which was recovered by Shara and Moffat 1982).

Associated with the central object, which is below the limit of the Palomar charts (Shara and Moffat, 1982), are two faint nebulosities at 5" or 6" from the nova candidate, displaying spectra similar to those of the nova ejecta, plus other fainter nebulosities. Two images obtained in the light of Hα and in the nearby continuum show that the nebulae are visible only in the first one; i.e. (Figures 6.71 a,b) the continuum is absent or too faint (Shara et al., 1985).

The nebulosities in the light of Hα and S II, after subtraction of the continuum are shown in Figures 6.72 and 6.73 together with their isointensity maps. The spectra of the nebulosities indicated in Figure 6.72 with 1,2,3, and 5, are shown in Figures 6.74 a-d. Figure 6.75 shows an expanded part of the spectrum of nebulosity 1 in the region of Hα. The strength of [N II] 6584 is impressive. It is the strongest line, followed by a blend of Hα and [N II] 6548. Also the intensities of [S II] 6716, and 6730 are remarkable. According to Cohen (1985), these spectral peculiarities are rather more characteristic of a supernova remnant than a nova. However, the low expansion velocity and the small size of the shell (less than 10") indicate that CK Vul is a slow nova. Cohen suggests that the similarity with the supernova spectrum can be due to the fact that CK Vul, being much older than all the other novae for which the nebular spectrum is known, has swept up more than its own ejected mass (estimated to be about 10^{-4} solar masses, see Cohen and Rosenthal, 1983) in the interstellar material. Hence, the emission may be from shock-heated gas at the interface between the expanding shell and the interstellar medium, rather than from the standard mechanisms prevailing in low-density nova shells.

According to Shara et al. (1985), the spectra of the equatorial and polar ejecta are similar to those of the slow recurrent nova T Pyx, but with lower excitation.

Shara et al. (1985) discuss the possibility that CK Vul is a different kind of object than an old nova. In fact, its very low luminosity is comparable to those of the faintest dwarf novae (M_R = 10.4+/-0.8) and certainly much lower than that typical of old novae (M_V = +4.5, Warner, 1976; Patterson, 1984). This luminosity can be explained by a normal red dwarf M3-M5 with no contribution from the white dwarf or from the accretion disk. This may indicate that mass transfer has probably stopped in the system. This luminosity could also be explained by an accretion disk with mass-accretion rate as low as 10^{-12} solar masses /year. Shara et al. examine the possibility that CK Vul is a young planetary nebula, or a Herbig-Haro object. But in the first case, the central star would be fainter by two orders of magnitude than any other known nucleus of planetary nebula, and the nebula mass is two orders of magnitude lower than that typical of planetary nebulae. In the second case, although the expansion velocity is similar to that of jets around HH objects, there are no young objects in the vicinity of CK Vul; moreover, its chemical composition, e.g., the nitrogen overabundance, indicates that CK Vul is an evolved object. The conclusion is that CK Vul has been a genuine classical nova, and if it is typical of classical novae in the thousand years between eruptions, their faintness makes them very difficult to find. Hence, our statistics on the space density of old novae may be grossly underestimated.

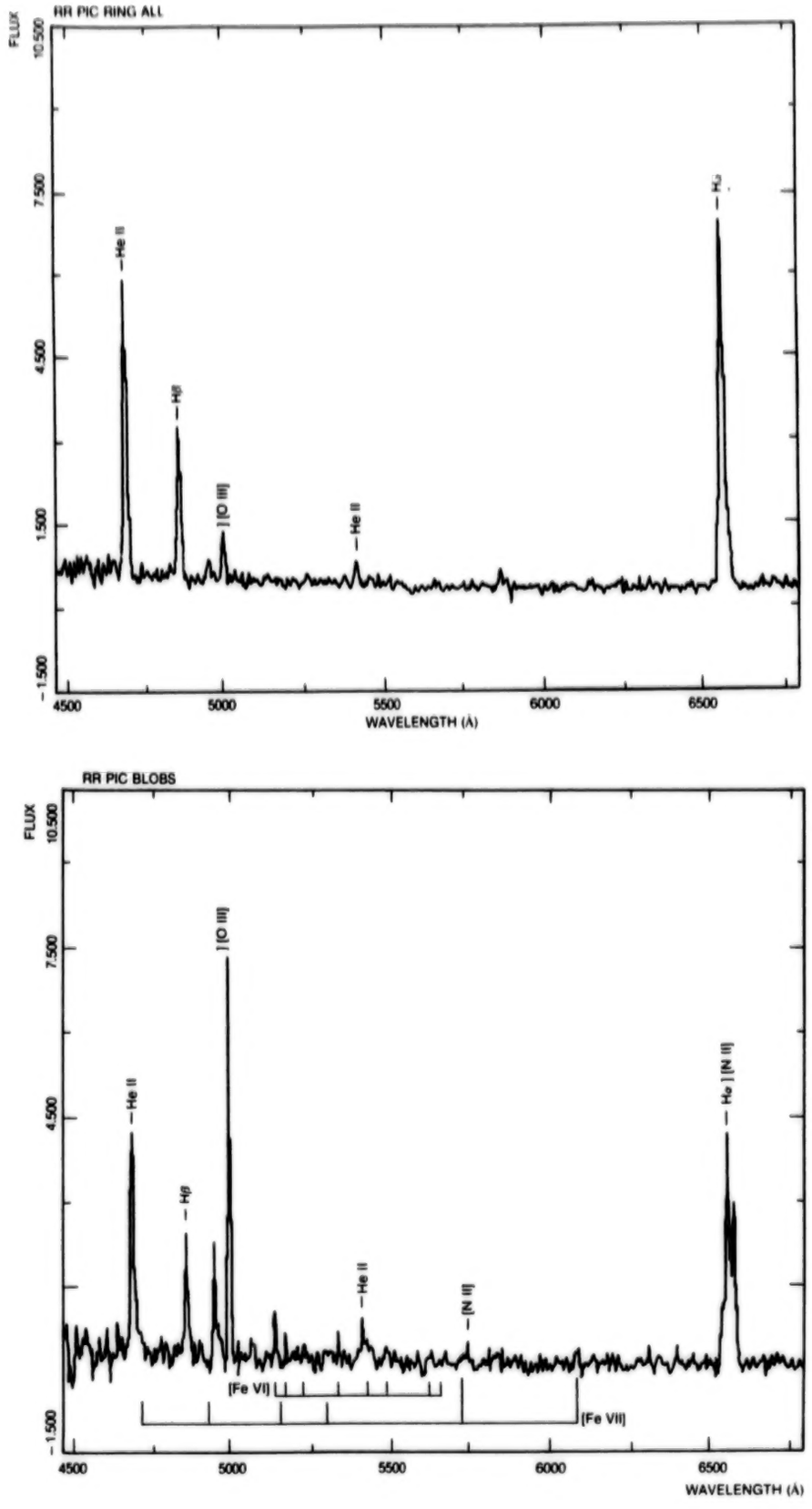


Figure 6-70. The optical spectrum of the polar blobs and the equatorial ring of the shell of RR Pic, observed with a Cassegrain spectrograph + CCD at the ESO 2.2 m telescope.

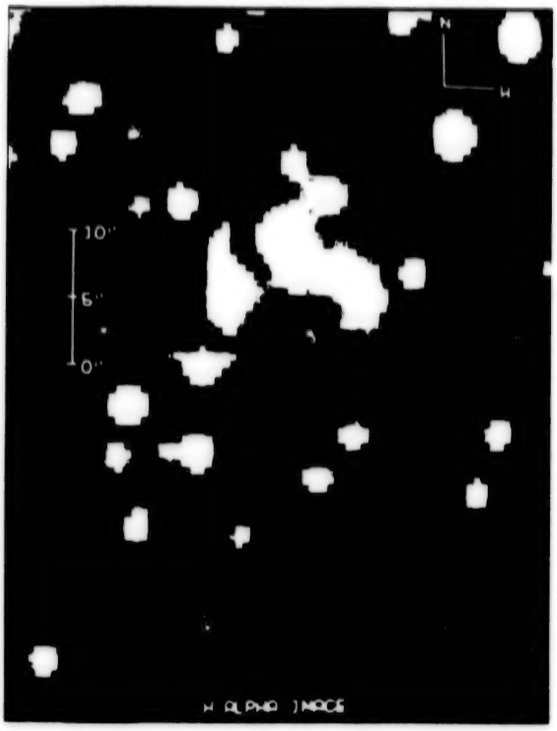


Figure 6-71. The nebulosities in the vicinity of the old nova CK Vul 1970. Image in the light of Hα. (from Shara et al., 1985)

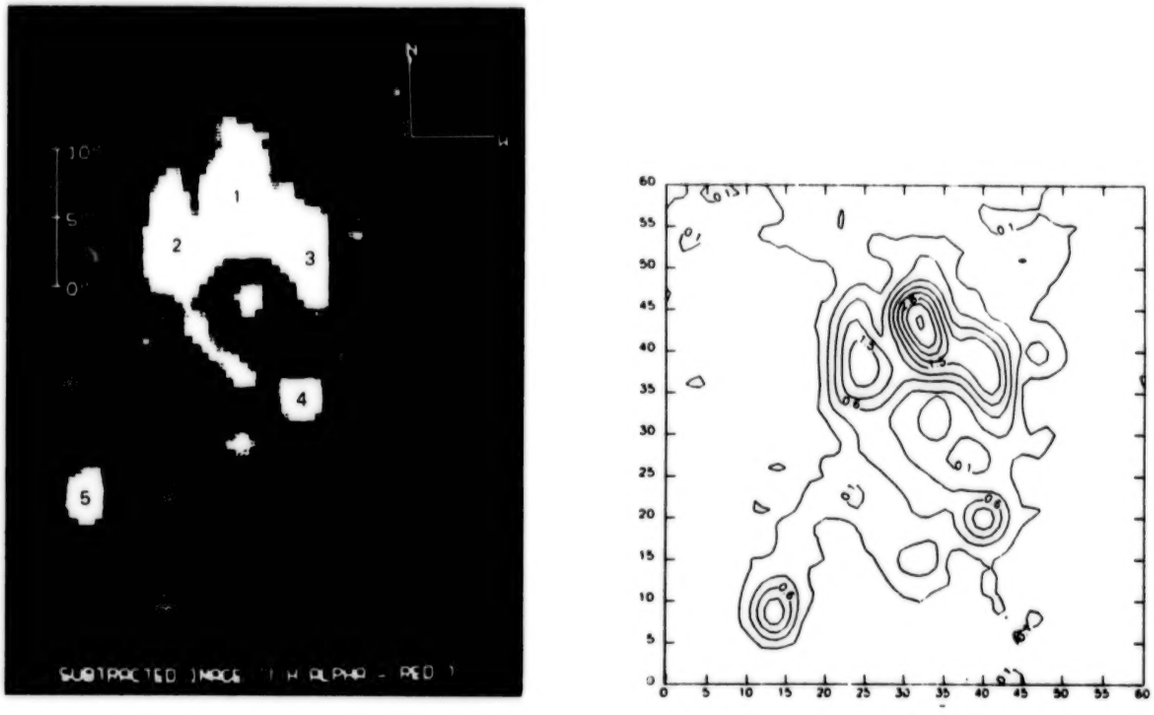


Figure 6-72. The same nebulosities shown in Figure 6-71, after substraction of the continuum, in the light of Hα, and the relative isointensity map. (from Shara et al., 1985)

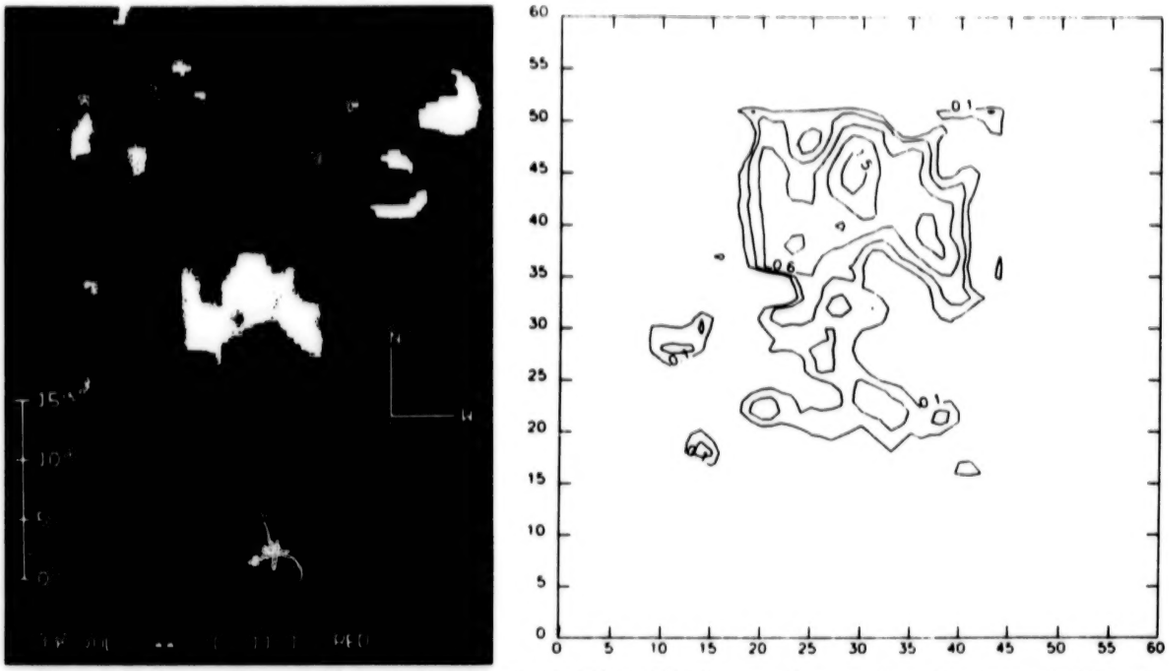


Figure 6-73. Same as Figure 6-72, but in the light of [S II] 6716+6730. The central star and knot 5 are strong in Hα and absent in the light of [S II]; knot 4 is much weaker than in Hα.
(from Shara et al., 1985)

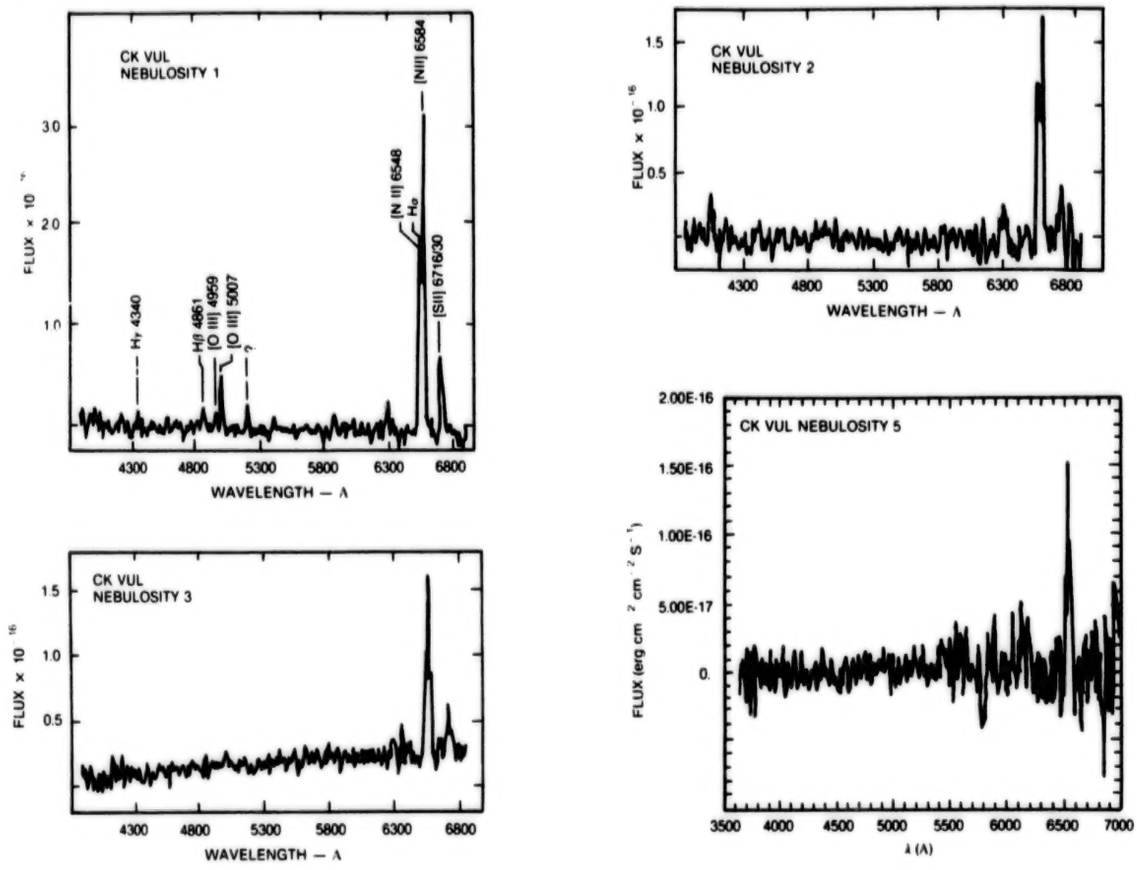


Figure 6-74. a) The spectrum of the nebulosity labeled 1 in Figure 6-72; b) the same for nebulosity labeled 2; c) the same for the nebulosity labeled 3; d) the same for the nebulosity labeled 5.
(from Shara et al., 1985)

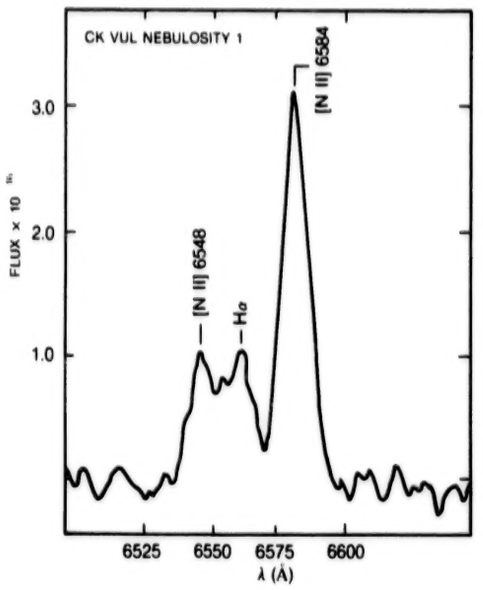


Figure 6-75. Expanded portion of the spectrum of nebulosity labeled 1 in the Hα region. from Shara et al., 1985)

VIII. RADIOASTRONOMICAL OBSERVATIONS OF NOVA ENVELOPES
(written by Hack)

Radioemission from novae has been observed in few cases: Wendker (1978 and successive updating) has collected data published before 1980. Positive detections have been obtained for the very slow nova HR Del 1967, the exceptional fast nova V 1500 Cyg 1975, the fast nova V 368 Sct 1970, and the moderately slow nova FH Ser 1970. Other novae have been searched for radioemission, (T CrB, DQ Her, V 533 Her, Nova Cep 1971), but with negative results.

A high-sensitivity radio survey of classical novae has been made with VLA by Bode et al. (1987a) at 1.5 GHz and 4.9 GHz. Of the over 26 objects observed, including very old novae like CK Vul 1670 and recent novae like V1370 Aql 1982 and V 4077 Sgr 1982, only two were detected: NQ Vul 1976 and V 4077 Sgr 1982. The radio "light curves" for HR Del, FH Ser, and V 1500 Cyg are given in Figure 6-76. The spectra are consistent with thermal radiation of expanding envelopes of ionized gas at high emission measures (where the emission measure E is given by N_e^2 x s with s dimension of the emitting body, N_e electron density, and is measured in pc cm^{-6}) as shown by Hjellming and Wade (1970). Altunin (1976) has measured a flare at 989 MHz from V 1500 Cyg. It exceeds by more than three orders of magnitude the flux expected at the same frequency and about the same date from the thermal spectrum; it can be explained by nonthermal synchrotron radiation.

An extended discussion of the radio observations for these three best studied novae is given Hjellming et al. (1979). The most important conclusion from this study is that the radio emission comes from the nova shell, as indicated by the fact that it reaches its maximum much later than the optical and also than the infrared maximum. If we identify with t(o) the beginning of the outburst, the maximum radio emission from the very fast nova V 1500 Cyg is reached at t-t(o) between 100 and 200 days, and for the moderately slow nova FH Ser, between 400 and 600 days. The observations of the very slow nova HR Del started almost at the epoch of maximum radioemission, which can be placed at a t-t(o) of about 1000 days.

In no case was the radio emission observable earlier than 50 days after outburst.

Hjellming et al (1979) show that a spherical symmetric isothermal model defined by three parameters-mass, inner velocity, and outer velocity-fits reasonably well the observed "radio light curves." Masses of 8.6 x 10^{-5}, 4.5 x 10^{-5}, and 2.4 x 10^{-4} solar masses, inner velocities of 200, 48, and 200 km/s and outer velocities of 450, 1000 and 5600 km/s have been found for HR Del, FH Ser, and V 1500 Cyg, respectively. A detailed discussion of these models will be given in Chapter 7.

We remark that slow novae like FH Ser and very fast novae like V 1500 Cyg present very similar radio "light curves" and radio spectra. Hence, the way their gas shells expand is very similar. Their dust shells, on the contrary, behave very differently as indicated by their infrared fluxes and their variation with time from outburst.

Chevalier (1977) predicted that also old novae should be observable radio emitters, but at rather low levels (<1 mJy). In the attempt to verify this prediction, Reynolds and Chevalier (1984) have observed GK Per 1901 with the VLA at wave-

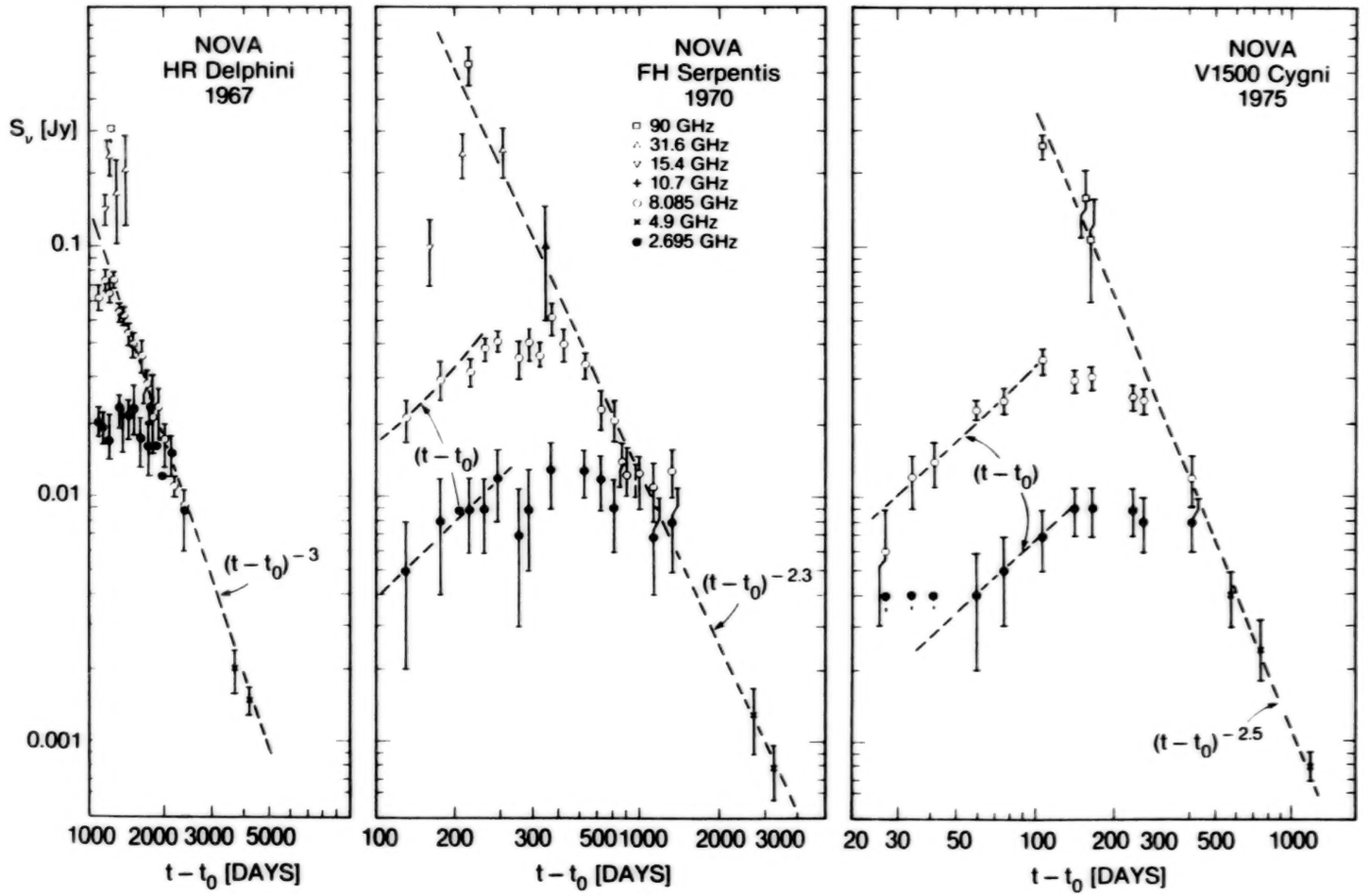


Figure 6-76. Radio "light curves" for HR Del, FH Ser, V 1500 Cyg. Also plotted are lines showing the power laws indicated for the rising and decaying radio curves.
(from Hjellming et al., 1979)

lengths of 20.5 and 6.2 cm. They detected an extended radio source within 40 are seconds of the nova position at both wavelengths (Figure 6-77). The nova was in eccentric position but within

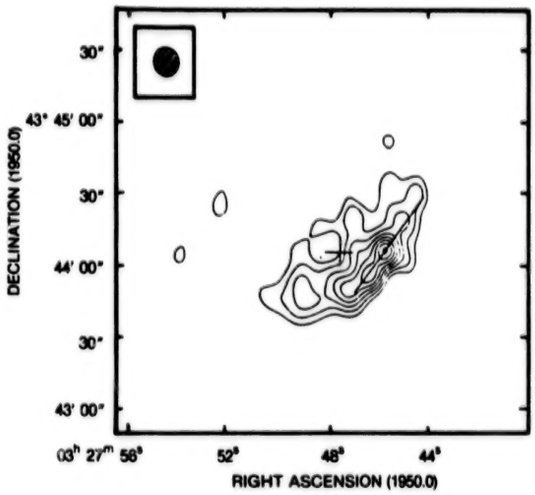


Figure 6-77. VLA map at 6 cm of the shell of GK Per. The plus sign indicated the position of the star GK Per itself.
(from Reynolds and Chevalier, 1984).

the radio source. The radio source has the shape of a partial shell and strongly resembles the optical nebulosity observable on the Palomar Observatory Sky Survey. The flux density dependence on the frequency is given by the relation $S \propto \nu^{-\alpha}$, with $\alpha = 0.67$ indicating that the emission is clearly non-thermal (differing from that observed from classical novae a few months after outburst). Although the dominant emission is synchrotron radiation, a thermal component at 6 cm cannot be ruled out. The shell ridge has several peaks qualitatively corresponding to the bright knots in the optical image.

The VLA survey by Bode et al. (1987a) of 26 classical novae has indicated no positive detection at 1.5 GHz over 18 objects observed, and two positive detections at 4.9 GHz over 8 objects observed. The value of the flux densities is the same for the two objects- the slow novae NQ Vul 1976 and V 4077 Sgr 1982- 0.6 mJy, i.e., of the same order as those observed previously by Hjellming et al. for HR Del, V 1500 Cyg, and FH Ser at similar frequencies. This fact, together with the high frequency at which the detection has been made, suggest the thermal origin of the radio emission. Since V 4077 Sgr is more distant (≈ 4100 pcs) than NQ Vul (≈ 1200 pcs), the radio luminosity of V 4077 Sgr is about one order of magnitude larger. This difference can be attributed to the fact that NQ Vul was observed when about 2000 days more than for V 4077 Sgr were elapsed from the date of the outburst. Figure 6-76 actually shows that the decline in the flux density in 2000 days for HR Del, FH Ser, and V 1500 Cyg is of one order of magnitude. However, a recent nova like N Sct 1981 placed at half the distance of V 4077 Sgr shows no measurable flux at 4.9 GHz.

As we have noted above, radio emission from classical novae has been observed not earlier than 50 days after outburst.

Observations of the recurrent nova T Cr B gave negative results. The first recurrent nova for which radio emission was detectable is RS Oph (Padin et al, 1985). The observations begin only 18 days after the recent outburst of 1985 and show a radio "light curve" different from that of classical novae. The brightness temperature is about 10^7 K, against the value of 10^4 K observed in classical novae, and therefore indicates a nonthermal origin for the radio emission. From this unique representative of recurrent novae, it seems that their radio properties are very different from those of classical novae. It is possible that the ejecta interaction with circumstellar material produces acceleration of electrons and enhancement of magnetic fields necessary to produce the synchrotron radiation. A similar mechanism was invoked by Chevalier (1982) for explaining type II supernovae. This interaction would explain also the presence of very strong coronal lines generally observed in the spectra of recurrent novae. Hence, the main difference between radio properties of classical novae and recurrent novae could be explained by the absence of circumstellar material in the first case and presence of it in the second case. This absence or presence of circumstellar material would be correlated to the fact that binary systems that explode as classical novae are composed of a white dwarf and a red dwarf, while over five recurrent novae, at least three have a late-type

companion, which is a red giant whose wind produces the circumstellar matter. A model for the radio and X-ray emission of RS Oph is proposed by Bode and Kahn (1985) and will be discussed in Chapter 7.

In concluding our discussion on radio observations of novae, we note that the data are for a very small number of objects for permitting us to generalize these results. We can just say the following:

1) the few novae observed months after outburst become thermal radiosources (expanding gas at T≈ 10^4). Their behavior is similar if they are either slow or fast novae, in contrast with their IR behavior.

2) the old nova GK Per shows a radio spectrum $S \propto \nu^{-\alpha}$ $\nu^{-\alpha}$, which is typical of synchrotron radiation. No other novae have been found with similar properties. GK Per might be a special case since there might be interaction with strong interstellar or circumstellar material. An ancient planetary nebula surrounding GK Per was suspected recently in IRAS data (Bode et al 1987b).

3) the recurrent nova RS Oph shows a brightness temperature of 10^7 K in the radio range.

Only one recurrent nova has been detected in the radio spectral range and we cannot say if the high brightness temperature (T ~ 10^7 against the value of 10^4 observed for four classical novae is a common property of all recurrent novae, distinguishing them from all classical novae. However, it is possible that this difference between the observed classical novae and RS Oph is related to the fact that all classical novae, known to be members of a binary system, have for companion a cool dwarf, while RS Oph (as well as T CrB and V 1017 Sgr) have a red giant for companion. Now red giants are known to have winds, which, interacting with the ejecta, could explain the high brightness temperature and nonthermal emission (White, 1985). Hence, the negative result for T CrB may probably be related to the long interval elapsed from the last outburst.

N95
27073
UNCLAS

N95- 27073

7

MODELS OF CLASSICAL AND RECURRENT NOVAE

M. Friedjung and H. Duerbeck

I. INTRODUCTION.

I.A. BASIC THINGS TO BE EXPLAINED

The behavior of novae may be divided roughly into two separate stages: quiescence and outburst. However, at closer inspection, both stages cannot be completely separated. The presumed accretion disc and companion star, determining the nova behavior at quiescence, may also play a more or less important role during outburst due to their interaction with the ejected shell or the "bloated dwarf", which is formed in the explosion. On the other hand, the outburst stage gently merges into the quiescent stage, and it is possible that special features observed at quiescence are still influenced by effects from an outburst that lies more than 50 years in the past. It should be attempted to explain features in both stages with a similar model.

Due to the faintness of exnovae and the long time scales involved, the behavior of novae in the quiescent stage is only poorly known. Time scales for which observations are available are short compared with the whole interval of quiescence, which may last for ten thousands of years. Thus, our observations of classical novae are confined to a configuration shortly before outburst (and data of this stage are scarce, for obvious reasons) to a situation shortly (relatively speaking) after outburst. Therefore, statistical arguments and observations of some nova-like systems believed to be novae in quiescence in historical times must supplement our study of novae in quiescence. As will be seen in Section V.C, statistical arguments and the recent "hibernation" theory give arguments concerning the possible identification of nova-likes or dwarf novae with novae in the middle of their quiescent stage.

This section will mainly deal with the discussion of models explaining the outburst behavior.

The concept of a nova "explosion" signals that we deal with a short-lived event, which seems to be determined by the phenomena that, according to our present understanding, occur in a thermonuclear runaway that lasts only minutes. In its aftermath, the outbursts of different novae show features that may not be completely determined at the moment of explosion. A closer look into the phenomenon shows that the outburst activity lasts a long time, at least weeks, if not years and decades.

I.B. THE LIGHT CURVE

The *optical* light curve shows a rapid rise, followed by a slower decline at variable rates for different novae. For some fast novae, oscillations occur in later phases; for some slow novae, they are found around maximum and later; a deep minimum is observed in the declining phase of some slow novae. In the *UV*, the maximum is delayed for smaller wavelengths. In the *IR*, excesses are sometimes seen after months, in general, coinciding with deep optical minima. In the *radio*, maximum occurs months after outburst and is delayed for large wavelengths. The *bolometric* light curve shows a much more gentle decline than the optical one. For some time, the nova radiates near the Eddington limit (or for fast novae, above it). A M_{max}-t_3-relation exists in the optical, where t_3 is the time in days to decline three magnitudes from maximum.

PRECEDING PAGE BLANK NOT FILMED

We first need to explain the light curve of novae, or, to be more precise, the variation of flux, integrated over all wavelengths, as well as its spectral distribution, with time. The variety of light curves observed for different novae (or even the differences between the light curves of two outbursts of a recurrent nova!) must be explained. The rise of the rate of nova energy production, the global optical decline, and the shift of the maximum of the distribution of radiation are compatible with a central object undergoing a thermonuclear runaway and suffering a strong mass loss, where matter is exhausted after a shorter or longer time. The detailed physics and the fine structure of a nova light curve are, however, hardly understood. In a few cases, brightness fluctuations with approximately the period of the underlying binary in early stages of the outburst are observed (V1500 Cyg, probably also V1668 Cyg). Repeated brightness (and possibly mass ejection) bursts, leading to secondary maxima and to short fadings and shifts of the energy distribution towards shorter wavelengths in the course of a prolonged maximum, are found in some novae (NQ Vul, QU Vul). Light oscillations in the transition phase occur mainly in a fraction of fast novae (GK Per, V603 Aql). Final declines show different gradients in the visual.

I.C. THE SPECTRAL EVOLUTION

The spectrum of a nova in outburst consists of superposed P Cyg profiles of different expansion velocities. In the early stages, the *blueshifted* absorption lines dominate; in intermediate stages, the spectrum has a typical P Cyg character; in the late stages, the continuum fades much more than the emission lines. The general evolution of the spectrum of a nova can be explained by the ejection of a large amount of mass, which starts at a well-defined time and declines in strength more or less slowly. This is indicated by the blueshifted absorptions, which are explained by the Doppler effect. The occurrence of lines of higher excitation and ionization in later stages of the outburst can be understood by the shrinkage of the photosphere, which becomes hotter at smaller radii if no large decrease in bolometric luminosity occurs. The gradual thinning of the shell leads to the emergence of nebular lines, as will be seen in Sections II.D and IV.E. Complications occur, as can be noted from the observation of superposed P Cyg profiles of different expansion velocities, because of the interaction of material ejected at different times with different velocities (higher excitation lines, higher velocity components appear later.) The main bulk of matter, however, is ejected at the time of maximum: the line widths in the nebular stage correspond to velocity shifts observed in the principal spectrum. A velocity-t_3-relation, and therefore a velocity-luminosity relation, exists.

An interpretation of the spectroscopic generalities derived from a comparative study of seven novae was carried out by McLaughlin (1943), where the spectral stages of the nova outburst are clearly described in much detail. A summary is found in McLaughlin (1942). This sequence was also adopted as a classification scheme by the IAU (Oort 1950). The systems listed in Table 7-1 seem to be normal in ordinary novae. Q indicates a spectral classification scheme, where each nova has a spectral Class Q, while subclasses are reached at various stages of the outburst (some may be skipped). A detailed description is found in Chapter 6.

I.D. THE EXPANDING NEBULA

For a small group of generally bright novae, expanding nebulae were observed in late stages. Structures at low resolution are, in general, spherical (contrary to jet-shaped). At high resolution or at later phases, they exhibit a wealth of detail: deviations from spherical symmetry are frequent; the shells appear often elliptical. The majority of shells shows the existence of equatorial rings and polar condensations. Additional structures are observed, e.g., the fragmentation of the shell into many cloudlets, or extended haloes.

Observational evidence shows that spherical symmetry for mass loss and velocity, often assumed in outburst models, is, in most cases, not correct. The observed ellipticity of the shell and the ring/blob structure may be connected with the underlying binary system, the fragmentation,

TABLE 7-1. SPECTRAL STAGES OF NOVAE

Spectrum	Absorption	Emission	Q
Prenova			0
Premaximum	I	I	1
Principal	II	II	2
Diffuse enhanced	III	III	3
Orion	IV	IV	4
N III (4640)	V	V	5
Eta Car = [Fe II]		VI	6
Nebular		VII	7
Wolf-Rayet		VIII	8
Final			9=0

with some sort of instability occurring in the ejected shell, the outer shell, with the survival of high-velocity material ejected in late stages of the outburst or with shock waves extending into the interstellar material.

The deceleration of nova shells observed in very late stages, decades after outburst, seems to be established. It is presumably caused by the interaction of the shell with the surrounding interstellar material.

It is often found that different regions of a nova shell have a different spectral appearance. A careful analysis must establish whether this is due to a different chemical composition, a different physical property (temperature, density), or, closely connected with it, different excitation conditions by the radiation field of the central object. This field probably has an axis of symmetry, but certainly deviates from spherical symmetry. Such "directional excitation" was suggested as early as 1937 by Grotrian in the case of DQ Her.

I.E. THE EXNOVA

Results of the few novae that have been observed at minimum are best interpreted in the framework of a close binary composed of a white dwarf and a low mass main sequence star. The nova explosion is a thermonuclear runaway in the electron degenerate hydrogen rich material close to the surface of the white dwarf, which was accreted (via a disk) from the late-type companion that suffers a Roche lobe overflow. It is usually assumed that the disk luminosity dominates all other contributions (white dwarf, late-type companion, hot spot) in classical nova systems at quiescence. Indeed, disk luminosities appear to have only little scatter if the different observational aspects are taken into account.

Recent detailed studies of the minimum visual magnitude of classical novae by Warner (1986, 1987) indicate that they have the same absolute magnitude at minimum, but are seen at different accretion disk inclinations. Warner showed that the histogram of minimum magnitudes can be explained by a mean absolute magnitude [M_V(i

= 0°) = 3.3], a random distribution of inclinations, and a scatter (intrinsic or observational) of 1^m. He argues that the minimum magnitude does not depend on nova speed class, or orbital period, or any other parameter besides the inclination i.

A study by Duerbeck (1986) indicates that minimum magnitudes do depend on speed class or light curve type, e.g., that slow novae (light curve Type D) are generally several magnitudes brighter than the rest. The very old novae CK Vul and WY Sge (Kenyon and Berriman, 1988) appear to be much fainter than an average, more recent exnova.

Spectroscopic studies of novae at minimum are only carried out for a very small percentage of the now identified objects at minimum. For some of them, radial velocity studies have been carried out. Preliminary results of a spectroscopic survey were reported by Duerbeck and Seitter (1987). The continua are frequently heavily reddened by interstellar extinction; weak to strong emission lines, mostly of the Balmer lines and notably He II 4686, are observed.

I.F. THE MANIFOLD OF NOVAE-SIMILARITIES, DIFFERENCES, AND THEIR POSSIBLE CAUSES

Despite the variety of light curve forms, spectroscopic development, and other features, there are similarities between different objects. Relations exist between the absolute magnitude at maximum and the t_3-time and, less clearly, between the absolute magnitude at minimum and the light curve form, or between the velocity of expansion of the shell and the t_3-time. This indicates that underlying systematics exist in novae. Possible "hidden parameters" that determine absolute magnitudes at maximum, ejection velocities, forms of light curves or shells are e.g.:

- The mass of white dwarf.
- The chemical composition of the white dwarf.
- The mass of accreted material.
- The accretion rate.
- The degree of mixing of white dwarf material into accreted hydrogen-rich shell material (or a deviation of the composition of accreted material from the solar value).
- Orbital elements.
- The presence and strength of a magnetic field in the white dwarf.
- The inclination of the orbit.

Unfortunately, the statistics of data derived from minimum observations (orbital elements, properties of the binary components, and the shell) are poor, contrary to data on light curves and spectroscopic data obtained during outburst, or to minimum data for dwarf novae. Thus, hardly anything can be said about the importance of the above parameters for the characteristics or evolution of the outburst.

II. SHORT HISTORY

II.A. EARLY IDEAS TO 1930

Because of their sudden, spectacular appearance in the sky and their fading into oblivion, novae have been the object of speculation and theoretical approaches since earliest times. Quite often, the most advanced physical theories were used to explain the nova phenomenon. As an early example, Newton (1713) might be quoted, who, investigating the stability of cometary orbits, proposed that novae are old, burnt-out stars, whose supply of combustible material is replenished by the impact of comets. Another proposal that an aging star undergoes a nova event is due to Zöllner (1865). He thought that cracks in the surface of a cooling star allow magma from the interior to reach the surface, leading to a brightening. We see that novae were no more considered as "new stars" by some astronomers of the 18th and 19th centuries.

Theories of the nova phenomenon can be divided into two categories: one is the attempt to explain the underlying cause of the nova outburst; the other, the attempt to explain the photometric and spectroscopic features observed during outburst. We will first deal with the second question.

Increasing observational evidence, especially the availability of more and more detailed spectroscopic material, led to a reduction of the large number of explanations of the nova phe-

nomenon that were at hand in earlier centuries. When observing visually the spectrum of the (recurrent) nova T CrB, Huggins and Miller (1866) noted the appearance of bright and dark lines in the spectrum, without being able to note that the dark lines are blueshifted. They interpreted the bright H lines as a result of a gas explosion, a chemical combustion of hydrogen.

Blueshifted absorption lines were first observed in T Aur by Huggins (1892), Campbell (1892) and Vogel (1893), and shortly afterwards in IL Nor (Pickering 1894). Among the numerous collision scenarios, which were proposed to explain the two sets of lines of different radial velocity in nova spectra, the most influential one is that of Seeliger (1892,1893,1909). He assumed the penetration of a star into an interstellar gas or dust cloud, a scenario that won much favor after the light echo phenomena observed in the vicinity of nova GK Per (1901). The simultaneous occurrence of blueshifted absorption and stationary emission line as being caused by an extended, expanding envelope of gas was first proposed in a somewhat obscure way by Pickering (1894), then by Halm (1901) and finally by Lau (1906). However, in the early decades of nova spectroscopy, the blueshift of the dark lines was not unequivocally thought to be caused by the Doppler effect. A good survey of early theories is given by Stratton (1928).

The suddenness of the brightening, in combination with the different radial velocities of the dark- and bright-line spectrum, was always used as an argument for the collision hypothesis, i.e., the collision of a star and an interstellar cloud, two stars, a star and a comet, an asteroid, or a whole solar system. The extended premaximum stage of RR Pic and the postmaximum appearance of bright lines led Hartmann (1925) to the view that a single star "expands, explodes." In his second note, Hartmann (1926) states: "we conclude that the nova phenomenon is one which has its cause in the interior of certain stars. It is a disturbance of the physical-chemical equilibrium which occurs, without exterior cause, in a critical point of evolution, and leads to a rapid, explosive transformation of the whole celestial object. This disturbance is possibly a radioactive transformation of atoms." Previous theories, especially the collision scenario, could not explain the delayed maximum of RR Pic and quickly fell into oblivion.

II.B. THE SEARCH FOR THE UNDERLYING CAUSE

After the external cause of a nova explosion had been discarded, and stellar structure became tractable, several outburst mechanisms were proposed. A good historical summary is found in Schatzman (1965).

Milne (1931) thought that the energy for the outburst is that of a star collapsing into a white dwarf. The energy is given (order of magnitude) by $\Delta E = G M^{*2} (1/R_2 - 1/R_1)$, which is 10^3 to 10^4 times higher than that observed. From the frequency of nova explosions, one can derive that a star must undergo about 10 nova explosions; i.e., a subset must show even more frequent eruptions. The hypothesis by Milne was relaxed by Vorontsow-Veljaminow (1940), who assumed that a sequence of nova outbursts of different strength leads to a transformation of a main sequence into a white dwarf.

Unsöld (1930), in investigating layers near the stellar surface for stability against convection, argued that the nova phenomenon is caused by the sudden onset of convection. One of his arguments was that the energy released in a nova explosion is much too small to be caused by dramatic changes in the interior, but he argued for a surface phenomenon.

Biermann (1939) thought that the explosion occurs because of an instability in a hydrogen-poor subdwarf. An instability develops at a certain depth where radiant equilibrium changes over to adiabatic equilibrium. In this case, the star should be poor in H and He, and the changes occurring lead to a release of ionization energy.

In 1946, Rosseland (1946), Lebedinskii (1946) and Schatzman (1946) thought of the nova explosion as a shock wave in the stellar interior, and Rosseland came up with some sort of atomic bomb explosion, specified later by Schatzman

(1950, 1951), who postulated as the energy source the conversion of ^{3}He into ^{4}He. Gurevich and Lebedinskii (1947a,b) assumed that a nova explosion results from explosive low-temperature nuclear reactions taking place in the peripheral layers of a star, which produces energy by the CNO cycle.

Mestel (1952) examined accretion of interstellar matter onto hot white dwarfs and postulated either continuous burning or supernova-type explosions.

The discovery by Walker (1954) that the famous nova DQ Her is a close binary was soon generalized by Struve (1955) and Huang (1956) to the possibility that all novae and nova-like stars are binaries. Kraft (1963, 1964) came up with the still-favored model: that the nova is a close binary composed of a white dwarf and a low-mass main sequence star. The nova explosion is a thermonuclear runaway in the electron degenerate hydrogen-rich material close to the surface of the white dwarf, which was accreted (via the accretion disk) from the late-type companion overflowing its Roche lobe. The binarity and the inclusion of an accretion disk led nova research out of a dilemma that still intrigued Payne-Gaposchkin (1957): novae at minimum are blue objects at $M_v \approx +4$; this always leads to objects below the main sequence, but above the white dwarf region, i.e., to subdwarfs, similar to the central stars of planetary nebulae.

An early nova model including a close binary is due to Schatzman (1958). He suggested that in one of the components, nonradial forced oscillations are produced by orbital motion. If there is a resonance between the orbital period and one of the periods of nonradial oscillation, the amplitude of the force oscillation is finite unless the damping constant vanishes or is negative. When this happens (as a consequence of the secular evolution of the star), the forced oscillation may become an explosive process. The damping constant can vanish if the energy sources are close enough to the surface of the star. One can predict the ejection of matter along polar caps and one or several belts or zones. The pole of the system is in the direction of the perturbing star. This is one of the first models (and nearly the only one) that make predictions about the directional dependence of mass loss.

In the 1960s, a clearer understanding of the structure of the binary components in nova systems led to a more realistic scenario for nova explosion: A Roche-lobe overflowing, unevolved star is losing H-rich material, and a fraction, if not almost all, of this material is accreted by the white dwarf companion. As accretion continues, a layer of H-rich material is built up on the surface of the white dwarf, and the bottom of this layer will be gradually compressed and heated until it reaches ignition temperatures of H-burning reactions. Hydrodynamic studies [Giannone and Weigert (1967), Rose (1968), Starrfield (1971a, 1971b)] have shown that a thermonuclear runaway will occur in the H-rich envelope, which can produce the observed energies and can reach temperatures and energy-generation rates at which dynamic effects become important (Starrfield 1971a, 1971b).

II.C. MECHANISMS OF MASS EJECTION

Despite the fact that the energy source for the nova explosion remained obscure for a long time, different mechanisms for mass ejection were investigated: shock ejection, pressure ejection, radiation pressure, and pulsational mass loss. It is now believed that the first three can act during various stages of the nova outburst. While shock ejection seems to play a predominant role in fast and recurrent novae, thick stellar wind driven by radiation pressure is important for slow novae.

II.C.1. MASS EJECTION BY EXPLOSIVE EVENTS

Rosseland (1946) proposed a central explosion (due to some "subnuclear mechanism"). The observed phenomena (several maxima) can be interpreted by the effects of a shock wave reaching the surface. Shock ejection was also proposed by Lebedinsky (1946). Schatzman (1946, 1949) also assumed that mass loss of novae is due to the propagation of a shock wave.

When energy is generated in a region in a time interval that is shorter than the sound travel time across that region, a shock wave is generated at the bottom of the region, which propagates outward. As the wave moves outward into less dense material, the shock wave accelerates. After the passage of the shock, the ejected material is left with a steep velocity gradient (Figure 7-1), see also Hazlehurst, 1962; Sparks, 1969). Shock ejection mechanisms lead to a temporal behavior of mass loss velocities, which shows a marked decrease of speed. In general, this is contrary to observations of classical novae, except perhaps for material of the premaximum absorption system.

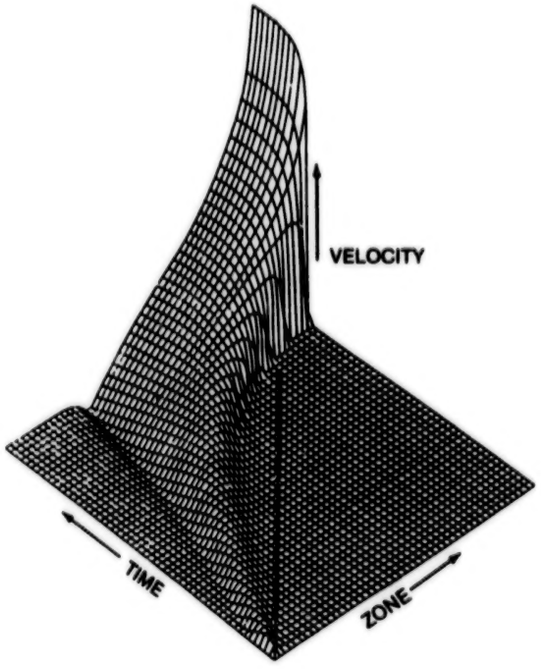


Figure 7-1. A three-dimensional plot of the velocity of material as a function of time in various zones of a star for shock ejection. The increase of the shock velocity and strength and the steepening of the shock front can be seen, as the shock wave propagates outward to zones of lower density. After the shock wave has passed through, the material has a large differential velocity. The trough on the left is due to material which did not reach escape velocity and is falling back onto the star (Sparks, 1969).

II.C.2. PRESSURE EJECTION

If the energy is deposited in a region during a time interval that is longer than the sound travel time across that region, but shorter than the time interval of radiation diffusion of the region, a "pressure" wave develops, which ejects all the material above the region with roughly the same velocity; i.e., the velocity gradient is much smaller than in the case of shock ejection (Figure 7-2). This mechanism was investigated in detail by Sparks (1969).

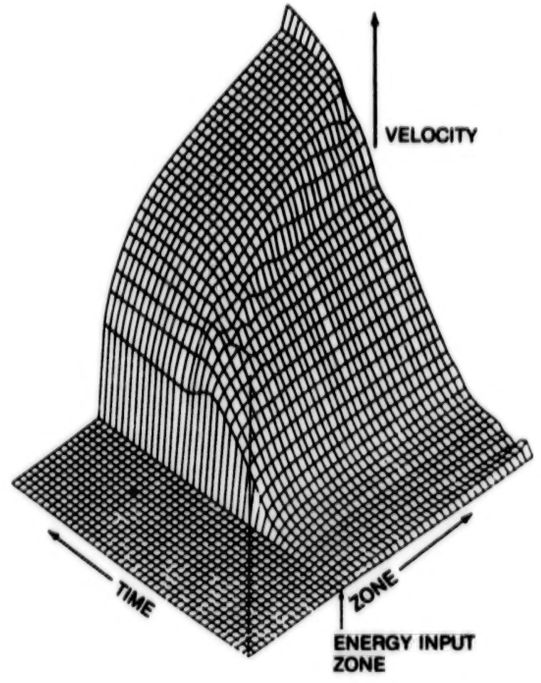


Figure 7-2. A three-dimensional plot of the velocity of material as a function of time in various zones of a star for pressure ejection. A pressure front is formed which ejects all material above the energy-input zone with roughly the same velocity. The slight increase in the velocity of the outer zones is due to the outward-propagating shock wave (Sparks, 1969).

II.C.3. RADIATION PRESSURE

The importance of radiation pressure by electron scattering for stars of high luminosity was pointed out by Eddington (1921). Radiation pressure in spectral lines was studied by Milne (1926), who derived limiting velocities of the order of 1600 km s^{-1}. It was further discussed by McCrea (1937), and in more recent times by Friedjung (1966a,b,c), Finzi (1973), and Nariai (1974), and in the optically thick wind models by Bath and Shaviv (1976) and Bath (1978).

II.C.4. PULSATION MASS LOSS

Problems encountered with shock ejection led Rose (1968) to investigate pulsational instabilities. Assuming thermally unstable H burning, a hot white dwarf becomes pulsationally unstable. The dissipation of pulsationally produced shock waves appeared to be a plausible means of surface heating; however, the calculations do not show how this extended envelope is ejected (Rose and Smith, 1972). In a later study, Sastri and Simon (1973) investigated multimodal radial pulsational instability in a prenova model. Predictions to test these models are, however, lacking.

II.D. CONTINUOUS EJECTION

First ideas on continuous ejection and the existence of a photosphere that shrinks in the later stages of the outburst, while the temperature increases, are found in Halm (1904) and Pike (1928, 1929). Whipple and Payne-Gaposchkin (1936) applied the theory of continuous ejection to DQ Her. These early studies found it difficult to distinguish observationally the process of continuous ejection from the expansion of a shell, both processes suggested already by Halm (1904). The process of continued ejection is favored by Whipple and Payne-Gaposchkin for the following reasons: if the continuous spectrum and the absorption lines are both produced in an expanding shell, the smallness of the observed changes in the absorption spectrum and in the energy distribution of the nova in its rise to maximum would require a continuous balance between the total radiation and the radius of the initial shell, unless one considers the shell so thick that it dams back the radiation for a considerable time. If the shell were as thick as this, one should expect the absorption lines to be broadened, because they would be formed near the surface of the rising photosphere. On the other hand, the observed narrowness of the lines indicates that the absorption must be produced so far above the effective photosphere that only a small solid angle is subtended at the center of the star by the material producing the absorption spectrum. For a thin shell, the intensity of the absorption lines might be expected to decrease with time but observations of DQ Her show that the intensity of the H lines increased.

II.E. SUPER-EDDINGTON LUMINOSITY

Finzi (1973) showed that the radiant energy of a nova in the course of its outburst cannot be stored and released by the ejected evelope, and concludes that the energy radiated in a nova outburst, i.e., 10^{45} erg, is released after the explosion by the central star. The luminosities of some novae at maximum exceed the "critical" or Eddington luminosity

$$L_{CRIT} = \frac{4\pi c\, GM_\odot}{\kappa_{TH}} \frac{M}{M_\odot} = 6.5\times10^4 \frac{1}{1+X} \frac{M}{M_\odot} L_\odot$$

where X is the relative H abundance in the external shell of the nova and $\kappa_{Th} = 0.2\ (1 + X)$ is the Thomson opacity, the opacity of fully ionized matter at low density, $c = 3 \times 10^{10}$ cm/s, $G = 6.67 \cdot 10^{-8}$ dyn cm^2/g^2, and $M_\odot = 2 \cdot 10^{33}$ g. The corresponding limit to the absolute bolometric magnitude is about $-6.8 - 2.5 \log_{10} (M/M_\odot)$ for $X \approx 0.7$. The critical luminosity is an upper limit to the luminosity of a star in hydrostatic equilibrium (Eddington, 1921). Finzi found that the luminosities of all postnovae (at least shortly after outburst) are larger than the critical luminosity and that their photospheres are steadily flowing out. Below this radiative atmosphere, Finzi assumed a convective hydrogen-rich shell. The concept of novae radiating above or near the Eddington luminosity plays an important role in subsequent nova wind models by Bath and Shaviv (1976) and Bath (1978).

II.F. HISTORY AND RESULTS OF MODELLING (FROM 1930)

Grotrian (1930), and Menzel and Payne (1933) found evidence, mainly from the appearance of forbidden lines, that diminishing pressure, rapidly rising temperature of the region in which the ionizing radiation originates, and dilution of radiation can account for the order of appearance of spectral lines of successive stages of excitation and ionization, as well as the appearance of lines originating by transitions from metastable levels.

The interpretation of observational results of nova DQ Her (1934) led to a new approach to the question of the time interval during which shell ejection occurs. Practically at the same time, and likely independently, Gordeladse (1937), Grotrian (1937) and Whipple and Payne-Gaposchkin (1936) put forward models with continuous mass outflow to explain some of the features of the slow nova DQ Her.

McLaughlin (1943) pictured the rise to maximum as an eruption of a spherical shell of gas sufficiently dense and deep to be opaque and to behave like an expanding star. The photosphere is only an optical level in the outward-rushing cloud, and as it expands, the individual atoms migrate from subphotosphere through the photosphere to the reversing layer. Finally, at maximum light, the cloud, which is now detached from the star, suddenly becomes transparent. In the early postmaximum stage, there are conspicuous bright bands that originate in gases located all around the star. The emission originates, however, mainly in the inner layers of the shell-almost on its inner surface-while absorption is produced throughout a great depth.

McLaughlin thought that the rate of mass ejection shows a variation similar to and almost in phase with the light curve, anticipating the latter very slightly. The model involves a main burst, followed by continuous expulsion of matter at a steadily decreasing rate. It requires a sharp reduction of the rate at the end of the main burst. The mass loss then drops slowly and continuously.

Qualitatively, this model has expansion accompanied by cooling. The shell acts initially as an (expanding) photosphere and mimics, after a short time from outburst, a spectral type of late B or early A with extended atmosphere. In a short time, τ_{vis} in the shell becomes less than unity; the shell becomes optically thin and ceases to radiate like a photosphere. The visual continuum fades and its color temperature increases. Further expansion of the shell produces

a. Less absorption of stellar radiation, thus transformation of P Cyg profiles into emission profiles.
b. Dilution of radiation, with accumulation of atoms in metastable states.
c. Time intervals between collisions greater than the lifetimes of metastable states: forbidden lines can be formed.

There is also formation of a subsequent system of shells, closer to the star, that are explained as being due to the tail of the ejection rates after the main burst (see Figure 7-3a and 7-3b). McLaughlin's model is indeed one with continuous ejection over a period of years (1943, p.188 ff.)

On the other hand, Pottasch's model (1959 a,b,c,d) is based on a spherically symmetric main burst only. Thus it offered the possibility to be tractable. The following assumptions were made:

a. The geometrical thickness of the shell is small compared to the radius of the shell.

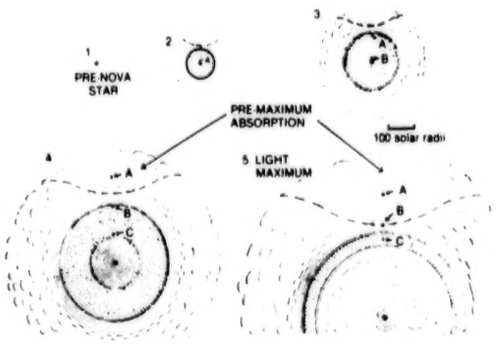


Figure 7-3a. Cross sections of a nova during the rise to maximum, as envisaged by McLaughlin (1950). The observer is looking from the top of the figure. The large black dot is the main body of the star. Stippled area represents the densest part of the ejected shell, concentric circles represent the optically thinner photospheric layers, which merge into the cloudy forms that represent the true atmosphere. On each drawing, a heavy dashed line outlines the region that is effective in producing the observed absorption spectrum. Successively ejected atoms A, B, and C are shown. With expansion, the layer containing A, and later that containing B, become transparent. By light maximum, the ejection has diminished and the shell, still opaque, has become detached from the star.

b. The density of the shell is always uniform and varies inversely as the volume of the shell.
c.The photosphere of the star remains at the

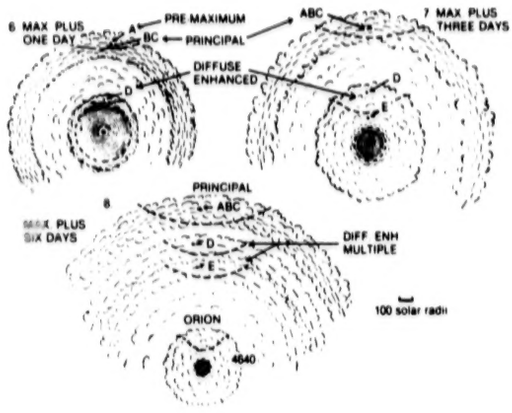


Figure 7-3b. Cross sections of a nova during early decline, as envisaged by McLaughlin (1950). Symbols have the same meaning as in Figure 7-3a. In section 6, the shell has just become transparent. Atoms B and C, owing to acceleration of the inner layers, have overtaken A, and the resultant shell is the principal one, the premaximum spectrum having disappeared with the engulfment of the outer layers (A) in the accelerated inner ones (B and C). Atom D is contributing to the diffuse enhanced absorption. In section 7, the inner cloud has become more extensive and the diffuse enhanced absorption is correspondingly stronger. Atom E is entering the region of absorption. In section 8, the gas ejected in the diffuse enhanced stage is in the form of two detached shells, overtaking the principal shell, while the inner cloud has developed into the Orion and the 4640 spectral stage.

initial temperature of the shell. As a result the inner surface of the shell receives stellar radiation diminishing as the inverse square of the time.

d.Energy is transferred by radiative processes.

A numerical solution was carried out for the following conditions: shell mass $M = 5 \cdot 10^{-3} M_{\odot}$, velocity = 800 km/s, central star temperature = 200,000 K, and radius 0.3 $R_{\odot}$. The computation was carried out until the shell has an optical depth low enough to question the basic assumptions. The model reproduces the essential features of a (fast) nova light curve with even the premaximum halt.

Pottasch's results are

1)The absolute magnitude of about -8.0, which the light curve attains before the shell becomes optically thin, is reasonable for a fast nova.

2)The temperatures observed during days 2 and 3 are similar to those observed.

3)The initial "bump" may be identified with the premaximum halt, the physical reason being that the shell is assumed to be initially isothermal at the surface temperature of the star from which it came, and the shell initially cools faster than the radiation can be transferred through the shell. Thus, the initial loss of energy occurs quickly and then subsides. The transfer of the energy of the star to the surface occurs more slowly; the combination of the two curves has a bump (more details are given in section III.A).

II.G. VELOCITY GRADIENTS

A plot of measured radial velocities of absorption versus time tends to increase, also when the feature is attributed to the same "system," which may form in a given layer. Furthermore, later spectral systems (diffuse-enhanced and Orion) always show larger radial velocities of absorption lines or wider emission lines. Thus, different parts of the shell move with different velocities. The diffuse-enhanced and Orion systems are attributed to the inner region surrounding the nova, while the original emission and absorption systems belong to the principal shell, which has moved outward in the meantime. Thus, we expect interactions with previously ejected material.

Arguments for the "inside origin" of the diffuse-enhanced and Orion feature have been outlined by McLaughlin (1947):

1)Some novae have secondary light variations, and the diffuse-enhanced absorption undergoes marked changes of intensity and of structure and position related to the light variations, while the principal spectrum responds only slightly with changes of intensity or excitation, but without changes of displacement.

2)The broad emissions of the diffuse-enhanced system extend across the emission and

absorption of the same lines from the principal shell. Nevertheless, the principal absorption remains strong and well-defined, without the filling-in that would occur if the atoms that produce the diffuse-enhanced spectrum were outermost.

3)There are numerous examples of partial or complete obliteration of absorption lines of the diffuse-enhanced spectrum by overheating emissions of the principal spectrum (further discussed in Section IV.A).

4)The same arguments apply also to the Orion spectrum.

According to McLaughlin, the high-speed atoms must eventually overtake the principal shell. Those that produced the Orion spectrum form a haze so rarefied that it would probably have no observable effects.Those of the diffuse-enhanced spectrum are present early enough to overtake the principal shell, while absorptions are still distinct. The collision of clouds should cause sudden disappearance of components of the diffuse-enhanced system, the appearance of new components, and acceleration of the principal shell. The principal shell is probably more massive than all the matter ejected later, so that large accelerations by collision are not to be expected. The principal shell continues to move outward until it becomes a quasi-planetary nebula. After a few decades, this has become too faint to be observable.

II.H. DETERMINATION OF T_{COL}, T_{ION}, T_{EXC}, T_E, N_E

The appearance of the bright nova DQ Her, in 1934, marked a decisive point in the study of novae, since at that time, the tools of stellar and nebular diagnostics were already well developed. Color temperatures T_{col} were most extensively determined (see McLaughlin, 1960, for a summary). Ionization temperatures T_{ion} were determined using Zanstra's (1931) method; the first to use it was Beals (1932) for V603 Aql, later determinations were made for CP Lac (McKellar, 1937) and DK Lac (Larsson-Leander, 1953, 1954). As a general rule, ionization temperatures are systematically much higher than color temperatures, and values based on He II and N III are approximately double those of H, while the nebular lines give values somewhat lower than hydrogen.

Excitation temperatures T_{exc} are calculated mainly from the relative intensities of [O III] and H lines (Stoy, 1933) and from the ratio He II 4686/Hβ (Ambarzumian, 1932). Both methods yield temperatures near or larger than the Zanstra temperatures. Oehler (1936) applied these methods to the nebular spectrum of DQ Her.

Electron temperatures T_e traditionally were mainly derived from the ratio of the [O III] lines (5007 + 4959)/4363. For all novae in which the ratio has been measured, T_e ranges between 6000 and 10,000 K, with a tendency to decrease as the nova fades (gain of strength of the nebular lines over the auroral transition 4363). Early applications to novae were made by Popper (1940) and Gaposchkin and Payne-Gaposchkin (1942).

The electron density is derived from the linear size of the nebula, and the surface brightness (or flux) of a hydrogen line with negligible self-absorption (Ambarzumian Kosirev, 1933; Sayer, 1940; Whipple and Payne-Gaposchkin, 1936, Payne-Gaposchkin and Gaposchkin, 1942), which turned out to range from 10^9 cm^{-3} in the early postmaximum stage to 10^6 cm^{-3} in the early nebular stage. With the assumption of $N_e = N_H$, the density of hydrogen ions, total nova masses were calculated by the above-mentioned authors.

II.I. ABUNDANCE DETERMINATIONS BY CURVE OF GROWTH OR NEBULAR LINES

The similarity of some nova spectra at maximum with those of supergiants led Mustel and Boyarchuk (1959) to attempt coarse analysis of nova spectra to determine excitation temperatures, microturbulent velocities, and chemical abundances. A number of analyses, mainly on slow novae, were carried out in subsequent years.

Another way of determining abundance of nova shells is by analyzing their nebular emission line spectrum. A wide range of ionization conditions is commonly observed in nova envelopes. Because of the large ejection velocities, emission lines are often wide, making line identifications sometimes problematic. The procedure employed to determine the chemical composition of nova shells is the same as that employed in abundance analyses of planetary nebulae. The first large-scale analysis of nebular spectra of the novae V603 Aql, RR Pic, GK Per, CP Lac, and DQ Her was carried out by Pottasch (1959e). He found that the abundances of O, N, S, Ca, and Ne seem to be a factor of 5 greater than cosmic.

III. SIMPLE MODELS TO EXPLAIN OBSERVATIONS

Various simple models to explain the observed light and spectral observations during post optical maximum activity are conceivable. Such models were described by Friedjung (1977a). They all describe stars that eject high-velocity gas during a limited time and that have a temporary increase in brightness. The geometry and the kinematics differ from model to model. As will be seen, the true situation is more complex, and though one simple model may be more helpful in explaining many phenomena, others may be needed to interpret other aspects. However, each of these models is conceptually very useful. Five of these models will be described.

III. A. INSTANTANEOUS EJECTION I

In instantaneous ejection models, all or nearly all material is ejected in a time that is short, compared with the duration of postoptical maximum activity. The observed changes occur in previously ejected gas, which at first is optically thick in the continuum (an expanding atmosphere is seen), and which later becomes optically thin. Instantaneous ejection type I models are those where the ejected material is in a fairly thin shell, the thickness of which remains small. Supposing that the outer radius of the shell at optical maximum is r_o and its thickness is Δr_o, while the corresponding values at a time near the end of activity are r_1 and Δr_1, instantaneous ejection type I supposes that, as $r_o \ll r_1$,

$$\Delta r_o \text{ and } \Delta r_1 \text{ both are} \ll \quad r_1 - r_o \approx r_1 \qquad (7.1)$$

To satisfy this condition, it is necessary for the expansion velocity of the shell to be much larger than the velocity of increase of thickness of the shell.

Assuming spherical symmetry and density of the shell to vary as 1/volume, this density will vary as $r^2/\Delta r$, r and Δr being the shell radius and thickness at any time. For a constant expansion velocity, the density will vary as t^{-2} at time t from outburst, as long as Δr is constant; it will vary as t^{-3} if Δr increases with a constant velocity from a value of zero at time zero. The shell surface area will vary as t^2 for a constant expansion velocity.

It can be supposed that the ejected shell is optically thick in the beginning; its surface area is then that of an expanding photosphere. After optical maximum, the bolometric luminosity does not increase, so if instantaneous ejection Type I with an optically thick shell were true, one would expect the temperature of the latter to fall. Once it became optically thin, the central object would become visible. The emission measure at this later stage varies as $r^{-2}/\Delta r$, so for a constant expansion velocity and shell thickness, it varies as t^{-2}; when Δr also increases from zero with a constant velocity from time zero, the emission measure varies as t^{-3}.

Instantaneous ejection Type I was extensively studied by Pottasch (1959 a,b,c,d). The shell thickness was supposed to increase from zero at ejection with a velocity equal to $2a/(\gamma - 1)$, where a is the speed of sound and γ, the ratio of specific heats equal to 5/3. This is a theoretical rate of expansion into free space.

In spite of the shortcomings of the model, which will be described later, Pottasch had some successes in explaining observations. First, he was able to explain the shape of the light curve before optical maximum including the premaximum halt, taking account of the fact that in early stages the optically very thick shell should not

be in radiative equilibrium (Pottasch 1959b). Moreover, this result appeared in a calculation for a shell mass of 10^{29} g ejected at 800 km s^{-1} surrounding a central star with a constant temperature of $2 \cdot 10^5$ K and radius of $2 \cdot 10^{10}$ cm (Figure 7-4). In Pottasch (1959c), early theory (largely neglecting velocity fields) was used to calculate the flux of the Hα line, when it was optically thick, as a function of electron density. He used the thickness of the shell given by this model to compute its mass, which could be compared with a mass calculated in late stages when the shell is expected to be optically thin

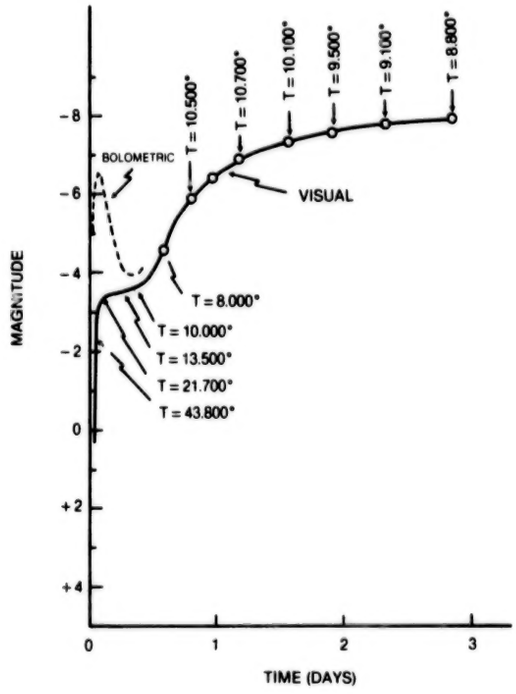


Figure 7-4. Light curve of the expanding nova shell according to computations by Pottasch (1959b). The energy emitted by the shell is shown as a continuous line as visual magnitude, the broken line gives the bolometric magnitude. The surface temperature is given at different stages. Note the presence of a pre-maximum halt in the visual light curve.

in the Lyman continuum (all hydrogen ionized) and in Hα. In spite of the various assumptions and approximations (including, for instance, that the Hα flux was three times that of Hβ, which unlike Hα was observed in all the studied novae), order of magnitude for the two masses determinations was reached for four out of five novae.

It may be noted that even Pottasch's (1959d) calculations indicate that part of the story was missing from his model. Temperatures of the central objects were found from the ratio of line emission emitted by ionized helium to that emitted by hydrogen, assuming photoionization by a Planckian continuum. The radius of the photosphere could then be determined from the total flux of photons emitted shortwards of 912 A, taken as equal to the total flux of Balmer emission photons. The calculated photospheric radii, for dates as soon as 10 days after ejection of the postulated shell, were much smaller than the latter, which for consistency needed already to be optically thin longwards of the Lyman limit. In addition, these radii decreased with time, suggesting that a constant radius "nova remnant" was not seen. It is this varying central object that first suggested that another sort of model needs to be invoked.

III.B. INSTANTANEOUS EJECTION TYPE II (SOMETIMES CALLED "HUBBLE FLOW")

In this model, a thick envelope is ejected instantaneously. This envelope remains thick as different parts have different velocities. In the simplest situation, where the velocity of any particular mass remains constant, the distance travelled by it at a particular time is proportional to the velocity. Thus, the outermost parts of the envelope have the largest velocity and the innermost parts, the smallest one. As expansion occurs, the optical thickness decreases, and the radius below which the deeper layers are not visible (which equals the photospheric radius) shrinks. It can be much smaller than the envelope.

When different parts of the envelope have the same density and each part a constant velocity, the density will vary as t^{-3} and the emission will measure as t^{-3}, t being the time since ejection. This behavior is the same as that of a thin shell whose thickness uniformly increases from zero at the time of ejection.

In the framework of instantaneous ejection Type II, one can imagine a much higher density in inner than in outer parts of the envelope. In this case, inner regions could remain optically thick for a

long time. However, they would produce strong line emission, because emission due to recombinations (and also collisional excitation) is proportional to the square of the density. As the radius of the photosphere decreases, regions with lower and lower expansion velocities would become visible, and the emission line profile would be more and more dominated by slowly expanding material. One might then expect the FWHM of emission lines to decrease with time, and the violet shift of P Cyg absorption components to decrease as well.

The type of situation just described is believed to be true for supernovae. Violet shifts of absorption lines have been seen to decrease in Type II supernova spectra (Chugai, 1975). Supernova 1987A in the LMC is a very good example (For instance, see Hanuschik and Dachs, 1987, and Henbest, 1987). The model has been reasonably successful. However, this situation does not seem to be true for nearly all classical novae, except perhaps before optical maximum, when the premaximum system can have behavior characteristic of instantaneous ejection Type II.

In spite of this, such models have sometimes been suggested for classical novae, including, for instance, Sobolev (1960). Nariai (1974) calculated the position of the photosphere, taking into account gravitational deceleration. In early stages, when the radius of the photosphere is large and the effective temperature is low, hydrogen is not ionized, and the radius of the photosphere is predicted to vary as $t^{-0.7}$. At a later stage, hydrogen is predicted to become ionized and the photospheric radius, to decrease very rapidly, as shown in Figure 7-5. Instantaneous ejection Type II or a "Hubble flow" was invoked by Seaquist and Palimaka (1977) to explain the radio emission of FH Ser. It may be noted that the regions from which radio emission is detected are much larger than those of the optical and ultraviolet photosphere (because of the free-free absorption coefficient), thus a simple model as the one given here gives a better description for the radio observations, as compared to optical and ultraviolet observations.

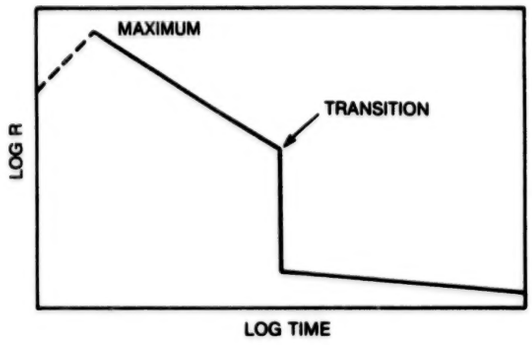


Figure 7-5. This schematic diagram gives the position of the photosphere, assuming constant luminosity, according to Nariai (1974). His study describes the slope of the curve from maximum to the transition phase, and also the sudden decline. After transition, the light curve is produced by the surface of the remnant in quasi-static contraction.

III. C. CONTINUED EJECTION A

Continued ejection models emphasize the importance of winds from the nova after optical maximum. When continued ejection A occurs, most of the emission of the continuous spectrum in the optical and ultraviolet comes from an optically thick wind. The photosphere (sometimes called quasi-photosphere) is located in the wind. The radius of this photosphere is directly related to the mass loss rate. The optical fading is readily associated with a drop in this mass loss rate, leading to a smaller photospheric radius, and if the bolometric luminosity does not decrease very rapidly, the photosphere will become hotter as it shrinks. The photosphere is much smaller than the ejected envelope for continuous ejection A, except near optical maximum. Material ejected near optical maximum will produce what is later an optically thin density peak near the outer edge, while the density will also be high in the inner regions containing material that has not expanded very much. This kind of model for instance, has been supported by Whipple and Payne-Gaposchkin (1936), Friedjung (1966 a,b,c), Bath and Shaviv (1976), and by Bath (1978).

Early quantitative formulations of continued ejection used the theory of Kosirev (1934) and Chandrasekhar (1934) for extended grey atmospheres in Local Thermodynamic Equi-

librium (LTE). Simple opacity laws were assumed such as a constant opacity (electron scattering dominant) or a mean photoelectric opacity law. As suggested by observation, the time scale of variations was supposed to be long, compared with the time for ejected material to travel from the mass losing star to the photosphere; therefore, the density in optically thick regions was supposed to vary as r^{-2}, r being the radial distance from the centre.

Making an Eddington approximation, one obtains

$$B=\frac{3}{4}\pi F r^2 \int_0^{\tau} \frac{d\tau}{r^2}, \qquad (7.2)$$

where B is the intensity of black body radiation emitted at a distance r from the centre, πF is the radiation flux, and τ is the optical depth. In LTE,

$$\pi B = \frac{1}{4} a c T^4, \qquad (7.3)$$

with T being the temperature. Supposing that the mean absorption coefficient is given by

$$\kappa = \kappa_0 P_e T^{-n}, \qquad (7.4)$$

with P_e the electron pressure, and that the number of free electrons per nucleus is a constant $1/\alpha$, one obtains that

$$T \text{ varies as } r^{-s/(n+3)} \qquad (7.5)$$

In an electron scattering case, κ is replaced by a constant σ, and

$$T \text{ varies as } r^{-3/4} \qquad (7.6)$$

Having obtained a temperature law, one can calculate the flux that should be observed at each wavelength by integrating emission from different directions at different optical depths, if one supposes that local emission is always Planckian. It may be noted that in regions where electron scattering dominates, this would not be correct even if all other hypotheses were valid. The result of such calculations is a way to interpret observations of continuum flux and color temperature in terms of photospheric radii and effective temperatures. Put in another way, one can correct temperatures and radii determined, assuming that the photosphere has a Plankian energy distribution.

If one knows the photospheric radius and temperature, the mass flux can be calculated. Putting the outflow velocity equal to V (assumed constant), the photospheric radius and temperature equal to R_P and T_P, respectively, and assuming for a first approximation an optical depth at the photosphere of 2/3, the mass loss rate is

$$\dot{m}=\sqrt{\frac{32}{3}\frac{(2n-14)}{(n+3)}\frac{\mu(\alpha+1)}{RK_o}}\pi V T_P^{(n-1)/2} R_P^{3/2}, \qquad (7.7)$$

(photoelectric κ)

or

$$\dot{m}=\frac{8\pi}{3} V \frac{\mu\alpha}{\sigma} R_P, \quad \text{(electron scattering)} \qquad (7.8)$$

Here R is the ideal gas constant, and μ the molecular weight.

This highly simplified theory illustrates some important features of continued ejection A. The characteristics of the continuous spectrum are directly related to the mass loss rate. If fading is rapid, R_P and $\dot{m}$ decrease rapidly. The time variation of the ejection rate derived from a good theory of an optically thick wind can be compared with other constraints to test continued ejection A. Such constraints, as shall be seen later, are connected with collisions betwen different parts of a nova envelope moving at different velocities, accelerating, for instance, the slower material.

Bath and Shaviv (1976) considered continued ejection A from a slightly different point of view. They supposed that during post optical maximum activity, the luminosity is close to the Eddington limit. The luminosity needs to reach this limit for radiation pressure to accelerate an optically thick wind, while a larger luminosity would lead to a breakdown of hy-

drostatic stability of the central mass losing star. In the case of constant luminosity L,

$$T_p = R_p^{1/2} (L/\pi ac)^{1/4} , \qquad (7.9)$$

with T_p the photospheric temperature, taken as equal to an "effective temperature" for the present approximation. The density in the photosphere ρ_p is given by

$$\rho_p = 2\sqrt{\frac{2}{3}\frac{\mu(\alpha+1)}{RK_O}\frac{(2n-14)}{(n+3)}}\; T_p^{(n-1)/2}\, R_p^{-1/2},$$

(photoelectric κ) (7.10)

or

$$\rho_p = \frac{2}{3}\frac{1}{\sigma RP} . \qquad \text{(electron scattering) (7.11)}$$

Combining Equation (7.9) with Equation (7.10) or (7.11), one sees that if L is constant, there are one to one correlations between photospheric density, temperature, and radius. These physical conditions are for constant L, which if LTE is valid, is also correlated with visual luminosity. In this way Bath and Shaviv (1976) were able to explain the frequent correlations of physical quantities with visual brightness during the decline of a nova from visual maximum.

Other models including continued ejection A were developed. Bath (1978) improved opacities. When electron scattering dominates (as is generally the case), he assumed an effective opacity of $(\kappa\sigma)^{1/2}$ in our notation, κ being a Cox and Steward opacity, quoted by Bath, as taking account of the fit and extension due to Christy (1966). The difference between scattering and absorption was thus taken into account, and some results are shown in Figure 7.6 Harkness (1983) calculated radiative transfer rigorously for non-grey optically thick winds; results are shown in Figure 7-7. However, these winds were not only in LTE, but they also had a solar composition and a constant luminosity at the Eddington limit. Such assumptions are at least partially wrong, as shall be seen.

Friedjung (1966c) showed that the optically thick winds required for continued ejection A could be accelerated by radiation pressure at very large optical depths. More detailed hydrodynamic calculations were performed by Ruggles and Bath (1979), while Friedjung (1981) studied observational consequences for acceleration of a wind for a luminosity far above the Eddington limit. We shall return to these questions later.

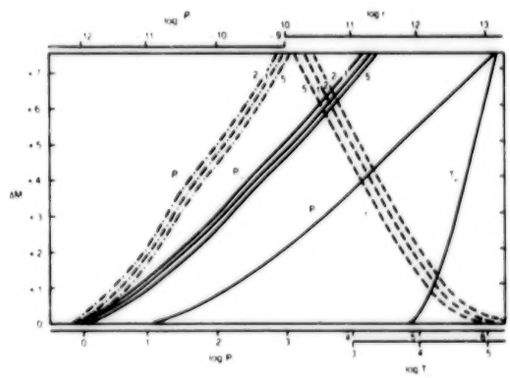


Figure 7-6. Variation of photospheric density, pressure, radius and temperature for outflowing nova winds as a function of delta Mv, the decline in visual magnitudes, for a blackbody continuum at constant luminosity in a nova model of Bath (1978). Three luminosities, 0.5 L_{ed}, L_{ed}, and 2 L_{ed}, are considered.

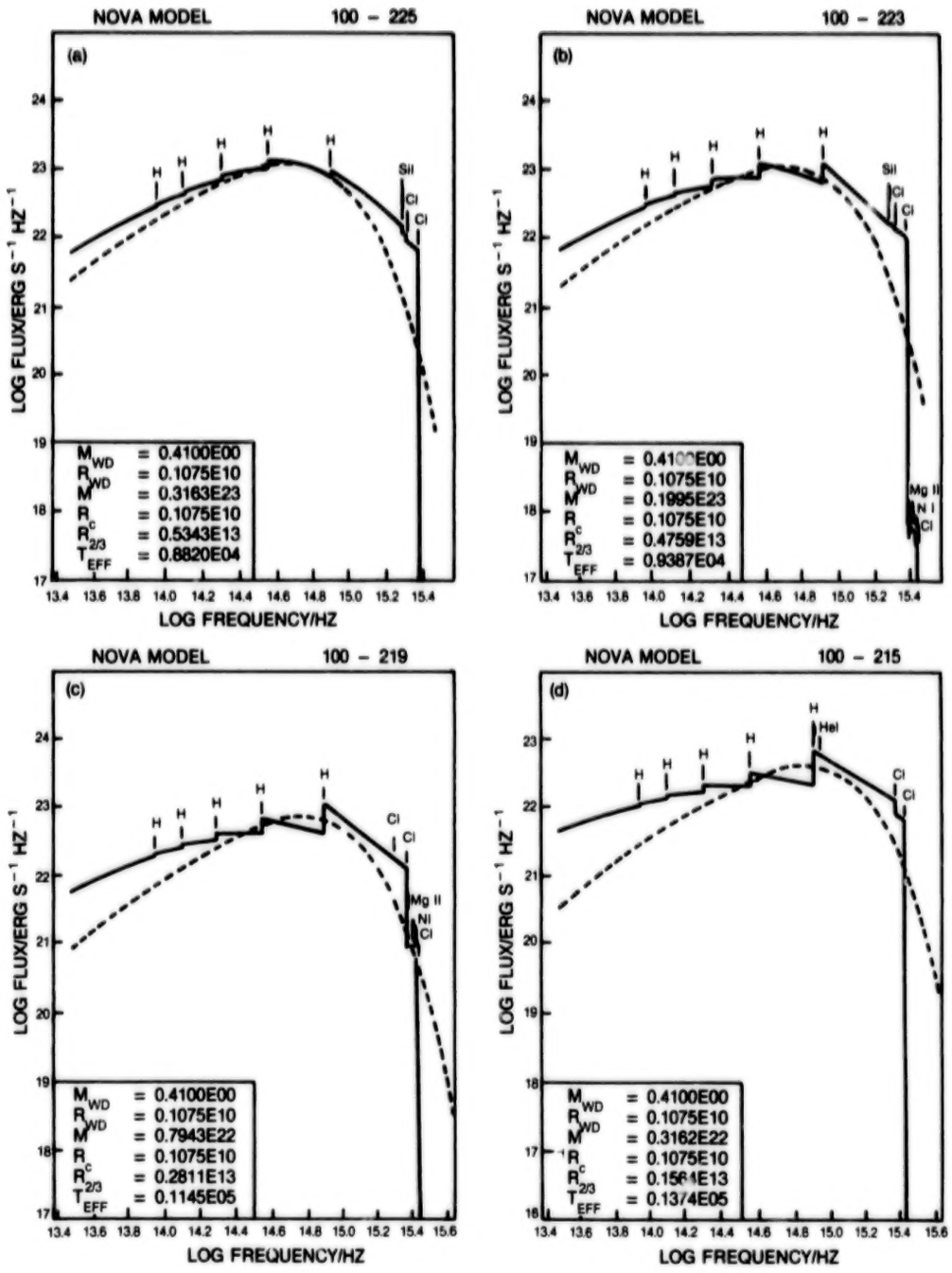


Figure 7-7. Emergent flux distributions for steady-state nova winds with (a) log $\dot{m}$ = 22.5, (b) log $\dot{m}$= 22.3, (c) log $\dot{m}$= 21.9 and (d) log $\dot{m}$ = 21.5 g s^{-1} (Harkness, 1983).

III. D. CONTINUED EJECTION B

A form of continued ejection is possible, where most luminosity arises from previously ejected material, ejected at a time when the mass-loss rate was very high. Such a model, therefore, resembles instantaneous ejection Type I with an envelope of constant thickness, if the ejection velocity is constant at the time when most of the ejection takes place. The observational consequences are very similar.

Continued ejection B can be expected to occur when the mass-loss rate decreases rapidly. A necessary (but not sufficient) condition for continued ejection B can be derived from Friedjung (1966a), if the mass-loss rate $\dot{m}$ varies as the power of ejection time t_0 from optical maximum (except of course for times close to the latter), then

$$\dot{m} = \dot{m}_0 \, t_0^{-\alpha} \qquad (7.12)$$

In the case when continuum emission in optically thin regions is due to recombinations at constant temperature and is proportional to the density squared, the necessary condition for continued ejection B to be valid for continuum radiation is

$$\left(\frac{R_P}{R_i}\right)\left(\frac{R_O}{R_O - R_i}\right)^{2\alpha} > 1 . \qquad (7.13)$$

Here R_i is either the outer radius of the part of the envelope where hydrogen is completely ionized, or the radius at which the power law of Equation (7.12) breaks down when the latter is smaller. R_o is the outer radius of the envelope. When $R_o - R_i > R_p$, condition (7.12) requires $\alpha > 0.5$. In addition, condition (7.13) suggests that continued ejection B is unlikely unless the hydrogen in the envelope is ionized almost to the outer edge.

The conditions for line emission need not be the same as for continuum emission. Strong lines, including in particular Balmer lines, though formed by recombination, may be optically very thick. Photons scattered many times in optically very thick lines can be lost through other processes. In view of such effects, line emission from outer parts of the envelope might dominate, even in situations where the continuum from such regions is relatively weak.

III.E. CENTRAL STAR DOMINANT MODELS

Ejection is supposed to occur from one of the components of the central binary, and one can imagine a general swelling of one of the components, so that something resembling a normal, almost stationary, stellar photosphere is observed after optical maximum. In this case, the high velocity expanding layers whose presence is deduced from the spectrum must be optically thin in the continuum. This type of model, which played a role in the history of nova models, more recently became attractive to those theoreticians who do not examine observational constraints in great detail.

A summary of older work on central star dominant models was given by Mustel, (1957). Figure 7.8 is taken from his work to illustrate the model. A fundamental change was supposed to take place at optical maximum with the detachment of the outer parts of an ex-

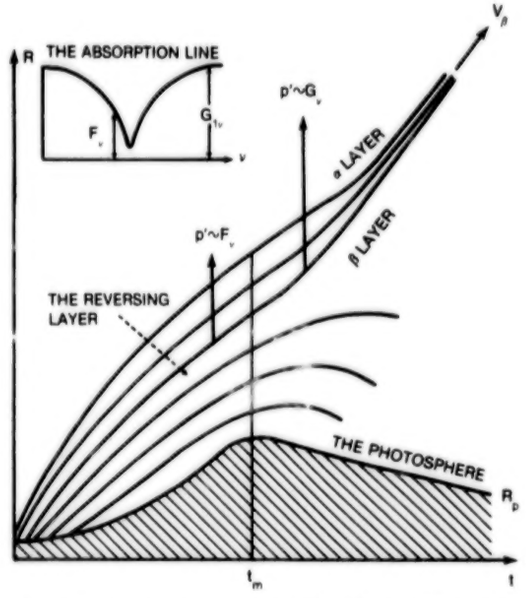


Figure 7-8. A representation of Mustel's (1957) model, in which the outer parts of the extended reversing layer of the nova continue to rise in the form of an envelope, while the star contracts.

tended reversing layer. Mustel considered the reason for the detachment to be a different radiation pressure, though in a later paper (Mustel 1962), cosmic ray pressure was proposed. In this model, the shell sweeps up preexisting premaximum system material, the shell itself being where the principal system is formed. The star itself then contracts after optical maximum.

Theoretical work to be described later suggests that the white dwarf component of the underlying binary expands during an outburst. Such a white dwarf can reach giant dimensions after having engulfed its companion, and its photosphere could give rise to the continuum emission. Any continued ejection would resemble the winds of "normal" hot stars, which are optically thin in the visual continuum. Indeed, in view of the large luminosity of a nova for a long time after optical maximum, strong winds of this kind are expected to be present.

Central star dominant models run into a major difficulty because of the usual lack of unshifted absorption lines and of relatively narrow unshifted emission lines from the region where the wind might be accelerated. One might expect to most easily observe photospheric absorption lines at times and for lines for which the line emission due to the expanding layers is relatively weak. One attempt to detect the strong unshifted absorption lines expected for FH Ser, if it had the photosphere of a normal giant with the same temperature and luminosity, indicated that such lines were not present (Friedjung (1977b).

In the framework of a central-star-dominant model, as well as for continued ejection A, the change in the energy distribution of a nova as it fades needs to be interpreted by an increase in photospheric temperature. In fact, lines of more highly ionized states are seen later. If a central-star-dominated model were true, one expects to see the lines of a high state of ionization formed in the photosphere (unshifted absorption lines) or in a chromosphere (narrow emission lines), at stages when no contribution to the line profiles from expanding material is seen. In fact, such a situation is never observed, and, as we shall discuss later (and have discussed before), the most central regions have the highest velocities.

According to McLaughlin (1943), faint nondisplaced absorption lines briefly existed around maximum light in the spectra of DN Gem, GK Per, and perhaps also V603 Aql. McLaughlin considered such lines circumstellar (seen because of radiative excitation of their lower levels near nova maximum), and in any case, one might expect their appearance in a much more systematic way, if they were the photospheric absorption lines of central-star-dominated models. Narrow line emission was seen in the spectrum of HR Del *before* optical maximum. One can wonder whether during this stage, not seen for other well-observed novae, a central-star-dominant model may not be the best way of describing the situation.

If we summarize the discussion of these simple models, instantaneous ejection Type II and central-star-dominant models put strong constraints on the velocity distributions; according to them, the lowest velocities must be near the centre of the envelope. The velocity distributions of such models encounter observational objections, which will be mentioned in more detail later. Instantaneous ejection Type I would require the continuum to be formed either in a thin shell or in a "nova remnant"; blueshifted P Cyg absorption components should be very wide in the first case and very narrow in the second one. In the first case, one would not expect to see absorption of the continuum by expanding material inside the shell; as will be seen, major difficulties are encountered for this type of model. Continued ejection A has also strong constraints; the continuum brightness is directly related to the mass-loss rate, and, if the inner regions have higher velocities than the outer ones, collisions between faster and slower moving material should accelerate the later following momentum transfer.

III.F. COMBINATION OF SIMPLE MODELS

The foregoing discussion suggests that the most fruitful way of making progress is to combine the approaches of continued ejection A and the presence of a thin shell. In many cases, at least, most radiation of the continuous spectrum is understood most easily as coming from an optically thick wind, while most line radiation may, at least sometimes rather come from a shell. Other reasons and considerations will be given later.

It can be noted that it is possible to combine continued ejection A with a central-star-dominant model, if electron scattering is much larger than pure continuous absorption. In such a case, P Cyg lines would only be seen clearly for those layer that are optically thin to electron scattering, while the continuous spectrum would come from deeper layers, which would have a lower velocity. Such a situation was proposed by Turolla et al. (1988) to occur in Wolf-Rayet stars. Presently, reasons will be given against this type of interpretation in the case of novae, but its possibility should be kept in mind in future studies.

It may be useful in this connection to emphasize the differences between novae and Wolf-Rayet stars, which like novae in outburst, also appear to have a very large mass-loss rate. In particular, Wolf-Rayet stars show signs of a velocity gradient in their winds. The shifts of the violet-displaced absorption components are correlated with line excitation potential but not so simply related to the ionization potential. This can be understood if the lines are formed in an accelerated wind (Willis and Garmany, 1987). A tendency is thought to exist for ionization to be frozen in such winds, explaining the contradictory results when one attempts to correlate velocity with ionization potential. As shall be seen, the picture that emerges for novae is rather different, though the lines of the Orion absorption system need to be studied in more detail to completely eliminate the possibility of such effects for them.

The higher velocities of later ejected material observed near the centre of the envelope suggest another model (Friedjung, 1987b), which can be considered a theoretical development of the consequences of continued ejection A, to be compared with the observations. A high-velocity wind is supposed to interact with slower moving material ejected before optical maximum, the latter being expected to produce the premaximum absorption system. A thin shell is formed by a snowplough effect associated with the collision of the two regions. This shell is assumed to be the seat of the principal absorption system and its associated emission, and when the postoptical maximum activity of a nova ceases, this shell can be expected to contain most of the ejected mass.

The model described is in many ways a combination of the simple models described previously. The premaximum system material, ejected before optical maximum and then swept up, might be partly described at least by instantaneous ejection Type II, the shell by instantaneous ejection Type I, and the wind by continued ejection A.

To predict the consequences of the model, the theory of the interaction of a stellar wind with the interstellar medium, described, for instance, in the review of McCray (1983), can be used. In early stages, densities are high, and the shocked material cools rapidly, directly transmitting momentum to the shell. In later stages, the time scale for cooling becomes longer than the characteristic time for the density of the wind near the shell to decrease because of the expansion of the latter. Shocked plasma then stays hot, exerting a thermal pressure on the shell, and also tends to fill a large proportion of the volume inside the shell. The condition for the transition between the two situations is estimated using order of magnitude arguments by Friedjung (1987b) as

$$t_a \geq \frac{8.0\times10^{-21}\,T^{-1/2}}{m_\mu^{\,2}} \frac{\dot{\bar{m}}}{V_P\,(V_W - V_P)^2\,f}, \qquad (7.14)$$

with $\dot{\bar{m}}$ being a mean mass-loss rate for the wind; T, the hot plasma temperature; m_μ, a mean mass for the atoms and ions present; V_W,

the wind velocity; and V_p, the shell velocity. t_a is the time since ejection when the transition takes place, the hot plasma then filling a fraction f of the volume inside the shell. In this expression, the formula of Kahn, (1976), which approximates the cooling rate of Raymond et al. (1976) was used. Taking f = 0.3, and $V_p = V_w - V_p = 1 \cdot 10^8$ cm s^{-1}, t_a is found to be 5. x 10^5 s. In this calculation, $\dot{m} = 10^{22}$ g s^{-1}, T = 3 x 10^7 K and m_μ = 3 x 10^{-24} g. Such a result however, is sensitive to both the numerical values and the physical assumptions used.

A model of this kind leads to a number of predictions. The shell should be accelerated by the pressure exerted on it. In addition, one can explain why the velocity of the premaximum system appears to increase after optical maximum. For instance, if the ejection of the material of this system takes place according to instantaneous ejection Type II, the fastest material is at the outside and is swept up last. One can precisely calculate when material, having the velocity of the last seen premaximum system, should have been ejected, assuming that it suffered no acceleration. The result can be compared with the time when material having this velocity was first seen before optical maximum for the few novae well observed in this stage. Finally, the shocked plasma should emit X ray and coronal emission lines: the former might be expected to be strongly absorbed by the shell in earlier stages. Calculations of the predicted X-ray and coronal line emission that should be observable indicated that they might be rather weak, being so masked by emission produced by other processes.

Other models involving collisions have also been previously proposed. Bychkova and Bychkov (1976) considered the collision between principal and premaximum system material, with the production of inward and outward propagating shocks. Bychkova (1982) later considered collisions between continuously ejected material and that of the principal system. Both regions were supposed to be extremely inhomogeneous, so collisions occurred between fast and slow-moving blobs. The diffuse-enhanced and Orion absorptions were supposed to be produced in shocked plasma, while most of the radiation of the continuous spectrum was also supposed to be produced by the colliding material. Therefore, the observed phenomena would be due to processes near the outer edge of the envelope. It would then be difficult to explain rapid variations such as those observed for DK Lac several months after maximum, over time scales of the order of 10^{-2} of the time elapsed since maximum. In addition, the author of these lines has difficulty in understanding how an apparently optically thick continuum energy distribution for emitted radiation could then be produced for novae.

In any case spherically symmetric collision models are probably too simple. The observed deviations from spherical symmetry need to be taken into account. An early attempt to do this was made by Hutchings (1972). Certain velocities were supposed to occur only in certain directions in order to explain the observed emission line profiles. Slow-moving principal system material, after interaction with the companion star, might only occur in polar cones. It should be noted, however, that the principal absorption system is always seen in the spectra of classical novae; this suggests that the material associated with it is present in all directions around a nova. The densities etc. are, of course, presumably dependent on the directions, and the orientation of the structure of the envelope, with respect to the observer, needs to be taken into account much more than in the past.

III.G. RECURRENT NOVA MODELS

The observed characteristics of recurrent novae in general, and of RS Oph and T CrB in particular, are rather different from those of classical novae; thus, models for these stars need not be the same. Let us recall that, in the course of an outburst, the observed expansion velocity of the absorption lines and the associated wide emission lines of RS Oph and T CrB decrease with time. Narrow emission components seen in the spectrum of RS Oph disappear during the same development.

These observations led Pottasch (1967) to propose a different kind of model for RS Oph.

An ejected shell was slowed down by a pre-existing circumstellar envelope, the latter being where the narrow emission lines were formed. He made quantitative estimates of the envelope mass assuming the same type of increasing envelope thickness as for a classical nova (the electron temperature and the shell thickness increase were assumed to be slightly higher). Knowing the thickness and the radius of the shell, hydrogen and helium fluxes gave the total mass, following theoretical expressions for the emission line intensities. Assuming momentum conservation, the density distribution of the preexisting circumstellar envelope could be determined. Pottasch found that it appeared to be in hydrostatic equilibrium, with a density distribution characteristic of a temperature of 10^4 K in inner regions and 10^3 K in outer regions. The resulting mass of the central star was 0.7 $M_\odot$.

T CrB and RS Oph are at present thought to be closely related to symbiotic stars, which are now considered to be binaries consisting of a cool giant and a more compact companion. Cool giants have strong winds, and the material of this wind would be swept up by the ejected material of a nova explosion. The basic idea of Pottasch's (1967) model is therefore attractive, even though details may be considerably different.

Pottasch's ideas were further developed by Gorbatskii (1972, 1973). The formation of a shock in the circumstellar envelope ahead of the shell was considered. Coronal line emission was studied, taking into account the different time variation of electron and ion temperature of the model. Gorbatskii (1977) suggested that similar ideas could also explain the narrowing of emission lines in the classical novae V1500 Cyg and CP Pup; red giants, however, are not present in these objects, and instantaneous ejection Type II may best describe the development of a large part of the envelopes of these exceptionally fast classical novae. Hydrodynamic calculations of what happens when high velocity ejection takes place in a low velocity wind were performed by Bode and Kahn (1985). They considered a model similar to that of supernova remnants: A spherical envelope expands into the wind of a cool giant, and forward and backward shocks are generated. Matter that has passed through the reverse shock is well cooled, forming small condensations following a Rayleigh-Taylor instability. In what the authors call Phase II, the movement of the backward shock confines unshocked gas to a progressively smaller volume in the middle, while, at the outside, a blast wave advances into the wind. The newly shocked outside gas is very hot and does not radiate much of its energy. In Phase III, cooling of the outer shock dominates and condensations are again formed, which can break loose and move at high velocity in the wind. The model was applied to explain X-ray and non-thermal radio emission.

The authors calculated that the first X-ray observations were made at a transition between Phase II and Phase III, the temperature from the shock being between 0 and 5.7 x 10^6 K. Analysis of the X-ray observations seemed to require a "metal" overabundance of about 5 in the *red giant wind*. The authors also concluded that the presence of optical emission lines throughout the development of RS Oph requires parts of the shocked gas to cool earlier; they supposed that denser condensations were produced by a magnetic field. This giant wind magnetic field was calculated to be 0.01 G ahead of the shock, and 0.04 G in the shocked gas; relativistic electrons moving in the field would then have produced the radio emission non-thermally.

Even if this type of model stands the tests of more observations and can be developed further, it probably cannot be applied to all recurrent novae. Not all of them appear to have cool giant companions; however, it is not clear to what extent classical nova models can be applied to recurrent novae without giants.

IV. EMPIRICAL APPROACH

At this point, we need to see whether observational results can be pushed further, in order to give a more precise indication of what is happening. Without already having a detailed

model, is it possible to do basic diagnosis? This type of approach will now be described.

IV.A. VELOCITY STRATIFICATION FOR CLASSICAL NOVAE

The different absorption components observed, which can sometimes be very numerous, suggest that motions are not simple. However, observations do suggest a definite stratification, often not taken into account in models.

Evidence from the study of the optical lines was summarized by McLaughlin (1947). He stated that in practically all detailed studies of classical novae, four absorption systems can be recognized, which are the pre-maximum, the principal, the diffuse-enhanced, and the Orion systems. These systems can be split into subsystems, so that in certain situations the total number is much greater, but this does not invalidate McLaughlin's classification. In any case, this classification is both chronological and in order of velocity; the premaximum system appears first with the lowest velocity and the Orion system last with the highest velocity, already indicating that low-velocity material is ejected first and so is further from the ejecting star at a given time than high-velocity material ejected at a later time.

McLaughlin (1947) was guided by three main considerations: (1) superposition of line profiles of different systems, (2) response to disturbances originating in the ejecting star, and (3) excitation and other physical processes. Considerations of the first type could be applied when diffuse-enhanced or Orion components of line profiles were superposed on lower velocity components. Principal system absorption components were not filled in by diffuse-enhanced or Orion emission from the profiles of other lines: a striking example was that of DQ Her, where the principal absorptions of Sc II 4247 Å remained strong and sharp when superposed on the longward wing of the Fe II 4233 Å diffuse-enhanced emission; similary, Orion N III emission did not fill in principal and diffuse-enhanced absorption. On the other hand, diffuse-enhanced absorption lines were often partially or completely obliterated by overlying principal emission. McLaughlin quotes examples for DQ Her. Cases of Orion absorption being disturbed by overlying principal emission were also quoted; in the case of V603 Aql, each Orion absorption component of the N III pair near Hδ weakened in turn as it coincided with the maximum of O II principal system emission. All this clearly suggests that higher velocity material is *below* that of lower velocity.

The other considerations of McLaughlin (1947) also pointed to the same conclusion. When secondary oscillations of light occur, the Orion absorptions, unlike other absorptions at such stages, show close wavelength correlations with brightness changes; as will be seen, this is also true if the brightness of the continuous spectrum is considered. In the framework of a continued ejection A model, this would suggest a correlation of a Orion system velocity and the ejection rate. Finally, the higher ionization of the Orion system suggests an origin in the inner parts of the envelope, if photoionization by radiation from the central photosphere dominates. McLaughlin explained the disappearance of high ionization bands in the principal spectrum during "flaring" of the 4640 A and other bands, supposing complete absorption of high-frequency radiation by the inner envelope during such stages.

As a careful experienced analyst of optical spectra, McLaughlin's arguments carry great weight, and his conclusions are very probably correct. However, future studies of line superpositions need to be quantitative. The interpretation is not always obvious. In addition, it may also be noted that emission not only fills in absorption lines produced in deeper layers, but can also fill in absorption lines in another line of sight. Large deviations from spherical symmetry are necessary for this to be important.

Since the classical work of McLaughlin, very high-velocity absorption components (up to 10^4 km s^{-1}) have been detected in the satellite ultraviolet spectra of some novae. It is not yet

completely certain whether they can be fitted into the classification for optical spectra. However, the highest velocity systems of V1370 Aql varied on a time scale of a few hours, suggesting line formation in the inner envelope.

Other points concerning velocity stratification need to be made. Absorption components of the principal absorption system are always seen for classical novae; this means that deviations from spherical symmetry do not appear to be large enough to prevent the formation of the system in any direction. High-velocity systems are also generally seen; there has been some uncertainty in the case of V1500 Cyg; however, even in the case of this exceptionally fast nova, Duerbeck and Wolf (1977) identified the presence of diffuse-enhanced absorption about one day after maximum. Therefore, limits are also placed to possible deviations from spherical symmetry for the high-velocity systems.

If the velocity identification of McLaughlin is accepted, this places strong constraints on the region of production of the continous spectrum. A large part of the continuous spectrum *at least* must be produced below the level where any strong absorption line is formed. Therefore, when strong Orion N III absorption components are seen, at least a large part of the continuum must be produced in more inner regions, a condition compatible with continued ejection A or central-star-dominant models. Such was the case for V603 Aql (Friedjung 1968). However, extrapolations of such conclusions to other epochs of nova development carry some uncertainty; as will be seen below, the best way is to reason from regularities in the time variation of the continuum flux.

IV.B. ANALYSIS OF THE REGIONS WHERE THE CONTINUOUS SPECTRUM IS PRODUCED

In continued ejection A and central star dominant models, most of the continuum is emitted by a photosphere, although in the former case, one has a "quasi-photosphere" formed by an optically thick wind. However, it should be noted that infrared emission is not included in such considerations; the outer parts of the envelope may be expected to be optically much thicker in the infrared than in the optical because of free-free (and sometimes dust) opacity.

The basic ideas of analysis have already been given in Section III.C. Photospheric temperatures and radii can be found, which, when continued ejection A is assumed, can be converted into mass-loss rates. However, all calculations made up to now are extremely approximate and of dubious physical consistency. Among temperature determinations, color temperatures are probably the easiest to interpret; other methods such as Zanstra-type temperatures do not only make assumptions about the relation of the energy distribution of emitted radiation to the photospheric effective temperature, but also about the excitation of emission lines. The latter temperatures assume production of line emission by photoionization, followed by recombinations and cascades to the ground state, all ionizing photons being absorbed by the line-emitting medium.

In view of this, we shall emphasize analysis, which is close to observational data and which should be easily reinterpretable in the future using better theory. The first step is to see what optical continuum fluxes (expressed as magnitudes) can tell us. When continuum magnitudes are plotted against log time from maximum, the graphs obtained have often linear portions; this means that flux varies as a power of the time from maximum (or perhaps rather from the initial explosion, which occurred not much earlier). Such graphs are shown in Figure 7.9, 7.10 and 7.11. The first two of these are for V603 Aql and GK Per, which showed oscillations during their declines; these oscillations were between parallel lines associated with early and late decline. The difference between the continuum flux magnitude and the visual magnitude, which includes the effects of emission lines, can be seen by comparing Figures 7.9 and 7.12, the lines not being parallel in the latter figure. The linearity of such graphs for visual magnitudes was shown by Vorontsov-Velyaminov (1940).

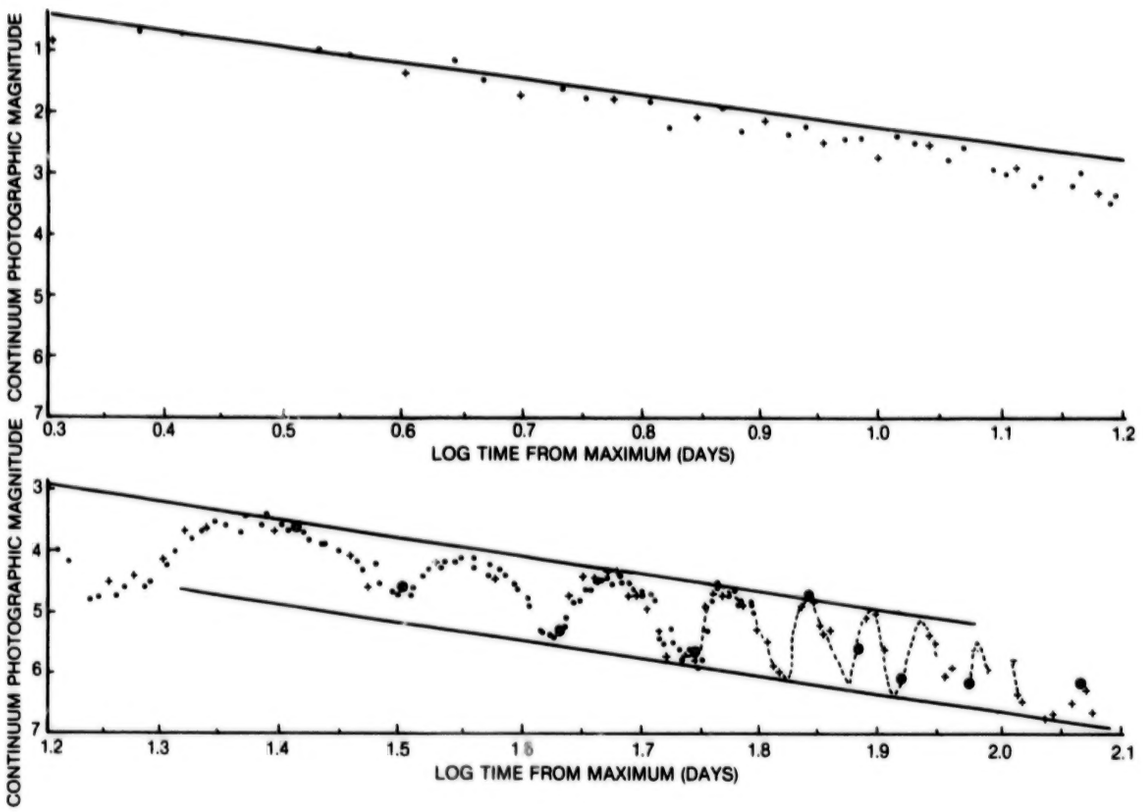


Figure 7-9. The continuum magnitude of V603 Aql versus log time from maximum (Friedjung, 1966a).

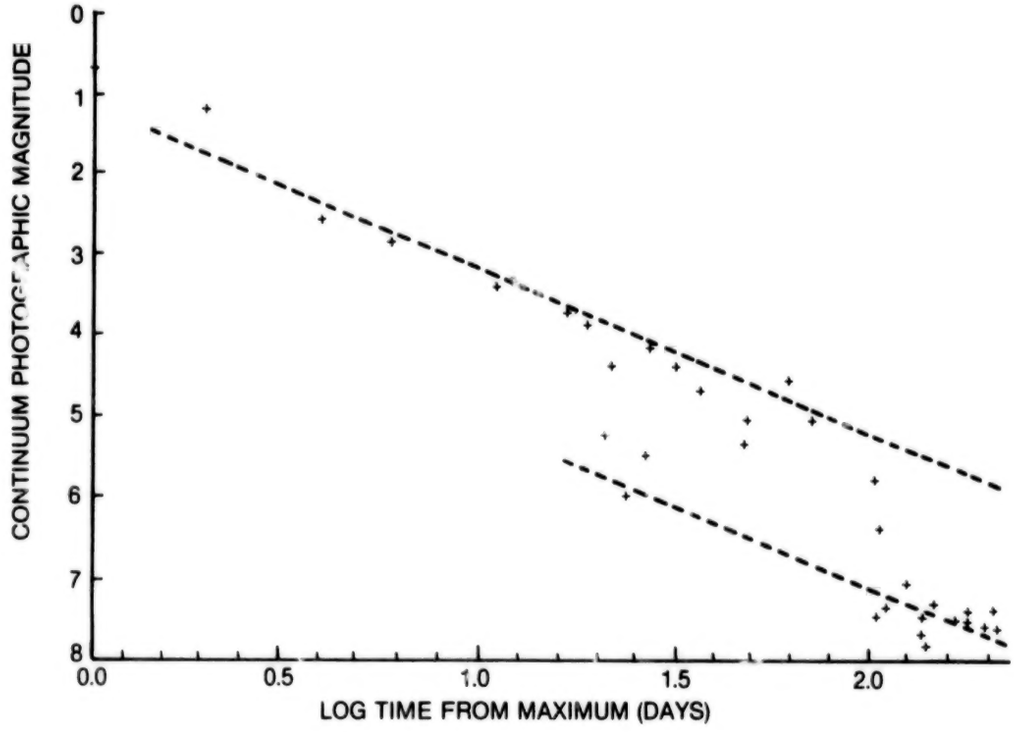


Figure 7-10. The continuum magnitude of GK Per versus log time from maximum (Friedjung, 1966a).

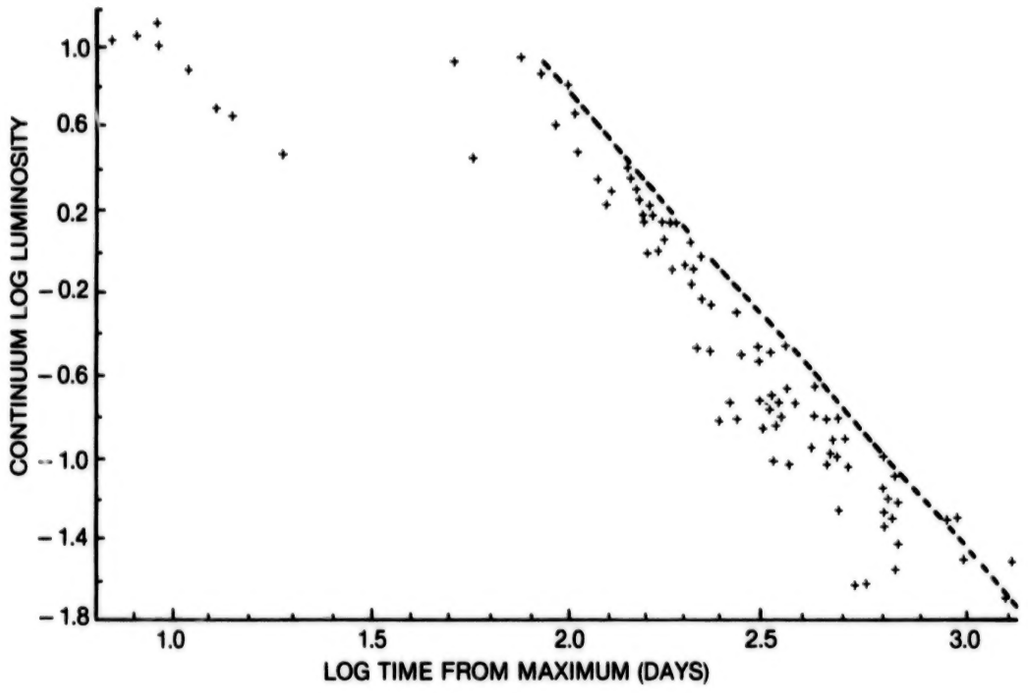


Figure 7-11. The continuum magnitude of RR Pic versus log time from maximum (Friedjung, 1966a).

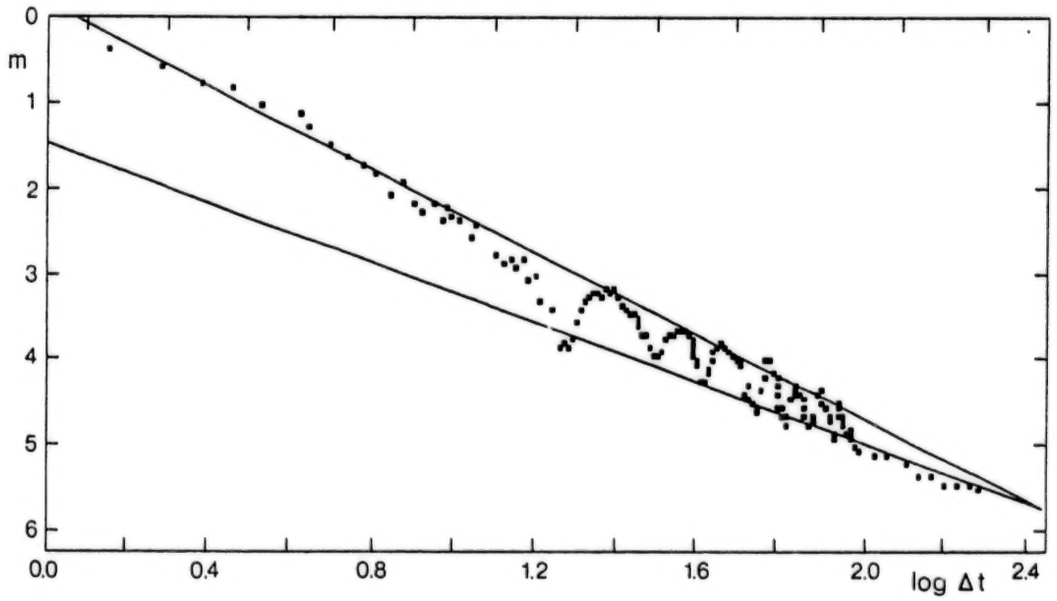


Figure 7-12. The visual magnitude of V603 Aql versus log time from maximum. The behaviour of the oscillation can be clearly seen (Friedjung, unpublished).

For novae such as V603 Aql and GK Per, one can conclude that when, during the decline, the continuum magnitude varies as the same power of the time, the basic physics and hence the most suitable model very probably do not change. In addition, if oscillations occur between parallel lines, as in that graphs described in the last paragraph, it is tempting to conclude that similar physical processes occur at both maxima and minima. However, the last conclusion is much less certain.

Continuum magnitudes combined with Zanstra temperatures were used by Friedjung (1966b) to derive radii, assuming a Planckian energy distribution for the photosphere. These radii appeared to have the same type of power law variation as the continuum fluxes. In spite of the doubts that can be cast on such a calculation, it may be that the conclusion concerning the power-law time variation is not strongly dependent on the assumptions. Such a hypothesis needs obviously to be confirmed. If the radii follow a power-law time variation, there is moreover a good chance that the same is true for the mass-loss rate.

In view of the lack of a reliable theoretical model to give the whole distribution of energy emitted by a nova, the observations in other spectral regions are needed for the determination of basic data, e.g., those concerning the total luminosity. The combination of observations in different spectral regions shows that the total luminosity declines much more slowly than in the optical, and indeed may stay almost constant for a long time. Gallagher and Code (1974) studied the time variation of the radiation from FH Ser between 1550 and 5480 A, and found it almost constant for more than a month after optical maximum (Figure 7.13). However, if one attempts to correct for emission in other spectral regions indications of a decline are seen (Friedjung 1977b) while, in any case, conclusions are sensitive to the reddening corrections. More recent results for other novae are shown in Figures 6-46 and 6-50. The slowness of the decline of integrated flux is obvious.

The total luminosity of novae was also studied by Duerbeck (1980), using ground-based data. Absolute magnitudes were determined from newly found distances and interstellar extinctions. A bolometric correction corresponding to a mean spectral type of F5Ia (-0.25) at optical maximum was used to obtain the luminosity at optical maximum. Duerbeck found that fast or moderately fast novae with smooth declines (except for transition-stage oscillations in some cases) had luminosities well above the Eddington limit, while slower novae had luminosities in the region of the Eddington luminosity. In any case, this type of calculation is still extremely approximate.

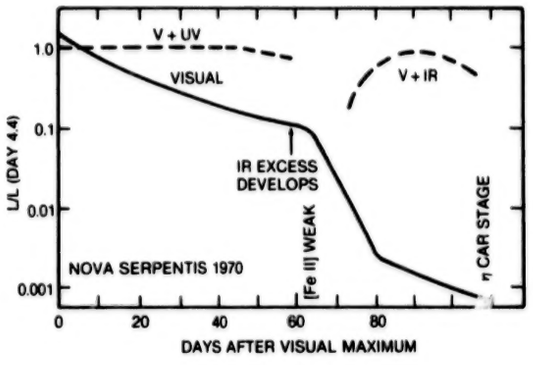


Figure 7-13. Energy budget of FH Ser as a function of time, based on ultraviolet, optical, and infrared data. For a distance of 650 pc, the day 4.4 luminosity is 1.6 x 10^4 $L_\odot$. The postmaximum luminosity plateau, the correlation between optical spectral, and light curve features and the development of the thermal infrared excess are shown (Gallagher, 1977).

Novae for which multifrequency observations are available can be studied further. One can not only attempt to determine the total radiative luminosity, but also the luminosity associated with the kinetic energy of the wind, which is large for continued ejection A. Such an attempt was made by Friedjung (1987a) for FH Ser, using rather approximate theory. The energy distribution had been studied from the infrared to the ultraviolet, and an examination of observed energy distribution indicated that a blackbody fit was not too bad, thus enabling a photospheric color temperature to be defined. A corresponding blackbody photospheric radius R_P could then be derived. If the optical depth in the photosphere is assumed to be 2/3,

the kinetic energy flux is

$$F_K = \frac{4\pi}{3} \frac{R_P V_P^3}{\kappa}, \qquad (7.15)$$

with V_P the ejection velocity, and κ the opacity supposed to be dominated by electron scattering. V_P was taken to be the higher of the observed absorption component velocities, because, as seen above, higher velocity material appears to be closer to the photosphere. Friedjung (1987a) obtained what are probably rather minimum values of F_K, as the measured V_P corresponding to the mean absorption component radial velocity was an average of ejection velocity components in the direction of the observer, while a maximum κ of 0.15, suggested by the calculation of Bath (1978), was taken. The total radiative and kinetic energy luminosity found and shown in Table 7-2 appears to remain for a long time above the Eddington limit of $2.07 \cdot 10^{38}$ erg s^{-1} for a 1 $M_\odot$ star with a chemical composition characteristic of a nova as given by Stickland et al. (1981). This result however, is approximate in view of the assumptions mentioned, while it is also clear that the maximum κ is sensitive to the various element abundances. Therefore, this type of calculation needs to be repeated with better theory in the future.

Other conclusion that can be drawn from Table 7-2 should also be emphasized. The kinetic energy flux is of the same order as, and indeed somewhat larger than, the radiative flux. In view of the fact that the velocity of the continuously ejected wind appears to be of the order of 0.005 the velocity of light, the ratio of the momenta of radiation emitted in unit time to that of material ejected in unit time is of the order of 3×10^{-3}. The ratio of the radiative energy per unit volume to the kinetic energy per unit volume is not much larger near the photosphere. This suggests that, unless the estimates of Table 7-2 are wildly wrong, acceleration of the wind by radiation pressure to the observed velocities cannot be produced at small optical depths. Acceleration by radiation pressure in the lines appears to be quite insufficient. However, radiation pressure can act in another way. Equations 7-5 and 7-6 indicate that the ratio of energy densities can be much larger at large optical depths; when electron scattering dominates, Equation 7.6 leads to a variation as r^{-1} for a constant velocity, so the ratio would be of order unity at 10^{-3} to 10^{-2} of the photospheric radius.

It is at such radii that radiation pressure migh be responsible for accelerating the continuously ejected material. It is for this type of reason, that the combination of continued ejection A and the formation of the continuous spectrum in a low-velocity photosphere, described above, is hard to reconcile with acceleration by radiation pressure.

Similar conclusions were previously reached by Friedjung (1966c), these being, however, based on temperatures and radii deduced only from ground based observations. The improved multifrequency photospheric temperatures and radii have not changed the situation radically, and one might perhaps doubt whether better diagnostics could really make such a large difference, in spite of the present approximations.

The velocity variations of the absorption lines of the Orion system can be closely related to the behaviour of the continuous spectrum. Very often there seems to be a correlation between the velocity of the Orion system and the brightness of the continuum. Correlations of velocity squared with 1/radius from Friedjung (1966c) are shown in Figures 7-14, 7-15, and 7-16. The radii of V603 Aql and RR Pic derived from Zanstra temperatures assuming a blackbody energy distribution and those from color temperatures of DQ Her show almost linear correlations. What is also very striking is that the velocity at infinite radius corresponds to that of the diffuse-enhanced system. This suggests that both absorption systems are due to the same physical process, best understood as continued ejection.

It may be noted that GK Per, another nova showing like the previous ones postoptical maximum oscillations, did not appear to have a velocity-radius correlation, according to Friedjung (1966c). It now seems (Bianchini et al., 1988) that its velocity at a given time has oscillations with twice the instantaneous period of the postmaximum light oscillations.

TABLE 7.2 PHOTOSPHERIC PROPERTIES OF FH SER

day from 1970 Feb. 14.0	L in 10^{38} [erg s^{-1}]	T_C [K]	R_P 10^{12} [cm]	mean measured high vel. [10^2 km s^{-1}]	low vel.	F_K(min) [10^{38} erg s-1]	F_K(min)+L
6.39	2.65	5250	22.0	most hydrogen neutral			
8.41	2.39	5370	20.1	—	—	—	—
15.85	1.32	7410	7.8	13.1	6.7	4.9	6.2
22.05	1.05	9120	4.6	15.1	7.1	4.4	5.5
27.34	0.92	9770	3.7	16.3	7.3	4.5	5.4
29.34	1.39	8320:	6.3:	16.8	7.4	8.3:	9.7:
31.87	0.91	9200	4.3	17.2	7.4	6.1	7.0
49.83	0.73:	14800:	1.5	18.5	7.6	2.7:	3.4:
57.49	0.64	18600:	0.84:	18.7	7.7	1.5:	2.2:

L = radiative luminosity; T_C = color temperature, R_P = photospheric radius; vel. = (expansion) velocity; F_K = kinetic energy flux.

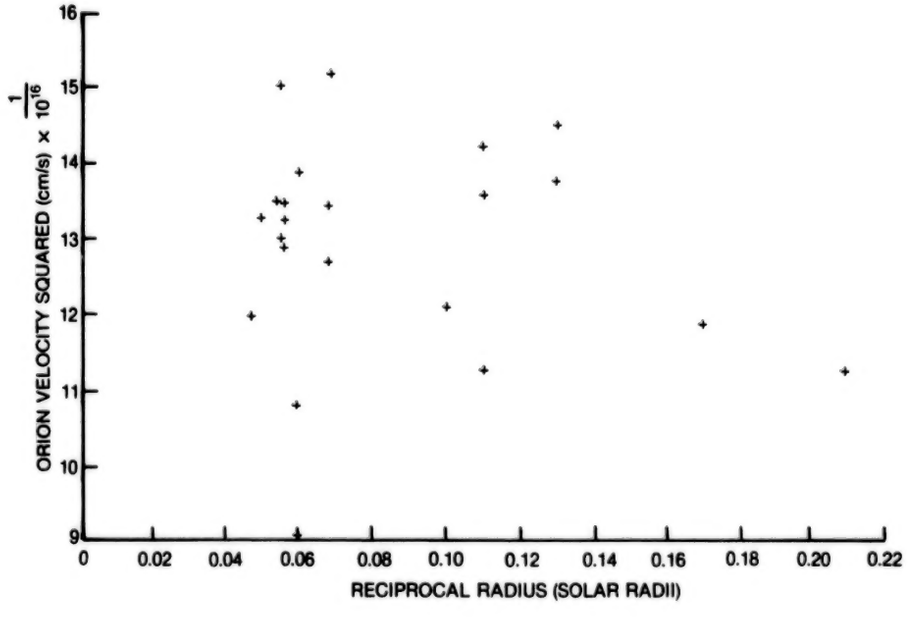


Figure 7-14. The relation between velocity squared and reciprocal radius for GK Per (Friedjung, 1966c).

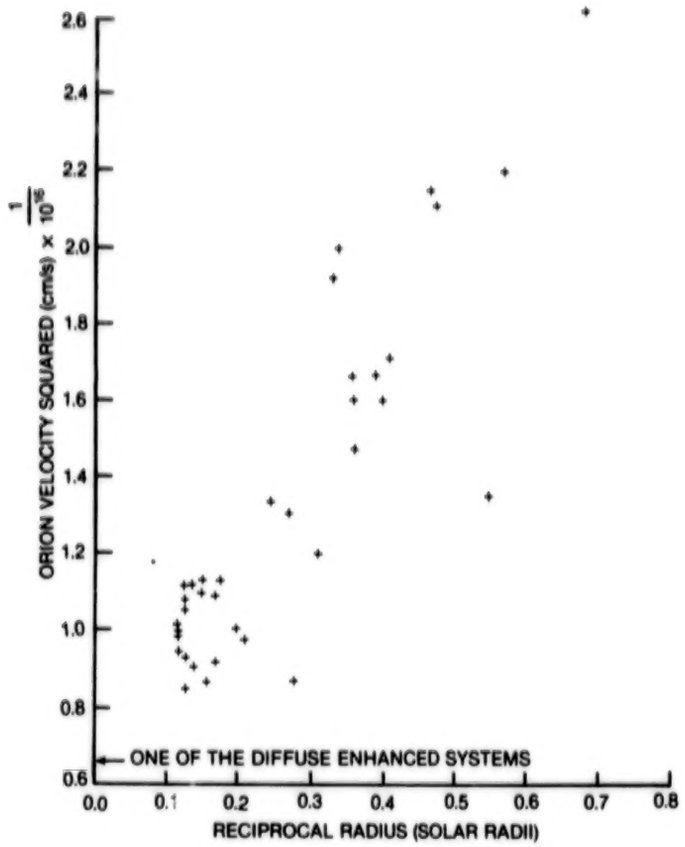


Figure 7-15. The relation between velocity squared and reciprocal radius for RR Pic (Friedjung 1966c).

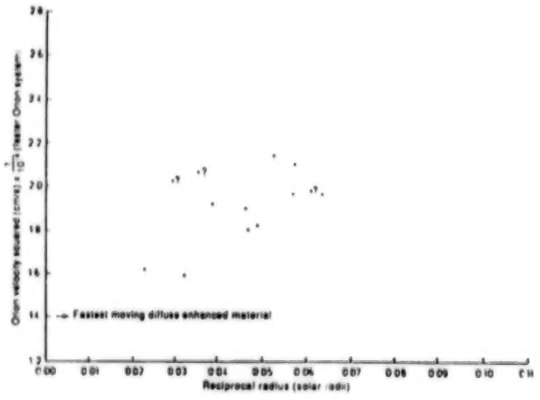


Figure 7-16. The relation between velocity squared and reciprocal radius for DQ Her (Friedjung 1966c).

The most attractive picture that emerges from these considerations seems to be one of wind acceleration by radiation pressure at large optical depths, where the total luminosity, at least in a limited region, is above the Eddington limit. Part of this total luminosity is converted to kinetic energy. It is clear that such a process, if it exists, cannot be thermal! Its possibility will be discussed later.

IV. C. ELEMENT ABUNDANCES IN NOVA EJECTA: CURVE OF GROWTH METHOD

Study of emission and absorption lines in principle, can give information about abundances. Sometimes, extremely abnormal abundances have been determined. Nevertheless, such determinations have traps, which should not be neglected.

Two types of method can be considered. The first uses absorption components of lines, and applies curve of growth methods to derive abundances. The second uses emission lines, which, particularly in the nebular stage, should be formed under conditions similar to those of planetary nebulae, for which one knows how to determine abundances. Older work is summarized by Collin-Souffrin (1977) and by Williams (1977). The subject has expanded very

C-6.

much since these reviews.

In the analyses of Mustel and his coworkers, using absorption lines and the curve of growth method, nova spectra were compared with those of stars with "similar spectral classes" (F supergiants). The narrowness of the observed nova absorption components suggested that they could be treated in the same way as the lines or normal stars, in spite of the blueshift due to the expansion (in fact, such narrowness could be produced when absorption lines are formed in an envelope where most line absorption is at a radius much larger than that of the photosphere). A systematic introduction to the curve of growth method can be found in Mustel (1964). The partial curves of growth are constructed, using equivalent widths of certain ions, are shifted in abscissa to make them coincide, and then are compared with theoretical curves of growth. A problem is encountered with the excitation temperature, Texc. The diagram showing multiplet strength versus excitation potential does not result in a straight line, whose slope is given by Texc, but shows an overexcitation of levels with high excitation potential, which might be explained by a temperature variation in the extended layer, or by isolated high-temperature cells in the extended atmosphere.

The curve of growth method was applied to the novae DQ Her, HR Del, and V1500 Cyg. Mustel and Boyarchuk (1959), Mustel and Baranova (1965), Antipova (1974) and Mustel (1974) based their analysis on the premaximum system of DQ Her, Mustel and Baranova (1966) analyzed the principal absorption system of this nova one week after optical maximum. HR Del was analyzed by Ruusalepp and Luud (1971), Antipova (1974) and Yamashita (1975). Premaximum and maximum spectra of the fast nova V1500 Cyg were analyzed by Boyarchuk et al. (1977). Another approach, based on simple synthetic premaximum spectra assuming LTE, was carried out by Stickland (1983). Generally, overabundances in C, N and O were found [though Stickland (1983) found C solar], while the heavier elements had almost normal abundances. Figure 7-17 (Antipova 1974) shows the abundances of DQ Her compared with solar ones.

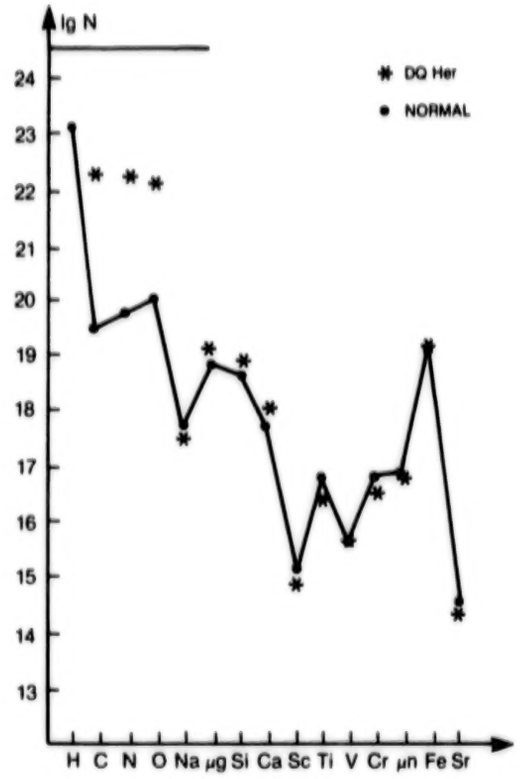


Figure 7-17. The chemical composition of the envelope of DQ Her, derived from outburst spectra, and compared with solar values (Antipova 1974).

It is rather dangerous to apply classical curve of growth theory in a situation where non-LTE and nonthermal effects can be expected. The similarity of the nova spectrum with that of an F supergiant may be deceptive, as can be seen when the above discussion of possible models is kept in mind. The more detailed examination of Williams (1977) leads to other criticisms. The CNO abundances were derived from very few lines (at most, 5 per element); indeed, there were only enough lines to construct separate curves of growth for the ions Fe I, Fe II, Ti II and Cr II. Mustel and his co-workers assumed the same curve of growth for all ions with the same "microturbulent" velocity, and the same law of atom/ion population variation with excitation potential. They had to assume that the latter deviated from a Boltzmann distribution, Texc increasing with excitation potential. Such assumptions can lead to very uncertain abundances, especially

when derived for H, C, N, and O, with lines having a high excitation potential. Though the measurements appear to be consistent with the mentioned assumptions and also with the use of the Saha equation, results derived from the curve of growth method should be viewed with much caution.

The absorption spectrum of DQ Her has also been studied in another way by Sneden and Lambert (1975). This nova showed CN absorptions during early postmaximum development, and spectral synthesis could be used to obtain information about isotopic ratios. The CN lines of the first six vibrational bands of the $\Delta\upsilon$-1 sequence of this molecule were analyzed, assuming formation in a scattering layer (fractional transmission proportional to $e^{-\tau}$ with τ being the optical depth). Thermal equilibrium was assumed for the molecule, with an arbitrary microturbulence of 5 km s^{-1}, atomic lines being neglected. The isotopic ratios obtained were $^{12}C/^{13}C \geq 1.5$ and $^{14}N/^{15}N \geq 2$, which can be compared with the corresponding solar system values of 89 and 273.

IV.D. ELEMENT ABUNDANCES IN NOVA EJECTA: NEBULAR LINES

In the post maximum stage, the spectrum of a nova exhibits a large number of emission lines, which in principle, can, be used to derive physical and chemical properties of the ejected envelope (or merely, the ejected shells that may be interacting), as well as properties of the central object. In general, lines originating from transitions requiring lower densities and higher levels of ionization appear at later stages of the development.

When the nova enters the nebular stage, it is generally not spatially resolved. Integrated intensities of different emission lines, which refer to the entire envelope as if it were a homogeneous nebula, are used for the analysis. This assumption is certainly not correct and leads to the most serious objection to an uncritical application of plasma diagnostics. A remedy would be a high resolution spectrophotometric study of emission lines, resolving at least the structure in the line of sight. Previously such observations have been very scarce.

The flux emitted by any line depends on how it is excited; knowing the physical conditions, one can deduce the abundance of the ion to which it belongs. Basically one uses the following equation (Collin-Souffrin, 1977):

$$I_\lambda = \frac{1}{4\pi d^2} \int f_\lambda (T_e, n_e)\, n(X_{ij})\, dV, \quad (7.16)$$

where I_λ is the absolute flux of the line (ergs cm^{-2} s^{-1}) at the earth, d is the distance of the nova, V is the volume of the envelope, $n(X_{ij})$ is the number density of the ion X_i in the jth state of excitation giving rise to the line, and f_λ is the emissivity of the line at an electron temperature T_e and an electron density n_e. This equation needs to be corrected for reddening and line self-absorption when present. It is clear that the observed inhomogeneities can pose very serious problems when trying to apply Equation (7.16). In addition one needs to know the abundances of all ions of an element in order to determine the total abundance; states of ionization not giving rise to lines in observed spectral regions are difficult to include in calculations, particularly when there are uncertainties concerning the ionization. The values of T_e and n_e are derived from line ratios that are sensitive to either of the parameters, e.g., ([O III] 4959, 5007)/([O III] 4363,([O III] 4959, 5007)/[Ne III] 3869), ([O III] 4959, 5007)/(He I 5876). The ionization fractions are assumed to be time-invariant (Seaton, 1975; Ferland and Shields 1978b; Lance et al., 1988). The relevant atomic constants can be taken from a compilation by Mendoza (1983).

Studies of abundances, like studies of the physical conditions in general of regions of emission line formation, are best based on results from many different parts of the spectrum. Combinations of satellite ultraviolet observations with optical ones are better than those based only upon the latter.

Filling factors in nova shells appear to be low, since most of the high-density material responsible for the emission is in clumps, filaments, of thin sheets, while the material in

between is at much lower densities and presumably higher temperatures. Masses in the past might have been overestimated by a factor of 10 (Peimbert and Sarmiento, 1984). However, the in-between material would be hard to detect, and its mass could be underestimated.

IV.E. INTERPRETATION OF INFRARED OBSERVATIONS

Infrared observations in different stages yield the following results:

Around optical maximum, the infrared flux of a nova yields the Rayleigh-Jeans tail of the pseudophotosphere, usually at a temperature of 7,000 - 10,000 K. In early decline, it transforms into an optically thin free-free (thermal Bremsstrahlung) flux distribution. At this phase, emission lines (or emission bands) often are superimposed on the continuum (see below for details). In many cases, this free-free emission is replaced by blackbody radiation from a circumstellar dust cloud of a temperature of typically 1,000 K. It condenses from the nova ejecta, or (as an alternative explanation, which encounters more difficulties), is a cloud of preexisting dust, heated by the radiation of the outburst.

Soon after the peculiar drop in the light curve of DQ Her, McLaughlin (1935, 1937) suggested that a cloud of dust had suddenly formed from the ejecta, producing the dramatic fading of the visual flux. However, since no infrared observations were made at that time, the suppression of the redshifted components of the emission lines, which is also today considered as a good criterium for dust formation, was then the only evidence for the existence of such a dust cloud.

Only in 1970, with the thorough study of the energy distribution of FH Ser in different stages of the outburst did the explanation of light curve disturbances by dust won acceptance: a fading of optical and ultraviolet flux coincided with the emergence of strong infrared continuum emission, balancing the energy output completely.

Bode and Evans (1983) sorted the novae according to their infrared development into three classes:

Class X: novae for which, at a certain stage, the infrared luminosity is nearly the luminosity of the underlying object. These novae invariably have a pronounced discontinuity in the visual light curve, which coincides with the onset of infrared development. The temperature of the dust shell attains a minimum before rising to a plateau—the so-called isothermal phase (example: NQ Vul).

Class Y: novae for which the infrared luminosity is below 10% that of the underlying object. The light curve is smooth and the dust shell temperature decreases monotonically (example: V1668 Cyg).

Class Z: novae with little or no infrared excess, i.e., little or no dust. The visual light curve is usually smooth. The excess can easily be attributed to line emission in the infrared (example: V1500 Cyg).

As has been shown by Bode and Evans (1981), the onset of infrared excess occurs (if it occurs) usually when the nova has declined by 4 magnitudes, and shortly after the transition phase of spectral development.

IV.E.1 GRAIN GROWTH

In the model of Clayton and Wickramasinghe (1976), grains can only condense from ejecta once the temperature of condensation is such that the saturated vapour pressure of the grain material is less than the partial pressure of the ambient monomer gas. This condition is fulfilled at 2,000 K, and grains begin to grow. Their temperature declines for two reasons: first, the distance to the central object is increasing, and second, the absorption efficiency of the grains increases as grains grow. Growth of an individual grain is essentially complete in a few days, and maximum grain size is 2 μm.

Because the photospheric temperature of novae increases after outburst, the distance at

which grains can condense recedes from the nova. Dust formation thus depends on the question whether the ejecta, which are obviously also receding, can overtake the condensation distance. If so, grain formation is possible; otherwise, the nova environment is always too hot. Futhermore, as the ejecta disperse, their density declines, and unless grain growth is initiated at an early stage, the amount of dust eventually formed is negligible.

Gallagher (1977) developed an idealistic model by assuming that the condensation of grains is controlled by the radiation field of the nova, which radiates at constant luminosity. Its surface temperature can be estimated to be

$$T_* = 5100\,(L_{CL}/L_\odot)^{1/4}\,K, \qquad (7.17)$$

where L_{CL} is the luminosity at outburst. The temperature of a grain can be written as

$$T_g^4 = \frac{1}{4\sigma}\frac{L_{CL}}{4\pi R^2}\frac{Q(T_*,a)}{Q(T_g,a)}, \qquad (7.18)$$

where Q is the Planck mean absorption cross section for grains of radius a and temperature T_g in a radiation field characterized by the stellar photospheric temperature T_*. Assuming that the early grains are simple,

$$T_g \approx (L_{CL}/4\,\pi\sigma r^2)^{1/4}, \qquad (7.19)$$

This can be written in terms of the time t_d at which dust initially becomes observable:

$$t_d \approx \frac{2}{T_g^2(0)}\sqrt{\frac{L_{CL}}{4\pi\sigma}}\frac{1}{V}, \qquad (7.20)$$

where V is the expansion velocity.

Calibrating this formula with FH Ser, adopting $T_g(0) = 1300$ K, this yields:

$$t_d = (320/V)\sqrt{(L_{CL}/L_\odot)}\ \text{days}, \qquad (7.21)$$

Fast novae have several properties that limit grain formation. First, the ejection velocities are larger than in slower novae, producing lower gas densities at a given time (especially since there is no evidence for the ejection of larger masses in fast novae). Second, fast novae produce substantial stellar winds, i.e., high-velocity material, that may give rise to shocks that might disrupt the grain nucleation process. Third, ionization might be higher.

The ionization time scale is given by Gallagher to be

$$t_i = 2.2\cdot10^6/V(L_{CL}/L_\odot)^{1/3}\ \text{days}. \qquad (7.22)$$

The ratio of t_i/t_d is independent of the expansion velocity and depends only on the luminosity or speed class of novae. For fast and very fast novae, $t_i < t_d$, and dust does not form. In moderately slow and slow novae, the equation for t_d gives a reasonable estimate for the time of dust formation. In this picture, HR Del, as well as most other slow novae, are not understood, because they form too little dust for their slow speed.

IV.E.2. LINE OR BAND EMISSION

The most spectacular line in the infrared observed until now is the 12.8 μm [Ne II] emission in QU Vul, originating from the transition $P_{1/2}$ - $P_{3/2}$, which amounted to 0.1% of the outburst luminosity at a given date (Gehrz et al., 1985, 1986). From Ne III and Ne IV lines in the ultraviolet simultaneously present, a high overabundance of Ne could be derived. Together with SiO features observed at 10 μm and the suspicion that an overabundance of Mg is hidden in the 10 and 20 μm features, QU Vul is a good candidate for a TNR on an O-Ne-Mg white dwarf (see Chapter 7, Section V.A.) with a large amount of white dwarf material mixed into the ejected shell.

Less spectacular features are the 5 μm emission, a short-lived feature in the early free-free phase, which was observed in V1668 Cyg and LW Ser. It is attributed to CO (Ferland et al., 1979). A fairly mysterious broad emission feature around 10 μm occurred in V1301 Aql, which is attributed to SiC or possibly CS.

IV.F. INTERPRETATION OF RADIO OBSERVATIONS

Radio emission from novae (HR Del and FH Ser) was first discovered in 1970 (Hjellming and Wade, 1970).

The radio light curve for novae develops much more slowly than the optical one. Let us assume a thermal absorption coefficient k_ν, which should take into account the usual chemical composition of the nova shell (e.g., Scheuer, 1960).

The radial optical depth is given by

$$\tau_\nu = \int \kappa_\nu \, dr. \qquad (7.23)$$

At a fixed date t, $\tau_\nu(t)$ behaves like ν^{-2}, and at a fixed ν, it behaves like t^{-5}, assuming expansion in the form of a Hubble flow (instantaneous ejection II).

For ν and t sufficiently small, i.e., at radio wavelengths, we have $T_\nu(t) \gg 1$, and the nova radiates like a blackbody:

$$S_\nu = \pi \left(\frac{R}{r} \right)^2 B_\nu(T_e) \qquad (7.24)$$

(thermal emission for $\tau_\nu \gg 1$),

where R is the outer radius of the shell and r, the distance. For ν and t sufficiently large, $\tau_\nu \ll 1$, and

$$S_\nu = \int_{\text{volume}} \kappa_\nu B_\nu \frac{dV}{r^2} \qquad (7.25)$$

(thermal emission for $\tau_\nu \ll 1$)

Thus, for Hubble flow expansion, at this stage, $S_\nu \sim D^{-3}$.

Hjellming et al. (1979) have calculated the radio development of an outburst and compared models with observed radio light curves. From this comparison, they derived information regarding mass, velocity, and radio thickness of the shell of V1500 Cyg. The assumed model is spherically symmetrical, with sudden ejection of an isothermal (T_e = 10,000 K) shell with a velocity gradient. For V1500 Cyg, the model gives a mass of $2.4\ 10^{-4}\ M_\odot$, the velocities are 200 and 5600 km s^{-1} at the inner and outer radii, respectively. The shell becomes radio thin after some 100 days. Infrared fluxes and their evolution in time are also well predicted.

Hjellming et al.'s models of slower novae give lower velocities of ejecta, lower masses of the shell, and greater time elapsed from outburst for the shell to become radio thin.

IV.G. STRUCTURE OF NOVA SHELLS

For a few nearby old novae, shells have been observed in quite some detail, and deviations from spherical symmetry are always encountered. Nonspherical envelopes were explained by

- Magnetic guiding of material (Mustel and Boyarchuk, 1970).
- Nonradial stellar pulsations, which is still a very debatable assumption (Warner, 1972).
- Interaction of the expanding nebula with the secondary component: blobs ejected perpendicular to the orbital plane (Hutchings, 1972; Pilyugin, 1986).
- Interaction of the expanding nebula with the accretion disk (Gorbatskii, 1974; Sparks and Starrfield, 1973).
- Effects of stellar rotation, gravitational braking, and radiative acceleration (Phillips and Reay, 1977)
- Rayleigh-Taylor instabilities at the beginning of the expansion (Chevalier and Klein, 1978)
- Stellar rotation only; TNR proceeds at the same rate at all latitudes; radial ejection velocity is the same at all latitudes. The oblateness of shells of about 1.5 can be explained with a rotating white dwarf with

a period of the order of minutes. No radiative acceleration is needed; it could also be shown that the accretion disk, hardly, and the secondary, only to a small extent, influence the kinematics of the (principal) ejection. As the shell expands, it must initially cool rapidly and may be subject to thermal instabilities. This tends to form concentrations of characteristic size about $(c/v_{ejecta})r$. Since the Mach number of the ejecta is probably initially about 1, the shell should contain only a few condensations (Fiedler and Jones, 1980).

V. CAUSES OF NOVA OUTBURSTS

The theory at present accepted by almost all workers in the field is one where hydrogen is accreted by the white dwarf component of the binary from its companion, and where this hydrogen undergoes a thermonuclear runaway. The detailed description of the theory is beyond the scope of this book devoted to atmospheres; what will be emphasized is the impact of it on observable properties. More details will be found in the reviews by Sparks et al. (1977), Starrfield and Sparks (1987), and Starrfied (1988).

V.A. MODELS FOR CLASSICAL NOVAE

Hydrogen accreted by a white dwarf will tend to be ignited, and as this process accelerates, a thermonuclear runaway can eventually occur. This is possible because there should be no significant transport of energy into the interior of the white dwarf from the outer regions where hydrogen is burning. The strength of the outburst is determined by a proper pressure at the core-envelope interface of the white dwarf

$$p=\frac{GM}{R^2}\frac{\Delta M}{4\pi R^2}, \qquad (7.26)$$

the right-hand side being the gravitational attraction multiplied by the mass of the accreted material per unit area. In this expression, ΔM is the envelope mass, M is that of the white dwarf, and R its radius. MacDonald (1983) and Fujimoto (1982) found that a value of p of 10^{20} dynes cm^{-2} is necessary for a fast nova outburst. Using a white dwarf mass-radius relation, one deduces a relation between the envelope mass and the white dwarf mass required for a fast nova outburst; the envelope mass decreases as the white dwarf mass increases. It becomes easier to produce a nova outburst when the white dwarf is more massive.

In reality, the situation is less simple. The mass accretion rate, the chemical composition, and the white dwarf luminosity all influence the evolution of what will give rise to an outburst. The influence of the mass accretion rate on the development of accreting white dwarfs having a solar composition will be discussed in chapter 12, where possible models for symbiotic stars are considered; the theory is not relevant only for classical novae. When the accretion rate of the white dwarf component increases, the mass of the accreted envelope decreases (cf., MacDonald, 1980) because of the gravitational compression of the accreted material, which produces energy that accelerates the thermonuclear runaway. It appears, moreover, that classical nova explosion are not produced for high accretion rates above 10^{-8} $M_\odot$ yr^{-1} unless the white dwarf mass is very close to the Chandrasekhar limit; in view of the observational evidence for such accretion rates, this poses a problem we will discuss in more detail.

While variation in the mass accretion rate is associated with variation in the energy release due to gravitational compression of accreted material by white dwarf components, the abundances of CNO are also very important for the physics of nova explosions. This can be understood theoretically because of the influence of the β unstable nuclei ^{13}N, ^{14}O, ^{15}O, ^{17}F. At first their lifetimes (863, 102, 176, and 925 s) are shorter than the CNO nucleus lifetime against proton capture, so the β unstable nuclei can quickly decay without holding up the following nuclear reactions. At later stages in the development of a prenova, the temperature rises, the proton captures that precede and succeed β decays are more rapid, and a β decay bottleneck

can build up. The energy generation is proportional to the CNO initial abundance at this point, where the temperature is approximately 10^8 K, as new CNO nuclei are not created but only redistributed. We should also note that the time delay between the creation of the β unstable nuclei and their decay leads to the storage of energy, so energy can be released after the envelope has begun to expand (10^2 - 10^3 s after production of the β unstable nuclei). In fact, the calculations suggest that an overabundance of CNO is necessary for a fast nova outburst, i.e., mixing of CNO into the envelope from the interior occurs. This is perhaps the place where theory and observation of novae come closest, and where many would begin at least to suspect that they are not talking of completely different things.

According to present theory, the initial luminosity of the white dwarf has no influence on the amount of accreted mass, when it is low. Energy is then generated from the proton-proton chain for which secular evolution of the envelope is very slow. When the time scale for nuclear burning is larger than that for accretion, the rate of evolution of a prenova is determined by the rate of mass accretion. However, for a higher initial luminosity, nuclear burning is from CNO reactions and their time scale can be shorter, thus influencing the mass accreted before a thermonuclear runaway.

For a thermonuclear runaway to produce ejection, the material of the shell source must be electron degenerate. The kinetic temperature of the gas must rise and exceed the Fermi temperature before expansion can occur and cool the gas. The Fermi temperature is given by Starrfield et al. (1985) as equal to

$$T_F = 3 \times 10^7 \left(\frac{\rho_3}{\mu_E} \right)^{2/3}, \qquad (7.27)$$

with ρ_3 the density in units of 10^3 g cm^{-3} and μ_E the mean molecular weight multiplied by the ratio of the number of all particles to that of electrons. If the temperature is rising rapidly, expansion only begins to stop the temperature rise when the temperature is much larger than T_F. The calculations indicate that convection is present during evolution to the peak of the outburst. The convection turnover time scale is of the order of 10^2 s, and β unstable nuclei reach the surface before decaying. Fresh unburnt material is brought into the hot shell source by the convection, and the β unstable nuclei are the most abundant of the CNO nuclei at outburst peak.

Very many calculations of models have been carried out and will not be described here. Detailed calculations, for instance were carried out by Starrfield et al. (1978), Sparks et al. (1979), and by Starrfield et al. (1985, 1986). Realistic velocities and ejected masses were obtained; however, this is not sufficient to demonstrate the validity of these models. Their description of postoptical maximum development will be perhaps a more sensitive test of future models.

Up to now, calculations suggest an expansion of the white dwarf component after the initial explosion. This component should engulf its companion and radiate at a luminosity not far from the Eddington limit for quite a long time. Therefore, this type of theory appears to be most compatible with central star-dominant models describing postoptical maximum evolution. Such a central star could have a strong wind like more "normal" hot stars; however, as already described, novae generally appear not to be like this. Another effect can be expected if the secondary revolves inside an extended white dwarf. Gravitational stirring would take place with extra energy generation, and perhaps the total luminosity could then exceed the Eddington limit. This last situation has been discussed by MacDonald (1980) and MacDonald et al. (1985), but such calculations are still too simple. In particular, deviations from spherical symmetry need to be properly taken into account. It is in the framework of such considerations that there is a possibility of understanding the production of an optically thick wind at large optical depths. Future work may or may not confirm this.

Various developments of thermonuclear

runaway theory have occurred in the 1980s. The observed apparent overabundances of Ne, Mg, etc., for some novae have lead to a certain amount of work on this second class of nova outburst. Delbourgo-Salvador et al. (1985) and Starrfield et al. (1986) explain them by nova outbursts of O-Ne-Mg white dwarfs. Such white dwarfs are expected to have masses close to the Chandrasekhar limit, the lower limit to their masses being somewhat uncertain. Only a small proportion of white dwarf components (on the order of a few percent) should be of the O-Ne-Mg class. The calculations indicate, however, that nova outbursts would be more frequent, so as many as 20% of observed outbursts could be of this type. Material of the white dwarf, as for other types of novae, would be mixed into the envelope. These stars are expected to be more massive, leading to runaways with less accreted mass and so occurring more frequently.

V.B. NONSPHERICAL MODELS

Accretion is not spherically symmetric, and this lack of spherical symmetry should play a role in the development of a prenova. Kippenhahn and Thomas (1978) considered the formation of a rapidly rotating belt following accretion; its chemical composition and angular momentum are then mixed with the underlying white dwarf material. Marginal stability, with respect to the Richardson criterion for shear instability, was assumed to be maintained by mixing, the amount of mixing at a certain time depending on the position and depth inside the belt. Hydrogen would be eventually ignited at the bottom of the belt according to this scenario. Kutter and Sparks (1987) and Sparks and Kutter (1987) considered accretion of material possessing angular momentum with fewer assumptions than Kippenhahn and Thomas, but still including marginal instability against shear mixing. Various cases between radial accretion and material accreted having a full Keplerian orbital velocity were considered. Unfortunately,a 1 $M_{\odot}$ white dwarf did not produce nova-like mass ejection under these conditions. The authors explain this lack of success, compared with other types of model, to the support the centrifugal force gave to the accreted matter, diminishing pressure confinement and the strength of the runaway. Kutter and Sparks considered that other physical effects needed to be taken into account in later work.

Shaviv and Starrfield (1987) considered another aspect of deviation from spherical symmetry. The boundary layer between the accretion disk and the white dwarf can (and was also supposed to) cause heating—a nuclear burning region in the whole accreted envelope was produced, and the latter become completely convective. Unfortunately, "no dynamical effect occurred during the evolution." By adding another badly known parameter, the degree of heat flow inward from the boundary layer, the authors admit to "have complicated an already cloudy situation." It is clear that much work needs to be done.

V.C. OTHER EFFECTS AND HIBERNATION

Another feature of some models of the mid-1980s for classical novae also needs to be discussed. Some observational and statistical evidence suggests that novae "hibernate" during outbursts, i.e., that very old novae become very faint for millenia and brighten again before the following thermonuclear runaway. Such ideas were suggested by the accretion rates in old novae, deduced from their energy distribution, which appear to be too high for nova explosions, according to the simple model previously discussed. In addition very old novae appear to be fainter than more recent novae, while, at one time, the lack of X-ray sources expected for a large population of old novae was considered to be a problem.

Hibernation models have been reviewed by Livio (1987). It is supposed that, following a nova explosion, the separation of the binary increases. At first, the secondary continues to transfer mass because it is strongly irradiated. This mass transfer then strongly decreases because the secondary underfills its Roche lobe, allowing previously accreted material to

cool, diffuse, and become degenerate so that a strong thermonuclear runaway is possible at a later time. The separation of the binary however, is reduced by magnetic braking (if the period is above the cataclysmic binary period gap) and returns to its original value and a high mass accretion rate on a time scale

(7.28)

$$\tau = 5000 \left(\frac{f}{0.7} \right)^2 \left(\frac{r_g}{0.45} \right) \left(\frac{R_{WD}}{6 \times 10^8 \text{ cm}} \right)^4 M^{-4/3} P_4^{-0.06} \text{ yr.}$$

Here f is a parameter of the order of 0.7, and r_g is the gyration radius of the secondary. R_{wd} is the radius of the white dwarf in cm, M is the total mass of the system in $M_\odot$, and P_4 is the period in units of 4 hours. It is after such a time that the white dwarf resumes accretion to produce a new thermonuclear runaway. At stages when the mass transfer is still relatively low, dwarf nova outbursts should be possible if disk instability models are a valid explanation for them, so classical and dwarf novae would be the same objects. Livio (1987) indeed lists eight old classical novae with post outburst eruptions similar to those of dwarf novae.

According to Shara et al. (1986), the separation increase of the binary is due to the mass ejection in the nova explosion, and this effect is larger than that due to angular momentum loss produced by interaction of the revolving secondary with the mass ejected by the nova. This was supposed by the period increase observed for one nova (BT Mon); suitable data do not exist for other novae. Such a discussion clearly neglects the possibility of the white dwarf expansion and the engulfment of its companion.

The present situation concerning the relevance of hibernation models is not clear. Recent results may indicate a much smaller effect on the mass transfer than previously thought. If the atmosphere of the companion is isothermal due to irradiation by the white dwarf, a mass transfer decrease by a factor of the order of 10 - 100 can be expected, but if the atmosphere is convective, the decrease is at most by a factor of 2. In the former case of "mild hibernation," the mechanism still works (Livio 1988a). If there is no hibernation, it may be necessary to suppose the accretion rates deduced from the luminosities of old novae wrong; the white dwarf could be exceptionally bright before and after the explosion, and its radiation could be reprocessed by the accretion disk (Friedjung 1985, Livio 1988b).

If we consider thermonuclear runaway theories in general, some success has been achieved. As predicted, fast novae have overabundances in CNO, the overabundance being correlated with the speed of development of a nova. Even the CNO overabundances of the slow nova DQ Her can be explained by the exceptionally low mass of the white dwarf. Postmaximum activity is probably also compatible with such models, but detailed predictions do not exist. However, when one attempts to take account of other physical effects, difficulties are encountered. A theory that explains most observations is still far away. In any case, theoretical prejudices should not be used as a pretext for rejecting models based on observations.

Unlike with other types of variable stars, the determination of the space density of novae is extremely difficult to determine, since year after year, new nova explosions are discovered. Thus, a straightforward density of observed novae that showed outbursts would be an ever increasing function of time. A parameter that can more easily be determined is the space/time density ρ^*, that is the number of nova explosions per cubic parsec per year. A determination of this parameter, as well as the scale height of the nova distribution in the Galaxy, is given by Duerbeck (1984).

To derive the true space density ρ, the mean time interval $\Delta\tau$ between two nova outbursts must be known. This value is extremely uncertain, and the only safe statement is that it is obviously larger than 100 years for classical novae.

If we assume that the nova state is a steady one, with the matter ejected during outburst being equal to the mass accreted between out-

bursts, values of $\Delta\tau$ between 1,000 and 10,000 years are derived for the observed shell masses and accretion rates. However, Prialnik (1986) and Kato (1988) have argued from calculations of nova outbursts that a secular loss of matter from the white dwarf that undergoes nova explosions takes place, thus shortening the interval between explosions. On the other hand, theoretical arguments for orbit changes during outbursts, the impossibility of TNRs under highly degenerate conditions at the accretion rates observed, and observational findings from the (unfortunately few) very old novae lead to the suspicion that mass transfer rates may diminish noticeably or may even cease. Thus, for a shorter or longer time between outbursts, the exnova transforms into a cataclysmic binary with possible disk instabilities (i.e., a dwarf nova), or even in a detached system, consisting only of the red dwarf and the white dwarf, with the accretion disk completely absent. Such systems would appear as red dwarfs with UV excess (possibly eclipsing) and rapid rotation, properties that are not obvious in low-dispersion spectral surveys. Such a decrease in mass transfer rate would increase the outburst interval.

Taking a mean outburst interval (without hibernation) to be 3,000 years, a space density of

$$\rho_0 = 1.27 \cdot 10^{-6} \text{ pc}^{-3} \qquad (7.29)$$

is derived for classical novae, which can be compared to that of dwarf novae, 0.95×10^{-6} pc^{-3}, and symbiotic stars, 0.00094×10^{-6} pc^{-3}, the scale height of the latter however, being very different from the first two groups.

If these assumptions are correct, one should find, if the nova brightness between outbursts stays at V = +4.2, 6×10^{-2} objects in the bright star catalogue (brighter 6^m), 5 - 6 objects in the Durchmusterung catalogues (brighter 9.5^m), and 36 objects brighter than 11^m. While there are some 'novalikes' in the brightness range of 9^m - 11^m their number and type makes them not too well suited for nova candidates.

However, the hibernation scenario is not a good scenario out of the dilemma. Decreasing the accretion rate means decreasing the absolute magnitude, thus decreasing the volume of space where the objects are found. On the other hand, a lower accretion rate means that the intervals become longer, and the space density of the objects must be increased to result in the same—observed—outburst density ρ^*.

V.D. CAUSES OF RECURRENT NOVA OUTBURSTS

Recurrent novae to a certain extent are intermediate between classical and dwarf novae. Indeed, there has sometimes been a certain amount of confusion about whether a particular star is a recurrent nova or a dwarf nova. To clearly make the distinction, Webbink et al. (1987) consider that a recurrent nova has two or more recorded outbursts with a maximum absolute magnitude comparable to that of a classical nova ($M_V \leq -5.5$) and ejection of a discrete shell in outburst with an expansion velocity of ≥ 300 km s^{-1}. These criteria also distinguish recurrent novae from various types of symbiotic stars. Even with such criteria, recurrent novae seem to be rather heterogeneous; the outbursts of some are now explained by theories similar to those for classical novae, while the outbursts of others are explained by theories bearing some resemblance to those of dwarf novae.

If we try to invoke a mechanism similar to that for classical novae, i.e., involving a thermonuclear runaway, rather stringent conditions need to be fulfilled. One can see from equation (7.26) that the pressure at the core interface is inversely proportional to the fourth power of the radius of the white dwarf; this will increase very rapidly near the Chandrasekhar limit, where the white dwarf radius becomes very small. Hence, a runaway will be produced for a relatively small amount of accreted mass, so if the accretion rate is supposed not to change very much, much shorter recurrence times are possible near the Chandrasekhar limit. In this way, short recurrence times are possible without the accretion rate becoming too high, to produce a strong outburst.

An increase of the white dwarf luminosity also leads to shorter recurrence times. Starrfield et al. (1985) for a limiting mass of 1.38 $M_\odot$, a luminosity of 0.1 $L_\odot$ and an accretion rate of 1.7 x 10^{-8} $M_\odot$ yr^{-1}, were able, to obtain a recurrence time of only 33 years. A rather high accretion rate would lead to a high accretion disk luminosity, detectable between outbursts, supposing naturally that accretion proceeds via a disk, Webbink et al. (1987) give for a 1.38 $M_\odot$ white dwarf:

(7.30)

$$\frac{L_{bol}}{L_\odot} \approx \frac{GM_{WD}\dot{M}}{R_{WD}} \approx \frac{160(M_{WD}/1.38\,M_{WD})}{R_{WD}/1.9\cdot10^{8}\,cm} \frac{\dot{M}}{10^{-8}M_\odot/yr},$$

with $\dot{M}$ the accretion rate, L the stellar luminosity, M_{WD} the stellar mass and R_{WD} the stellar radius.

As in the case of dwarf novae, recurrent novae, in principle, can, also be produced by accretion events. Such events might be powered by an instability of the cool component, or by a disk instability, or they might occur at periastron if the companion had an eccentric orbit. In the last case, the eccentricity must exceed the ratio of the pressure scale height near the inner Lagrangian point at periastron to the radius of the star losing mass by Roche lobe overflow. It can be noted that when accretion events occur, unlike in a thermonuclear runaway, the accretor need not be a white dwarf with a mass below the Chandrasekhar limit. It can be a main sequence star, as is indeed indicated by the most probable compact star mass above the Chandrasekhar limit for T CrB (see Chapter 9 of this volume).

Different accretion event mechanisms for recurrent novae can be examined in more detail as was done by Livio (1988). According to him, the accretion rate $\dot{M}$ must obey the condition for disk instability to occur:

$$\dot{M} \geq 3\cdot10^{-9}\left(\frac{P_4}{4}\right)^{1.8} M_\odot\ yr^{-1}, \qquad (7.31)$$

with P_4 the period in units of 4 hours. So for a period of 230 days (T CrB, RS Oph), $\dot{M} \leq 10^{-6}$ $M_\odot$ yr^{-1}. Disk instability models, however, may run into recurrence time problems; to obtain times of the order of those observed, a viscosity parameter α of the order of 10^{-1} is required (for the cold state of the disk).

A more relevant accretion event mechanism according to Webbink et al. (1987) and Livio (1988a) for some recurrent novae involves a sudden instability of the cool component with ejection of 10^{-3} to 10^{-4} $M_\odot$. This mechanism is supposed to be particularly relevant for T CrB and RS Oph, and according to Edwards and Pringle (1987) to be possible for Roche lobe filling giants. The collision of the ejected material with itself, with the cool giant wind, or with the accreting star can be associated with high-velocity shock ejection, when no well-developed accretion disk exists before the event. According to Livio et al. (1986), the shock velocity is given by

(7.32)

$$V_{shock} = \left(\frac{2\,GM}{R}\right)\left(\frac{\rho_{circum}}{\rho_{stream}}\right)^{-\left[2+\left(2\gamma/(\gamma-1)^{0.5}\right)^{-1}\right]}$$

The first factor, giving the free fall velocity from zero at distance R from a star of mass M, is multiplied by the second factor, including the ratio of the density of circumstellar material ρ_{circum} to that of the stream of accreted material ρ_{stream}, which collides with it. As usually, γ is the ratio of specific heats, and G, the gravitational constant. Therefore, the highest shock velocity occurs if the stream collides with very low-density material in the vicinity of the accreting star. The accreted material can then form a temporary bright disk (whose absence before outburst would pose a problem for thermonuclear runaway models), explaining the secondary maximum of T CrB, or it can easily collide with the accreting star if it is bloated, following considerable accretion at a high rate (suggested for RS Oph). It should be noted that 10^{-4} of the accreted material (according to the low envelope mass estimate of Bode and Kahn (1985) for RS Oph) needs to be ejected at a velocity of 10 times the free fall ve-

locity of RS Oph (of the model of Livio et al., 1986, with R equal to 8.2 x 10^{11} cm), so then requiring only a high efficiency for the conversion of the kinetic energy of the accreted material of the order of 10^{-2}. This type of mechanism clearly needs to be studied in more detail.

Webbink et al. (1987) support thermonuclear runaway models for T Pyx and U Sco. The former, to some extent, resembles a classical slow nova. The presence of bright accretion disks, characteristic as an accretion rate preceding a thermonuclear runaway, is compatible with observations for both these recurrent novae, though Webbink et al., suggest that most of the quiescent luminosity of T Pyx has another source (continuing nuclear burning?). In a later paper, however, Truran et al. (1988) are not so certain about U Sco; observations appear to indicate a high He/H ratio for which it is difficult to produce a nova-like outburst following a thermonuclear runaway. These authors suggest that a high helium abundance could favor an accretion disk instability even for a hot accretion disk.

One can conclude that models for recurrent novae need to be compared with results for individual stars. The situation for recurrent novae is not clear; one may wonder whether other possible mechanisms for outbursts have not been neglected. One tends to gather the impression that at a give time, theorists are too certain about their mechanisms.

N95
27074
UNCLAS

N95- 27074

8

TYPICAL EXAMPLES OF CLASSICAL NOVAE

M. Hack, P. L. Selvelli, A. Bianchini, H. Duerbeck

I. INTRODUCTION

Because of the very complicated individualistic behavior of each nova, we think it necessary to review the observations of a few well-observed individuals. We have selected a few objects of different speed classes, which have been extensively observed.

They are:

V1500 Cygni 1975, very fast nova. t_3 = 3.6 d.
Range of the light curve Δm = 2.2 B-21.5p; light curve of Duerbeck type A (smooth, fast decline without major disturbances).
Quiescence: It presents short period variations.
Characteristics: Large outburst amplitude.

V603 Aql 1918, fast nova. t_3 = 8 d.
Δm = −1.1V-12.0V; light curve type Ao (smooth, fast decline without major disturbances, oscillations in the transition stage).
Spectroscopic binary P = 0.13854 d; eclipsing binary?

CP Pup 1942, fast nova. t_3 = 8 d.
Δm = 0.5V-15.0V; light curve type A.
Spectroscopic binary with P=0.061429 d; light variations with P = 0.06196 d.
Characteristics: It has the shortest binary period among novae; slightly different spectroscopic and photometric periods.

GK Per 1901, fast nova. t_3 = 13d.
Δm = 0.2V-11.8...14.0V; light curve type Ao.
Spectroscopic binary, P =1.996803 d.
Characteristics: Many unusual characteristics; minor outbursts at quiescence; it has the longest orbital period among novae.

V 1668 Cyg 1978, moderately fast nova. t_3 = 23 d.
Δm = 6.7p- 20.0p; light curve type Ba (decline with standstills or other minor fluctuations).
Quiescence: It shows short period variations.

FH Ser 1970, slow nova. t_3 = 62 d.
Δm = 4.5V- 16.2p; light curve type Cb (strong brightness decline before the onset of the transition minimum).
Characteristics: Dust formation; the bolometric magnitude remains constant for a period much longer than the optical one.

DQ Her 1934, slow nova. t_3 =94 d.
Δm = 1.3V -14.5V (var); light curve type Ca (small variation of visual brightness at maximum).
Spectroscopic and eclipsing binary with P = 0.193621 d
Characteristics: Pronounced dust formation; unusual occurrence of molecular lines in premaximum spectrum.

T Aur 1891, slow nova.t_3 = 100 d.
Δm 4.2p-15.2p; light curve type Ca.
Characteristics: Great similarity with DQ Her.

RR Pic 1925, slow nova. t_3 = 150 d.
Δm = 1.0V-11.9p; light curve type D (slow development, extended premaximum, maximum often with several brightness peaks).
Characteristics: Spectroscopic binary, P = 0.1450255d.
Light variations with the same period: eclipses shallow or absent.

HR Del 1967, very slow nova. t_3 = 230 d.
Δm = 3.5 V-12.0 V; light curve type D.
Spectroscopic binary, P = 0.2141674.
Characteristics: Extremely slow nova, with no appreciable formation of dust.

A catalogue of all observed novae, from the two oldest ones, CK Vul 1670 and WY Sge 1783 to Nova Cyg 1986, has been prepared by Duerbeck (1987c). For most objects, brightness ranges, accurate positions, finding charts, and bibliographies on light curves, spectroscopy, UV, IR, radio observations, nebular shells variability in quiescence and evidences for duplicity are given.

II. V1500 CYGNI 1975: A VERY FAST NOVA

(written by Hack)

It was discovered on August 29, 1975, and it is one of the most extensively observed novae. A large number of spectroscopic and photometric observations are collected in the issue of the Astron. Zh.54, May-June 1977 (Sov. Astron. 21, No.3). At maximum brightness, reached on August 30, V was equal to 1.7. Nova Cyg 1975 is peculiar for several reasons: a) It is an extremely fast nova, with t_3 = 3.9 days, t_7 = 45 days (Figure 8.1). b) It presented a very large light amplitude, V = 19 mag, with an absolute visual magnitude at maximum of about -10 (as derived by Becker and Duerbeck, 1980, from its nebular expansion parallax), which makes it the brightest of all galactic and extragalactic novae ever observed, with the exception of CP Pup, which reached M_v = -11.5 (Duerbeck and Seitter, 1979). Generally, novae at maximum are less bright than M_V = -8.5. The amplitudes of the outburst of both V1500 Cyg and CP Pup are more typical of supernovae than novae; however, their expansional velocities have the typical values of very fast novae. c) The absolute magnitude of V1500 Cyg at minimum before outburst was about +9 or fainter, which makes it similar to the U Gem stars, while the majority of novae are about 5 mag brighter. This value of M_V at minimum was deduced from the fact that superposition of the blue Palomar survey with the field of V1500 Cyg (Beardsley et al., 1975) indicates no star brighter than mag 21 on the print. However, the outburst started when the star was 5 mag brighter than the normal prenova luminosity. This increase in luminosity was observed on August 5, 1975. The color, during the pre outburst phase was B-V = 1.3 and V-R = 2.5, suggesting a color temperature of about 4,000 K, i.e., a K- or M-type star. d) At maximum, the spectral type was B2 Ia, the earliest spectral type ever observed for novae. e) The absorption spectrum shows broad diffuse bands; the two systems, diffuse-enhanced and orion, were not evident.

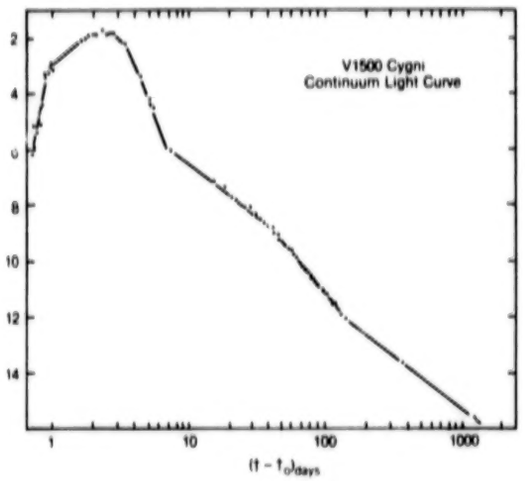


Figure 8-1. V 1500 Cygni: continuum light curve. (from Ferland et al., 1986)

In fact, the diffuse-enhanced spectrum appeared at 0.3 days after optical maximum with an expansion velocity of -3,850 km/s; it

reached its greatest strength 0.9 days later and lasted slightly more than 1 day as an absorption feature. For this reason, many observers have not detected it (Ferland, 1977a). Also, the high value of the Doppler broadening can make the detection of the various components difficult, blending them together.

The penetration of the principal shell by the diffuse—enhanced occurred without any noticeable interaction, because the principal spectrum did not show any appreciable variation. The interpretation may be that the great majority of the material was expelled in one explosive event almost instantaneously. f) The expansional velocity of the principal spectrum was very high, much higher than in normal novae (Boyarchuk et al., 1977), as indicated below:

August 29: absorption expansional velocity V = -1300 km/s,
Total (Emission + Absorption) Doppler broadening ΔV =2200 km/s
August 30: V = -1700 km/s, ΔV = 4000 km/s.
August 31: V = -2200 km/s, ΔV =6100 km/s.

II.A. MASS LOST IN THE OUTBURST

A lower limit of the mass ejected in the outburst has been computed by Wolf (1977). From the equivalent widths of the Balmer absorption lines, the column density $n_{02}\ \Delta r$ (*) is computed, and from the observed temperature at maximum, by assuming a plausible value of the electron density, one gets $n_1\ \Delta r = 4.2 \times 10^{23}$ cm^{-2} using the Boltzmann and Saha equations.

From $n_1\ \Delta r$ and $N_e \approx n_1$, a value of $\Delta r = 4.2 \times 10^{13}$ cm = 600 solar radii is derived. Hence, the mass lost in the outburst is given by $\Delta m = 4\pi(\Delta r)^2 \Delta r n_1\ m_H = 1.5 \times 10^{28}$ g $= 10^{-5}\ m_\odot$. As we shall see later, infrared observations by Gallagher and Ney (1976) and by Ennis et al. (1977) estimate $10^{-5}\ m_\odot < \Delta m < 10^{-3}\ m_\odot$. From this value of the mass lost in the outburst and the expansional velocity, it follows that the kinetic energy liberated in the explosion is $E_{kin} \geq 10.^{28}$ g x $(2 \times 10^8$ cm/s$)^2 = 4 \times 10^{44}$ erg comparable to the energy radiated away, $E_{rad} \approx 10^{45}$ erg.

(*) $W\lambda = \frac{\lambda \pi e^2}{mc^2} f n_{02}\ \Delta r$ valid for an optically thin layer (Doppler branch of the curve of growth).

II.B. SPECTRAL VARIATIONS

The spectral variations were as follows: August 29 B2Ia+, T (pseudo-photosphere = T continuum) $\simeq$ 30,000 K,T(envelope) $\simeq$ 20,000 K. August 30-31 A2Ia+. The lines show P Cyg profiles with faint emission wings; the latter increase fast in intensity.

September 1, almost all the absorption features have disappeared. From September 1 to September 10, metallic emission lines appear first and He I, He II, N III, plus several forbidden lines later on. The nebular stage was reached 9 days after maximum (Figure 8-2). From September 2, 1975, to January 5, 1976, the Balmer emission lines present several peaks at almost constant velocity: -1050, -580, +150 + 600 km/s. A similar behavior is shown also by the O I 8446 A permitted line and 6300 A forbidden line. The four peaks have a different relative intensity and they are not all observable in the high excitation lines of [Fe X], Fe XI], and [S VIII] (Figure 8-3, 8-4, and 8-5). High dispersion spectra of the photographic range have been obtained from September 2 to October 2 by Sanyal and Willson (1980). Rush and Thompson (1977) have made spectrophotometric observations with time resolution of 3-15 minutes. All the hydrogen lines observed from September 7 to 11 show that the relative intensity of the four peaks change simultaneously in each Balmer line on a time scale of 5 minutes. Following a model suggested by Weaver (1974) for V603 Aql, they assume that four blobs of matter were ejected simultaneously in two opposite directions, two at higher velocities and two at lower velocities. Since each peak is produced in a separate blob, a sudden change in the radiation from the stellar pseudophotosphere will produce a change in the ionization of the hydrogen in the blob.

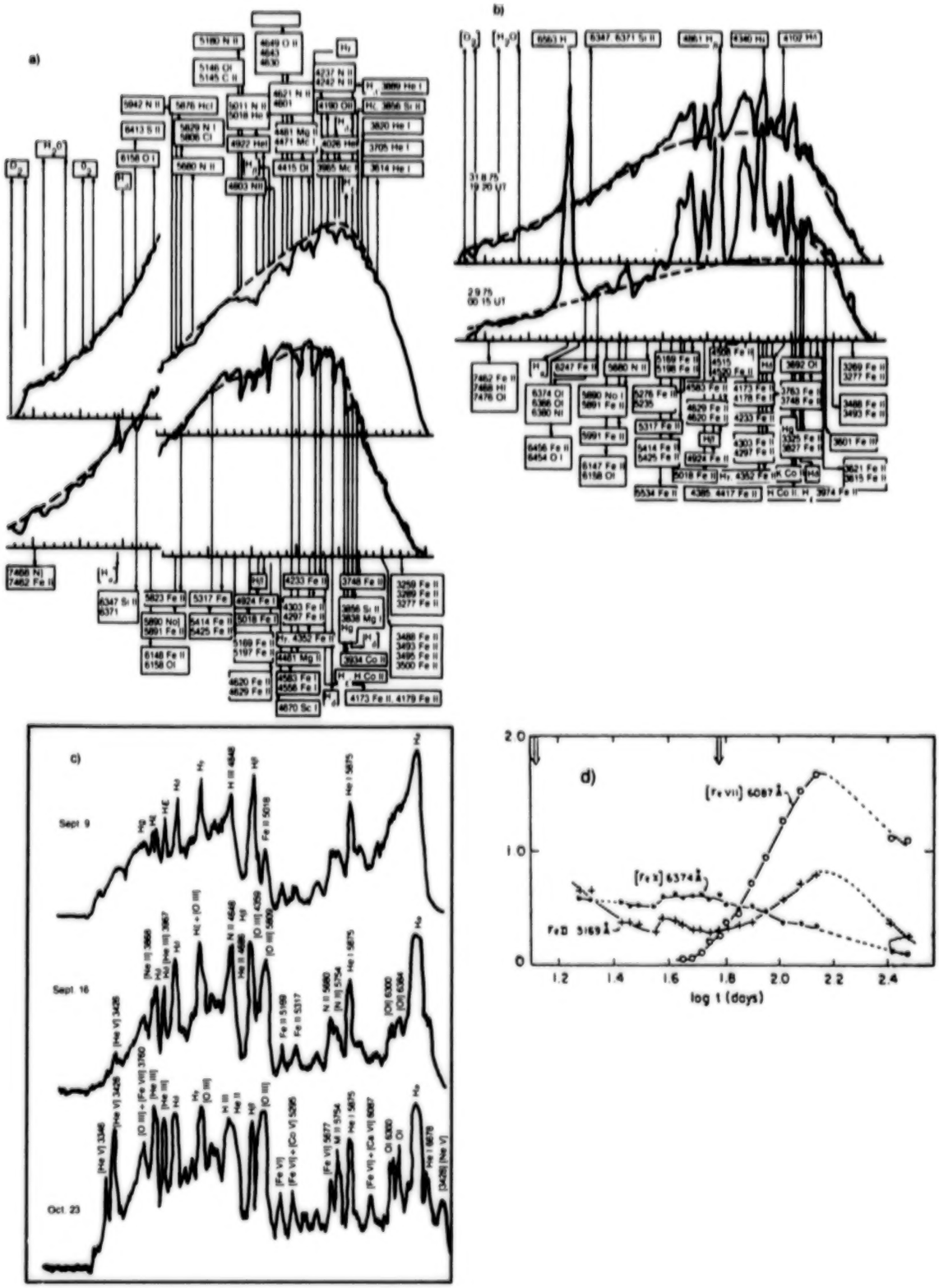


Figure 8-2. The spectrum of V 1500 Cyg: a) August 29 and 30: the absorption lines dominate the spectrum. P Cyg profiles appear on August 30; b) August 31 and September 2: the emission lines dominate the spectrum (from Voloshina and Doroshenko, 1977); c) The spectrum from the beginning of September to the end of October (from Rosino and Tempesti, 1977); d) Line intensity variation with time after maximum light (from Ferland et al., 1977).

ORIGINAL PAGE IS
OF POOR QUALITY

However, the assumption that all the blobs are ejected toward and away from the observer in the direction of the line of sight seems not very plausible. It seems more plausible to assume that the blobs are ejected in several directions at about the same velocity and that the observed differences in radial velocity are rather due to projection effects.

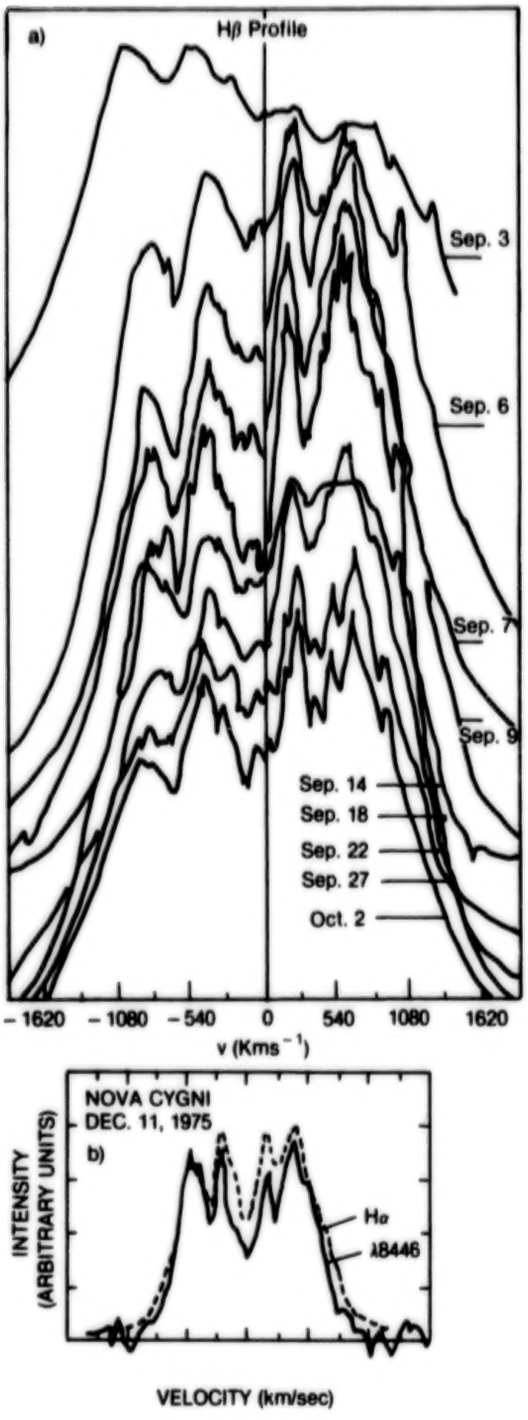


Figure 8-3a. Line profiles of Hβ at different epochs (from Sanyal and Willson, 1980). b) Line profiles of Hα and O I 8446 (from Strittmatter et al., 1977).

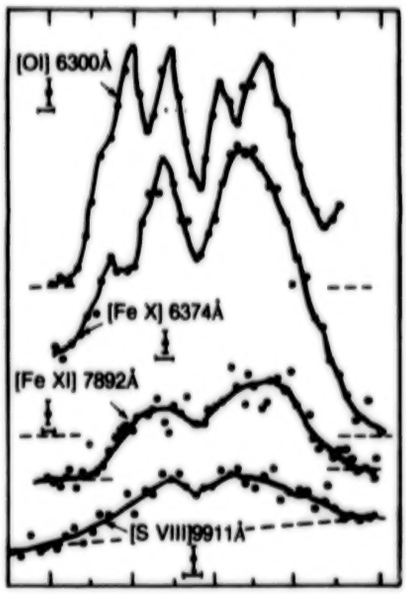


Figure 8-4. Line profiles for [OI] 6300 (Oct. 9), [Fe X] (Oct. 5 and 9), [Fe XI] 7892 (Oct. 2, 5 and 9), [S VIII] 9911 (Oct. 5, 9, 12, 15, 19, 27 and Nov. 7) (from Ferland et al. 1977).

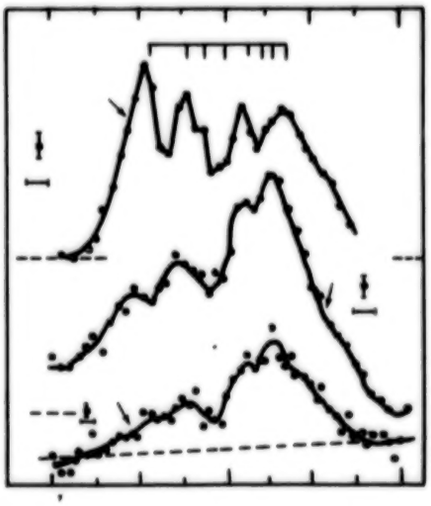


Figure 8-5. Line profiles for [OI] 6300 (Oct. 9), [FeX] (Oct. 5, 19, 23, and 27), [Fe XI] (Oct. 15, 19, 23 and 27) (from Ferland et al. 1977).

II.C. PERIODIC LIGHT AND RADIAL VELOCITY VARIABILITY

V1500 Cyg has shown periodic light variability with a period of 3.3 hours since early postmaximum (Hutchings, 1979b). The amplitude has remained in the range 0.15-0.5 mag, while the mean brightness was changing by a factor of 60,000 (about 12 mag). As we have seen in Chapter 6, the period decreased by 2% during the first year from outburst and then increased slightly and then stabilized. Flickering with time scale of 100 s was observed, i.e., a behavior typical of cataclysmic variables (Figure 8-6). Ultraviolet observations made with the photometric Astronomical Netherland Satellite (ANS) confirm the light variability with P = 0.14 days (Wu and Kester, 1977).

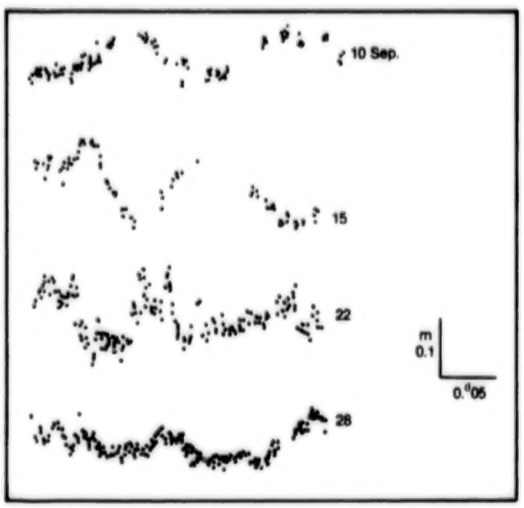


Figure 8-6. Blue light curves of V 1500 Cyg observed in Sep. 1975. The light curves are not aligned by time or by phase.
(from Ambruster et al. 1977).

Spectra taken in 1977 (Hutchings, 1979b) show the characteristic nebular emisssion lines of [O III] 4959 + 5007 and 4363, [Ne III] at 3868 and 3967 and, in addition, several permitted emissions of H I, He II, N III. The permitted lines, and especially 4686 He II, present radial velocity variations with a period of 3.3 hours like the photometric period and semiamplitude K of 350 km/s. Such a large value of K in a simple binary model would imply a large value of the mass function, and therefore—for reasonable values of the mass ratio—of the masses, which is not in agreement with the typical low masses of novae. Moreover, the Balmer lines present a different radial velocity variation than 4686 He II. These observations, therefore, suggest that they do not represent an orbital motion only, but rather stream motions or a combination of the two. A mass function consistent with the expected masses would give K = 150 km/s. Hence, the line emissions appear to originate in fast-moving streams and confirm the binary nature of the object but do not reveal anything about the orbital parameters. This is a problem common to several classes of close binaries, where streams, accretion disk, and envelopes surrounding the whole system, produce their own spectra with their own peculiar motions superposed on the orbital motions.

The system appears to have a mean radial velocity about 400 km/s more positive than the mean velocity of the nebular lines, which, therefore, indicate that the region where they are formed is an expanding envelope.

A model for explaining the behavior of the binary V1500 Cyg has been proposed by Hutchings (1979b). He suggests that the light variations can be linked to the disk, which is probably the most luminous element of the system, and the period changes may be linked to a precession of the bright and dark side of the accretion disk, partly due to nonsynchronous rotation of the white dwarf after the nova outburst. In fact, the irregularity of the light curve suggests that an eclipse of the white dwarf from the companion is not the most plausible hypothesis.

II.D. ULTRAVIOLET OBSERVATIONS

As we have seen in Chapter 6, V1500 Cyg was observed with the ultraviolet satellites ANS and Copernicus. The channels at 1800, 2200, and 2500 A of ANS are free from strong emissions, and the continuum radiation from the nova shell is negligible. Hence, the continuum of the hot nova remnant could be observed and the interstellar reddening estimated from the dip at 2200 A. A color excess E(B-V) = 0.69

has been found, nearly equal to that determined for 55 Cyg, which is nearby V1500 Cyg. From a comparision of the intensity of the emission lines of the Balmer and Paschen series, Ferland (1977b) found E(B-V) = 0.50 +/- 0.05 consistent with the strength of the interstellar lines. This value gives a distance of 1.95 kpc +/-0.02 kpc, higher than the value of 1.35 kpc given by the nebular expansion parallax. The latter is probably more reliable, because methods based on the interstellar extinction and interstellar lines are affected from the irregular distribution of the dust and gas in the interstellar medium.

Copernicus observations, at a spectral resolution of 0.4 A, were made from September 1 to September 9 (Jenkins et al., 1977). The spectrum was not detectable at $\lambda < 2700$ A. Broad Mg II emissions were observed. After the 9th, the nova was no longer detectable with Copernicus. These authors discuss the absence of measurable ultraviolet radiation at shorter wavelengths: it suggests that the Mg II lines are formed by collisional excitation in the outer layers of the shell at $T \simeq 4{,}000$ K, and the absence of emission lines of the abundant multiionized atoms indicate that the material at temperature between 25,000 and 50,000 K is less than 0.001 that producing the Mg II emission. They point out also that it is strange that no emission was observable as λ 1302 A, corresponding to the O I resonance line, while 8446 O I is a strong emission line. In fact, both these lines are explained with Ly Beta fluorescence: Ly Beta emission (1025.72 A, upper E.P. level 12.04 eV) overpopulates the upper level of 1025.72 O I (upper E.P. level 12.03 eV), and from that level $3d^3\ D^0$ a cascade down to $3p^3$ P and then to $3s^3\ S^0$ explains the emissions at 11287 A and at 8446 A; then a cascade down to $2p^4\ ^3p$ will produce the 1302 A emission. Now from the infrared observations of Gallagher and Ney (1976) and from the ultraviolet spectroscopic observations of Jenkins et al. (1977), one derives that the flux at the Earth of λ 8446 is of about 4×10^3 photons $cm^{-2}\ s^{-1}$, while the upper limit for λ 1302, after correction for the interstellar extinction is less than 31 photons $cm^{-2}\ s^{-1}$.

These two fluxes are irreconcilable. From the average luminosity of the central remnant of novae Strittmatter et al. (1977) estimated the number of ionizing photons emitted by the central source of V1500 Cyg and the optical depth of Ly Alpha. This is so high that a random walk of photons in the nebula will be accomplished in a time long compared with the age of the nova. For this reason, no strong Ly Alpha emission is expected, in agreement with Copernicus observations. For the same reason, one also expects that the optical depth at 1302 O I is high enough for the 1302 photons to have an escape time that is long compared with the age of the nova at the time of Copernicus observations, therefore explaining why this emission was not observable.

II.E. INFRARED OBSERVATIONS

Observations at 2 μm (Ennis et al., 1977) show that the Brackett Gamma line changes from absorption to emission about 5 days after maximum. It is in absorption when the 1-20 μm continuum is that of a black body and changes to emission when the continuum becomes that typical of free-free radiation.

Starting on September 16, several coronal lines were detected: [Fe X] 6374, [Fe XI] 7892 and [S VIII] 9911 are present from late September 1975 to January 1976; [Fe XIV] was not observed (Ferland et al., 1977) Hence, according to them, the temperature was placed between 10^6 and less than 2×10^6 K. As the coronal lines became fainter, the [Fe VII] 6087 strenghtened, indicating $T \simeq 2 \times 10^5$ K. O I and H Alpha are clearly formed in the same region of the envelope as indicated by the strict similarity of the profiles (see Figure 8.3) while the forbidden lines of multiionized iron have different profiles and must be formed in different layers (see Figure 8.4 and 8.5).

As we have seen in Chapter 6, the infrared light curves of V1500 Cyg indicate that the energy distribution until 3.2 days after outburst

is that typical of a blackbody with T varying from 10^4 to about 5,000 K. Later, the energy distribution curve changes gradually from that typical of a blackbody (approximated in the infrared by the Rayleigh-Jeans relation $F_\nu \propto \nu^2$) to that typical of free-free radiation ($F \sim$ constant). Figure 8-7 gives the flux at the Earth of Nova Cyg 1975 and, for comparison, the flux of Alpha Cyg.

The spectral energy distribution from near UV (as measured by Copernicus) to IR on September 2 is shown in Figure 8-8. The position of the maximum at about 0.8 μm indicates a color temperature of about 4,000 K.

The maximum in the light curve is reached at progressively later epochs with increasing wavelengths, according to the empirical relation Fmax = 31.31 August 1975 (UT) + 0.681 λ (μm).

During the phases of the thick shell, it is possible to estimate the distance of the nova by the following considerations (Gallagher and Ney, 1976): the flux at the Earth F_λ is known directly from the observations; the flux B_λ emitted per surface unit by the shell is found by fitting the observed energy curve with the planckian curve for the corresponding temperature. Hence, it follows: $F_\lambda = \theta^2 B_\lambda$ with θ angular radius of the shell. Now $\theta = R/d$, $d\theta/dt = (1/d)\, dR/dt = v/d$, where R is the linear radius of the shell, d is the distance of the nova, and v, the expansional velocity of the shell. The observations give θ, dθ/dt, and v; hence, the distance d can be derived. Since the expansional velocities range from 1300 to 2500 km/s, it is found 1.2 kpc < d < 2.3 kpc (i.e., a value including that derived by the nebular expansion as well as that derived from the 2200 dip—see Chapter 8, Sections II.D and II.G. Figure 8-9 gives the values of T and θ and the absolute magnitude computed for a distance of 1.5 kpc. At 3.2 days after outburst, when the shell is still optically thick and fits the blackbody curve for T = 5,000 K from 0.5 to 5 μm, the radius (for a distance of 1.5 kpc) is equal to 3 AU and the area of the shell is 3×10^{28} cm^2. If σ is the mass above each cm^2 of photosphere, since the shell is optically thick, but just about to become optically thin, it

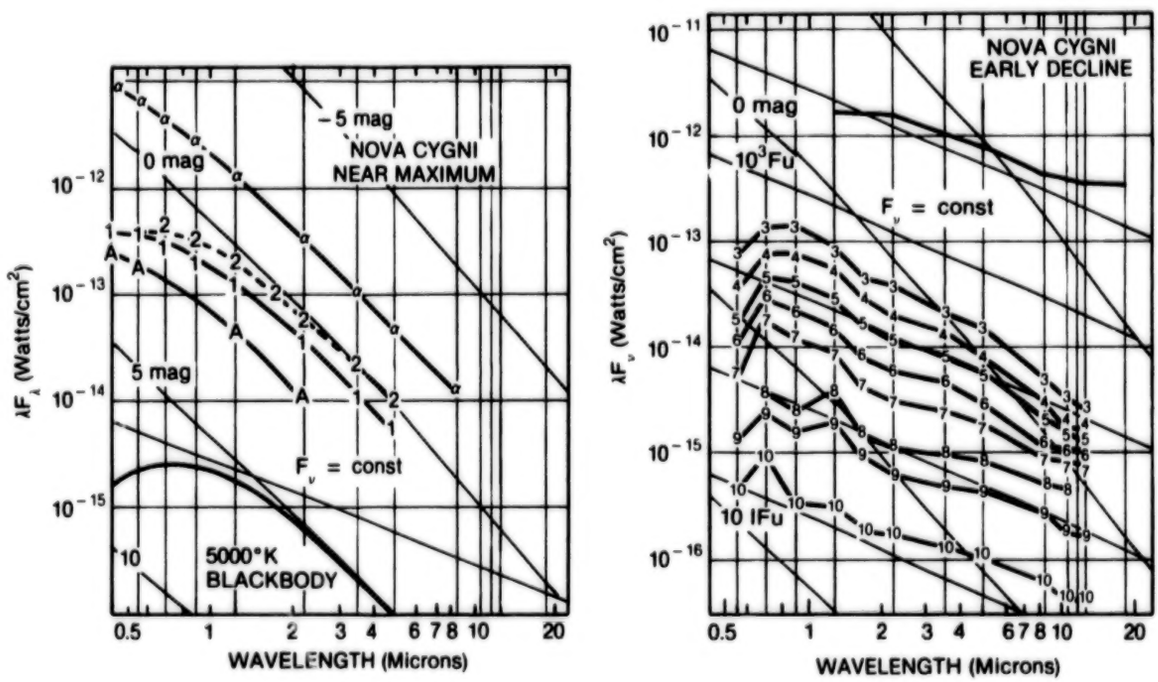


Figure 8-7. Energy spectra for V 1500 Cyg near maximum and during early decline. A:Aug. 29.8; 1:Aug.30.3; 2:Sep.1.1; α:α Cygni shifted by -2.5 mag; 3:Sep.2.0; 4:Sep. 2.4; 5:Sep.4.0; 6:Sep.6.1.; 7:Sep.9.1; 8:Sep.16.2; 9:Sep.24-25; 10:Oct.18-21. The transition from Black Body to free-free radiation is evident by comparing spectra no. 3 and No. 5. (from Gallagher et al. 1976).

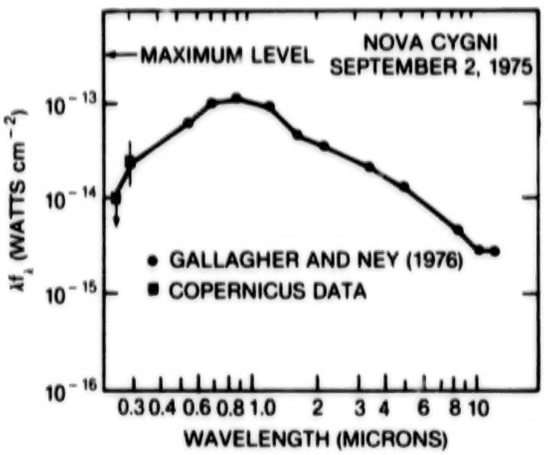


Figure 8-8. Spectral energy distribution for V 1500 Cyg measured on Sep. 2, 1975.
(from Jenkins et al., 1977).

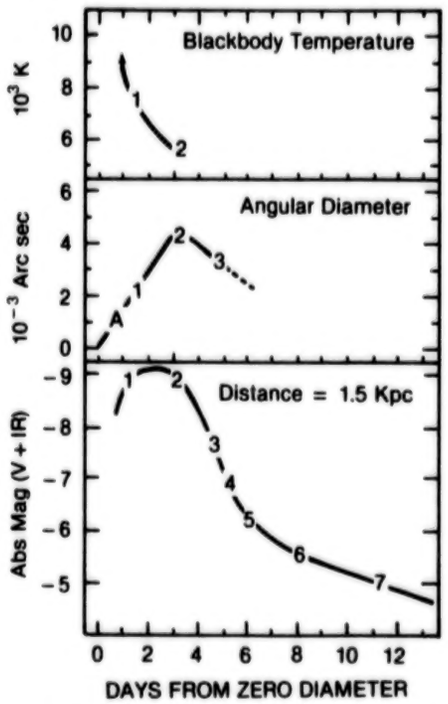


Figure 8-9. Black body temperature and angular diameter versus day from the zero expansion date (Aug. 28.9) and corresponding absolute magnitude (V+IR) for d= 1.5 kpc.
(from Gallagher et al., 1976).

is reasonable to assume $\tau = \kappa\sigma \approx 1$. Hence, the mass of the ejected shell is about $3 \times 10^{28} \times (\tau/\kappa)$. For temperatures of about 5,000 K and density of the order of 10^9 cm^{-3}, $k \simeq 0.01$. If the gas in the outer parts of the shell becomes ionized, then $k \simeq 2$. Hence, the two limits for the mass of the ejected shell are obtained: 1.5×10^{28} g $< m < 3 \times 10^{30}$ g; the lower limit is in good agreement with the value derived by Wolf (1977) from the Balmer lines.

By combining all the available observations in the different spectral ranges at different epochs it is found that the luminosity of V1500 Cyg passed from 5×10^5 $L_\odot$ at maximum to 3×10^4 $L_\odot$ 100 days later. These values give a bolometric amplitude $\Delta m_{bol} = 3.05$ against a visual amplitude $\Delta m_v = 7.5$. Figure 8-10 gives the infrared light curves. The infrared energy distribution from August 30 to October 15 is shown in Figure 6.27c.

Although V1500 Cyg is generally considered a dustless nova, it shows a slight IR excess at 10 μm about 100 days after outburst. An excess is detectable also at 3.5 μm (Ennis et al., 1977; Szkody, 1977; Tempesti, 1979).

According to Bode and Evans (1985), this excess is consistent with the heating of dust close to the nova during the eruption. No significant excess is observed for $t < 120$ days. Between days 200 and 400, the excess increases monotonically. The dust temperature is of the order of 200 K. A previous interpretation of the IR excess at 10 μm was given by Ferland and Schields (1978a) who attributed it to a [Ne II] emission at 12.8 μm; in this case, however, the excess at lower wavelengths is not explained. A summary of all the observations made at the McDonald Observatory since the outburst through one year later is given by Ferland et al. (1986) (see Figure 6.14). They found that the remnant became a dominant contributor to the optical continuum only one year after outburst, while it was detectable in the ultraviolet, with the Astronomical Netherland satellite (ANS) by day 100 (Wu and Kester, 1977). Both the UV continuum on day 100 and the optical continuum on day 368 fit the same Rayleigh-Jeans tail ($F_\nu \propto \nu^2$) indicating: a) that the underlaying hot body radiates like a blackbody at $T > 10^5$, and b) that the hot body maintained almost constant luminosity and energy distribution for at least 268 days. The continuum emission in the optical and infrared, on the contrary, shows a flat distribution ($F \approx$ con-

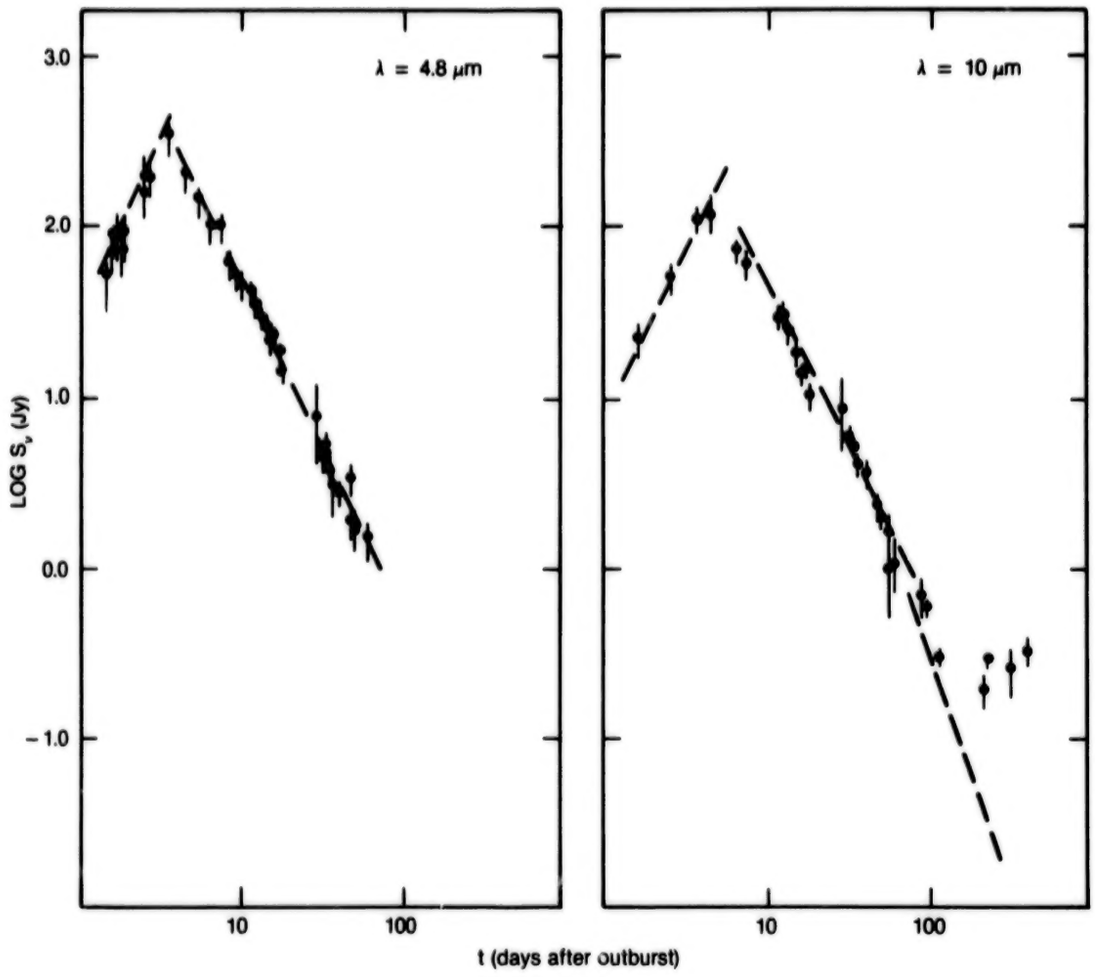


Figure 8-10. Infrared light curves for V 1500 Cyg. After day 300 from outburst an infrared excess is observed, especially evident at 10 μm, suggesting the formation of a dust shell. (from Ennis et al., 1977).

stant) (see Figure 8-11 from Ferland et al., 1986) dominating the nova spectrum from day 10 to day 100. Ferland et al. show that the gas at $T \approx 10^4$ responsible for the nebular spectrum is insufficient to explain this continuum and suggest that a contribution from the coronal line region, as well as the central object, must be added. In fact, from the H Alpha intensity, one can derive the combined free-free + bound-free emission of a low-density gas at temperatures $t=T/10^4$ for $0.5 \leq t \leq 2$: $\nu F(4800\ A) / F(H\alpha) = 1.23\ t^2\ e^{-0.663\ t}$ (see Osterbrock, 1974). Now Figure 8-12 from Ferland et al. shows that the free-free + bound-free contribution predicted from the intensity of H Alpha is lower by a factor of about 3 than the observed continuum emission. The hot underlying body gives also a contribution, which, by comparing the amplitude of the 3-hour-period light variation when the continuum is produced by the hot body only with that when the flat continuum was present, can be estimated to be of 10%. The only other contributor to the flat continuum is then bremsstrahlung from the hot gas ($T \approx 10^6$) originating the coronal lines. Figure 8-13 from Ferland et al. shows that the contributions of the hot body, the nebular, and the coronal gas are able to explain the observed continuum.

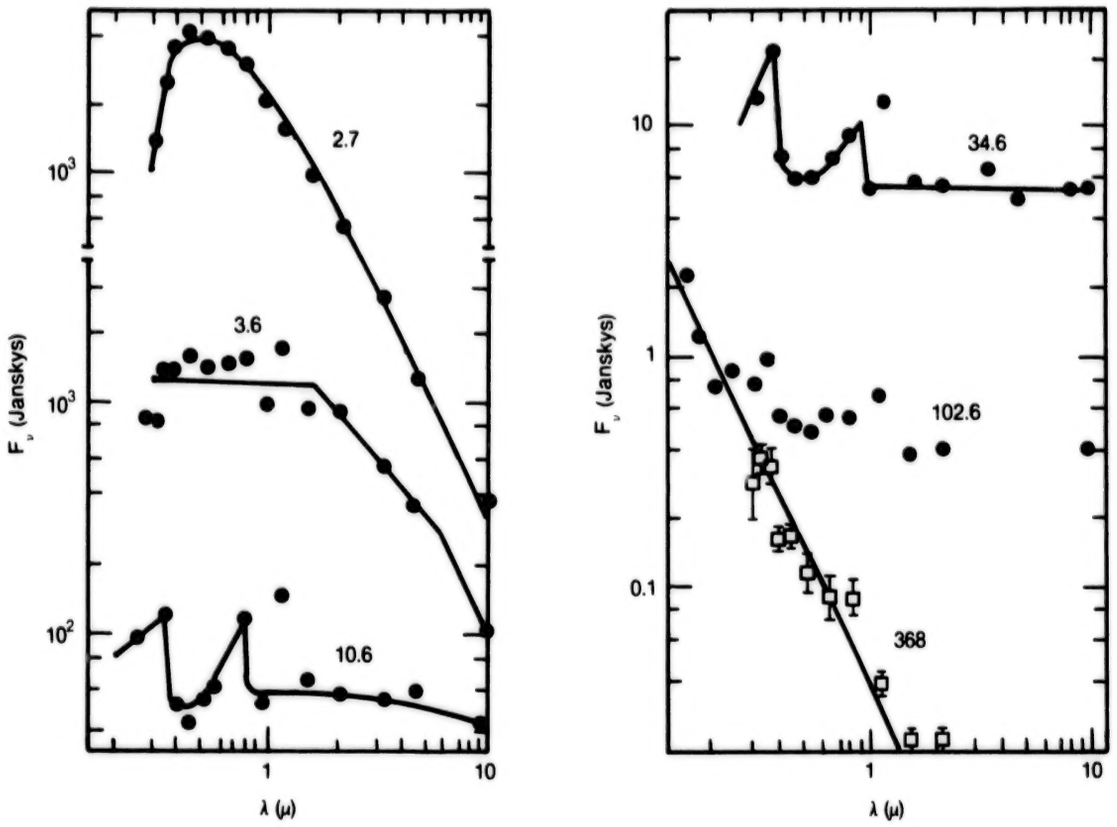


Figure 8-11. The composite energy distribution of the nova continuum is shown throughout the decline. The data are corrected for insterstellar reddening, and are taken from Ferland et al., 1986, from Wu and Kester, 1977 and from Ennis et al. 1977. The days after outburst are indicated. The squares and error bars are the data for day 368.

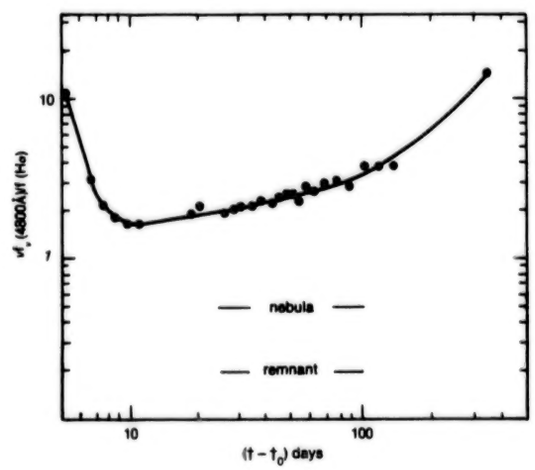


Figure 8-12. Ratio of the 4800 continuum to Hα as a function of time. The intensity of H α is used to predict the contribution of the nebula, and the intensity of the remnant continuum is predicted from Zanstra arguments. It is evident that a third contribution is required to fully account for the optical continuum.
(from Ferland et al. 1986).

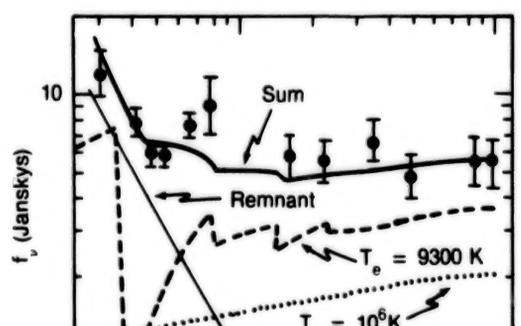


Figure 8-13. Continuum deconvolution for day 34.6. Reddening—corrected infrared and optical data are plotted. The contribution of a warm gas at 9300 K, plotted as a dashed line is predicted from the strength of Hα. A similar contribution from coronal gas at T≈10⁶K, plotted as dotted line is fitted by matching the infrared continuum points; a hot Rayleigh - Jeans tail is added to fit the UV observations (solid line). The sum of all these contributions fits the observed data in a very satisfactory way.
(from Ferland et al. 1986)

II.F. RADIO SPECTRUM OF V1500 CYG

V1500 Cyg was observed at different frequencies with different radiotelescopes (see Figure 6.76): at 0.6, 1.4, and 5.0 GHz with the Westerbork Synthesis Radio Telescope, at 2.7 and 8.1 GHz with the Greenbank interferometer, at 10.5 and 22.5 GHz with the Algonquin 46-meter telescope, and at 90 GHz with the NRAO 11 m radiotelescope on Kitt Peak. Seaquist et al. (1980) show that the data are consistent with thermal bremsstrahlung from an expanding cloud of ionized gas. Radio and infrared observations can be interpreted not in terms of a shell of constant mass, but rather as an ionized zone moving outward through the shell.

II.G. THE SHELL OF NOVA CYG 1975

The shell became observable for the first time on direct photograph on August 27, 1979 (Becker and Duerbeck, 1980). The image of the nova (Figure 8-14) displays an extension into the NW quadrant, Since Beardsley et al. (1975) have excluded the existence of any star brighter than 21 mag in a circle of 10 inches around the position of the nova, this feature cannot be a close companion, but must be identified with the brightest part of the ejected shell. Hence, the mass ejection was strongly asymmetric, a behavior seen in other novae, in particular, in the fast nova GK Per. The mean expansion rate of 0.25 inch per year, compared with the expansional radial velocity of the principal spectrum, gives the distance of 1350 pc quoted above. Speckle interferometry of V1500 Cyg made by Blazit et al. (1977) 45 days after outburst gives an expansion rate of 0.26 inch per year in excellent agreement with the value obtained at a distance of 4 years from the outburst.

II.H. THE ELEMENT ABUNDANCE IN THE SHELL OF V1500 CYG

Ferland and Schields (1978b) have derived the chemical composition of the envelope by comparing the measured intensities of the emission lines of the nebular spectrum (observed between days 40 and 120 after the outburst) corrected for interstellar reddening E(B-V) = 0.51 with those predicted for an equilibrium photoionization model. The authors observe that the steady-state assumption is reasonably good during this phase of the outburst, because the recombination time scale is always short compared with the rate of decline of the nova. Several line ratios are indicators of the electron temperature and electron density, which vary between about 9500 K and 8400 K, and between 1.5×10^8 and 10^7 cm^{-3}, respectively, The model successfully predicts the intensities of He I, [OIII] and [Ne III], but underestimates the strengths of [Ne V] and [Fe VII], which may be produced in a mechanically heated "subcoronal" region. Table 8-1 gives the abundances derived from the nebular spectrum. Moreover, Ferland et al. (1986), using the determination of electron temperature and density made by Ferland and Shields (1978b) derive the abundance of argon from the only line present in their spectra, 7136 [Ar III].

Table 8-1. Chemical abundances of V1500 Cyg

Element	$\log N(V1500\ Cyg)/N_{\odot}$		
He/H	0.0		
C/H	1.4	+/-	0.2
N/H	2.0		0.2
O/H	1.3		0.1
Ne/H	1.3		0.2
A/H	<0.9		
Fe/H	0.1		0.3

Hence, helium and iron have solar abundances, while carbon, nitrogen, oxygen, and neon are strongly overabundant, and argon is less than a factor of eight of the solar value. The normal helium abundance is a characteristic common to several novae and not easily reconcilable with the excess of CNO. Colvin et al. (1977) suggest that the overabundant C,O,Ne are the result of convective mixing of the outer layer of the white dwarf with its carbon core. Helium and iron, on the contrary, would have the abundance of the material transferred from

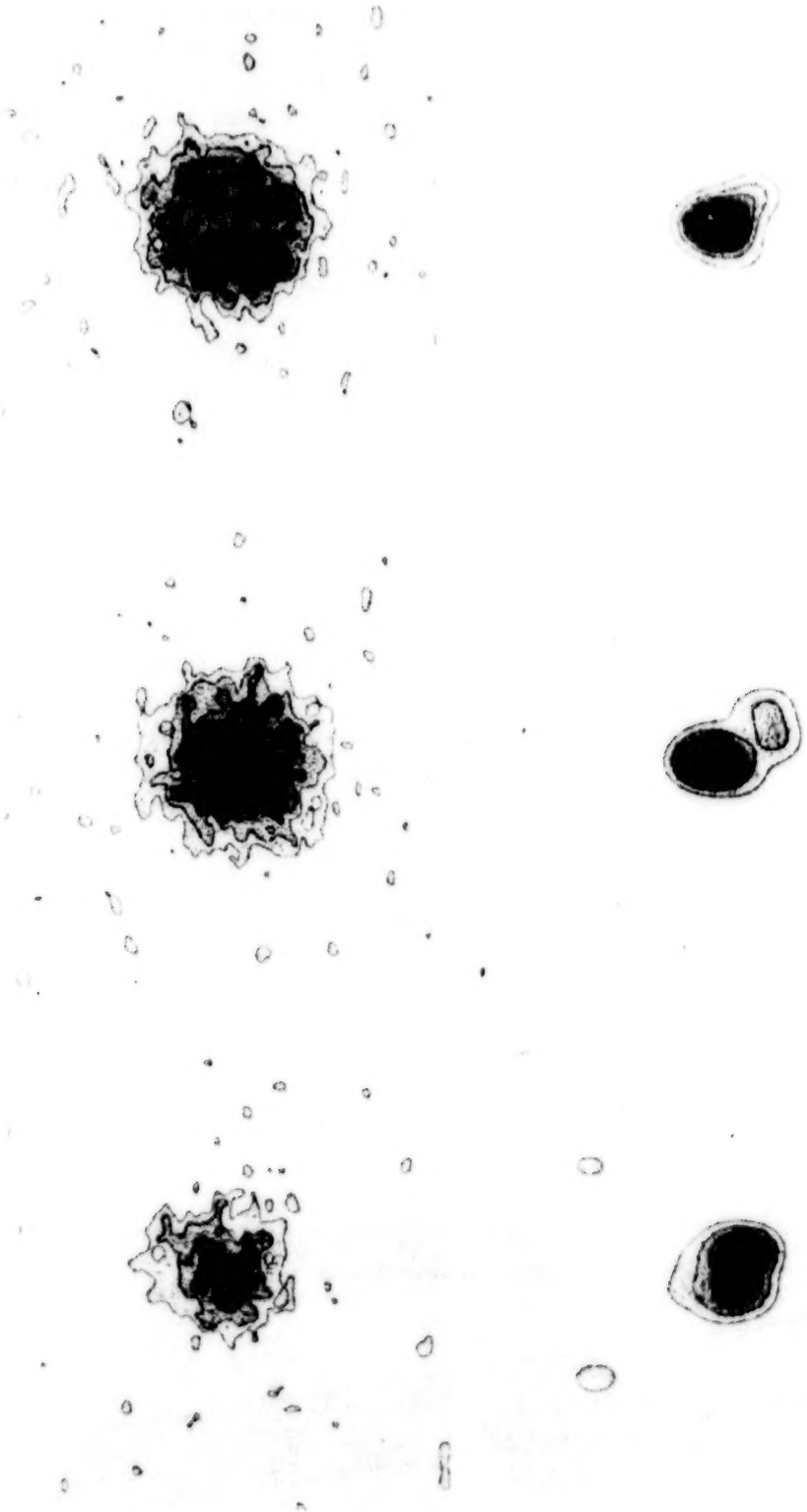


Figure 8-14. Density profiles (left) and deconvolved images (right) of the bright comparison star, the nova and the fainter comparison star (from top to bottom). North is up, west is to the right.
(from Becker and Duerbeck, 1980).

the companion to the white dwarf. The large abundance of nitrogen may result from proton capture during the thermonuclear runaway. For a complete discussion of these suggestions and theories of the origin of the outburst, see Chapter 7.

III. V603 AQL - AN HISTORY SURVEY
(written by Selvelli)

III.A. THE LIGHT CURVE

V603 Aql is the brightest member of the "classical" nova class having reached $m_v = -1.1$ at maximum and having now $m_v \sim 11.6$.

The light curve of its outburst, which started near June 9, 1918, was studied by Campbell (1919). Figure 8-15 illustrates the light curve of V603 Aql in the first 100 days after maximum. The "very fast" nova character of V603 Aql is based on the very short (2-day) time interval between the prenova phase and the maximum phase.

It is noteworthy that the maximum luminosity phase lasted a few hours only and was anticipated by a premaximum halt. The first decline phases were quite smoothed, with t_3 of the order of 10 days, and were followed by the oscillation phase, which lasted about 100 days and was characterized by the regularity of the oscillations with P~11 days. The last decline phases were instead characterized by a constant or weak variation in the light curve.

The luminosity of V603 Aql during the outburst phases has been studied by Payne-Gaposchkin (1941, 1957). Since the ejected shell is optically thick and Teff 10^4 K near maximum, the visual maximum luminosity provides a good estimate of the peak bolometric luminosity; the bolometric correction is small at this stage.

Figure 8-16 (from Gallagher and Starrfield, 1976) shows that if the maximum luminosity is to be maintained for a time of 100 days after maximum, the bolometric correction must be

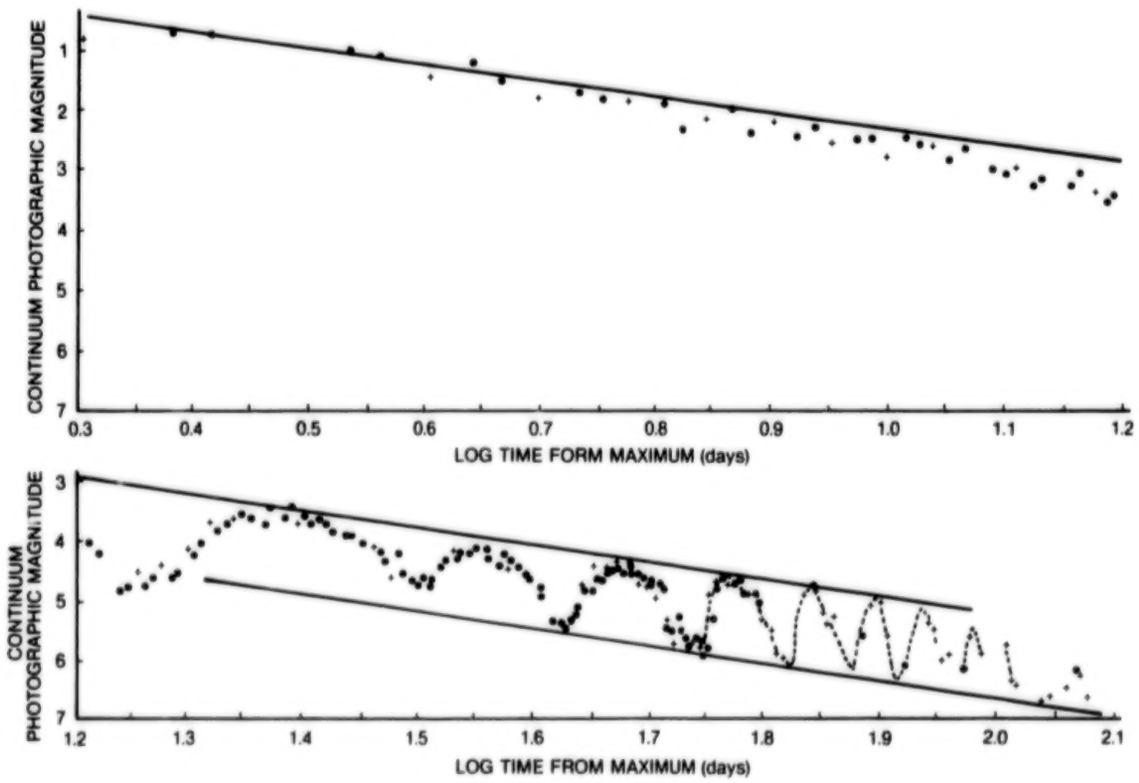


Figure 8-15. The continuum magnitude of V 603 Aql against log t from maximum. (From Friedjung, 1966a).

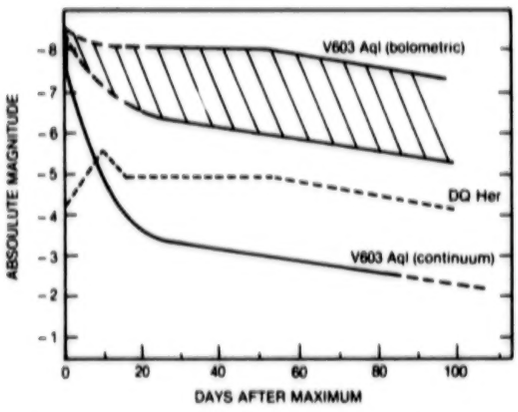


Figure 8-16. Smoothed photographic light curves of V 603 Aql and allowed range of bolometric absolute magnitudes. (From Gallagher and Starrfield, 1976).

higher than 6 magnitudes. Gallagher and Starrfield interpreted this as an indication of a decline in total luminosity, although the total amount of energy radiated under the assumption of constant L_{bol} of the order of L_{max} was estimated at about 8×10^{45} erg, a value which is approximately three times the total amount of kinetic energy and is similar to that found for slow novae (~10 times). Only the assumption M_{bol} ~7 during the interval from 10 to 100 days after maximum would give a ratio radiative energy/kinetic energy larger than one. If no bolometric correction is applied, this ratio is only one-tenth.

III.B. THE SPECTRUM IN OUTBURST

Objective spectra of the pre nova were reported by Cannon (1920). The energy distribution seemed to indicate a rather high temperature, but there was no evidence of emission lines. Several sharp absorption lines were seen, probably of hydrogen, and the spectral type was classified near Class A I. V603 Aql was also observed spectrographically during the first outburst phases. Absorption lines at maximum were violet-shifted by about -1300km s^{-1}. This spectrum was followed by the principal absorption spectrum, which showed similar features (resembling an F I star) but with higher velocities v_{out} ~-1500 km s^{-1} , thus producing an aspect of duplicity in the lines. Nearly at the same time with the presence of the principal absorption, bright emission lines of low excitation (H, NaI, CaII, FeII, etc.) appeared as superimposed to the absorption spectrum. This principal emission was gradually replaced by lines of increasing ionization and excitation. Ultimately, emission lines of NIII, NeIII, OIII, HeII, etc., appeared in the emission spectrum.

Gallagher and Starrfield (1976), using selected spectral features reported by Wyse (1939), have outlined the increasing level of ionization with the decline in luminosity (Figure 8-17). Lines from ions which appear shortly

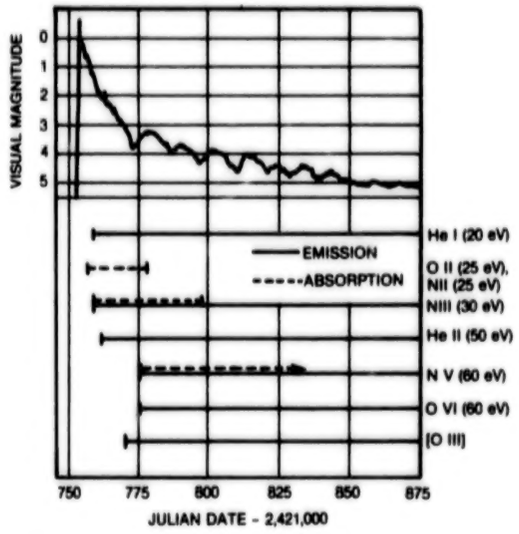


Figure 8-17. The appearance times for lines from major ions are compared with the visual light curve for V603 Aql. All of the data are from Wyse (1939). The pattern of increasing excitation with declining light is observed in most novae and suggests that ultraviolet energy redistribution following maximum commonly occurs.
(from Gallagher and Starrfield, 1976).

after maximum have excitation and ionization potentials of the order of 20 eV or less, while later features require much higher potentials (>50 eV).

The new system of lines of the diffuse-enhanced spectrum showed absorption features which were violet-shifted by about -2200 km s^{-1} , almost twice as much as in the premaximum spectrum. An even higher outflow velocity was present in the Orion Spectrum, which showed absorption lines (typically HeI, NII, OII) with velocities up to -4000 km s^{-1} Figure 8-18).

Payne-Gaposchkin (1957) has given a detailed description of the complex behaviour of the various absorption and emission systems.

As the nova faded, forbidden emissions became prominent, with a progressive strengthening with respect to the permitted ones. McLaughlin (1960), has provided a comprehensive description of the postnova emissions of V 603 Aql, including a detailed description of the behaviour of the HeII λ 4686 Paschen line emission. Nitrogen flaring, a secondary fluorescence originated from HeII Lyman alpha λ 303 was related to the increase in intensity of the 4686 emission line and was evident from the appearance of two wide and hazy emissions at 4100 Å and 4640 Å. It is remarkable that, as noted by Wyse (1940), most of the nebular light in 1919 and 1920 came from the OIII λ 4959-5007 doublet and, in second place, from the NII λ 6548-6584 doublet.

Payne-Gaposchkin and Gaposchkin (1941), from the absolute intensities of some lines and from the distance derived from the nebular expansion, have estimated the line luminosity for

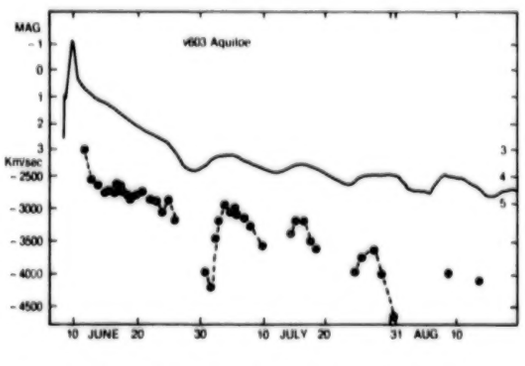


Figure 8-18. Radial velocities of Orion absorption system of V 603 Aql, correlated with light curve. (from Friedjung, 1966b).

H delta (log H_8 36.65, Δ m = 3, and 35.85, Δ m = 6 with Δm counted from maximum) and for the [OIII] λ 5000 emission (36.99 at maximum).

Electron temperatures have been calculated from the usual OIII ratio (5007 + 4959) / 4363, and values of about 6500 K were derived. Estimates of the electron density, based on the surface brightness of H delta and the nebular radius, gave values ranging from 1 x 10^9 cm^{-3}, in the early phases, to 1 x 10^6 cm^{-3} in the early nebular stages. With the assumption $N_e \sim N_{H^+}$, a lower limit to the mass of the shell ejected in the outburst was estimated in 10^{29} g.

Friedjung (1966b) has given a set of determinations of temperatures and radii of the ejected shell in the first months after the outburst. The estimates of the temperature were made using the methods developed by Zanstra, Ambartzumian, and Stoy and data from the literature and from archives. From this study, Friedjung found support in favour of an inverse T-R correlation. A clear relation between the characteristic velocities of the diffuse-enhanced and Orion spectra and the corresponding radii was also found (Figure 8-19).

III.C. THE STRUCTURE OF THE EJECTED SHELL

The expansion of the ejected shell and the nebular structure has been studied quite carefully by various authors. About 4 months after maximum, Barnard (1919) detected a nebular shell with a diameter on the order of 1" that expanded at a uniform rate. Wyse (1940), in his protracted photographic and spectroscopic monitoring, showed that the expansion rate was at about 1"00 per year during some 20 years. Wright (1919), from a series of exposures made by rotating the spectrograph, was able to demonstrate that the expanding shell was not spherically symmetric. From studies on spectrograms taken at Lick Observatory with the slit at different position angles, Baade (1947) proposed the presence of a system of three rings (equatorial belts) in parallel plans, and of two very large polar caps (blobs, condensations) that were apparently ejected in opposite directions along a common symmetry axis pointing nearly (16°) toward the sun.

Weaver (1974) has made the most exhaustive study on the development of the shell. From the slit-spectrograph images taken with the slit in a number of different position angles, he reconstructed the structure of the ejecta. The model he derived describes the nebula in terms of cones of emitting material and two polar jets. The axis of the cone system and the line of

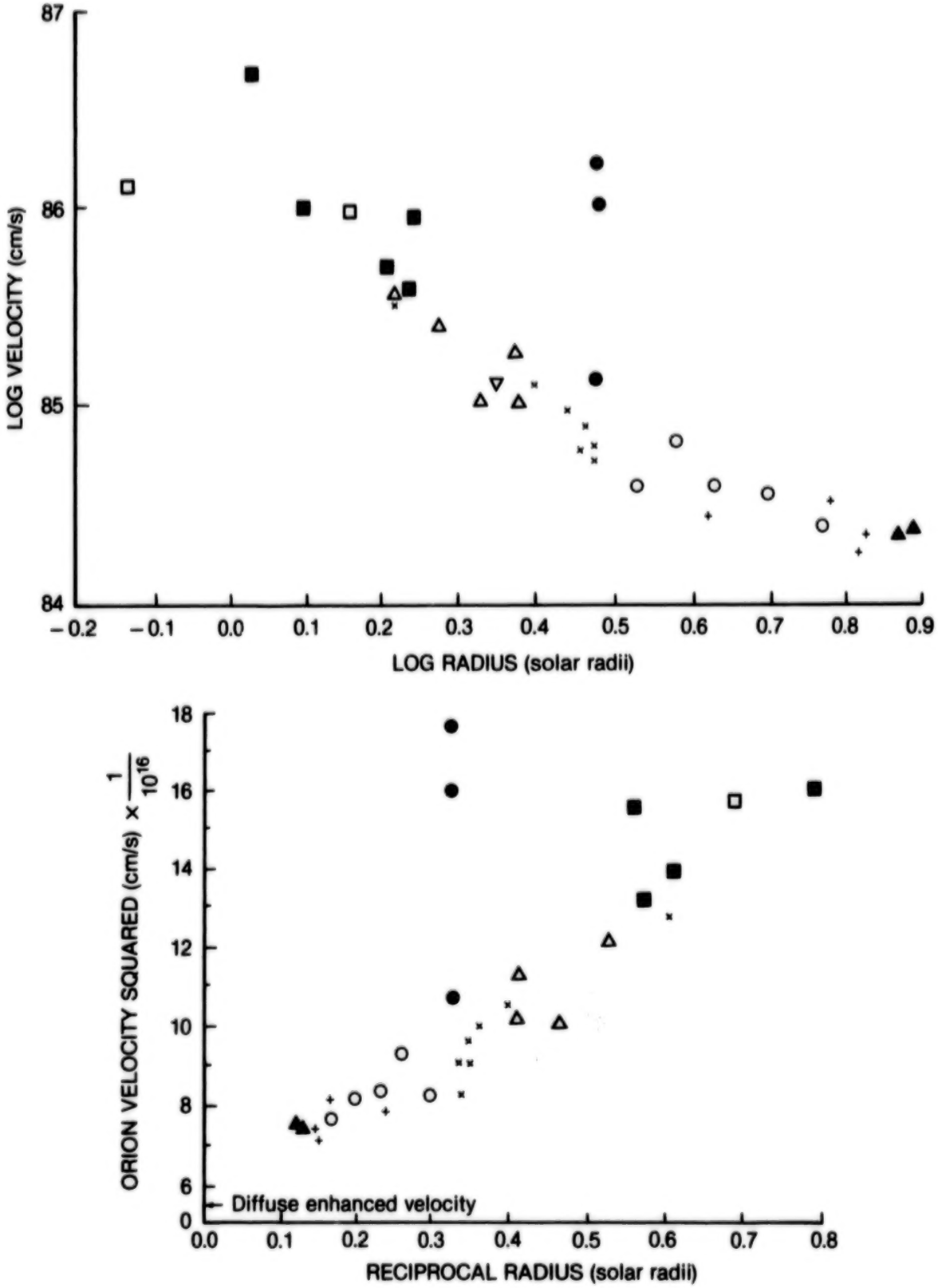


Figure 8-19. a) The relation of Orion velocity to radius for V 603 Aql.log t included between less than 0.80 (black triangles) and larger than 1.60 (black squares) and 1.73 (white squares). b) Relation between the velocity squared and reciprocal radius. Symbols for different epochs are the same as in a)
(from Friedjung, 1966b).

sight are nearly perfectly aligned (angle less than 1°). Figure 8-20 gives a sketch of the morphology of the ejecta.

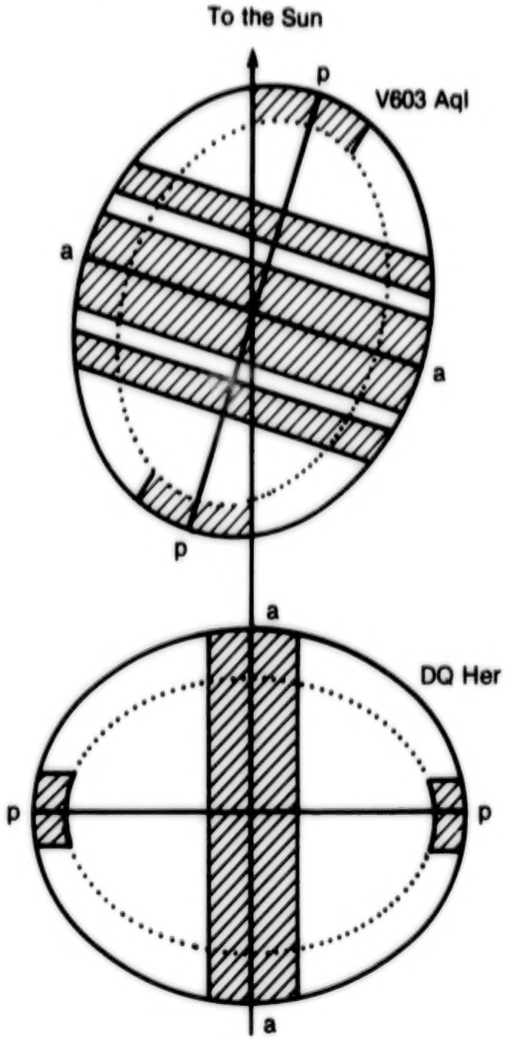


Figure 8-20. Morphological models of the principal envelopes of V 603 Aql and DQ Her.pp is the polar axis and aa the equatorial belt. (from Mustel and Boyarchuk, 1970).

III.D. UV AND X-RAY OBSERVATIONS OF V 603 AQL

The first UV observations of the old nova were made by Gallagher and Holm in 1974 (1974), using the 8-inch photometric telescopes of the OAO-2 Wisconsin Experiment Package (WEP).

They attempted also to observe other quiescent novae, but only V 603 Aql and RR Pic were positively detected. From the observed distribution, after correction for $E_{B-V} = 0.07$, Gallagher and Holm were able to estimate an empirical color temperature of about 25,000 K.

From the observed continuum distribution and the knowledge of the distance, a lower limit for the luminosity of about 8 $L_{\odot}$ was derived.

After the launch of IUE, V603 Aql was observed by several authors: Selvelli and Cassatella (1981), Drechsel et al. (1981), Lambert et al. (1980), Duerbeck et al. (1980a), Krautter et al. (1981), Ferland et al. (1982a), etc. (Figure 6-36 shows a typical IUE spectrum of V603 Aql.)

The remarkable differences from author to author in the temperature fitting to the continuum distribution have already been mentioned in Chapter 6. In this respect, it is worth mentioning that Lambert et al. (1980) in the first IUE observations of V 603 Aql noted a systematic disagreement between the OAO-2 and IUE values shortward of λ 1600 and suggested real variability in the continuum of the hot component.

Duerbeck et al. (1980) reported that the CIV 1550 emission was accompanied by a blue-shifted absorption indicating mass outflow. Selvelli and Cassatella (1981) used low-resolution archive data and original high-resolution spectra to look for a possible phase dependence in the continuum distribution (which could explain the differences in temperatures found in previous works) and to check the reality of the presence of P Cyg profiles in the resonance lines of CIV and SiIV reported by Krautter et al. (1981). One of the results of this study was the suggestion of the presence of rapid variations in the far UV and "eclipse-like" effect in the near UV for the high excitation lines, which seemed correlated with the orbital phase.

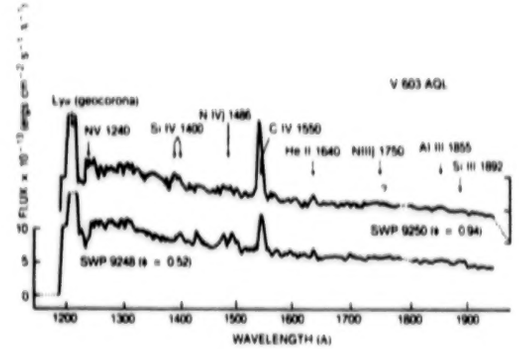
The high-resolution SWP spectrum was slightly underexposed. However, three emissions were clearly present, i.e., SiIV 1400, CIV

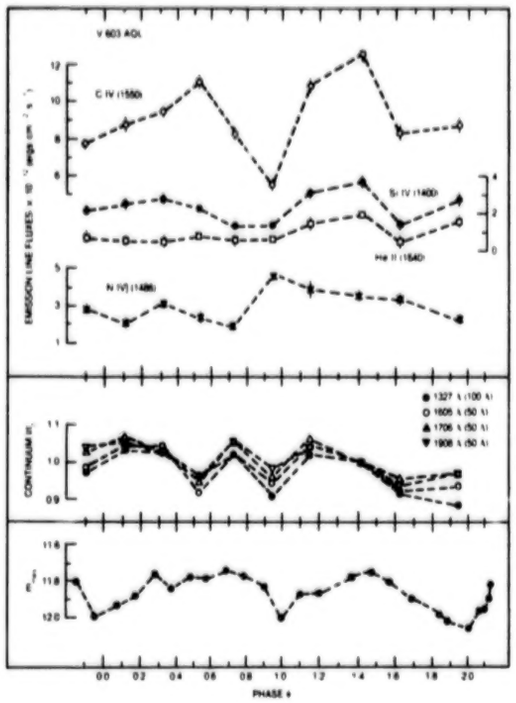
1550, and HeII 1640. They all present the same kind of profile, which appears to be a wide and shallow emission centered at the nominal wavelength. The half-half widths indicate velocities of around 900 km s^{-1} that cannot be ascribed to the orbital motion, which has lower velocities. It is remarkable that this high-resolution, deep-exposure spectrum (420 minutes) has not revealed any additional emission line besides the three emissions mentioned above (see also Figure 6-42) that are clearly evident in the low-resolution spectra. The absence of (sharp) intercombination emissions was interpreted as an indication that the nebular shell had essentially vanished.

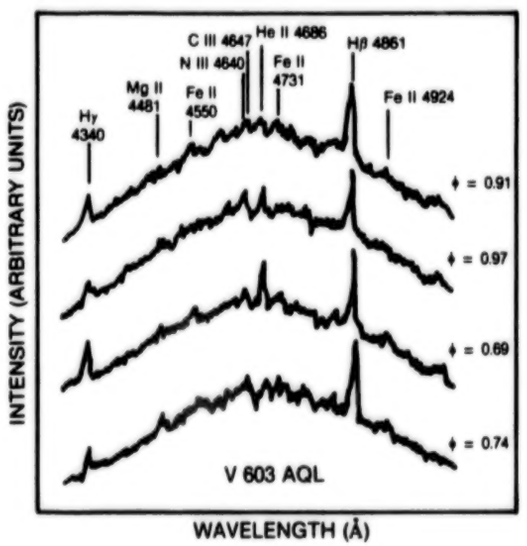
The main shortcoming of this study was in the inhomogeneity of the data: the IUE spectra used were taken at different epochs, and phases were reconstructed assuming Kraft's (1964) period. Drechsel et al. (1981), instead, made an extensive set of observations monitoring the nova during almost two complete cycles, one entire IUE shift. A total of 8 SWP and 2 LWR spectrograms were obtained. UV (and optical) changes with a period in agreement with that of Kraft were detected and interpreted as related to the phase of the binary system. The emission line spectrum consists of two distinct groups: quite strong resonance lines such as SiIV, CIV, AlIII, MgII, and much weaker semiforbidden lines such as NIV 1486, NIII 1750, CIII 1908, and CII 2326. The presence of these latter lines, if confirmed, would indicate that the system is surrounded by highly diluted (nebular) matter. The strongest feature is the CIV resonance doublet λ 1550. Phase-dependent variations (by a factor of up to two) in the line intensity are clearly evident, especially for CIV, SiIV, HeII, and NIV 1486. The most pronounced changes occur near maximum light at about $\phi = 0.5$. The intensity is instead minimum near orbital phase 0 (Figure 8-21). The continuum variations with phase are smaller than the 0.3 mag observed in the visual (FES) light-curve. The fact that the variations in the optical continuum, UV continuum, and UV line emission are strongly correlated suggests that the main source of UV and optical radiation are located in about the same region of the system. This behaviour is in agreement with the optical photometric observations of Panek (1979), who showed gray variations in the light-curve. "Eclipse-like" effects (near phase 0.0) are not evident in the semi forbidden lines. This was interpreted as an evidence for the presence of diluted gas surrounding the whole system. These results are in disagreement with those by Selvelli and Cassatella (1981) who did not show presence of nebular lines.

A study similar to that of Drechsel et al. but focused on the LWR range (which was covered by two observations only in that study), was performed by Selvelli and Cassatella (1982). Five LWR spectra at low resolution were taken in a close sequence, to monitor the phase-related variations (since they covered about one orbital period), and one high-resolution LWR spectrum was taken in order to provide correct identifications and information on the emission lines shape. Actually, no stellar lines, either in emission or in absorption, were detected in the high-resolution spectrum, probably partly because of the fact that it was underexposed by a factor of about two, and mainly because the possible features, being very broad and shallow as in the high-resolution SWP spectrum described previously by Selvelli and Cassatella (1981), were not detectable. The five low-resolution spectra, on the contrary, have permitted an easy estimate of the presence or absence of spectral features. These data indicate that the emission lines are probably formed in the accretion disk and that there is no trace of any nebular contribution from the envelope ejected at the time of the outburst. (Figure 8-22)

About three fourths of the emission lines have been identified or tentatively identified as belonging to permitted, semiforbidden, and forbidden transitions of medium-high ionization species. The strongest emissions are Mg II λ 2800, OIII λ 2320, OII λ 2470, Al II λ 2669, probably Fe XII λ 2568 and 2578, O III λ 3047 and a few unidentified lines. In addition, all the lines of the He II Paschen series are present, together with the O III lines produced by the Bowen flourescent mechanism involving He Lyα λ 303.







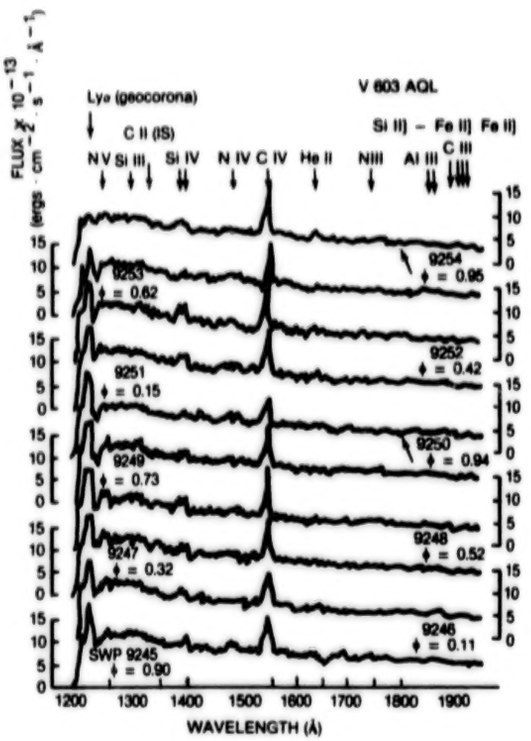


Figure 8-21. a) Two selected IUE short wavelength spectrograms of V 603 Aql obtained at orbital phase 0.52 and during the supposed eclipse at phase 0.94. Pronounced variations of the strengths of C IV 1550, Si IV 1400 and He II 1640 as well as N IV / 1486 - but in the opposite sense are evident. b) Comparison of the visual light curve (obtained with the Fine Error Sensor on board of IUE), at the bottom, with the emission line flux of four ions (top) and ultraviolet continuum light curves (center). c) IUE short wavelength spectrograms obtained during more than two complete orbital cycles. d) optical observations obtained with the ESO 3.6 meters telescope. Variations in the line strengths (e.g. He II 4686) and line profiles (e.g. H gamma) are noticeable.
(from Drechsel et al, 1980: Figs a, d; Drechsel et al. 1981: Figs b, c.)

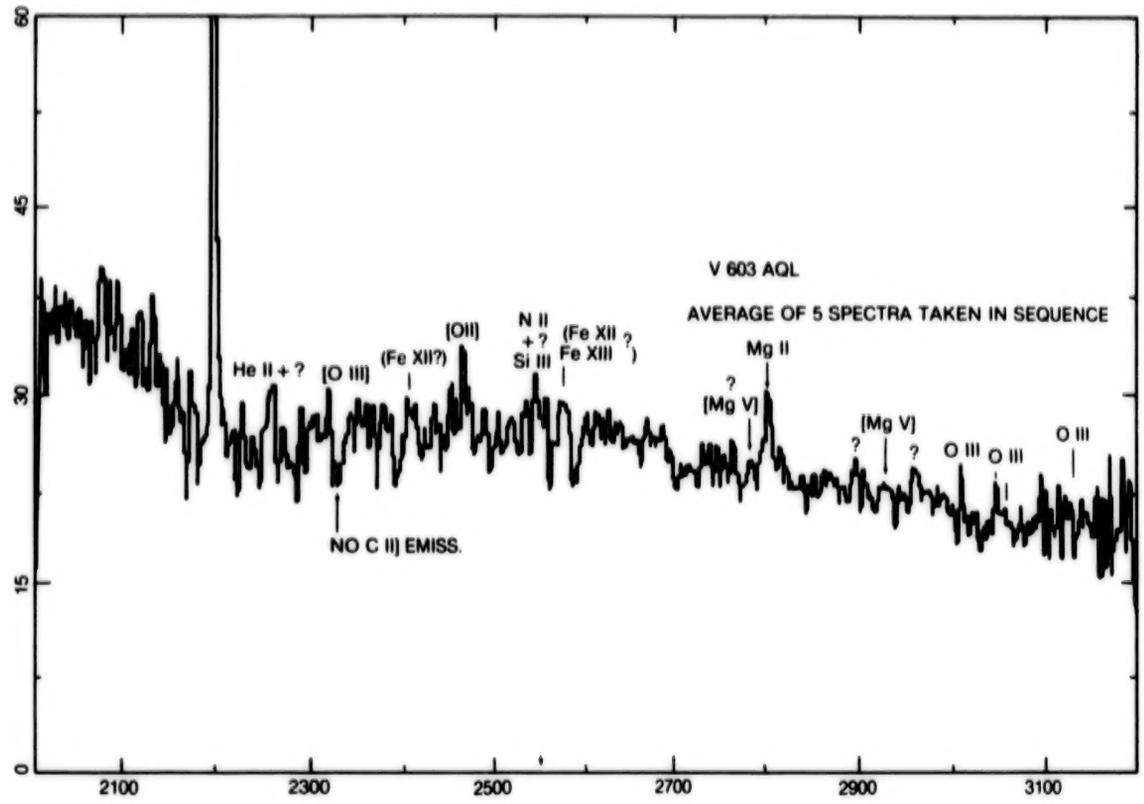


Figure 8-22. Average of 5 spectra of V 603 Aql taken in sequence in the IUE long wave range (2000-3100 A).

Selvelli and Cassatella (1982) have attributed to coronal lines many emission features lacking any other reasonable identification.

Actually, of the dozen coronal lines reported in the near UV range of the solar spectrum, all but one (Fe XI 2649) might be present in V603 Aql.

Figure 8-23 reports the values (not corrected for reddening) of the total flux below the continuum (i.e., $\int_{2000}^{3200} F_{\lambda}^{C} \, d\lambda$ in ergs cm^{-2} s^{-1}) of the Mg II emission intensity (erg cm^{-2} s^{-1}) and of the visual magnitude derived from the FES counts as function of the orbital phase (seeTable 8-2).

For the ephemeris, the value of P=0.1383d and the time of the principal minimum given by Herczeg (1982) have been assumed.

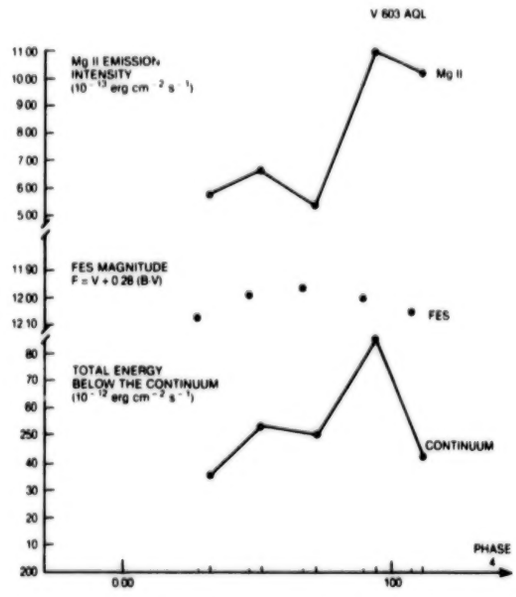


Figure 8-23. The variations observed in 5 spectra taken in strict sequence, in the long wavelength region.

There are variations both in the lines (by a factor of ≃ 2) and in the continuum (by a factor of ≃ 1.3) in spectra taken in close sequence. It is questionable, however, whether these variations are intrinsically phase-related. The observed maximum of the Mg II emission and of the continuum around phase ~ 0 might be attributed to a transient phenomenon. This might explain the disagreement with the visible data and the previous far UV observations.

TABLE 8-2.

VALUES OF VISUAL MAGNITUDE M_V(FES), MG II EMISSION, AND TOTAL FLUX BELOW THE CONTINUUM, FOR V 603 AQL AT DIFFERENT ORBITAL PHASES.

Phase*	m_v (FES)	MgII Emission (10^{-13} erg cm^{-2} s^{-1})	Total Flux below the continuum (10^{-12} erg cm^{-2} s^{-1})
0.281	12.11		
0.325		5.75	235
0.479	12.03		
0.522		6.70	253
0.678	12.00		
0.722		5.10	252
0.899	12.04		
0.942		11.00	285
1.097	12.09		
1.140		10.25	242

Surprisingly, the maximum in the near UV total flux and in the Mg II emission intensity occurs near phase = 0 (principal minimum in the visible), while at the other phases, the values of the quantities under study do not differ very much from each other.

Ferland et al. (1982) have made a quantitative analysis of the physical conditions in the continuum and line-emitting region of the system. After correction for E(B-V) = 0.07, the continuum follows a power-law close to the $\lambda^{-2.33}$ value expected from a "standard" disk. If the distance is of 380 pc, the total luminosity is of the order of 5 x 10^{34} erg s^{-1}. If this luminosity is generated in the accretion disk, the mass-accretion rate can be derived: $\dot{M} \sim 10^{18}$ gr s^{-1}.

A study of the emission lines from ions like H, He, C, N, O, has led the authors to suggest that these lines are formed in a circumstellar "corona" with size comparable with the binary separation. The "corona" is heated by the hot radiation from the accretion disk. The large radius of the "corona" is required by the emission measure of the gas and by the presence of the NIV 1486 line, which has a critical density of about $10^{10.5}$. Ferland et al. (1982a) pointed out that several features of the model, in principle, were open to direct observational test. For HeII (produced across much of the corona) they expected a broad line with a fill-in center, while for lines such as C IV (produced only across an annulus), they expected a narrower, saddle-shaped profile.

Ferland et al. (1982) studied also the optical spectrum of V 603 Aql (Figure 8-24). The hydrogen emission lines show a flat Balmer decrement:

$H\alpha = 0.99$, $H_\beta = 1.00$, $H\gamma = 0.86$, $H\delta = 0.92$, etc.

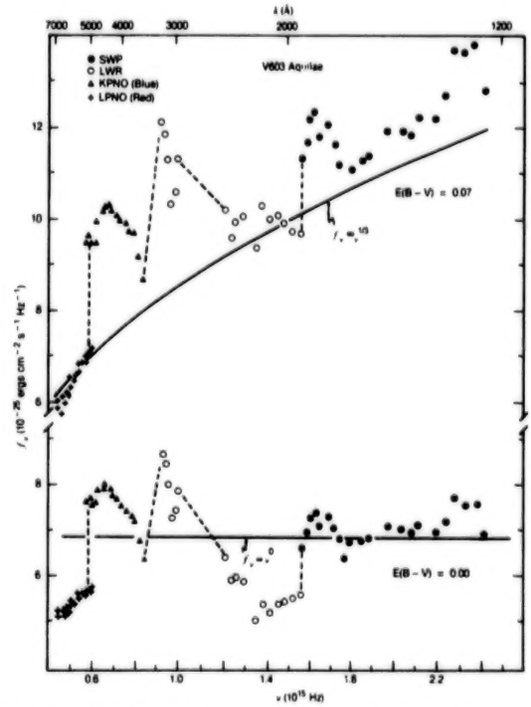


Figure 8-24. The lower panel shows the observed optical - ultraviolet continuous energy distribution. The upper panel shows the energy distribution after applying an interstellar reddening correction E(B-V)=0.07 mag. This reddening correction, which is consistent with the object's galactic position, brings the continuum to the form predicted for an optically thin accretion disk.
(from Ferland et al, 1982a)

*ϕ=0 corresponds to the principal minimum of the visible light curve. The phase associated with m (FES) is that corresponding to about 2 minutes before the beginning of the exposure. The phase associated with the spectral quantities is that of mid-exposure. (4 June 1981, GMT = 23y 09m 35s = JD 2444760.4652).

This anomalous behavior was interpreted in terms of emission from a small volume of dense gas (10^{13} cm^{-3}) on the surface of an accretion disk. The presence of N IV 1486 ($N_e^{crit} = 10^{10.5}$) however, is disturbing.

III.E. V603 AQL IN QUIESCENCE: HOW MANY PERIODS IN V 603 AQL ?

The binary character of V 603 Aql was discovered by Kraft (1964), by using high-resolution Palomar coude spectrograms at 38 Å/mm. From the RV changes in the Hγ and Hδ emissions, he determined a period of 3^h 19.5^m (0.13854 days). The RV curve has 2K = 75 km s^{-1}, and the emission lines have an intrinsic broadening of approximately 240 km/s (half-half width). The low 2K value suggested low system inclination, and, therefore eclipses or occultation effects were not expected.

The first photometric observations never covered one entire period; they just revealed strong flickering activity. (Walker, 1963; Robinson and Nather, 1977)

Time-resolved spectrophotometry (Panek, 1979) has shown that differences of 0.3 mag over time scales of ~10 minutes are common in V603 Aql. These variations are gray.

Rahe et al. (1980), during an 8-hour observing run with the IUE satellite, monitored the optical photometric behavior of V603 Aql by using the FES instrument (5.1-second integration times and about 20 points in the curve, separated by intervals of about 20 minutes).

The light curve they found (Figure 8-25) reveals the presence of three pronounced minima separated by a time interval, which is in agreement with the spectroscopic period found by Kraft. The presence of these minima was tentatively interpreted in terms of a partial eclipse of the accretion disk around the white dwarf by the late main-sequence component, or as an occultation of the hot spot by the disk itself.

Slovak (1981) made high-speed photometric observations of V 603 Aql starting on 15 June 1980, 5 days after Rahe's observations. The

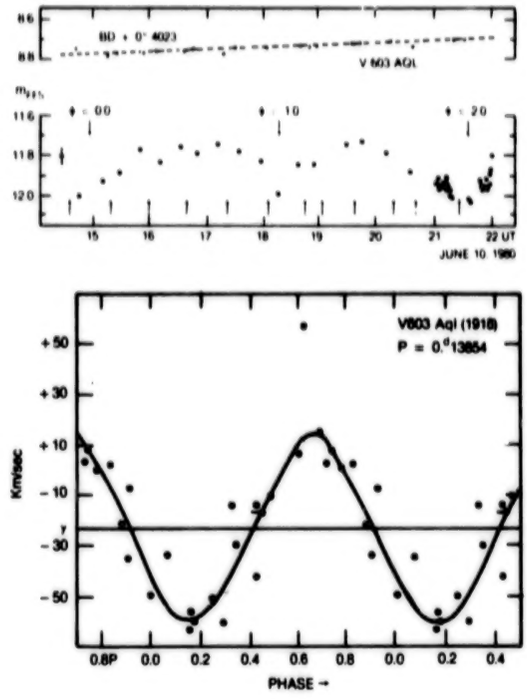


Figure 8-25. Visual light curve obtained with the FES (from Drechsel et al, 1980) and RV curve (only H gamma and H delta have been measured) (from Drechsel et al, 1983b).

new data were reduced, using a cross-correlation analysis, and power spectra were calculated to search for low-amplitude rapid oscillations, of the kind detected in DQ Her and V533 Her.

During the five observing runs, no evidence for regular eclipses or any other periodic feature was found. (Figure 8-26) This fact led to the conclusion that the variations reported by Rahe et al. (1980) may arise from the formation of transient features in the accretion disk.

This failure in the attempt to find regular eclipses was interpreted as a support to the indications of low system inclination derived from the spectroscopic data of Kraft and from the study of the nebula by Weaver (1974). Similar arguments were also adopted by Cook (1981) to reject the eclipse explanation of the minima observed in the light curve.

Surprisingly, new photometric observations by Haefner (1981) in summer 1981, revealed a repeating hump structure in the light curve. A periodogram analysis gave a period of

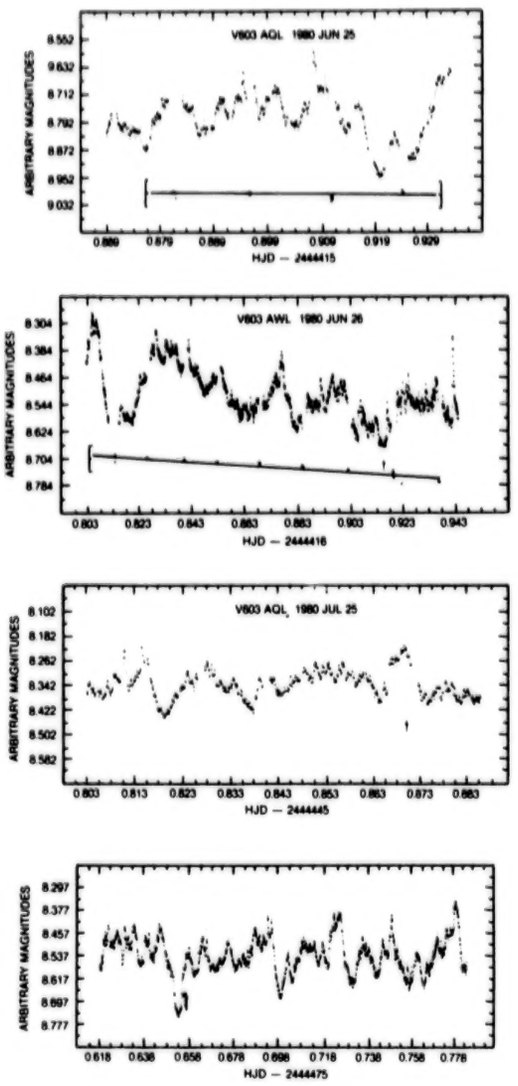


Figure 8-26. Light curves of V 603 Aql obtained during several nights, with a resolution of 6 s per point. Solid arrows denote predicted time of minimum light. On July 25 a hump occurs rather than an eclipse. (from Slovack, 1981).

0.144854 days, about 5% larger than the spectroscopic one. Haefner suggested that periodic features only can be identified when the mean light level of the system is low (V~11.9); otherwise, they might be masked by a strong flickering activity. In this respect, it is worth remarking that the observations by Slovak indicated V~11.4. New observations were made by Herczeg (1982) who also used data obtained in previous works in his attempt to clearly define the photometric period. He found, beyond any doubt, clear evidence of minima in the light-curve and suggested 0.13816 days as the best value for the period, leaving, however, a possibility for P = 0.13822 and P = 0.13828. Also, he pointed out the considerable observational difficulties produced by the strong photometric disturbances the star presents.

More recently, Haefner and Metz (1985) have presented a careful analysis of the data taken in mid summer 1981 with the ESO 50 cm telescope during long observing runs. The preliminary results presented by Haefner (1981) were confirmed: hump-like features instead of eclipse-like features, and a period of 3^h 28.8 (0.144854 days), which is about 10 minutes (5%) larger than the spectroscopic one [Kraft 3^h $18^m.9$].

No periodic variations during the whole observing time interval, which covered 117 periods, were detected. The observed hump structure (Figure 8-27) in view of the low inclination of the system, cannot find an easy explanation. Haefner and Metz have made also polarimetric observations. The measurements of linear and circular (P_c~$2.7\ 10^{-4}$) polarization revealed an unexpected, new period of 2^h 48^m.

There are, therefore, at least three periods that characterize the various observing modes of V 603 Aql.

On the basis of these results, Haefner and Metz (1985) have proposed a detailed model of intermediate polar, combined with a transitory eccentric disc to explain the different periodicities present in the system. A magnetic field of the order of 10^6 Gauss was derived from the degree of circular polarization.

Optical observations obtained in 1980 and with the ESO 3.6 m. telescope (Drechsel et al., 1983b) together with previous data taken by Kraft, have been used to determine more precisely the spectroscopic period. (Figure 8-28).

The power-spectrum analysis yielded P = $0^d.1381545$ in good agreement with the early determination of Kraft: P = 0.13854.

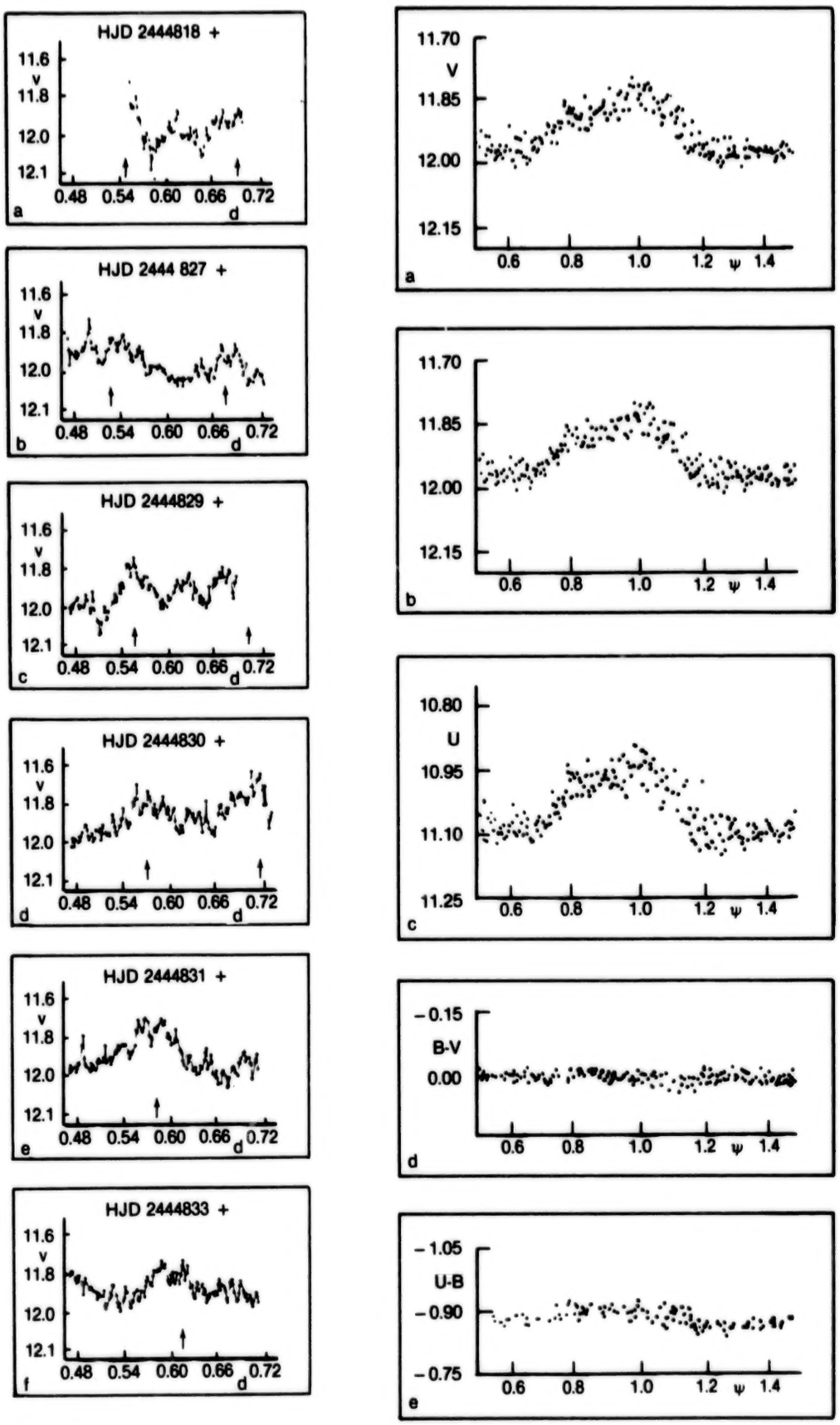


Figure 8-27. a) Selected photometric runs in chronological order V vs JD. Arrows indicate the predicted time of maxima. b) Average light curves and colors. (from Haefner and Metz, 1985).

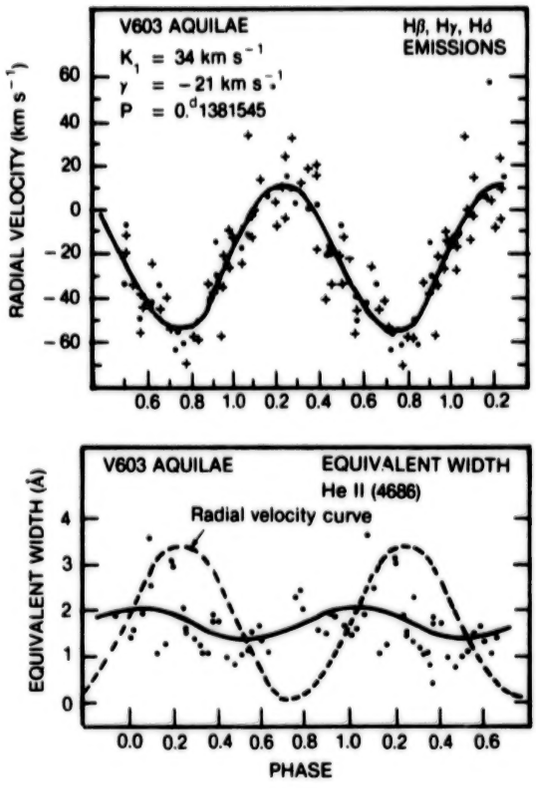


Figure 8-28. a) Radial velocity curve of the primary component of V603 Aql (crosses H Beta and H Gamma emission lines measured by Drechsel et al, 1983b), while the dots are earlier measurements by Kraft. b) equivalent widths of He II 4686 vs the phase. The dashed line is the RV curve shown in a). (from Drechsel et al, 1983b).

IV. CP PUP

(written by Bianchini)

IV.A. INTRODUCTION

CP Pup is one of the two brightest galactic novae ever observed; the other one is nova Cygni 1975. It reached photographic magnitude 0.5 on JD 2430675, rising from fainter than 17th magnitude. A large outburst amplitude, a very rapid development, though with modest expansion velocities, high terminal excitations with the simultaneous presence of very low excitation lines, such were the first peculiarities observed in nova Puppis 1942 (Payne-Gaposchkin, 1957). At light minimum, the nova has been found to be a close binary system having an unusually short orbital period below the 2-3 hour period gap for all cataclysmic variables (Bianchini et al., 1985a,b; Warner, 1985; Duerbeck et al., 1987).

We shall report here some relevant data for this nova at outburst and at minimum.

IV.B. THE OUTBURST

The outburst light curve of CP Pup shows a smooth early decline and a transition phase without oscillations (Figure 8-29). The star rose from fainter than 17th magnitude and so, at least after the rise, it had the largest range recorded for a nova. Now the old nova standstills at $m_v \sim 15$. The nova at maximum reached absolute magnitude −11.5 (Duerbeck,1981), so that it radiated for a large fraction of the outburst with a luminosity that surpassed the Eddington luminosity by two orders of magnitude. The velocity of decline of the light curve was as high as 0.37 mag/day. Such a large velocity of decline has been reached by the more recent very bright nova Cygni 1975 and also by the far less energetic recurrent nova T CrB, which also presented a similar rapid spectral development.

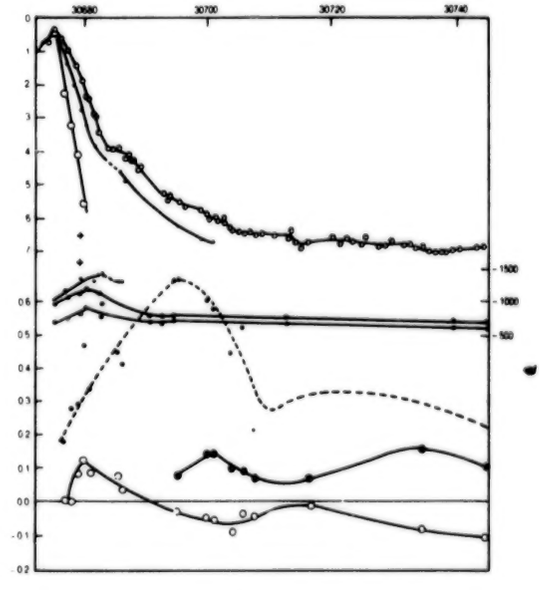


Figure 8-29. Above, the light curve of CP Pup 1942 in the photographic (dots), the visual (small circles), and the continuum (large circles). Middle, radial velocities from absorption lines (dots), red edge (half-filled circles) and violet edge (also half-filled circles) of bright lines. Ordinates are shown on the right. Bottom, logarithm of the ratio Hβ/Hγ (dots and broken line), the ratio V/R for the HeII 4686 (circled crosses) and for the Balmer lines (circle). Note that the curve of the HeII lines changes in the opposite sense to those of the Balmer lines. (from Payne-Gaposchkin, 1957).

Soon after the maximum, the spectra of CP Pup showed the presence of high-excitation lines of [OIII], [CaVII], [[CrIII], [MnVI], [FeVIII], [FeX] and [FeXI]. However, the same spectra revealed bright lines of [OI] OI, Na, CaII, Si, FeII, and [FeII], indicating the presence of a stratification of the ionized atoms around the star. We recall here the fact that high-excitation coronal lines are observed also in recurrent novae like, for example, T CrB. This demonstrates that the velocity of the photometric and of the spectroscopic development and the appearance of high-excitation emission lines are not related only to the rate of the energy output by the explosion. In fact, low-energy outbursts with large expansion velocities of very thin envelopes should also favor the formation of high-excitation lines. Moreover there exists only a very general correlation between the velocity of decline and the expansion velocity of the envelope of classical novae. Actually, the velocities derived from the diffused-enhanced spectrum and the Orion spectrum of CP Pup were not particularly large: –1600 km/s and –2000 km/s, respectively. When the envelope became optically thin, we observed a doubling of the nebular lines, due to the layers expanding towards us and those expanding in the opposite direction. These emission lines yielded an even lower value of the expansion velocity: 1100 km/s. The velocity derived from P Cyg profiles was of 1400 km/s. These differences can be attributed to the fact that the expansion velocity of the observed nebula is often lower than that derived from the blue-shifted absorption features that characterize the so called continuous wind-ejection phase of the decline. It is then possible that the bulge of the matter lost by the nova was not principally formed by the high-velocity wind produced during this relatively well-extended phase of the nova outburst.

However, the spectral development of CP Pup was really very fast. The diffuse-enhanced spectrum appeared four days and the Orion spectrum, five days after light maximum. The absorption spectrum was recorded for only fifteen days: it disappeared at the beginning of the transition phase, when the spectrum of a nova starts changing from a more stellar to a purely nebular one. This could suggest that the expanding envelope of CP Pup was not very massive.

The behaviour of the V/R reversals for the Balmer lines and for the HeII λ4686 emission is peculiar. The V/R ratio of the HeII line changes with time in the opposite sense to that of the hydrogen lines, but with the violet edge always the stronger. All this is shown in Figure 8-29. The V/R ratios for the H lines are initially larger than unity and become unity at approximately the end of the transition phase, just when the HeII λ 4686 emission becomes visible. It is then evident that hydrogen and HeII lines are produced in different regions around the hot central object. All these phenomena are actually the consequence of a unique basic physical process, that is the dilution of the expanding envelope and the consequent variation of the optical depths and the velocities of the regions that are responsible for the emission of the different ions. In 1947, the nebular spectrum was still strong, with very structured emission lines.

IV.C. THE NEBULA

The expanding nebula was for the first time observed by Zwicky (1956) when it had a radius of 2.78". Distance determinations based on several methods, including the nebular parallax, have been discussed by Duerbeck (1981), who gives the revised value of 1500 pc, based on new photographs of the nova (Duerbeck and Seitter, 1979). The nebula is shown in Figure 8-30. Its structure is, according to Williams (1982), "moderately symmetric, reminiscent of a wheel with spokes emanating from the center and extending out to a roughly circular rim." Williams (1982) has given a detailed spectroscopic study of the nebula when it was 14" in diameter. Two hours of exposure spectra of the nebula, taken in the blue and in the red spectral region, are presented in Figure 8-31. Table 8-3 gives the emission line fluxes.

Williams emphasized two peculiarities of the spectrum of the nebula.



Figure 8-30. The shell of CP Pup 1942. H_α + [NII] CCD image taken by H W. Duerbeck with the 2.2 m ESO telescope.

The first is the presence of a broad emission feature at about λ3600, which might originate from Balmer continuum recombination of low-velocity electrons. If it is that, then the temperature of the nebula would be rather low, T = 800 K, for collisional excitation of the observed forbidden lines.

The second observed peculiarity is that the nebula contains permitted and forbidden lines of NII with comparable fluxes. Normally, forbidden lines of nebular spectra are 10^3 times the intensities of the permitted lines. The solution suggested by Williams is that excitation of all the levels occurs by recombination. Table 8-4 lists those transitions of the C,N,O elements which may produce the strongest optical lines in the recombination spectra of each of the five lowest ionization stages. Quantitative estimates can be made for the relative abundances of the H, He, and N elements, since line identifications and fluxes were well determined for ions of these elements. Assuming that lines are formed by recombination, and that the resonance lines are optically thin due to the very large differential expansion velocities for nova

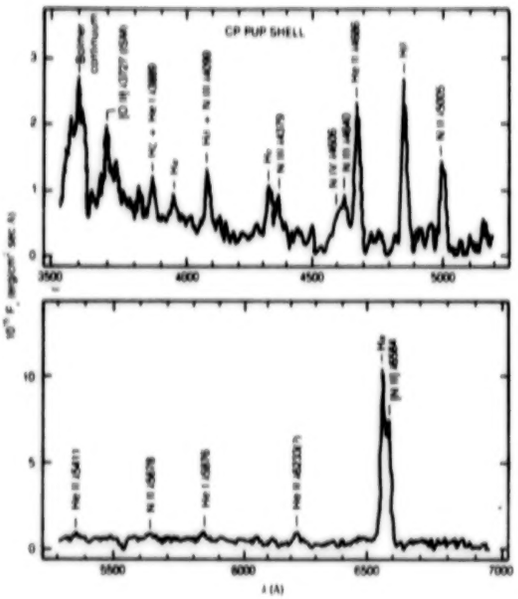


Figure 8-31. Blue (top) and red (bottom) spectral scans of the expanding shell of CP Pup obtained by R P Williams. Line fluxes are given in Table 1. (From Williams, 1982).

TABLE 8.3 (*)

EMISSION-LINE FLUXES FOR THE CP PUPPIS SHELL

Measured Wavelength (Å)	Line Identification	Relative Flux [3] (Hβ=100)
3638	H I Balmer cont.	...
3720	[O II] λ3727 (ISM)	21
3886	Hζ+He I λ3889	20
3969	Hε	13
4101	Hδ+N III λ4099	28
4341	Hγ	26
4380	N III λ4379	19
4608	N IV λ4606	
4640	N III λ4640	52
4682	He II λ4686	92
4860	Hβ	100
5004	N II λ5005	44
5407	He II λ5411	7
5672	N II λ5678	9
5875	He I λ5876	19
6233	He II λ6233 (?)	23
6560	Hα	300:
6580	[N II] λ6584	200:

[3]Fluxes of lines in the red (scan (λ >5300 Å) have been arbitrarily normalized such that Hα = 300. The absolute H β flux of the portion of the shell we sampled (~20% of the entire shell) was $F_{H\beta} = 5.8 \times 10^{-15}$ ergs cm^{-2} s^{-1}.

(*) From Williams (1982)

TABLE 8.4 (*)

STRONGEST OPITCAL RECOMBINATION LINES FROM CNO IONS[a]

Carbon	Nitrogen	Oxygen
C I ($2p^2\ ^3P$):	N I ($2p^3\ ^4S^0$):	O I ($2p^4\ ^3P$):
Triplets: none in visible	Quartets: $3s^4P$–$3p^4D^0$ λ8692	Quintets: $3s^5S^0$–$3p^5P$ λ7773
Singlets: $2p^2\ ^1P$–^1D [λ9849]	Doublets: $2p^3\ ^4S^0$–$^2D^0$ [λ5200]	Triplets: $3s\ ^5S^0$–$3p\ ^3P$ λ8446
C II ($2p\ ^2P^0$):	N II ($2p^2\ ^3P$):	O II ($2p^3\ ^4S^0$):
Doublets: $3d^2\ D$–$4f\ ^2F^0$ λ4267	Triplets: $3p^3\ D$–3d $^1F^0$ λ5005	Quarters: $3s\ ^4P$–3p $^4D^0$ λ4652
	Singlets: $2p^2\ ^1P$–^1D [λ6584]	Doublets: $2p^3\ ^4S^0$–$^2D^0$ [λ3727]
C III ($2s^2\ ^1S$):	N III ($2p^2\ P^0$):	O III ($2p^2\ ^3P$):
Triplets: $4f\ ^3F$–$5g\ ^3G$ λ4069	Doublets: $4f\ ^2F^0$–$5g\ ^2G$ λ4379	Triplets: $3p\ ^3D$–$3d\ ^3F^0$ λ3266
		Singlets: $2p^2\ ^1P$–^1D [λ5007]
C IV ($2s\ ^2S$):	N IV ($2s^2\ ^1S$):	O IV ($2p\ ^2P^0$):
Doublets: $5g\ ^2G$–$6h\ ^2H^0$ λ4660	Triplets: $5g\ ^1G$–$6h\ ^1H^0$ λ4606	Doublets: $5g\ ^2G$–$6h\ ^2H^0$ λ4633
C V ($1s^2\ ^1S$):	N V ($2s^2S$):	O V ($2s^2\ ^1S$)
Triplets: $6h\ ^1H^0$–$7i\ ^1I$ λ4946	Doublets: $6h\ ^2H^0$–$7i\ ^2I$ λ4946	Triplets: $6h\ ^1H^0$–$7i\ ^1I$ λ4932

[a]The ground-state configuration of each ion is given in parentheses.

(*) From Williams (1982)

shells, Williams found that, for $T=10^3$ K, the He/H relative abundance of the CP Pup envelope is 0.12. Similarly, it resulted in N/H > 0.1. The strong abundance of N is characteristic of every classical nova.

IV.D. THE NOVA AT LIGHT MINIMUM-THE BINARY SYSTEM

The postoutburst apparent magnitude of CP Pup is ~ 15.0 mag; that is, at least three magnitudes brighter than it was before the outburst. This fact seems to be an exception, since Robinson (1975) has shown that the luminosities of novae before and after the outbursts are essentially the same. It is quite interesting, however, to note that a similar situation is occurring also to nova Cyg 1975. Why should these two very fast novae take such a long time to reach light minimum? It is possible that after an outburst, these systems remain for some time in a perturbed state either due to the secondary (high mass-loss), or to the white dwarf component.

CP Pup is a strong soft X-Ray source (Becker, Marshall, 1981; Cordova, et al., 1981a) and might be also variable by a factor of 10, at least, with a softer spectrum associated with a higher flux.

The old nova is now known to be a very-short-period binary system having the characteristics of the intermediate polar subclass of cataclysmic variables. This situation might perhaps explain the suggested excited state of the system, since one of the characteristics of intermediate polars is the presence in the system of some particular active regions that greatly contribute to the emitted radiation field.

Spectroscopic observations of CP Pup were carried out at the European Southern Observatory, La Silla, by Bianchini et al. (1985 a), Duerbeck et al. (1987) and Krautter (unpublished data).

The orbital period of CP Pup was independently discovered by the spectroscopic observations performed by Bianchini et al. (1985 a, b; see also Figure 6-2), and by the photometric observations carried out by Warner (1985b). Due to the poor signal to noise ratio of the spectra and also to the intrinsic strong variability of the nova, the modulation observed in the radial velocity curve couldn't give a precise determination of the period. For this reason, Bianchini et al. used several methods: line baricenters gave P = 0.0605 and P = 0.0571 days while line peaks gave 0.06115 days. The latter fit was probably clearer than the other ones and was adopted.

High-speed photometry performed by Warner (1985b) revealed a light curve whose morphology looks very similar to that of V 1500 Cyg (nova Cygni 1975), having a period of 0.06614 or 0.06196 days, that is slightly longer than the spectroscopic one (Figure 8-32).

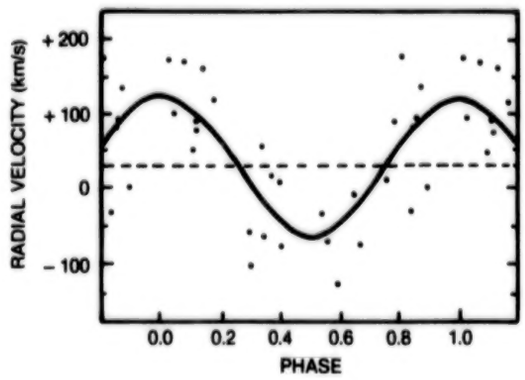


Figure 8-32. The radial velocity curve for the emission lines of CP Pup. (from Duerbeck et al., 1987).

Duerbeck et al. (1987) used Bianchini et al.'s (radial) velocities and 29 other ones determined from IDS spectra taken in December 1982. The spectroscopic period could then be refined to 0.061422 ± 0.000025 days, which is definitely shorter than the photometric period (1% and 7% shorter than the shorter and, respectively, the longer period found by Warner, and close to the original period proposed by Bianchini et al., see Figure 8.32). Thus, the behavior of CP Pup reminds us of Su Uma systems during superoutbursts, when the observed photometric periods of superhumps are systematically different by a few percent from the spectroscopic (i.e., orbital) ones (Warner, 1985b). Warner and Livio (1987) have sug-

gested that the period distribution of CVs below the period gap is characterized by a clustering of SU Uma's and Polars into separate period ranges. According to this scheme, the observed orbital period of CP Pup would fall in one of the period ranges favored by polars.

The amplitude of the radial velocity curve is determined by Duerbeck et al. (1987) to be 91.6 ± 17.6 Km/s (new data only), or 68.3 ± 11.0 Km/s (all radial velocity data). If this period and amplitude are interpreted as orbital motion, and since no eclipses were observed by Warner, Duerbeck et al. derive the following masses:

M (secondary) = 0.14 $M_\odot$, approximately an M7 V star

M (primary) $\leq$ 0.86 $M_\odot$ (all data)

$\leq$ 0.50 $M_\odot$ (new data only).

If the inclination of the system is estimated to coincide with some nebula features, i ≈ 30 ± 5°, then these authors obtain

M (primary) = 0.27 $M_\odot$ (all data)

= 0.12 $M_\odot$ (new data only).

These values are very low, much too low for any theoretical model of a white dwarf experiencing a TNR.

V. GK PER 1901
(written by Bianchini)

V.A. INTRODUCTION

Nova GK Per 1901 has been the first classical nova to be adequately observed from the early to the late stage. It was discovered by Rev. T. D. Anderson on February 21, 1901, before the light maximum, which was reached two days later, at visual magnitude 0.2. A detailed comparative description of all the available observational data of the nova during the outburst has been given by McLaughlin (1969). The photometric and spectroscopic evolution was that of a fast nova, with a speed of decline of about 0.13 magnitudes per day, an outburst amplitude of about 13.0 magnitudes, and an expansion velocity of the ejecta which ranged from 1000 km/s, for the Absorption I system, to 3800 km/s, for the Orion system. During the "transition phase", i.e., between 3.5 and 6.0 magnitudes below the light maximum, the nova presented strong light fluctuations which, unlike for other novae, were not correlated with the variations of the Orion absorption system velocity (Friedjung 1966c). The nebular shell surrounding the old nova presents an asymmetric shape, probably due to its interaction with a dense and structured circumstellar environment in which Bode et al. (1987b) have discovered the presence, around the nova, of an ancient planetary nebula remnant. The return of GK Per to light minimum was complicated by strong light fluctuations that lasted until the forties. Later, the old nova settled down to a more quiescent state, at about magnitude 13.0, but, since that epoch, the nova has shown occasional well-defined optical outbursts. Several of the peculiarities of GK Per at light minimum have been reviewed by Bianchini et al. (1986).

Probably, the most peculiar characteristics of GK Per as an old nova are its relatively long orbital period, almost two days (but this is still subject of controversy), and its dwarf nova-like behavior, which would place this object between the classical novae and the dwarf novae subclasses of cataclysmic variables.

From the beginning, GK Per was seen to be an exceptional object, and we can assert today that the study of the many peculiarities shown by this nova, both during the main outburst and at quiescence, has strongly contributed to the understanding of the nova phenomenon and of the long-term evolution of cataclysmic variables.

We wish here to emphasize some of the more unique aspects of this important nova.

V.B. PECULIARITIES OF GK PER DURING THE 1901 OUTBURST

Following the chronology of the events, the first peculiarity can be found by analyzing the behavior of the nova during the so-called tran-

sition phase which started at 3.5 magnitudes below maximum, when strong light fluctuations with a range from 1 to 1.5 mag and a period from 3 to 5 days suddenly appeared (Figure 8-33). This phenomenon lasted for more than 3 months. At each minimum of the light curve, the spectrum of the nova changed towards the nebular type with a weaker continuum and stronger high-excitation emission lines of [NeIII], [OIII] NIII, HeII, and the unidentified band at λ4726. At light maxima, these lines were weaker or even disappeared, indicating decreased temperatures and increased densities in the line-emitting region. In particular, the [NeIII] λ3869 and the [OIII] λ5007 emission showed variations of two kinds: (1) they invariably weakened at light maxima and became very strong in coincidence of the minima; (2) at each succeeding light minimum, these forbidden lines emerged in greater strength, and at each succeeding light maximum, their extinction was less complete.

At the end off the transition phase, the spectrum of the nova was purely nebular.

These phenomena are believed to be common to all those novae that show oscillations during their transition phase.

Two aspects of the oscillatory phenomenon in GK Per however, are, quite unusual and then worthy of note. The first is that the time intervals between successive light maxima varied with time in a sinusoidal fashion and that the period, amplitude, and mean value of this sinusoid increased with time. In other words, the light fluctuations had a period that was oscillating between two extreme values that were monotonically increasing with time, as shown in Figure 8-33.

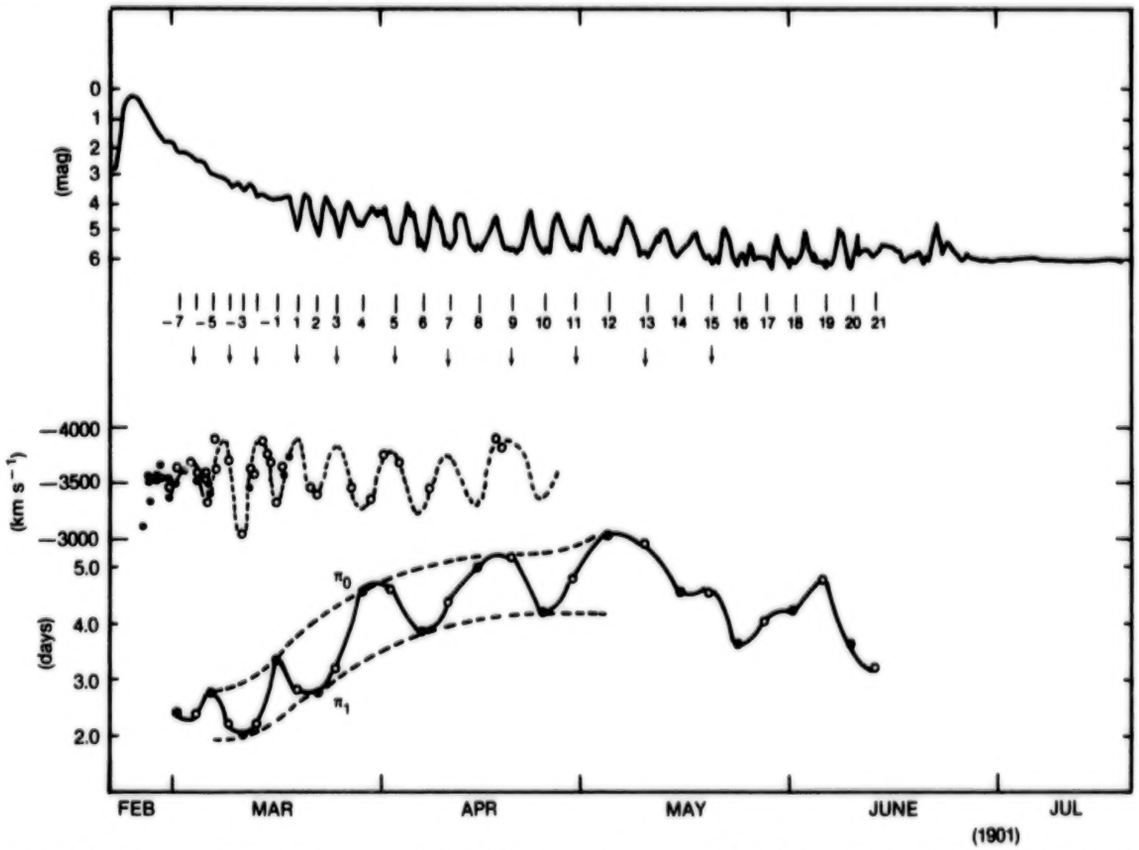


Figure 8-33. The oscillatory phenomenon during the transition phase of GK Per. Top pannel: the light curve of the early decline shows small amplitude oscillations, which might be correlated with the stronger oscillations of the transition phase. - Central pannel: the variations of Orion velocities (from McLaughlin, 1969) show that the negative maxima of the velocity of the ejected wind occur every two minima of the light curve. - Bottom pannel: the sinusoidal variation with time of the period of the oscillations. The period oscillates between two extreme values (dashed lines), which could represent the fundamental period and the first overtone of an n=3 radially pulsating, slowly expanding (v~2 Km/s) polytrope.

The second peculiarity of the transition phase of GK Per is that the radial velocity variations of the highly blueshifted absorption components of the diffuse-enhanced spectrum and of the Orion spectrum are not correlated with the light oscillations in the same way as for other novae. Friedjung (1966c) showed that the observed negative Orion velocities and the calculated photospheric radii—or the magnitudes—of some novae during the oscillations of the transition phase were inversely—directly, respectively—correlated; the only known exception seemed to be GK Per (see Figures 7-14, 7-15, and 7-16). A reanalysis of the photometric and spectroscopic data has revealed that a correlation similar to that known for other novae is still possibe for GK Per, provided that we assume that the negative maxima of the Orion velocities of this nova have a period that is all the time twice that of the light fluctuations. In Figure 8-33, we can, in fact, see that the negative maxima of the Orion velocities occur every two minima of the light curve. We can also note that the first decline of the light curve is not smooth but shows small amplitude oscillations that might represent the ideal backward extrapolation of the stronger oscillatory phenomenon of the transition phase. In fact, both the dependence with time of the maxima during the early decline and the correlation between the light minima and the negative maxima of the Orion velocities seem to have the same character as observed during the transition phase. Besides their different amplitudes, the principal difference between the small light fluctuations of the early decline and the larger ones of the transition phase is the appearance during the deeper minima of the latter phase of a genuine nebular spectrum. Thus, what we probably observe is the combined effect of an oscillatory phenomenon that starts immediately after the explosion of the nova and of the constant decrease with time of the density of the expanding shell. When a critical value of the density is reached, the outer expanding envelope becomes optically thin and the underlying pulsating object, whatever it might be, can be finally observed. This picture could actually agree with the fact that the two portions of the light curve immediately before and after the transition phase cannot be reconciled with a unique continuum slope. In fact, the first decline would fit only the maxima, while the second portion of the light curve seems to follow the slope indicated by the minima.

Since the light oscillation are not correlated in a simple way with the velocity changes of the Orion spectrum, we suggest that, at least in the case of GK Per, the light variations cannot be directly caused by changes in the velocity of the continuously ejected optically thick wind, as it is usually suggested for the other novae. The fact that the radial velocity changes of the Orion spectrum appeared rather large, even during the early decline, when only minor light oscillations were observed, could support the previous conclusion. Looking at Figure 8-33, one could even argue that these light oscillations start soon after the explosion with a period of about 2 days, which is close to the orbital period of the underlying binary system. Thus, the possibility arises that the luminosity fluctuations are triggered by binary motion inside a pulsating extended atmosphere, which is sustained by the radiation pressure produced by the hot central object. However, we do not observe the spectrum of such an expanded object but, more probably, that produced by a structured optically thick wind. We must then conclude that the physical mechanism responsible for the particular photometric and spectroscopic behaviours so far described is still not understood.

After the transition phase, GK Per settled down to a very slow decline towards its minimum light, which was reached several years later. As we have said, the spectroscopic evolution was typical of a fast nova with the normal sequence of slow changes from the nebular spectrum, where the [OIII] lines are predominant, to that typical of a cataclysmic variable, leaving the λ4686 and the Balmer emission as the strongest lines. A rapid fading of the nebula relative to the star was observed at the end of 1903 and during 1904, as shown by the weakening of [Ne III] relative to hydrogen and by the disappearance of [O III]. The historical mini-

mum of the visual light curve of the nova, m_v ~15, was reached in 1916. However, as we will see later on, since the mid-forties, the magnitude of the quiescent nova has remained at about m_v ~13.1.

V.C. THE PECULIAR EXPANDING NEBULA AND CIRCUMSTELLAR ENVIRONMENT

Another peculiarity of GK Per appeared in the autumn of 1901, when an apparent shell was seen to be expanding from the star at roughly the speed of light, such a high velocity being inferred from the apparent expansion velocity of the shell and an estimate of the lower limit of the distance to the nova that does not show any parallax effect. This shell is distinct from the shell of gaseous ejecta that was clearly seen only two decades later. Ka-pteyn first proposed that the high-velocity shell was due to a "light echo" from the burst of the nova light being reflected by interstellar dust. In all generality, such an apparently expanding nebula could be produced by the illumination of a sheet of material anywhere either beyond the nova or between it and the earth. In 1939, Couderc (1939) refined this model, showing that the illuminated dust seen by the earth at any time must describe an ellipsoid of revolution whose foci are the nova and the observer. On this principle, Couderc had calculated the location of the illuminated nebula, which resulted in a plane sheet placed between the nova and the observer at about 46 light-years from the nova and inclined about 45° to the line of sight. Actually, the presence of much circumstellar material is confirmed by the measures of the reddening, which can be easily determined from the intensity of the λ2200 dip observed in the UV spectra of the nova (Bianchini et al., 1986). The E(B-V) result was of the order of 0.35. The light echo was mainly visible south of the nova.

But the important discovery by Bode et al. (1987b) of an ancient planetary nebula surrounding the old nova has provided the basis for a new interpretation of the circumstellar environment and, obviously, of the evolutionary history of this interesting close binary system. The nebula was discovered by analysing several Infrared Astronomical Satellite (IRAS) images of the GK Per region. Extended emission was detected in both the 60- and 100-μm bands. Figure 8-34 shows the 100-μm map of the region with a superimposed sketch of the disposition of the mentioned 1901 light-eco. Bode et al. (1987) have estimated a grain temperature of about 22°K, a density of 2.2 g cm^{-3} and a total mass of the emitting dust of 0.058 $M_\odot$, which would imply a large mass for the gaseous component. Actually, new 21-cm HI observations performed by Seaquist et al. (in preparation) led to an HI mass of $\geq$0.6 $M_\odot$. This mass is 10^4 - 10^5 times greater than that found in classical nova envelopes. According to Bode et al. (1987), the $\leq$5 Km s^{-1} expansion velocity of the gas would suggest that GK Per, as a nova, is a relatively young object, not much older than 10^5 years, and the 1901 outburst might have been the first one from this system.

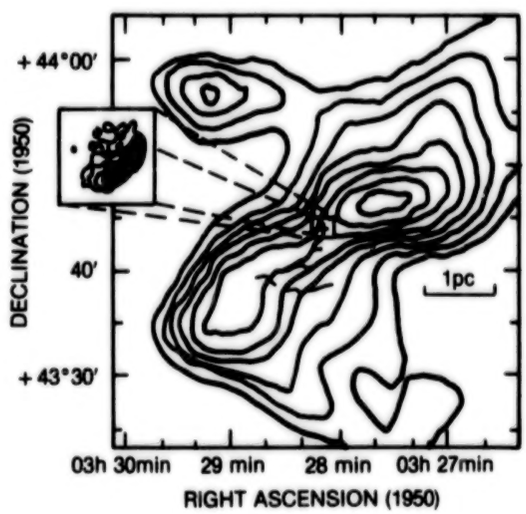


Figure 8-34. IRAS 100-μm map of the region around GK Per. Contours range from 1.5 MJy sr^{-1} to 5[illegible] MJy sr^{-1}. The position of the nova is marked. The inset shows a 5-GHz radio map of the nonthermal radio emission of the central interaction region of the expanding shell. Superimposed is also a sketch of the disposition of reflection nebulosity from a Lick Observatory plate taken on 12-13 November 1901 (from Bode et al., 1987b).

The nebula ejected by GK Per during its nova outburst is also peculiar. It has the shape of a prolate ellipsoid (Figure 8-35), but with

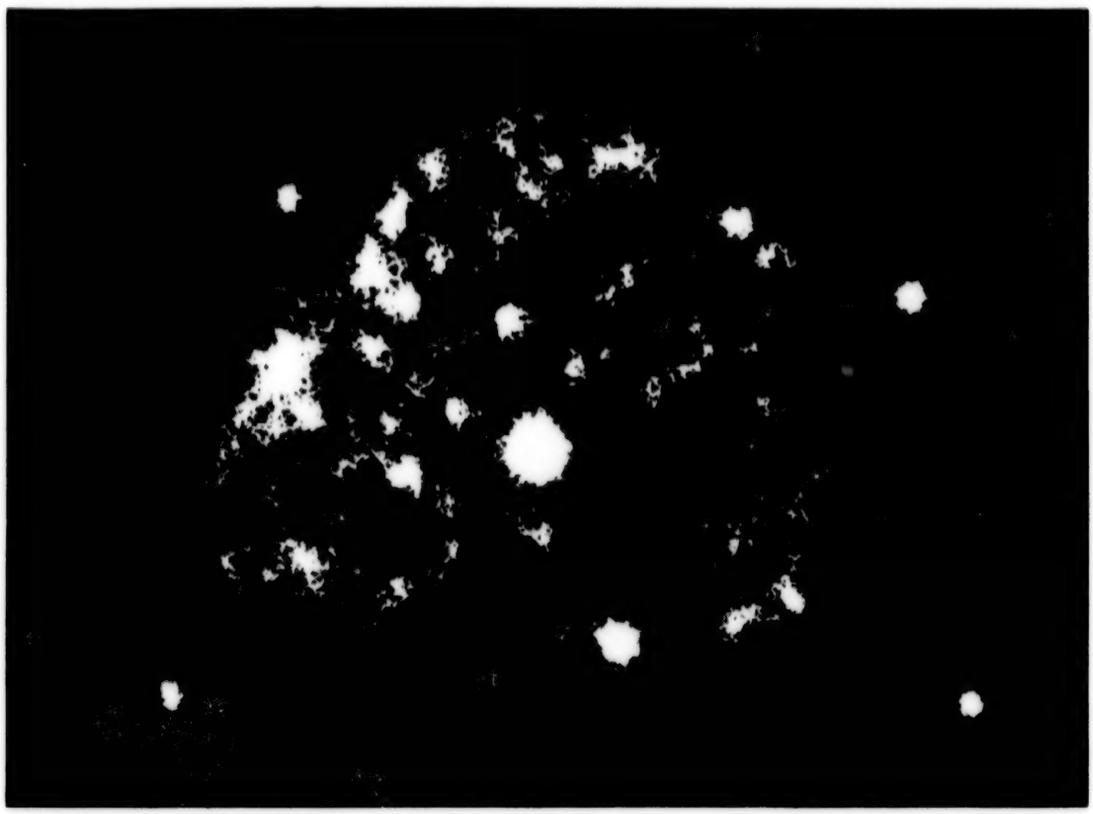


Figure 8-35. The nebula of GK Per. The distribution of matter is asymmetric and the material is concentrated into blobs. The interaction of the shell with the interstellar medium is responsible for the formation of the S-W front

the matter non equally distributed, the southwest portion of it being the more luminous. The material of the shell looks concentrated into blobs of variable size whose trajectories during the expansion can be determined by comparison of plate images taken at different epochs. The interaction of the expanding nova shell with the interstellar medium was discussed by Duerbeck (1987a) who determined the deceleration of the shell and more reliable distance to the nova: 390 pc. A detailed reconstruction of the three-dimensional image of the shell of GK Per was obtained, using more than 200 blobs, by Seitter and Duerbeck (in "An Atlas of Nova Shells", in preparation; see also Seitter and Duerbeck, 1987). Monochromatic images of the nebula taken by these authors revealed differences in the distribution of light concentrations from the different ions that do not exclude different chemistries for polar and equatorial regions as shown in Figure 8-36. Radio (Reynolds and Chevalier, 1984) and optical (Williams and Ferguson, 1983) observations revealed the presence on the nebula of shocks and turbulent processes which are similar, although far less energetic, to those acting in supernova remnants. In particular, the radio map of the shell (see Figure 6-77), shows that the emission is concentrated in the southern region of the sky around the nova, in complete analogy with all the preceeding results. It is then possible that the interaction of the ejecta with the interstellar material is, at least partially, responsible for the observed energetics.



Figure 8-36. The [OIII] image subtracted from the Hα + [N II] image of the nebula of GK Per. North is to the left, west to the top (from Seitter and Duerbeck, 1987).

V.D. PECULIARITIES OF GK PER AS A CATACLYSMIC BINARY

The old nova GK Per was discovered to be a Close Binary System by Kraft (1964).

The results obtained by several authors have demonstrated that, among classical old novae, GK Per can be considered an exceptional object for the following reasons:

1) The most probable orbital period is unusually long. It has been subject of controversy (Kraft, 1964; Paczynski, 1965). Bianchini et al. (1981) found an eccentric orbit (e=0.4) and an orbital period quite close to that given by Kraft (P = 1.904 days). A more extended and detailed spectroscopic study of the radial velocity variations of both the white dwarf and the K2 secondary, done by Crampton et al. (1986), revealed circular orbits and a period of 1.996803 days (Figure 8-37). According to these authors, since no eclipse has ever been observed, the inclination of the system should be < 73° so that the most probable masses for the two components are M(K2) = 0.25 $M_\odot$ and M(WD) = 0.9 $M_\odot$ (Figure 8-38). Thus, apparently, only about one-quarter of the original mass of the K star remains. This also implies that the secondary is a slightly evolved star, perhaps stripped to its helium core.

More recently, this already uncertain scenario has been further complicated by a reanalysis of Crampton et al.'s original data carried out by Kurochkin and Karitskaya (1986). These authors found that the two-day variation itself is modulated with a period of 0.131623 days. The amplitudes of these smaller radial velocity variations are of only 15 Km/s for the absorption lines and 20 Km/s for the emission lines. If this shorter period is orbital, the masses of the two components could be 0.8 $M_\odot$ for the white dwarf, and 0.6 $M_\odot$ for the K star. Should this result be confirmed, then the two-day periodicity could be tentatively ascribed to the preces-

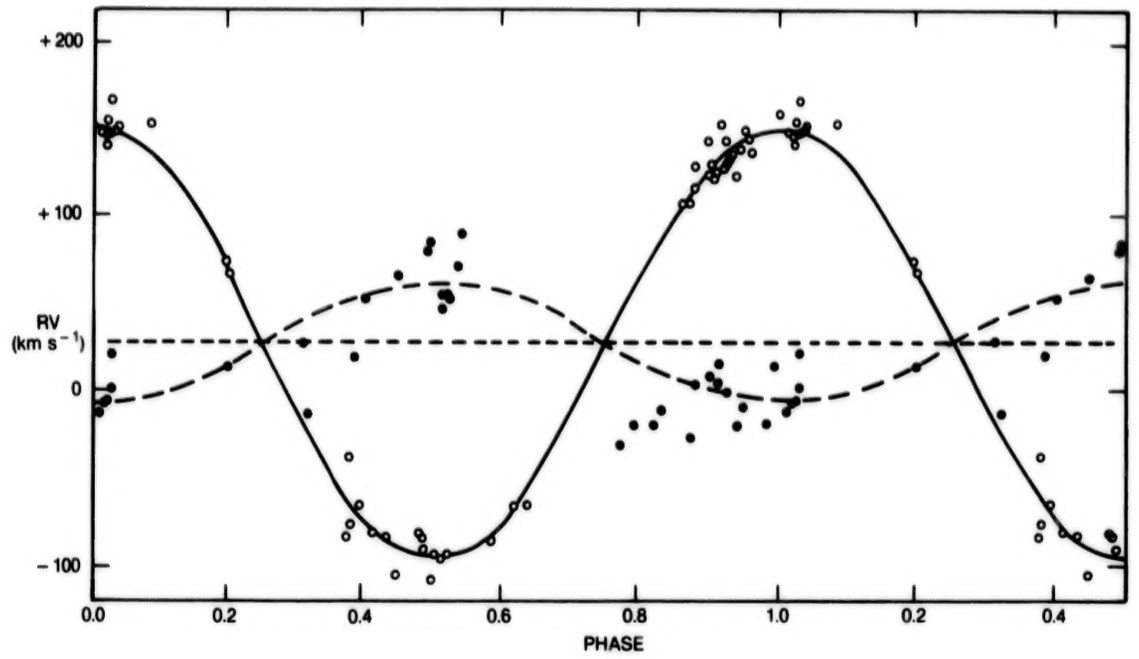


Figure 8-37. The radial velocity variation as a function of the orbital phase. Open circles represent the absorption lines, filled circles are measures of the positions of the wings of Hβ. Least-squares orbital fits are also shown (from Crampton et al., 1986).

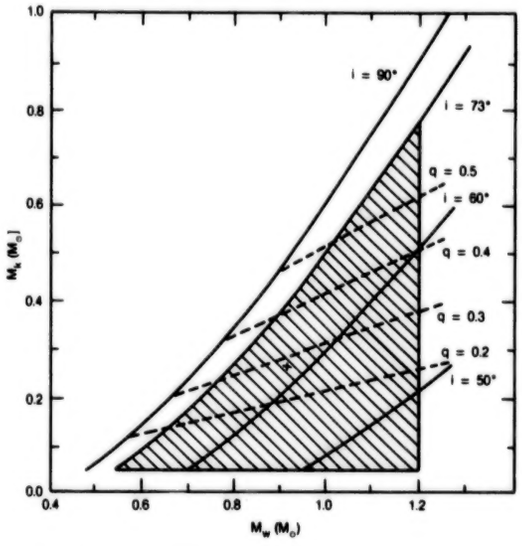


Figure 8-38. A diagram showing how the mass of the K star (M_k) varies with the mass of the white dwarf component (M_w) for different values of the inclination and mass ratio. Since eclipses have not been observed, i ≤73°, and M_w must be less than the Chandrasekhar limit, 1.2$M_\odot$. The cross marks the position of the most probable masses of the components (see text). (from Cramper et al., 1986).

sion of the eccentric, e = 0.4, orbit or to the presence of a third body. Needless to say, further detailed spectroscopic observations are badly required.

2) The nova at quiescence presents an outburst activity reminiscent of that of certain long-period dwarf novae, e.g., BV Cen. As an example, Figure 8-39 shows the light curve of the novae in the years 1969-1983. The duration of the optical outburst of GK Per is one or two months. The amplitudes range from one to three magnitudes. The outburst profiles tend to be symmetric, especially for the largest outbursts. The observed recurrence times are variable, but all of them seem to be submultiples of 2400 days. This sort of quasi-periodicity is illustrated in Figure 8-40. A classification scheme for the outbursts is suggested in Figure 8-41.

According to Bianchini et al. (1986) and Cannizzo and Kenyon (1986), most of the observational characteristics of the optical outbursts of GK Per can be explained by disc instability episodes starting from the inner edge of the accretion disc, where an unstable transition region is formed if the mass transfer rate from the secondary is slightly larger than $10^{16}gs^{-1}$. However, as we will see, some observational facts are suggesting that we are probably still missing the correct interpretation of the out-

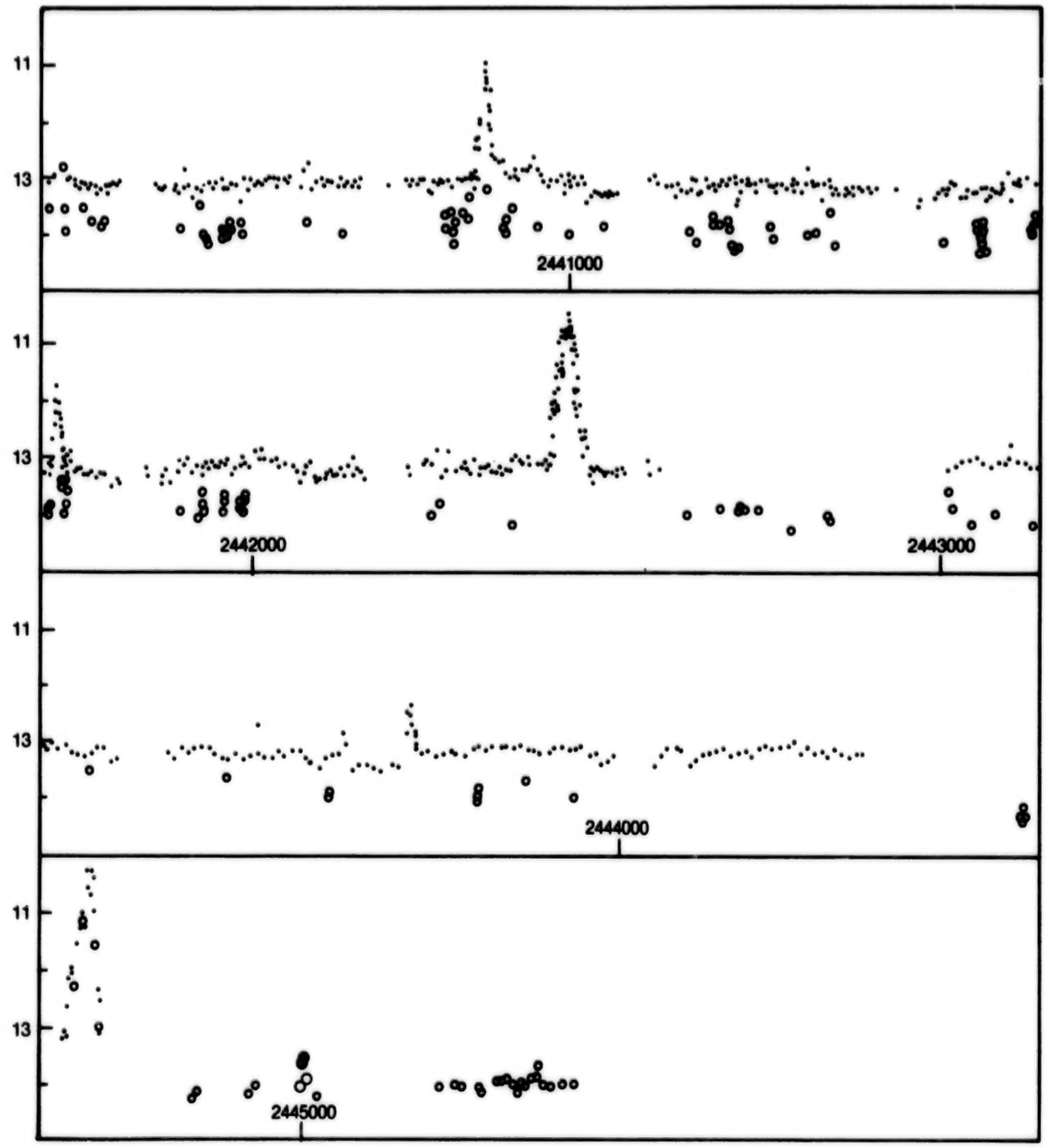


Figure 8-39. The light curve of GK Per in the years 1969-1983. Optical outbursts occurring in 1970, 1973, 1975, 1978, and 1981 are clearly visible (from Sabbadin and Bianchini, 1983). Circles: B; dots: v.

burst phenomenon in GK Per. The phenomenology connected to this important property of the old nova will be discussed further on in this review.

3) While most old novae are completely dominated in the blue spectral region by light coming from the accretion disc and the boundary layer, the spectrum of GK Per at light minimum (Figure 8-42), shows also the presence of a K2 IV-V companion (Kraft, 1964; Gallagher and Oinas, 1974). We note that the spectroscopic detectability of the secondary might be consistent with the assumption of the longest orbital period, since this would require the presence of a larger and brighter Roche-lobe filling secondary. It might be consistent also with the suggested low mass accretion rate, since this would imply a relatively low luminosity of the disc, at least compared to that of other classical old novae (Warner 1987a).

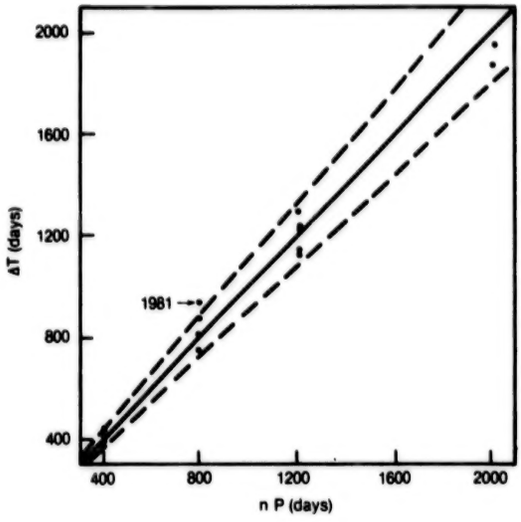
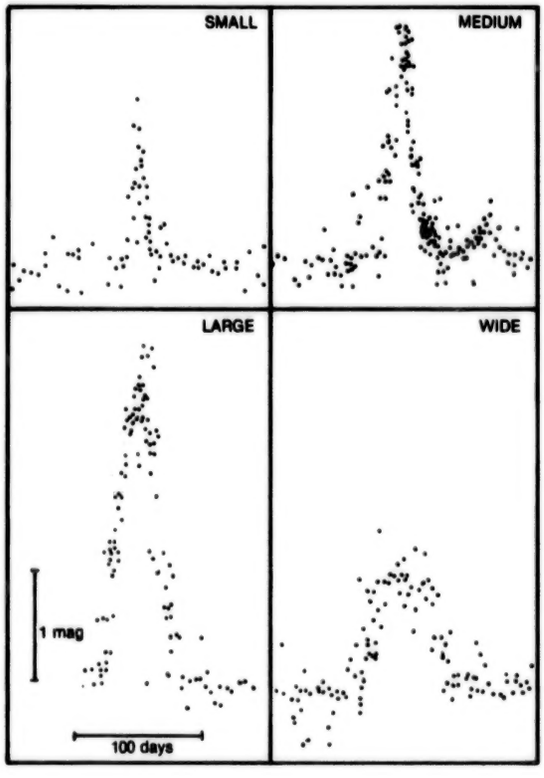


Figure 8-40. The $\Delta T=n(400\mp40)$ days relation between successive outbursts; only the 1981 outburst is clearly outside the error bar of ∓40 days (from Bianchini et al., 1986; except the point relative to the 1986 outburst).

4) In spite of the presence of high excitation emission lines, the UV continuum from the nova is unusually weak and flat. Bianchini and Sabbadin (1983) showed that the UV to IR continuum energy distribution, corrected for E(B-V) = 0.15, is peaked at λ3600. However, even applying a correction for E(B-V) = 0.35, as derived from the UV spectra of the nova in outburst, the continuum energy distribution in the UV remains rather flat and approximates that expected from the standard model of a semiinfinite accretion disc, i.e., F proportional to $\lambda^{-2.33}$, only during the optical outbursts (see Figure 8-43). Bianchini and Sabbadin (1983) suggested that the particular spectrum emitted by GK Per could be explained by assuming that the accretion onto the white dwarf is controlled by a magnetic field that is strong enough to disrupt the inner part of the accretion disc. Bianchini et al. (1986) suggested that the probable value of the mass transfer rate at quiescence is about 10^{16} gs^{-1}. This value of the mass transfer rate is rather low for a classical nova, but it would correspond to that needed by the theory if we assume that the outburst is produced by the disc instability mechanism starting near the inner edge of the disc and propagating outward as explained in Section V.E.4.

a)



b)

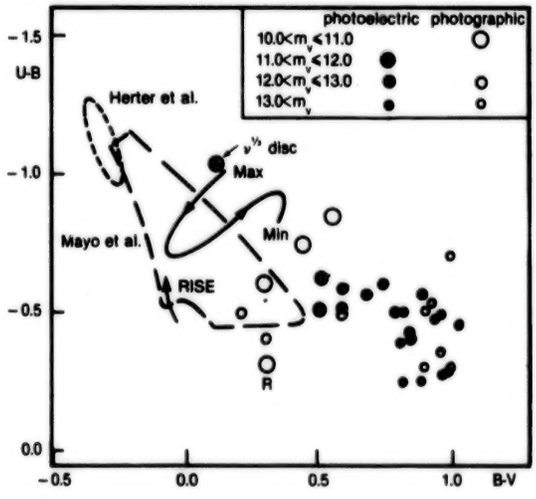


Figure 8-41. a) Average photometric properties of the four types of outbursts identified in the light curve of GK Per (from Bianchini et al., 1986). b) two color diagram.

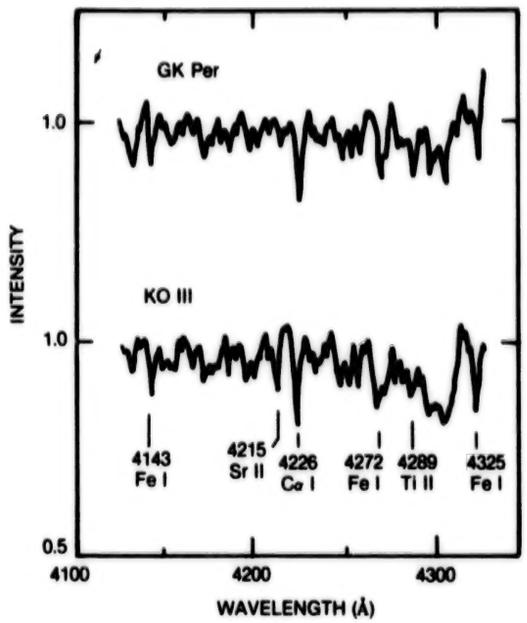


Figure 8-42. Portion of the mean spectrum of GK Per (upper) compared to that of a KO III star (lower) (from Crampton et al., 1986).

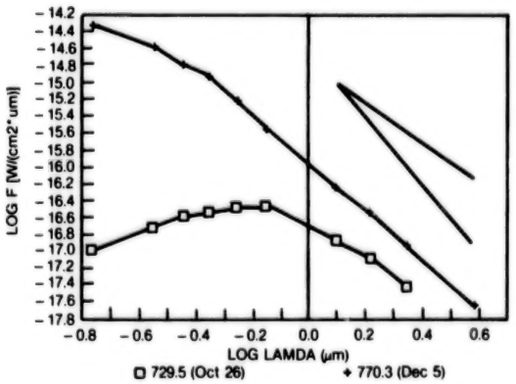


Figure 8-43. The UV to IR continuum energy distribution of GK Per at quiescence, corrected for E(B-V) = .1, and during the 1986 light peak, corrected for E(B-V) = 0.35. If we adopt E(B-V) = 0.35 also at light minimum the continuum in the UV becomes flat (see text). The $\lambda^{-2.33}$ and the λ^{-4} slopes are also shown.

5) GK Per is a hard x-ray transient. Although the near UV is faint, the x-ray emission from the nova is particularly strong and increases during the optical outbursts (King et al., 1979; Cordova et al., 1981b; Watson et al., 1985). The hard x-ray luminosity of the old nova at quiescence is between 2 x 10^{32} erg s^{-1} (Cordova and Mason, 1984) and 7 x 10^{33}erg s^{-1} (Bianchini and Sabbadin 1983). During an optical outburst, it can amount to about 10^{34} erg s^{-1} (King et al., 1979; Watson et al., 1985).

6) The old nova GK Per is an intermediate polar. During the 1983 large outburst, the nova was observed with the EXOSAT instrument by Watson et al. (1985), who detected a strong coherent modulation of the hard x-ray flux of about 80%, having a period of 351 s. Superposed to this, a longer term modulation on time scales of 0.8÷1.5hr was also observed (see Figure 8-44). The detection of the shorter highly coherent periodicity would then identify GK Per as a member of the so called 'intermediate polar' subclass of magnetic cataclysmic variables.

7) Part of the infrared radiation emitted by the system could come from the outer cooler regions of the accretion disc. Infrared observations (JHKL) performed by Sherrington and Jameson (1983) were interpreted in terms of the infrared radiation coming from the cool companion. However, several JHKL flux determinations secured at Asiago and TIRGO Observatories by F. Stafella and D. Lorenzetti show that, at some epochs, the nova may vary on time scales of few hours over a range of a few tenths of magnitude. As shown previously in Figure 8-43 the slope of the continuum energy distribution in the infrared does not change too much during an outburst and approximately fits that of the "standard" accretion disc model (a quite different behavior is observed in the UV). So we argue the infrared continuum is not principally produced by the cool secondary component of the binary system; most probably, the cooler outer regions of the large accretion disc, which is formed around the collapsed object, may give a significant contribution to the IR radiation field also

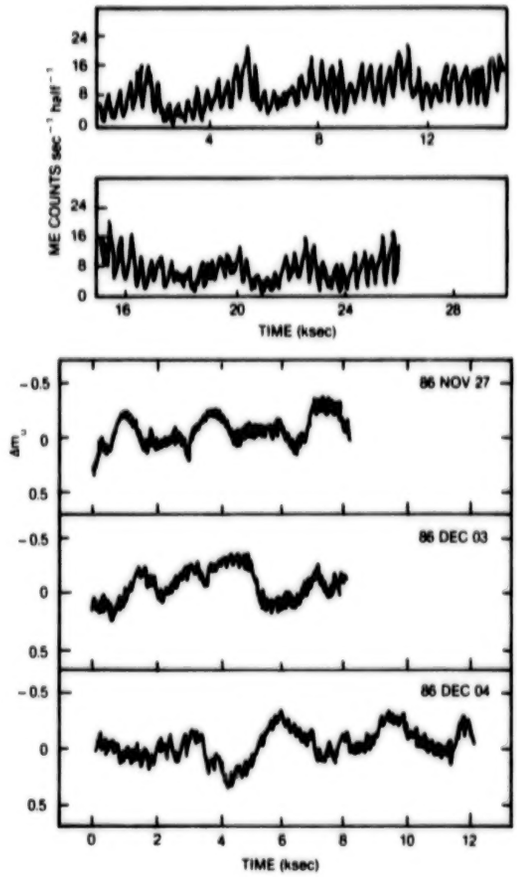


Figure 8-44. The EXOSAT hard X-ray light curve of GK Per during the 1986 outburst (from Watson et al., 1985) compared to the optical one (Stagni et al., in preparation). The 351 s coherent modulation is observed only in the X-ray region. The flickering observed in the U band, in fact, does not show any clear and steady periodicity. A .8-1.5-hr modulation can be seen both in the x-ray and in the optical.

at quiescence. This would again play in favour of the longest orbital period.

V.E. THE SMALL POSTNOVA OPTICAL OUTBURSTS OF GK PER

The most striking characteristic of the light curve of GK Per at quiescence is its nonquiescent character and, in particular, its "dwarf-nova-like" behavior. The amplitude, duration, rise, and decay times of the optical outbursts vary from case to case. As shown back in Figure 8-41, we can identify four types of outbursts. The rise to decay-time ratio is about 0.5 for "small" outbursts, like those that occurred in 1973 and 1978 ($\Delta m \sim 1.0$ mag); 0.7 for "medium" outbursts, like those of 1949, 1966, and 1970 ($\Delta m \sim 1.0$ mag), 2.0 for "large" outbursts, like those of 1967, 1948 (?), and 1950 (?) ($\Delta m \sim 2.0$ mag); and 1.0 for the "very large" ones, like those observed in 1975, 1981, 1983, and 1986 ($\Delta m \sim 3.0$ mag).

The best studied outbursts are those of 1981, 1983, and 1986. In particular, during the last one, coordinated UV, optical, and IR observations have been performed. In the following, we will discuss some of the main observational results so far obtained, pointing out those aspects of the known phenomenological scenario that we feel are more relevant to a physical interpretation of the outburst phenomenon.

Due to the long time intervals between two subsequent outbursts and the nonstrictly periodic nature of the phenomenon, most of our knowledge of the long-term light curve of GK Per comes from visual, photographic, and even photometric observations by amateur astronomers whose precious collaboration should be emphasized more often.

V.E.1. ON THE MULTIWAVELENGTH BEHAVIOR DURING THE OUTBURSTS

The only outburst for which extensive x-ray monitoring of the nova has been performed is that of 1978 (King et al. 1979). A reanalysis of all the available x-ray and optical data showed that, at least in that case, the x-ray flux reached its maximum level about 30 days before the rise in the optical (Bianchini an Sabbadin 1985). This cannot be simply explained as the effect of enhanced mass transfer rate produced by the disc instability mechanism. In fact, for inside-outbursts, like those observed in GK Per, the V and the x-ray light curves should present almost contemporary rising branches (Cannizzo et al., 1986).

Another peculiarity of the x-ray behavior is represented by the fact that during the 1978 one-magnitude outbursts, the luminosity of the nova in the 2 - 10 KeV range was $\simeq 5 \times 10^{33}$erg s^{-1} (King et al., 1979), which is comparable to that observed by EXOSAT, in the same energy

interval, during the larger outburst of 1983, that is when the star was two magnitudes brighter than in 1978!

IUE spectra of the nova taken by A. Cassatella during the 1986 outburst revealed that, although this optical maximum, in the visual, was only 0.2 - 0.3 magnitudes brighter than that of 1981, the UV fluxes of the continuum were brighter by a factor of two. The same occurred for the UV emission lines whose intensities resulted, on the average, twice as much as those observed in 1981.

These results are not completely accounted for by the standard disc instability model. In general, they only fit in the already proposed phenomenological scenario in which the outbursts should occur mainly in the inner, denser, and hotter regions of the accretion disc, probably starting near the boundary layer and the surface of the mass-accreting white dwarf (see also Section V.E.4.).

The visual and infrared light curves of the 1986 outburst are shown in Figure 8-45. No time delay between the two light curves can be clearly detected. We recall that no time delay was seen also between the visual and the UV light curves of the 1983 outburst (Bianchini et al. 1986). IUE observations of the nova during the 1986 outburst confirm this result.

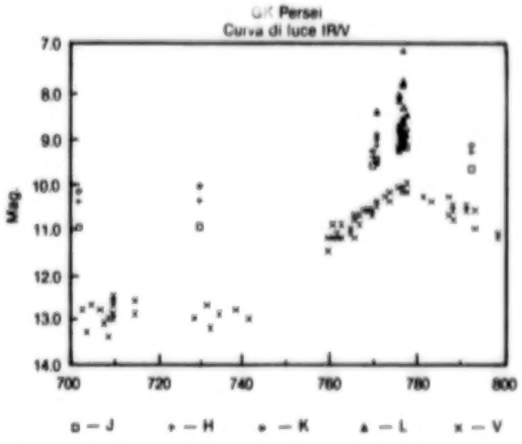


Figure 8-45. Visual, J, H, and K light curves of the 1986 optical outburst. No time delay is observed.

The UV to IR continuum energy distributions of the nova at quiescence and at the 1986 light peak, corrected for E(B-V) = 0.1 and E(B-V) = 0.35, respectively, are shown in Figure 8-43. At light maximum, the slope is not too far from that predicted by the theory for a semi-infinite disc even in the infrared, suggesting that the accretion disc of GK Per is quite extended and that a large portion of it has low temperatures also during an outburst. Alternatively, part of the infrared emission could come from the secondary, from the cold outer rim of the accretion disc and from the circumstellar material.

The pattern of the nova in the U-B vs B-V plane looks rather complicated, as shown by Bianchini et al. (1986). (Figure 8.41b).

V.E.2. SPECTRAL CHANGES DURING THE OUTBURSTS

Few optical spectroscopic observations are available for the 1986 outburst. More data were given for the 1981 and 1983 events. A description of the main spectroscopic changes observed in the optical region is given by Szkody et al. (1985) and Bianchini et al. (1986). The general trend is that of a strengthening of the central intensities of the high-excitation emission lines together with a general decrease of their equivalent widths. In other words, the outbursts occurred more in the continuum than in the emission lines. Bianchini and Sabbadin (1982) suggested also that the observed change in the width of the Hα profile might indicate that the radius of the outer optically thin portion of the accretion disc is about 8×10^{10}cm at quiescence, and 2×10^{11}cm during an outburst (Bianchini et al. 1982), as required by the disc instability model. In fact, a burst of the mass-transfer rate from the secondary would cause the disc to shrink and not to expand.

A particularly interesting behavior of the nova during light maxima is suggested by two optical spectra taken at the Asiago Observatory during the 1975 and 1983 light peaks. These two spectra show the presence of an unusual emission feature at λ4842. This does not seem to be a high radial velocity component of Hβ, since it is not observed at Hα; it can be tenta-

tively identified as the A1O head, similar to what is observed in Miras at maximum (Iwanoska et al. 1960). A portion of one of the two spectra indicating the line is displayed in Figure 8-46. Figure 8-47 reproduces a calibrated spectrum of the nova at light maximum taken by Szkody et al. (1985) in which the λ4842 emission might perhaps appear blended with that of H_β. We estimate that the line has a width of about 14 Å (FWHM) and an intensity about 0.3 that of H_β. The line has never been observed in any of the spectra taken after light maxima and at quiescence.

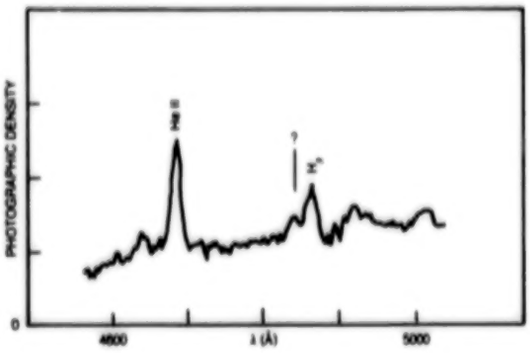


Figure 8-46. Portion of the plate spectrum taken with the 182-cm reflector of the Asiago Observatory during the light peak of 1975. The unusual emission at λ4842 is shown.

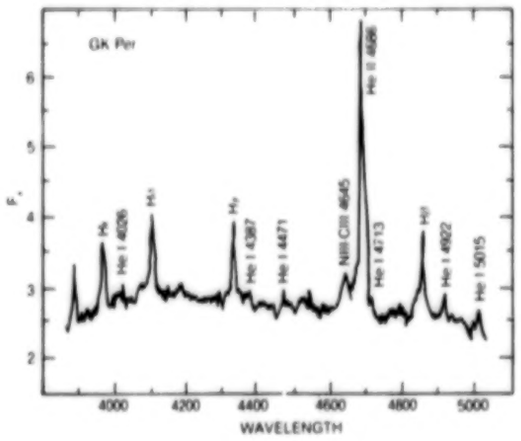


Figure 8-47. The spectrum of GK Per at the 1983 outburst maximum on 1983 August 15 UT (from Szkody et al., 1985).

IUE spectra of the nova taken during the 1981 (Bianchini et al., 1986) and the 1986 (Cassatella et al., work in preparation) large optical outbursts confirm the main character of the spectroscopic variability already observed in the optical region. In fact, only the central intensities, and not the equivalent widths of the principal UV emission lines, follow the outburst profile. An exception is represented by the NIV, SiIV, and OIII lines which have a dip at the very beginning of the rise; whereas, the UV continuum has a flare. Traces of [NeIV] 2423 and OV 1371 are observed during the rise and the light maximum. In general, the indication is that of an increase of the ionization during the rise to maximum. The constant presence throughout the outburst of the lower-excitation emission lines of [OIII] λ2471, [NIII] λ1750, [NIV] λ1487, and MgII λ2800 demonstrates that a stratification of the ionized elements is produced at all times. This requires the presence of an extended circumstellar envelope and /or of an anisotropy in the high-temperature ionizing source. We note, however, that the MgII chromospheric emisssion was almost absent during the UV spectra of the 1986 outburst, perhaps due to the presence of a much stronger UV ionizing radiation field. An IUE spectrum of the nova taken at the 1986 light peak is shown in Figure 8-48.

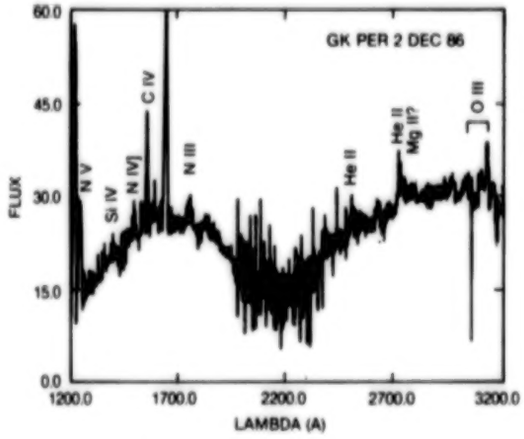


Figure 8-48. IUE spectrum of GK Per during the 1986 light maximum taken by A. Cassatella. The λ2200 dip suggests E(B-V)=0.35. At light minimum the dip seems to be less pronounced but the spectrum presents a rather poor signal to noise ratio so no conclusion can be driven.

Analysis of the behavior presented by some of the UV emission lines can give important information on the physics of the small outbursts of GK Per. The intensity ratios of resonance lines CIV (λ1549): NV (λ1238):SiIV (λ1394, λ1403) are changing during the outburst being

1:0.4:0.28 at light minimum, and 1:1:0.4 at light maximum. Bianchini and Sabbadin(1987) have tentatively explained this behavior by assuming that at light minimum, these three resonant lines are produced in a small volume around the white dwarf, having a radius of the order of that of the inner edge of the accretion disc, a temperature of a few 10^4 K, and a density of $Ne > 10^{12} cm^{-3}$. At light maximum, instead, a stratification of the ionization would imply for the different ions much larger but different emitting volumes.

Additional information about the physical mechanism of the outbursts is provided by the behavior of the OIII λλ3047,3133 and the [ArIII] λ3109 lines. The I(λ3133)/I(λ3047) intensity ratio is about unity at light minimum, at the start and at the end of the outburst, and about 6.0 during the rise and light maximum. For the OIII lines coming from the excitation of the oxygen by the HeII λ303.8 Ly_α (Bowen fluorescence mechanism), a typical I(λ3133)/ I(λ3047) ratio is about 5.6 (Saraph and Seaton, 1980). Our results suggest that the Bowen fluorescence mechanism might be operating only during the rise and the light maximum, while at quiescence and at the start of the outburst, the OIII energy levels could be selectively excited by collisions. In the spectrum of February 14, taken at the start of the 1981 outburst, we observe a bright emission of [ArIII] λ3109. This line is virtually absent in all the other spectra. Seven IUE spectra taken by A. Cassatella throughout the 1986 outburst (Cassatella et al., work in preparation) seem to confirm this particular behavior of the nova, because the [ArIII] λ3109 emission is detected only in one spectrum of the early rise. Since the ionization potential of ArIII is close to that of OIII, the ArIII forbidden line should come from the same region that also produces the OIII permitted line. However, collisions will prevent radiative decays from the ArIII metastable level for densities $Ne > 10^8 cm^{-3}$. For this reason, Bianchini and Sabbadin (1987) suggested that, at quiescence and during light maxima, the OIII emission lines are emitted by regions where the density is high enough to prevent the production of the ArIII forbidden lines. In particular, at quiescence, the OIII line-emitting region should be more concentrated around the white dwarf and the inner regions of the accretion disc, where densities can be relatively high so as to prevent the formation of the ArIII forbidden line. At the start of an outburst, instead, the luminosity and temperature of the central ionizing source increase, and the OIII ionization regions should be immediately pushed further out, towards lower-density regions, where the AIII forbidden line can be finally produced. This situation could be also favored by the suggested existence in the system of a very hot region, which explains the observed high-energy precursor to the 1978 optical outburst. However, if we assume that an outburst can also produce an increase of the wind from the inner regions of the accretion disc it is then possible that, soon after the start of an outburst, a substantial increase of the wind and, consequently, of the density of the circumstellar material might again prevent radiative decays from the ArIII metastable level. We note here that the lack of a P Cyg profile in the resonant lines during light maxima can be understood if we recall that a wind is predominantly emitted in directions perpendicular to the disc plane and that it can be observed only if the accretion disc is seen almost pole-on, i. e., the inclination of the binary system is rather low.

The 1986 IUE observations of the nova confirm the large color excess derived from the obervations of the 1981 outburst (Figure 8-48). The E(B-V), derived from the intensity of the λ2200 dip of the continuum, is about 0.35. It is not clear, however, whether such a reddening can be attributed also to the nova at light minimum (Bianchini et al. 1986).

As already mentioned, a rather peculiar difference was found between the UV spectra of the 1981 and the 1986 outbursts, that is the almost total absence in the 1986 outburst, of the MgII λ2800 chromospheric emission and its only appearance during the late decline. This particular behavior is perhaps understandable for what already has been said. In fact, the 1986 outburst implied much stronger UV, and possibly also x-ray, fluxes than the 1981 one. This

must have produced a higher level of ionization in most of the line-emitting regions included, perhaps, the region responsible for the chromospheric emission, i.e., the disc or the cool secondary star.

V.E.3. SHORT TERM PHOTOMETRIC VARIABILITY DURING THE OPTICAL OUTBURSTS

High-speed photometry of the old nova GK Per has been occasionally performed by different observers (Nather; Robinson; Bianchini; unpublished data), and the result was that the light curve could appear either smooth or flickered. Unfortunately, no systematic photometry has been performed before the 1983 optical outburst, when Mazeh et al. (1985b) and Steinle and Pietsch (1987) tried to detect the optical counterpart of the x-ray 351 s coherent modulation discovered by Watson et al. (1985) during the same outburst. Some small amplitude (~3%) periodicities in the optical, to be compared with the 80% modulation observed in the x-ray region, were actually detected, more often at slightly larger frequencies (360, 390, and 410 seconds), or close to the 350 s period but lasting only for a few cycles. High-speed photometry of the nova during the 1986 outburst (Stagni et al. 1987, work in preparation) didn't show any clear evidence for the existence of such periodicities. However, inspection of the light curves obtained in the different nights (an example is given in Figure 8-44) reveals the presence of periodicities of the order of 400 seconds lasting only for a few cycles, as found by Steinle and Pietsch.

This behavior means that the region producing the 351 s oscillations is very small and hot, as expected for the emission coming from the polar caps of a rotating magnetic white dwarf. The smaller amplitude of the modulation seen in the optical and its nonstrictly periodic nature could be attributed to the fact that the optical modulation originates from x-ray heating of a feature of the accretion disc that is not completely fixed or stable in the rotation frame.

The EXOSAT observations of the 1983 outburst (Mazeh et al. 1985b) revealed also the presence of a modulation of the x-ray flux on typical time scales of 0.8 hour. High-speed photometry performed by Stagni et al. during the 1986 outburst definitely confirms the presence of such a modulation as shown in Figure 8-44. Mazeh et al. (1985b) suggested that it might be generated by a bulge inside the disc, rotating around the compact star with its Keplerian velocity, and reprocessing the x-ray oscillation in the optical wavelengths. The observed periodicity should then be the beat frequency of the bulge orbital period and the x-ray one. Alternatively, Duschl et al. (1985) suggested the onset of the inner disc of a region that is unstable with respect to the mass flow rate which crosses it. The theoretical time scale of the modulation of the accretion rate should be of the order of 0.7 hour.

V.E.4. THE ORIGIN OF THE OPTICAL OUTBURSTS

Whether the optical outbursts of GK Per are to be considered as a genuine dwarf nova-like behavior is still a matter of discussion. Obviously, much depends on the definitions, classification schemes, and also on the particular theoretical models adopted to explain the dwarf nova phenomenon.

Two basic competing models are proposed to explain the dwarf-nova phenomenon (see also Chapter 4). The first model (Bath, 1973; Bath and Pringle, 1981) explains the brightening of the accretion disc as due to a sudden increase of the mass-transfer rate from the secondary component. The second model suggests that accretion discs themselves may be unstable (Smak, 1971; Osaki, 1974; Hoshi, 1979; Meyer and Meyer-Hofmeister, 1981, 1982; Cannizzo et. al., 1982; Mineshige and Osaki, 1983; Faulkner et al., 1983; see also Chapter 4.III).

We have already said that the disc instability model can account for most of the observational properties of GK Per during the optical outbursts. Cannizzo and Kenyon (1986) pro-

posed for GK Per an accretion disc limit cycle mechanism and placed the transition region, which is responsible for the onset of the outburst, at the very inner edge of the disc. Bianchini et al. (1986) proposed that the mass-transfer rate within the binary system is modulated by the presence in the secondary of some kind of activity, and that the unstable transition region in the inner regions of the accretion disc could be formed only when the mass-transfer rate from the secondary becomes larger than $10^{16} gs^{-1}$.

For bursts starting at small radii of the disc, the light curves observed at different wavelengths should have more rounded and symmetric profiles with no relevant time delays between them (Cannizzo et al. 1986). Actually, the outbursts of GK Per tend to be symmetric, and no appreciable time delay has been observed between the UV, the visual, and the infrared light curves. We know that smaller outbursts have a more asymmetric profile but, unfortunately, only their visual light curves have been observed so far.

However, we have seen that some observational results seem to contradict the standard disc instability model. For example, the detection of strong hard x-ray fluxes prior to the onset of the 1978 optical outburst strongly indicates that the outburst originates in the hotter central regions of the accretion disc or on the surface of the white dwarf, but also contradicts the theoretical prediction that no relevant time delay of the outburst profile should be seen at any wavelength. Other important discrepancies between the theory and the observations have been already pointed out in Section V.A.

The $T = n(400 \mp 40)$ days relation (n = 1,2,3,5; as we have seen, 4 seems to be absent), which gives the observed time intervals between two consecutive outbursts, suggests the existence of a mechanism capable of producing these particular recurrence times. This mechanism could be represented by the presence in the secondary of cycles of activity that modulate the mass-transfer rate and trigger the onset of the disc instability mechanism with the observed recurrence times.

However, we must be very cautious when applying the standard disc instability model to the very inner regions of the accretion disc of GK Per. In fact, the inner radius of the disc is controlled by the magnetic field and could be close to the corotation radius (Duschl et al., 1985). Thus, the physical situation in this region must be rather complicated, and much more refined models are required.

V.F. THE LONG TERM LIGHT OSCILLATIONS OF GK PER AT QUIESCENCE

The return of the nova to light minimum did not occur monotonically but through a number of strong light fluctuations. The historical light curve covering the years 1901-1983 is discussed by Sabbadin and Bianchini (1983). The main characteristics of the long-term light curve of GK Per at minimum can be summarized as follows:

1) The preoutburst light curve (Robinson, 1975) shows that the nova was fainter than 13.8 mag for several years and that it brightened in the range of 12.8-13.4 mag in the two years just prior to its eruption. We can then conclude that the nova had essentially the same luminosity before and after the explosion and that variations of, at least, 2 magnitudes were probably present also in the preoutburst light curve.

2) The historical minimum, $m_v \sim 15$, was reached in 1916, but this low luminosity does not correspond to that of the normal quiescent state of the nova, which is 2 magnitudes brighter. Instead, it is surprisingly close to the reddened apparent visual magnitude of a K2 IV-V star at the distance of the nova. Thus, we suggest that GK Per, at the end of the explosive episode, passed through a sort of mini-hibernation phase with little or no mass-transfer rate from the secondary. In fact it is possible that the strong heating of the deep layers of the secondary by hard radiation emitted during the nova explosion enhanced the mass loss from the secondary so much that at the end of the explosion the star had to shrink inside its Roche-lobe. The light fluctuations observed at that time should then

be mainly caused by intrinsic variability of the secondary while it was trying to fill again its Roche-lobe.

3) During the twenties and thirties, the visual magnitude of the nova was continuously fluctuating between magnitudes 14.2 and 12.0 on typical time scales of 40, 80, and 400 days. During this period of time, we observe an increase of the nova mean luminosity and, during the forties, the nova was hardly found fainter than magnitude 13.

4) From 1948 till the present time, we see a very slow decline of the luminosity; now the nova spends most of its time in quiescence and, at intervals of hundreds of days, shows enhanced outbursts. As an example, Figure 8-39, shows the light curve of the nova in the years 1969-1983.

5) The analysis of the data, including the more recent 1986 outburst, indicates that the observed optical maxima present a particular type of semiperiodicity, in the sense that the intervals, ΔT, between two consecutive outbursts can be expressed by the relation: $\Delta T = n(400 \pm 40)$, where n ranges from 1 to 5, although 4 seems to be excluded. Figure 8-40, presents the suggested relationship and shows that all points, except the 1981 outburst, which occurred 984 days after the 1978 one, are within their error bars of $\simeq$ 40 days.

6) The plot of the annual mean magnitude in the period 1917-1986 (see Figure 8-49) might suggest the presence of a longer term modulation of the outburst activity of GK Per. Fourier analysis revealed the presence of a main cycle of about 2500 days, but a smaller modulation at about 1300 days is also possible. This result has been tentatively interpreted by Bianchini (1988) as the effect of the presence in the secondary of a solar-type cycle capable of changing the mass-transfer rate within the binary system by a factor of 2.8. The cycle is more evident in the light curve of the period 1917-1940, that is, while the nova was recovering from the historical minimum. This might be due to the fact that solar-type cycles in CVs are better observed in systems having low-mass accretion rates (Bianchini, 1988). During the seventies and the eighties, the magnitude of the nova has been around 13.15, still oscillating on time scales of 1300 and 2600 days between magnitudes 13.0 and 13.2. However, in the period 1950-1988, a slow decline of the out of outburst-luminosity, at a rate of 0.018 mag/yr, could also be suggested. We note here that the observed 2400-, 1200-, 800-, and 400-day, time intervals between the optical outbursts of GK Per could well be connected with the 2400- and 1300-day modulations observed in the long term light curve of the nova. In other words, it is probable that all these periodicities are physically correlated. For example, they could be explained as the effect of the presence in the secondary of solar-type cycles. Bianchini et al. (1986) proposed that since 1950, the accretion disc of GK Per, due to the particularly low-mass transfer rate from the secondary, is fully convective and stable most of the time and that a cyclic increase of the mass transfer rate from the secondary is responsible for the onset of the unstable transition region near the inner edge of the accretion disc. In particular, a cyclic increase of the mass transfer rate might be caused by the periodic alignment of nonradial g-modes on the surface of the cool star. As a consequence, several periodicities should be observed, in coincidence with the periodic alignments of different groups of sets of modes. These periodicities should result in submultiples of the time interval between two consecutive alignments of all the sets. Such a long period could be tentatively identified with the observed 2400-day light modulation.

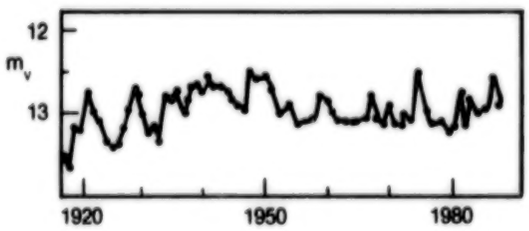


Figure 8-49. Annual mean visual magnitude of GK Per in the years 1917-1986. Fourier analysis reveals the presence of a quasi periodicity at about 2400 days. Similar periodicities have been found also in other Cataclysmic Variables. They could be ascribed to the effect of solar-type cycles in the secondary.

VI. V1668 CYGNI 1978, A MODERATELY FAST NOVA

(written by Hack)

V1668 Cyg 1978 was discovered on September 9, 1978, independently by Collins (1978) and by Shao (1978). It is the first nova whose development has been followed completely, from premaximum to the nebular phase, both in the ultraviolet with IUE and in the infrared.

VI.A. PHOTOMETRIC OBSERVATIONS

It reached maximum brightness on September 12, 20 with V = 6.2 (Kolotilov, 1980). The absolute magnitude is very uncertain; from the degree of interstellar reddening, values ranging between -6.2 and -8.3 are derived (Klare et al., 1980), while the relation between the fastness of light decrease and absolute visual magnitude $M_v = -11.5 + 2.5 \log t_3$ gives $M_v = -8$. In about 3 months, the nova decreased from V = 6 to V = 11, and the energy radiated amounted to about 3×10^{44} ergs. The photometric observations in U,B,V by Duerbeck et al. (1980b) show how the position of the nova varies in the two-color diagram (Figures 8-50 and 8-51). The temperatures derived by the colors, together with the values of the luminosity, permit to derive the loci occupied by the nova in the logT-logR diagram (Figure 8-52), where T and R represent the values of the pseudophotosphere. During the first 8 days after maximum, T varies from 8,000 K and 18,000 K, and R, between 100 and 25 solar radii, while the luminosity remains almost constant. On September 12-14, the UV and visual continuum energy distribution is similar to that of an F5 star.

Photoelectric observations in UBV were obtained in 1978 by Piccioni et al. (1984) from 2 to 60 days after outburst , and others were obtained in August 1981, when the magnitude was about 17, showing the presence of fluctuations of a few hundreths of magnitude (Figure 8-53) and time scales ranging from a few minutes to 2 hours.

Kaler (1986) has made simultaneous observations in the visual continuum (y magnitude in the Stroemgren system) and with the wide H

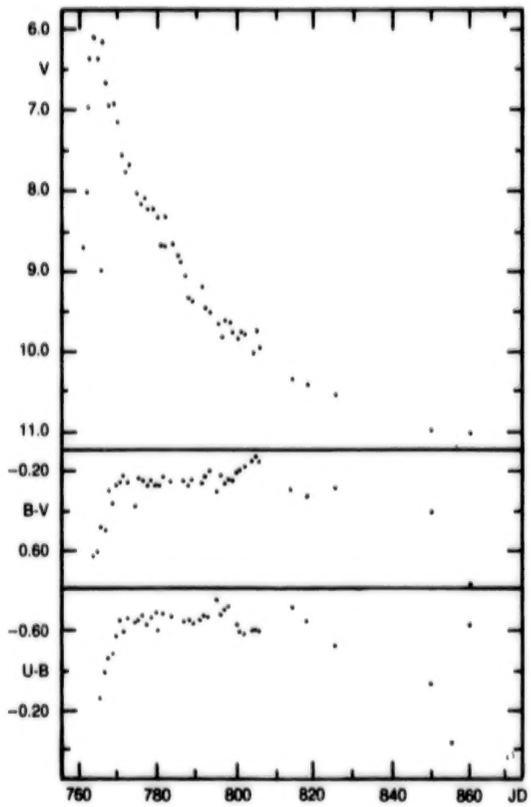


Figure 8-50. Light and color curves of Nova Cygni 1978.
(from Duerbeck et al., 1980b).

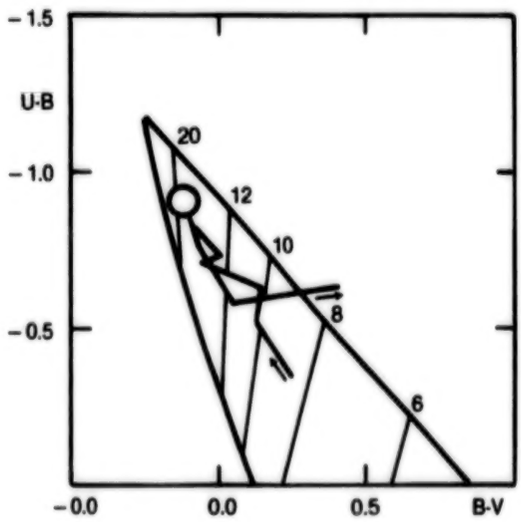


Figure 8-51. Path of Nova Cygni 1978 in the two-color diagram, corrected for interstellar extinction. Supergiant and blackbody sequences, and lines of constant temperature (in 10^3 K are shown.
(from Duerbeck et al., 1980b).

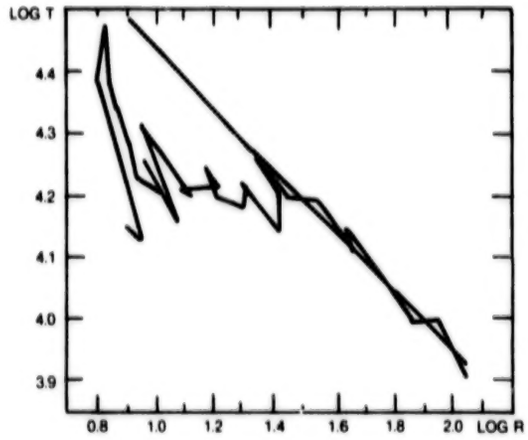


Figure 8-52. Nova Cygni 1978 in the T-log R diagram. For 8 days after maximum the nova stays at constant luminosity (corresponding to a line with a slope of 45°). (from Duerbeck et al., 1980b).

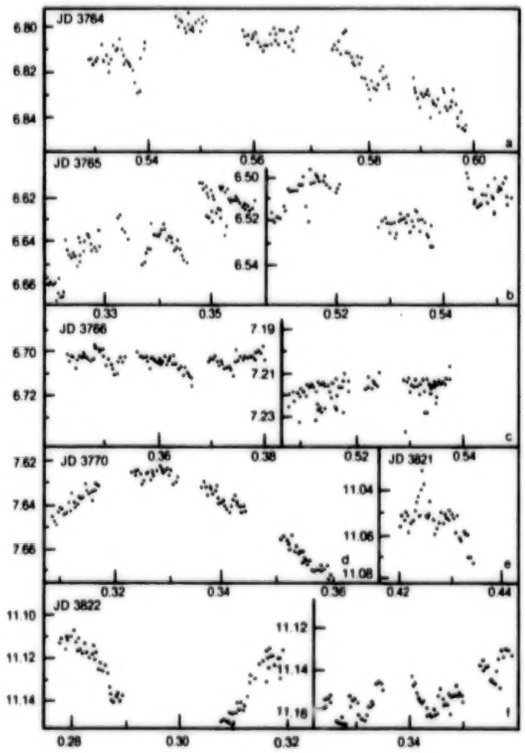


Figure 8-53. Examples of B light variations of Nova Cygni 1978 during its early decline. Each dot represents the mean magnitude over one minute. (from Piccioni et al., 1984).

Beta filter w (including the H beta and [O III] emissions). The two light curves separate rapidly after 50 days from outburst (Figure 8-54). At 311 days after outburst, the continuum has declined by 9 mag while the w emission has declined by 4.7 mag only. Hence, the decline of

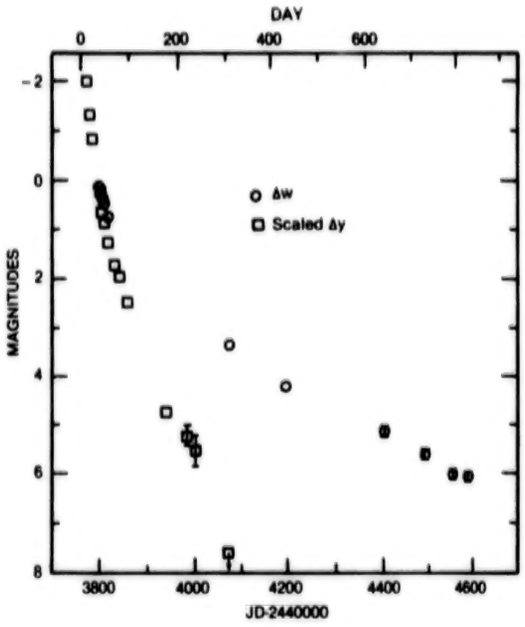


Figure 8-54. Hβ-wide (Δw) and Stroemgren y (Δy) light curves for Nova Cygni 1978. The ordinates are the nova minus comparison magnitude differences. The Δy curve is scaled to Δw for September 26, 1978, to show the differences between the two. The decline of Hβ is much slower than that of the y continuum. (from Kaler, 1986).

the star (indicated by y) is much faster than that of the nebula where [OIII] is produced.

Polarization measurements have been made by Piirola and Korhonen (1979) from 6 to 55 days after outburst. They observe an increase of polarization from 1.6% to 1.9% between October 1 and 11, 1978. i.e., in the same period when the dust formation phase (October 7-15), indicated by the infrared observations (Gehrz et al. 1978) started.

VI.B. SPECTROSCOPIC OBSERVATIONS

Spectra obtained near maximum and for several weeks after outburst have been obtained by Kolotilov (1980), Ortolani et al. (1978) and by Klare et al. (1980). The latter show the full sequence of spectra from September 13 to December 18, giving an instructive example of the kind of variations occurring in the spectrum of a nova (Figures 8-55 and 8-56). Three main emission components at about -500,- 45, and + 500 km/s are observed for several weeks on

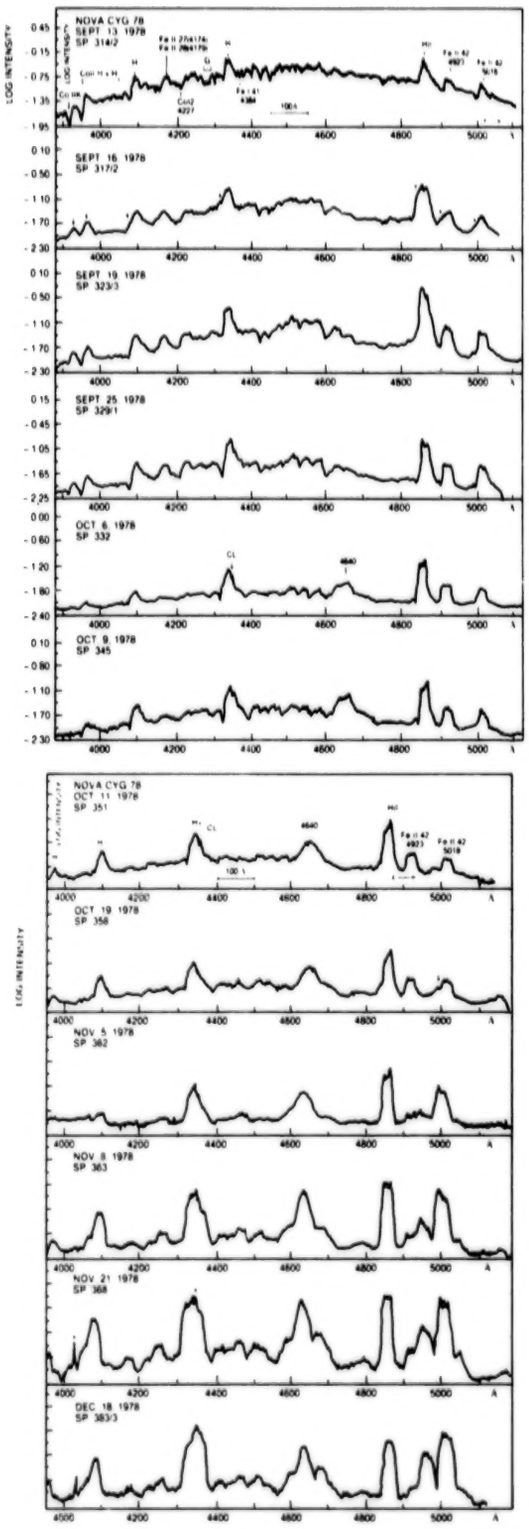


Figure 8-55. The photographic spectrum of V 1668 Cyg: a) from September 13 to October 9. CL = Emissions due to city light. b) The same spectral region, from October 11 to December 18. A P Cyg profile is still visible on October 11 at H Beta, Gamma, and Delta and is completely disappeared on November 5. The multiple structure of the emissions is evident. (from Klare et al., 1980).

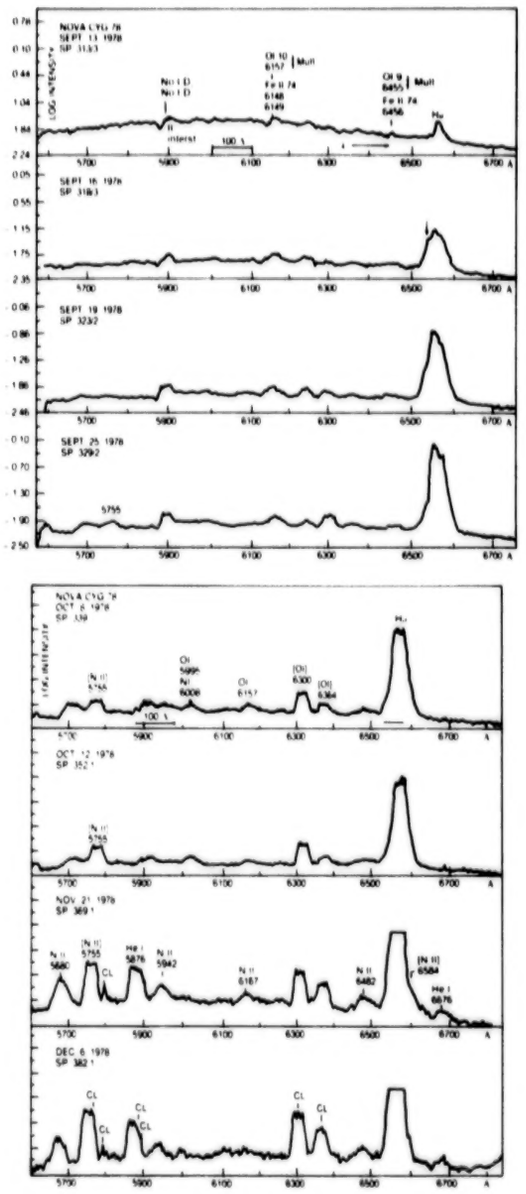


Figure 8-56. The red spectrum of V 1668 Cyg. a) from September 13 to September 25, b) from October 8 to December 6. CL = emissions due to city light. (from Klare et al., 1980).

October and November (Kolotilov, 1980), and more complex structures, indicating the presence of two main shells expanding at about 500 and 150 km/s, are evident along the 3 months after outburst (see Klare et al. 1980). During the first few days from outburst, P Cyg profiles are evident, with expansion velocities increasing from -600 km/s (principal spectrum), to -1700 (diffuse-enhanced) and -2100 km/s (Orion spectrum).

Comparison of the visual and ultraviolet

spectra show that lines of comparable excitation appear at about the same epochs in both wavelength ranges. The only exception is 1640 He II (E.P. 48.3 eV), which is present already on the spectrum of September 19 (7th from the outburst), while 4686 He II (E.P. 50.8 eV) only appears at November 5 (54th from the outburst), reaches maximum intensity on Novermber 21, and is still strong on December 18. However, the low-resolution spectra of IUE show that on September 19 (Figure 8-57a), the O I line at 1302 is present. Hence, it is possible that the emission at 1640 is due, totally or partially, to the semiforbidden line of O I at 1641. Figure 8.57 and 8.58 show the low-resolution UV spectrum on September 19 and October 17, 1978. The great strength of the ultraviolet nitrogen lines is noticeable. Comparison of the nebular spectrum of the nova with those of planetary nebulae suggests that nitrogen is in excess in the nova ejecta by a factor of 200 (Stickland et al., 1981) relative to the solar abundance.

Ultraviolet observations were made on the early phases of the outburst by Wu et al. (1978), who observed the nova on September 13.4 and then from September 15 to October 8; by Cassatella et al. (1979), who observed it on September 14.98 and then on September 28 and October 10 (Figures 8-59, 8-60, 8-61), and by Stickland et al. (1979), who obtained an extended series of spectra from September 11.7 to March 24, obtaining spectra preoutburst, at early decline, in the transitional stage and the nebular stage, which are the object of the quoted paper (Stickland et al. 1981). From visual data obtained on September 12-14, Ortolani et al. (1978) estimated a spectral type F5 Ib, which agrees with the UV energy distribution. On the same dates, the narrow absorption lines have an expansion velocity of -630 km/s. On September 16-17, Ortolani et al. observe only wide diffuse absorptions at the blue edge of the emissions with velocity of -630, -700 km/s. On September 28, emission lines of Fe II, Cr II, and Mn II are broad and symmetric. The half width (FWHM) of the Balmer lines indicates a larger expansion velocity, -1550 km/s. At least another system of emission lines, characterized by an expansion velocity of 525 km/s is present through the O III fluorescence lines at 2688, 2984, and 3333 Å. The structure of the Mg II resonance doublet (Figure 8.61) is complex, with two absorption components, one sharp (FWHM = 55 km/s) and shortward shifted by - 80 km/s; the other is broader (FWHM=270 km/s) and shortward shifted by -1160 km/s with an emission wing. The presence of a few resonance lines of Mn II, Fe II, Mg I, which are very sharp (FWHM = 30 km/s, just slightly above the resolving power of the IUE camera) and shortward shifted by -95 km/s, suggests that an outer shell is present.

The spectrum in October shows a higher degree of excitation and ionization (as indicated by the presence of emissions of 1640 He II, Fe III, Si III, O III) and the flux in the continuum is about twice as strong as that in September, indicating the usually observed shift of the flux to the ultraviolet, probably due to the unveiling of the hot object as the ejected envelope becomes optically thin.

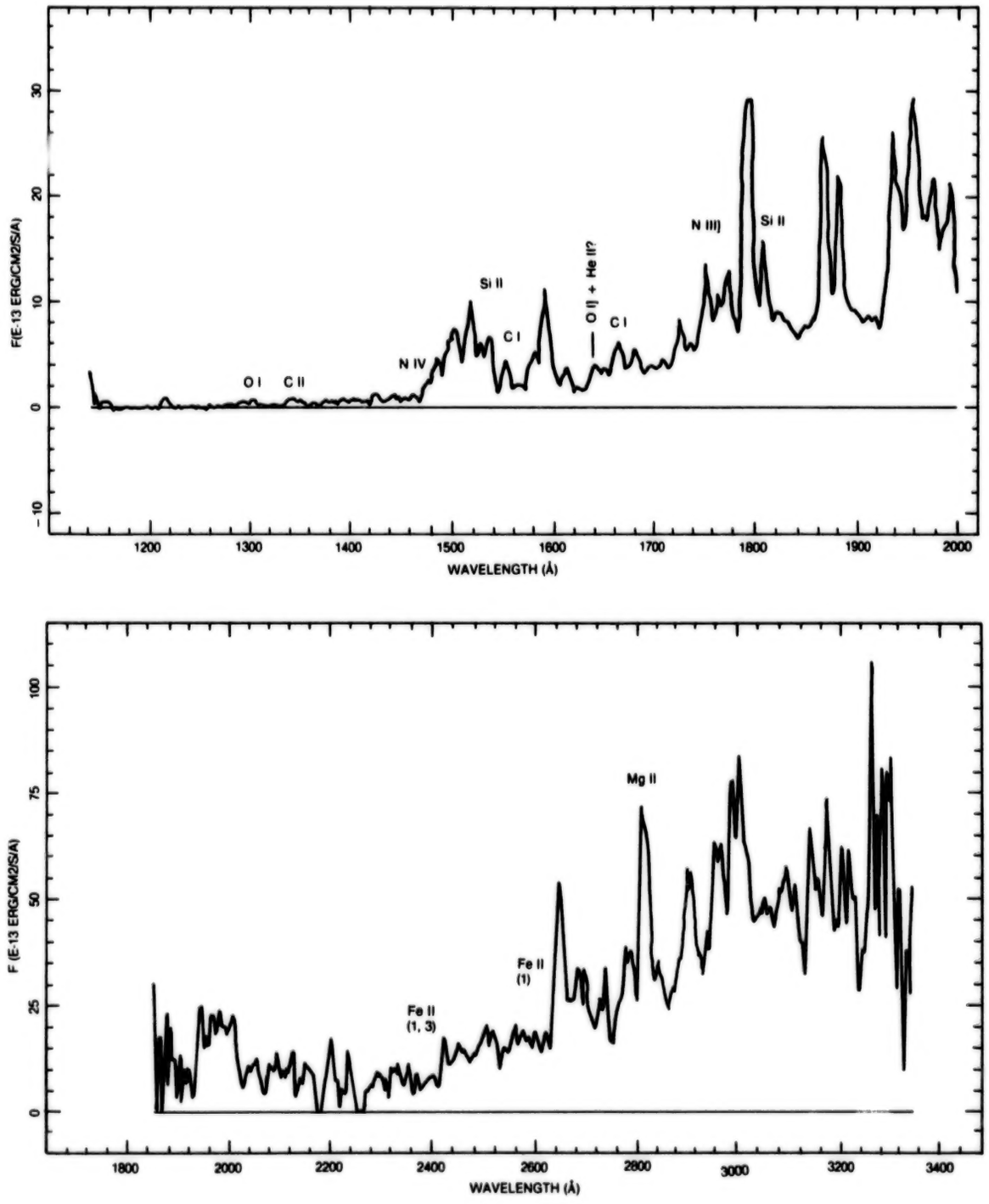


Figure 8-57. The ultraviolet spectrum (obtained with IUE) of V 1668 Cyg in the early decline stage (day 7 from maximum). a) short-wave range, b) long-wave range.
(from Stickland et al., 1979).

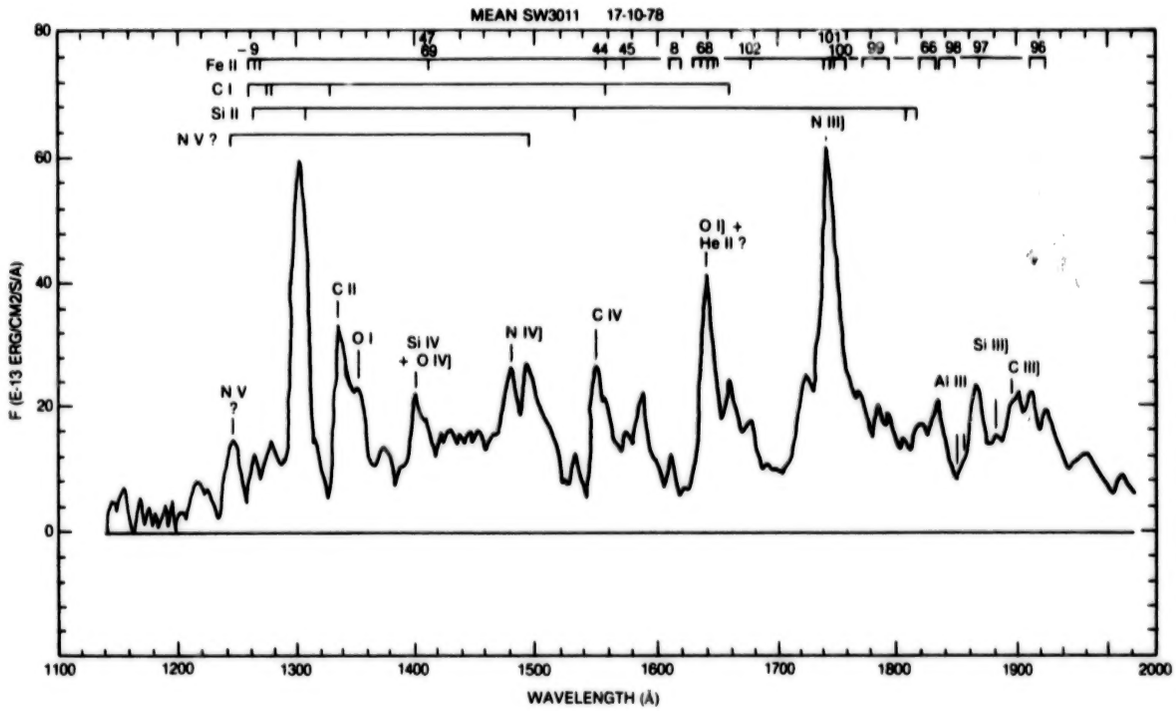


Figure 8-58. Short-wave spectrum of V 1668 Cyg in the transition state (day 35). (from Stickland et al., 1979).

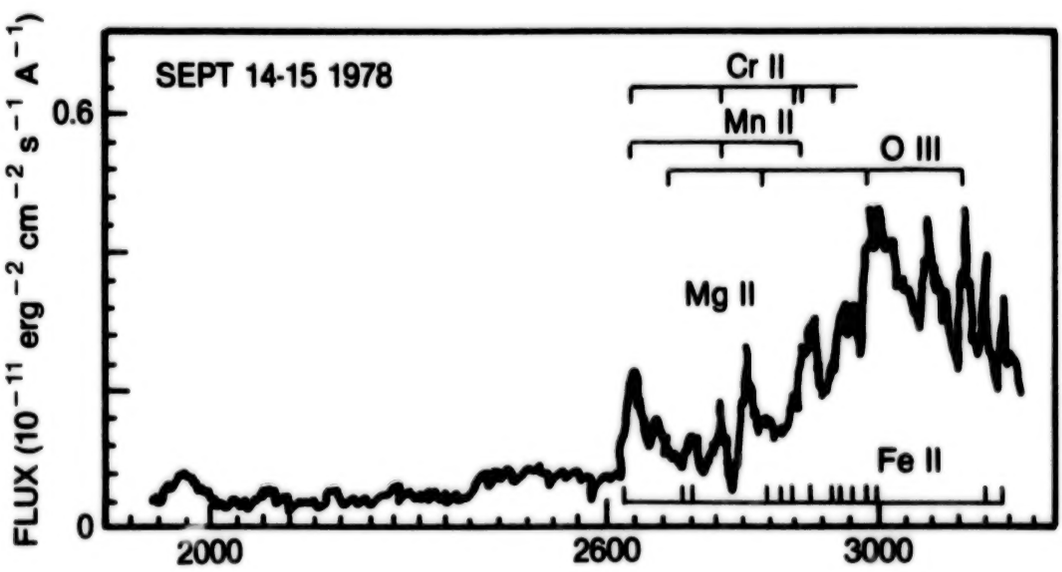


Figure 8-59. The absolute energy distribution (not corrected for reddening) in the IUE long-wave range, two days from maximum. (from Cassatella et al., 1979).

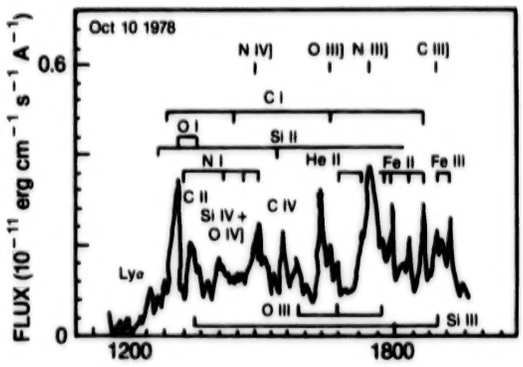


Figure 8-60. The absolute energy distribution (not corrected for reddening) in the IUE short-wave range on October 10. (from Cassatella et al., 1979).

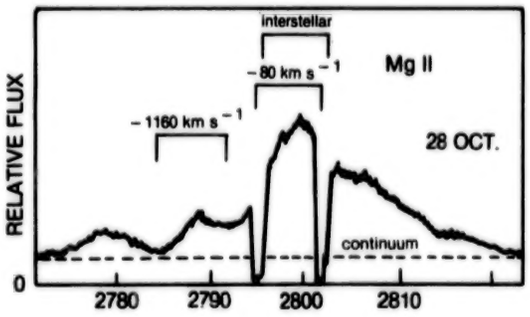


Figure 8-61. The Mg II doublet feature from the IUE high-resolution spectrum of September 28. The two broad Mg II lines at -1160 km/s are very broad, with a half-width at half maximum of 815 km/s. (from Cassatella et al., 1979).

VI.C. THE NEBULAR PHASE

The results of the study of the nebular spectrum (the first nebular spectrum was observed on November 6, 56 days after maximum) are summarized by Stickland et al. (1981). Their main results are the following. The reddening derived by the λ2200 feature is E(B-V) = 0.40 +/- 0.10 in good agreement with the value derived by the optical observations, which gives a mean value of 0.35 +/- 0.08. Electron temperature, electron density, and abundances are derived by the ratios of several nebular emission lines.

Collisionally excited lines are sensitive to the electron temperature while recombination lines are only very slightly dependent on T_e. Hence, the ratio between a line formed by recombination and another formed by collisional excitation of a same ion is independent of the abundance and of N_e (if collisional deexcitation is negligible), and dependent only on T_e. In the case of forbidden lines, which are present in the visual spectrum of novae, collisional deexcitation is not negligible; hence, the ratio of permitted to forbidden line of a same ion depends also on N_e. The situation is better in the UV. Stickland et al. (1981) used the following ratios to derive T_e: C II 1335/C II 2326 and CIII 2297/C III 1909, where the permitted lines are formed by recombination and the intercombination lines are formed by collisional excitation. Temperatures in the range 2 x 10^4 and 5 x 10^5 K are found. Although this method may seem the best way to derive the electron temperature, the application of it to planetary nebulae gives too high values. Another method is to use the ratio of the recombination line of 1717 N IV to the collisionally excited line 1240 N V. These three ratios give values of the electron temperature ranging from 9200 to 13,300 K on day 70 from outburst; from 9810 to 15,100 K on day 88 and from 8440 to 13,700 K on day 304.

Electron densities are derived by the ratios of intercombination lines to forbidden lines. Since intercombination lines fall in the ultraviolet and forbidden lines in the visual, lines from the two spectral ranges must be used. The ratios 2140 N II]/ 5755 [N II] and 1663 O III] / 5007 [O III] give N_e = 8 x 10^7 cm^{-3} on day 88.

The abundances of C, N, and O relative to He are obtained from the UV spectra, while the optical observations by Klare et al. (1980) have been used to derive the helium ionization and the He/H ratio. From these data, it is found that the ratio of CNO atoms in the shell relative to H is larger than the solar value by a factor of 30.N, in particular, is enhanced by a factor of 200.

Figure 8-62 shows the UV nebular spectrum.

Starrfield et al. (1978) have predicted that the rate of energy produced during the runaway is determined by the initial abundance of the CNO elements, and that the ejection of a shell becomes possible only if the CNO abundances

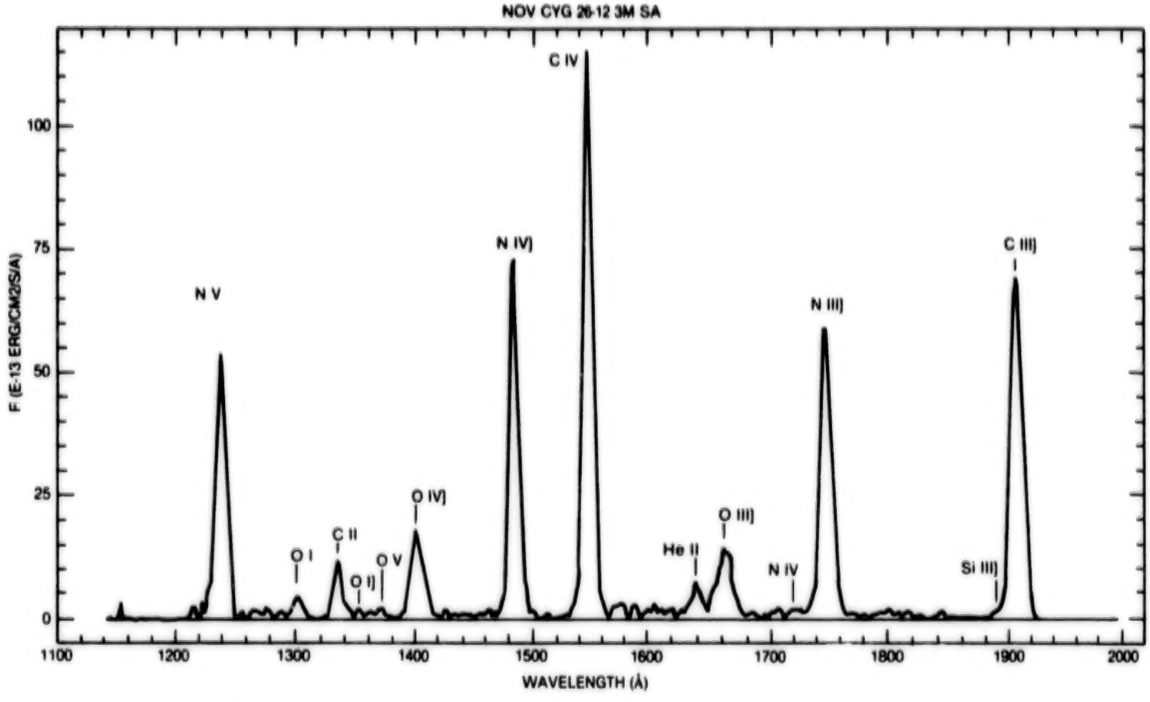


Figure 8-62. Short-wave spectrum of V 1668 Cyg in the nebular stage (day 105 from outburst). (from Stickland et al., 1979)

are substantially larger than the solar abundances. If this mechanism is operative, their computations show that the ejected material will have enhanced CNO abundances, and the abundance of N will be relatively enhanced to C and O: hence, the results found for Nova Cyg 1978 seem to confirm the theory of the thermonuclear runaway. The total luminosity of the remnant has an approximate constant value L = $1.7 \times 10^4 L_\odot$ from day 13 to day 27 after outburst, with an output of radiant energy of 8×10^{43} ergs. A total energy of about 3×10^{44} ergs has been emitted since the instant of the outburst. The mass of the ionized gas in the ejected shell is about 10^{29} g, and its kinetic energy of the order of 6×10^{44} ergs.

VI.D. INFRARED OBSERVATIONS

Gehrz et al. (1980b) have monitored V 1668 Cyg from the visual band V to 19.5 μm for 120 days after outburst. We have seen in Chapter 6 that V1668 Cyg is an intermediate case between slow novae-like FH Ser or NQ Vul (type DQ Her) which exhibit a transition phase with a deep minimum in their light curve and very fast novae-like V1500 Cyg. V1668 Cyg presents an intermediate behavior also in the infrared. In fact, infrared observations have shown that the formation of a thick dust shell in slow novae explains the deep minimum during the transition phase of the light curves. While the majority of slow novae form a thick dust shell, and fast novae do not show evidence of it, V1668 Cyg gives evidence of the formation of a thin dust shell. Figure 8-63 shows the infrared light curves. At the beginning of the expansion (4.5 days after outburst), the energy distribution was characteristic of emission from an optically thick photosphere at T = 7400 K (see Figure 8-64), and the luminosity in this phase varies as t^2 : in fact the flux at a given wavelength is $F_\lambda = 4\pi R^2 B_\lambda$, where B_λ is the Planck function and $R \approx vt$ with v expansion velocity; it follows that $F \propto t^2$. Then the expansion continues and the envelope becomes optically thin. Now in a thin shell of constant thickness and expanding at constant velocity, the flux varies at t^{-2}. In fact, the radius is still given by R = vt; the volume of the shell $V = 4\pi R^2 dR = 4\pi(vt)^2 dR$; the density of the shell $\rho = M/V \propto t^{-2}$. Now, the flux of a thin shell is proportional to its optical depth and therefore to its density; it follows $F \propto t^{-2}$. Hence, we have a first period

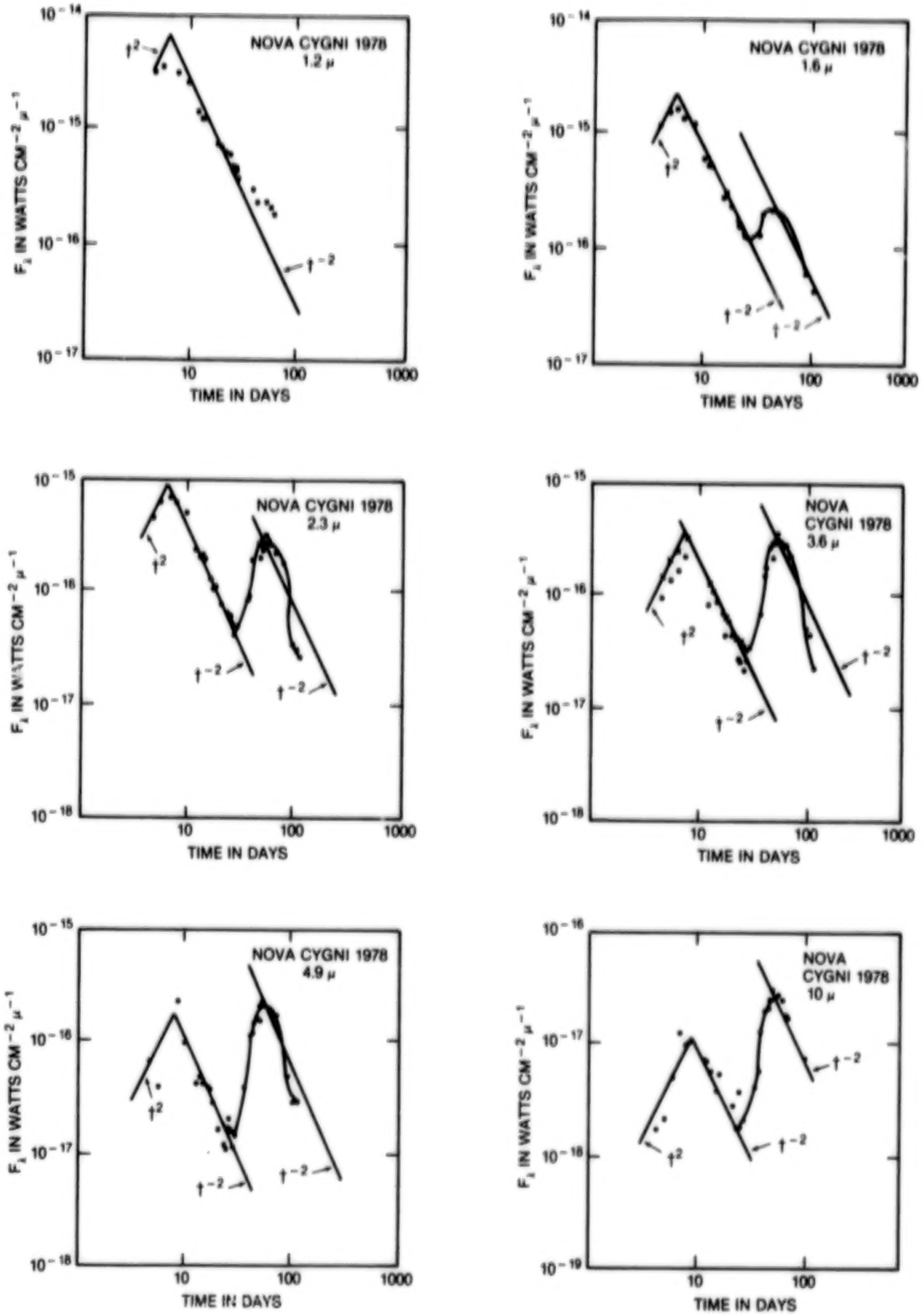


Figure 8-63. Flux versus time at different infrared wavelengths. The straight lines indicate the periods where F varies at t^2 or as t^{-2}.
(from Gehrz et al., 1980b).

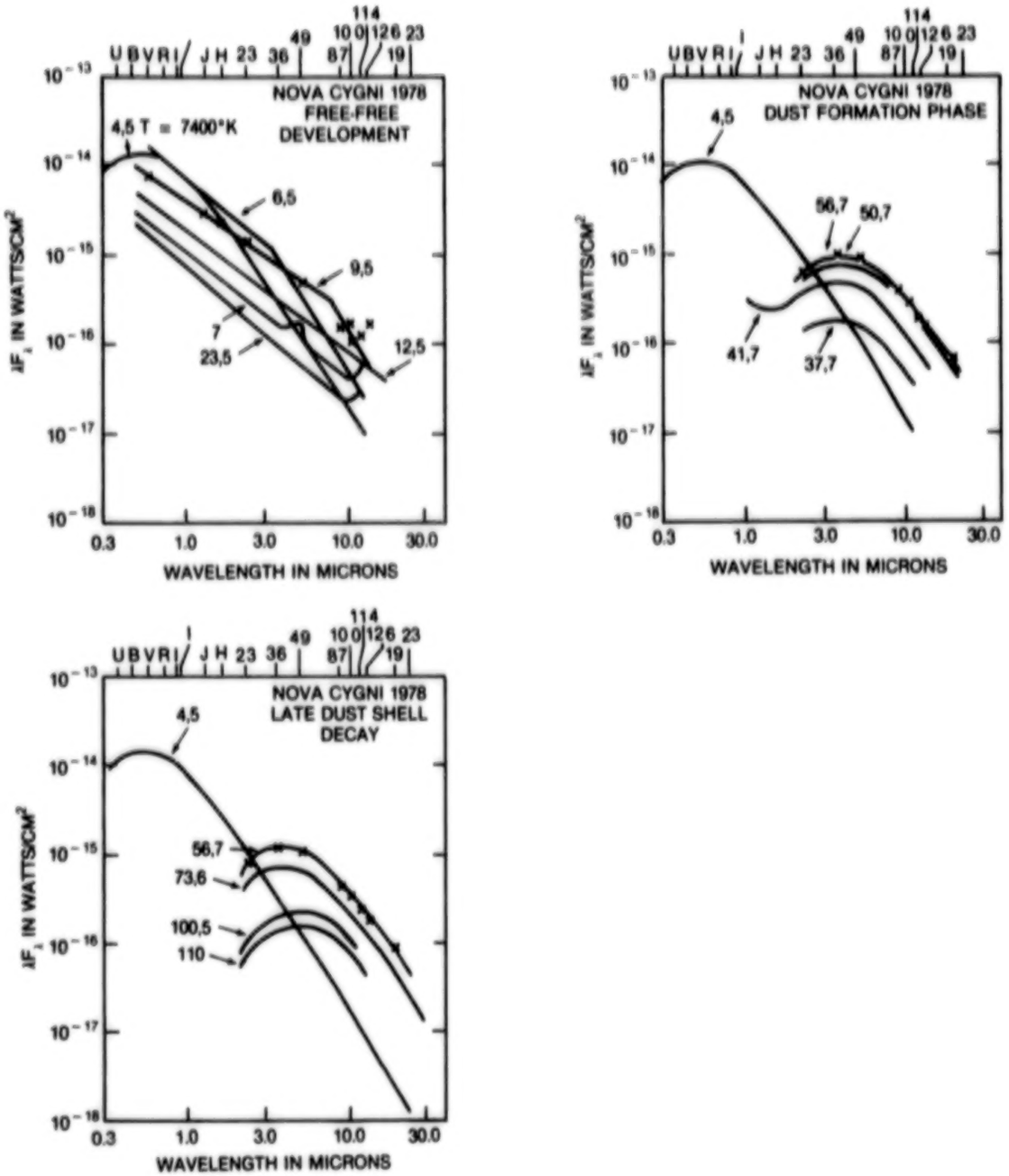


Figure 8-64. Following the expansion of the optically thick gas (the pseudophotosphere-when the energy curve is well fitted by a 7400K blackbody), three major phases follow: a) free-free development; the shell became optically thin at short wavelengths on day 6. During day 6 to day 10 the Rayleigh-Jeans tail advances towards the long wavelengths as the shell density decreases because of the expansion. By day 12.5 the spectrum 1.2 μm to 20 μm is that of a thin free-free emitting gas. b) Dust formation phase; dust grains are condensing by day 35 when the shell temperature has fallen to 1100K. From day 35 on the spectrum is that of a cool blackbody. c) late dust shell decay: after maximum infrared light, the flux from the shell decays because grain growth ceases and the shell optical depth decreases due to expansion. The shell has cooled to 850 K by day 110.
(from Gehrz et al., 1980b)

when the pseudophotosphere emits like a blackbody at T = 7400 K. The temperature remains constant, and the radius increases until day 6. From day 6.5 to day 12.5, we have a free-free emission phase; the energy distribution gradually evolves into spectrum typical of an optically thin gas. Since the absorption coefficient of a thin gas increases with the wavelength, the gas of a given density behaves like a thin gas at short wavelengths and as a thick gas at long wavelengths. Hence, the Rayleigh-Jeans tail moves toward longer wavelengths as the shell becomes less dense because of the expansion. Figure 8-64 shows that on day 6.5, the Rayleigh-Jeans tail starts at about 3.5 μm, while on day 9.5, the Rayleigh-Jeans tail start at about 8.7 μm, and 12.5 days after outburst, the spectrum has the characteristic shape of that of a thin shell in the whole observed infrared range. After day 35, we observe the start of the grain condensation phase: the flux increases again with time (see Figure 8-63) and the energy curve is represented by a blackbody curve for T = 1100 K (Figure 8-64). Hence, the angular diameter Θ_{BB} can be derived by the observed flux at the earth F and the blackbody flux B: $F = B\,(R/d)^2 = B\,\Theta^2$ (Figure 8-65). As

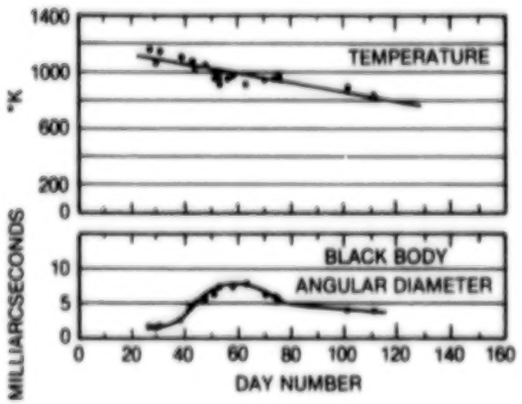


Figure 8-65. Shell temperature and angular diameter variations.
(from Gehrz et al., 1980b).

grain growth progresses, the shell flux reaches a maximum on day 60. After maximum infrared flux, there is a decay as the grain growth ceases and the optical depth of the shell decreases due to the expansion: the flux decreases again as t^{-2} (see Figure 8.63).

VII. FH SER

(written by Duerbeck)

VII.A. THE LIGHT CURVE

The outburst of FH Ser (N Ser 1970) was discovered on February 16, 1970 by M. Honda. It is a moderately fast nova with a DQ Her-type light curve, fairly similar to the nova XX Tau, and it is the first nova to be observed in the UV, optical, infrared, and radio regions more or less continuously.

The prenova magnitude was V = 16.1. FH Ser was discovered on its rise to maximum, which was reached at visual magnitude 4.4 on February 18.5. The decline occurred smoothly until about April 16, when it became very dramatic. An UBV light curve between outburst and 1979, making use of all previously published data and new ones, is shown in Rosino, Ciatti, and della Valle (1986) (Figure 8-66, 8-67, 8-68).

VII.B. SPECTROSCOPY

Spectroscopic studies of FH Ser were carried out by Wagner et al. (1971); Anderson, Borra, and Dubas (1971); Burkhead, Penhallow, and Honeycutt (1971); Walborn (1971); Hutchings, Smolinski, and Grygar (1971); Ciatti and Mammano (1972); Stefl and Grygar (1981); Rosino, Ciatti, and della Valle (1986). The absorption spectrum shows two main components, the principal and the diffuse-enhanced spectrum. Each of these has two subcomponents. (Figure 8-69). A general increase of the radial velocity was observed in the first 60 days, i.e., before the onset of dust formation, with an acceleration of about 0.02 m s^{-2}. The redshifted emission components of the Balmer and nebular lines lost much of their strength during the dust-forming phase, and in most other lines (O II, Fe II, N II...), there were no detectable redward components (Hutchings and Fisher, 1973; Rosino et al., 1986). This indicates that the dust formation occurred in the shell itself, i.e., the radiation from the receding layers was severely absorbed by dust in the approaching layers.

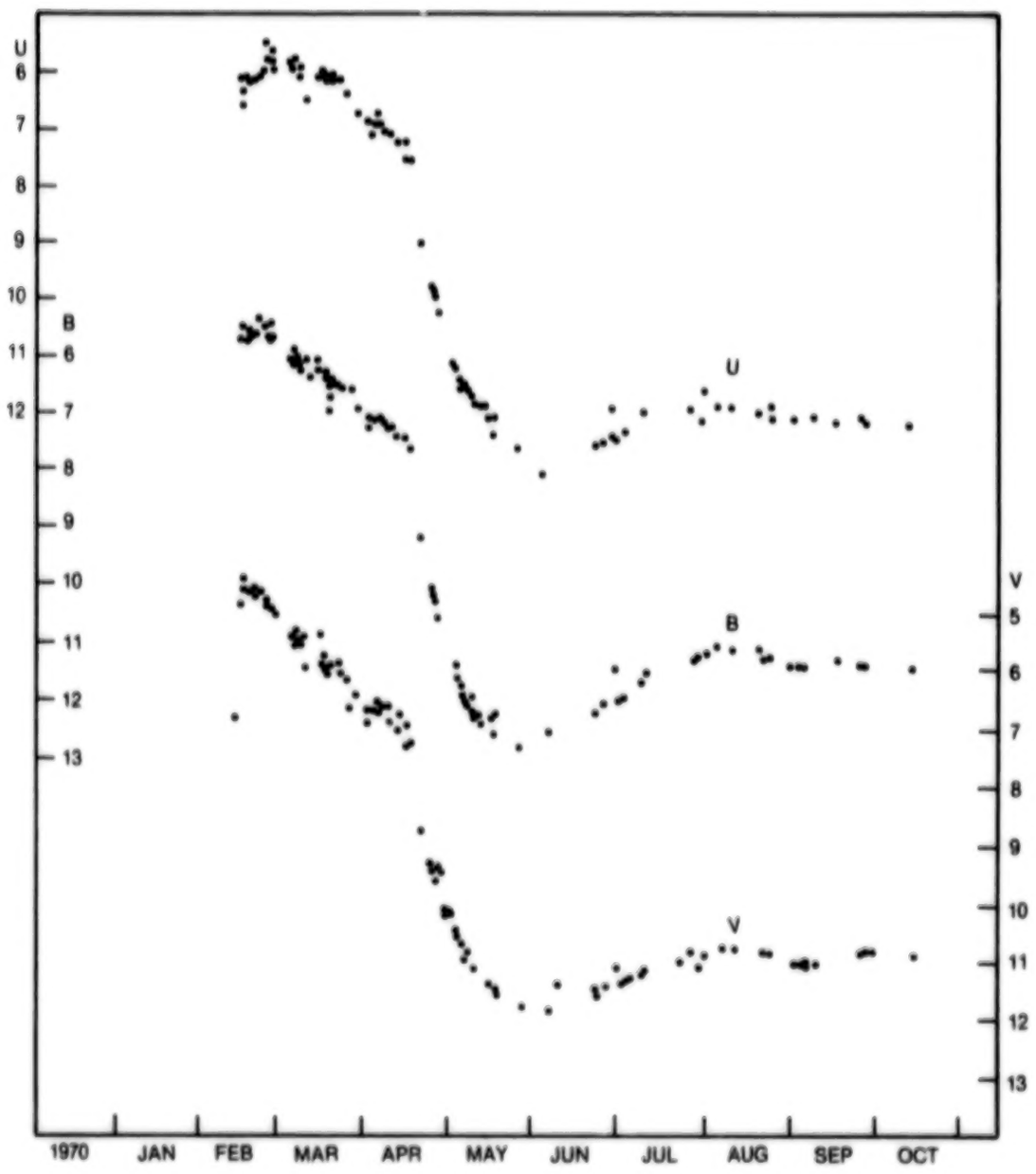


Figure 8-66. UBV light curves of FH Ser around maximum (Rosino et al., 1986).

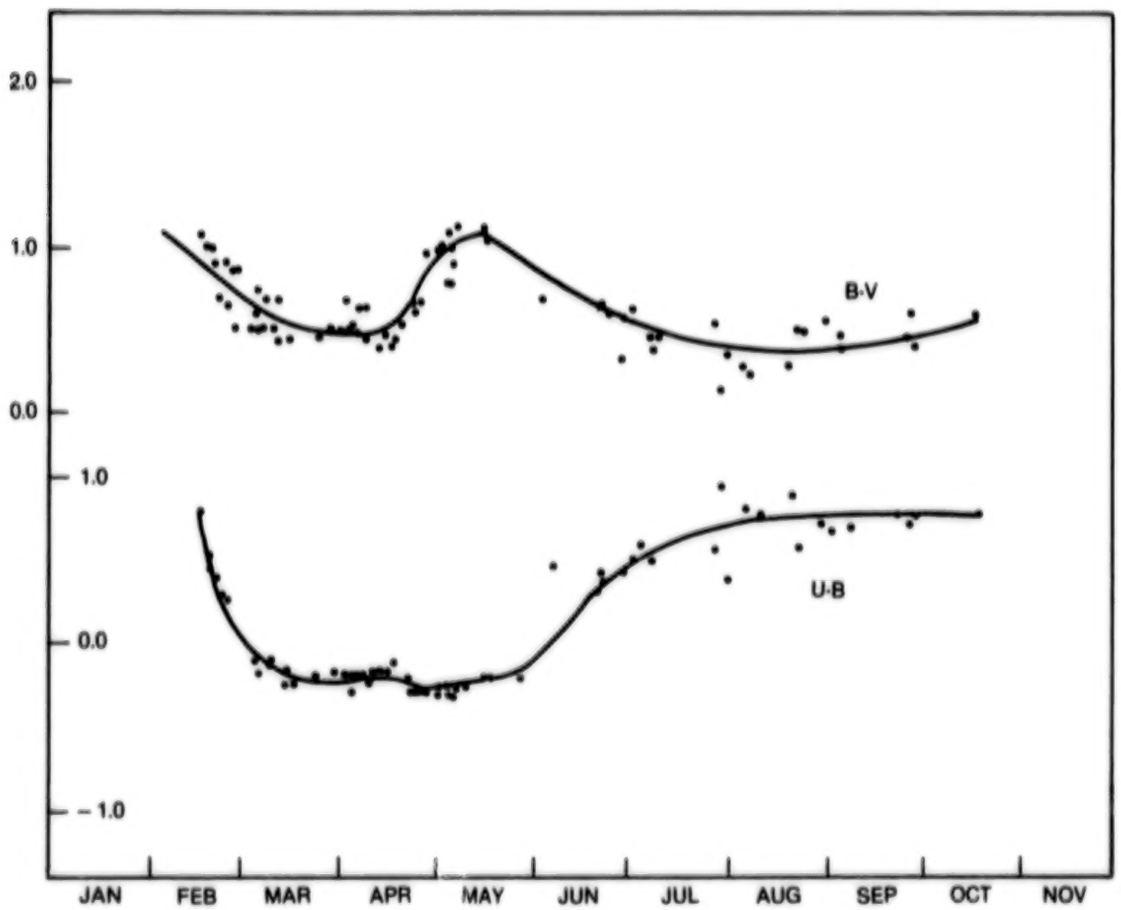


Figure 8-67. Colour curves of FH Ser around maximum (Rosino et al., 1986).

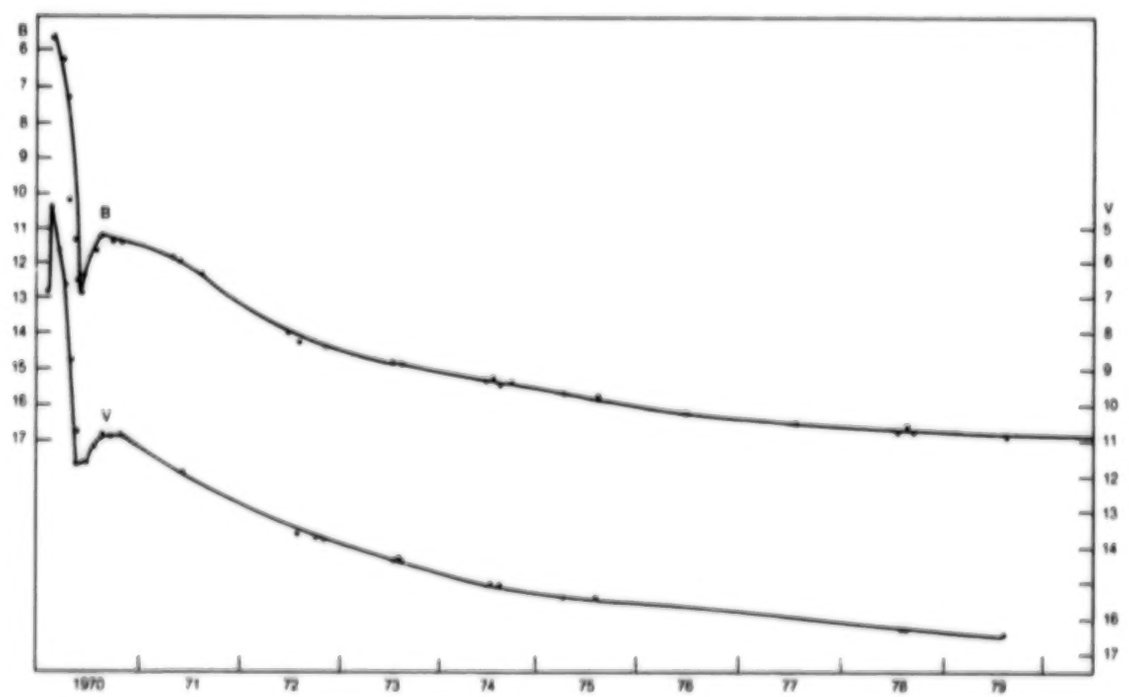


Figure 8-68. Extended B, V curves of FH Ser (Rosino et al. 1986).

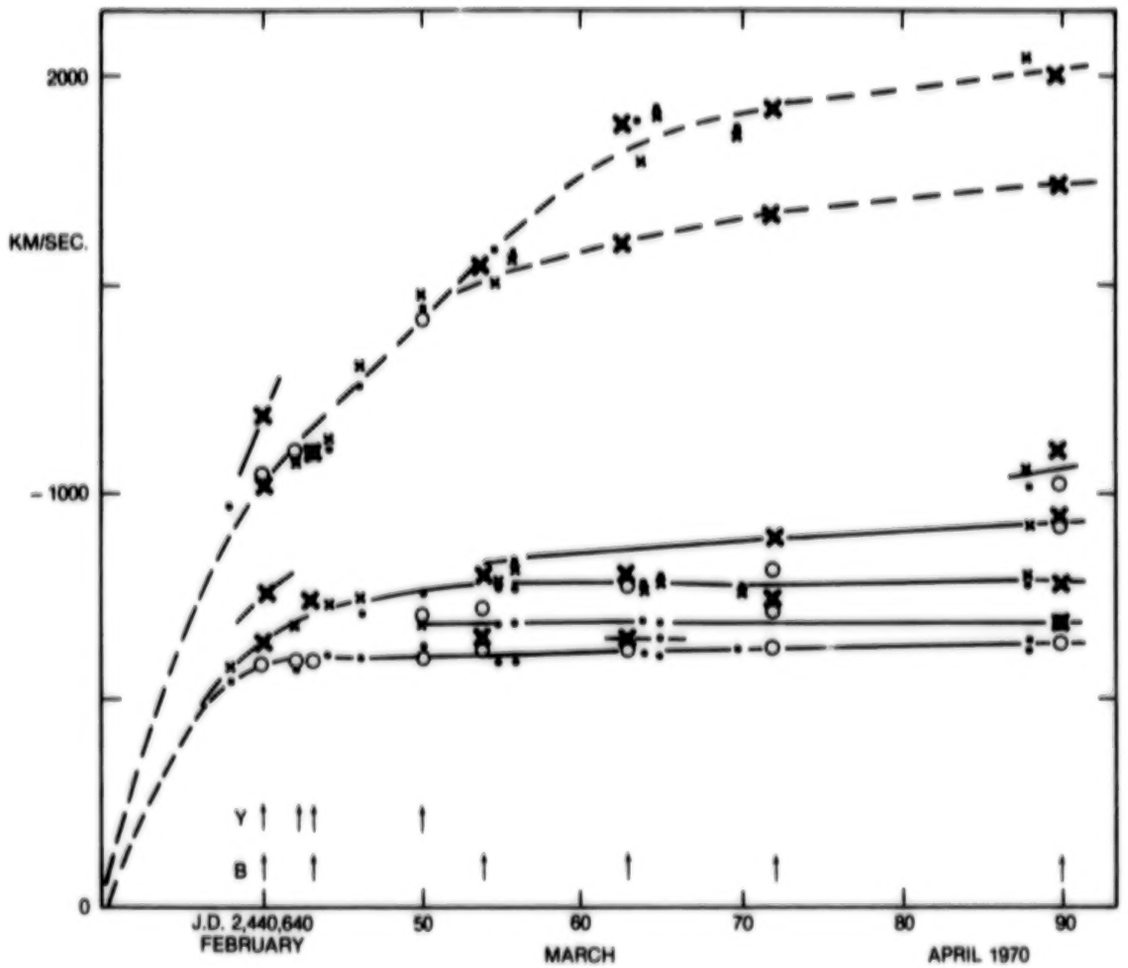


Figure 8-69. Absorption velocities in FH Ser. Crosses refer to Balmer lines, dots to metallic lines. The splitting of the principal and diffuse enhanced spectra into two (and later into four) components is clearly seen (Hutching et al., 1971).

A coronal line, [A X] 5535, was suspected by Anderson et al. (1971) on a spectrum taken August 13, 1970. Rosino et al. (1986) note that the nova attained its highest degree of ionization in March 1971, when they suspect lines of [Ni VIII] 4446, 4493, [Ni IX] 4332, 4404, [Fe XIV] 5303, and [A X] 5535. [O III] were also very strong in that phase.

VII.C. INFRARED OBSERVATIONS

Infrared observations were carried out by Hyland and Neugebauer (1970) and Geisel, Kleinmann, and Low (1970). Geisel et al. present light curves for .5, 1.25, 1.65, 2.2, 3.4, 5, 10, and 22 μm, which show clearly that the luminosity longward of 2 μm increases at the time when the light decreases at shorter wavelengths, which can be explained by formation of dust, which is heated by the central source. At peak infrared luminosity, the nova can be described as a spherical shell of unit emissivity radiating at 900 K, and having a diameter of 6.5 x 10^{14} cm (= 0.07") at a distance of 1.2 kpc, which may be an upper limit. Data taken from a more recent study are found in Section VII.F.

VII.D. RADIO OBSERVATIONS

Radio observations of FH Ser by Hjellming were analyzed by Seaquist and Palimaka (1977), and by Hjellming et al. (1979). They assumed a model in which the entire shell is ejected instantaneously and thickens as a consequence of velocity dispersion in the shell

(Hubble flow model). Two different geometrical assumptions, a spherical model and one consisting only of two polar caps, lead Seaquist and Palimaka to acceptable fits to the observed temporal change of radio radiation at 8.1 and 2.7 GHz, and to the spectral distribution of the nova remnant at a given moment (see Figure 6-76).

From the radio data and a Hubble flow model, a mass of 4.3 x 10^{-5} $M_{\odot}$ is deduced for the spherical shell, which has a temperature of 10^4 K and a distance of 730 pc.

VII.E. ULTRAVIOLET OBSERVATIONS

Ultraviolet filter photometry in the ranges of 1430 and 4250 Å and low-resolution spectral scans in the range of 2500 - 3600 A was carried out by the OAO-2 satellite (Gallagher and Code, 1974). The measurements were obtained from maximum to the onset of the rapid decline in April. (Figures 8-70, 8-71, 8-72, 8-73). Some additional UV lines are identified here.

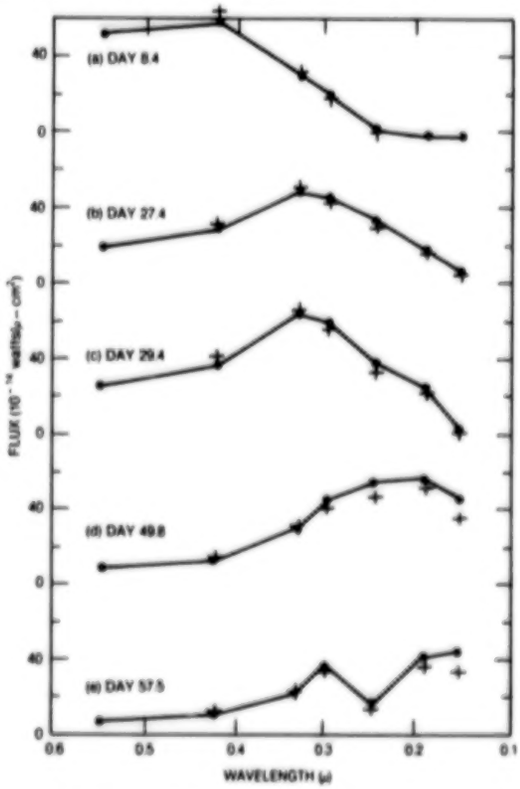


Figure 8-70. Flux distribution of FH Ser as measured by WEP photometry on board of OAO-2, corrected for an extinction of E(B-V) = 0.8. Crosses and dots refer to old and new calibrations (Gallagher and Code 1974).

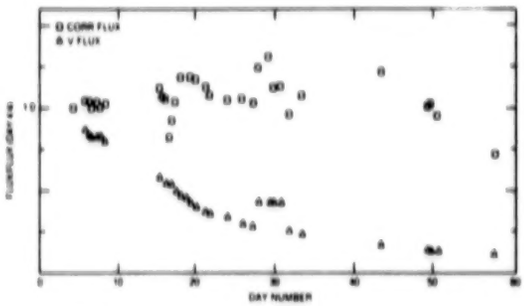


Figure 8-71. Integrated total flux as measured between 1550 aand 5460 A and corrected for extinction (open squares), and V flux (open triangles) (Gallagher and Code 1974).

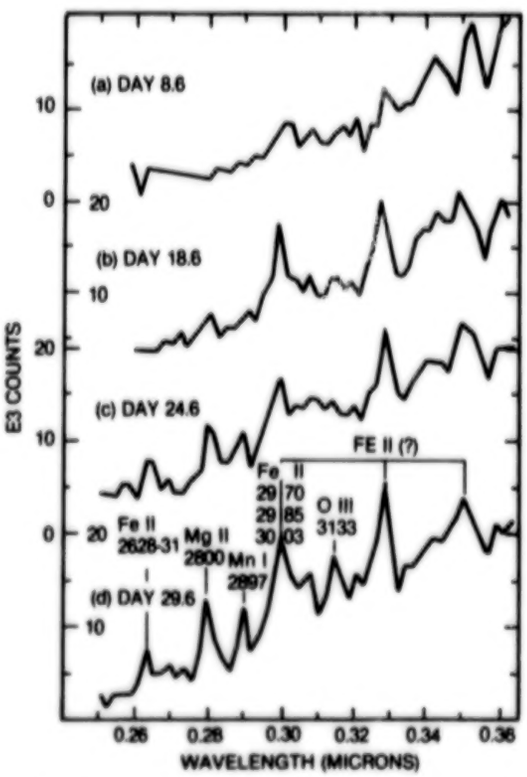


Figure 8-7 Spectral scans of FH Ser made with the spectrometer 1 on board of OAO-2 for times up to and including the "flare" in the light curve. The data have been corrected for the relative response of the scanner (Gallagher and Code 1974). Additional lines are identified.

VII.F. DISCUSSION

The most important result is that the nova did not decrease in total luminosity by a factor of 10 some 53 days after visual maximum, as implied by the V observations, but continued at almost constant luminosity. As the visible light declined, a compensating redistribution in flux

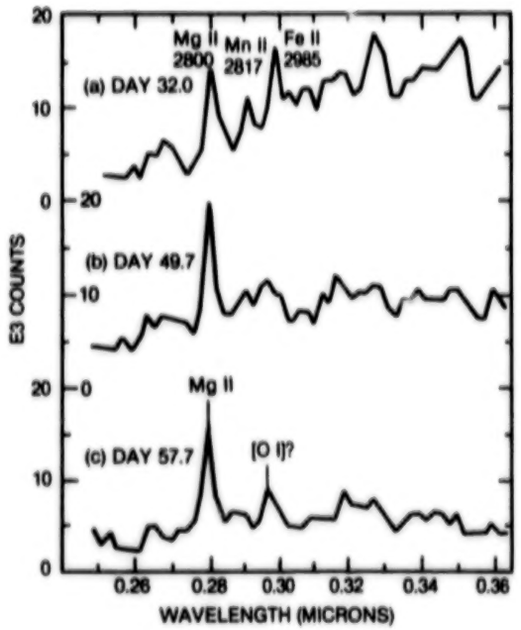


Figure 8-73. Spectral scans of FH Ser made with the spectrometer I on board of OAO-2 after the flare stage showing the increased dominance of Mg II. The data have been corrected for the relative response of the scanner (Gallagher and Code 1974). Additional lines are identified.

to the ultraviolet occurred (the correction for interstellar reddening must be accurate). The increase in IR flux, e.g., the peak in luminosity at wavelengths between 2.2 and 22 μm, which occurred about 100^d after maximum, is explained in terms of the observed trend for more energy radiated at shorter wavelengths, if efficient conversion of far-UV flux in the heating of grains occurs (see Figure 8-74).

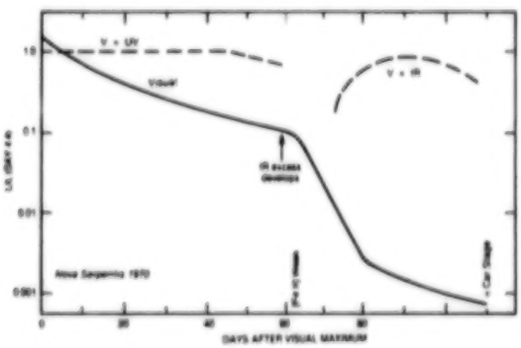


Figure 8-74. Smoothed energy budget for FH Ser as a function of time based on ultraviolet, optical and infrared data. The data show the postmaximum luminosity plateau, and the correlation between optical light curve as well as spectral features and the development of the thermal infrared excess (Gallagher and Starrfield 1978).

A more detailed study, taking into account infrared observations obtained more than 500 days after outburst, shows that from day 60 to 111, the light curve can be explained by rapid grain growth, and from day 111 to 129, by grain destruction. The luminosity appears to remain constant until day 200, after which it fell inversely proportional with t (Mitchell et al., (1985). (See Figures 6-28 and 6-29).

FH Ser is a good example for a nova to be a constant-luminosity system for a period of at least 10^7 sec after visual maximum. The hypothesis that the light curve changes are primarily due to the effective photosphere of the star, which in term is dominated by the mass-ejection rate, can explain the observed features.

From the strength of the IS lines, Huchings et al. estimated a distance of 750 pc, and an interstellar extinction $A_v = 1.5$; thus, the absolute magnitude of the nova was $M_v = -6.5$.

VII.G. THE REMNANT

A CCD image of the resolved shell of FH Ser is given by Seitter and Duerbeck (1987). The frame taken in mid-August 1984 shows an oval shell (with some indications of polar condensations at the end of the larger axis with a size of 3.9" x 3.1". The nebular expansion parallax is ambiguous due to the variable radial velocity observed during outburst; a good guess of 550 km/s (also based on emission line widths) leads to a distance of 825 pc. If the fairly strong expansion velocity component with 1100 km/s is used, the distance would not be reconcilable with other distance estimates (see Section VII.F.).

The orbital motion of FH Ser is unknown. Vogt (1981) estimates from the dereddened colors of the nova that the orbital period is of the order of 7.5 hours.

VIII. DQ HER 1934: A SLOW NOVA
(written by Hack)

DQ Her — a typical slow nova — has been observed very extensively, and its history has been reported in great detail by Beer (1974).

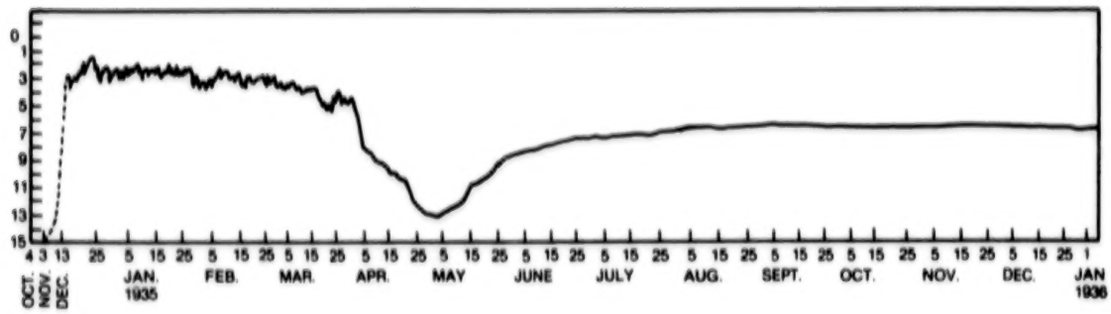


Figure 8-75. The light curve of Nova DQ Her, covering the period 1934-1936. (from Beer, 1935, 1936).

This history is very instructive as a detailed example of the complexity of the spectrum of a nova.

The magnitude before outburst was about 15. It rose to mag 3 on December 13, 1934, and reached maximum brightness 10 days later with mag 1.3. It went back to mag 3 on December 25 and then decreased slowly, with several oscillations, to reach mag 5 at the beginning of April, when the deep minimum, which is a common feature of the light curves of several slow novae, started. At the beginning of May, the magnitude was about 13, then the light increased again, and on June 15, it was about 7.5 and the phase of smooth decline began (Figure 8-75).

VIII.A. SPECTRAL VARIATIONS DURING OUTBURST

The premaximum spectrum (Abs.I and Em.I) changed from type B to type A during the day of discovery. A second shell (Abs.II and Em.II) was seen on December 23, a day after maximum brightness. Then several shells appeared: III and IV with multilple components; shell V, on January 13; shell VI on January 23; shell VIII, on March 23-25; shell IX, in the second half of March; shell X, on March 20-24; shell XI, in January. These shells are identified by the various systems of lines having the same radial velocities and are subject to different interpretations. For instance, McLaughlin, in his study (1937), identified shells II, III = VII, IV, V, VI, VIII, IX, X, and XI, while in his successive interpretation of 1954, he identified just shells II, III with several components, IV and V.

The expansional velocities range between 300 and 1000 km/s. Shortly before the start of the deep light minimum, the emergence of [FeII] emissions was observed. The same phenomenon was observed in other novae having the same type of light curve. It is evident that the expanding envelope has reached a sufficiently low density for the forbidden lines to appear.

It is interesting to recall that Struve in 1947 expressed the idea that the nebulosity where [Fe II] is formed is not purely gaseous but contains also iron-rich dust particles; Stratton (1945) suggested that the deep minimum in the nova light curves is due to an obscuring cloud formed inside the main outer shell. Now infrared observations have shown that these suggestions were fundamentally correct and that a dust shell is actually formed in moderately slow novae, just coinciding with the dip in the light curve.

Before the deep minimum, the emission bands in DQ Her spectrum started to show two maxima (Figure 8-76). During the deep minimum (from the beginning of April to the end of May), the longward components faded and disappeared, suggesting that the increasing opacity of the shell permitted the observation only of that part of the envelope expanding toward us. At the end of the deep minimum, the longward emission reappeared.

Interactions between different shells seem evident from the observational data. These are described in detail by Beer (1974). Let us consider just one significant example, quoting from Beer:

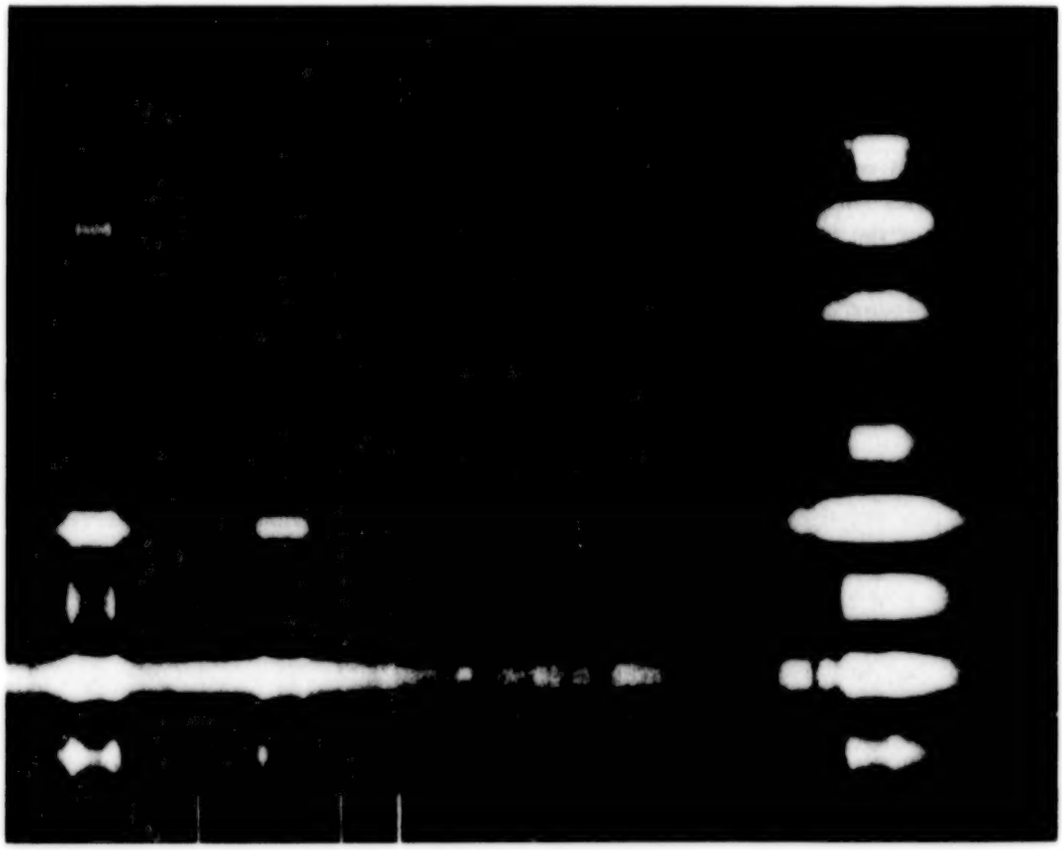


Figure 8-76. DQ Her: the structure of Hα between January 12, 1935 and March 24, 1935 (adapted from Stratton and Manning, 1939).

"With regard to the later shells McLaughlin (1947) pointed out that while the atoms of the shells giving the Orion spectrum were so rarified as to be unlikely to produce any results on the outer shells, the atoms from the diffuse enhanced shells III and IV might overtake the principal shell II before they get too rarified. We might observe an acceleration of the principal shell and possibly the disappearance or a retardation of the later component. McLaughlin (1954, p. 135) has discussed in more detail the problem of shells overtaking each other with special reference to shell III and shell IV overtaking shell II. The view that the particles in the different clouds continue to move outwards at a constant or slightly increasing speed is strongly supported by the presence of separate narrow components in the second half of March...Let us first consider the question on what date shell III should have collided with shell II. McLaughlin gives 1934 December 26 as the date of emergence of shell II. An independent study of early plates (Stratton, 1936, p. 148) suggests December 24. Let us accept December 25. Taking a mean velocity of 317 km/s for 1934 December 25 to 1935, January 15, of 323 km/s for January 15-25, and of 333 km/s for Jamuary 25-29, we find that by January 29 the original particles of shell II would have travelled outwards 9.6 x 10^8 km".

"For shell III McLaughlin gives January 8 as the date of emergence; a study of the Stratton and Manning Atlas (1934) and of the Cambridge plates suggests January 10. Let us accept January 9, the date of a maximum in the light curve. Then with an average velocity of 569 km/s the original atoms of shell III would have travelled 9.7 x 10^8 km by January 29. We may note also that the largest increase of velocity of

shell II occurred between January 26 and 30. It seems reasonable to accept the view that shell III overtook shell II on or a little before January 29. McLaughlin's date for this event is January 23 . In support of January 29 we may add that according to Rottenberg (1952), when an inner shell overtakes an outer shell, the peaks in the emission bands should strengthen relatively to the centres of the bands. Emission maxima in the Fe II bands shortward of H Beta are first detected on January 29 and rapidly strengthen though they are visible in the H and K bands of Ca II a few days earlier, suggestive again of stratification, the Ca II atoms being ahead of the Fe II atoms. We may further note that Absorption III faded out on January 25 and did not reappear until February 3".

"This was probably mainly due to the strengthening of the emission from shell IV: The emission bands widened on both wings during the last few days of January. By this time the leading atoms of shell III and shell IVi were closely intermingled with each other and with shell II. Taking the date of emergence of shell IVi as January 12 and its mean outward velocity as 674 km/s, the date of collision of shells III and IVi becomes January 28. By this date Absorption IVii had become the strongest absorption".

"1935 January 19 (another maximum in the light curve) is McLaughlin's date for the emergence of shell IVii and his mean velocity is 800 km/s. Cambridge plates give January 20 and 779 km/s. Both sets of figures agree in giving February 5 as the date when shell IVii overtakes shell II, by which date absorption IViii had become the strongest component. During the first week of February there was a further increase of velocity of shell II."

"Absorption IViii was measured on Mount Wilson plates as early as January 20, but it was not clearly separated on Cambridge plates until January 28. McLaughlin gives January 24 as the date of emergence and 900 km/s as the mean outward velocity. This gives February 10 as the date on which the initial particles of shell IViii would overtake shell II, a date coinciding with another increase of velocity of shell II. If shell V can be regarded as starting on January 27 with a velocity of 1100 km/s, it would overtake shell II about the same time as shell IViii, thus accentuating the effect on the outward velocity of shell II. By this time, however, the picture is getting very complicated and the conclusions to be drawn from these figures must be regarded with considerable caution".

"Shell VI would not have reached shell II before deep minimum : Absorption VIII was too fitful in appearance and strength to be discussed in connection with collisions; all that can be said is that its shell was outside shell VI late in March, as its absorptions completely wiped out emissions of shell VI. Shell XIi, if it started on February 16, would have overtaken shell II about March 5, and it was in the first week in March that shell II increased again in velocity. Shell XIii which emerged early in March would not have reached shells III and IV by March 18, and its emission might have provided the background for the narrow absorption lines of shells III and IV measured around that date. But this is a hazardous speculation and would require the spectroscopically active region of shell XIii to be close to the star. All that can really be said on the idea of shells overtaking one another is that it is a crude simplification of "what is really a very complicated state of affairs, but that it is not inconsistent with a number of changes during the first three months of the observed history of the nova."

This decription of the spectral evolution of DQ Her gives an idea of how complicated the spectrum of a nova can be and how difficult is its interpretation.

Spectra taken after 1942 show a strong ultraviolet continuum due to the central star and line emission profiles showing double maxima, clearly indicating that they are produced in the expanding optically thin envelope. The double maxima are especially clearly observable for the hydrogen lines and for 4686 He II (Figure 8-77).

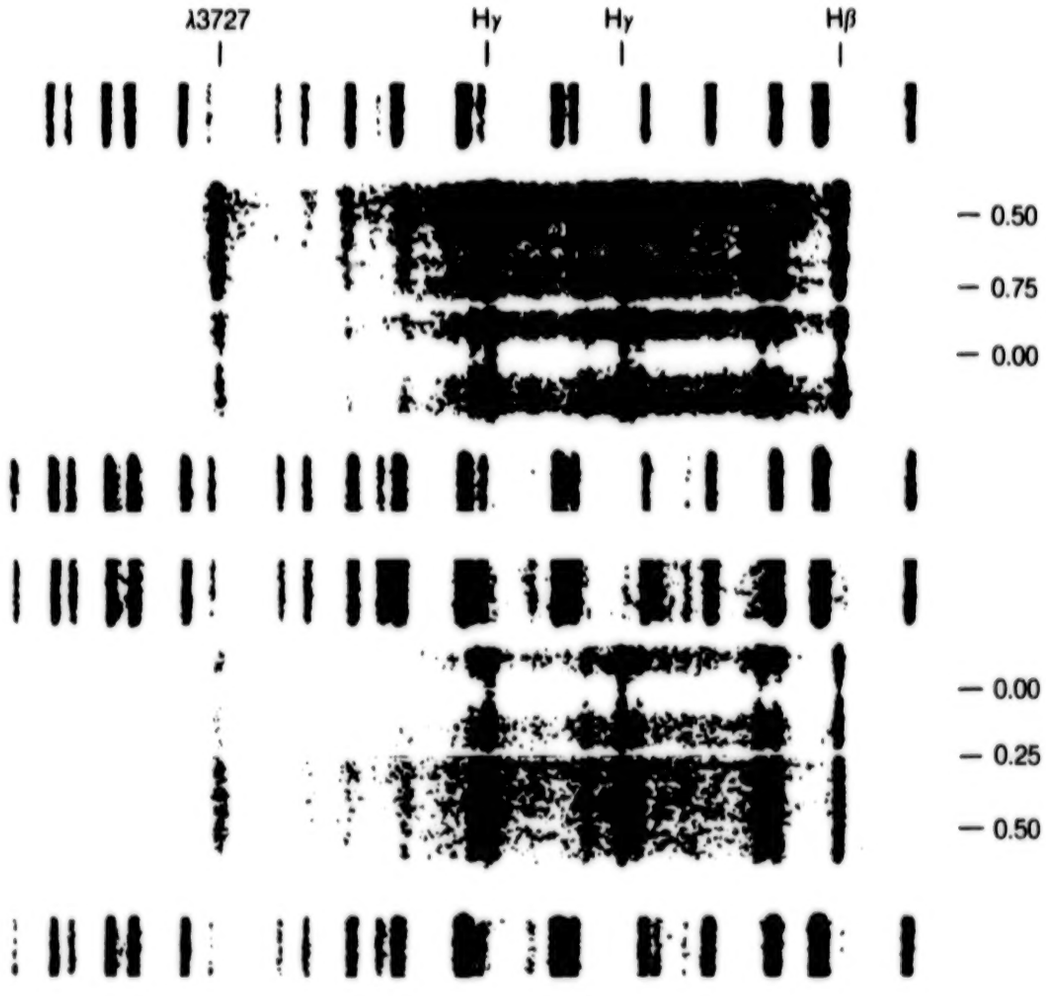


Figure 8-77. The central star of DQ Her in 1955.
(from pictures taken by G. Herbig, Lick Observatory).

VIII.B. CHEMICAL COMPOSITION AND EXTENDED ENVELOPE CHARACTERISTICS

Curve of growth analysis of the absorption lines in the pre-maximum spectrum (Abs.I) and in the principal spectrum (Abs.II) were made by Mustel (1956, 1958, 1963), by Mustel and coworkers (1958, 1959, 1965, 1966, 1972), by Gorbatsky (1958, 1962) and by Gorbatsky and Minin (1963). The chemical composition of the absorption-line region at maximum light and at other dates is practically the same and it is compared with the average chemical composition of normal stars. The relative abundance of metals is normal; instead, carbon, nitrogen and oxygen are more than 100 times higher than in normal stars. Although this kind of analysis is very uncertain, because the intensity of the absorption lines may be seriously affected by the presence of the emission components and especially because the pseudophotosphere is very far from the condition of LTE, Pottasch (1967) confirmed this result by measuring the emission forbidden lines of these elements. He gave the average abundances of CNO for five novae including DQ Her, and found an excess by at least a factor of 10.

Direct photographs of DQ Her taken on July 6, 1945, in the light of [OIII] lines of 4959 and 5007 A and in the light of [NII] lines at 6548 and 6584 A, look very different from each other. Both are similar to a planetary nebula, but the image in the light of [OIII] (Figure 8-78) shows an elongated ring surrounding the

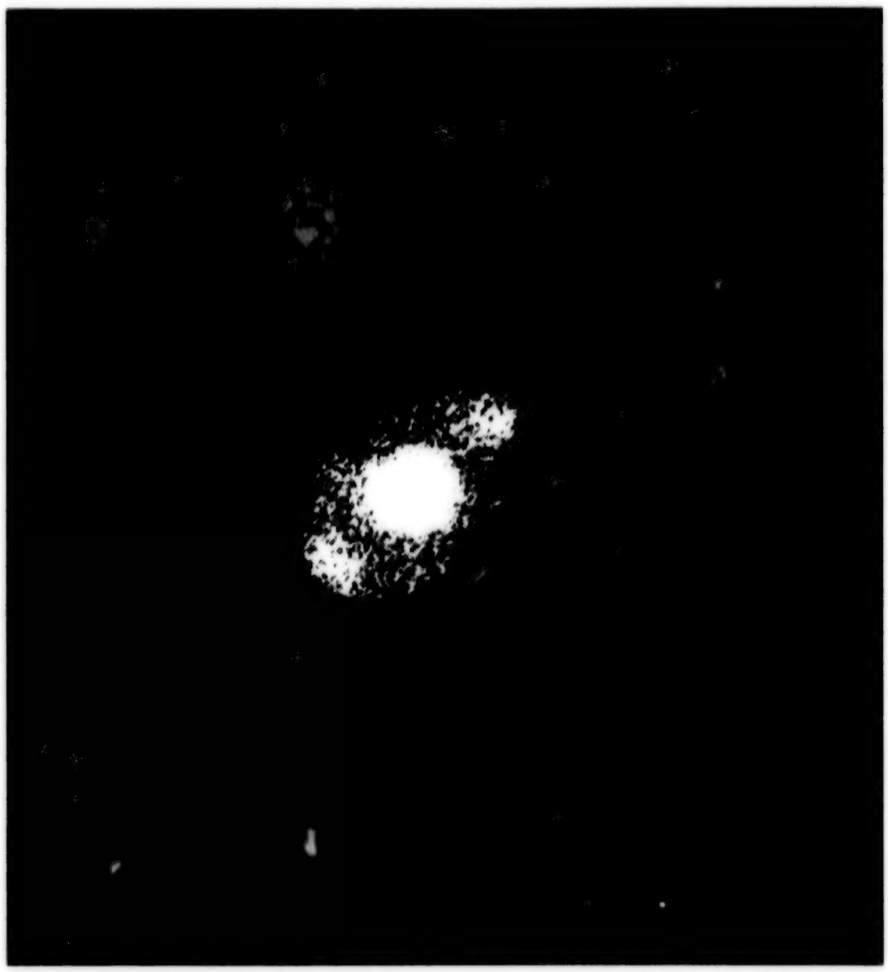


Figure 8-78. The envelope of DQ Her in the light of the /O III/ lines at 4959 A and 5007 A, photographed by W. Baade on July 6, 1945 with the M. Wilson 100 inch telescope.

central source, with two slightly stronger blobs in the direction of the major axis; the image in the light of [NII] (Figure 8-79), on the contrary, shows three strong condensations along the minor axis. Spectra taken with different orientations of the slit indicate that each line shows longward and shortward displacements, highest at the center of the slit and least at the two ends of the slit: expansional velocities of the order of 70 km/s and of 300 km/s were found at the border and at the center of the expanding nebula respectively.

Figure 8-80 shows the monochromatic image of the nova shell surrounding DQ Her in the light of H Alpha obtained more than 40 years after outburst. The circles indicate the regions where the spectra given in Figure 8-81 were taken (Williams et al., 1978). These spectra are very similar to those of a typical planetary nebula. However, certain permitted recombination lines of C and N are unusually strong for a typical planetary nebula, while 5007 [OIII] is not present. A strong emission feature at 3646 A is attributed to the Balmer continuum, formed at the very low electron temperature of about 500 K.

Muste[illegible] and Boyarchuck (1970) noted that the 4959, 5007 lines of [OIII] weakened already during the 1940s and had practically disappeared by 1950. This weakening was attributed to a drastic decrease of the temperature, as confirmed by the strong Balmer jump observed by Williams et al. (1978) indicating $T_e \simeq 500$ K. The gas in the envelope presented the sharp Balmer jump already in old spectra obtained in 1956-58 (Greenstein and Kraft, 1959). On the other hand, the emissions of C II 4267 and N II 4237 and 4242 indicate an elec-

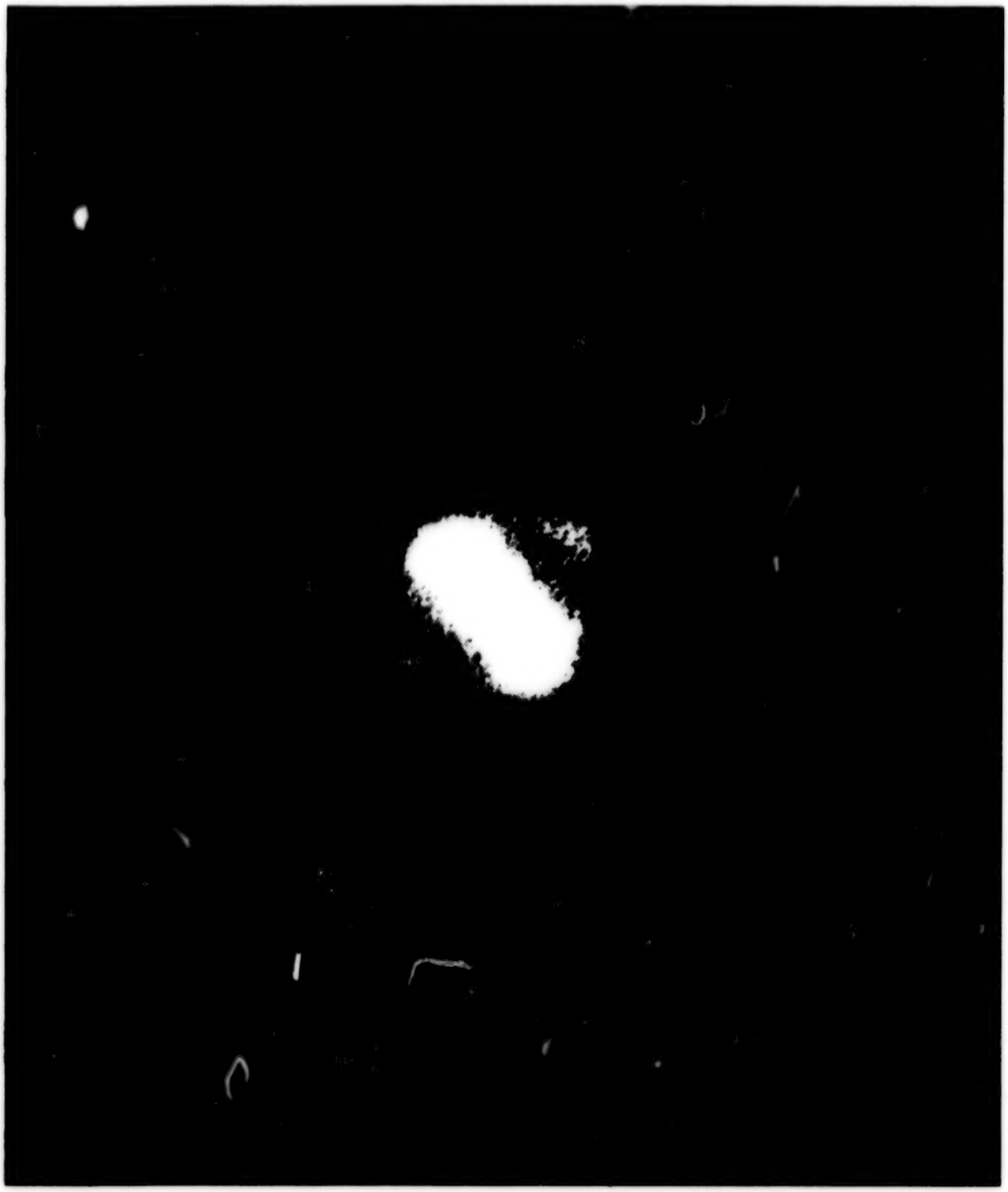


Figure 8-79. Same as Figure 8-78, but in the light of [N II] lines at 6548 and 6584 A.

tron temperature of about 10^4 K, and their strength is about one or two order of magnitude greater than in planetary nebulae.

These data suggest that the shell contains two regions: one that is hot and the other that is cold. The C II and N II permitted lines are pure recombination lines, because they originate in levels high above the ground state (20 eV), which are not directly coupled to the ground state by permitted transitions. Hence, radiative or collisional excitation from the ground line is very unlikely. Since the emission coefficients of the C II and N II lines have about the same temperature and density dependence as the Balmer recombination lines, the relative intensities depend only on the relative abundance of the emitting ions integrated over the emitting region. It is found that $C/H \simeq 10^{-3}$ and $N/H \simeq 10^{-2}$. Hence, C and N appear to be enhanced relatively to H by factors of 20 and 100, respectively, in comparison with the solar values. The He abundance derived by 4471 He I appears to be essentially solar. The determina-

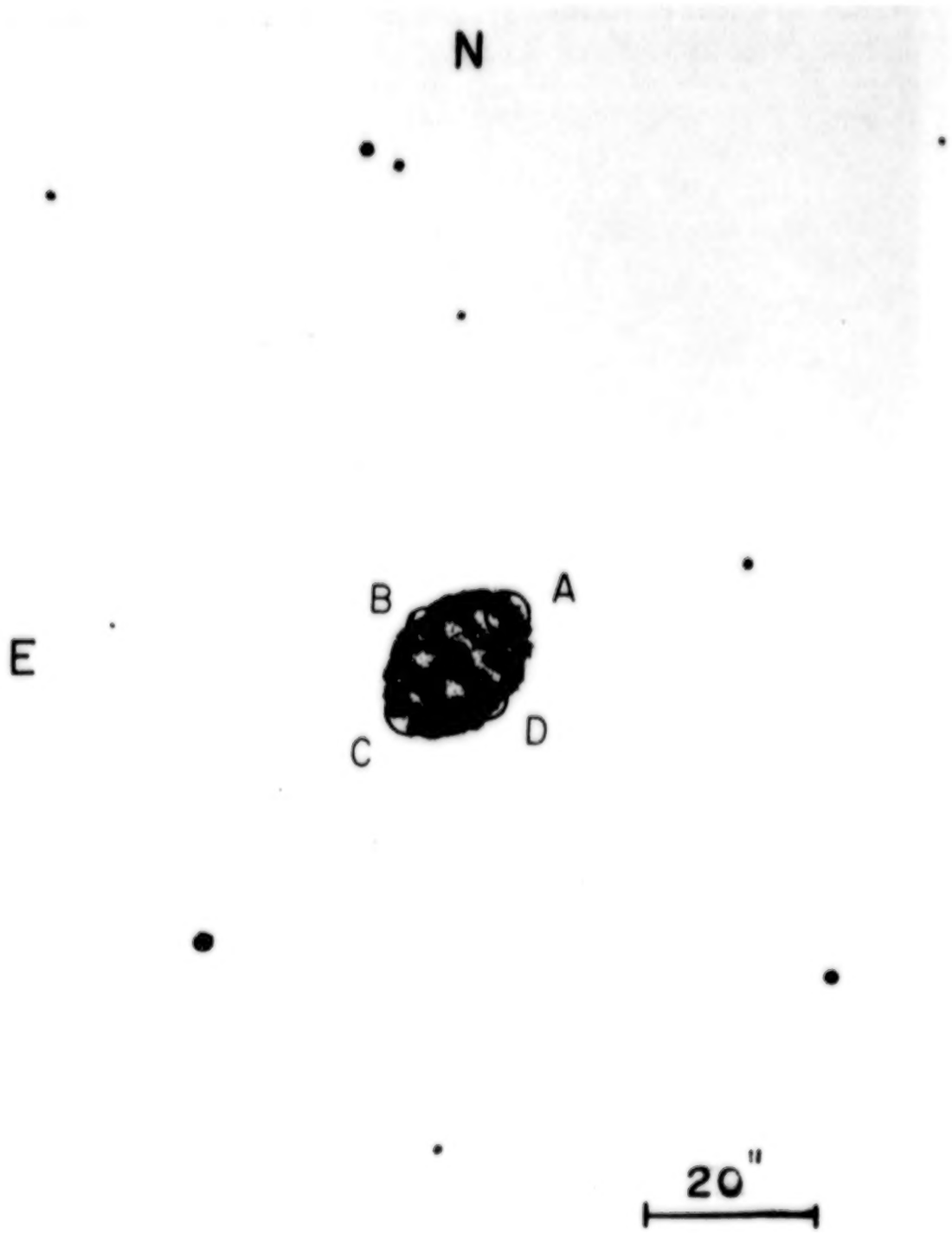


Figure 8-80. Monochromatic photograph of the shell surrounding DQ Her in the light of Hα. The circles indicate the regions where spectra were obtained. (from Williams et al., 1978).

tion of the oxygen abundance is difficult because no recombination lines are observable, but only forbidden lines whose intensity depends strongly on the assumed electron temperature.

Now the problem is to understand why the electron temperature in the shell is so low as indicated by the sharp Balmer jump and by the absence of collisionally excited forbidden lines and why strong (C,N) once-ionized recombina-

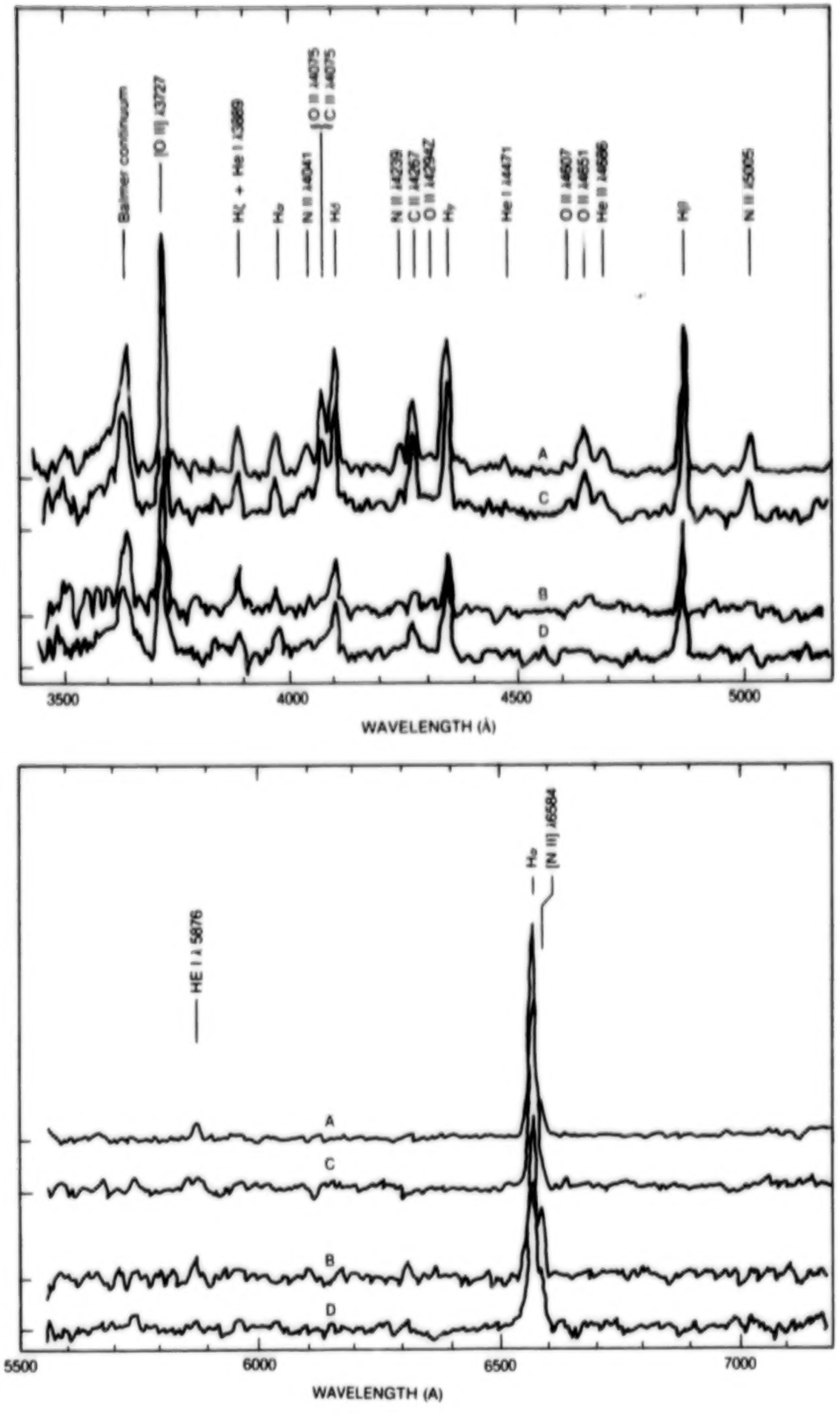


Figure 8-81. a) blue spectral scans of the regions indicated in Figure 8-80; b) red spectral scans of the same four regions. (from Williams et al., 1978).

tion lines are present, which indicate a temperature of at least 10^4.

One can think of various possibilities: the ionization of the gas is a relic of an earlier phase, the gas expands more rapidly then it recombines as suggested by Williams et al. (1978).

Or alternatively, the radiation field emitted by a hot central object (e.g., an X-ray source produced by matter accreting on the white dwarf) ionizes the shell producing very little heating, as suggested by Ferland and Truran (1981). However, both these hypotheses have been discussed by Ferland et al. (1984), who were able to show that both are not acceptable. On the contrary, the large overabundance of heavy elements indicated by the nebular spectrum explains the low temperature and the strength of the recombination lines.

But let us see in more detail the conclusions of this latter work. Ferland et al. have used the infrared, optical, ultraviolet and X-ray observations of the nebula and the central object. The composite spectrum is derived by ground-based observations in the optical and infrared range obtained by Schneider and Greenstein (1979) by ultraviolet observations obtained with IUE and x-ray observations obtained by Cordova et al. (1981b) with EINSTEIN. According to the generally accepted model, the continuum is essentially due to the central object and is shown in Figure 8-82 (corrected for interstellar extinction). The emission line spectrum is due to an accretion disk and to the shell. The UV emissions originating in the shell are spatially resolved on the two-dimensional image obtained through the large aperture of IUE (10" x 20"). The only feature clearly originating in the shell is 1335 C II. The optical emissions and their intensity relative to H Beta are given in Table 2 of Ferland et al. (1984). From these data, the authors show that the recombination time for 4686 He II, which has been always present in the nebula spectrum, is of the order of 20 years (for T_e = 500 K and N_e = 100 cm^{-3}). The low value of T is confirmed also from the ratio of the two lines of C II: I(1335)/ I(4267). For temperatures included

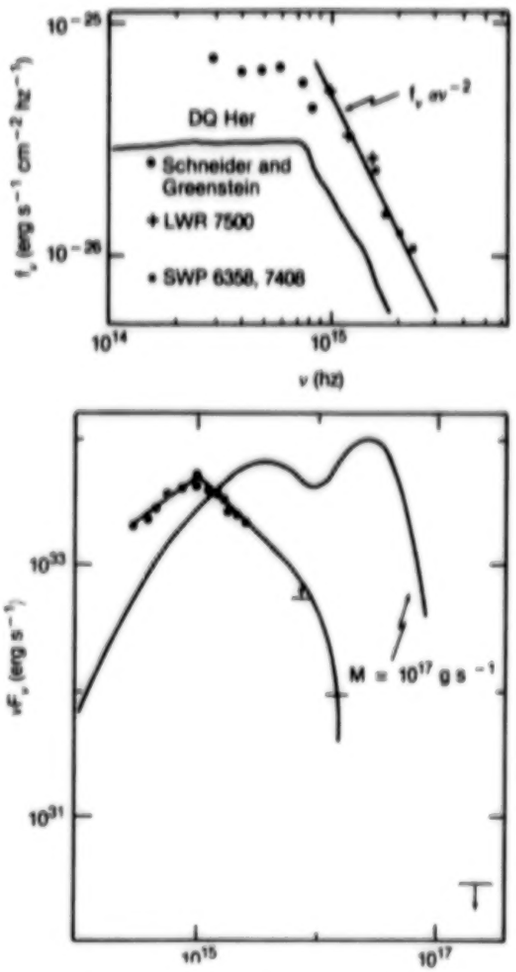


Figure 8-82. a) Composite ultraviolet-infrared continuum. The points are reddening-corrected fluxes and are averages over emission-line free continuum intervals. A line corresponding to a power law with spectral index -2 is drawn for comparison, it fits well the UV continuum. b) The dereddened observed continuum, for E(B-V) = 0.12, corrected for the assumed geometry (a flat disk seen at inclination of 80°) is compared with the theoretical continuum for an accretion disk with mass transfer of 10^{17} g s^{-1}.
(from Ferland et al., 1984).

between 7000 and 15,000 K, this ratio varies only from 56.3 and 59.8 (Storey, 1981; Seaton, 1978b). It becomes much lower for $T<10^3$. Since the observed ratio is 9, the value of $T_e \approx$ 500 K is confirmed. The value of N_e is indicated by the volume of the shell and the H Beta luminosity. The expansion time for the nebula is of the order of 50 years. Hence, the continuous presence of 4686 He II indicates that the gas is being ionized continuously since the epoch of the outburst, contrary to the assumption by Williams et al. (1978).

The observed continuum for the central object (Figure 8-82b) is very different from that expected from an accretion disk and a mass-transfer rate of 10^{17} g s^{-1} (Smak, 1982) and also the following section), and especially the EINSTEIN observations have shown that DQ Her (as well as the other quiescent novae) are not strong X-ray sources. Hence, the model by Ferland and Truran (1981) is not acceptable. Instead, photoionization calculations indicate that for a wide variety of ionizing radiation fields, the nebula will stay at $T < 10^{4}$ K if the heavy elements are overabundant and the density low enough.

Actually Ferland et al. (1984) show that the low density and an enhanced oxygen abundance permit the production of low electron temperature. Infrared fine-structure lines of carbon, nitrogen, and oxygen are very efficient coolants for low-density nebulae. It is shown that at the ionization conditions and chemical composition of the nebula surrounding DQ Her, the IR lines at 88 μm and 52 μm of [O III] can easily cool the gas at 500 K. Table 3 from their paper and Figure 8.83 show the electron temperature which is reached for different oxygen overabundances through these two IR lines. For O/H varying between 10 and 100 times the solar value, the electron temperature varies between 1150 and 180 K. The graph gives the electron temperature versus the density, computed for a given $\dot{M} = 10^{17}$ gs^{-1} and a ratio U of photon density to electron density equal to 10^{-3}. (Here $U = Q(H) / 4\pi r^2 Nc$.) Q(H) is the number of ionizing photons emitted by the central object per second, r is the separation between the source and the nebula, (which is of the order of 4×10^{16} cm, as estimated from the angular diameter of the nebula and the distance of the system), and N and c are the density of the gas and the speed of light.

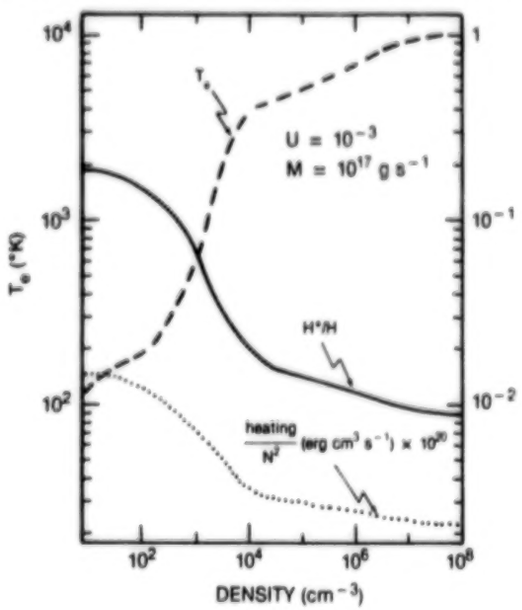


Figure 8-83. Dependence of the electronic temperature on the gas density in the shell. The temperature falls dramatically at N<1000 particles per cc because the infrared fine structure lines become efficient coolants. (adapted from Ferland et al., 1984).

In fact, for a luminosity of the central object of the order of 10^{32} erg/s, and assuming that the ionizing photons correspond to wavelength lower than 3500 A, it follows that $L = h \nu \times Q(H)$, $Q(H) = 7 \times 10^{41}$, $U = 10^{-3}$. The observed photoionizing continuum and the observed electron density permit us to predict the intensities of the emission lines and to compare them with the observations (see Tables 2 and 3 of Ferland et al. (1984)). The agreement is satisfactory and gives a positive test of this model. However, the predicted intensities of the 88 μm and 52 μm lines should be revealed by the IRAS observations. Instead, very few of the observed novae show measurable far IR flux.

The hydrogen emission in the envelope has been used by several investigators to derive the mass of the envelope; its value is found to be included between 1.4×10^{28} and 10^{29} g (7×10^{-6} and 5×10^{-5} solar masses). If we estimate the mass fraction of carbon, oxygen, nitrogen, and neon, we find that half of the mass is due to these elements.

VIII.C. DQ HER PARALLAX FROM NEBULAR EXPANSION

Observations of the nebula made by Williams et al. (1978) in 1977 have been used by Ferland (1980) for deriving the distance of the nova from the nebular expansion. The distance derived in 1940, when the size of the nebula was estimated at about 3", gave d = 230 pcs. According to Ferland, this value was probably overestimated, because the value derived about

40 years later was 15", implying a deceleration on the expansion. Such a deceleration due to interaction with the interstellar medium should produce high temperature in the nebula. However, the absence of coronal lines through 1940 rules out high temperatures. Ferland concludes that the size of the nebula was overestimated in 1940. On this assumption, the present size gives a distance of 420 +/- 100pcs, i.e., considerably larger than that previously estimated. This new value of the distance brings the absolute magnitude of DQ Her at maximum light to Mv = -7.1 +/- 0.7 and Mv on the broad plateau at -5.9 +/- 0.7. With this revision of the distance the luminosity at maximum become close to the Eddington limit for one solar mass star.

VIII. D. THE ECLIPSING BINARY DQ HER

In 1954, Walker discovered that the nova is an eclipsing binary of the Algol type with the very short period of 4h39m (Figure 8-84). After this discovery, Ahnert (1960) measured 27 Sonnenberg plates taken in the years 1930-1934 in the field of the prenova, and found that DQ Her was an eclipsing binary with a period of 0.1932084 days, while, according to Walker, after the explosion, the period was 0.19362060. From this value of dP/dt, Ahnert estimates a mass ejection during the eruption of 1.6×10^{-3} solar masses, two orders of magnitude larger than that derived by the spectral emissions. However, we remark that if there are both mass loss and mass exchange, as is probably the case, it is impossible to derive them simply from dP/dt. Moreover, Schaefer and Patterson (1983), using the archival plates of Harvard college Observatory, did not confirm the period given by Ahnert for the prenova. The Fourier transform of 50 prenova observations does not have any significant peaks. According to them, this is because there are too few observations with too long exposures to detect the eclipse. The same authors were able to derive the mass of the ejecta for another nova, BT Mon, by comparing its orbital period before (0.3338010 d) and after (0.3338141 d) erup-

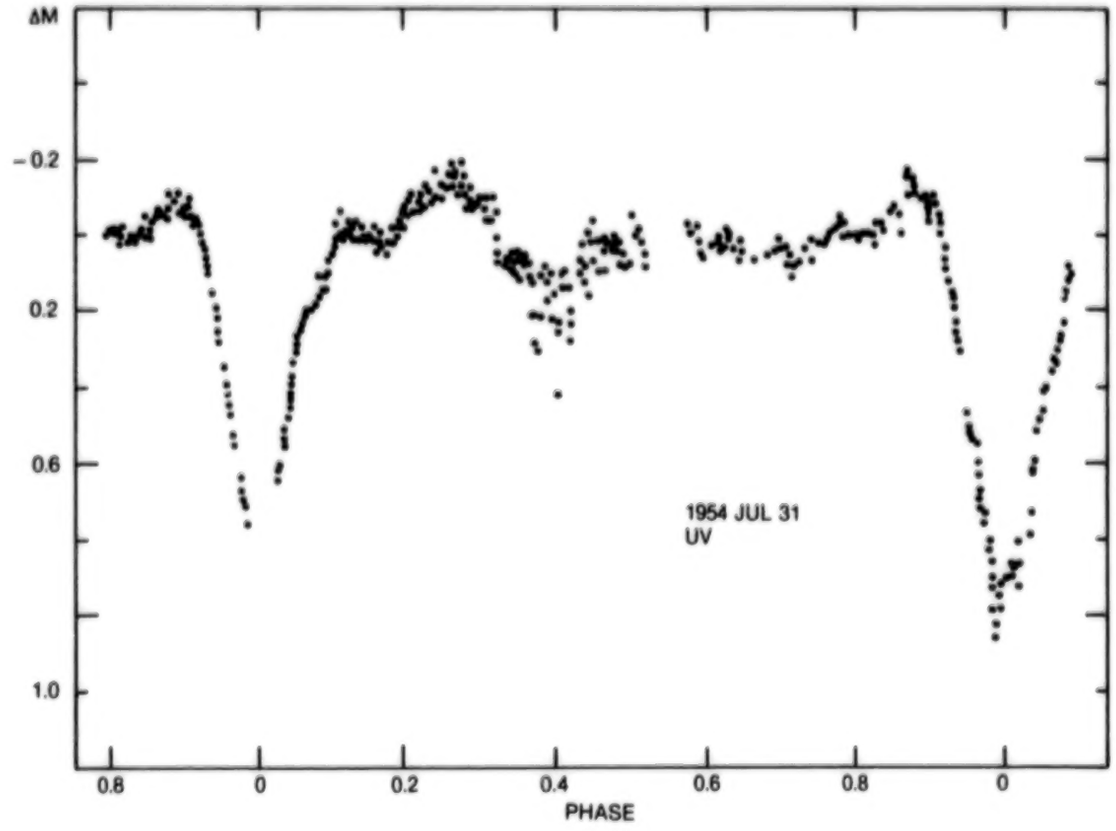


Figure 8-84. Photometric observations of DQ Her (from Walker, 1956).

tion. They found a reasonable value, 3 x 10^5 solar masses. However, the variation of the period depends also on the mass lost from the system and not only from mass transfer. Hence, these determinations are not very reliable.

According to the Ritter catalog (1987), the masses of the two components are 0.62 +/- 0.09 for the hot primary and 0.44 +/- 0.02 for the secondary.

Spectra of the old nova obtained by Herbig (see Figure 8.77) in 1955 show that the permitted lines of C II, C III, NII, and He II and the continuum are greatly weakened during primary eclipse, while the Balmer lines H Alpha, H Beta, H Gamma, and the forbidden lines of [OII] and [OIII] do not change in strength and, therefore, are formed in an extended envelope or in an expanding gas unaffected by the eclipse.

The variation of the emission lines H Beta, H Gamma, and 4686 He II during eclipse has been studied by Young and Schneider (1980), who took spectra with an exposure time of 300 seconds at phases included between 0.80 and 0.15 P. The radial velocity curve given by 4686 He II presents the classical rotation disturbance: the velocity jumps to +400 km/s before eclipse, when only part of the eclipsed body (which can be an accretion disk) that is rotating outward from us is not yet eclipsed, and to more than -200 km/s after the eclipse, when the part of the eclipsed body rotating toward us is already out of eclipse. The Balmer lines are eclipsed slightly before the He II lines, and go out of eclipse slightly later, this fact suggesting that they are formed farther out in the disk.

The UV spectrum of DQ Her has been observed with IUE at various phases. In contrast to other old novae, it is flat, $F_\lambda \propto \lambda^0$.

This flat continuum may indicate that, because of the high inclination of the system (according to Ritter, 1987, i = 70° +/-17°), we are observing the outer and cooler parts of the disk.

The UV line spectrum shows strong emissions of N V and C IV and fainter emissions of He II and Si IV. All these features vary with the orbital phase, being all fainter at phase zero. He II practically disappears during the eclipse.

We recall that a peculiarity of the photometric behavior of DQ Her is the presence of coherent oscillations with a 71-second period. These are low-amplitude sinusoidal variations remaining coherent for several years. The reciprocal of the period variation $(\dot{P})^{-1} \approx 10^{12}$ suggests that we are dealing with the rotation of a solid body, e.g., the white dwarf. Now a peculiar behavior of these oscillations is shown during the eclipse: at eclipse ingress (phase 0.91), the oscillations begin to come earlier and earlier, until at mid eclipse, they jump from 90° early to 90° late, and then gradually come back to the phase they had originally when the eclipse ends (phase 1.08). Petterson (1979, 1980) proposes the following model to explain this behavior: He suggests that the oscillating light is not coming directly from the white dwarf, but the illuminating beam on the white dwarf surface is reflected by the accretion disk. This is because the phase shift has the same duration of the eclipse itself. Moreover, the variation of the phase shift can be explained by assuming that the reflecting point is located in the backside of the disk. By assuming different inclinations of the orbital plane, the phase shift and the oscillation amplitude vary (see also Chapter 4. Section III.F.2).

IX. THE OLD SLOW NOVA T AUR 1891

(written by Hack)

T Aur is the oldest galactic nova for which a complete record of the outburst is available and which was observed by photographic spectroscopy (see Payne-Gaposchkin, 1957, pp. 93-97, for complete references). The visual magnitude range is $V_{max} = 4.1$ and $V_{min} = 15.8$; the absolute magnitude at maximum-derived from the nebular expansion parallax- is -4.2 or -5.7, if we assume the expansion velocity equal to 500 or to 1000 km/s^{-1} (i.e., velocities included between those oberved for the more recent observed novae; in fact, in 1891 no high-resolution spectra were obtained, permitting us to

measure the expansional radial velocity), and neglecting the interstellar extinction.

T Aur is very similar to DQ Her, concerning both the light curve and the spectroscopic appearance and spectral variations. It was this strict similarity which suggested to Walker (1963) to search whether it was also an eclipsing binary like DQ Her. He was successful in his expectations and found that T Aur is an eclipsing binary with period of 0.2043786 days. The eclipsing light curve is in many ways reminiscent of dwarf nova light curves. Its main characteristics are:

1) short period,

2) Algol type,

3) absence of detectable secondary eclipse,

4) asymmetry of the rising branch of the eclipsing curve,

5) occurrence of a bright shoulder before and somtimes after eclipse,

6) occasional presence of a depression in the light curve at 0.7 P,

7) occurence of intrinsic variations outside of eclipse (Figure 8-85).

Moreover, the colors B-V = +0.28 and U-B = -0.64 place it in the same position as dwarf novae in the two-color diagram and correspond to the colors of a composite object sdO+dK.

The distorted light curve does not permit one to find any geometrical solution of the kind obtained for detached binaries, but only indicates that both components must be small and dense. Differently from DQ Her, T Aur does not show any coherent oscillations, but just rapid flickering.

The spectrum of the nova at minimum was described by Humason (1938) as dominated by weak emission lines of hydrogen and He II and a continuum well extended in the ultraviolet.

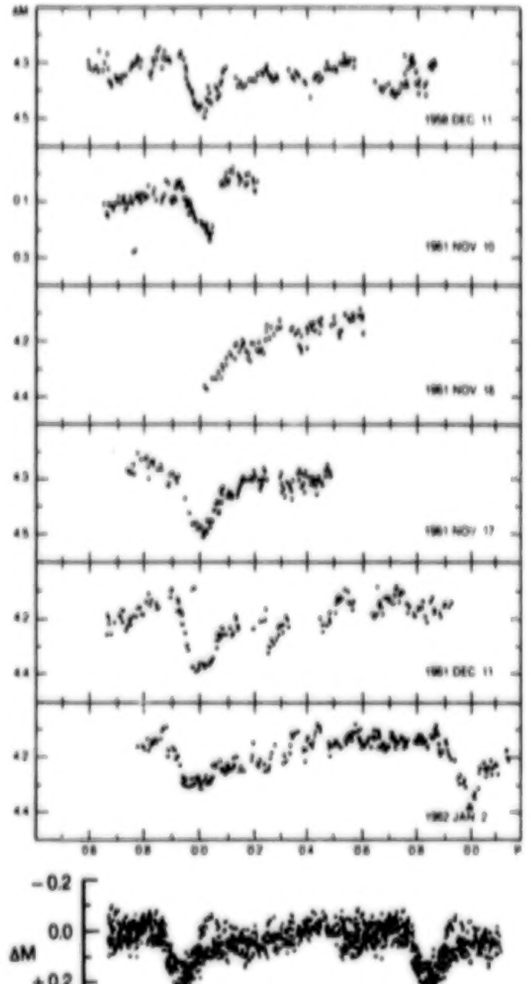


Figure 8-85. a) Light curves of T Aur; b) Composite light curve. Zero point of the magnitude scale is the average brightness of the system outside the eclipse. The phases are computed from the elements derived by Walker (1963).
(from Walker, 1963).

No other detailed spectroscopic observations were made since the recent ones by Bianchini (1980). Study of the variations of the 4686 He profile along the 4h54m period shows that the emission lines reach a maximum at phase 0.85, when the light curve presents, a hump, and a minimum at phase 0.53 (Figures 8-86 a,b). Phases 0.0 is at the epoch of the Algol-type minimum. This behavior indicates the presence of a hot spot observable in its full size at phase 0.85 in the light of He II. A broad absorption

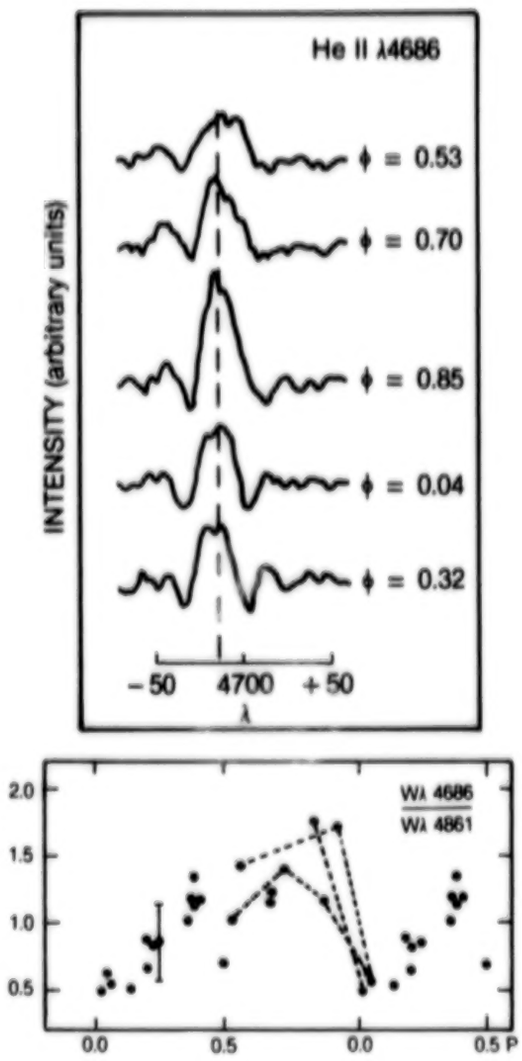


Figure 8-86. a) He II 4686 emission line profiles at selected orbital phases. b) Plot of the ratio W(4686 He II)/W(Hβ) versus the orbital phase. Observations made during the same orbital phase are connected by the dashed lines.
(from Bianchini, 1980).

line is detectable, underlying the emission, and suggests the presence of an optically thick body (stellar atmosphere or accretion disk). This absorption line is more evident around phase 0.00 (Figure 8-86a). Low-resolution (R = 6A) ultraviolet spectra have been obtained with IUE (SWP 21454 and 21456, LWP 2268) and combined together (Figure 8-87). The exposures needed to obtain a measurable signal are too long to detect spectral variations related to the phase.

The S/N is low, but it is evident that the flux increases toward shorter wavelengths, and the energy distribution is very different from the flat spectrum of DQ Her, in spite of the other many similarities of the two objects.

An interesting spectrophotometric study of the faint nebula surrounding T Aur has been made by Gallagher et al . (1980). The nebula is faint and has an ellipsoidal ring-like shape with a major axis of 26" (see Figure 6-68). This nebula is very similar to that produced by DQ Her. In both nebular spectra, recombination lines dominate over forbidden lines: The spectrum of T Aur presents recombination lines of once-ionized helium, twice-ionized nitrogen and oxygen, while forbidden lines are faint (Figure 8-88).

After correction for interstellar extinction, the abundance ratio of helium to hydrogen can be evaluated from the ratio I (5876)/ I(4861) according to the relation

$$\frac{N(He^+)}{N(H^+)} = \frac{\alpha_{i\beta}(T_e)\, h\nu_{4861}\, I(\lambda 5876)}{\alpha_{5876}(T_e)\, h\nu_{5876}\, I(H\beta)}$$

where the α are the effective recombination-line coefficients at electron temperature T_e (Osterbrock, 1974). Helium is found to be overabundant by a factor of 2 or 3, like most slow novae. Also, nitrogen and oxygen are found overabundant by factors of 60 and 25 (by number), respectively, over cosmic abundance.

Like DQ Her, T Aur also shows regions of the nebula where the electron temperature is low, but not so extremely low as in the case of DQ Her. From the ratio 4651 O II/5007 [O III], a value of T_e lower than 3000 K is derived. The nebula surrounding T Aur has a substantially lower content of heavy elements than that around DQ Her, in spite of the great similarity of the two novae, which is reflected not only in their light curve, but also in the manner in which their ejecta have evolved.

The evolution of the nebulae of old novae presents several problems. For instance, T Aur and DQ Her extend their similarities in the outburst to the similarities in how their nebulae

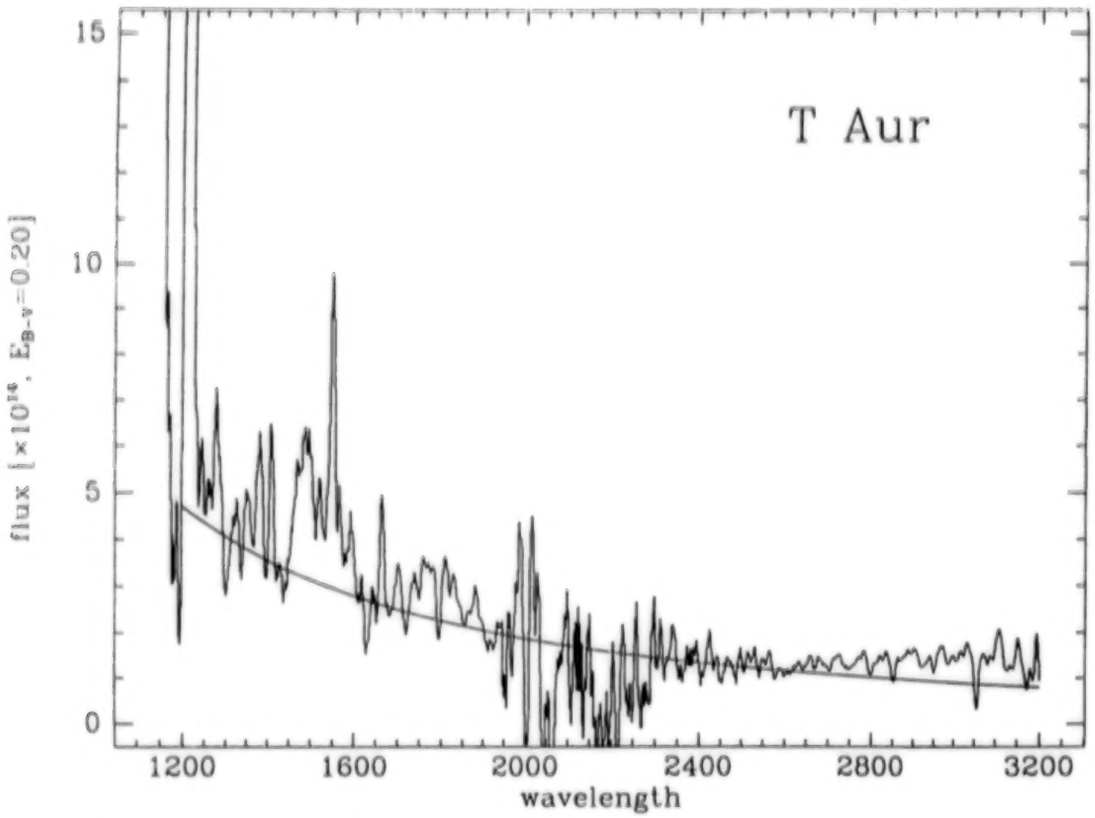


Figure 8-87. The low resolution IUE spectrum of T Aur, obtained combining the short wave spectra SWP 21454 at phase 0.92 and SWP 21456 at phase 0.74 and the long wave spectrum LWP 2268 at phase 0.24. Although the noise is strong, and the region 1950-2500 is completely drowned in the noise, it is evident that the flux increases from 1600 A toward shorter wavelengths.
(from the IUE data bank).

evolved. RR Pic, on the other hand, is an older nebula than DQ Her, but presents higher T_e and high ionization. Therefore, it is very important to follow the development of nebulae of recent well-observed novae.

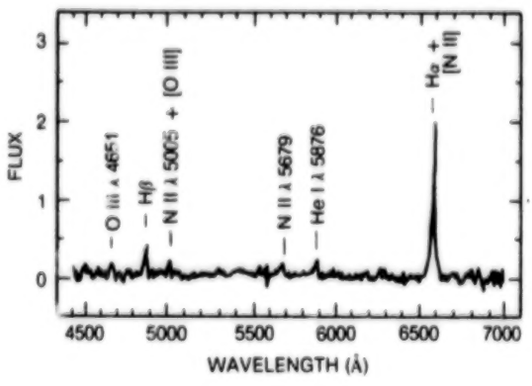


Figure 8-88. The optical spectrum of T Aur obtained by summing several spectral scans. The flux units are 10^{-16} ergs cm^{-2} s^{-1} A^{-1}. (from Gallagher et al., 1980)

X. RR PIC

(written by Selvelli)

X.A. THE HISTORICAL OUTBURST

The outburst of RR Pic was first noticed by R. Watson, on May 25 1925, when the star reached magnitude 2.4, while the maximum (m= 1.0 - 1.2) was reached on June 9, 1925. The light curve was characteristic of a "slow" nova with t_3 ~ 150 (182) days. The light curve has been studied by several authors: e.g., Spencer Jones (1931), Campbell (1929) and Payne-Gaposchkin (1957). Characteristic were the large oscillations during the early decline, with several maxima of nearly equal magnitude (Figure 8-89). It is notable that the preoutburst magnitude was estimated as 12.8 (12.7, 13.3) and that the present magnitude is 12.3 (12.1). Sixty years after outburst, the star has not yet returned to its preoutburst magnitude. This

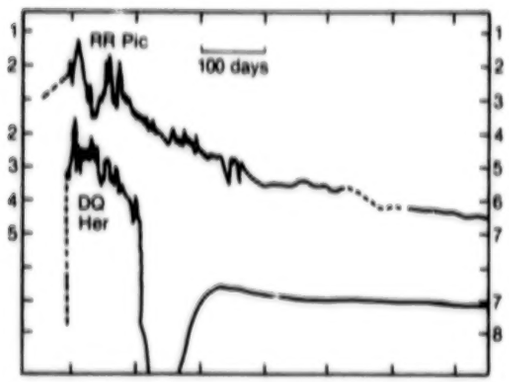


Figure 8-89. The light curve of the slow nova RR Pic, and, for comparison, the light curve of the other slow nova DQ Her. The typical dip in the light curve, characteristics of several slow novae, is missing in RR Pic, as well as in the extremely slow nova HR Del (see next section 8-11).
(from McLaughlin 1960).

behavior seems in contrast with the general conclusion by Robinson (1975) that novae before and after outburst are characterized by the same m_v value.

The spectral type of the nova at the time of the first spectroscopic observations was estimated as F2, while at maximum it was F8. This behavior reflects that of slow novae, which near maximum display a later spectral class than fast novae (F2-F8, instead of A0-A5).

The premaximum and maximum spectra have shown outflow velocities of the order of -100 km s^{-1}, while velocities of up to -400 km s^{-1} have been observed at the end of the evolution of the principal spectrum during the first 10 months after outburst.

The spectral behavior after maximum has shown a very complex behavior and has been

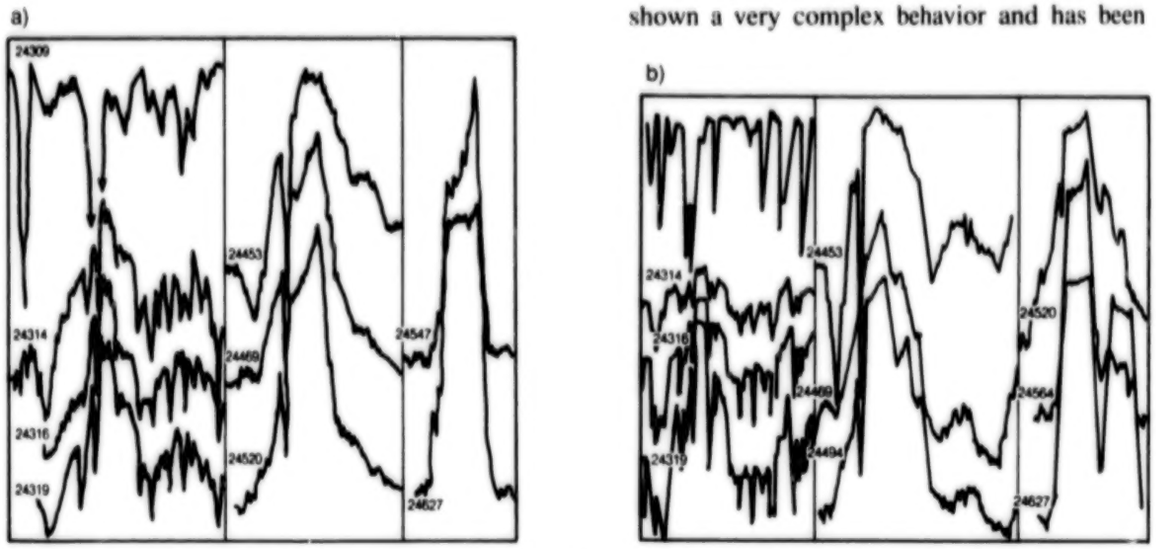


Figure 8-90. a) RR Pictoris, changes in the spectrum near Hd 4101 over about 320 days; tracings from Lick spectra, not reduced to intensities. Left strip, top to bottom: JD 24309 (date of maximum; for clarity the deep center of the hydrogen line is omitted), 24314, 24316, 24319; center strip; JD 24453, 24469, 24520; right strip: JD 24541, 24627. The development is similar to that shown in Figure 4, but the later spectra are less complicated by emissions other than that of hydrogen. Note that all the dates on the two figures are not identical. Violet is to the left .
(from C.P. Gaposchkin in HP 51 / 752) 1958.

b) RR Pictoris, changes in the spectrum near Hg 4340 over about 320 days; tracings from Lick spectra, not reduced to intensities. Left strip, top to bottom: JD 24309 (date of maximum), 24314, 24316, 24319; middle strip: JD 24453, 24469, 24474; right string JD 24520, 24564, 24627. The first tracing shows only the pre-maximum spectrum. In the subsequent tracings, the principal spectrum emerges and strengthens to the violet of the pre-maximum spectrum, which gradually fades. In the second strip the principal spectrum, and the intense, more highly-displaced spectra of hydrogen dominate the absorptions, and the bright redward edge, associated principally with the highly-displayed spectrum, becomes conspicuous. By JD 24469 the bright line has developed a distinctive structure, with a strong redward edge; the violetward and redward edges of the Fe II line at l 4351 have also become prominent. In the third strip, the hydrogen absorptions are diminishing in intensity, the bright lines displacing more structure. On JD 24564 the absorptions are almost gone, and the violetward and redward edges of the [O III] line l 4363 are superimposed on those of the Fe II line. On JD 24627, only the lines of hydrogen and [O III] are discernible, each with complex structure. Note that the two last tracings cross. Violet is to the left.

described in great detail by H. Spencer Jones (1931), by W.H. Right (1925), and by C. Payne-Gaposchkin (1957). Outflow velocities were lower than in other novae, and the Orion spectrum showed absorption displacements of up to -1500 km s^{-1}. A peculiarity of RR Pic has been the extreme weakness of the N III λ4100 lines during the Orion stage. These lines are usually associated with the "nitrogen flaring," the secondary fluorescence produced after the excitation of the 3d P° level of O III by He II Lyα.

Another distinction between fast and slow novae during the Orion stage is the presence of numerous [FeII] emissions in slow novae and their weakness or absence in fast novae (McLaughlin, 1960, p.585). It is also remarkable that RR Pic, during the nebular stage, has shown unusually weak lines of [O III] λ4957 and 5007.

The nebula surrounding RR Pic has shown an expansion rate of 0.18 arc sec yr^{-1}. The fact that the nebula of RR Pic was not strictly spherically symmetric was reported by Payne-Gaposchkin (1957). In a direct photography of the remnant, taken by Duerbeck and Seitter (1979) at the prime focus of the ESO 3.6 m. telescope, the ex-nova is surrounded by a structured nebulosity; an equatorial ring(s) and double "polar caps" or "knots" are clearly evident on opposite sides of the remnant, in a structure which somehow resembles that surrounding the slow nova DQ Her (see Figure 6-69).

Williams and Gallagher (1979) have studied the nebula surrounding RR Pic using the Cerro Tololo Vidicon spectrometer. The filaments have spectra very similar to those of high excitation planetary nebulae, and show also prominent [Fe V] emissions. The source of excitation of the nebula is in the UV radiation field of the hot component of the system (Figure 8-91; see also Figure 6-70).

Photoionization models suggest temperatures of the order of 2.5 x 10^5 K and L(Star) ~ 4.4 x 10^{34} erg. s^{-1}. An enhancement of Helium

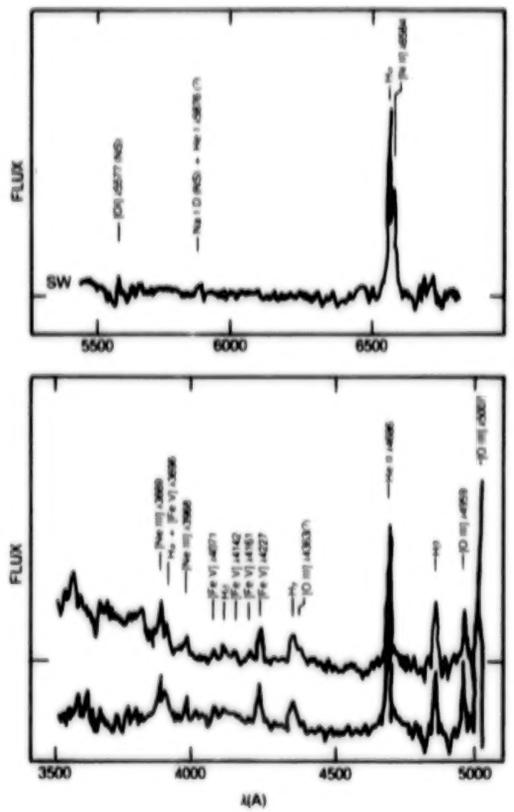


Figure 8-91. Spectral scans of the nebular condensations to the NE and SW of RR Pic. The zero flux levels of the scans are indicated on the ordinate axis. (from Williams and Gallagher, 1979).

by at least a factor of two over the solar abundances is required to explain the He II λ4686 emissions flux.

Moreover, the fact that the low-ionization line [N II] λ6584 Å is seen with moderate strength indicates overabundances of nitrogen by a factor of at least 10, while oxygen is probably underabundant.

The dimensions of the nebula are presently 18" x 23".

X.B. RR PIC IN QUIESCENCE: OF HUMPS AND DIPS IN THE LIGHT CURVE

The first photoelectric observations of RR Pic were made by Van Houten (1966), who found a light curve with a period of approximately 3.5 hours and suggested the presence of an eclipse. This period was confirmed by the observations of Mumford (1971). Vogt (1975)

made an extensive set of observations with the purpose of determining a more accurate period and confirming the presence of eclipse. The determination of the photometric period by Vogt was made difficult by the near absence of features repeating at equal phases. The light curve was characterized by a broad hump with amplitude 0.3 magnitudes that lasted more than half period. The low amplitude and the singular shape of this hump made difficult its use for the determination of the period. Fortunately, the hump was found to always end in a sudden dip, near minimum brightness; this feature was used to determine the period:

JD (MAX) =2 438 815 379 + 0.1450255

$\varphi = 0$ corresponds to the main brightness maximum.

The (B-V) and (U-B) curves show that the bluest parts of the curves are reached near phase 0.0, the reddest, near phase = 0.5 (Figure 8-92).

A drop near $\varphi = 0.4$ seems to be always present, also in the V curve. Since this behavior repeated fairly well from cycle to cycle, it was associated by Vogt to orbital motion.

It is remarkable for what follows that in

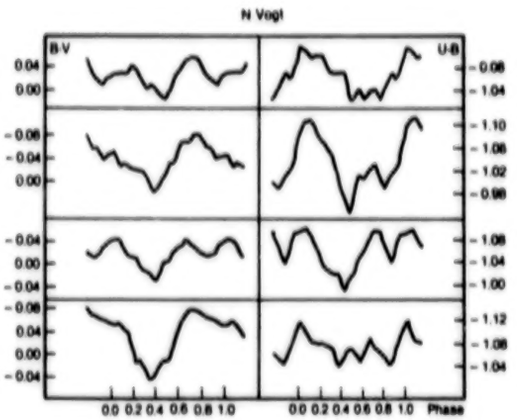


Figure 8-92. Mean colors as a function of phase during December 1972.
(from Vogt, 1975).

Vogt observation, a blue peak, especially pronounced in (B-V), is present near phase 0.75 (Figure 8-93). Vogt also found that, generally, a flickering was superimposed on the light curve with a typical time-scale of 5-15 min and amplitude of 0.05 ÷ 0.10 magnitudes. Also time-resolved observations by Warner (1981) have revealed the presence of occasional multiperiodic rapid oscillations, which were present in about one-quarter of the observing runs. The periodogram analysis showed periods in the range of 20-40 s, with a more persistent one with P = 32 s. Schoembs and Stolz (1981) have

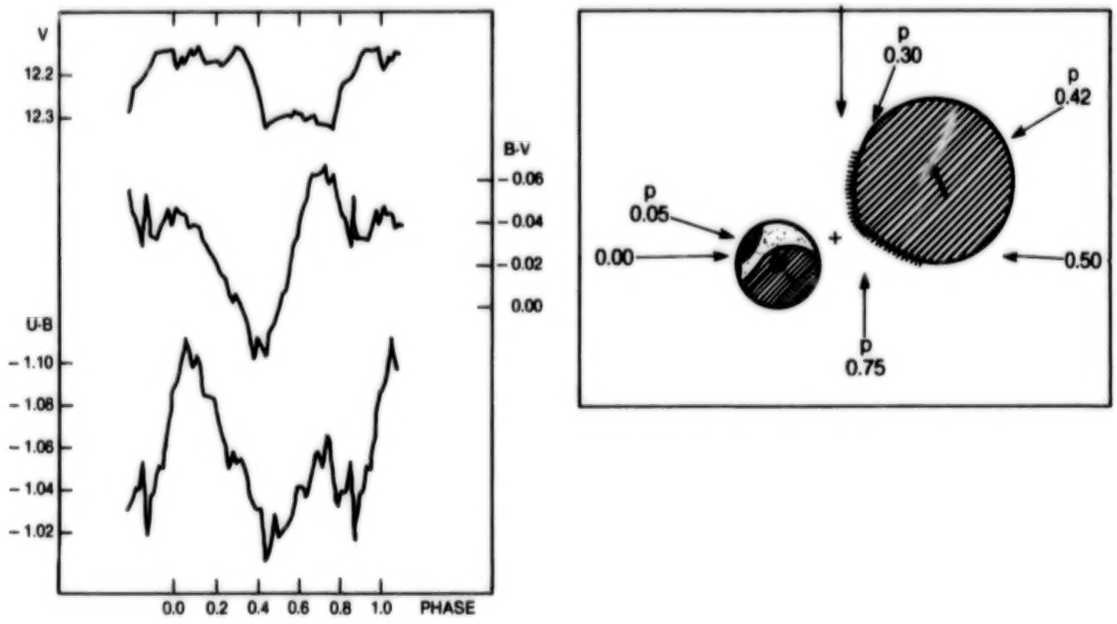


Figure 8-93. Left: Mean light curves and colors versus phase for all observations of Dec. 1972 averaged in 0.02 P intervals. Right: the phases are indicated in this schematic model for RR Pic.
(from Vogt 1975).

confirmed the presence of such rapid oscillation with P=32 s.

New UBV measurements by Haefner and Metz (1982) have confirmed the period of Vogt and have also indicated the high stability of the period, with $\frac{dP}{P} = 1.4 \times 10^{-11}$.

However, they found a quite different behavior in the light curve with a "w" shape as a characteristic feature of *all* light curves (Figure 8-94), and much more pronounced than in Vogt's observations. Different curves behave similarly and show minima near phase 0.43 and phase 0.74 (deeper). This behavior is in contrast with that described by Vogt who reported

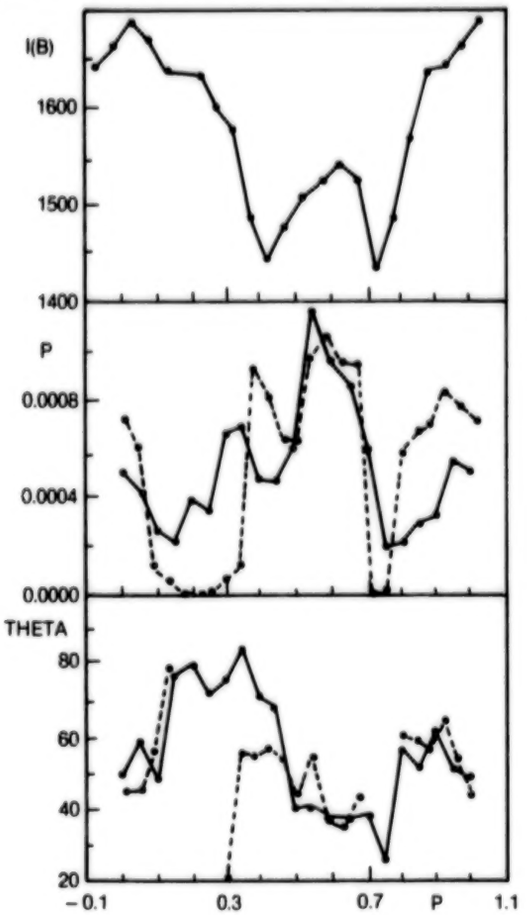


Figure 8-94. Top:B intensity derived by averaging the B light curve within a phase interval of 0.05 and represented by arbitrary count numbers. Middle and bottom: the hot spot polarization percentage and angle, respectively. Solid line: derived from the observations, dashed line: numerical approximation (θ is indefinite for phase 0.0P).
(from Haefner and Metz, 1982).

the presence of a blue peak near φ=0.75. Spectroscopic observations by Wyckhoff and Wehinger (1977) have revealed the presence of radial-velocity variations in the He II λ4686 emission. These variations are nearly sinusoidal with 2K ~120 km s^{-1}. The minimum in this spectroscopic curve is quite close to $\varphi = 0$, the principal maximum of Vogt's observations. Combining their photometric results with these radial-velocity observations, Haefner and Metz (1982) have suggested that, since φ = 0.75 corresponds to the orbital condition in which the red component is in front of the white dwarf, the minima they observed near φ= 0.74 were caused by occultations (eclipses) of the hot component (white dwarf, accretion disk).

This suggestion was supported by the fact that optical spectra showed that the Hβ emission was weaker near φ =0.7. (But He II λ4686 remained constant.)

The suggestion reported above is in contrast, however, with the indications of Vogt (1975) who found the presence of a blue peak near φ = 0.75.

New observations by Kubiak (1984) confirmed the shape of the V curve found by Vogt. The U curve, however, suggested the presence of an eclipse beginning near φ = 0.8 and lasting until φ= 0.96. In the V and B bands, the eclipse was less evident. The system appeared bluest at the beginning of the "eclipse."

Kubiak claimed the presence of coherent brightness modulation in all bands with a period of about 15 min. A study by Haefner and Schoembs (1985) of a large amount of photometric data has not confirmed the permanent existence of this period. They suggested that the 15-min period found by Kubiak was attributable to transient phenomena in the disk.

The new observations by Warner (1986a) have not confirmed the periodicity either. Power spectra of its extensive observations have not detected the periodicities found by Kubiak, nor the presence of any other period larger than 1 min (except for the orbital one).

Probably most of the contradictory indications reported above are attributable to real intrinsic changes with time in the photometric behavior. Warner (1986a) has also recently pointed out that in the last years, the variations in the light curve have had a smaller range and that more evident flickering activity has been present (see Figure 6-4). A comparison of these curves clearly indicates that from 1975 to 1984 there has been a reduction both in the amplitude and in the phase interval of the hump. This has coincided with a decline in the mean brightness of the system.

RR Pic is currently at m_v ~12.3 and is still declining in luminosity.

The light curve in recent observations (Warner 1986a) is characterized by repetitive but singular "eclipse-like" features superimposed on a highly variable background.. The minimum near φ~0.42 reported by Haefner and Metz (1982) is now scarcely evident; whereas, that near φ~0.74 is the dominant feature. The interpretation of this complex behavior is not straightforward and unequivocal. The origin of the hump, its progressive decay, the reality of the interpretations of the dips (minima) as eclipses needs further investigations.

X.C. THE UV BEHAVIOR OF RR PIC

UV observations of RR Pic can set some constraints on the physical parameters and the location of the region where the (hot) radiation emitted by the system is produced.

Optical observations by Vogt (1976) showed that the ex-nova had a blue continuum with He II 4686 as the strongest emission line, with W ~ 8Å.

Other (fainter) emissions are the hydrogen Balmer lines, the Pickering series of He II, and the CIII 4650 line. These features are typical signatures of a high-temperature object.

The first UV observations of RR Pic were made by Gallagher and Holm (1974) using the 8-inch photometric telescope of the OAO-2 Wisconsin Experiment Package. Fair data were obtained for RR Pic, which indicated a quite high (color) temperature, in excess of 35,000 K, and a bolometric luminosity of the order of 10 $L_\odot$. Variations of the order of 0.5 mag in two observations separated by about 1.7 hours (~ 0.5 P) seemed also to be present.

Duerbeck et al. (1980a) and Krautter et al. (1981) have reported on the first IUE observations of RR Pic (see Figure 6-36). Krautter et al. estimated UV temperatures of about 28,000 K and suggested the presence of P Cyg profiles (although much weaker than in HR Del) in the NV 1240, CII 1335, and Al III 1860 lines.

He II 1640 and NV 1240 are the strongest emissions in the spectrum, confirming the high-temperature character revealed in the optical emissions.

Krautter et al. (1981) have found temperatures on the order of 28,000 - 40,000 K, or, alternatively, they have made a fitting to the continuum distribution with a power-law λ^{α} , where $\alpha = 1.81 \pm 0.03$.

The UV luminosity was estimated at 4.4 $L_\odot$. Krautter et al. (1981) noticed the presence of two absorption components in the P Cyg profiles with velocities of -2500 km s^{-1} and -4600 km s^{-1}, respectively.

Wargau et al. (1982), using the same spectra, attempted an alternative fit to the continuum distribution and suggested a superposition of two blackbodies, one with T = 14,000 K (originated in the disk) and the other with T = 90,000 K (attributed to the boundary layer).

RR Pic has been also studied by Rosino et al. (1982). The continuum distribution has been interpreted as a combination of two blackbodies with temperatures of 20,000 K and 35,000 K. They detected the presence of (pure) absorption lines of Si II, Si III, Si IV, and S II, but did not confirm the presence of the P Cyg profiles. The width of the emission lines was interpreted in terms of expansion velocity of the shell, and a value of about 1700 km s^{-1} was derived.

RR Pic has been the target of an UV monitor-

ing that covered almost two complete cycles (Selvelli, 1982). A sequence of alternate exposures with the short λ and long λ cameras has made it possible to obtain 12 low-resolution spectra in about 6.5 hours, thus providing a reasonable time-resolution for the detection of φ-related variations. (The typical exposure time was 18 min). After correction for reddening (E (B-V)~ 0.05), the continuum fits quite closely the $\lambda^{-7/3}$ relation, although the index α ranges actually from 1.7 to 2.1 for different spectra. Figure 8-95 shows two fits to the continuum at different phases. Note that the mean time separation between two successive SWP and LWR spectra (which are merged together) is of about 30 min., which corresponds to Δφ~ 0.14.

Having several (6) spectra at disposal for each range, it is easier to detect faint lines (which in a single spectrum could be masked by noise) and to ascertain the reality of doubtful features. A careful examination of the spectra has led to the detection of a wealth of emission lines over the entire range.

The spectrum is characterized by strong permitted transitions of high-ionization species such as N V 1240, Si IV 1400, C IV 1550, He II 1640. Among the low-ionization species, only Mg II is present, while O I 1300, Al II 1670, C II 1335, Si II 1810 and similar species are definitely absent. The intersystem lines are rather weak: O V] 1218, N IV] 1486, O III] 1666, N III] 1750, Al II] 2669, or absent: Si III] 1892, C III] 1909, CII] 2326). [Ne V] 1575. [O II] 2469, and [Mg V] 2784 are probably present although faint.

The lines of the He II Paschen series are clearly present (note that the line of the Pickering series were reported in the optical by Vogt), together with some O III lines, notably 2836, produced in the Bowen fluorescent mechanism originated by He II Lyα.

Some emission features lacking any reasonable identification, such as λ 2575, λ 2405, λ 1446, have been attributed to "coronal lines," although the absence of a few of the strongest coronal lines in the solar spectrum, such as Fe XI 2648.73 and Fe XII 2565.99, poses a serious problem regarding the reality of these proposed identifications.

There is definitely no evidence of P Cyg profiles, neither for the lines proposed by Krautter et al. (1981) nor for any other line. Nor is there evidence of the absorption lines reported by Rosino et al. (1982), except for the feature near λ 1295, attributable to Si III UV 4, which seems to be variable.

C-7

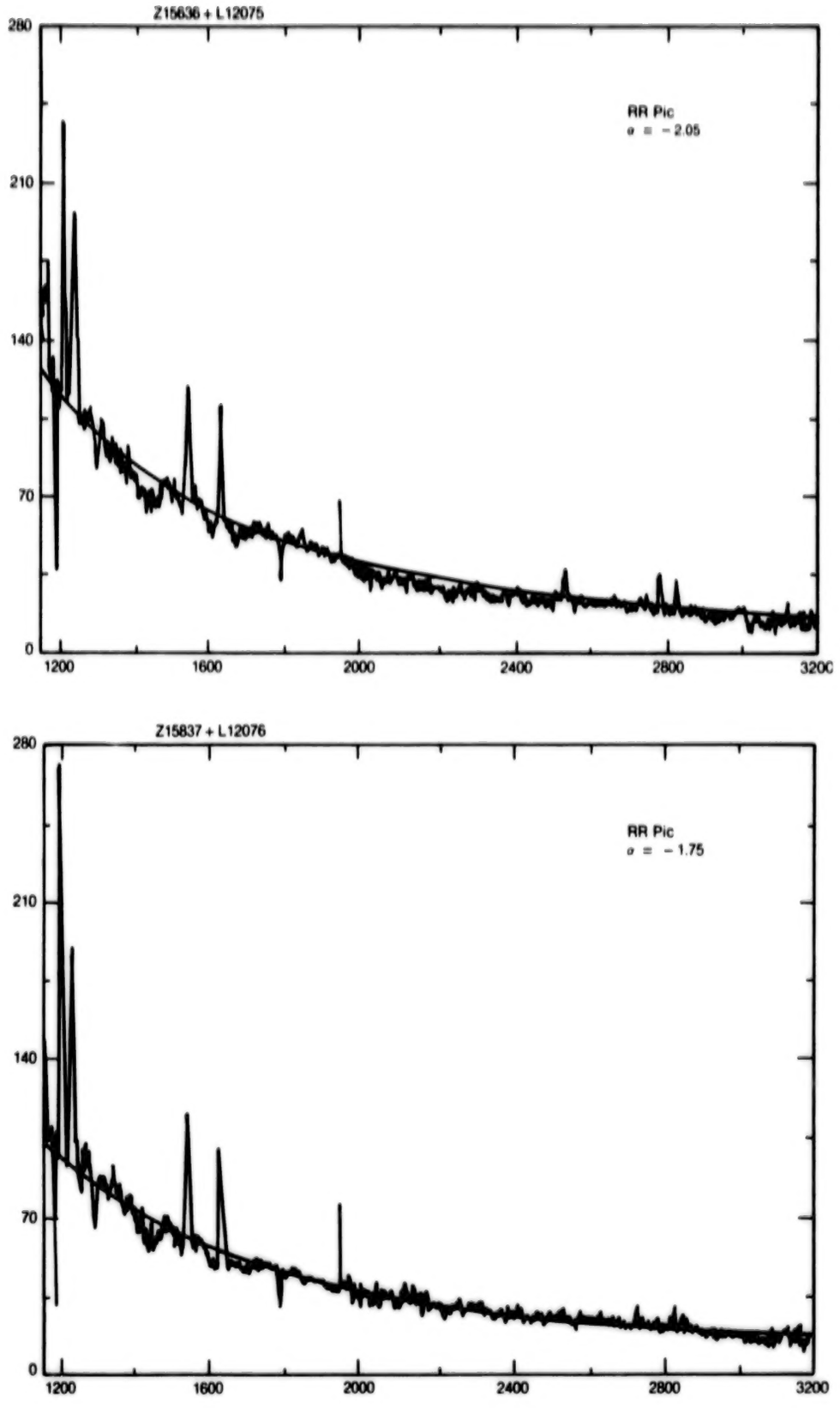


Figure 8-95. Low resolution IUE spectrum of RR Pic and comparison with a power-law spectrum with α = -2.05 (top) and -1.75 (bottom).

X.C.1. THE UV SPECTRAL VARIATIONS

The continuum, as well as the emission lines, shows significant variations in the various spectra that have been taken.

As is customary, the various spectral quantities have been ordered as a function of the phase φ, using the ephemeris given by Vogt (1975). The continuum does not vary significantly in shape, and, therefore, only the total flux in the continuum for the SWP asn LWR regions, respectively, has been reported. Variations as large as 1.5 have been found between the weakest and the strongest continua. The line spectrum shows stronger variations, especially in the near UV region, where variations around a factor of 5 have been observed for some lines.

Figure 8-96 reports the phase-related variations of the following quantities: m_v (FES), $\int_{1200}^{2000} F_\lambda^C d\lambda$ and $\int_{2000}^{3200} F_\lambda^C d\lambda$ (in erg cm^{-2} s^{-1}), line-emission intensities (in erg cm^{-2} s^{-1}) for N V, C IV, He II, Mg II, and O III 2836. The phase φ associated with each spectrum is that of mid-exposure. The phase associated with the m(FES) is that of ~ 2 min before the beginning of the exposure. In accordance with Vogt (1975), φ = 0 corresponds to the main maximum in the visible light curve, which has a minimum around φ = 0.42 (center of the eclipse). Schoembs and Stolz (1981) have found minima also around φ = 0.6. Haefner and Metz (1982), on the other hand, give φ = 0.75 for the primary eclipse (in accordance with the He II R.V. curve).

The mean continuum flux in the $\lambda\lambda$1200 - 3000 range is of 6.8 x 10^{-10} erg cm^{-2} s^{-1}. Assuming a distance of 440 pc, the mean UV luminosity results in 1.7 x 10^{34} erg s^{-1} ~ 5$L_\odot$.

From the IUE data, it is easy to see that a maximum common to the above-mentioned quantities falls between φ = 1.6 + 1.9, while a minimum for most quantities occurs around φ = 1.1. + 1.5. These results are in partial agreement with those of Vogt (1975), who found minima around φ ~ 0.4, but the occurrence of maxima centered around φ = 1.75 is in complete contradiction with all previous findings. In addition, the different behavior of the above quantities at about the same phase in two different periods is remarkable. See, for instance, the dramatic changes for Mg II and O III between φ = 0.687 (deep minimum) and φ =1.752.

On the other hand, Kubiak (1984) claims that the "eclipse" occurs between φ = 0.80 and φ = 0.95.

The UV data are in contradiction with conclusions drawn from the behavior in the optical and clearly rule out possible eclipse of the hot component. If the interpretation based on the R.V. curve of the He II λ 4686 line is correct, such eclipses are expected near φ= 0.75 when the companion is in front of the hot component. The UV data, on the other side, indicate that neither the continuum nor the emission lines, which are likely to be formed close to the hot component, become weaker near φ = 0.75. One more indication against a high inclination of the system comes from the considerations of Warner (1986b). Systems with high inclination, seen edge on, are expected to have a flatter UV continuum that RR Pic actually has. Probably, a key to understand both the behavior in the UV and the discrepancies about the phases of the various humps and dips in the light curve at different epochs is the presence of transient phenomena, which are superimposed to the periodic-phase-related changes.

Simultaneous IUE and ground-based observations covering at least two cycles are required.

The x-ray luminosity of RR Pic in the range (0.15 - 4.5 Kev) has been determined by Becker and Marshall (1981) using the Einstein IPC value 2.3 x 10^{31} erg s^{-1}, which is close, although weaker to the mean value of the few old novae detected in the x-ray range.

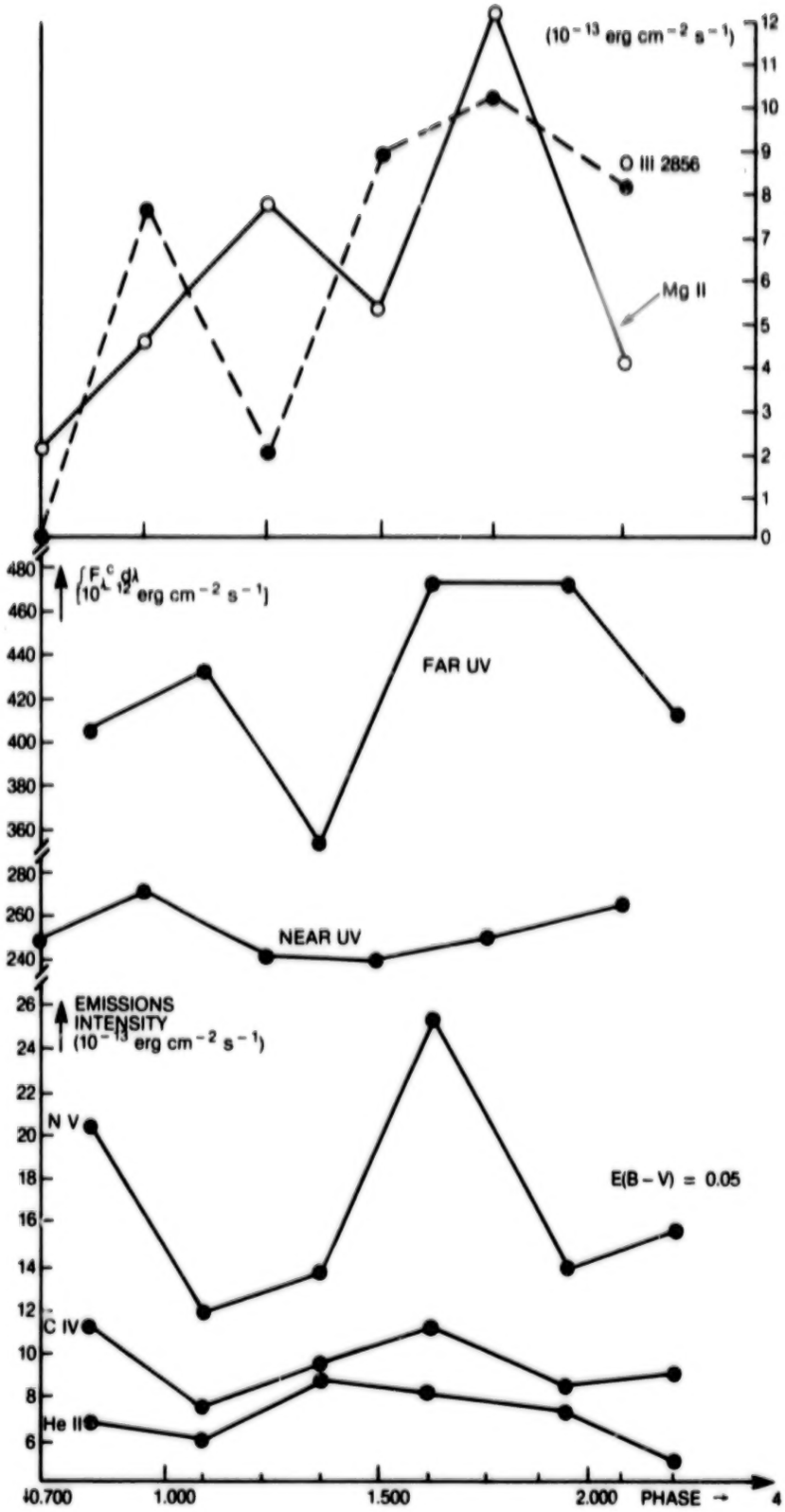


Figure 8-96. Phase variations of the flux in the emission lines of O III 2836, the 2800 resonance doublet of Mg II, the 1240 resonance doublet of N V and the 1550 resonance doublet of C IV, He II 1640, and the integrated continuum flux in the far UV and in the near UV, dereddened for E(B-V)=0.05.

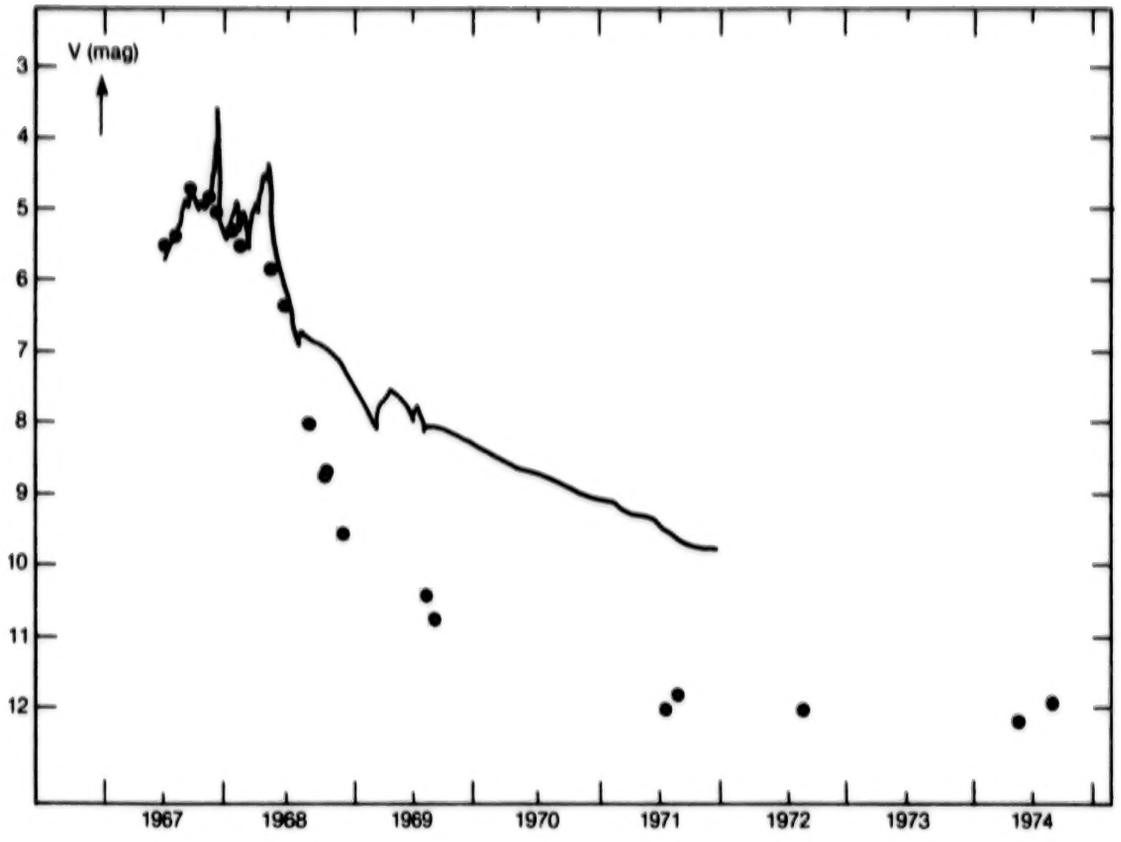


Figure 8-97. The photoelectric and the visual continuum light curve of HR Del (Drechsel et al., 1977).

XI. HR DEL

(written by Duerbeck)

XI.A. THE LIGHT CURVE

The outburst of HR Del (N Del 1967) was discovered by G. Alcock on 1967 July 8. The brightness of the star increased, starting from 1967 June 3, from the prenova magnitude of 12.0 to to a premaximum halt at 5.0; the peak brightness of 3.4 was reached on 1967 December 12. A secondary maximum of 4.3 occured in May 1968, and thereafter, the nova declined gradually. By 1975, it had returned to nearly 12.0 The light curve is well-covered, it shows similarities to that of the slow nova RR Pic, whose early rise however, was, missed.

A visual light curve from the beginning of the outburst to the end of 1971 is given in Drechsel et al. (1977). It shows the broadband V magnitude, which includes continuum + emisssion line light, as well as the continuum magnitude. The continuum magnitude declined much more rapidly, reaching 12.0 in mid-1971 (Figure 8-97).

XI.B. SPECTRAL STUDIES

High-dispersion spectroscopic studies were made by Sobotka and Grygar (1979), by Hutchings (1969), by Yamashita (1968, 1975), by Barlt and Szumiejko (1975), and by various astronomers using coude spectra of the Haute Provence Observatory (Andrillat and Houziaux 1970a, 1970b, 1971, Andrillat, Fehrenbach and Hou-ziaux 1974, Andrillat and Fehrenbach 1981, Friedjung (1977), Malakpur (1973), Antipova, 1977). Medium-dispersion studies were made by Galeotti and Pasinetti (1970), and by Rafanelli and Rosino (1978). Low-dispersion studies were reported by Seitter (1969, 1974) and Woszczyk et al. (1968). Spectrophotometric studies based on objective spectra were published by Drechsel et al. (1977).

XI.C. THE REMNANT

Models of the evolutionary remnant were computed and compared with observations by Tylenda (1977, 1978, 1979).

The nebular remnant was spatially resolved on direct photographs by Kohoutek (1981). Observations in 1981 show an oval shell with a size 3.7" x 2.5". The nebular expansion parallax yields a distance of 850 ± 50 pc.

A kinematical model was developed by Solf (1983) from the study of spatially resolved coude spectra. The main body of the material is found in an equatorial ring and two "polar" rings (rings at higher azimuthal angle). The polar axis is seen at position angle 45° and has an inclination of 38° with respect to the celestial sphere (Figure 8-98).

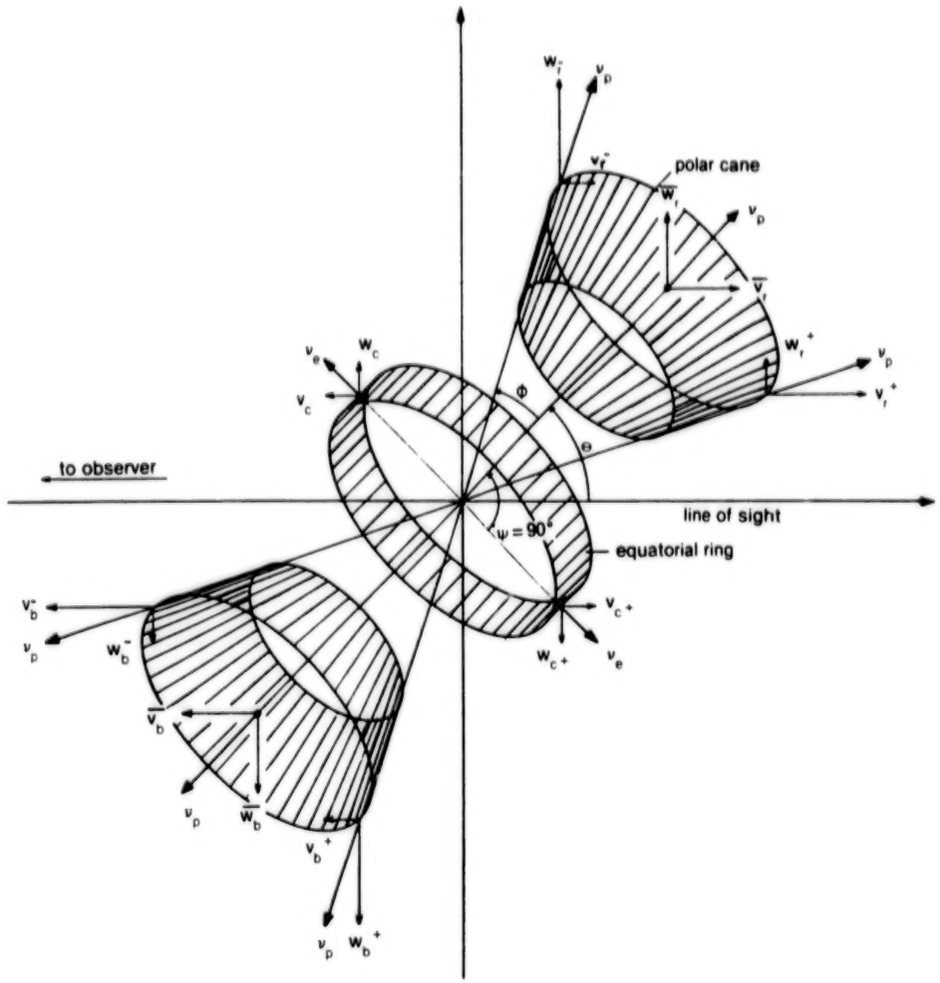


Figure 8-98. A geometrical and kinematical model of the shell of HR Del, consisting of two polar caps (sketched by truncated cones) and an equatorial ring (radial thickness not sketched). Radial (V_b) and tangential (W_b) components of the polar (V_p) and equatorial (V_e) expansion velocities, occurring on the near (−) or the far (+) side of the shell. Also indicated are the velocity components of the bulk motion of the caps (V_r, W_r). The caps and the ring are filled with matter which is heavily clumped (Solf 1983).

XI.D. HR DEL AS A CLOSE BINARY

The most complete study of the binary motion was made by Bruch (1982), using his own and previously published material. The period is unambiguously determined to be 0.2141674 days; the amplitude of radial velocity of the He II 4686 line is 104 km/s, and only 34 km/s for Hβ (Figure 8-99). No trace of the secondary could be detected. The orbital inclination was estimated to be near 41°, which yields for HR Del the most plausible properties of a cataclysmic binary (e.g., mass ratio). This inclination is in good agreement with the results of the study of the nebular shell, assuming that the polar axis of the nebula is perpendicular to the orbital plane. A combination of Kepler's third law, Paczynski's (1971) analytical expression for Roche-lobe geometry, and Lacy's (1977) mass radius relation for low-mass main-sequence stars yields for the late-type component

$$M_2 = 7.7 \cdot 10^{-5} P^{1.142}$$

with P measured in seconds, M_2 in solar masses. In the case of HR Del, $M_2 = 0.58 \pm 0.01\ M_\odot$.

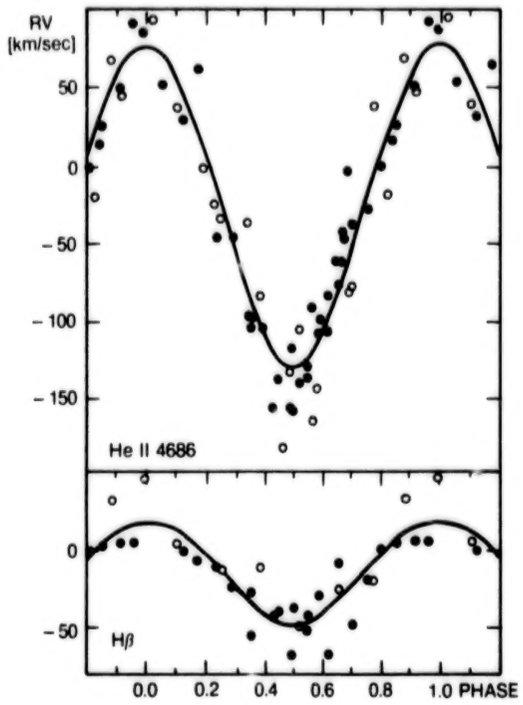


Figure 8-99. Radial velocity curves of HR Del for He II 4686 and Hβ. Filled and open circles are data from various sources (Bruch 1982).

From the observed radial velocity amplitude and the inclination angle, for the compact component, $M_1 = 0.9 \pm 0.1\ M_\odot$.

XI.E. EVOLUTION OF THE OUTBURST

As is typical for slow novae, the spectral evolution was quite complex; the results of radial velocity measurements of absorption lines is shown in Figure 8-100.

Following Hutchings (1969), the outburst is divided into three phases:

Phases I: Pre-maximum.

June - early December, 1967. The light curve is smooth, levelling off at about 5 m, and shows long term (time scale: weeks) fluctuations of 0.5. The spectrum shows lines normal for the early stages of the nova, and smoothly varying line displacements: The strongest lines are those of H, Fe II, Cr II, and Ti II; during the course of evolution, more lines of lower excitation and ionization appeared (Figure 8-101). The shortward displacement of the absorption lines gradually decreased with time; Malakpur (1973c) identifies the broad main absorption, whose radial velocity decreased from 625 to 230 km/s in this time interval, with the premaximum spectrum. Furthermore, a sharp, stationary emission component was visible. The Ca II H and K lines were strong and showed four narrow highly-displaced absorption components in addition to the broad main absorption, which disappeared on December 12, 1967. They are suspected to originate in pre-existing circumstellar material (Figure 8-102).

Phase II. Maximum.

December 1967 - May 1968. The phase begins with a rapid, short—lived brightening up to 3.5 on December 14. The light curve varies rapidly and irregularly by up to 1.2 and as fast as 0.5 within one night. The spectrum shows equally rapid changes, and each line has several sharp absorption components and a strong, variable emission. The strong lines displayed a number of sharp absorption components, which appeared individually and irregularly, fading away during a period of a few weeks. Malakpur (1973c) notes that the princi-

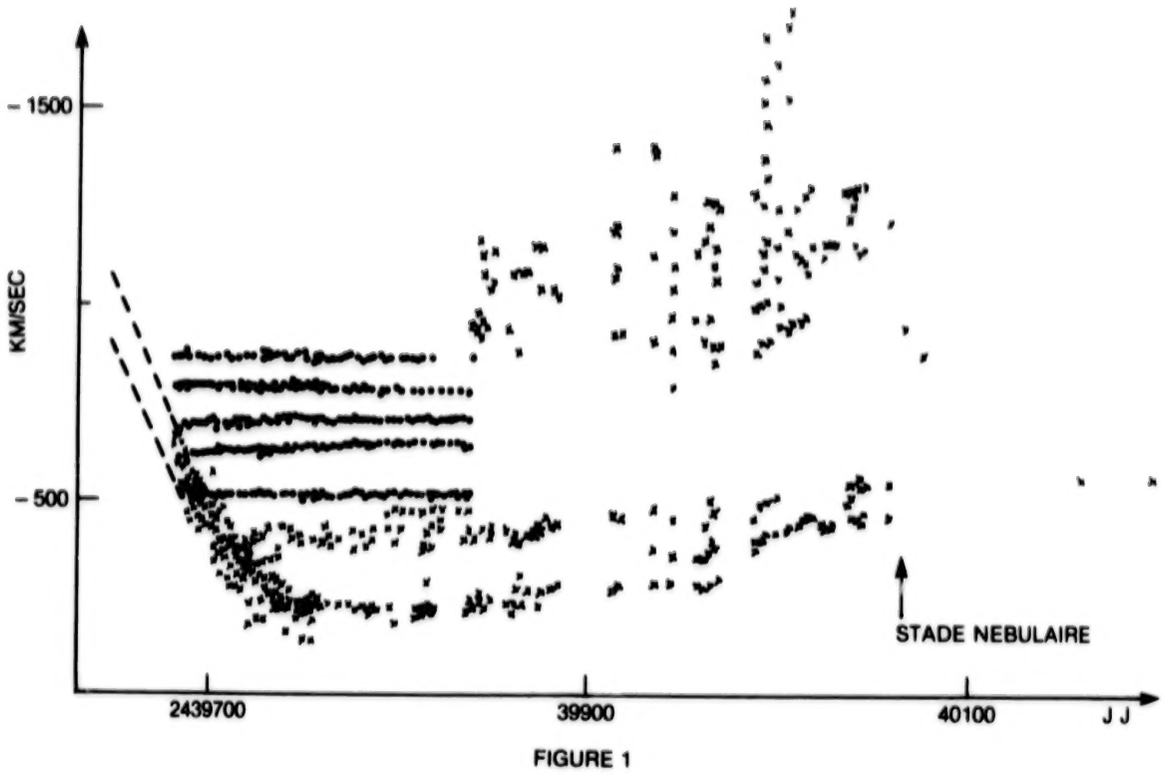


FIGURE 1

Figure 8-100. Radial velocity data of absorption lines in the spectrum of HR Del from the premaximum to the nebular stage (Malakpur 1973c).

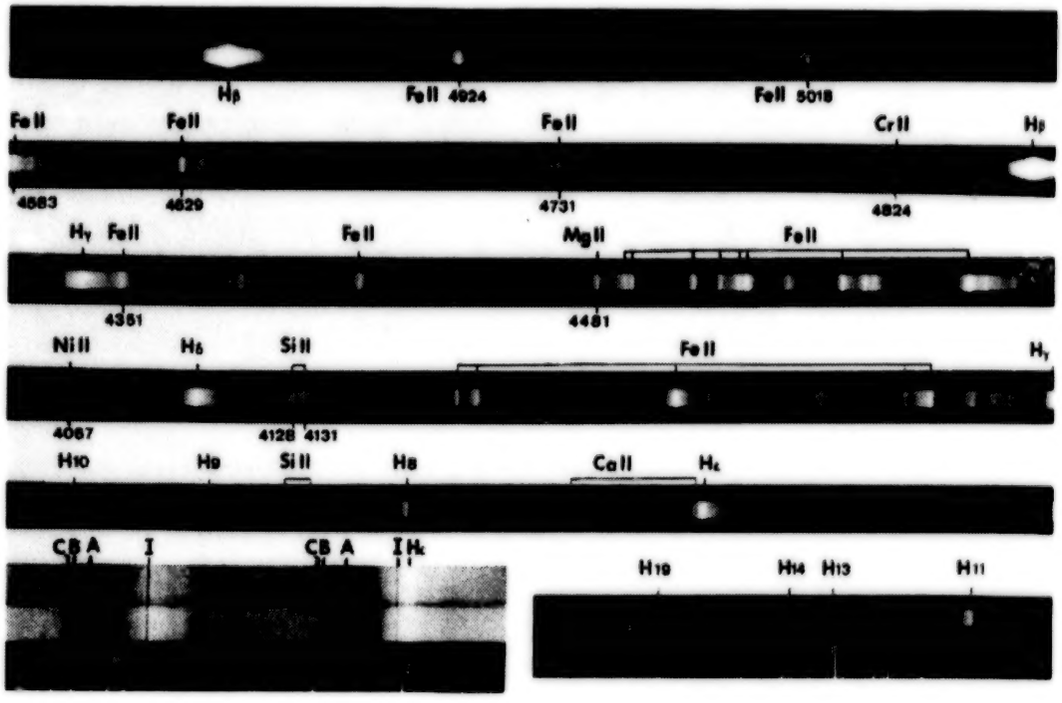


Figure 8-101. The spectrum of HR Del from Hβ to the Balmer limit three days after outburst. On the bottom at left: enlargement of the Ca II H and K region showing the absorption components A, B and C and the interstellar components I. (Courtesy of Ch. Fehrenbach and P. Veron. Observatoire de Haute Provence du Conseil National de la Recherche Scientifique (CNRS)).

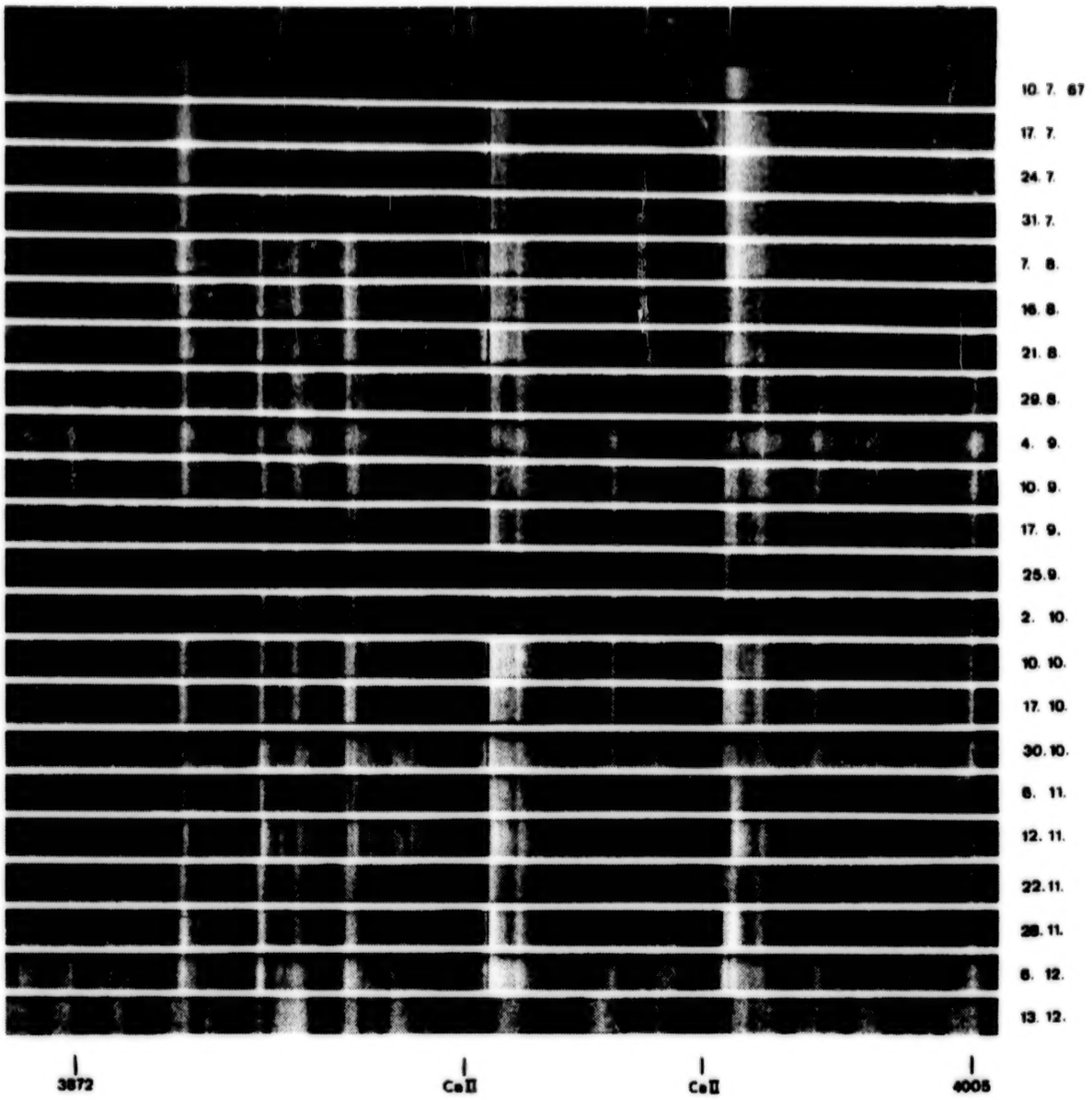


Figure 8-102a. Spectral variations of HR Del from 1967 July 10 to December 13, spectral range λλ 3872-4005. Note the sharp interstellar absorption lines of Ca II, the broad stellar absorption components showing expansion velocities decreasing from -660 to -300 km/s from early July to September, and increasing again to -400 km/s in December. Note also the sharp absorption components which are violet-shifted with respect to the broad absorption line. The emission components, formed in an outer extended envelope, are stationary. For details, see Fehrenbach and Petit (1969). (Courtesy of Ch. Fehrenbach and P. Veron. Observatoire de Haute Provence du Conseil National de la Recherche Scientifique (CNRS)).

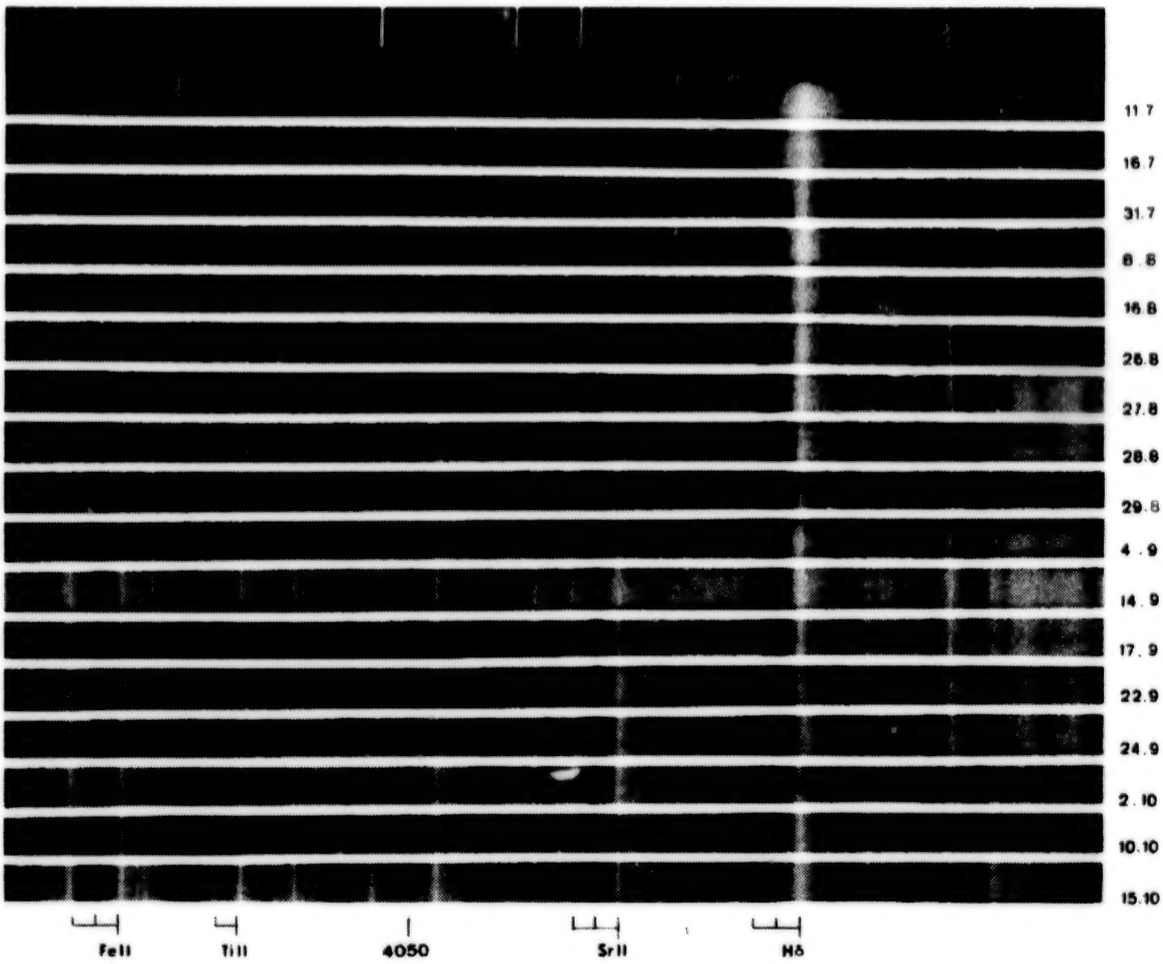


Figure 8-102b. See Figure 8-102b spectral range λλ 4000 - 4150. Note the very remarkable increase in intensity of the emission and absorption lines of Ti II and Sr II and the presence of three absorption components on 1967 August 28 and 29. For details, see Fehrenbach et al. (1968a). and Fehrenbach et al, (1968b). (Courtesy of Ch. Fehrenbach and P. Veron. Observatoire de Haute Provence du Conseil National de la Recherche Scientifique (CNRS)).

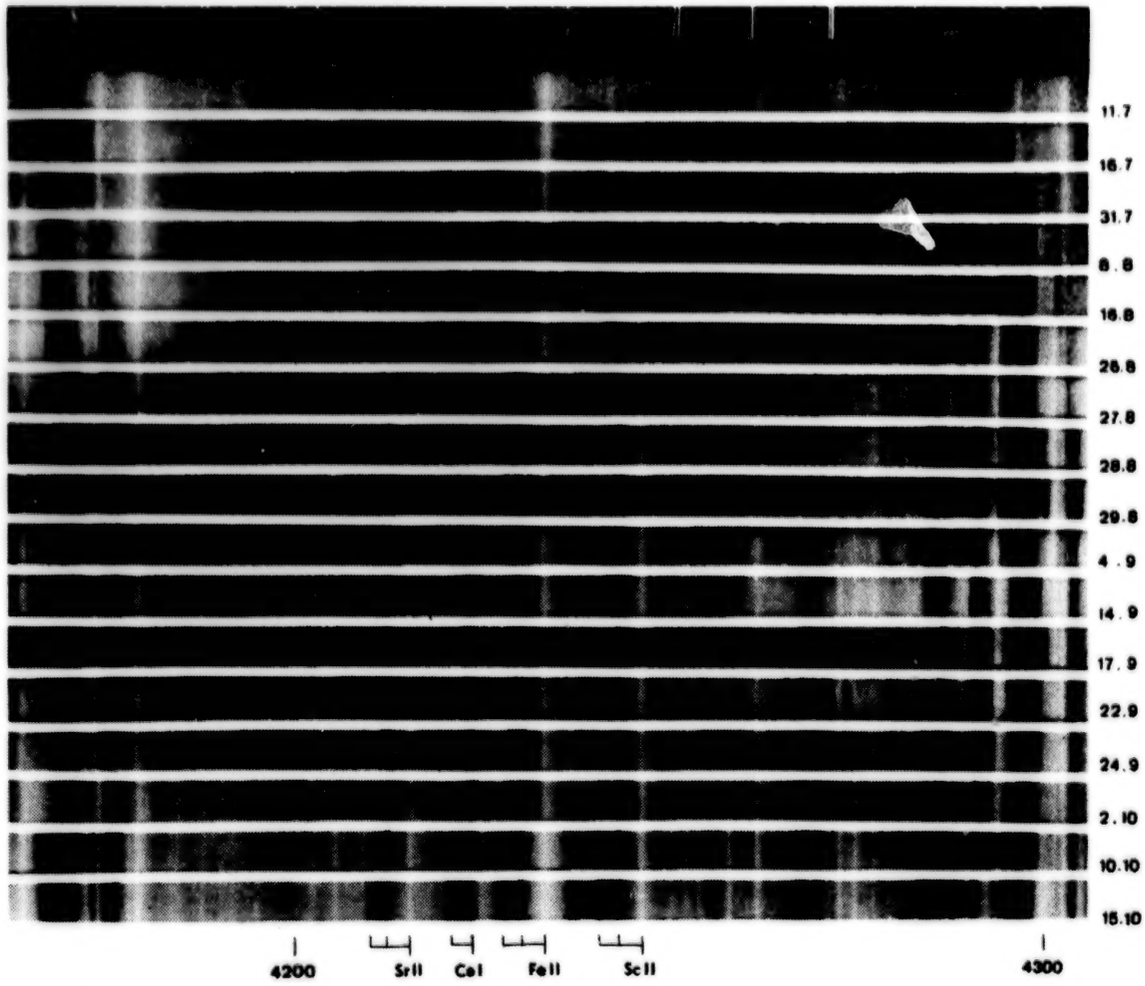


Figure 8-102c. See Figure 8-102a spectral range λλ 4140 - 4300. (Courtesy of Ch. Fehrenbach and P. Veron. Observatoire de Haute Provence du Conseil National de la Recherche Scientifique (CNRS)).

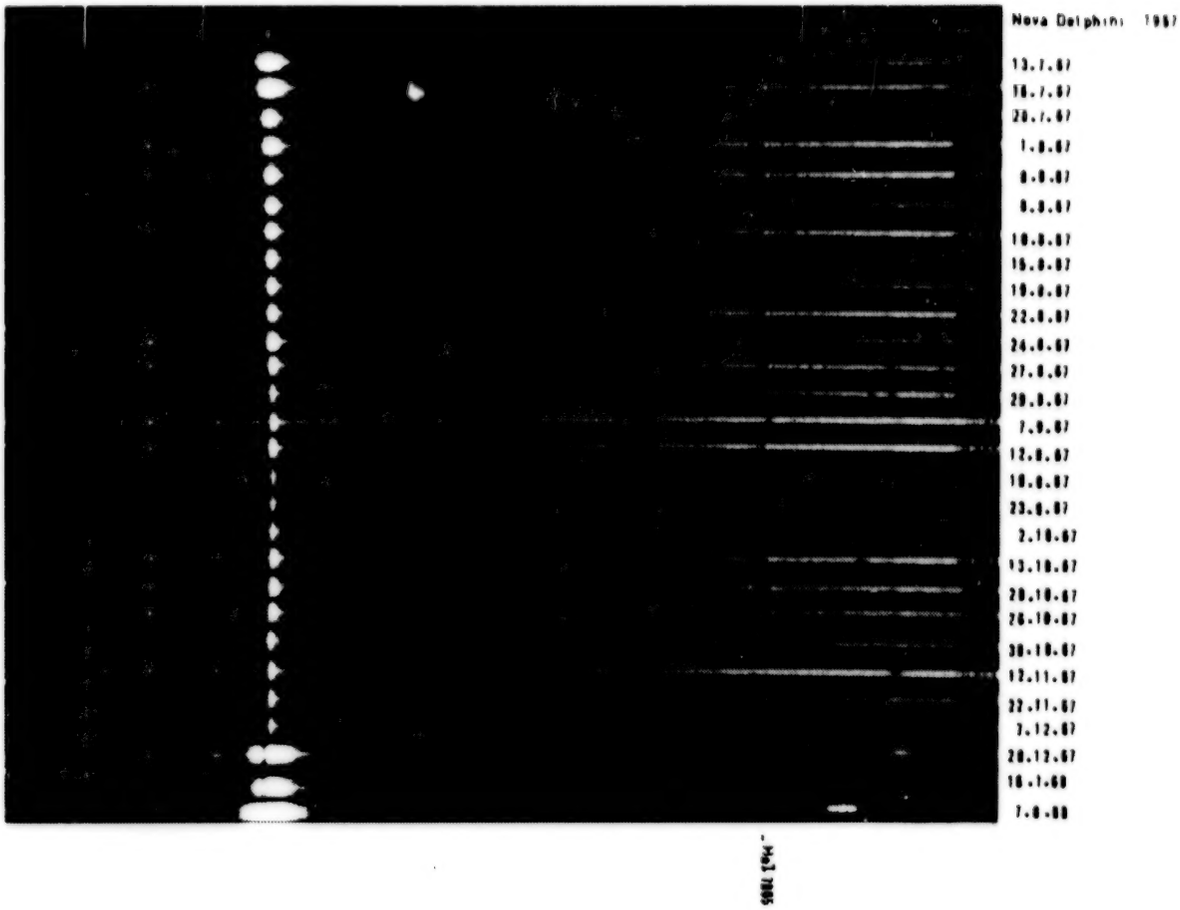


Figure 8-102d. The red spectrum of HR Del: Hα to λ 7400. (Courtesy of Ch. Fehrenbach and P. Veron. Observatoire de Haute Provence du Conseil National de la Recherche Scientifique (CNRS)).

ORIGINAL PAGE IS
OF POOR QUALITY

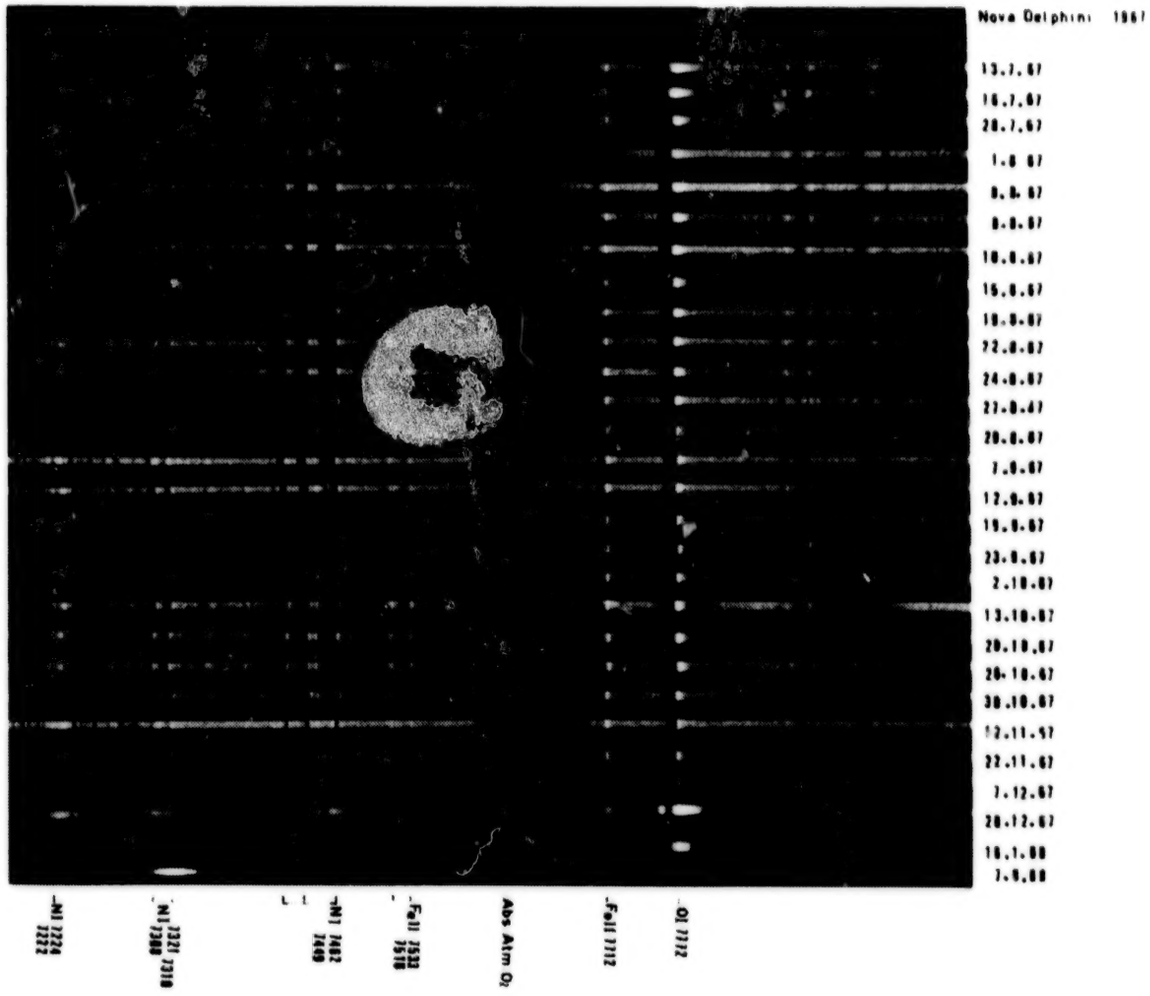


Figure 8-102e. The infrared spectrum of HR Del: λλ 7200 - 8000. (Courtesy of Ch. Fehrenbach and P. Veron. Observatoire de Haute Provence du Conseil National de la Recherche Scientifique (CNRS)).

pal spectrum, visible since August 27, 1967, experienced a sudden increase in velocity on April 21, 1968, (Figure 8-103), when the diffuse-enhanced system, visible since December 17, 1967, merged with it. The emission components were much stronger than during Phase I, and appeared to be a blend of several contributing emissions, each of which was intially sharp and narrow but which gradually spread in wavelength while diminishing in central intensity, again over a period of several weeks. The velocities of some components are in excess of 1700 km/s. The correlation between luminosity and spectrum changes is not clear.

The composition of the spectrum in Phase II is similar to that at the beginning of Phase I. It appears to arise from a number of successive shells each with slightly different temperature, and possibly composition. While the excitation state of lines during Phase I corresponded to excitation potentials of 1 to 5 eV, the excitation state here appears to cover the potentials of 2 to 3 eV in the high-velocity shell (up to 1000 km/s), and of 0.5 to 3 eV in the low-velocity shells.

Malakpur (1973c) notes that the Orion system had its first appearance on May 11, 1968 (Figure 8-104).

Phase III. Transition and nebular stage.

Phase III begins in June, 1968, with the cessation of irregular activity. The light curve falls smoothly to m = 8, and the spectrum changes rapidly through the Orion to the nebular stage, where is characterized by strong, multiple-peaked emissions. Malakpur (1973c) determined the beginning of the nebular stage to be around July 28, 1968. No shells were ejected after May, the spectrum began to change rapidly, going through stages of increasing excitation and dilution, to the final nebular stage, in about 10 weeks. The continuum became very blue and then faded, while the emission line strength increased. The emission lines split into three components, and the relative intensities differed between allowed and forbidden lines.

During August, the continuous spectrum continued to fade. Starting from that date, until 1972, various coronal lines could be seen in the spectrum: [A X], [Fe X], [Fe XI], [Fe XIV], [Fe XV], [Ni XII], and [Ni XV] (Andrillat and Houziaux, 1970a; Rafanelli and Rosino, 1978).

The radio light curve is well covered in the later stages. A Hubble flow model yields a good fit to the observations at several frequencies (Seaquist et al., 1979) (see Figure 6-76).

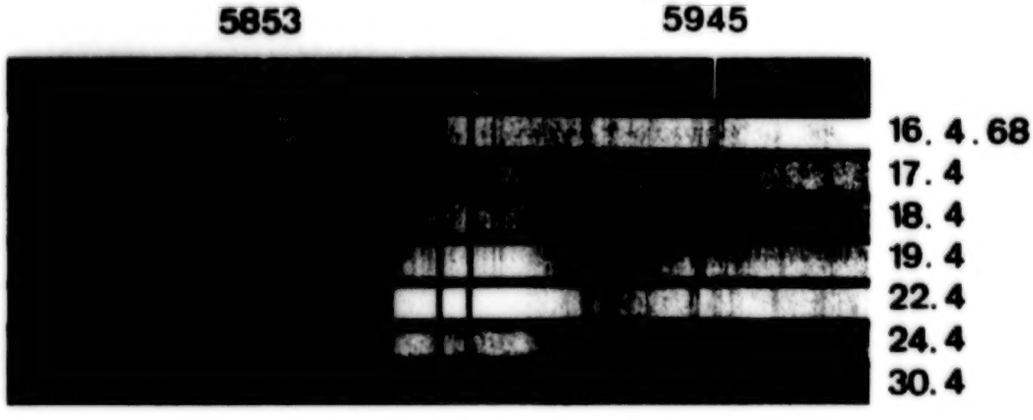


Figure 8-103. Spectral variations of HR Del in 1968 April in the region λλ 5800 - 5950. Note the strong interstellar D lines of Na I and the violet shifted stellar D lines. (Courtesy of Ch. Fehrenbach and P. Veron. Observatoire de Haute Provence du Conseil National de la Recherche Scientifique (CNRS)).

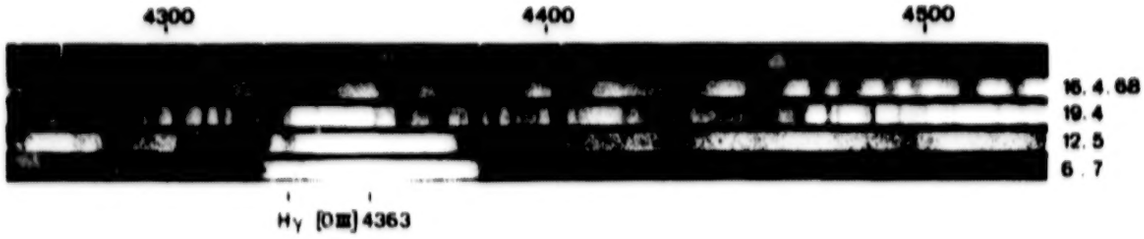


Figure 8-104. Th spectral variations of HR Del from 1968 April to 1968 July (Courtesy of Ch. Fehrenbach and P. Veron. Observatoire de Haute Provence du Conseil National de la Recherche Scientifique (CNRS)).

XI.F. CHEMICAL COMPOSITION

Table 8-5 shows the results of various determinations of the chemical composition of HR Del.

The abundance dererminations of Antipova (1977) Raikova (1977), and of Ruusalepp and Luud (1971) are derived from the curve of growth method applied to the absorption lines of the principal spectrum (August - December 1967), and using the usual equations by Boltzmann and Saha, i.e., by assuming that the pseudophotosphere of the nova is in LTE, a condition very far from its real state. The determinations by Tylenda (1979) are more reliable because they are based on the emission lines of the envelope during the nebular stage (1971-72 and August 1975), using two different models (A and B). Tylenda (1978) shows that the observed line intensities of the envelope in the nebular stage cannot be fitted by models that assume that the central source of the ionizing photons radiates as a single star with blackbody spectrum (Tylenda 1978). The theoretical line intensities are 4 to 100 times fainter than the observed ones. Instead, a good fit with the observations is obtained by assuming that the central source of ionizing photons consists of two components. An ionizing radiation, being the sum of two blackbody distributions with almost equal luminosities and temperatures of about 4×10^4 K and 2.5×10^5 K, is adopted. The input parameters of the two source models A and B and the comparison with the observations are given in Tables 3 and 4 of Tylenda (1978).

In spite of the different models and assumptions, all determinations agree in obtaining a CNO excess. Tylenda (1978) gives C(HR Del)/C(Sun) = 25, N(HR Del)/N(Sun) = 630, O(HR Del) O (Sun) = 125, Ne (HR Del)/N(Sun) =37. These values are in good agreement with the average values found for novae (Collin-Souffrin, 1977).

Table 8.5 — The table shows the results of various determinations of the chemical composition of HR Del

element	Antipova	Raikova	Ruusaleep	Tylenda (A)	(B)	Sun
H	24.64		25.49	26.40	25.77	25.0
He				25.83	25.20	23.8
C	22.98	22.42	23.56	23.00	23.00	21.6
N	23.14	22.53	22.80	23.94	23.50	20.9
O	23.59	23.87		24.08	23.70	21.8
Ne				22.78	22.37	21.0
Mg	20.34	20.71	20.28			20.6
Al	19.34					19.5
Si	21.02	20.92	21.52			20.7
Ca	19.02	20.48				19.3
Sc	15.90	16.64	16.83			16.1
Ti	17.72	18.26	18.73			18.1
V	16.60	17.18	17.51			17.0
Cr	18.37	18.22	19.57			18.3
Mn	17.61	18.97				18.0
Fe	20.83	20.83	19.98			20.5
Sr	15.85	16.67	15.36			15.9
Y	15.56	15.97				15.1
Zr	15.37	16.22				15.7
Ba	14.85	15.62				15.1
La	14.64					14.4

N95
27075
UNCLAS

N95- 27075

9

RECURRENT NOVAE

M. Hack and P. L. Selvelli

I. THE KNOWN RECURRENT NOVAE

Recurrent novae seem to be a rather inhomogeneous group: T CrB is a binary with a M III companion; U Sco probably has a late dwarf as companion. Three are fast novae; two are slow novae. Some of them appear to have normal chemical composition; others may present He and CNO excess. Some present a mass-loss that is lower by two orders of magnitude than classical novae. However, our sample is too small for saying whether there are several classes of recurrent novae, which may be related to the various classes of classical novae, or whether the low mass-loss is a general property of the class or just a peculiarity of one member of the larger class of classical novae and recurrent novae.

Five recurrent novae have been observed up to now (Table 9.1).

It is an open problem whether the well known relation between amplitude and cycle length existing for dwarf novae may be extended to recurrent novae, especially since the gap existing between the greatest cycle length

TABLE 9-1. KNOWN RECURRENT NOVAE

Name	Epochs of outbursts	Apparent magnitudes Min - Max	Light Curve Class	Spectrum (quiescence)	Notes
U Sco	1863,1906, 1936,1979, 1987	19.2v-8.8v	Fast	GO V	
T Pyx	1890,1902, 1920,1944, 1966	15.3p-6.5p	Slow	Very blue	
RS Oph	1898,1933, 1958,1967, 1985	12.5v-4.3v	Fast	M III	
V1017Sgr	1901,1919 1973	14.7B-7.2p	Slow	G5 IIIp	Symbiotic?
T CrB	1866,1946	11.3p-2.0p	Fast	M3 III	Sp.bin P = 227.3d

in dwarf novae* (about 1.5 years) and the smallest one in recurrent novae (about 20 years) has been filled by WZ Sge, of which the outburst properties are typical of dwarf novae, but which has a cycle length of about 33 years, and by the recurrent nova RS Oph which has outburst properties typical of a nova, but which has exhibited outbursts at intervals less than 10 years.

A recent compilation of amplitudes A and cycle lengths C for dwarf novae and recurrent novae, including three X-ray recurrent novae, has produced the graph published by Richter (1986) (Figure 9-1).

This superposition in cycle length has posed some problems in defining recurrent novae. Webbink et al. (1987) give the following criteria for defining a recurrent nova unambiguously:

1) Two or more recorded outbursts, reaching absolute magnitude at maximum compa-

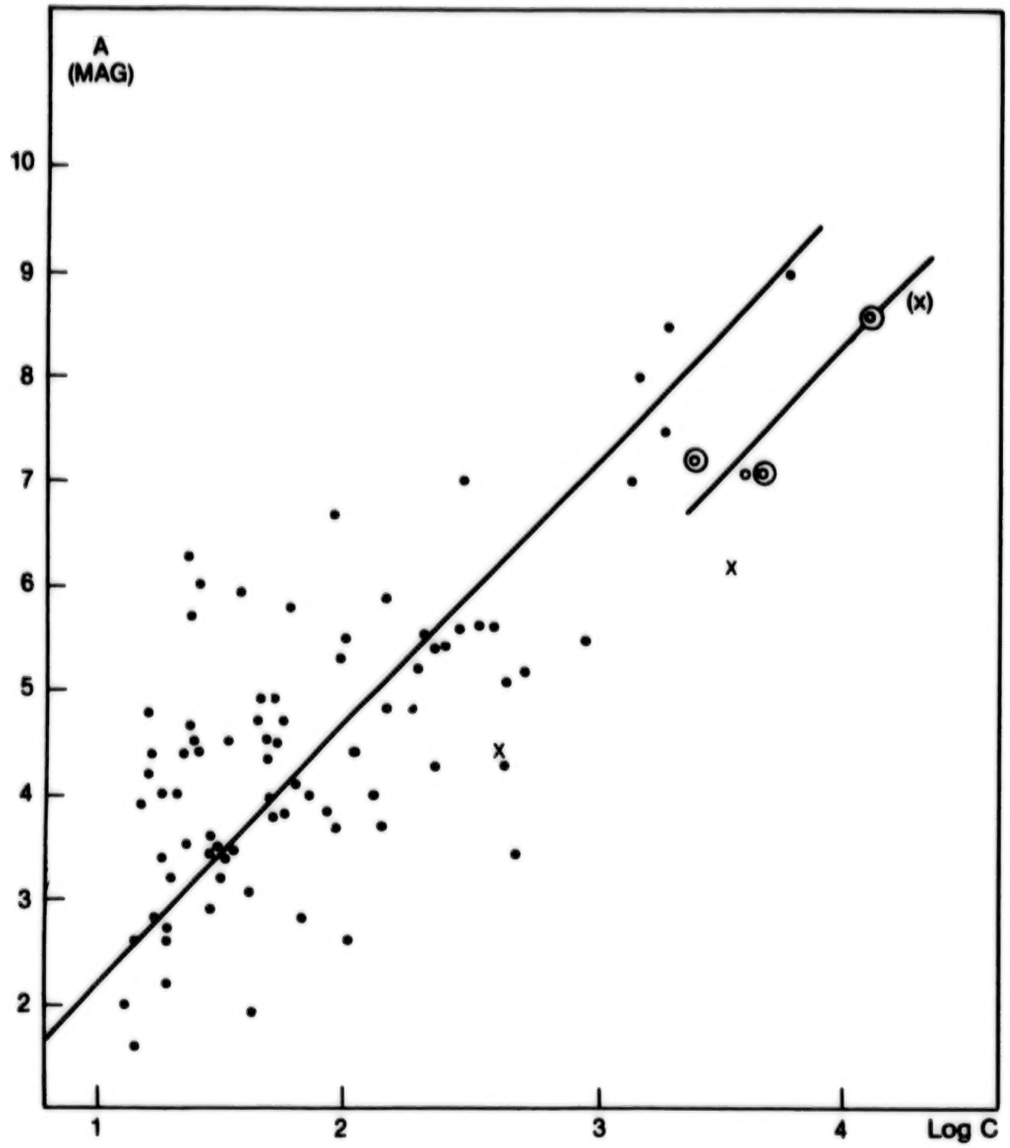


Figure 9-1. Amplitude-Cycle length relationship of cataclysmic variables. Dots: dwarf novae; circles: recurrent novae; crosses: recurrent X-ray novae. Very uncertain values are in brackets. (from Richter, 1986).

*See also Chapter 2, II.A.3 on Dwarf Novae. Actually, if we consider Dwarf Novae alone the scatter is very large.

rable with those of classical novae (i.e., $M_V \leq -5.5$).

2) Ejection of a discrete shell in outburst, at velocities comparable with those of classical novae ($V_{exp} \geq 300$km/s).

The first criterion distinguishes recurrent novae from both classical and dwarf novae and also from symbiotic novae. The second distinguishes them from the remaining symbiotics stars, many of which show bright, multiple outbursts, but without high-velocity shell ejection.

We will report in detail the results of the observations of the five objects: U Sco, T Cr B, RS Oph, T Pyx, and V 1017 Sgr, and we will compare these objects among themselves, and with classical novae.

II. U SCO

The recurrent nova has undergone recorded outbursts in 1863, 1906, 1936, 1979, and another in 1987. At quiescence, it is very faint (V = 19.2) and reaches V = 8.8 at maximum. On May 5.55, 1987, V was equal to 15.5. There are no observations between May 10, when V = 13, and May 16.08 when V = 10.8 (see IAU Circular No. 4395 of May 18, 1987). It is, therefore, probable that the maximum of 8.8 was reached during this gap (on May 13.5, 1987 according to Rosino and Iijima, 1988). Five superposed visual light curves are shown in Figure 9-2 from their paper.

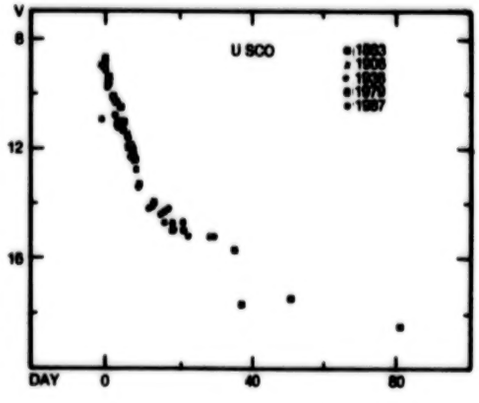


Figure 9-2. Five superposed visual light curves of U Sco.
(from Rosino and Iijima, 1988).

The light curve is typical of very fast nova, with $t_3 = 6^d$ and with a smooth decline (Figure 9.2).

Two spectra taken during the 1987 outburst are shown by Rosino and Iijima (1988). The first one, obtained on May 22, is characterized by the presence of a relatively weak continuum and emission lines of H, He II ,N III, N IV, N V, C III, C IV, Si III, Fe III, O IV, and O VI, indicating a very high degree of excitation. The second spectrum obtained about 24 hours later is similar to the first except for the drastic fading of the λ 4640 blend, which was very strong the night before.

Reports on the previous outbursts were given by Pogson (1908) and by Thomas (1940). A complete spectrophotometric study in the visual and ultraviolet range was made during the 1979 outburst by Barlow et al. (1981) and by Williams et al. (1981). Spectroscopic observations in the range accessible from the ground were obtained during the whole outburst. In addition, a preoutburst spectrum was taken on March 26, 1979 (Figure 9-3). The maximum brightness was reached on June 24, and an early outburst spectrum was obtained by Duerbeck and Seitter (1980) on June 28.95 U.T. The preoutburst spectrum and one obtained on July 12, 1979, when the visual magnitude was about 15, are very similar. They do not present strong emission and absorption features, with the exception of the He II emission at 4686 A, which is always dominant (see also the spectrum taken by Williams-Williams et al. 1981 in March 1980, Figure 9.7). On July 2 and 3, the strong He II emission shows a double-peaked profile; H Beta and H Gamma show a broad emission - full width at zero intensity (FWZI) ≃ 10000 km/s, and a narrow asymmetric feature, split in two to four components, separated by about 500 km/s, while the FWZI is 1600 km/s (Figure 9-4). A very broad strong emission feature is present on July 2 in the spectral interval 4500-4700 Å , and it diminishes rapidly in intensity. It is probably a blend of N III, N V, C III, C IV and He II emissions.

Such broad complex profiles of the Balmer emissions clearly indicate expansion velocities

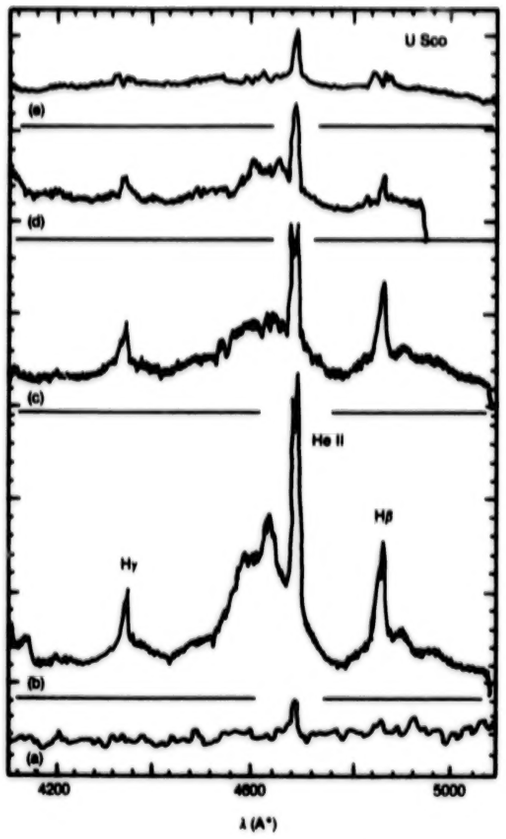


Figure 9-3. Early evolution of the spectrum of U Sco through the 1979 outburst. The dates, from bottom to top are: March 26, July 2, July 3, July 6 and July 12, 1979. (from Barlow et al., 1981).

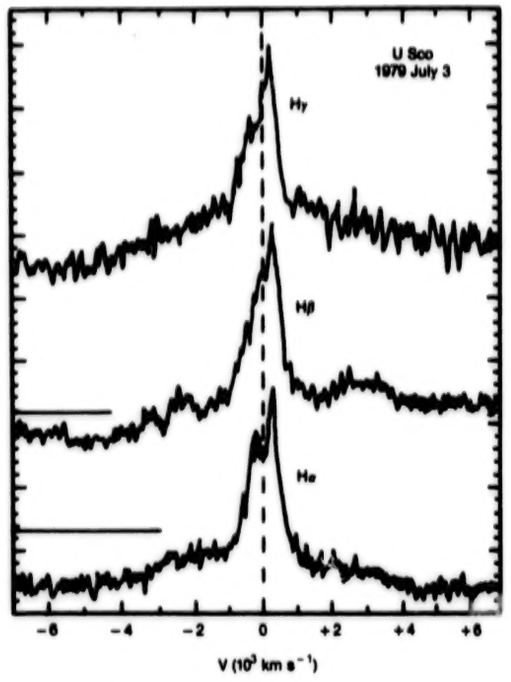


Figure 9-4. The profiles of the Balmer lines on July 3, 1979 plotted on velocity scale. (from Barlow et al., 1981)

of the ejecta as large as 5000 km/s, much larger than those usually found in classical novae, which rarely are larger than 2000 km/s (Figures 9.4 and 9.5). The expansion velocities indicated by the ultraviolet spectrum are much larger than the visual ones.

On August 13, U Sco had faded to magnitude 17. One absorption feature is observable at 5175 Å and can be attributed to the Mg I triplet at 5167-5183. Since this feature is dominant in spectral types later than G0, it is possible that it is due to a late-type underlying star (Figure 9.6). Another spectrum was obtained by Williams in March 1980 (Figure 9.7) when the star was back to its quiescent magnitude: it still shows the strong He II emission at 4686 A. Two fainter but clearly detectable emissions at 5411 and 6560 are attributed to He II and to H +He II. 3781 and 4200 He II are also detectable. A nonidentified emission feature at 6250 is rather

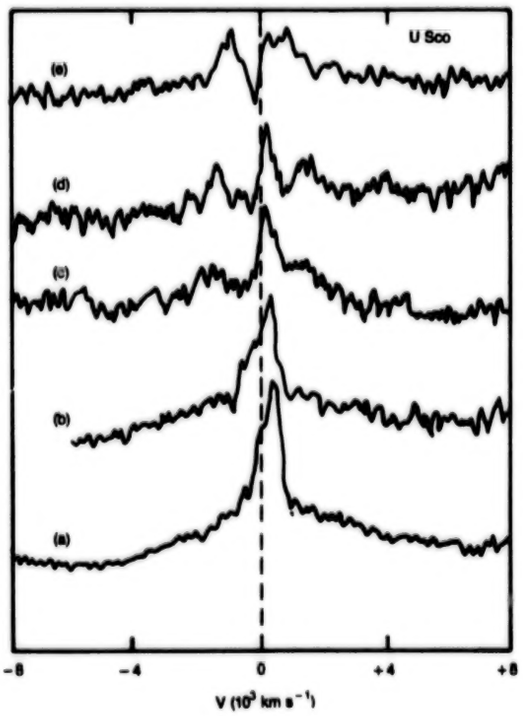


Figure 9-5. The H Gamma profile of U Sco at various epochs, plotted on velocity scale. The dates from the bottom to top are July 2, July 3, July 6, July 8 and July 12, 1979. (from Barlow et al., 1981).

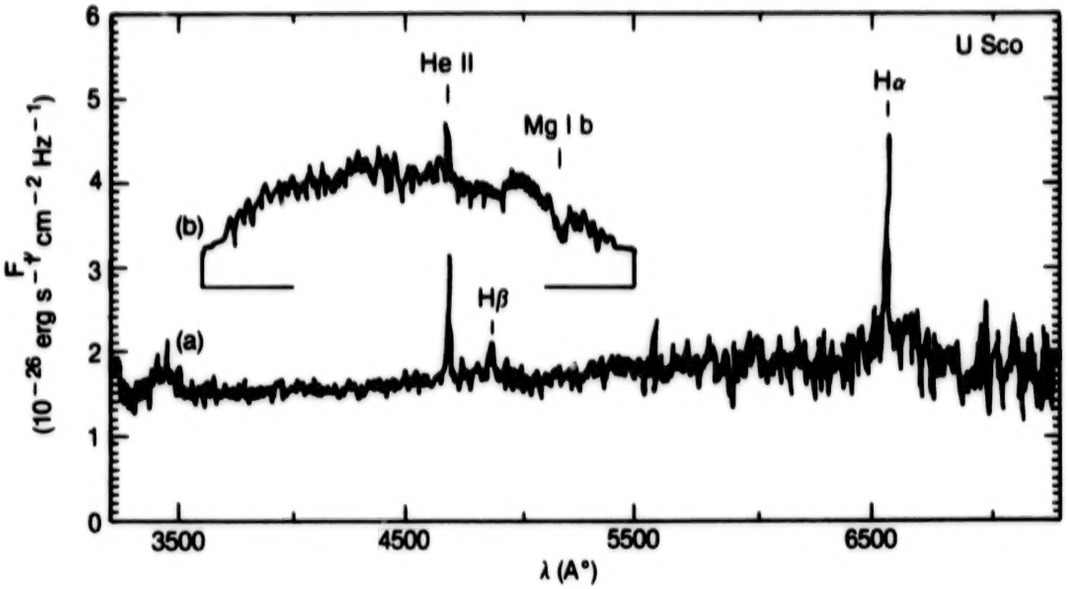


Figure 9-6. The spectrum of U Sco late in the outburst. (from Barlow et al., 1981).

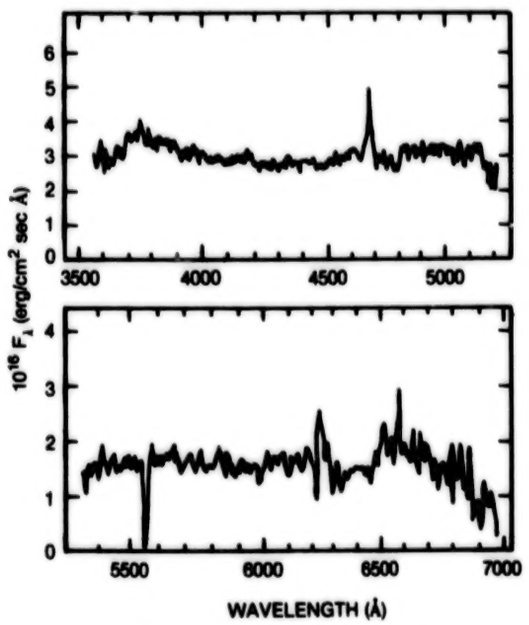


Figure 9-7. Optical spectrum of U Sco obtained in March 1980 after the nova had returned to quiescence. (from Williams et al., 1981)

strong. There is no evidence for the presence of the Balmer lines. It is not possible to say whether some absorption lines are present. Another postoutburst spectrum was observed by Hanes (1985) in June 1982, with a resolution of about 8 A, when the visual magnitude was about 17.85. The flux distribution observed in March 1979, about 3 months before outburst, and the observed in June 1982 are identical, although in 1979, the star was about 2 magnitudes brighter (Figure 9-8). The line spectrum presents emission lines of He II 4200, 4542, 4686, and 5412 A, the absorption lines H and K of Ca II and of the Mg I triplet at 5167, 5173, and 5184 A, and a depression at the Balmer limit, which, however, cannot be attributed to H I since no Balmer lines are observable either in absorption or in emission (Figure 9.9-a). This depression is very probably due to a blend of metallic lines. This feature, togther with the presence of the Mg I absorption triplet, and the comparison with the spectra of 70 Oph (K0V), Mu Ara (G5V) and 58 Oph (F7V) sug-

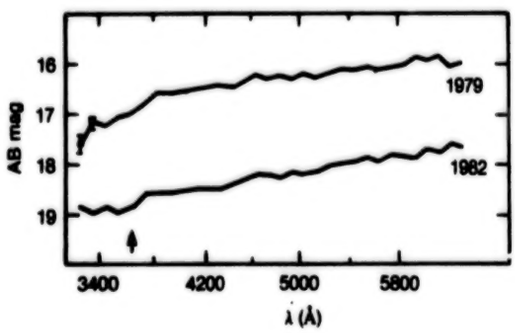


Figure 9-8. The flux distribution for U Sco in 1982 and 1979. The scale for the 1982 curve is AB Mag = -2.5 log f(nu) -48.60. The spectrum of 1979 has been arbitrarily shifted vertically. The arrow indicated the position of the Balmer discontinuity at 3636 A. (from Hanes, 1985).

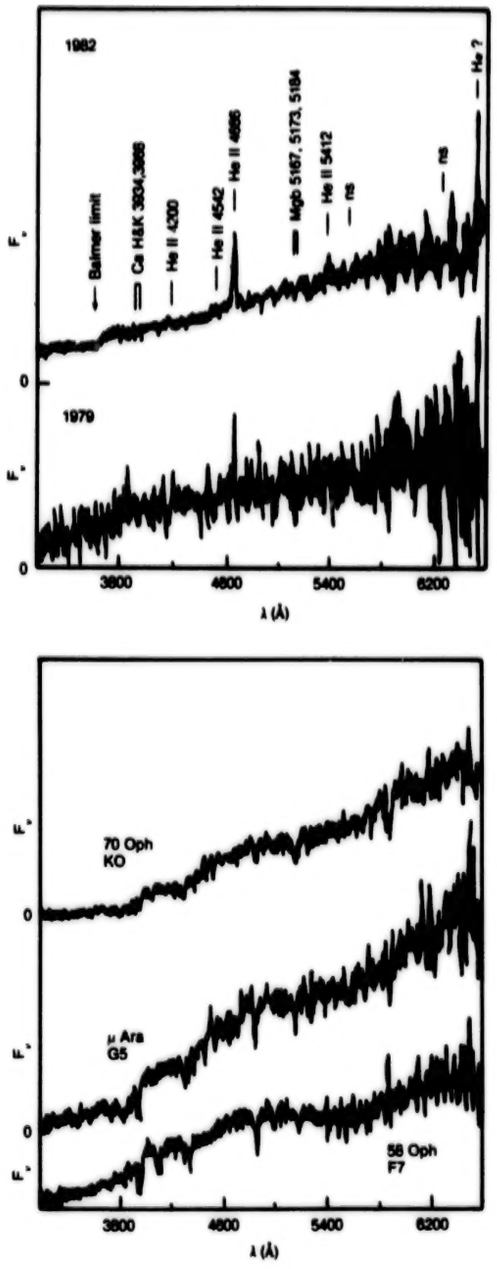


Figure 9-9. a) The narrow-slit spectrum of U Sco in 1982 obtained with an integration time of 14000 s. Below is shown the 1979 spectrum obtained with an integration time of 1000 s. The ordinate scale is in units of flux per unit frequency and is linear. The zero point for each spectrum is shown. b) The spectra of three main-sequence stars are shown. The spectra were obtained with the same instrumentation as for U Sco. The ordinate and abscissa scales are the same. The comparison of the spectrum of U Sco with those of the standard stars suggests a spectral type F7-GO. (from Hanes, 1985).

gest a spectral type G0 +/- 5 (Figure 9-9b). By plotting the infrared colors of U Sco in the two diagrams (H-K) vs (J-H) and (V-K) vs (J-H) and comparing the position of U Sco with those of main sequence stars, it appears that U Sco is a G0 or a late F main sequence star (Figure 9-10).

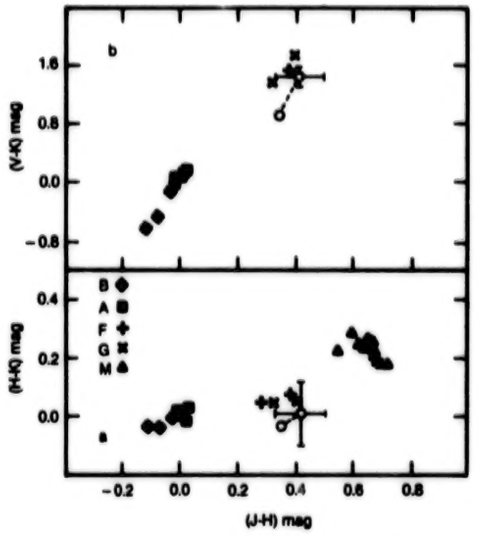


Figure 9-10. The position of U Sco (circle with error bars) in the (H-K), (J-K) two infrared color diagram is very close to that of F and G stars. (from Hanes, 1985).

II.A. ULTRAVIOLET OBSERVATIONS

Several far-ultraviolet, low-resolution spectra were also obtained with IUE during the 1979 outburst, mainly by Willliams et al. (1981) plus one by Barlow et al. (1981) during the period June 28 to July 11, 1979. The main characteristic is the strong emission 1240 N V, which is much stronger than 1550 C IV. The latter presents a strong shortward absorption component on June 28, which is fainter on June 30 and absent on July 2. On June 28 also, low- or relatively low-ionization features, like C II or Si IV, are present, but they have disappeared by July 2 (see Figure 6-52).

Simultaneous observations of U Sco in the ultraviolet (1175-2000 Å) and in the visual range were obtained by Barlow et al (1981) on July 6. These observations permitted Barlow et al. to derive the energy distribution (Figure 9-11). However, no data for the near-ultraviolet

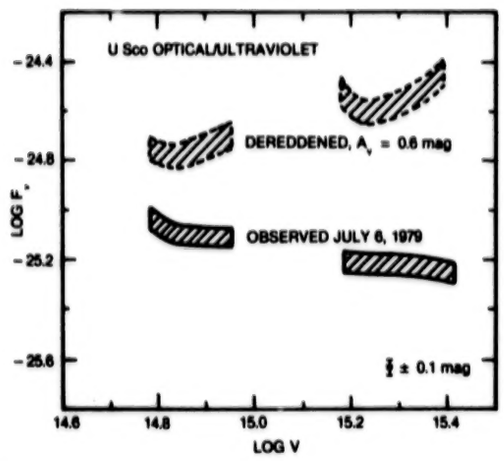


Figure 9-11. The observed continuum flux (in erg cm^{-2} s^{-1} Hz^{-1}) of U Sco on July 6, 1979. (from Barlow et al., 1981).

were obtained that would allow a direct measurement of the interstellar reddening by means of the 2200 Å feature.

An estimate of this was made by using the 1640 He II/4686 He II ratio, which is not very sensitive to either density or temperature. A value of E(B-V) = 0.2 and A_V = 3.1 E (B-V) = 0.6 was found. Figure 9-11 illustrates how strongly the energy distribution depends on the dereddening.

Other data obtained from June 26 to July 6 in the I-R-V-B-U bands show that the energy distribution remains remarkably constant from June 29 to July 6. This behavior is different from that of classical novae, which show a shift to the ultraviolet with time after maximum.

II.B. ABUNDANCES IN THE EJECTA

Abundances in the ejecta were derived from the visual (Barlow et al., 1981) and the ultraviolet (Williams et al., 1981) spectra. The presence of many strong lines of N III and N IV in the visual spectrum probably indicates an excess of nitrogen. The ratio H/He can be derived quantitatively by the ratio of the even to the odd members of the Pickering series. In fact, it is well known that the even members of He II Pickering series are almost coincident with the Balmer series. If we assume that the higher members of the series are optically thin, the fluxes are proportional to the numbers of the emitting ions: F(even)/F(odd) = (H^+ + He^{2+}) / He^{2+}. By this method H^+/He^{2+} = H^+/He^{2+} = H/He = 0.5 is found.

The ultraviolet spectrum permits us to derive the H/He abundance from the ratio Ly Alpha/ 1640 He II with considerable accuracy, since the two lines are both formed by recombination and, hence, the ratio is not strongly dependent upon other parameters. A difficulty, however, is to disentangle the stellar Ly Alpha from the geocoronal Ly Alpha emission.

Relative abundances of carbon, nitrogen, and oxygen can be derived reliably, because all the ultraviolet lines of these ions are transitions from collisionally excited levels which, therefore, present the same dependence on temperature and density. By assuming that the ionization degrees of C,N,O are similar, i.e., that C^{3+}/ N^{3+} = C/N and N^{2+}/O^{2+} = N/O, then approximate abundance ratios can be derived by the ratios 1550 C IV/1486 N IV], and 1750 N III/ 1663 O III]. C/N = 0.1 and N/O = 0.9 are found and H/He < 0.1 is estimated. The abundance ratio nitrogen to helium, which is derived by the ratio 1240/1640 is very uncertain. This ratio, in fact, is affected strongly by the value assumed for the electron temperature. The abundance ratio CNO/ (H+He) varies from 4 for $T_e = 10^4$ to 2 x 10^{-3} for T_e = 2.5 x 10^4. The temperature independent ratios He/H and N/CNO are higher than the solar value, indicating that the material in the ejecta has experienced substantial CNO burning. Not only the ultraviolet and visual spectra of U Sco in outburst are characterized by the great strength of the He II lines. Also the spectrum of U Sco at quiescence, obtained by Williams in March 1980 (see Figure 9-7), is characterized by the strength of the He II emission relative to the Balmer lines. In this respect, the quiescent spectrum of U Sco is very different from the spectra of other quiescent novae. The classical novae present some helium enhancement, but not as much as that observed for U Sco (Y = 0.9 and X = 0.1). The high abundance of helium poses several prob-

lems that have been discussed by Webbink et al. (1987).

II.C. MASS LOSS

The mass of the shell can be estimated if the gas density, the distance, and the filling factor* are known. However, Williams et al (1981) show that when the optically thick resonance lines present in the ultraviolet can be observed, the mass of the shell can be derived by the knowledge of the optical thickness of the shell, and it is not necessary to know the distance and the filling factor.

Optical observations of the Balmer emissions provide the mass of the shell by the relation $F(H\beta) \propto N_e N_i R^3_S \simeq \epsilon N_e^2 R_S^3$ which requires the knowledge of the distance in order to obtain the flux at the stellar surface from the observed flux at the earth.

N_e can be derived from the spectral observations, hence the mass given by the product mass density ρ by R_S^3 can be derived.

The new method proposed by Williams et al. and making use of the ultraviolet observations is related only to the optical thickness of the shell along the line of sight and does not require to know the distance, the filling factor, and the density. Let us suppose that the shell of radius R_S is formed of n clouds of mean radius r. Then $\epsilon = nr^3/ R_S^3$; $t_i = N_i a_o r$ is the optical depth of one internal cloud and the optical depth of the whole shell, $\tau_i = N_i a_o R_S \epsilon$, where N_i is the number density of the absorbing ions, a_o the absorption cross-section at the line center per ion, given by $a_O = \sqrt{\pi}\ e^2 f_i \lambda_i^2 / m_e c^2 \Delta\lambda_D$.

Now if we call the mean free path between clouds $l=r/\epsilon$, it follows that $\tau = t_i(R_S/l) = N_i a_o r (R_S/l)$, hence $\epsilon = n(r/R_S^3) = \tau_i/N_i a_o R_S = r/l$. $M_s = (4/3)\pi R^3$, and $\rho = (N_H + 4N_{He}) m_H = N_{He} m_H (N_H/N_{He} + 4)$ and finally, $M_s = (4/3)\ \pi R_s^3 m_H N_{He} (N_H/N_{He} + 4)\epsilon$.

*The filling factor ε is defined as the ratio nr^3/R_S^3 where n is the number of clouds of mean radius r and R_S is the radius of the shell.

Since the observations suggest that $N_{He}/N_H \simeq 2$, we have $M_S = (4/3)\pi R^3_S m_H N_{He} \times 4.5$ $(\tau_i/N_i a_o R_S) = 6\pi m_H (N_{He}/N_i)(\tau_i/a_o) R^2_S$, where R_S is given by the product of the expansion radial velocity by the time elapsed from the outburst.

The optical depth on the center of the strong absorption resonance lines of C IV (observable on June 28 and 30) is assumed equal to 1, since there is some residual radiation even in the center of the line. This is the advantage of using the ultraviolet range of the spectrum, where absorption lines like those of C IV are present, but the assumption that τ_i is equal to one is also the weak point of the method. Another weak point in this procedure is the determination of the ratio N_{He}/N_i, in this case the ratio of helium atoms to the absorbing ion C^{3+}. It can be derived from the spectrum but it is strongly affected by the assumed value of the electron temperature.

With all these causes of uncertainty in mind, the mass of the shell can be computed. It is found to be of the order of $10^{-7} M_\odot$. This value is much smaller than the typical values of the shells of classical novae, which have masses of the order of $10^{-4} M_\odot$.

II.D. ON THE NATURE OF THE HYPOTHETIC COMPANION OF U SCO AND AN ESTIMATE OF THE DISTANCE OF U SCO

The quiescent magnitude of U Sco estimated on a survey plate is V = 19.3 +/- 0.5 (Barlow et al., 1981). If we assume that this is the apparent magnitude of the cool companion, and if we assume that it is a giant (as is the case for T CrB, for a reddening E(B-V) = 0.2, A_v = 0.6 mag), then we have a distance modulus of 18.5 +/- 1 mag, corresponding to a distance in the range of 30-80 kpcs, which is unacceptably high and not consistent with the moderate reddening. If we assume the companion to be a subgiant in the spectral range G5-M5, the distance estimate is 13 kpcs, which is still very large. Hence, it seems more reasonable to assume that the companion of U Sco is a main sequence star, thus obtaining an independent

confirmation of the spectral type indicated by the colors and by the comparison with some main sequence stars in the spectral range F7-K0 (Hanes, 1985). For $M_v = 4.5$, corresponding to a spectral type G0 or late F, it follows d = 6.9 kpcs. This distance is in good agreement with the estimate by Williams et al. (1981), by making the assumption that the luminosity of the star at outburst is equal or larger than the Eddington luminosity for one solar mass.

In conclusion, it seems reasonable to assume that the quiescent spectrum of U Sco is G0 V.

III. T PYXIDIS

Among the five accepted recurrent novae, T Pyx is that with the shortest mean period (19 years) and with the hottest spectrum at minimum. Five outbursts were observed: in 1890, 1902,1920,1944, and 1966. However, none of them was observed extensively, with the exception of the last one, during which members of the Variable Star Section of the Royal Astronomical Society of New Zealand (Circulars 123 ad 125) visually observed the light curve, and Catchpole (1969) obtained nine spectrograms between 12.6 and 412.5 days after the initial halt.

The light curve, as those previously observed, rises rapidly to a maximum at about 7.9 (the initial halt); then rise slowly to 7.4 during the next eight days, fall rapidly by 0.5 mag, and rise again to the principal maximum at 6.5 mag 30 days after the inital halt. Thereafter, the brightness decreases smoothly at a rate of 1 mag/34.7 days, with fluctuations of 0.5 mag around the mean, similar to those observed in several classical novae. Hence, this is the only example of a recurrent nova showing the characteristics of a slow nova.

The strict similarity from event to event is remarkable.

The spectra obtained during the first 12 and 16 days after halt are characterized by P Cyg profiles of the Balmer lines. The absorptions are sharp, while the emissions have a width of about 300 km/s. Spectra taken 66 and 85 days after halt are dominated by strong Balmer emissions and other emissions of He I, He II, N II, O II, Fe II and [Fe II] with half-widths of about 2000 km/s (Figure 9-12). The other spectra obtained between 92 and 412 days after the halt are typical nebular spectra dominated by emissions of the Balmer lines, O III, N III and at least in the plate obtained 142 days after halt a faint feature at 5297 A, which may be identified with 5303 [Fe XIV], first observed by Joy in 1945 (Figure 9-13). At that time (outburst of 1944), Joy (1945) observed only one spectrum 130 days after maximum when the star had faded at 11 mag. He saw several emissions of H I, He I, He II, N II, [N II], N III, [OI], [OII], O III, [OIII], [NeIII], [Ne IV], [SII], [FeV], [FeVI], [Fe VII], [Fe X], and [Fe XIV]. The expansion velocity from the half-widths of the lines was about 1700 km/s, similar to that observed in 1966. Figure 9-14 shows the variation of the profile of H Beta.

III.A. QUIESCENT STATE

The spectrum at minimum was observed by Humason (1938), 14 years after the 1920 outburst. He saw a continuum with strong 4686 He II, moderate Balmer lines and weak 5007 [OIII]. Elvey and Babcock (1943) obtained one underexposed spectrum when the star was at 15th mag. They observed only a faint continuum and no detectable emission lines. Catchpole (1969), on the contrary, observed no continuum, a strong 5007 [OIII], a very weak H Beta and a doubtful 4686 He II. It seems probable that this spectrum, taken one year and half after outburst is not a true minimum but represents an advanced nebular stage.

The colors at minimum are B-V = 0.12, U-B = -0.96 and become redder during the rise to visual maximum: (B-V)max = +0.31 and (U-B)max = -0.08 (Eggen et al., 1967), a behavior characteristic of an expanding photosphere, common to classical novae.

Ultraviolet observations give the color excess by the 2200 depression in the continuum: E(B-V) = 0.35 +/- 0.05 (Bruch et al., 1981).

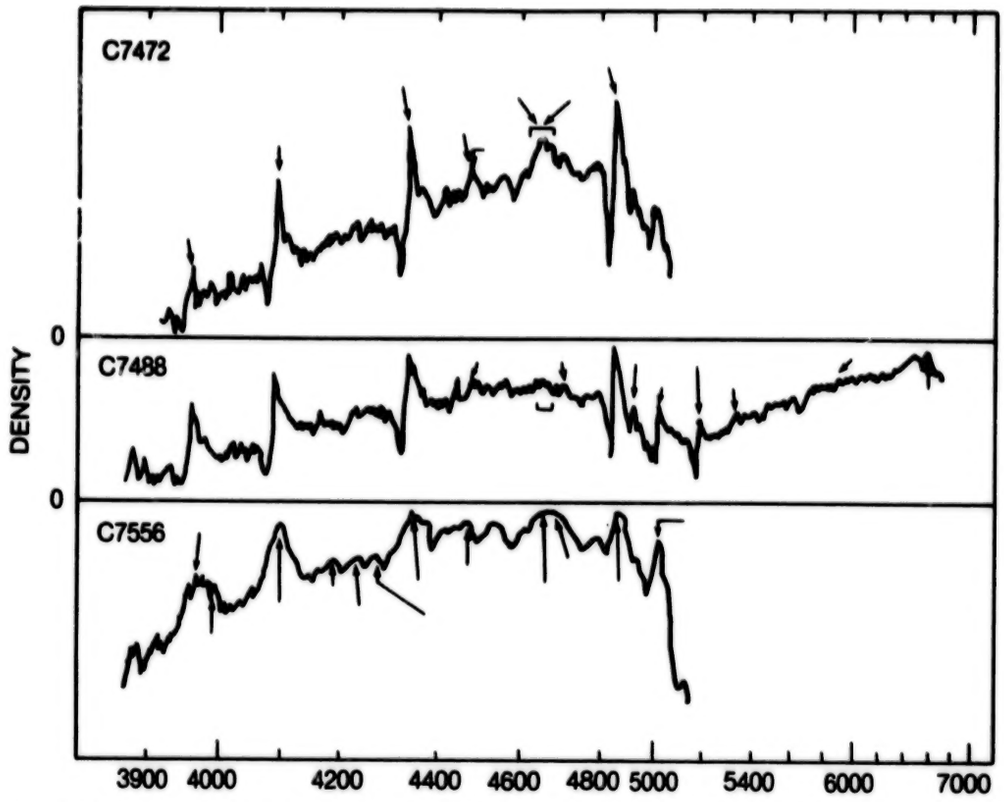


Figure 9-12. The evolution of the spectrum of T Pyx from 12.6 days after outburst (top) to 85.3 days after outburst (bottom). (from Catchpole, 1969).

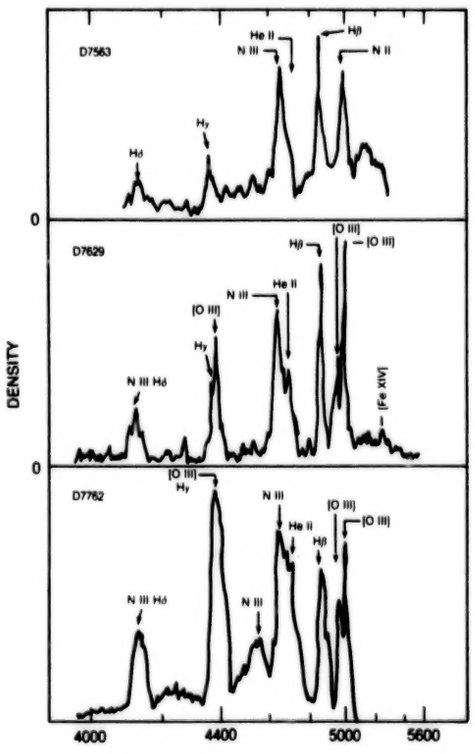


Figure 9-13. The evolution of the spectrum of T Pyx from 92.3 days (top) to 191.2 days after outburst (bottom). (from Catchpole, 1969).

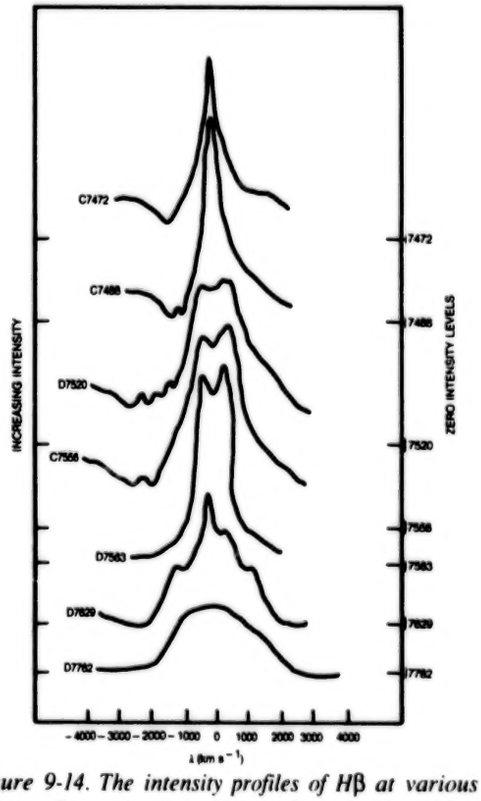


Figure 9-14. The intensity profiles of Hβ at various epochs. Top to bottom: 12.6, 16.5, 66.5, 85.3, 92.3, 142.3, 191.2 days from outburst. (from Catchpole, 1969).

Hence, $(B-V)_0$ = -0.23, $(U-B)_0$ = -1.31. Hence, T Pyx at minimum is extremely blue. Also, the dereddened colors at maximum, $(B-V)o^{max}$ = -0.05 and $(U-B)o^{max}$ = -1.06, are bluer than those of typical novae at maximum.

The low-resolution, far-ultraviolet spectrum shows a hot Rayleigh-Jeans tail. Emission lines of C II 1335, C IV 1550, He II 1640, NIII] 1750 are detectable. The complete absence of 2800 Mg II is remarkable. This fact, together with the extremely blue colors, are indications that no red star is present in the system. (Figure 9-15; see also Figure 6-44).

interstellar extinction Av = 3xE(B-V), gives Mv at maximum of -4.55. Using the Arp relation between the time of decline through the three magnitudes and the absolute magnitude at maximum, valid for classical novae, an absolute magnitude -6.5 is obtained. Hence, we have two possibilities: either the Arp relation can be applied to recurrent novae, and the interstellar calcium is weak in the direction of T Pyx (and in this case the absolute magnitude at minimum is about 2 mag, i.e., three magnitudes brighter than for classical novae at minimum) or it is not applicable to recurrent novae (and in this case the absolute magnitude at

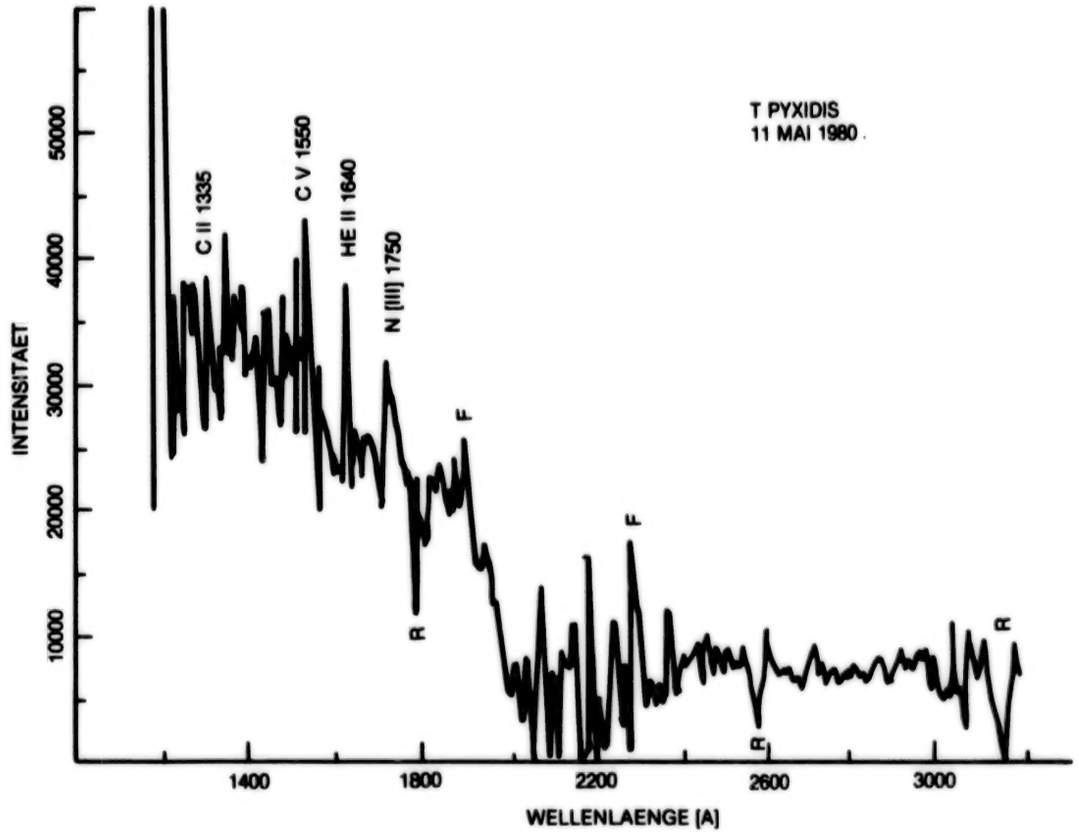


Figure 9-15. The IUE ultraviolet spectrum of T Pyx in quiescence (May 11, 1980). (from Bruch et al., 1981).

III.B. DISTANCE

The absolute magnitude of T Pyx is estimated by the intensity of the interstellar lines of Ca II. A distance of 1050 pcs is obtained, which, coupled with the apparent magnitude at maximum of 6.5 and taking into account the minimum, approximately 4.3, is comparable to that of classical novae).

III.C. THE ENVELOPE SURROUNDING T PYXIDIS

T Pyx is surrounded by a strong remnant nebulosity. Observations of this shell have

been made in 1979. 0, in 1980.2, and in 1982.9 (Seitter, 1987; Williams, 1982). Isophotes of this shell in 1979.0 and 1982.9 show remarkable differences. The relative intensities across a scan line through the center of the star in the image of 1982.9 is given by Seitter (Figure 9-16). The intensity distribution suggests that we are observing the remanants of several previous explosions. A spectral scan of the northern part of the shell is given by Williams (1982). The intensities of [OIII] 5007 and 4363, using the nebular theory (Osterbrock, 1974) gives an electron temperature of 29000 K. The ratio H/He can be derived by the ratios 5876 He I/H Alpha and 4686 He II/ H Beta, which give the He^{+} and He^{++} abundances relative to hydrogen in the hypothesis that all of the lines are formed by recombination. The result is $(He^{+} + He^{++})/H = 0.04 + 0.02 = 0.06$, i.e., a helium abundance, which, within the uncertainties of the assumptions, indicates a slight deficiency of helium (in contrast to the determinations for other recurrent novae, which show an excess of helium). Although an exact determination of the abundances of CNO is not possible, there is no evidence of an enhancement of these elements, an enhancement that is a general property of classical novae, but which has not been found in the recurrent nova U Sco.

Seitter (1987) comparing the images of the envelope obtained in 1979.0 and in 1982.9, observes that the two images can be superposed after a rotation of about 20 degrees (Figure 9-17 by Seitter). She observes that a real rotation would imply velocities of 6000 km/s at large distance from the star, which must have transferred the angular momentum to the shell; hence, the central velocities are too large. She suggests that the rotation is apparent and the changes in intensity are not associated with real nebular motions,

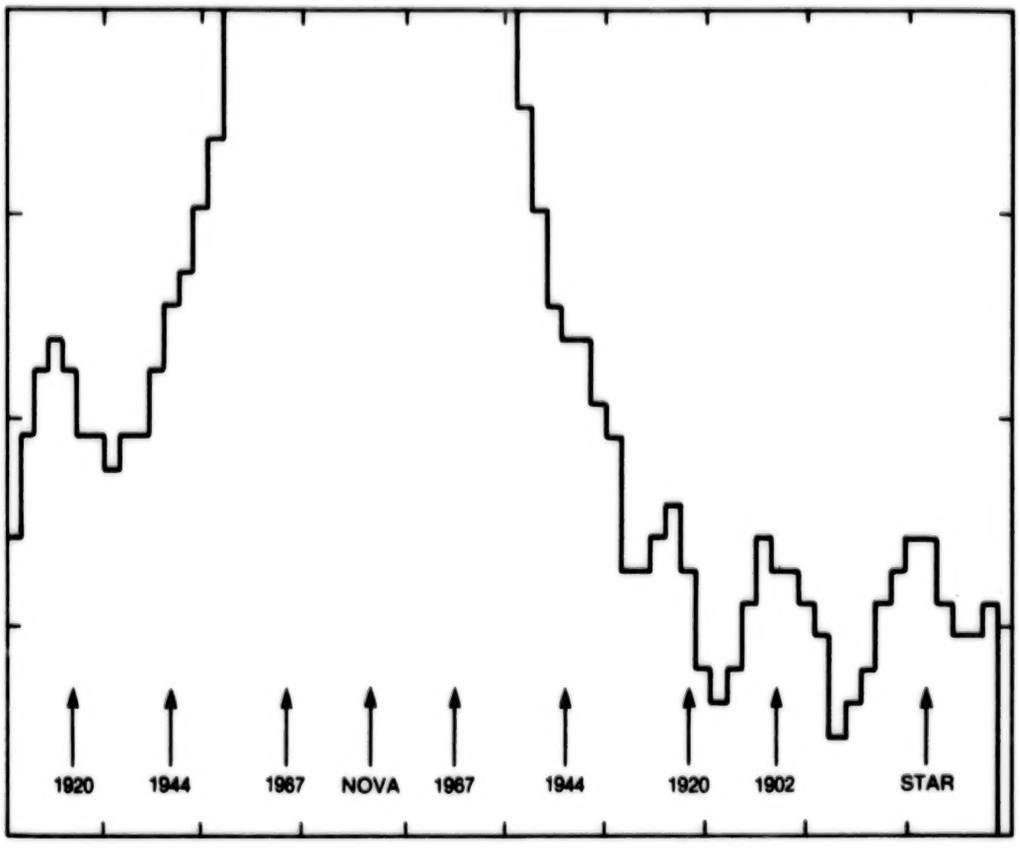


Figure 9-16. Scan line showing shell features of various outburst of T Pyx. (from Seitter, 1987).

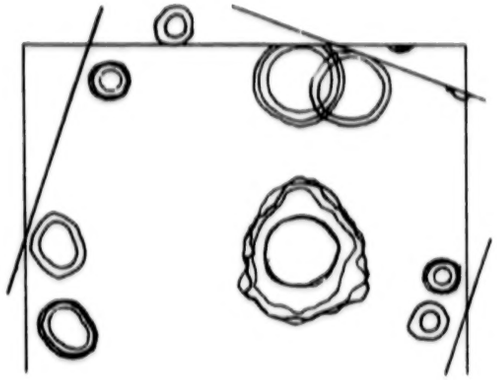


Figure 9-17. Superimposed images of T Pyx from 1979.0 and 1982.9. The earlier image was rotated relative to the later one until the inner isophotes of T Pyx matched best.
(from Seitter, 1987).

but are due to changing illumination from the central star. These changes can be explained by assuming an illuminating source situated at one of the poles, changing orientation relative to the nebula because of precession. Since the directional changes amount to 20 degrees in 4 years, the precession period is of about 72 years, which suggests the presence of an unseen companion orbiting with a period of about 100 days, according to the relation between orbital and precession periods (Kopal 1985, private communication; see Seitter, 1987).

IV. RS OPHIUCHI

Outbursts were recorded in 1898, 1933, 1958, 1967, and 1985. RS Oph in quiescence is an 11th magnitude star. It is very similar to T CrB. It shows very high ejection velocities at maximum; it is a very fast nova (but not so fast as T CrB); it develops high-excitation forbidden emission lines during late decline. The main difference is that the outburst light curve of RS Oph does not present a secondary maximum, as is the case for T CrB (*).

(*) A full conference has been devoted to RS Oph on Dec. 1985. The proceedings have been published by the VNU Science Press: "RS Ophiuchi (1985) and the recurrent nova phenomenon," ed. M.F. Bode, 1987.

IV.A. THE OUTBURST EPISODES

The outburst of 1958 was the most extensively observed in the past, while that of 1985 was observed almost simultaneously in the X-rays, ultraviolet, optical, infrared, and radio waves at many epochs.

IV A.1. THE OUTBURST OF 1898

Emission lines of H, He I, He II, and N III were observed by Pickering (1905) in two spectra obtained in 1898, July 14 and 15. The star was of 7.7 mag on June 30 and declined steeply in July and August. Extrapolating the light curve, by assuming that it was similar to those observed in the successive outbursts, the maximum must have occurred around June 19, with mag 4 or 5.

IV.A.2 THE OUTBURST OF 1933

On August 12, 1933, RS Oph was observed by an amateur astronomer, E. Loreta (see Rosino, 1987), to have reached the visual magnitude of 4.3. The spectral evolution was described by Adams and Joy (1933) and by Joy and Swings (1945).

Emission lines of H, He, Fe II, Ca II, and Na I were observed from August 16 to September 11, with a faint P Cyg absorption component. The strongest emissions were about 25 A wide, corresponding to about 1500 km/s. Comparatively sharp nebular lines appeared in the following order: 4362 [O III] on August 18, 5006 [O III], 4640 N III, and 4686 He II on August 29, 3868 [Ne III], 3967 [NeIII], and 4959 [O III] on August 30, [Fe II] on September 11, and 4068 [S II] on October 1. The coronal lines were definitely identified on October 2. At the end of October, 5303 [Fe XIV] was comparable in intensity to H Beta, and 6374 [Fe X] was twice as strong as 5875 He I. In March 1934, the coronal lines had disappeared.

IV.A.3 THE OUTBURST OF 1958

The maximum occurred on July 14.5. The development of the outburst of 1958 has been observed since the first night, and it was very similar to the previous one of 1933. During the first six days, the decrement was of 0.35 mag/day (Tolbert et al., 1967). The very red color of the star during the first day and the comparison of the observed Balmer decrement with the theoretical one (although classical models can only be applied with difficulty to nova envelopes) suggest that the star is strongly reddened (see Walker, 1977; Dufay and Bloch, 1964). Recent ultraviolet observations made with IUE actually indicate E(B-V) = 0.73 from the 2200 feature. However, the galactic position of RS Oph makes it difficult to justify this strong reddening (Svolopulos, 1966). It is possible that it has circumstellar origin. However, this reddening is similar to that of the Cepheid Y Oph, which lies close to the same line of sight, and this fact suggests that the reddening is mainly interstellar (see Evans, 1987).

One year after outburst, the continuum was cut by several absorption lines typical of a late-type star, and the color temperature (without correction for reddening) was of the order of 3900 K (Dufay and Bloch, 1964). Since the absolute photographic magnitude of the nova at maximum was about -8.7 (from the Arp relation between rate of decline and magnitude at maximum, assuming it applicable to recurrent novae) and it brightened by about 7 magnitudes, the absolute magnitude at minimum is about -1.7, thus suggesting that the late-type star is a giant, as in the case of T CrB. However, as we shall see in the following (see Section IV.C.4), the distances inferred from the interstellar extinction and from the interstellar line absorptions do not agree with the value derived from the Arp relation and indicate a value of M_v max less bright than -5. It follows that the absolute visual magnitude at minimum is included between -1.7 and +2.

A detailed description of the spectrum and its variation from the outburst to about one year later is given by Wallerstein (1958) and by Dufay et al. (1964). Just before maximum, the spectrum appeared very flat and almost featureless, with the exception of the Balmer line emissions, which, however, were very broad and flat. The profiles of the Balmer emissions, in contrast to those of classical novae, had a much simpler structure as shown by Figure 9-18.

The night of July 14, 1958, the star was of 5th mag, while the day before, Peltier reported that the magnitude was 11.1 (see Sky and Telescope 17,555,1958). On the first night, one observed very broad hydrogen emissions (about 1000 km/s wide) and superposed on them very sharp emissions and equally sharp violet-shifted absorptions. Broad, hazy absorption features are also present, violet-shifted by -3000 to -3600 km/s (and by about -1000 km/s on the following days).

The nonmetastable lines 4471 He I and 4481 Mg II were present in absorption on the first day only; the sharp H Alpha emission and absorption disappeared on the 8th day. The sharp absorption due to He I 3888 remained present until the 14th day after the outburst. All the sharp absorption lines showed no change in velocity during the nights following the outburst. Hence, they cannot be formed in the violently expanding nova shell, but in a slowly expanding envelope (the radial velocity of these lines is about -60 km/s) surrounding the whole system, which was probably present before the explosion. The broad emissions and absorptions, on the contrary, are formed in the nova envelope. The size of the nova envelope can be evaluated from the expansional velocity at the time of the outburst, about -3000 km/s and the time of disappearance of the sharp absorption lines, when the nova shell reaches the region of the cirsumstellar shell, where the sharp lines are formed. It is found that the region of absorption of Mg II and He I has a size of about 1.7 A.U., that of the H I absorptions, of about 7 A.U., and that of the metastable line 3888He I, of about 22 A.U.

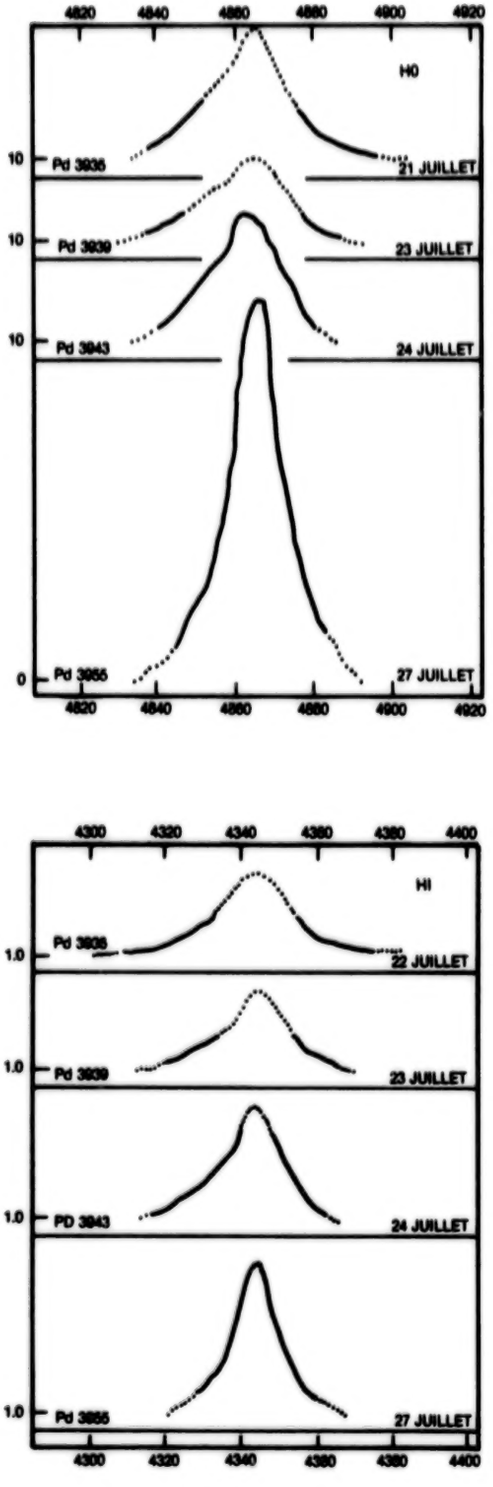
Emissions of Fe II, [Fe II], [Fe III] appeared on the second, fourth, and seventh night, re-

spectively, and have all the same velocities, suggesting that they are all formed in the same place in the envelope.

Numerous coronal lines appeared in August and September: [Fe X], [Fe XIV], [A X], [A XI], [Ni XII], [NiXV]. From February to June 1959, the coronal lines disappeared completely, while the forbidden lines of O I, O III, and N II were rather strong but less than the permitted lines.

The very similar spectral evolution in 1933 and 1958 suggests that the outbursts give rise to a well-regulated mechanism able to reproduce a sequence of several complex phenomena in all their details and in the same chronologicial sequence.

Figures 9-19 through 9-25 show the evolution of the spectrum of RS Oph from the night of the outburst (July 14, 1958) to Oct. 19 of that year.



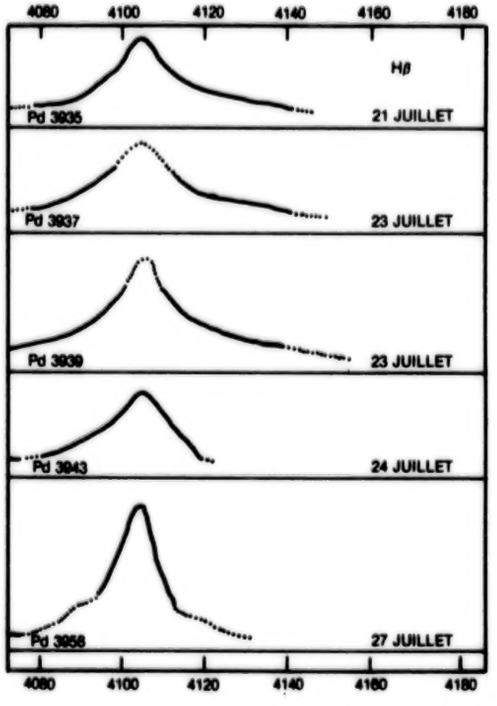


Figure 9-18. The profiles of H Beta (a), H Gamma (b), and H Delta (c) of RS Oph for the period July 21-27, 1958 during the second week following the outburst.
(from Folkart et al., 1964).

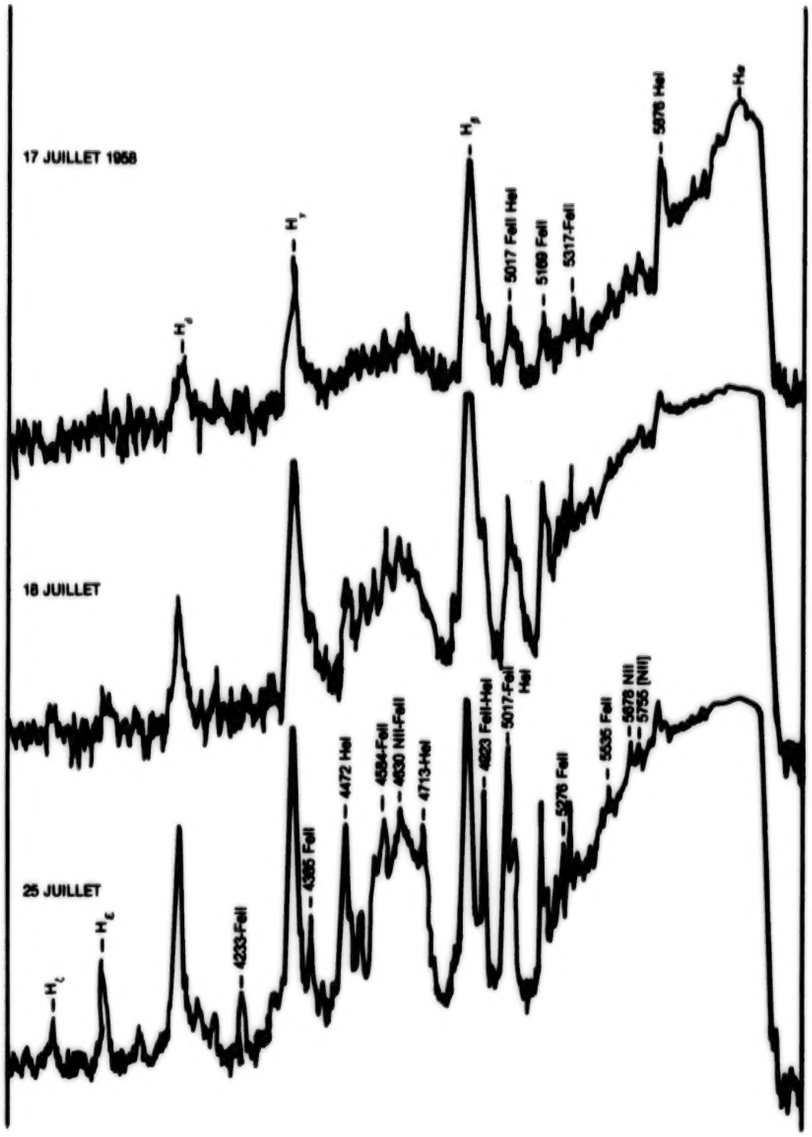


Figure 9-19. Evolution of the spectrum of RS Oph. Region H Alpha-H epsilon. (from Dufay et al., 1964).

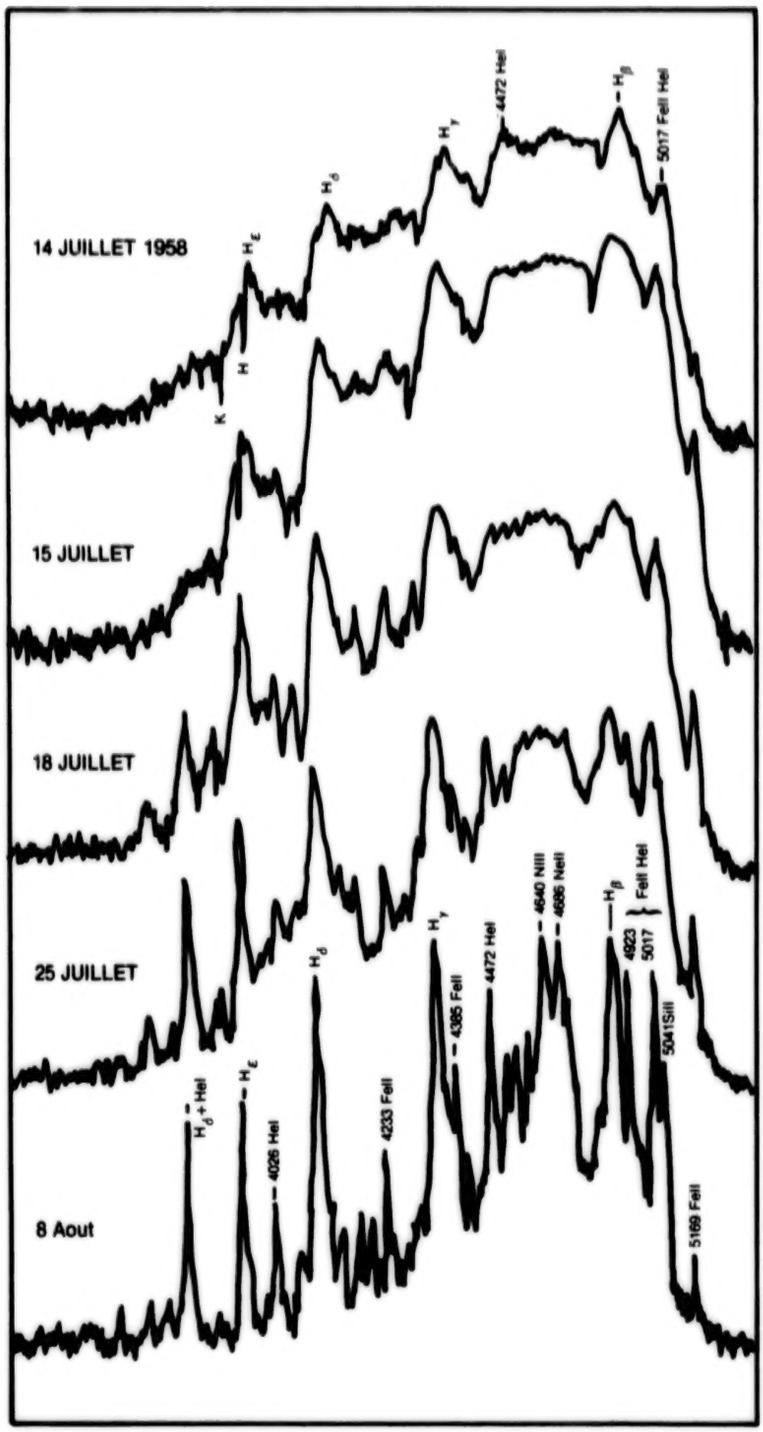


Figure 9-20. Evolution of the spectrum of RS Oph. Blue region. (from Dufay et al., 1964).

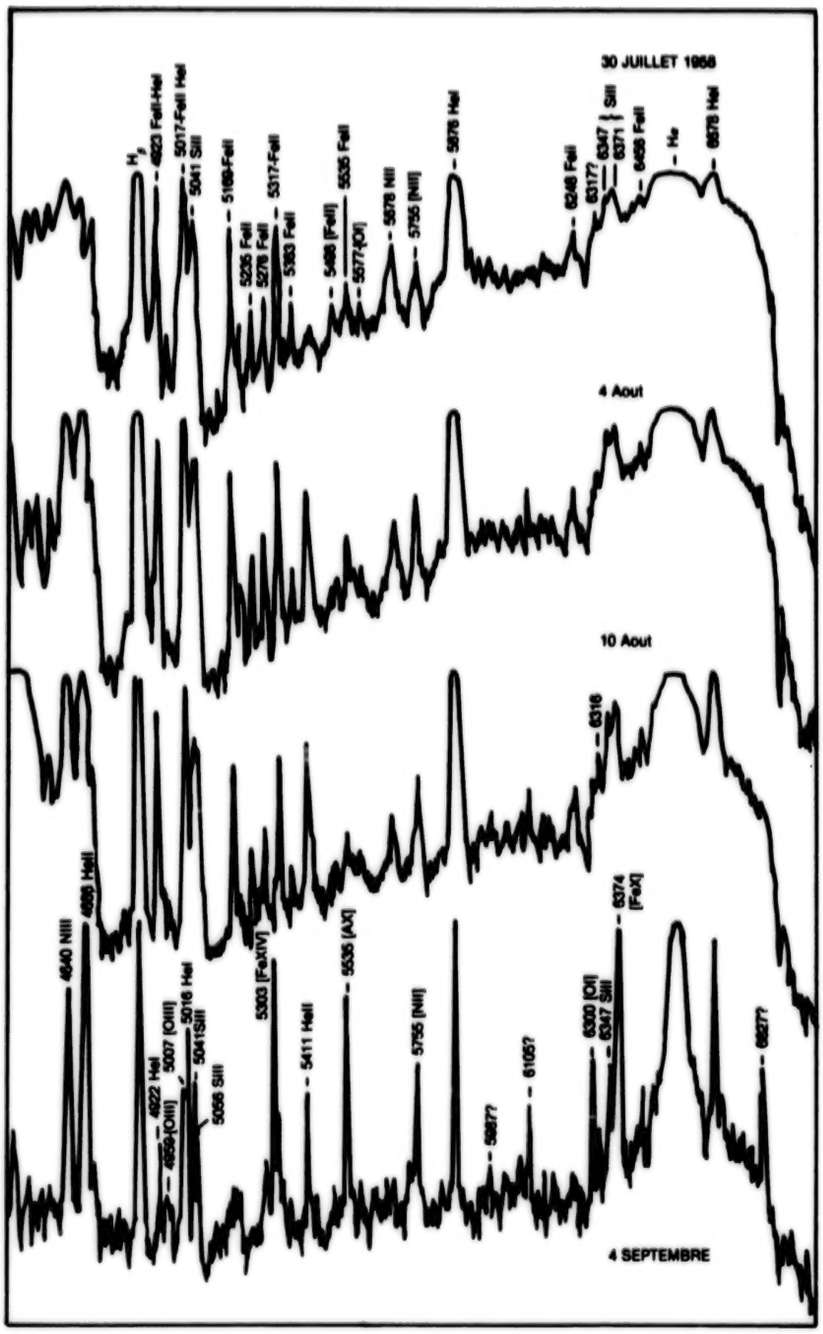


Figure 9-21. Evolution of the spectrum of RS Oph from July 30 to September 4. Region 4600-6800 A. (from Dufay et al., 1964).

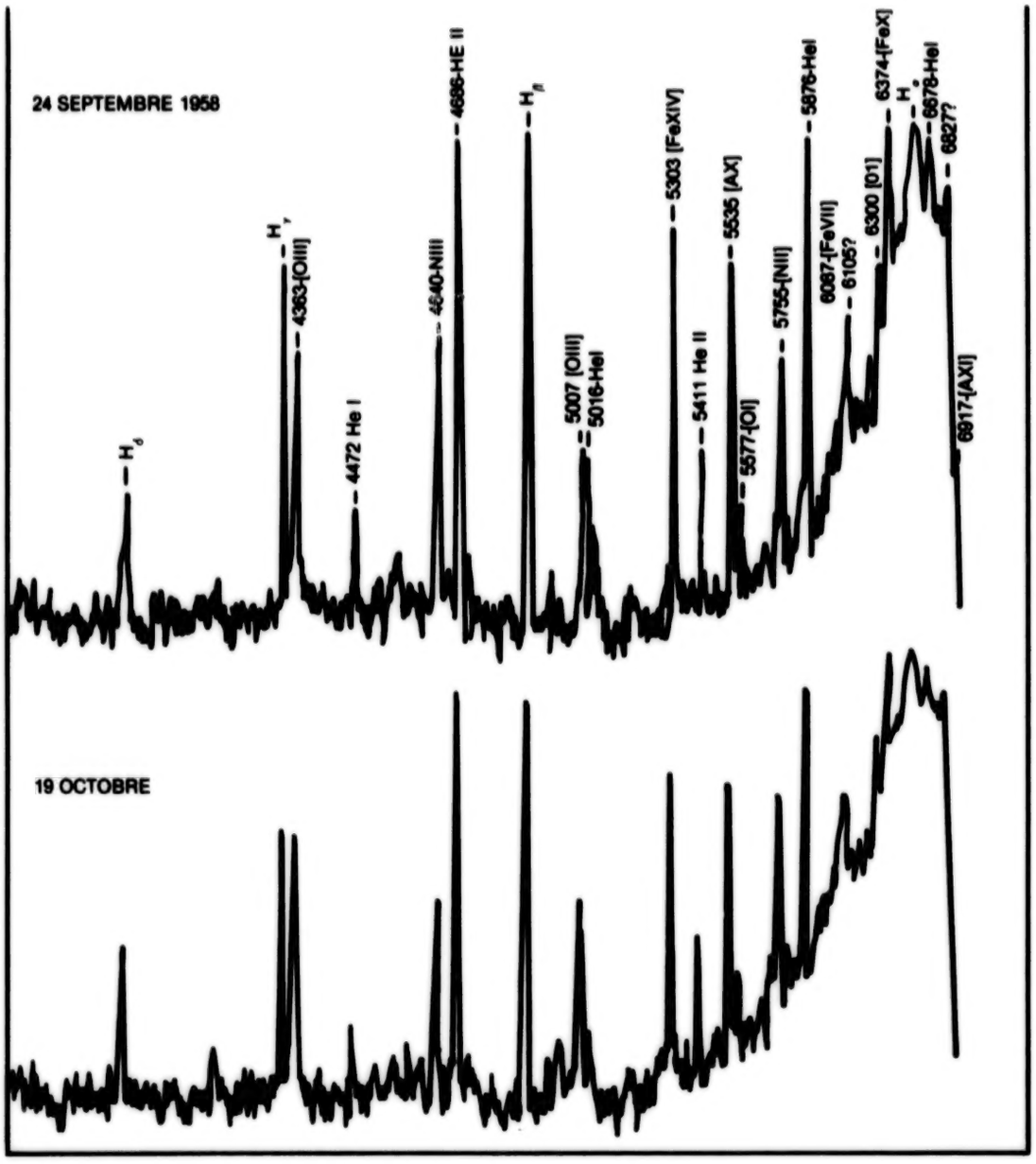


Figure 9-22. Evolution of the red region of the spectrum of RS Oph in September and October 1958. (from Dufay et al., 1964).

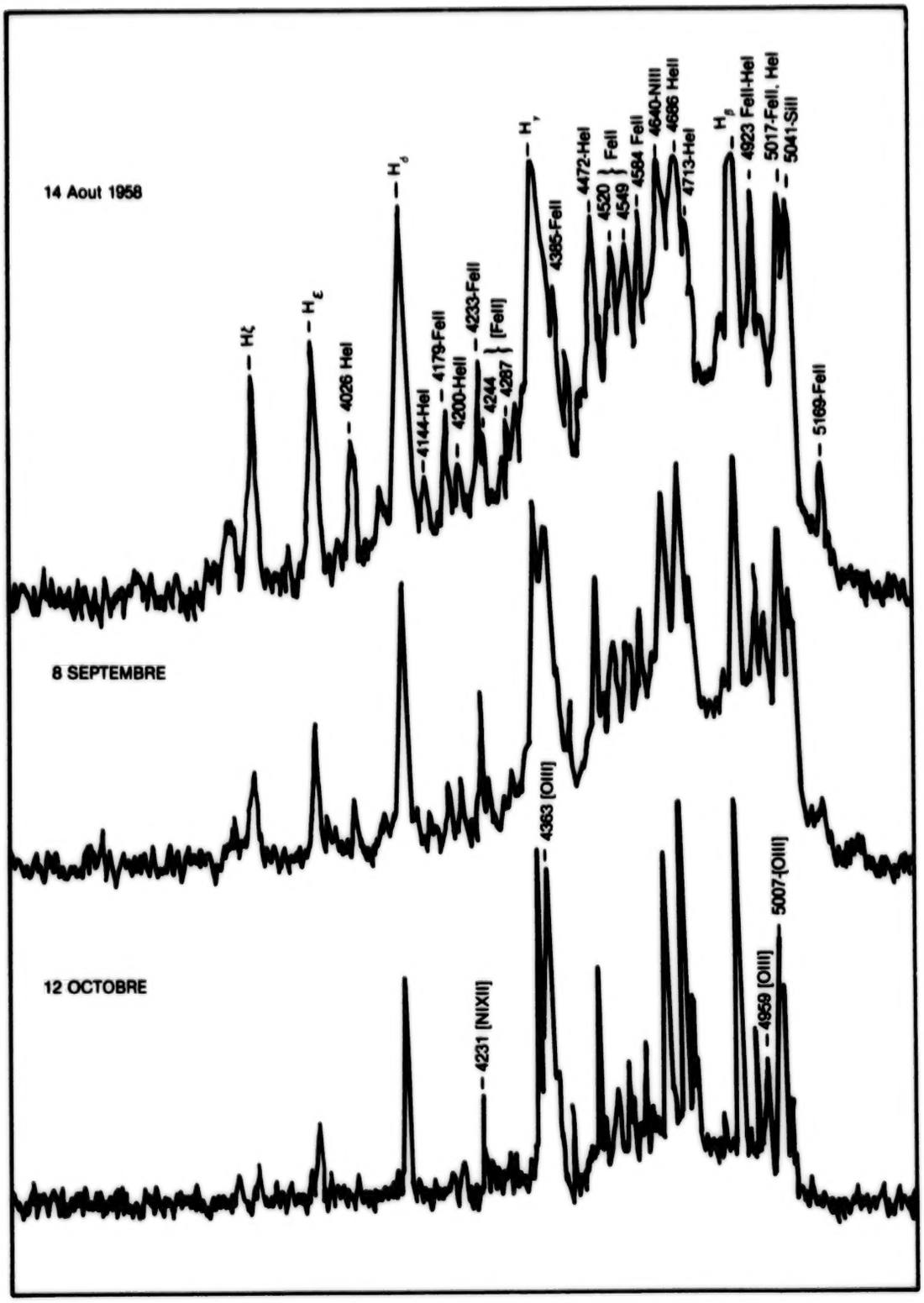


Figure 9-23. Evolution of the blue spectrum of RS Oph from Aug. 14 to Oct. 12, 1958. (from Dufay et al., 1964).

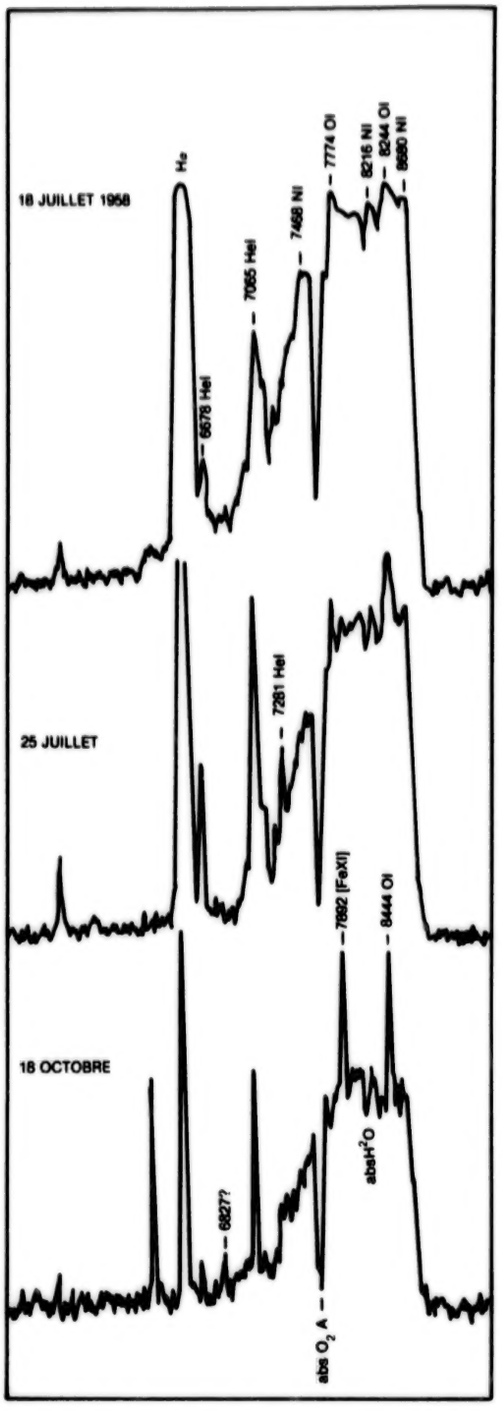


Figure 9-24. The infrared spectrum of RS Oph from July 18 to October 18, 1958.
(from Dufay et al., 1964).

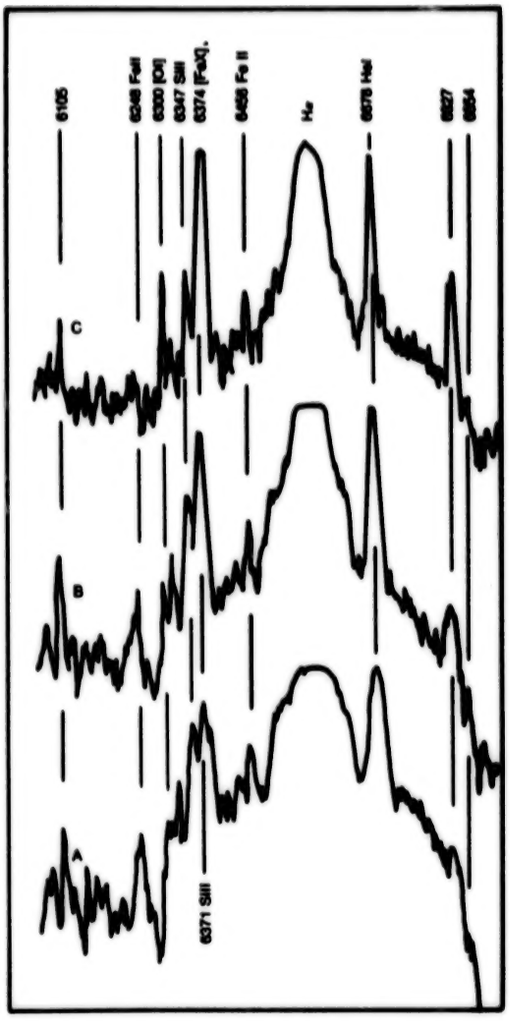


Figure 9-25. Appearance of the forbidden lines 6374 Fe X, 6827 Ca X (?), 6855 Ca X (?). A: August 10, 1958; B: August 12, 1958; C: September 4, 1958.
(from Dufay et al., 1964).

IV.A.4. THE OUTBURST OF 1967

The outburst started on October 26,1967, was observed spectroscopically in Asiago from October 27 to the beginning of November when the star was very low on the horizon (Rosino, 1987). Broad emission bands of hydrogen and helium with two absorption systems violet-shifted by -3600 and -2700 km/s were observed on October 27. Near the center of each emission band, a sharp emission with a narrow P Cyg absorption at -40 km/s was present. Four to five days after maximum, the broad absorptions become weaker and then disappeared, while the He emissions become dominant. At the beginning of November, forbidden lines of O III, Ne III, and Fe X were present. In February 1986, when it was possible to observe the nova again, the spectrum showed strong and wide Balmer emissions, He I and He II emissions, and coronal lines of [A X], [Fe X], and [Fe XIV].

IV.B. OBSERVATIONS IN QUIESCENCE

A few spectroscopic observations were made by Wallerstein (1963) in 1960-62 in correspondence of a minor outburst to mag 10. Also, in this almost quiescent period, the spectra present emission and absorption lines characteristic of a shell; that is : Balmer lines observable in absorption up to H 30, absence of the non-metastable, high-excitation line of Mg II at 4481 A, Fe II lines in emission, strong absorption lines of Ti II, and a few emissions of [Fe II], but no nebular lines.

From these observations, Wallerstein (1963) underlines the following points:

a) No late-type spectrum is visible in the blue region; even 4226 Ca I is not present. Hence, at this time RS Oph is similar to T CrB.

b) The spectrum in 1960-62 was practically the same as that observed by Sanford (1947b). This means that the basic physical processes occurring at minimum were not changed by the 1958 outburst. The two magnitude changes that occurred in 1960-62 were not accompanied by significant spectral changes.

c) The absorption lines H and K of Ca II are more negative by 10 km/s relative to the other shell lines, suggesting that an expanding circumstellar envelope is still present.

d) Emission lines of hydrogen and Fe II have shown an abrupt violet shift between 1960 and 1961 (H gamma and H delta from about +25 to -230, Fe II from about -30 to -90) showing a sort of activity taking place. No similar effect was shown by He I and [Fe II] lines.

IV.C. THE OUTBURST OF 1985

The last outburst of 1985 was observed from space with EXOSAT, IUE, and IRAS; also, radio and infrared observations were made from the ground beside, of course, optical observations.

IV.C.1. OPTICAL OBSERVATIONS

On January 26.47 U.T., the visual magnitude was 6.8; on January 28. 45, it was 5.2 (Morrison, 1985). On March 6.22 it was 9.4 (Medway, 1985). An extended series of spectroscopic observations was made in Asiago (Rosino and Iijima, 1987). Their main conclusions of this study are the following: The 1985 outburst has the same characteristics of the previous ones; i.e., the rapid decline, the very high velocity of the ejecta (-1650 to -3500 km/s), the presence of extremely strong coronal lines, the persistence of high excitation lines for almost nine months.

The first spectra were obtained on February 10, two weeks after maximum and continued to November 1985 with dispersions of 60 to 125 A/mm in the spectral range 3900-6600 A and 6500 to 9000 A.

From days 14 to 29, the spectra were characterized by a strong continuum and broad emissions of H and He, accompanied by two systems of faint P Cyg absorptions at -3500 and -1650 km/s, and narrow permitted and forbidden emisssions of Fe II and O I. At day 17 a very weak coronal line, 6374 Fe X, appeared.

From days 52 to 72, when the magnitude had declined to 9.5-9.7, very strong coronal lines of Fe XIV, Fe X, Fe XI, and A X were present, beside the emissions of H, He I, and He II.

At the end of April, when the magnitude was approaching its normal minimum value, the degree of excitation began to decrease. In the second half of May, all the coronal lines, with the exception of Fe X and Fe XI, have disappeared.

In June, the nova had reached the minimum of 12 mag, but the spectra still showed evidence of the past outburst, i.e., emissions of H Alpha, H Beta, 5876 and 7065 He I, 4686 He II, and the nebular lines of O III and N II. The only coronal line still observable was 6374 Fe X.

In October-November, only the Balmer

lines and the [OIII] doublet at 5007 and 4959 are present; the 4686 He II was not more detectable. Wallerstein and Garnavich (1986) have also made spectroscopic observations of RS Oph from days 65 to 73 after outburst and have measured the radial velocity of several low and moderate excitation lines, like H I, He I, He II, [NII], [OIII], Si II, Ti II, Fe II. Radial velocities of about -20 to -30 km/s were found while He I and He II show two components at about -20, -30, and at -170, -200 km/s. Several forbidden lines of Fe IV, Fe VI, and Fe VII, and the coronal lines of Fe XI, Fe XIV, Ni XIII, Ni XV, and Ni XVI have radial velocities included between -10 and -70 km/s, while A X, A XI, and Fe X have two components at about -20, -40, and another at about -200 km/s. These authors give a full identification list, the measured fluxes and the fluxes corrected for the interstellar reddening of all the emission lines between 3312 A and 6918 A.

IV.C.2. INFRARED OBSERVATIONS

The near infrared colors of RS Oph between outbursts place it close to the region of Mira variables in the two-color diagram (J-H)-(H-K), while it lies close to the normal giant-supergiant sequence in the two-color diagram (J-K)-(K-L) (Figure 9-26a,b) (Evans, 1987). According to Feast and Glass (1974), this discrepancy could be resolved assuming a reddening E(B-V) = 1.8, which is in contrast with that deduced by pre and postoutburst ultraviolet observations that give E(B-V) = 0.73. Hence, the colors of RS Oph are not completely normal, probably because the M0 III secondary color may be modified by the presence of an accretion disk or by circumstellar material, result of previous outburst. RS Oph was detected at 12μm with the infrared satellite IRAS in the course of the IRAS survey in 1983 (IRAS Point Source Catalogue, 1985; Evans, 1987). Fluxes measured by IRAS photometry at 12 and 25 μm and JHKL (*) photometry obtained by Whittet and Evans in 1981 (see Evans, 1987) are plotted in Figure 9-27 together with the planckian curve for T = 3000 K and with the near infrared spectrum of an M0 III star (Strecker et al., 1979). The excess at the IRAS wavelengths is evident. If this excess is attributed to the presence of dust in the RS Oph system, a dust temperature of 350 K is derived. A similar excess was observed by

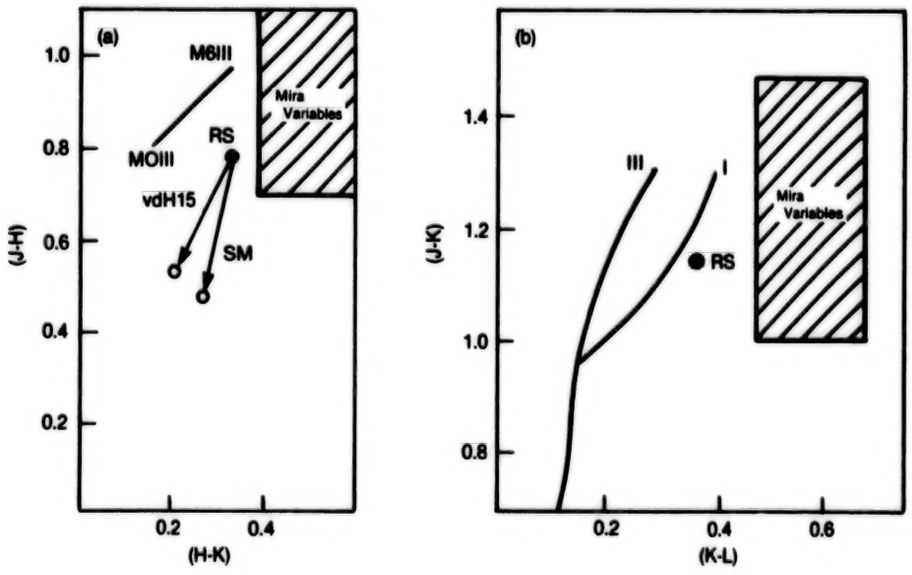


Figure 9-26. Infrared two-color diagrams for RS Oph (based on Feast and Glass, 1974). Arrows denote dereddening of E(B-V)=0.73.
(from Evans, 1987).

J: λ_0 = 1.25 μm; H: λ_0 = 1.62 μm; K: λ_0 = 2.2 μm, L: λ_0 = 3.5 μm

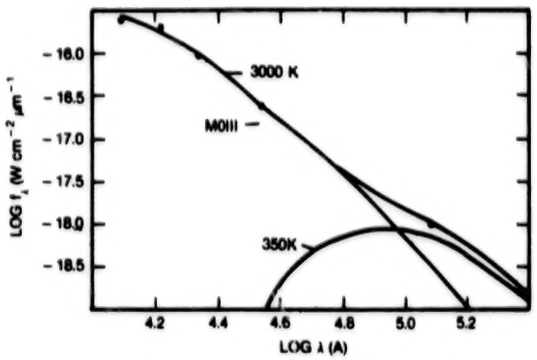


Figure 9-27. Pre-outburst photometry at JHKL and from IRAS survey for RS Oph; a good fitting is obtained with an M0 III + 350 K black body energy distribution.
(from Evans, 1987).

Geisel et al. (1970) for RS Oph in quiescence. This is another point of difference with T CrB, which, on the contrary, presents a negligible infrared excess.

Infrared photometry during outburst by D. Lancy (1985) indicates a strong flux in the J band, possibly due to the He I line at 10830 A, and dust excess at longer wavelengths. Evans (1987) reports the results of infrared observations made during the 1985 outburst. The position of RS Oph in the two-color diagram (J-H)-(H-K) after dereddening indicates that the He I line at 10830 A is dominant (Figure 9-28), at least during the first days. The variation of (J-H) with time (Figure 9-29) indicates that the He I line starts decreasing about 35 days from outburst. The two-color diagram of Figure 9-30 shows that the position of RS Oph is consistent with the presence of two components, one at 4000-5000 K and another at 1500 K. If we assume that the component at 1500 K is due to circumstellar dust, the shock associated with the outburst could be responsible for its heating.

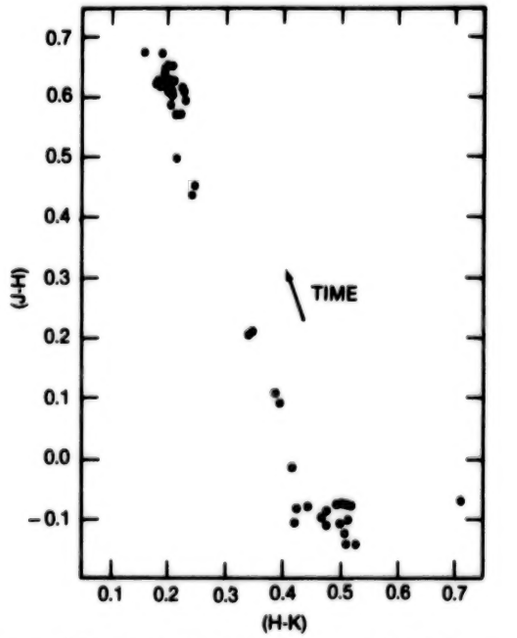


Figure 9-28. (J-K)-(H-K) diagram for RS Oph during the 1985 outburst.
(from Evans, 1987).

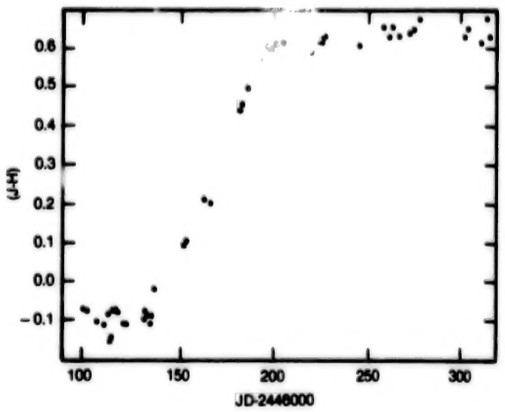


Figure 9-29. Variation of (J-K) (corrected for reddening) with time during the 1985 outburst.
(from Evans, 1987).

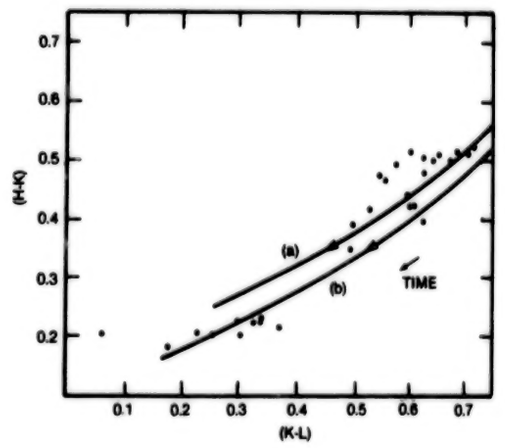


Figure 9-30. Positions of RS Oph in the (H-K)-(K-L) diagram during the 1985 outburst. The data are corrected for reddening. Curve (a) is a 4000 K + 1500 K black body combination, curve (b) a 5000 K + 1500 K combination.
(from Evans, 1987).

The light curve at 1.25 μm (J) is shown in Figure 9-31.

Infrared spectroscopy during outburst has

been made by Bailey et al. (1985) with resolution $\lambda/\Delta\lambda$ = 100. On the assumption that the continuum is mainly due to free-free emission, one spectrum obtained on February 21, 1985, simultaneously with ultraviolet observations with IUE (Snijders, 1987a) indicates that an electron temperature of 1.1 x 10^5 K fits ultraviolet and near infrared observations while an excess relative to free-free emission is evident at longer wavelengths, i.e, longer than 1.6 μm. (Figure 9-32). This excess can be explained with a blackbody at 600 K, only at wavelengths shorter than 3 μm; at 3.4 μm, it is lower than predicted by a factor of 4. Hence, blackbody emission by dust must be ruled out. The excess could be explained by the vibration-rotation transition of CO at 2.3 μm possibly excited by the shockwave from the expanding envelope in the circumnova H II region.

High-resolution spectra ($\lambda/\Delta\lambda$) = 1000 obtained on June 24, 1985, are compared with the low-resolution spectra taken in February and April (Figure 9-33). In the April spectrum, we observe the hydrogen emission lines and a very strong 10830 He I line.

The highest excitation lines observed in the high-resolution June spectrum are [Si VI] 1.961 μm and [Si VII] 2.461 μm. It is not surprising that no coronal lines are observable, because the maximum intensity of coronal lines in the optical range was reached in April and then declined significantly (Rosino and Iijima, 1987). However, the apparent absence of coronal lines in earlier infrared spectra is surprising. Unfortunately, no high-dispersion spectra were available.

A noticeable characteristic observed in the high-resolution spectrograms is the CO band in the spectrum of the M0 giant (see Figure 9-33).

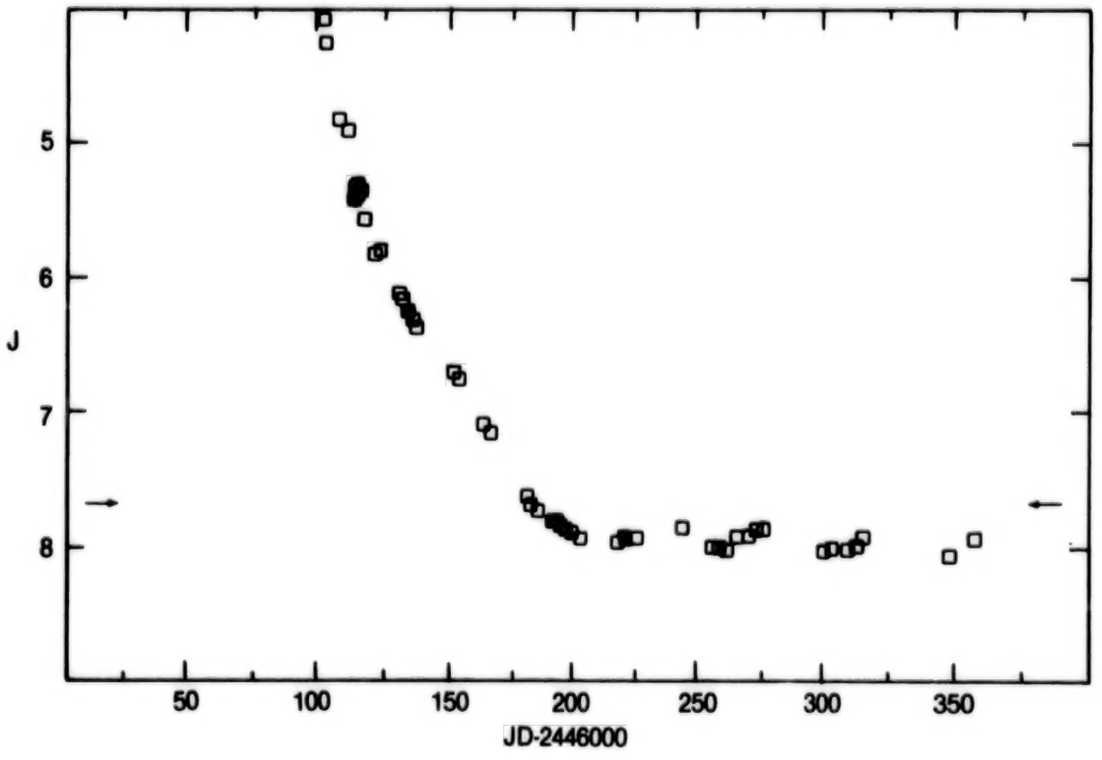


Figure 9-31. J(1.25 μm) light curve of RS Oph for 1985 outburst. The arrows show the pre-outburst J magnitude. (from Evans, 1987).

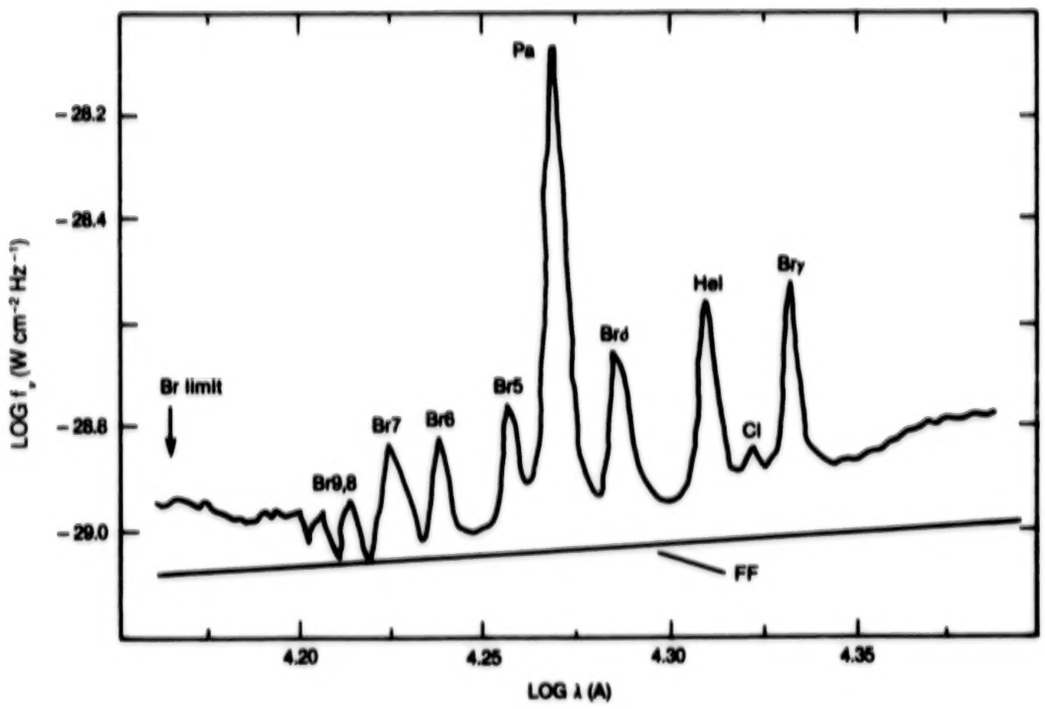


Figure 9-32. Infrared spectrum (1.5-2.4 μm) of RS Oph obtained on February 21, 1985. The line labelled FF is the nebular continuum.
(from Evans, 1987).

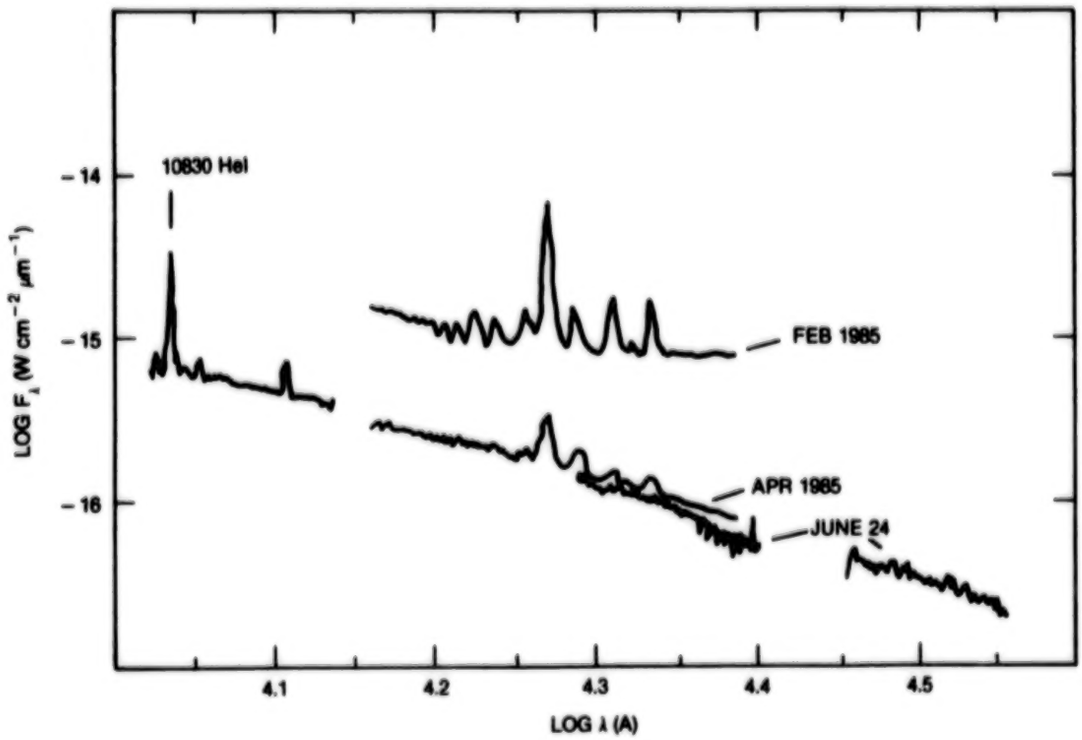


Figure 9-33. Low resolution (λ/Δλ=100) spectra of RS Oph obtained on February and April 1985 and the high resolution spectrum (λ/Δλ=1000) obtained on June 24, where the CO bands of the M giant are clearly visible.
(from Evans, 1987).

RS Oph has been detected also at radio waves (Padin et al., 1985), and details are described by Davis (1987). This is the first detection of radio emission from an outburst of a recurrent nova. Radio emissions from classical novae have been detected in several cases, but never earlier than 50 days from outburst. In this case, on the contrary, the emission was observed 18 days from outburst at a density flux of 23 mJy at 5 GHz. Two days later, on February 15, the density flux was 30 mJy. If the assumption is made that the radio-emitting layers are expanding at about 1000 km/s as indicated by the optical spectrum, and assuming a distance to the nova of 1.6 kpc (confirmed by an interstellar absorption measure of the HI 21 cm line), these measurements indicate a brightness temperature larger than 10^7 K. This is another important difference with classical novae. In fact, the radio envelopes of the latter have a brightness temperature of 10000 K, typical of an envelope of ionized hydrogen. The high value of the brightness temperatúre suggests a nonthermal origin for the radio emission.

Figure 9-34a shows the radio "light-curve" at 5 GHz. Initially there is a rapid increase in flux density at the rate of about 4 mJy per day until February 18. Then there is a slower linear increase, which, projected back to the time of the outburst t_0 , gives a $(t-t_0)$ dependence of 1.7 mJy per day, characteristic common to the observed classical novae. The maximum of about 70 mJy was reached 37 days from outburst and then the decay started and a value of 30 mJy was reached on day 77 from outburst.

Spoelstra et al. (1987) have observed RS Oph with the Westerbork Synthesis Radio telescope (WSRT) at 327 MHz and with the Cambridge 5 km radio telescope at 5 GHz. A remarkable event was observed by Spoelstra et al. at 5 GHz: a radio flare occurred 41 days after outburst, about 3 days after the maximum of radio flux. The intensity of the flare was 80 mJy, and it lasted more than 1 hour and less than 1 day (Figure 9-34b).

The spectrum on day 48 from outburst (March 15, 1985) is shown in Figure 9.35a. The data are from WSRT, Cambridge 5-km telescope, Jodrell Bank and VLA.

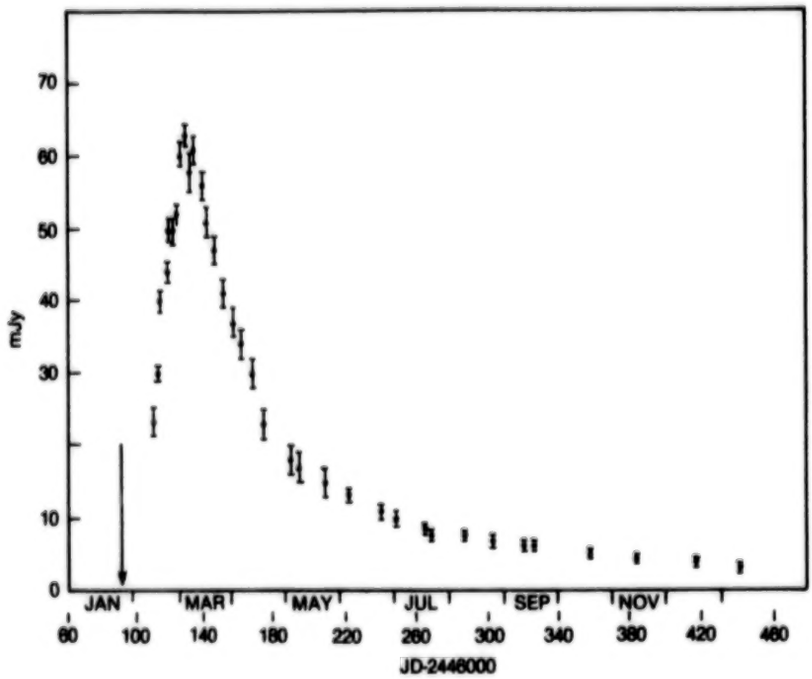


Figure 9-34. a) The 4.9 GHz "light curve" of RS Oph during the 1985 outburst (from Davis, 1987).

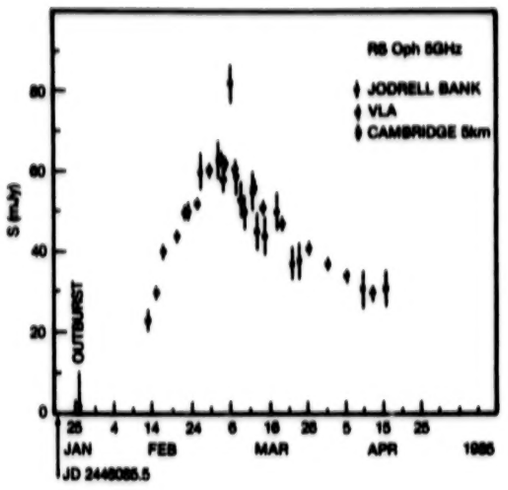
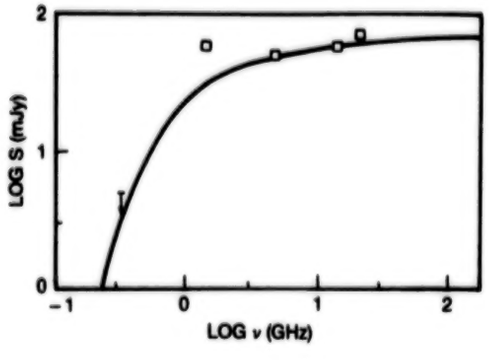


Figure 9-34. b) The 5 GHz "light curve" for RS Oph showing the "radio flare" occurred 41 days after outburst.
(from Spoelstra et al., 1987).

Davis reports the variation of the spectral behavior, which is very complex and is represented by a power law $s \approx \mu^{+\alpha}$. The variation with time of the spectral index α is shown in Figure 9.35b for the high-frequency range (15 to 22.5 GHz) and low-frequency range (1.5 to 5 GHz). The interpretation of these variations is not straightforward.

Porcas et al. (1987) observed RS Oph using the technique of very long baseline interferometry on March 8 and on April 13. The latter observation permitted them to obtain a map of the structure of RS Oph at 1.7 GHz, when the density flux was 30 mJy. Figure 9-36 reproduces the measured visibility data, and from these data the following conclusions are drawn: a) more than 80% of the total flux of the source is present in this radio image; b) the emission is not spherically symmetric but elongated in position angle 84° ; c) the extensions along the major axis reach about 100 milliarcseconds. For an assumed distance of 2.0 kpc, this corresponds to 200 A.U. and an average expansion velocity of 4000 km/s over the 77 days from the outburst.



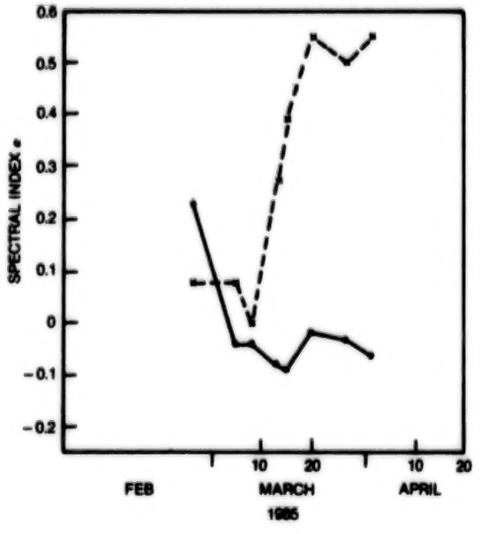


Figure 9-35. a) The radio spectrum of RS Oph on March 15, 1985. The curve is normalized to 68.5 mJy at 111 GHz. (from Spoelstra et al., 1987) b) Variation of the spectral index α for the initial phase of the outburst. dots: 1.5-5 GHz; crosses: 15-22.5 GHz (from Davis, 1987).

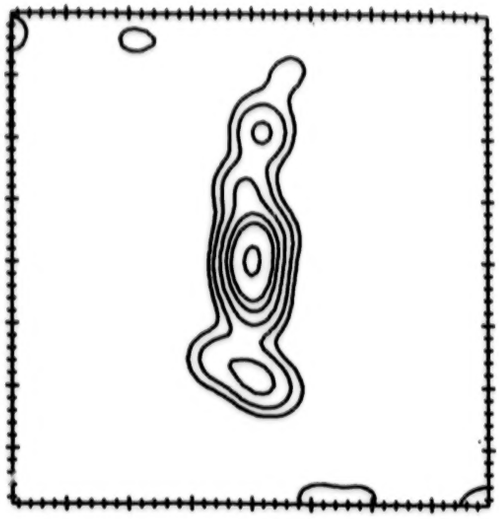


Figure 9-36. Map of the structure of RS Oph with resolution 35 milliarc sec. Contour interval: 5, 10, 20, 35, 50 and 90% of the peak brightness.
(from Porcas et al., 1987)

IV.C.4. ULTRAVIOLET OBSERVATIONS

Ultraviolet observations have been made with IUE both in quiescence (Rosino et al., 1982) and in outburst (Cassatella et al., 1985). The ultraviolet quiescent spectrum indicates a state of low excitation in agreement with the indications from the optical spectrum. However, rapid changes of brightness, accompanied by the appearance of He II emission lines, are observed between two major outbursts (see, for instance, Figure 9-37 from Cassatella et al.): the 2900 Å flux was a factor of 35 higher in October 1982 than in April 1981. The recent outburst of 1985 has been monitored with IUE during the first 3 months by Cassatella et al. (1985). Spectra before outburst (of 1981 and 1982) are compared with those obtained 12 days after outburst (see Figure 9.37): the energy distribution does not change appreciably, although the flux has increased by factors between 100 and

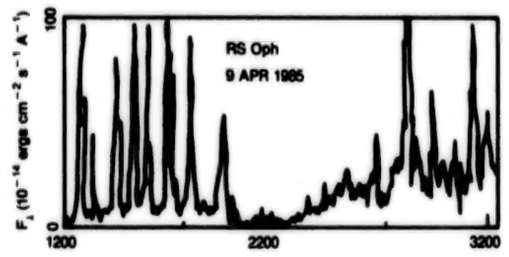


Figure 9-38. IUE low resolution spectrum of RS Oph on April 9, 1985.
(from Cassatella et al., 1985)

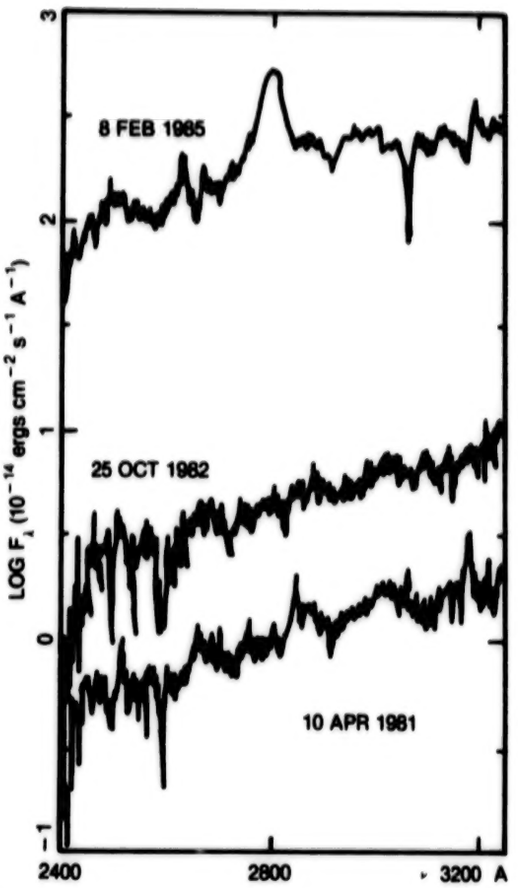


Figure 9-37. Comparison between pre-outburst and outburst ultraviolet spectra of RS Oph.
(from Cassatella et al., 1985).

300. The presence of a very strong emission of Mg II is remarkable. On April 9 (Figure 9-38), about 70 days after outburst, the spectrum is dominated by strong emissions, including several coronal lines. The most prominent are Fe XI 1467 and 2649, Fe XII 1350, 2406, and 2568. It is interesting to note that the emissions from highly ionized species peak at a later stage in the decline than those for lower excitation species (see Figure 6-58). The strenghtening of the high-ionization lines is accompanied by the decrease of the electron density, which is indicated by the decrease of the ratio 1893 Si III/1909 C III. This behavior is common to classical novae. High-resolution spectra, obtained with IUE, show the complex structure of the emission of C IV and 1486 N IV. It is evident that more than one component contributes to the observed profiles (Figure 9-39).

An estimate of the distance of RS Oph is made using the interstellar extinction and the

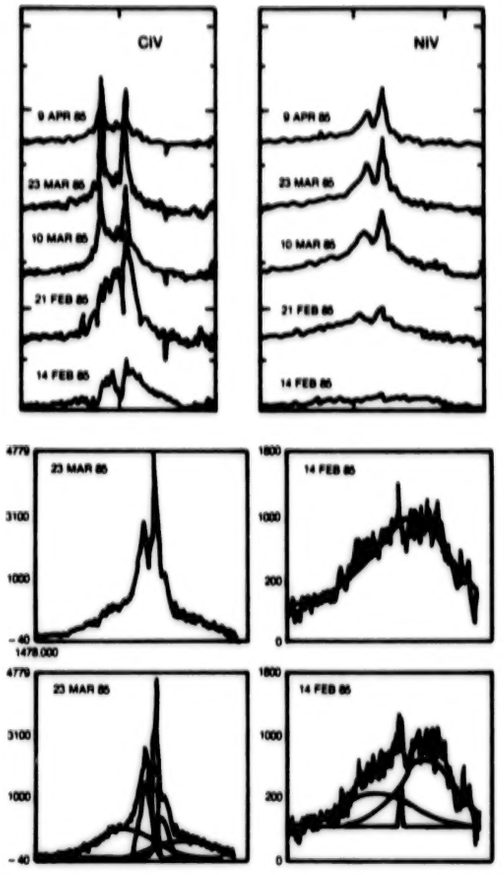


Figure 9-39. a) Variation of the CIV and NIV] line profiles, from IUE high resolution spectra. b) Attempt to represent the NIV] line at 1486 A with three or five gaussian components at two different dates. (from Cassatella et al., 1985).

interstellar line absorption (Snijders, 1987). The interstellar extinction derived by the 2175 feature in the quiescent and outburst phase gives E(B-V) = 0.73 +/- 0.10. The flux ratio of the He II lines at 1640 and 3203, combined with the theoretical recombination line ratios (Seaton, 1978a), gives E(B-V) = 0.73 +/-0.06, in very good agreement with the E(B-V) = 0.76 derived by Svolopoulos (1966). The interstellar absorption lines present in the ultraviolet spectrum are very numerous but all at velocities typical for our spiral arm and none at velocities typical for the Carina arm in the direction of the nova, at +19 km/s. This puts an upper limit of two kpcs to the distance and M_v (max) equal or less bright than -5.

Hjellming et al. (1986) derive 1.6 kpc from the strength of the 21-cm absorption observed in an object nearby RS Oph.

The total luminosity derived by ultraviolet, optical, and infrared data (the X-ray contribution, as observed with the european satellite EXOSAT, is 0.5 to 10% of the total flux emitted on day 51, and the radio contribution is always less than 1%) is shown in (Figure 9-40) versus the time from outburst. This bolometric light curve is very similar to those of classical novae (Stickland et al., 1981; Snijders et al., 1984). On this subject, it is important to note that the decline in the ultraviolet is much slower than in the optical (see Figure 9.40).

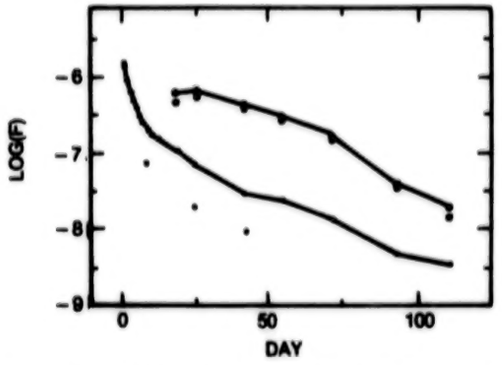


Figure 9-40. The luminosity as a function of time: small black dots infrared; curve in the middle optical; larger black dots ultraviolet, and upper curve total luminosity. (from Snijders, 1987).

An estimate of the abundances from the IUE spectra can be made using selected line ratios. Snijders (1987) derived several abundance ratios using the method employed by Williams et al. (1981). The ratio N III] 1750 / O III] 1663 is time independent from day 43 and gives O/N=1.10 +/-0.17. The C IV 1549/ N IV] 1486 can be used only on days 94 and 111 because at earlier epochs C IV has absorption components: It gives C/N = 0.16 +/-0.04. The ratio N V 1240/He II 1640 is subject to self-absorption of N V even at day 111; moreover, it is strongly dependent on the temperature. From these data it can be estimated that the ratio He/N is included between 3 and 40. There is no doubt that nitrogen is strongly overabundant, and this indicates that nuclear runaway has occurred. However preoutburst ultraviolet spectra show a very strong N III] line. This may indicate that the material transferred from the red giant is nitrogen-enriched or that we are observing the result of a previous outburst.

IV.C.5. X-RAY OBSERVATIONS

RS Oph was observed with the european satellite EXOSAT at the earliest opportunity, i.e., on March 22, 1985, 54 days after optical maximum. At earliest dates the star was too close to the sun. The observations were made with the low-energy telescope and broadband filters that gave limited spectral information in the energy range 0.04 to 2.0 keV. Additional spectral information was obtained in the medium energy range, from 1.5 to 15 keV. Six observations were made from March to October. Figure 9-41 gives the low-energy flux

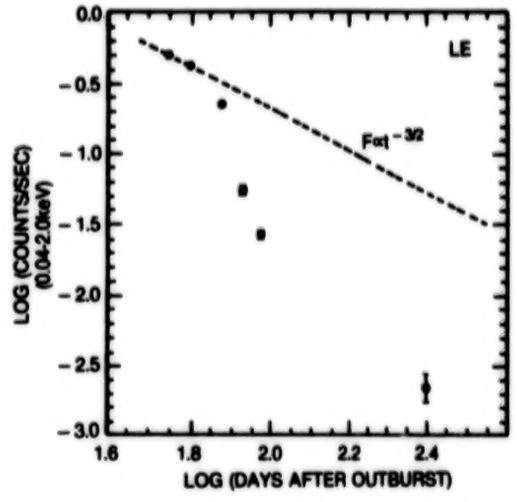


Figure 9-41. EXOSAT count rate as a function of time since the optical outburst. The dashed line is the expected decay rate of the X-ray flux according to the model of Bode and Kahn (1985).
(from Mason et al., 1987).

variation from day 54 to day 250 and, for comparison, the decay expected, according to a theory by Bode and Kahn (1985). They have calculated the expected decay of the flux due to a shock wave expanding in a medium whose density falls as r^{-2}, i.e., the expanding wind of the red giant. It is evident that the decay is much faster than their theoretical prediction. However, there are several indications that the origin of the X-ray emission is due to circumstellar gas heated by the shock wave produced by the nova outburst. In fact, the X-ray emission lasts a long time after the optical outburst, at least 250 days; there is no detectable short-time variability, indicating that the source is extended; the observed expansion velocity 50 days after outburst, as indicated by the optical emission line widths is about 500 km/s. In this case, the temperature expected from the optical emission lines of the gas is consistent with the characteristic temperature of the X-ray spectrum; i.e., the flux in the coronal lines observed on March 18 is consistent with the flux observed in the X-ray range on March 22.

At the latest date of X-ray observations, on day 250 from outburst, IUE simultaneous observations were made. Then the ultraviolet spectrum was very faint and the only emission lines observable were N III] 1750 and a very faint Mg II 2800. It is difficult to understand why a well measurable X-ray flux was detected and no trace of it was observable in the far UV.

The X-ray spectrum is shown in Figure 9-42, and the relation of the low and medium energy measurements at the various epochs is shown in Figure 9-43.

Mason et al. (1987) observe that the strong soft X-ray flux detected from RS Oph about two months after outburst can be interpreted as thermal emission from the circumstellar gas heated by the passage of the shock wave from the nova explosion. In this respect, the environments of RS Oph are similar to those of a mini-supernova whose evolution can be studied on time scales of months instead of hundred or thousands of years. The rapid decay of the X-ray flux, in contrast with the theoretical predictions, can be explained if the shock wave has reached the edge

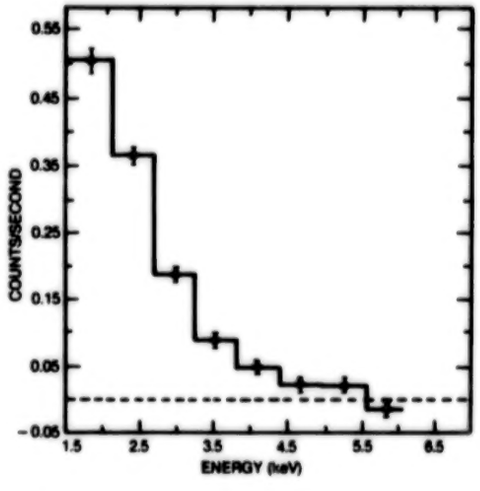


Figure 9-42. EXOSAT background-substracted count spectrum of RS Oph on March 22, 1985.
(from Mason et al., 1987).

of the cavity filled by the stellar wind of the red giant since the last nova explosion.

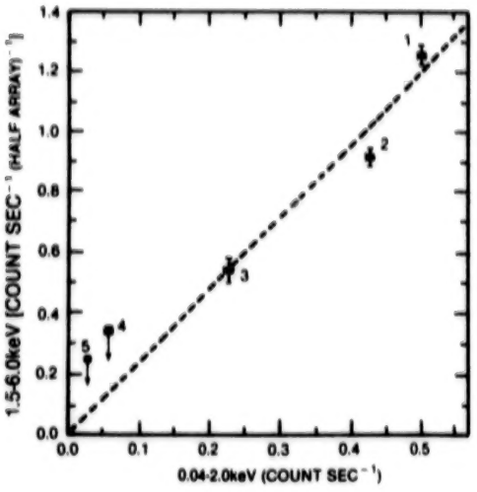


Figure 9-43. 1.5-6.0 keV count rate versus 0.04-2.0 keV count rate for the first five EXOSAT observations of RS Oph. (from Mason et al., 1987).

V. V 1017 SAGITTARII

V 1017 Sgr is an atypical recurrent nova. It has suffered three outbursts in this century: in 1901, in 1919, and in 1973. By contrast to the other recurrent novae, these outbursts have different amplitudes. The nova is of 15th magnitude at minimum, and reached mag 11 in 1901 and 1973, while in 1919 it reached mag 7. The two minor outbursts of 1901 and 1973 have an amplitude typical of a symbiotic star rather than a nova. For this reason, it is uncertain whether V 1017 Sgr must be classified among recurrent novae or rather among symbiotics.

The light curve from 1897 to 1929 is shown in Figure 9-44, and the light curves at the epochs of the three maxima, in Figure 9-45.

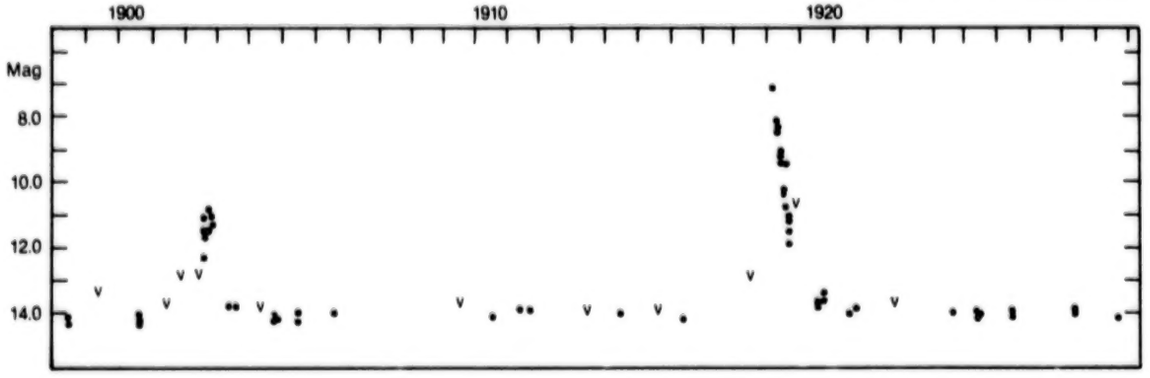


Figure 9-44. Light curve of Nova Sgr 1919. The complete curve for the interval 1897-1929. (from McLaughlin, 1946).

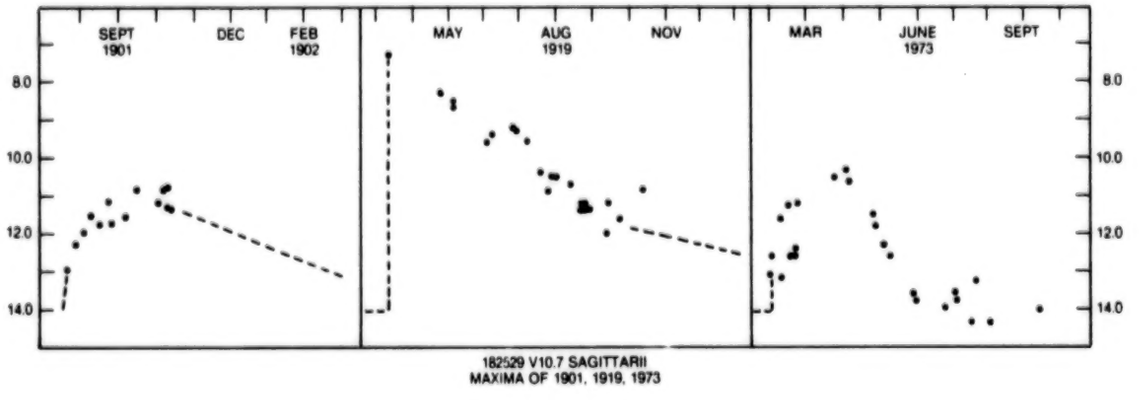


Figure 9-45. The light curves of the three observed outburst of V1017 Sgr. (from Mattei, 1974).

V.A. THE QUIESCENT SPECTRUM OF V 1017 SGR

The spectra at minimum show variations. Spectra obtained by Humason (1938) presented a strong continuum extending to the violet with no absorption or emission lines; Kraft (1964), on the contrary, reported the presence of wide Balmer emission lines in several spectra and their absence in another. The absorption spectrum suggested a spectral type G5 III.

Photoelectrical photometry at minimum has been made in the optical and infrared (for references see Webbink et al., 1987). Mumford (1971) and Walker (1977) found it to be rapidly variable in blue light by about 0.2 mag in less than one hour. The reddening, derived from the VRIJK photometry, assuming the intrinsic color of a G5 III star, is E(B-V) = 0.39 +/- 0.03.

V.B. THE SPECTRUM DURING THE OUTBURST OF 1973

Vidal and Rodgers (1974) observed the spectrum of V 1017 Sgr during the outburst of 1973. There are no reports of spectra obtained during the two previous outburst.

One spectrum at premaximum, one at maximum, and one at postmaximum with dispersion of 200 Å/mm were taken during the last outburst. All three spectra are characterized by broad emission lines. The premaximum spectrum (when the star was 0.5 mag below maximum) shows a weak emission blend at 4640 and He II 4686. Some weak and broad absorption features due to Ca II H and K, a blend at 4140 (due to He I, Fe II, and Si II), the G band, He I 4388, and H beta are detectable. The spectrum taken at maximum shows no absorptions, H Alpha and H Beta emissions, and other weak emissions of [Fe II], and blends of He I+ Fe II and FeII+[Fe II]. The third spectrum taken almost at minimum does not show the forbidden lines of Fe II while the blends of Fe II+ He I at 4923 and 5017 and He I 5047 are strengthened. Similar variations, however, were observed also during quiescent periods, as observed in the previous section.

VI. T CORONAE BOREALIS

(written by Selvelli)

VI.A. HISTORICAL OUTLINE

T CrB is a double-line spectroscopic binary, with period P = 227.5 days (Kraft, 1958; Paczynski, 1965), containing an M3 giant and a hotter companion whose nature has been so far rather elusive. This companion is responsible for the hydrogen and other emission lines and for the variable hot continuum, which, are superimposed over the M spectrum that dominates the optical region.

Because of these features, T CrB can also be classified as a symbiotic star. The classification as recurrent nova is based on the occurence of two historical outbursts in 1866 and 1946, during which the star has suddenly risen from a quiescent magnitude fainter than 9.5 to magnitudes 2 and 3, respectively.

Recently, Webbink et al. (1987) have identified two subclasses of recurrent novae on the basis of their outburst mechanism:

1) those powered by thermonuclear runaway on a white dwarf;
2) those powered by the transfer of a burst of matter from a red giant to a main sequence star. One of the conclusions of the Webbink et al. study (based also on previous models and observations) has been the interpretation of the behavior of T CrB in terms of accretion onto a main-sequence star.

It is remarkable that during the two historical outburst, the photometric and spectroscopic behaviors of T CrB were impressively similar (Pettit, 1946a), thus indicating a similarity in the physical processes responsible for the explosions. Expansion velocities of up to -5000 km/s have been reported for the H lines observed near the 1946 maximum (Sanford, 1947a; Herbig and Neubauer, 1946). In the light curve, the extremely

fast initial rise was followed (Pettit, 1946 b,c) by a rapid decline with $t_3 = 5^d$. A peculiar characteristic of the light curve was that the principal maximum ($m_v \approx 2.0$) was followed in both outbursts, and with nearly the same time separation, by a secondary maximum ($m_v \approx 8.0$). (Figure 9-46).

It is also remarkable that the two observed outbursts occurred at nearly the same orbital phase. The relevance of this fact on the model for T CrB has been pointed out by Webbink et al. (1987).

A detailed description of the outburst spectrum and its variation is given by Bloch et al. (1946), Herbig and Neubauer (1946), Sanford (1947), and by C. Payne-Gaposchkin in her book *The Galactic Novae* (1957). What is remarkable is the enormous initial expansional velocity of 4500 km/s, (or 5000 km/s if we consider the violet edge of the lines).

Sixty spectrograms were obtained at the Haute Provence Observatory by Bloch et al. (1946) during the period February 12 (three days after outburst, which occurred on February 9.25 UT) to July 15, 1946. The evolution of the spectrum is shown in Figure 9-47. We note the presence of the forbidden coronal lines 6374 Fe [X] and 5303 Fe [XIV], which are present on February 12, reach their maximum on February 16, and disappear completely between February 20 (λ5303) and March 18 (λ6374). Figure 9.47 shows clearly the progressive weakening of the permitted lines and the strenghtening of the forbidden ones from February 13 to April 7.

The spectroscopic observations made by Bloch et al. during the 1946 outburst permit us to draw some general remarks: the appearance of the forbidden lines and the strengthening of the high-excitation permitted lines (He II, 54 eV; N III, 47 eV;), which were observed from February 20 to April 30, are a common characteristic observed in classical novae. But a secondary maximum was observed in June; the continuum becomes stronger again and masks almost completely the TiO bands of the red giant and at the same time almost overwhelms the high-excitation lines (both forbidden and permitted). Moreover, a "shell" spectrum (blue continuum and sharp absorption lines of ionized metals) was observed in the photographic region (Sanford, 1947, Herbig and Neubauer, 1946). This phenomenon is not generally observed in classical fast novae, and classical slow novae at the moment of the secondary maximum show a nebular spectrum. The behavior of T CrB is instead rather similar to that

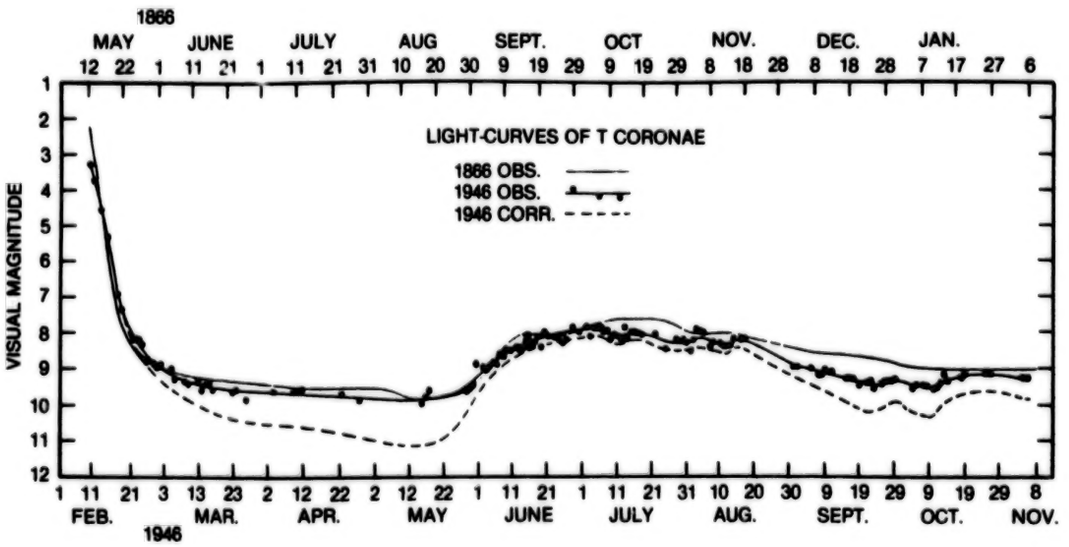


Figure 9-46. The light line is the mean light-curve for the year 1866. The heavy line is the mean light-curve for the year 1946 representing the observational points. The heavy dashed line is the 1946 curve corrected for an M-type companion of magnitude 10.2. The first point for February 9, is an observation by Armin Deutsch. (from Pettit, 1946).

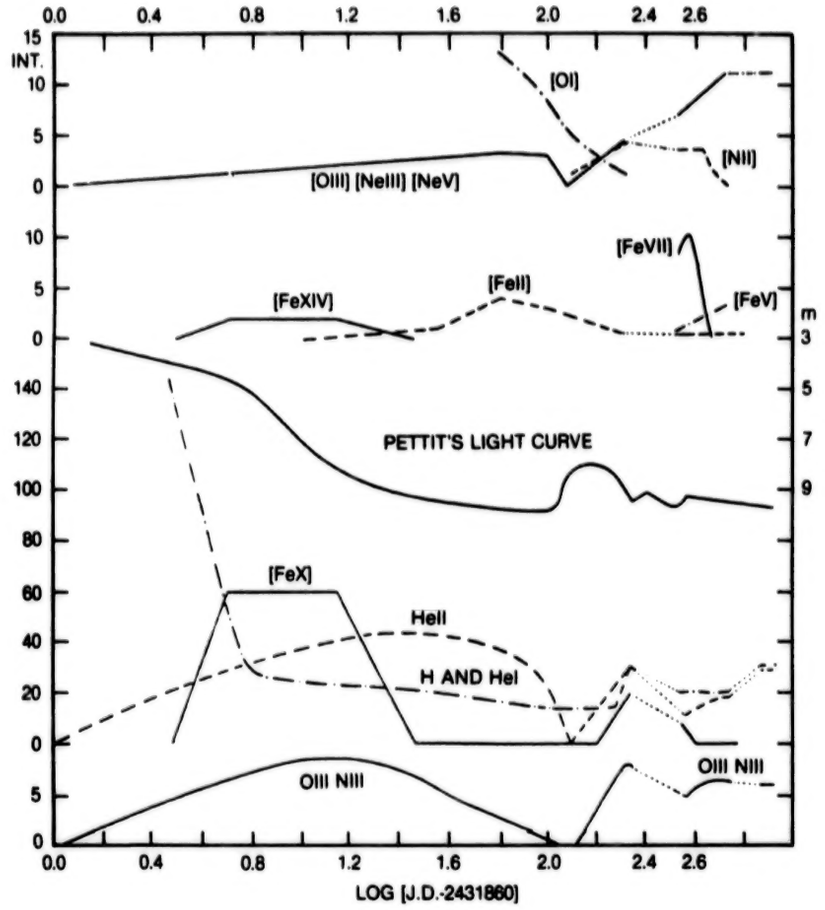


Figure 9-47. Curves of intensity for emission lines in T CrB. Abscissae are logarithms of the number of days after JD2431860. Ordinates are intensities by comparison with He 4686, assigned intensity 10. Curves for [Fe X], He II, H, and He I have ordinates compressed to one-quarter the scale of the other curves. Dotted lines join successive observing seasons. The magnitude scale for Petit's light-curve is on the right.
(from Sanford, 1949).

of some symbiotic stars in outburst, like, for instance, CH Cyg (however, which, does not show high-excitation lines).

Moreover, in slow classical novae the deep minimum is due to dust enveloping the system, as shown by the infrared observations. In the case of T CrB, on the contrary, during the interval between principal and secondary maximum, the spectrum of the M3 giant is clearly visible and not veiled by dust.

The temporary presence of coronal lines seems to be a common characteristic of recurrent novae: they have been observed in T CrB, in RS Oph, and in T Pyx. The only exception is U Sco where no forbidden lines, either of low or high excitation have been observed, and V 1017 Sgr, however, which has several characteristics of symbiotic rather than nova.

During the outburst of 1946, T CrB brightened from $m_v \approx 9.6$ to $m_v \approx 3.0$, with an increase of a factor of 500 in luminosity. The relation F_λ (vis) = $3.68 \times 10^{-9} \times 10^{-mv/2.5}$ gives $F_{\lambda Outb}$ (vis)=2.3×10^{-10} (erg cm^{-2} s^{-1} A^{-1}) at maximum. With a distance of 1300 pc, L_{Outb} (vis) is therefore of the order of 4.6×10^{37} erg s^{-1} A^{-1} . This value sets a lower limit for the bolometric luminosity during outburst: $L_{Outb} \gtrsim 10^{38}$ (erg s^{-1}). The luminosity at maximum was, therefore, close to that of 2×10^{38} erg s^{-1} , corresponding to the Eddington limit for a 1.5 $m_\odot$ star.

VI.B. T CRB IN QUIESCENCE

The optical spectrum of T CrB is a typical M3 III dominated by strong TiO absorption bands. A major step in the understanding of the nature of T CrB was the discovery of its binary nature (Kraft, 1958). The radial velocity data, revised by Paczynski (1965), indicate a double-line spectroscopic binary with P ≈ 227 .6 and $m_{hot} > 1.6\ m_{\odot}$ and $m_{giant} > 2.2\ m_{\odot}$ (Figure 9-48). These values, however, might be affected by the uncertainties in the determination of K_2.

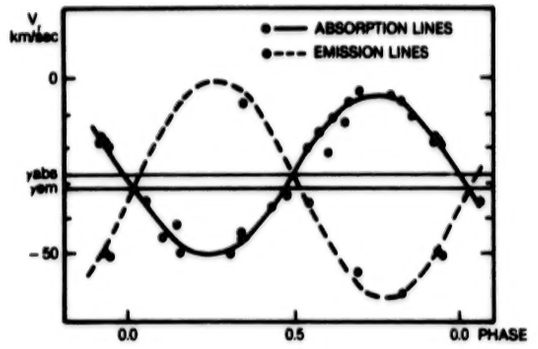


Figure 9-48. The radial velocity curves for T Coronae Borealis.
(from Paczynski, 1965).

Recently, a series of new spectra has been obtained by Kenyon and Garcia (1986) with the purpose of obtaining an improved orbital solution. In this study they have substantially confirmed the K_1 value without attempting, however, to redetermine K_2, whose measurement is made quite difficult by the composite structure of the H emissions. In their spectra, in addition to the typical lines of the M giant, strong hydrogen, He I, and [Ne III] 3868 emissions were present (Figure 9-49). The spectra obtained by Blair et al. (1983), instead, do not show He I emissions. This

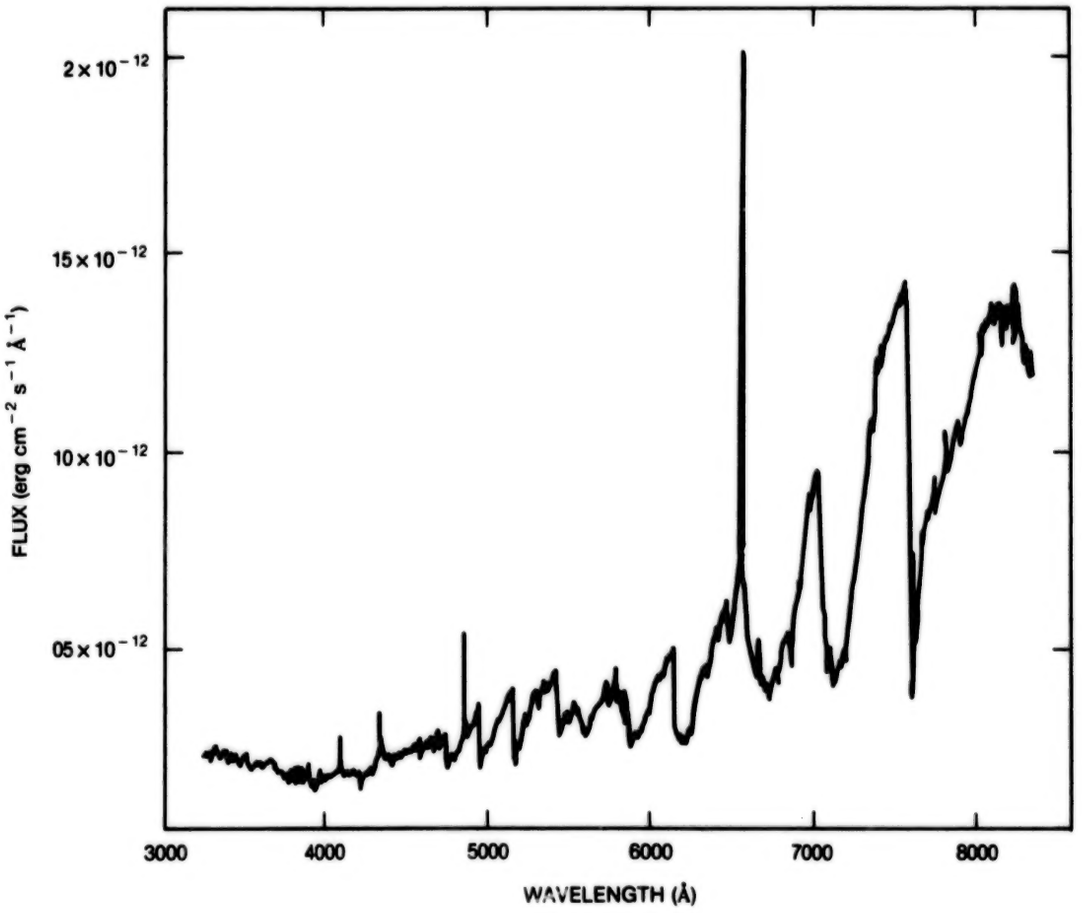


Figure 9-49. Optical spectrum of T CrB. TiO absorption bands and H I emission lines are very prominent on this April 1984 spectrum.
(from Kenyon and Garcia, 1986)

behavior indicates variations in the excitation conditions, related to changes in the temperature of the hot component. Similar variations in the spectrum were noticed and described as early as in the late thirties and in the forties by several authors (e.g., Joy 1938, Swings and Struve 1941, 1943).

The first time-resolved photometric observations during quiescent phases have detected rapid variations in the U light (M.F. Walker 1954). The star was reobserved several years later (1975) by A.R. Walker (1977), who detected a U flickering with a time scale shorter than 15 s and variations of about 0.5 magnitudes from the mean level (Figure 9-50). Bianchini and Middletich (1976) also found comparable UV flickering at nearly the same period, but they reported a marked absence of such activity for 1976. A similar behavior has been reported also by Oskanyan (1983).

These variations are very similar to the flickering exhibited by many dwarf novae that are known to have a white dwarf as companion.

A consequence of the RV observations of Kraft (1958) and Paczinsky (1965), which indicated that the secondary was a main-sequence star, was to rule out thermonuclear runaway models for the outburst of T CrB. After the study by Paczinski and Sienkiewicz (1972), who found that Roche lobe overflow from a giant with a deep convective envelope could lead to extremly high $\dot{M}$ on a (very short) dynamical time scale, Plavec et al. (1973) suggested that T CrB was in a rapid phase of convective mass-loss and that the outburst was caused by the interaction between the mass-accreting star and the large amount of material falling on it. The two historical outbursts were, therefore, attributed to two episodes of extremely high mass transfer triggered by an instability in the red giant.

Webbink (1976) has considered in greater detail the outburst behavior of T CrB and has also interpreted the outburst in terms of episodic accretion phenomena from a giant onto a main-sequence star. He suggested that the outburst was caused by the transfer of a burst of matter ejected by the giant and by the subsequent dissipation of the excess energy of this parcel of transferred mass (of $5 \times 10^{-4}\ M_{\odot}$) when its originally eccentric orbit around the secondary is made circular dynamically by supersonic collisions within the

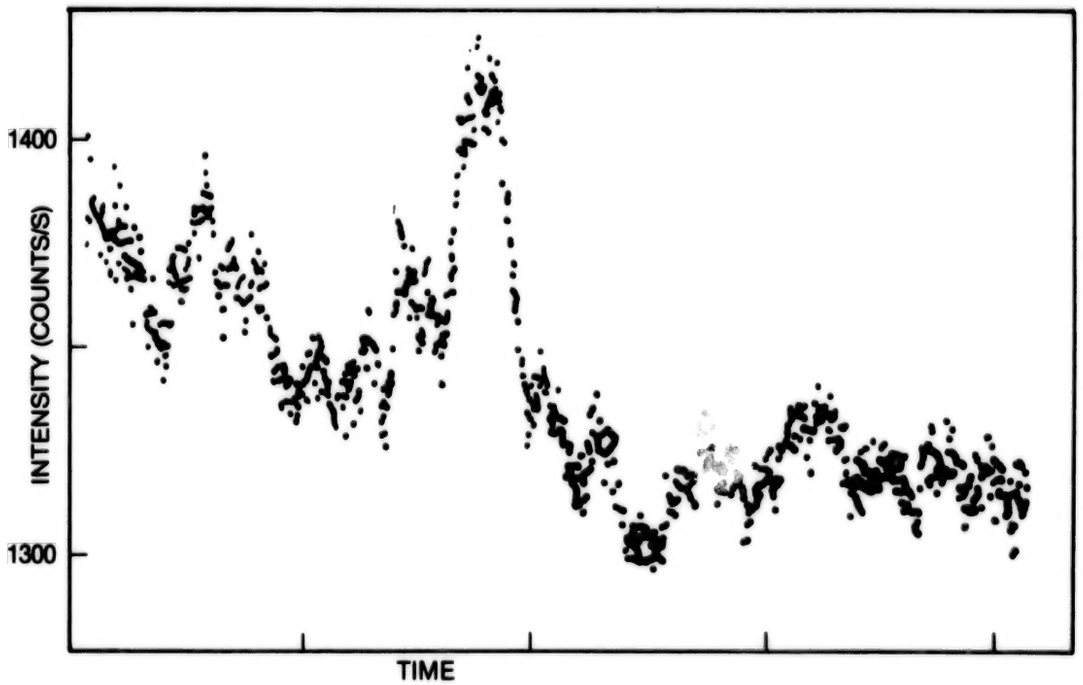


Figure 9-50. Light curve of T CrB through a U filter. The data have been corrected for extinction and the sky background has been removed. Time marks are 1000s apart. The observation was made on JD2442578. (from Walker, 1977).

orbiting material, thus producing a ring. The secondary maximum, instead, is produced when the inner edge of the disk (produced by the broadening of the ring by viscous dissipation) strikes the surface of the (main-sequence) accreting star.

With this model Webbink (1976) was able to explain the presence of the two maxima in the light curve, the time interval between them and their relative amplitude. Spectroscopic observations made at the time of the second maximum have shown, however, the appearance of a "shell" absorption spectrum and the weakening or disappearance of the emission lines (including He II 4686) in disagreement with the increase in excitation (expecially in He II) expected on the basis of Webbink's (1976) explanation of the secondary maximum. Additional considerations in favor of an accretion event onto a main-sequence star as responsible for the outburst of T CrB have been reported in the extensive study on the nature of recurrent novae by Webbink et al. (1987).

After Webbink (1976), Livio et al. (1986), Starrfield et al. (1985), and Webbink et al. (1987) consider (in general) both accretion events onto main-sequence stars and thermonuclear runaways on white dwarfs as possible mechanisms for the outbursts of recurrent novae. The accretion model appeals to dynamical phenomena, similar to those proposed by Webbink (1976), to reproduce the very rapid rise of the light curve in outburst in some recurrent novae. These accretion-powered novae require shock-type events to produce the observed super Eddington luminosities and the very-high-excitation coronal-line emission observed during decline.

Thermonuclear runaways models, instead, require a very massive ($m_{WD} \approx 1.38\ m_\odot$), low-luminosity ($L \approx 0.1\ L_\odot$) white dwarf, and a very high accretion rate ($>1.7 \times 10^{-8}\ M_\odot\ yr^{-1}$) to produce thermonuclear runaway outburst with the short recurrence time scales compatible with those observed in recurrent novae ($\leq 10^2$ years).

Under the above conditions, an accreted envelope mass as low as $5 \times 10^{-7}\ M_\odot$ (much smaller than in normal classical novae, $10^{-5}\ M_\odot$) is sufficient to trigger a thermonuclear runaway (Starrfield et al., 1985). For more details about these models, the reader is referred also to Kenyon (1988). and Livio (1988a).

The above constraints reported on $\dot{M}$ and on M_{env} have been used by Webbink et al. (1987) to define some criteria which would enable observers to distinguish between accretion-powered and thermonuclear runaway-powered recurrent novae: 1). The required high $\dot{M}$ implies that thermonuclear runaway-powered recurrent novae must have high-accretion rates ($> 1.7\ 10^{-8}\ M_\odot\ yr^{-1}$) and, therefore, high-accretion luminosities ($L_{accr} > 100\ L_\odot$) at minimum. Because of the presence of a white dwarf accretor, the bulk of this luminosity is emitted in the UV, and therefore thermonuclear runaway-powered recurrent novae are expected to be luminous UV sources and to display high excitation emission lines (He II,CIV, N V) in their UV spectra.

2) Unlike most classical novae, thermonuclear-runaway-recurrent novae are expected to be emission-line objects at maximum of the outburst because the envelope mass at the time of the runaway is less massive than in classical novae.

Webbink et al. (1987) have used these two "criteria" to give additional arguments against the presence of a white dwarf in T CrB. In particular, from the weakness of the UV spectra they have examined, they have derived a $\dot{M}$ of $10^{-6}\ M_\odot\ yr^{-1}$ for a main-sequence star (or of $10^{-8}\ M_\odot\ yr^{-1}$ for a white dwarf, a value too low, in their opinion, to refuel a thermonuclear runaway model with a recurrence time of 80 years).

Recently, Selvelli, Cassatella, and Gilmozzi (1990) have described the results of 9 years of UV observations of T CrB with the IUE satellite. The main conclusion of this study (which is briefly reported in the following paragraph) is that the overall behavior of T CrB in the UV (and also in the other spectral ranges) finds a self-consistent interpretation in terms of accretion onto a (massive) white dwarf.

VI.C. UV OBSERVATIONS OF T CRB

Previous studies on IUE spectra of T CrB have been presented by Krautter et al. (1981), Kenyon and Webbink (1984), Kenyon and Garcia (1986). Kenyon and Webbink have made an attempt to fit the form of the observed continuous-flux distribution to their synthetic spectra, but were unable to find a consistent model in light of the variability. Their conclusion was that accretion disks around a white dwarf or a main-sequence star could not give a consistent explanation for the UV continuum of T CrB as a function of time. Kenyon and Garcia (1986), instead, excluded the presence of a white dwarf on the basis of the relatively flat UV continuum they observed and of the overall weakness of the high-excitation lines. Tentatively, they ascribed the observed UV variations (IUE) to fluctuations within an optically thin disk orbiting a main-sequence star, fueled by matter streaming from a lobe-filling M3 III star at 10^{-6} $M_{\odot}$ yr^{-1}.

Selvelli, Cassatella, and Gilmozzi (1989) have observed T CrB with IUE from the early days of IUE's life until very recently. Some short progress report of this study have been presented by Cassatella et al. (1982, 1986); Gilmozzi et al. (1987), and Selvelli et al. (1988).

VI.C.1. THE UV CONTINUUM

After correction for reddening, E(B-V) = 0.15, the continuum can be represented, at the various epochs, by a single power-law spectrum $F(\lambda) = A\lambda^{-\alpha}$ over the entire IUE range. The UV spectral index α ranges from 0.7 to 2.0, with a mean value of 1.25. Some examples of the continuum variability are provided in Figure 9-51. The flat spectrum corresponds with a minimum in the UV flux (March, 1979).

In general, when the flux is high, the continuum becomes steeper. One should note that the Balmer emission continuum (peaking around 2800 - 3200 Å in the IUE range) is not negligible in T CrB (Kenyon and Garcia, 1986) and could substantially distort the shape of the long wavelength IUE spectra, causing the derived power-law index to appear flatter, at least when the object is weak (see also Figure 9-52).

The UV continuum from 1200 to 3200 Å is variable by a factor of up to 10.

Certainly, a distinctive peculiarity of T CrB is the lack of significant optical variations (as calculated from the FES-Fine Error Sensor-instrument onboard IUE) correlated to the UV ones. In particular, at the time of the UV minimum (March 1979), the FES magnitude was 9.9, while during the UV maximum of May 1983, the magnitude was 10, indicating that the bulk of the variability is restricted to the UV, in agreement with observations by Walker (1977), Bianchini and Middleditch (1976), and Oskanyan (1983), who could detect variability only in the ground U band. Also the "flares" reported for the years 1963 and 1975 by Palmer and Africano (1982) were present in the (ground) U only.

The changes in the continuum show no obvious dependance on the orbital phase. The deepest minimum (March 1979) occurred at phase ≈ 0.34. Near phase 0.50 (red giant in front), possible occultation effects could be present. However, at phase 0.48 and at phase 0.54 no decrease was observed.

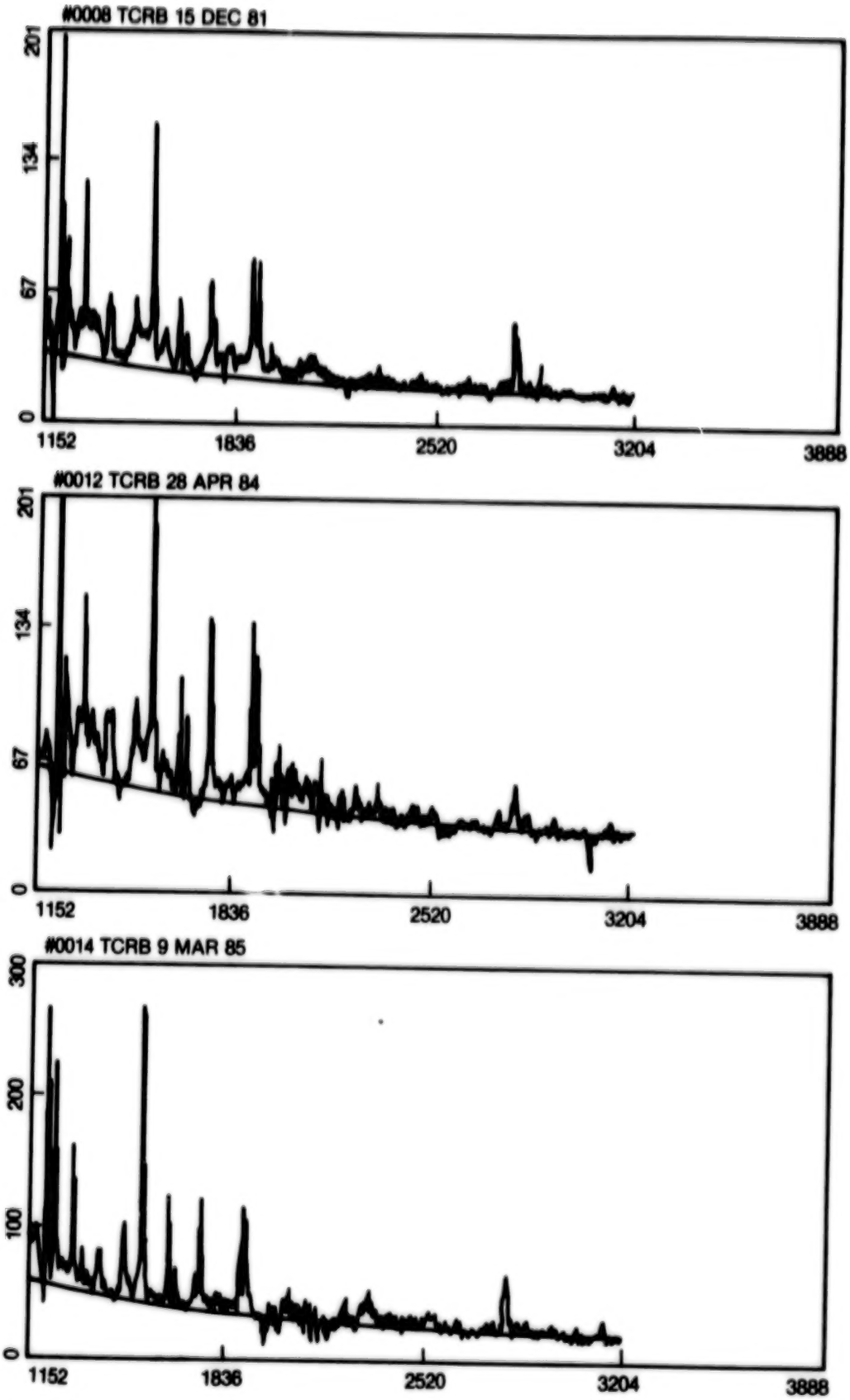


Figure 9-51. The spectrum of T CrB in three different epochs. The power-law ($\lambda^{-\alpha}$) fits of the continuum have $\alpha = 0.60$, 0.65, and 1.0 (from top to bottom).

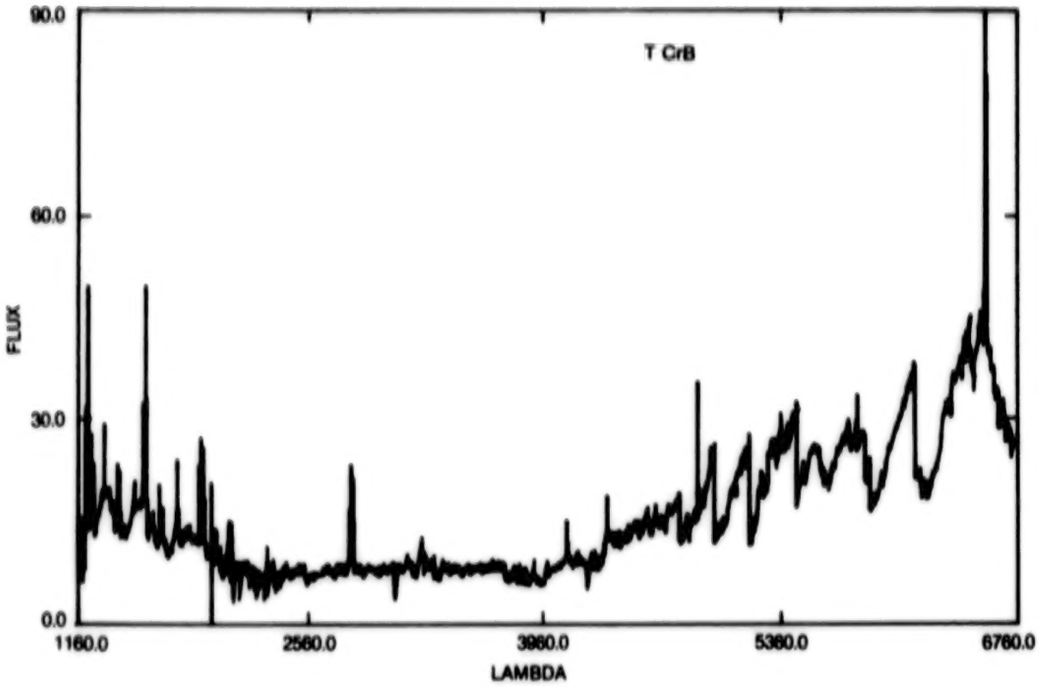


Figure 9-52. A composite spectrum of T CrB from λ1200 to λ5700. (from Cassatella et al., in preparation).

VI.C.2. THE EMISSION LINES

A typical UV spectrum of T CrB is shown in Figure 9-53. The emission lines are remarkably intense in comparison with classical novae in quiescence and include strong intercombination transitions (e.g., Si III, C III, N IV, O III, etc.) and the Mg II doublet, which are usually absent in classical novae.

Table 9-2 lists the most important emission lines observed in the UV spectrum of T CrB. Most lines are straightforwardly identified and are typical of symbiotic stars.

Figure 9-54 shows the time variability of the continuum and of the strongest emission lines. It is evident that the variations of the emission lines, both of low and high degree of ionization, are correlated with the continuum variations, showing as well no dependence on the orbital phase. This suggests that photoionization is the main energy input mechanism, as in the symbiotic stars Z And, AG Car, and HBV 475, and unlike in CH Cyg. The general lack of significant changes in the line fluxes near phase 0.5 seems to rule out the possibility of a partial eclipse of the hot component (which would be most readily detected in the emission lines because of their origin in a larger region than the continuum).

There is marginal indication, in some spectra, of a possible P Cygni profile in the NV line, although it cannot be excluded that this effect is only apparent and due to the Lyα being either variable in width or not filled in, at these epochs, by the geocoronal Lyα. If true, the P Cygni profile would indicate an outflow velocity larger than 2000 km/s, in analogy to the case of AG Dra (Viotti et al., 1984).

High-resolution spectra, although partially underexposed, clearly indicate that the high-excitation lines (C IV 1550, He II 1640) have a shallow and broad profile (HWZI ≥ 1000 km/s). The Si III λ 1892 and C III λ 1909 emissions have instead narrow cores and broad wings. The FWHM corresponding to the broad components are comparable to the ones derived by Kraft (1958) for the Hβ line (330 km/s), while the narrow component is only instrumentally broadened.

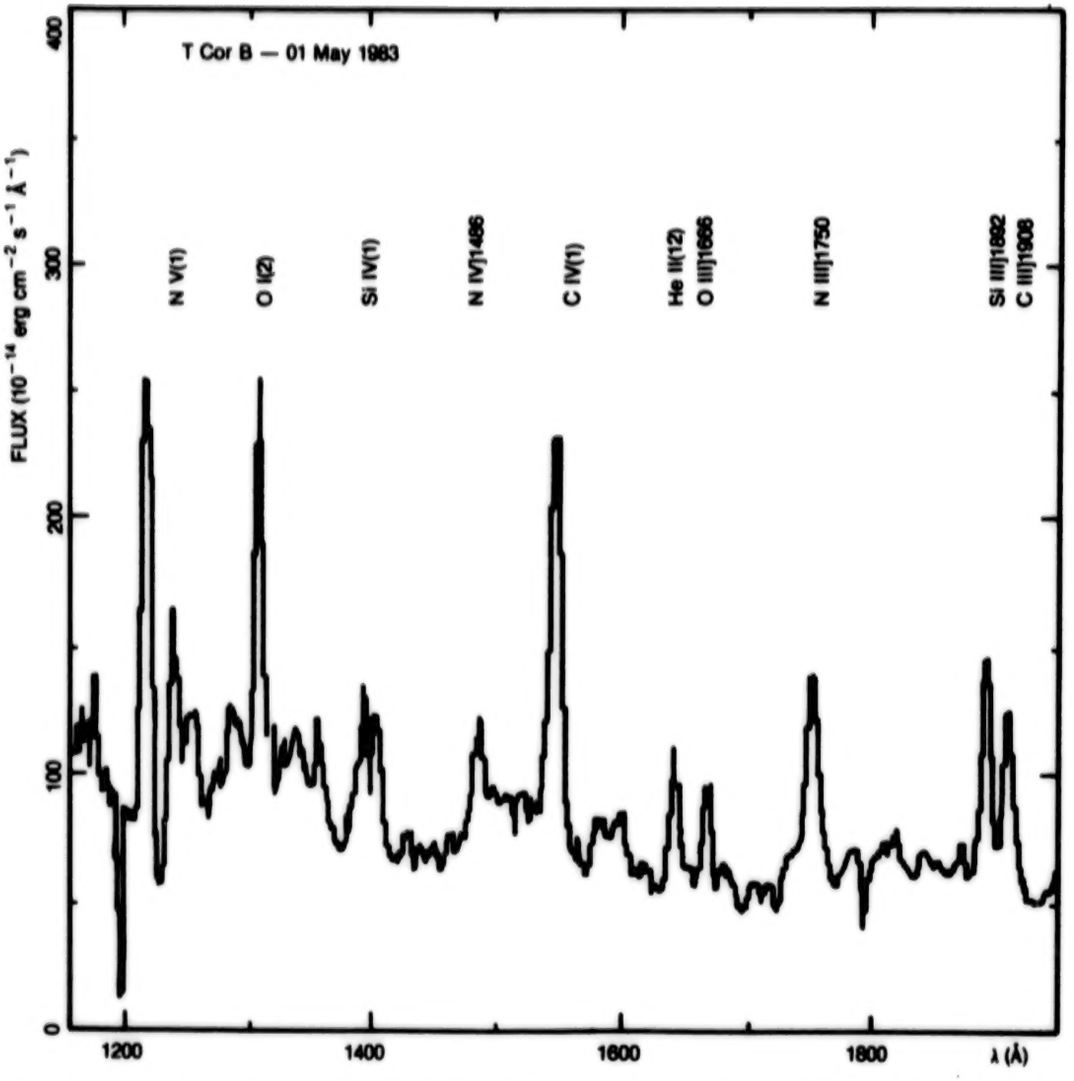


Figure 9-53. A short wavelength IUE spectrum of T CrB taken on May 1, 1983, with typical emission lines. The high excitation NV line is a prominent feature.

TABLE 9-2 THE UV EMISSION SPECTRUM OF T COR B

	Identif.		
1240	NV (1)	1665	OIII
1285	?	1750	NIII (0.07)
1304	OI (2)	1892	SiIII (1)
1335	CII (1)	1908	CIII (0.01)
1355	OI (1)	2330	CII + SiII
1400	SiIV (1) (+0IV)	2670	AlII (1)
1485	NIV (0.01)	2735	HeII
1530	?	2800	MgII (1)
1550	CIV (1)	2835	OIII (Bowen)
1594	?	3133	OIII (Bowen)
1640	HeII (12)	3188	HeI (3)

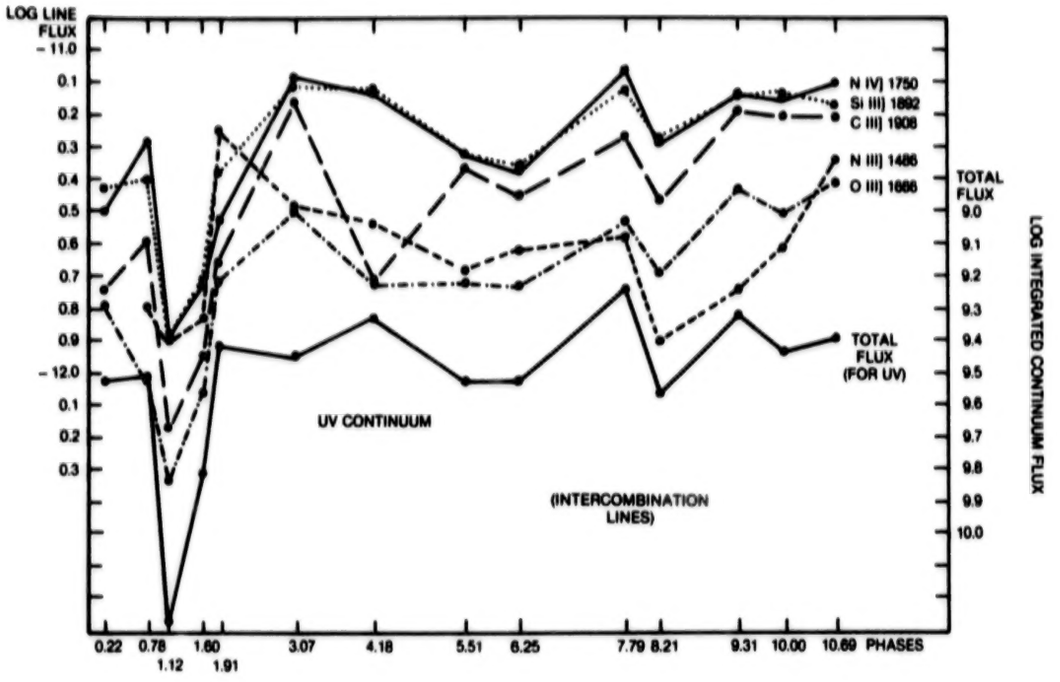


Figure 9-54a. Time variability of the emission line fluxes and of the integrated continuum flux 1152-3200 A from 1978 to 1985. A deep minimum occurred in March 1979. Intercombination lines.

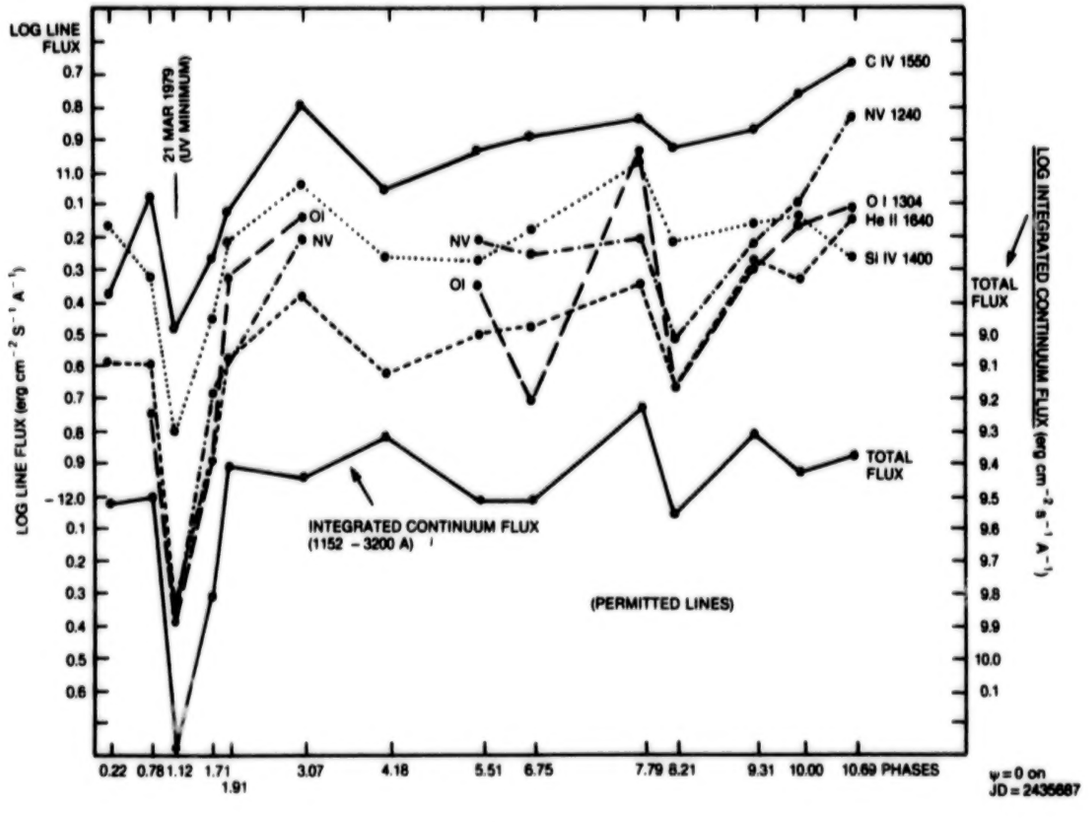


Figure 9-54b. Same as Figure 9-54a. Permitted lines.

VI.C.3. THE ABSORPTION LINES

Absorption lines are generally present in all the spectra of T CrB, although their intensity has shown considerable variations with time.

The overall UV absorption spectrum of T CrB is, at some epochs, very similar to that of late B and early A supergiants, with lines mainly of once-ionized metals (Fe II, Ni II, Cr II...). This seems to be a typical signature of symbiotic stars during activity phases and mimics an optically thick cool shell surrounding the hot component (Sahade and Wood, 1978). Kenyon (1986) has also reported recently a similar behavior for the symbiotic star PU Vul.

A high-resolution, near ultraviolet (2000-3000 Å) spectrum obtained on April 30, 1982, has confirmed the presence of many absorption lines from once-ionized metals (mainly Fe II).

VI.D. THE HYDROGEN RECOMBINATION CONTINUUM

The hydrogen free-free and free-bound emissions are generally an important component of the observed UV energy distribution in symbiotic stars with which T CrB has been sometimes associated. A determination of this contribution is not, in general, possible for the lack of simultaneous optical and UV observations. However, for the epoch February 1981, a rough estimation can be made from the observed Hβ flux (1.05 10^{-12} erg cm^{-2} s^{-1} , Blair et al. 1983) in the assumption that the emitting volumes are the same. This gives an expected flux at 2800 A of 5.3 × 10^{-15}erg cm^{-2} s^{-1} A^{-1}, a value below the IUE detection limit for the exposure time used.

On the other hand, Kenyon and Garcia (1986), have obtained optical spectra in which the Balmer jump is clearly present in emission. This is confirmed by recent UV and optical spectra (Cassatella et al. 1988). Probably, the recombination continuum is either variable or it was masked by the strong far UV component during the high state of February 1981.

VI.E. DIAGNOSTICS

VI.E.1. THE ELECTRON DENSITY

The electron density in the line-emitting region has been derived from the intensity ratio of the Si III] 1892 and C III] 1909 intercombination lines, both strong in the spectra of T CrB. Calculations of the Si III]/C III] ratio from Nussbaumer and Stencel (1987) were adopted. In addition, it was assumed that

(1) The ionization fraction [N(Si III)/N(Si I)]/N(C III)/N(C I) is about 0.5.
(2) The Si and C abundances are solar.
(3) The electron temperature of the emitting region is 15000 K (see following).

The mean value of the electron density since January 1979 is 2.8 x 10^{10} cm^{-3}. The highest density (1.2 x 10^{11} cm^{-3}) corresponds to the peculiar spectrum of February 1981, while the lowest value (1.8 x 10^{10} cm^{-3}) is recorded on March 9, 1985.

An independent estimate of the electron density can be made using the N III] multiplet around 1750 A, whose line components could be detected in two high-resolution spectra. From the measured fluxes of these lines, and the calculations by Altamore et al. (1981), it results N_e = 1.7 x 10^{10} cm^{-3} on June 1980, and N_e=1.3 x 10^{10} cm^{-3} on February 1981, in agreement with the low-resolution estimates.

VI.E.2. ELECTRON TEMPERATURE

The electron temperatures of the line-emitting regions can be determined from the low-resolution spectra by making use of the N IV 1718 / N V 1240 and the C III 1176 / C III] 1909 flux ratio between lines produced by dielectronic recombination and lines produced by collisional excitation, following the calculations by Nussbaumer and Storey (1984).

The measured line ratios, corrected for reddening, and the derived electron temperatures give a mean value of about 13000 K +/-1000 K.

The C III 1176 / C III] 1909 flux ratio provides values which are systematically higher than those derived from the N IV 1718 / N V 1240 ratio.

Note, however, that the C III 1176 emission falls near the camera sensitivity cutoff, and it is, therefore, difficult to measure accurately.

VI.E.3. DETERMINATION OF $\dot{M}$ FROM THE UV LUMINOSITY

Accretion onto a compact object is a commonly accepted mechanism for producing the observed UV luminosity in Cataclismic Variables. In most cases (semidetached systems), the mass transfer is achieved through Roche-lobe overflow but wind accretion can also be effective, especially for detached systems containing a mass-losing primary. In the absence of (strong) magnetic fields, matter accretes on the compact object forming an accretion disk. Mass loss can be estimated if the disk luminosity and the nature of the accreting object are known or assumed. In this case $\dot{M} = 2RL/GM$, where R and M refer to the accreting object.

This value of $\dot{M}$ is not model-dependent but requires the knowledge of the bolometric accretion luminosity. In general, therefore, it underestimates the mass-loss accretion rate if only a limited spectral range is available. Assuming a distance to T CrB of 1300 pc, the reddening corrected IUE integrated luminosity ranges from 2.6×10^{34} erg/s (21 March 1979, deep minimum) to 2.6×10^{35} erg/s (1 May 1983, maximum). An average value of the integrated UV luminosity is 2.2×10^{35} erg/s. The IUE observations have shown that the disk luminosity is radiated mostly in the UV with a negligible contribution to the optical. This is a strong indication in favor of a white dwarf accretor: a main sequence accretor is expected to emit mostly in the optical region in contrast with the observed behavior of T CrB.

The presence of a quite strong He II 1640 emission requires a very hot continuum with a temperature of the order of 10^5 K . This value also is hardly compatible with a main-sequence accretor and suggests in itself the presence of a compact accreting object (see also the following sections). Taking indicative values of a white dwarf ($M = 1\ M_\odot$ and $R = 0.01\ R_\odot$), the derived accretion rate is $\dot{M} = 4 \times 10^{-8}\ M_\odot$/yr (= $2.5\ 10^{18}$ gr/s.) An independent check for $\dot{M}$ can be made through the $\dot{M}$ - λ1640 intensity relation given by Patterson and Raymond (1985b). Their Table II gives $\dot{M} \approx 10^{19}$ g/s for $L(1640) = 10^{33}$ erg/s and $M = 1 M_\odot$ for the white dwarf, in good agreement with our estimate based on the UV continuum. The same model gives, for this $\dot{M}$, a boundary layer temperature of about 4×10^5 K with a luminosity of 10^{36} erg/s.

VI.E.4. THE ZANSTRA TEMPERATURE FROM HE II 1640

The He II 1640 emission, as a recombination line of an ion requiring 55.4 eV for ionization, is an unambiguous and useful indicator for the presence of high-energy radiation in the spectrum. This line, together with the λ4686 emission, has long been known as a typical signature of X-ray binaries (Patterson and Raymond, 1985a). It is remarkable that λ1640 is often absent in dwarf novae (Szkody, 1985), while it is present in AM Her stars and intermediate polars.

Because of the high energy of its lower level, it is unlikely that the He II 1640 line is formed by a mechanism other than recombination after radiative ionization. This seems indeed to be the case of T CrB, as indicated by the positive correlation between the He II 1640 and the UV continuum fluxes. Whatever the nature of the ionizing source is, it is possible to estimate its temperature using the Zanstra method under the assumption that the ionizing source radiates as a blackbody and that the He II emitting region is optically thick to the continuum of the blackbody source shortward of 228 A (ionization limit of He II). With the assumption that the reddening corrected flux of T CrB at 1300 A, F(λ1300) is entirely contributed by the blackbody source, the flux ratio F(λ1640) / F(λ1300A) provides a direct indication of the Zanstra temperature (see, e.g., Pottash, 1985). The He II Zanstra temperature

was substantially constant over the period covered by the UV observations: T(Z) = 66000 K, on average.

Because of the assumptions implicit in the definition of the Zanstra temperature, the above value is actually a lower limit to the temperature of the ionizing source.

VI.F. THE EUV/SOFT X-RAY LUMINOSITY

The 1640 intensity can be used to determine the number of photons with energies higher than 55.4 eV, to provide an estimate of the EUV/soft X-ray flux in T CrB. The average value of the He II 1640 line intensity is 5×10^{-12} erg s^{-1} cm^{-2}. Since the distance to T CrB is 1300 pc, the average λ1640 luminosity is 1.3×10^{33} erg/s. Assuming case B recombination and assuming that all EUV photons are able to ionize He II, it is possible to estimate the number Q4 of photons with energies higher than $4h\nu$ = 55.4 eV (See also Pottasch, 1985):

$$Q4 = \int_{4\nu_0}^{\infty} \frac{L_\nu d\nu}{h\nu} = \frac{\alpha(B,tot)}{\alpha(eff)} \frac{He^{++}}{1640} \frac{L(1640)}{h\nu(1640)}.$$

Taking α(B, tot) = 2.6×10^{-13}, α (eff 1640) = 8×10^{-14}, $h\nu$ (1640) = 7.5 eV, it results that Q4 ≈ 3.3 10^{44} photons. Assigning an average typical energy of 100 eV to these photons, the obtained luminosity is about 5×10^{34} erg/s. This is, however, a lower limit for L(EUV), since it seems unlikely that all photons ionize He II and also that we are in a spherically symmetrical situation. A value of a few 10^{35} erg/s seems realistic (~ 100 $L_\odot$).

From this, one can obtain a rough (but indicative estimate of the dimensions of the region involved from the simple relation $L = 4\pi R^2 \sigma T^4$ with $T \sim 10^5$ K; $R \approx 1.2 \times 10^4$ Km. It is tempting to relate this value to a region associated with a white dwarf.

VI.G. THE RELATIVE OPTICAL+UV+ X-RAY CONTRIBUTION TO THE TOTAL LUMINOSITY

The hot component (disk) luminosity contributes to the satellite UV mostly. At some epochs (Bianchini and Middletich, 1976; Walker, 1977; Oskanyan, 1983) there has been a contribution by the hot source to the ground U at best, but never to the B or V, as confirmed also by the FES photometry that has shown no correlation with the significant far UV variations. On the other hand, if the observed far UV continuum slope ($\lambda^{-\alpha}$ with α = 1.2 on the average) is extrapolated toward the visible, a contribution of a few percent to the giant optical luminosity (100 $L_\odot$) is expected and should be detectable by the FES photometry. Evidently, the above power-law approximation breaks down at longer wavelengths, probably because the disk becomes optically thin in its cooler outermost layers, thus truncating its contribution to the optical. In practice, the disk-hot component emits only in the satellite UV and, at some epochs, in the ground U, while the giant emits mostly at longer wavelengths.

It is remarkable that the soft x-ray luminosity, as estimated from the He II emission intensity gives a power comparable to that of the UV:

L (disk) ≥ 2×10^{35} erg/s = L (UV)
L (EUV—soft x) ≥ 10^{35} erg/s; L (hard x)≈ 10^{31} erg/s.

VI.H. THE NATURE OF THE COMPANION

A white dwarf companion has been explicitly or implicitly assumed in the previous considerations. There are, in fact, several observational indications which are hardly compatible with the presence of a main-sequence companion:

1) The bulk of the disk luminosity is emitted in the UV, with a negligible contribution in the optical range (L(UV)~2×10^{35} erg/s and $F_\lambda(UV) \sim \lambda^{-1.2}$). This UV luminosity is larger than that found in old novae. It is difficult to explain at the same time this UV luminosity and its spectral distribution with a main sequence accretor, because this would require a very high accretion rate and, as a consequence, the disk would emit mostly in the optical, contrary to what is observed. With the white dwarf assumption, the observed UV

continuum luminosity (a lower limit of the total disk luminosity) gives $\dot{M} \geq 2.5\ 10^{18}$ gr/ s. 2) A rather strong He II λ1640 emission is generally present: L (1640) ≈ 1.2×10^{33} erg/ s. (N V is also present, although weaker). These emissions are indicative of temperatures of the order of 10^5 K, and are naturally associated with the boundary layer. The semi-empirical estimates of Patterson and Raymond (1985), who assume a white dwarf, associate to this He II 1640 luminosity a mass-accretion rate of 8 x 10^{18} gr/ s , in good agreement with that derived directly from the UV luminosity. It is also remarkable that only a white dwarf accretor, at the calculated $\dot{M}$, can explain at the same time both the observed UV luminosity and the high temperature required to produce the He II 1640 emission intensity.

3) The X-ray luminosity (Cordova, et al., 1981) from the Einstein satellite in the range 0.2-4.5 KeV is L = 5×10^{31} erg/ s , of the same order of that found in the X-ray brightest old novae (mean value 6 x 10^{31} erg/ s from Patterson and Raymond, 1985a).

4) The EUV luminosity emitted below λ228 A, as estimated from the He II 1640 emission is ≥ 5 x 10^{34} erg/ s, that is, comparable with the observed UV luminosity L(UV) ≈ 2 x 10^{35} erg/ s . If L(UV) is attributed to the disk and L(EUV) to the boundary layer, it is evident that the power emitted by the disk is on the same order of magnitude as that emitted by the boundary layer, in agreement with the theoretical predictions for a "standard" disk around a white dwarf accretor (Patterson and Raymond, 1985b). They also predict that when $\dot{M}$ is larger than 10^{16} gr/s, then only a small fraction of the bolometric luminosity is emitted as "hard" X-rays (0.2-4.5 KeV), as actually observed, (point 3: $L_x \approx 1.5\ 10^{31}$ erg/ s).

5) The shape of the C IV 1550 (and He II 1640) emission lines in high-resolution spectra is very wide and shallow. C IV, the strongest UV line in low-resolution spectra, is hardly evident at high resolution, while weaker lines (e.g., the semi-forbidden lines of CIII and Si III) are sharper and clearly present.

This indicates that C IV and He II are strongly broadened by rotation, probably because they originate in the innermost disk region. The (HWZI) for C IV gives v sin i larger than 1000 km/s, a value not compatible with a main-sequence star.

Two other indications for the presence of a white dwarf in T CrB are the presence of flickering (Walker, 1977; Bianchini and Middletich, 1976) and the fact that in the 1946 outburst the expansion velocity reached -5000 km/s (Herbig and Neubauer, 1946), a value of the order of the escape velocity from a white dwarf.

All these arguments in favor of the white dwarf are "disturbed" by the results of the orbital data for T CrB, which suggest a mass for the companion higher than that acceptable for a white dwarf (Kraft, 1958; Paczynski, 1965).

The problem of the radial velocity is of critical importance. Radial velocity variations in the giant's lines were first noted by Sanford (1949) who proposed a period of 230 days. A subsequent investigation by Kraft (1958) led to an improved period (227.6) and to the detection of radial velocity variations also in the H emissions whose considerable width (300 km/s) together with their small velocity range (K_2 =30 km/s), prevented Sanford to detect the radial velocity changes. Kraft used several plates for the determination of K_1 (23 km/s), but seven plates only for the detection of K_2. Paczynsky (1965), using the same data as Kraft improved the curves obtaining K_1 =22.9, K_2 = 31.3+/- 2, and $q = M_1/M_2 = 1.4$ +/-2. Adopting i = 68°, the results for the masses were $M_1 \approx 2.6\ M_\odot$, and $M_2 \approx 1.9\ M_\odot$, thus placing the hot component above the Chandrasekhar limit. This fundamental conclusion has remained unchecked since then. It must be stressed that:

1) The H emissions of T CrB are quite wide (300 km/ s) and severely distorted by the absorptions of the giant and show a composite structure; are they necessarily associated with the orbital motion of the hot component?

2) An entire period of the emission lines was covered by only seven points (plates) in all,

and only two plates were close to quadratures (velocity maxima).

3) About 30 years have elapsed since these radial velocity determinations. Even nowadays, in spite of the considerable improving in the measuring techniques, the problem of how to measure K_{em} is serious and difficult. For a critical analysis of the detection of K_{em} see, for example, Wade (1985), p. 307; Shafter (1985), p. 355; and Gilliland et al. (1986).

4) Kraft himself (1958), after the laborious operations for reconstruction of the emission profile, explicitly stated (p.629) that "a non negligible degree of error might still exist in the orbit derived from the H emissions."

Under all these circumstances, an error of 8 km/s in excess for the K_2 value by Kraft (1958), whose measurement is substantially based on two points only (and of critical determination), is not unlikely. A reduction of K_2 by this amount would yield $K_1 \approx K_2 \approx 23$ km/s and a solution $M_1 \simeq M_2 \simeq 1.4\ M_\odot$ for the masses, thus allowing the accreting object to be a degenerate dwarf near the Chandrasekhar limit.

Note that this is the sole solution compatible with $q \geq 1$, $M_2 \leq 1.4\ M_\odot$ and $i = 68°$ ($q = M_1/M_2$).

Recently, Kenyon and Garcia (1986) have accurately remeasured K_1 (= 23.3), confirming substantially the value proposed by Paczynsky (1965). They have not attempted, however, to remeasure the emission line radial velocity and, in their new determination of the orbital parameters, they either have assumed q = 1.2, or have used indirect methods to give evidence that $q \approx 1.3$. How can the discrepancy between the UV observations (which clearly indicate a white dwarf companion) and the radial velocity studies (which indicate a companion more massive than $1.4\ M_\odot$) be reconciled? Two possible scenarios can be envisaged:

1) The radial system is triple, composed of a "normal" binary nova and the giant. The mass of the "companion" of the giant is the mass of the nova system ($M_{Tot} \approx 1.8\ M_\odot$), compatible with the presence of a $0.5\ M_\odot$ red dwarf and of a rather massive ($\sim 1.3\ M_\odot$) white dwarf.

2) The radial velocity results are (slightly) wrong: K_2 is smaller and of the order of $K_1 \simeq 23$ km/s. In this assumption, the radial velocities would be compatible with the presence of a $M_1 \simeq 1.4\ M_\odot$ giant, and of a very massive ($M_2 \simeq 1.4\ M_\odot$) white dwarf.

It is remarkable that theoretical considerations (Starrfield et al., 1986) require the presence of a massive white dwarf in recurrent novae. It is also remarkable that the $\dot{M}$ derived from the UV observations ($\dot{M} \simeq 4 \times 10^{-8}\ M_\odot$/yr) is exactly that requested to produce a recurrence time of the order of 100 years (or slightly less) for the outbursts in a massive ($1.4\ M_\odot$) white dwarf (Kenyon, 1988, Livio, 1988).

New, accurate, radial-velocity measurements of the emission lines associated with the hot component are clearly required. Unfortunately, in the optical most hydrogen lines are contaminated by the cool component, and the He lines are rather weak. The UV range offers a line (He II λ1640), which is a good candidate for the measurements of K_2: beyond any doubt, it is associated with the hot component and, thanks to the high excitation (40.8 e V) of its lower level, it is not affected by reabsorption.

The acquisition of a series of high-resolution spectra with good signal-to-noise ratio of this line however, is, a task that only the Space Telescope can successfully perform.

VII. CONCLUSIONS

The detailed description of the observed characteristics of the five known recurrent novae proves the statement made in the first section of this chapter: They are a rather inhomogeneous group. T CrB and RS Oph are very similar: a) both have a quiescent visual spectral type M III; b) both are fast novae; c) both have spectra in outburst characterized by strong emissions and strong coronal lines; d) both have been detected with the IRAS and present a low infrared excess; e) both present variable ultraviolet spectra, but

we cannot say if their shape and variability are similar or very different—as it appears from the available observations—because T CrB has been observed for several years during its quiescent state, while only few observations have been made for RS Oph in quiescence and in outburst.

U Sco is a fast nova like T CrB and RS Oph, but has very different characteristics: Its visual spectrum at minimum is G0 V, and it does not present forbidden and coronal lines during outburst. The ultraviolet spectrum in outburst is completely flat with superposed permitted and semipermitted emissions.

T Pyx and V 1017 Sgr are both slow novae. However, this is the only common characteristic. T Pyx is a typical recurrent nova, whose outbursts are very similar to each other (and this is true also for the other recurrent novae with the exception of V 1017 Sgr), while V 1017 Sgr has presented outbursts of different amplitudes. T Pyx has a very blue spectrum at minimum, while the minimum spectrum of V 1017 Sgr is G5 III. The spectrum of T Pyx in outburst is characterized by the presence of several strong forbidden and coronal emissions, while V 1017 Sgr presents no forbidden lines with exception of weak [Fe II] lines.

The chemical composition of the ejecta of the recurrent novae is not homogeneous, suggesting that different processes originate the outbursts. For instance, the scanty available determinations indicate that U Sco presents He and N excess, RS Oph presents N excess, while T Pyx shows no evidence of CNO excess and presents a slight deficiency of He. No data are available for T CrB and V 1017 Sgr.

The meaning of the abundances of the ejecta and their relation to the mechanisms producing the outburst have been discussed in chapter 7.

10
SUMMARY

M. Hack and M. Friedjung

We summarize here the main results and the several open questions on classical and recurrent novae, both from the observational and theoretical side.

I. THE OBSERVATIONS

The observations indicate that three main periods can be recognized in the nova phenomenon: the quiescent stage, when the object behaves like a typical dwarf nova; the outburst, when the more or less rapid increase of luminosity is accompanied by expulsion of several envelopes producing the premaximum, the principal, the Orion, and the diffuse-enhanced spectrum; and the nebular phase, when the envelope becomes sufficiently rarefied to give a pure emission-line spectrum and becomes spatially resolvable a few years after the outburst.

The space era has offered the possibility of measuring almost the whole electromagnetic spectrum of celestial objects. What has been the gain in knowledge we have obtained in the special case of novae?

As it was observed for the first time for FH Ser, the bolometric magnitude remains constant for a longer time interval or presents a much slower decline than the visual magnitude.

As we have seen in Chapter 6, ultraviolet and X-ray observations have strengthened the previous evidences that all novae are close binary systems and confirmed the presence of a white dwarf and an accretion disk in classical novae, and probably also in all recurrent novae, although some doubt that the companion is a dwarf nova or a main-sequence star still exists for some systems (e.g., see discussion on T CrB in Chapter 9).

Infrared measurements, both from the ground and space, have clarified the reason for the presence of the dip in the light curve of slow novae, i.e., formation of dust in the ejecta, although it is not still clear which is the mechanism of formation. Several examples suggest that these mechanisms are more efficient in slow novae than in fast novae, but they seem not efficient in very slow novae like HR Del or RR Pic, which do not present any dip in their light curve.

Radio observations, together with imaging and spectroscopy have given information on the extension, shape, density, temperature, and motions of the envelope and the rate of mass loss.

There are some indications that the old nova remnants need very long time intervals to go back to the preoutburst state remaining brighter than their prenova magnitudes for several tens of years. For this reason, it is very important to find and to observe the remnants of historical novae like WY Sge 1783 and CK Vul 1670. The sensitivity of the new electronic detectors can be of great help in finding very faint traces of past outbursts. The IUE satellite has permitted us to observe several quiescent novae and to monitor some of them for time intervals sufficiently long for studying their variability, thus permitting us to detect periodical, quasi-cyclical and irregular variability.

PRECEDING PAGE BLANK NOT FILMED

Moreover, several outbursts of novae have been monitored with IUE. Combined optical and ultraviolet observations of novae in outburst have permitted us to derive more accurate abundances in the ejecta, because of the possibility of observing lines of several elements in different ionization states. The previous results, that CNO are enhanced, and that enhancement is generally stronger in fast than in slow novae, are confirmed: none of the novae studied with IUE have ejecta with solar abundance. A very important result is the discovery of another class of novae (Starrfield and Snijders, 1987). The members at present are three: V693 CrA 1981, V1370 Aql 1982, and Nova Vul 1984 # 2.

In V693 Cr A, all the intermediate mass elements, from nitrogen to aluminum are enhanced by a factor of about 100. In V 1370 Aql, the elements up to sulphur are enhanced, and neon is the most abundant element in the ejecta. Also Nova Vul 1984 # 2 shows a large overabundance of neon in the ejecta. Recent developments of the thermonuclear runaway theory (Starrfield et al. 1985, 1986) have shown that these observations are explained by the ejection of core material from an oxygen, neon, magnesium white dwarf. Hence, we can distinguish novae with CO white dwarfs and novae with ONeMg white dwarfs in close binary systems. The main distinguishing feature is the emission line [Ne IV] 1602. If it is present at late times in the outburst, the ejecta are neon rich (Starrfield and Snijders, 1987).

The evidence that all the well-studied objects are close binaries may explain the large variety of behavior of novae. In fact, we dispose of a larger number of parameters than one can have with a single star, and this explains, at least qualitatively, such a large variety of phenomena observed among members of a same class. However, a large number of questions must still be answered. Let us summarize some puzzling observations.

All nova systems have periods larger than 2.82 hours and shorter than 1 day with just two exceptions: CP Pup, period P = 1.58 hours (the only nova known to have a period below the gap) and GK Per, P = 1.9 days (the only nova known to have a period longer than one day). Light curves are not exactly repeatable, and when they present minima, they are not always simply interpretable as an eclipse of the hot companion, because the epochs of the minima are sometimes varying. The variability in light curves, and especially the varying epochs of the minima both seem to validate the idea that it is the eclipse of an unstable structure like a hot spot on the accretion disk that we are observing, and not the hot star itself.

The part devoted to dwarf novae and nova-like stars shows the great similarity of these two classes of cataclysmic variables with that of these quiescent novae. Actually, several quiescent novae are members of a specific class of dwarf novae. Hence it remains an open question whether all dwarf novae have suffered or will suffer a nova outburst. We still do not know why systems with practically identical properties may or may not develop an outburst phase.

The observations that the properties of a nova before and after outburst remain the same is a proof that the outburst, although so impressive from the observational side, affects only the "skin" and not the internal structure of the system.

We can ask why the spectral and photometric characteristics of quiescent novae are so similar to each other, and why they develop such macroscopically different characteristics in outburst: very fast and very slow evolution of the outburst, expansion velocities up to several thousand km/s or a few hundred km/s, fast novae with smooth light curves, or curves presenting oscillations during the decline, slow novae with a secondary maximum, generally absent in fast novae, etc.

Why do few quiescent novae present coherent oscillations, while the majority of the others present flickering?

Why does the general rule—valid for dwarf novae—that the spectrum of the cold companion is detectable only for orbital periods greater than six hours seem not to be valid for all old novae?

Are some slight differences observed—on the average—among the spectra of dwarf novae, nova-like, and quiescent novae real? Or are they due only to the low number of observations of a same individual with highly variable spectrum? A better understanding of these phenomena could be obtained by long series of observations of a few selected objects, rather than by a few scattered observations of a large number of individuals (see, for example, the important results obtained by the long series of optical observations of GK Per—see Chapter 8—and of UV observations of T CrB—see Chapter 9).

Two important physical quantities that are badly known are the masses of the two members of a nova system. Moderately high-resolution spectra of these faint objects, in the ultraviolet and in the infrared, could improve our knowledge on this fundamental parameter, which is one of the basic assumptions in the theories of thermonuclear runaway. An outburst can be reproduced by these theories if the mass of the white dwarf is larger than the average mass of single white dwarfs (about 0.6 solar masses). Now the existing data (Ritter catalogue, 1987) suggest that white dwarfs in nova systems are included between 0.6 and 1 solar masses, while dwarf novae and nova-like have both lower and higher values, ranging between 0.1 and 1.25 solar masses. However, the sample is much smaller for novae than for the two other groups. Is the frequency of fast and slow novae really different in our galaxy (fast novae represent more than 70% of all novae) and the Andromeda galaxy, where the slow novae are more abundant, according to Arp? Unfortunately we do not have ample statistics on the frequency of various types of novae in outer galaxies.

Another open question is: What are the physical differences that distinguish classical novae from recurrent novae? Some recurrent novae, like T CrB and RS Oph, have a red giant in the system, instead of a red dwarf. This could be a good reason for the difference. But we know that U Sco and T Pyx have a dwarf companion, just as classical novae.

Several novae have been observed in the X-ray range, with the satellites EINSTEIN and EXOSAT. They are rather weak sources in this spectral range. The average X-ray luminosity is about 6×10^{31} erg/s, while the average UV luminosity is 10^{34} - 10^{35}. There is some evidence (but based on a relatively small number of individuals) that fast novae are brighter X-ray sources than slow novae.

GK Per, during the minor outburst of August 9, 1983, was an exceptionally strong X-ray source in the range 2-20 keV, $L_x \sim 10^{34}$ erg s^{-1}.

This same nova was exceptional also in the radio range. Its spectrum indicates a non-thermal origin of the emission, in contrast to all the other classical novae. Interaction with an old planetary nebula in its surrounding could be the reason for this peculiarity.

Thermal radio emission from the envelopes of classical novae has been observed in few cases, and always later than 100 days from outburst for fast novae and as late as 1000 days for the very slow nova HR Del. Instead the recurrent nova RS Oph was found to be a non thermal radio source as soon as 18 days after its last outburst of 1985. A possible explanation could be the interaction of the expanding envelope with the previous ejecta. To this point, it is interesting to note that the recurrent nova T Pyx has an envelope presenting several shells, probably produced in different outbursts. This property is not shared by the envelopes of classical novae, which present polar or equatorial blobs with different chemical and physical properties, but not multiple shells.

II. THE THEORIES

Even though novae have been known and studied for a very long time, the subject is still extremely controversial. Many apparently complex phenomena are observed, and their interpretation is uncertain.

Before its outburst, a classical nova very much resembles a dwarf nova or "nova-like" binary. A component on or very near the lower main sequence in almost all cases appears to lose mass to a companion, usually via an accretion disk. The companion is most easily understood as being a white dwarf. Sudden brightening occurs, followed by a slower fading to a brightness nearly always close to that shortly before the outburst. Examination of the spectrum during an outburst shows spectral line profiles characteristic of a medium in expansion, different layers having different expansion velocities. The brightening can therefore be understood as due to expansion of an initially optically thick envelope, which is ejected at high velocities. The envelope becomes optically thinner with time and eventually has the properties of an expanding nebula, which can be studied in the radio and, even resolved spatially in very late stages. The nova remains active for a long time after the start of the outburst, its bolometric brightness declines very slowly, with most radiation being radiated at shorter and shorter wavelengths (ultraviolet and X rays) in later stages. This bolometric luminosity is not far from the Eddington limit; approximate calculations suggest that the total (radiative and kinetic energy) flux of FH Ser at least may have stayed for some time well above the Eddington limit.

Sometimes a large infrared excess is observed, interpreted as due to dust condensation. The dust appears to be sometimes optically thick, absorbing and reemitting radiation from the centre of the expanding envelope. Absorption by it can also affect emission line profiles. Overabundances in CNO and sometimes in heavier elements, which have been found particularly from studies of the nebular stage, appear to be real. The overabundances are probably related to the speed with which a nova undergoes its development during outburst. A clear anticorrelation between the O/H ratio and the time to decline 3 magnitudes (t_3) was found by Pacheco and Codina (1985).

However, many of the things that happen during an outburst are not clear. In the development of an outburst, higher velocity material appears later and is almost certainly nearer the center of the envelope. It is hard to avoid the conclusion that continued ejection occurs, and the apparent absence of detectable low-velocity material near the centre of the envelope would appear to indicate that the wind is optically thick. The last conclusion is not always accepted, and one future aim must be to test this further. In any case, it is not easy to explain the presence of many layers, having different expansion velocities. A high-velocity wind would form a dense shell by a snowplow effect, following collision with slower moving material ejected at the beginning of an outburst, but usually more layers at different velocities are seen. Collisions between parts of the wind not ejected at the same time with different velocities are possible, while various instabilities may lead to the formation of cool clouds in the line of sight. The dynamics of such processes, including the formation of hot plasma, needs a lot of detailed study. It remains to be seen whether part of the physics is still missing from present ideas. Another point to be emphasized is that ejected material is not spherically symmetric, the origin of polar caps, equatorial rings, etc. is not understood.

Though nobody who works in the field now challenges the theory that the classical nova outbursts are due to thermonuclear runaways in the hydrogen accreted by the white dwarf component of the binary, many problems still remain. The great success of the theory was the prediction that a fast nova, i.e., a nova that undergoes its outburst development rapidly, must have CNO overabundances. The overabundances sometimes observed in heavier elements may be explainable if the outburst then occurs on a very massive white dwarf having a different composition. However, it is difficult to take account of the deviation from spherical symmetry in the accretion process of the white dwarf. In addition, complex processes can be expected during outburst in the general framework of the theory. The outer layers of the white dwarf should expand and engulf the companion star, the motion of the latter in the envelope should generate an extra luminosity, and the result might be a total luminosity

above the Eddington limit. In that case, the radiation pressure associated with the luminosity could accelerate an optically thick wind at large optical depth. Other problems also exist for the theory of nova outbursts. In particular, do novae "hibernate" during outbursts?

It is not clear how different recurrent novae are from classical novae. Recurrent novae do not form a homogeneous group, and it is to be hoped that the number of classes of recurrent novae does not become larger than five, the number of recurrent novae known at the time of this writing! Two (T CrB and RS Oph) have an orbital period of about 200 days, which is much longer than that of classical novae, while the stellar companion is a red giant. These recurrent novae show no clear sign of continued ejection. The outburst spectrum of RS Oph shows the presence of both a low-velocity and a high-velocity component, the latter having a decreasing velocity with time. The spectral development, as well as the observed X-ray emission, have been successfully explained by the interaction of the envelope ejected at high velocity, and the low-velocity wind of the companion red-giant star into which it is ejected. A similar model may work for T CrB, but the three other recurrent novae are different; T Pyx, for instance, cannot have a red giant binary companion. As far as the outburst mechanism is concerned, the situation for recurrent novae is not at all clear. Thermonuclear events have been challenged in the cases of T CrB and RS Oph, for which accretion events have been proposed. However, at the time of this writing there is no consensus about this.

REFERENCES

Adams, W.S., and Joy, A.H. 1933, Pub. A.S.P., 45, 249.

Ahnert, Von P. 1960, Astr. Nach., 285, 191.

Alcock, K.G. 1967, Brit. Astron. Assoc. Circ. 488.

Allen, C.W. 1973, Astrophysical Quantities, London, Athlone Press.

Aller, L.H. 1978, in "IAU Coll.no 76, Planetary Nebulae" ed. Y. Terzian, Dordrecht, Reidel p.225.

Aller, L.H. 1984, "Physics of Thermal Gaseous Nebulae" (Dordrecht: Reidel).

Altamore, A., Baratta, G.B., Cassatella, A., Friedjung, M., Giangrande, A., and Viotti, R.1981, Ap.J. 245, 630.

Altunin, V. I.1976, Soviet Astr. (Letters), 2, 116.

Ambarzumian, V.A. 1932, Pulkovo Circ., 4, .8.

Ambarzumian, V.A. and Kosirev, N. 1933, Z.f. Ap. 7, 320.

Ambruster, C.W., Blitzstein, W, Hull, A.B., and Koch, R.H. 1977, Soviet. Astr., 21, 336.

Anderson, P.H., Borra, E.F., and Dubas O.V. 1971, Pub. A.S.P., 83, 5.

Anderson, C.M., Gallagher, J.S. 1977, Pub. A.S.P., 89,264.

Andrillat, Y., and Fehrenbach, C. 1981, Ap. Space Sci, 76, 149.

Andrillat, Y., Fehrenbach, C., and Houziaux, L. 1974, Ap. Space Sci., 31, 169.

Andrillat, Y., Friedjung, G.M.,and Puget, P. 1982, Proceed. of 3rd European IUE Confer. ESA SP 176, p.191.

Andrillat, Y., and Houziaux, L. 1970a, Ap. Space Sci, 6, 36.

Andrillat, Y., and Houziaux, L. 1970b, Ap. Space Sci, 9, 410.

Andrillat, Y., and Houziaux, L. 1971, Ap. Space Sci., 13, 100.

Antipova, L.I. 1971, Astr. Zh., 48, 288.

Antipova, L.I. 1974, Highlights of Astronomy, 3., ed. G. Contopoulos, (Dordrecht: Reidel), p. 501.

Antipova, L.I. 1977, Astr. Zh., 54, 68 = Soviet Astr., 21, 38.

Arp, H.C. 1956, A.J., 61, 15.

Baade, W. 1947, Pub. A.S.P., 53, 319.

Baade, W., and Zwicky, F. 1934, Proc. Nat. Acad. Sci., 20, 259.

Barlow, M.J., Brodie, J.P., Brunt, C.C., Hanes, D.A., Hill, P.W., Mayo, S.K., Pringle, J.E., Ward, M.J., Watson, M.G., Whelan, J.A.J., and Willis, A.J. 1981, M.N.R.A.S., 195, 61.

Barnard, E.E. 1919, Ap.J., 49, 199.

Bartl, E., and Szumiejko, E. 1975, Acta Astr., 25, 265.

Bath, G.T. 1973, Nature Phys. Sci, 246, 84.

Bath, G.T. 1978, M.N.R.A.S., 182, 35.

Bath, G.T., and Pringle, J.E. 1981, M.N.R.A.S., 194, 964.

Bath, G.T., and Shaviv, G. 1976, M.N.R.A.S., 175, 305.

Bath, G.T., and Shaviv, G. 1978, M.N.R.A.S., 183, 515.

Bayley, J., Hyland, A.R., and Hillier, M. 1985, A.A.O., 34.

Beals, C.S. 1932, M.N.R.A.S., 92, 677.

Beardsley, W.B., King, M.W., Russell, J.L., and Stein, J.W. 1975, Pub. A.S.P., 87, 943.

Becker, R.H. 1981, Ap. J., 251, 626.

Becker, H.J., and Duerbeck, H.W. 1980, Pub. A.S.P., 92, 792.

Becker, R.H., and Marshall, F.E. 1981, Ap. J. (Letters), 244, L93.

Beer, A. 1935, M.N.R.A.S., 93, 538.

Beer, A. 1936, M.N.R.A.S., 96, 238.

Beer, A. 1974, Vistas in Astr., 16, 179.

Bertsch, D.L., Fichtel, C.E., Reames, D.V. 1972, Ap.J. 171, 169.

Bianchini, A. 1980, M.N.R.A.S.,192, 127.

Bianchini, A. 1988, IBVS, No. 3136.

Bianchini, A., Friedjung, M., and Brinkmann, W. 1988, in preparation.

Bianchini, A., Friedjung, M., and Sabbadin, F. 1985a, Inf. Bull. Var. Stars, No. 2650.

Bianchini, A., Friedjung, M., and Sabbadin, F. 1985b, in Recent Results on Cataclysmic Variables, ed. W. Burke, ESA SP-236, 77.

Bianchini, A., Hamzaoglu, E., and Sabbadin, F. 1981, Astr. Ap., 99, 392.

Bianchini, A., and Middletich, J. 1976, IBVS

PRECEDING PAGE BLANK NOT FILMED

1151.
Bianchini, A., and Sabbadin, F. 1982, ESA SP-176, p.187.
Bianchini, A., and Sabbadin, F. 1983, Astr. Ap., 125, 112.
Bianchini, A., and Sabbadin, F. 1985, Inf. Bull. Var. Stars., No. 2751.
Bianchini, A., and Sabbadin, F. 1987, in HE - UHE Behaviour of Accreting X-Ray Sources, Vulcano Workshop 1986, eds. F. Giovanelli and G. Mannocchi, (Bologna: Soc. It. di Fis.), p.53.
Bianchini, A., Sabbadin, F., Favero, G.C., and Dalmeri, I. 1986, Astr. Ap., 160, 367.
Bianchini, A., Sabbadin, F., and Hamzaoglu, E. 1982, Astr. Ap. 106, 176.
Biermann, L., 1939, Z. Astrophys., 18, 344.
Blair, W.P., Stencel. R.E., Feibelman, W.A., and Michalitsianos, A.G. 1983, Ap.J.Suppl. 53, 573.
Blazit, A., Bonneu, D., Koechlin, L., and Labeyrie, A. 1977, Ap. J. (Letters), 214, L79.
Bloch, M., Dufay, J., Fehrenbach, Ch., and Tcheng, M.L. 1946, Ann.Ap. 9,156.
Bode, M.F.(editor) 1987, in RS Ophiuchi (1985) and the Recurrent Nova Phenomenon, (Utrecht:VNU Science Press).
Bode, M.F., Duerbeck, H.D., Seitter, W.C., Albinson, S., and Evans, A., 1988, ESA SP-281, vol. 1, 183.
Bode, M.F., and Evans, A. 1981, M.N.R.A.S., 197, 1055.
Bode, M.F., and Evans, A. 1983, Q.J. R.A.S., 24, 83.
Bode, M.F., and Evans, A. 1985, Astr. Ap., 151, 452.
Bode, M.F., Evans, A.,Whittet, D.C.B., Aitken, D.K., Roche, P.F., and Whitmore, B. 1984, M.N.R.A.S., 207, 897.
Bode, M.F., and Kahn, F.D. 1985, M.N.R.A.S., 217, 205.
Bode, M.F., Seaquist, E.R., and Evans, A. 1987a, M.N.R.A.S., 228, 217.
Bode, M.F., Seaquist, E.R., Frail, D.A., Roberts, J.A., Whittet, D.C.B., Evans, A., and Albison, J.S. 1987b, Nature, 329, 519.
Boggess, A., Bohlin, R.C., Evans, D.C., Freeman, H.R., Gull, T.R., Heap, S.R., Klinglesmith, D.A., Longanecker, G.R., Sparks, W., West, D.K., Holm, A.V., Perry, P.M., Schiffer III, F.H., Turnrose, B.E., Wu, C.C., Lane, A.L., Linsky, J.L., Savage, B.D., Benvenuti, P., Cassatella, A., Clavel, J., Heck, A., Macchetto, F., Penston, M.V., Selvelli, P.L., Dunford, E., Gondhalekar, P., Oliver, M.B., Sanford, M.C.W., Stickland, D., Boksenberg, A., Coleman, C.I., Snijders, M.A.J., and Wilson, R. 1978, Nature, 275, 377.
Boyarchuk, A.A., Galkina, T.S., Gershberg, R.E., Krasnobabtsev, V.I., Rachkovshaya, T.I., and Shakhovskaya, N.S. 1977, Soviet Astr., 21., 257.
Bruch, A. 1980, IBVS, No. 1805.
Bruch, A. 1982, Pub. A.S.P., 94, 916.
Bruch, A., Duerbeck, H.W., and Seitter, W.G. 1981, Astr. Gesell. Mitt. 52, 34.
Burkhead, M.S., Penhallow, W.S., and Honeycutt, R.K. 1971, Pub. A.S.P., 83, 338.
Bychkova, V.S. 1982, Astrofiz. Issl. -Izv. Spets. Astrofiz. Obs., 15, 3.
Bychova, V.S., and Bychkov, K.V. 1976, Astr. Zh., 53, 1196. = Sov. Astr., 20, 675.
Callus, C.M., Albison, J.S., Evans, A., and Bode, M.F. 1986, Light on Dark Matter, ed. F.P. Israel (Dordrecht: Reidel), p. 149.
Campbell, B. 1975, IAU Circ., No. 2839.
Campbell, B. 1976, Ap. J. (Letters), 207, L41.
Campbell, L. 1919, Harv. Ann., 81, 113.
Campbell, L. 1929, Harvard Bull., 835.
Campbell, W.W. 1892, Astr. Ap., 11. 799 (previously The Sidereal Messenger).
Campolonghi, F., Gilmozzi, R., Guidoni, U., Messi, R., Natali, G., and Wells, J, 1980, Astr. Ap., 85, L4.
Cannizzo, J.K., Ghosh, P., and Wheeler, J.C. 1982, Ap. J. (Letters), 260, L83.
Cannizzo, J.K., and Kenyon, S.J. 1986, Ap. J. (Letters), 309, L43.
Cannizzo, J.K., Wheeler, J.C., and Polidan P.S. 1986, Ap. J., 301, 634.
Cannon, A.J. 1920, Harv. Ann., 81, 179.
Carone, T.E., Polidan, R.S., and Wade, R.A., 1985, Proc. of the Ninth North American Workshop on CV'S, ed. P. Szkody (Depart. of Astron. Univ. of Washington), p. 11.

Cassatella, A., Benvenuti, P., Clavel, J., Heck, A., Penston, M., Selvelli, P.L., and Macchetto, F. 1979, Astr. Ap., 74, L18.

Cassatella, A., Gilmozzi, R., and Selvelli, P.L. 1986, "New Insight in Astrophysics", (ESA-SP 263), p. 277.

Cassatella, A., Gilmozzi, R, and Selvelli, P.L. 1990, in prep.

Cassatella, A., and Gonzales Riestra, R. 1988, Physics of Formation of FeII lines outside LTE, eds. R.Viotti et al. (Dordrecht, Reidel), p. 115.

Cassatella, A., Hassal, B.J.M., Harris, A., and Snijders, M.A.J. 1985, Proc. ESA Workshop, Recent Results on Cataclysmic Variables, (Bamberg, ESA SP-236), p. 281.

Cassatella, A., Patriarchi, P., Selvelli, P.L., Bianchi, L., Cacciari, C., Heck, A., Perryman, M., and Wamsteker, W. 1982, Proc. of Third Europ. Conf. (ESA-SP 176), p. 229.

Castor, J.I., and Lamers, H.J.G.L.M. 1979, Ap. J. Suppl., 39, 481.

Catchpole, R.M. 1969, M.N.R.A.S., 142, 119.

Chandrasekhar, S. 1934, M.N.R.A.S., 94, 444.

Chevalier, R.A. 1977, Astr. Ap., 59, 289.

Chevalier, R.A. 1982, Ap. J., 259, 302.

Chevalier, R.A., and Klein, R.I. 1978, Ap. J., 219, 994.

Christy, R.F. 1966, Ap. J., 144, 108.

Chugaj, N.N. 1975, Astr. Zh., 52, 197. = Sov. Astr., 19,119.

Ciardullo, R., Ford, H., and Jacoby, G. 1983, Ap. J., 272, 92.

Ciatti, F., and Mammano, A. 1972, Atti Acad. Naz. Lincei Ser., 8, 52 Fasc. 1, 62.

Clayton, D.D., and Wickramasinghe, N.C. 1976, Ap. Space Sci., 42, 463.

Code, A.D. 1971, The Scientifics Results from OAO-2 (NASA SP-310), p.535.

Cohen, J.G. 1985, Ap. J., 292, 90.

Cohen, J.G., and Rosenthal, A.J. 1983, Ap. J., 268, 689.

Collin-Souffrin, S. 1977, in "Novae and Related Stars", ed. M. Friedjung, (Dordrecht: Reidel), p.123.

Collins, P.L. 1978, IAU Circ., No. 3263.

Colvin, J.D., Van Horn, H.M., Starrfield, S.G. and Truran, J.W. 1977, Ap. J. 212,791.

Cook, M.C. 1981, M.N.R.A.S., 195, 51P.

Cordova, F.A., Jensen, K.A., and Nugent, J.J. 1981a, M.N.R.A.S., 196,1.

Cordova, F.A., and Mason, K.O. 1982, Ap. J., 260, 716.

Cordova, F.A., and Mason, K.O. 1984, M.N.R.A.S., 206, 879.

Cordova, F.A., and Mason, K.O. 1985, Ap. J., 290, 671.

Cordova, F.A., Mason, K.O., and Nelson, J.E. 1981b, Ap. J., 245, 609.

Couderc, P. 1939, Phys. Ber. Leipzig, 20, 2177.

Crampton, D., Cowley, A.P., and Fisher, W.A. 1986, Ap. J., 300, 788.

Crampton, D., Cowley, A.P., and Hutchings, J.B. 1983, IAU Colloquium 72, Cataclysmic Variables and Related Objects, eds. M. Livio and G. Shaviv (Dordrecht, Reidel), p. 25.

Davis, R.J. 1987, in RS Ophiuchi (1985) and the Recurrent Nova Phenomenon, ed. M.F. Bode (Utrecht:VNU Science Press).

Delbourgo-Salvador, P., Mochkovitch, R., and Vangioni-Flam, E. 1985, ESA SP-236, p. 229.

Dinerstein, H.L. 1986, Astr. J., 92, 1381.

Dmitrienko, E.S., and Cherepashchuk, A.M. 1980, Soviet Astr., 24, 432.

Doroshenko, V.T. 1968, Soviet Astr., 12, 95.

Drechsel, H., Rahe,J, Duerbeck, H.W., Kohoutek, L., and Seitter, W.C. 1977, Astr. Ap. Suppl., 30, 323.

Drechsel, H., Rahe, J., Holm, A., and Krautter, J. 1980, The Messenger No 22, p. 10.

Drechsel, H., Rahe, J., Holm, A., and Krautter, J. 1981, Astr. Ap., 99, 166.

Drechsel, H., Rahe, J., Seward, F.D., Wang, Z.R., and Wargau, W. 1983a, Astr. Ap., 126, 357.

Drechsel, H., Rahe, J., and Wargau, W. 1983b, The Messenger, 32, p. 35.

Drechsel, H., Wargau, W., Rahe, J. 1984, Astr. Space Science 99, 85.

Duerbeck, H.W. 1980, Habilitation thesis, Bonn University.

Duerbeck, H.W. 1981, Pub. A.S.P., 93, 165.

Duerbeck, H.W. 1984, Astroph. Space Science, 99, 363.

Duerbeck, H.W. 1986, Mitt. Astron. Ges., 67, 309.
Duerbeck, H.W. 1987a, Ap Space Sci, 131, 461.
Duerbeck, H.W. 1987b, ESO Messenger, 50, 8.
Duerbeck, H.W. 1987c, Space Sci. Rev., 45, 1.
Duerbeck, H.W., Klare, G., Krautter, J., Wolf, B., Seitter, W.C., and Wargan, W. 1980a, Proced. 2 IUE Conf. ESA S.P., 157, p. 91.
Duerbeck, H.W., Rindermann, K., and Seitter, W.C. 1980b, Astr. Ap. 81, 157.
Duerbeck, H.W., and Seitter, W.C. 1979, ESO Messenger, 17, 1.
Duerbeck, H.W., and Seitter, W.C. 1980, IBVS.
Duerbeck, H.W., and Seitter, W.C. 1987, Ap. Space Sci, 131, 467.
Duerbeck, H.W., Seitter, W.C., and Duemmler, R. 1987, M.N.R.A.S., 229, 653.
Duerbeck, H.W., and Wolf, B. 1977, Astr. Ap. Suppl., 29, 297.
Dufay, J., and Bloch, M. 1964, Ann. Ap., 27, 462.
Dufay, J., Bloch, M., Bertaud, Ch., and Dufay, M. 1964, Ann. Ap., 27, 555.
Dultzin-Hacyan, D., Andrillat, Y., Audouze, J., Friedjung, M., Gordon, C., Rocca-Volmerange, B., and Stasinska, G. 1980, Proceed. of 2nd Europ. IUE Cong., (ESA SP-157), p. 87.
Duschl, W.J., Meyer-Hofmeister, E., and Meyer, F. 1985, in Recent Results on Cataclysmic Variables, ESA SP-236, 221.
Eddington, A.S. 1921, Zs. Physik, 7, 351.
Edward, D.A., and Pringle J.E., 1987, M.N.R.A.S. 229, 383.
Eggen, O.J., Matheson, D.S., and Serkowski, K. 1967, Nature, 213, 216.
Elvey, C.T., and Babcock, H.W. 1943, Ap. J., 97, 412.
Ennis, D., Becklin, E.E., Beckwith, S., Elias, J., Gatley, I., Matthews, K., Neugebauer, G., and Willner, S.P. 1977, Ap. J. 214, 478.
Evans, A. 1985, Observatory, 105, 6.
Evans, A. 1987, in RS Ophiuchi (1985) and the Recurrent Nova Phenomenon, ed. M.F. Bode, (Utrecht: VNU Science Press).
Faulkner, J., Lin, D.N.C., and Papapaloizou, J. 1983, M.N.R.A.S., 205, 359.
Feast, M.W., and Glass, I.S. 1974, M.N.R.A.S., 167, 81.
Fehrenbach, Ch., Andrillat, Y., and Bloch, M. 1967, Publ. Obs. Haute Provence, 9, No. 19.
Fehrenbach, Ch., Andrillat, Y., and Bloch, M. 1968a, Publ. Obs. Haute Provence, 9, No. 25.
Fehrenbach, Ch., Andrillat, Y., Bloch, M. and Houziaux, L. 1968b, Publ. Obs. Haute Provence, 10, No. 7.
Fehrenbach, Ch., and Petit, M. 1969, Astr. Ap., 1, 403.
Ferland, G.J. 1977a, Ap. J. (Letters), 212, L21.
Ferland, G.J. 1977b, Ap. J., 215, 873.
Ferland, G.J. 1980, Observatory, 100, 166.
Ferland, G.J., Lambert, D.L., Netser, H., Hall, D.N.B., Ridgeway, S.T. 1979, Ap. J. 227, 489.
Ferland, G.J., Lambert, D.L., Mc.Call, M.L., Shields, G.A., and Slovak, M.H. 1982 a, Ap. J., 260, 794.
Ferland, G.J., Lambert, D.L., Netzer, H., Hall, D.N.B., and Ridgway, S.T. 1979, Ap. J. 227, 489
Ferland, G.J., Lambert, D.L., and Woodman, J.H. 1977, Ap. J., 213, 132.
Ferland, G.J., Lambert, D.L., and Woodman, J.H. 1986, Ap. J. Suppl., 60, 375.
Ferland, G.J., Longer, S.H., Mac Donald, J., Pepper, G.H., Shaviv, G., and Truran, J.W. 1982b, Ap. J., 262, L53.
Ferland, G.J., and Shields, G.A., 1978a, Ap. J. (Letters), 224, L15.
Ferland, G.J., and Shields, G.A. 1978b, Ap. J., 226, 172.
Ferland, G.J., and Truran, J.W. 1981, Ap. J., 244, 1022.
Ferland, G.J., Williams, R.E., Lambert, D.L., Schields, G.A., Slovak, M., Gondhalekar, P.M., and Truran, J.W. 1984, Ap. J., 281, 194.
Fiedler, R.L., and Jones, T.W. 1980, Ap. J., 239, 253.
Finzi, A. 1973, Ap. J., 183, 183.
Folkart, B., Pecker, J.C., and Pottasch, S.R. 1964, Ann. Ap., 27, 249.
Folkart, B., Pecker, J.C., and Pottasch, S.R. 1964, Ann. Ap., 27, 252.
Fried, J.W. 1980, Astr. Ap., 81, 182.
Friedjung, M. 1966a, M.N.R.A.S., 131, 447.
Friedjung, M. 1966b, M.N.R.A.S., 132, 143.
Friedjung, M. 1966c, M.N.R.A.S., 132, 317.
Friedjung, M. 1968, Astroph. Lett. 2, 121.

Friedjung, M. 1977a, Novae and Related Stars, ed. M. Friedjung. (Dordrecht, Netherlands), p. 61.
Friedjung, M. 1977b, in Novae and Related Stars, ed. M. Friedjung, (Dordrecht: Reidel), p. 95.
Friedjung, M. 1981a, Acta Astr., 31, 373.
Friedjung, M. 1981b, Astr. Ap., 93, 320.
Friedjung, M. 1985, in Multifrequency Behavior of Galactic Accreting Sources, ed. F. Giovanelli, (CSN: Frascati), p. 65.
Friedjung, M. 1987a, Astr. Ap., 180, 155.
Friedjung, M. 1987b, Astr. Ap., 179, 164.
Friedjung, M. 1988, Classical Novae, eds. M.F. Bode and A. Evans, (Wiley Interscience).
Friedjung, M., Andrillat, Y, and Puget, P. 1982, Astr. Ap., 114, 351.
Friedjung, M., and Smith, M.G. 1966, M.N.R.A.S., 132, 239.
Fujimoto, M.Y. 1982, Ap. J., 257, 752 and 767.
Galeotti, P., and Pasinetti, L.E. 1970, Contr. Oss. Astr. Milano-Merate N.S., Nos. 328, 329.
Gallagher, J.S. 1977, Astr. J., 82, 209.
Gallagher, J.S. and Code, A.D. 1974, Ap. J., 189, 303.
Gallagher, J.S., Hege, E.K., Kopriva, D.A., Williams, R.E., and Butcher, H.R. 1980, Ap. J., 237, 55.
Gallagher, J.S., and Holm, A.V. 1974, Ap. J., 189, L123..
Gallagher, J.S., and Ney, E.P. 1976, Ap. J. (Letters), 204, L35.
Gallagher, J.S., and Oinas, V. 1974, Pub. A.S.P., 86, 952.
Gallagher, J.S., and Starrfield, S. 1976, M.N.R.A.S., 176, 53.
Gallagher, J.S., and Starrfield, S. 1978, Ann. Rev. Astr. Ap., 16, 171.
Gehrz, R.D., Grasdalen, G.L., Hackwell, J.A., and Ney, E.P. 1978, IAU Circ. 3296.
Gehrz, R.D., Grasdalen, G.L., Hackwell, J.A., and Ney, E.P. 1980a Ap. J., 237, 855.
Gehrz, R.D., Grasdalen, G.L., and Hackwell, J.A. 1985, Ap. J. (Letters), 298, L47.
Gehrz, R.D., Grasdalen, G.L., Greenhouse, M., Hackwell, J.A., Hayward, T., and Bentley, A.F. 1986, Ap. J. (Letters), 308, L63.
Gehrz, R.D., Hackwell, J.A., Grasdalen, G.L., Ney, E.P., Neugebauer, G., and Sellgren, K. 1980b, Ap. J., 239, 570.
Geisel, S.L., Kleinmann, D.E., and Low, F.J. 1970, Ap. J. (Letters), 161, L101.
Gershberg, R.E. 1964, Izv. Krym. Astrofiz., 32, 133.
Giacconi, R., Branduardi, G., Briel, U., Epstein, A., Fabricant, D., Feigelson, E., Forman, W., Gorenstein, P., Grindlay, J., Gursky, H., Harnder, Jr., F.R., Henry, J.P., Jones, C., Kellogg, E., Koch, D., Murray, S., Schreier, E., Seward, F., Tananbaum, H., Topka, K., Van Speybroek, L., Holt, S.S., Becker, R.H., Boldt, E.A., Serlemitsos, P.J., Clark, G., Canizares, C., Markert, T., Novick, R., Helfand, D, and Long, K. 1979, Ap. J., 230, 540.
Giannone, P., and Weigert, A. 1967, Zs. Astrophys., 67, 41.
Gilliland, R.L., Kemper, E., and Suntzeff, N. 1986, Ap. J., 301, 252.
Gilmozzi, R., Cassatella, A. and Selvelli, P.L. 1987, in Proc. of Vulcano Workshop 1986, He-UHE Behaviour of Accreting X-Ray Sources, eds. F. Giovanelli and G. Mannocchi, (Italian Physical Society Conference Proceedings), Vol. 8, p. 49.
Giuricin, G., Mardirossian, F., Mezzetti, M., Pucillo, M., Santin, P., and Sedmak, G. 1979, Astr. Ap., 80, 9.
Gorbatskii, V.G. 1958, Scientific Notes of the Leningrad State Univ., No. 273, Math. Section, No. 34, p. 30.
Gorbatskii, V.G. 1962, Scientific Notes of the Leningrad State Univ., No. 307, Math. Section, No. 36, p. 45.
Gorbatskii, V.G. 1972, Astr. Zh., 49, 42. = Sov. Astr., 16, 32.
Gorbatskii, V.G. 1973, Astr. Zh., 50, 19. = Sov. Astr., 17, 11.
Gorbatskii, V.G. 1974, Astrophysic, 8, 220.
Gorbatskii, V.G. 1977 Astr. Zh. 54, 1036; Sov. Astr. 21, 587.
Gorbatskii, V.G., and Minin, I.N. 1963, in Non Stable Stars, (Moscow: State Pub. House), p. 355.
Gordeladse, Sh.G. 1937, Byull. Abastumani Astrofiz. Obs., 1, 55.
Greenstein, J.L. 1960, Stellar Atmospheres, ed. J.L. Greenstein, (Univ. of Chicago), p. 676.
Greenstein, J.L., and Kraft, R.P. 1959, Ap. J.,

130, 99.
Grotrian, W. 1930, Zs. Astrophys., 2. 78.
Grotrian, W. 1937, Zs. Astrophys., 13, 215.
Gurevich, L.E., and Lebedinskii, A.I. 1947a, Doklady AN SSSR 56, No. 1, 2.
Gurevich, L.E., and Lebedinskii, A.I. 1947b, Zhurn, Eksperim. i Teor. Fiz., 17, 792.
Gyldenkerne, K., Meydahl, V., and West, R.M. 1969, Pub. Mindre Medd. Kobenhavns Obs., No. 201.
Haefner, R. 1981, IBVS, No. 2045.
Haefner, R., and Metz, K. 1982, Astr. Ap., 109, 171.
Haefner, R., and Metz, K. 1985, Astr. Ap., 145, 311.
Haefner, R., and Schoembs, R. 1985, Astr. Ap., 150, 325.
Halm, J. 1901, Astr. Nachr., 156, 147.
Halm, J. 1904, Proc. Roy. Soc. Edinburgh, 25, 513.
Hanes, D.A. 1985, M.N.R.A.S., 213, 443.
Hanuschik, R.W., and Dachs, J. 1987, in ESO Workshop on the SN 1987 A, ed. I.J. Danziger, p. 153.
Harkness, R.P. 1983, M.N.R.A.S., 204, 45.
Hartmann, J. 1925, Astr. Nachr., 226, 63.
Hartmann, J. 1926, Astr. Nachr., 226, 203.
Hazlehurst, J. 1962, Advances in Astr. Ap., 2, ed. Z. Kopal, (New York and London: Academic Press), p. 1.
Henbest, N. 1987, New Scientist 116, No. 1585, p. 52.
Herbig, G. 1955, (see Beer 1974) in Vistas, 16, 179, p. 259.
Herbig, G.H., and Neubauer F.J. 1946, Pub. A.S.P., 58, 196.
Herczeg, T. 1982, IBVS, No. 2078.
Hjellming, R.M., van Gorkom, J.H., Taylor, A.R., Seaquist, E.R., Padin, S., Davis, R.J., and Bode, M.F. 1986, Ap. J. (Letters), 305, L71.
Hjellming, R.M., and Wade, C.M. 1970, Ap. J. (Letters), 162, L1.
Hjellming, R.M., Wade, C.M., Vandenberg, N.R., and Newell, E.B. 1979, Astron. J., 84., 1619.
Hoffmann, J.A., Lewin, W.H.G., Brecher, K. Buff, J., Clark, G.W., Joss, P.C., and Matilsky, T. 1976, Nature 261, 208.
Holm, A., and Crabb, W. 1979, NASA IUE (Letter 7), p. 40.
Honda, M. 1982, IAU Circ. No. 3661.
Hoshi, R. 1979, Prog. Theor. Phys., 61, 1307.
Huang, S.S. 1956, Astron. J. 61, 49.
Hudec, R. 1978, Bull. Astr. Inst. Czech., 32, 93.
Huggins, W., 1892, Astr. Ap., 11, 571.
Huggins, W., and Miller, W.A. 1866, Proc. Roy. Soc. London 15, 146. - M.N.R.A.S., 26, 275.
Humason, M.L. 1938, Ap. J., 88, 228.
Hutchings, J.B. 1969, Pub. Dom. Ap. Obs., 13, 14 and 16.
Hutchings, J.B. 1972, M.N.R.A.S., 158, 177.
Hutchings, J.B. 1979a, Pub. A.S.P., 91, 661.
Hutchings, J.B. 1979b, Ap. J., 230, 162.
Hutchings, J.B. 1980, Pub. A.S.P., 92, 458.
Hutchings, J.B., and Fisher, W.A. 1973, Pub. A.S.P., 85, 122.
Hutchings, J.B., Smolinski, J., and Grygar, J. 1971, Pub. A.S.P., 83, 15.
Hyland, A.R., and Neugebauer, G. 1970, Ap. J. (Letters) 160, L177.
Iben, Jr., I., and Tutukov, A.V. 1984, Ap. J. Suppl., 54, 335.
Iwanoska, W., Mitchell, W.E., and Keenan, P.C. 1960, Ap. J., 132, 271.
Jenkins, E.B., Snow, T.P., Upson, W.L., Starrfield, S.G., Gallagher, J.S., Friedjung, M., Linsky, J.L., Anderson, R., Henry, R.C., and Moos, H.W., Ap. J. 1977, 212, 198.
Jensen, K.A. 1984, Ap. J. 278, 278.
Jensen, K.A. 1985, Cataclysmic Variables and Low Mass X-Ray Binaries, eds. D.Q. Lamb and J. Patterson (Dordrecht: Reidel), p. 407.
Joy, A.H., 1938, Pub. A.S.P., 50, 300.
Joy, A.H., 1945, Pub. A.S.P., 57, 171.
Joy, A.H., and Swings, P. 1945, Ap. J., 102, 353.
Kahn, F.D. 1976, Astr. Ap., 50, 145.
Kaler, J.B. 1986, Pub. A.S.P., 98, 243.
Kaplan, S.A., and Pikelner, S.B. 1970, The Interstellar Medium, (Cambridge: Cambridge Univ. Press.), p. 19.
Kato, M. 1983, Publ. Astron. Soc. Japan 39, 507.
Kato, M., and Hachisu, I. 1988 Ap. J. 329, 808.

Kenyon S.J. 1986, Astr. J., 91, 503.
Kenyon, S.J. 1988, in IAU Colloquium 103, The Symbiotic Phenomenon, eds. J. Mikolajewska, M. Friedjung, S.J. Kenyon and R. Viotti, (Kluwer Academic Publish.), p. 161.
Kenyon, S.J., and Berriman, G. 1988, Astr. J., 95, 526.
Kenyon, S.J., and Garcia, M.R. 1986, Astr. J., 91, 125.
Kenyon, S.J., and Webbink, R.F. 1984, Ap. J. 279, 252.
King, A.R., Ricketts, M.J., and Warwick, R.S. 1979, M.N.R.A.S., 187, 77P.
Kippenhahn R., and Thomas, H.C. 1978, Astr. Ap. 63, 265.
Klare, G., Wolf, B., and Krautter, J. 1980, Astr. Ap., 89, 282.
Kleine, T., and Kohoutek, L. 1979, Astr. Ap., 76, 133.
Kohoutek, L. 1981, M.N.R.A.S., 196, 87p.
Kohoutek, L., and Pauls, R. 1980, Astr. Ap., 92, 200.
Kolotilov, E.A., 1980, Soviet Astr. (Letters), 6, 268.
Kopal, Z. 1987, Private Communication to Seitter in RS Ophiuchi (1985) and the Recurrent Nova Phenomenon, ed. M.F. Bode, (Utrecht: VNU Science Press), p. 63.
Kosirev, N.A. 1934, M.N.R.A.S., 94, 430.
Kraft, R.P. 1958, Ap. J., 127, 625.
Kraft, R.P. 1959, Ap. J., 130, 110.
Kraft, R.P. 1963, Advances in Astronomy and Astrophysics 2, ed. Z. Kopal, (New York and London: Academic Press), p. 43.
Kraft, R.P. 1964, Ap. J., 139, 457.
Krautter, J. 1986, Proceedings IUE Conference: New Insights in Astrophysics, (ESA SP-263), p. 275.
Krautter, J., Beuermann, K., Leitherer, C., Oliva, E., Moorwood, A.F.M., Deul, E., Wargau, W., Klare, G., Kohoutek, L., Van Paradijs, J., and Wolf, B. 1984, Astr. Ap., 137, 307.
Krautter, J., Beuermann, K., and Ogelman, H. 1985, Space Sci Rev., 40, 156.
Krautter, J., Klaas, U., and Radons, G. 1987, Astr. Ap., 181, 373.
Krautter, J., Klare, G., Wolf, B., Duerbeck, H.W., Rahe, J., Vogt, N., and Wargau, W. 1981, Astr. Ap., 102, 337.
Kruszewski, A., Semeniuk, I., and Duerbeck, H.W. 1983, Acta Astr. 33, 339.
Kubiak, M. 1984, Acta Astr., 34, 331.
Kupo, I., and Leibowitz, E.M. 1977, Astr. Ap., 56, 181.
Kurochkin, N.E., and Karitskaya, E.A. 1986, Astr. Tsirk., No. 1441, 7.
Kurucz, R.L. 1979, Ap. J. Suppl., 40, P1.
Kutter, G.S., and Sparks, W.M. 1987, in press.
Kylafis, N.D., and Lamb, 1982, Ap. J., 48, 239.
Lacy, C.H. 1977, Ap. J. Suppl. 34, 479.
Lambert, D.L. 1978, M.N.R.A.S. 182, 249.
Lambert, D.L., Slovak, M.H., and Shields, G.A. 1980, NASA Conf. Publ. 2171, The Universe at UV wavelengths, (Greenbelt, Maryland), p. 461.
Lance, C.M., McCall, M.L., and Uomoto, A.K. 1988, Ap. J. Suppl., 66, 151.
Lancy, D. 1985, IAU Circ., No. 4036.
Larsson-Leander, G. 1953, Stockholm Ann. 17, No. 8.
Larsson-Leander, G. 1954, Stockholm Ann. 18, No. 4.
Lau, H.E. 1906, Bull. Astr., 23, 297.
Law, W.Y., and Ritter, H. 1983, Astr. Ap., 123, 33.
Lebedinskii, A.I. 1946, Astr. Zh., 23, 15.
Lewin, W.H.G., Doty, J., Clark, G.W., Rappaport, S.A., Bradt, H.V.D., Doksey, R., Hearn, D.R., Hoffmann, J.A., Jernigan, J.G., Li, F.K., Mayer, W., McClintock, J., Primini, F., and Richardson, J. 1976, Ap. J. (Letters) 207, L95.
Livio, M. 1987, Comments Astrophys., 12, 87.
Livio, M. 1988a, in IAU Colloquium 103, The Symbiotic Phenomenon, eds. J. Mikolajewsha, M. Friedjung, S.J. Kenyon, R. Viotti, (Kluwer Academic Publ.), p. 323.
Livio, M. 1988b, in IAU Colloquium 108, Atmospheric Diagnostics of Stellar Evolution, K. Nomoto, ed., p. 226.
Livio, M., Truran, J.W., and Webbink, R. 1986, Ap. J., 308, 736.
Lockwood, G.W., and Millis, R.L. 1976, Pub. A.S.P., 88, 235.
Loreta, E. 1987, in Rosino, RS Ophiuchi (1985)

and the Recurrent Nova Phenomenon, ed. M.F. Bode, (Utrecht: VNU Science Press), p. 4.
Lynden-Bell, D. 1969, Nature, 223, 690.
MacDonald, J. 1980, M.N.R.A.S., 191, 933.
MacDonald, J. 1983, Ap. J., 273, 289.
MacDonald, J. 1986, Ap. J., 305, 251.
MacDonald, J., Fujimoto, M.Y., and Truran, J.W. 1985, Ap. J., 294, 263.
Malakpur, I. 1973a, Astr. Ap., 24, 125.
Malakpur, I. 1973b, Astr. Ap., 28, 393.
Malakpur, I. 1973c, Astroph. Space Sci. 24, 577.
Malakpur, I. 1980, Ap. Space Sci., 72, 143.
Marino, B.F., and Walker, M.F. 1982, Publ. Var. Star Section, Roy. Astr. Soc. (New Zealand).
Mason, K.O., Cordova, F.A., Bode, M.F., and Barr, P. 1987, RS Ophiuchi (1985) and the Recurrent Nova Phenomenon, ed. M.F. Bode, (Utrecht: VNU Science Press), p. 167.
Mattei-Akyuz, J. 1974, J.R.A.S. Canada, 68, 22.
Mazeh, T., Netzer, H., Shaviv, G., Drechsel, H., Rahe, J., Wargau, W., Blades, J.C., Cacciari, C., and Wamsteker, W. 1985 a, Astr. Ap., 149, 83.
Mazeh, T., Tal, Y., Shaviv, G., Bruch, A., and Budell, R. 1985b, Astr. Ap., 149, 470.
McCray, R. 1983, in Highlights of Astronomy 6, ed. R.M. West, p. 565.
McCrea, W.H. 1937, Observatory, 60, 277.
McKellar, A. 1937, Publ. Dom. Ap. Obs., 6, 353.
McLaughlin, D.B. 1935, Publ. Am. Astron. Soc., 8, 145.
McLaughlin, D.B. 1937, Publ. Obs. Univ. Michigan, 6, No. 12, 107.
McLaughlin, D.B. 1942, Ap. J., 95, 428.
McLaughlin, D.B. 1943, Publ. Obs. Univ. Michigan, 8, No. 12, 149.
McLaughlin, D.B. 1945, Pub. A.S.P., 57, 69.
McLaughlin, D.B. 1946, Pub. A.S.P., 58, 46.
McLaughlin, D.B. 1947, Pub. A.S.P., 59, 244.
McLaughlin, D.B. 1950, Pub. A.S.P., 62, 185.
McLaughlin, D.B. 1954, Ap. J., 119, 124.
McLaughlin, D.B. 1960, in Stars and Stellar Systems VI, ed. J.L. Greenstein, Stellar Atmospheres, (Chicago: Univ. of Chicago Press) p. 585.
McLaughlin, D.B. 1969, Pub. Obs. Univ. Michigan, vol. IX, No. 3.
Medway, K. 1985, IAU Circ., No. 4048.
Meinel, A.B. 1963, Ap. J., 137, 834.
Mendoza, C. 1983, in IAU Symposium 103, Planetary Nebulae, ed. D.R. Flower, (Dordrecht: Reidel), p. 143.
Menzel, D.H., and Payne, C. 1933, Wash. Nat. Acad. Proc., 19, 641.
Mestel, L. 1952, M.N.R.A.S., 112, 598.
Meyer, F., and Meyer-Hofmeister, E. 1981, Astr. Ap. (Letters), 104, L10.
Meyer, F., and Meyer-Hofmeister, E. 1982, Astr. Ap., 106, 34.
Middleditch,J.,and Nelson,J.1979,Bull. AAS, 11, 664.
Middleditch, J., and Nelson, J. 1980, Bull. AAS, 12, 848.
Milne, E.A. 1926, M.N.R.A.S., 86, 459.
Milne, E.A. 1931, M.N.R.A.S., 91, 4. - Observatory, 54, 140.
Mineshige, S., and Osaki, Y. 1983. Pub. Astr. Soc. Japan, 35, 377.
Mitchell, R.M., Evans, A., and Albinson, J.S. 1986, M.N.R.A.S. 221, 663.
Mitchell, R.M., Robinson, G., Hyland, A.R., and Neugebauer, G. 1985, M.N.R.A.S., 216, 1057.
Morrison, W. 1985, IAU Circ., No. 4030.
Mumford, G.S. 1966a, Ap. J., 146, 111.
Mumford, G.S. 1966b, Ap. J., 146, 962.
Mumford, G.S. 1971, Ap. J., 165, 369.
Mustel, E.R. 1957, in IAU Symposium 3, Non-Stable Stars, ed. G.H. Herbig, (Cambridge: Univ. of Cambridge Press), p. 57.
Mustel, E.R. 1956, The mechanism of ejection of matter from novae, Vistas in Astr., ed. A. Beer, 2, p. 1496.
Mustel, E.R. 1958, in IAU Symposium 6, Electromagnetic Phenomena in Cosmical Physics, ed. B. Lehnert, London, Cambridge Univ. p. 193.
Mustel, E.R. 1962, Astr. Zh., 39, 185.
Mustel, E.R. 1964, Soviet Astr., 7, 772.
Mustel, E.R. 1974 in IAU Symposium 66, Late Stages of Stellar Evolution, R.J. Tayler and J.E. Hesser, eds., Reidel.
Mustel, E.R. 1978, Problems of Physics and Evolution of the Universe, Pub. Armenic. Ac.

of Sciences, p. 221, 233.
Mustel, E.R., and Antipova, L.I. 1971, Nauchn. Inf., 19, 32.
Mustel, E.R., and Antipova, L.I. 1972, Scient. Inform. Astr. Council USSR, (Moscow: Academy of Sciences), 19, 32.
Mustel, E.R., and Baranova, L.I. 1965, Astr. Zh., 42, 42.
Mustel, E.R., and Baranova, L.I. 1966, Soviet Astr., 43, 488.
Mustel, E.R., and Boyarchuk, A.A. 1958, Izv. Krymsk. Astrofiz., 20, 86.
Mustel, E.R., and Boyarchuk, A.A. 1959, Astr. Zh., 36, 762.
Mustel, E.R., and Boyarchuk, A.A. 1970, Ap. Space Sci., 6, 183.
Nariai, K. 1974, Astr. Ap., 36, 231.
Neckel, Th., and Klare, G. 1980, Astr. Ap. Suppl., 42., 251.
Neff, J.S., Smith, V.V., and Ketelsen, D.A. 1978, Ap. J. Suppl., 38, 89.
Newton, I. 1713, Principia Mathematica Philosophiae Naturalis, second Ed., 3rd book, section 5., p. 541.
Ney, E.P., and Hatfield, B.F. 1978, Ap. J. 219, L111.
Nussbaumer, H., and Stencel, R.E. 1987, Exploring the Universe with the IUE Satellite, ed. Y. Kondo, (Dordrecht, Reidel), p. 203.
Nussbaumer, H., and Storey, P.J. 1984, Astr. Ap. Suppl., 56, 293.
Oehler H. 1936, Z. Astroph. 12, 281.
Ogelman, H., Beuermann, K., and Krautter, J. 1984, Ap. J., 287, L31.
Ogelman, H., Krautter, J., and Beuermann, K. 1987, Ap. Space Sci. 130, 279.
Ogelman, H., Krautter, J., and Beuermann, K. 1987, Astron. Astroph. 177, 110.
Oke, J.B., and Wade, R.A. 1982, A. J., 87, 670.
Oort, J.H. 1946, M.N.R.A.S., 106, 159.
Oort, J. 1950, Ed., IAU Trans. VII, (Cambridge: Cambridge Univ. Press), p. 305.
Oort, J.H. 1951, in "Problems of cosmical aerodynamics", Dayton, OH 1951, p. 118.
Ortolani, S., Rafanelli, P., Rosino, L., and Vittone, A. 1978, IAU Circ. 3276.
Osaki, Y. 1974, Pub. Astr. Soc. Japan, 26, 429.
Oskanyan, A.V. 1983, IBVS, No. 2349.
Osterbrock, D.E. 1974, "Astrophysics of Gaseous Nebulae", (San Francisco: Freeman).
Pacheco, J.A., and Codina, L.S. 1985, M.N.R.A.S. 214, 481.
Paczynski, B. 1965, Acta Astr., 15, 197.
Paczinski, B. 1971, Ann. Rev. Astronom. Astroph. 9, 183.
Paczinsky, B., and Sienkiewicz, R. 1972, Acta astr., 22, 73.
Padin, S., Davis, R.J., and Bode, M.F. 1985, Nature, 315, 306.
Palmer, L.H. and Africano, J.L. 1982, IBVS, No. 2069.
Panek, R.J. 1979, Ap. J. 234, 1016.
Patterson, J. 1978, Ap. J., 225, 954.
Patterson, J. 1979a, Ap. J. (Letters), 233, L13.
Patterson, J. 1979b, Ap, J., 231, 789.
Patterson, J. 1980, Ap. J., 241, 235.
Patterson, J. 1984, Ap. J. Suppl. 54, 443.
Patterson, J., and Raymond, J.C. 1985a, Ap. J., 292, 535.
Patterson, J. and Raymond, J.C. 1985b, Ap. J. 292, 550.
Pavlenko, E.P. 1983 , Soviet Astr. Lett., 9, 119.
Payne-Gaposchkin, C. 1957, Galactic Novae, Pub. North-Holland.
Payne-Gaposchkin, C., and Gaposchkin, S. 1942, Harv. Circ., 445.
Payne-Gaposchkin, C., and Whipple, F.L. 1939, Harv. Circ., 433.
Payne-Gaposchkin, C., and Menzel, D.H. 1938, Harv. Circ., 428.
Peimbert, M. and Sarmiento, A. 1984, Astr. Express, 1, 97.
Peltier, L. 1958, Sky and Telescope, 17, 555.
Pettit, E. 1946a, Publ. A.S.P., 58, 159.
Pettit, E. 1946b, Publ. A.S.P., 58, 255.
Pettit, E. 1946c, Publ. A.S.P., 58, 359.
Petterson, J.A. 1979, IAU Colloquium 53, White Dwarfs and Variable Degenerate Stars, ed. H.M. Van Horn and V. Weidemann, (Publ. University of Rochester) p. 412.
Petterson, J.A. 1980, Ap. J., 241, 247.
Pfau, W. 1976, Astr. Ap., 50, 113.
Phillips, J.P., and Reay, N.K. 1977, Astr. Ap., 59, 91.
Piccioni, A., Guarnieri, A., and Bartolini, C. 1984, Acta Astr. 34, 473.

Pickering, E.C. 1905, Harv. Circ., 99.
Pickering, W.H. 1894, Astr. Ap. 13, 201.
Piirola, V., and Korhonen, T. 1979, Astr. Ap., 79, 254.
Pike, S.R. 1928, Proc. Leeds Philos. and Literary Soc.
Pike, S.R. 1929, M.N.R.A.S., 89, 538.
Pilyugin, S.L. 1986, Astrophysics, 23, 527.
Plavec, M., Ulrich, R.K., and Polidan, R.S. 1973, Pub. A.S.P., 85, 769.
Pogson, R.N., 1908, Mem. RAS, 58, 90.
Popper, D. 1940, Ap. J. 92, 262.
Porcas, R.W., Davis, R.J., and Graham, D.A. 1987, in RS Ophiuchi (1985) and the Recurrent Nova Phenomenon, ed. M.F. Bode, (Utrecht: VNU Science Press), p. 203.
Pottasch, S.R. 1959a, Ann. Astrophys., 22, 297.
Pottasch, S.R. 1959b, Ann. Astrophys., 22, 310.
Pottasch, S.R. 1959c, Ann. Astrophys., 22, 318.
Pottasch, S.R. 1959d, Ann. Astrophys., 22, 394.
Pottasch, S.R. 1959e, Ann. Astrophys., 22. 412.
Pottasch, S.R. 1967, Bull. Astr. Inst. Neth., 19, 227.
Pottasch, S.R. 1985, "Planetary Nebulae" (Reidel Publ. Company).
Prialnik, D. 1986, Astrophys. J., 310, 222.
Rafanelli, P., and Rosino, L. 1978, Astr. Ap. Suppl., 31, 337.
Rahe, J., Boggess, A., Drechsel, H., Holm, A., and Krautter, J. 1980, Astr. Ap. (Letters), 88, L9.
Raikova, D.V. 1977, Soviet Astr., 21, 30.
Raymond, J.C., Cox, D.P., and Smith, B.W. 1976, Ap. J., 204, 290.
Reimers, D. and Cassatella, A. 1985, Ap. J., 297, 275.
Reynolds, S.P., and Chevalier, R.A. 1984, Ap. J. (Letters), 281, L33.
Richter, G.A. 1986, Astr. Nach., 307, 221.
Right, W.H. 1925, Pub. A.S.P., 37, 235.
Rinsland, C.P., and Wing, R.F. 1982, Ap. J. 262, 201.
Ritter, H. 1987, Astr. Ap. Suppl., 70, 335.
Robbins, R.R., and Sanyal, A. 1978, Ap. J., 219, 985.
Robinson, E.L. 1975, Astr. J., 80, 515.
Robinson, E.L. 1976, Ann. Review Astr. Ap., 14, 119.
Robinson, E.L., and Nather, R.E. 1977, Pub. A.S.P., 89, 572.
Robinson, R.L., and Nather, R.E. 1983, Ap. J., 273, 255.
Robinson, R.L., Nather, R.E., and Kepler, S.O. 1982, Ap. J., 254, 646.
Robinson, E.L., Nather, R.E., and Patterson, J. 1978, Ap. J., 219, 168.
Rose, W.K. 1968, Ap. J., 152, 245.
Rose, W.K., and Smith, R.L. 1972, Ap. J., 172, 699.
Rosino, L. 1964, Ann. Ap., 50, 113.
Rosino, L. 1973, Astr. Ap. Suppl., 9, 347.
Rosino, L. 1987, in RS Ophiuchi (1985) and the Recurrent Nova Phenomenon, ed. M.F. Bode (Utrecht: VNU Science Press) p.1.
Rosino, L., Bianchini, A., and Rafanelli, P. 1982, Astr. Ap., 108, 243.
Rosino, L., Ciatti, F., and della Valle, M. 1986, Astr. Ap., 158, 34.
Rosino, L., and Iijima, T. 1987, in RS Ophiuchi (1985) and the Recurrent Nova Phenomenon, ed. M.F. Bode, (Utrecht: VNU Science Press), p. 27.
Rosino, L., and Iijima, T. 1988, Astr. Ap. 201, 89
Rosino, L., Taffara, S., and Pinto, G. 1960, Mem. SAIt, 31, 3.
Rosino, L., and Tempesti, P. 1977, Soviet Astr., 21, 291.
Rosseland, S. 1946, Ap. J., 104, 324.
Rottenberg, J.A. 1952, M.N.R.A.S., 112. 125.
Ruggles, C.L.N., and Bath, G.T. 1979, Astr. Ap., 80. 97.
Rush, W.F., and Thompson, R.W. 1977, Ap. J., 211, 184.
Ruusalepp, M., and Luud, L. 1971, Tartu Publ., 39, 89.
Sabbadin, F., and Bianchini, A. 1983, Astr. Ap. Suppl., 54, 393.
Sahade, J., and Wood, F.B. 1978, in "Interacting Binary Stars" (Pergamon Press), p. 114.
Sandlin, G.D., Brueckner, G.E., and Tousey,

R. 1977, Ap. J. 214, 898
Sanford, R.F. 1947a, Publ. A.S.P., 59, 87.
Sanford, R.F. 1947b, Pub. A.S.P., 59, 331.
Sanford, R.F. 1949, Ap. J., 109, 81.
Sanyal, A., and Willson, L.A. 1980, Ap. J., 237, 529.
Saraph, H., and Seaton, M.J. 1980, M.N.R.A.S., 193, 617.
Sastri, V.K., and Simon, N.R. 1973, Ap. J., 186, 997.
Sayer, A.R. 1937, Ann. Harv. Coll. Obs., 105, 21.
Schaefer, B.E., and Patterson, J. 1983, Ap. J., 268, 710.
Schatzmann, E. 1946, Ann. Astrophys., 9, 199.
Schatzmann, E. 1949, Ann. Astrophys., 12, 281.
Schatzmann, E. 1950, Ann. Astrophys., 13, 384.
Schatzmann, E. 1951, Ann. Astrophys., 14, 305.
Schatzmann, E. 1958, Ann. Astrophys., 21, 1.
Schatzmann, E. 1965, in Stars and Stellar System 8, eds. L.H. Aller and D.B. McLaughlin, (Chicago: Univ. of Chicago Press), p. 327.
Scheuer, P.A.G. 1960, M.N.R.A.S., 120, 231.
Schmidt-Kaler, Th. 1965, (private commun.).
Schneider, D.P., and Greenstein, J.L. 1979, Ap. J., 233, 935.
Schoembs, R., and Stolz, B. 1981, IBVS, No. 1986.
Seaquist, E.R., Duric, N., Israel, F.P., Spoelstra, T.A.T., Ulich, B.L., and Gregory, P.C. 1980, Astr. J., 85, 283.
Seaquist, E.R., and Palimaka, J. 1977, Ap. J., 217, 781.
Seaton, M.J. 1975, M.N.R.A.S. 170, 475.
Seaton, M.J. 1978 a, M.N.R.A.S., 185, 5P.
Seaton, M.J. 1978 b, in Planetary Nebulae: Observations and Theory, ed. Y. Terzian, p. 131.
Seaton, M.J. 1979, M.N.R.A.S., 187, 73p.
Seeliger, H.V. 1892, Astr. Nachr., 130, 393.
Seeliger, H.V. 1893, Astr. Nachr., 133, 305.
Seeliger, H.V. 1909, Astr. Nachr., 181, 81.
Seitter, W.C. 1969, in IAU Colloquium, Non-Periodic Phenomena in Variable Stars, ed. L. Detre, (Reidel, Dordrecht), p. 277.
Seitter, W.C. 1971, in IAU Colloquium 15, "Veroff. Remeis Sternw.", Bamberg 9, No. 100, p. 268.
Seitter, W.C. 1974, Proc. First European Meeting, Stars and the Milky Way System, ed. L.N. Mavridis, (Berlin: Springer), 2, p. 39.
Seitter, W.C. 1985, ESO Workshop on Production and Distribution of C,N,O Elements, p. 253.
Seitter, W.C. 1987, in RS Ophiuchi (1985) and the Recurrent Nova Phenomenon", ed. M.F. Bode, (Utrecht: VNU Science Press), p. 63.
Seitter, W.C., and Duerbeck, H.W. 1987, in RS Oph (1985) and the Recurrent Nova Phenomenon, ed. M.F. Bode, (VNU Press, Amsterdam), p. 71.
Selvelli, P.L. 1982, Proceed. of Third European IUE Conf. (ESA SP- 176), p. 197.
Selvelli, P.L., and Cassatella, A. 1981, IAU Colloquium 59, Effects of Mass Loss on Stellar Evolution, eds. C. Chiosi, and R. Stalio, (Dordrecht, Reidel), p. 515.
Selvelli, P.L., and Cassatella, A. 1982, Proceed. of Third European IUE Conf. (ESA SP-170), p. 201.
Selvelli, P.L., Cassatella, A., and Gilmozzi, R. 1990, Mem. Soc. Astr. Ital., 60, 151.
Selvelli, P.L., Cassatella, A., and Gilmozzi, R. 1990, The Nature of the Recurrent Nova T CrB, submitted to Ap. J.
Shaffer, A.W. 1985, in Cataclysmic Variables and Low Mass X-Ray Binaries", ed. D.Q. Lamb and T. Patterson, (Reidel Publ. Company), p. 355.
Shao, C.Y. 1978, IAU Circ., No. 3263.
Shara, M.M. 1981, Ap. J., 243, 268.
Shara, M.M., Livio, M., Moffat, A.F.J., and Orio, M. 1986, Ap. J. 311, 163.
Shara, M.M., and Moffat, A.F.J. 1982, Ap. J. (Letters), 258, L41.
Shara, M.M., and Moffat, A.F.J. 1983, Ap. J. 264, 560.
Shara, M.M., Moffat, A.F.J., Mc Graw, J.T., Dearborn, D.S., Bond, H.E., Kemper, E., and Lamontagne, R. 1984, Ap. J., 282, 763.
Shara, M.M., Moffat, A.F.J., and Webbink, R.F. 1985, Ap. J. 294, 277.
Shaviv, G. 1987, Ap. Space Sci, 130, 303.
Shaviv, G., and Starrfield, S. 1987, Ap. J.

(Letters), 321, L51.
Sherrington, M.F., and Jameson, R.F. 1983, M.N.R.A.S., 205, 265.
Slovak, M.H. 1980, IAU Circ. No. 3493.
Slovak, M.H. 1981, Ap. J., 248, 1059.
Smak, J. 1971, Acta Astr., 21, 15.
Smak, J. 1982, Acta Astr., 32, 213.
Smak, J. 1987, Proceed. of the Vulcano Workshop 1986: HE-UHE Behaviour of Accreting *X*-Ray Sources, eds. F. Giovannelli, and G. Mannocchi, (Italian Physical Soc. Conf. Proc. Vol. 8), p.3.
Sneden, C., and Lambert, D.L., 1975, M.N.R.A.S., 170, 533.
Snijders, M.A.J. 1987, in RS Ophiuchi (1985) and the Recurrent Nova Phenomenon, ed. M.F. Bode, (Utrecht: VNU Science Press), p. 54.
Snijders, M.A.J., Batt, T.J., Roche, P.E., Seaton, M.J., Morton, D.C., Spoelstra, T.A.T., and Blades, J.C. 1987, M.N.R.A.S., 228, 329.
Snijders, M.A.J., Batt, T.J., Seaton, M.J., Blades, J.C., and Morton, D.C. 1984, M.N.R.A.S., 211, 7P.
Sobolev, V.V. 1960, Moving Envelopes of Stars, (Cambridge: Harvard).
Sobotka, M., and Grygar, J. 1979, Bull. Astr. Inst. Czechosl., 30, 129.
Solf, J. 1983, Ap. J., 273, 647.
Sparks, W.M., 1969 Ap. J.156, 569.
Sparks, W.M., and Kutter, G.S. 1987, Ap. J. 321, 394.
Sparks, W.M., and Starrfield, S. 1973, M.N.R.A.S., 164, 1P.
Sparks, W.M., Starrfield, S., and Truran, J.W. 1977, in Novae and Related Stars, ed. M. Friedjung, (Dordrecht: Reidel). p.189.
Sparks, W.M., Starrfield, S., and Truran, J.W. 1978, Ap. J., 220, 1063.
Sparks, W.M., Starrfield, S., Wyckcoff, S., Williams, R.E. Truran, J.W., and Ney E.P. 1982, NASA CP 2238, p. 478.
Sparks, W.M., Wu, C.C. Holm, A.V., and Shiffer III, F.H. 1980, IAU Highlights of Astronomy, ed. P.A. Wayman, Vol. 5, p. 285.
Spencer Jones, H. 1931, Annals Cape Obs., 10, No. 9.
Spoelstra, T.A.T., Taylor, A.R., Pooley, G.G. Evans, A., and Albinson, J.S. 1987, M.N.R.A.S., 224, 791.
Starrfield, S. 1971a, M.N.R.A.S., 152, 307.
Starrfield, S. 1971b, M.N.R.A.S., 155, 129.
Starrfield, S. 1985, in Radiation Hydrodynamics in Stars and Compact Objects, K.H.A. Winkler, ed., Lecture Notes in Physics (Berlin, Springer), p. 255.
Starrfield, S. 1988, in The Classical Nova, eds. M.F. Bode and A. Evans, (Chichester: Wiley).
Starrfield, S., and Snijders, M.A.J. 1987, Exploring the Universe with the IUE Satellite, ed. J. Kondo, (Dordrecht, Reidel), p. 377.
Starrfield, S., and Sparks, W.M. 1987, Ap. Space Sci., 131, 379.
Starrfield, S., Sparks, W.M., and Truran, J.W. 1985, Ap. J. 291, 136.
Starrfield, S., Sparks, W.M., and Truran, J.W. 1986 Ap. J. (Letters), 303, L5.
Starrfield, S., Sparks, W.M., and Williams, R.E. 1982, Advances in UV Astronomy, 4 Years of IUE Research, (NASA C.P. 2238), p. 470.
Starrfield S.G., Truran, J.W., and Sparks, W.M. 1977 in CNO isotopes in Astrophysics. ed. J. Audouze, p. 49.
Starrfield, S., Truran, J.W., and Sparks, W.M. 1978, Ap. J. 226, 186.
Stefl, S., and Grygar, J. 1981, Bull. Astr. Inst. Czechosl., 33, 116.
Steinle, H., and Pietsch, W. 1987, Ap. Space Sci., 131, 485.
Stephenson, C.B. 1967, Pub. A.S.P., 79, 584.
Stephenson, C.B., and Herr, R.B. 1963, Pub. A.S.P., 75, 253.
Stickland, D.J. 1983, Astrophy. Sp. Sci. 92, 197.
Stickland, D.J., Penn, C.J., Seaton, M.J., Snijders, M.A.J., Storey,P.J. and C.R.Kitchin, 1979 in The first year of IUE, p.63 ed. A.J. Willis.
Stickland, D.J., Penn, C.J., Seaton, M.J., Snijders, M.A.J., and Storey, P.J. 1981, M.N.R.A.S., 195, 27p.
Storey, P.J.1981, M.M.R.A.S. 195, 27P.
Stoy, R.H. 1933, M.N.R.A.S., 93, 588.
Stratton, F.J.M. 1928, in Handbuch der Astrophysik 6, 251.

Stratton, F.J.M. 1936, M.N.R.A.S., 96, 373.
Stratton, F.J.M. 1945, M.N.R.A.S., 105, 275.
Stratton, F.J.M., and Manning, W.H. 1934, Atlas of Spectra of Nova Herculis, 1939, The Solar Physics (Observatory: Cambridge, Eveyland).
Strecker, D.W., Erickson, E.F., and Witteborn, F.C. 1979, Ap. J. Suppl., 41, 501.
Strittmatter, P.A., Woolf, N.J., Thompson, R.I., Wilkerson, S., Angel, J.R.P., Stockman, H.S., Gilbert, G., Grandi, S.A., Larson, H., and Fink, U. 1977, Ap. J. 216, 23.
Struve, O. 1947, Science, 106, 149.
Struve, O. 1955, Sky Telesc., 14, 275.
Svolopoulos, S.N. 1966, Pub. A.S.P., 78, 157.
Swings, P. and Struve, O. 1941, Ap. J., 94, 291.
Swings, P. and Struve, O. 1943, Ap. J., 98, 91.
Szkody, P. 1977, Ap. J., 217, 140.
Szkody, P. 1985, in "Cataclysmic Variables and Low-Mass X-Ray Binaries", ed. D.Q. Lamb and J. Patterson, (Reidel Publ. Company), p. 385.
Szkody, P., Mattei, J.A., and Mateo, M. 1985, Pub. A.S.P., 97, 264.
Takalo, L.O., and Nousek,J.A. 1985, Publ.A.S.P. 97,570
Tempesti, P. 1975, IAU Circ. No. 2834.
Tempesti, P. 1979, Astr. Nach., 300, 51.
Thomas, H.L. 1940, Harv. Bull., 912, 11.
Tolbert, C.R., Pecker, J.C., and Pottasch S.R. 1967, BAN, 19, 17.
Truran, J.W. 1985, Nucleosynthesis: Challenges and new Developments, eds. W.D. Arnett, and J.W. Truran, Univ. of Chicago press. (Chicago).
Truran, J.W., Livio, M., Hayes, J., Starrfield, S., Sparks, W.M. 1988, Ap. J. 324, 345.
Turolla, R., Nobili, L., and Calvani, M. 1988, Ap. J., 324, 899.
Tylenda, R. 1977, Acta Astr., 27. 389.
Tylenda, R. 1978, Acta Astr., 28, 333.
Tylenda, R. 1979, Acta Astr., 29, 55.
Unsöld, A. 1930, Zs. Astrophys., 1, 138.
Van den Bergh, S., and Pritchet, C.J. 1986, Pub. A.S.P., 98, 110.
Van den Bergh, S., and Youngh, P.F. 1987, Astr. Ap. Suppl., 70, 125.
Van Houten, C.J. 1966, B.A.N., 18, 439.
de Vaucouleurs, G. 1978, Ap. J., 223, 351.
Verbunt, F. 1987, Astr. Ap. Suppl. Series, 71, 339.
Verbunt, F., and Wade, R.A. 1984, Astr. Ap. Suppl., 57, 193.
Vidal, N.V., and Rodgers, A.W. 1974, Pub. A.S.P., 86, 26.
Viotti, R., Altamore, A., Baratta, G.B., Cassatella, A, and Freidjung, M. 1984, Ap. J., 283, 226.
Vogel, H.C. 1893, Abh. Konigl. Preuss. Akad. Wiss. Berlin.
Vogt, N. 1975, Astr. Ap., 41, 15.
Vogt, N. 1976, in IAU Symposium No. 73, Structure and Evolution of Close Binaries, Eds. P. Eggleton, S. Mitton, and J. Whelau (Dordrecht:Reidel), p. 147.
Vogt, N. 1981, Mitt. Astr. Ges., 57, 79.
Voloshina, I.B., and Doroshenko, V.T. 1977, Soviet Astr., 21, 313.
Vorontsov-Velyaminov, B.A. 1940, Byull. Inst. Sternberg. Moskva, No. 1.
Vorontsov-Velyaminov, B.A. 1948, "Gasovye tumannosti i novye zvezdy" (Moskva-Leningrad: Izd. Akad. Nauk).
Vorontsov-Velyaminov, B.A. 1953, "Gasnebel und Neue Sterne" (Berlin: Kultur und Fortschritt).
Wade, R.A. 1984, M.N.R.A.S., 208, 381.
Wade, R.A. 1985, in "Interacting Binaries", ed. P.P Eggleton and J.E. Pringle, (Reidel Publ. Company), p. 289.
Wagner, R.L., Gull, R.G., Byrd, G.G., and Loren, R.B. 1971, Ap. J., 165, 431.
Walborn, N.R. 1971, Pub. A.S.P., 83, 813.
Walker, A.R. 1977, M.N.R.A.S., 179, 587.
Walker, M.F. 1954, Pub. A.S.P., 66, 230.
Walker, M.F. 1956, Ap. J., 123, 68.
Walker, M.F. 1957 in IAU Symposium 3, Non-Stable Stars, ed. G.H. Herbig, (Cambridge: Univ. Press.), p. 46.
Walker, M.F. 1963, Ap. J., 138, 313.
Wallerstein, G. 1958, Pub. A.S.P., 70, 537.
Wallerstein, G. 1963, Pub. A.S.P., 75, 26.
Wallerstein, G., and Garnavich, P.M. 1986, Pub. A.S.P., 98, 875.
Wargau, W., Drechsel, H., and Rahe, J. 1982, Proc. 3 European IUE Conference ESA S.P., 176, p. 215.

Wargau, W., Drechsel, H., and Rahe, J. 1983, Acta Astr., 33, 149.
Warner, B. 1971, Pub. A.S.P., 83, 817.
Warner, B. 1972, M.N.R.A.S., 160, 35P.
Warner, B. 1976 in IAU Symposium No 73, Structure and Evolution of Close Binary Systems, Eds. P.Eggleton, S.Mitton, and J.Whelau (Dordrecht:Reidel) p. 85.
Warner, B. 1981, M.N.R.A.S., 195, 101.
Warner, B. 1985 a, Proced. ESA Workshop, "Recent Results on Cataclysmic Variables", ESA S.P., 236, 1.
Warner, B. 1985 b, M.N.R.A.S., 217, 1P.
Warner, B. 1986a, M.N.R.A.S., 219, 751.
Warner, B. 1986b, Ap. Space Sci., 118, 271.
Warner, B. 1986c, M.N.R.A.S., 222, 11.
Warner, B. 1987a, M.N.R.A.S., 212, 917.
Warner, B. 1987b, M.N.R.A.S., 227, 23.
Warner, B., and Livio, M. 1987, Ap. J. (Letters), 322, 95L.
Watson, M.G., King, A.R., and Osborne, J. 1985, M.N.R.A.S., 212, 917.
Watson, R. 1925, Harvard Bull. 820.
Weaver, H.F. 1951, Ap. J., 113, 320.
Weaver, H.F. 1974, IAU Highlights of Astronomy, ed. G. Contopoulos, (Dordrecht: Reidel), 3, 509.
Webbink, R.F. 1976, Nature, 262, 271.
Webbink,R., Livio, M.,Truran, J.W. and Orio, M. 1987, Ap.J., 314, 653.
Wendker, H.J. 1978, Catalogue of Radio Stars, (preprint).
Whipple, F.L., and Payne-Gaposchkin, C. 1936, Harv. Circ. 413.
Whipple, F.L., and Payne-Gaposchkin, C. 1937, Harv. Circ. 414.
White, R.L. 1985, Radio Stars, eds. R.M. Hjellming, and D.M. Gibson, (Dordrecht, Reidel), p. 45.
Whitelock, P.A., Carter, B.S., Feast, M.W., Glass, I.S., Laney, D., Menzies, J.W., Walsh, J.W., and Williams, P.M. 1984, M.N.R.A.S., 211, 421.
Williams, G. 1983, Ap. J. Suppl., 53, 523.
Williams, R.E. 1977, in IAU Colloquium 42, The Interaction of Variable Stars with Their Environment, ed. R. Kippenhahn, J. Rahe, and W. Strohmeier (Bamberg: Schadel) p. 242.
Williams, R.E. 1982, Ap. J., 261, 170.
Williams, R.E., and Ferguson, D.H. 1983, in IAU Colloquium 72, Cataclysmic Variables and Related Objects, eds. M. Livio and G. Shaviv, (Dordrecht:Reidel), p. 97.
Williams, R.E., and Gallagher, J.S. 1979, Ap. J. 228, 482.
Williams, R.E., Ney, E.P., Sparks, W.M., Starrfield, S.G., Wyckoff, S., and Truran, J.W. 1985, M.N.R.A.S., 212, 753.
Williams, R.E., Sparks, W.M., Gallagher, J.S., Ney, E.P., Starrfield, S.G., and Truran, J.W. 1981, Ap. J., 251, 221.
Williams, R.E., Woolf, N.J., Hege, E.K., Moore, R.L., and Kopriva, D.A. 1978, Ap. J., 224, 171.
Willis, A.J., and Garmany, C.D. 1987, in Exploring the Universe with the IUE Satellite, ed. Y. Kondo, (Dordrecht: Reidel).
Wilson, R. 1935, Ap. J., 82, 233.
Wolf, B. 1977, IAU Colloquium No 42, The Interaction of Variable Stars with Their Environment, ed. R. Kippenhahn, J. Rahe, and W. Strohmeier, (Bamberg) p. 151.
Woszczyk, A., Smolinski, J., Maron, N., Strobel, A., and Krempec, J. 1968, Ap. Space Sci, 1, 264.
Wright, W.H. 1919, Lick Obs. Bull., 10, 30.
Wu, C.C., Boggess, A., Holm, A.V., Perri, P.M., Schiffer, F.H., III, Turnrose, B.E. and West, D.K. 1978, Bull. Am. Astr. Soc., 10, 687.
Wu, C.C., and Kester, Do 1977, Astr. Ap., 58, 331.
Wychoff, S., and Wehinger, P.A. 1977, Proceed. IAU Colloquium 42, eds. R. Kippenhahn, J. Rahe, and W. Strohmeier, (Bamberg, Sept. 6-9), p.201.
Wyse, A.B., 1939, Lick Pub., 14, 93.
Wyse, A.B. 1940, Publ. A.S.P. 52, 334.
Yamashita, Y. 1968, Pub. Astr. Soc. Japan, 20, 183.
Yamashita, Y. 1975, Ann. Tokyo Astr. Obs. 2nd Ser., 15, 1.
Young, P., and Schneider,D.P. 1980, Ap.J. 238,955.
Zanstra, H. 1931, Pub. Dom. Ap. Obs., 4, 209.
Zollner, J.C.F. 1865, Photometrische Untersuchungen, Leipzig, p. 241.
Zwicky, F. 1956, Astr. J., 61, 328.

PART III

SYMBIOTIC STARS

Written by

Michael Friedjung

Roberto Viotti

N95
27076
UNCLAS

N95- 27076

11

OVERVIEW OF THE OBSERVATIONS OF SYMBIOTIC STARS

R. Viotti

I. INTRODUCING THE SYMBIOTIC STARS

Symbiotic stars represent a rather poor category--better to say: "collection"--of astrophysical objects. But the simultaneous presence of at least two apparently conflicting spectral features, and their peculiar light curves, have long since attracted the attention of many researchers and resulted in a large amount of observational and theoretical work. At present, this field is still very lively, and the prospects for the future are even more promising. Therefore, this monograph comes at the right time to give a *"coup d'oeil"* on what is going on in this field, in a rather untraditional way.

The term *Symbiotic Stars* commonly denotes variable stars whose optical spectra simultaneously present a *cool absorption* spectrum (typically TiO absorption bands) and emission lines of high ionization energy, such as HeII 4686 A, [OIII] 4363 A, and 5007 A, etc. Historically, it was Merrill and Humason (1932) who first called attention to the existence of a small group of stars with symbiotic spectrum: CI Cyg, RW Hya, and AX Per. The word "symbiotic" was introduced later by Merrill (1944) when describing the spectrum of BF Cyg, and this term is now currently used for the category of variable stars with composite spectrum. Figure 11-1 shows some typical optical spectra of symbiotic stars.

As illustrated in the figure, the main spectral features of these objects are: (1) the presence of a red continuum typical of a cool star, (2) the rich emission line spectrum, and (3) the UV excess, frequently with the Balmer continuum in emission. These two latter features are characteristic of the emission from a hot, low-density plasma, such as the gaseous and planetary nebulae. In addition to the peculiar spectrum, the very irregular *photometric* and *spectroscopic variability* is the major feature of the symbiotic stars, which also distinguishes them from both normal cool stars and gaseous nebulae. Moreover, the light curve is basic to identify the different phases of *activity* in a symbiotic star, as discussed in detail in the next section.

At present, 100 to 200 astrophysical objects have been classified as symbiotic (Allen 1979, 1982, 1984b; Kenyon 1986), but it is not clear whether they really represent a homogeneous group of objects. Actually, as we shall see in this chapter, there is a large variety of phenomenology that is hard to include in a coherent scheme.

Our problem is to find out the physical mechanisms that cause the symbiotic phenomenon and its variety. Probably, the same mechanisms are working with different strengths and ways in different objects. This may imply that, in some cases, one mechanism dominates over the others, and it is the one mainly responsible for the symbiotic phenomenon. Conversely, other mechanisms may be dominant in other objects. Clearly, these so far unknown mechanisms largely depend on the physical conditions that are present in symbiotic stars. A change in one basic parameter such as density or temperature makes one mechanism dominant or negligible with respect to the others.

Let us better clarify this point, which is also the basic point of this monograph series. We have observed an astronomical phenomenon character-

PRECEDING PAGE BLANK NOT FILMED

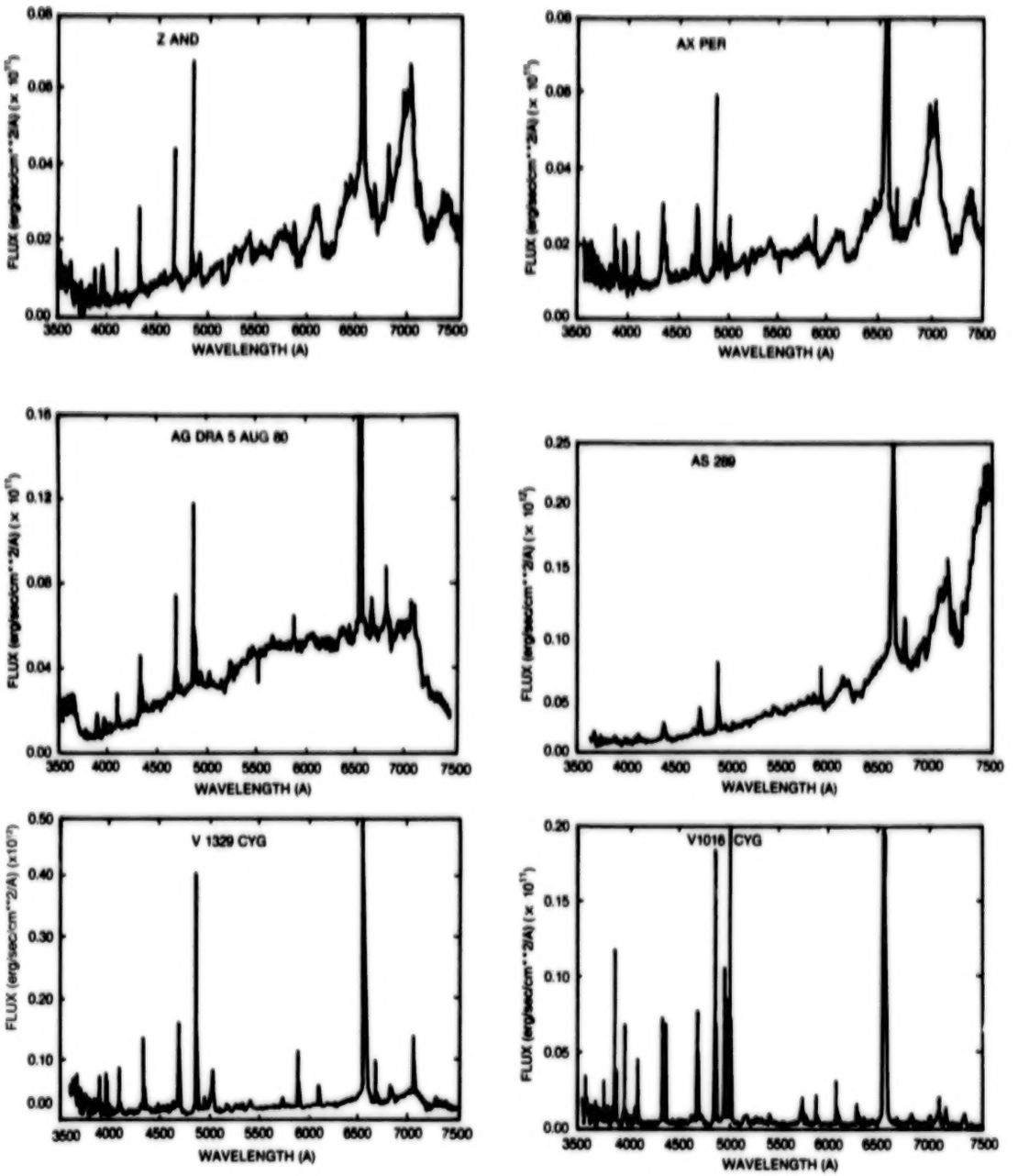


Figure 11.1. The optical spectrum of symbiotic stars Z And, AX Per, AG Dra, AS 289, V1329 Cyg, and V1016 Cyg (Blair et al., 1983).

ized by: (1) a composite stellar spectrum with two apparently conflicting features, and (2) large variability. This is what is generally defined as the *symbiotic phenomenon* (cf. Friedjung and Viotti 1982, p.227). We want to find out the origin of this behavior, and, in particular, to identify and measure the physical mechanism(s) which is (are) responsible for the observed phenomena. We could try a statistical approach to the problem. That is to analyze the observational data of as many symbiotic objects as possible. For instance, we may study the position in the color-color using optical and IR photometry. However, this may easily be misleading, since 100 or 200 objects certainly include objects that have nothing to do with the symbiotic phenomenon, such as unresolved planetary nebulae or extreme VV Cep variables. In addition, these diagrams generally

do not tell us anything about the symbiotic mechanism. The sample could also be largely affected by strong selection effects, as many symbiotic objects are close to the Galactic Plane.

Finally, symbiotic stars are variable. That is, the same object may occupy very different places in an observational diagram during different phases of its activity. Thus, a single "event" (i.e., one symbiotic star) is not represented in this diagram by a single point, but by a complex curve. This *representative curve* varies from object to object, and indicates that the physical mechanisms responsible for the symbiotic phenomenon have different weights and shapes in different objects. In other words, *variability is one of the basic observational parameters of a symbiotic object*, and perhaps *the most important one*.[1] In fact, we shall show later that a large progress concerning the symbiotic phenomenon has been made through the analysis of the variability in all the wavelength ranges. For those objects, the majority, which have been observed only a few times or even only once, the information is too poor to be included in a consistent study of the symbiotic phenomenon. This is true even if the observations cover a wide frequency range.

In this chapter, we shall give an overview of the observations of symbiotic stars in different spectral regions. In Chapter 12, we shall discuss the models for symbiotic stars, while Chapter 13 will be devoted to the description of a few well-studied symbiotic objects and discuss their observations in the light of possible models. We finally summarize our present knowledge about the symbiotic phenomenon. This review is not intended to give a full account of all the studies on the symbiotic stars so far made, but only to illustrate the different aspects of the symbiotic phenomenon and to stimulate future researches, Thus, in many cases, we shall quote only a limited number of articles that appeared essential to illustrate the problem. Extensive lists of references can be found in the *Proceedings of the IAU Colloquium 70* (Friedjung and Viotti 1982) and *Colloquium 103* (Mikolajewska et al., 1988), and in Kenyon 1983a; 1983b). Among the several reviews on symbiotic stars, we should quote: Swings (1970), Boyarchuk (1983), Allen (1984a), Kenyon (1986), and Fernandez-Castro (1988).

(1) We must note that frequently symbiotic stars remain at a nearly constant luminosity for a long period of time, even for several years. This is, for instance, the case of Z And during quiescence, and of a number of symbiotic novae (V1016 Cyg, HM Sge, etc.) some years after the outburst. Because of the lack of long enough observations, one symbiotic star could appear stable for a long time only because we have missed the outburst. But this does not disprove that variability is a major feature of the symbiotic phenomenon.

II. GENERAL OVERVIEW OF THE OBSERVATIONS

Observation in different spectral regions essentially gives information about different parts of the atmospheric envelope(s) of a symbiotic object. For instance, as we shall show in the following, the red and near-IR regions are in most cases dominated by what appears to be a cool star's spectrum, while the far-IR is generally associated with thermal dust emission. On the other side, the radio flux provides information about the ionized cloud surrounding the system. The near-UV and the emission lines also are typical features of the diffuse ionized gas near the star(s), while the far-UV and the X-rays are probably associated with a hot star and/or with an accretion disk.

In this chapter, we shall follow the traditional way of first discussing the optical observations, which have provided the distinguishing characteristics of the symbiotic stars. Then the analysis is extended to longer (IR and radio) and shorter wavelengths (UV and X-rays). In addition, a full section will be devoted to polarimetry, since, although this field is so far not well investigated, it should give fundamental information on the structure of the circumstellar environment.

III. THE LIGHT HISTORY OF SYMBIOTIC STARS

III.A. INTRODUCTION

The light history of the symbiotic stars is basic to recognize their different activity phases, to find

periodicities which could be related to the presence of a binary (or multiple) system, and, more in general, to separate the different physical subgroups. It should be considered that an obvious reason to use visual photometry, instead of IR or UV, is that it always covers a much longer period of time, and the basic time scales of the symbiotic phenomena are of the order of several hundred days to decades. Perhaps, the ungoing programs of continuous IR and UV monitoring of symbiotic stars will considerably change this viewpoint. In the study of the light curves, a special warning should be made concerning the large contribution to the broad-band photometry of the emission lines whose integrated flux sometimes exceeds that of the continuum. Therefore, the light curves might represent the time-behavior of the nebular region, rather than that of a central stellar object.

Symbiotic stars display in the visible a large variety of light curves, with one or several nova-like outbursts, quasi-periodic oscillations, long periods of relative quiescence at minimum or at maximum luminosity, short-time variability (e.g., flickering), etc. The same object, if observed for a long enough period of time, may present many different kinds of variability. It is therefore impossible to fit all the light curves of symbiotic stars into a common scheme. We might only say that the main character of the variations is that they are *irregular, of moderate amplitude* (one to few magnitudes) with respect to classical novae and cataclysmic variables, and mostly on *long-time scales* (several days to years). But, as illustrated below, small amplitude and short-time scale variations are also present.

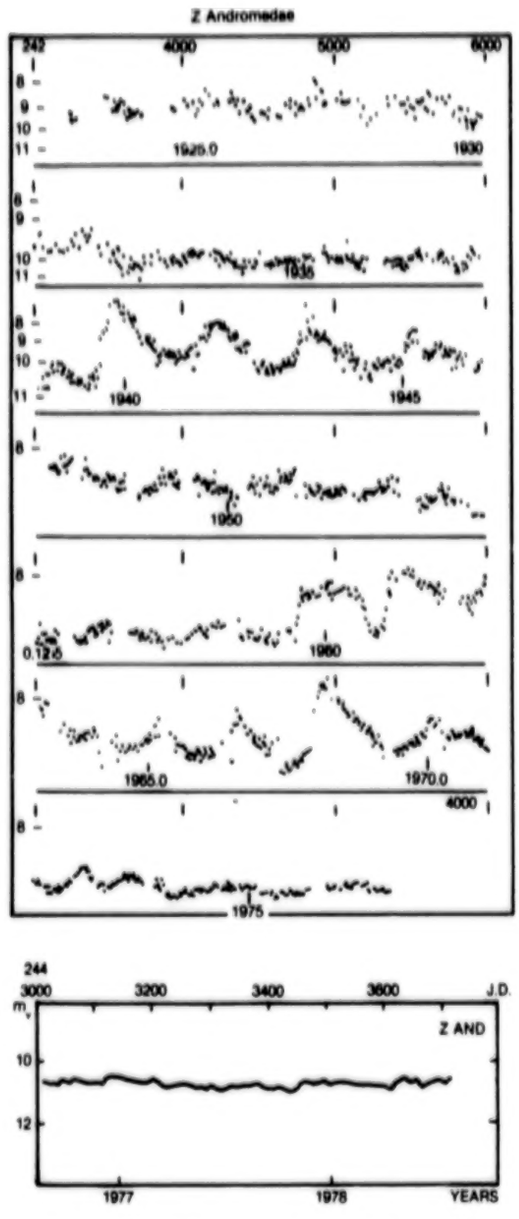


Figure 11.2 The light curve of Z And from 1923 to 1978 (Mattei, 1978) showing a sequence of maxima (or outbursts) separated by 1-2 years, which characterize the active phases of the star, and long-lasting periods of minimum luminosity (quiescence).

III.B. LONG-TERM LIGHT VARIATIONS

The light history of one of the best-studied symbiotic stars, *Z And*, is shown in Figure 11.2.

This light curve, which for a long time has been the ground for many theoretical works on symbiotic stars, is quite irregular. However, two main "trends", or *phases*, can be recognized: as follows (1) a sequence of large amplitude (1-2 magnitudes) oscillations of gradually decreasing amplitude, and (2) quiescent phases with the star near minimum luminosity.

In Z And four and maybe five active phases (1895-1905 and 1914-1923, not in Figure 11.2, 1939-1947 and 1959-1972) have been so far identified in its historical light curve (e.g., Kenyon, 1986). A new minor outburst occurred in March-April 1984 (Mattei, 1987; Viotti et al., 1984), and

the star was still active in 1986. At the time of writing this report, it was not yet clear whether this was the beginning of a new active phase, or the 1984 and 1986 maxima were isolated events. The active phases start either abruptly with a rise to maximum (V = 8 or 9) in a few weeks or months, or the main outburst is preceeded by a smaller light maximum. The time interval between two successive light maxima (or minima) is not constant, but varies from 310 to 790 days, with a mean value of 632 days (Mattei, 1978). It should be considered that long-term variations, but with a smaller amplitude, have also been observed during quiescence, especially in the U-band. In this case, these oscillations seem to be periodic, with a mean period of about 757 days (Kenyon and Webbink, 1984) and the maxima are not in phase with the above "outbursts." This behavior will be discussed in more detail in the next section. In the following, we shall describe the period when a symbiotic star is at minimum luminosity (in the visible) as *quiescence* or *quiescent phase*, and the period when the star is highly variable and brighter as *activity* or *active phase*.

Several symbiotic stars show light curves resembling that of Z And with active and quiescent phases. During the last one hundred years, the high-velocity star *AG Dra* underwent several outbursts, reaching a peak magnitude around m_{phot} ~11 (V~10). The maxima are separated by 240 to 710 days (see Robinson, 1969) without evidence of a periodic recurrence of the outbursts. In addition, as in Z And, there are long lasting periods of quiescence from 11 to more than 37 years. During the quiescent phases, the magnitude of AG Dra presents small scale fluctuations (e.g., Belyakina, 1969). The amplitude of these fluctuations increases from visual to near UV, and appears to be periodic with a period of 554 d (Meinunger, 1979).

Another typical case is *CI Cyg*, a symbiotic star showing both outbursts and recurrent minima (see Figure 11-5). Since the beginning of this century, this star displayed five outbursts, the last one in 1975 when it brightened from V = 11 to 8.4 in a few weeks (Belyakina, 1979). Two months later, the luminosity fell to V~11.3 and remained at minimum for about 60 days. CI Cyg brightened again to V~9 at the end of 1975 then gradually faded to V~11 in 1980. The behavior in 1975 is qualitatively similar to that of Z And at the beginning of its active phases. This similarity, however, is only apparent. In fact, the deep 1975 minimum is in phase with several other periodic minima (period of 855 days) recorded in the light curve of CI Cyg, and should be attributed to an eclipse of a binary system, rather than to a phase of minimum activity in between two successive outbursts. If we neglect these periodic eclipses, the overall light curve of CI Cyg during the recent active phases was characterized by a rapid brightening of about two magnitudes in 1979, followed by a four-year decline to the present quiescent phase. This behavior is rather similar to that of the symbiotic novae, which will be discussed later in this section.

In many respects, the classical symbiotic star *BF Cyg* is similar to CI Cyg for showing semiregular minima about one magnitude deep with a period of about 757 d (Pucinskas, 1970), overposed on a much slower trend. As illustrated in Figure 11.3, BF Cyg brightened from m_{pg} = 12-13 to 10 between 1891 and 1894 (Jacchia, 1941). This unrecorded outburst was followed by a very slow fading, interrupted during the active phase around 1916-1922, and continued to present.

Long-term light variations are also observed in the brightest symbiotic star *CH Cyg*. In recent years, this star has varied between V = 6 and 8 (see Figure 22 in Chapter 13). In general, the variations are slow and the fading and brightening phases take several months. However, a much faster luminosity variation took place in September 1984, when the visual light dropped by about 1.5 mag in a few days. This event, associated with a strong radio outburst will be discussed on Section VII.D. Irregular variations on short (~10^2 days, e.g., Kenyon, 1986), and very short (minutes, see Section III.C.) time scales are also present in CH Cyg, and suggest the presence of different mechanisms of variability.

Among symbiotic stars there is a small group of objects showing a light curve quite different from those previously described, which actually characterize the large majority of the stars com-

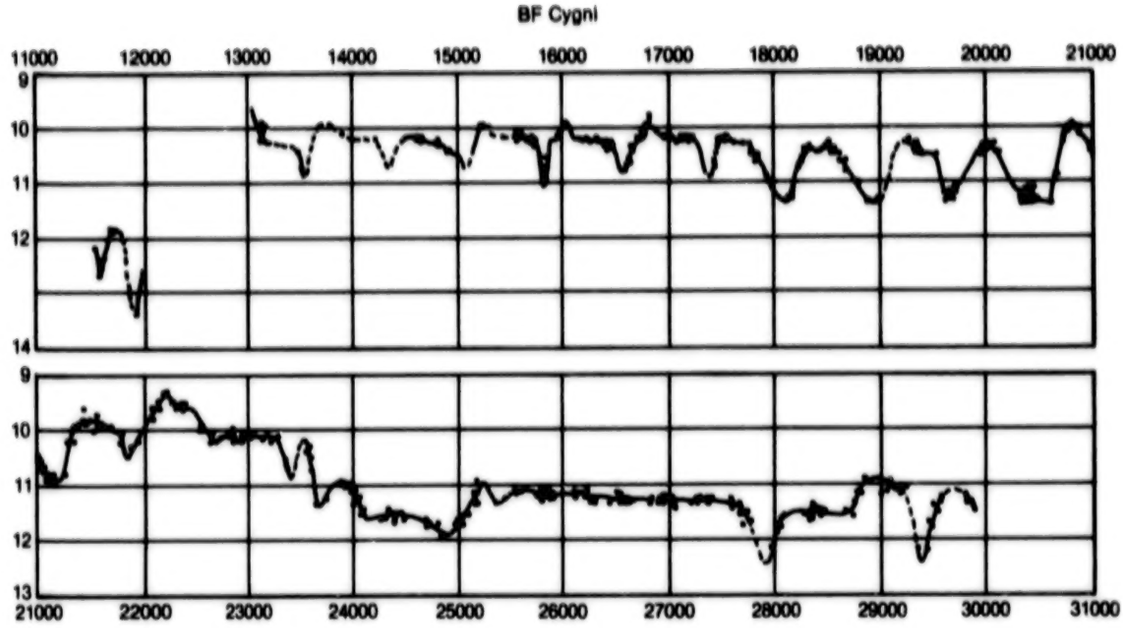


Figure 11-3 The light curve of BF Cyg (Jacchia, 1941). There is a secular decrease of luminosity since the end of the last century interrupted by the active phase around 1916-22, and a sequence of quasi-regular minima atttributed to eclipses in a binary system with a period of 757 d.

monly called symbiotic. They are the *symbiotic novae*. In 1964, a nova-like event was recorded in Cygnus (FitzGerald et al., 1966) in a faint (B~ *15*^{m}) M star, *MHα 328-116*, known to have strong Hα in emission (Merrill and Burwell, 1950). The luminosity of this object, better known as *V1016 Cyg*, gradually increased in the following years until B = 11 mag at the beginning of 1968 (see Figure 11-4). Since that time, the luminosity of V1016 Cyg has remained nearly constant. This behavior (and the associated spectral variations, which will be discussed in the next section) is reminiscent of that of novae, but with a smaller amplitude and an exceptionally long time scale. In addition, in V1016 Cyg, no decline in the optical luminosity of this star was observed until now. A similar behavior was more recently displayed by *HM Sge*. This star brightened from V>17 to 11 mag in a few months, and still is at maximum at the time of writing this report. Both stars, V1016 Cyg and HM Sge, have been included among symbiotic stars because of their very rich emission line spectrum, and their red-near IR excess showing marginal presence of molecular (TiO) absorption bands, confirming their symbiotic nature.

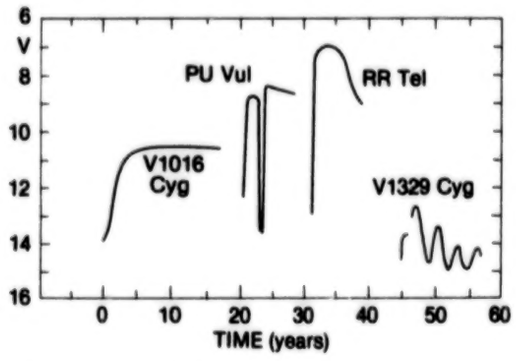


Figure 11-4 . Schematic light curves of the symbiotic novae. V1016 Cyg, PU Vul, RR Tel, and V1329 Cyg (=HBV 475).

There are a few more symbiotic stars that had a historical light curve with one single major outburst. Allen (1980) listed seven stars having the character of very slow novae, or of *symbiotic novae*: AG Peg, RT Ser, RR Tel V1016 Cyg, V1329 Cyg, HM Sge, and AS 239 (V2110 Oph). To this list, we have to add the nova-like variable PU Vul, which "exploded" in 1978. In these objects, the rise to maximum is much slower than in the classical novae (but in two cases, RR Tel and HM Sge the brightening phase was not recorded). The following phase of luminosity decrease is even slower and took from one decade to more than one century. In fact, no decline has so far

been observed in V1016 Cyg, HM Sge, and PU Vul. The fading in RR Tel and probably AG Peg was gradual, while in V1329 Cyg, it was characterized by large light oscillations. In PU Vul, a deep minimum was observed just one year after its outburst. In these two objects, the minima could be caused by eclipses in a binary system, but the PU Vul deep minimum could be due to temporary occultation by dust (Friedjung et al., 1984). In any case, as illustrated by Figure 11-4, we can hardly speak of a typical light curve of symbiotic novae, except for the fairly steep and large brightening with respect to the other symbiotic stars. These objects will be discussed in Chapter 13, Section IV.

III.C. SHORT TIME VARIATIONS

The light curve of symbiotic stars is characterized by irregular variations of short (days and minutes) time scales overimposed on the long-term trend described above. In general, this variability is poorly known and in many cases its reality is questionable. In fact, our knowledge on the light behavior of symbiotic stars, in most cases, is based on visual estimates that are intrinsically uncertain by a few tenths of magnitudes. Actually, only a few objects are included in current monitoring programs using standard procedures of observation and reduction. In most cases, our knowledge is based on visual estimates that are uncertain by a few tenths of a magnitude. For instance, the light curve of Z And shows several small amplitude fluctuations besides the already discussed long-term behavior, which are probable real. Night-to-night UBV variations in CI Cyg have been claimed by Burchi et al. (1984) and Chochol et al. (1984). The amplitude seems to be larger at shorter wavelengths.

Intermediate filter photometry is more appropriate for the study of the nature of the rapid variations (Kenyon 1986). Short-term fluctuations on a time scale of minutes have been observed in CH Cyg by Cester (1968) and Wallerstein (1968). As in the case of CI Cyg, the amplitude increases with decreasing wavelength. The phenomenon is similar to the "flickering" observed in dwarf novae, and could be a means to investigate the nature of the hot component in symbiotic systems. However, a survey of Walker (1977) suggests that the majority of symbiotic stars are constant to 1 *per cent* over time scales of 20 minutes to 2 hours. We finally note that a large flickering is present in the recurrent novae T CrB and RS Oph, stars that are frequently included among symbiotic stars.

III.D. PERIODIC LIGHT VARIATIONS

As discussed above, in some light curves, one can identify a series of minima occurring at regular, or quasi-regular time intervals. About one dozen periodic minima were discovered by Hoffleit (1968) in the Maria Mitchell Observatory plots of CI Cyg covering the period 1916-1967 (Figure 11-5). The periodicity of 855 d was confirmed by new extensive photometric studies carried out among others by Belyakina (1974). As in other symbiotic stars, during these minima CI Cyg becomes redder, suggesting that the light decrease is associated with fadings or eclipses of the blue spectral component. Periodic minima were also discovered in the southern sky symbiotic AR Pav by Mayall (1937), who derived a period of 605 d. Semiregular variations are also present in BF Cyg as discussed above (see Figure 11-3), while in other cases, such as Z And during its active phases, the light minima do not suggest a periodic trend.

It would be of crucial importance, for understanding the symbiotic stars, to find out any periodic phenomenon in the observations that could be associated with orbital motion in a binary system, or with stellar rotation or pulsation. The problem is to separate any "regular trend" from the irregular variations associated with the large scale activity, and with the microvariability illustrated in the previous sections. For instance, the minima of CI Cyg are clearly present in the whole recorded light curve, independently on the "activity." This is best illustrated in Figure 11-5 that show the recent light curve of CI Cyg.

During quiescence the recurrent minima are difficult to identify, since the star's minimum luminosity (V ~ 11.1) is only a few tenths of a magnitude fainter that the mean luminosity at

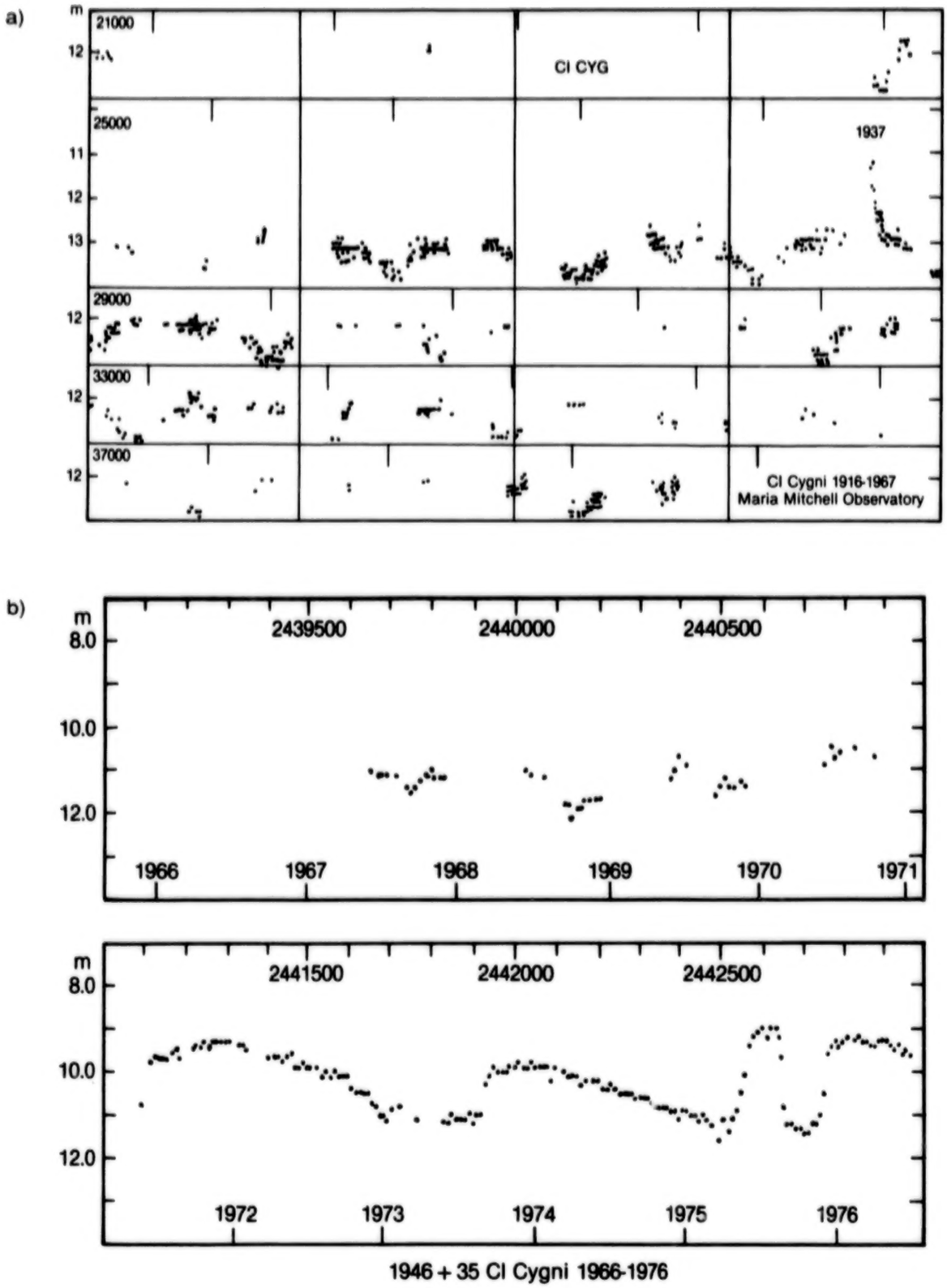


Figure 11-5. The light curve of CI Cyg: (a) from 1916 to 1967 (Hoffleit, 1968), and (b) from 1967 to 1976 (Mattei, 1976).

quiescence (V ~ 10.8-11.0), and this difference is of the same order of magnitude as the observational errors and as the irregular light fluctuations. On the contrary, when CI Cyg is in outburst, the minima are very deep. It is worth noting that during these phases, the star attains the same minimum magnitude as during the minima in quiescence. Thus, the minimum luminosity is independent on the phase of activity, and might suggest complete eclipse of the variable hot component, as also confirmed by Belyakina (1979) results that the minima are deeper in the U-band.

During quiescence, the light curves of many symbiotic stars present quasi regular long term fluctuations. Figure 11-6 shows the light curve of AG Peg during 1964-1984 characterized by several recurrent minima separated by about 827 d (Belyakina, 1985). The amplitude is larger in B and U. A similar behavior was found in other symbiotics such as AG Dra (Meinunger, 1979), AX Per (Kenyon, 1982), SY Mus (Kenyon and Bateson, 1984). Also, these variations can be attributed to partial eclipses of a binary system. Small-scale periodic oscillations of the visual luminosity of RR Tel are, on the contrary, attributed to the pulsation of its Mira component (Heck and Manfroid, 198[illegible]; Kenyon and Bateson, 1984).

BX Mon represents an extreme case of quasi-periodic variability. From a study of a collection of Harvard plates taken between 1890 and 1940, Mayall (1940) concluded that BX Mon was a very long period variable with P = 1380 d, m_{pg} (max) = 10.02 and m_{pg} (min) = 13.05. Thus, this star should be an extreme Mira-type variable with prominent symbiotic characteristics. However, the periodicity has not been confirmed (Iijima, 1985), and the large amplitude photometric variations could be attributed to the hot component activity, rather than to a Mira variable (Viotti et al., 1986).

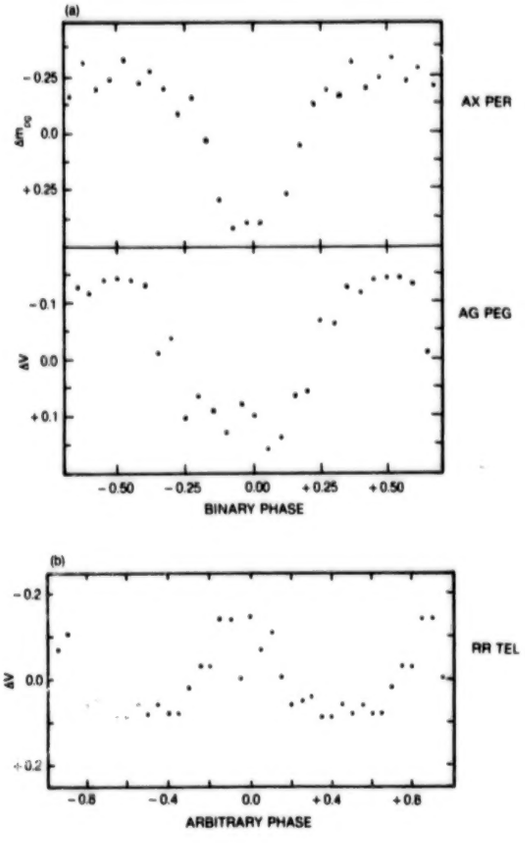


FIGURE 1.

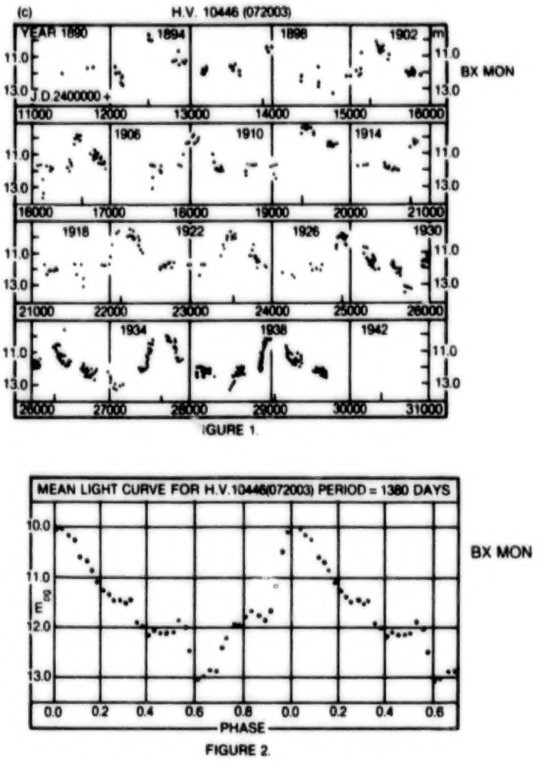


FIGURE 2.

Figure 11-6. Periodic light variations of symbiotic stars: AX Per, AG Peg, RR Tel (Kenyon, 1986), and BX Mon (Mayall, 1940).

It is clear from the above considerations that the presence of periodic light variations does not represent an evidence of binarity. Only observations in different ranges can provide an answer to this problem. Table 11-1 summarizes the main parameters of the regular, or quasi-regular light variation observed in symbiotic stars.

clearly distinguish among the two, irregular and periodic, types of long-term variation, since they are associated with two different phenomena. Most symbiotic stars show small amplitude (one-tenth of magnitude) fluctuations on time scales from days to minutes. In many cases, the photometric accuracy is not large enough to confirm

TABLE 11-1. BASIC DATA ON THE OPTICAL LIGHT VARIATIONS IN SYMBIOTIC STARS.

Star		Maximum (JD) 2400000+	Period days	Ref.
Z	And		756.85	1
EG	And	43200.5	470	2
CI	Cyg	11902	855.25	3,4
AG	Dra		554	5
RW	Hya	21519.2±4.2	372.45±0.3	1
BX	Mon		1380	6
SY	Mus	35175.7±15.7	627.0 ±1.2	7
AR	Pav		605	8
AG	Peg	42710.1 ±6.0	816.5 ±0.9	9
RR	Tel	42550.7±18.7	374.2 ±3.8	10

Notes to the table. (1) Kenyon and Webbink (1984). (2) Smith (1980). (3) Greenstein (1937). (4) Belyakina (1974). (5) Meinunger (1979). (6) Mayall (1940). (9) Fernie (1985). (10) Kenyon and Bateson (1984).

As a conclusion of this section on the light history of symbiotic stars, there is a large variety of shape, amplitude, and time scale in the light curves of different objects. But also, the same object generally displays different types of variability at different epochs, and variations on long and very long time scales to short and very short ones. The "secular" behaviour is known only in a relatively small number of objects (a few dozen), obviously because it requires observations for several decades. But also observations for more than one century for a few objects have not helped the understanding of their long-term behavior. The variations are, in general, irregular. The regular or quasi-regular fluctuations found in several objects are attributed to recurrent eclipses of a binary system. In many cases, this has been confirmed by the spectroscopic observations. It is important in any study of symbiotic stars to these variations and their behavior, but the amplitude seems to generally increase towards shorter wavelengths. Much work is still to be done in this field.

IV. THE VISIBLE SPECTRUM

In this section we shall describe the main features of the visible spectrum of symbiotic stars, pointing out both the spectral anomalies and the features that are commonly seen in "normal" stellar spectra. In general, three main spectral components are identified in the optical spectrum of symbiotic stars: (1) the cool stellar spectrum, (2) the blue continuum excess, (3) and the rich emission line spectrum. These components can be easily seen in the spectra reproduced in Figure 11-7. In the following we shall separately describe the three spectral features.

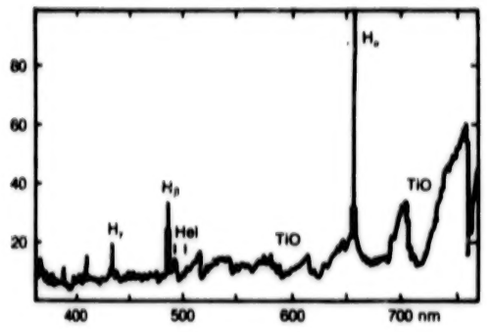


Figure 11-7 The optical spectrum of BX Mon from 3800 to 7600 A (Viotti et al, 1986). The TiO absorption bands are clearly visible in the red part of the spectrum. Shortwards of about 6000 A, the late type spectrum is masked by the blue continuum. Note the prominent emission lines of hydrogen and helium.

IV.A. THE RED COMPONENT

Most of the symbiotic stars have a red continuum that rises towards longer wavelengths. Metallic absorption lines (e.g., of FeI) or bands of molecular species (e.g., TiO, VO, C2) that are attributed to photospheric absorptions on a cool-star continuum have been identified in these continua. In Figure 11.7, the prominent TiO bands typical of an intermediate M-type giant are clearly seen in BX Mon.

The cool-star spectral features are easily seen in the red, near-IR where the cool spectrum normally dominates. As discussed later, these objects have visual/IR color indices typical of a late-type star and are therefore called S-type symbiotics (where S stands for "stellar"). In many cases also, absorptions from the resonance lines of CaI and CaII have been identified in the blue, but normally these lines are masked by the strong blue continuum excess.

A major problem is represented by the blue continuum, which is variable and extends to longer wavelengths. Thus the cool-star absorption lines are *veiled*, i.e., their central depth is reduced by an amount, that depends on the wavelength and that is variable in time. This is illustrated in Figure 11-8, which shows the high-resolution spectrum of CH Cyg during different epochs.

CI Cyg is another example of variable veiling of the blue spectral component which could mimic an apparent time variability of the cool spectral component. From the analysis of the 1975 spectrum of this star, Audouze et al. (1981) claimed the occurrence of an s-process episode with the considerable enhancement of the elements produced from the s-process. However, their observations refer to a phase of minimum luminosity when the blue region was dominated by the cool spectral component. Therefore, the observed large spectral change was only due to the disappearance of the blue, shell-type spectrum formed during the outburst, dominated by singly ionized metal lines, and the emerging of the M-spectrum with several FeI lines, wrongly identified by Audouze et al. as lines of rare earths (Kenyon et al. 1982).

Several authors have provided the spectral classification of symbiotic stars, but frequently there is a large spread in the individual classifications for the same star. For instance, AG Dra has been variously classified as K1II, G5, K3III, or K0I (Kenyon, 1986), and one could argue that the cool component of AG Dra is highly variable, but this has not been confirmed by recent accurate studies. More probably, the spectral classification of this star is largely affected by the variable blue spectral component, as discussed above for the cases of CH Cyg and CI Cyg. Actually, the classical (old) criteria of spectral classification are based on the relative strength of absorption lines and bands in the blue region, while only recently the yellow-red region has been more extensively used for the cool stars. Most of the reported classification of symbiotic stars were based on blue spectra, where the absorption features are seriously masked by the variable blue continuum and by the emission lines. Thus, one should take care of these classifications, especially the oldest ones.

Spectral classification of the cool components of the symbiotic stars mostly based on near-IR spectrophotometry, has been performed by, among others, Kenyon and Fernandez-Castro (1987), and Schulte-Ladbeck (1988). Typically, the symbiotic stars show deep TiO absorption bands whose strength suggests a spectral type from early M (e.g., AG Peg) to intermediate M (Z

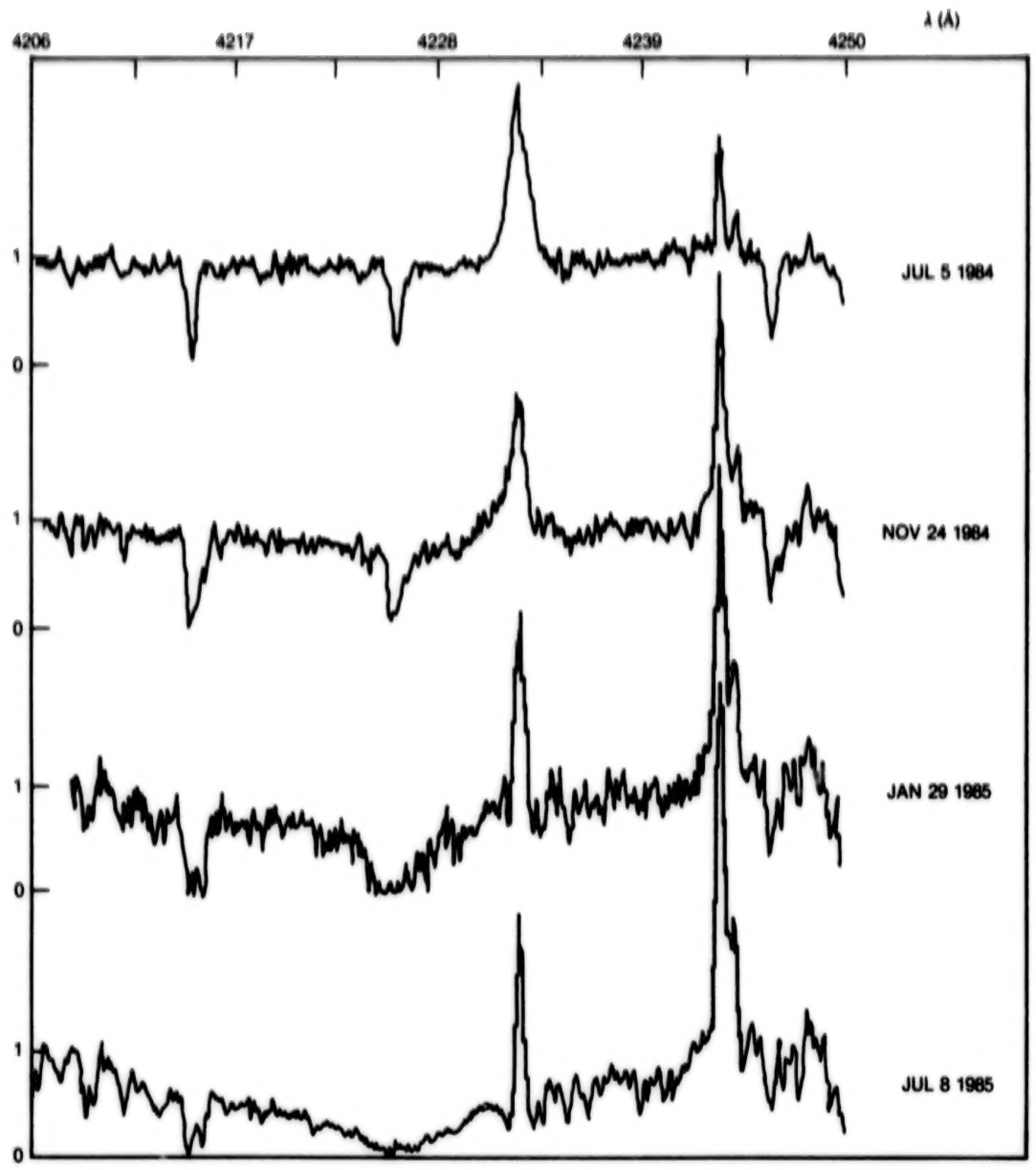
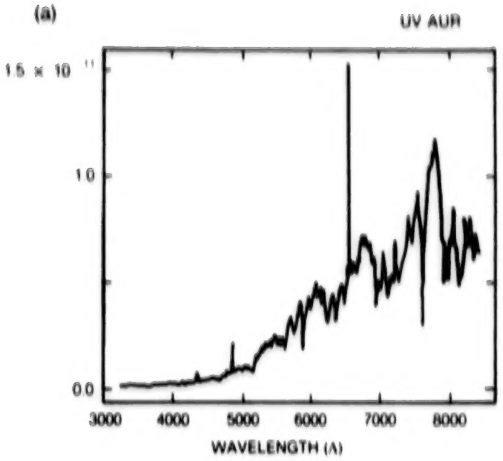


Figure 11-8. The high resolution spectrum of CH Cyg during two different luminosity phases: (a) 5 July 1984) (V~6.0); (b) 8 July 1985 (V~7.8). The broad CaI absorption, associated with the spectrum of the M component is strong at minimum, but invisible at maximum. Note the strong "shell" absorptions of FeI present all the time and the prominent FeII emission at 4233 A (courtesy of M. Hack).

And, CI Cyg) and late M-type (e.g., V1329 Cyg). A few objects included in the symbiotic category have a hotter cool components of type F or G. Examples are M1-2 (type G2), HD 330036 (F5III-IV, Lutz, 1984), and HD 149427 (F-type, Webster, 1966). These stars have been called "yellow symbiotics" by Glass and Webster (1973). They are also known, from their IR spectrum, as D'-type symbiotics (Allen, 1982). Another case is the symbiotic star AG Dra which, as seen above, is characterized by a K-giant spectral component. This star is interesting also for its large radial velocity (-140 kms^{-1}, Roman, 1953), and high galactic latitude (+41°). Thus AG Dra is a typical Pop II object, and probably not the only one, among symbiotic stars, as we shall discuss in the summary section of this chapter.

C-8.



In a few symbiotic objects, molecular carbon bands, instead of TiO ones, have been identified. This is, for instance, the case of the bright galactic object UV Aur (Figure 11-9). Other examples are UKS Ce-1 and Weaver's star in our Galaxy (Schulte-Ladbeck et al., 1988), and S63 in the Large Magellanic Cloud (Figure 11-9). The latter is one of the two symbiotic objects so far identified in the LMC (Allen, 1982) and could suggest a higher frequency of carbon symbiotics in LMC than in our Galaxy. Actually, it is well known that in the LMC, the frequency of carbon stars among late-type stars is much larger

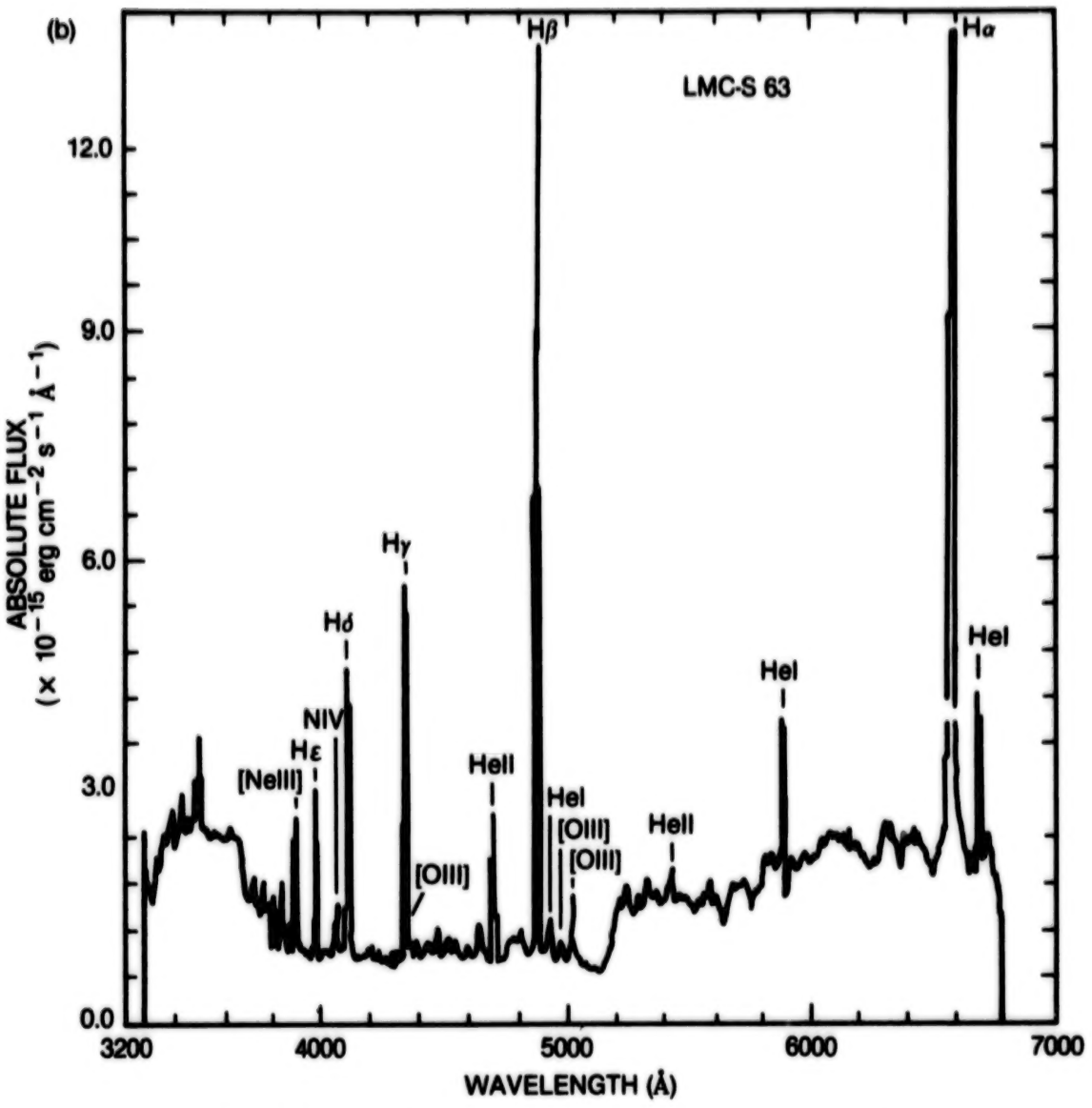


Figure 11-9. The optical spectrum of two carbon symbiotic stars, UV Aur (Kenyon, 1986), and S63 in the Large Magellanic Cloud (Kafatos et al., 1983).

than in our Galaxy. It would be important to investigate in the future if the frequency of carbon spectra in the LMC symbiotics is higher by a similar amount. This could provide crucial information about the origin of symbiotic stars.

In some symbiotic stars, the red continuum is an extension of the IR excess, which is attributed to thermal dust emission (the so-called D-type symbiotic stars, see Section VI). This is, for instance, the case of V1016 Cyg (Figure 11-1), where the contribution to the red of a cool photospheric spectrum should be small and the photospheric absorption features hard to identify. Actually, in this star, the molecular absorption bands seem to be present but very weak (Mammano and Ciatti, 1975). Also, in other D-type symbiotic stars such as RR Tel and HM Sge, the M-type features are hard to be seen (e.g., Thackeray, 1977). We shall come back to the problem of the spectral classification of the cool stellar spectrun in Section VI devoted to the IR observations.

IV.B. THE BLUE SPECTRUM

As discussed above, the main spectral feature that distinguishes the symbiotic stars from normal cool giants, is the presence in their visible spectrum of strong emission lines and of a "blue" continuum. In normal late-type stars, emission lines are present at the shortest wavelengths of the visible spectrum, and in the space ultraviolet, where the photospheric continuum rapidly drops. In the Sun, the photospheric spectrum extends to about 2000 A, where it turns to a rich emission line spectrum. In symbiotic stars, emission lines—of both low and high ionization species, and not only the Balmer series—are already seen in the visible spectrum, and around 4,000-5,000 A, there is a gradual transition from the cool photospheric spectrum, which dominates the longer wavelength region, to a "blue" continuum. This continuum extends to shorter wavelengths and to the space ultraviolet, and frequently presents a Balmer continuum excess. Typical cases of symbiotic stars with a positive Balmer discontinuity are Z And, BF Cyg, V1016 Cyg (Figure 11-1), AG Dra, V443 Her, SY Mus, AG Peg, ect. (see O'Dell 1967; Blair et al., 1983; Allen, 1984b; and Kenyon, 1986). The blue continuum of the symbiotic nova V1329 Cyg (Figure 11-10) is peculiar not only for the large Balmer discontinuity, but also for the presence of several very broad humps. Crampton et al. (1970) attributed them to emission lines typical of a Wolf Rayet star of type WN5. These features have also been observed by Baratta et al. (1974) in their objective prism spectra. In general, the violet end of the visible spectrum is not well recorded in the great majority of the observations, while this should give precious information about the structure of the emitting region or about the hot star atmosphere.

The blue continuum is highly variable (with respect to the cool spectrum), and its variability is mainly responsible for the behavior of the visual light curve of the symbiotic stars. Generally, symbiotic stars near maximum become bluer, while their colors are redder at minimum. But their trend is not well established, and red maxima have also been observed. During the maxima, the cool spectrum may be completely veiled by the enhanced blue continuum, and the photospheric absorptions disappear, while the color indices become bluer. If an eclipse occurs, the blue continuum disappears, and the red spectrum emerges, making the color index redder, as, for instance, observed in CI Cyg.

IV.C. THE OPTICAL EMISSION LINE SPECTRUM

Emission lines, both permitted and forbidden, belonging to a wide range of ionization energy and line strength have been identified in the optical spectrum of symbiotic stars. From neutral species up to six times ionized iron and calcium have been observed in the spectrum of the same object. Table 11-2 gives the atomic species identified in the emission spectrum of two well-studied symbiotic stars, Z And and RR Tel.

These species are commonly identified in the spectrum of symbiotic stars during quiescence and in symbiotic novae some time (months or years) after the beginning of the outburst. Most emission lines are those observed in the spectra of diffuse and planetary nebulae, and for this reason some authors suggested a physical link between symbiotic stars and planetary nebulae. Indeed,

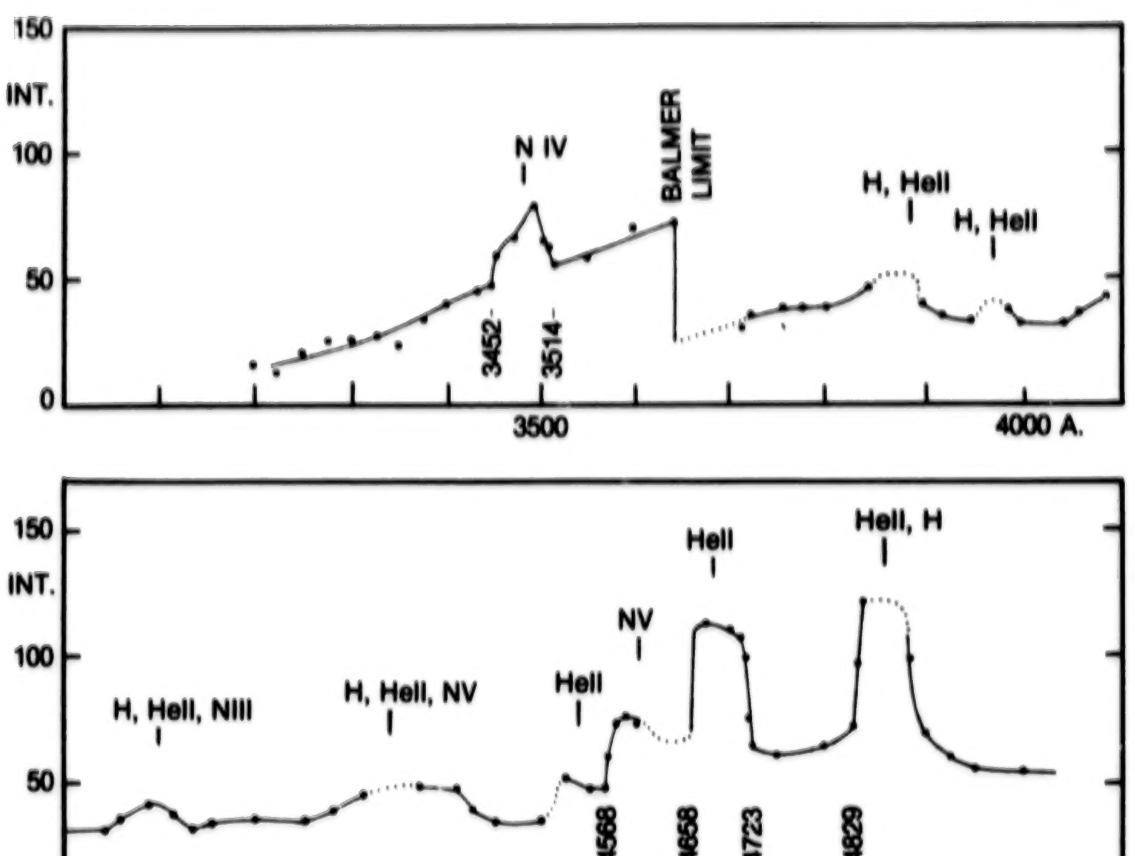


Figure 11-10. The blue continuum of V1329 Cyg in November 1969 (Crampton et al., 1970). Several WR features and the Balmer discontinuity are clearly visible.

TABLE 11-2. ATOMIC SPECIES IDENTIFIED IN EMISSION AND ABSORPTION IN THE OPTICAL SPECTRUM OF THE SYMBIOTIC STARS Z AND AND RR TEL.

Star	Emission Lines	Ref.	Abs. Lines	Ref.
Z And	H, HeI,II, CII,III,IV NIII, OII,III, NeIII,V, MgII, CaII, TiII, FeII,III?,VII, 6380 A	1,2,3	TiO, VO:	1,2
RR Tel	H, HeI,II, CII,III,IV NII,III,V, OI,II,III,IV NeIII,IV,V, MgI,II, SiII, SII,III, C1 IV:, AIII,IV,V, KIV,V, CaII,IV:,V, MnIV,V?, MnVI?, FeII,III,IV,V,VI,VII, 6830 A	4	TiO	4

References: (1) Swings and Struve (1941); (2) Boyarchuk (1968a,b); (3) Altamore et al. (1974); (4) Thackeray (1977).

the observation of intense forbidden lines indicates the presence of a diluted, highly ionized medium near or around the symbiotic object. Strong high-ionization lines (HeII, NIII, [OIII], [NeIII], [NeV], [FeVII]) have, in fact, been identified in the spectra of many symbiotics, and have long since raised the problem of their origin, e.g., whether collisionally or radiatively ionized (for instance, Ilowaisky and Wallerstein, 1968). Of particular interest is the intriguing problem of the still unidentified broad features at 6830 and 7088 A. These emission lines are present in the optical spectrum of symbiotic stars with the highest ionization level, such as RR Tel, He 2-38, and H 2-38, and probably are associated with a so far unknown highly ionized species (Allen, 1980a). It should be noted that in RR Tel and in other symbiotic novae, these features appeared in the latest stages of their spectral evolution, when the optical spectrum displayed the highest ionization level. Also, in some cases coronal lines have been observed: [FeX] has been reported in CI Cyg (Swings and Struve, 1940), and possibly in RX Pup (Swings and Klutz, 1976), while [FeXIII] has been identified in R Aqr by Zirin (1976). We should recall that still higher ionization levels have been observed in the recurrent novae T CrB ([FeX], [FeXIV]), and RS Oph ([FeX], [FeXI], [FeXIV], [AX], and [NiXII]; see Kenyon, 1986). These latter objects have, in fact, been often included in the category of symbiotic stars.

A major problem of the symbiotic phenomenon is the simultaneous presence of both high (e.g., [FeVII])-and low (e.g., FeII, [FeII])-ionization emission lines, implying the existence of a very wide temperature range in the environment of symbiotic stars. In this regard, their spectrum resembles fairly well that of the solar chromosphere, transition region and corona, and this could again suggest that a similar physical process is acting in the environment of the Sun and of, at least, some symbiotic stars.

Emission lines are variable, in both intensity and shape. As a rule, the line excitation is higher when the star is at minimum luminosity, and *vice versa*. RX Pup, during its bright stage of 1960-75 (V=8.5), showed in the optical hydrogen and ionized iron emission lines, while at minimum (in 1905, 1940, and 1981 to present, V~13), the star displayed a large ionization range up to [NeV] and [FeVII] (Allen and Wright, 1988). During outburst, the mean line excitation generally decreases, and P Cygni profiles are seen with absorption components displaced to shorter wavelengths by a few hundreds of km s^{-1}. Swings and Struve (1941) measured in Z And velocities from -83 to -186 km s^{-1}. At maximum, the spectrum of CI Cyg and RR Tel resembled that of an F supergiant with a few emission lines (hydrogen and helium) and absorption lines of singly ionized metals (Thackeray, 1950; Belyakina, 1979). Larger P Cygni velocities have occasionally been observed in a number of objects, such as BI Cru (Henize and Carlson, 1980), AG Peg (Merrill, 1951), RX Pup (Klutz, 1979), and RR Tel (Pottasch and Varsawsky, 1960). Radial velocities of the absorption components range from few to several hundreds km s^{-1}. After the outburst, during the fading phase and at minimum, the degree of ionization increases with the gradual appearance of higher and higher ionization lines (e.g., Thackeray, 1977). Thus, the behavior is rather similar to that of novae, except for the much shorter time scales. Spectral variability in individual objects will be discussed in more detail in Chapter 13.

In additon to the spectroscopic changes associated with the long-term light variability, many authors have noticed spectral variations on short time scales. For instance, night-to-night fluctuations of emission-line intensities have been observed in Z And (Kenyon, 1986). Scanner observations of CH Cyg by Walker et al. (1969) revealed that the Balmer excess is rapidly varying on time scales of minutes. Several other examples can be found in the literature (most of which are reported in Kenyon's thesis and book (Kenyon 1983b, 1986)), but in the majority of cases, the observations are too scattered, and the authors do not provide a quantitative picture of the phenomenon. So, it is not possible at this stage to have a clear idea about amplitudes, time scales, and trends of these fluctuations. This is one field that should require more observational (and systematic) work in the future.

IV.D. LINE PROFILES

The high-resolution spectroscopy of most symbiotic stars has revealed the existence of emission lines with a very complex profile. This is best illustrated by the Hα line, which presents a large variety of shapes in different objects, and, for the same object, in different epochs. Figure 11-11 shows the Hα profiles in a number of symbiotic stars.

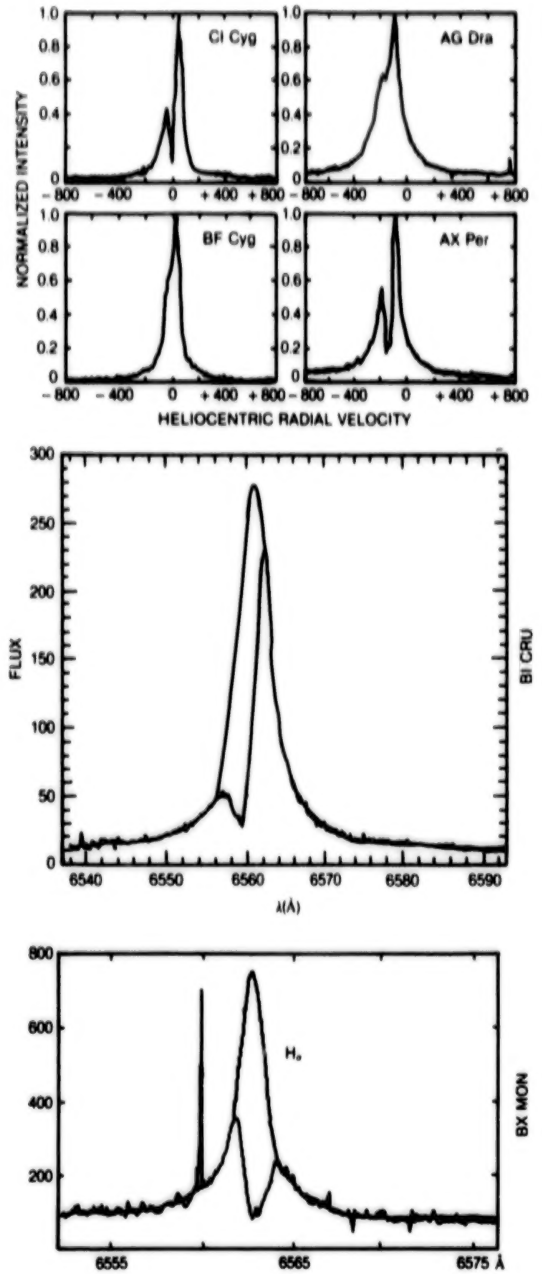


Figure 11-11. Hα profiles in symbiotic stars (Kenyon, 1986; Viotti et al., 1986 Rossi et al., 1988).

Hα profiles in individual objects were studied among others by Smith and Bopp (1981: AG Dra), Oliversen et al. (1985: EG And), Viotti et al. (1986: BX Mon), Rossi et al. (1988: BI Cru), etc. Generally Hα is characterized by a central peak broadened by one to a few 100 km s^{-1} (FWHM). A P Cygni profile is frequently observed again with an absorption component violet-shifted by -100 ÷ -300 km s^{-1}, although sometimes red-shifted absorptions have also been found. In many of those objects where the P Cygni absorption is not seen, the Hα peak appears asymmetric, sometimes with a bump in the emission wing. Hα is generally variable in intensity and shape on a long time scale, probably as the result of the stellar "activity" and/or orbital motion. Oliversen and Anderson (1982b) described the change for the Hα profile in AG Dra as a function of the phase of the U-band photometric curve. Iijima (1985) noted that in BX Mon, Hα changed from direct to inverse P Cygni profile. Oliversen et al. (1985) studied the Hα profile variation in EG And during one cycle of the suggested 470-day period. They found dramatic variations of the line equivalent width and profile, with the line changing from strong emission peak to broad central absorption with weak side emissions (Figure 11-12).

Extended broad wings are another frequently observed feature of Hα; they are generally better seen in the middle resolution spectrograms. Broad wings are also seen in other strong emission lines, but a systematic study of these features has not yet been made, mostly because of the lack of high S/N optical spectra. As discussed later in this chapter, these features are also present in the ultraviolet spectra of several symbiotics. P Cygni profiles have been observed in several optical lines (H, HeI, FeII, etc.) during different phases of the history of symbiotic stars. For this reason, many authors classified some symbiotics as Be or P Cygni stars (e.g., Beals, 1951). The displacement of the P Cygni absorptions is from one to several hundreds of km s^{-1}, again depending on the symbiotic phase. In 1950, the HeI 3888 line in AG Peg developed multiple absorption components at velocities from -72 to -382 km s^{-1}, a behavior similar to that of novae (Kenyon, 1986).

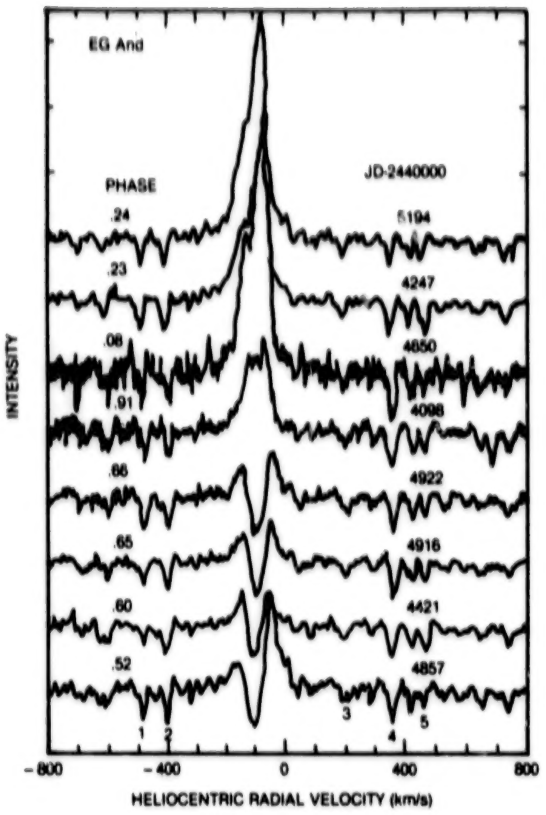


Figure 11-12. Variation of the Hα profile in EG And during August 1979 to August 1982 as a function of the phase of the Smith (1980) curve (Oliversen et al., 1985). Photospheric absorption features of neutral elements are seen on the stellar red continuum.

As regards the "narrow" emission components, at high resolution their width is of the order of a few to several 10 km s^{-1}. When measured with great accuracy, the width appears different in different ionic species. For instance, Muratorio and Friedjung (1982) found that in V1016 Cyg, the FWHM of the emission lines varies from 40-60 km s^{-1} for the singly ionized metal lines to 110-150 km s^{-1} for the highly ionized lines of [NeIII], [AIV], [NeIV], and [FeVII].

V1329 Cyg, RX Pup, HM Sge, RR Tel, and other symbiotics display, or have displayed during some phases of their history WR features (Crampton et al., 1970; Thackeray and Webster, 1974; Brown et al. 1978), but not the OVI characteristic of very high excitation (see Allen, 1980). As discussed above, V1329 Cyg presents very broad WR features, which are better seen at low resolution. Similar features could be present in other symbiotic objects but are difficult to observe. This raises again the need of high-quality observational data.

At high resolution, the strongest emission lines frequently exhibit a multiple structure sometimes similar to that observed in the decline phase of novae. A typical example is again V1329 Cyg. According to Crampton et al. (1970), after the outburst, this star displayed [NeIII] and [OIII] lines with a dozen or more narrow emission components from -240 km s^{-1} to +250 km s^{-1}. This multiple structure is still present to date (Figure 11-13) and indicates that the feature was not episodic and only related to the outburst.

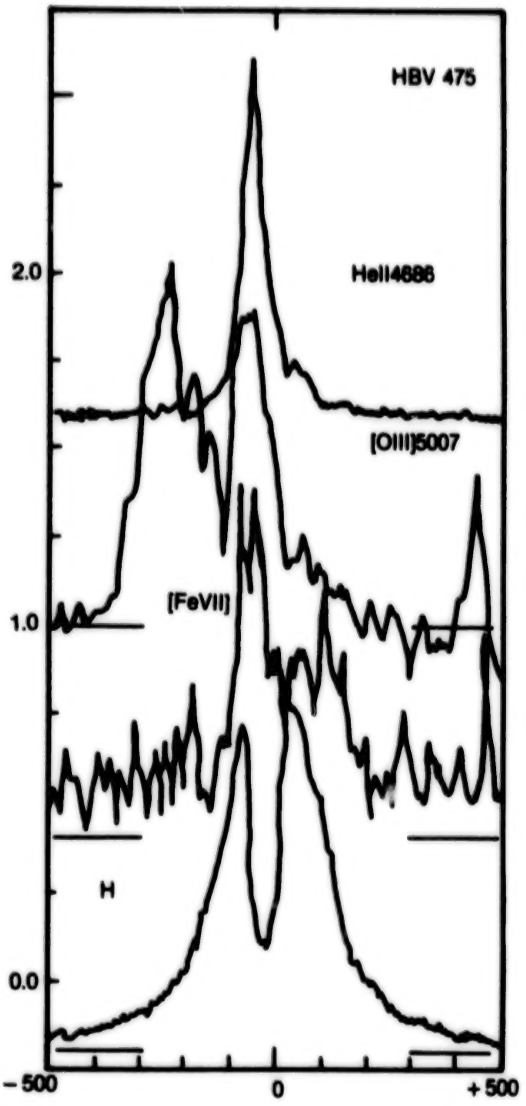


Figure 11-13. Emission line profiles in V1329 Cyg (Tamura 1988). Note the very different shape of lines of different species.

IV.E. RADIAL VELOCITY

The knowledge of the radial velocity of a symbiotic system is basic for the determination to which populations it belongs, but also to find any periodicity related to the orbital motion of a binary system. However, it is difficult to observe the cool star absorption lines at high enough resolution. The narrow FeI lines are rather weak and frequently masked in the blue-yellow region by the hot continuum. In many symbiotics, the radial velocity is close to zero, but a high velocity of about -140 km s^{-1} was found in AG Dra (Roman, 1953), which, together with its high galactic latitude, +41°, is strongly suggestive of a Pop II object. We should add that AG Dra is not unique for its high radial velocity. There are other cases in which the *emission lines* have high (positive or negative) radial velocity, which is probably associated with a high radial velocity of the system, rather than to the orbital motion of the components. For instance, a high radial velocity was found for the symbiotic novae V1016 Cyg (-68 km s^{-1}, FitzGerald and Pilavaki, 1974; Wallerstein et al., 1984); and RR Tel (-61 km s^{-1}, Thackeray, 1977). Large absolute values were also found in RT Ser (+92 km s^{-1}), AS 296 (+100 km s^{-1}), EG And (-95 km s^{-1}), and AX Per (-109 km s^{-1}) (Wallerstein, 1981; see also Section X). In CH Cyg, the radial velocity of the photospheric absorption lines and of the FeII, [FeII], and [OI] emissions is variable (Faraggiana and Hack, 1971), but the average value of -60 km s^{-1} is again very different from the local standard of rest. Wallerstein (1981) assembled the radial velocity of 19 symbiotic stars, and found a large velocity dispersion of 63±14 km s^{-1} (or 51±14 km s^{-1}, if AG Dra is omitted), similar to that of an old disk population such as long-period variables.

A systematic variability of the M-type absorption lines was found by Thackeray and Hutchings (1974) for the eclipsing symbiotic AR Pav, with a period in agreement with the period of the eclipses. A similar result was obtained by Hutchings et al. (1975) from the study of the cool star photospheric lines in AG Peg. More recently, Garcia (1986) performed a systematic study of the radial velocity in a number of symbiotic stars, using a cross-correlation technique. He found a periodic variation in AG Dra, EG And, T CrB, TX CVn, and RW Hya. This result has been confirmed by Garcia and Kenyon (1988; see Figure 11-14).

Presently, many observational programs are devoted to this crucial point, and there is growing evidence of periodic radial velocity variability in many symbiotic stars (see Section X).

IV.F. MAGNETIC FIELDS

The eruptive character of symbiotic stars might suggest the presence of intense surface activity in their dominant (= cool) spectral component. This, in turn, could be associated with the presence of strong magnetic fields. These fields should be variable according to their "activity," to possible stellar rotation and to different line-of-sight observations during the orbital motion, if the symbiotic object is binary. In the latter case, the hotter component could be a white dwarf, and these stars frequently have very intense magnetic fields. The search for magnetic fields and their time variability, in symbiotic stars, is therefore of no small importance in order to provide crucial information on the nature of the components. At present, however, the results are quite scanty and controversial, and further work is needed in the field. Two symbiotic stars—EG And and AG Peg—were included in the pioneering survey of Babcock (1958). Magnetic measurements in the blue spectral region of these two stars during 1949-55 gave a strong and variable magnetic field, with extreme values ranging from -1050 to +1100 gauss for EG And and from -1800 to +300 gauss for AG Peg. Babcock also noted that appreciable changes occurred in a few weeks.

Slovak (1982a) observed again the two symbiotic stars in 1978 with a photoelectric Zeeman analyzer measuring two spectral regions centered at 6129 and 6555 A; the first region contains many absorption lines, while the second includes Hα with emission and absorption components. Slovak did not confirm the kilogauss fields of Babcock, and provided a mean magnetic field of -3±49 and -66±36 gauss for EG And and AG Peg, respectively. He also noted a lack of magnetic line broadening in the two stars. Observations of

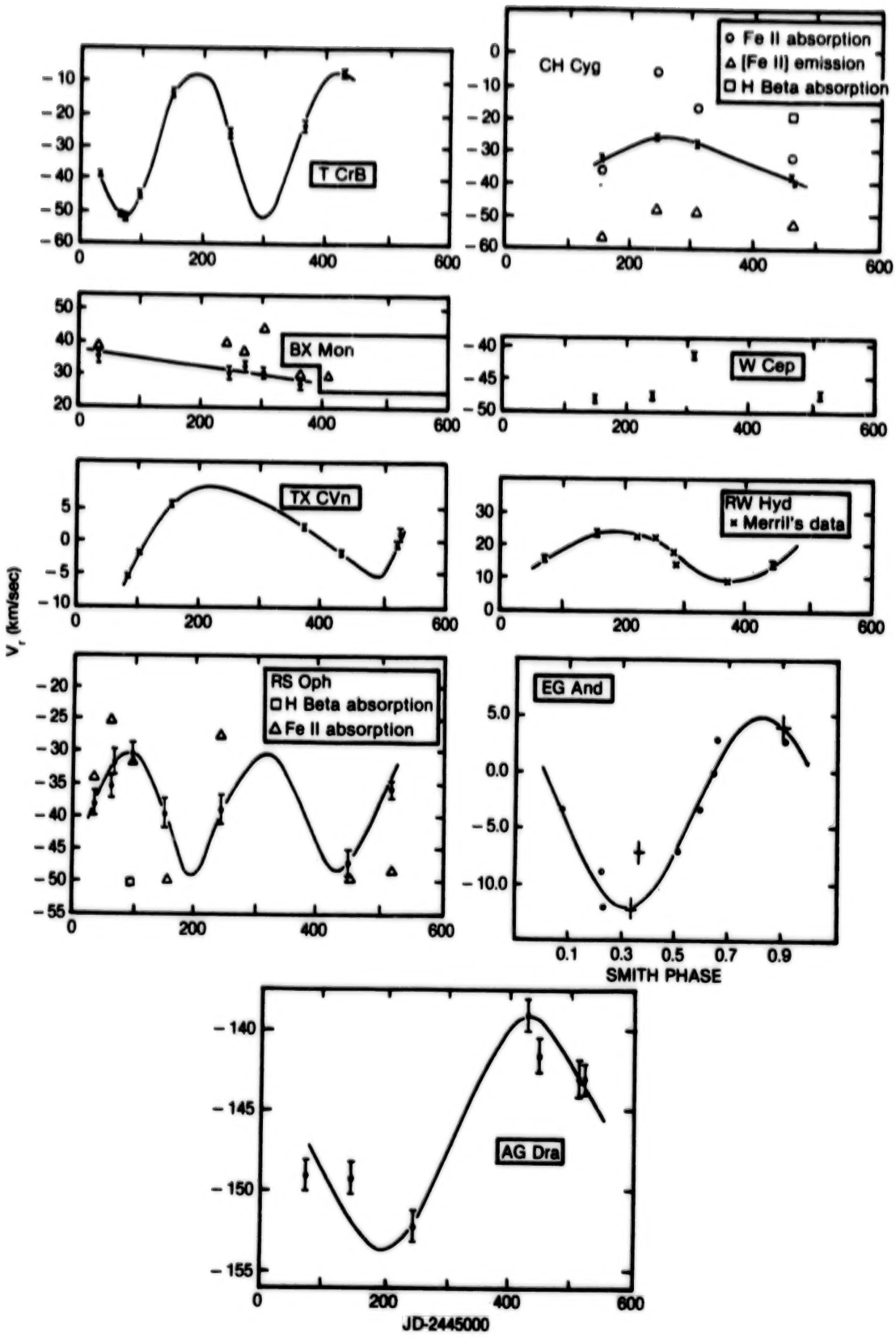


Figure 11-14. The radial velocity curves in symbiotic stars (Garcia and Kenyon 1988).

AG Peg separated by about one year do not give evidence of significant field variability in disagreement with Babcock results. Slovak also observed CH Cyg in 1978 and 1979 during its bright (V=6-7) phase, and again found a null result (+23±132 gauss, and no significant magnetic broadening in any of his spectra).

Luud (1986) discussed the results of Babcock and Slovak, which were based on measurements in two different spectral regions. The disagreement could then be related to the fact that two different physical regions were actually observed. Luud noted that the large (~ 10^3 gauss) magnetic fields of Babcock were observed close to the phase zero (hot star behind the red giant) of the orbital motion, just before ingress for EG And, and just after egress for AG Peg. Intense magnetic fields could be present in symbiotic stars only at certain phases of their orbital motion and of their activity. Therefore, future work should cover a period of several years to unveil this problem.

V. POLARIZATION

Polarization of the stellar radiation is, in general, an indication of deviation from spherical symmetry. Linear polarization has been measured in many stars surrounded by extended atmospheric envelopes and circumstellar matter, such as WR and Be stars, T Tau stars, novae and luminous red variables, as well as in some interacting binaries. Therefore, it is to be expected that also symbiotic stars should present a significant amount of polarization, since their spectral features clearly suggest the presence in most of them of extended, asymmetric atmospheres, of dusty circumstellar envelopes, disks, etc. This polarization should be variable with time according to the activity of the star, and/or to the orbital phase, and the study of its time variability should give precious information about the structure of the stellar envelope(s), as well as a better insight into their suggested binary nature. Symbiotic stars however, are, in general, rather faint in the visual, so that it is difficult to achieve a high enough accuracy in the polarimetric measurements. In addition, these objects are normally reddened by a significant amount of interstellar extinction, and in some cases, the intrinsic component of the polarization cannot be distinguished from the larger interstellar polarization, especially in the absence of variability. Only in very recent years has systematic polarimetry of symbiotic stars been undertaken, and still the amount of observations is too spare (at the time of writing this report) to draw clear conclusions on the polarization properties of symbiotic stars. An overview of the problem was recently given by Magalhaes (1988).

CH Cyg is one of the best studied symbiotic stars, being one of the brightest objects. This star, which is described in detail in Chapter 13, has an M6III spectrum and a variable blue continuum which fills the M photospheric absorption lines, and extends to the space ultraviolet (Hack and Selvelli 1982). CH Cyg was at minimum luminosity (about V=8) until the end of 1976, then brightened to V=7 in 1977 and to V=6 in 1981. A sudden drop of luminosity of one magnitude occurred in July 1984, then in 1985 the star faded to the preoutburst minimum of V=8.

Broad band polarimetry of CH Cyg was made throughout the whole recent light history. Rodriguez (1988) found that during the preoutburst phase, the degree of polarization was maximum in the blue (nearly 2 *per cent*), decreasing to 0.5 *per cent* in the red. A polarization increase was noted between 1974 and 1976 with a change of the position angle (Figure 11-15). Piirola (1982, 1983) measured the linear polarization of CH Cyg in the UBVRI bands during 1977-82, during the gradual brightening of the star. In 1978, the polarimetry in the UBV bands was again characterized by a larger polarization towards shorter wavelengths, with nearly constant position angle. After 1979, a different wavelength dependence was found with a strong rotation of the position angle with wavelength. Later, the blue-UV polarization decreased, but it was still larger than in the visual, where there was a minimum of polarization and an increase towards the red-near infrared. In 1981, the polarization in the longer wavelengths decreased, and the maximum polarization was in the blue. Rodriguez (1988) observed CH Cyg in September-October 1984 just after the luminosity drop: He measured a large decrease of the degree of polarization and a weaker depend-

ence on wavelength than before (Figure 11-15). This peculiar behavior of CH Cyg can be explained by strong changes in the structure and geometry of the scattering envelope(s). In particular, the increase of the polarization of CH Cyg in 1980 in the R and I bands could be attributed to the presence of large ($a \sim 1\mu m$) particles (Piirola, 1983), while the 1984 decrease should be caused by the contribution of the hot radiation source (Rodriguez, 1988).

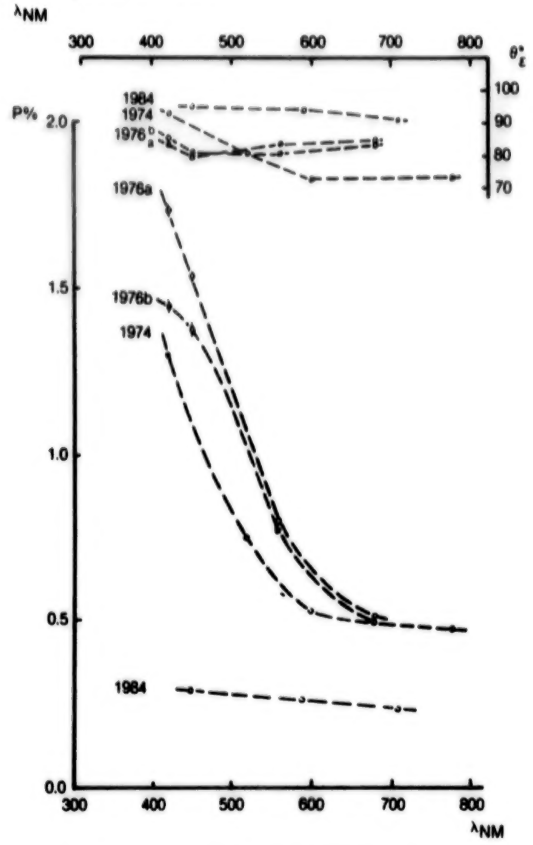


Figure 11-15. Linear polarization measurements of CH Cyg in 1974, 1976, and 1984 (Rodriguez, 1988).

The polarization of the symbiotic Mira R Aqr has been widely studied by several authors. This star is interesting for its relative nearness and for the many peculiarities, which will be discussed in detail in Chapter 13. Serkowski (1970) studied the time variability of the linear polarization of this star during the cycle of the Mira variable, and found large variations that suggest modulation of the structure of the circumstellar envelope by the Mira pulsation. He also found a large increase of the polarization towards the near ultraviolet. More recently, Aspin et al. (1985) discovered a remarkable structure of the polarization in the optical spectrum of R Aqr. The polarization increases across the TiO absorption bands and decreases in the emission lines (Figure 11-16).

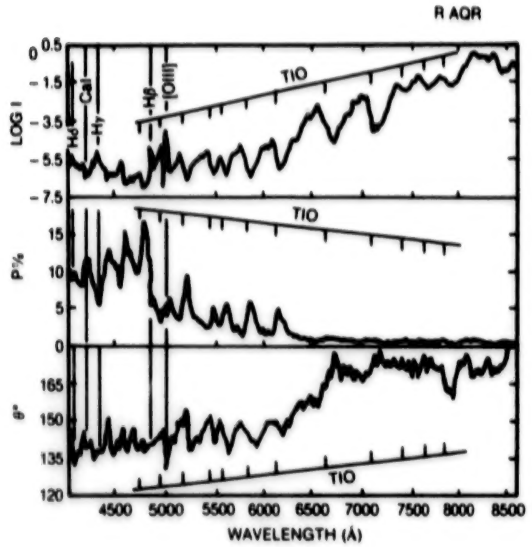


Figure 11-16. Intensity and polarization spectra in the Mira-type symbiotic R Aqr (Aspin et al., 1985).

CH Cyg and R Aqr are affected by a small amount of interstellar reddening (see Table 11-7), so that the linear polarization in these objects arises in the symbiotic system. Other symbiotic stars like CI Cyg are significantly reddened. In the eclipsing binary CI Cyg, the polarization appeared variable and was characterized by a strong rotation of the position angle with wavelength (Figure 11-17), which gives a clear evidence of the presence of an intrinsic polarization.

In general, the interstellar polarization could be quite large, but, since the observed polarization is the *vectorial sum* of intrinsic and interstellar polarization the stellar component can still be determined even if it is smaller than the interstellar one, in the case that the intrinsic and interstellar components are nearly orthogonal. The latter can be measured in nearby stars, which have no intrinsic polarization, and can be vectorially subtracted from the polarization measured in the symbiotic star.

Extensive polarimetry of symbiotic stars has been recently performed by Schulte-Ladbeck (1985) and Schulte-Ladbeck and Magalhaes (1986) (Figure 11-18). Some results of those observations are summarized in Table 11-3. It has

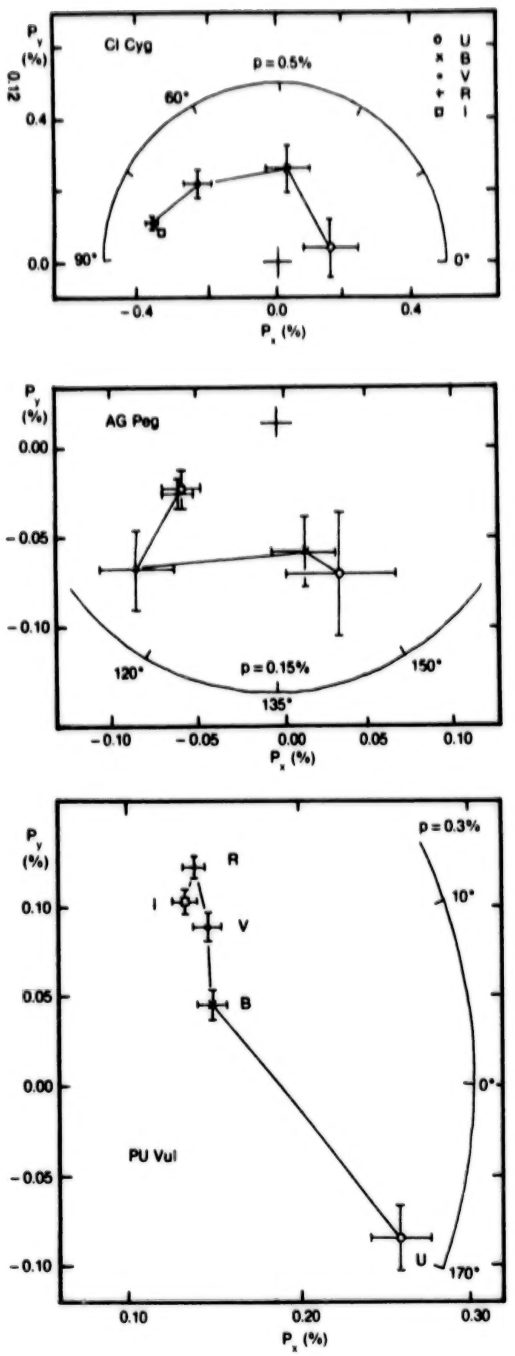


Figure 11-17. The wavelength dependence of the linear polarization in CI Cyg, AG Peg, and PU Vul (Piirola, 1983).

been found that some stars, namely V1016 Cyg, AS 338, and HM Sge, possess intrinsic polarization, while for the majority of the symbiotic stars, the observed polarization is interstellar. In general, the amount and nature of the polarization in symbiotic stars is not well known. In addition, nothing is known about the polarization near the emission lines and in the IR, and on the circular polarization. New extensive polarimetry of symbiotic stars is needed to gain precious information about their nature.

VI. INFRARED OBSERVATIONS

The first systematic infrared observations of symbiotic stars (e.g., Stein et al., 1969; Swings and Allen, 1972) revealed the presence of strong fluxes, which can be attributed to a cool component with a temperature around 3,000 K or less, and to circumstellar dust. Since then, a large amount of IR data on these objects has been accumulated also thanks to space observations with the IRAS satellite. These data are providing a fundamental ground for understanding the nature of the cool components of the symbiotic systems. They represent a real progress on the study of the symbiotic phenomenon, as is illustrated below. Two main categories of symbiotic stars were clearly identified, thanks the IR observations: the S- and D-type systems, which are characterized by different energy distribution and time behavior. (Actually, there is another category, or subgroup of symbiotic stars called D'-type, which significantly differ from the D-type objects).

The discovery of this *bimodal distribution* of symbiotic stars in the near-IR has been one fundamental step to understand the nature of the symbiotic phenomenon. In particular this IR behavior is correlated with properties of the stars at other wavelengths. It has also been noted that the D-type systems have, in general, a higher level of excitation of the emission line spectrum. In the following sections we shall discuss the energy distribution and the main spectral features of these groups and analyze their time behavior.

VI.A. ENERGY DISTRIBUTION

The infrared observations of symbiotic stars have proved to be a fundamental tool to investigate the nature of these objects. The first IR observations of symbiotic stars were made by Swings and Allen (1972), who found that these objects have color indices similar to those of late-type stars. Later on, Webster and Allen (1975) recognized the presence among symbiotics of two

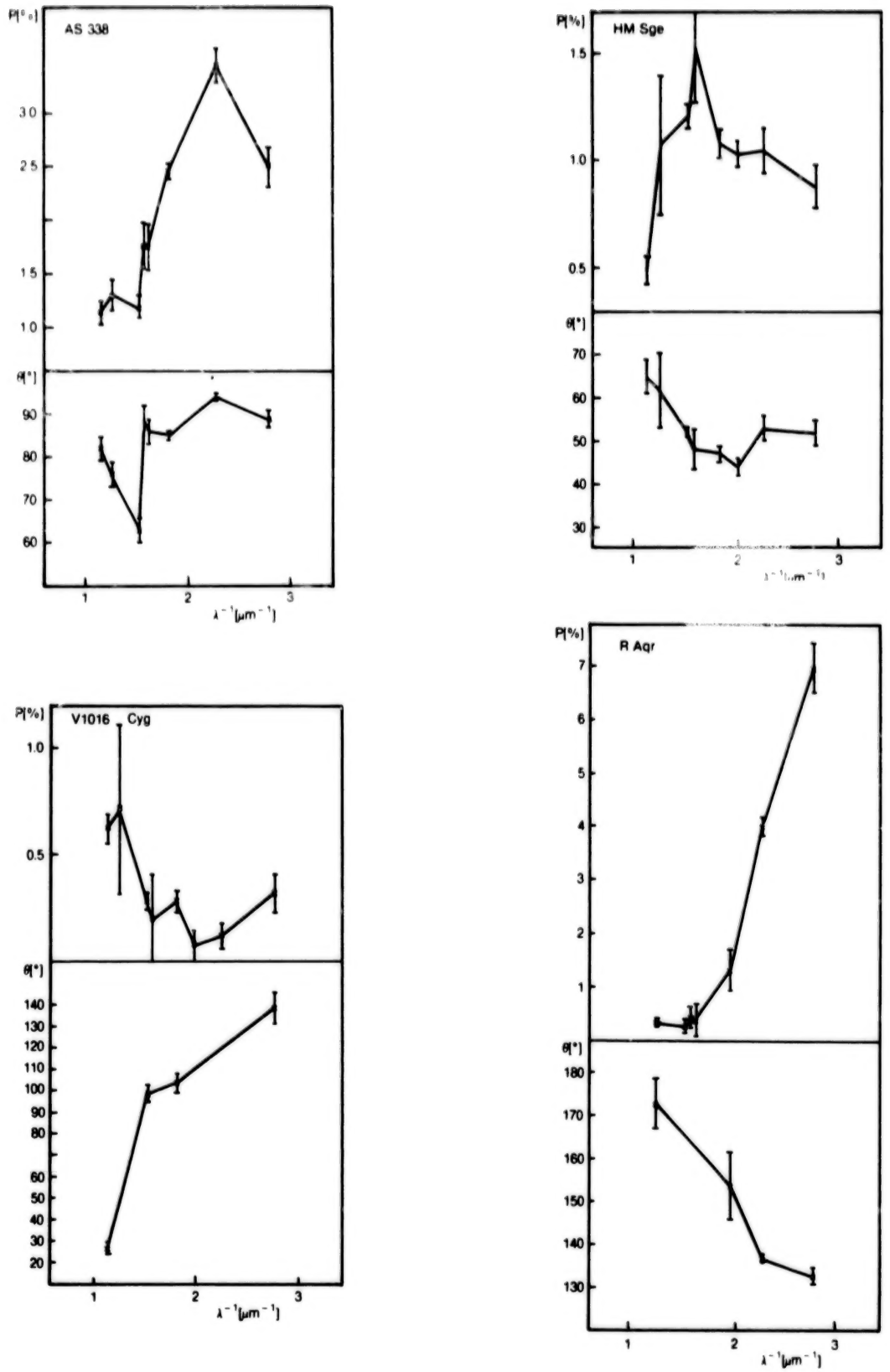


Figure 11-18. The wavelength dependence of the linear polarization in some symbiotic stars (Schulte-Ladbeck 1985).

TABLE 11-3. LINEAR POLARIZATION IN SYMBIOTIC STARS.

Object	Sp	IR	Polarization (P,θ)			Remarks
			1.5μm^{-1}	2.5 μm^{-1}	3. μm^{-1}	
R Aqr	M7	D		4.02,137°		var,7,8,3,4
CH Cyg	M6	S	0.2-0.5	0.3-1.8	1.3-2.0	var,5,6
CI Cyg	M4	S	0.3,81°	0.5,95°	0.7,153°	8,9
			0.43,90°		0.33,	7
			0.3,70°	0.25,40°	0.15, 5°	5
V1016 Cyg	M	D	0.28,104°	0.12 -		7
AG Peg	M2	S	0.1,115°	0.07,140°	0.10, 117°	5
RX Pup	M	D	1.8,123°	1.9, 118°	1.65, 113°)	1
HM Sge	M	D	1.08,47°	1.05, 53°		2,7
PU Vul	F+M	S	0.13	0.15	0.3	5
AS 338	M5	S	2.46,85°	3.44,94°		7

References: (1) Barbier and Swings (1982); (2) Efimov 1979); (3) McCall and Hough (1980); (4) Nikitin and Khudyakova (1979); (5) Piirola (1982, 1983); (6) Rodriguez (1988); (7) Schulte-Ladbeck (1985), (8) Serkowski (1970); (9) Szkody et al. (1982).

groups of objects with different energy distribution, the S- and D-type symbiotic stars. The general behavior of the two categories is described in detail by Allen (1979, 1982).

Figure 11-19 shows the near-IR energy distribution of a number of symbiotic stars. Some objects, such as Z And and CI Cyg, present a sharp rise from the visual to the near-IR with a broad maximum at 1-2 μm, and a gradual slope at longer wavelengths. This is the typical iR spectrum of the S-type symbiotic stars. In the two-color diagram (Figure 11-20), these stars are grouped near the locus of the late-type stars with J-H = ~ +0.8 to +1.5 and H-K= ~ +0.2 to +0.5 (Allen, 1982). This fact is immediately interpreted as due to the presence of a late star— typically an M giant—in the S-type symbiotics, and several authors succeeded in fitting their energy distribution from the visual (if not affected by the hot continuum and the emission lines) to the mid-IR with the spectrum of normal late-type stars (e.g., Kenyon et al., 1986; Viotti et al., 1986). As discussed below, the far-IR observations with the IRAS satellite have given a further support to this interpretation.

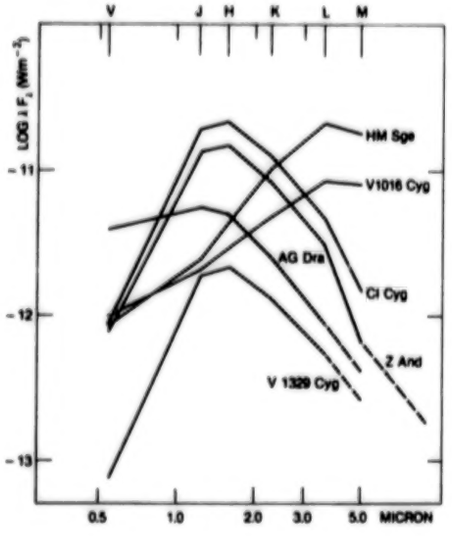


Figure 11-19. The visual-near infrared energy spectrum of some symbiotic stars (Eiroa et al., 1982). Two separate categories of objects are recognized showing respectively a maximum in the near-IR (the so-called S-type symbiotics) or a gradual rise to the mid-IR (the D-type ones).

A different behavior is displayed by the so-called D-type symbiotics. These objects represent a rather small subgroup, being about 20 *percent* of the total in current catalogs of symbiotic stars. Typical members of this subgroup are RR Tel, V1016 Cyg, HM Sge, and RX Pup. Their red continua have a smaller slope than in the S-type symbiotics, but the energy distribution peaks at longer wavelengths and is much redder than in normal M-type stars (Figure 11-

19). The H-K color index ranges from +0.5 to +1.8 (Allen, 1982; Figure 11-20). These values are characteristic of objects such as carbon stars and highly reddened nebular objects, where the extreme red color is attributed to a large intrinsic reddening and to thermal emission from circumstellar dust. Actually, the IR excess in the D-type symbiotics is commonly interpreted as due to dust emission, hence the name "D." However, it should be considered that, in general, it is difficult to fit the observed near-IR spectrum with a single temperature component.

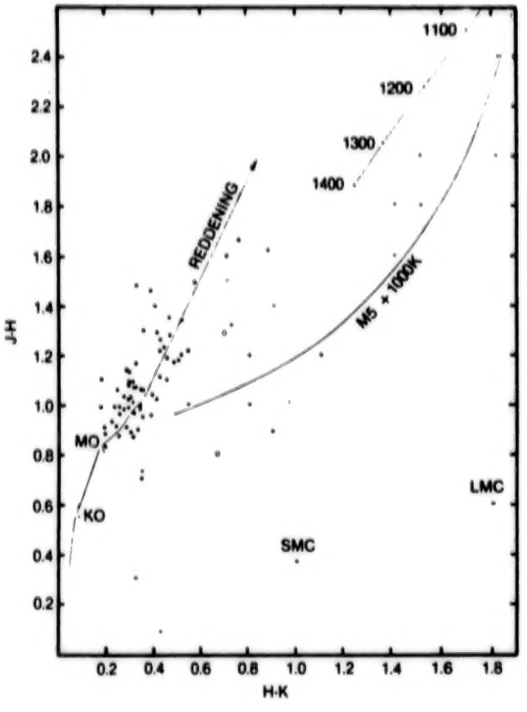


Figure 11-20. The two-color IR diagram for the symbiotic stars (Allen 1982).

A small number of symbiotics have a large excess longwards of 2-3 μm. Their IR energy distribution suggests a lower color temperature than in D-type symbiotics. Generally, the optical spectra are earlier than in other objects, F- or G-type, and were called by Glass and Webster (1973) as "yellow symbiotics." Allen (1982) defined these systems as D'-type symbiotic stars. Some examples are M1-2, AS 201 and HD 149427.

A new insight on the problem of symbiotic stars was recently provided by the IRAS observations (IRAS, 1985). Kenyon et al. (1988) reported that 34 S-type and 28 D-type objects were successfully detected. The frequency of D-type systems is thus larger than in the catalogs, as expected from their larger IR excesses. Four D-type symbiotics—R Aqr, V471 Per, RR Tel, and AS 201—were also detected at 100 μm. Because of their far-IR weak fluxes, only a few S-type systems were detected at 25 and 60 μm. A particularly interesting case is EG And. This star is rather faint in the IR, but has the chance of being placed close to M31, the Andromeda galaxy. Since IRAS has accumulated a long observing time for the galaxy, the limiting flux for IR sources in the field, including EG And, is much lower than in the IRAS Point Source Catalogue. The detected fluxes of EG And were: 4.6, 1.2, and 0.23 Jy at 12, 25, and 60 μm, respectively, while there is an upper limit of 0.7 Jy at 100 μm (Kenyon et al., 1986; 1988).

In the IRAS two-color diagram (Whitelock, 1987; 1988; Kenyon et al., 1988), the S-type systems are placed in a rather limited locus, close to cool stars, while the D-type systems are distributed in a large region of the HR diagram, including the loci of the Mira variables and of the planetary nebulae (see also Persi et al., 1987).

The IR energy distribution of the best observed S- and D-type symbiotics, based on ground and space (IRAS) observations is depicted in Figure 11-21. The mid-IR of the S-type systems is close to the Rayleigh-Jeans tail of the cool star spectrum with a modest or no indication of far-IR excess due to dust emission. This result is confirmed by the detailed study of the IRAS data by Kenyon et al. (1988). The large mid-IR excess of the D-type systems, in principle, would imply the presence of a strong thermal dust emission (e.g., Allen 1982). Circumstellar dust should be heated by the stellar photons (more probably, from the cool giant) at a temperature around 10^3 K. But Kenyon et al. (1986) suggested that in these systems the cool component, the giant star, is heavily reddened ($A_v \sim 1$-2) by dense circumstellar dust envelope. In this case, the observed spectrum is not thermal dust emission, but instead the reddened cool giant spectrum.

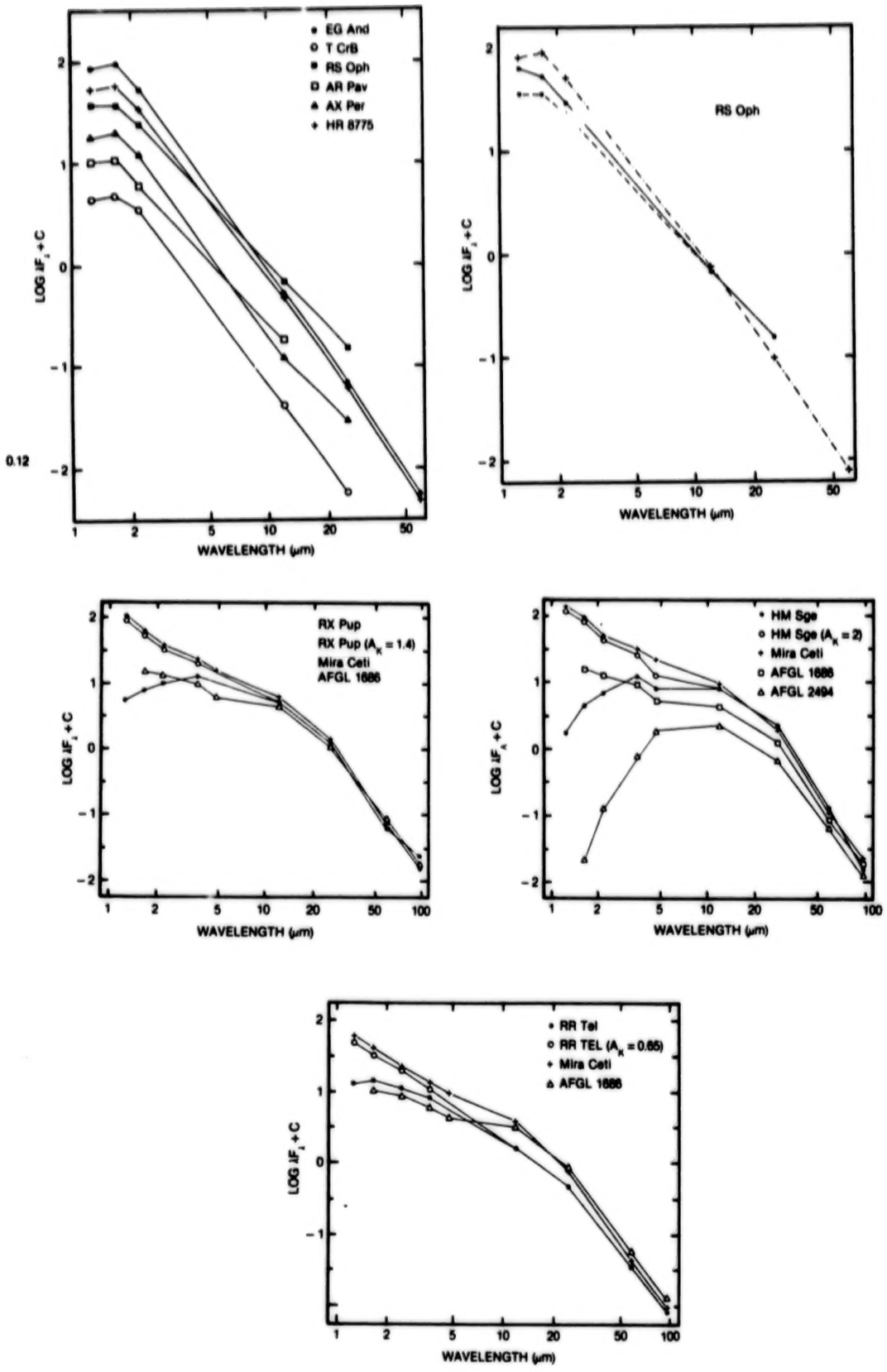


Figure 11-21. The infrared energy distribution of S-type (a) and D-type (b) symbiotic systems (Kenyon et al., 1986).

VI.B. SPECTRAL FEATURES

The major spectral features in the near-IR spectra of late-type giants and supergiants are the CO and H_2O absorption bands at 1.6, 2.3, 4.7 μm and 1.4, 1.9, 2.7 μm, respectively. The strength of these features depends on the temperature and luminosity of the cool star, and can thus be used to classify the cool components of the symbiotic systems and ultimately to derive their distance. CO and steam absorption features have been observed in several symbiotic stars. Kenyon and Gallagher (1983) have investigated the low-resolution IR spectra of symbiotic stars and find evidence of the 2.3 μm CO band in 12 S-type symbiotics and in R Aqr. By comparison with normal M-stars, Kenyon and Gallagher have derived the basic properties (temperature, luminosity, and distance) of the cool components for a number of symbiotic stars.

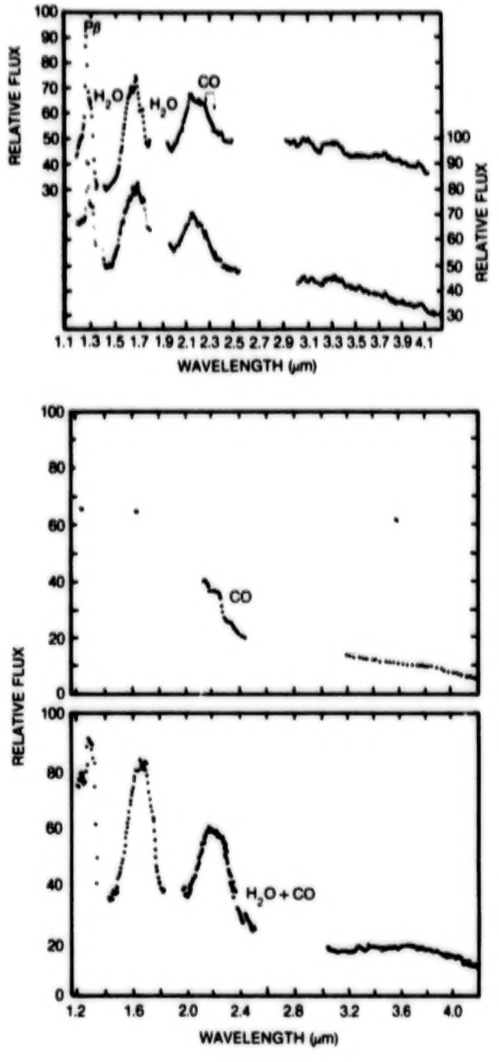


Figure 11-22. The near-infrared spectrum of symbiotic stars (Whitelock et al., 1983a).

Since TiO bands have been identified in the optical spectra of these stars, the IR provides a further proof of the presence of a late-type star, whose energy spectrum is the dominant contributor to the red-near IR spectrum of S-type symbiotics. Another evidence is provided by the Mira-type IR pulsation as discussed below. We should finally recall that the 2.3 μm CO band was observed in emission in the Mira-type symbiotic BI Cru (Whitelock et al., 1983c).

VI.C. VARIABILITY

Another important distinguishing feature of D-type symbiotics is their large IR variability. First, Harvey (1974) discovered that V1016 Cyg presented a long-time scale variation in all the IR photometric bands, from 1.2 to 10 μm, with a maximum amplitude of about 1 magnitude at K and of $1^m.5$ at H. This result should provide a direct evidence for the presence of a Mira-type variable star in V1016 Cyg. Harvey's work has, in the meantime, shown the importance for a continuous monitoring of symbiotic stars, which should give important information on the nature of the cool component. However, we had to wait almost one decade to have a real progress in this problem.

In fact, systematic photometry of southern symbiotic stars, especially at the South Africa Observatory, led to the discovery of large amplitude periodic variations in the IR of D-type symbiotics: RR Tel (Feast et al., 1983a). RX Pup (Whitelock et al., 1983a), and in the similar Mira system R Aqr (Whitelock et al. 1983b). Feast et al. (1983b) also found Mira-type variability in three more D-type systems: He2-106, He2-38, and He2-34. Some typical light curves are shown in Figure 11-23. As far as the northern systems are concerned, Taranova and Yudin (1983) confirmed the Mira-type variability in V1016 Cyg

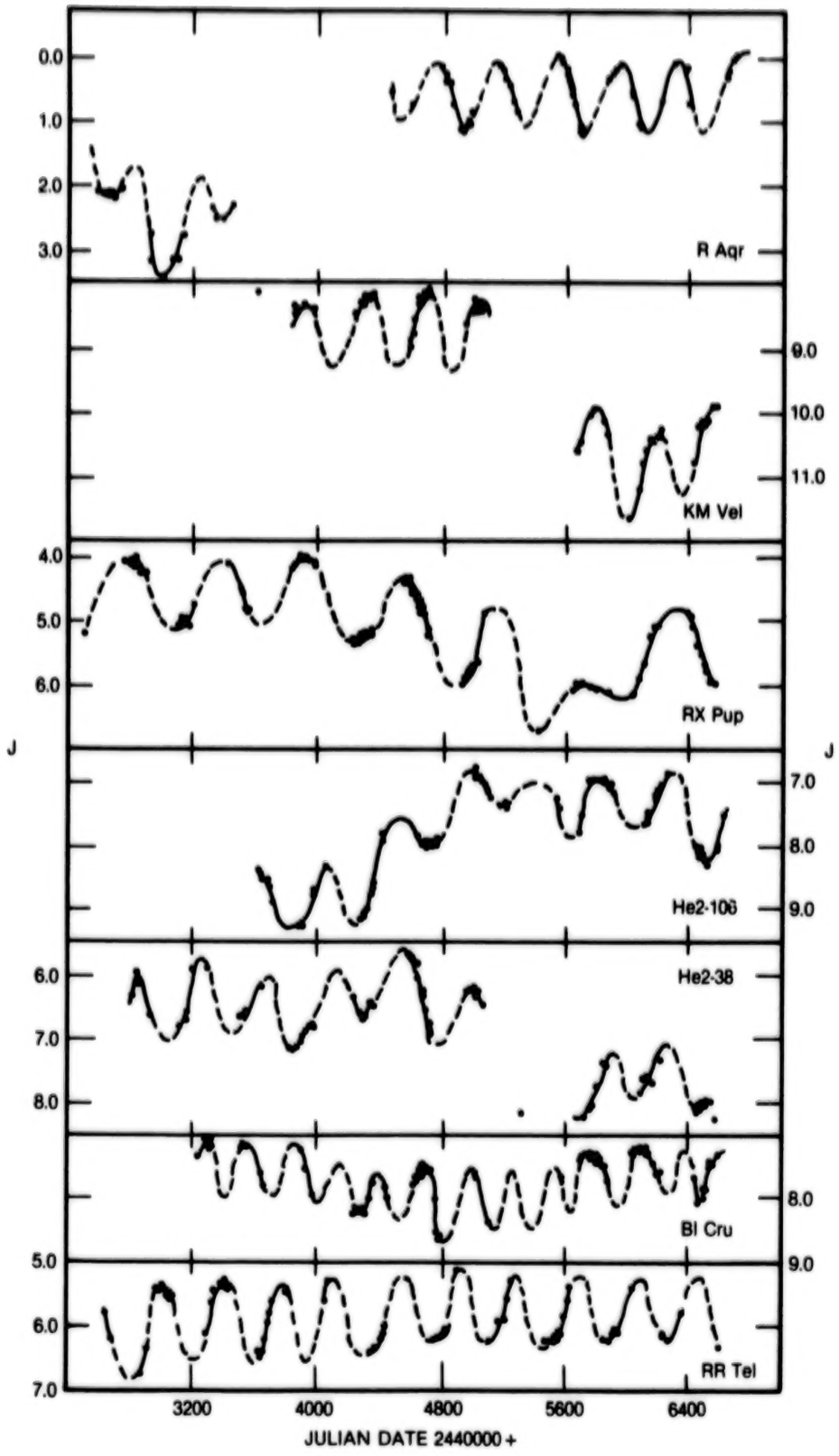


Figure 11-23. The infrared variability of Mira (D)-type symbiotic stars (Whitelock, 1987).

and found similar amplitude and time scale in HM Sge. The periods and amplitudes of the IR variability are summarized in Table 11-4. The derived periods range from about 300 to 600 days and correspond to the long-period Miras, which also have larger amplitudes in the IR (see Feast et al., 1982). These periods are of the same order of magnitude of the orbital periods observed or expected for the symbiotic systems. Thus, care should be taken to recognize the different nature of the two kinds of periodic variability.

A long-time scale trend has been found for the IR maximum luminosity in R Aqr, RX Pup, He2-34 and He2-106, which could be explained by variable dust obscuration (Feast et al., 1983b; Whitelock et al., 1983a).

In the S-type symbiotic systems the IR variability is generally of smaller amplitude and irregular. Systematic observations of the northern objects have been especially undertaken by O.G Taranova and B.F. Yudin in Crimea (e.g., Taranova and Yudin, 1983). In this regard, it should be remembered that all M giants and supergiants later than M4 are variable. The IR variability of the stellar-type symbiotics is thus not unusual, but confirms the rule and shows again that their cool components behave like a normal single star.

Finally, we recall that most of the above observations have been made during quiescent phases of the symbiotic stars. It is also important to study the behavior during an active phase and to look for possible correlations. In fact, some models for symbiotic stars assume that the cool star activity, possibly associated with an increased rate of mass transfer to the dwarf companion, could be responsible for the observed symbiotic activity. Both the classical symbiotic stars Z And and AG Dra underwent outbursts in recent times, and are suitable for considering more thoroughly this problem. The IR photometry of these events led to the conclusion that no large change of the IR spectrum occurred during the outbursts (Cassatella et al., 1984; Viotti et al., 1985; Cassatella et al., 1988a). A similar result was found for the symbiotic nova PU Vul. This star, after its 1978 outburst, suffered a deep luminosity fading in 1980. Simultaneous ultraviolet

TABLE 11-4. INFRARED VARIABILITY OF SYMBIOTIC STARS.

Object	ΔJ (mag)	ΔK (mag)	T(days)	Ref.
D-type symbiotic stars				
V1016 Cyg	1.0	1.0	450	1,2
BI Cru	1.0	0.8	280	3
RX Pup	1.2	1.0	580	4
HM Sge	1.2	1.5	500:	2
RR TEL	1.5	1.0	387	5
He 2-34	0.8	0.5	370	3
He 2-38	1.0	0.8	433	3
He 2-106	1.5	0.9	400	3
S-type symbiotic stars				
Z And	0.2:	0.3:	=	6
CI Cyg	0.5:	0.5:	=	6,7
AG Peg	0.2	0.1	=	8
Related objects				
R Aqr	1.0	0.8	387	9

References: 1. Harvey (1974). 2. Taranova and Yudin (1983). 3. Feast et al. (1983b). 4. Whitelock et al. (1983b). 5. Feast et al. (1983a). 6. Taranova and Yudin (1981). 7. Baratta and Viotti (1983). 8. Feast et al. (1983b). 9. Whitelock et al. (1983a).

and infrared observations made by Friedjung et al. (1984) showed that while the ultraviolet flux largely decreased during the minimum, the infrared remained nearly the same, indicating that the source of the IR radiation (the cool giant) was not affected by the event. The amount of IR observations of symbiotic stars during outburst is still poor to make a general conclusion. But all the above results are in favor of a cool component that is not directly involved in the symbiotic activity. Actually, the observed IR variability seems to be a peculiarity of the cool component, not necessarily associated with the symbiotic phenomena.

VII. RADIO OBSERVATIONS

VII.A. INTRODUCTION

Radio observations provide a probe of the large scale structures from a few stellar radii to the typical sizes of planetary nebulae. It is therefore a useful tool to investigate stellar winds, accretion structures, and ejecta. Symbiotic objects generally are weak radio emitters. Thus, a significant progress in this field was made only when large area radio telescopes began to be available. A comprehensive summary of the radio observations of symbiotic stars can be found in the book on Radio Stars (Hjellming and Gibson, 1985). The first object successfully detected at radio wavelengths was V1329 Cyg (HBV 475), which was pointed by the 100 m MPI Bonn radio telescope in October 1972 at 10.63 Ghz (Altenhoff and Wendker, 1973). This star is known for having brightened in 1966. A rather weak flux (~ 10mJy; 1 Jy=1.10^{-26} watt m^{-2} Hz^{-1}) was detected in this star known to have exploded in 1967. A larger flux was found by Purton et al. (1973) in another symbiotic nova, V1016 Cyg, which exploded in 1964. This latter observation is of particular importance, not only for the large impact of radio observations on the understanding the symbiotic phenomenon, but more in general for the modelling of stars with optically thick winds. In fact, after the first detection of V1016 Cyg at 10.63 Ghz, observations at other frequencies, from 26.95 to 10.70 Ghz, revealed that the radio spectrum was remarkably linear, with a mean slope of about 0.75, a value significantly smaller than the value of 2.0 expected for a uniform slab of optically thick gas emitting by the free-free process, and larger than the optically thin case, which is nearly independent of the frequency. Figure 11-24 shows the radio spectrum of V1016 Cyg.

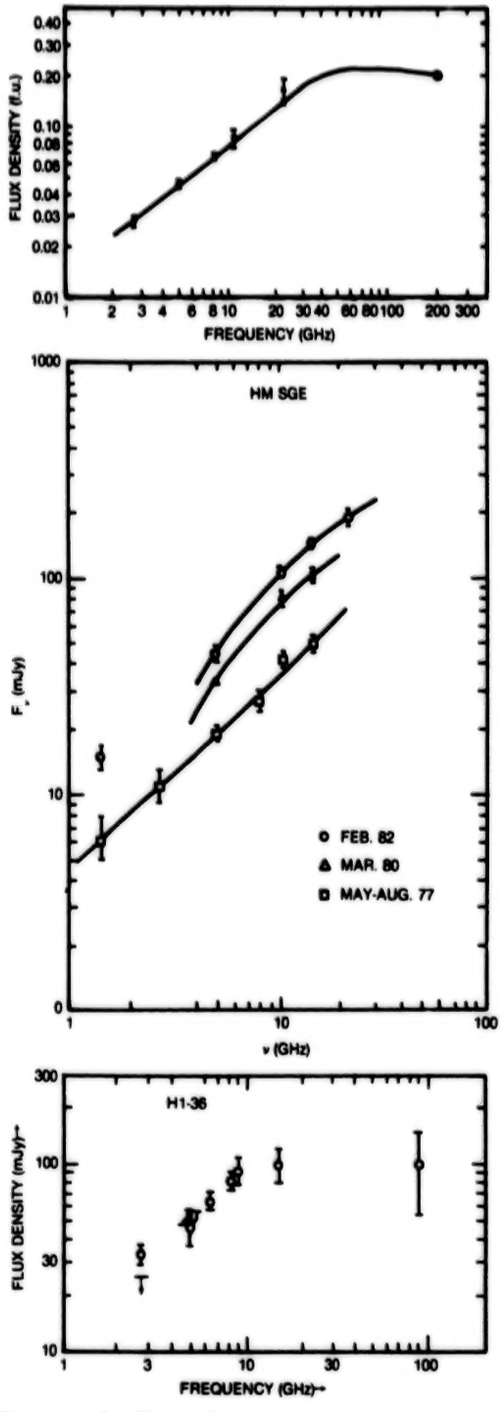


Figure 11-24. The radio spectrum of symbiotic stars. (a) V 1016 Cyg (Marsh et al., 1976); (b) HM Sge at different epochs after its 1975 outburst (Kwok et al., 1984); (c) HI-36 (Purton et al., 1977).

Seaquist and Gregory (1973) found that the observed slopes rather support a model in which the central object is undergoing a continuous mass ejection (i.e., it has a stellar wind). Therefore, the radio flux at a given frequency provides a measure of the mass-loss rate (under certain assumptions about the electron temperature and the structure of the wind, and if the distance is known). The model of an optically thick (at radio wavelengths) ionized wind from a hot central star was later developed by Panagia and Felli (1975) and Wright and Barlow (1975).

Following the first observations of V1329 Cyg and V1016 Cyg, several symbiotic stars were pointed to with radio telescopes, with varying (positive and negative detection) results. For instance, Wendker et al. (1973) failed to detect AG Peg and Z And, while intense radio emission was found from the D-type symbiotic nova HM Sge two years after its outburst, which is continuously rising (Purton et al., 1982). An extensive radio survey of Wright and Allen (1978) of 91 targets led to the discovery (or confirmation) of only 9 sources, all but one (AG Peg) belonging to the D-type subgroup discussed in the previous Section VI. A particularly intense flux was found for HM Sge, RR Tel, and H1-36, which is the most intense one (91 mJy at 14.5 and 8.9 Ghz). Wright and Allen also found a clear correlation between the 14.5 Ghz flux and the dust emission at 10 μm. This is shown in Figure 11-25.

The opening of the Very Large Array (VLA) radio telescope of Socorro, New Mexico, in 1981 afforded the opportunity of a basic improvement of our knowledge of radio emission from symbiotic stars. A survey of 59 symbiotic stars at 4.9 Ghz was carried out by Seaquist et al. (1984) who found 17 positive detections, including several S-type systems not observed before. A compendium of the radio observations at 6 cm (4.9 Ghz) from different sources is given in Table 11-5. In general D-type systems have stronger radio emission than the S-type ones. It is, however, difficult to find an immediate interpretation of this result, since it could be affected by unknown selection effects, and obviously by the uncertainty on the distance.

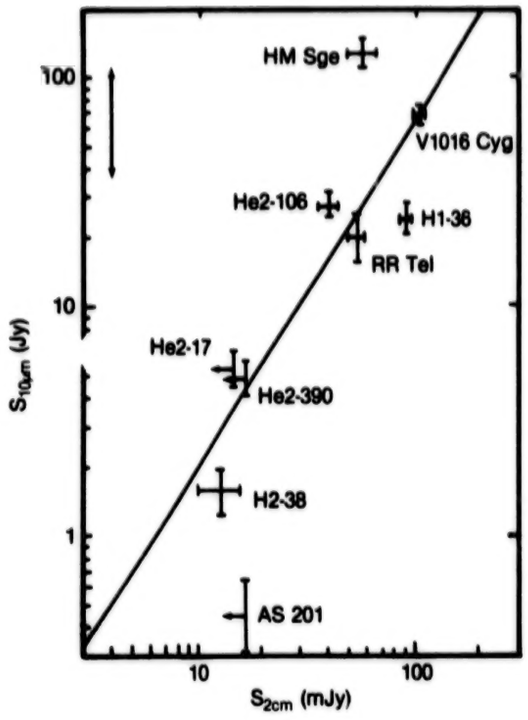


Figure 11-25. The radio flux at 14.5 Ghz versus the 10 μm emissions in D-type symbiotic stars (Wright and Allen, 1978).

VII.B. RADIO VARIABILITY

A few objects have been repetitively observed over a long time interval, and this could provide information about the long-term variability and possible correlation with the optical behavior. After its first detection, V1329 Cyg was irregularly observed at radio wavelengths for several years. During 1972 to 1978, its radio flux probably remained at a nearly constant flux of 12-14 mJy at 10.7 Ghz (Purton et al., 1982). The star was not detected at 4.89 Ghz in 1980 (Kwok et al., 1981), while two years later Seaquist et al. (1984) reported a flux level of 2.16±0.44 mJy at the same frequency. It should be considered that the 1980 radio observation was made near a luminosity maximum of the star (phase 0.48, according to the Iijima (1981) parameters). At that phase, the emission line and UV continuum fluxes are at maximum (e.g., Nussbaumer and Schmutz, 1983). RX Pup is a D-type symbiotic characterized by a large radio variability, but with a still unknown time behavior (Seaquist and Taylor,

TABLE 11-5. 6 CM RADIO OBSERVATIONS OF SYMBIOTIC STARS

Object	Flux (mJy)	Slope (α)	Size([8]) (arcsec)	Ref.
D-type symbiotics				
V1016 Cyg	61	+0.8	0.5	1,2
RX Pup	34 var	+0.72	0.50	3
HM Sge	40-90 var	+0.78	0.36x0.24	4
RR Tel	28			2
S-type symbiotics				
Z And	1.2	+0.62	<0.6	5
BF Cyg	2.1	+0.98	<0.7	5
CH Cyg	0.4-18 var	(see ref 6)	1.5	6
CI Cyg	<0.42			5
V1329 Cyg	2-5 var		<2.8	5,7
AG Dra	0.5			5,8
YY Her	<0.35			5
AG Peg	8.2		1.5	5
related objects:				
R Aqr	12.5	+0.6	100	11
RS Oph	20-82 var	(see ref 13)	0.2	12,13
RT Ser	1.3	+0.73		5
H1-36	46	+1.05	5.0	14

Notes to the table. ([8]) *Data on angular sizes (generally at 6 cm) are from Seaquist et al. (1984), Hjellming and Gibson (1985), and Taylor (1988).*

References: (1) Purton et al. (1973). (2) Purton et al. (1982). (3) Seaquist and Taylor (1987). (4) Kwok et al. (1984). (5) Seaquist et al. (1984). (6) Taylor et al. (1986, 1988). (7) Altenhoff and Wendker (1973). (8) Torbett and Campbell (1987). (11) Hollis et al. (1985, 1987). (12) Padin et al. (1985). (13) Spoelstra et al. (1987). (14) Purton et al. (1977).

1987). The D-type symbiotic nova V1016 Cyg was continuously monitored at 2.8 cm since 1973, but only marginal evidence of variation was found (Purton et al., 1981; Becker and White, 1985). The star may have reached a stationary stage after the 1964-66 outburst, and this is in agreement with the spectroscopic and photometric results. It must be noted that in 1969, M. B. Bell, E. R. Seaquist, and W. J. Webster failed to detect V1016 Cyg, with an upper limit of about 100 and 70 mJy at 4.6 and 11 cm, respectively (see FitzGerald and Houk, 1970). These upper limits are a factor of two larger than the radio fluxes detected later; thus, they cannot be used as an indication of a rise of the radio luminosity. Also, no variability was found in the strong source H1-36 (Allen, 1983). A different situation holds in the case of HM Sge, which underwent its outburst in 1975 and was first radio-detected in 1977. Since then, the star has been frequently monitored, and a gradual increase of the radio flux was found (see Figure 11-24 and Table 11-6). The radio spectrum remained optically thick over all the observed frequency range, and this fact provided means to estimate the expansion velocity of the optically thick surface (which is not necessarily the wind velocity) of about 100 km s^{-1} (Kwok, 1982). This time evolution can be com-

pared to that of the recurrent nova RS Oph, which, after its 1982 outburst, rapidly increased its radio flux up to 63 mJy in a few weeks (Padin et al., 1985). The fact that no variability was found in the similar object V1016 Cyg has to be related to the more time elapsed since the outburst in the latter one. Thus, we expect HM Sge to reach a constant radio luminosity in few years. The radio variability in symbiotic objects is summarized in Table 11-6.

VII.C. RADIO IMAGERY

Radio observations have represented and for a long time will represent a unique way to make very high spatial resolution imagery of circumstellar envelopes of different categories of astrophysical objects. For instance, the Socorro radio telescope in its most extended (35 km) configuration can reach an angular resolution of 0.07" at 1.3 cm. This resolution is one order of magnitude larger than that achievable at optical wavelengths for diffuse sources. A few symbiotic objects have been so far observed at high spatial resolution, and the radio observations have disclosed quite a variety of structures, such as shells, halos, jets, and bipolar nebulae. A special case is the radio source associated with the Mira variable R Aqr which will be discussed in Chapter 13, which is devoted to the detailed discussion of this star. A description of the radio nebulae in symbiotic stars can be found in the volume Radio Stars (Hjellming and Gibson, 1985) and in Taylor (1988).

The radio emission from V1016 Cyg has been resolved into two lobes separated by about 0.10" in the NE-SW direction (Figure 11-26). As discussed above, this star has been considered the classical example of a radio source produced by thermal emission from a stellar wind (Seaquist and Gregory, 1973). These observations seem instead to suggest a rather different model, with ejection of matter preferentially in polar directions as in the bipolar nebulae. Such a radio structure can hardly be resolved in the optical region from ground-based telescopes. However, Solf

TABLE 11-6. RADIO VARIABILITY OF SYMBIOTIC STARS

Object	Date	Nu(Ghz)	Flux (mJy)	Reference
V1329 Cyg	1972.8	10.7	10 ± 2	1
.....	1978:	4.9	5 ± 1	2
.....	1980.2	4.9	<1.	3
.....	1982.1	4.9	2.2 ± .4	3
HM Sge	1977.4	10.6	40	4
.....	1980.3	10.6	80	4
.....	1981.x	10.6	90	4
.....	1983.8	4.9	51 ± 3	5
CH Cyg	1984.9	15.0	9.3	6
.....	1985.1	15.0	25.8	6
.....	1985.9	15.0	44.0	7
.....	1986.2	15.0	24.3	7
.....	1987.0	15.0	8.2	7
RS Oph	1982.1	5.	<0.32	3
.....	1985.12-.17	5.	20 to 63	8,9
.....	1987.18	5.	82	9
.....	1985.17-.46	5.	59 to 22	9

Notes to the Table. (1) Altenhoff and Wendker (1973). (2) Hjellming (1981). (3) Seaquist et al. (1985). (4) Kwok et al. (1981). (5) Becker and White (1985). (6) Taylor et al. (1986). (7 Taylor et al. (1988. (8 Padin et al. (1985). (9) Spoelstra et al. (1987).

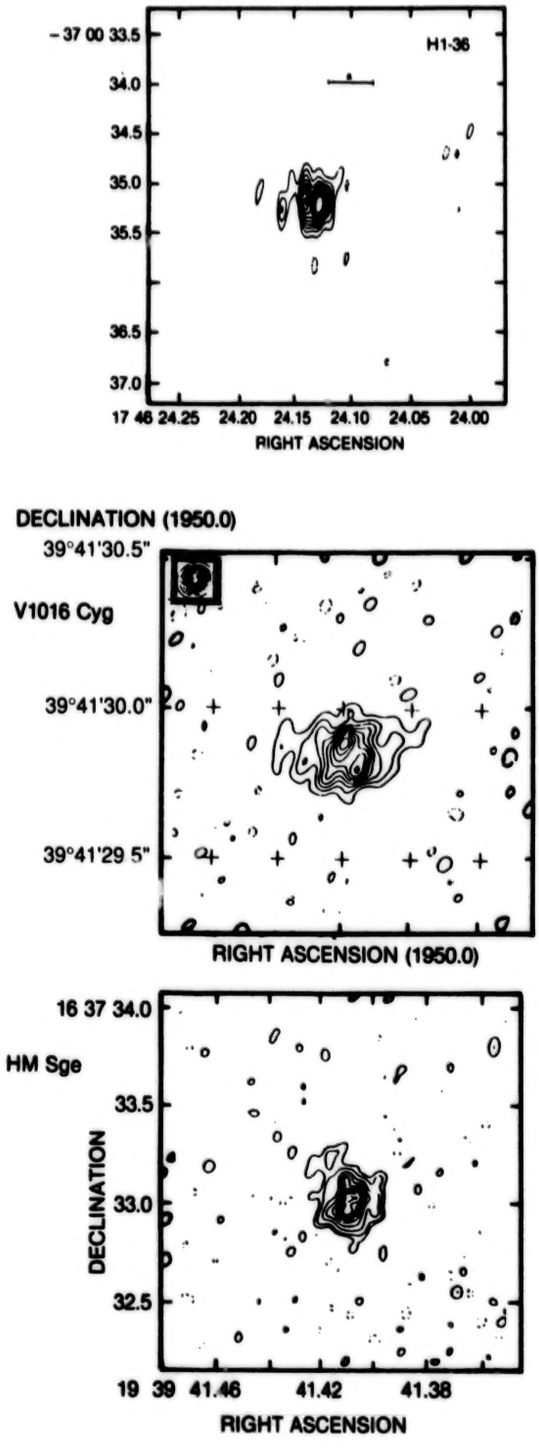


Figure 11-26. Radio images of symbiotic stars (Taylor, 1988).

(1983) succeeded in separating the two components of V 1016 Cyg, using high-spatial, high-spectral resolution observations near the [NII] 6583 A emission line.

The high-resolution radio image of HM Sge (Figure 11-26) shows a diffuse symmetrical emission, or *halo*, with a size of about 0.5" at 1.3 cm (22 Ghz), and a central bipolar structure similar to that of V1016 Cyg with an extension NS of 0.15. Both stars—HM Sge and V1016 Cyg— are known for their recent outburst, and for the peculiar bipolar radio structure. An even more complex structure is shown by the S-type symbiotic star AG Peg, in which three separate structures can be identified: a spherical nebulosity, a compact core (θ<0.1" at 15 Ghz), and a possible jet-like structure 0.8" long, extending from the central core through the halo (Figure 11-26). Like the previous two objects, AG Peg has also suffered a major nova-like outburst. The question is whether the present radio structure is associated with this behavior (see Viotti 1987a). Table 11-5 summarizes the maximum angular size at radio wavelengths of some symbiotic stars.

VII.D. THE RADIO OUTBURST OF CH CYGNI

CH Cyg represents a unique example of evolution of a radio nebula. This star recently underwent a radio outburst followed by the appearance of ejecta (Taylor et al., 1986). During April 1984 to May 1985, the radio flux increased by about a factor of 35, while VLA 2 cm observations on 8 November 1984 disclosed the presence of two radio knots separated by 0.18". Taylor et al. (1986) also found that 75 days later, the radio image evolved into a three-component structure with a total separation of 0.4" (Figure 11-27).

This radio outburst of CH Cyg was associated to a luminosity decline of the star of about 1.5 mag (Tomov, 1984). In the same time, Selvelli and Hack (1985) observed a dramatic increase of the line excitation in the ultraviolet. Taylor et al. (1986) explained the radio evolution of CH Cyg as the result of formation of ejecta, which are moving away from the central object at a very high speed, about 1.1 arsec/yr, corresponding to a projected velocity of about 1000 km s^{-1}. The thin lines in Figure 11-27 connect the corresponding knots according to this hypothesis. This conclusion also seems to be supported by the large width of the hydrogen lines. Thus, CH Cyg could

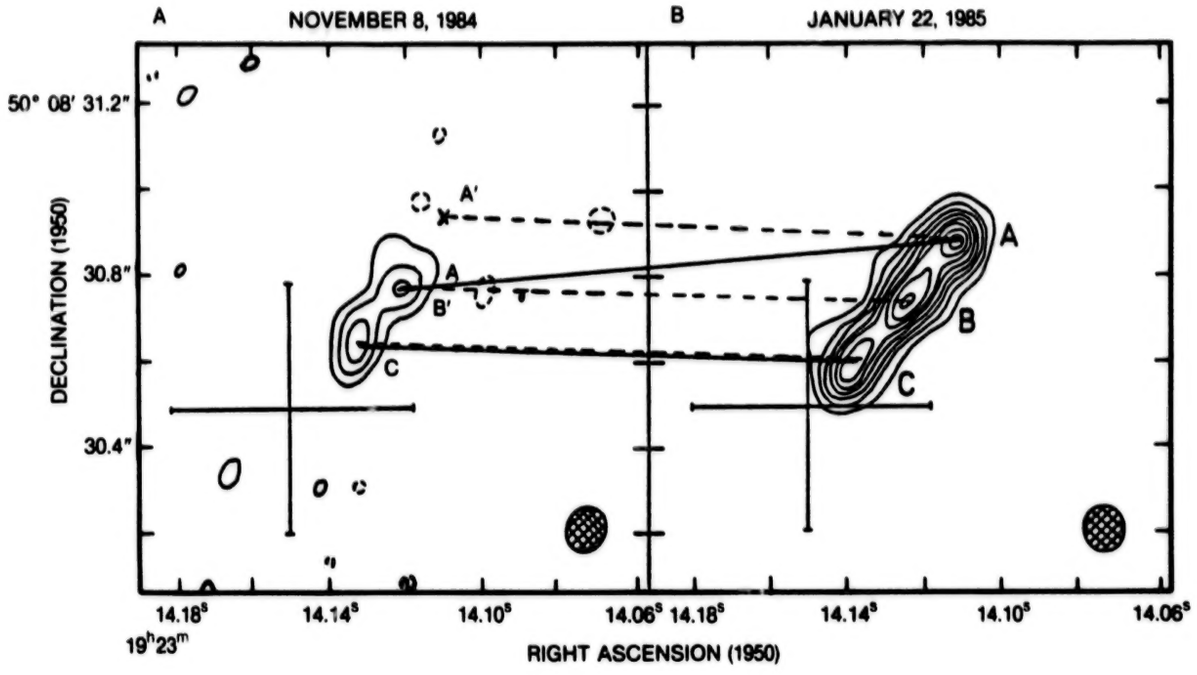
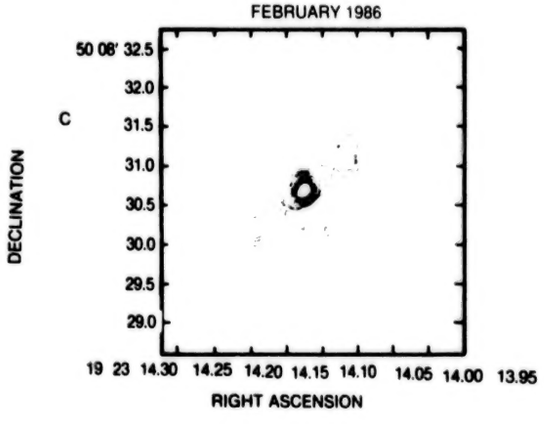


Figure 11-27. The radio map of CH Cyg after the 1984 radio outburst: (a) 8 November 1984; (b) 22 January 1985 (Taylor et al., 1986); (c) February 1986 (Taylor et al., 1988).



be considered as the best example of jet activity. There is , however, an alternative and simpler explanation of the observations: the two sources observed in November 1984 (labelled A and C in Figure 11-27a) would correspond not to the sources A and C of Figure 11-27b), but to B and C, respectively. This correspondence is indicated in the figure by dashed lines. In such a hypothesis the apparent motion of the radio structures, especially of knot A, would be much lower than that claimed by Taylor et al. (1988) and possibly equal to zero. Also, the broadness of the Lyα emission, shown in the following Figure 11-29, is more easily explained by a very large optical thickness so that the observed wings are the damping wings of the emission lines, rather than related to Doppler broadening. The appearance of the radio jets in CH Cyg could be associated with a sudden increase of the flux of ionizing photons from the central object in mid-1984, followed by the propagation of an ionizing front through the preexisting circumstellar matter. The .increase of the line ionization in the UV and the detection of an X-ray emission (Leahy and Taylor, 1987) give further support to this intepretation.

VII.E. MASER EMISSION

The observation of radio lines of molecular species from late-type stars is an important tool to investigate their outer envelopes. Maser emission of OH, H_2O, and SiO has been detected at radio wavelengths in several objects, including M supergiants, carbon and S stars, and Mira variables (e.g., Lepine et al., 1978, and references therein). Most of the SiO sources are Mira variables, and there is evidence that most, if not all, Miras are SiO emitters. This maser emission is, therefore, important for the investigation of the characteristics of the cool component of symbiotic stars. In particular, we should expect maser emission in the D-type symbiotics for the presence in most of

them, as discussed in the previous section, of a Mira-type variability. SiO is also an important cooling agent in the outer atmospheres of oxygen-rich red giants, and is the first step toward the production of circumstellar dust (Muchmore et al., 1987). Therefore, the observation of the molecule in symbiotic objects surrounded by dust envelopes, such as the D-types, is important for the study of the process of dust formation. However, so far the results are far from being satisfying. Extensive search of SiO maser emission was made by Cohen and Ghigo (1980). They were able to positively detect only one object: the symbiotic Mira R Aqr, whose SiO emission was already observed by Lepine et al. (1978) in their survey of cool stars. This star was also observed in the OH and H_2O maser lines, but with negative results (Wilson and Barrett, 1972; Dickinson, 1976). According to Lepine et al. (1978), the SiO emission is probably less affected by the presence of a hot companion, since it is formed in deeper and denser parts of the cool star envelope. This effect was, in fact, already noted in the case of the Mira binaries o Ceti and R Hya (Lepine and Paes de Barros, 1977). More recently, Hollis et al. (1986) observed the 86.24337 Ghz line of SiO from R Aqr with a 2.6 x 3.6" beam width, and found that the SiO emission is unresolved and placed about 1" away from the central star and from the central HII region (see Figure 13-17). For a reasonable assumption on the distance of R Aqr (about 300 pc), Hollis et al. (1986) found that the emisssion is formed too far (about 4.5 x 10^{15} cm) from the red giant envelope. SiO emission is more probably formed in the circumbinary nebulosity, pumped by the hot star radiation. We also point out the fact that the SiO emission originates in the region opposite to the jet, where no strong radio sources were detected. Probably in this region, the gas is denser and less ionized and/or there is a larger amount of dust and molecules. Mapping of this region in radio and infrared should provide a fundamental basis for understanding the origin of maser emission in circumstellar envelopes and its association with dust and with the nature of the central object.

To conclude this chapter on the radio observations, let us make a more general remark about a major problem: the exact location of the optical counterpart. In fact, the coordinates of the radio source can be derived with very high accuracy (a few milliarcsec), while the astrometric position of the optical counterpart is normally known with much lower precision. It is possible that the radio emission is not coming from the visual star, but from a nearby region (an invisible companion or a small nebula). This is a very important point, since the relative position of the radio and optical sources has strong consequences on the model. Very precise determinations of the astrometric position of these stars are thus urgently needed.

VIII. THE ULTRAVIOLET SPECTRUM OF SYMBIOTIC STARS

VIII.A. INTRODUCTION

The basic problem of the symbiotic phenomenon is to explain the origin of the emission lines and of the strong blue continuum, which should be associated with an ionized region close to the cool star. Can this region be identified with an exceptionally extended transition-region/corona around the cool star, or with a circumstellar nebula ionized by the UV radiation from a hot companion? How can we decide among the different possibilities?

Before the advent of the ultraviolet satellites, several attempts were made to explain the presence of the nebular component in the optical spectrum of symbiotic stars by the presence of a hot star. In particular, Boyarchuk (1966, 1968) made a detailed analysis of the optical energy distribution of symbiotic stars during different activity phases. He was able to identify three spectral components: a stable M giant, a nebular component, and a hot dwarf star, the latter two variable in time. These results clearly anticipate the presence of a strong hot continuum in the UV spectrum of symbiotic stars. But there still was the problem of the unknown amount of the interstellar extinction and the relative faintness of symbiotic stars in the visual.

AG Peg was the first symbiotic star observed in the UV. The Orbiting Astronomical Observatory OAO-2 pointed the star on May 11, 1970, and

discovered a strong UV flux with a steep rise to the shortest wavelengths, implying the presence of a luminous hot source, probably a WN6 star with a bolometric luminosity brighter than that of the M3III visible star (Gallagher et al., 1979). The successful launch of the IUE satellite on January 26, 1978 represents an important progress in our knowledge of the nature of the symbiotic phenomenon because of the large amount of new and frequently unexpected results. In particular, the long life-time of this satellite, and its wide and well-balanced use by the astronomical community has been the great advantage of this facility.

In the following, we shall discuss separately the main progresses reached in the fields of the interstellar extinction, continuum energy distribution and emission line spectrum, and of their time variability. We shall also use the expressions "near-UV" and "far-UV" for the 2000-3200 A and 1200-2000 A regions, respectively, which coincide with the long and short wavelength modes of the IUE satellite.

VIII.B. INTERSTELLAR EXTINCTION

Ultraviolet observations have been proved in a number of cases to be the best and even the unique means of determining the interstellar extinction, which is a basic parameter for any model fitting of the observational data. In most symbiotic stars the mid-UV continuum is strong enough to allow the measurement of the interstellar absorption band at 2200 A, which is a prominent feature in the UV extinction curve, and is well correlated with E(B-V). The estimated errors in the corresponding E(B-V) values are around ±0.03/0.05. Figure 11-28 shows some examples of the UV spectra of symbiotic stars showing the 2200 A feature.

For this procedure, the mean galactic extinction curve is generally used. Variations of the interstellar extinction from the mean galactic one are possible, especially for the Large Magellanic Cloud members, and for those objects that are known (or are thought) to be surrounded by dense dust clouds. Different criteria are thus needed for the latter cases and to reduce the estimated errors.

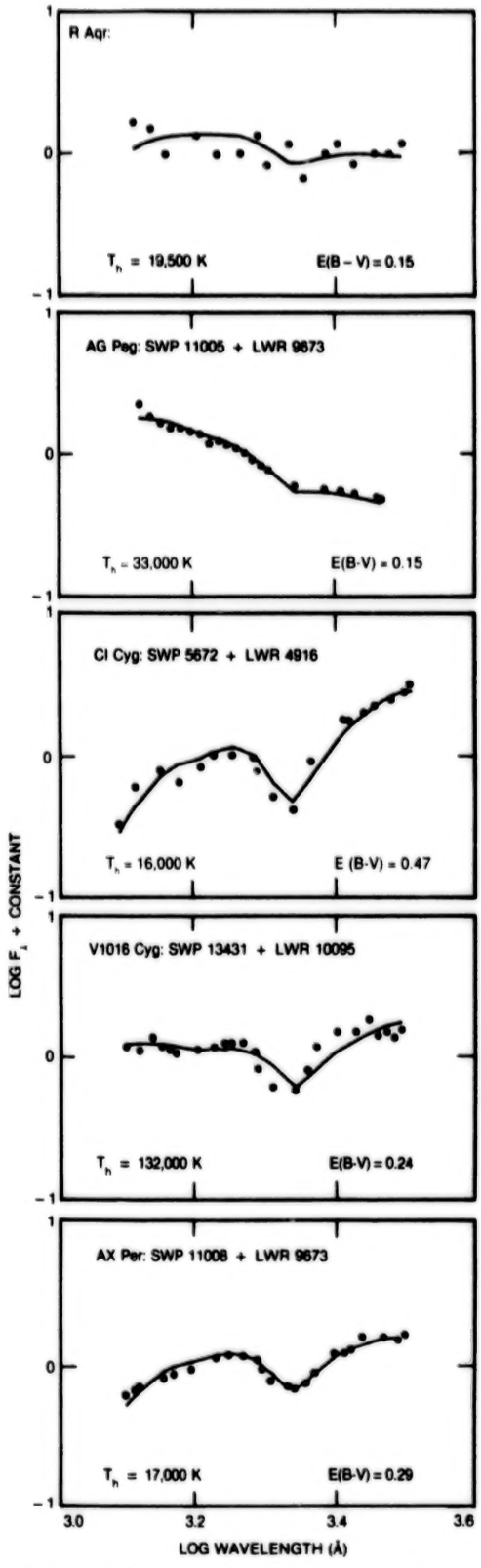


Figure 11-28. Correction for the interstellare extinction in symbiotic stars using the depth of the 2200 A band (Kenyon, 1983a). The hot star fitting temperature T_h and the color excess E(B-V) for a standard extinction curve are indicated.

An independent determination of the i.s. extinction can be derived from the relative intensity of the emission lines in the UV range, or of lines belonging to the UV and optical regions. From the [NeV] and HeII lines in the UV spectrum of V1016 Cyg, Nussbaumer and Schild (1981) obtained E(B-V) =0.3 to be compared with E(B-V)=0.25 as derived from the 2200 A band. For AG Dra, the relative intensity of the HeII lines in the UV provided E(B-V) = ~ 0.05 in agreement with E(B-V) = 0.06 ±0.02 as derived from the i.s. band (Viotti et al. 1983a, 1984a). In this latter star, the far UV continuum is so strong that the region can be observed at high resolution. Several i.s. absorption lines have been identified in spite of the low reddening of this star. The i.s. Lyα line is present as a broad absorption, and from the extension of the wings, a column density of log N(HI) = 20.2±0.2 [N (HI) in cm^{-2}] was derived by Viotti et al. (1983), which again agrees with the above value if one takes into account a lower portion of the i.s. hydrogen in form of H_2 at the high galactic latitude of AG Dra (b = +41°).

In the case of CH Cyg, a prominent Lyα emission line appeared in 1985 (Selvelli and Hack, 1985; Selvelli, 1988; see Figure 11-29a). This line is doubled by a broad absorption due to the

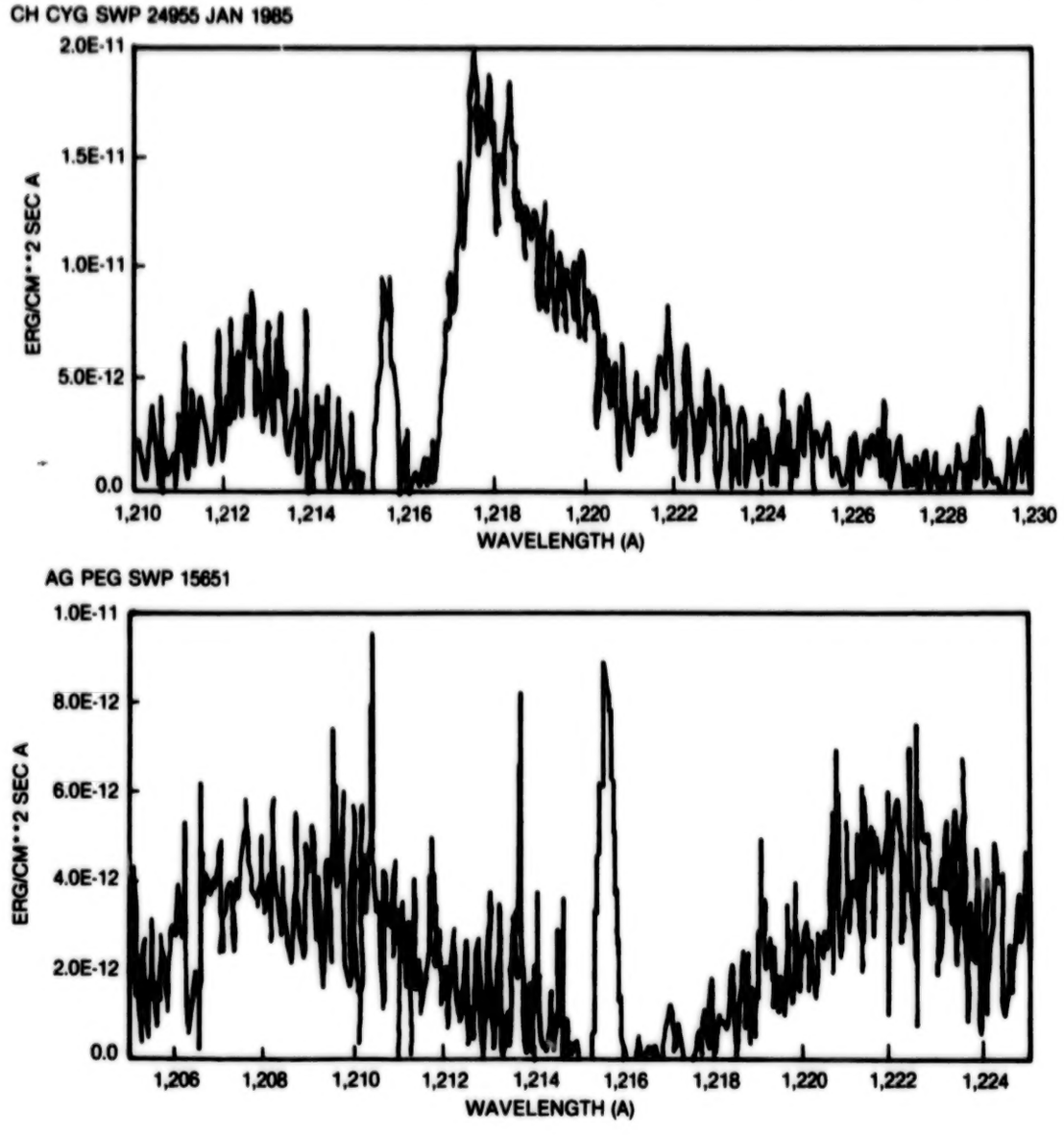


Figure 11-29. Interstellar lines in the high resolution UV spectrum of symbiotic stars. (a) The Lyα region in CH Cyg and AG Peg.

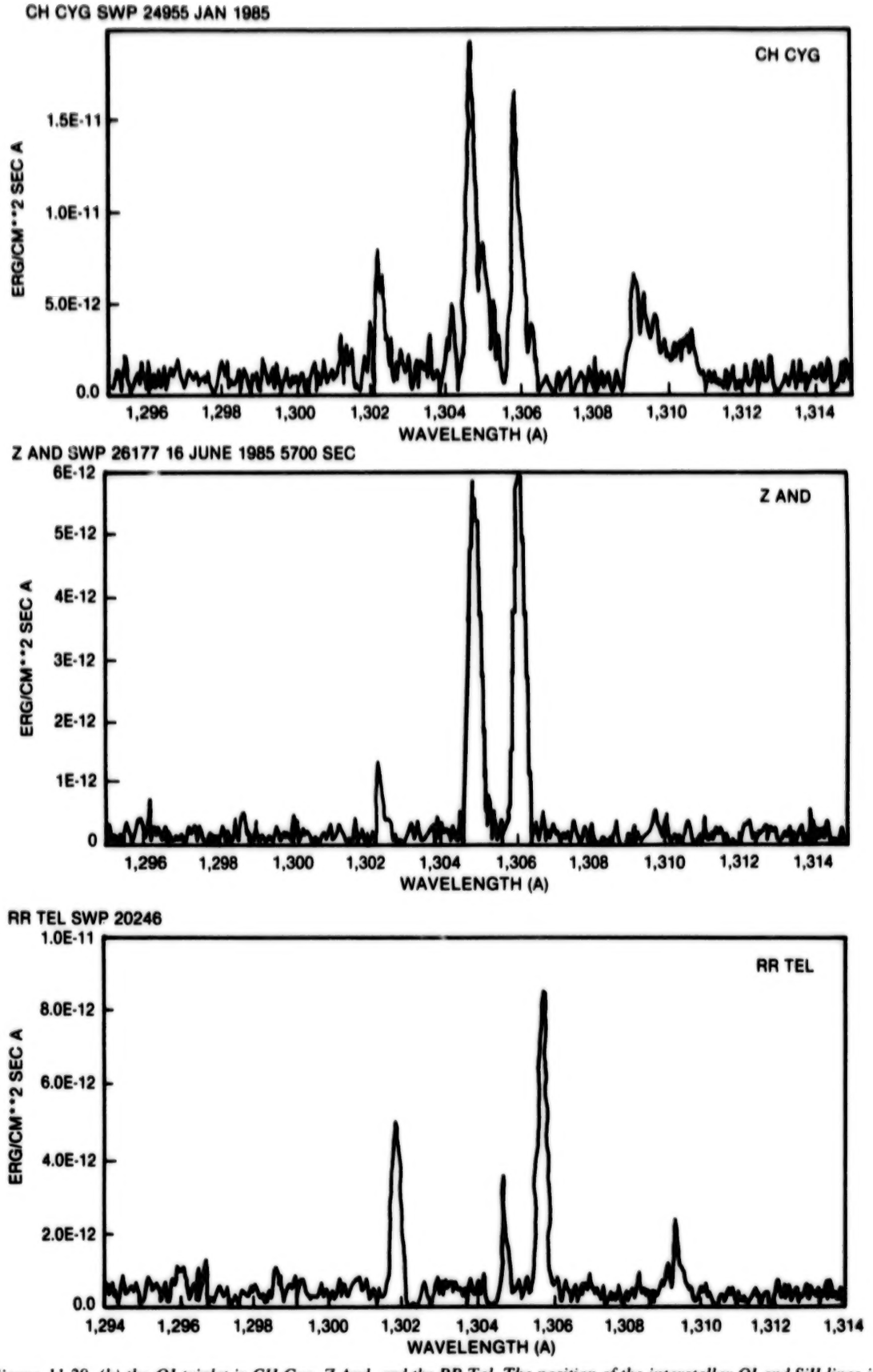


Figure 11-29. (b) the OI triplet in CH Cyg, Z And, and the RR Tel. The position of the interstellar OI and SiII lines is indicated. Note the high negative radial velocity of RR Tel (-61 km s^{-1}).

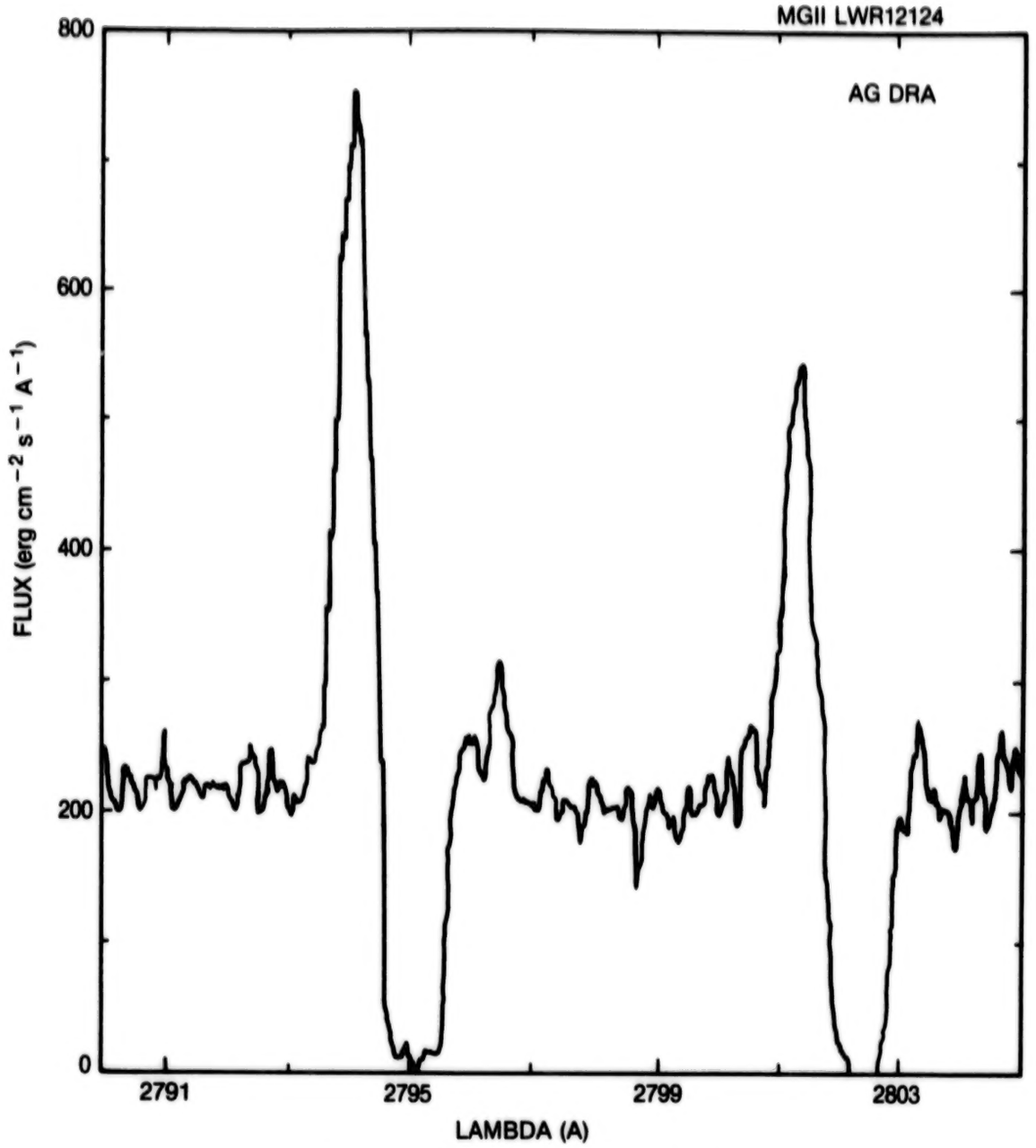


Figure 11-29. (c) The MgII doublet in AG Dra.

interstellar Lyα, whose strength corresponds to logN(HI) = 19.7, or E(B-V) = 0.015 (Viotti, 1988a). Frequently, the interstellar lines fall close to emission lines, and may largely affect its intensity and profile. This may sometimes lead to wrong conclusions. For instance, in Z And, as well as in many other symbiotic stars such as CH Cyg and V1016 Cyg, the OI line near 1302 A is completely absent (see Figure 11-29b), while the other two lines of the resonance triplet are present and strong in emission. The absence of the strongest component of the OI triplet has been frequently interpreted as the result of some rather strange excitation mechanism, or of radiative transfer in the emitting envelope, while the simplest explanation is that the line is missing because of the absorption by the interstellar line (while the other two lines have no i.s. components, being slightly excited transitions). In fact, as soon as the stellar radial velocity is different enough from the i.s. one, the OI 1302 emission line reappears. This is, for instance, the case of the high-velocity stars RR Tel (Figure 11-29b) and AG Dra, whose radial velocities are -61 and -140

km s^{-1}, respectively, so that the i.s. OI 1302 A line falls to the red of the stellar emission line. But it is curious to note that in these stars, the second component of the OI multiplet at 1305 A is much weaker than expected. It is easy to find that in this case, the emission line is coincident in wavelength with the interstellar SiII line at 1304 A. Again, we have an indirect evidence for the presence of an interstellar absorption line, although its true intensity is very hard to be determined with the present spectral resolution of the UV spectra. AG Dra has another interesting feature. In this star, the MgII doublet is characterized by a kind of "inverse P Cygni profile" (Figure 11-29c). Obviously, this is not a real stellar effect, which should be very peculiar for a symbiotic star, but an accidental combination of the blue-shifted stellar emission lines and of the unshifted interstellar components of the same doublet. A similar longward absorption of interstellar origin is seen in the red wing of the CIV 1548 line in the high-velocity (-95 km s^{-1}) symbiotic star EG And (Oliversen et al., 1985). Concerning the resonance doublets, we should finally note that in the case of no wavelength shift between stellar and i.s. lines, the relative strength of the two emission components could be affected by the i.s. absorption, which reduces the stronger component more than the other one, an effect which has been noted for the CIV doublet as discussed below in Section VIII.D.

Table 11-7 summarizes the different determination of the i.s. extinction toward several symbiotic objects derived from UV and optical studies. In general, the UV determinations appear to be in agreement or slightly lower than the optical ones. In some cases, the agreement is poor, being the optical E(B-V) much larger. In these cases, we preferred the UV determinations. It should be finally observed that most of the symbiotic stars are little reddened, which makes these objects good targets for future space observations beyond Lyα in the far-UV, as also discussed below.

VIII.C. THE ULTRAVIOLET CONTINUUM

Figure 11.30 shows the low resolution IUE spector of some symbiotic stars. The majority of them display a smooth continuum which is rather flat in the near-UV, but with a clear far-UV excess. Once the fluxes are corrected for the i.s. extinction, the continuum gradient in the far-UV becomes quite steep and frequently approaches the Rayleigh-Jeans tail of a black body radiation, which corresponds to black body temperatures $\geq$ 40,000 K. This implies that the size of the "hot source" could be as small as one-tenth of a solar radius or even less, close to the size of a hot subdwarf. In addition, most of its energy is radiated outside the IUE range shortwards the Lyman continuum. It is then difficult to have a precise estimate of the bolometric luminosity of the hot source, unless we use other methods. In fact, as for the central stars of the planetary nebulae, we can derive the Zanstra temperature from the emission line fluxes. For instance, the intensity of the HeII line at 1640 A provides a measure of the photon flux shortwards of the helium ionization limit at 228 A. For more details on the method, the reader should refer to the many publications on the matter (e.g., Osterbrock, 1974; Pottasch, 1984) and to the papers on individual symbiotic stars. One not negligible problem is the true energy distribution of the far-UV spectrum of the hot source, which is fairly different from that of a black-body. The hot source itself could be not a star but the innermost layers of an accretion disk, or even a "hot spot" somewhere in the environment of the symbiotic object, or on the cool star surface. It is difficult at this stage to distinguish among all these possibilities, although, as we shall show later, energy balance considerations and, especially, the time variability may help to solve this problem.

If the far-UV continuum is produced by the photosphere of a hot dwarf star, we should expect to see some photospheric absorption lines. The typical features that could be seen at low resolution for effective temperatures of 40,000 K or more, are the resonance doublets of NV, CIV, and SiIV, and the excited lines of HeII 1640 A, NIV 1718 A, and OV 1371 A. The resonance lines and the HeII line are always coincident with prominent emission lines of the symbiotic spectrum, and any contribution from a photospheric absorption is thus masked. The subordinate lines of NIV and OV are generally not seen (or present as weak emissions). The most promising feature associ-

TABLE 11-7. INTERSTELLAR EXTINCTION TOWARD SYMBIOTIC STARS

Object	E(B-V) (mag)	LogN(H) (a) (cm^{-2})	Method (b) (Reference)
Z And	0.35	==	2200 (1)
EG And	0.07	==	UVc (2)
CH Cyg	0.015	19.7	Lyα (3)
CI Cyg	0.40	==	2200 (4)
V1016 Cyg	0.28	==	2200, UV1(5), opt (6)
V1329 Cyg	0.37	==	2200, opt+UV1 (7)
AG Dra	0.06±.02	20.2	Lyα, 2200, UV1 (8)
YY Her	0.18	==	2200 (2)
V443 Her	0.31±.04	==	UVc (2)
BX Mon	0.20±.05	==	opt (9)
SY Mus	0.40	==	2200 (10)
AR Pav	0.30	==	2200 (8,11), radio (12)
AX Per	0.29	==	2200 (2)
AG Peg	0.12±.03	==	2200 (2,13), radio (12)
RX Pup	0.3-1.0	==	opt (14), 2200 (8,15)
HM Sge	0.6	==	2200 (2,16), opt (17)
RR Tel	0.10±.03	==	2200,UVI (18)
PU Vul	0.49	==	UVc (19)
R Aqr	<0.10	<20.2	Xray,opt (20), 2200 (2)
RS Oph	0.73±.10	21.0	UV (21), Xray (22)

Notes to the table: (a) Neutral hydrogen column density from radio or X-ray observations. (b) 2200: depth of the 2200 A interstellar band; Lyα: extension of the i.s. Lyα absorption; UVc: UV energy distribution; UV1: flux ratio of UV emission lines; opt: flux ratio of optical emission lines; Xray: X-ray spectrum; radio: radio maps.

References: (1) Viotti et al., 1982. (2) Kenyon, 1983a. (3) Viotti, 1988a. (4) Baratta et al., 1982. (5) Nussbaumer and Schild, 1981. (6) Ahern, 1978. (7) Muller et al., 1986. (7) Viotti et al., 1983; Viotti et al., 1984a (8) Kenyon and Webbink, 1984. (9) Viotti et al., 1986. (10) Michalitsianos and Kafatos, 1984. (11) Slovak, 1982b. (12) Burnstein and Heiles, 1982. (13) Penston and Allen, 1985. (14) Klutz et al., 1979. (15) Kafatos et al., 1982; Kafatos et al., 1985. (16) Mueller and Nussbaumer, 1985. (17) Willson et al., 1984. (18) Penston et al., 1983. (19) Friedjung et al., 1984. (20) Viotti et al., 1987. (21) Snijders, 1987. (22) Mason et al., 1987.

ated with a hot photosphere could be the FeIV-FeV blend near 1400 A, which is seen in many hot subdwarfs (e.g., Bruhweiler et al., 1981; Rossi et al., 1984). These absorptions have also been identified in the UV spectrum of WR stars (Fitzpatrick, 1982). So far, there is no indication of this blend in the UV spectrum of symbiotic stars, but certainly a careful analysis of high S/N spectrograms should give a more precise answer on this regard. We should also consider that the hot component of a symbiotic system might be subject to an intense high-velocity wind producing strong and wide P Cygni profiles in the resonance and subordinate lines, which should easily be seen also at low resolution. But, as discussed below, P Cygni profiles are rather rare among symbiotic stars.

The continuum of symbiotic stars is generally too weak to be observed at high resolution with IUE, with two important exceptions: AG Dra and CH Cyg. AG Dra has a very intense UV continuum that can be detected at high resolution in less than one hour. The continuum appears featureless, apart from the many interstellar lines discussed in the previous section, and the narrow P Cygni absorption of the NV 1240 A doublet. In particular, there is no trace of the FeIV-FeV, which, as discussed above, should be present in

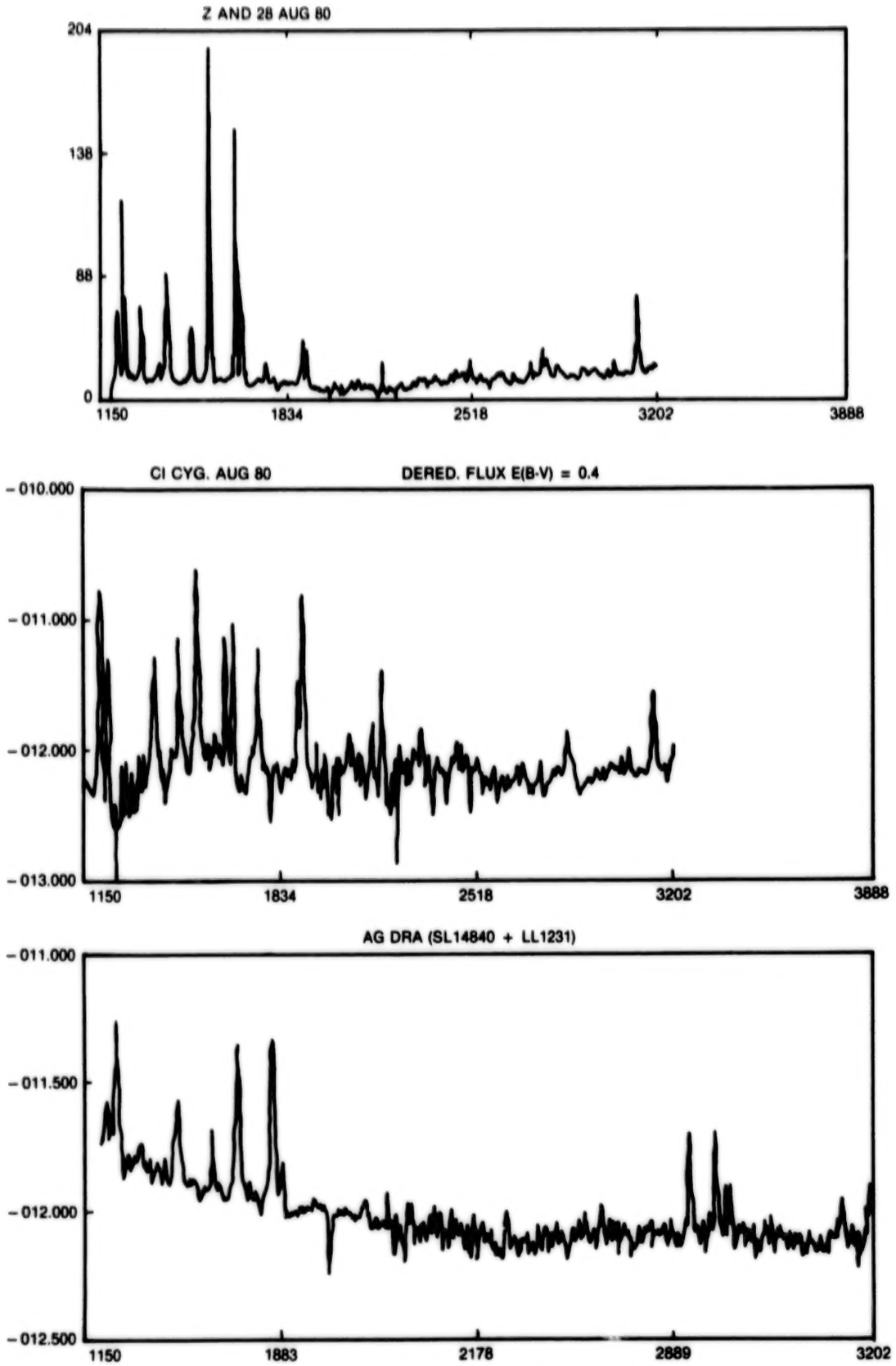


Figure 11-30. The low-resolution ultraviolet spectrum of symbiotic stars observed with the IUE satellite.

the photospheric spectrum of a star with a temperature similar to that of the UV continuum of AG Dra. More complex is the case of CH Cyg, which displays (during the light maximum) a rich absorption line spectrum. The lines—mostly of FeII, NiII, and of other singly ionized metals—appear rather narrow and slightly violet-shifted, which should be an indication of lines formed in a diluted medium, rather than in a stellar photosphere. The large spectral variability of this star is also suggestive of a nonphotospheric origin of the observed features.

To summarize, so far, there is no direct evidence for photospheric features in the far-UV continuum of symbiotic stars, that could support the hot subdwarf hypothesis. But again, these could have been masked by the rich emission line spectrum. Or, more simply, the "photospheric spectrum" actually is a kind of "mild" P Cygni-type spectrum like the central stars of planetary nebulae, but with a lower expansion velocity of the atmosphere.

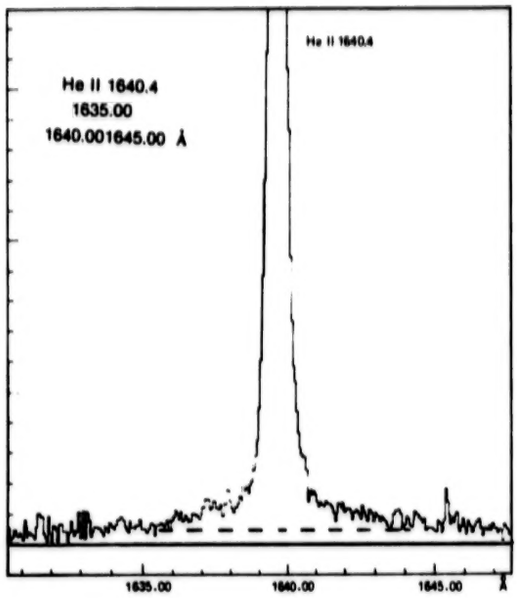
The near-UV continuum generally appears flat and featureless and could be considered as a continuation of the Balmer continuum. Thus, it is probably produced in an optically thin or thick "nebular" region, i.e., in the ionized parts of the circumstellar gaseous envelope. Several attempts have been made to fit the UV continuum of symbiotic stars with a two-component model (e.g., Slovak, 1982; Penston et al., 1983; Kenyon and Webbink, 1984; Cassatella et al., 1988b; Fernandez-Castro et al., 1988). In general, the derived parameters largely depend on the assumed values for the hot star temperatures, so that there is a large uncertainty on the physical structure of the system. In particular, in the majority of cases, it appeared hard to discriminate among the two most favored models: hot star or accretion disk. In other words, we have so far no *direct* proofs of the presence of a hot stellar component (i.e., a hot star) in a symbiotic system, nor, as we shall discuss later, of an accretion disk surrounding a dwarf star.

VIII.D. THE EMISSION LINE SPECTRUM

As in the optical region, the UV spectrum of symbiotic stars in characterized by a great number of emission lines belonging to a wide range of ionization energies. In most objects, very prominent are the resonance lines of NV, CIV, SiII, SiIV, AlII, AlIII, and MgII, and the intercombination lines of CII, CIII, OI (λ 1641), OIII, SiIII, NIII, and NIV. HeII is present with the strong line at 1640 A, and with the weaker Pickering series, in the near-UV range. The highest ionization energy species are represented by OV, NV,[MgV], and [CaVI] (e.g., Penston et al., 1983). But FeII is also frequently observed in the UV spectra of symbiotic stars. A very rich FeII spectrum is displayed by RR Tel (Penston et al., 1983) and by CH Cyg after the outburst (Marsi and Selvelli, 1987). It may be noted that the emission lines are frequently so intense as to be easily detected with IUE at high resolution with very short exposure times. We may thus have an accurate measure of the flux ratios and of the line profiles. Line profiles may, in fact, provide a means to derive the velocity fields in the stellar environments. P Cygni profiles are difficult to see because of the weakness of the continuum, which, in general, cannot be observed with IUE at high resolution. The presence of a shortward displaced absorption can be indirectly inferred by the asymmetry of the emission line profile, or from the doublet intensity ratios, as discussed in Chapter 13. In the case of AG Dra, a P Cygni profile is clearly visible in the NV doublet, with an absorption component shifted by -120 km s^{-1} and extending to -170 km s^{-1} (Viotti et al. 1983, 1984; Figure 11-31a). This component is not seen in the lower energy CIV and SiIV doublets and might suggest a very high temperature (>1-2x10^5K) for the expanding envelope (however, see later the discussion of models).

As can be seen in Table 11-8, frequently the flux ratio of the components of the resonance doublets of NV, CIV, SiIV, and MgII largely deviates from the optically thin value of two. The anomalous resonance doublet ratio in symbiotic stars (and related objects) was noted and discussed among others by Nussbaumer and Schild (1981), Feibelman (1983), Kafatos et al. (1985), and especially Michalitsianos et al. (1988).

The HeII 1640 A line is the strongest emission in the UV spectrum in many symbiotic stars. In



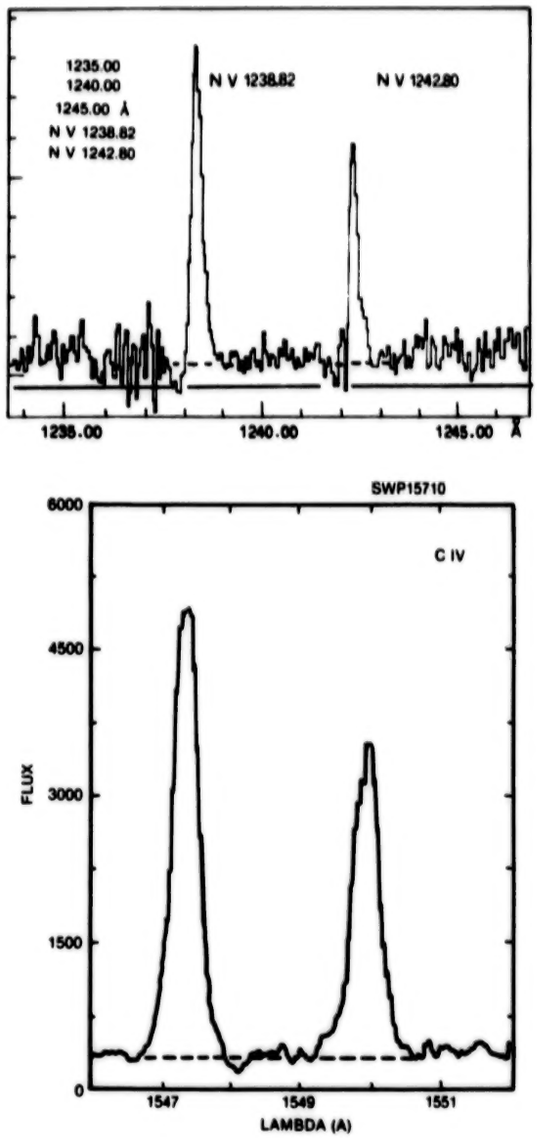


Figure 11-31. The UV emission line profiles in symbiotic stars. (a) NV, CIV, and HeII in AG Dra. (b) NV, CIV, and HeII in RR Tel with broad wings. HeII is flanked by the narrow OI forbidden line. (c) NV, NIV], CIV, and HeII in AG Peg. The central absorption in NIV] is a processing artifact.

AG Dra, the line appears as a narrow peak, with a FWHM of 0.50 A, and very broad emission wings with a FWHM of about 6 A (Viotti et al., 1983; Figure 11-31a). Broad wings have also been observed for the strongest emission lines (CIV, HeII, NV, and CIII) in RR Tel (Ponz et al., 1982 Figure 11-31b), V1016 Cyg (Kindl et al., 1982), and in the outburst spectrum of Z And (Cassatella et al., 1988a). These broad features could be produced by Thomson scattering in the emitting region. Alternatively, if Doppler broadened, the wings should indicate the presence of a high-velocity (rotational or expansion velocity) region, which could be identified with the accretion disk or with matter streaming in the system. Note that in the accretion disk hypothesis, the wings of the higher temperature lines should be broader.

In RR Tel Penston et al. (1983) found a systematic increase of the line width of the narrow emission lines with ionization potential from 40 to 86 km s^{-1}. A similar behavior is present in AG Dra (Viotti et al., 1983) and HM Sge (Mueller and Nussbaumer, 1985). This result again, if confirmed, should be an important element to understand where emission lines are formed.

A rather extreme case is represented by AG Peg, whose UV spectrum shows quite a variety of line profiles (see Figure 11-31c) that are also variable in time. As discussed by Keyes and Plavec (1980) and by Penston and Allen (1985), in 1979, the HeII 1640 line appeared very broad with a triangular shape and a FWHM of 4 A. The CIV line was represented by a narrow peak, while the 1551 component displayed a broad red wing. Later, in January 1985, the CIV doublet was characterized by two asymmetric peaks of about equal intensity, low velocity P Cygni absorption components, and broad wings (Figure 11-31c). It should finally be remarked that in this star also the intercombination line of NIV at 1486 A presents a broad wing below the strong emission peak.

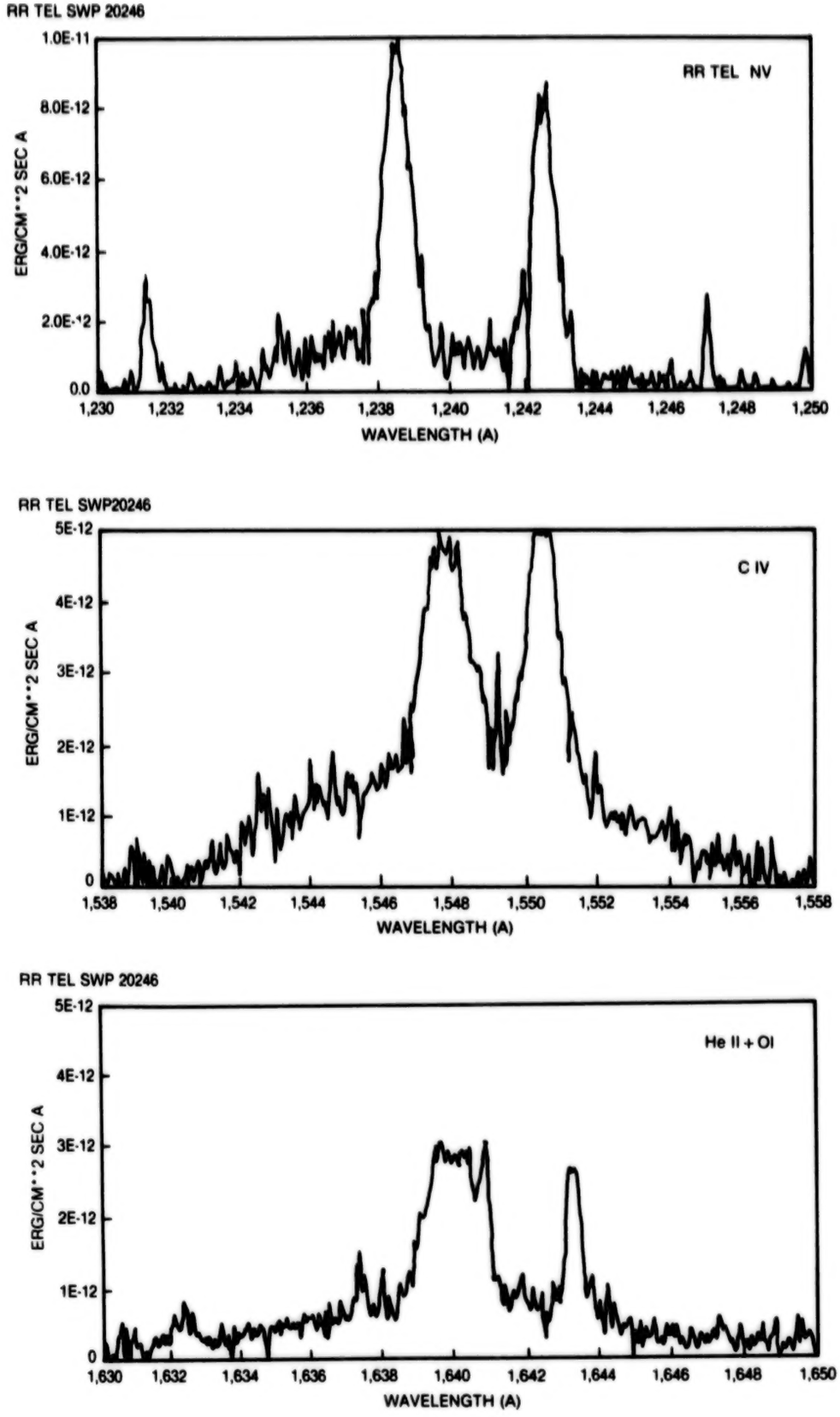


Figure 11-31. (b)

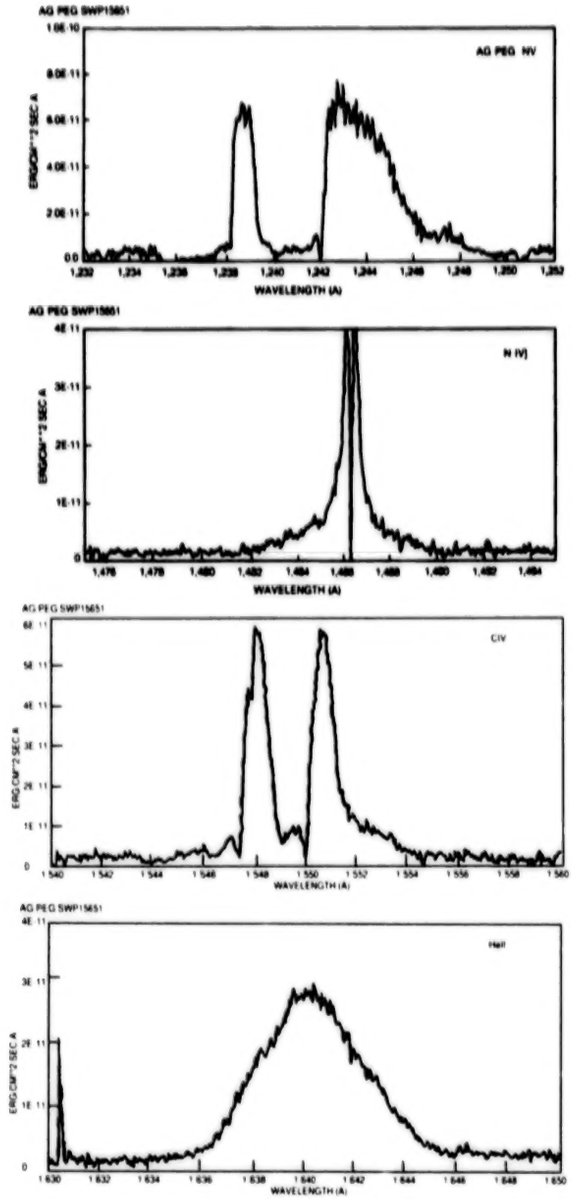


Figure 11-31. (c)

VIII.E. UV VARIABILITY

The very long lifetime of the IUE satellite has so far represented a unique occasion to collect the UV spectra of many symbiotic stars on a time scale of one decade. It was thus possible to follow spectral changes possibly associated with the long-term symbiotic activity, and with any orbital motion. Since the start of full operation of IUE (April 1978) a number of "outbursts" occurred in the following symbiotic stars: PU Vul (1978; first observed in 1979), AG Dra (three outbursts in 1980, 1985, and 1986), Z And (two outbursts in 1984 and 1985), CH Cyg (the 1984 "radio outburst"), and AX Per (1988). These outbursts were followed by a variety of spectral evolution without a clear common trend. For instance, the 1984 outburst of Z And, which was of small amplitude with respect to its light history, was characterized by a slight decrease of the UV emission line and continuum temperature (Viotti et al., 1984b; Cassatella et al., 1988a). The visual fading of CH Cyg after the radio brightening was followed by a fading of the UV continuum and a large increase of the line excitation with the appearance of high temperature lines and a rich FeII emission line

TABLE 11-8. EMISSION LINE INTENSITIES IN THE ULTRAVIOLET SPECTRUM OF SYMBIOTIC STARS

Wavel.[1]	ion	Emission Line Fluxes[2] Z And (3)	CH Cyg (4)	V1016 Cyg (5)	AG Dra (6)	RR Tel (7)	AG Peg (8)
1215.67	Lyα	=	2160.:	=	=	=	=
1238.80	NV	88.4	15.0	170	26.4pc	p	3500n
1242.78	NV	47.6	17.8	100	>13.5pc	p	bl
1371.29	OV	=	=	=	3.0n	80n	420n
1393.73	SiIV	20.9	35.4	49	3.2	260	312n
1402.73	SiIV	12.4	85.7	42	2.6	172	195n
1401.16	OIV]	24.9	=	94	8.1	442	36
1404.81	OIV]	9.4	=	50	3.3	233	34
1486.50	NIV	>29.9s	5.0	140	6.5	514	2250n
1548.20	CIV	>177.0s	57.9	650	29.2	384	6780n
1550.77	CIV	115.0	101.3	460	16.8	210	bl
1640.43	HeII	212.0	47.5	510	160.0nw	1880nw	5800n
1641.3	OI]	7.4	35.0	17	=	92	=
1666.15	OIII]	28.0	43.4	100	3.1	427	880
1718.52	NIV	=	=	4.2	=	13.6	1070n
1749.67	NIII]	9.6	8.0	43	0.4	93	190
1753.99	NIII]	3.1	=	7.5	0.2	26.3	=
1785.26	FeII	=	145.7	=	=	5.5	p
1892.03	SiIII]	22.4	25.7	100	1.4	280	350
1906.68	CIII]	=	2.1	<=10	=	11.1	=
1908.73	CIII]	33.5	138.8	500	0.6	1130	500
2325.40	CII]	p	41.9	58	=	52.8	=
2326.93	CII]	=	19.0	=	=	18.5	=
2506.43	FeII	=	97.4	=	=	26.8	=
2508.34	FeII	=	88.1	=	=	40.6	=
2733.30	HeII	7.8	=	27	4.1	70.8	330
2782.7	MgV]	=	=	88	=	446	=
2795.52	MgII	p	s	82	3.8	488	p
2802.70	MgII	p	s	79	3.1	320	p
2926.58	FeII	2.7	149.3	3.0	=	8.5	p
3132.86	OIII	40.2	=	240	...	473	13
3203.04	HeII	p	=	66	11.7	p	530n

Notes to the table: (1) Wavelengths in A (in vacuum below 2000 A). (2) Fluxes in 10^{-13} erg cm^{-2} s^{-1}, not corrected for the reddening, Other symbols: p: present; s: strong and saturated; bl: blended; n: broad line (FWHM>0.3A); w: broad wings (FWHM = 2 - 6 A); pc: P Cygni profile, (3) Altamore et al., 1981. (4) Selvelli and Hack, 1985; Marsi and Selvelli, 1987. (5) Nussbaumer and Schild, 1981. (6) Viotti et al., 1983. (7) Penston et al., 1983. (8) Penston and Allen, 1985; line fluxes include both broad and narrow components.

spectrum (Selvelli and Hack, 1985). The large brightening of AG Dra of November 1980 was associated in the UV with a large increase of the UV line and continuum flux, but the line excitation remained the same as at minimum, as indicated by the nearly constant NV/CIV resonance doublet ratio (Viotti et al., 1984a). Also, the P Cygni profile of NV discussed in the previous section remained nearly unchanged before, during, and after the light maximum. The rising

phase of the symbiotic nova PU Vul was not observed with IUE, but the deep fading of 1980 and the subsequent recovery did not display a significant change of the near-UV spectrum, which is dominated by the A-type component (Friedjung et al., 1984). It is obvious to conclude from the above examples that different mechanisms should be responsible for the observed phenomena and that each event should be treated individually. It is also evident that UV observations alone cannot provide an unambiguous model of the outburst and that multifrequency observations are always needed for an effective discrimination among possible mechanisms.

Spectral variations in the ultraviolet were occasionally observed by several authors also when the star was in a quiescent phase. In some cases, when the star was monitored by IUE for a long enough time, periodic or quasi-periodic variations of the continuum and emission line intensity were clearly identified. For instance, Viotti et al. (1984a) found that AG Dra, during the period before the main 1980 outburst, underwent a large change of the UV spectrum in phase with the U-band periodic variations discovered by Meinunger (1979). For V1329 Cyg, Nussbaumer et al. (1986) found a periodic ("modulation") of both the flux and wavelength position of the emission lines. The derived period of 964 days is in agreement with the optical light curve. In the case of RR Tel, Hayes and Nussbaumer (1986) found a gradual decrease of the UV line fluxes during the period 1978-1984, without evidence of periodicity. The best example is probably represented by the prototype Z And. The star was observed many times with IUE during the long quiescent period preceding the minor 1984 outburst. From a study of the UV spectrum of Z And during 1978-1982 Fernandez-Castro et al. (1984) found large amplitude periodic changes of the intensity of the ultraviolet emission lines and of the Balmer and far-UV continuum. These variations appeared in phase with the optical photometry (Taranova and Yudin, 1981; Belyakina, 1985) and suggested a period of about two years. A different case is that of the eclipsing binary CI Cyg, which was monitored by IUE during its 1980 and 1982 eclipses. The star, however, was at minimum activity, so that the variations during eclipse were of small amplitude in all the wavelength ranges. Stencel et al. (1982) found that during the 1980 eclipse, the HeII 1640 emission line largely faded, while NV, which should be formed in the same region, did not change. A decrease of the UV continuum by about a factor 2.5 was noted by Baratta et al. (1982).

From a high dispersion study of the D-type symbiotic RX Pup, Kafatos et al. (1985) discovered a large variability of the emission line profiles. HeII 1640 and NIV] 1486 appeared sometimes double, while the CIV resonance lines were characterized by a variable 1548/1550 doublet flux ratio, frequently below the optically thick value of unity (Figure 11-32). This peculiarity is a mean to investigate the structure and temporal behavior of winds in symbiotic stars and similar objects, as discussed by Michalitsianos et al. (1988). Long-term variation of the emission line fluxes was also found by Kafatos et al. (1986) in the "jet" of R Aqr. They also observed that the variations were not correlated with the Mira light curve of R Aqr, and the time scale of about one year and a half was larger than the Mira period.

More details about the UV spectral variations will be given in Chapter 13 devoted to the description of individual objects.

VIII.F. FAR-UV OBSERVATIONS

As discussed above, many symbiotic stars display in the SWP range of IUE a strong continuum that should extend far beyond the IUE short wavelength limit. The presence of prominent high-ionization emission lines also requires high-energy photons from a very hot continuum. Therefore, it is expected that symbiotic stars should be strong EUV sources, also because of the small interstellar extinction found in many of them. Several symbiotic stars were, in fact, pointed by the Voyager 1 and 2 experiments (Holdberg and Polidan, 1987). These spacecrafts are well known for their exploration of the outer solar system objects. Each Voyager brings a low-resolution spectrometer that is sensitive in the range 500 to 1700 A, with an effective resolution of 25 A (Broadfoot et al., 1981), a region that

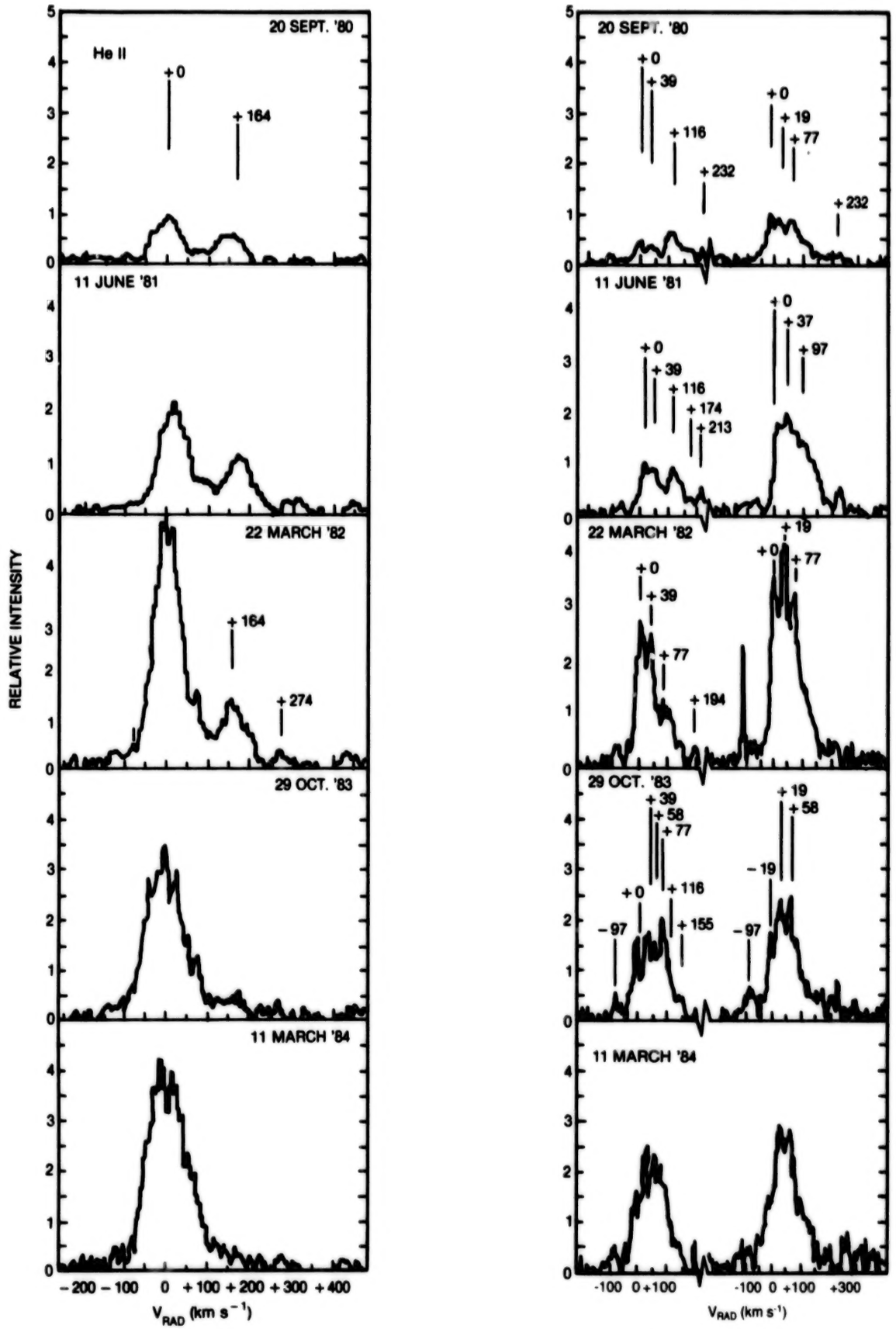


Figure 11-32. Time variability of the HeII and CIV profiles in RX Pup (Kafatos et al, 1985).

includes the Lyman continuum and several important transitions such as the Lyman series and the OVI 1032 A line. Although the Voyager spectra have not yet been published at the time of writing this report, we have been informed that, in spite of the rather low sensitivity of the instruments (flux limit of about 10^{-12} erg cm^{-2} s^{-1} A^{-1}), the observations were quite successful. The analysis that is in progress will provide important information about the high-ionization emitting regions and the temperature of the hot continuum.

IX. X-RAY OBSERVATIONS OF SYMBIOTIC STARS

IX.A. INTRODUCTION

The spectrum of symbiotic stars is dominated by a large number of prominent emission lines belonging to species with very high ionization energies up to more than 100 eV. Forbidden and intercombination lines of MgV, OV, and CaVI have been identified, for instance, in the well-studied object RR Tel (Penston et al., 1983), while [FeVII] and the unidentified emission at 6830 A, generally attributed to a highly ionized ion (Allen, 1980), are present in the optical region (Thackeray, 1977). This fact may suggest the existence of efficient ionization processes somewhere around the symbiotics that could be associated with high temperature plasmas. Therefore, we expect that some symbiotics, namely those displaying emission lines with the highest ionization stages and, which are, obviously, not too faint and not too reddened, should be X-ray sources. There are other "model-dependent" arguments. For instance, X-rays could be produced by the tail of the very hot and luminous UV continuum found in many symbiotic stars, such as AG Dra. In a binary system, accretion processes may lead to the formation of a hot disk and boundary layer around the dwarf component. Accretion onto the surface of a degenerate star could produce thermonuclear burning of the hydrogen-rich accreted shell. At any event, we should expect a strong dependence of the X-ray flux on the symbiotic activity.

The X-ray astronomy has largely profited from the extensive survey with the HEAO-2 satellite (the Einstein Observatory), which has greatly increased the number of different categories of stellar X-ray sources. Several symbiotics have been pointed at with HEAO-2, but only in a few cases, that is, 5 out of about 20, X-ray emission was detected. The positive detection includes 3 D-type, nova-like symbiotics: V1016 Cyg, HM Sge, and RR Tel (Allen, 1981), the S-type AG Dra (Anderson et al., 1981), and one related object GX 1+4 = 4U 1728-24 (Davidsen et al., 1977). All but one (GX 1+4) are soft X-ray sources. One star, HM Sge, was observed three times (Willson et al., 1984). HEAO-2 also provided the upper limits to the X-ray flux for about 15-20 more objects (Allen, 1981; Wallerstein, quoted in Willson et al., 1984; Seward, 1985) including CH Cyg, which will be discussed below. In the case of the symbiotic Mira R Aqr and of Mira itself, Jura and Helfand (1984) claimed a marginal but positive detection, while a reanalysis of the HEAO-2 data led to the conclusion that one can only put an upper limit (Seward, 1985; Viotti et al., 1986b, 1987).

New observations were carried out during 1984-86 with the EXOSAT satellite, and two new positive detections were added: R Aqr (Viotti et al., 1985) and CH Cyg (Leahy and Taylor, 1987). In addition, the strong source in AG Dra was monitored during three different phases of its recent activity. Figure 11-33 shows the EXOSAT map of R Aqr in June 1985. We shall discuss in the following the results of these observations. Table 11-9 summarizes the main X-ray observations of symbiotic stars based on HEAO-2 and EXOSAT observations.

IX.B. THE SYMBIOTIC NOVAE

The three symbiotic novae—RR Tel, V1016 Cyg, and HM Sge—were first observed in X-rays in 1979 with the Image Photon Counter (IPC) onboard of HEAO-2 (Allen, 1981). The detected fluxes are weak, but Allen noted that in the more recently exploded objects V1016 Cyg and HM Sge, the flux was larger than in the older symbiotic nova RR Tel. This may suggest a secular decrease of the X-ray luminosity after the outburst, with an e-folding time of about 7 years.

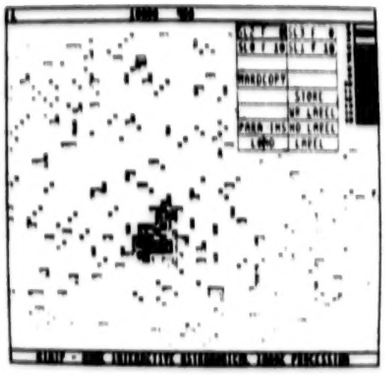


Figure 11-33. X-ray observations of the Mira-type symbiotic R Aqr with the EXOSAT satellite (Low-Energy LE1 detector, Thin Lexan filter) in June 1985.

Willson et al. (1984) have reanalysed the data on HM Sge and RR Tel and added a new observation of HM Sge obtained in 1981. They noted a decrease of the X-ray flux of the latter star. The change of the luminosity of HM Sge and the comparison of the data for the three stars are again consistent with a similar X-ray luminosity at the outburst followed by a decline with a decay time in the range from 5 to 50 years. Kwok and Leahy (1984) have further analyzed the HEAO-2 1979 data of the symbiotic novae and concluded that the observed spectra can be fitted with a thermal bremsstrahlung from circumstellar gas at about 0.4 to 1.5 keV. They propose that the hot region is shocked gas, resulting from the collision of the winds from the hot and cool star of a binary. After the outburst, the shocked region expands and produces the observed gradual decrease of the X-ray luminosity.

Although three different papers come to the same conclusion, one should pay attention to the

TABLE 11-9. X-RAY OBSERVATIONS OF SYMBIOTIC STARS

Object	Instr.	Date	Phase	X-ray Source				Ref.
				Range	Flux	N(H)	Flux	
	(a)		(b)	(c)	(d)	(e)	(f)	
RR Tel	HEAO	79/4/9	decl	.1-3.	3.	2.	3-4	1
....	....	.....	...	.2-4.	4.8	2.2	6.7	2
....	EXO	84/5/4	...	.02-1.	<14.	==	==	3
V1016Cyg	HEAO	79/11/24	max	.2-4.	4.3	4.6	8.2	2
HM Sge	HEAO	79/4/9	max	.2-4.	36.	6.2	50.	2
....	....	.....	...	.1-3.	28.	17.	480.	1
....	....	81/4/8	...	...	17.	23.	36.	1
AG Dra	HEAO	80/4/11	min	.2-1.	21.	23.	36.	4
....	EXO	85/3/15	out	.02-2.5		weak		5
....	EXO	85/6/5	min	...		strong		5
....	EXO	85/11/5	min	...		strong		5
....	EXO	86/2/14	out	...		no detect		5
R Aqu	HEAO	80/6/21	min	.2-3.5	<3.	==	==	6,7
....	EXO	85/6/14	max	.2-1.		1.5	200.	7
....	EXO	85/12/24	min	...		1.5	200.	7
CH Cyg	HEAO	79/10/ 29	max	.2-4.	<1.4	==	==	8
....	EXO	85/5/24	min	.02-2.5		4.	120.	8

Notes: (a) HEAO:HEAO-2 (Einstein Observatory) observations; EXO: EXOSAT observations. (b) Symbiotic phase: out = outburst; max = light maximum; min = light minimum, or quiescence; decl= decline phase after the outburst. (c) X-ray energy range in keV. (d) Fluxes in 10^{-13} erg cm^{-2} s^{-1} integrated for the given energy range. (e) Hydrogen column density in 10^{20} cm^{-2}. (f) Fluxes in 10^{-13} erg cm^{-2} s^{-1} corrected for the interstellar absorption.

References: (1) Willson et al. (1984). (2) Kwok and Leahy (1984). (3) Cassatella et al. (1985). (4) Anderson et al. (1981, 1982). (5) Cassatella et al. (1987). See Figure 11-34. (6) Jura and Helfand (1984). (7) Viotti et al. (1987). (8) Leahy and Taylor (1987).

fact that the result largely depends on the assumptions of the distance and the interstellar absorption. As discussed in the previous Section VIII, two of the three stars have a rather low reddening, with E(B-V) = 0.1 to 0.3 (see Table 11-7). But in the X-ray range, the dependence of the observed spectrum on the hydrogen column density is very high, also at low reddening values, and especially for the soft X-ray spectra like those of the symbiotic stars. Even more uncertain is the distance of these objects. The only case for which more than one HEAO-2 observation is available—HM Sge—the observed variation (see Table 11-9) is not much larger than the observational uncertainties. Taking into account other possible sources of variability (e.g., the stellar "activity" or the orbital motion, as discussed above for the variations observed in other wavelength ranges), the presence of a secular decay of the X-ray flux in these nova-like symbiotics is still a weak possibility.

IX.C. AG DRACONIS

The high-velocity star AG Dra was first observed with HEAO -2 on 11 April 1980 at a minimum luminosity phase of the star V~ 9.7). Anderson et al. (1981) reported the discovery of a strong X-ray flux of 2.1×10^{-12} erg cm^{-2} s^{-1} (in the energy range 0.2 to 1.0 keV). The spectrum appears soft and, if fitted with a bremsstrahlung spectrum, corresponds to a temperature of 1.1×10^{6}K and to an emission measure of EM=2.6×10^{55}cm^{-3} (Anderson et al. 1982). The integrated X-ray luminosity is then L_x(0.2-1.0 keV) = 5×10^{32} erg s^{-1}, for N(H)= 3×10^{20} cm^{-2}.

This star was observed again with the European EXOSAT satellite during 1985-86 by F.A. Cordova and R. Viotti and their collaborators. The first observation was made on 15 March 1985, a few weeks after a minor outburst of AG Dra, and the derived count rate was much lower than expected according to the rather large X-ray flux observed in April 1980 (see Cassatella et al., 1987). Within the EXOSAT accuracy, the X-ray source is point-like and centered on the star within the uncertainty of the EXOSAT satellite. The EXOSAT observations were repeated on 5 June and 5 November 1985, when AG Dra was again at minimum (V~9.8), and a larger X-ray flux was found, in much better agreement with the 1980 results. These EXOSAT observations show that the X-ray spectrum of AG Dra is very soft, with a temperature of about 3×10^{5}K (Piro et al., 1985; Cassatella et al., 1987). These two latter EXOSAT observations were made at two different phases (0.22 and 0.50) of the U-light curve discovered by Meinunger (1979), in order to search for any phase dependence of the X-ray flux and for a possible eclipse of the hot source at phase 0.5. The results, however, indicate no flux change between June and November 1985, and, therefore, do not support a U-phase dependence of the X-ray flux. In January 1986, AG Dra underwent a new outburst, and EXOSAT observations were repeated on February 14th when the star was still at near maximum luminosity. No X-ray flux was detected in spite of the large increase of the UV flux, as illustrated in Figure 11-34. At the same time, the UV spectrum showed only small variations, except for a large increase of the high-excitation HeII 1641 A line in 1986. The optical, ultraviolet, and X-ray observations of AG Dra during 1985-86 are shown in Figure 11-34.

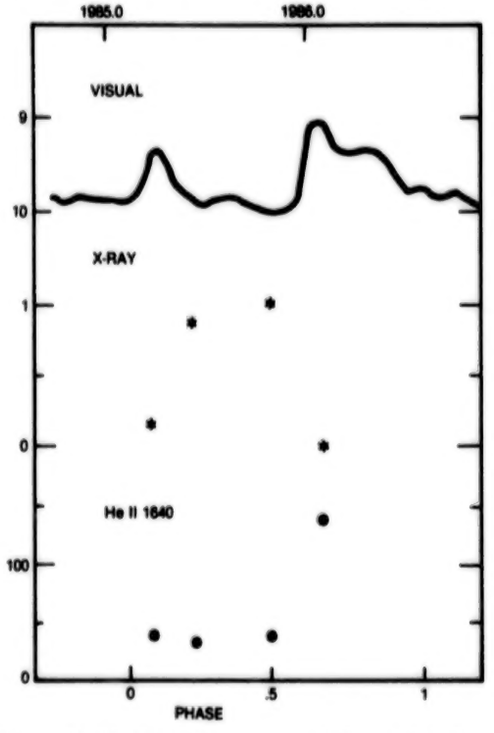


Figure 11-34. Optical, X-ray , and ultraviolet observations of AG Dra from March 1985 to Febraray 1986. From top to botttom: the visual light curve (Mattei, 1987), the EXOSAT X-ray flux (low enery, thin lexan filter; arbitrary units, and flux variation of the HeII 1640 A emission line.

It is clear that there exists a kind of anticorrelation of the X-ray emission with the stellar activity (where for "activity," we refer to the optical luminosity of the star). Furthermore, the X-ray fading was not followed by a simultaneous decrease of the emission line ionization, which is a frequent feature of symbiotic stars during outburst. However, also during the 1980 major outburst, no change of the ionization level of the UV emission line spectrum was noted (Viotti et al., 1984a).

IX.D. CH CYGNI

CH Cyg was detected as X-ray source with EXOSAT on 24 May 1985 by Leahy and Taylor (1987) when the star was in a phase of enhanced activity, characterized by a radio outburst and an increase of the ionization of the emission line spectrum, while the visual luminosity faded (Taylor et al., 1986). Previous observations with the HEAO-2 IPC detector gave only an upper limit, two orders of magnitude smaller than the EXOSAT flux (Leahy and Taylor, 1987, see their Table 2.11). There is an unidentified X-ray source in the HEAO-A2 experiment (Marshall et al., 1979) close to the position of CH Cyg, but, as discussed by Leahy and Taylor (1987), its identification with the symbiotic star is doubtful. Thus, the EXOSAT observations well probably represent the first X-ray detection of CH Cyg. This also implies that the star has largely increased its X-ray flux after the 1984 radio outburst, which puts it close to the small group of symbiotic novae, whose X-ray emission has been discussed above. From the analysis of the EXOSAT data, Leahy and Taylor concluded that the source is soft, with an integrated flux in the energy range 0.02-2.5 keV of about 1.3×10^{-11} erg cm^{-2} s^{-1}. As for the previous cases, we must consider that the derived fluxes critically depend on the assumed hydrogen column density and on the model used to fit the observational data. In particular, in the case of CH Cyg, the value $N(H)=4 \times 10^{20}$ cm^{-2} adopted by Leahy and Taylor is probably too high in comparison with the much lower column density that can be derived from the interstellar Lyα absorption, as discussed in their Section 2.6.2 (see their Table 2-8). Finally, EXOSAT observations seem to indicate a possible short-time variability during the 15 minutes of observations with the Thin Lexan filter of the LE1 telescope, with a time scale of the order of 5 minutes. If confirmed, this value, close to the flickering time scale of 5 to 7 minutes found by Slovak and Africano (1978) could support a model of X-ray emission from an inner boundary layer of an accretion disk (Leahy and Taylor, 1987). We shall come back to this problem in the following Chapter 12.

IX.E. R AQUARII

R Aqr is the second of the two symbiotic stars first detected in X-rays with EXOSAT. This is a Mira variable with a symbiotic spectrum and several other peculiarities, such as the anomalies of the Mira light curve, the strong radio emission and the radio jet-like features, the small planetary nebula around it, and the rich emission line spectrum. All these features will be discussed in details in Chapter 13, Section V. The many peculiarities and the relative vicinity (about 300 pc) make R Aqr an obvious target for X-ray satellites. The star was, in fact, observed with HEAO-2 on 1 June 1979, using the High Resolution Imagery (HRI), and on 21 June 1980, using IPC. In both cases, R Aqr was close to the minimum of its Mira light curve (about V=10). While there was no detection in the HRI image of June 1979 (Seward, 1985), a "marginal" flux was measured by Jura and Helfand (1984) from the more sensitive IPC observation of June 1980. However, a reanalysis of the original HEAO-2 observations using an improved data processing software available at the Center for Astrophysics of Cambridge, led Viotti et al. (1986b, 1987) to conclude that there is no evidence in the June 1980 IPC image of any X-ray source at the position of R Aqr. The estimated count rate upper limit was 0.010 s^{-1} for the broad (0.2-3.5 keV) energy range of IPC. The disagreement between Viotti et al. and Jura and Helfand again should be attributed to the different ways these data can be treated and the dependence of the results on the techniques, especially in the case of low fluxes as in the case of R Aqr. One should also consider that Jura and Helfand (1984)

also derived a marginal flux for the prototype of the Mira variables o Ceti, which should be a crucial result for understanding the nonthermal processes in Mira variables. However, also in this case it should be considered only as an upper limit, rather than a real detection (Seward, 1985).

R Aqr was observed with EXOSAT on June 14 and December 24, 1985, during two different phases (0 and 0.5) of the Mira light curve, and a weak flux was detected with the LE1 detector equipped with a Thin Lexan filter, Viotti et al. (1987) measured a background corrected count rate of 5.4 and 4.6×10^{-3} s^{-1} for the June and December 1985 observations, respectively. Within the errors, the count rates at the two epochs are the same, in spite of the large change of the visual magnitude of the Mira (V = 6.1 and 8.2, according to the IUE FES, Viotti et al., 1987). Therefore, the observed X-ray emission is not directly related to the pulsation of the Mira giant. Assuming a low reddening (logN(H)=20.2) and a soft X-ray spectrum ($T = 2\text{-}3 \times 10^{3}$K), Viotti et al. derived an X-ray flux of about 2×10^{-11} erg cm^{-2} s^{-1} in the 0.2-1 keV range. At a distance of 300 pc, the X-ray luminosity is 1×10^{30} erg s^{-1}. This value is close to the HEAO-2 upper limit reported above, and implies that at least the X-ray flux did not decrease between 1980 and 1985. Figure 11-33 shows the X-ray EXOSAT map of R Aqr. The source is point-like within the errors, but there is in both the June and December 1985 images an indication of an elongation of the image in the NE-SW direction, nearly the same as the orientation of the radio "ejecta" discussed by Hollis et al. (1986). Viotti et al. (1987) discussed these observations and, also on the basis of the IUE observations showing the high-temperature lines of NV and HeII in the spectrum of the jet stronger than in the spectrum of the central star, concluded that X-rays are mostly emitted from the jet. Clearly, high spatial resolution X-ray imagery is needed to better clarify this point.

X. SUMMARY OF THE OBSERVATIONS

X.A. THE SYMBIOTIC PHENOMENON

The symbiotic stars enbody features that are typical of many different categories of astrophysical objects: planetary nebulae, bipolar nebulae and jets, cocoon objects, ζ Aur and VV Cep stars, Mira and OH-IR variables, peculiar Be stars, novae, and cataclysmic variables. In addition, there is evidence for phenomena possibly associated with physical processes such as stellar winds, mass transfer and accretion, disks and streams, thermonuclear outbursts, dust condensation, and shocks. These are the many aspects of *the symbiotic phenomenon*. It should be clear to the reader, at this point, that the study of the symbiotic phenomenon can have a great impact on the understanding of a large amount of phenomena, which are relevant to many different classes of astrophysical objects. To proceed in our investigation, we have first to put the above described variety of information in a quantitative scheme and to determine the physical properties of our targets. In particular, we have to find a basis, a "counter stone" for our picture, and to provide a simplified scheme of the time behavior of the different phenomena. We shall try to do this in the following sections.

X.B THE COOL COMPONENT

The energy distribution of symbiotic stars typically presents three spectral components (e.g., Boyarchuk, 1969). The UV-to-IR spectrum of the S-type symbiotic BF Cyg is shown in Figure 11-35a. It is evident that for this star the visual range is a minimum of the energy spectrum.

As discussed above, in symbiotic stars, the cool spectral component is the most common feature, which generally leaves little doubt about its origin. This belief is based on the energy distribution showing, in most cases, a maximum in the

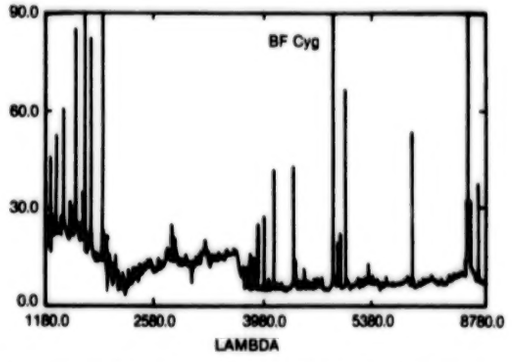


Figure 11.35a. The ultraviolet-to-infrared energy distribution of the symbiotic star BF Cyg (Cassatella et al., 1988b).

red-near IR, and on the presence of "photospheric" absorption lines and bands, especially in S-type symbiotics. It has been argued that the TiO bands and the absorption features could be formed in an outer cool absorbing layer like in the Mira variables, rather than in a stellar atmosphere. However, as already discussed in the previous section, this hypothesis is hard to maintain. Therefore, the cool component is the only characteristic of a symbiotic object that could be directly related to a "normal" stellar atmosphere. In the visible, the spectrum of a symbiotic star appears "peculiar" (See Figure 11-35b), but if our eyes and our instrumentation were sensitive only to the near-IR range, i.e., between 7000-8000 A and 1-2 μm, we would find, in most cases, a normal M-type spectrum with small amplitude irregular variations (in S-type systems), or with periodic Mira-type oscillations (for the D-type ones). Perhaps we might see some emission lines, especially in the latter objects, but this would be considered not unexpected because of the presence of a pulsating star. Certainly, we should not have the need to introduce a second star. The situation changes as soon as we move beyond the near-IR region, where the "peculiarities' emerge, and this is the case of the visual.

Let us better clarify this important point. For any scientific investigation, we have to decide about the best starting point. This should possibly be a well-established physical property of our phenomenon. In the case of the symbiotic stars, the classical approach is first to describe their behavior in the visual, but as shown in this chapter, for most objects, this is very confusing and difficult to put into a coherent picture. On the other hand, the near-IR is much simpler: in the S-type symbiotics, the cool spectral component is represented by a normal late-type photospheric spectrum. IR monitoring has disclosed the presence of irregular, small amplitude variations, (generally uncorrelated with optical and UV "activity"), which are not unusual among the majority of the "nonsymbiotic" late-type giants and supergiants.

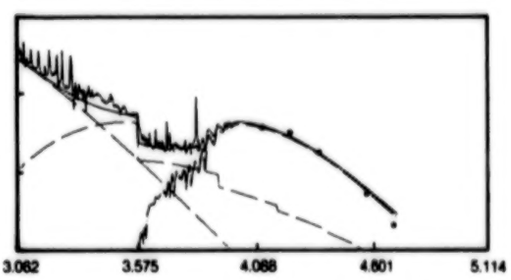


Figure 11.35b. Preliminary model of the energy distribution of BF Cyg. The main spectral components are included (Cassatella et al., 1988b).

Let us thus make the following statements: (1) the cool spectral component of the S-type symbiotics is a *cool star*, and (2) it behaves (near the maximum of its energy spectrum) like a *normal* cool star.

In the case of the (fewer) D-type symbiotics, there is no doubt about the presence of Mira-type periodicity, with a somewnat irregular light curve and possible secular trends, for all those objects which have been studied in the IR for long enough. Their light curves are rather irregular, which is, however, a common feature of the light curves of the "normal" Miras. The amplitude of the variations in J and K is, in general, rather large (up to about one magnitude) in fair agreement with the amplitudes observed in "normal" Miras (see Feast et al., 1982). This implies that most of the radiation in the 1-3 μm range comes from the cool variable source, while other possible contributors, especially emission from circumstellar dust, are less important. There is the problem of the difficulty of detecting the spectral features associated with a Mira star, such as the TiO bands in the visual. This could be explained by the small contribution of the cool component continuum to the visual region because of the dominant hot continuum. However, this molecula has been clearly identified in the classical D-type symbiotic RR Tel at 8206 A and elsewhere (Thackeray, 1977; note added in proofs). As discussed in Section VI.B. steam absorption bands have been observed in the IR of this star near 3 μm, where the cool spectrum dominates.

Again, we are brought to the conclusion, which is probably less firm than in the previous case of the S-type symbiotics, that also for the D-type symbiotics, the cool spectral component is *a cool star that is a Mira variable*. Therefore, following the suggestion of Whitelock (1988), it would be more appropriate to call them *symbiotic Miras* or *Mira-type symbiotic stars*. However, we have to recall that we are considering here only those stars for which there are enough infrared observations, and not all those objects that are included in the list of D-type symbiotics.

Now we have a good starting point for our study (1).

The next step would be to assume that these cool stellar components of the symbiotic systems have the same bolometric luminosity as the "nonsymbiotic' cool stars with the same spectral features. So far, there is no evidence against this assumption. But if the peculiarity of the symbiotic stars were associated with a higher chromospheric/coronal activity of the cool star, it would be possible that the enhanced activity would affect the relationship between bolometric magnitude and spectral type and luminosity class. However, so far, we have little ability to probe the chromospheric activity of the cool star, because it is very difficult to separate the stellar chromospheric spectral features from those originating in the hot circumstellar environment or nebula, or in the same cool star's atmosphere heated by the hot source's radiation. Probably, high resolution, high S/N spectrophotometry of some emission and photospheric absorption lines during the whole cycle of variability of a symbiotic star, should provide clear information about the place where the lines are formed and about the structure of the cool star's atmosphere and, eventually, about the presence and extension of a chromosphere. Fourier Transform Spectroscopy (FTS) observations in the near-IR would be of particular relevance for the problem. At this stage, the comparison of the apparent (dereddened) luminosity of the cool stellar component of a symbiotic star with the bolometric luminosity of a normal cool star seems to be the best and the most correct way we have to derive the distance of a symbiotic star.

D-type symbiotics are thought to be surrounded by extensive dust envelopes that are heated by the stellar radiation(s). It is also possible that the cool star is somewhat or largely obscured by the circumstellar dust, for instance, as suggested by Kenyon et al. (1986). So the apparent luminosity of the Mira could be underestimated, and the distance overestimated. For instance, Rossi et al. (1988) derived for the D-type southern symbiotic BI Cru a distance of 3800 pc. This value should be reduced by a factor of about 2 in the case of the presence of a thick dust envelope around the Mira component. This fact and the larger uncertainty in the absolute magnitude of the field Miras make the determination of the distances of the D-type symbiotics more uncertain than those of the S-type ones. Table 11-10 gives the spectral types of the cool components of symbiotic stars. Once the spectral type is known, the distance can be derived from the K-magnitude (if not variable) and from A_k, the interstellar extinction at 2.2 μm ($A_k = 0.112 \times A_v = 0.346 \times E(B-V)$, e.g., Rieke and Lebofsky, 1985), assuming for the cool star the same absolute K-magnitude of a non-emission line, non-variable star with the same spectral type and luminosity class. The reddening of the symbiotic stars was discussed in Section VIII.B. Table 11-11 summarizes the reddening and distance estimates for many symbiotic stars.

X.C. VARIABILITY

The second main distinguishing feature of the symbiotic phenomenon is the photometric and spectroscopic variability in all the frequency ranges. From the previous discussions, it appears quite hard to give a consistent picture of the observed variability, for both the large differences from star to star and for the changes between different phases in the same star. In general, we can state that variations are: (1) very irregular, (2) the dominant variation is on a long time scale (several months to years), and (iii) the amplitude of the long time scale variation is of the order of one to a few magnitudes, and is larger towards smaller wavelengths. In addition, periodic variations have been observed in a number of objects, and the associated periods are of the order of several hundred days. Short (days) or very short (minutes or seconds) time scale variations are also present, but so far they have not been investigated enough.

The symbiotic phenomenon is, therefore, mainly characterized by the long and irregular photometric variability. The behavior is not the same in different spectral regions. In particular, as described above, in the IR, a Mira-type vari-

(1) However, we should consider that the above "paradigma" that there is a cool star inside a symbiotic system needs to be checked "a posteriori" for each individual star. In particular we must verify whether the cool stellar components are placed in the H-R diagram in the same place as the normal cool giants and supergiants.

TABLE 11-10. SPECTRAL TYPES OF THE COOL COMPONENTS OF SYMBIOTIC STARS.

Star	IR Type	Spectrum			Remarks	Ref.
Z And	S	M	3.5	III		1
EG And	S	M	2.4	III		1
R Aqr	S	M	7	III	Mira	1
UV Aur	S	N			carbon star	2
TX CVn	S	K	5.3	III		1
T CrB	S	M	4.1	III	recurrent nova	1
BF Cyg	S	M	5	III		1
CH Cyg	S	M	6.5	III	radio-active	1
CI Cyg	S	M	4.9	II		1
AG Dra	S	K	3	III		3
YY Her	S	M	3.0	III		1
V443 Her	S	M	5.1	III		1
RW Hya	S	M	1.1	III		1
BX Mon	S	M	4.6	III	(Mira)	1,4
SY Mus	S	M	4			5
RS Oph	S	K	5.7	I-II	recurrent nova	1
AR Pav	S	M	3-4	II-III		1
AG Peg	S	M	3.0	III	symbiotic nova	1,5
AX Per	S	M	5.2	II-III		1
RT Ser	S	M	5.5		symbiotic nova	1
PU Vul	S	M	4-5		symbiotic nova	1
LMC S63	S	R			carbon star	6
BI Cru	D	M			Mira	7
V1016 Cyg	D	>	M4		Mira, symbiotic nova	1
V1329 Cyg	D	>	M4		symbiotic nova	1
RX Pup	D	>	M5		Mira	5
HM Sge	D	>	M4		Mira, symbiotic nova	1
RR Tel	D	>	M5		Mira, symbiotic nova	5
He 2-38	D	>	M5			5
M1-2	D'	G	2			8
HD 149427	D'	F				9
HD 330036	D'	F	5	III-IV		10

Notes: (a) S, D, D' infrared types as from Allen (1982). (b) Mira: Mira-type IR variability (e.g., Whitelock, 1987). Recurrent nova: see Kenyon (1986). Symbiotic nova: see Viotti (1988b).

References: (1) Kenyon and Fernandez-Castro (1987). (2) Nassau and Blanco (1954). (3) Viotti et al. (1983). (4) Viotti et al. (1986). (5) Schulte-Ladbeck (1988). (6) Allen (1979). (7) See discussion of Rossi et al. (1988). (8) O'Dell (1966). (9) Webster (1966). (10) Lutz (1984); see also Webster (1966).

ability was discovered in all the D-type symbiotics that were observed for long enough time. In some cases, the Mira pulsations have also been found in the visual, although with a much smaller amplitude and during quiescence. But the main photometric characteristics of the visual variability are the nova-like brightenings of the symbiotic novae, such as RR Tel, and the recurrent, but not

clearly periodic, long-term oscillations like those observed in Z And. The first type of behavior is clearly to be associated with some kind of "Cataclysma," whose repetition time--if the event is recurrent--should be very long (>> 10-10^2 y).While the Z And-type quasi-periodic oscillations could be related to a softer and repetitive process, such as stellar surface activity, pulsation, instability of an accretion disk or stream, etc., or to the orbital motion of a binary system, or to both. In between the RR Tel-type variability and the Z And-type one, there is a large range of different behaviors, as described in the previous sections, which are hard to classify, unless more information is available on the individual objects.

X.D. BINARITY AND ORBITAL GEOMETRY

The next step of our study is to determine whether the symbiotic phenomenon is associated with the presence of a close interacting binary system. First, we have to find out if we are dealing with two stars. Then, if the system is subject to strong gravitational and radiative interactions, and to mass exchange, or at least if the binarity has or has had at least partly a fundamental role in the present atmospheric structure of each component, for instance, on their chromospheric/coronal activity. In fact, even if the stars were at present far enough to not strongly interact, their physical properties (e.g., rotation) could have been influenced by the earlier evolutionary stages of the system, when the stars were closer. Thus in any case binarity is an important parameter to be determined in symbiotic objects.

For visually unresolved double star systems, the classical criteria of binarity are: periodic variations in the radial velocity curve of the photospheric lines (spectroscopic binaries) and periodic light variations associated with partial or total eclipses of one star by the other and with reflection effects (Leibowitz and Formiggini 1988). Both criteria work if the orbital plane is not too inclined with respect to the line of sight. Thus, even if all the symbiotic objects were binaries, we should expect to directly identify the binarity only for some of them. There are statistical means to estimate the "a priori" fraction of positive detections, but these computations are based on some assumptions about the orbital parameters and the stellar sizes that are rather uncertain. Conversely, there are other "indirect" ways to decide about binarity, which will be discussed later.

Periodic variation of the radial velocity of the photospheric lines of the cool star, possibly associated with phase-shifted luminosity variation, appears the best criterion of binarity. As discussed in Section IV.E, Garcia (1986, see also Garcia and Kenyon, 1988) has found periodic cool-component radial velocity variations in several S-type symbiotics. These results are generally in agreement with long-period photometric variability, and strongly support their binary nature. Two notable exceptions are Z And and RW Hya, whose photometric and spectroscopic curves have not the expected phase difference. This suggests rather complex geometric effects (Garcia and Kenyon, 1988).

Let us now discuss the long-time scale light oscillations found in different wavelength regions. There is no doubt that the large IR variations found in D-type symbiotics are associated with a pulsating star, rather than with eclipses. The latter hypothesis must be excluded, especially because of the large size of the eclipsed object, if it is a cool giant. Small amplitude long-term variations have been found in several symbiotic stars belonging to both types. These variations are generally seen during a quiescent phase of the symbiotic object, but still could be a residual of the symbiotic activity that is characterized by time scales of the same order. This might also be suggested by the associated spectral variability, such as the long term Hα (Altamore et al., 1979) and UV variations (Fernandez-Castro et al., 1988). However, these photometric (and associated spectroscopic) long-term variations of symbiotic stars could simply be explained by periodic eclipses or reflection effects in a binary system; and the discovery of periodic radial velocity changes in many symbiotics makes this interpretation the most plausible, for these systems at least.

Given the period and the radial velocity curve,

TABLE 11-11. ORBITAL PARAMETERS OF SYMBIOTIC SYSTEMS.

Object	T (a)	Vo (b)	K (c)	e (d)	Ref
Z And	750	+2	8.1	(0.0)	1
EG And	482	-95	5.1	0.17	2
.....	492	-94	7.1	(0.0)	1
UV Aur	388	+6	5.1	(0.0)	1
TX CVn	199	+2	6.1	0.2	1
CH Cyg	5700:	-58	4.9	0.47	3
CI Cyg	812	+18	6.5	(0.0)	1
AG Dra	530	-146	5.3	(0.0)	1
RW Hya	366	+14	8.7	(0.0)	1
AG Peg	819	-16	5.0	0.28	4
.....	796	-14	6.4	(0.0)	1
AX Per	601	-114	6.7	(0.0)	1

Notes to the table.

(a) Orbital period. (b) Radial velocity of the system (in km s^{-1}). (c) Half amplitude of the radial velocity curve (in km s^{-1}). (d) Eccentricity. Garcia and Kenyon (1988) found, for most of their stars, not enough data to justify fitting with an eccentric orbit.

References: (1) Garcia and Kenyon (1988). (2) Skopal et al . (1988). (3) Mikolajewski et al. (1988). (4) Slovak et al. (1988).

it is possible to infer some basic parameters of the binary system. Table 11-11 gives the orbital elements of some symbiotic systems. The corresponding mass functions are in the range 0.003 to 0.042 M (Garcia and Kenyon, 1988). Note that there is a number of cases where a significant eccentricity of the orbit seems to be present. Although the orbital constants need to be confirmed, there is now a fairly convincing ground that most symbiotic objects—especially the S-type ones—are wide binary systems.

X.E. STATISTICAL CONSIDERATIONS

When one deals with a group of objects showing a certain number of common characteristics as in the case of the symbiotic stars, two main questions have to be posed: (1) Do they constitute a homogeneuos group of objects so that we can speak of symbiotic stars as a whole? That is, do they represent a well-defined stage of the stellar evolution? (2) Which are the mean physical parameters defining this group?

As already discussed in the previous sections, symbiotic stars do not seem to represent a homogeneous stellar group, unless we restrict ourselves on some smaller samples, such as the symbiotic novae. Moreover, for most of the objects so far classified as symbiotic, the available information is not sufficient to define their nature to some extent. We, therefore, shall restrict our discussion to a comparison of the symbiotic objects with other categories of astrophysical objects. Most of the classification criteria are based on the optical multicolor photometry. But in the case of symbiotic stars the broad-band magnitudes are strongly affected by the emission lines, whose strength and relative intensity are largely variable from star to star and from epoch to epoch for the same star. In the near-IR, the emission lines are generally weaker with respect to the continuum. Thus, the IR photometry may provide some more physical information. The color-color diagrams in the near and far (=IRAS) infrared (e.g., Allen 1982; Whitelock, 1987, 1988; Kenyon et al., 1988) permit one to separate the symbiotic objects into at least two categories: those falling in the region of the late-type giants, and those spread out on a more extended region generally occupied by the Mira variables, the

TABLE 11-12. BASIC DATA ON SYMBIOTIC STARS AND RELATED OBJECTS (*).

Object	l (1)	b	IR (2)	Spectrum (3)	V (4)	K (5)	E(B-V) (6)	Dist. (7)
Z And	110	0	S	M3.5III	10.8	5.0	0.35	1.12
EG And	122	-22	S	M2.4III	7.5	2.6	0.07	0.63
AE Ara	344	-9	S	M 2	12.5	6.3		
UV Aur	174	-23	S	N	7.9	2.1		
BI Cru	300	0	D	M	12.3v	4.8v	1.5	3.8
BF Cyg	63	7	S	M 5 III	12.3	6.3	0.49	
CH Cyg	82	16	S	M6.5III	8.2	-0.7	0.02	
CI CYG	71	5	S	M4.9 II	11.0	4.5	0.40	
V1016 Cyg	75	6	D	> M 4	10.5	4.5v	0.28	
V1329 Cyg	78	-5	S	> M 4	13.7	6.8v	0.37	
AG Dra	10	41	S	K 3 III	9.9	6.2	0.06	0.70
YY Her	48	17	S	M3.0III	13.6	8.0	0.18	
RW Hya	315	36	S	M1.1III	10.	4.7	0.03	
BX Mon	220	6	S	M4.6III	11.9	5.7	0.20	2.80
SY Mus	295	-4	S	M2	11.2	4.7	0.40	
AR Pav	328	-22	S	M3-4II/III	11.	7.2	0.30	
AG Peg	69	-31	S	M3.0III	8.6	3.6	0.12	0.50
AX Per	130	-8	S	M5.2II/III	11.9	5.5	0.29	2.82
RX Pup	259	-4	D	> M 5	10.9	2.0v	0.7	1.0
HM Sge	54	-3	D	> M 4	10.7	3.6v	0.5	1.0
RR Tel	342	-32	D	> M 5	10.5	4.1v	0.10	
PU Vul	63	-9	S	M4-5III	8.8	5.9	0.49	
LMC S63	--	--	S	R	14.7	11.3	<0.02	55.0
Related Objects								
R Aqr	67	-70	S	M 7 III	6-11	-1.0V	<0.10	0.30
T CrB	42	48	S	M4.1III	10.2	4.8	0.15	1.43
RS Oph	20	10	S	K5-7 I-II	11.4	6.5	0.6	
RT Ser	14	10	S	M5.5	13.	7.0		

Notes to the table:

(*) Data collected mostly from Allen (1982, 1984), Kenyon (1986) and Mueller and Nussbaumer (1988). For individual objects: BI Cru: Rossi et al. (1988); BX Mon: Viotti et al. (1986); RX Pup: Allen and Wright (1988); LMC S63: Kafatos et al. (1983).

(1) Galactic coordinates (Allen, 1984).

(2) IR type (Allen, 1982).

(3) Spectral type of the cool component (Table 11-10).

(4) Visual magnitude at min (for S-type symbiotics) or after outburst (for D-type symbiotics). In many cases, the magnitudes are derived from the data published by the AAVSO bulletins (Mattei, 2988).

(5) K-magnitude (maximum value if variable).

(6) Interstellar colour excess (Table 11-7).

(7) Distance (in kpc).

OH-IR masers, and the compact planetary nebulae.

Emission line intensities, especially in the ultraviolet spectra, generally suggest line formation in rather dense (10^6-10^{10} cm^{-3}) regions, denser than in the classical planetary and gaseous nebulae. Schwarz (1988) applied to the symbiotic stars the classification method of Baldwin et al. (1981), which is based on the [OIII] 5007/Hβ and [OII] 3727/[OIII] 5007 line ratios. In the diagram 5007/ 4861 against 3727/5007, planetary nebulae and HII regions occupy two well-defined regions. Schwarz found that most symbiotic stars (both S, and D-D'-types) are spread out in the diagram, but the D, D' types are closer to the planetary nebulae region.

A different approach can be made by using the radial velocities (and proper motion if available), together with the galactic coordinates. Wallerstein (1981) first noted that the radial velocity dispersion of the (few) symbiotic stars in his sample is rather high (63±14 km s^{-1}, averaged on 19 objects). This value remains high even if the peculiar high-velocity star AG Dra is not included.

The galactic distribution (Figure 11-36) shows a fairly strong concentration towards the galactic plane and the galactic center, and suggests an old disk population (Boyarchuck, 1975; Wallerstein, 1981; Kenyon, 1986). This conclusion, however, should be taken with some care. For instance one should consider that one of the most representative symbiotic objects, AG Dra, for its high-velocity and high-galactic latitude, is clearly a halo object.

An ultraviolet color-color (C1, C2) diagram was recently proposed by Kenyon and Webbink (1984). This diagram is based on the UV fluxes near four continuum regions (1300 A, 1700 A, 2200 A, and 2600 A), and is useful as diagnostics of the hot and nebular components (which, as discussed in Section VIII.C, generally dominate the SW and LW spectral regions of IUE, respectively), and eventually the accretion rate. The

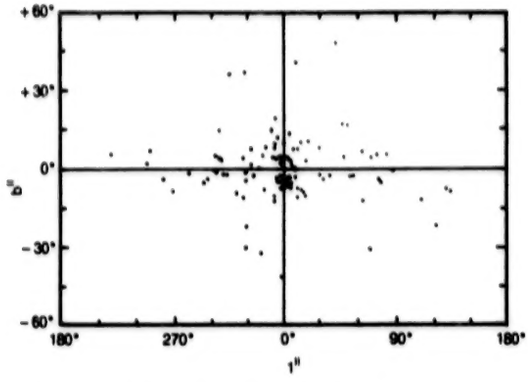


Figure 11-36. Distribution of symbiotic stars in galactic coordinates (Kenyon, 1976).

comparison of the observed colors with computed trajectories (Figure 11.37) seems to suggest that symbiotic stars possess either accreting main-sequence stars, or hot stellar sources (Kenyon and Webbink, 1984; Kenyon 1986).

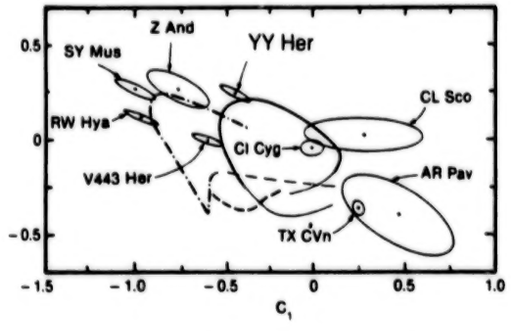


Figure 11-37. The C1-C2 diagram for symbiotic stars (Kenyon and Webbink, 1984; Kenyon,1986).

The problem of the classification of symbiotic stars is still open. But the above examples illustrate the need for new methods of statistical analysis (not only for the symbiotic stars), and the need to focus on those observational parameters that can provide information on which process is going on. The previous Table 11-12 summarizes the basis observational data on the symbiotic stars.

N95
27077
UNCLAS

N95- 27077

12

MODELS OF SYMBIOTIC STARS

M. Friedjung

I. GENERAL INTRODUCTION

As it can be seen from Chapter 11 of this monograph, we need to explain many features of symbiotic stars. One of the most important is the coexistence of a cool spectral component that is apparently very similar to the spectrum of a cool giant, with at least one hot continuum, and emission lines from very different stages of ionization. The cool component dominates the infrared spectrum of S-type symbiotics; it tends to be veiled in this wavelength range by what appears to be excess emission in D-type symbiotics, this excess usually being attributed to circumstellar dust. The hot continuum (or continua) dominates the ultraviolet. X-rays have sometimes also been observed.

Another important feature of symbiotic stars that needs to be explained is the *variability*. Different forms occur, some variability being periodic. This type of variability can, in a few cases, strongly suggest the presence of eclipses of a binary system. One of the most characteristic forms of variablility is that characterizing the active phases. This basic form of variation is traditionally associated in the optical with the veiling of the cool spectrum and the disappearance of high-ionization emission lines, the latter progressively appearing (in classical cases, reappearing) later. Such spectral changes recall those of novae, but spectroscopic signatures of the high-ejection velocities observed for novae are not usually detected in symbiotic stars. However, the light curves of the "symbiotic nova" subclass recall those of novae. We may also mention in this connection that radio observations (or, in a few cases, optical observations) of nebulae indicate *ejection* from symbiotic stars, with deviations from spherical symmetry.

In the following, we shall give a historical overview of the proposed models for symbiotic stars and make a critical analysis in the light of the observations discussed in Chapter 11. Then we describe the empirical approach to models and use the observational data to diagnose the physical conditions in the symbiotics stars. Finally, we compare the results of this empirical approach with existing models and discuss unresolved problems requiring new observational and theoretical work.

II. HISTORY AND OVERVIEW OF SIMPLE MODELS

Several types of model are conceivable, if one takes as a starting point the fact that the spectra are composite. For instance, it can be supposed that one has a single object with several regions whose physical properties are very different or that one has a binary. Following Friedjung (1982), we shall broadly classify simple models into the following categories:

(a) Single-star models having a hot central object surrounded by a cool envelope.
(b) Single-star models having a cool central object surrounded by a hot envelope.
(c) Binary models.

PRECEDING PAGE BLANK NOT FILMED

It must be noted that single-star models without spherical symmetry are also possible and have sometimes been suggested.

The simplest sort of explanation is of type (c), and this was the one the first suggested. It was proposed by Berman (1932) for several stars, and by Hogg (1934) for Z And. Berman suggested the presence of an extremely faint O star that would be too faint to be seen, enclosed by a small nebular shell of high excitation. Binary motion and the proximity of the nebular shell were supposed to be possibly responsible for the observed variations. He thought that duplicity might be directly seen using a powerful instrument. Hogg (1934) proposed that Z And consisted of a normal M giant and a variable very hot dwarf that excited a nebular envelope, perhaps ejected in nova-like outbursts.

Kuiper (1941) suggested that stars such as Z And, VV Cep, T CrB, CI Cyg, AX Per, etc., might be examples of what he called ejection of type A in binaries. To use present day language, a giant fills its Roche lobe, and material is ejected near the inner Lagragian point, tending to go into orbit around a compact companion. A binary model for BF Cyg, proposed by Aller (1954a) is illustrated in Figure 12-1.

However, it is generally not easy to find direct evidence of binarity for symbiotic stars, so various single-star models were proposed. Menzel (1946) suggested a hot central star with cool envelope model for different kinds of giant star. He proposed that the cool envelope of R Aqr lay only over the poles or only around the equator.

In a similar way Sobolev (1960) gave an explanation for cool stars with emission lines,

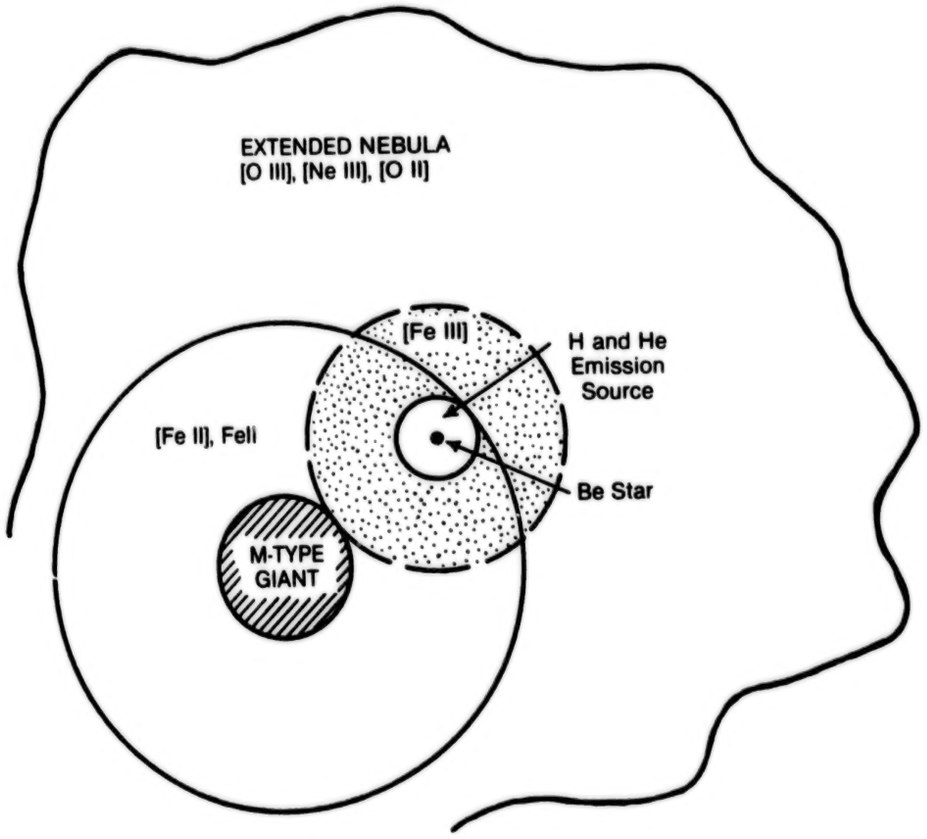


Figure 12-1. A binary model proposed for the symbiotic star BF Cyg (Aller, 1954a).

which symbiotic stars can be considered to resemble at certain times in certain wavelength ranges. According to Sobolev, such stars had a hot nucleus surrounded by an envelope with a significant optical thickness in subordinate continua like the Balmer continuum of hydrogen, giving rise to a cool absorption line spectrum.

The Sun and similar stars can from a certain point of view, also be thought of as "symbiotic". The same star has a relatively cool spectrum in the optical and high-ionization emission lines in the far-UV. This is explained in the solar case by the presence of a hot chromosphere, transition region and corona above a fairly cool photosphere, and quite a number of attempts have been made to explain symbiotic stars with this kind of model. Aller (1954b) suggested that such a picture with heating produced by the dissipation of shock waves could be an alternative to a binary model. Gauzit (1955 a,b) tried to explain observations of the symbiotic star AX Per using this kind of model. His studies of relative line-intensity variations appeared to him hard to explain using a binary model. However, it may be noted that stratification effects can be complex, particularly in a binary system.

Wood (1974) made theoretical calculations concerning a model with a cool photosphere and hot chromosphere. An asymptotic-branch giant star had pulsations and relaxation oscillations; noise from shocks heated the chromosphere.

A new impulse was given to binary models by the work of Boyarchuk (1966, 1967a, 1968, 1969a, 1969b, 1975, 1976b). Energy distributions of a number of symbiotics were studied and interpreted as due to three components: a cool giant, a small hot star with a temperature near 10^5 K, and an ionized nebula. The hot star was assumed to radiate as a blackbody, while the nebula was supposed to be optically thick to photons with wavelengths less than 912 A, and optically thin at longer wavelengths. Optical range energy distributions were explained for a number of stars, including AG Peg and Z And. The variations of Z And were interpreted by changes in the temperature of the hot star at almost constant bolometric magnitude.

At present, workers in the field of symbiotic stars with few exceptions consider that almost all symbiotics, if not all, are interacting binaries. The question now is since about 1980, to find out *which processes dominate in which stars*. One major reason for this shift in attitude is the impact of ultraviolet observations with the IUE satellite, which cannot be easily explained in the framework of single star models. In the following we shall give a more detailed description of models and how they can be tested.

III. SINGLE STAR MODELS

III.A. HOT STAR WITH COOL ENVELOPE

We shall consider two forms of such a model. The first form to which the already mentioned historical models belong has dense envelopes, with a nonnegligible optical thickness in the continuum at most wavelengths. Without detailed calculations, it is possible to make simple predictions for the behavior of symbiotic stars that would be described by the first form of the model, these appearing, in general, to be contradicted by the observations.

Firstly, as we have already seen in Chapter 11, the cool spectral component very much resembles that of a cool star without signs of abnormalities. We shall come back to this point in Section III.B. In addition, a cool envelope might be expected to consist of cool regions of the wind of the late-type central star. As will be seen, the source of the hot continuum needs to come from a rather small object, which would be a subdwarf in the present case. A wind velocity on the order of the stellar escape velocity (around 1-3 10^3 km s^{-1}) might then be expected. Neither emission lines with a corresponding Doppler width nor absorption lines with a corresponding blue shift are usually observed, AG Peg perhaps being an exception. In addition, both line and continuum absorption of the hot continuum by the cool envelope

might be expected unless there were large deviations from spherical symmetry. No indications of a modification of emission line fluxes in the optical because of overlying absorption are seen as pointed out by Boyarchuk (1969b). Similarly, as discussed in Section 11.VIII.C, no clear sign of hot continuum absorption by non-interstellar excited neutral absorption lines has been reported in high dispersion UV observations. Moreover, when low excitation lines are seen in the near UV, they do not appear to be associated with the spectrum resembling that of a cool star. For instance, Faraggiana and Hack (1971) found that the M6III-type absorption spectrum of CH Cyg was veiled by the blue continuum present in 1967. Johnson (1982), however, claimed that continuum absorption by amorphous silicate smoke might occur in the UV of R Aqr. Nevertheless, as pointed out by Johnson, even this could be explained by a binary model with absorption of hot continuum radiation by the cool star's wind.

Absorption of the hot continuum might be less important if there were deviations from spherical symmetry, such as in the model suggested by Menzel (1969), further extending his 1946 proposal, with a cool ring formed by a magnetic field around the hot star. However, as previously seen, the cool component observed in symbiotic stars appears very normal. Also, no magnetic fields were detected by Slovak (1978) for symbiotic stars.

Another argument was given by Boyarchuk (1982). "If we propose that a symbiotic star is a hot star with a hot nebula, and that TiO-bands and other absorption features are formed in other parts of this nebula, we should note that in the spectra of many symbiotic stars we observe the absorption line of CaI 4227 A. This line has very extended 'wings' which is normal for a cool star spectrum. But, if we calculate the column density which is needed to produce such wings in a nebula, and multiply by the surface of the nebula which is huge, then we will obtain the mass of the absorption envelope that is equal to several solar masses. It is difficult to understand how such envelope could exist".

The second form of the hot central star with cool envelope model is to suppose that one has an object rather like a compact planetary nebula. This sort of explanation can be attempted for D-type symbiotics for which indications of the presence of the cool spectral component are less clear in the visual. Nussbaumer and Schild (1981) made a proposal of this kind for V1016 Cyg. They calculate the emission line fluxes with their model; emission came from a shell with a mass of ionized hydrogen of 3×10^{-4} $M_\odot$ surrounding a hot star with an effective temperature of 1.6×10^5 K and a radius of 0.06 $R_\odot$. Other single star models for this object exist, such as those discussed by Baratta et al. (1974) and Ahern et al. (1977).

The objection connected with the absence of spectroscopic signatures of a high-velocity wind have less importance for the last kind of model. This is because a low-velocity envelope, in principle, could have been ejected from a previously existing red giant with a much lower escape velocity, this giant then having become a subdwarf (see Figure 12-2). Indeed according to the mechanism of Kwok et al. (1978) a planetary nebula might be formed as a result of the collision of the wind of a subdwarf and that of the pre-existing red giant. However the evidence for the existence of a cool star spectral component even for D-type symbiotic stars seems to contradict planetary nebula types of model.

III.B. COOL STAR WITH HOT ENVELOPE

As for the previously considered single-star models, rather simple considerations lead to major problems for cool star with hot envelope models. It is hard for the present models to produce the strong observed hot continua already studied by Boyarchuk (1967a, 1968, 1969a) in the optical, and in more recent years, well-studied in the satellite ultraviolet. The energy radiated in different forms will be discussed later, but we can anticipate by stating that the energy radiated by the hot continuum and the emission lines is of the same order as that due to the cool spectral component. Let us

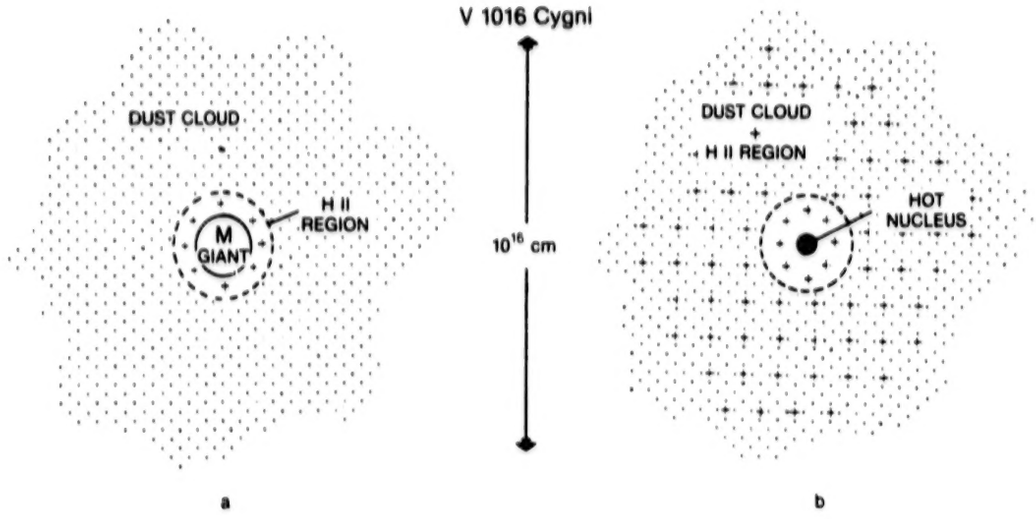


Figure 12-2. Single-star model proposed for the symbiotic nova V1016 Cyg: a Mira-type variable red giant loses its outer envelope and becomes a hot subdwarf, whose radiation ionizes the low-velocity circumstellar nebula produced by the red giant wind during the preoutburst phase (Baratta et al., 1974).

also mention a calculation performed by Altamore et al. (1981) for Z And; the regions producing the emission lines of highly ionized atoms seen in the UV could not produce the strong UV continuum observed in Z And. This result does not appear very easy to change, even with other assumptions for the calculations.

One can try to avoid some of the problems associated with the production of the hot continuum, if it is assumed to be produced by optically thick spots of the cool star's photosphere resembling solar faculae. Wdowiak (1977) suggested a model of this type for CH Cyg involving magnetic heating following a prediction of kilogauss surface magnetic fields, while Oliversen et al. (1982) suggested the presence of a large spot with associated magnetic activity to explain the phenomena of AG Dra. The lack of detection of coherent magnetic fields for CH Cyg, AG Peg and, EG And by Slovak (1978), however, poses a special problem for this form of model.

Other types of arguments against models of cool stars surrounded by coronae have been given by Kenyon (1986, p.13). He based his reasoning on results obtained by Hartman et al. (1981, 1982) concerning more "normal" late type stars. In the latter, the flux of the HeII 1640 A line is correlated with X-ray emission observed using the Einstein satellite, as expected if a substantial part of the double photoionization of helium is due to X-ray radiation from a hot corona with temperatures above 10^6 K. Kenyon points out that T CrB and V1017 Sgr have X-ray emission without HeII 1640 A, while R Aqr and AG Dra show X-ray emission that is one to two orders of magnitude less than that predicted from HeII. The two former stars are usually considered rather to be recurrent novae, and perhaps, they may be different from most of the stars considered in this chapter, while the results from the two latter stars indicate either a different mechanism for photoionizing helium (e.g., the photosphere of a hot star) or a relatively cool corona. Kenyon (1986, p.13) also argues from the NV 1240 A/CIV 1550 A flux ratio observed for "normal stars"; this ratio can be much lower in symbiotic star spectra. One may conclude, perhaps, in the light of the arguments given by Kenyon, that any symbiotic star corona, if present, would have to be rather unusual.

If we consider single-star models in general, we also see that the explanation of the variations is not clear. How can one produce what appear to be eclipses, while though it might not be impossible to explain active phases, explanations of them appear rather vague? In any

case, in view of what has been said, single-star models seem difficult to support, unless rather artificial assumptions are made. Therefore, we shall not pay very much more attention to them in the following discussion.

IV. BINARY MODELS

Binarity is very common among stars, and interaction between components can lead to many effects when these components are close. As we shall see, binary models have a strong predictive power. In any case, it is immediately obvious that composite spectra and eclipses are straightforwardly explained in the framework of such models. The main signature of close binarity, radial velocity variations, has been discussed in Section 11.X.D. Evidence for the presence of such variations has been rapidly improving.

Instead of considering particular models, it is more useful to consider the different processes that can occur in binaries. Several processes could be responsible for the phenomena in symbiotic stars: the question will be which process is dominant. In addition, the physics of these processes is often still badly understood, and different possibly conflicting phenomena need to be mentioned.

In all the following discussion, we shall suppose, as discussed in Section 11.X.B, that the cool spectral component is really produced by a cool giant star. The different processes and phenomena lead to conflicting interpretations of the nature of the hot component and concern the interactions between the components. We shall now consider the different processes and possible phenomena.

IV.A. HOT COMPONENT AS A SUBDWARF OR A REJUVENATED WHITE DWARF

The simplest interpretation is that the hot continuum comes directly from a hot star similar to the nucleus of a planetary nebula. In this case, we can predict the form of the continuum. In addition, if the emission line fluxes and radio emission come from an HII region, we can, in principle, obtain information about unobservable wavelength ranges of the continuum that photoionizes the HII region. In this way, analysis of the observations leads to the deduction of the characteristics of the hot star. This type of analysis, to be described later, was performed by Kenyon and Webbink (1984).

If such an interpretation is accepted, active phases must be linked to changes in the properties of the hot component. In fact, a fair amount of theoretical work has been done, supposing that the hot component is an accreting white dwarf undergoing thermonuclear events or even continuous shell burning. The accreted material then comes from the stellar companion by processes that will be considered later. According to Iben (1982), the condition for steady hydrogen burning is

$$\dot{M} \gtrsim 1.32 \times 10^{-7}\ M_{wd}^{3.57}\ M_{\odot}\ yr^{-1},$$

where $\dot{M}$ is the mass accretion rate in solar masses per year and M_{wd}, the white dwarf mass in solar masses. For an $\dot{M}$ above a slightly larger limit, the envelope of the accreting star expands so it resembles a giant, while for smaller rates, recurrent outbursts occur.

The different forms of possible behavior of an accreting white dwarf were studied in detail by Fujimoto (1982a, b), and are summarized in Figure 12-3 taken from the second of these papers.

In general, two types of stable configuration of accreting white dwarf exist, according to Fujimoto. In one, nuclear shell burning compensates for energy losses; in the other, gravitational energy release balances the radiative energy loss. Steady burning occurs in the former configuration, which has a lower limit to the mass of the hydrogen-rich envelope. For lower accretion rates, transitions occur between these two configurations, which are not stable. Starting from the second configuration, accretion leads to an increase in the mass of the hydrogen-rich envelope. A "hydrogen shell flash" then occurs, associated with a transition

to the other configuration. If energy losses are larger than thermonuclear energy generation, this new state does not last, and the white dwarf returns to its initial state. The cycle is then repeated.

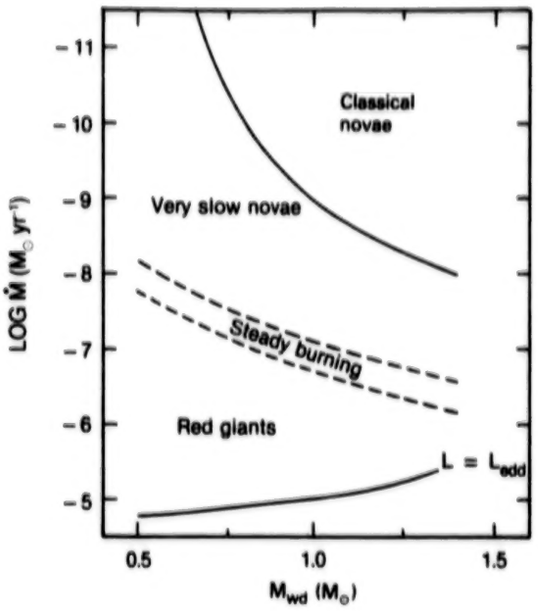


Figure 12-3. Behavior of accreting white dwarfs in a graph of white dwarf mass against the accretion rate, according to Fujimoto (1982b).

Examining in more detail Figure 12-3, one sees first the region at the bottom of the figure; that is where the envelope of the white dwarf expands, so as to make it like a giant. The star will then fill its Roche lobe; if the companion also fills its Roche lobe a sort of contact binary will be formed; otherwise, the system will be semi-detached with mass transfer *from* the expanded white dwarf *to* its companion. For lower accretion rates, steady state burning occurs, and the expanded white dwarf will be a strong source in the extreme UV. Even lower accretion rates are associated with recurrent events, their nature depending on the extent to which the white dwarf expands. It expands during hydrogen burning to less than a solar radius for higher accretion rates, and to larger radii for lower rates. Finally, for very low accretion rates, the white dwarf envelope expands at high velocity during a shell flash, and a nova explosion occurs. However, the limits of this theory should be noted; in particular, a simple interpretation of observations of classical novae in quiescence suggests higher accretion rates than would be possible, according to the calculations of Fujimoto.

Fujimoto (1982b) also calculates time scales. During a shell flash, the duration of burning is

$$\tau = \Delta M_1 / (\dot{M}_{ex} - \dot{M}),$$

where M is the mass of the accreted envelope, $\dot{M}_{ex}$ the minimum mass accretion rate for steady burning, and $\dot{M}$ the actual rate. Hence, for ΔM_1 equal at ignition to 10^{-6} $M_\odot$ and a value of $(\dot{M}_{ex} - \dot{M})$ of 3×10^{-7} $M_\odot$ yr^{-1}, τ is 3 years.

Explanations of symbiotic stars using such models were proposed by Tutukov and Yungelson (1976), Paczynski and Zytkow (1978), Paczynski and Rudak (1980), and by Kenyon and Truran (1983). Paczynski and Rudak divided symbiotic stars into two classes. In *type I* symbiotic stars, the luminosity was produced in a stable burning hydrogen shell; small variations of accretion rate led to changes of radius and effective temperature of the expanding white dwarf at constant bolometric magnitude. Thus, an active phase of this type of symbiotic star was associated with a small increase of the accretion rate; the effective temperature dropped while the radius increased, causing an increase of the visual brightness over a time scale of the order of $\Delta M_1/\dot{M}_{ex}$ (using our previous notation), estimated by Paczynski and Rudak as of the order of 2.5 years. *Type II* symbiotic stars, according to the explanation of Paczynski and Rudak, have an accretion rate below $\dot{M}_{ex}$, and therefore, are undergoing recurring shell flashes. This explanation was used for symbiotic novae.

Shell flashes were also discussed by Kenyon and Truran (1983) and by Kenyon (1986) to explain the symbiotic novae phenomenon. The rise to visual maximum is characterized by two phases illustrated in Figure 12-4.

A rapid increase in bolometric luminosity at

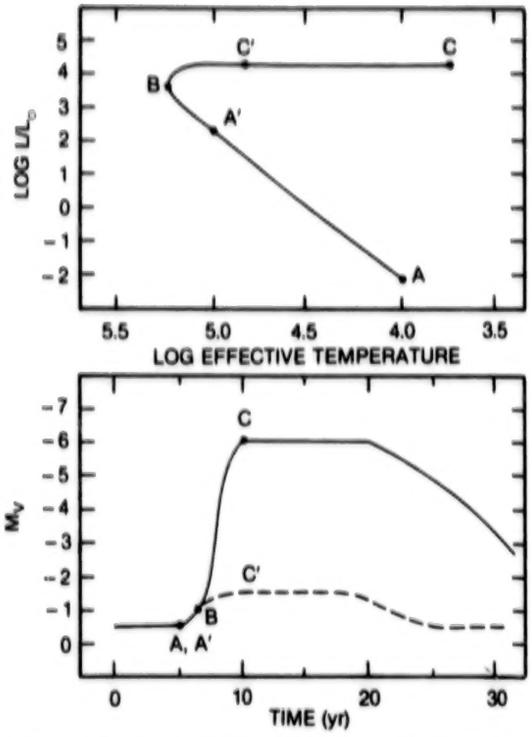


Figure 12-4. Time evolution of a white dwarf undergoing a thermonuclear flash. (a) The path in the H-R diagram. (b) The visual light curve (Kenyon 1986): A C, strong flash; A C', weaker flash.

almost constant radius (A to A' in Figure 12-4) is followed by a phase at nearly constant bolometric luminosity (C to C' in the figure). In the first phase, the visual brightness is almost constant while the effective temperature of the star increases, so being able to strongly ionize any surrounding nebula. In the later phase, however, the temperature drops and the visual brightness rises (see Figure 12-4b). Weaker flashes lead to shorter tracks in the H-R diagram (for instance to C' in the figures). Kenyon and Truran (1983) divided symbiotic novae into two classes. RR Tel, RT Ser, and perhaps AG Peg had strong flashes, showing like classical novae B-F supergiant spectra at maximum, characteristic of not very high temperatures. V1016 Cyg, V1329 Cyg, and HM Sge were considered to be examples of weak shell flashes; they did not evolve into F supergiants and had planetary nebula-type spectra even at maximum. We shall discuss this point again in Chapter 13, Section IV.C.

We can conclude this section by stating that binary models containing an expanded white dwarf component appear promising in certain respects at least. Future work will show whether they really represent the observations well.

IV.B. ACCRETION PROCESSES

Accretion has already been invoked in the discussion about expanded white dwarfs. It can play a dominant role in other ways, and we shall now discuss them. Two simple sorts of accretion are conceivable, (1) via a disk following Roche lobe overflow, and (2) from the wind of the companion star.

The former type of accretion has already been extensively discussed for dwarf novae, novae in quiescence, and nova-like cataclysmic variables in this volume. In a classical case, material flows from the inner Lagragian point in a stream that strikes the accretion disk at a bright spot. Angular momentum is lost in the disk and a boundary layer is formed between the disk and the mass gaining star. As in the previous situation where the hot continuum came directly from a star, one can calculate a theoretical energy distribution for observable and also unobservable spectral regions able to photoionize various atoms. The methods of calculating the energy distribution are the same as for dwarf novae, novae in quiescence and nova-like cataclysmic variables.

Kenyon and Webbink (1984) have calculated theoretical energy distributions for symbiotic stars, supposing that the hot component was due to accretion. They assumed that radiation was emitted by a disk locally radiating as a blackbody (that is, by a disk consisting of a sum of blackbodies at different temperatures) and a boundary layer radiating as a blackbody at one temperature. The inclination of the disk and occultation of part of the boundary layer were taken into account. Kenyon and Webbink considered accretion both onto a white dwarf, and onto a main sequence star, and found no example of the former case when comparing theory and observations. For stars whose continuum energy distribution suggested a main

sequence accretor model, difficulties were encountered in explaining emission line intensities as due to photoionization. This type of approach will be considered in more detail below, but it is already clear that it needs to be refined in future work.

In cataclysmic binaries, emission line formation in or near a disk leads to double peaked profiles for large inclinations (Smak, 1981). A bright spot, if present, would lead to an S wave profile as for cataclysmic binaries (see Section 2.III.B.1.e), and variations in the ratio of the violet to the red peak over the orbital cycle.

Eclipses of an accretion disk should also lead to characteristic time variations of the continuum and the emission line profiles, as seen for cataclysmic binaries. This is because an accretion disk does not have the same brightness distribution at a given wavelength as a star, while different parts having different rotational velocities contribute to different parts of line profiles, eclipsed at different times. (The theory of this is described in Section 4.III of this Monograph).

When accretion occurs from a wind, disk formation is difficult, because only a small amount of angular momentum should be accreted. The three-dimensional theory has been treated by Livio et al. (1986a,b). The second of these papers describes the results of calculations in three dimensions, taking account of pressure. Conditions necessary for the formation of a disk were obtained in that paper. Enough angular momentum must be accreted for material to be able to rotate at a Keplerian velocity at the radius of the accretor at least. Livio et al. (1986b) give a condition for the formation of a disk in their equation (21):

$$V_{rel} \leqq 3.7\times10^{8}(\xi/0.2)^{1/4}(M_{wd}/0.6)^{3/8}(P/10y)^{1/4}$$
$$(R_{wd}/4.5\times10^{8}\,cm)^{-1/8} \qquad (12.1)$$

Here V_{rel} is the relative velocity of the wind and the accreting object, $\xi = l/l_{BH}$ is the ratio of the accreted angular momentum to that deposited at the radius of accretion, according to the classical theory of Bondi and Hoyle (1944), M_{wd} the mass of the accreting star (taken to be a white dwarf by Livio et al.), R_{wd} the radius of the accreting star, and P the orbital period. The calculations of Livio et al. (their Table 1) give values of ξ ranging form 0.10 to 0.23, depending on the assumed Mach number and ratio of specific heats. For a symbiotic star having a period of 2 years, ξ equal to 0.15, a white dwarf accretor with a mass of 1.0 $M_{\odot}$ and a radius of 9.5×10^{8} cm, the condition is $V_{rel} < 28$ km s^{-1}. For a main sequence accretor with a radius of 6×10^{10} cm, this condition becomes $V_{rel} < 17$ km s^{-1}. Wind velocities of red giants can be expected to be very low; if the orbital part of V_{rel} is near 20 km s^{-1}, formation of a disk around a white dwarf may be possible following wind accretion. Livio (1988) found that a disk could be formed by wind accretion round a white dwarf accretor of the symbiotic star AG Dra.

There are, however, many uncertainties in the theory of disk formation from winds. For instance, the two dimensional calculations of Matsuda et al. (1987) found nonsteady behavior with the accreted angular momentum being able to change sign. More work remains to be done, before one can be sure when disks can be formed by accretion from a wind.

Accretion processes can also be invoked to explain the active phases of symbiotic stars. The models are fairly similar to those for the outbursts of dwarf novae, described in Chapter 3. As for the latter, one can conceive both of instabilities of the secondary leading to times when the mass transfer rate is enhanced, and of instabilities of the accretion disk, if one is present.

In addition to the dwarf nova type of instability proposed by Bath (1975, 1977) for a cool component of such a binary, another type of instability was suggested by Kenyon (1986), associated with recurrent helium shell flashes. A cool giant in a double shell phase of evolution is modeled with secular combustions in two shells; an outer shell burning hydrogen to helium and an inner shell burning helium. The latter is unstable because of the presence of a

convective envelope above it, preventing expansion associated with an increase of thermal energy. Such an increase leads to a sudden increase of energy generation of the helium shell and a large expansion, which temporarily extinguishes the hydrogen binary shell. Such events should not have much effect on the surface properties of a single red giant, but according to Kenyon (1986), the small predicted increase in photospheric radius could power a mass transfer instability. The phenomenon is predicted to be periodic with a period P in years given by

$$\log P = 3.05 - 4.5\,(M_{core} - 1.0M_{\odot}) \qquad (12.2)$$

Kenyon fitted this expression to observed activity of R Aqr; a 44-year period would correspond to a core mass of 1.3 $M_{\odot}$ and a bolometric magnitude of -7. This was thought tolerably close to the observed one of symbiotic stars, considering both the theoretical uncertainties and the uncertainty in the distance of the star.

It may be noted that periodic mass transfer events could also occur at periastron, if the orbits were eccentric. Determinations of the eccentricity of orbits by Garcia and Kenyon (1988) suggest that in some, but not all, cases, the orbits are fairly circular (see Section 11.X.D), rendering such a mechanism fairly unlikely for those stars at least.

Disk instability calculations were made by Duschl (1983,1986a,b). In the latter of these papers, calculations were made in cases of accretion by a one-solar mass main sequence star. The limit cycle instability model led to heating and cooling fronts crossing the disk; reflection of a front of one type led to propagation of a front of the opposite type. Conditions for this type of model to work for symbiotic stars indicated breakdown of the model as follows (Duschl 1986b):

- A: The description breaks down, as the disks are no longer geometrically thin.
- B: The disks are too large, so that the outbursts are too rare to be consistent with the observations.
- C: The outbursts occur too rarely, as the mass transfer rate is too low.
- D: No outbursts occur at all, as the unstable branch does not appear within the disk; i.e., the disk can be everywhere stationary on the upper branch.
- E: Maximum brightness is too small to be consistent with observations.

The regions in which disk instabilities are possible are shown in a diagram of the accretion rate and the disk radius, according to Duschl, in Figure 12-5.

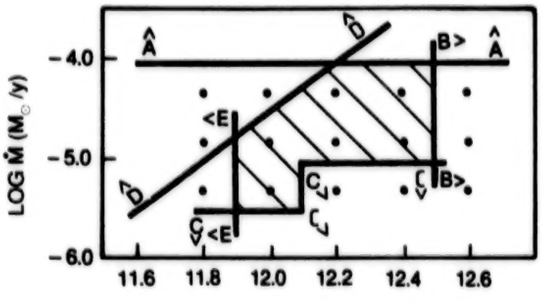


Figure 12-5. Location of possible models for symbiotic stars (shaded area), according to Duschl (1986b). The restrictions AA to EE are those described in the text. Abscissae are log of the outer radius of the disk s_Q, and ordinates log of the mass transfer rate.

In situations where accretion from a wind occurs, the accretion rate varies inversely as the fourth power of the relative (wind + orbital) velocity of the accretor and the wind. A decrease in the wind velocity would, therefore, cause an increase in the accretion luminosity. However, it is very difficult for a high enough luminosity to be produced for a main sequence accretor, because the calculations of Kenyon and Webbink (1984) indicate accretion rates of $\sim 10^{-5}\ M_{\odot}\ yr^{-1}$ in such cases, and the mass-loss rate of a cool giant wind would have to be even greater.

It is hard to assess the relevance of models involving accretion rate changes. In general, simple models would predict that activity is associated with temperature increases of the disk and, hence, a flux increase at all wavelengths. However, the behavior of the boundary layer in particular needs also to be taken

into account. The theories of disks plus boundary layers are sufficiently uncertain that it is not sure whether accretion events can be ruled out when observations clearly indicate that the hot source cools during an outburst. Therefore, it is premature to make a judgement of this type of theory.

IV. C. WINDS FROM BOTH COMPONENTS

The strong wind expected from the cool giant component of a symbiotic binary should have important effects. Emission lines and, in certain conditions, absorption lines can be produced; indeed, it can be what is sometimes called the "nebula".

The winds of normal cool giants have rather low velocities of the order of 10^1 km s^{-1}, and can be expected to give rise to rather narrow emission lines. Radiative transfer in an expanding medium can be expected to produce radial velocity differences between the centers of optically very thick resonance and optically thin lines. This is because a multiply scattered photon inside the profile of an optically thick line formed in such a medium will be somewhat redshifted by each scattering, producing a net redshift of the emission line. In addition, if the continuous spectrum is not too weak, this type of line will also have a blueshifted P Cygni absorption component eating into the blue wing of the emisssion line, and so increasing the mean redshift of the observed line emission. Such a difference between the radial velocitites of high-ionization resonance lines and semiforbidden lines has been observed in the ultraviolet spectra of a number of symbiotic stars (Friedjung et al., 1983).

Photoionization can be expected to be due to the hot companion, which is not at the center of the cool component's wind. Ionization models must take this lack of spherical symmetry into account. The consequences of this were first calculated for the interpretation of radio observations by Seaquist et al. (1984) and by Taylor and Seaquist (1984). In these papers, the geometry of the ionizaton boundary is calculated as a function of f(u, θ) with u a radial distance centered on the hot star and normalized to the binary separation, and θ the angle between a line joining a point to the central star and that joining the two stars. Then f(u, θ) was set equal to X at the boundary, where

$$X = 4\pi\mu^2 m_H^2/\alpha\, a\, L_{ph}\, (\dot{M}/V)^{-2} \qquad (12.3)$$

Here $\dot{M}$ is the cool component mass loss rate, V is the wind velocity assumed constant, a is the distance between the two stars, L_{ph} is the flux of hydrogen ionizing photons per second emitted by the hot component, α is the recombination coefficient, m_H is the mass of a hydrogen atom, and μ the molecular weight. Finally, the expressions given by equations (12.4) were used for f(u, θ).

The relative orbital motion of the stars is neglected, and velocities are supposed low enough that local ionization is in equilibrium. The results of calculations of the form of the ionized region and the resulting radio spectrum are shown in Figure 12-6 from Seaquist et al. (1984).

This type of model has been extended by Nussbaumer and Schmutz (1983), Nussbaumer et al. (1986), and by Nussbaumer and Vogel (1987). The most detailed calculations are in the last of these papers. The wind is supposed to be accelerated with a velocity law of the form:

$$V_r = (1-R/r)^{\beta} V_\infty$$

Where r is the distance from the star's cen-

$$f(u,\theta)=\begin{cases} \dfrac{1}{3(1-u)^3}-\dfrac{u}{(1-u)^2}-\dfrac{1}{3}; & \theta=0 \\ \dfrac{(2\cos^2\theta-1)u-\cos\theta}{2\sin^2\theta(u-\cos\theta)^2}+\dfrac{1}{2\sin^3\theta}\left[\tan^{-1}\left(\dfrac{u-\cos\theta}{\sin\theta}\right)+\tan^{-1}(\cot\theta)\right]+\dfrac{\cos\theta}{2\sin^2\theta}; & \theta\neq 0,\pi \\ \dfrac{1}{3}-\dfrac{u}{(1+u)^2}-\dfrac{1}{3(1+u)^3}; & \theta=\pi. \end{cases} \qquad (12.4)$$

ter and R, the radius for the origin of the wind, while the constant β was assumed equal to 1. Emission line profiles were calculated assuming the lines optically thin. Nussbaumer and Vogel considered the non-validity of this assumption to be responsible for the calculated HeII 1640 A flux of V1329 Cyg, being too strong at minimum brightness.

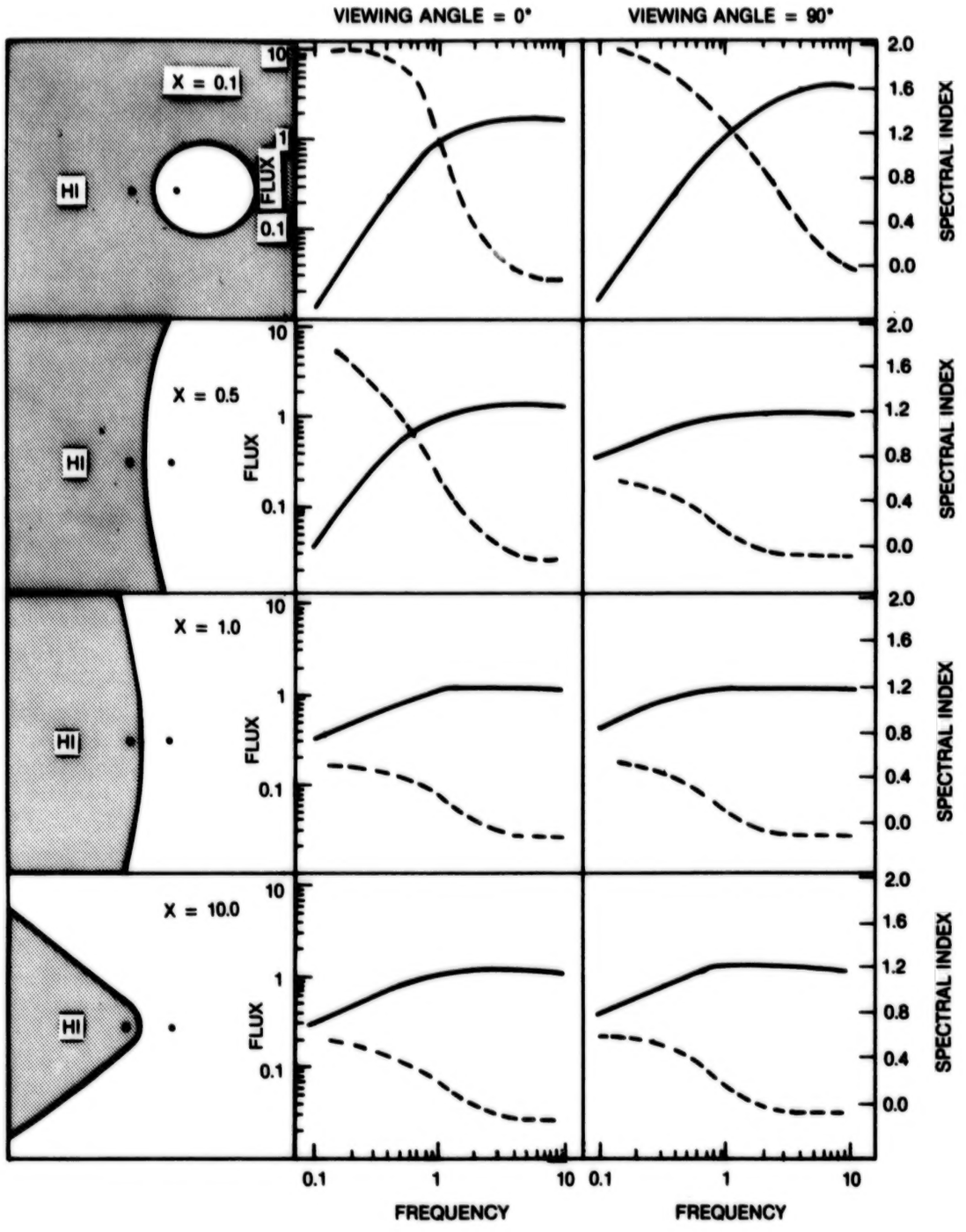


Figure 12-6. Left: the shape of the ionization front for various values of the parameter X (eq. 12.3). The position of the red giant (left) and hot star (right) is also shown. Centre and right: the radio spectra for two viewing angles, along the axis joining the two stars (α=0°), and at right angles (α=90°). Solid lines are flux densities, while dashed lines are the spectral indices.

Nussbaumer and Vogel (1987) also propose an explanation for what happens when a symbiotic star becomes active. According to them, the mass-loss rate from the cool star then increases, causing a change in the geometry of the ionized regions and, hence, a variation of emission line and continuum radiation due to recombinations. Clearly, such a mechanism cannot work in a situation where the initially present hot continuum cools or disappears.

The compact conponent's wind needs also to be taken into consideration. This could either be from the stellar companion or from an accretion disk if one is present. The velocity can be expected to be much higher than that of the wind of the cool giant and could produce wide emission components and wide P Cygni absorption components with a large blue shift, as indeed is seen for cataclysmic variables. There is also a possibility of collimation of a wind from a disk, and so a bipolar flow can be formed. For instance, Kenyon (1987) has proposed that such a wind could be driven by Alfven waves and have a much larger velocity perpendicular to the disk than in other directions.

If two winds are present, collisions can be expected to occur between them. A number of papers have been written based on such models (Kwok et al, 1984; Wallerstein et al., 1984; Willson et al., 1984; Kwok and Leahy, 1984; Girard and Willson, 1987; and Kwok, 1988). The model is applied to symbiotic novae, for which the compact component is supposed to produce a high-velocity wind during the outburst, while the physical model has been derived in most detail by Girard and Willson 1987).

The situation is shown in Figure 12-7. Material accumulates on the boundary where the winds meet, and the nebular shell produced will be deformed as can be seen in the figure. Different regions of this shell will have different ionizations and so emit in different emission lines, which will not, therefore, necessarily have the same profile. The situation in the immediate vicinity of the binary is shown in the

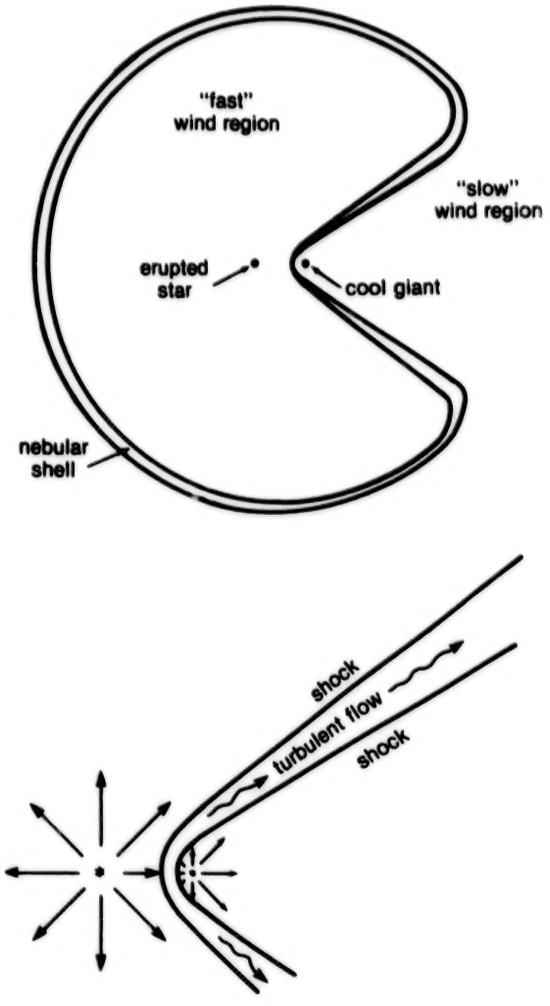


Figure 12-7. Colliding wind geometry, according to the model of Girard and Willson (1987).

lower part of the figure. A steady state configuration is reached there. This steady state was studied by Girard and Willson (1987), who first ignored the orbital motion of the binary and assumed the wind interaction region thin. Equations were derived based on mass and momentum conservation. The authors found that the shape of the shell only depended on the product $m.w$, where m is the ratio of the mass loss rates and w the ratio of the wind velocities. The steady state solutions indicate that the wind interaction occurred on the surfaces of truncated cones. The forms of these for different values of $m.w$ are shown in Figure 12-8.

Girard and Willson then calculated a dynamical shell model including orbital motion,

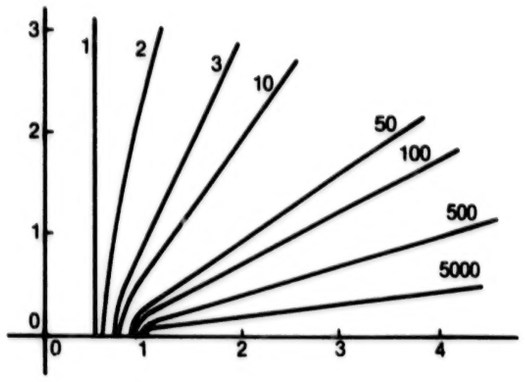


Figure 12-8. Steady state colliding wind solutions from Girard and Willson (1987). The star with the high velocity wind is at the origin of the coordinate system, while its companion is one unit away on the abscissae. The curves represent the sections of the interaction surfaces which have the form of truncated cones. Each curve is labelled with a value of m.w.

and assuming a sudden turn on of the high-velocity wind. The orbits were circular, and the stars of equal mass. The results of calculations for a stellar separation of 20 a.u., an orbital period of 60 years, wind velocities of 500 and 20 km s^{-1} and a high-velocity to low-velocity mass-loss rate ratio m of 2 are shown in Figure 12-9.

Certain forms might even mimic bipolar flows to some extent. The authors also speculated on the possibility of higher velocities of material in the hot shocked region near the apex of a cone than in other parts of this cone.

Kwok and Leahy (1984) calculated properties of X-ray emission from colliding winds. The emission is deduced to be from thermal bremstrahlung of plasma at 10^7K characteristic of colliding winds. Girard and Willson (1987) also discussed X-ray emission; they were unable, however, to make a detailed prediction, as it was not clear what proportion of the available energy flux was radiated. In general, colliding wind models seem to need more physics.

IV.D. ENHANCED SOLAR-TYPE ACTIVITY OF THE COOL STELLAR COMPONENT

Another possibility is that the symbiotic phenomenon is due to increased solar-type activity of the cool stellar component (Altamore et al., 1981; Friedjung et al., 1983; Friedjung, 1988). This could be associated with a higher rotational velocity than for normal cool giants because of tidal locking of the rotational and orbital periods. A region similar to the solar transition region might then produce the high-ionization emission lines observed, while small variations in the wind from the cool giant could cause large changes in the accretion rate to the compact component, and, hence, in the nature of any accretion disk. The model was proposed because early IUE observations of Z And suggested that the hot continuum was not hot enough to produce the highest ionization lines in photoionized regions, while some lines, at least, were formed in a region where high-temperature radiation was diluted, a region that is far from that where the hot continuum was formed. In addition, a certain form of reasoning suggested that this region was thin. The fact that high-ionization resonance lines of CI Cyg, unlike other lines of this star were little or not eclipsed also seemed to support the model. However, it now appears that enough high-energy radiation is generally present for photoionization. Mikolajewska (1986) showed that the high-ionization emisssion lines of CI Cyg had radial velocity variations, probably in phase with those of the compact component, and first results on the widths of absorption lines of the cool component of CI Cyg (Bensammar et al., 1988), suggest that the rotation of CI Cyg may not be tidally locked to its orbital period. The model may also have other problems. However, even if effects of increased activity of the cool giant are less important than originally proposed, the possibility of their presence should not be forgotten in future interpretations.

IV.E. CONCLUSIONS ABOUT THE MODELS

It appears that, in principle, it should be possible to learn a lot if one assumes the presence of accretion in interactive binaries either from Roche lobe overflow or from a wind. Such processes need not be steady; not only can the

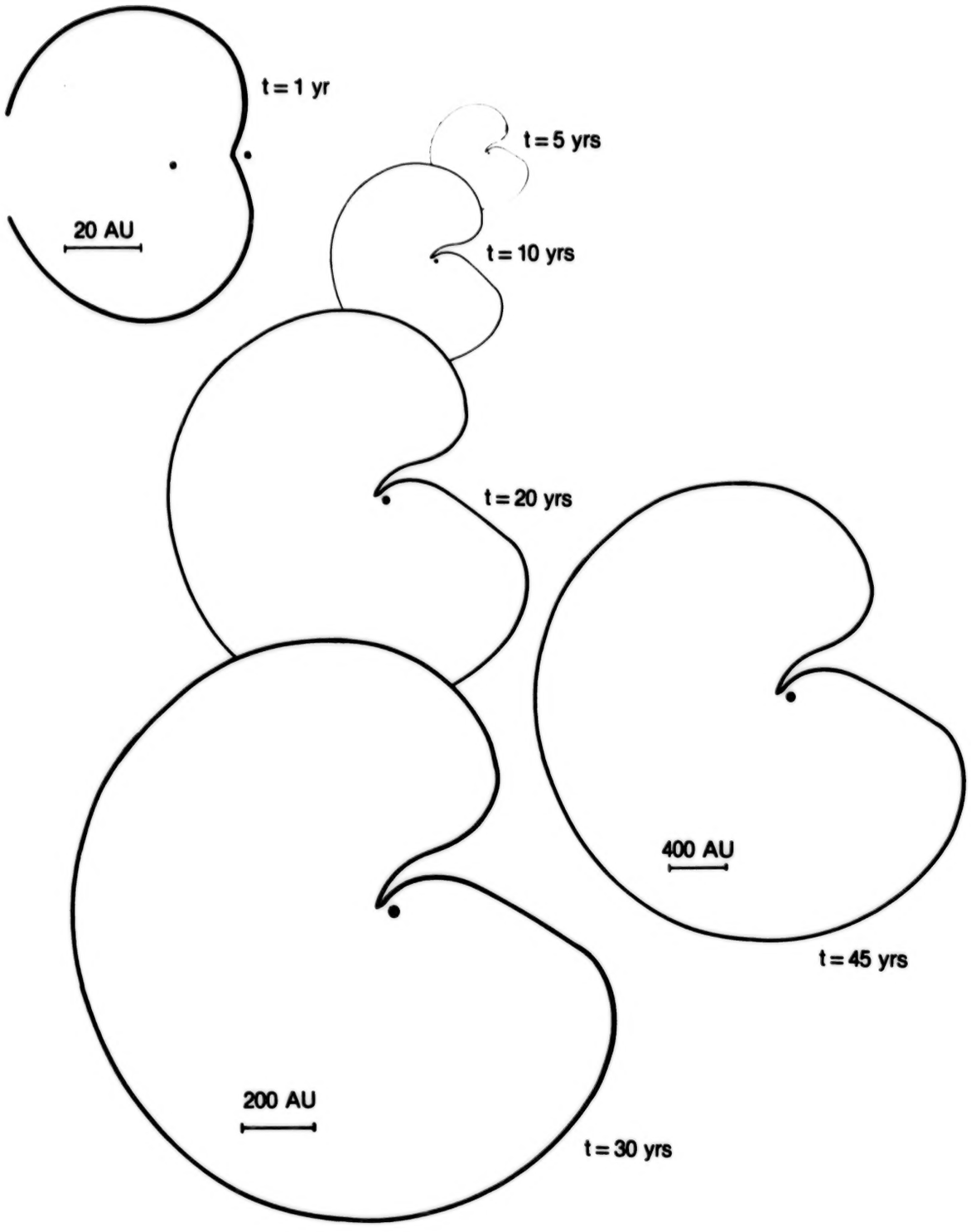


Figure 12-9. Evolution of colliding winds from Girard and Willson (1987).

rate of accretion change, but also thermonuclear flashes can occur.

All the binary models considered emphasize one physical process, and it is clear that several processes occur either simultaneously or at least in different symbiotic stars. A realistic theory needs to consider, at the same time, all the processes mentioned. In addition, the physics of several of them is still not very well understood and needs further study before more definite conclusions can be drawn.

N95
27078
UNCLAS

N95-27078

13

DISCUSSION ON SELECTED SYMBIOTIC STARS

R. Viotti and M. Hack

I. INTRODUCTION

Because of its large variety of aspects, the symbiotic phenomenon is not very suitable for a statistical treatment. It is also not clear whether symbiotic stars really represent a homogeneous group of astrophysical objects or a collection of objects of different natures but showing similar phenomena. However, as already discussed in the introduction to the symbiotic stars, in this monograph we are especially interested in the *symbiotic phenomenon*, i.e., in those physical processes occurring in the atmosphere of each individual object and in their time dependence. Such a research can be performed through the detailed analysis of individual objects. This study should be done for a time long enough to cover all the different phases of their activity, in all the spectral ranges. Since the typical time scale of the symbiotic phenomena is up to several years and decades, this represents a problem since, for instance, making astronomy outside the visual region is a quite new field of research. It was a fortunate case that a few symbiotic stars (Z And, AG Dra, CH Cyg, AX Per, and PU Vul) had undergone remarkable light variations (or "outbursts") in recent years, which could have been followed in the space ultraviolet with IUE, and simultaneously in the optical and IR with ground-based telescopes. But, in general, the time coverage of most of the symbiotic objects is too short to have a complete picture of their behavior. In this regard, one should recall Mayall's remark about the light curve of Z And: "Z Andromedae is another variable that shows it will requires several *hundred* years of observations before a good analysis can be made of its variations" (Mayall, 1969).

This pessimistic remark should be considered as a note of caution for those involved in the interpretation of the observations. In the following, we shall discuss a number of individual symbiotic stars for which the amount of observational data is large enough to draw a rather complete picture of their general behavior and to make consistent models. We shall especially illustrate the necessary steps toward an empirical model and take the discussion of the individual objects as a useful occasion to describe different techniques of diagnosis.

II. Z ANDROMEDAE AND THE DIAGNOSTICS OF THE SYMBIOTIC STARS

II.A. INTRODUCTION

Z And has been considered as the prototype of the symbiotic stars, from its light history and the spectral variation during outburst. For a long time, its light curve has been the basis for theoretical studies of the symbiotic stars. The optical spectrum of the star has been studied extensively since the pioneer work of Plaskett (1928). Of particular interest is the work of Swings and Struve (1941; see also Swings, 1970) describing the spectral evolution during and after 1939 outburst, and of Boyarchuck (1968), who discussed the 1960 outburst and the following decline phase. Ultraviolet observations started after the launch of the International Ultraviolet Explorer (Altamore et al., 1981) and continued to the time of writing the present review. In particular, this allowed the study in the UV of the two minor outbursts that

occurred in 1984 and 1985. These observations, together with the extensive monitoring of the IR and of the emission line profiles, still make Z And one of the best-studied symbiotic stars, and an ideal target for investigation the symbiotic phenomenon.

The visual luminosity of Z And is variable between V = 8 to 11 on time scales from a few days to several months, without clear evidence of any periodicity. The full light curve is reproduced in Figure 11-2 in Chapter 11. Figure 13-1 is a condensed plot of 100-day means of photographic and visual observations from 1887 to 1969 (Mayall, 1969).

The light curve is characterized by (1) four main phases of higher luminosity starting in 1895, 1914, 1939, and 1959, and by (2) periods of low luminosity lasting roughly one decade in between. In the following, we shall discuss the behavior of Z And during quiescence and activity.

II.B. THE BEHAVIOR OF Z AND DURING QUIESCENCE

The most recent quiescent phase (1972 to about 1984) of Z And was also the longest, and this fact has allowed a detailed study of the behavior of a symbiotic star during minimum light. The optical-ultraviolet spectrum of Z And at minimum is rich in strong and narrow emission lines of several different atomic species and with a large range of ionization energy. A compendium of the ions whose transitions have been identified in the optical spectrum of Z And was given in Table 11-2. Both permitted and forbidden transitions are present, as well as lines typical of stellar chromospheres, Be, Of, and WR stars, planetary nebulae, coronal regions, etc. These features are also seen in the ultraviolet. Altamore et al. (1981) identified low-excitation lines of OI, MgII, and FeII, and high-ionization lines of HeII, OV, and MgV]. But the main result is that the intensity of the emission lines is largely variable on long time scale. Variation of Hα was reported by Altamore et al. (1979), while Altamore et al. (1982) found that in November 1982, the UV continuum and emission lines were about 40 percent stronger than in August 1980. They also noted that the IR spectrum did not show a significant change since 1981. From a more thorough analysis of the UV observations collected since 1978 with the IUE satellite, Fernandez-Castro et al. (1988) found that the UV continuum and the emission line fluxes vary quasi-periodically on a time scale of about 760 days. The amplitude is larger for the Balmer near-UV continuum and for most of the emission lines, and lower for the far-UV continuum and the CIII] line. The time variation of the SiIII]/CIII] ratio suggests a variable mean electron density of the emitting region from 0.6 to 2.2 x 10^{10} cm^{-3} in phase with the UV light curve. At maximum, the density and the emission measure are larger, while the effective emitting volume is smaller. Thus at maximum, the emission mostly comes from a compact

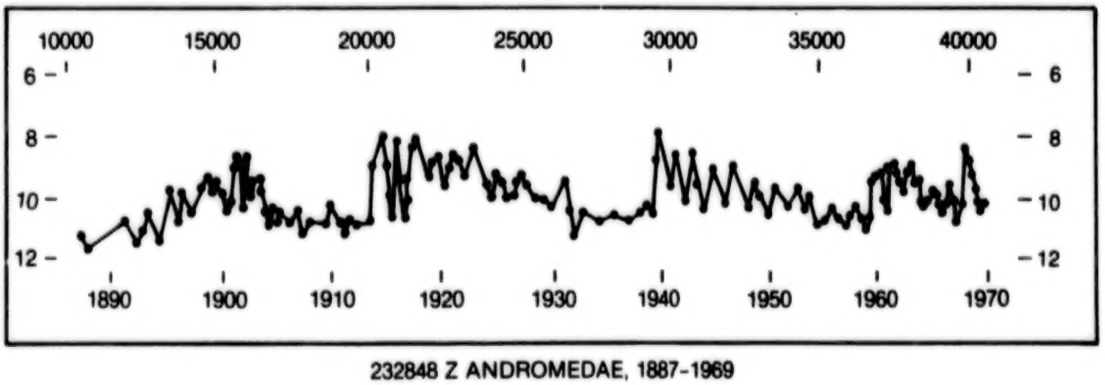


Figure 13-1. Plot of the 100-day average magnitudes of Z And during 1887 to 1969 (from Mayall, 1969).

region, and at minimum, the emitting volume is more diluted. These observations are consistent with a model of highly ionized diffuse region that is periodically occulted, leaving visible only the outer low-density regions.

Much about the nature of Z And can be learned from the simultaneous study in different wavelength regions. Figure 13-2 illustrates the variations of Z And from UV to IR during the last quiescent phase.

The large UV variability is clearly present in the U-band and in the Hα-variation and can be traced back to before the first ultraviolet observation. The variation is less evident in the visual. During minimum, V varied between 10.2 and 11.0 in an apparently irregular mode. This variation during minimum has been noted by several authors, (see Kenyon, 1986), and Kenyon and Webbink (1984), from the analysis of all the minima during quiescence, found that they are clearly periodic with a mean period of 756.85 days in agreement with the UV and Hα results. The radial velocity of the M-giant component was measured by Garcia and Kenyon (1988) over about 6 years. They found a smoothed sinusoidal curve with a period of 750 ± 8 days, and a semiamplitude of K = 8.1 ± 0.5 km s^{-1}. This fact provides further evidence of binarity, but the radial velocity and photometric curves do not have the relative phasing (a quarter of phase) expected from eclipse or reflection effects. This might suggest a more complex geometry of the system, as also suggested by the ultraviolet observations as discussed below. Finally, concerning the infrared, Taranova and Yudin (1981) and others reported small fluctuations, clearly not in phase with the UV variations. These can be attributed to the irregular behavior of the late-type component that is a common feature of the normal (normal = not a symbiotic or peculiar system) late-type giant and supergiant stars. The little variability of the cool component was also noted by Altamore et al. (1979, 1981) who, from their analysis of a collection of blue-infrared objective prism plates taken during October 1977 to June 1979, found that the near-IR continuum remained constant within ±0.1 mag. Larger variations seem to be present at longer wavelengths, but this needs to be confirmed by future observations.

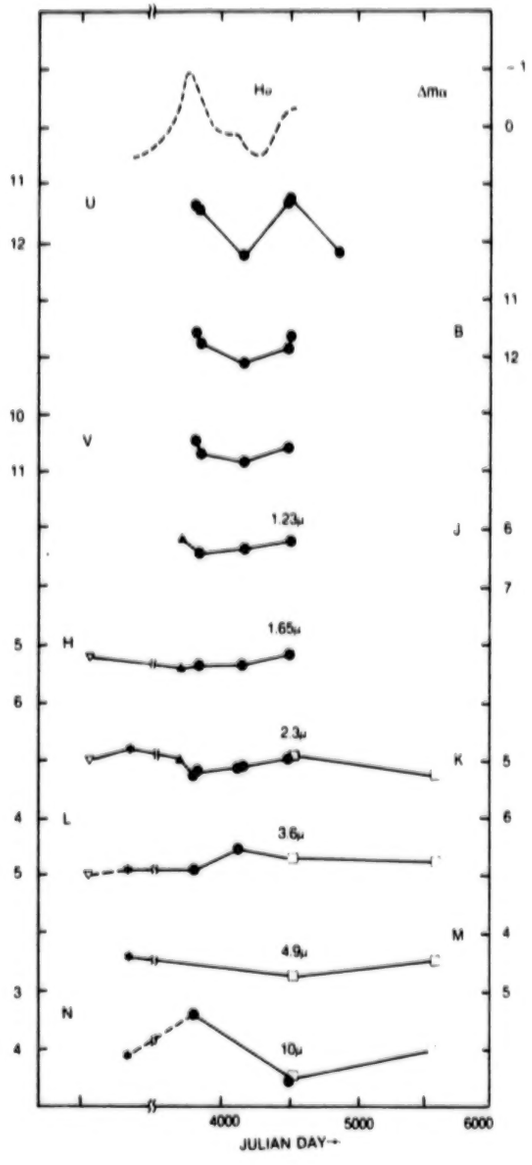
II.C. THE ACTIVE PHASES OF Z AND

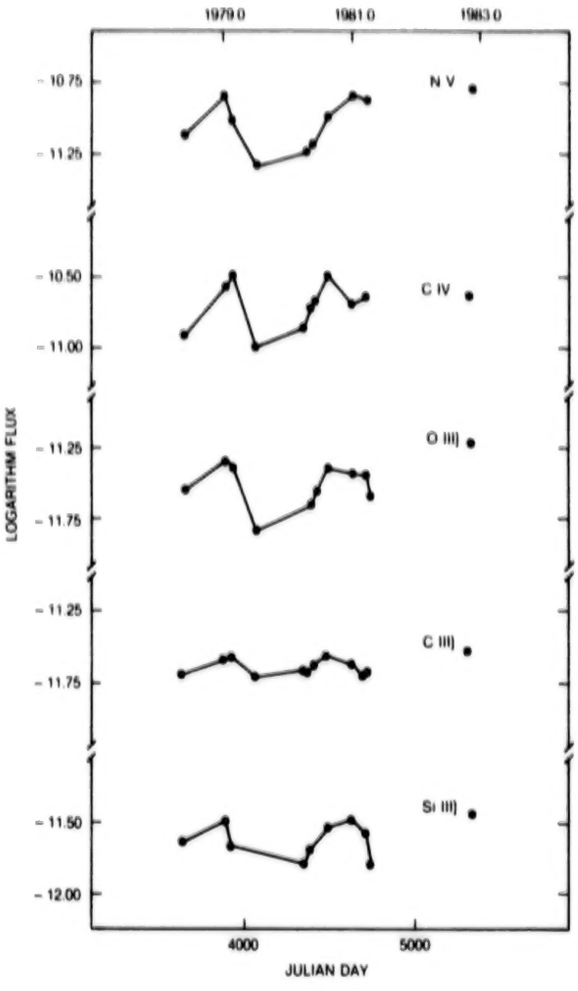
The active phase is characterized mostly by an increase of one to two magnitudes of the visual magnitude after a long-lasting quiescent phase. The brightening is rather slow, the rise time being about 100 days/mag, even compared with the slow novae. This "outburst" is generally followed by a sequence of minima and maxima resembling a damped oscillator. The time interval between two successive maxima (or minima) is not constant, but varies from 310 to 790 days (Mattei 1978) in an irregular way and is not in phase with the UV-variability during quiescence discussed above.

During the rise to outburst and the subsequent oscillations, the optical spectrum undergoes large changes, which have been extensively described in a number of papers. As the stellar luminosity increases, the high-ionization lines fade, and at maximum light, the spectrum displays a strong blue continuum with prominent hydrogen emission. These lines have absorption cores that dominate the emission at the higher members of the Balmer series. In some cases, P Cygni profiles are present in the H and HeI lines. At maximum, the absorption bands of the M spectrum are hardly visible. However, the weakening of the cool spectrum is only apparent since, as it has been found, for instance Boyarchuck (1968), the TiO bands are only veiled by the enhanced blue continuum, while the luminosity of the cool component has not changed within the errors. The high-ionization lines and the TiO absorption bands strengthen again as the blue continuum decreases during the light fading.

Recently, two minor outbursts of Z And were reported. After nearly 12 years of quiescence, the star brightened to V = 9.6 in March 1984 and again to V = 10.1 in September 1985 (Mattei, 1984, 1985). The 1984 outburst displayed a general rise of the line intensity. The largest increase was measured for the high-

ionization lines of HeII, CIV, and OIII, while NV remained unchanged. Of particular interest is the behavior of the continuum: longwards 1400 A the flux appeared larger than previously, while it was weaker in the far-UV, indicating a general decrease of the continuum temperature. This result is not unexpected, since, as discussed above, generally at outburst the excitation of the spectrum decreases. However, this behavior was not followed by the OI emission triplet at 1302-06 A, which markedly faded during outburst. This result could





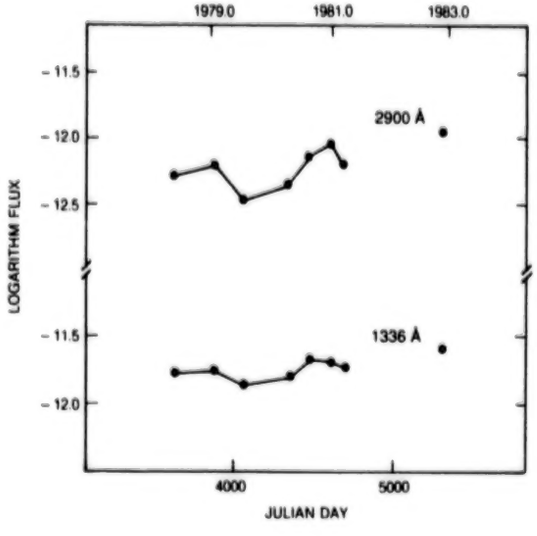


Figure 13-2. Multifrequency monitoring of Z And during quiescence. (a) Near-UV to IR photometry and Hα intensity (Altamore et al., 1979). Taranova and Yudin (1981). Lunel (see Altamore et al., 1981). Ultraviolet line and continuum fluxes during 1978-1982 (Fernandez-Castro et al., 1988).

probably be related to the fact that the 1984 event was not similar to the main outbursts observed in the past. In the months following the outbursts, after the luminosity decline, OI and NV strengthened in the UV (Cassatella et al., 1984). At high resolution, the blue wings of CIV and NV displayed an absorption line at −120 km s^{-1}, which suggests the presence of a low-velocity, warm wind like that observed in AG Dra (Viotti et al., 1983). The high-resolution UV monitoring of Z And after the outburst revealed large variation of the emission line profiles which have been noted since April 1984. Figure 13-3 shows the evolution of the CIV doublet since the 1984 outburst (Cassatella et al., 1988). Evident in the figure is the different shape of the lines at different epochs. P Cygni absorptions are clearly present in three spectra. The intensity ratio of 1548/1551 is smaller than the optically thin value of two, and in one case, even smaller than one (February 1986). This result will be discussed below in Section II.D. Strong broad wings are evident in the June 1985 spectrum, while in the other phases, they are much weaker.

II.D. DIAGNOSTICS

Once a consistent amount of homogeneous data is available for a given target, including also its time behavior (and taking into account all the possible time scales), it is then possible to make the next step, that is, to try to build up an empirical model. In general, the IUE archives provide for most of the symbiotic objects (and for many other categories of astrophysical objects as well) the best homogeneous

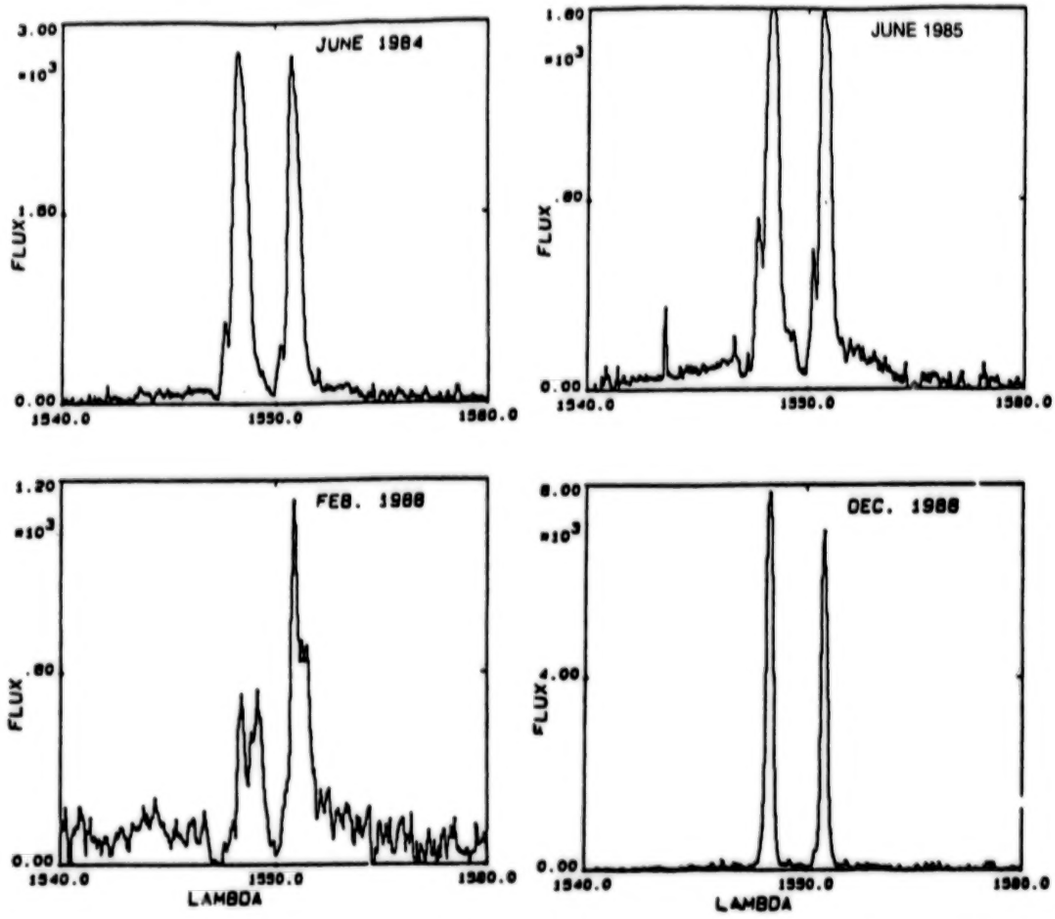


Figure 13-3. Evolution of the CIV doublet in Z And after the March 1984 outburst (Cassatella et al., 1988). Note the P Cygni absorptions which are clearly present in three spectra, and the strong emission wings in June 1985. In February 1986 the 1548/1551 line flux ratio is smaller than the optically thick limiting value of one.

set of calibrated, good quality data. In the meantime, several theoretical computations of the atomic parameters of important UV transitions have been recently performed, so that the line intensities can be used to derive the physical parameters of the emitting region. In the following, we shall discuss the case of Z And also as an illustration of the impact of the new UV observations on our knowledge of the nature of peculiar objects such as the symbiotic stars.

As discussed above, the optical and UV spectrum of Z And includes prominent emission lines of both permitted and intercombination or forbidden transition of different ions. In principle, this should be used to determine the electron density of the emitting region(s). In addition, the presence of different ionization stages of the same element and of ions of different elements can be used as diagnostics of the temperature and chemical composition. Table 13-1 summarizes the main line ratios, that can be used to derive the physical parameters of the symbiotic system.

Altamore et al. (1981) analyzed the NIII] multiplet near 1750 A and determined an electron density (for the N++ region) of (1.7 ± 0.9) x 10^{10} cm^{-3} (Figure 13-4). The line ratio of this multiplet is sensitive to changes in the electron density in the range from 10^{+9} to 10^{11} cm^{-3}, but is rather independent of the electron temperature (Nussbaumer and Storey, 1979). For instance, the NIII] line intensities in the symbiotic novae RR Tel and V1016 Cyg suggest a smaller density of 1.5 x 10^{+9} (Altamore et al., 1981) and of about 10^{+9} cm^{-3} (Nussbaumer and Schild, 1981), for RR Tel and V1016 Cyg, respectively. As shown in Table 13.1, the electron density can also be determined from the relative intensity of the OIV] and CII] multiplets. From the observed OIV] 1404.81/1401.16 ratio of 0.38, Altamore et al. derived log N_e = 10.1, in good agreement with the NIII] estimate. The CII] multiplet is too weak in Z And for density diagnostics. Only the high-density component of the CIII] doublet is visible in the UV spectrum of Z And, which provides a lower limit to Ne of about 10^{+6} cm^{-3}

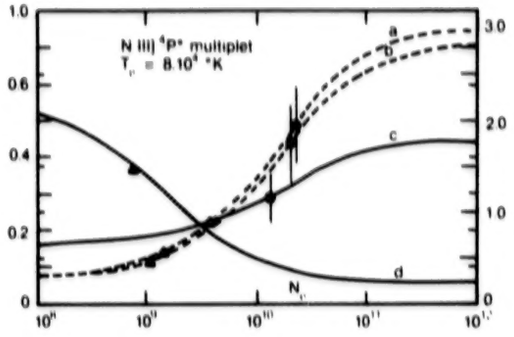


Figure 13-4. The NIII multiplet ratio in Z And and RR Tel (Altamore et al., 1981). The different curves give as a function of the electron density for Te=8x10^4 K the theoretical line ratios: (a) 1754.0/1752.2; (b) 1748.7/1749.7 (dashed curves, right-hand scale); (c) 1748.7/1749.7; (d) 1746.8/1748.7 (solid curves, left-hand scale). The observed ratios for Z And (dots) and RR Tel (triangles) are indicated.

(Nussbaumer and Schild, 1979). This is again in agreement with the above results, and might also suggest that all the intercombination lines are formed in the same region. This may not be true for all the symbiotic stars. In fact, Nussbaumer and Schild (1981), in their analysis of the UV spectrum of the symbiotic nova V1016 Cyg, found from the CIII] and NIV] double ratios an electron density of 2 x 10^6 and 4 x 10^6 cm^{-3}, respectively. But the intensity of the NIII] multiplet would require a much higher N_e of about 10^{+9} cm^{-3}, which could be related either to a large density gradient in the emitting region or to a particular excitation mechanism.

Altamore et al.(1981) also considered the CIII]/NIII] intensity ratio, and found an electron density of 1.9 x 10^{10} and 1.2 x 10^{+9} cm^{-3} for Z And and RR Tel, respectively, consistent with the results obtained from the NIII] multiplet. More recently, Fernandez-Castro et al. (1988) have used the SiIII]/CIII] flux ratio in Z And to give an estimate of the electron density during different phases of its UV variability. They found N_e to be variable in the range from 0.56 to 2.2 x 10^{10} cm^{-3}, again in agreement with Altamore et al. results. However, when the flux ratios of the lines of different ions are used, the derived density estimates largely depend on the adopted electron temperature, as well as on the ionization equilibrium of each ion and on the C/N abundance ratio. Singly ionized carbon

TABLE 13-1. ULTRAVIOLET INDICATORS OF THE PHYSICAL PARAMETERS IN SYMBIOTIC STARS.

ions	lines	parameter	range	ref.
CII]	2325.4/2328.1	N_e	10^7 - 10^9	(1)
....	2325.4/2326.9		.....	
....	2324.7/2326.9		.....	
NIII]	1754.0/1752.0	N_e	10^9 - 10^{11}	(2)
....	1748.7/1752.0		.....	
....	1748.7/1749.0		.....	
....	1748.7/1746.8		10^8 - 10^{10}	
OIV]	1407.4/1401.2	N_e	10^3-10^5 ; $10^{9.5}$-10^{11}	(3)
	1401.2/1404.8		10^3-10^5 ; 10^9-$10^{10.5}$	
CIII]	1908.7/1906.7	N_e	10^3 - 10^6	(4)
NIV]	1486.4/1483.3	N_e	10^4 - 10^{10}	(5)
SiIII]	1892.0/1882.7	N_e	3.10^3 - 3.10^5	(6)
[NeIV]	1601/2423	N_e	10^4 - 10^8	(7)
	.....	T_e	(for $N_e<10^4$ or $N_e>10^8$)	
[FeVII]	2015/3759	N_e	10^7 - 10^{10}	(7)
	.....	T_e	(for $N_e<10^7$ or $>10^{10}$)	
NIII]/CIII]	1749.7/1908.7	N_e	10^9 - 10^{11}	(1)
SiIII]/CIII]	1892.0/1908.7	N_e	10^9 = 10^{11}	(1)
CII/CIII]	1336/1909	T_e		(9) (10)
CIII]/CIV		T_e	10^4 - $3x10^4$	(9) (10)
	1718/1240			
NIV]/NV		T_e		(9) (10)
OIII]/[OIII]	1661/6300	T_e		(5)
SiIII/SiIII]	1299/1892	T_e	1.2 - 6.10^4 K	(6)
			(for N_e = 10^6-10^{10})	
HeII	1640.4/Fc(1336)	T*		(11)

Notes to the table. (1) Stencel et al. (1981). (2) Altamore et al. (1981). (3) Nussbaumer and Storey (1982). (4) Nussbaumer and Schild (1979). (5) Nussbaumer and Schild (1981). (6) Nussbaumer (1986). (7) Nussbaumer (1982). (8) Nussbaumer and Stencel (1987). (9) Stikland et al. (1981). (10) Nussbaumer and Storey (1984). (11) Fernandez-Castro et al. (1988).

and nitrogen have ionization energies of 24 and 30 eV respectively, which are different enough to give significant differences in the ionization fractions C++/C and N++/N. This also depends on whether the ionization is by electron collisions or by photoionization. Altamore et al. (1981) have computed the CIII]/NIII] ratio assuming ionization by electron impact like that in the solar transition region, and for a cosmic C/N abundance ratio. This last assumption can be justified from the fact that the study of several symbiotics—including Z And—by Boyarchuk (1970) in the optical, and by Nussbaumer et al. (1988) in the ultraviolet generally suggest a close to cosmic abundance for the emitting regions in symbiotics. Altamore et al. also found that the CIII]/NIII] ratio could be largely affected by radiation field (e.g., the diluted hot stellar radiation). The flux ratio observed in Z And would imply an upper limit of 1.5×10^{-16} erg cm^{-3} Hz^{-1} for this radiation in the N++ emitting region, or a dilution factor smaller than 7.5×10^{-5}.

In a planetary nebula-like model of symbiotic stars, such as the one proposed by Nussbaumer and Schild (1981) for V1016 Cyg, the electron temperature should be close to 10^4 K. Photoionization models for Z And were discussed by Fernandez-Castro et al. (1988) and Nussbaumer and Vogel (1988). Alternatively, the high-ionization lines could be produced in a solar-type transition region with much larger T_e, as for instance suggested by Altamore et al. (1981) for Z And. This latter hypothesis is based on several arguments: the small width of the emission lines implies formation in a low-velocity dense region (which excludes line formation in a high-velocity hot star wind, and in a rotating disk). Comparison of the derived CIII] emitting volume of $1 \times 10^{+37}$ cm^3 with the SiIV maximum line thickness indicates that the emission should come from a thin shell, rather than from an extended sphere. In addition, as discussed above, the stellar radiation in the NIII] emitting region should be very weak, hence the region far from the hot star.

Another observable which could put constraints on the possible models is the radial velocity difference between the high-ionization resonance lines and the intercombination lines. From a study of several symbiotics Friedjung et al. (1983) found a systematic redshift of the former lines with respect to the latter, of the order of +10 to +20 km s^{-1}. They interpreted this as the result of radiative transfer in a warm, low-velocity expanding medium, which should be identified with either the cool star wind, or with its base. This model is also supported by the larger width of the higher ionization lines observed in some symbiotics, as discussed in Chapter 11 Sections IV.D. and VIII.D. Friedjung et al. found that in Z And, the radial velocity difference is probably variable but always positive well beyond the measurement errors. Fernandez-Castro et al. (1988) confirmed this result and found a range of variability between +15 to +30 km s^{-1}, but without a clear correlation with the UV line and continuum flux variations.

To decide about possible models, better would be to have a direct estimate of the electron temperature. In most cases, this is difficult, since the temperature indicators generally are weak lines, and their flux ratio may also depend on other parameters. Stikland et al. (1981), Nussbaumer (1982), and Nussbaumer and Storey (1984) discussed, among others, methods of electron temperature determination from emission line ratios. Some useful T_e indicators are listed in Table 13.1. Fernandez-Castro et al. (1988) derived the electron temperature for Z And from the NIV 1718/NV 1240, CII 1336/CIII] 1909, and CIII 1176/CIII] 1909 flux ratios. They found $T_e \simeq 15{,}000$ K, lower than the value assumed by Altamore et al., (1981) which seems to favor a photoionization model. However, the above flux ratios involved emission lines that are rather faint in the UV spectrum of Z And. Thus, the T_e estimates of Fernandez-Castro et al. are rather uncertain, and could well be lower limits.

Once the electron density and temperature are known, the line fluxes can be used to derive the total amount of the emitting ions, and the size of the emitting regions. Altamore et al. (1981), assuming the C++ and N++ regions

homogeneous and transparent, obtained an emitting volume of 1.0×10^{36} and 8.2×10^{35} cm^3 for C++ an N++ respectively. These values obviously depend on their assumption of a solar-type emitting region with $T_e \simeq$ 80,000 K. It is easy to see that such a warm region cannot be responsible for the ultraviolet continuum observed in Z And. This implies the presence of an optically thick region (or disk) or a hot star with a radius of about 2×10^{10} cm. The temperature of the hot source can be obtained using the Zanstra method. Assuming that the emitting region is optically thick to the hot source continuum Fc shortward of 912 Å (ionization from the ground level of H) and of 228 A (He+ ionization), and that the hot component of Z And radiates as a blackbody, we have for a case B He++ recombination (Fernandez-Castro et al., 1988):

$$\frac{I(HeII\ 1640)}{Fc(\lambda')} = 3.303 x 10^{-28}\ T^3 \times f(\lambda^0, T)\lambda'^5\left(e^{hc/\lambda' T} - 1\right) \qquad (13.1)$$

where it is assumed that the HeII 1640 A line is optically thin, and $f(\lambda^o,T)$ is the relative number of photons provided by a blackbody at a temperature T between $\lambda = 0$ to $\lambda^o = 228$ A. Using the continuum flux at $\lambda' = 1336$ A and the HeII 1640 A intensity, dereddened for E(B-V) = 0.35, Fernandez-Castro et al. (1988) derived a HeII temperature of about 10^5 K. This temperature remained nearly constant in spite of the large UV variability. In fact, the NV/CIV flux ratio, which can be considered as an ionization temperature indicator, did not significantly change during the period studied by Fernandez-Castro et al.

The hot continuum is responsible for the short wavelength UV continuum. But there is an excess of the continuum flux in the range from 1500 A to the visual that can be attributed to bound-free and free-free hydrogen emission, as indicated by the marked Balmer discontinuity at 3650 A (Altamore et al., 1981; Blair et al., 1983). Continuum recombination from He++ may also contribute to the UV. Fitting of the observed Balmer continuum with hydrogen and helium continua provides an estimate of the emission measure Ne^2V. Assuming T_e = 15,000 K, Fernandez-Castro et al. (1988) found Ne^2V equal to about 2-6 x 10^{+59} cm^{-3}, a value much larger than the above derived value of 4 x 10^{+57} cm^{-3} for C++, N++ region, assuming cosmic abundance (Altamore et al., 1981). Perhaps the intercombination lines and the Balmer continuum are formed in different regions.

Variability may give important information, especially about the spatial structure of the system, if the variations are associated with an orbital motion of a binary system. In fact, observations at different epochs allow one to observe the system with different lines of sight. The best period is when the symbiotic system is in quiescence, so that the periodic phenomena are not masked by the symbiotic activity, whose time scale is generally comparable with the orbital period. Fernandez-Castro et al. (1988) investigated the periodic UV variability during quiescence and found that the UV continuum and emission line fluxes are variable on a time scale of about 760 days, with maxima and minima in phase with the UBV and Hα variability (see Figure 13-2). From the time variability of the SiIII]/CIII] flux ratio, Fernandez-Castro et al. suggested that the mean electron density in the emitting region varied from 0.6 to 2.2 x 10^{10} cm^{-3}, being higher at maximum. This can be explained with a model of line formation in an asymmetric nebula near the cool giant, which is photoionized by the UV photons of the hot star. This nebula is occulted at minimum, and emission is seen only from the outer, less dense parts. This fact and the small size and high density of the emitting region suggest that it can be identified with the inner parts of the cool giant wind ionized by the hot star radiation. Therefore, the UV emission lines are mostly formed in the cool giant wind, as also is suggested by the systematic radial velocity difference between the high ionization resonance lines and the intercombination lines discussed above.

II.E. POSSIBLE MODELS FOR Z ANDROMEDAE

Let us summarize our present knowledge about the Z And system. The UV to IR energy distribution is characterized by two maxima, one in the near-IR, and another in the unseen EUV (Fernandez-Castro et al., 1988). During the active phases, the second maximum is shifted to longer wavelengths in the UV or in the optical. In the latter case, the apparent "outburst" in the visual is larger. According to Fernandez-Castro et al., the integrated fluxes of the two spectral "bumps" are comparable, around 450 and 880 $L_\odot$ for the hot and cool components, respectively. The "nebular" f-f and b-f continuum contributes another 44-141 $L_\odot$ to the total power from Z And. Therefore, the radiative power emitted in the UV is not a small amount of the visual-IR power. As discussed in Chapter 12, this point rules out the model of active cool star, in which the emission line spectrum and blue continuum are the result of a large surface activity of the cool giant. Thus, the double-bump energy distribution is strongly suggestive of *binarity*. This hypothesis is also supported by the optical and UV variability during quiescence, and by the long-term radial velocity variations of the cool component, even if the phasing is not the expected one. An important point for the following discussion is whether the cool component is filling its Roche lobe. Taking into account the proposed orbital period of 750 d, the luminosity class of the cool component, which implies that its mass should be of a few solar masses (Querci, 1986), and assuming for the hot component the mass of a white dwarf, it can be easily found that the cool giant is well inside its critical Roche surface. A different conclusion will be drawn in the case that the Z And system contains a cool bright giant, for instance, as suggested by the IR spectroscopic observations of Kenyon and Gallagher (1983). This again stresses the importance of future detailed studies of the cool spectral component, in order to derive its surface gravity.

The nature of the hot component is so far unveiled, but a model of a hot subdwarf, or of a rejuvenated white dwarf is favored. In any case, its structure could have been largely affected by the mass-transfer processes during the earlier stages of evolution of the binary system. In particular, we do not know if it presently has the same mass and radius of a white dwarf, and this makes our modelling rather uncertain. In Z And, the dwarf component seems to accrete mass from the cool star wind, not through Roche lobe overflow. The accreted matter could form a disk around the dwarf star. But so far, there is no evidence of an accretion disk in Z And, whose presence could, for instance, be indicated by broad high-ionization emission lines. This problem will probably be solved with future high-quality observations of the emission line profiles in the visual and UV. Mass accretion M_a onto the degenerate star results in an increased luminosity L_{acc} of the star. The actual values of M_a and L_{acc} critically depend on many poorly known parameters, the mass-loss rate and wind velocity of the cool giant, the orbital parameters, the mass and radius of the dwarf star. Thus, our picture of Z And (and of all the other symbiotic stars, as well) is necessarily limited because of the *a priori* assumptions we have to make. The matter flowing from the red giant is ionized by the hot star radiation, and emits in the radio. The radio flux from Z And observed by Seaquist et al. (1984) has a spectral index $\alpha = +0.62$, close to the theoretical value for a photoionized wind (cf. Seaquist and Gregory, 1973). Using the formulations of Wright and Barlow (1975) and taking for the wind velocity the value of 40 km s^{-1}, and the observed radio flux at 4.885 Ghz, Fernandez-Castro et al. (1988) derived for the cool giant a mass-loss rate of about 2×10^{-7} $M_\odot$ yr^{-1}, in good agreement with the typical values of M giants (e.g., Goldberg, 1986). Using their parameters for the Z And system, Fernandez-Castro et al. also derived an accretion rate of 4.5×10^{-9} $M_\odot$ yr^{-1}, and an accretion luminosity of 1.2 $L_\odot$. This luminosity is about two orders of magnitude lower than the recombination continuum, and, therefore, it cannot be accounted for by accretion processes. Conversely, accretion seems not to play an important role in the energy budget of Z And. It can anyhow be responsible for some of the symbi-

otic phenomena, and, in particular for the recurrent "outbursts". In fact, the above derived accretion rate is well below the minimum accretion rate for steady burning discussed in Section 12.IV.A, but implies occurrence of recurrent thermonuclear events.

A schematic model for Z And during quiescence is shown in Figure 13-5. The UV photons from the hot component ionize the cool-star wind until a limiting surface which is separating the HI and HII regions. According to Taylor and Seaquist (1984), the shape of this surface is determined by a parameter X defined as:

$$X = (4\,\pi\,a\,L_{ph}/\alpha) \cdot \mu^2 m_H^2 (V/\dot{M})^2, \qquad (13.2)$$

where a is the binary separation, L_{ph}, the number of hydrogen ionizing photons per second from the hot component, α, the recombination coefficient to all but the ground state of hydrogen, μ, the mean molecular weight, m_H, the hydrogen mass, and V and $\dot{M}$, the red giant's wind velocity and mass-loss rate, respectively. For Z And, Fernandez-Castro et al. (1988) obtained X = 14, implying that the ionization front is close to the red giant surface with a shape as shown in the figure. It should be considered that the particle density in the wind rapidly falls down outwards. Since the continuum and line emission in the HII region is proportional to N_e^2, the regions near the ionization front are the main contributors to the nebular spectrum. Therefore, in deriving the physical parameters of the emitting region, it is crucial to take into account the geometry, which could be far from homogeneity and from spherical symmetry. In addition, because of the different dependence on the electron density, the mean regions of formation of different emission lines and continua could be significantly different. The corresponding electron densities and emission measures, therefore, can be largely different, even if the lines are formed in the same medium. This can explain the different values found in Z And, as discussed above, and in many other symbiotic stars as well. Formation of emission lines in a low-velocity medium, such as the red giant's wind, is also in agreement with the line narrowness. According to Fernandez-Castro et al., the observed time variability of the line fluxes should be the result of the orbital motion: the effective emitting volume is different, if the line of sight is different. As discussed by Nussbaumer et al. (1986) for V1329 Cyg, one should thus expect a "modulation" of the line profile with the orbital phase. Observations have not yet shown this effect, at least during quies-

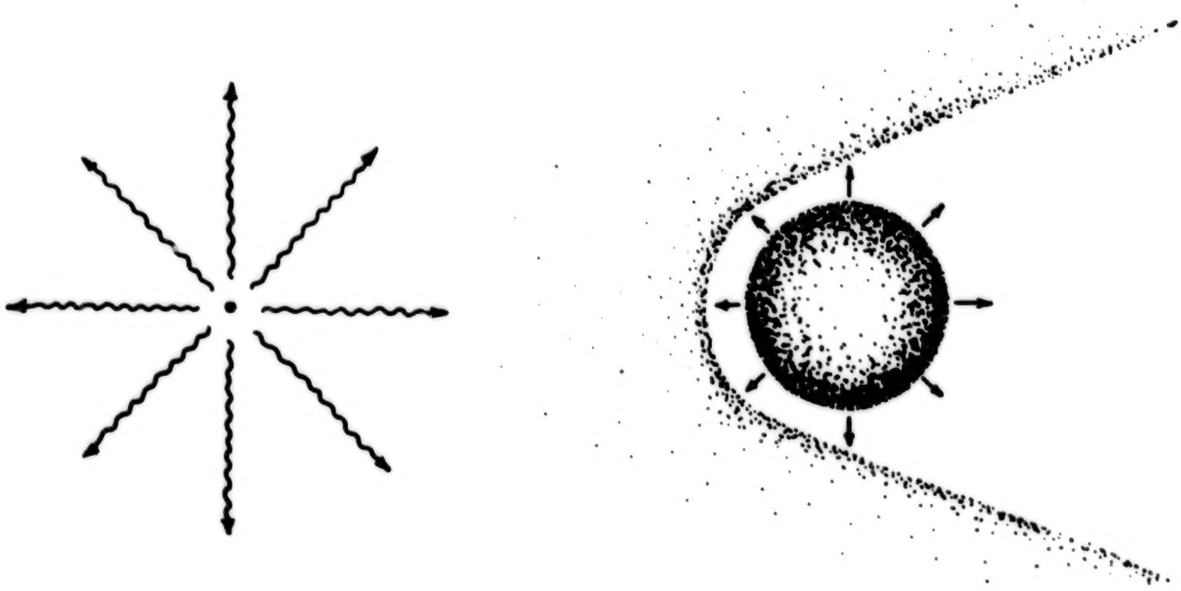


Figure 13-5. Schematic binary model for Z And, according to Fernandez-Castro et al. (1988).

cence, probably because of their fairly poor quality. [Profile changes as those reported by Cassatella et al. (1988) should be attributed to the stellar "activity", rather than to orbital motion.] Partial occultation from the red giant may partly account for the observed flux variability. The effect obviously depends on the (unknown) inclination. Alternatively, the orbit could be *eccentric*: in this case, one would expect a larger nebular emission and a higher electron density at the passage near the periastron, as observed. However, it is hard to fit all the observational data with this fairly simplified model. Nussbaumer and Vogel (1988) recently showed that the coexistence of two winds can substantially modify the ionization structure. The presence of two winds will also modify eclipse effects in different ionization stages.

In conclusion, the binary model may account for many of the properties of Z And. Being a detached system, the stellar wind(s) play an important role, both during "quiescence" and during the "outbursts". Many of the system parameters-inclination, stellar masses, etc.—are uncertain and prevent a more thorough study of the Z And complex. Yet the object appears a very promising target for the study of many important aspects of the symbiotic phenomenon. But high quality observations are essential for a real progress on the matter.

III. THE HIGH-VELOCITY SYMBIOTIC STAR AG DRACONIS

III.A. INTRODUCTION

The symbiotic star AG Dra has many interesting peculiarities with respect to what is generally considered as a "classical" symbiotic. First, it is a high-velocity (Roman, 1955), high-galactic latitude object (b= +41^0, Table 11-12); i.e., it belongs to *Pop II*. Its cool spectral component appears less cool (K-type) than in most other symbiotic stars, whereas the excitation of the emission line spectrum is quite high, as indicated by the high-ionization lines of NV, and SV in the UV, and of [FeV], [FeVI], and the 6830 A feature in the visible. HeII is quite strong in emission in both the spectral domains. Also, the far-UV continuum is very hot and intense. Moving to even shorter wavelengths, we find an intense X-ray flux, the most intense among symbiotic stars (taking into account the X-ray spectrum and the interstellar absorption). This is also in contrast with the fact that X-rays were mostly detected in D-type symbiotics, while AG Dra is S-type. Perhaps, the most interesting aspect of this object concerns the major outburst (followed by three other ones of lesser strength), which occurred in recent times, allowing a detailed study of a symbiotic star during the whole duration of an active phase.

III.B. THE LIGHT HISTORY

The light history of AG Dra is quite similar to that of Z And, in spite of the several differences between the two objects, as discussed below. Robinson (1969), from a detailed study of its light curve, identified 11 outbursts between 1890 and 1966. Since then, AG Dra remained at minimum until the end of 1980, when it brightened again from V = 9.8 to 8.5 in a few days. During the following fading phase, the star had a new minor maximum in 1982, then it reached the minimum luminosity in mid-1983. More recently, two new low-amplitude "outbursts" were observed in March 1985 and January 1986 (Mattei, 1987). The schematic light curve of the star is show in Figure 13-6.

This long-term behavior is close to that of Z And, i.e., recurrent phases of activity followed by long periods of quiescence. As in Z And, small amplitude variations were found in AG Dra during quiescence, with an amplitude increasing towards shorter wavelengths (Belyakina, 1969; Meinunger, 1979), and which are possibly periodic with a period of about 554 days (Meinunger, 1979). This behavior is also present in the space-UV, where large amplitude UV variations were observed before and after the 1980-82 outburst (Viotti et al., 1984a; Viotti, 1988a). Recently, Kaler (1987)

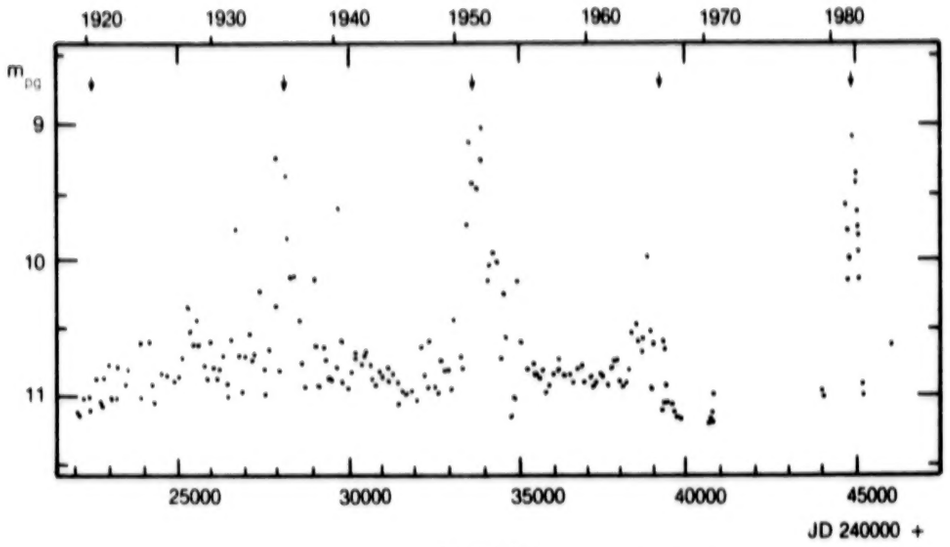
studied the variation of AG Dra in 11 intermediate and narrow photometric bands, between 3473 A and 8200 A. The observations were made from March 1977 to October 1980, during the quiescent phase preceeding the recent active phase, and covered about 2.4 cycles. The periodic variations are present in several bands and are by far the largest in the near-UV with an amplitude of about 1 mag. The amplitude decreases towards the red, but the variations are also present to some extent in the narrow bands centered on strong emission lines. Kaler also noted indications of a "secondary eclipse" of the K giant at some wavelengths.

Of particular interest is the recent activity of the star with one major outburst in 1980 and three minor maxima in 1982, 1985, and 1986 (see Figure 13-6). These events occurred at the right time to perform multifrequency observations of a symbiotic star during activity from both ground-based and space observatories. This active phase, in fact, occurred when the IUE satellite was fully operational, which gave the opportunity to collect a complete set of ultraviolet spectra throughout the whole light curve (Viotti et al., 1984a; Lutz et al., 1987). In addition, two X-ray satellites, HEAO-2 and EXOSAT, were operating during this period, and, as discussed in Section 11.IX, X-rays from AG Dra were positively detected on four different occasions (Anderson et al., 1981; Cassatella et al., 1987).

III.C. THE OPTICAL AND ULTRAVIOLET SPECTRUM

Near minimum, the yellow-red spectrum of AG Dra presents the absorption line spectrum typical of a luminous K-type star, with several narrow absorptions of neutral and ionized metals (e.g., Huang, 1982; Lutz et al., 1987). The relative strength of these absorptions suggests an early-K spectral type and a luminosity class III. However, some anomalies are present, such as the strength of the BaII and SrII lines, which might imply a higher luminosity class, for instance, as suggested by Huang (1982), or, more probably, a composition anomaly as discussed by Lutz et al. (1987). In this regard, Iijima et al. (1987) found that the absorption spectrum can be classified as G7V, in agreement with earlier classifications (e.g., Wilson, 1943), but not in agreement with the red-IR colors. They attributed this discrepancy to a metal deficiency of the cool star, as also suggested by its Pop II nature, which may affect the usual spectral classification criteria. The optical-IR energy distribution at minimum is, in fact, consistent with a K-giant spectrum. Viotti et al. (1983a) derived a K3-5III spectral type from the broad-band photometry. During outburst, the K-type spectrum is veiled (Huang, 1982) by the intense blue continuum.

The optical spectrum of AG Dra (Figure 13-7) shows prominent emissions of H, HeI, HeII, OIII, and of iron, from FeII up to [FeV] and [FeVI], and the unidentified high-excitation features at 6830 and 7088 A (Boyarchuk 1966; Bopp and Smith, 1981; Huang, 1982; Blair et al., 1983; Iijima et al., 1987. Hα is very strong in emission. Smith and Bopp (1981) and Oliversen and Anderson (1982) found large profile variations of the line which they attributed to activity on the K-star surface. In the UV, the star displays weak intercombination lines of CIII, OIII, OIV, and SiIII, and strong permitted lines of NV, CIV, and especially HeII 1640 A (Figure 11-31a). Other identified species include the low-ionization OI and MgII lines, and the high-ionization OV and SV lines (Viotti et al., 1983). The HeII 1640 A line presents extended wings, while the NV doublet displays a P Cygni profile with absorption components extending to -170 km s^{-1} (Viotti et al., 1984a). Two separate components can be identified in the UV continuum: in the near-UV, a flat continuum probably of nebular origin, and shortwards of 1600 A, a steep and strong continuum, close to the Rayleigh-Jeans tail of the energy spectrum of a hot star (Figure 11-30). However, the high-resolution observations do not reveal any absorption of possible photospheric origin. Actually, at such an effective temperature we should expect to observe strong photospheric absorptions of HeII 1640 A and of the high-ionization resonance lines of NV and CIV. These features should be completely hidden by



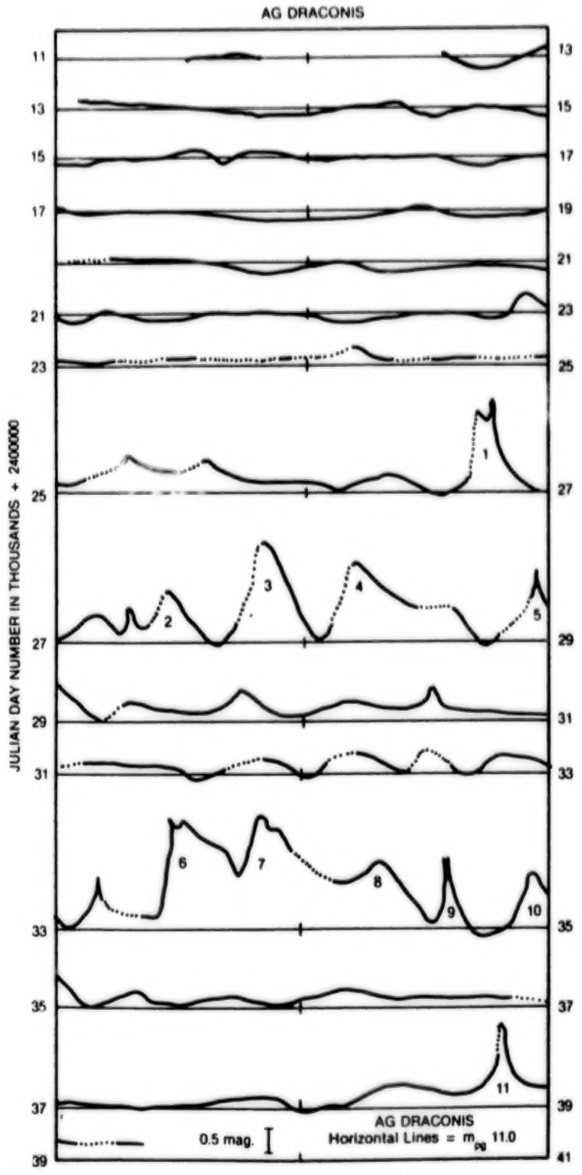


Figure 13-6. (a) The light history of AG Dra from 1890 to 1966 (Robinson, 1966).

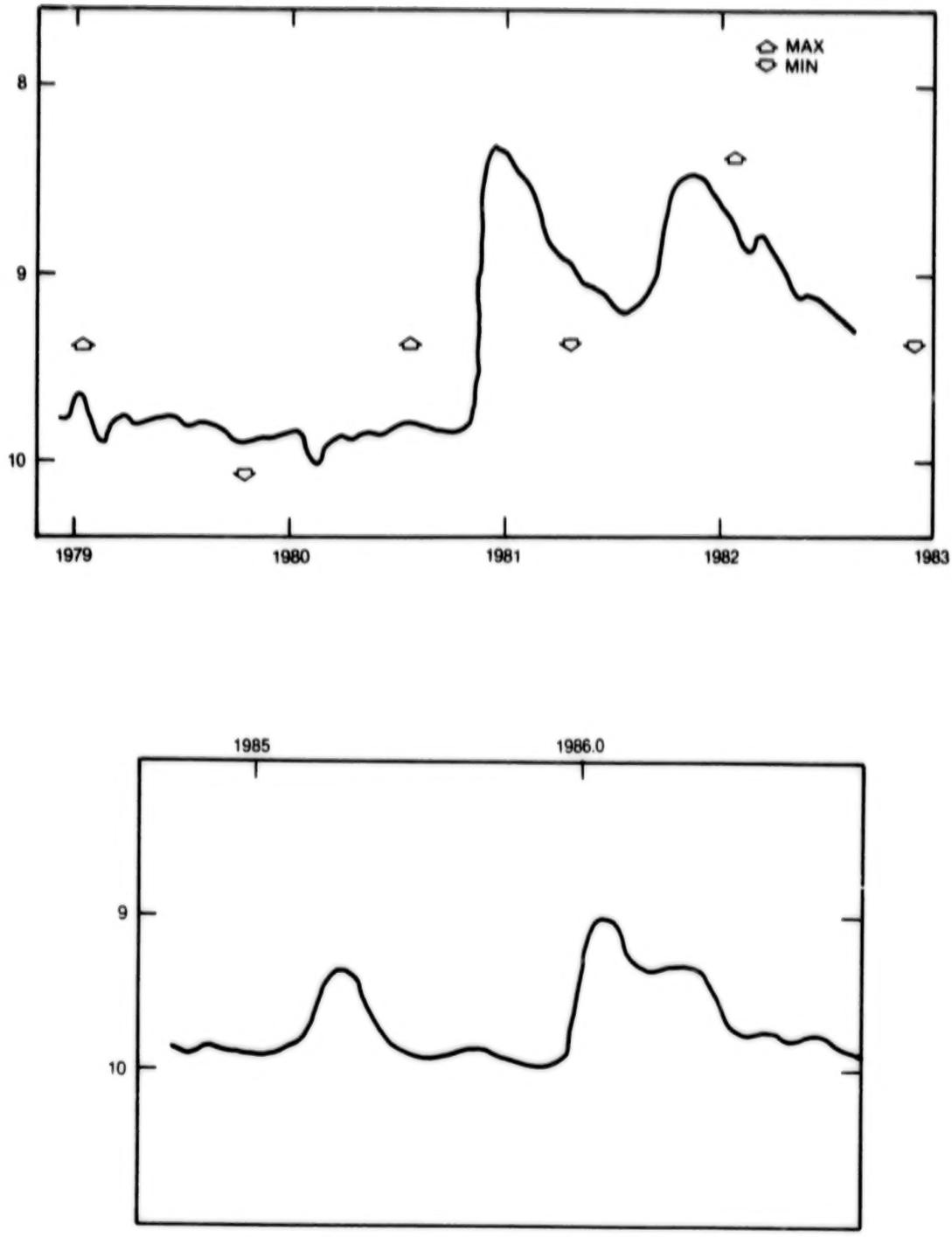


Figure 13-6. (b) The recent light curve of AG Dra from 1979 to 1986 (Mattei, 1987). Three outbursts have been recorded in November 1980, February 1985, and January 1986. The vertical arrows show the epochs of ultraviolet (IUE) and X-ray (HEAO-2, EXOSAT) observations.

the prominent nebular emissions. But, according to the IUE observations of hot subdwarfs of Rossi et al. (1984), we should also expect to observe excited lines of highly ionized C, N, and O, and especially FeIV and FeV near 1400 A, which have not been seen in the UV spectra of AG Dra. The only absorptions are the interstellar ones (see Figure 11-29c), which are rather strong indeed if compared with the low interstellar extinction of E(B-V) = 0.06 of the star (Viotti et al., 1983). This fact, however, is not unusual among halo stars.

The radial velocity of the absorption lines is high, about -140 ÷ -146 km s^{-1} (Roman, 1953; Garcia and Kenyon, 1988). This point and the high galactic latitude clearly indicate that AG Dra is a *halo object*. Huang (1982) observed a variability of the absorption and emission line radial velocity. More recently, Garcia (1986) and Garcia and Kenyon (1988) found that the K-star lines vary periodically, with an amplitude of K = 5.3 ± 0.3 and with about the same period as that of the photometric one (see Figure 11-14). In this case the phase shift between the radial velocity and photometric curves is the expected one and clearly confirms the binarity of the object.

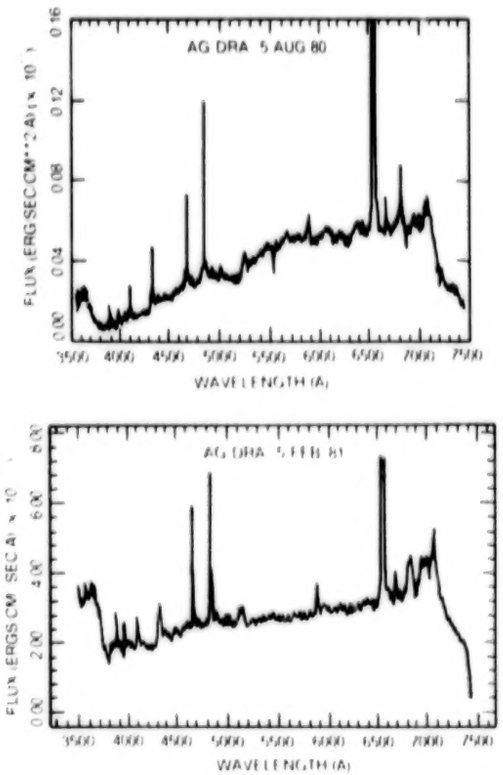


Figure 13-7. The optical spectrum of AG Dra at two different activity phases: August 6, 1980 and February 6, 1981. Note the strength of the HeII 4686 A line, and of the Balmer discontinuity in both spectra (Blair et al., 1983).

III.D. THE RECENT OUTBURSTS

The main outburst that occurred in November 1980 represented an excellent occasion to study in many spectral regions the behavior of a symbiotic star during an active phase. The optical photometric variations during outburst and those of the UV spectrum are described among others by Kaler et al. (1987) and Viotti et al. (1984a), respectively. The outburst was most energetic in the ultraviolet. The amplitude of the first rise was of two magnitudes in the u band (near 3500 A), and only 0.5 A at 8200 A (Kaler et al., 1987). The IUE observations (Viotti et al., 1984a) show that the UV continuum underwent a large increase between October and November 1980, at the time of the optical outburst, with a subsequent further increase until January 1981. The overall rise was of about a factor 10, much larger than in the visual (Figure 13-8a). In the following months, the trend in the UV nearly followed the visual, with a minimum by mid-1981, and a second maximum in December. Then, the continuum flux gradually faded to minimum. A similar trend was displayed by the emission lines. The main difference was the absence of the secondary minimum in the high-ionization NV doublet, and the constancy of the ionization before and after the outburst, as indicated by the NV/CIV line ratio (Figure 13-8b). This behavior of AG Dra was confirmed by the optical observations showing the persistence of the high-ionization emission lines (e.g., the HeII 4686 A line) also after the outburst (see Figure 13-7).

An intense X-ray flux from AG Dra was first detected with HEAO-2 in April 1980 when the star was at minimum (Anderson et al. 1981). The star was pointed to again with HEAO-2 after November 1980, but a technical problem prevented the observations (Seward, 1985).

More recently, AG Dra was observed with EXOSAT during the 1985 and 1986 outbursts and during the minimum phase in between. These observations, already described in Section 11.IX.C, indicate a modulation of the X-ray flux by the stellar activity, while there is no indication of a dependence on the 554-day period.

It is interesting to note that IR observations collected before and after the outburst only showed small variation, indicating that the K star remained substantially stable during this period (Viotti et al., 1983b, Piro et al., 1985).

Radio emission at 6 cm was first detected from AG Dra in June 1986 by Torbett and Campbell (1987) who found a flux larger than 0.5 mJy. Previously, Seaquist et al. (1984) reported only an upper limit of 0.41 mJy, for a 6-cm observation made in February 1982. Torbett and Campbell also resolved AG Dra into two close components separated by about 1.3". This increased radio activity, and the presence of a structure could be related to the recent activity of AG Dra. It would be interesting to follow the further development of this star in the radio.

III.E. INTERPRETATION

In contrast with the majority of the other symbiotic object, our observational data on AG Dra are fairly complete to make a clear picture of the system. First, AG Dra is binary. The cool component is a K giant, which, taking into account the orbital parameters, is not filling its Roche lobe. Assuming that it has the same absolute luminosity of single red giants, for E(B-V) = 0.06, a distance of 730 pc is derived, 500 pc above the galactic plane (Friedjung, 1988). It should be considered that, if one assumes that the cool component fills its Roche lobe, it should be a bright giant with a distance of about 3 kpc. Such a large distance and the corresponding large height on the galactic plane are, however, in contrast with the weakness of the interstellar CIV lines in the UV. Concerning the other stellar component of the

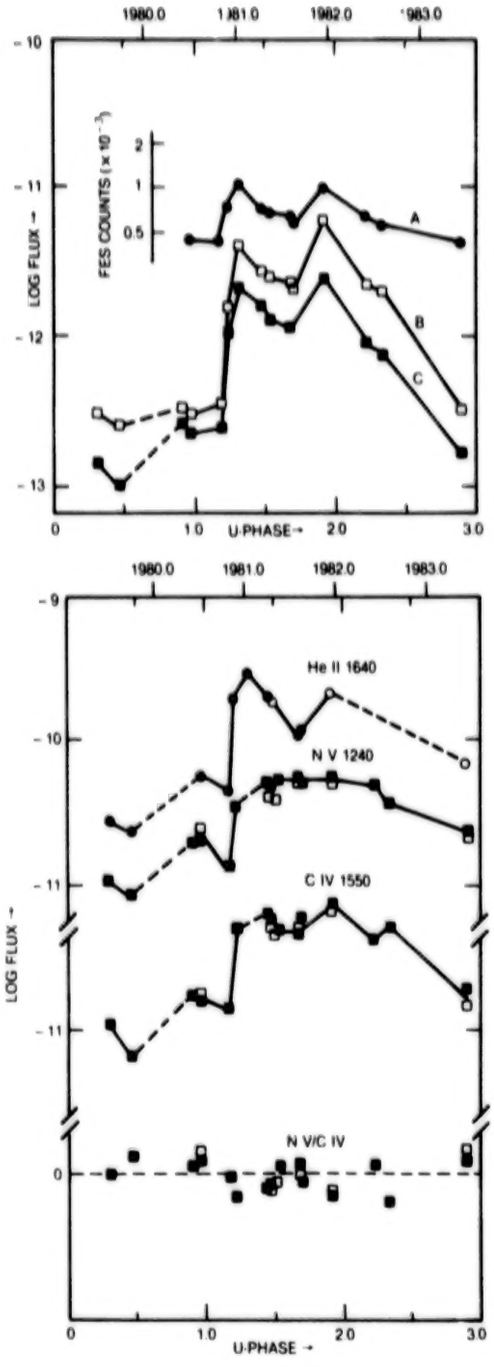


Figure 13-8. The ultraviolet variations of AG Dra during 1979 to 1983 (Viotti et al., 1984). (a) The UV continuum near 1340 A (curve B) and 2860 A (curve C) compared with the visual light curve (curve A) derived from the IUE FES count rates. (b) The variation of the high ionization UV emission lines and of the NV/CIV line flux ratio.

system, Kenyon and Webbink (1984) interpreted the UV energy distribution of AG Dra as due to a hot star without an accretion disk. In-

deed, the fact that the red giant does not fill its Roche lobe implies that the accretion rate is too low to produce a disk. According to Viotti et al. (1983), the temperature of the hot component is about 100,000 K. The corresponding effective radius in mid-1981 was 0.02 $R_{\odot}$, typical of a white dwarf. A higher temperature of about 160,000 K was also determined by Kenyon and Webbink (1984), and Iijima et al. (1987). However, the hot component of AG Dra cannot be considered a normal hot star, since, as discussed above, no "photospheric" absorption lines have been so far identified.

Let us turn our attention to the "nebular" component. Emission lines and the strong Balmer continuum can be attributed to a nebula excited by the hot star radiation (Boyarchuk, 1966b). Such a simple nebular model, however, fails to explain the large ionization range observed in AG Dra, with neutral to several times ionized species. Other "ingredients" need to be added to explain the many peculiarities. The HeII 1640 A line has broad wings which, according to Viotti et al. (1983), seem not to be produced by Thomson scattering. Another possibility is that the wings are formed in an accretion disk, or in a high velocity (10^3 km s^{-1}) warm wind. To verify these possibilities, high S/N observations of the emission line profiles are required, which are not available with IUE. The P Cygni profile of NV, which is present during all the (orbital and activity) phases of AG Dra, and the simultaneous absence of such a profile in CIV, suggests the existence of a low-velocity (-170 km s^{-1}) warm wind in the system (Viotti et al., 1984a). This velocity is too low to be associated with a stellar wind from the hot star, which should have a much larger velocity, unless the structure of its atmosphere is very peculiar because of the accretion processes. As discussed by Viotti et al., a dense, "torrid" wind (with a temperature higher than 10^5 K), for instance, could be produced from the polar regions, or near hot spots. Since all nitrogen is in the form of at least NIV, no NV lines are formed there. At a certain distance from the star's surface, the wind slows down. This fact causes a decrease of the density with the radial distance r slower than r^{-2}; that, together with the geometrical dilution and the increased far-UV opacity, would contribute to recombine nitrogen ions to NV and would then produce the observed P Cygni profile. Still further out, in almost stationary regions, the CIV ions are produced that would not show a P Cygni profile. In this case, the absence of CIV could also be a geometrical effect, for the more extended CIV region is not homogeneous and would not hide the stellar disk. It should be considered that, according to this model, we should expect the OVI lines in the far-UV to have a P Cygni profile broader than that of NV. This is an interesting study for future astronomical satellites.

A more plausible model for the low-velocity wind observed in NV is ejection from the cool giant surface. The observed wind velocity of about 170 km s^{-1} is close to the stellar escape velocity, but quite large with respect to the wind velocities generally observed in normal cool giants. The high ionization should be the result of the presence of an extended solar-type transition region or, more probably, of ionization from the hot star radiation. Like the model proposed for Z And, the near-UV continuum and the emission lines are probably mostly emitted from an extended region of the cool star, and their emission is modulated by the orbital motion of the system as a result of variation of the visibility of the region (e.g., Viotti et al., 1984a). The variability during quiescence can also be explained if the orbit is elliptical. In this regard Iijima (1987) suggested that the photometric variations are due to variation of the mass-transfer rate during the orbital cycle. However, the results of Garcia (1986) and Garcia and Kenyon (1988) are in better agreement with a low eccentricity of the system.

The light history of AG Dra was characterized by recurrent phases of activity and long periods of quiescence. By combining the photographic magnitude estimates of AG Dra since 1920, Iijima et al. (1987) suggested a recurrence period of the outbursts of roughly 15 years, corresponding to about ten 554 d cycles. Iijima et al. suggest that the outbursts are pro-

duced by mild hydrogen flashes on a massive (~1.2 $M_\odot$) white dwarf undergoing large mass accretion (~10^{-7} $M_\odot$ yr^{-1}). However, such an accretion rate is not conceivable for AG Dra, since the cool star seems not to fill its Roche lobe. IUE observations have shown that during the 1980 outburst, the far-UV continuum increased significantly. Viotti et al. (1984a) found that the variation occurred at nearly constant temperature, implying that the effective stellar radius should have increased by a factor of two to three during outburst. Kenyon and Webbink (1984) considered that the 1980 outburst was thermonuclear, but substantially less developed than the large-scale events observed in other symbiotic stars, such as the symbiotic novae. The white dwarf would not have developed a very extended envelope, so that its effective temperature would have remained high. It should be important to find possible probes of the hot star structure close to the time of the outburst. Figure 13-9 shows the variation of the ratio of the flux of the HeII 1640 A emission line and of the far-UV continuum at 1340 A before and after the 1980 outburst (Viotti et al. 1984a). This ratio, as discussed in the previous sections, is a measure of the far-UV temperature of the star, if one assumes that the HeII line is radiatively excited and that the 1340 A continuum belongs to the hot star. The figure shows that the ratio was the same just before and after the outburst (the observations were made in October 23 and November 15, respectively, when, according to Viotti et al., the visual magnitude changed by -0.7 mag, and the UV fluxes by -1.6 mag). The HeII/Fc(1340A) ratio largely decreased in the period following the first light rise, and reached again the preoutburst value in 1984. The 1982 minimum can be explained by a lower color temperature of the hot star (about 80,000 K), after the outburst, but it remains difficult to explain the long delay of the change. It should be considered that before the outburst, there was a slight increase of the HeII/Fc(1340A) ratio, which could be an indication of a heating of the stellar surface before the event, which can be associated with the onset of the thermonuclear outburst.

Unlike the other S-type symbiotics, AG Dra is a strong X-ray source. The X-ray spectrum is very soft, with an integrated luminosity of 2.1 x 10^{-12} erg cm^{-2} s^{-1} in the 0.2-1.0 keV range (Anderson et al., 1981). If the X-rays are produced by the cool giant, the ratio of the X-ray flux to the bolometric flux (in the usual units for the HEAO-2 observations) is equal to 2.1 x 10^{-4}, which is three orders of magnitude larger than that observed in the Hyades K giants (Stern et al., 1981a). AG Dra should have an exceptionally enhanced chromospheric activity giving origin to an extended corona, for instance, as observed in some dwarf stars (Stern et al. 1981b.). From the analysis of the HEAO-2 data, Anderson et al. (1982) obtained a plasma temperature of 1.1 x 10^6 K, and an emission measure of 2.6 x 10^{55} cm^{-3}, much lower than that derived from the HeII 1640 A line, but close to the values for the intercombination lines (e.g., Viotti et al., 1983). Alternatively, X-rays are formed in a hot "area" emitting as a black body with a temperature of 1.5 x 10^5 K, and a radius of 1.4 x 10^3 km (Anderson et al., 1982). This area can be identified with an active region on the K-giant surface. Actually, Oliversen and Anderson (1982b) proposed for AG Dra a model of a (single) star with active regions of enhanced surface brightness to explain the modulation of the U-light curve. Although we cannot exclude that the cool component in symbiotic system has some kind of enhanced activity (and this point needs to be further investigated), it is difficult to accept that this activity regards a large fraction of the stellar energy output.

Garcia (1986) considered the X-ray luminosity as converted gravitational energy due to capture of matter from the cool star's wind. But the required mass-loss rate from the K giant turned out to be too high for a normal giant (10^{-7} $M_\odot$ yr^{-1}). The X-rays are most easily explained as the high-energy tail of the hot component spectrum. Slovak et al. (1987) found that HEAO-2 and far-UV IUE data (during the quiescent phase of mid-April 1980) can be fitted by a black-body with a temperature of 191,000 K and a luminosity of 174 $L_\odot$. AG Dra

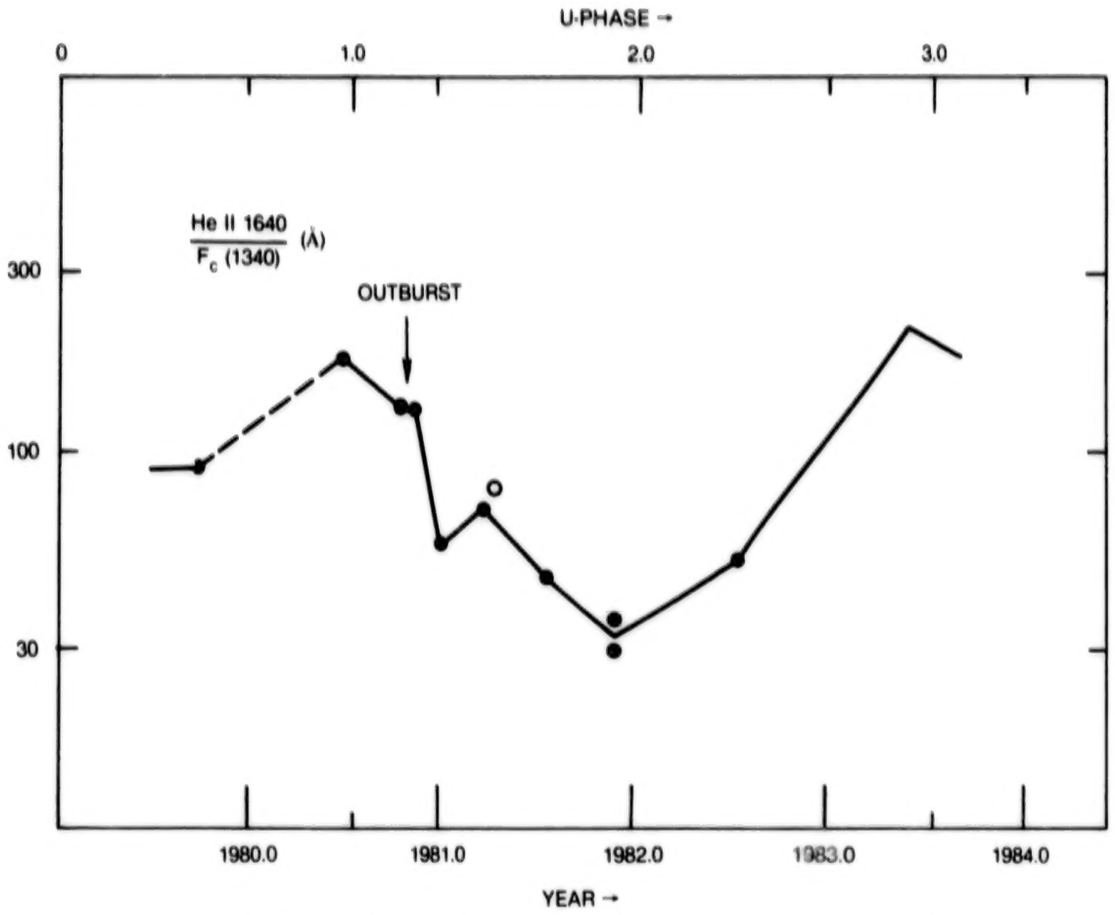


Figure 13-9. The HeII 1640A/Fc (1340A) flux ratio in AG Dra before and after the 1980 outburst.

was observed again with EXOSAT in June 1985 by Piro et al. (1985), who found that the observations can be fitted with a Bremsstrahlung model with log N(H) = 20.2, kT = 24 keV and a flux of 3.4 x 10^{-13} erg cm^{-2} s^{-1} in the 0.2-1.0 keV range. (It should be recalled that all these flux estimates strongly depend on the adopted interstellar extinction. For instance, Anderson et al. (1982) assumed log N(H) = 20.5, while Slovak et al. (1987) have made no reddening corrections. Piro et al. used the N(H) value derived by Viotti et al. (1983) from the interstellar Lyα). If the X-rays are produced near the hot component, and if the orbit of the AG Dra system is seen nearly edge-on, we should expect an eclipse at phase 0.5 of the Meinunger's light curve. In fact, AG Dra was observed again with EXOSAT in November 1985, at the time of the expected eclipse, but the X-ray flux was the same (Cassatella et al., 1987). Cassatella et al. also found a large decrease of the flux during the small outbursts of 1985 and 1986, without a similar decrease of the ionization of the emission line spectrum (see Figure 11-34). The cause of this rather unexpected behavior is not clear, but seems to suggest that X-rays do not represent the tail of the hot star spectrum. They are probably produced in nearby region. If the region is heated by the stellar radiation, its angular extension should be small, so as to capture only a small fraction of the stellar EUV photons, in agreement with the very large HeII/X-ray emission measure ratio.

To summarize, the presently available observational material on AG Dra is best interpreted in the framework of a detached binary model, formed by a rather normal K-type giant, and a degenerate star that is "heated" by slow mass accretion from the giant's wind. The accretion is probably responsible for the recurrent outburst. The K-giant could be peculiar for

having an anomalous chemical abundance, in agreement with its Pop II nature, and a rather high-velocity wind. But it is not clear whether these facts are associated with the symbiotic phenomenon. It is also not yet clarified if there is any enhanced surface activity of the giant. More detailed models of the AG Dra system require a careful analysis of the available and future data, especially the time variability in different frequencies. Of particular importance would be the systematic study of the cool spectrum at high resolution, to derive the basic data (abundance, surface gravity, turbulence, rotation, etc.), but also to improve the orbital parameters of the system, and high-quality emission line profiles collected during the orbital cycles and at different activity phases.

IV. THE SYMBIOTIC NOVAE

IV.A. INTRODUCTION

In describing the light curves of symbiotic stars in Section 11.III, we have shown that there exists a small group of objects characterized by the fact that they have undergone *one single outburst* in their known light history. This group (or subgroup) was first identified by Allen (1980b), who called them *symbiotic novae*. Attention was directed onto these stars after the recent outburst of a few northern objects, namely V1016 Cyg, V1329 Cyg, and HM Sge, whose behavior was found to be similar to those of slow novae. These objects were extensively studied in all the wavelength ranges for several years after their outburst. Thus our present knowledge of their behavior is rather complete. Other objects have displayed, in the past, a similar behavior, the most remarkable ones are RR Tel, which will be discussed in the next section, and AG Peg. AG Peg is the oldest known symbiotic nova. In the middle of the past century, the star underwent a major nova-like outburst, with a very slow increase of the visual luminosity from the 9th to the 6th magnitude in one to two decades, and a still longer decline to the present magnitude, which is close to the reported preoutburst luminosity (Figure 13-10).

At present, AG Peg displays a typical symbiotic spectrum with a cool (red) continuum and strong TiO absorption bands. The emission lines of low and high ionization are very prominent in the visible and UV spectrum, with a hot continuum extending to the far-UV (e.g., Boyarchuck, 1967; Hutchings et al., 1975). AG Peg was the first symbiotic star observed in the ultraviolet with OAO-2 (Gallagher et al., 1979). The star was extensively studied with the IUE satellite (e.g., Keyes and Plavec, 1980; Penston and Allen, 1985). Some high-resolution profiles of UV features are shown in Figure 11.31c. In many respects, the emission line spectrum is similar to that of a WN6 star, and AG Peg is often classified as M+WR, although the luminosity of the hot spectral component actually is lower than that of normal WR stars. The WR features are more probably associated with interactive phenomena in a binary system, as discussed later. It should be noted that without the knowledge of the light curve of AG Peg so many years ago, its nova-like nature would not have been recognized on the basis of its

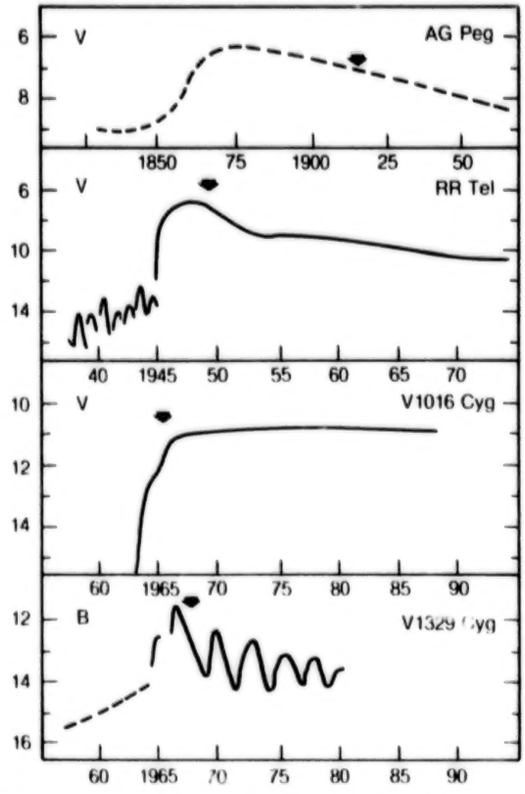


Figure 13-10. The comparative light curves of some symbiotic novae: AG Peg, RR Tel, V1016 Cyg, and V1329 Cyg (= HBV 475).

present behavior alone. The star is, in fact, quite different from the other "classical" symbiotic novae, such as RR Tel, V1016 Cyg, and HM Sge, all of which are D-type without the prominent M-spectrum of AG Peg. It is quite conceivable that several other symbiotic objects actually belong to the category of symbiotic novae, because they underwent in the past a nova-like outburst. But, owing to the long time scale involved, and the low frequency of the phenomenon, their main outburst has not been recorded.

Allen (1980b) listed seven stars having the character of very slow novae: AG Peg, RT Ser, RR Tel, V1016 Cyg (MHα328-116), V1329 Cyg, (HBV 475), HM Sge and V2110 Oph (AS 239). More recently, a new event—the outburst of PU Vul—was recorded, and the star added to this small class of objects. Figure 13-10 shows the schematic light curves of some symbiotic novae. The basic parameters are summarized in Table 13-2 (from Viotti, 1988b). In the following, we shall discuss in detail the case of RR Tel, which, for its luminosity and spectral evolution, can be considered as the best representative of the category of symbiotic novae. The main observational properties of most of these object were already presented in the different sections of Chapter 11. The general properties of symbiotic novae, for instance, were discussed by Kenyon (1986a), and Viotti (1988b, 1989).

IV.B. RR TELESCOPII

RR Tel was discovered as variable by Mrs. Fleming (1908) many decades before its main outburst. The light curve, based on 600 Harvard observations from 1889 to 1947 was described by Mayall (1949), and is schematically shown in Figure 13-10. According to Mrs. Mayall, RR Tel showed little evidence of periodic variations from 1889 to 1930, the observed range being about 1.5 mag with maxima ranging from 12.5 to 14 mag. After 1930, the periodicity of the variation became clearer, and a mean period of about 387 days could be derived with an amplitude of about 3 magnitudes. This behavior is typical of a long-period variable, and is presently barely visible at optical wavelengths with a period of about 374 d (Heck and Manfroid, 1982; Kenyon and Bateson, 1984). The period, however, seems to be variable between 350 and 410 d (Heck and Manfroid, 1985). As already discussed in Section 11.F, the Mira-type pulsation is evident at IR frequencies (Feast et al., 1983a). In late 1944, the periodicity stopped and the star rapidly brightened from m_{pg} = 14 to 10 in a few days, then rose to 7 mag by mid-1945. In the

TABLE 13-2. THE SYMBIOTIC NOVAE

Star	To[1]	Tmax[2]	Magnitude			Spectrum		Type
			pre[3]	max[4]	post[5]	cool	max	IR
AG Peg	1855	1871	9	6	8.3	M3		S
RT Ser	1909:	1923:	>16	9.5	13	M5.5	A8	S
V2110 Oph	.....	1940:		11:	22	>M3		D
RR Tel	1944	1948	14v	6	11	M5	F5	D
V1016 Cyg	1964	1967	14	11	11	>M4	neb	D
V1329 Cyg	1966	1967	14v	11.5	13-14	>M4	neb	S
HM Sge	1975	1975	>17	11	11	>M4	neb	D
PU Vul	1978	1982-83	15v	8.8	8.8	M4	A7	S

Notes to the table. (1) Year of beginning of the outburst. (2) Year of maximum luminosity. (3) Preoutburst magnitude. (4) Maximum luminosity. (5) Present (1986-88) postoutburst magnitude.

following years, RR Tel remained at maximum luminosity until 1949, reaching the sixth magnitude during 1948. Then the star gradually faded to the present V = 10 in about 14 years (see Kenyon, 1986). Although the star was quite bright at maximum it was discovered only in 1949, three years after the outburst. Therefore no spectroscopic information is available on the early development of RR Tel. Nevertheless, since late 1949 the star underwent a major spectral evolution which was followed at the Bosque Alegre (Argentina) and Radcliffe (South Africa) observatories. Figure 13-11 illustrates the spectral evolution of RR Tel between April 1949 to July 1971 based on a collection of spectra obtained at Bosque Alegre.

The first spectrum taken at Bosque Alegre in April 1949 showed a strong continuum with many absorption lines of singly ionized metals. Some absorptions are flanked at longer wavelengths by a weak emission component, indicating a marginal P Cygni profile. This emission became more prominent in July 1949. By mid-September, the continuum appeared weaker and the emission lines dominated the spectrum of RR Tel, although the mean line excitation was still low. The first spectra taken at the Radcliffe Observatory of South Africa were discussed by Thackeray (1950), who found strong absorption of CaII and hydrogen in June-August 1949. TiII was present in absorption, and Hβ was absent, probably filled in by emission. Mayall (1949) reports on low-quality, low-dispersion spectra taken when RR Tel was at maximum brightness. All these earlier observations agree in giving an F-supergiant spectral type (cF5, according to Thackeray, 1950). In a later paper, Thackeray (1977) reports that the relative shift of the absorption lines was - 100 km s^{-1}. The remarkable spectral change, which occurred between August and September 1949, was first noted by Thackeray (1950), where reported that in his spectra all the absorption lines disappeared and a rich emission - line spectrum appeared with prominent hydrogen, CaII and especially FeII emission, close resembling the spectrum of the peculiar variable Eta Car (Thackeray, 1953). According to the Bosque Alegre spectra shown in Figure 13-11, the spectral variations should have taken place in *less than one week*, and maybe in a few days.

The spectral evolution of RR Tel in the following years is best described by A. D. Thackeray's review (Thackeray, 1977). Since 1949, the star has shown a gradual increase of the mean ionization of the emission line spectrum. HeII and NIII appeared around August 1950 (see also Pottasch and Varsavsky, 1960). These authors also identified HeI absorption with a velocity of -685 km s^{-1} (in 1951) and -865 km s^{-1} (in 1952). Then, between 1951 and 1952, [OIII] and [NeIII] flared while the permitted FeII lines faded (Thackeray, 1953). The increase of the level of ionization continued through 1953 and 1954 and is best illustrated by the sequential appearance of higher and higher ionization stages of iron, from FeIII to FeVII. This sequence is shown in Figure 13-12. First, the spectrum only showed the low-ionization lines of permitted FeII. Then, the forbidden [FeII] lines appeared and gradually strengthened with respect to FeII, indicating a decrease of the density of the emitting medium (cf. Viotti 1976).

The sequence continued with [FeIII], whose lines brightened in 1952; [FeIV] (1952-53); [FeV] (1954-56); [FeVI] (1956-59); and finally [FeVII] (1959-64). This behavior is similar to that found in novae after the optical maximum, but with the important differences that in RR Tel (and in other symbiotic novae), the trend was much slower. In any case, RR Tel was the first nova-like object in which this phenomenon was studied in such detail. It should also be noted that at the time of Thackeray's observations, the spectrum of three to five times ionized metals was very poorly known. His careful study of the spectral evolution of RR Tel, and the theoretical computations of B. Edlen and R.H. Garstang led to the first identification of many forbidden lines of FeIV to FeVI, and of other highly ionized metals. From this point of view, RR Tel has also been a good laboratory for atomic spectroscopy.

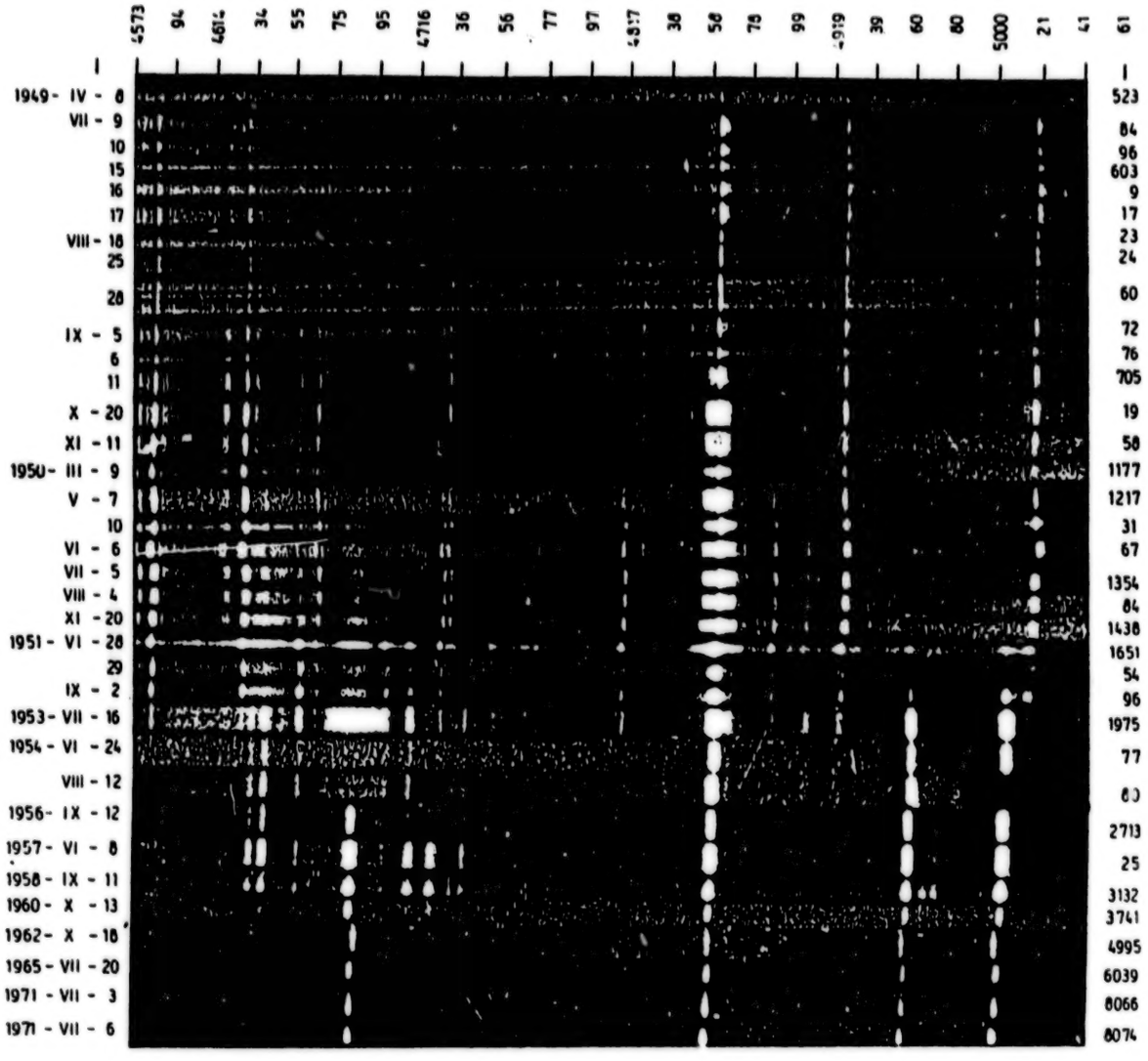


Figure 13-11. (Plate) the blue spectrum of the symbiotic nova RR Tel between April 1949 and July 1971. This is a reproduction of spectrograms taken at the 150-cm telescope of Bosque Alegre Observatory (Argentina). The original reciprocal dispersion is 41 A mm^{-1}. Note the dramatic spectral change occurred in September 1949. Courtesy of Professor Jorge Sahade.

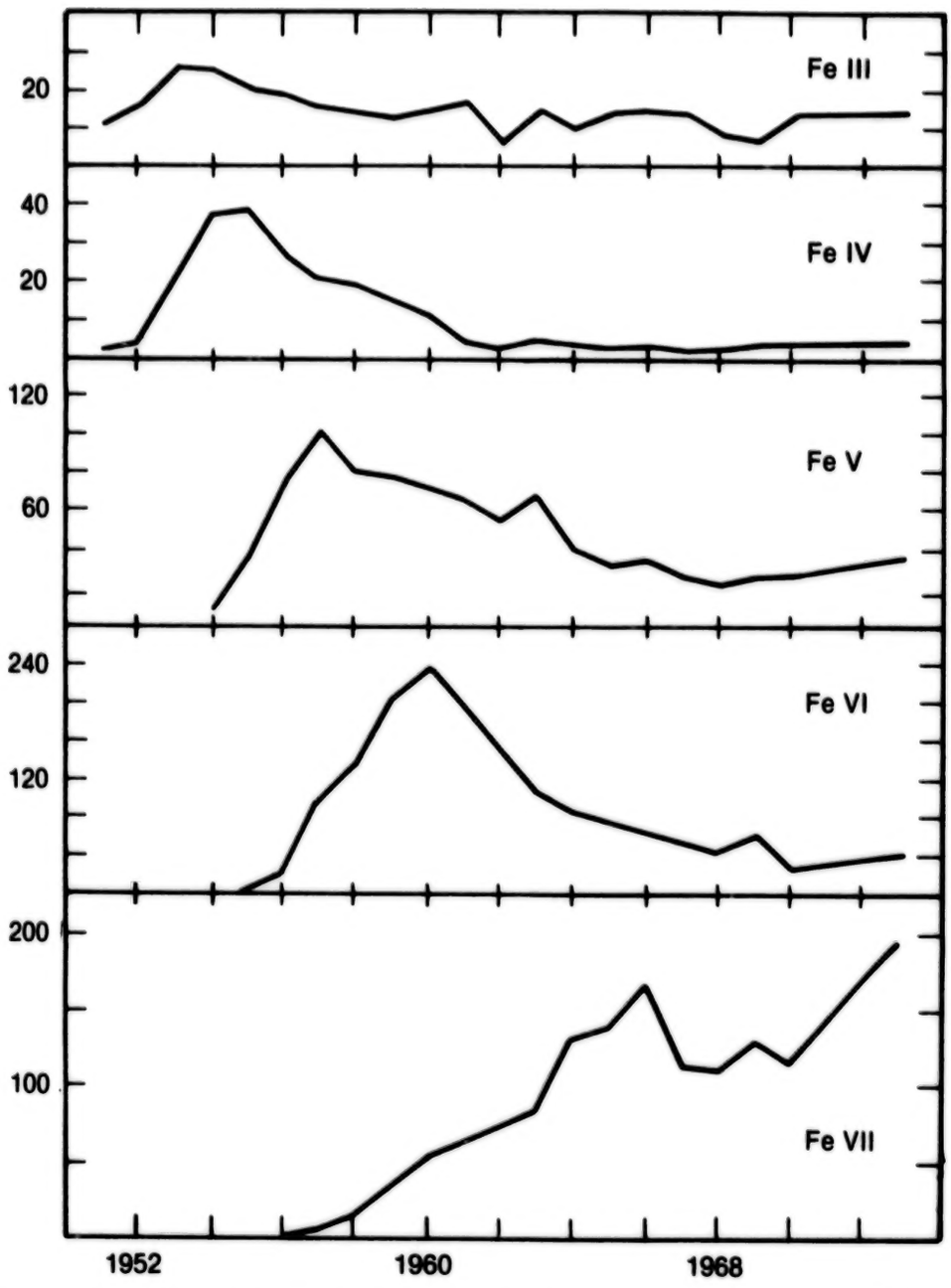


Figure 13-12. The evolution of the intensity of the lines of the different ionization stages of iron in RR Tel during 1952 to 1964 as described by Thackerary (1977). Note the gradual increase of the ionization of the emitting envelope as indicated by the appearance of the evolution of the successive ionization stages of iron (Viotti, 1987).

In the ultraviolet, the star presents a very rich emission spectrum with a wide range of ionization, from neutral species to five times ionized calcium (Penston et al., 1983). More recently, Raassen (1985) suggested the identification of a line at 2648.9 A with the $3P^2$ - $1D^2$ transition of [FeXI], which could thus be the highest ionization stage so far observed in RR Tel (possibly excluding the yet unidentified high-temperature features at 6830 and 7088 A). Penston et al. (1983) found that the width of the emission lines varies between different atomic species and increases from 40 to about 80km s^{-1} from low- to high-ionization lines. Similar correlation between line width and ionization energy was previously reported by Friedjung (1966) and Thackeray (1977) for the optical lines. This behavior was also found in other

symbiotic novae, such as V1016 Cyg and HM Sge.

IV.C. GENERAL PROPERTIES OF THE SYMBIOTIC NOVAE

Like RR Tel, the other symbiotic novae also have the common property of having undergone a single major outburst and of showing a symbiotic spectrum. Since there exists in the few objects classified as symbiotic novae a large variety of behavior, it is important to investigate their general properties and whether they represent an extreme case of symbiotic stars or have to be associated with the category of novae. In the following, we summarize the different aspects of the phenomenon.

a. The preoutburst phase and the red component.

The preoutburst phase is known in some detail only for V1329 Cyg and RR Tel. Both appeared largely variable, on a long time scale. In V1329 Cyg, the variability is interpreted as due to eclipses of a binary system, and this is also supported by recent radial velocity measurements (e.g., Grygar et al., 1979; Nussbaumer et al., 1986). On the contrary, in the cases of RR Tel, the long-term variability is attributed to a Mira-type pulsation, as also confirmed by the recent optical and IR monitoring (Heck and Manfroid, 1982; Feast et al., 1983a). The orbital period of RR Tel, as in other D-type symbiotics, is believed to be much longer.

In these two objects and in V1016 Cyg, the preoutburst spectrum was M-type. It is quite possible that the luminosity (and spectrum) of the preoutburst M star was the same as that of the present red component of the symbiotic systems. This obviously implies that the outburst was not (at least directly) caused by the red star, but rather by its companion. An M-giant spectrum was also observed during the deep 1980 minimum of PU Vul, and in AG Peg and RT Ser after decline from maximum. In V1016 Cyg and HM Sge, which have not (yet) declined, the M spectrum in the visible is masked by the strong continuum and line emission from the circumstellar regions. In these stars, the presence of a late-type component is supported by the Mira-type variations in the near-IR. As in RR Tel, the Mira star could be hidden by a dense circumstellar dust shell (Kenyon et al., 1986). Indeed, in the D-type symbiotic novae, the Mira component should be subject to large mass overflow, followed by formation of dense gas and dust clouds. Table 13-3 (from Viotti, 1988b) summarizes the typical time scales of the cool components of symbiotic novae. The spectral types found from the literature are given in Table 13-2. The luminosity class is III for AG Peg and PU Vul, and for the Mira components of the D-type objects as well.

b. The outburst.

As seen in Figure 13-10 and in Table 13.3, the rise to maximum was fast in V1329 Cyg, HM Sge, and RR Tel, and very slow in V1016 Cyg and especially in AG Peg and RT Ser. It is noticeable that the rise time is apparently not related to the other features (e.g., the IR-type) of the symbiotic novae. The amplitude of the outburst, ranges from 3 mag (AG Peg) to more than 6 mag (HM Sge, RT Ser). It is also important to consider that this difference is not due (or not only due) to the actual amplitude of the outburst, but rather to the relative brightness of the late-type component (with respect to the luminosity of the symbiotic nova at maximum), which is high in AG Peg and V1329 Cyg, and very low in RT Ser, V2110 Oph, and HM Sge. The actual visual luminosity increase of the red-giant companion is unknown.

The spectrum at maximum is another intriguing problem. As in classical novae, some objects (RT Ser, RR Tel, and PU Vul) displayed an intermediate (A-F) equivalent spectral type, possibly of supergiant class, but without the highly violet-displaced absorption lines

TABLE 13-3. CHARACTERISTICS TIME SCALES OF SYMBIOTIC NOVAE.

Star	Rise (a)	Decay (b)	Mira (c)	Orbit (d)	K (e)
AG Peg	16	40	==	816.5	5.1
RT Ser	14	7:	==	==	==
RR Tel	<0.3	9	374.2	==	==
V1016 Cyg	2-3	>125	472	==	==
V1329 Cyg	0.3	12-20	==	950	62
HM Sge	<0.4	>65	500-600	==	==
PU Vul	1	>38	==	==	==

Notes to the table. (a) Rise time of the visual luminosity in years. (b) The e-folding decay time of the visual luminosity in years. (c) Period (in days) of the Mira pulsation. (d) Orbital period (in days). (e) Semiamplitude of the radial velocity curve (in km s^{-1}).

that are seen in novae. No similar absorption spectra have been observed in the other symbiotic novae. The simplest explanation is that the absorption-spectrum phase occurred during a period not covered by the observations, and we missed it. In fact, V1016 Cyg was first observed spectroscopically near the end of its long-lasting rise to maximum (indicated by an arrow in Figure 13-10). The first spectra of V1329 Cyg were taken at the end of 1969, one year after its light maximum, and showed a rich emission line spectrum, which could be compared with the post-maximum spectrum of classical novae. In this regard, RR Tel represents a rather fortunate case, since its A-type spectrum suddenly disappeared in late 1949, just a few months after the discovery that the star had "exploded". Suppose that the discovery would have been made 4-5 months later, in late September or in October 1949, instead of in April. We would have missed the absorption-spectrum phase, and perhaps have placed RR Tel in a different subcategory of symbiotic novae (see, e.g., Kenyon and Truran, 1983). Thus it is important to take into account these selection effects in any modeling of the phenomenon.

Like the classical novae, the symbiotic novae after the outburst display a rich emission line spectrum with wide ionization energy range. But unlike novae, the emission line profiles are narrow, in general, indicating a low expansion velocity of the main emitting region. There are, however, a number of interesting exceptions. Crampton et al. (1970) found in V1329 Cyg the [OIII] and [NeIII] lines having a multiple structure, with emission peaks ranging from -240 to +250 km s^{-1}. This line multiplicity was also present in later spectra of the star (Grygar et al., 1979; Tamura, 1988) (Figure 13-13; see also Figure 11-13).

As discovered by Crampton et al. (1970) and confirmed by Baratta et al. (1974), the low-resolution spectra of the star show several broad and shallow emission features, which were identified with WN5-type lines having an expansion velocity of about 2300 km s^{-1} (figure 11-10). As discussed above, broad WR structures have also been seen in AG Peg and RR Tel, while high-velocity P Cygni profiles were observed in RR Tel during decline. Therefore, in some symbiotic novae, at least, there is evidence for the presence of high temperature, high-expansion velocity regions, but this should only represent a small portion of their emitting envelope. This result is probably related to the velocity gradient found in some objects from the analysis of the line width of the narrow emissions, with the higher energy ions (and the corresponding higher temperature-emitting regions) having larger expansion velocity, as suggested by the observed correlation between emission line width and ionization energy (see Chapter 11 Section VIII.D) It

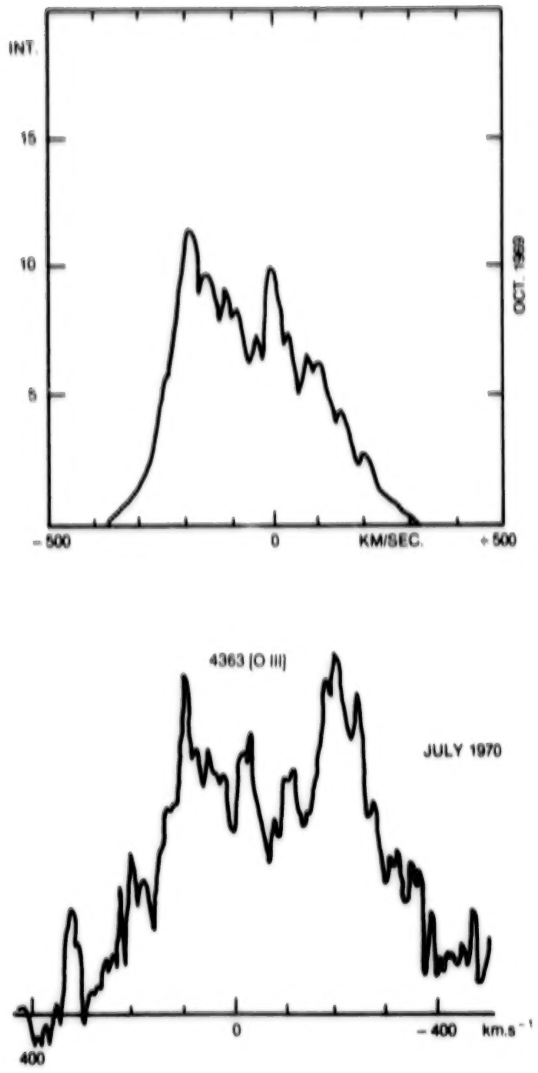


Figure 13-13. Emission line profiles of the forbidden lines in the spectrum of the symbiotic nova V1329 Cyg. Top: Mean profile of [O III] and [Ne III] lines in October 1969 (Crampton et al., 1970). Bottom: profile of the /O III/ 4363 line in July 1979 (Grygar etal., 1979).

is also conceivable that the WR features observed, especially in V1329 Cyg, originate in a dense expanding envelope or wind of the hot star, which behaves like some WR-type nuclei of Planetary Nebulae. In view of possible models, it would be interesting to know if these WR features are present far away in time from the outburst, or in the spectroscopic records of the preoutburst phase.

The emission line spectrum should be formed in an extended circumstellar or circumsystem nebula, which is supposed to be ionized by the radiation of a hot source (a hot star or the hottest parts of an accretion disk) in the system. Collisional ionization is another possible mechanism to explain the very high ionization features and the X-rays. It might occur in shocks formed by the interaction of the winds of the two stellar components, for instance, as suggested by Willson et al. (1984), or by collision of the stellar wind(s) with the circumstellar matter. In general, the analysis of the high-ionization emission line fluxes and of the far-UV continuum leads to a model of a hot central source with temperatures (around 10^5K) and radii (0.1 $R_\odot$ or less) typical of the nuclei of Planetary Nebulae (e.g. Nussbaumer and Schild, 1981; Tamura 1981; Mueller and Nussbaumer, 1985; Hayes and Nussbaumer, 1986).

c. The decline phase.

The behavior of symbiotic novae after the outburst is very different from case to case. Four objects showed a gradual fading of the visual luminosity that took several years to decades (Figure 13-10). The e-folding decline time varied from 7-9 years for RT Ser and RR Tel to 12-20 years for V1329 Cyg and 40 years for AG Peg (Table 13-3). In the case of V1329 Cyg, the decline time was derived from a fit of the UV emission line flux variation, taking into account the 950 d periodicity (Nussbaumer et al., 1986). We recall that Allen (1981) and Willson et al. (1984), from the analysis of the X-ray flux in three symbiotic novae, V1016 Cyg, HM Sge, and RR Tel, suggested a very slow decrease of the X-ray flux after the outburst, with an e-folding decay time of 5 to 50 years. But this result needs to be confirmed.

Three recent symbiotic novae, V1016 Cyg, HM Sge, and PU Vul, have not significantly faded since their outburst, although a small visual luminosity decrease has been recently noted for PU Vul (Gershberg and Shakhovskoj, 1988). Their decay time is probably similar to that of AG Peg, or even much larger. Once again we recollect that in symbiotic stars, emission lines largely contribute to the broad-band photometry, so that the observed light

C-9.

curve of an object does not necessarily describe its global time behavior, but should also reflect local fluctuations of the physical structure of the emitting envelope. Therefore, it is possible that some precious information remains masked in the broadband light history.

As in RR Tel and in classical novae, the spectral evolution of V1016 Cyg and HM Sge was characterized by the gradual increase of the ionization level of the emission line spectrum. WR features were first detected in HM Sge two years after the outburst (Ciatti et al., 1978). As these faded, HeII and [FeVII] emerged with very intense lines (Blair et al., 1981). We recall that, unlike in the novae, the spectral evolution of V1016 Cyg and HM Sge occurred at nearly constant visual luminosity.

Symbiotic novae were also followed at radio wavelengths, sometimes over a period of several years (see Section 11.VII). Radio observations of HM Sge started in 1977, two years after the outburst, and disclosed a gradual evolution, with a steady increase of the radio flux at 15 GHz from 40 mJy in 1977 to 150 mJy in 1985. The radio spectrum remained optically thick all the time, indicating that, unlike classical novae, the expanding HII region was still dense several years after the outburst (Kwok et al., 1981; Kwok, 1988). An optically thick radio spectrum is also displayed by V1016 Cyg. The star was first observed in 1973, nine years after the outburst, but no significant flux change has been detected since then. Probably it reached a stationary stage before 1973. We finally recall the large and probably irregular radio variability of the other symbiotic nova V1329 Cyg.

One particular case is PU Vul. This star, after the main brightening phase that took about 1 year, remained at maximum for another year, showing an F-supergiant spectrum (e.g., Nakagiri and Yamashita, 1982; Kolotilov, 1983). Then, during the first half of 1980, the visual luminosity gradually dropped from V = 8.8 to 13.5 (Figure 13-14), and the M-type spectrum appeared. PU Vul remained at minimum for about 200 days, then gradually flared up again to V = 8.5, followed by the very slow decline discussed above. During this phase, the visual and ultraviolet spectrum remained dominated by the hot component, but with a gradual evolution from F5 to A2 during 1983-1986 (Gershberg and Shakhovskoj, 1988). In late 1987, Maitzen et al. (1987) noticed an increase of the emission line strength. The 1980 minimum was also followed by Friedjung et al. (1984) beyond the visual range. As shown in Figure 13-14, the amplitude of the minimum was much larger at shorter wavelengths, and just detectable in the near infrared. Also the duration of the eclipse was longer in the UV. Friedjung et al. interpreted the deep minimum as a result of temporary obscuration of the "exploded" star by dust condensated from the ejected shell. Dust might also have been produced by the red giant. Alternatively, the hotter star has been eclipsed by the M giant (Kenyon, 1986b). From the duration of the minimum, Kenyon derived an orbital period of about 700 years. In both hypotheses, the M spectrum observed at minimum should be that of the cool giant component of the system, which at maximum is completely masked by the radiation of the early type component.

IV.D. POSSIBLE MODELS FOR SYMBIOTIC NOVAE

Let us now examine the above "main properties" of symbiotic novae in the light of possible models. Other aspects of the problem are discussed in Viotti (1989). Although the preoutburst phase is very poorly known, it is clear that the large increase of the visual luminosity, mostly due to the appearance and strengthening of emission lines, was associated with a sudden increase of the flux of far-UV photons from the M-giant's companion. The hot source should have largely increased its brightness temperature and bolometric luminosity with respect to the previous unknown stage. As discussed in Section 12.IV.A, such an event can be explained as a result of sudden thermonuclear burning of the hydrogen-rich matter accreted by a degenerate star from the red giant wind. According to the models developed, among others, by Paczynski and Rudak (1980), Fujimoto (1982a,b), Kenyon and Truran (1983),

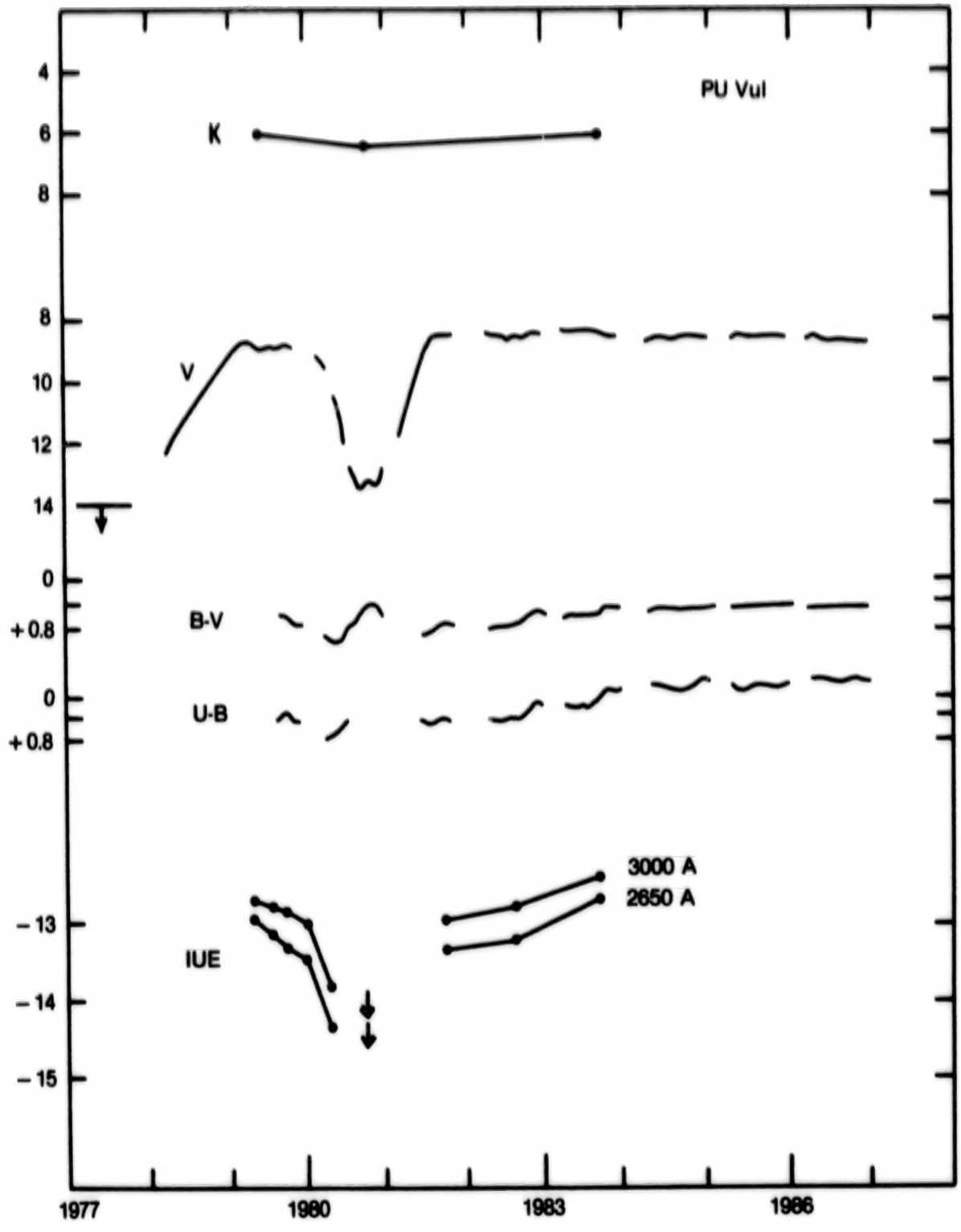


Figure 13-14. The infrared, optical, and ultraviolet light curve of PU Vul during the recent outburst (Friedjung et al., 1984; and Kenyon, 1986, adapted).

Kenyon (1988), and Livio et al. (1989), the accretion rate should be smaller than that required to have a stable burning of the matter as it is accreted, and larger than that which characterizes the classical nova outburst. Since the first case is supposed to occur in at least some Z And-type symbiotic stars, symbiotic novae should represent the dividing line between Z And-type variables and classical novae. Due to the larger separation of the components in

symbiotic novae, the accretion from the red-giant wind (the systems are clearly detached) should be smaller than in other symbiotic systems, even if we expect denser winds in those symbiotic novae containing a Mira.

According to Kenyon (1988), thermonuclear flash models imply that, if the accretion rate is fairly low, the white dwarf envelope is completely degenerate. Under these conditions, the luminosity of the star first increases at nearly constant radius, then a slow expansion at constant bolometric luminosity follows until an A-F supergiant configuration is reached (see Figure 12-4). Later, after a rather long time, the star evolves again to high effective temperatures. This *degenerate flash* model possibly applies to AG Peg, RT Ser, RR Tel, and especially PU Vul. However, in the case of RR Tel, it is difficult to explain the rapid evolution of its spectrum from F-supergiant to emission line.

If the accretion rate onto the white dwarf is larger, the accretion results in a non-degenerate envelope, and produces a relatively weak shell flash. These weak *non-degenerate flashes* (Kenyon, 1988) do not evolve into the A-F supergiant stage discussed above, but the star remains hot throughout the eruption. This could be the case of V1016 Cyg, V1329 Cyg, and HM Sge, which have probably not developed the intermediate-type spectrum in the earlier stages of their outburst. In any event, such a phase, if it occurred during an early unobserved phase, should have lasted quite a short time, one year or less, which is difficult to explain in the light of the proposed models. The amplitude of the outburst in the visual should be larger in the former case of a degenerate outburst, as a consequence of the small bolometric correction at maximum. Although the amplitude of some well-documentated objects (RR Tel and PU Vul, on one side, V1016 Cyg and V1329 Cyg, on the other) apparently seems to support this model, in the reality, the preoutburst visual magnitude in all these objects is that of the red giant, since the preoutburst spectrum is M. The actual amplitude of the white dwarf outburst should be larger, and probably much larger, than that given in Table 13-2. We finally consider that during the high-temperature phase, the exploded star should have a dense hot wind, which might have produced the WR features observed in several cases. This point, however, has not yet been investigated in detail, especially in order to find possible differences with the hot components of symbiotic systems whose high surface temperature is not the result of accretion processes. In particular, the chemical composition of the wind should reflect the recent violent history of the star, and this problem should require more studies.

The outburst of symbiotic novae might be explained by instabilities of an accretion disk (cf., Duschl, 1986b), but this model should require high accretion rates, which do not appear to be realistic for detached systems. Alternately, the outburst can be the result of a sudden onset of a strong stellar wind from the cool giant (Nussbaumer and Vogel, 1988). The wind will produce an extended envelope surrounding the system. The luminosity increase is the result of the ionization of the envelope by the UV radiation of the hot stellar component. This model has to be worked out in more detail, with special attention to the time scales involved in the processes. Periodic enhancements of the accretion rate could occur if the orbit is highly eccentric, and the red giant is going to fill its Roche lobe at periastron. Such a model was proposed by Kafatos and Michalitsianos (1982) to explain the outbursts of R Aqr (See the next section V.), but obviously it does not apply to those symbiotic novae, AG Peg and V1329 Cyg, whose period appears too short for the time scale involved in the symbiotic nova phenomenon. Other observational and theoretical aspects of the phenomenon that need to be further investigated are the identification of other symbiotic novae whose main outburst has not been observed, the recurrence of the phenomenon, and the structure of the circumstellar nebula. But we especially need the basic parameters of the binary systems.

V. R AQUARII: A SYMBIOTIC MIRA WITH JET

R Aqr is one of the most peculiar astrophysi-

cal objects, since the characteristics of many different astrophysical categories are present in the same object (Michalitsianos, 1984). R Aqr is symbiotic for its composite spectrum characterized in the visual by many emission lines and a late-type MIII component. R Aqr is also a Mira-type variable with a period of 387 days, but the light curve presents important irregularities. A SiO maser emission was also detected. The star is interesting for being at the center of a planetary nebula with a mid-ionization nebular spectrum. The central part of the nebula, studied at radio wavelengths, is highly variable with jet-like features. Finally, as discussed in Chapter 11 Section IX.E, R Aqr was recently detected as X-ray source with EXOSAT (Viotti et al., 1987). Thus, it is difficult to put R Aqr in one specific category. In addition, the star is rather different from the "classical" concept of symbiotic stars. However, we may consider that the symbiotic phenomenon is particularly evident in this object and that its study could give an important contribution to the problems that we are discussing in this monograph. This is the reason for having devoted a full section to this interesting object. Many aspects of R Aqr have also been discussed by Querci (1986) in the previous volume on M-stars of this monograph series.

V.A. THE MIRA VARIABLE

R Aqr, as indicated by the letter "R", was the first variable discovered in the Aquarius constellation. It was found as variable by Harding in early 1800, and since then it has been studied by several astronomers. Thus, its light history has been fairly well known for almost two centuries. The light curve from 1887 to 1980 is reproduced in Figure 13-15.

R Aqr is a red giant that shows large and quasi-regular light variations rather typical of a Mira variable. The mean period is 387 days. The mean light curve generally presents a broad minimum lasting 6-7 months, followed by a rapid rise to maximum. There are ample variations from cycle to cycle, in both the shape and amplitude of the light curve. In some cases the variability nearly disappeared. For instance, this has happened in the years 1905-10, 1928-30, and 1974-78. Thus, the light curve presents a kind of a long time scale "modulation" of the amplitude of oscillation. Willson et al. (1981) suggested that these irregularities should be caused by eclipses of a close binary system orbiting in a highly eccentric orbit with a period of 44 years.

R Aqr was monitored in the infrared (JHKL) at SAAO during 1975 to 1981 (Catchpole et al., 1979; Whitelock et al. 1983b). These observations confirmed the visual periodicity of 387 days. The light curve in the L-band (about 3.6 μm) is slightly different from the visual curve, with a steeper decline after maximum, and a slower rise to maximum, which is reached slightly later than in the visual. This is fairly normal for a Mira variable. Whitelock et al. (1983b) noted that the infrared fluxes appeared depressed during 1975-78. They attributed this to an obscuration by an opaque dust cloud as suggested by Willson et al. (1981).

The Mira character of R Aqr is also indicated by the positive detection of SiO maser emission (Lepine et al., 1978), which is normally associated with LPV's. So far, R Aqr is the only symbiotic star showing detectable maser emission (Lepine et al. 1978, Cohen and Ghigo, 1980). The negative detection of OH (Wilson and Barrett, 1972) and H_2O lines (Dickinson, 1976) is probably related to the inhibition by the hot close companion of the Mira. More recently, Hollis et al. (1986) reported interferometer SiO observations indicating that the maser emission occurs in the nebulosity about one arcsec away from the optical position of the Mira (see Figure 13-17). This result is clearly in disagreement with a model of collisionally pumped SiO emission (e.g., Elitzur, 1981).

V.B. THE NEBULA

The planetary nebula around R Aqr is essentially composed of two distinct structures: the outer nebula with an oval shape with is formed by two arcs symmetrically extending to the

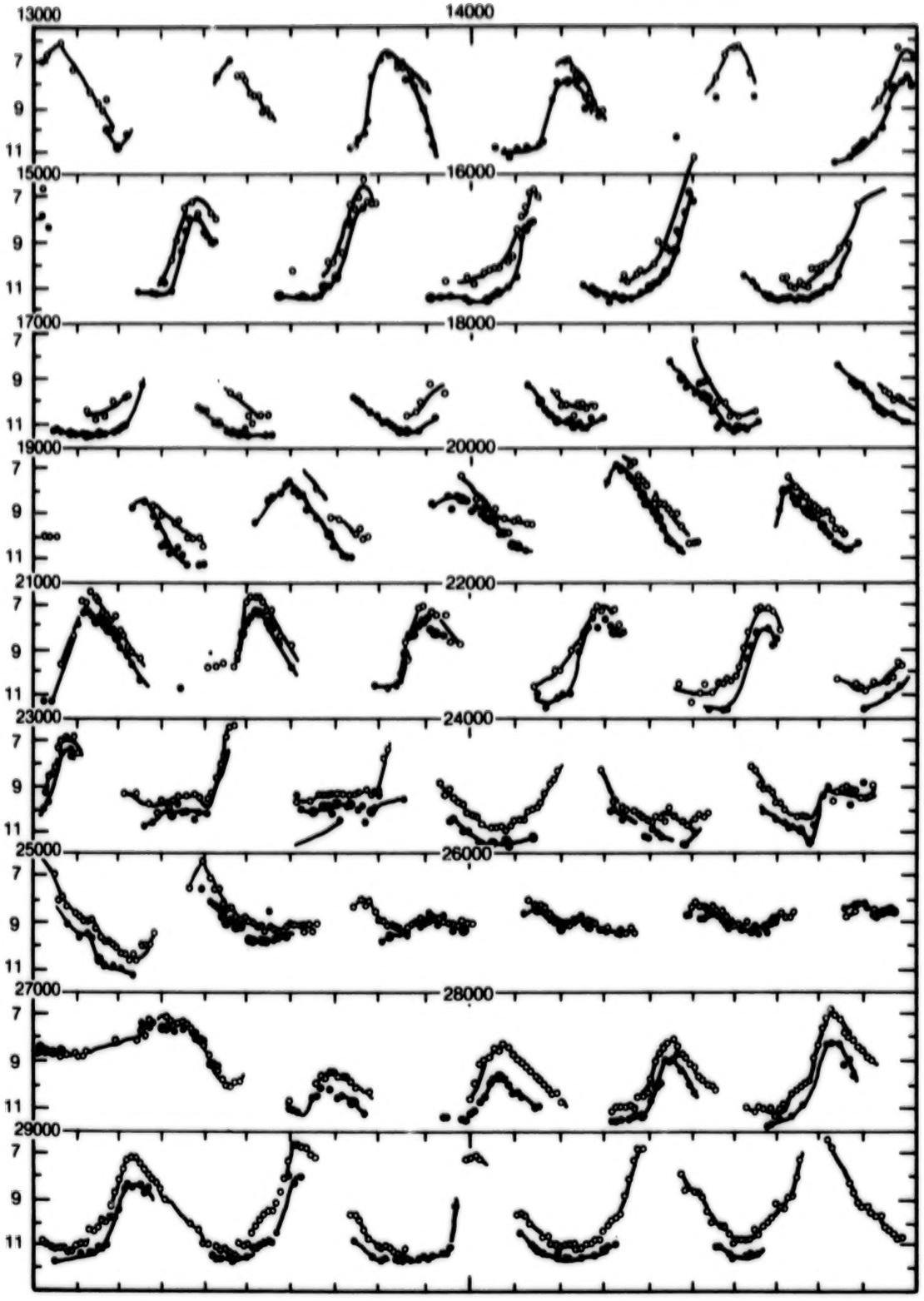


Figure 13-15. The light curve of R Aqr from 1895 to 1941 Mattei, 1979). The visual magnitude is periodically variable between V = 6 and V = 11, with large variations from cycle to cycle. Note, in particular, the anomalies during 1905-10, 1928-30, and 1974-78, which could be associated with enhanced activity of the hot component. The mean Mira period is 387 days.

East and West from the central star giving to the nebula the aspect of a double lens (Figure 13-16).

The R Aqr nebula has been recently studied by Solf and Ulrich (1983) who found that the nebula is composed of two separate shells, which are expanding at velocity of 30-50 km s^{-1}. These shells should have been ejected from the central object 185 and 640 years ago. The spectrum of the nebula is typical of a (low excitation) planetary nebula. The problem is to find the central ionizing source, which could be identified with the unobserved hot companion of the red giant.

A few years ago Wallerstein and Greenstein (1980) first reported the detection in a 1977 plate of R Aqr of a "spike" of emission nebulosity that appeared as an elongation of the stellar image towards North-East, never reported previously. Using Lick plates, Herbig (1980) and Sopka et al. (1982) confirmed the jet-like feature that was, however, not present in a 1970 plate of R Aqr. Therefore, the jet should have appeared between 1970 and 1977. Sopka et al. also found the presence of an elongation in the radio map at 6 cm at the position of the optical jet. Later, higher spatial resolution radio observations obtained with the NRAO VLA of Socorro led to the identification of five separate radio sources (Figure 13-17), the "jet" (source B), a second jet closer to R Aqr, (A), a "counter-jet" (A'), while the central source C was resolved in two components separated by 0.5" (Hollis et al, 1985; 1986).

The radio jet is cospatial with the optical jet, and, because of the higher spatial resolution, can be studied with much more accuracy. Radio observations suggest an ordered geometry of ejecta: the distance of each knot, C2, A and B, from the central source C1 is linearly dependent on position angle (Hollis et al, 1986), and this should be associated with the mode of expulsion of the jets. According to Kafatos et al. (1986), components B, A, and C2 were formed during successive outbursts of the system, C2 being the most recent ejection, probably related to the mid-1970s event discussed above, while the two further ones should have been ejected long ago, during previous active phases of the object. At any rate, it should be considered that no expansion of the radio knots has been so far detected (e.g., Hollis et al. 1985).

High-resolution optical imagery of the R Aqr complex should provide precious complementary information on the nebula. Michalitsianos et al. (1988b) have recently studied the large-scale structure of the nebula using a CCD camera and narrow-band interference filters. Paresce et al. (1988) used a coronograph in conjunction with narrow band filters to imagine the immediate surroundings of R Aqr (1 to about 15 arcsec) at subarcsec spatial resolution. These observations have put in evidence an S-shaped bipolar shape which comprises the



Figure 13-16. (Plate) The planetary nebula around the symbiotic-Mira R Aqr (Kafatos and Michalitsianos, 1984).

radio jet features described above. The optical image is extended in both directions and at much larger distances than observable at radio wavelengths. Observations have also revealed the presence of several knots, including one not seen at radio wavelengths. This bipolar symmetry of the R Aqr inner nebula suggests a symmetric collimated flow from R Aqr, associated with a rotation or precession of the central object. For any consideration of this kind, the knowledge of the precise position of the star-like counterpart is very important. Michalitsianos et al. (1988b) derived the astrometric position of the Mira variable within about ±0.05". The star position is about 0.15" SW of the central radio source C1 (Figure 13-17) and provides clues to the origin and ionization structure of the HII region surrounding the R Aqr system. As discussed above, the SiO maser source is not coincident with the astrometric position of the Mira variable, as one would have been expected, but it is placed 1" SE from C1 and LPV, in the opposite direction of the radio jets. Again, this result has to be further investigated and compared with observations with similar accuracy of other symbiotic and Mira variables.

V.C. THE SYMBIOTIC SPECTRUM

The optical spectrum of R Aqr is rich in emission lines which are difficult to observe when the star is near maximum light. The hydrogen lines and the nebular [OIII] and [NeIII] are strong in emission. As in other symbiotics, the energy range is wide, as indicated by the presence of low- (FeII, [FeII], etc.) and high-ionization lines (HeII, NIII, CIII). During the optical outbursts, the latter ones become stronger and broader. Zirin (1976) reported the identification of the coronal [FeXIII] line at 10747 A in spectra made in 1970-71. But there are no other observations of this line.

The UV spectrum of R Aqr has been investigated since 1979 and has revealed the presence

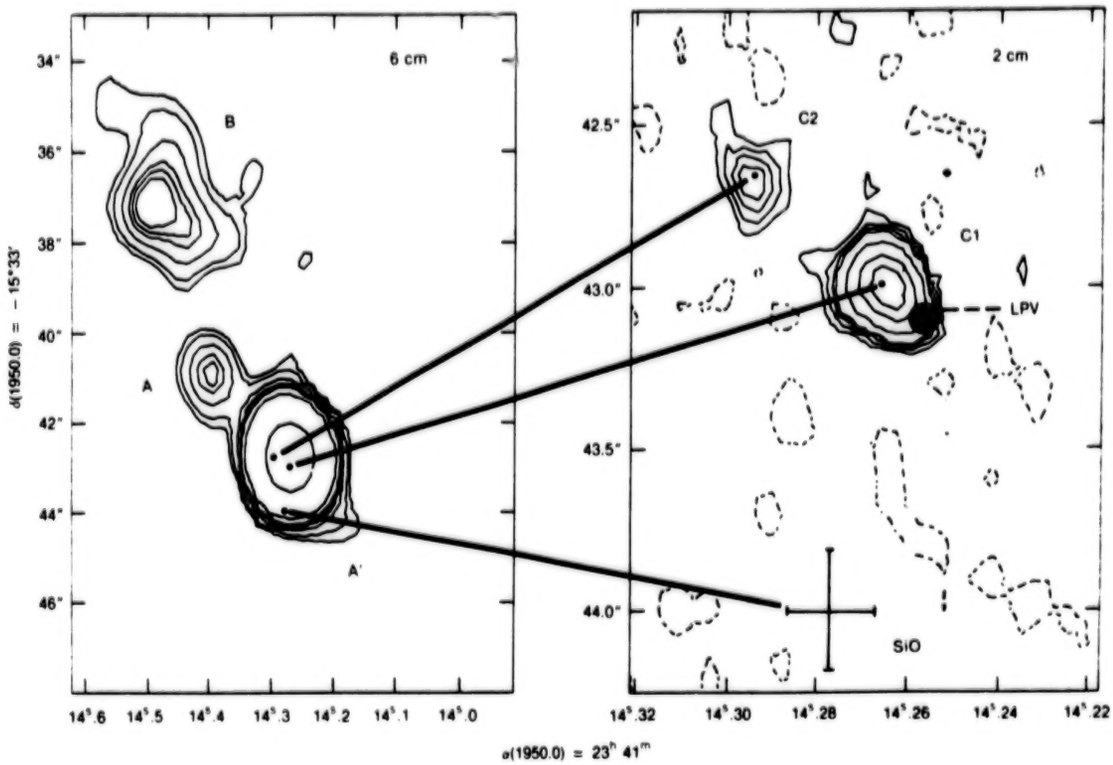


Figure 13-17. The high-resolution radio map of the central region of R Aqr. Left is the 6 cm map showing the "jet-like" features A and B, and, marginally, the counterjet A. Right the central source is resolved into two components—C1 and C2. The astrometric position of the Mira variable (LPV) and of the SiO maser emission is also indicated (from Michalitsianos et al., 1988).

of moderate-excitation emission lines with prominent CIII] and CIV, and weaker OI, CII, SiIV, OIV], and NIII] emissions. The overall far-UV spectrum is remarkably similar to that of Mira itself as described by Reimers and Cassatella (1985). The high-ionization lines of NV and HeII are weakly present. Kafatos et al. (1986) found that the line intensities for the central HII region are rather stable, in spite of the large Mira variations in the visual. On the contrary, the UV emission lines are largely variable in the jet A and B features. The high-ionization lines of NV and HeII were greatly intensified in the jet in 1982 and became even stronger than in the spectrum of the central source. Kafatos et al. (1986) noted that this increase of the ionization could be related to the first detection of X-rays from R Aqr (Viotti et al., 1987). During 1982-1986 the emission line intensities varied in a quasi-periodic way, with minima in 1983 and 1985, and maxima in early 1984 and possibly in late 1986 (Kafatos et al, 1986, and unpublished results). This one-and-half year modulation is larger than the Mira pulsation period, but could be related to it. In fact, if one takes into account the relative motion of the binary system following the recent close approach, the increasing distance between the two stars should cause a delay of the time of arrival of the matter from the Mira wind.

Emission line profiles observed at high resolution can tell us about the dynamical structure of the system. For this reason and to have as much information as possible on R Aqr, Michalitsianos et al. (1988a) recently attempted to obtain high-resolution ultraviolet images of R Aqr and its NE jet. Because of the faintness of the sources, these observations required about half a day of exposure, but the results were quite instructive. Michalitsianos et al. found that the CIV doublet in the nebula appeared broad, possibly double, with a FWHM of about 250 km s^{-1}. The doublet intensity ratio I(1548/I(1550) was close to the optically thin value of 2. In the central R Aqr core, the CIV doublet presented some multicomponent structure with 2 or 3 sharp components separated by about 40 km s^{-1}. In the core, the doublet intensity ratio I(1548)/I(1550) was found equal to about 0.5, i.e., much lower than the optically thick limit of unity. This anomalous *CIV doublet ratio intensity effect* has been observed in other symbiotic stars at least during some phases of their activity, such as in the case of CH Cyg (Marsi and Selvelli, 1987; see Table 11-8). Michalitsianos et al. (1988a) found that in RX Pup, the ratio I(1548)/I(1550) is variable in time, and that it is inversely correlated with the CIV line intensity, as well as with the visual luminosity. In Z And, Cassatella et al. (1988a) noted that the CIV doublet ratio was much smaller than one in February 1986, i.e., during the active phase started in September 1985, while it was slightly larger than one during minimum. An anomalous intensity for the NV resonance doublet was observed in the 1979 spectrum of AG Peg (Figure 11-31c). The "anomalous" doublet ratio intensity cannot be explained by simple considerations on the line opacity. In some cases, it could be the result of intense high-temperature interstellar lines, since in this case, the stronger emission component of the multiplet should also be the more depressed one by the interstellar line. Actually, we have already noted in Section 11.VIII.B that, in some cases, the anomalous intensity ratios of the OI resonance multiplet observed in the UV spectrum of some symbiotic stars has to be attributed to the interstellar line absorption. In R Aqr, the interstellar lines are weak. We cannot exclude that they could be partly responsible for the CIV structure in the core and in the nebula, but this possibility is excluded for the largely anomalous CIV doublet ratio in the core. As Michalitsianos et al. (1988a) discussed, to explain the observed profile complex, radiative transfer effects should be considered, which require a complete analysis under multiscattering conditions. According to spherically symmetric wind models for hot stars computed by Olson (1982) for resonance doublets whose separation is comparable to, or smaller than, the wind velocity, the source function of the longer wavelength doublet component depends on non local values of the shorter wavelength source function. Radiation scattered in our line of sight by the blue compo-

nent can be scattered again by the red line, enhancing emission in the red wing of the 1550 A line.

The presence of a high-velocity wind can be put in evidence by overlapping the two doublet components as shown in Figure 13-18. In the figure, the shaded area represents those points of the line profile, in velocity space, where the monochromatic flux of the 1548 A line is smaller than that of the 1550 A line. Taking into account the wavelength shift between the components, the shaded area corresponds to a velocity range from about -500 to -700 km s^{-1}. This should be the range of the P Cygni absorption of the 1550 A line in order to reduce the emission of the 1548 A line. Similar wind velocities can be derived for the other symbiotic stars showing this anomaly and represent an indirect evidence for the presence of high-velocity winds in symbiotic systems.

V.D. POSSIBLE MODELS FOR R AQR

The large amount of available data on R Aqr in all the spectral range should in principle aid in building detailed models of the system. However, it is difficult to find models which are capable of describing in a consistent way the whole observational information. In addition, some fundamental parameters such as the distance of R Aqr and the interstellar extinction are still uncertain. In the framework of binary models, the Mira should have an unseen companion producing the high-energy photons that ionize the compact central HII region, and the nebula (Michalitsianos, 1984). The hot companion is probably hidden by a disk or by opaque matter in the orbital plane which is seen nearly edge-on (Figure 13-19), and/or by circumstellar dust. Its nature is still uncertain: present infor-

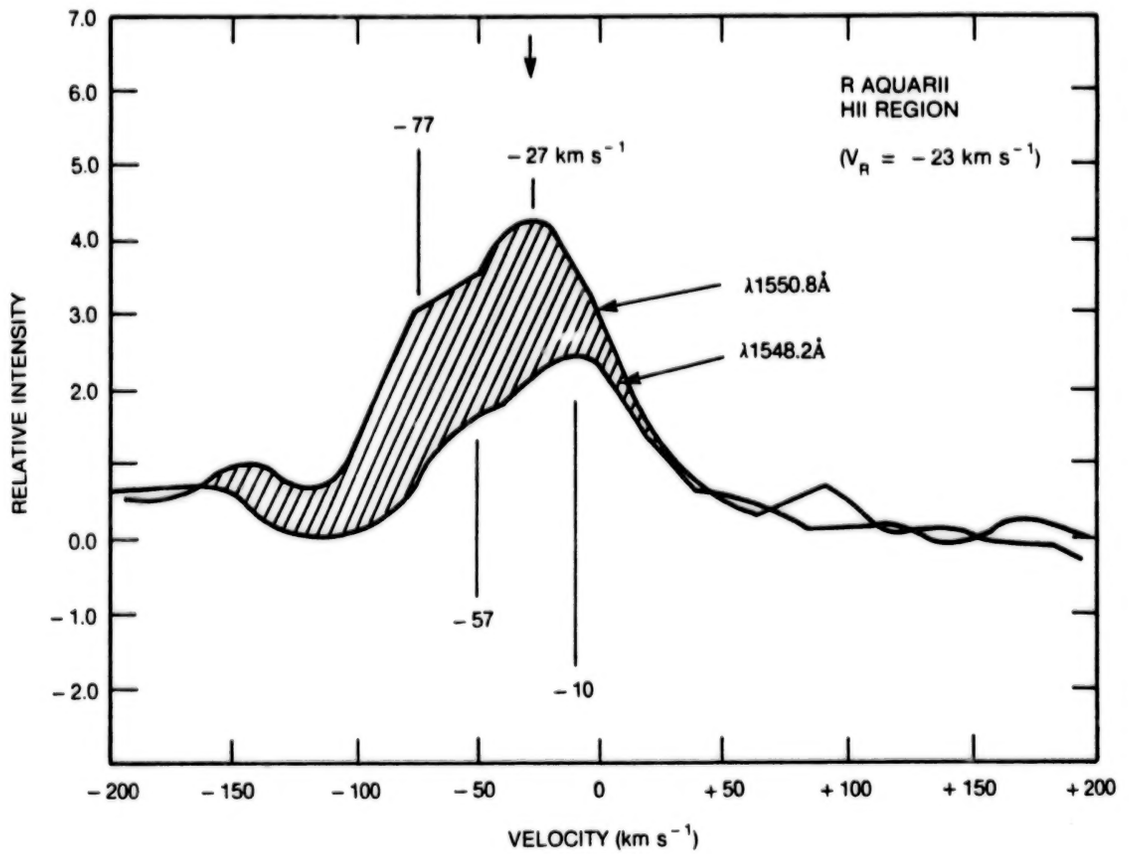


Figure 13-18. Comparison of the profile of the two components of the CIV doublet in the spectrum of the central core of R Aqr. The 1548 A line appears much fainter than the 1550 A line. Probably as the result of absorption by a high-velocity (500-700 km s^{-1}) wind. The shaded area indicates the region in the velocity space over which I(1548) /I(1550)< 1 (Michalitsianos et al., 1988a).

mation is not sufficient to decide whether the high-temperature source is a hot, possibly rejuvenated dwarf or the inner boundaries of an accretion disk. In any case, the disk would be considerably extended in the outer regions, where it should be much cooler and probably cause the temporary obscuration of the Mira discussed by Whitelock et al. (1983 a and b). The radiation from the central source is largely absorbed by the circumstellar matter. Therefore, in order to explain the highly ionized nebula, and the X-rays emerging from it, one has to suppose that the ionizing photons are mostly emitted perpendicularly to the line of sight, from regions that are less occulted (Viotti et al., 1987). Indeed, Kafatos et al. (1986)

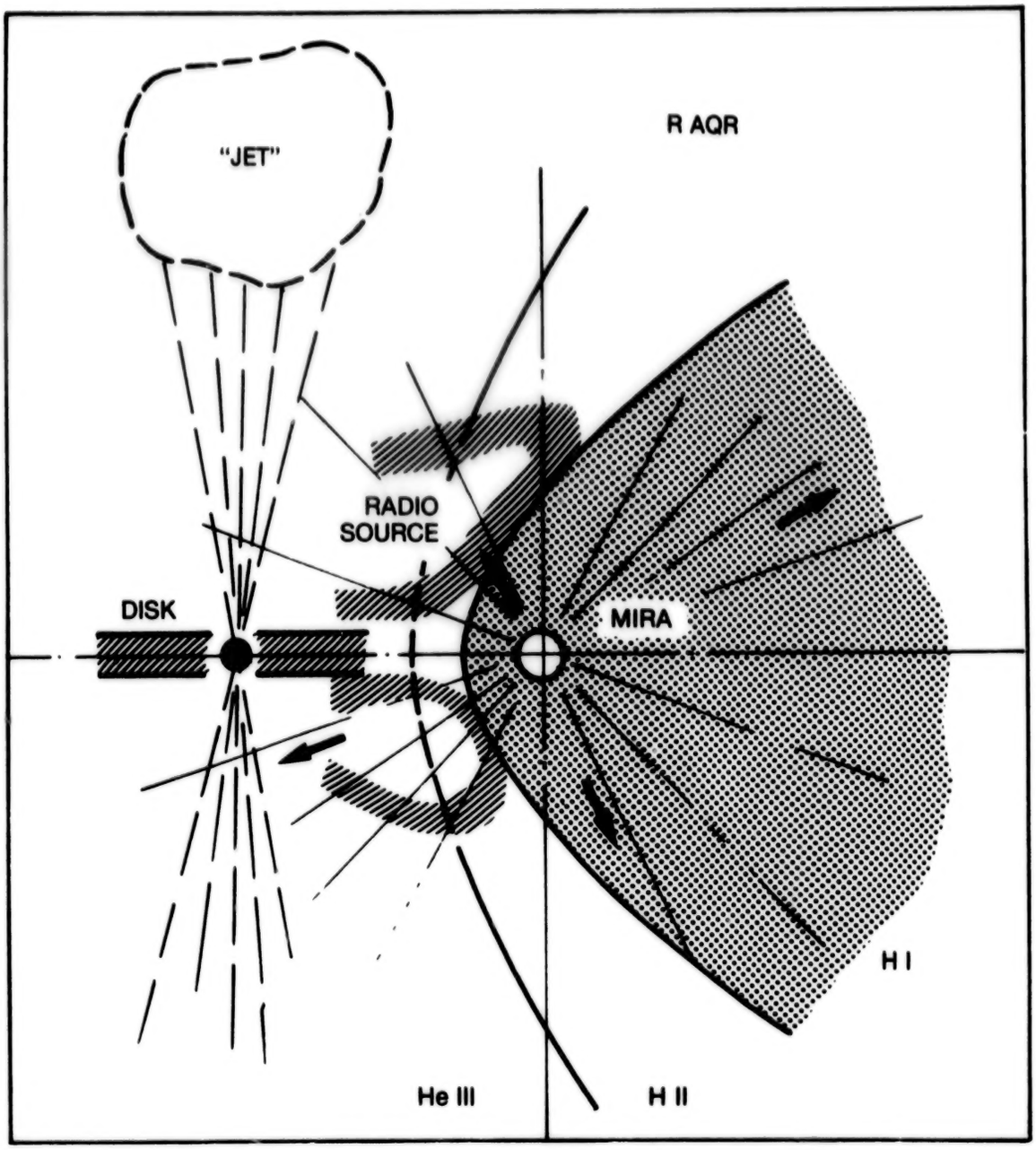


Figure 13-19. A model for R Aqr. The neutral wind from the Mira giant is ionized by the UV radiation from the hot subdwarf and /or the accretion disk, and originates the intense central radio source. The hot source is obscured in the direction of the line of sight (perpendicular to the figure) by the accretion disk or by matter in the equatorial plane. Intense ionizing radiation is emitted from the poles inside a cone, and hits the circumstellar cloud (the 'jets'), producing the high-ionization features (NV, HeII) and X-rays. Alternatively, the jets could be heated by shocks produced by the interaction of the hot source wind with the circumstellar environment.

explained the peculiar radio morphology of R Aqr as a consequence of photoionization of ejected material lying inside an ionizing radiation cone, whose axis is perpendicular to the orbital plane, and having an opening angle of about 150°. The hot source might also generate the high-velocity wind revealed by the anomalous CIV resonance doublet discussed above.

The high-temperature emission from the nebula can be alternatively interpreted as emission from a hot plasma, which can be heated material previously ejected from the central hot star. But, taking the electron density on the jet of 4×10^4 cm^{-3} derived by Kafatos et al. (1986) and an electron temperature of 3×10^5 K, the cooling time should be around 5×10^6 s, much shorter than the supposed time elapsed since the ejection. Such a warm matter, therefore, would cool in a rather short time. A possible heating mechanism could be the interaction of the ejected material with the circumstellar environment, producing shock waves. Viotti et al. (1988) found that, in this case, the emission measure of the HeII emitting region, assumed to have a temperature of 3×10^5 K, would be close to that derived from the X-ray flux assumed to be optically thin thermal emission at the same temperature. The low-electron temperature derived by Kafatos et al. (1986) using the CII] and CIII] line ratios would then be referred to cooler, not shocked parts of the nebula. A shockwave heating (or photoionization by a power law continuum) is also suggested by the [NII]/Hα ratio of 1.2 to 1.8 found by Paresce et al. (1988) in the nebula. But so far, it is not possible to decide which is the dominant heating mechanism of the jets.

The orbital elements of the R Aqr system are unknown. The period might be of several decades, as suggested by the modulation of the light curve (Willson et al., 1981). Such a period seems to be supported by radial velocity measurements (Andarao et al., 1985; Wallerstein, 1986). The separation of the stellar components should be large to account for a large mass transfer from the Mira to the dwarf star, and to feed the hot source. To overcome this problem, Kafatos and Michalitsianos (1982) proposed a high eccentricity of the orbit, in order to allow large mass accretion through Roche lobe overflow at the periastron passage. A geometrically accretion disk formed during this phase would produce at its inner boundary high-temperature photons, and possibly periodic ejection of matter. The intensified radiation field would also cause ejecta from previous outburst to brighten (Kafatos et al., 1986). This might explain the sudden (but apparent) appearance of the A and B jets around 1970, while according to Kafatos et al., the feature C2 (Figure 13-17) would represent the most recent ejection. The disk may also be formed by the capture of the Mira wind, which is enhanced during some periods by the close passage of the binary components in a moderately eccentric ($e \lesssim 0.5$) orbit (Kafatos et al., 1986). Again, such a model better explains the episodic outbursts and ejections observed in R Aqr. To give a better insight into this problem, accurate measurements of the Mira radial velocity over a few decades are needed.

V.E. PLANS FOR FUTURE OBSERVATIONS

R Aqr, for its relatively close distance (180-300 pc). and the many peculiarities represents an ideal target for future observations involving space experiments and high-technology ground telescopes. In particular, of special importance will be the high-resolution imagery at different wavelengths.

Figure 3-20 shows a set of CCD images of R Aqr obtained using the Space Telescope Science Institute coronograph, which occults the bright central star, thus, allowing a detailed study of the nebula very close to R Aqr with a subarcsec spatial resolution. Figure 13-21 shows the derived contour maps in the light of Hα and [NII] 6584 emission lines, where many emission knots are easily detected. Ultraviolet and visual images and polarimetry with subarcsec resolution will be possible with the Faint Object Camera of the Hubble Space Telescope, and should provide information about the location and physical structure of the high-temperature regions, including the X-ray source, and about the presence and nature of circumstellar dust. Concerning this prob-

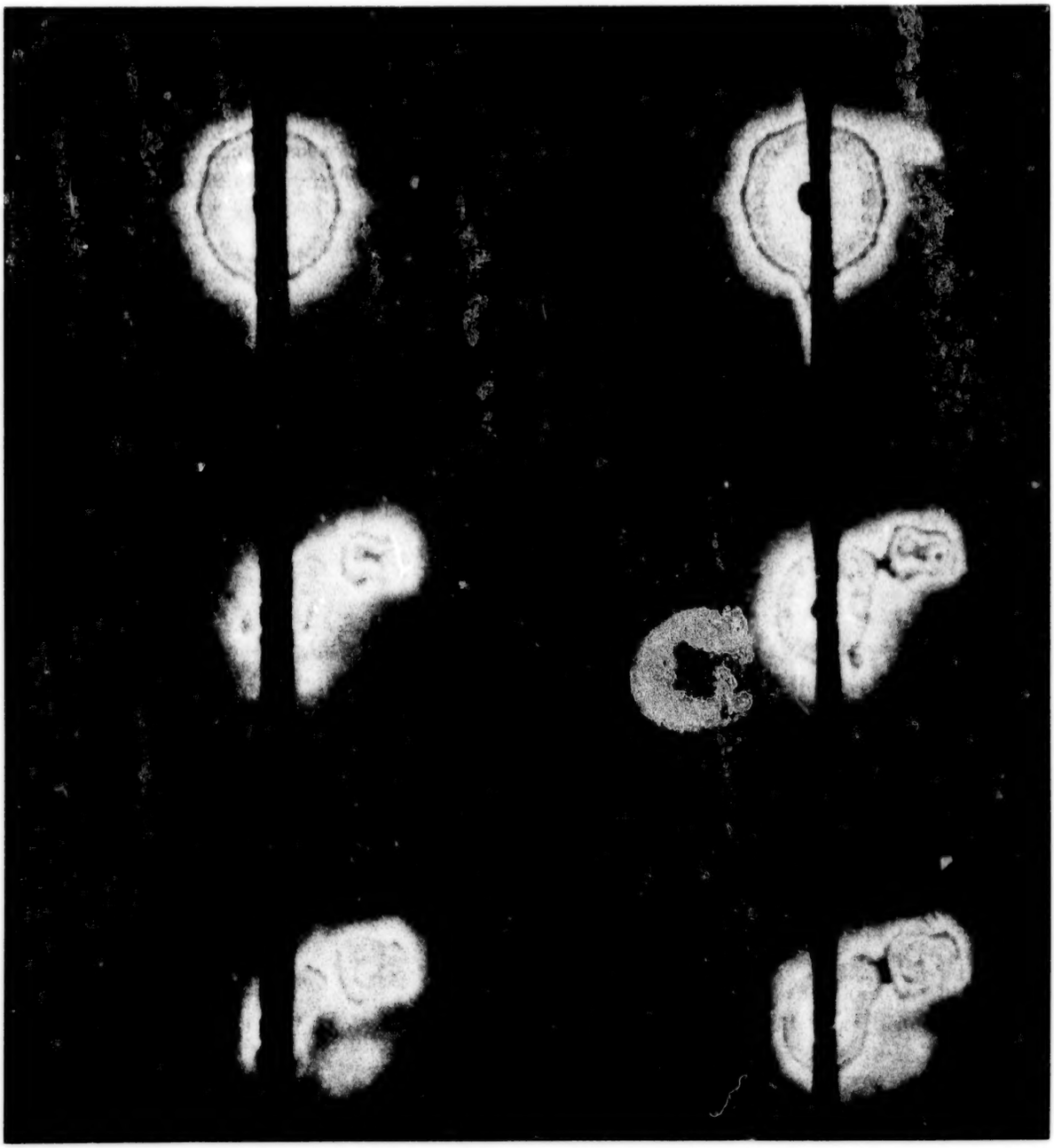


Figure 13-20. CCD images of R Aqr in a broadband R filter (left), and in narrowband filters centered on Hα (center) and [N II] 6584 (right). North is up and East to the left. Top row: original images, bottom row: final images in which the emission line contribution is subtracted from the R filter image, and the glow from the central star is subtracted from the narrowband filters (from Paresce et al., 1988).

lem, we expect very interesting results from the new high-quality infrared arrays. Recent IR imagery of R Aqr at 3.45 μm led to the discovery of an extended spherically symmetric halo that extends to about 15 arcsec from the central star (Schwarz et al., 1987.) Higher resolution IR imagery is needed to determine the spatial distribution of the cool matter and dust. In this regard, R Aqr probably represents a unique target to study the nature and structure of circumstellar dust, and the interaction of the stellar radiation and wind with the circumstellar environment in an evolved object.

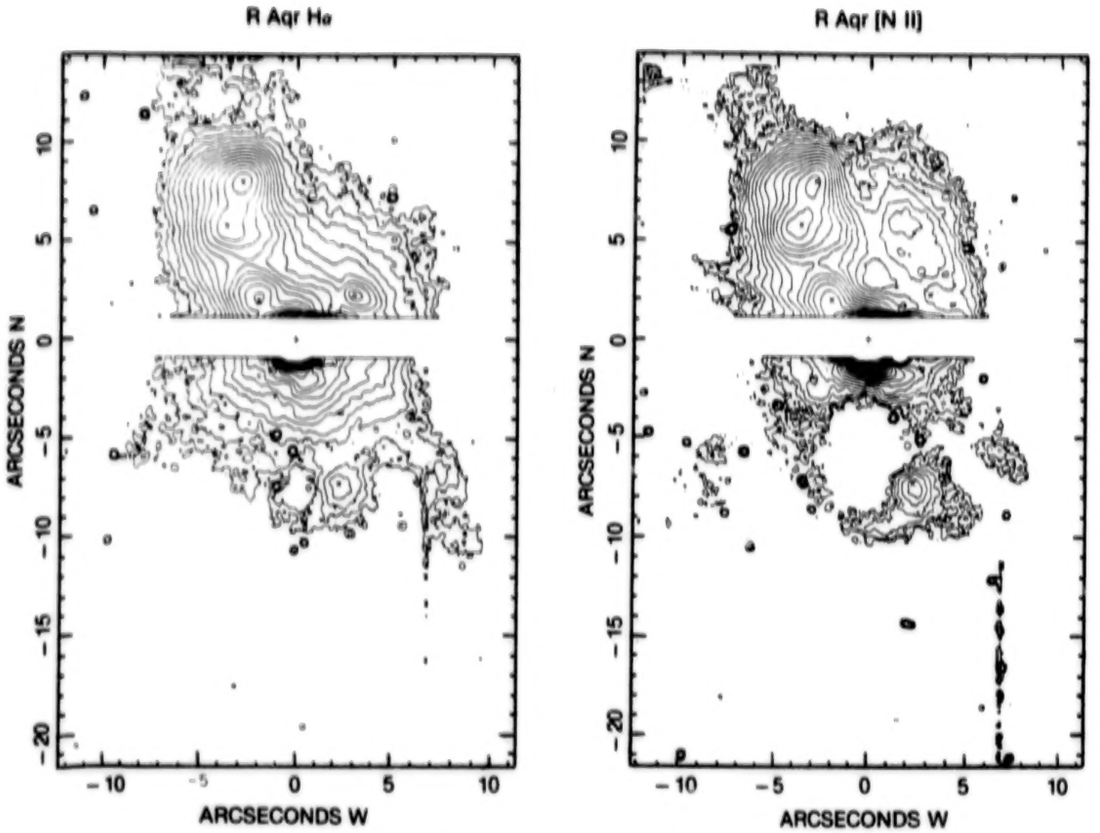


Figure 13-21. Contour maps of R Aqr in the light of Hα (left) and [NII] 6584 (right) as derived from the images in Fig 3-20 (Paresce et al., 1988).

VI. CH CYGNI: ANOTHER SYMBIOTIC VARIABLE WITH A JET

VI.A. INTRODUCTION

CH Cyg is classified as an Mb star in the HD catalogue. It has long been known for its semiregular light variability with a period ranging from 97 to 101 days (Wilson, 1942; Gaposchkin, 1952; Payne-Gaposchkin, 1954) and was classified M6 III. Beside this short-time variability, a long cycle of 4700 days or 12.8 years was found, not very different from that recently derived by using all the radial velocity measurements found in the literature by Yamashita and Maehara (1979) of 5750 ± 250 d and by Hack et al. (1986) of 5,000 ± 450 days. According to C. Payne-Gaposchkin (1954), the median maximum photographic magnitude was 7.97 and the median minimum, 8.44. Joy (1942) measured the radial velocity at different epochs and found an almost constant velocity (from -51 to -59 km/sec) for the M6 absorption lines. No emission lines were present in his spectra. Smak (1964) observed CH Cyg using narrow filter photometry during a period of 82 days. The visual magnitude varies from 7.06 to 6.64, and the color indices indicate that the star was bluer when fainter. This behavior is common to all M-type variables and could be ascribed to the TiO absorption bands, that affect the magnitudes B and V but not U, and are stronger at minimum. The photographic magnitude has been observed to vary between 7.9 and 9.1.

All the existing observations of CH Cyg before 1963 indicate a normal M6 III semiregular variable. In September 1963, Deutsch (1964) observed that CH Cyg "showed a composite spectrum. A hot, blue continuum was superposed over the late-type spectrum, together with emission lines of H (strong and wide), He I (weak and wide), [Fe II] (strong and narrow) and Ca II (also strong and narrow). The spectrum of the recurrent nova T Cr B closely resembled this in June 1945, a few months before the outburst of 1946. No doubt, there is a nova-like variable star in CH Cyg

system,too. However, a spectrogram of March 1961 showed no trace of the hot spectrum, which has faded appreciably since its discovery in September 1963." One high-resolution spectrum taken at the Haute Provence Observatory in August 1965 (Faraggiana and Hack, 1969) shows no evidence of symbiotic characteristics. The only peculiarity was an emission at H alpha and H beta and possibly at H gamma.

A second symbiotic episode started in June 1967 (Deutsch, 1967) and was over by late autumn 1970. A third episode started in 1977 and is almost over at the time of writing this report (July 1988). Luud et al. (1978) detected no trace of H alpha emission in spectra taken on May 1976, but in May 1977, H alpha and H beta showed a double emission peak with V/R>1. In August 1977, the presence of a blue continuum and of several emission lines was evident (Fehrenbach, 1977; Morris, 1977).

Spectra taken in July 1986 show the presence of numerous strong emissions, although the hot continuum has practically disappeared between November 1984 and January 1985. The emissions are fainter in 1987, but they are still easily detectable. In 1988, only Hα and Hβ are strong in emission. The strongest [Fe II] emissions are very faint, while the Fe II permitted emission lines have almost completely disappeared.

This last outburst episode has been observed with the IUE satellite since April 1978 (see Section VI.D.3 on the UV spectrum).

VI.B. THE LIGHT CURVE OF CH CYGNI

The light curve of CH Cyg from 1899 to 1975 has been described by Gusev (1976) and is illustrated in Figure 13-22. Until 1960, only small amplitude variations are present. The following period is described by Hopp and Witzigmann (1981), by Duschl (1983), Panov et al. (1985), and Mikolajewski and Tomov (1986). After the 1963 outburst, the oscillations became more evident and regular with a mean period of 700-800 days during 1967 to 1977. During the third outburst, the semiregular variations were no more detectable; the star reached V = 6.4 at the beginning of the outburst, and after three years at almost constant magnitude, reached V = 5.6 at the end of 1981 and remained close to this value until mid-1984. A sudden luminosity drop of about one magnitude occurred between July and August 1984 and was accompanied by strong spectral variation (for instance, weakening of the blue continuum, see Section VI.D.1)

The variation of the B-V and U-B colors from 1967 to 1985 are described by Hopp and Witzigmann; by Panov et al. and by Mikolajewski and Tomov.

In the period of quiescence 1970-1976, B-V is generally bluer at minimum as it was observed by Smak. In general, U-B is in phase with B-V with stronger fluctuations. Both indices become smaller (star bluer) at the beginning of the third outburst. During the outburst, B-V fluctuated between 0.4 and 0.6 and increased from 0.49 to 0.82 from Aug. 10, 1984, to September 30, 1984. U-B varies from 0.6 in mid-1976 to about -0.4 during the outburst, with oscillations between -0.3 and -0.7. After July 1984, U-B gradually increased. On November 24, 1984, it was equal to -0.29, and in May 1985, to about 0.0. (see Figure 13-22, light curve and color variation).

In addition to these long-period variations, which are typical of semiregular late-type variables, short-time scale (minutes), small amplitude variability has been observed during the periods of activity and will be described in the following sections.

VI.C. THE 1967 OUTBURST

The outburst of 1967-70 was followed both photometrically and spectroscopically by several observers.

A detailed description of the spectral variations from July 1967 to December 1970, covering the whole duration of the second observed outburst, has been given by Faraggiana and Hack (1971). Photometric observations during the same period have been made by several authors,

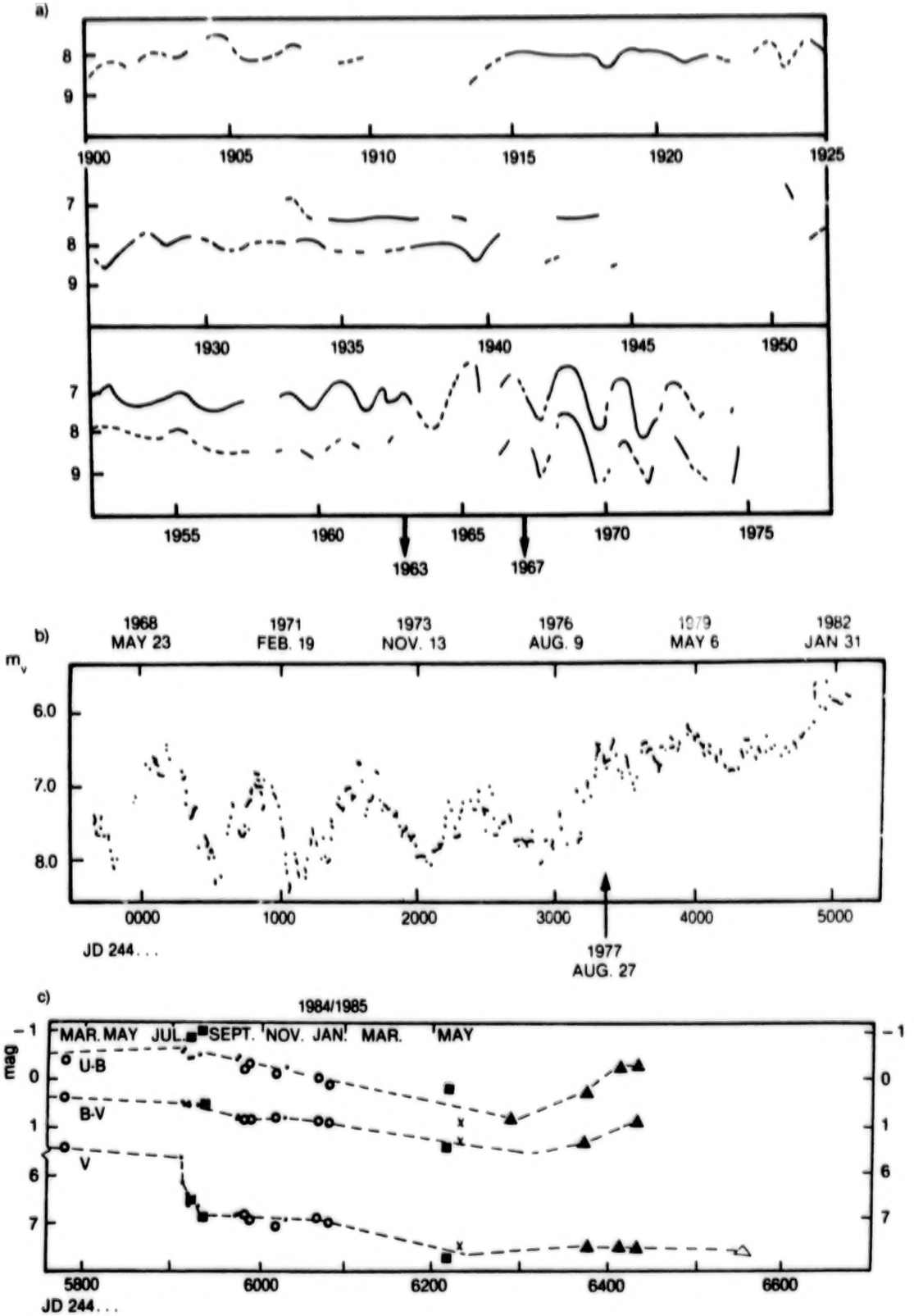
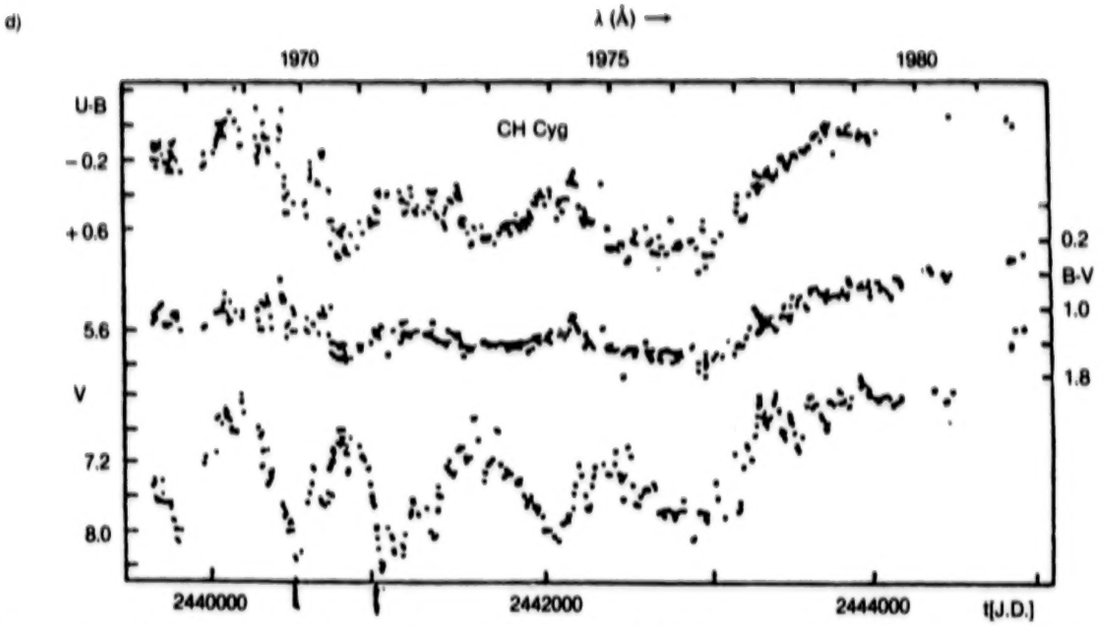


Figure 13-22. a) The visual light curve of CH Cyg from 1900 to 1975. The arrows indicate the epoch of starting of the two outbursts of 1963 and 1967. b) Visual light curve from 1968 to 1981. The arrow indicates the starting of the outburst of 1977. c) Visual light curve and B-V, U-B variation in 1984-1985. d) light curve and U-B variation from 1967 to 1982 (from Gusev, 1976; Duschl, 1983; Mikolajewski and Tomov, 1986; Mikolajewski, 1985; Panov et al., 1985; Mikolajewski and Wikierski, 1986; Hopp and Witzigmann, 1981).



The rapid variations (flickering) were first noted by Cester (1968) and by Wallerstein (1968). The amplitude was of the order of 0.1 mag on a few minutes time scale. Cester (1969) found that the variations were strongly correlated in different colors, and the color indices were quite different from those typical of an M6 III star: B-V oscillates between +1.3 and +1.0, and U-B, between –0.05 and -0.6. As a rule, the amplitude of the flickering is larger at shorter wavelengths. For instance, Shao and Liller (1971) reported variations of 32% at 3,200 A and of only 2% at 7,000 A. Figure 13.23 shows the flickering observed in U by Luud et al. (1970) on November 5, 1968. Walker et al. (1969) made photoelectric spectral scans from 3300 to 5000 A during August 1967. Figure 13.23 shows the excess continuum radiation relative to the standard M6 IIIab spectrum of 45 Ari for several scans made during the night of August 3, 1967. Variations on time scale of a few minutes are evident.

The main characteristics of the spectrum and its variations during the second outburst can be summarized as follows (Faraggiana and Hack, 1971):

a) The M6 spectrum is veiled by a continuum that partially fills the absorption lines and increases in intensity toward the violet. This continuum was absent in August 1965 and in September 1970; it appeared in June 1967 (Deutsch, 1967) and reached a maximum in August 1968. The color temperature of the blue continuum was about 10,000 K. No measurable Balmer discontinuity was observable.

b) Emission lines of He I, Fe II, [FeII] and [SII] are present. The Balmer lines and the H and K lines of Ca II present a P Cygni profile. In July and August, H and K presented two sharp absorption cores at radial velocity of about -75 and -160 km/s, while the radial velocity of the photospheric lines (TiO bands and nonresonance lines of neutral metallic atoms) ranges between -50 and -60. In July 1968, the nebular line 5007 [OIII] appeared; 4959 and 4363 [OIII] were not visible. The emissions reached maximum intensity in August 1968 and again in August 1969. In 1965 and 1966 and in September-December 1970, the spectrum was a normal M6 III type, except that H alpha and H beta presented emission components.

c) Low-excitation absorption lines of metallic ions appeared in the ultraviolet continuum in July 1968. In May 1970, several lines of neutral elements appeared. At this epoch, the ultraviolet lines of low excitation ions and the strong resonance lines give radial velocities more negative than the other lines having the same low level by about 20 km/s and are not filled in by the blue continuum. This may suggest that they were formed in the blue continuum like a kind

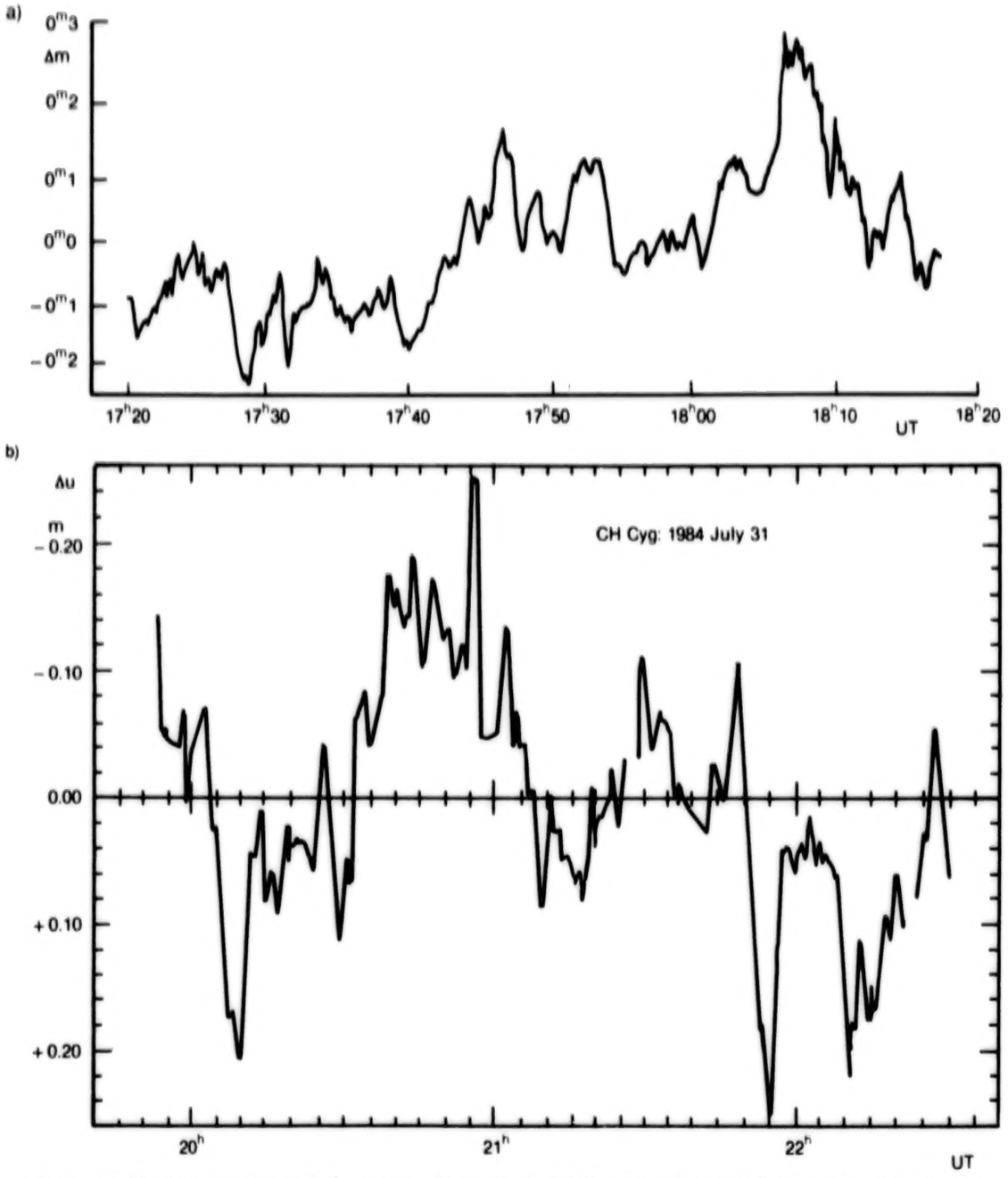


Figure 13-23. a) Observations of U flickering on November 5, 1968 (from Luud et al., 1970), b) and on July 31, 1984 (from Panov et al., 1985.

of shell absorption. Significant spectral variations have been observed over a few days. For instance, the Balmer lines were in emission on May 13, 1970, and in absorption on May 16, 1970.

The ratio [FeII]/Fe II is constant during the whole outburst, indicating no change in density, while the line intensity was variable.

VI.D. THE OUTBURST STARTED IN 1977

The last outburst began in 1977 and was followed by several observers in a wide spectral range from UV and X-rays to optical, infrared, and radio.

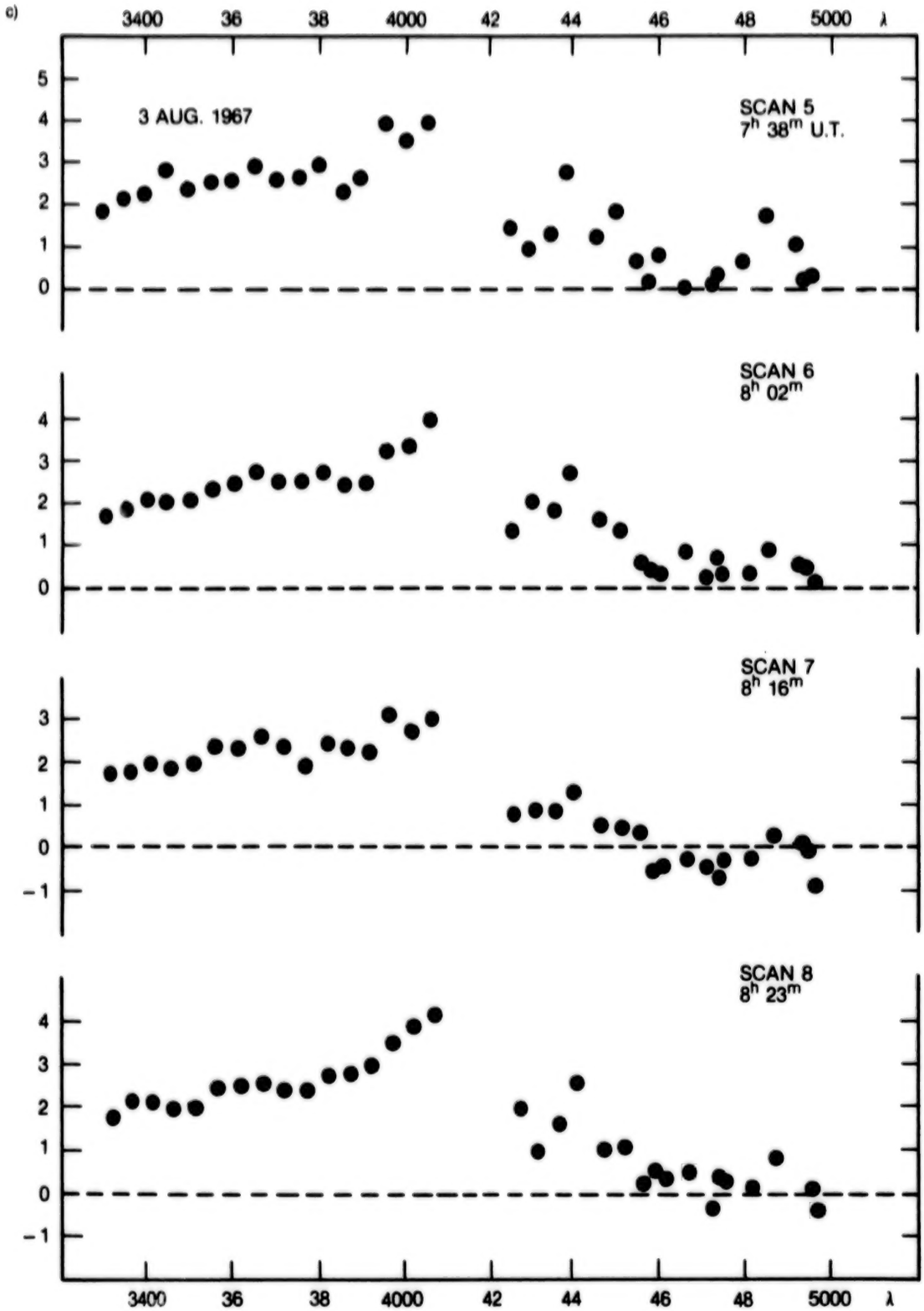


Figure 13-23. c) Excess continuum radiation in the spectrum of CH Cyg relative to the standard M6IIIab spectrum of 45 Ari, for twelve scans taken on the night of August 3, 1967. Ordinate is in flux units with an arbitrary scale factor applied (from Walker et al., 1969).

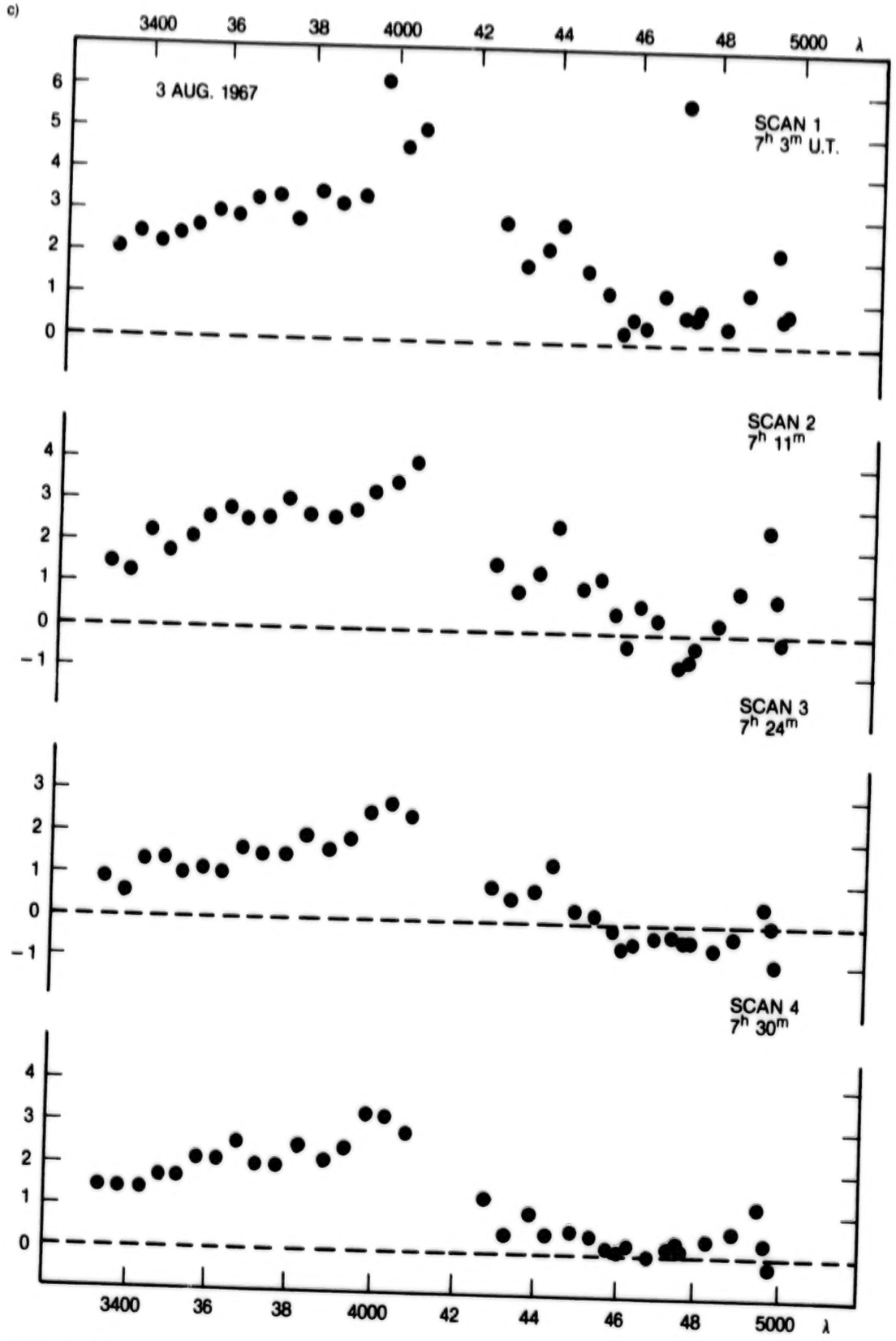


Figure 13-23. c) continued.

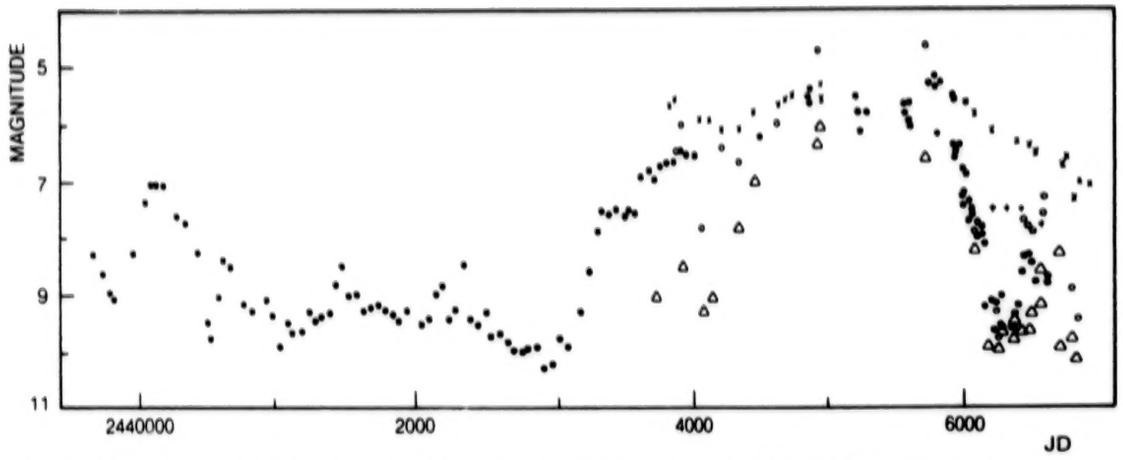


Figure 13-24. Ultraviolet light curve of CH Cyg showing the two minima in 1969 and 1985. (●) U magnitude, + V magnitude measured from the ground (x) V magnitude measured with the Faint Error Sensor, (FES) aboard IUE, (o) m (3000 A) derived from the IUE fluxes: m(3000) = -2.5 log F(3000) -22; (Δ) m(1440) = -2.5 log F(1440) -22. The constant 22 has been arbitrarily chosen.

The International Ultraviolet Explorer (IUE) has given us the opportunity of follow the outburst in the ultraviolet since April 1978.

VI.D.1. PHOTOMETRIC OBSERVATIONS

As we have observed in Section VI.B, the semiregular light variations with a period of 700-800 days disappeared during the third outburst when V gradually rose to 6.4 at the beginning of the outburst, then rose to 5.6 and remained at this value until July 1984, when its brightness dropped by about one magnitude (Mikolajewski and Tomov, 1986). One year later, V was equal to 7.8.

The U magnitude and the ultraviolet flux measured with IUE displayed a different behavior (Mikolajewski et al., 1987; Mikolajewski et al., 1988), i.e., a minimum lasting about 150 days (May - Oct. 1985). A broad minimum, especially in the U band (Cester, 1972; Luud et al., 1977), was observed in 1969. The possibility has been suggested that these two minima—separated by about 5700 days—were two consecutive eclipses of the hot companion of a binary system (Mikolajewski et al., 1987) (Figure 13-24).

Although the evidence of orbital motion given by radial velocities measured from 1942 to 1986 is weak because of the large scatter due to the irregular radial velocity variations, which are typically observed in late-type giants and supergiants, these measurements suggest a period of 13 to 15.5 years (Yamashita and Maehara, 1979; Hack et al., 1986). Our last observations, added to all those existing since 1961, suggest P = 14.4 years or 5250 days, not very far from the value suggested above. (see Figure 13-27, radial velocity curve). High-speed photometry confirmed the presence of flickering during the present phase. Slovak and Africano (1978) observed an amplitude of about 0.10 mag in the ultraviolet and violet light (u and v filters) and of only 0.03 mag in y filter. Actually, two features characterize the light curve: rapid flickering on time scale of 5 min and amplitude 0.02-0.04 mag and slow, large amplitude flares (0.10 mag) lasting 15-20 minutes. Panov et al. (1985) give a summary of the flickering amplitudes observed during this outburst (Table 13-4). The data obtained by Cester (1969) during the outburst of 1967 are given for comparison.

After the drop in brightness of July 1984, a drastic change in the spectrum was observed at the end of 1984, with the almost complete disappearance of the hot continuum (see next section), while a large rise of the radio flux was observed between April 1984 and May 1985 (Taylor and Seaquist, 1985; Taylor et al., 1986).

A fresh outbreak of activity (the end of the eclipse?) is indicated by the photometric observa-

TABLE 13-4. FLICKERING AMPLITUDES OF CH CYGNI FROM 1977 TO 1984 (FROM PANOV ET AL., 1985) AND IN 1968 (CESTER 1969).

Observers	δu	δB	δV
Slovak and Africano (1978)	0.10		0.03
Ichimura et al. (1979)	0.18	0.13	0.10
Luud et al. (1982)	0.20		
Spiesman (1984)	0.23	0.21	0.15
Reshetnikov and Khudyakova (1984)	0.20	0.20	0.20
Panov et al. (July 31, 1984)	0.6		
Panov et al. (Nov. 24, 1984)	0.24	0.17	0.12
Cester, 1969 (July 13, 1968 UT 23h 15)	0.24	0.24	
Cester, 1969 (Aug. 20, 1968 21h 45)	0.24	0.12	
Cester, 1969 (Aug. 24, 1968 22h 28)	0.44	0.24	
Cester, 1969 (Aug. 25, 1968 23h 05)	0.24	0.12	
Cester, 1969 (Aug. 25, 1968 24h 00)	0.36	0.24	

tions of Panov et al. (1985): On August 17, 1985, U = 7.38, U-B = 0.97, i.e., the color normally observed for CH Cyg in quiescence (Smak, 1964), as well as for several late-type semiregular variables. On December 9, 1985, U = 7.31, U-B = -0.021. As we shall also see in the following, the spectral changes confirm a slight strenghtening of the blue continuum, which was very weak in January 1985.

VI.D.2. SPECTROSCOPIC OBSERVATIONS

High-resolution spectroscopic observations of CH Cygni during the period 1977-1986 were made by several groups (Hack et al., 1982; 1986; 1988; Mikolajewski and Biernikowicz, 1986; Mikolajewski et al., 1987; Tomov and Luud 1984; Wallerstein, 1981; 1983; Wallerstein et al., 1986; Yoo and Yamashita, 1984). A general description of the visual spectrum and its variations was given by Hack et al. (1986, 1988). The spectrum, from the beginning of the outburst, in May 1977 to November 1984 is characterized by a continuum, that is stronger at shorter wavelengths but is also present in the red part of the spectrum, and partially or almost completely veils the M6 absorption features. The strength of this continuum is evident when comparing the regions of the TiO band heads or that of the broad absorption of Ca I at 4227 A observed during the outburst with those observed in 1970, after the end of the second outburst, or in 1988, when the outburst was almost over (Figure 13-25).

The prelude to the end of the outburst was observed from December 1984 to January 1985, when the visual spectrum became again that typical for an M6 III star, after the disappearance of the blue continuum. The emission lines, however, were still present and prominent; moreover, beside the emission lines of H I, Fe II, [Fe II], [O I], He I, [SII], emissions of [O III] and [Ne III] appeared in November 1984 and rapidly increased in intensity. The complex vari-

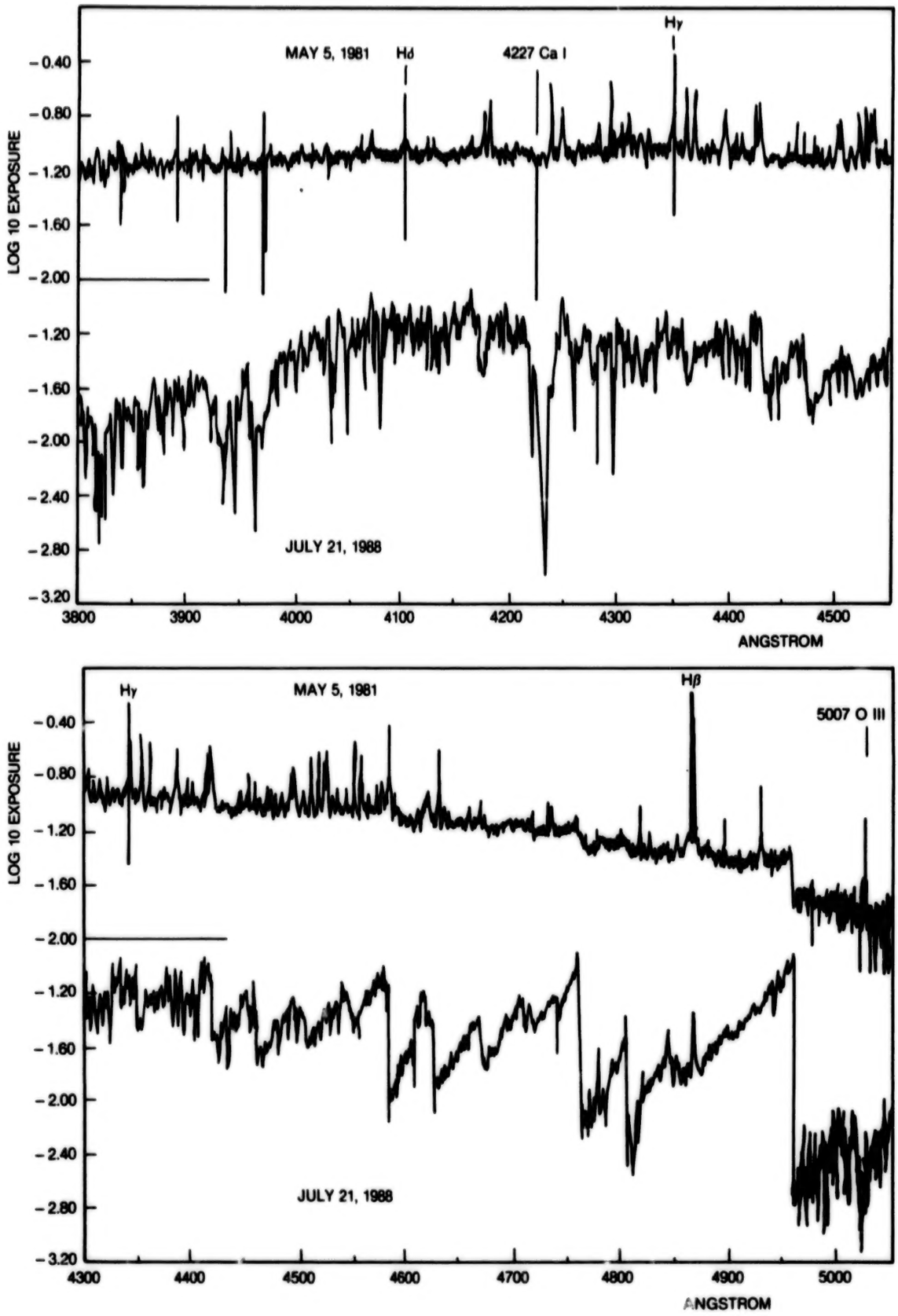


Figure 13-25. Intensity tracings of two spectra obtained on May 5, 1981 during the outburst and in July 21,1988, when the outburst is almost finished (Spectra obtained at the Haute Provence Observatory).

ability of the line intensities, line profiles, and radial velocities is described by Hack et al. (1986, 1988). Figures 11-8, and 13-26 give some examples of line variability.

It should be noted that the M6III photospheric lines and the forbidden and permitted Fe II emission lines have radial velocities that are 180° out of phase, suggesting that the Fe II emissions are associated with the companion (Figure 13-27). The relative amplitudes of the two curves suggests a mass ratio of the two components close to 1. Also, the absorption cores of the inverse P Cygni profiles of the metallic ions give radial velocities 180° out of phase with the primary photospheric lines (Figure 13-28). Mikolajewski et al. (1987), by the metallic ion absorption lines, derive $3 < m1/m2 < 4$. However, the radial velocities of the inverse P Cygni absorptions are affected by the presence of the emission wings, which partly mask the absorption cores affecting their measured shifts.

The most characteristic features that distinguish the second and third outburst are the following:

1) A similar behavior of the blue continuum, ...ever, it was bluer in 1977-84.

2) At certain epochs during the outburst, several metallic ions and Balmer lines showed direct P Cygni profiles in 1967-70 and inverse P Cygni profiles in 1977-84.

3) The Ca II H and K lines, on the contrary, displayed the same behavior during the two outburst showing one or two, occasionally three, violet-shifted absorption components and always direct P Cyg profiles, which clearly indicate the existence of one or several expanding envelopes. The highest observed expansion velocity is -100 km/s.

4) In both outbursts, emission lines of fairly high excitation were observed, i.e., He I during the whole outburst and [O III] at some phases. [Ne III] 3868,74 was observed only during the latter outburst.

5) The ratio between Fe II and [FeII] remained

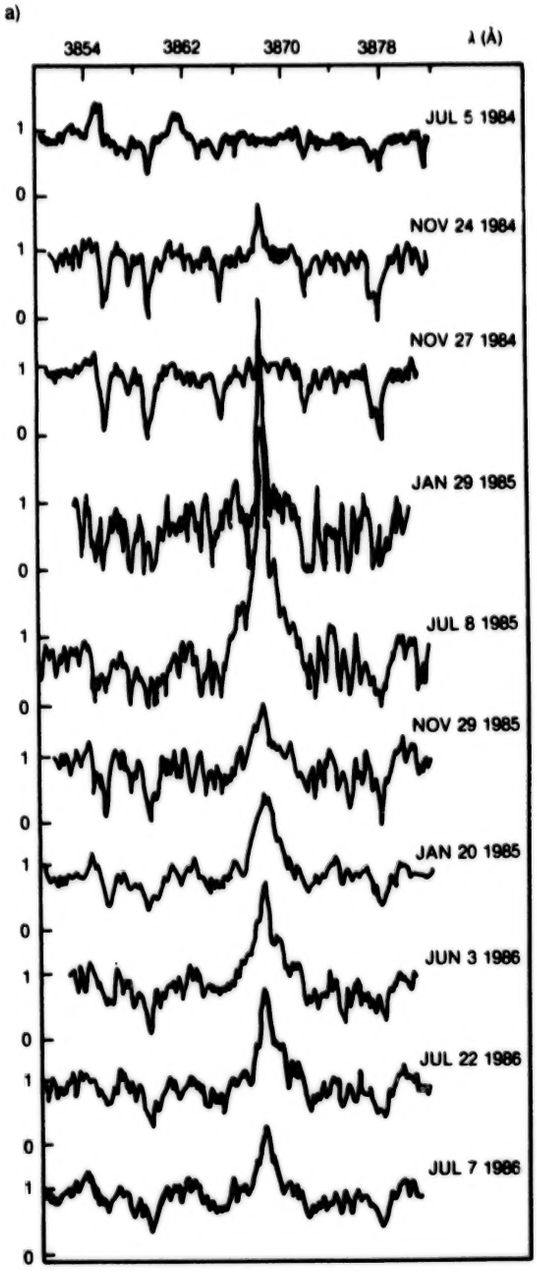
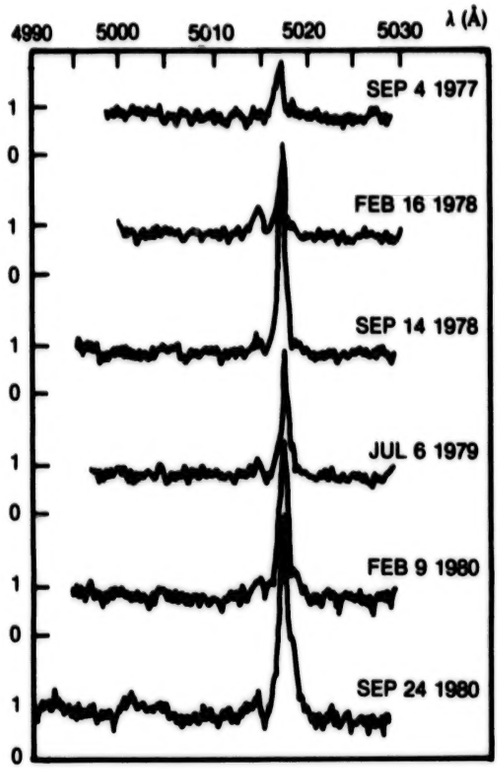
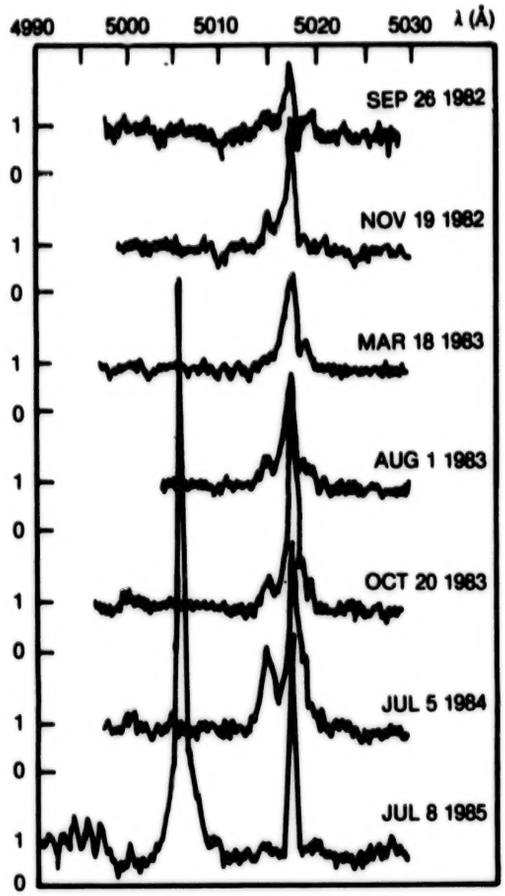


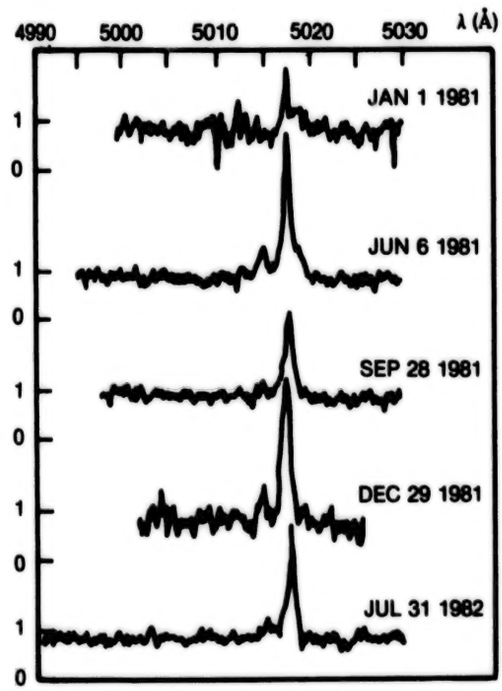
Figure 13-26. a) The region of 3868 [Ne III] from July 5, 1984, to July 7, 1986. b) The region of 5006.84 [O III], 5015.675 He I and 5018.434 Fe II (Spectra obtained at the Haute Provence Observatory).

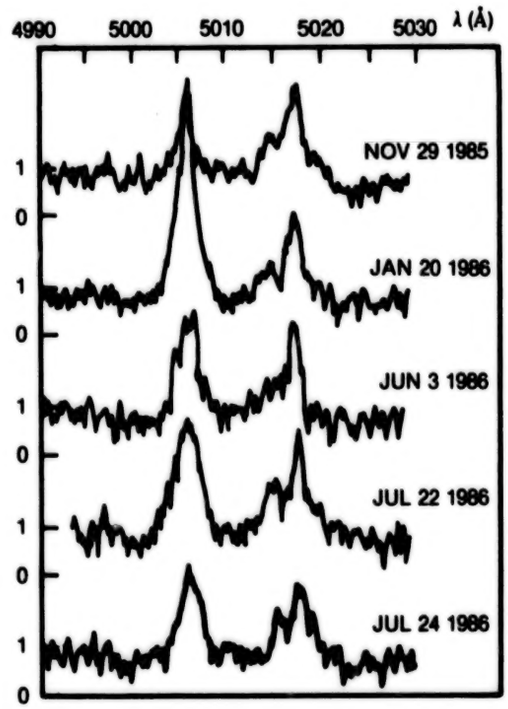
constant during the 1967-70 outburst, while during the 1977 outburst, it was variable with a significant decrease at the end of the outburst. These ratios indicate that the density in the region where the permitted and forbidden lines of Fe II are formed was lower in 1967-70 than during the latter outburst. The presence of the lines of [O I] at 6300, 6363 A indicate a density of about 10^6 cm^{-3}, while [FeII] indicates 10^8 -10^9 cm^{-3}.

b)


4990
5000
5010
5020
5030
λ (Å)
SEP 4 1977
FEB 16 1978
SEP 14 1978
JUL 6 1979
FEB 9 1980
SEP 24 1980
1
0


4990
5000
5010
5020
5030
λ (Å)
SEP 26 1982
NOV 19 1982
MAR 18 1983
AUG 1 1983
OCT 20 1983
JUL 5 1984
JUL 8 1985
1
0


4990
5000
5010
5020
5030
λ (Å)
JAN 1 1981
JUN 6 1981
SEP 28 1981
DEC 29 1981
JUL 31 1982
1
0


4990
5000
5010
5020
5030
λ (Å)
NOV 29 1985
JAN 20 1986
JUN 3 1986
JUL 22 1986
JUL 24 1986
1
0

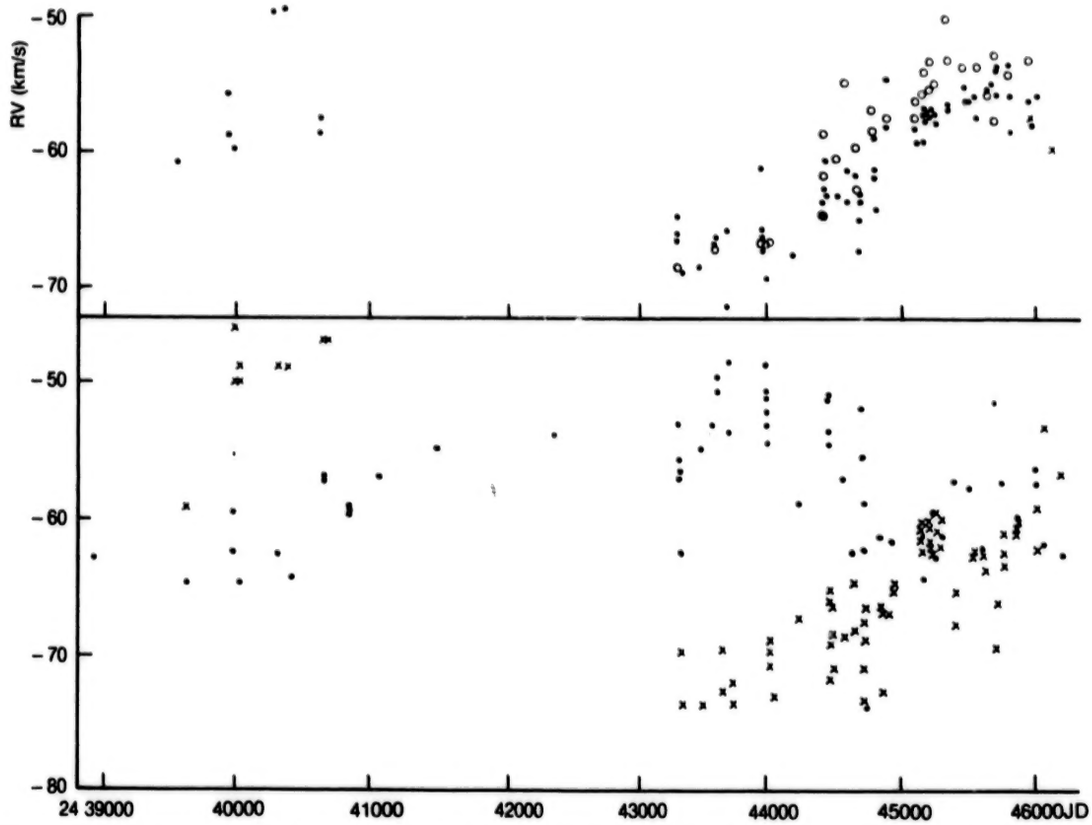


Figure 13-27. Bottom: radial velocities of the M6 III photospheric lines (●) and of Fe II permitted emission lines (x) vs. J.D. Top: Radial velocities of the forbidden lines of Fe II (●), O I (o) and O III (x), from Hack et al., 1986).

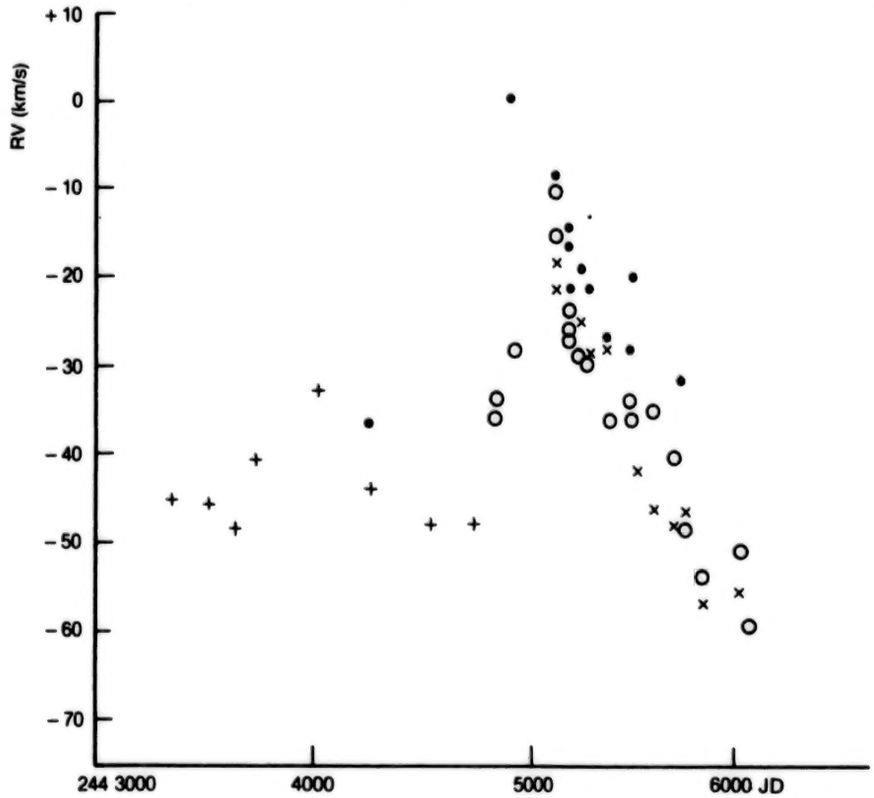


Figure 13-28. Radial velocities of the absorption cores of Fe II (o), Ti II (●), Mg I (x) and mean of Ti II, V II, Cr II, Mn II (+) (from Hack et al., 1986).

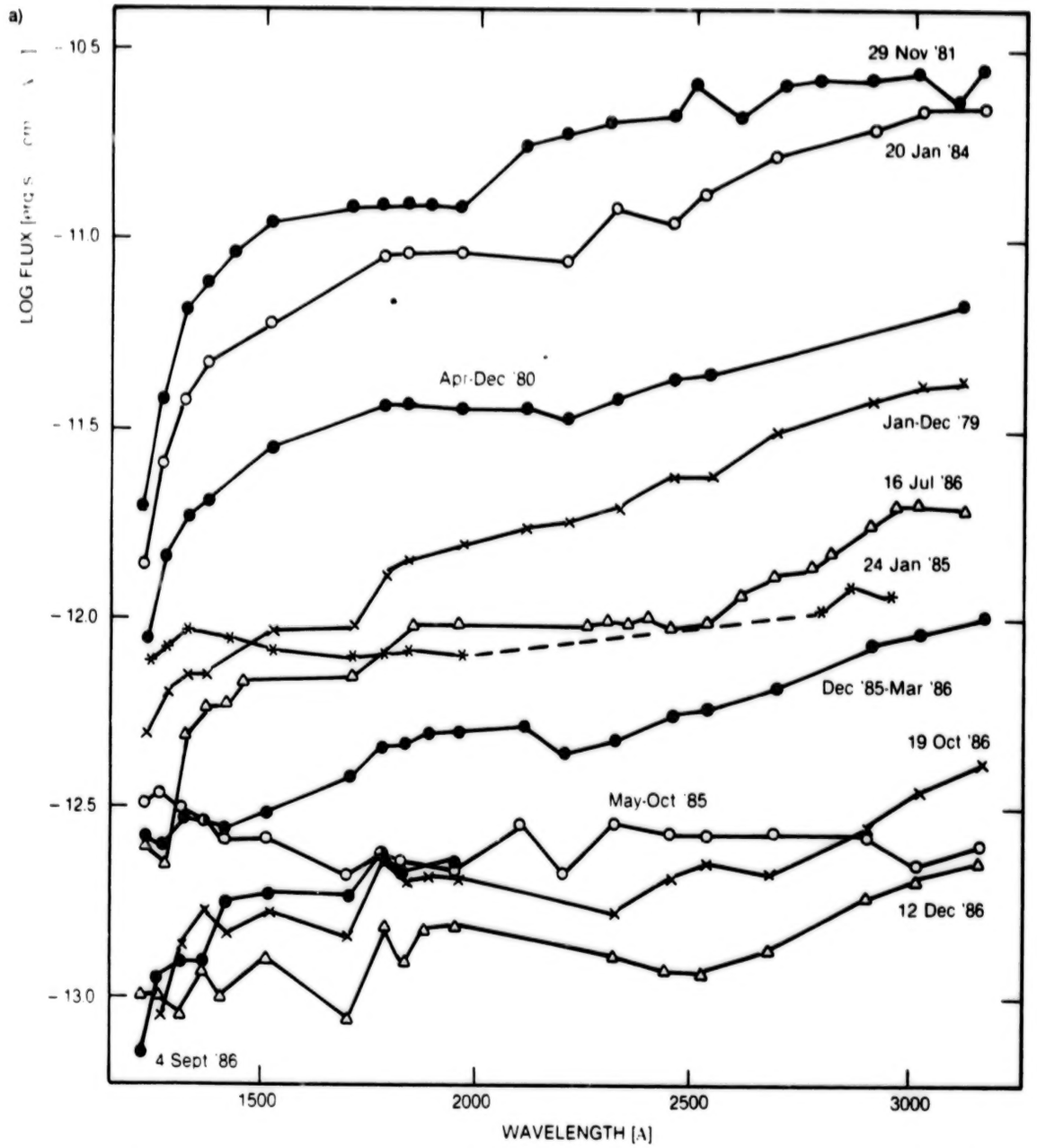
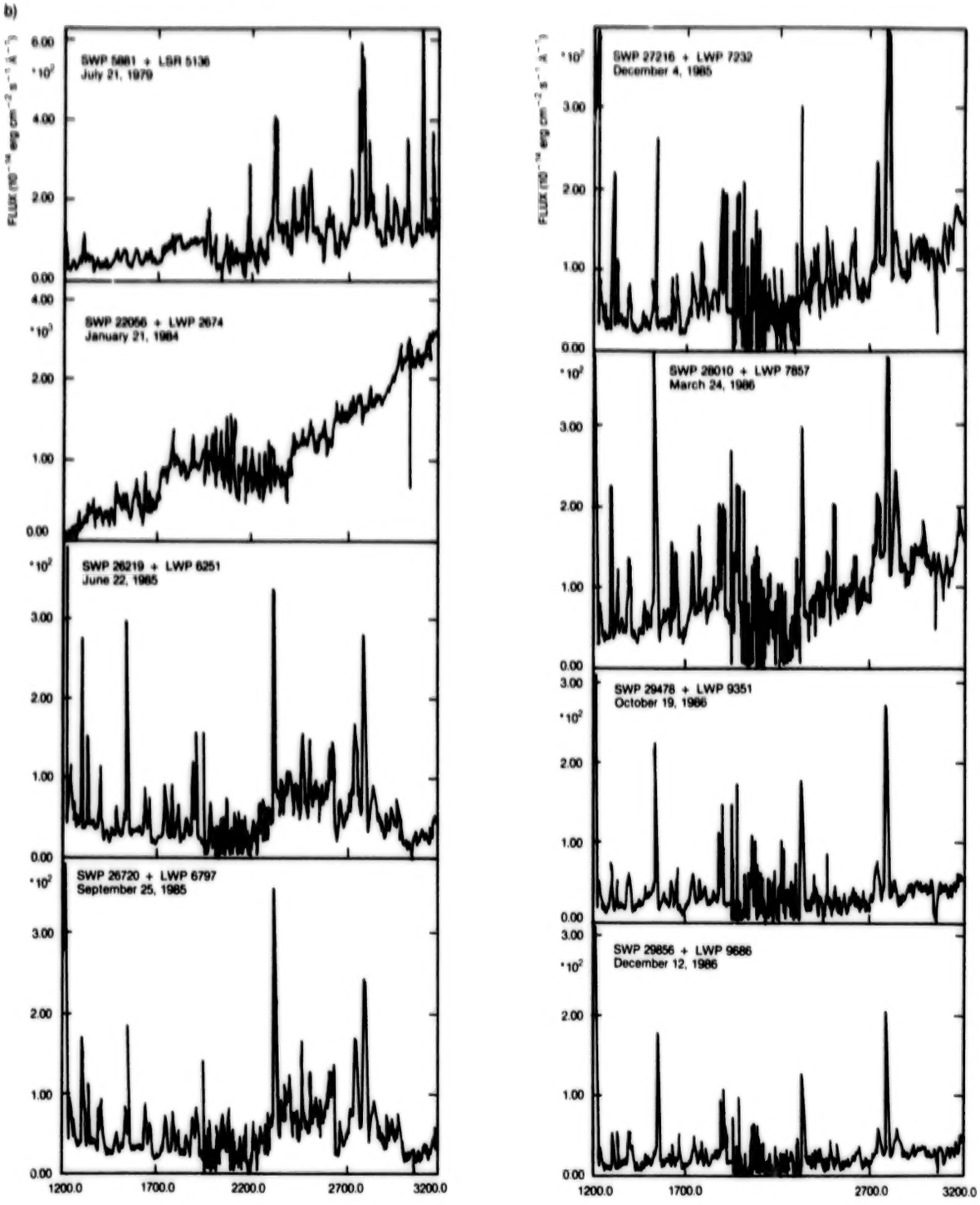


Figure 13-29. a) Continuum energy distribution in CH Cyg; b) Combined UV low-resolution spectra (1200-3200 A) of CH Cyg; c) Far UV low-resolution specta of CH Cyg. (from Mikolajewska et al., 1988).

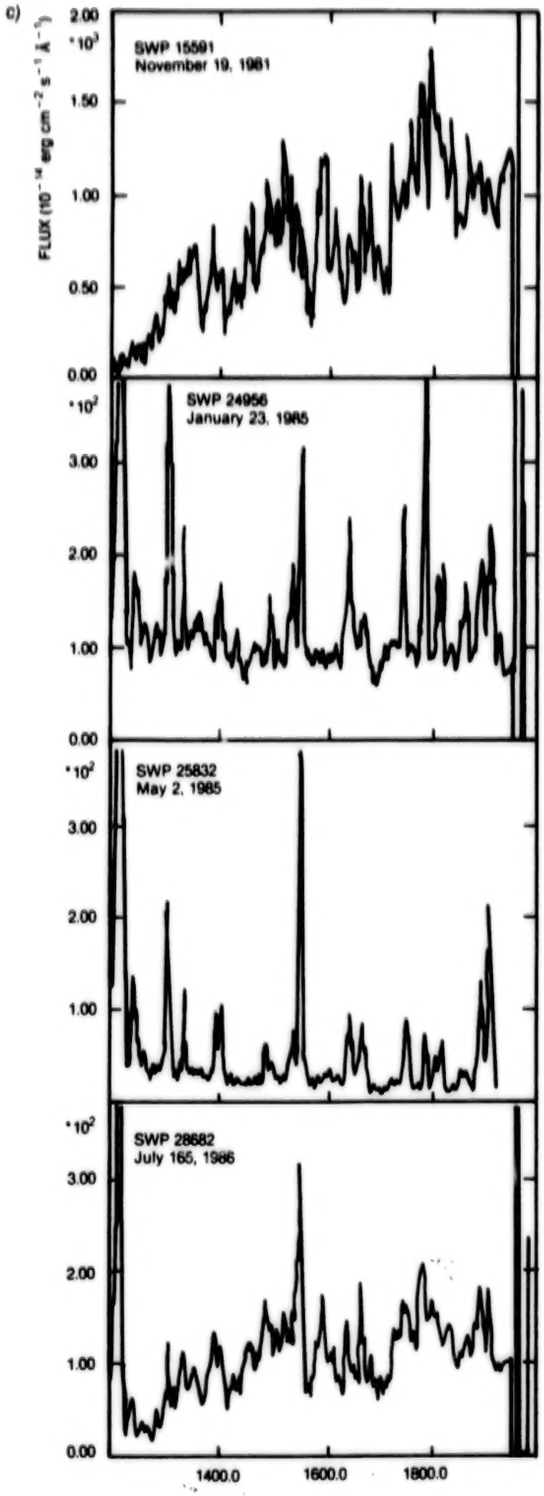
VI.D.3. THE ULTRAVIOLET SPECTRUM

The ultraviolet spectrum was also observed during the whole outburst with IUE in the low-resolution mode (6 A) and, when possible, also in the high-resolution mode (0.2A). The variation of the UV continuous flux from 1200 to 3200 A during the period 1978 to 1986 was studied by Mikolajewska et al. (1987, 1988). Figure 13-29 shows the ultraviolet energy distribution and its strong variation with time. Not only the flux varies but also the shape of the continuum, which becomes completely flat in January 1985, remains flat to October 1985 and starts increasing toward the longer wavelengths in December 1985. A drop in the flux intensity by a factor of three was observed between January 24, 1985, and May 27, 1985. Unfortunately, no other IUE observations were made during the rest of 1984. Hence, we cannot decide whether the drop observed in visual light in August 1984



was also present in the UV. In December 1985, the far ultraviolet flux started to rise again (in concomitance with the increase of the continuum observed in the visual) and reached a secondary maximum in July 1986, while in Septemper 1986 it declined back to the level of October 1985 (see also Figure 13-24). In 1988, the flux in the far UV had decreased considerably (to about 20 times weaker than in 1986), but it is interesting to note that at λ 1300 A, there is evidence of a slight increase of the flux toward the shorter wavelengths, suggesting that we are now observing the Rayleigh-Jeans tail of a hot-body radiation, a tail whose presence had been previously excluded on the basis of observations obtained until 1986-1987.

The ultraviolet line spectrum and its variations



during the outburst are described by Hack (1979), Hack et al. (1982), Hack and Selvelli (1982), Boehm et al. (1984), Persic et al. (1984) and by Selvelli and Hack (1985a,b). High-resolution spectra were obtained for the first time on March 1979 in the near UV (2000-3200 Å) and on September 1980 in the far UV (1200-2000 Å). The spectrum was characterized by the presence of both emission and absorption lines. We observed the emission lines of O I 1304 and O I] 1641, C III] 1909. 73, Si III] 1892, the multiplet 191 of Fe II at 1785, while all the other Fe II lines in the far UV were in absorption. Other absorption lines present in the spectrum of September 1980 were C IV, Si IV, Al II resonance lines, and a large number of ground level lines of Ni II. The strong Fe III lines from excited levels were not present. The Mg II resonance doublet presented a P Cygni profile with two absorption components, one at almost the rest velocity, probably of interstellar origin, and another shortward-shifted by about -110 km/s.

Hack and Selvelli (1982) discuss the excitation mechanisms for the O I and Fe II lines, which present some intriguing problems. For instance, the semiforbidden line 1641 O I] has about the same intensity as the strongest of the three permitted O I lines at 1302-1306 A, and the observed intensity ratio within the triplet 1302, 1304, and 1306 in September 1980 was 1:9.4:6.5 instead of the theoretical one of 5:3:1. The large optical thickness indicated by the strength of the permitted multiplet means that the 1304 photons will scatter many times before escaping from the region of neutral oxygen. Substantial reabsorption will occur mostly from the 0.00 eV level, and, therefore, the 1302 line will be weaker than the two other lines. There is a small but finite chance that at each coherent resonance scattering, decay from the upper term 3s $^3S^o$ will occur through the 1641 line, which shares the upper term with the 1304 multiplet. Hence, the great optical depth of the 1304 multiplet has the effect of converting the resonantly trapped photons into 1641 photons, which will escape easily. This phenomenon is observed in several emission line stars, like Z And, V 1016 Cyg, RR Tel, HD 45667: all present an anomalous intensity ratio in the 1304 triplet and the strong 1641 emission. Another characteristic common to several stars with extended envelopes is the presence of multiplet 191 of Fe II in emission, while the other far ultraviolet Fe II lines are in absorption. In this

case, we have a resonance fluorescence mechanism, i.e., absorption in the far ultraviolet followed by reemission at longer wavelengths:

a^6D ----> x^6P^o (UV mult. 9, λ~ 1260 in absorption)

x^6P^o ----> a^6S (UV mult. 191, λ~ 1785 in emission)

a^6S ----> a^6D (opt. mult. 7F, 4287-4475 in emission)

The spectrum observed in the high-resolution mode at the end of 1981 has about the same general appearance as it had in September 1980. It is noticeable the presence of practically all the Ni II absorption lines up to multiplet 30 (low EP=2.8 eV).

Unfortunately, no observations were made from the end of 1981 to January 1984. The spectrum in 1984 shows that the multiplet at 1303 of OI 1302-6). The high-resolution spectra are dominated by numerous and strong emission lines the same as in 1981. A spectacular change was detected in Junuary 1985, at about the same epoch of the disappearance of the blue continuum in the visual range (Selvelli and Hack, 1985a). The continuum in January 1985 has become completely flat, and the line spectrum has dramatically changed from an absorption-like to an emission-like spectrum (Figures 13-30 and 13-31); see also Figure 11-29a Lyα, and Figure 11-29b OI 1302-6). The high-resolution spectra are dominated by numerous and strong emission lines whose peak intensity rises to about 100 times the continuum. No absorptions are observable, also due to the weakness of the continuum. The emissions range from neutral species like O I and N I to highly ionized species like C IV, N V, and Si IV. New remarkable characteristics of the 1985 spectrum are:

a) The appearance of a strong and wide Ly Alpha emission (Full width at zero intensity = 16.4 A). The emission is cut by an absorption centered at rest wavelength (possibly of interstellar origin) 3.8 A wide.

b) The appearance of the other faint C III] line at 1906.68; all the other spectra only showed the strongest line of the doublet at 1908.73. The intensity ratio of the two lines indicates a decrease of the electron density to about 5 x 10^6 cm^{-3}.

The N V resonance doublet, which was never observed before either in emission or in absorption, and C IV, and Si IV, which were previouly present in absorption, are now in emission. The strong multiplet 34 of Fe III is present in emission. Fe II, which before January 1985 was one of the principal components of the absorption line spectrum in the far UV, starting with January 1985, changed completely to emission.

VI.D.4. INFRARED, RADIO AND X-RAY OBSERVATIONS

IR (1-20 μm) observations during the outburst have been made by Ipatov et al. (1984). The near-IR low-resolution spectrum of CH Cygni observed at different epochs in quiescence and in outburst remained nearly unchanged for wavelengths longer than 7000 A and is very similar to that of the M giants Alpha Her and g Her.

The light curve from 1978 to mid-1983 in J (1.25 μm) and in H (1.6 μm) shows long-term variability never exceeding 0.4 mag.

The IR energy distribution observed in 1982 is compared with the standard energy distribution of an M6 III star. An IR excess is present longward of 3.5 μm up to a factor of 10 at 20 μm.

The Infrared astronomical satellite (IRAS), which operated for 10 months in 1983, has observed CH Cygni (Kenyon et al., 1988), which allows us to extend its energy distribution curve in 1982 to 100 μm. The flux at 12 and 25 μm agrees well with the ground-based observations by Ipatov et al. at 10 and 20μm. The infrared excess in the IRAS range remains of the order of 10 with respect to the standard M6 III energy distribution (Figure 13-32). IR spectra (1.5-2.5 μm covering the time interval February 1979 to the end of 1984 have been made by Hinkle et al. (1985). The spectrum is that of a typical M giant, with the exception of very weak Brackett gamma emission. The velocities have been measured from the CO bands. It varies with a time scale of several hundred days but does not have a single

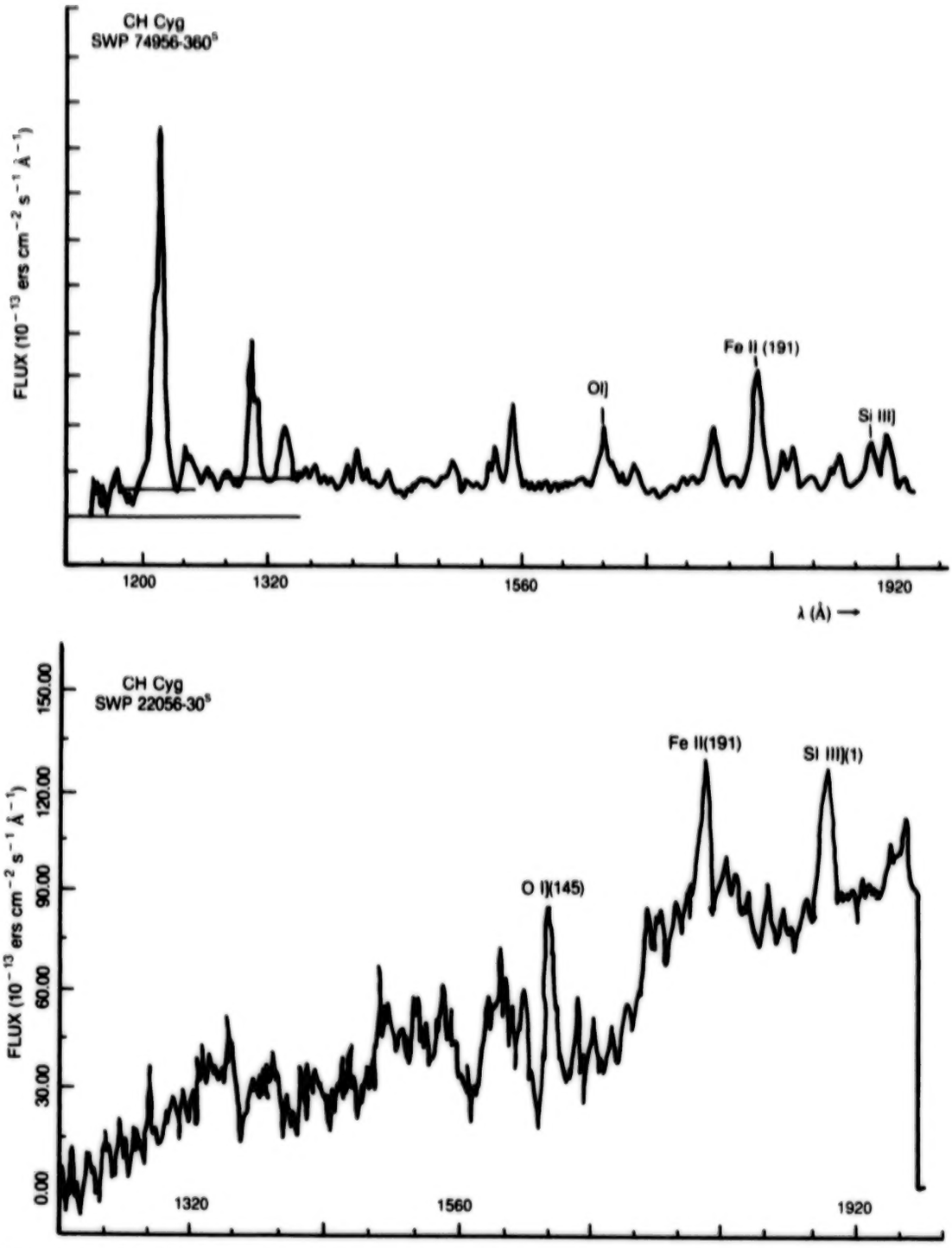


Figure 13-30. Far UV low-resolution spectra of CH Cyg taken on January 23, 1985 (top), and on January 20, 1984 (bottom).

periodicity, according to these authors. They found a median velocity of -63.5 km/s with an amplitude of 9 km/s, close to the values obtained from the visual region.

Hence, the IR observations do not show any clear evidence of the outburst that so strongly affects the optical and UV region. Observations in the radio range give more exciting results.

Taylor and Seaquist (1985) were monitoring several symbiotic stars. During the period April 1984 and May 1985, they discovered that CH Cyg underwent a strong radio outburst coincident

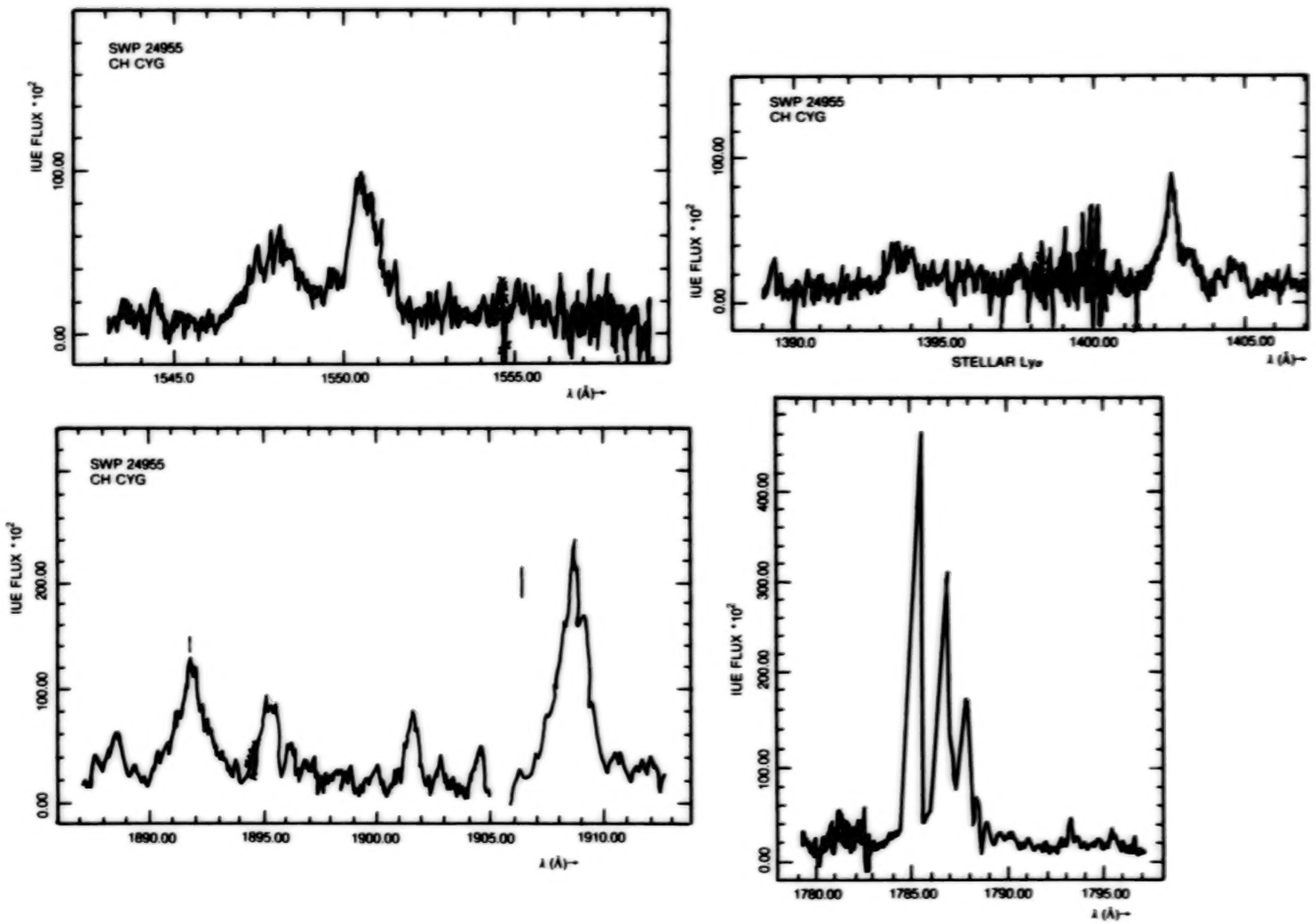


Figure 13-31. High-resolution UV line profiles observed in January 1985. a) C IV resonance doublet, b) Si IV resonance doublet; c) semiforbidden lines of C III at 1906 and 1909; d) the multiplet 191 of Fe II.

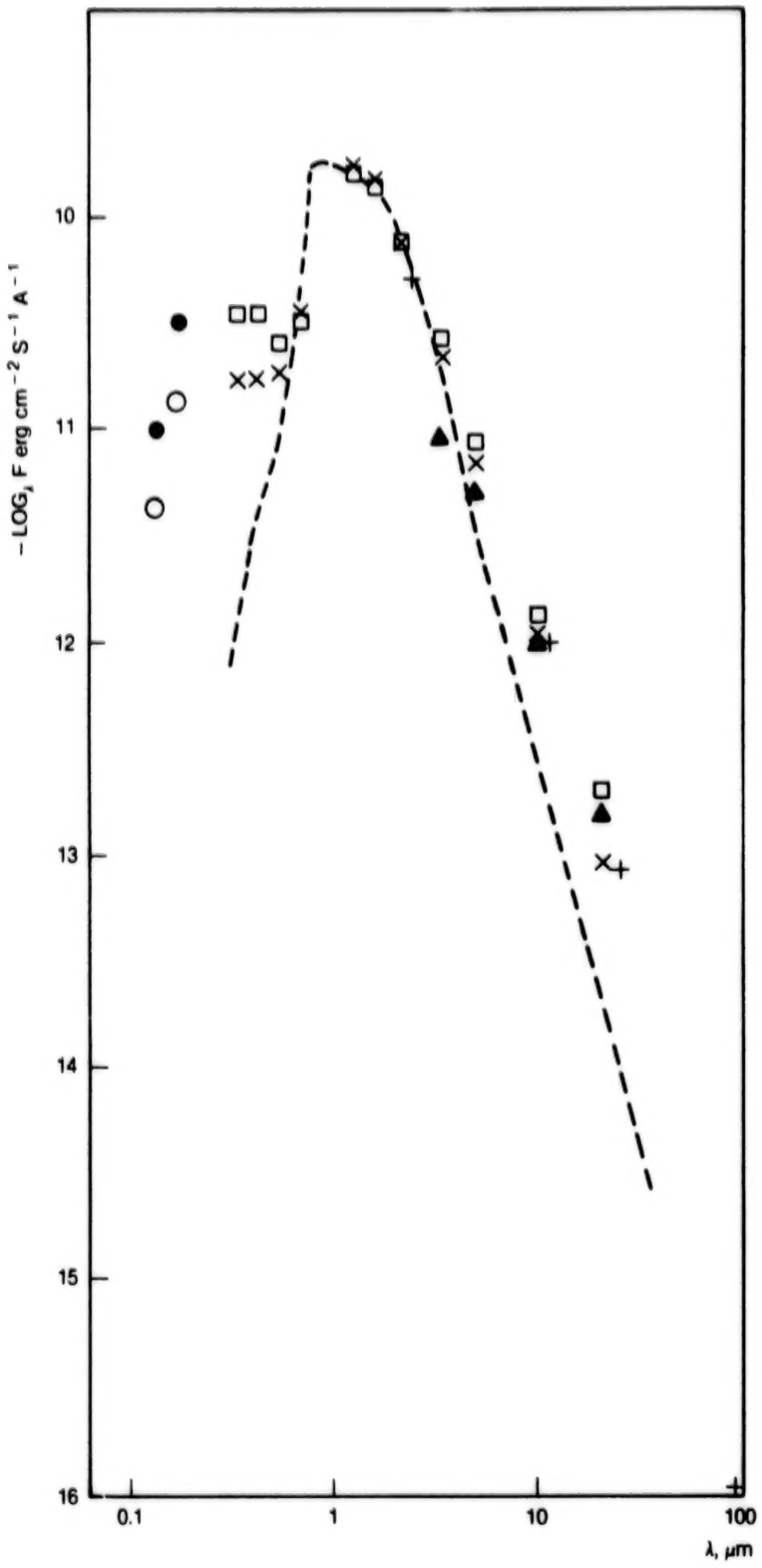


Figure 13-32. Composite energy distribution of CH Cygni corrected for an interstellar extinction of E(B- V) = 0.07 compared with a standard M6 III distribution (dashed line). o *September 1980;* □ *June 1981;* ● *December 1981; x May-June 1982,* ▲ *IR observations from Ipatov et al., 1984; + IR observations from IRAS (from Kenyon et al., 1988) (adapted from Ipatov et al., 1984)*

with the appearance of a multicomponent jet, expanding at a rate of 1.1 arc - s/yr (Taylor et al., 1986; also see Figure 11-27). The onset of the radio outburst coincided with the observed drop in visual light in July 1984. The radio light curve at 2-cm wavelength indicated a flux increase by a factor of about 50 from April 1984 to May 1985. The flux increased with increasing frequency, indicating a thermal origin. The expansional velocity was of the order of 2500 km/s, of the same order as the values given by the full widths of Lyα and the Balmer lines at about the same epochs: 3950 km/s for Ly alpha (Selvelli and Hack, 1985), 1200 km/s for H alpha and 1100 for H beta (Hack et al. 1986).

The radio jet from CH Cyg is an unusual and complex event. The only other symbiotic star known to show a jet-like feature is R Aqr: it was observed both at optical and radio wavelengths. Also in the case of CH Cyg, there is evidence of the presence of a jet emitting in the optical and- possibly- in the UV. Solf (1987) obtained high-resolution spectra of CH Cyg on September 1986. His data reveal a very compact nebulosity located about 1" northwest of the star and emitting in the light of [O III] at 5007 A, i.e., in the same direction as the radio jet. An attempt to observe it in the UV with the IUE satellite was made by Selvelli et al. (1987, IAU Circ. 4491) in November 1987, when the 20" slit was oriented in the same direction of the jet. By placing the star at one end of the slit, a stellar spectrum with P Cyg features was observed at one side, while at the other (at about 19 arcsec from the star), few emission features were observed (SiIII 1892, NIII 1750, OIII 1663). An attempt to observe the jet again in May 1988, when the slit had the same orientation, gave negative results.

Attempts to detect X-ray emission from CH Cygni were made with the X-ray satellite EINSTEIN with negative results. The european satellite EXOSAT observed again CH Cygni on May 24, 1985 (Leahy and Taylor, 1987), and at this time soft-X-ray flux was detected of 1.3×10^{-11} erg cm^{-2} s^{-1}.

Actually, there is some suspicion that CH Cygni is the optical counterpart of a hard X-ray source H1926+503, Int.= 1.22 count/s. In fact, it falls near the center of the error box of a hard-X-ray source measured by the satellite HEAO A-2 on November 1977 at 2-6 keV (about 3 Å) (Marshall et al., 1979). The doubt with this identification is that the other symbiotic stars that have been detected in the X-ray range are soft-X-ray emitters; none is known to emit in the hard-X-ray range.

VI.E. TOWARD A MODEL FOR CH CYG

The long and homogeneous series of spectroscopic observations made from 1965 to 1986 at the Haute Provence Observatory by Hack and collaborators, together with those made by Deutsch et al. (1974) since 1961, suggest that the radial velocity variations in the photospheric lines of the M6 III star are due to orbital motion on which are superposed some erratic variations commonly observed in giants and supergiants. The presence of a companion seems to be proved by the behavior of the permitted and forbidden emissions, showing radial velocity varying in antiphase with that of the M6 photospheric lines. The evidence for the presence of this companion is reinforced by the minimum in the U magnitude and in the UV flux observed in 1969 and in 1985, suggesting the occurrence of an eclipse of the companion by the cool star. Moreover, the detection of a slight increase of the flux toward wavelengths shorter than 1300 A observed in 1988 suggest that the accretion disk has become very thin, and we can observe the continuous spectrum of a faint hot companion.

A period of 16 years is not in disagreement with the values indicated by the radial velocity curve. However, the large scatter of the radial velocity data do not permit one to derive reliable parameters for the orbit, but just to estimate a mass ratio of about unity.

The observed flickering, with time scales of a few minutes, is a typical phenomenon observed in dwarf novae and quiescent novae and believed to arise in the hot spot where the mass flux from the cool star impinges on the accretion disk. The presence of flickering in CH Cyg and its higher

amplitude in the U magnitude are additional proofs that CH Cyg is a binary system and that the flickering occurs in the hot component of the system.

The ultraviolet continuum may be explained as superposition of a stellar continuum with T eff ranging between 8500 K (at maximum UV brightness) and 15, 000 K (at the end of the outburst) and b-f +f-f hydrogen emission (Mikolajewska et al., 1987; 1988).

However the indication obtained in 1988 of the presence of a Rayleigh-Jeans tail at λλ1200-1300 suggest the presence of a hotter object.

Assuming as reasonable values for the masses m(M6) = m(comp.) = 1 solar mass, and P = 15.7 yrs, the resulting distance of the two stars is of the order of 7.8 A.U. or 1.2 x 10^{14} cm, i.e., about 10 times the radius of the red giant. Hence, the system is detached, and if what we observe during the outburst is the spectrum of an accretion disk, it must be formed by accumulation of matter from the red giant wind. During the rising part of the outburst the disk becomes thicker and more extended as indicated: a) by the increasing intensity of the blue and UV continuum; b) by the appearance of absorption lines of once-ionized metals, and also of multi-ionized atoms (e.g., C IV, Si IV); c) by the increasing width of the Balmer lines. At the end of the outburst, the disk becomes less dense, as indicated by the ratio of forbidden to permitted lines of Fe II, the appearance of C III] 1906 and of [O III] 4959 and 5007, and by the diminution or disappearance of the UV-blue continuum. An indication of the decrease in density is also given by the transition of UV absorption-dominated spectrum (because the UV continuum is strong, the disk is optically thick in the UV) to an emission-dominated UV spectrum (because the disk become optically thin in the continuum). The appearance of Ly Alpha emission in January 85 probably has the same origin. The Ly Alpha absorption was not observable at earlier dates, probably because the continuum is very low at 1215 A on account of the low sensitivity of IUE at that wavelength and because of interstellar absorption.

The large widths of the Ly Alpha (about 4000 km/s), H alpha (about 1200 km/s) and H beta (about 1100 km/s) at the beginning of 1985 suggest that the disk becomes larger by expanding, and this has the effect of increasing the RV gradient in the disk and, hence, the broadening of the strong lines, and of decreasing the density. The EXOSAT detection of X-ray emission, while previous observations with EINSTEIN gave negative results, may indicate that the vanishing of the outer parts of the disk makes it possible to observe the inner hotter parts and, in 1988, also the Rayleigh-Jeans tail of the companion.

The duration of an outburst and the intervals between two consecutive outbursts may have very different lengths depending on the ellipticity of the orbit. If the critical mass for outburst in the disk is reached in the vicinity of periastron, the activity may be longer than if it is reached near apoastron, because of a larger accretion of matter through the stellar wind. The intervals between the two outbursts may be shorter if, at the end of one outburst, the star is near the periastron and may more rapidly replenish the disk or longer if, at the end of one outburst, the star is at the apoastron.

Although the orbital parameters derived by Yamashita and Maehara (1979) are very uncertain because of the scatter of the observed radial velocities, we have computed the phases of the epochs of the three observed outbursts. The outburst of 1963 occurred at phase 0.7 (counted from the epoch of periastron), and the outburst of 1967-70 started at phase 0.94. The 1977 outburst occurred at phase 0.58; it was near to the end in January 1985, at phase 0.05. Hence, the shorter time interval between the first and the second outbursts (4 years) and the longer interval between the end of the second and the beginning of the third outburst (7 years) may be justified by the above hypothesis. However, it is not easy to justify the strength and length of the third outburst, started when the companion was near to the apoastron.

To have a better explanation for the origin of the outburst, we need much longer series of radial

velocities for computing more reliable orbital data, and, hopefully, new outburst observations.

The model adopted by Warner (1972) to explain the luminosity of Mira Ceti B as due to accretion from the wind of Mira Ceti A can be applied to CH Cyg. Assuming $m_1 = m_2 = 1$ solar masses, P = 15.74 yrs, the semiaxis a of the orbit is equal to 7.75 A.U. or $1.16\ 10^{14}$ cm. For $m_1 = 1$ and $m_2 = 0.25$ (as suggested by Mikolajewski et al., 1987), a = 6.6 A.U.

The mass lost by the primary is given by $dm/dt = 4\ \pi a^2\ \rho\ V_{out}$ where Vout is the expansional velocity observed during the outburst. For an observed particle density of 10^6 (as indicated by the forbidden emissions appearing at the end of the outburst) or of 10^9 (as indicated by the forbidden and permitted emissions of Fe II at maximum outburst) and for V_{out} = 50 km/s, it follows $1.5\ 10^{-8}\ m_\odot$ /yr < dm/dt < $2.4\ 10^{-5}\ m_\odot$ / yr.

The radio structure observed by Taylor et al. (1986) from April 84 to January 85 indicates $dm/dt \approx 7\ 10^{-6}\ m_\odot$ /yr. The luminosity, due to accretion only, of the object which is gaining mass, is given by

$$L = \frac{G^1 m_2^1}{2(V_{rel}^2 + V_s^2)^{3/2}\ V_{out}\ \pi^2 a^2} dm/dt, \quad 13.3$$

where V_{rel} is the velocity of the companion moving at orbital velocity, relative to the wind of the companion, V_s is the sound velocity in the outflowing envelope, $V_s \approx$ 1km/s, m_2 is the mass, and r_2 the radius of the companion.

For $m_2 = 1$, $r_2 = 0.1$ (both in solar units), V_{orb} = 8km/s, $V_{rel} = V_{out}$ and $dm/dt = 10^{-5}\ m_\odot$/yr, it follows $L = 9.6\ 10^{33}$ erg/s. For $m_2 = 0.25$, V_{orb} =32 km/s, V_{rel} = 59 km/s, assuming $r_2 = 0.01$, it follows $L = 1.75\ 10^{33}$ erg/s.

Now, assuming that the flux due to the M6 giant is completely negligible below 1600 A, we observe that the flux at the Earth of the companion in the period of maximum activity in the interval of maximum emission, 1200-1600 A, is $F = 4\ 10^{-9}$ erg $cm^{-2}\ s^{-1}$. Hence, the luminosity L, assuming for the distance of CH Cyg about 250 or 300 parsecs, results equal to about 10^{34} erg/s. Hence, a mass loss of $10^{-5}\ m_\odot$ /yr, as indicated by the optical and radio observations, is sufficient to explain the observed luminosity of the companion of mass about 1 solar mass and radius about 1/10 the solar radius.

14

SUMMARY OF OUR PRESENT KNOWLEDGE ABOUT SYMBIOTIC STARS

M. Friedjung and R. Viotti

At the end of these Chapters 11, 12, and 13, where the different observational and theoretical aspects of the symbiotic stars have been discussed, with special attention to a few well-studied objects, it is now necessary to clarify to the reader the present status of our research, and to find out the lines for future work on the field. In the following, we shall summarize the main points concerning the symbiotic phenomenon.

I. SYMBIOTIC STARS AS INTERACTIVE BINARIES

There is now strong evidence that most, if not all, symbiotic stars are interactive binary systems. Indeed, this conclusion is so much believed by specialists, that if a star previously classified as symbiotic had been found not to be binary it would then have been classified as something else! One component is thought to accrete from the other. One, the mass loser, is supposed to be a cool giant, while the mass gainer should be a main sequence star or a white dwarf or possibly a neutron star. Accretion is supposed to occur either from Roche lobe overflow via a disk, or from the wind of the cool component. When the accretor is a white dwarf, the accreted hydrogen can be burned almost continuously or in shell flashes. However, even accepting this basic picture, many "details" are not understood, while it has to be related to the behavior of particular symbiotic stars.

In the case of S-type symbiotic systems, the evidence for binarity has grown. The orbital periods seem to be of the order of several hundred days. In some cases (e.g., CI Cyg and AR Pav), observations can be interpreted if there is a main sequence accretor surrounded by a disk. However, such a situation does not explain what is seen for many (probably most) S-type symbiotics. For these, wind accretion on to a white dwarf appears more probable. In the latter cases a high mass-loss rate from the cool giant might be suggested; actually, Kenyon and Fernandez-Castro (1987), Kenyon et al. (1988), and Kenyon (1988) found evidence of enhanced mass-loss rates compared with those of normal cool giants of the same types. The last conclusion is clearly dependent on the accuracy of the spectral classification, and especially on mass-loss rates determined from continuum radio emission and masses of dust present. Indeed, the accuracy of mass-loss rates is not so good; radio emission, in particular, needs to be modeled taking into account ionization of the cool-giant wind by radiation from the hot component (see Chapter 12). It can be noted that the mass-loss rate for the D-type symbiotic H1-36 found from the model of Taylor and Seaquist (1984), which is obtained by assuming the same wind velocity as those authors give, but with the distance from Kenyon et al. (1988), is two to eight times larger than that derived by Kenyon et al. if one assumes spherical symmetry.

For the D-type symbiotics such as RR Tel and V1016 Cyg, it has not been possible to derive an orbital period, although there are many reasons to state that they also are binary (e.g., from energy balance considerations). Their periods are often believed to be much larger than those of S-type systems (10^1 to 10^3 years), thus implying larger separations and less interaction phenomena unless the components are more "active." In fact, the cool giant in such systems appears to be a

PRECEDING PAGE BLANK NOT FILMED

Mira variable, having a larger mass-loss rate than that of other cool giants. It appears that it is the presence of a Mira which explains the different properties of such systems, and it now seems best to call them *symbiotic Miras* (Whitelock, 1988). Their large mass-loss rate is considered to be associated with the condensation of a large amount of dust. Indeed, the infrared properties of symbiotic Miras might be understood by supposing a much larger extinction of the light of the Mira than that of its companion, as the result of the presence of a massive circumstellar dust envelope (Kenyon et al., 1988).

When speaking of *interaction* in symbiotic binaries, we need to consider quite a number of different processes. These include (1) mass exchange following mass loss from one component leading to transfer and accretion by the companion, perhaps modulated by varying stellar separation during an orbital period; (2) possible nuclear burning of hydrogen accreted by a white dwarf; (3) interaction of radiation of one component with the environment of the other; (4) collision between the winds from each component, etc. The interaction of radiation of one component with the environment of the other can take many forms, including heating of a disk and/or of a companion's atmosphere, ionization of the wind and upper atmosphere of the cool component (this can well vary with time), heating and possible destruction of grains, and acceleration of the cool star's wind by radiation pressure in the lines, etc. Up to now, studies have concentrated on one process at a time, so that a proper global picture of interaction still does not exist.

II. NATURE OF THE COMPONENTS OF THE SYMBIOTIC SYSTEMS

To make consistent models of the phenomena here studied, we especially need to know the nature of the components. It is now clear that the cool component very much resembles a normal cool giant or bright giant, for S-type symbiotics, and a Mira for D-type symbiotics. Here by "normal" we mean that the cool component appears very much to resemble the corresponding type of single star. This result needs to be checked in much more detail in the future. The claim of an increased mass-loss rate for the cool components of S-type symbiotics should be verified using proper binary star modeling for infrared dust and radio emission. The atmospheric structure needs to be studied using high resolution infrared spectra (e.g., from Fourier Transform Spectroscopy), which can also be used to measure stellar surface gravity, turbulence, and rotation velocity.

It appears, however, that binarity is the main cause of the properties of symbiotic stars; it now is very likely that they can be ascribed to the peculiar properties of the cool component. Indeed, the normality of this component is largely used to derive the distances of symbiotic systems. These distances need to be refined, but almost certainly will not be substantially changed in the future.

The exact nature of the *hot component* is still more open and controversial. In some cases, it appears to be like a hot subdwarf, and can be understood as being an expanded white dwarf undergoing shell burning. Then it often is similar to the nucleus of a planetary nebula, and temperature and radius estimates are derived as for the latter from the ultraviolet energy distribution and emission line fluxes. The temperature can be so high that the observed ultraviolet continuum is quite insensitive to its exact value. The properties of certain hot components during outbursts (e.g., CH Cyg and PU Vul) somewhat resembling a supergiant of intermediate temperature, might then be explained by expansion of the outer layers of the white dwarf to supergiant dimensions, following a shell flash. However, in this case, the luminosity would have to be ~ 59250 ($M_{core}/M_\odot$ -0.522) $L_\odot$ (Kenyon, 1986). According to Mikolajewska et al. (1988), CH Cyg did not have a maximum luminosity of more than 10^3 $L_\odot$. Therefore, in order for this explanation to work for CH Cyg, the white dwarf core mass would have to be quite low, of the order of 0.54 $M_\odot$.

The hot component can sometimes be understood as an *accretion disk* plus boundary layer around a main sequence star. Such a disk may be

formed from Roche lobe overflow and sometimes from wind accretion, but in the latter case, a disk does not seem easy to be formed. In any case, the detailed interpretation of the hot component as a disk still involves a number of uncertainties because of the gaps in the present theory of disks. Studies assuming a disk to radiate as a sum of blackbodies or even as a sum of normal stellar atmospheres cannot lead to highly reliable results. Other physical effects can also be present. Among these, one should mention heating of the disk by a central stellar component, which can be an expanded white dwarf undergoing shell burning. The heated disk could reradiate as a result of the heating at a rate much larger than that due to gravitational dissipation in the disk. If the hot component is a disk, one can envisage an explanation of active phases of symbiotic stars, by mechanisms similar to those invoked for dwarf nova outbursts. In addition, it is not certain whether a disk, if formed, would always be present. For instance, it might temporarily appear during activity, if it were formed by accretion from the wind of the companion. The properties of the latter or the separation of the stellar components would have to change.

The presence of a disk should lead to observational consequences other than those exhibited if only an object similar to a hot star were present. Not only is the continuum energy distribution changed, but also the emisssion and absorption line profiles (or at least contributions to the profiles), as well as all the variations in eclipse, can be expected to have characteristic properties. High-quality observations, combined with better theory, should help to eliminate these problems. In any case, the correct identification of the nature of the hot component for a particular system is important for deducing which processes dominate. In addition, such information is essential for understanding the system's evolution.

III. EMISSION LINES

The picture just described obviously has a bearing on the formation of the emission lines. If formed by electron collisions or by cascade following recombination in an ionized region, one might, in the simplest situation, expect line formation near the hot component. In fact, the situation is more complex, as material does not appear to be distributed uniformly. The fairly narrow emission lines seen very often are most easily understood as formed in regions connected with the cool component (wind, outer atmosphere). Line narrowness implies formation in a low-velocity region far from any compact accreting object. In addition, a study of inter-combination lines of Z And and RR Tel indicated line formation where radiation coming from the hot component at 1176 and 772 A (Altamore et al., 1981) was diluted.

A similar kind of situation is believed to exist for zeta Aur binaries where a hot main sequence star appears to be immersed in the wind of a cool supergiant companion (Shroeder, 1988). The wind scatters photons from the hot main sequence star in resonance lines according to successful models for such stars, and information on wind velocities and mass-loss rates can be obtained. Such stars provide lessons for the study of symbiotic systems.

Symbiotic stars, however, are more complex. As discussed in Chapter 12, not only is the geometry of regions of the cool star wind ionized by the hot component complex, but other physical processes determine line formation regions also. Evidence of a high-velocity wind from the hot component, in particular, can be seen for AG Peg, this producing the broad component of line profiles. Collision between the two winds, when important, can also lead to another line formation region, whose properties really have not been studied up to now. Emission-line formation can occur near an accretion disk (plus perhaps a bright spot formed where a current from a companion losing mass by Roche lobe overflow strikes the disk). It may be noted that such a disk might also produce a wind. The influences of these and other effects on emission-line formation still need to be fully elucidated.

IV. CHEMICAL COMPOSITION

Some of the models discussed above imply that the matter in the symbiotic system should be processed. Abundances different from cosmic

values are also expected for the high-velocity objects, such as AG Dra. Therefore, the determination of the chemical composition of all the components of the symbiotic systems is a crucial parameter. Obviously, nothing can be directly said about the hot component, since no truly photospheric lines are visible. The spectrum of the cool component can be studied with the classical curve-of-growth method, provided that high-resolution, high-S/N spectrograms are available, which is not the case for the large majority of symbiotic stars. In addition, in order to avoid errors introduced by the veiling of the variable blue continuum (see Chapter 11, Section IV.A), the analysis should be made on high-resolution spectrograms taken in the red, or even in the near-IR, which is not so easy at present. So far, the abundance analyses of the brightest objects are very few. From a curve-of-growth analysis of the optical spectrum of the symbiotic nova PU Vul, Belyakina et al. (1984) found some chemical anomalies, such as Ca and Fe deficiency, and excess of the other iron group elements and of some rare earths (cf. Gershberg and Shakhovskoj, 1988). Lutz et al. (1987) found that in AG Dra, the BaII and SrII lines are probably enhanced. Unfortunately, these authors were unable to perform a detailed abundance analysis for lack of a good calibration of their echelle spectra.

Concerning the "nebular" emission-line spectrum, the abundance determinations are strongly model-dependent. Several estimates have been made based on the optical and UV line fluxes. The results of CNO abundance determinations from *IUE* are summarized by Nussbaumer et al. (1988), who used the emission-line fluxes of CIII, CIV, NIII, NIV and OIII, supposed to be formed in a common region. They also supposed the ionizing hot source to have an effective temperature equal to or larger than 10^5K, and the nebular regions to be uniform with an electron temperature of 12,000 K and an electron density of 10^{+9} cm^{-3}. Line emissivities were found to be insensitive to the assumed electron temperature, as well as to the assumed electron density, at least for N_e below 10^{+9} cm^{-3}. Nussbaumer et al. found that in symbiotic stars the abundance ratios are close to those for M giants, suggesting that the line-emitting material come originally from the cool-giant companion. The latter would have its abundances somewhat modified by CNO cycling. The only symbiotic system that shows clear signs of deviation is HM Sge, for which C/N/O ratios were found to be similar to that of novae. It would be important to extend these results to other ions, and to check to what extent the abundance estimates are dependent on the assumptions and on the adopted model. Future work on both (and simultaneously) the emission-and absorption-line spectra using high quality material are urgently required to make any progress in this field.

V. VARIABILITY

The variability of symbiotic stars is a fundamental property of these objects. It is the result of many mechanisms, which in many cases are far from being well-understood. Various time scales are involved, and we mention here (nearly in order of increasing time scale):

- The *flickering* of CH Cyg with time scales of 5 and 15-20 min seen during activity, which might be physically related to the flickering seen for cataclysmic variables.

- Variations during the orbital cycle, which may not be only geometrical (eclipses, reflection effects, etc.), but also physical, associated with a varying separation of the stellar components. In the latter case, the orbit must be *eccentric*. It should be noted that accretion variations due to varying separation cannot have much effect on the brightnesses of AG Dra, AX Per and AG Peg; otherwise, the determination of orbital elements from the reflection effect as discussed by Leibowitz and Formiggini (1988) would not work.

- When the cool companion is a Mira, variations occur over its pulsational period, which are of the same order as the *orbital* period, if it is an S-type system. Accretion and dust condensation might sometimes be modulated.

- Active phases can occur over time-scales of

decades. Within each, oscillations of activity can occur. Some, but probably not all, of the active phases, might be explainable by accretion events. The active phases of other symbiotics (e.g., AG Dra) may be hard to understand without invoking shell burning of a white dwarf.

- D-type symbiotics can have faint phases lasting one to several years. These are possibly due to dust obscuration, and/or to phenomena associated with the periastron passage.

- Only one outburst has been observed for each symbiotic nova. Such events have been explained by shell flashes of white dwarfs.

However, the explanations invoked for different events are not to be believed dogmatically. Certain dividing lines between different classes of event may turn out to be artificial.

VI. NEBULAE

Small nebulae have been discovered around many symbiotics, especially at radio wavelengths. Image deviations from circular (therefore from spherical) symmetry are observed, with indications of the presence of bipolar flows and jets (Taylor, 1988; Solf, 1988). According to Taylor, one should distinguish between ejecta and stellar winds. The former are clumpy and associated with a known outburst of the system, while the latter are smooth and featureless with an angular size that increases with frequency. It is the ejecta following outbursts that show bipolar flow (or jet-like) structures.

The physics behind the origin of nebular structure is not really known. For wind-produced nebulae, the ionization of the cool component's wind by the hot component and collision between winds from both components may play major roles. A system seen in the plane of its orbit could show apparently linear structure in certain cases because of these mechanisms. However, such an explanation is not expected to be generally true. Bipolar flows and jets are common in other astrophysical situations such as radio galaxies, active galactic nuclei, young stellar objects, etc. Their existence may be linked to the existence of disks, but it would be dangerous to extrapolate this type of "explanation" to symbiotic systems, and to conclude that disks are very often present. Conversely, the study of bipolar nebulae and ejecta in symbiotic systems might be useful to understand their nature. A large progress in this field is expected from the new astronomical technologies for imagery and polarimetry, and from HST.

REFERENCES

Ahern, F.J.: 1978, Astrophys. J. 223, 901.

Ahern, F.J., FitzGerald, M.P., Marsh, K.A., Purton, C.R.: 1977. Astron. Astrophys. 58, 35.

Allen, C.W.: 1973, Astrophysical Quantities, The Athlone Press.

Allen, D.A.: 1979, in 'Changing Trends in Variable Stars Research', IAU Colloquium No.46, F.M. Bateson, J. Smak and I.H. Urch eds., University of Waikoto, Hamilton, New Zealand, p. 125.

Allen, D.A.: 1980a, Mon. Not. R. Astr. Soc. *190*, 75.

Allen, D.A.: 1980b, Mon. Not. R. Astr. Soc. *192*, 524.

Allen, D.A.: 1981, Mon. Not. R. A. S. *197*, 739.

Allen, D.A.: 1982, in 'The Nature of Symbiotic Stars', IAU Colloguium 70, M. Friedjung and R. Viotti eds., D. Reidel, Dordrecht, p. 27.

Allen, D.A.: 1983, Mon. Not. R. A. S. *204*, 113.

Allen, D.A.: 1983, Mon. Not. R. Astr. Soc. *204*, 113.

Allen, D.A.: 1984a, Astrophys. Space Science, *99*, 101.

Allen, D.A.: 1984b, Proceed. Astron. Soc. Australia, *5*(3), 369.

Allen, D.A., Wright, A.E.: 1988, Mon. Not. R. Astr. Soc *232*, 683.

Aller, L.H.: 1954a, Publ. Dom. Astrophys. Obs. *9*, 321.

Aller, L.H.: 1954b, Astrophysics, Vol.2 'Nuclear Transformations, Stellar Interiors and Nebulae', Ronald Press, New York, p. 180.

Altamore, A., Baratta, G.B., Cassatella, A., Friedjung, M., Giangrande, A., Ricciardi, O., Viotti, R., 1981, Astrophys. J. *245*, 630.

Altamore, A., Baratta, G.B., Viotti, R.: 1979, Inf. Bull. Var. Stars No. 1636.

Altamore, A., Cassatella, A., Eiroa, C., Neckel, Th., Viotti, R.: 1982, IAU Circular No. 3750.

Altenhoff, W.J., Wendker, H.J.: 1973, Nature *241*, 37.

Andarao, B.G., Sahu, K.C., Desai, J.N.: 1985, Astrophys. Space Sci. *114*, 351.

Anderson, C.M., Cassinelli, J.P., Sanders, W.T.: 1981, Astrophys. J. (Letters) *247*, L127.

Aspin, C., Schwarz, H.E., McLean, I.S., Boyle, R.P.: 1985, Astron. Astrophys. *149*, L211.

Audouze, J., Bouchet, P., Fehrenbach, Ch, Wosczyck, A.: 1981, Astron. Astrophys. *93*, 1.

Babcock, H.W.: 1958, Astrophys. J. Supplem. Ser. *3*, 141.

Baldwin, J.A., Phillips, M.M., Terlevich, R,: 1981, Pub. Astr. Soc. Pacific *93*, 5.

Baratta, G.B., Altamore, A., Cassatella, A., Friedjung, M., Ponz, D., Viotti, R.: 1982, in 'The Nature of Symbiotic Stars', IAU Colloquium 70, M. Friedjung and R. Viotti eds., D. Reidel, Dordrecht, p. 145.

Baratta, G.B., Cassatella, A., Viotti, R.: 1974, Astrophys. J. *187*, 651.

Baratta, G.B., Viotti, R.: 1983, Mem. Soc. Astr. Ital. *54*, 493.

Barbier, R,, Swings, J.P.: 1982, in 'Be Stars', IAU Symposium 98, M. Jaschek, H.G. Groth Eds., Reidel, Dordrecht, p. 103.

Bath, G.T.: 1975, Mon. Not. R. Astr. Soc. *171*, 311.

PRECEDING PAGE BLANK NOT FILMED

Bath, G.T.: 1977, in "Novae and Related Stars", M. Friedjung, ed., p. 41.

Beals, C.S.: 1951, Publ. Dominion Astrophys. Obs. Victoria *9*, 1.

Becker, R.H., White, R.L.: 1985, in 'Radio Stars', R.H.H. Hjellming and P.M. Gibson eds., Reidel, Dordrecht, p. 139.

Belokon, E.T., Shulov, O.S.: 1974, Trudy Leningrad Astr. Obs *30*, 103.

Belyakina, T.S.: 1969, Izv. Krym. Astrofiz. Obs. *40*, 39.

Belyakina, T.S.: 1974, Izv. Krym. Astrofiz. Obs. *59*, 133.

Belyakina, T.S.: 1974, Izv. Krym. Astrofiz. Obs. *41-42*, 275.

Belyakina, T.S.: 1979, Inf. Bull. Var. Stars No. 1602.

Belyakina, T.S.: 1980, Inf. Bull. Var. Stars No. 1808.

Belyakina, T.S.: 1981, Inf. Bull. Var. Stars No. 1974.

Belyakina, T.S.: 1985, Inf. Bull. Var. Stars No. 2698.

Belyakina, T.S., Bondar, N.I., Chochol, D., Chuvaev, K.K., Efimov, Yu.S., Gershberg, R.E., Grygar, J., Ilric, L., Krasnobabtsev, V.I., Petrov, P.P., Piirola, V., Savanov, I.S., Shakhovskaja, N.I., Shakhovskoj, N.M., Sheavrin, V.I.: 1984, Astron. Astrophys. *132*, L12.

Belyakina, T.S., Gershberg, R.E., Efimov, Yu.S., Krasnobabtsev, V.I., Pavlenko, E.P., Petrov, P.P., Chuvaev, K.K., Shenavrin, V.I.: 1982, Soviet Astron. Zh. *59*, 302.

Bensammar, S., Friedjung, M., Letourneur, N., Maillard, J.P.: 1988, Astron. Astroph. *190*, L5.

Bensammar, S., Friedjung, M., Letourneur, N., Maillard, J.P.: 1988, in "The Symbiotic Phenomenon." IAU Colloquium 103, J. Mikolajewska, M. Friedjung, S. J. Kenyon, R. Viotti, eds., D. Reidel, Dordrecht, p. 193.

Berman, L.: 1932, Pub. Astr. Soc. Pacific *44*, 318.

Blair, W.P., Stencel, R.E., Shaviv, G., Feibelman, W.A.: 1981, Astron. Astrophys. *99*, 73.

Blair, W.P., Stencel, R.E., Feibelman, W.I., Michalitsianos, A.G.: 1983, Astrophys. J. Supplem. Series *53*, 573.

Boehm, C., Hack, M., Persic, M.: 1984, Fourth European IUE Conference, ESA SP 218, 407.

Bondi, H., Hoyle, P.: 1944, Mon. Not. R. Astr. Soc. *104*, 273.

Boyarchuk, A.A.: 1966a, Soviet Astronomy *10*, 783.

Boyarchuk, A.A.: 1966b, Astrofizika *2*, 101.

Boyarchuk, A.A.: 1967a, Soviet Astronomy *11*, 8.

Boyarchuk, A.A.: 1967b, Soviet Astronomy *11*, 818.

Boyarchuk, A.A.: 1968, Astrophysics *4*, 109.

Boyarchuk, A.A.: 1969a, Izv. Krymsk. Astrophys. Obs. *39*, 124.

Boyarchuk, A.A.: 1969b, in 'Non Periodic Phenomena in Variable Stars', L. Detre ed., Academic Press, Budapest, p. 395.

Boyarchuk, A.A.: 1970, Izv. Krymsk. Astrophys. Obs. *42*, 264.

Boyarchuk, A.A.: 1975, in 'Variable Stars and Stellar Evolution', IAU Symposium No.67, V.E. Sherwood and I. Plaut eds., D. Reidel, Dordrecht, p. 377.

Boyarchuk, A.A: 1982, in 'The Nature of Symbiotic Stars', IAU Colloquium 70, M. Friedjung and R. Viotti eds., D. Reidel, Dordrecht, p. 225.

Boyarchuk, A.A.: 1984, Astrophysiscs and Space Physics Reviews, R. Syunyaev Ed., Vol. 3, p. 123.

Broadfoot, A.L. et al.: 1981, J. Geophys. Research *86*, 8259.

Bruhweiler, P.C., Kondo, Y., McCluskey, G.E.: 1981, Astrophys. J. Supplem. Ser. *46*, 255.

Buerger, P.F.: 1972, Astrophys. J. *177*, 657.

Burnstein, D., Heiles, C.: 1982, Astr. J. *87*, 1165.

Capps, R.W., Coyne, G.V., Dick, H.M.: 1973, Astrophys. J. *184*, 173.

Cassatella, A., Cordova, F.A., Friedjung, M., Kenyon, S.J., Piro, I., Viotti, R.: 1987, Astrophys. Space Sci. *131*, 763, and preliminary results.

Cassatella, A., Eirca, C., Fernandez, T., Friedjung M., Pollard, G., Selvelli, P.L., Sims, M., Viotti, R.: 1984, Proc. Frascati Workshop 1984 'Multifrequency Behaviour of Galactic Accreting Socurces', F. Giovannelli ed., Istituto Astrofisica Spaziale, Frascati, p. 97.

Cassatella A., Femandez-Castro, T., Oliversen, N.: 1988a, in 'The Symbiotic Phenomenon', IAU Colloquium 103, J. Mikolajewska et al. eds., Kluwer Acad. Publ., Dordrecht, p. 181.

Cassatella, A., Gonzalez-Riestra, R., Fenandez-Castro, T., Puensalida, J., Gimenez, A.: 1988b, in "The Symbiotic Phenomenon', IAU Colloquium 103, J. Mikolajewska et al. eds., Kluwer Acad. Publ., Dordrecht, p. 301.

Catchpole, R.H., Robertson, B.S.C., LloydEvans, T.H.H., Feast, M.W., Glass, I.S., Carter, B.S.: 1979, Circ. SAAO. *1*, 61.

Cester, B.: 1968, IBVS 291.

Cester, B.: 1969, Astroph. Space Sci. 3, 198.

Cester, B.: 1972, Mem. Soc. Astron. It 43, 83.

Chochol, D., Vittone, A., Milano, L., Rusconi, L.: 1984, Astron. Astrophys. *140*, 91.

Ciatti, F., Mammano, A., Vittone, A.: 1978, Astron. Astrophys. *68*, 251.

Cohen, N.L., Ghigo, P.D.: 1980, Astron. J. *85*, 451.

Collins, G.W., Buerger, P.F.: 1974, in 'Planets, Stars and Nebulae studied with Photopolarimetry', T. Gehrels ed., The University of Arizona Press, p. 663.

Coyne, G.V.: 1970, Astrophys. J. *161*, 1011.

Coyne, G.V.: 1974, Astron. J. *79*, 565.

Coyne, G.V., McLean, I.S., 1982, in 'Be Stars', IAU Symposium 98, M. Jaschek and H.G. Groth eds., D. Reidel, Dordracht, p. 77.

Crampton, D., Grygar, J., Kohoutek, L., Viotti, R.: 1970, Astrophys. Lett. *6*, 5.

Davidsen, A., Malina, R., Bowyer, S.: 1977, Astrophys. J. *211*, 866.

Deutsch, A.J.: 1964, Ann. Report of Mt. Wilson and Palomar Obs., p. 11.

Deutsch, A.J., 1967: IAU Circ. 2020.

Deutsch, A.J., Lowen, L., Morris, S.C., Wallerstein, G.: 1974, Publ. Astron. Soc. Pacific *86*, 233.

Dickinson, D.F.: 1976, Astrophys. J. Supplem. Ser. *30*, 259.

Duschl, W.J.: 1983, Astron. Astroph. *119*, 248.

Duschl, W.J.: 1986a, Astron. Astroph. *163*, 56.

Duschl, W.J.: 1986b, Astron. Astroph. *163*, 61.

Eiroa, C., Hetele, H., Qian Zhong-yu: 1982, in 'The Nature of Symbiotic Stars', IAU Colloquium 70, M. Friedjung and K. Viotti eds., D. Reidel, Dordrecht, p. 43.

Elitzur, M.: 1981, in 'Physical Processes in Red Giants', I. Iben and A. Renzini eds., Reidel, Dordrecht, p. 363.

Faraggiana, R., Hack, M.: 1971, Astron. Astrophys. *15*, 55.

Faraggiana, R., Hack, M.: 1969, Astroph. Space Sci. *3*, 205.

Feast, M.W., Catchpole, R.M., Whitelock, P.A., Carter, B.S., Roberts, G.: 1983b, Mon. Not. R. Astr. Soc. *203*, 373.

Feast, M.W., Robertson, B.S.C., Catchpole, R.M., Lloyd Evans, T., Glass, I.S., Carter, B.S.: 1982, Mon. Not. R. Astr. Soc. *201*, 439.

Feast, M.W., Robertson, B.S.C., Catchpole, R.M.: 1977, Mon. Not. Roy. Astr. Soc. *179*, 499.

Feast, M.W., Whitelock, P.A., Catchpole, R.M., Roberts, G., Carter, B.S.: 1983a, Mon. Not. R. Astr. Soc. *202*, 951.

Fehrenbach, Ch.: 1977, IAU Circ. 3102.

Feibelman, W.A.: 1983, Astron. Astrophys. *122*, 335.

Femandez-Castro, T.: 1988, 'Observacion y analisis de estrallas binarias interactivas de tipo simbiotico', Thesis, Universidad Complutense de Madrid.

Femandez-Castro, T., Cassatella, A., Gimenez, A., Viotti, R.: 1988, Astrophys. J. *324*, 1016.

Femie, J.D., 1985, Pub. Astr. Soc. Pacific *97*, 653.

FitzGerald, M.P., Houck, N.: 1970, Astroph. J. *159*, 963.

FitzGerald, M.P., Houk, N., McCuskey, S.W.: 1966, Astrophys. J. *144*, 1135.

FitzGerald, M.P., Pilavaki, A.: 1974, Astrophys. J. Suppl. *28*, 147.

Fitzpatrick, B.L.: 1982, Astrophys. J. *261*, L91.

Fleming, W.P.: 1908, Circ. Harvard Coll. Obs. No. 143.

Flower, D.R., Nussbaumer, H., Schild, H.: 1979, Astron. Astrophys. *72*, Ll.

Friedjung, M.: 1966, Mon. Not. R. Astr. Soc. *133*, 401.

Friedjung, M.: 1982, in 'The Nature of Symbiotic Stars', IAU Colloquium 70, M. Friedjung and R. Viotti eds., D. Reidel, Dordrecht, p. 253.

Friedjung, M.: 1988, in 'The Symbiotic Phenomenon', IAU Colloquium 103, J. Mikolajewska et al. eds., Nuwer Ac. Publ., Dordrecht, p. 349.

Friedjung, M., Ferrari-Toniolo, M., Persi, P., Altamore, A., Cassatella, A., Viotti, R.: 1984, 'Future of Ultraviolet Astronomy Based on Six Years of IUE Research', NASA CP 2349, p. 305.

Friedjung, M., Stencel, R.E., Viotti, R., 1983, Astron. Astrophys., *126*, 407.

Friedjung, M., Viotti, R. (editors): 1982, 'The Nature of Symbiotic Stars', Proceedings IAU Colloquium No. 70. Reidel, Dordrecht.

Fujimoto, M.Y.: 1982a, Astrophys. J. *257*, 752.

Fujimoto, M.Y.: 1982b, Astrophys J. *257*, 767.

Gallagher, J.S., Holm, A.V., Anderson, C.M., Webbink, R.F.: 1979, Astrophys. J. *229*, 994.

Gaposchkin, S.: 1952, Ann. Harvard Obs. *118*, 155.

Garcia, M.: 1986, Astron. J. *91*, 1400.

Garcia, M., Kenyon, S.J.: 1988, 'The Symbiotic Phenomenon', IAU Colloquium 103, J. Mikolajewska et al. eds., Nuwer Ac. Publ., Dordrecht, p. 27.

Gauzit, J.: 1955a, Compte Rendu Ac. Sci. *241*, 793.

Gauzit, J.: 1955b, Ann. d'Astrophys. *8*, 354.

Gershberg, R.E., Shakhovskoj, N.M.: 1988, in 'The Symbiotic Phenomenon', IAU Colloquium no. 103, J. Mikoilajewska et al. eds., Kluwer Acad. Publ., Dordrecht, p. 279.

Girard, T., Willson, I.A.: 1987, Astron. Astrophys. *183*, 247.

Glass, I.S., Webster, B.L.: 1973, Mon. Not. R. astr. Soc. *165*, 77.

Goldberg, L.: 1986, in 'The M-Type Stars', Monograph Series on Nonthermal Phenomena in Stellar Atmospheres, NASA SP-492, p. 245.

Grygar, J., Hric, L., Chochol, D., Mammano, A.: 1979, Bull. astr. Inst. Czech. *30*, 308.

Gusev, E.B.: 1976, Astr. Tsirk. No. 901, 2.

Hack, M.: 1979, Nature *279*, 305.

Hack, M., Engin, S., Rusconi, L., Sedmak, G., Yilmaz, N., Boehm, C.: 1988, Astron. Astroph. Suppl. 72, 391.

Hack, M., Persic, M., Selvelli, P.L.: 1982, Third European IUE Conference, ESA SP 176, 193.

Hack, M., Rusconi, L., Sedmak, G., Aydin, C., Engin, S., Yilmaz, N.: 1986, Astron. Astroph. *159*, 117.

Hack, M., Rusconi, L., Sedmak, G., Engin, S., Yilmaz, N.: 1982, Astron. Astroph. *113*, 250.

Hack, M., Selvelli, P.L.: 1982, in 'The Nature of Symbiotic Stars', IAU Colloquium 70, M. Friedjung and R. Viotti eds., Reidel, Dordrecht, p. 131.

Hack, M., Selvelli, P.L:: 1982, Astron. Astroph. *107*, 200.

Hartmann, L., Dupree, A.K., Raymond, J.C.: 1982, Astrophys. J. *252*, 214.

Hartmann, L., Dupree, A.K., Raymond, J.C.: 1981, Astrophys. J. *246*, 193.

Harvey, P.H.: 1974, Astrophys. J. *188*, 95.

Hayes, M.A., Nussbaumer, H.: 1986, Astron. Astrophys. *161*, 287.

Heck, A., Manfroid, J.: 1985, Astron. Astrophys. *142*, 341.

Heck, A., Manfroid, J.: 1982, The Messenger *30*, 6.

Henize, K.G., Carlson, B.D.: 1980, Publ. astr. Soc. Pacific *92*, 479.

Herbig, G.: 1980, IAU Circular No. 3535.

Hinkle, K.H., Scharlach, W.W.G., Shaw-Hanson, A.D.: 1985, Bull. American Astron. Soc. *16*, 897.

Hjellming, R.M.: 1981, Proceedings of the North American Workshop on Symbiotic Stars, R.E. Stencel ed., National Bureau of Standards and University of Colorado, p. 15.

Hjellming, R.M., Gibson, D.M. (Editors): 1985, 'Radio Stars', Reidel, Dordrecht/Boston/ Lancaster.

Hjellming, R.M., Wade, C.M., Vandenberg, N.R., Newell, R.T.: 1979, Astron. J. *84*, 1619.

Hoffleit, D.: 1968, Irish Astron. J. *8*, 149.

Hogg, B.S.: 1934, Bull. Am. Astr. Soc. *8*, 14.

Holdberg, J.B., Polidan, R.S.: 1987, private communication.

Hollis, J.M., Kafatos, M., Michalitsianos, A.G., Oliversen, R.J., Yusef-Zedeh, I.: 1987, Astrophys. J. Letters *321*, L55.

Hollis, J.M., Kafatos, M., Michalitsianos, A.G., McAlister, H.A.: 1985, Astrophys. J. *289*, 763.

Hollis, J.M., Michalitsianos, A.G., Kafatos, M., Wright M.C.H., Welch, W.J.: 1986, Astrophys. J. Letters *309*, L57.

Hopp, U., Witzigmann, S.: 1981 IBVS 2048.

Huang, C.C.: 1982, in 'The Nature of Symbiotic Stars', IAU Colloquium No. 70, M. Friedjung and R. Viotti eds., Reidel, Dordrecht, p. 151.

Hutchings, J.E., Cowley, A.P., Redman, R.O.: 1975, Astrophys. J. *201*, 404.

Iben, I.: 1982, Astrophys. J. *259*, 244.

Ichimura, K., Shimizu, Y., Nakagiri, M., Yamashita, Y.: 1979, Tokio Astron. Bull. 2nd Series No. 258.

Iijima, T.: 1982, Astron. Astrophys. *116*, 210.

Iijima, T.: 1985, Astron. Astrophys. *153*, 35.

Iijima, T.: 1987, in 'Circumstellar Matter', I. Appenzeller and C. Jordan eds., Reidel, Dordrecht, p. 481.

Iijima, T., Mammano, A., Margoni, R.: 1981, Astrophys. Space Sci. *75*, 237.

Iijima, T., Vittone, A., Chochol, D.: 1987, Astron. Astrophys. *1 78*, 203.

Ilowaisky, S.A., Wallerstein, G.: 1968, Publ. astr. Soc. Pacific *80*, 155.

Ipatov, A.P., Taranova, O.G., Yudin, B.F.: 1984, Astron. Astroph. *135*, 325.

IRAS Point Source Catalog: 1985, Prepared by the Joint IRAS Science Working Group, US Government Printing Office, Washington D.C.

Jacchia, L.: 1941, Bull. Harvard College Obs. No. 915, p. 17.

Johnson, H.M.: 1982, Astroph. J. *253*, 224.

Joy, A.H.: 1942, Astroph. J. *96*, 344.

Jura, M., Helfanot, D.J.: 1984, Astroph. J. *287*, 785.

Kafatos, M., Michalitsianos, A.G.: Feibelman, W.A.: 1982, Astrophys. J. *257*, 204.

Kafatos, M., Michalitsianos, A.G., Fahey, R.P.: 1985, Astrophys. J. Supple. Ser. *59*, 785.

Kafatos, M., Michalitsianos, A.G.: 1984, Scientific American, Vol. 251 No. 1, p. 84.

Kafatos, M., Michalitsianos, A.G., 1982, Nature, *298*, 540.

Kafatos, M., Michalitsianos, A.G., Allen, D.A., Stencel, R.E.: 1983, Astrophys. J. *275*, 584.

Kafatos, M., Michalitsianos, A.G., Hollis, J.M.: 1986, Astrophys. J. Supple. Ser. *62*, 853.

Kaler, J.B.: 1987. Astron. J. *94*, 437.

Kaler, J.B., Stoher, C.A., Hartkopk, W.I., Shaw, R.A., Hufford, F., Olson, E.C., Shankar, A.: 1987, Astron. J. *94*, 453.

Kenyon, S.J.: 1982, Publ. Astr. Soc. Pacific *94*, 165.

Kenyon, SJ.: 1983a, 'The Physical Nature of the Symbiotic Stars', Part One, Ph. D. Thesis, University of Illinois at Urbana-Champaign.

Kenyon, S.J.: 1983b 'The Collected History of the Symbiotic Stars', Part Two, Ph.D. Thesis, University of Illinois at Urban-Cambridge.

Kenyon, S.J.: 1986a, 'The Symbiotic Stars', Cambridge University Press, Cambridge.

Kenyon, S.J.: 1986b, Astronomical J. *91*, 563.

Kenyon, S.J.: 1987, private communication.

Kenyon, S.J.: 1988, in 'The Symbiotic Phenomenon', IAU Colloquium 103, J. Michola-jewska et al. eds., Kluwer Ac. Publ., Dordrecht, p. 161.

Kenyon, S.J., Bateson, F.M.: 1984, Pub. astr. Soc. Pac. *96*, 321.

Kenyon, S.J., Fernandez-Castro, T., Stencel, R.E.: 1988, Astron. J. *95*, 1817.

Kenyon, S.J., Fernandez-Castro, T., Stencel, R.E.: 1986, Astron. J. *91*, 1118.

Kenyon, S.J., Fernandez-Castro, T.: 1987, Astron. J. *93*, 938.

Kenyon, S.J., Gallagher, J.S.: 1983, Astron. J. *88*, 666.

Kenyon, S.J., Truran, J.W.: 1983, Astrophys. J. *273*, 280.

Kenyon, S.J., Webbink, R.F.: 1984, Astrophys. J. *279*, 252.

Kenyon, S.J., Webbink, R.F., Gallagher, J.S., Truran, J.W.: 1982, Astron. Astrophys. *106*, 109.

Keyes, C.D., Plavec, M.: 1980, 'The Universe at Ultraviolet Wavelengths', NASA CP 2171, p. 443.

Kindl, C., Maxer, N., Nussbaumer, H.: 1982, Astron. Ap. *116*, 265.

Klutz, M.: 1979, Astron. Astroph. *73*, 244.

Klutz, M., Simonetto, D., Swings, J.P.: 1979, Astron. Astrophys. *66*, 283.

Kohoutek, L.: 1969, Inf. Bull. Var. Stars no. 384.

Kohoutek, L., Bossen, H.: 1970, Astrophys. Lett. *6*, 157.

Kolotilov, E.A.: 1983, Sov. Astr. J. *27*, 432.

Koonan, F.P., Dufton, P.L., Aggarwal, K.M., Kingston, A.E.: 1988, Astrophys. J. *324*, 1068.

Koorneef, J.: 1983, Astron. Astrophys. *119*, 326.

Kuiper, G.P.: 1941, Astrophys. J. *93*, 133.

Kwok, S.: 1982, in "The Nature of the Symbiotic Stars." M. Friedjung and R. Viotti, eds., D. Reidel, Dordrecht, p. 209.

Kwok, S.: 1988, in 'The Symbiotic Phenomenon', IAU Colloquium 103, J. Milkola-jewska et al. eds., Kluwer Ac. Publ., Dordrecht, p. 129.

Kwok, S., Bignell, R.C., Purton, C.R.: 1984, Astrophys. J. *279*, 188.

Kwok, S., Leahy, D.A., 1984, Astrophys. J. *283*, 675.

Kwok, S., Purton, C.R., Keenan, D.W.: 1981, Astrophys. J. *250*, 232.

Kwok, S., Purton, C.R., FitzGerald, M.P.: 1978, Astroph. J., Lett. *219*, L25.

Leahy, D.A., Taylor, A.R.: 1987, Astron. Astrophys. *176*, 262.

Leibowitz, E.W., Formiggini, L.: 1988, 'The Symbiotic Phenomenon', IAU Coll. 103, J. Mikolajewska et al. eds., Kluwer Ac. Publ., Dordrecht, p. 33.

Lepine, J.R.D., Le Squeren, A.M., Scalise, E., Jr.: 1978, Astrophys. J. *225*, 869.

Lepine, J.R.D., Paes de Barros, M.H.: 1977, Astron. Astrophys. *56*, 219.

Linsky, J.L., Haisch, B.M.: 1979, Astrophys. J. (Letters) *229*, L27.

Livio, M.: 1988, in 'The Symbiotic Phenomenon', IAU Colloquium 103, J. Mikola-jewska et al. eds., Kluwer Ac. Publ., Dordrecht, p. 149.

Livio, M., Prialnik, D., Regev, O.: 1989, Astrophys. J. *341*, 299.

Livio, M., Soker, N., de Kool, M., Savonije, G.J.: 1986b, Mon. Not. R. astr. Soc. *222*, 250.

Livio, M., Soker, N., de Kool, M., Savonije, G.J.: 1986a, Mon. Not. R. astr. Soc. *218*, 593.

Lutz, J.H.; 1984, Astrophys. J. *279*, 714.

Lutz, J.H., Lutz, T.E., Dule, J.D., Kolb, D.D.: 1987, Astron, J. *94*, 463.

Luud, L.: 1986, Proc. Academy of Sciences of the Estonian SSR, Physics-Mathematics, *35*, 184.

Luud, L.S., Ruusalepp, M., Vennik, J. :1977, Publ. Tartu Astroph: Obs. *45*, 113.

Luud, L.S., Ruusalepp, M., Kunsk, T.: 1970, Publ. Tartu Astroph. Obs. *39*, 106.

Luud, L.S., Tomov, T., Vennik, J., Panov, K.,: 1982, Pisma A.J. *8*, 476.

Luud, L.S. Vennik, J., Pehk, M.: 1978, Sov. Astroph. Len. *4*, 46.

Magalhaes, A.M.: 1988, in 'The Symbiotic Phenomenon', IAU Colloquium no. 103, J. Mikolajewska et al. eds., Kluwer Acad. Publ., Dordrecht, p. 89.

Maitzen, H.M., Schnell, A., Hron, J.: 1987, IAU Circular No. 4474.

Mammano, A., Ciatti, F.: 1975, Astron. Astrophys. *39*, 405.

Mammano, A., Rosino, L., Yildizdogdu, S.: 1975, in "Variable Stars and Stellar Evolution', IAU Symposium 67, V.E. Sherwood and L. Plaut eds., D. Reidel, Dordrecht, p. 401.

Marsh, K.A., Purton, C.R., Feldman, P.A.: 1976, Astron. Astrophys. *49*, 211.

Marshall, F.E., Boldt, E.A., Holt, S.S., Mushotzky, R.F., Pravdo, S.H., Rotschild, R.E., Serlemitsos, P.J.: 1979, Astrophys. J. Suppl. *40*, 657.

Marsi, C., Selvelli, P.L.: 1987, Astron. Astrophys. Suppl. *71*, 153.

Mason, K.C., Cordova, F.A., Bode, M.F., Barr, P.: 1987, in 'RS Ophiuci (1985) and the Recurrent Nova Phenomenon', M.F. Bode ed., VNU Science Press, Utrecht, p. 167.

Matsuda, T., Jnoye, M., Sawada, K.: 1987, Mon. Not. R. astr. Soc. *226*, 785.

Mattei, J.A.: 1978, J.R.A.S. Canada *72*, 61.

Mattei, J.A.: 1979, J.R.A.S. Canada *73*, 173.

Mattei, J.A.: 1984, IAU Circular No. 3932.

Mattei, J.A.: 1985, IAU Circular No. 4122.

Mattei, J.A.: 1986, private communication.

Mattei, J.A.: 1987, IAU Circular No.

Mattei, J.A.: 1988, private communication.

Mayall, M.W.: 1949, Harvard Bull. No. 919, p. 15.

Mayall, M.W.: 1969, J.B. Soc. Canada *63*, 321.

McCall, A., Hough, J.H.: 1980, Astron. Astrophys. Suppl. *42*, 141.

Meinunger, L.: 1979, Inf. Bull. Var. Stars, No. 1611.

Menzel, D.H.: 1946, Physica *12*, 768.

Menzel, D.H.: 1969, in 'Les Transitions Interdites dans les Spectres des Astres', 15me Colloque Astrophys. de Liege, p. 341.

Merrill, P.W.: 1951, Astrophys. J. *113*, 605.

Merrill, P.W.: 1958, Etoiles a Raies d'Emission, Institut d'Astrophysique, Cointe-Sclessin, p. 436.

Merrill, P.W., Burwell, C.G.: 1950, Astroph. J. *112*, 72.

Merrill, P.W., Humason, M.L.: 1932, Publ. astr. Soc. Pacific *44*, 56.

Michalitsianos, A.G., 1984, Comments on Modern Physics, Vol. 10, No. 3, 85.

Michalitsianos, A.G., Kafatos, M., Fahey, R.P., Viotti, R., Cassatella, A., Altamore, A.: 1988a Astrophys. J. *331*, 477.

Michalitsianos, A.G., Kafatos, M.: 1984, Mon. Not. R. Astr. Soc. *207*, 575.

Michalitsianos, A.G., Oliversen, R.J., Hollis, J.M., Kafatos, M., Crull, H.E., Miller, R.J.: 1988b, Astron. J. *95*, 1478.

Mikolajewska, J.: 1985, Acta Astronomica *35*, 65.

Mikolajewska, J.: 1987, Astroph. Space Sci. *131*, 713.

Mikolajewska, J., Friedjung, M., Kenyon, S.J., Viotti, R. (editors): 1988, Proceedings of IAU Colloquium No. 103 'The Symbiotic Phenomenon', Kluwer Academic Publishers, Dordrecht, The Netherlands.

Mikolajewska, J., Selvelli, P.L., Hack, M.: 1988, Astron. Astroph. *198*, 150.

Mikolajewska, J., Selvelli, P.L., Hack, M.: 1987, IAU Coll. 93, Astroph. Space Sci. *131*, 725.

Mikolajewski, M., Biernikowicz, R.: 1986, Astron. Astroph. *156*, 186.

Mikolajewski, M., Szczerba, R., Tomov, T.: 1988, in 'The Symbiotic Phenomenon', IAU Colloquium 103, J. Micholajewska et al. eds., Kluwer Ac. Puble., Dordrecht, p. 221.

Mikolajewski, M., Tomov, T., Mikolajewska, J.: 1987, IAU Coll. 93 Astroph. Space Sci. *131*, 733.

Mikolajewski, M., Tomov, T.: 1986, M.N.R.A.S. *219*, 13P.

Morris, S.C.: 1977, IAU Circ. 3101.

Muchmore, D.O., Nuth, J.A.III, Stencel, R.E.: 1987, Astrophys. J. (Letters) *315*, L141.

Mueller, B.E.A., Nussbaumer, H., Schmutz, W.: 1986, Astron. Astrophys. *154*, 313.

Mueller, B.E.A., Nussbaumer, H.: 1985, Astron. Astrophys. *145*, 144.

Muratorio, G., Friedjung, M.: 1982, in 'The Nature of Symbiotic Stars', IAU Colloquium 70, M. Friedjung and R. Viotti eds., D. Reidel, Dordrecht, p. 177.

Nakagiri, M., Yamashita, Y.: 1982, Ann. Tokyo Obs. *19*, 8.

Nassau, J.J., Blanco, V.M.: 1954, Astrophys. J. *120*, 129.

Nikitin, S.N., Khudyakova, T.N.: 1979, Sov. Astron. Letters 5, 327.

Nussbaumer, H.: 1982, in 'The Nature of Symbiotic Stars', M. Friedjung and R. Viotti eds., D. Reidel, Dordrecht, p. 85.

Nussbaumer, H.: 1986, Astron. Astrophys. *155*, 205.

Nussbaumer, H., Schild, H.: 1981, Astron. Astrophys. *101*, 118.

Nussbaumer, H., Schild, H., Schmid, H.M., Vogel, M.: 1988, Astron. Astrophys. *198*, 179.

Nussbaumer, H., Schild, H.: 1979, Astron. Astrophys. *75*, L17.

Nussbaumer, H., Schmutz, W., Vogel, M.: 1986, Astron. Astrophys. *169*, 154.

Nussbaumer, H., Schmutz, W.: 1983, Astron. Astrophys. *126*, 59.

Nussbaumer, H., Stencel, R.E.: 1987, in 'Exploring the Universe with the IUE Satellite', Y. Kondo ed., Reidel, Dordrecth, p. 203.

Nussbaumer, H., Storey, P.J.: 1982, Astron. Astrophys. *115*, 205.

Nussbaumer, H., Storey, P.J.: 1984, Astron. Astrophys. Supplem. Ser. *56*, 293.

Nussbaumer, H., Storey, P.J.: 1979, Astron. Astroph. *74*, 244.

Nussbaumer, H., Vogel, M.: 1989, Astron. Astrophys. *213*, 137.

Nussbaumer, H., Vogel, M.: 1988, in 'The Symbiotic Phenomenon', IAU Colloquium No. 103, J. Mikolajewska et al. eds., Kluwer Acad. Pub., p. 169.

Nussbaumer, H., Vogel, M.: 1987, Astron. Astrophys. *182*, 51.

O'Dell, C.R.: 1966, Astrophys. J. *145*, 487.

O'Dell, C.R.: 1967, Astrophys. J. *149*, 373.

Oliversen, N.A., Anderson, C.M.: 1982a, in 'The Nature of Symbiotic Stars', IAU Colloquium 70, M. Friedjung and R. Viotti eds., D. Reidel, Dordrecht, p.71.

Oliversen, N.A., Anderson, C.M.: 1988, Astron. Astrophys. *190*, L5

Oliversen, N.A., Anderson, C.M.: 1982b, in "The Nature of Symbiotic Stars" IAU Colloquium No. 70, M. Friedjung and R. Viotti, eds., D. Reidel, Dordrecht, p. 177.

Oliversen, N.A., Anderson, C.M., Stencel, R.E., Slovak, M.H.: 1985, Astroph. J. *295*, 620.

Olson, G.L.: 1982, Astrophys. J. *255*, 267.

Osterbrock, D.E.: 1974, 'Astrophysics of Gaseous Nebulae', W.H. Freeman and Co., San Francisco, USA.

Paczynski, B., Rudak, B.: 1980, Astron. Astrophys. *82*, 349.

Paczynski, B., Zytkov, A.N.: 1978, Astrophys. J. *222*, 604.

Padin, S., Davis, R.J., Bode, M.F.: 1985, Nature *315*, 306.

Panagia, N., Felli, M.: 1975, Astron. Astrophys. *39*, 1.

Panov, K., Ivanova, M., Kovachev, B.: 1985, IAU Circ. 4153.

Panov, K.P, Kovachev, B., Ivanova, M., Geyer, E.H.: 1985, Astroph. Space Sci. *116*, 355.

Paresce, F., Burrows, C., Horne, K.: 1988, Astrophys, J. 329, 318.

Payne-Gaposchkin, C.: 1946, Astrophys. J. *104*, 362.

Payne-Gaposchkin, C.: 1954, Ann. Harvard Obs. *113*, 1912.

Penston, M.V., Allen, D.A.: 1985, Mon. Not. R. astr. Soc. *212*, 939.

Penston, M.V., Benvenuti, P., Cassatella, A., Heck, A., Selvelli, P.L., Macchetto, F., Ponz, P., Jordan, C., Cramer, N., Rufener, F., Manfroid, J.: 1983, Mon. Not. R. Astr. Soc. *202*, 833.

Persi, P., Preite-Martinez, A., Ferrai-Toniolo, M., Spinoglio, L.: 1987, Vulcano Workshop 'Planetary and Proto-Planetary Nebulae: from IRAS to ISO', A. Preite-Martinez editor, Reidel, Dordrecht, p. 221.

Persic, M., Hack, M., Selvelli, P.L.: 1984, Astron. Astroph. *140*, 317.

Piirola, V.: 1982, 'The Nature of Symbiotic Stars', IAU Colloquium 70, M. Friedjung and R. Viotti eds., Reidel, Dordrecht, p. 139.

Piirola, V.: 1983, "Cataclysmic Variables and Related Objects", IAU Colloquium 72, M. Livio and G. Shaviv, eds., Reidel, Dordrecht, p. 211.

Piro, L., Cassatella, A., Spinoglio, L., Viotti, R., Altamore, A.: 1985, IAU Circular No. 4082.

Plaskett, H.H.: 1928, Pub. Dom. Astrophys. Obs. Victoria *4*, 119.

Poekert, R.: 1975, Astrophys. J. *196*, 777.

Ponz, D., Cassatella, A., Viotti, R.: 1982, "The Nature of Symbiotic Stars", IAU Colloquium 70, M. Friedjung and R. Viotti, eds., D. Reidel, Dordrecht, p. 217.

Pottasch, S.R.: 1984, "Planetary Nebulae", D. Reidel, Dordrecht, The Netherlands.

Pottasch, S.R., Varsavsky, C.M.: 1960, Ann. d'Astrophys. *23*, 516.

Pucinskas, A.: 1970, Bull. Vilnius Astroph. Obs. *27*, 24.

Purton, C.R., Allen, D.A., Feldman, P.A., Wright, A.E.: 1977, Mon. Not. R. Astr. Soc. *180*, 978.

Purton, C.R., Feldman, P.A., Marsh, K., Allen, D.A., Wright, A.E., 1982, Mon. Not. R. Astr. Soc. *198*, 321.

Purton, C.R., Feldman, P.A., Marsh, K.A.: 1973. Nature Phys. Sci. *245*, 5.

Purton, C.R., Kwok, S., Feldman, P.A., 1983, Astron. J. *88*, 1825.

Querci, F.R.: 1986, in 'The M-Type Stars', Monograph Series on Nonthermal Phenomena in Stellar Atmospheres, NASA SP-492, p. 1.

Raassen, A.J.J. 1985, Astrophys. J. *292*, 696.

Reimers, D., Cassatella, A.: 1985, Astrophys. J. *297*, 275.

Reshetnikov, V.P., Khudyakova, T.N.: 1984, Pisma A.J. *10*, 673.

Rieke, G.H., Leborsky, M.J.: 1985, Astrophys. J. *288*, 618.

Robinson, L.: 1969, Per. Sviosdi *16*, 507.

Rodriguez, M.H.: 1988, in 'The Symbiotic Phenomenon', IAU Colloquium No. 103, J. Mikolajewska et al. eds., Kluwer Acad, Publ., Dordrecht, p. 229.

Roman, N.G.: 1953, Astrophys. J. *117*, 467.

Roman, N.G.: 1955, Astrophys. J. Supplem. Ser. *2*, 195.

Rossi, C., Altamore, A., Viotti, R.: 1984, Astron. Astrophys. Supplem. Ser. *55*, 361

Rossi, C., Altamore, A., Ferrari-Toniolo, M., Persi, P., Viotti, R.: 1988, Astron. Astrophys. *206*, 279

Schroeder, K.P.: 1988, in 'The Symbiotic Phenomenon', IAU Colloquium 103, J. Mikolajewska et al. eds., Kluwer Ac. Publ., Dordrecht, p. 339.

Schulte-Ladbeck, R.: 1985, Astron. Astrophys. *142*, 333.

Schulte-Ladbeck, R.E.: 1988, Astron. Astrophys. *189*, 97.

Schulte-Ladbeck, R., Magalhaes, A.M.: 1987, Astron. Astrophys. *181*, 213.

Schwarz, H.E.: 1988, 'The Symbiotic Phenomenon', IAU Colloquium 103, J. Mikolajewska et al. eds., Kluwer Ac. Publ., Dordrecht, p. 123.

Schwarz, H.E., Aspin, C., Hanner, M., Zarnecki, J.: 1987, in 'Infrared Astronomy with Arrays', C.G. Wynn-Williams and E.E. Becklin eds., University of Hawaii, Institute for Astronomy, Honolulu, p. 312.

Schwarz, H.E., Aspin, C.: 1987, Proc. IAU Symp. 122, 'Circumstellar Matter', I. Appenzeller and C. Jordan eds., Reidel, Dodrecht, p. 471.

Seaquist, E.R., Gregory, P.C.: 1973, Nature Phys. Sci. *245*, 85.

Seaquist, E.R., Taylor, A.R., Button, S.: 1984, Astrophys. J. *284*, 202.

Seaquist, E.R., Taylor, A.R.: 1987, Astrophys. J. *312*, 813.

Selvelli, P.L.: 1988, in "The Symbiotic Phenomenon", IAU Colloquium 103, J. Mikolajewska, M. Friedjung, R. Viotti, eds., Kluwer, Acad. Publ., Dordrecht, p. 209.

Selvelli, P.L., Cassatella A., Hack M.: 1987 IAU Circ. 4491.

Selvelli, P.L., Hack, M.: 1985b, ESA SP 236, 207.

Selvelli, P.L., Hack, M.: 1985a, Astronomy Express *1*, 115.

Serkowski, K.: 1968, Astrophys. J., *154*, 1 15.

Serkowski, K.: 1970, Astrophys. J. *160*, 1083.

Serkowski, K.: 1973, Astrophys. J. (Letters) *179*, L101.

Serkowski, K., Mathewson, D.S., Ford, V.L.: 1975, Astrophys. J. *196*, 261.

Seward, F.D.: 1985, private communication to R. Viotti.

Shao, C. Y., Liller, W.: 1971, Bull. American Astron. Soc. *3*, 443.

Skopal, A., Chochol, D., Vittone, A., Mammano, A.: 1988, 'The Symbiotic Phenomenon', IAU Colloquium 103, J. Mikolajewska et al. eds., Kluwer Ac. Publ., Dordrecht, p. 289.

Slovak, M.H.: 1982a, Astrophys. J. *262*, 282

Slovak, M.H.: 1982b, Ph. D. Thesis, University of Texas.

Slovak, M.H., Africano, J.: 1978, Mon. Not. R. Astr. Soc. *185*, 591.

Slovak, M.H., Cassinelli, J P., Anderson, C.M., Lambert, D. I.: 1987, Astrophys. Space Sci. *131*, 765.

Slovak, M.H., Lambert, D.L.: 1988, in 'The Symbiotic Phenomenon', IAU Colloquium 103, J. Mikolajewska et al. eds., Kluwer Ac. Publ., Dordrecht, p. 265.

Smak, J.: 1964, Astroph. J. Suppl. *9*, 141.

Smak, J.: 1981, Acta Astron. *31*, 395.

Smith, S.E., Bopp, B.W.: 1981, Mon. Not. R. Astr. Soc. *195*, 733.

Snijders, M.A.J.: 1987, in 'RS Ophiuchi (1985) and the Recurrent Nova Phenomenon', M.F. Bode editor, VNU Science Press, Utrecht, p. 51.

Sobolev, V.V.: 1960, 'Moving Envelopes of Stars', Harvard University Press, Cambridge, USA.

Solf, J.: 1983, Astroph. J. Lett. *266*, L119.

Solf, J.: 1987, Astron. Astroph. *180*, 207.

Solf, J., Ulrich, H.: 1983, Mitt. Astron. Ges. *60*, 318.

Sopka, R.J., Herbig, G., Kafatos, M., Michalitsianos, A.G.: 1982, Astrophys. J. (Letters) *258*, L32.

Spiesman, W.J.: 1984, M.N.R.A.S. *206*, 77.

Spoelstra, T.A.T., Taylor, A.R.,Pooley, G.G., Evans, A., Allinson, J.S.: 1987, Mon. Not. R. Astr. Soc. *224*, 791.

Stencel, R.E., Linsky, J.L., Brown, A., Jordan, J.: 1981, Mon. Not. R. Astr. Soc. *196*, p. 47.

Stencel, R.E., Michalitsianos, A.G., Kafatos, M., Boyarchuk, A.A.: 1982, Astrophys. J. (Letters) *253*, 177.

Stern, R.A., Nousek, J.A., Nugent, J.J., Agraval, P.C., Riegler, G.R., Rosenthal, A., Pravdo, S.H., Garmire, G.P.: 1981b, Astrophys. J. (Letters) *251*, L105.

Stern, R.A., Zolcinski, M.C., Antiochos, S.P., Underwood, J.H.: 1981a, Astrophys. J. *249*, 647.

Stickland, D.J., Seaton, M.J., Snijders, M.A.J., Storey, P.J.: 1981, Mon. Not. R. Astr. Soc. *197*, 107.

Stienon, F.M., Chartrand III, M.R., Shao, C.V.: 1974, Astron. J. *79*, p. 47.

Swings, J.P., Allen, D.A.: 1972, Pub. astr. Soc. Pacific *84*, 523.

Swings, J.P., Klutz, M.: 1976, Astron. Astrophys. *46*, 303.

Swings, P.: 1970, in 'Spectroscopic Astrophysics', G.H. Herbig editor, University of California Press, Berkeley/Los Angeles/London, p. 189.

Swings, P., Struve, O.: 1941, Astrophys. J. *93*, 356.

Swings, P., Struve, O.: 1940, Astrophys. J. *91*. 546.

Szkody, P., Michalsky, J.J., Stokes, G.M.: 1982, Pub. Astron, Soc. Pacific *94*, 137

Tamura, S.: 1981, Pub. Astr. Soc. Japan *33*, 701.

Tamura, S.: 1988, in 'The Symbiotic Phenomenon', IAU Colloquium 103, J. Mikolajewska et al. eds., Kluwer Ac. Publ., Dordrecht, p. 285.

Taranova, O.C., Yudin, B.F.: 1983, Astron. Astrophys. *117*, 209.

Taranova, O.C., Yudin, B.F., 1981, Sov. Astron. *25*, 710.

Taylor, A.R.: 1988, in 'The Symbiotic Phenomenon', IAU Colloquium 103, J. Mikolajewska et al. eds., Kluwer Ac. Publ., Dordrecht, p. 77.

Taylor, A.R., Seaquist, E.R., Kenyon, S.J.: 1988, in 'The Symbiotic Phenomenon', IAU Colloquium 103, J. Mikolajewska et al. eds., Kluwer Ac. Publ., Dordrecht, p. 231.

Taylor, A.R., Seaquist, E.R.: 1984, Astrophys. J. *286*, 263.

Taylor, A.R., Seaquist, E.R. Mattei, J.A.: 1986, Nature *319*, 38.

Taylor, A.R., Seaquist, E.R.: 1985, IAU Circ. 4055.

Thackeray, A.D.: 1950, Mon. Not. R. Astr. Soc. *110*, 45.

Thackeray, A.D.: 1953, Mon. Not. R. Astr. Soc. *113*, 211.

Thackeray, A.D., 1977, Mem. R. Astr. Soc. *83*, 1.

Thackeray, A.D., Hutchings, J.B.: 1974, Mon. Not. R. Astr. Soc. *167*, 319.

Thackeray, A.D., Webster, B.L.: 1974, Mon. Not. R. Astr. Soc. *168*, 101.

Tomov, T.: 1984, Inf. Bull. Var. Stars No. 2610.

Tomov, T., Luud, L.S.: 1984, Astrofisika *20*, 99.

Torbett, M.V., Campbell, B.: 1987, Am. Astr. Soc. Bull., p. 917.

Tutukov, A.V., Yungelson, L.R.: 1976, Astrophysics, *12*, 342.

Vaiana, G.S., Cassinelli, J.P., Fabbiano, G., Giacconi, R., Golub, L., Gorenstein, P., Haish, B.M., Harnden, F.R. Jr., Johnson, H.M., Linsky, J.L., Maxson, C.W., Mewe, R., Rosner, R., Seward, F., Topka, K., Zwaan, C.: 1981, Astroph. J. *245*, 163.

Viotti, R.: 1976, Astrophys. J. *204*, 293.

Viotti, R.: 1987a, Vulcano Workshop 'Planetary and Protoplanetary Nebulae from IRAS to ISO', A. Preite-Martinez editor, Reidel, Dordrecht, p. 163.

Viotti, R.: 1987b, Proceed. 6th European Conference on White Dwarfs, F. D'Antona editor, Mem. Soc. Astr. Ital. Vol. *58*, 147.

Viotti, R.: 1988a, unpublished results.

Viotti, R.: 1988b, in 'The Symbiotic Phenomenon', IAU Colloquium 103, J. Mikolajewaska et al. eds., Kluwer Ac. Publ., Dordrecht, p. 269.

Viotti, R.: 1989, in 'Physics of Classical Novae', IAU Colloquium No. 122.

Viotti, R., Altamore, A., Ferrari-Toniolo, M., Friedjung, M., Persi, P., Rossi, C., Rossi, L.: 1986, Astron. Astrophys. *159*, 16.

Viotti, R., Altamore, A., Baratta, G.B., Cassatella, A., Friedjung, M., 1984a, Astrophys. J., *283*, 226.

Viotti, R., Cassatella, A., Altamore, A.: 1984b, ESA SP-218, 403.

Viotti, R., Eiroa, C., Cassatella, A., Altamore, A.: 1983b, IAU Circular No. 3855.

Viotti, R., Giangrande, A., Ricciardi, O., Cassatella, A.: 1982, in 'The Nature of Symbiotic Stars', IAU Colloquium 70, M. Friedjung and R. Viotti eds., D. Reidel, Dordrecht, p. 125.

Viotti, R., Piro, L., Friedjung, M., Cassatella, A.: 1987, Astrophys. J. (Letters), *319*, L7.

Viotti, R., Ricciardi, O., Ponz, D., Giangrande, A., Friedjung, M., Cassatella, A., Baratta, G.B., Altamore, A.: 1983a, Astron. Astrophys., *119*, 285.

Walker, G.A.H.: 1977, Mon Not. R. Astr. Soc. *179*, 587.

Walker, G.A.H., Morris, S.C., Younger, P.F.: 1969, Astrrophys. J. *156*, 117.

Wallerstein, G.N.: 1968, The Observatory *88*, 111.

Wallerstein, G.N.: 1981, The Observatory *101*, 172.

Wallerstein, G.N.: 1981, Publ. Astron. Soc. Pacific *98*, 330.

Wallerstein, G.N.: 1983, Publ. Astron. Soc. Pacific *95*, 135.

Wallerstein, G.N.: 1986, Publ. Astron. Soc. Pacific *98*, 118.

Wallerstein, G.N., Bolte, M., Whitehill-Bates, P., Mateo, M.: 1986, Publ. Astron. Soc. Pacific *98*, 330.

Wallerstein, G., Greenstein, J.L.: 1980, Pub. Astr. Soc. Pacific *92*, 275.

Wallerstein, G., Willson, L.A., Salzer, J., Brugel, E.: 1984, Astron. Astrpophys. *133*, 137.

Warner, B.: 1972, M.N.R.A.S. *159*, 95.

Wdowiak, T.J.: 1977, Publ. Astron. Soc. Pacific *89*, 569.

Webster, B.L.: 1966, Pub. Astr. Soc. Pacific *78*, 136.

Webster, B.L., Allen, D.A.: 1975, Mon. Not. R. Astr. Soc. *171*, 171.

Wendker, H.J., Baars, J.W.M., Altenhoff, W.J.: 1973, Nature Phys. Sci. *245*, 118.

Wenzel, W.: 1976, Inf. Bull. Var. Stars No. 1222.

Whitelock, P.A.: 1987, Pub. Astr. Soc. Pacific *99*, 573.

Whitelock, P.A.: 1988, in 'The Symbiotic Phenomenon', IAU Colloquium 103 J. Mikolajewska et al. eds., Kluwer Ac. Publ., Dordrecht, p. 47.

Whitelock, P.A., Catchpole, R.M., Feast, M.W., Roberts, G., Carter, B.S.: 1983a, Mon. Not. R. Astr. Soc. *203*, 373.

Whitelock, P.A., Feast, M.W., Roberts, G., Carter, B.S., Catchpole, R.M.: 1983c, Mon. Not. R. Astr. Soc. *205*, 1207.

Whitelock, P.A., Feast, M.W., Catchpole, R.M., Carter, B.S., Roberts, G.: 1983b, Mon. Not. R. Astr. Soc. *203*, 351.

Willson, L.A., Garnavich, P., Mattei, J.A.: 1981, Inf. Bull. Var. Stars No. 1961.

Willson, L.A., Wallerstein, G., Brugel, E.W., Stencel, R.E.: 1984, Astron. Astrophys., *133*, 154.

Wilson, R.E.: 1942, Astroph. J. *96*, 371.

Wilson, R.E.: 1943, Publ. Astr. Soc. Pacific *55*, 282.

Wilson, W.J., Barrett, A.H.: 1972, Astron. Astrophys. *17*, 385.

Wood, P.R.: 1974, Astrophys. J. *190*, 609.

Wright, A.E., Allen, D.A.: 1978, Mon. Not. R. Astr. Soc. *184*, 893.

Wright, A.E., Barlow, M.J.: 1975, Mon. Not. R. Astr. Soc. *170*, 41.

Yamashita, Y., Maehara, H.: 1979, Publ. Astron. Soc. Japan *31*, 307.

Yoo, K.H., Yamashita, Y.: 1984, Publ. Astron. Soc. Japan *36*, 567.

Zirin, H.: 1976, Nature *259*, 466.

15

PERSPECTIVES AND UNSOLVED PROBLEMS

M. Friedjung, M. Hack, C. la Dous and R. Viotti

PRECEDING PAGE BLANK NOT FILMED

In this book we reviewed the observations of dwarf novae, nova-like stars, novae, recurrent novae and symbiotic stars, and the current state of their interpretation. We tried to demonstrate the immense variety and variability of phenomena found in these objects.

As is probably true in all other fields of science, we are facing a dilemma. On one hand the availability of new observational material- from satellite telescopes as well as from ever more advanced and sophisticated ground-based devices - is opening our eyes to ever new phenomena in cataclysmic variables which help clarifying some questions. On the other hand, however, unexpected new questions and problems arise. The general picture becomes clearer; for instance there is little doubt left that in principle the Roche model is rather well suited for explaining the basic physics of cataclysmic variables (with the possible exception of symbiotic stars), but curious assumptions and concepts flourish if details of individual observations are to be explained. And, not surprisingly, conceptual understanding has evolved much further than our ability to carry out detailed, meaningful computations.

Let us consider dwarf novae and nova-like stars. A few intriguing statistical differences between the different sub-classes of these systems seem to exist, with respect to the distribution of orbital periods and the masses of the stellar components. Furthermore, judging from their spectroscopic and photometric appearance, nova-like stars belonging to the sub-class of UX Ursae Majoris stars, anti-dwarf novae and dwarf novae appear to be basically the same kind of objects. In most respects also the DQ Herculis stars are very similar to them. They are suspected, however, to possess a moderately strong magnetic white dwarf. And finally, the appearance and behavior of AM Herculis stars can be understood, if it is assumed that they also are basically the same kind of objects, but that their white dwarfs possess a very strong magnetic field. AM Canum Venaticorum stars, on the other hand, represent a different kind of system. The complete absence of hydrogen lines from their spectra, in conjunction with the extremely short orbital periods, suggest that these systems consist of two white dwarfs and, therefore, that their evolutionary history must be different than that of the other systems which are believed to consist of a white dwarf and a red dwarf.

Although nova-like stars are commonly believed to be dwarf novae in a permanent state of outburst, statistical differences in the photometric and spectroscopic appearance of members of both classes suggest that the physical differences between them might lie beyond mere outburst behavior.

In spite of the very large number of observations of dwarf novae, the very start of rise to an outburst, due to the unpredictability of the event, has so far escaped detailed observations. However, this particular phase in the activity cycle of dwarf novae is very likely to contain valuable clues to the structure and dynamics of the accretion discs. Thus, what is called for in order to help the situation is continuing monitoring of a few selected objects, both photometrically and spectroscopically, in as large a spectral range and over as long a time interval as possible.

In both dwarf novae and nova-like systems the companion stars are cool main-sequence stars which in all probability undergo solar-type activity cycles. These activities, in turn, are likely to influence the brightness variability of cataclysmic variables. Moreover, according to theoretical considerations, the secondary stars are forced to co-rotate with the binary orbit at a considerably higher velocity than normal for stars of this spectral type. It is not known yet what effect this has on the star, nor is it known what effect it must have for it to be confined to the non-spherical shape of the Roche lobe. All these problems should be taken into account by a new generation of theoretical models.

A weak point in the computation of models is also the structure of the accretion discs. So far only very simplified models have been consid-

ered. Two-dimensional hydrodynamics computations depend strongly on the assumptions about the viscosity. Moreover, the vertical stratification has been included in the computations only in a rather crude way, yielding correspondingly vague results. A further complication is presented by the hot spot. The geometrical structure and the position of it in the disc, which are a theoretical rather than a controversial issue, are bound to influence the structure and dynamics of the disc. Similarly, spectrum computations, too, severely suffer from the poorly known physical structure of the accretion discs.

Classical and recurrent novae, both in quiescence and in outburst, present plenty of open problems. We summarize here some of them, and will try to indicate which course to pursue for tackling them.

One main question is: are dwarf novae, nova-like stars and old novae the same class of objects, just seen in different stages of activity? Actually the only known statistical difference among these three groups, besides the outburst activity, is their absolute magnitude: the magnitudes at minimum of old classical novae cluster around +4.5, those of quiescent dwarf novae around +7, and the nova-like stars have magnitudes clustering around +5. This difference might be due to a weakening of the accretion disc in very old novae. Furthermore, there is some indication that very old novae, like CK Vul, are several magnitudes fainter than old novae just a few decades after the outburst. Also two of them, CK Vul, and WY Sge, are reminiscent in their photometric behavior of dwarf novae. Both these observations can be taken as a sugestion that dwarf novae merely are very old novae. It is not clear, however, where the apparently closely related nova-like variables fit into this picture.

Actually we observe 50 novae per year in M 31. In 15 billion years there should occur 7.5×10^{11} novae. Hence we have two possibilities. Either practically all stars in M 31 will become or have been novae, or each nova must suffer f outbursts (with f the ratio of the total number of stars in M 31 to the number of nova systems). Since we observe that only 1/1000 binary systems are formed of a close white dwarf plus a red dwarf, able to produce a nova outburst, the second possibility is the only one which can be accepted. The hibernation theory follows, according to which each nova will erupt thousand of times and stay in a low state for centuries between one outburst and the following one. Although many details are not completely explained, the hibernation theory gives a unifying picture of dwarf novae, nova-like stars and novae, explaining the change from one class of cataclysmic variables to another with the change of mass transfer over the millennia.

Another question is why novae are so similar to each other at minimum, and so different from each other in outburst? Actually it is difficult to say if an old nova behaved as a fast nova or a slow nova, just looking at its characteristics in quiescence.

Fundamental parameters like the masses of the two components, or even as basic as the orbital periods, of a cataclysmic variable system are badly known. There is a need for simultaneous as well as long-term observations of light curves and radial velocity curves, so far available for just a few individuals.

Still, careful analysis of observations indicates that the problem of deriving system parameters is not as straightforward as one might naively assume. Besides the technical problems of suitable data analysis, such as properly taking into account irradiation effects in the system, some difficulties seem to be even more basic, reflecting that the underlying physics probably is not quite as simple as would be desirable. For instance, in some systems the photometric periods seem to be variable on unreasonably short time-scales. In other systems the spectroscopic and photometric periods are different from each other.

It is very important to get better determinations of the chemical composition of the ejecta of novae, both for obtaining information on the phenomena occurring at the surface of the hot degenerate star when it accretes matter from the boundary layer of the accretion disc, and also for obtaining information on the characteristics of the white dwarf itself.

The impact of ultraviolet observations on our knowledge of cataclysmic variables has been very important. Not only because it has given us the possibility to obtain abundance determinations from ions not observable in the optical range, but also for having given us proofs of the reality of the existence of accretion discs from the shape of the continua, which are generally fitted by a power law. Only in few cases can a Rayleigh-Jeans tail, imputable to the hot member, be detected. The importance of extending the observations to shorter wavelengths than those accessible to IUE is clear. However the hope of detecting the spectrum of the hot companion at shorter wavelengths than those accessible with IUE will not necessarily be satisfied. In fact the few data from Voyager actually indicate that the same power law explaining the IUE range is not valid for the shorter wavelengths, but neither is it explicable by a hot black body emission. The spectrum instead is generally very flat.

Few nova outbursts have been observed in the near infrared. From these data it seems that a different behavior characterizes the fast novae (no appreciable formation of a dust shell), the intermediate novae (formation of an optically thin dust shell) and the slow novae (formation of a thick dust shell, although the few data for two very slow novae indicate absence of a dust shell). It is not yet clear how general these relations are. A larger sample is certainly needed, in order to firmly support the notion that these behaviors really are correlated to the speed class of a nova. The mechanism of dust formation is not clear either. Dust may be preexisting to the outburst or it may form in the envelope when it cools off.

The foremost problem with recurrent novae is one of classification, thus one of what one imagines their basic structure to be.

It is not obvious that they can be addressed as a reasonably homogeneous class at all. Only five individuals (*) are known which can be divided into at least three sub-classes: T Pyx and U Sco are similar to classical novae, V 1017 Sgr has a behavior more reminiscent of that of symbiotic stars, and finally, T CrB and RS Oph have a red giant in their system (rather than a red dwarf as the other cataclysmic variables). T Pyx, unlike other recurrent novae, presents a very steep rise of the ultraviolet flux toward the shortest wavelengths accessible to IUE.

Also, the distinction between novae and symbiotic stars is not as neat as one would like it to be. Symbiotic stars are known, like V 1016 Cyg and V 1329 Cyg, which behave much like classical novae. On the other hand RT Ser and RR Tel, both commonly classified as old novae, behave much like symbiotic stars.

Since the basic structures of novae and symbiotic stars might be rather different from each other, but since recurrent novae bear characteristics of both, their investigation might yield valuable clues to the nature of both, old novae and symbiotic stars.

Because of the length of the orbital periods of those symbiotics that have been ascertained to be binary systems, the interaction between the cool giant and its companion must occur, in the majority of cases, by accretion through winds rather than by overflow of the Roche lobe. It is possible that many characteristics of the outbursts are affected by the properties of the orbits, by their eccentricity, etc. It should be, therefore, necessary to obtain better determinations of the radial velocity curve, over long periods of time, covering more than one orbital period. In fact one main difficulty in obtaining reliable radial velocity curves is that the amplitudes are generally small and comparable with the irregular fluctuations often present in the atmospheres of cool giants and supergiants.

The problems of line blending of the wide Doppler broadened lines mean that outburst spectra in different spectral regions must be studied using spectral synthesis. The use of spectral synthesis requires the finding of parameters which are sensitive to unknown quantities connected

(*) A sixth recurrent nova has been recently discovered: V394 CrA 1949 which had a second outburst in 1987. It behaves similarly to T Pyx and U Sco. (Liller, 1987)

with the model, abundances, etc. A vague resemblance of the results of a calculation to what is observed is not sufficient.

Besides better observations we certainly need better and more realistic models.

Parameters which affect the absolute magnitudes at maximum, the shape of the outburst light curve, and the ejection velocities, etc. can be the mass and chemical composition of the white dwarf, the mass of the accreted material and the accretion rate, the degree of mixing of white dwarf material into accreted hydrogen-rich shell material, the orbital elements and the inclination of the orbit, and the presence and strength of magnetic fields, etc. Unfortunately the majority of these data are only poorly known or altogether unknown. Through extensive comparison between theoretical models and observations it should be possible to get a better handle on physically reasonable parameter ranges for more sophisticated models. Such new models then clearly should take into account non-LTE effects, circumstellar absorption and dust, and the hydrodynamics and thermodynamics of shocks, etc., before spectral synthesis is attempted.

As long as such a theory is not available or not usable, semi-empirical methods of analysis need to be further developed, among these the self-absorption curve method by Friedjung and Muratorio (1987) for studying spectra of ions where there are very many lines, such as Fe II, should be mentioned. In such methods the fit is made to assumed physical situations which, because of physical uncertainties involved, have more free parameters than a self-consistent theory.

Simultaneous or nearly simultaneous multifrequency observations are required for comparison with spectral synthesis leading to determination of the total bolometric luminosity, the mass-loss rate and velocity distribution of the continuously ejected wind, and the disc structure, etc.

Novae often go through post-maximum oscillations; and to understand their nature, multifrequency observations closely spaced in time are needed.

Observations of high spatial resolution in various spectral bands can give more information about the geometry of the ejected envelope, including deviations from spherical symmetry. It will be particularly interesting to resolve the envelope as early as possible after the outburst of a nova and to follow the evolution of its structure with time. Study of the spectrum of different parts of the nebula will not only give information about differences in physical conditions, but also about the velocity distribution in the line of sight (from line profiles), leading to the possibility of the three-dimensional reconstruction of envelope structure.

It must be emphasized that the study of nebular expansion, combined with knowledge of the expansion velocity, is the best method for determining the distance of a nova.

The theory of classical-nova outbursts needs to be further developed taking into account deviations from spherical symmetry and the influence of the companion.

In addition magnetic fields appear to be important for some old novae. The old nova V 1500 Cyg seems to be a polar object and GK Per an intermediate polar one. Strong fields should have a major effect on the outburst.

The causes of recurrent-nova outbursts are still not clear, and it is possible that some of the important physical processes involved are completely unknown. More work on accretion events and thermonuclear runaways at very short intervals of time may help to solve these problems.

A very large amount of work needs to be done before one can claim to understand novae reasonably well.

In the chapters devoted to the observation and modeling of symbiotic stars, attention has been focused on the *symbiotic phenomenon*, rather than on a group of stars. The reason was that (1) it is not clear whether symbiotic stars really represent a well-defined category of stars, and (2) our main interests are the physical processes occurring in the atmospheres of stars, rather than the nature of the stellar objects.

Actually, symbiotic stars represent only a comparatively small number of objects, and there should be no reason to dedicate so much time to their study, unless we expect from it - as is in fact the case- results of much wider interest.

We have shown in the previous chapters that symbiotic stars, as other cataclysmic variables, are characterized by non-LTE phenomena that have been observed in many different categories of astrophysical objects. These phenomena include: stellar chromospheres, mass loss and stellar winds, circumstellar nebulae, accretion phenomena in close binaries, superionization and X-ray emission, etc. These phenomena characterize several differents fields of astrophysics such as: formation of planetary nebulae, cool-and hot-star winds, circumstellar dust, jets, maser sources, pulsation, X-ray sources, accretion disks, thermonuclear runaway, and close binary evolution. Therefore, symbiotic stars are linked with many astrophysical categories of stars, including M-giants, Miras, Zeta Aur/VV Cep stars, hot subdwarfs, planetary nebulae, and obviously close binary systems, besides active galactic nuclei too. This is why symbiotic stars have always attracted the interest of so many investigators from different fields. Their hopes were, and are, to have a better insight into the physics of their own objects from the study of the symbiotic phenomenon, where the same mechanisms are probably present but with a larger strength, or on a different spatial scale.

On the other hand, we have found that the diagnostics of the symbiotic phenomenon are not very straightforward. First we need as complete an observational description of the phenomenon as possible. However, because of their long timescale variability, symbiotic stars must be studied for several decades, before a reasonably complete picture can be drawn. In addition coordinated observations in a broad frequency range are required, since, as discussed in previous chapters, different spectral regions involve different physical phenomena. In practice, this requirement was (at least partly) fullfilled in only a few cases.

On the other hand, a large amount of observational data on very broad samples of symbiotic stars has been collected in many different fields, from radio to X-rays, which in principle could be very useful for a statistical approach. But some concern should be expressed on the criteria which have been used in the selection of the targets in these surveys. It seems to us that these data have not yet been satisfactorily analyzed with the standard methods of statistical analysis. Thus new surveys, and extensive use of statistical methods, are aspects which require more work in the future. Selection effects will, however, have to be properly studied, and fully taken into account.

Another major problem is associated with the techniques of determination of the physical parameters from the observations. To develop an empirical model, we need to use diagnostics of the environment of the symbiotic stars derived from observational data. For instance, radio observations can provide information about ionized circumstellar envelopes, while the infrared rather gives information about the cool giant and circumstellar dust. Emission-line ratios provide first-approximation estimates of electron densities and electron temperatures in the line emitting regions. However, such regions are not uniform, which can explain differences in the parameters determined using different emission-line ratios; moreover the physical constants involved in the calculations are not too certain.

To overcome these type of difficulties, we need to calculate observable quantities from detailed models. The latter must take into account many different physical effects, including ionization of the wind of one stellar component by the other component, collision between winds, etc. These calculations use many unknowns, thus future work will have to involve convergence between models and observations. The ideas behind the former will have to be confronted by the facts provided by the latter.

In order to make progress from the observational point of view we need better orbital data about the binary systems. This requires the accurate determination of the radial-velocity variations of the cool component. *High resolution infrared spectra* will not only yield this, but will also provide information about the "normality" or "non normality" of the cool component. In addi-

tion, it may be noted that in this spectral region one can detect absorption between the observer and the cool component, so the envelope can be studied using absorption lines produced by it in such positions.

Diagnostic methods need to be enlarged. For instance, symbiotic stars are rich of Fe II emission lines which have proved to be very useful for the investigation of emission line objects. But still a large amount of data on this and other ions have not yet been studied. It should also be emphasized that the profiles of spectral lines formed by circumstellar material, rather than their radial velocities, needs to be examined. The radial velocity, in fact, gives only a kind of "integrated" information about the region of line formation, while the study of the line profile at high spectral resolution is basic for a detailed modeling. Finally, those systems showing *eclipses* can give a lot of information about the geometry and physical conditions of different regions.

Observations of *spatial structure* at *very high resolution* are essential. In this regard, we expect very exciting results from the Hubble Space Telescope as well as from the large ground-based telescopes equipped with new sophisticated instrumentation. In particular, information about jets and bipolar flows should be obtainable. *Polarization studies* will provide precious additional information on the geometry.

On the theroretical side, much is still to be understood about *accretion discs* in symbiotic systems, and in particular those formed following wind accretion. The reprocessing of radiation from a central object by a disc needs to be treated in a much more rigorous way than previously.

Effects of symbiotic binarity on the cool-star upper atmosphere and wind have not yet been fully studied. This aspect is obviously also linked to the uncertainties one still has about single cool giants. Perhaps the symbiotic phenomenon will be of help for a better understanding of the outer atmosphere of normal cool stars.

Colliding wind models need to be worked out in much more detail, in order, for instance, to better predict emission-line fluxes. Other situations where shock formation should occur also exist, and they must be carefully examined, in particular for wind accretion.

It is only when ideas based on much more careful research are confronted with better observations spanning many years that significant progress will be made about the symbiotic phenomenon.

Finally, along which lines should further reasearch be developed? We realize that new sophisticated observations really raise more questions than they yield answers. Each of us has made the claim "We need more observations". We surely do. But we need certain particular kinds of observations. We need observations involving a somewhat different approach than that which has been useful and appropriate so far. The traditional tendency to obtain bits and pieces of observations on as many objects as possible needs to be supplemented. There are many obvious gaps in the records of observation; many are even relatively easy to fill in. It is sobering to realize how little is actually known. For instance, we know little about spectra of dwarf novae during the outburst state, or about how they develop on time-scales of minutes or hours (rather than days), or what orbital photometric variations occur during outbursts, or whether they are of orbital (geometrical) origin or only occur on orbital time-scales. And we still don't know what triggers a dwarf nova outburst, or what causes many nova-like stars to drop in brightness. We believe the mass-transfer rate is responsible, but it is not clear why it changes in the first place; i.e., what the trigger is.

Furthermore, we now know that whatever observations of a system we obtain, these are not likely to be entirely characteristic of the particular brightness state we happened to monitor, but are likely to be merely one possible pattern. Observations at the same brightness level well may yield another result at some later time. Currently, we have only glimpses of the actual life of individual systems, without being able to appreciate how the most intricate interactions of all kinds of phenomena finally result in, for instance, the violent outburst events.

So what actullay is called for is long-term semi-continuous monitoring, in as many wavelength ranges and by as many means as possible. This has been tried for very few objects, with rather amazing, and quite unexpected results. Campaigns like these need to be repeated, and observing plans and schedules of the various working groups should be coordinated for observing times and for objects to be monitored. The priorities of committees for the allocation of telescope time need to be changed so that they finally realize that there is after all a lot of potential scientific merit in re-observing the same object over and over again. Results should be communicated quickly, rather than accumulating dust in offices and archives. Already existing material, belonging to individuals as well as hidden away in archives, needs to be made widely available and studied. And, last but not least, the countless amateur astronomers could and should be involved in systematic monitoring activities. They have the telescope time and the enthusiasm to observe, both of which many professional astronomers are lacking.

Astronomical satellites dedicated to the monitoring of stellar variability from X-ray to optical wavelengths are now being projected, and we hope they will soon be realized.

As for the theory, it seems that any possible progress heavily depends on observations to set limits to the nearly infinite number of possible combinations of parameters that govern computations of all aspects of cataclysmic variables. And here, at the current, still very general, state of the theory, it is necessary to resort to statistically significant samples of observations, in order to not mistake idiosynchrasies of individual systems for general patterns of the entire class. Investigations of this sort are still largely lacking. From comparison of features of such statistical samples with the theoretical results obtained from variations of parameters over wide limits (after parameters of only secondary importance have been ruled out beforehand) hopefully possible values can be limited to reasonably narrow ranges that then might yield realistic results; while most theoretically possible values can then be ruled out. Once such narrower limits will have been established, there is hope that computations could be used to actually determine systemic parameters from comparison with observations.

One further aspect of research in cataclysmic variables (but this is valid also for several other fields of research) should be changed, so work in later years can remain fruitful. The number and quality of publications should, in the first case decrease, in the second case increase. Over the last 20 years the number of papers, only restricted to the narrow field of cataclysmic variables and related stars, has increased almost exponentially, so that probably already by now a stage has been reached where it is practically impossible to read and fully assimilate all that is being published. Many fractional results are being turned out as individual publications, rather than as the results of complete investigations made available once all the work is done. Furthermore, there clearly is no need for publishing the same results several times in different journals or proceedings.

Our hope is that the monograph at hand will make it easy for theorists as well for observers to find their way into and through the jungle of results and papers. We tried to point out relations and gaps of knowledge. We hope this will become a useful reference book.

SUBJECT INDEX

abundances (see chemical composition)
absolute magnitude 5, 10-11
- dwarf novae and nova-like 4-5, 27-28, 161-162, 176, 216
- novae 5, 275-280, 294, 373
- symbiotics 5
accretion disk 3-4, 11, 351, 362
- column 188-192
- funnel 188
- hibernation model 294, 408-410
- inclination 294, 320, 373
- instability 3, 171-179, 181-184, 449-450
- luminosity 294, 320-321, 373, 411
- mass accretion rate 320-321, 406-408, 411-412
- models 320-321, 408
- pole 188-192
- power law 316-320
- shock 188-192
- symbotic 654-657
- ultraviolet spectrum 316-317, 319-324
- X-rays 342-345
Algol variables 146, 149, 216
alpha disk 154, 169-178
Alfven radius 153, 188, 191, 195
AM Canum Venaticorum stars 19-20, 95-96, 140-143, 178, 222, 229-230, 235
AM Herculis stars 19-20, 95-96, 125-140, 153, 188-191
anti-dwarf novae 19-20, 95-96, 102-112, 125, 172, 234
Bailey relation 27
Balmer continuum 593, 596
Balmer decrement 73, 135
Balmer jump 73, 81, 84, 110
Balmer lines (see spectrum)
banana diagram 56-57
beat period 50, 52, 123, 192
beat phenomena 50
Be stars 4, 599
binarity 6, 21, 145, 148, 150-151, 235
binary model 8-9, 589
binary period 9
binary system 6, 8-9, 418, 435-437, 442-443, 448-453, 485-487, 490-497, 523, 546-547, 556-558, 642, 651-661, 727-728
bipolar flow 658
black body disc 192-194
black dwarf 221-222
blue continuum 1, 593, 596
bolometric correction 164, 216
boundary layer 46, 73, 152, 154-155, 185-188, 194-195, 199, 207, 209, 212-214
BQ stars 4
B stars 207
bremsstrahlung 71-72, 188-189
bright spot (see hot spot)
carbon stars 594
Chandrasekhar limit 218, 220, 228, 410-411
chemical composition 170, 194, 207, 217-218, 220, 226-227, 315, 331-334, 336, 340, 341, 359-362, 381, 398, 400-403, 424, 426, 479-485, 510, 517, 562, 729-730
- CNO 330-331, 341, 359-361, 401-402, 407, 424, 522, 564
- neon 331, 334, 361, 404, 562
- O/H 360, 564
classical novae 11, 261-369, 371-410, 413-510
classification 1
- dwarf novae and nova like 15-17, 19, 234-235
- novae 262, 298-300
- symbiotics 583, 607-609
chromosphere-transition region-corona (see spectrum)
CN Orionis stars 16
colliding winds 656-661
color 32-35, 38-39, 41-42, 44-45, 47-48, 52-53, 69, 96, 98, 103-104, 112, 119, 121, 126-127, 134, 140, 147, 150, 160-161, 164, 171, 176, 178, 195, 199, 211-212
- of flickering 55
- of oscillations 58
- of superhump 52-53
- of X-rays (see hardness ratio)
combination spectrum 1
common envelope 217-219, 227-229
cool (late-type) component 592-596, 638-640
corona 65, 153, 155, 194, 199-200, 213
cycle-amplitude relation 511-512
cyclotron radiation 139, 188-190
decline 346-355, 587-588
degenerate star 222, 226-227, 229
descendants 215, 227-229
disc instability (see instability)
distance 7, 161-163, 212, 214, 351-352, 485-486, 518, 521
DQ Herculis stars 19-20, 95-96, 102, 112-124, 190, 234-235, 263, 317, 320, 485-487
D-type symbiotics 607-609 (see also classification)
D'-type symbiotics 607-609 (see also classification)
dust 300-303, 307-313, 403-404
- emission 404, 595
- formation 307, 408-404, 564
- opacity 394
dwarf novae 11, 15-94
eclipse 587, 589, 596, 601
eclipse mapping 163-164, 203-206, 209-212
eclipse, secondary 40-41, 44, 98, 102-103, 130-131
eclipsing binary 261, 485-487
Eddington limit 278-279, 329, 341, 371, 378, 385, 397-398, 400, 564-565
Einstein Observatory (see satellites)
electron density 381, 554
electron temperature 381, 554
energy
- distribution 420-421, 423, 446, 452, 465, 515, 517, 605
- radiative 5
- mechanical 5
envelope 5, 351-369, 372-373, 405-406, 424, 426, 428, 430, 440, 446-448, 467-470, 479-485, 501, 521-523, 13/18, 13/32-35, 731
evolutionary state 194, 214-231
EXOSAT (see satellites)
expansion velocity 5, 298-300, 414-415

extinction (reddening), interstellar 289, 320, 397, 623
extreme ultraviolet (EUV) 317, 320, 343
flare 42-43, 47, 97, 113, 117, 119, 121, 126, 128-129, 138
flickering 16, 35, 45, 50, 54-55, 60, 62, 78, 96-99, 103, 106, 113, 116, 118-119, 121, 126, 128-131, 140, 181, 262, 589
free-free
- emission 535, 554
- opacity 535, 554
gamma velocity 86-88, 92-94, 111, 138, 157, 184
gap (see period gap)
globular cluster 216
grain growth (see also dust) 403-404
gravitational radiation 163, 220, 222-231
hardness ration 71, 106
hibernation 230-231, 371, 408-410, 565
hot component 556-558, 622
hot spot 38, 46, 55, 64, 149, 152, 155-157, 164, 166, 168, 174, 187, 206
Hubble Space Telescope (see satellites)
hydrogen bound-free, free-free emission 554
imagery
- optical 424-425, 440, 475
- radio 617
individuality 3
instability
- disc 171-179, 181-184
- transfer 172, 178-181, 183-184
intermediate hump 35-36, 48
intermediate polar 119-124 (see also DQ Herculis stars)
interstellar absorption 65, 161-162, 216, 537
interstellar extinction (or interstellar reddening, see also extinction) 278, 320, 397, 623
ionization mechanism 596
IRAS (see satellites)
IUE (see satellites)
jets 693-694, 700
Keplerian velocity (see velocity)
Kukarkin-Parenago relation 26-27
K-velocity 79, 86-87, 94, 119, 138, 157-159, 161
late giant 4
late-type spectrum (see spectrum of the cool star)
light curve 371, 414, 427, 443-446, 460-461, 469, 491, 500, 513, 542, 544, 547, 585-592, 664, 666, 674-675, 679, 704-706, 710
limb darkening 194-195, 209
limit-cycle instability (see instability disc)
line profiles 417, 524-525, 598-599
- broad component, wings 593-594
- line width 599
- multiple structure 600
- P Cygni 2, 81-82, 84, 88, 90-91, 93, 99, 110-124, 155, 206-209, 213, 598-600
- WR features 596-599
LTE, non-LTE 195, 198, 206
luminosity
- bolometric 329-330, 341-342, 346-347, 371, 384, 397, 422, 475-476, 540, 547, 561, 564
- kinetic 398
magnetic accretion 124, 140, 188-192
magnetic braking 163, 219-220, 222-225, 228-229, 231
magnetic fields 96, 124, 139, 153-155, 165, 169, 184-186, 188-192, 199, 225, 230, 263, 593-595
maser emission 618-621
mass 9
- accretion 155,163, 207, 213-214, 222, 224, 227, 406
- determination 156
- ejection 376-378
- loss (see also P Cygni profiles) 94, 206-209, 218, 220, 223, 415, 517-518, 555
- ratio 1/9, 20-21, 157-158, 160-161, 184, 192, 199, 219-220, 222, 228
- stellar 21, 156-158, 160, 214, 216-219, 229
- throughput 163-164, 172, 193
- transfer 1, 5, 102, 154, 162, 164, 176, 178-179, 184, 186, 191, 193, 195, 199-201, 206, 211, 214, 222-225, 227-228, 230
Mira-type symbiotic stars 693
Mira variables 95, 694
models
- causes of outbursts 374-392
- central star dominant model 388-389
- combination of models 390-391
- continued ejection 342, 384-388, 564
- hibernation model 408, 565
- hidden parameters 374
- instantaneous ejection 382-384
- non-spherical models 408
- novae classical 378-391
- novae recurrent 391-392, 410
- nuclear burning 348
- snowplow 351
- symbiotic 647-661, 672-674, 679-683, 723-725
novae
- active phase 275-281, 296-300, 327-341
- catalogue 262
- distance 280, 351-352, 485
- general properties 261, 561-565
- infrared 299-314, 403-404, 419-423
- luminosity 268-270, 342
- masses 449, 502
- nebular phase 342-369, 466-467
- photometry 262-281
- quiescent phase 262-275, 281-296, 316-327
- remnant 561
- space density 409
- spectroscopy 281-299
- ultraviolet 315-342, 418-419
- variability on short time-scale 262-263, 266-268, 418
- X-ray 261, 342, 345-346, 405-406, 452
nova envelope (or shell) 351-356, 405-406, 424, 426, 446-448, 467-470, 501
- chemical composition 359-362, 381, 400-403, 424, 426, 479-485
- coolants 361, 489
- deceleration 351-355, 373,
- dust envelope 300-303
- expansion velocity 351-355
- filling factor 402
- masses 354-355, 403, 405, 410
- models 388, 405-406, 501
- morphology 356-359, 361, 372-373, 425, 428, 430, 440, 475
- radio emission 366-369, 405, 423-424
- recurrent novae circumstellar envelope 391-392
- snowplow model 353, 390

- spectra 360-363, 365-366, 439-440, 442
- structure 361, 364-365, 405-406
- temperature 361, 480
nova-like stars 1, 3, 95-144, 292
nova outburst
- absolute magnitude 275-281, 438, 459, 488, 491
- causes (classical novae) 406-410, 564-565
- causes (recurrent novae) 410-412, 565
- classification 275-279, 373
- energy (mechanical) 5, 297, 398
- energy (radiative) 5, 297, 408
- expansion velocity 298-300, 351-354, 374, 564
- extreme ultraviolet radiation (EUV) 343
- infrared emission 300-314, 467-470, 561
- light curves 275-280, 414, 427, 450, 491
- light curves bolometric 330, 332, 371, 468-469
- light curves infrared 302-304, 306, 308, 371, 468-469
- light curves optical 275-280, 348, 371, 383-384, 460-462, 471, 475, 500
- light curves radio 371, 473-474
- light curves ultraviolet 330, 371, 474
- light oscillations 393, 444
- speed class (see classification)
- ultraviolet radiation 327-342, 474
- X-ray radiation 346-347
nova outburst spectra 296-300, 372-373, 417, 426-428, 438-439, 460-461, 465-466, 470-475, 490-492, 500-510
- continuum 394-400
- coronal lines 298, 391-392, 510
- diffuse-enhanced 297, 373, 380, 391, 393
- nebular 297, 373, 380, 391, 393, 400
- orion 297, 373, 380-381, 391, 393, 509-510
- post-nova 298
- pre-maximum 297, 373, 380, 390, 393, 401, 502
- principal 297, 373, 380, 391-394, 401
- recurrent nova 337, 339-341
- stratification 393
- ultraviolet 327-342, 464
OAO-2 (see satellites)
OH/IR source (see maser)
old disk population 600-601
old nova (see quiescent nova)
orbit (see binary period)
oscillations (see also pulsation) 35, 54, 56-64, 113, 185, 192, 213, 234-235, 372
- coherent 54, 56-64, 98, 114, 116-119, 122, 124, 130, 185, 234, 262-263
- colors 58-59
- dwarf nova (see coherent oscillations)
- quasi-periodic 54, 58-64, 106-107, 119, 126, 129-130, 140-141, 185-186, 265-268
- white dwarf (see coherent oscillations)
O stars 207
outburst 5, 21, 586-588, 600
- anomalous 22-23, 34
- duration 5
- interval between 5
period 263, 589-592
- binary 9
- changes 45-46, 97-98, 111, 115, 119, 121, 124, 186-188, 264
- gap 9, 20, 24, 126, 163, 219, 222-226, 235
- orbital 9, 20-21, 193, 221-222, 226-227, 229
- outburst 17, 27-28
- jitter 140
photosphere (see quasi-photosphere or pseudo-photosphere)
planet 227, 229
planetary nebulae 228, 583-584, 596
polars (see AM Herculis stars)
polars intermediate (see DQ herculis stars)
polarization 64-65, 96, 98, 106, 113, 125, 127, 129-135, 140, 188, 190, 263, 461, 603-605
population 216
pre-cataclysmic variables (see also progenitors) 228
pre-nova 262, 281
primary star (see also white dwarf)
progenitors 215-216, 219, 227-229
pulsation (see also oscillations) 591
- white dwarf (see coherent oscillations)
- X-ray 60-61, 106-107, 124, 130, 213, 269
quasi-periodic oscillation (see oscillations)
quasi-photosphere (or pseudo-photosphere) 384, 394
- density 373
- mass-loss 394, 397
- pressure 373
- radii 385-386, 388
- temperature 386, 394
quiescent nova (see also nova) 262-275, 281-296, 373-374
- absolute magnitude 280, 374
- disc instabilities 411, 457
- light curve 264-265, 269-275, 435-437, 444
- orbital inclination 293-294, 501
- orbital periods 442, 448, 486, 502, 562
- oscillations 458-459, 476
- photometric properties 262-275, 435-438, 449-453, 457-459, 486, 487-488, 490-491, 562
- radial velocity 435, 438, 442, 449
- spectra 281-296, 373, 427, 441, 452, 455, 489-492
- ultraviolet line spectrum 324-325, 432-433, 490, 497
- ultraviolet radiation 315-320, 430-433
- ultraviolet spectral variability 324-326, 430-433, 495, 498
- X-rays 342-346, 442, 457, 484, 498, 563
quiescent recurrent nova 513-514, 519, 525-531, 542, 546-548
- photometry 547
- radial velocity 546
- spectrum 326-327, 515-516, 519-521, 538-540, 546
- UV spectrum 519, 521, 539-540, 549-554
- X-ray 556-557
radial velocity 35, 76, 78-81, 86-88, 92-93, 102, 109-110, 117, 119, 123-125, 134, 138-139, 142, 148, 150, 156-161, 187, 200, 202, 209, 212, 218, 600-601
radio emission 4, 65, 73, 119, 134
- from novae 366-369, 405, 473-474
- novae: emission mechanism 366-369
- novae: extended radio sources 366, 368
- novae: radio envelope masses 366
- novae: radio light curve 367, 405
- novae: radio spectra 369
radius, disc 160
radius primary star 153-160, 187, 199, 214, 216
- secondary star 156, 160-161, 219

R Coronae Borealis stars 147
recurrent nova 1-3, 511
- amplitude-cycle length 511-512
- chemical composition 517
- companion 518, 556-558
- definition 512-513
- distance 518, 521
- infrared spectrum 533-535
- mass-loss 517-518, 555
- model 547-548
- nebular spectrum 521-522
- orbital radial velocity 546
- outburst cause 410
- radio emission 369, 405, 537-538
- ultraviolet spectra 327-329, 334, 337, 339-340, 539-540, 550-552
- X-ray 392-393, 541-542
revurrent nova envelope 392, 521-523
recurrent nova outburst 523-532
- coronal lines 519, 524, 531, 544
- expansion velocity 513, 543
- light curve 513, 519, 542
- outburst mechanism 543
- spectrum 514-515, 519-531, 523, 536, 539-540, 541, 543-544, 546
- UV spectrum 516-517, 539-540
reddening (see extinction)
rejuvinated white dwarf 652-654
reversed X-ray mode 129, 131, 140
Roche model 3, 7, 38, 67, 92, 95, 145, 148, 150-153, 156, 163, 192-193, 209, 233, 235, 376
rotational braking (see magnetic braking)
rotational disturbance 102, 111, 117, 122, 296
RW Aurigae stars 95
satellites
- ANS = astronomical Netherlands satellite 329
- Ariel V 344
- COPERNICUS = OAO-3 329
- EINSTEIN = HEAO-2 261, 342-345, 484, 563
- EXOSAT 261, 269, 340, 344-346, 532, 563
- HEAO-1 = High Energy Astronomical Observatory-1 342
- HST = Hubble Space telescope 299
- IRAS = Infrared Astronomical Satellite 310-314, 532-534, 558
- IUE = International Ultraviolet Explorer 261, 263, 316- 317, 323-331, 333-336, 341, 361, 521, 532, 539-540, 561-562
- OAO-2 = Orbiting Astronomical Observatory-2 263, 329
- Voyager 320
S-curve 170, 172-178
shell (see envelope)
single star model 649-651
Sobolev approximation 202-203, 209
solar dynamo (see magnetic braking)
solar-type chromosphere 598
space density 7, 215, 228
space distribution 7-8, 214-216
spectrum 281-298, 416-417, 427-428, 461-466, 467, 490, 503-510, 540
- absorption 1/3, 73, 75, 78-83, 86-87, 117, 119, 134, 139, 151, 157, 161, 546, 550-552, 583, 592-595, 600
- emission line 1/3, 297-298, 441, 514-516, 519-520, 523- 531, 545, 550-552, 596-600, 627-630, 729
- high ionization 298, 466, 467, 490, 531, 661
- infrared 3, 299-314, 419-422, 531, 536, 605-613, 719-720, 722
- molecular 588, 592-595
- optical 665
- quiescent 4
- radio 3, 366-369, 424, 473-474, 519, 538, 613-618, 719-720, 722-723
- ultraviolet 2-3, 315-320, 418-419, 430-432, 466, 495-499, 516-517, 539-540, 550, 622-634, 664-671, 675, 678-683, 697-699, 703-704, 716-721
- variations 2, 415-417, 454-457, 470-475, 630-631, 710-711, 730-731
- X-ray 2-3, 342-346, 498-499, 541-542, 634-636, 681-682, 723
SS Cygni stars 16
standstill 16-18, 29, 31, 48, 56, 66, 84, 88, 234-235
Stark effect 147, 202, 206
statistics 7, 19
supercycle 29-31
superhump 16-18, 42, 49-54, 84, 86, 88, 113, 185
- color (see color)
- late 48-50, 184
- period 49-50
supermaximum (see superoutburst)
supernova 15, 216-218, 229
superoutburst 16-19, 21, 24, 29-32, 34, 48-54, 56, 60, 62, 68, 71-72, 94-88, 90-91, 235
- models 184-185
- period 30-32
surface brightness 162, 166
surface density 166, 168, 170-172
SU Ursae Majoris stars 16-21, 24, 29-32, 42, 48-54, 157, 184, 234-235
S-wave 80, 86, 91, 94, 102, 110, 122, 124, 137, 142
symbiotic novae 4, 296, 587-589, 596, 635-636, 683-693
symbotic stars 1, 3, 583-585, 728-729
- accretion processes (winds) 654-661
- activity phase 586, 665-667, 678-679
- binary models 651-654
- blue spectrum 596-598, 675, 706
- emission lines 596-600, 627-630, 697-699
- infrared observations 605-613, 719-720, 722
- light curves 585-592, 664, 666, 674-677, 704-706, 710
- line profiles 598-600, 627-630, 697-699
- magnetic fields 601-603
- maser emission 618-621
- models 647-651, 672-674, 679-683, 723-725
- polarization 603-605
- quiescent phase 586, 664-665
- radial velocity 600-601
- radio imagery 616-618
- radio observations 613-616
- red component 592-596, 638-640
- UV spectrum 622-634, 664-671, 675, 697-699, 703-704, 716-721
- X-ray 634-636, 681-682, 723
symbiotic phenomenon 583-584, 638
temperature 381, 392-393, 402
- color 381

- excitation 381
- ionization 381
- Zanstra 381, 394, 555-556
thermonuclear runaway (TNR) 3, 341, 371-373, 376, 406-412, 564
tidal forces 168, 184, 225, 228
transfer instability (see instability)
two-color diagram 32-34
type CV's (see classification)
U Geminorum stars 16-21, 230, 234, 235
ultraviolet delay 67-68
ultraviolet flare (see flare)
UV Per stars 16
UX Ursae Majoris stars 19-21, 95-102, 172, 230, 234
variability 1-2, 6, 261-262, 415-417, 583, 586
- irregular 586-587, 589
- long term 458-459, 586-589
- periodic 415-417, 589-592
- quasi-periodic 591
- secular 592
- short term 262-263, 266-268, 415-417, 457, 587, 589, 598
veiling 593, 596
velocity
- expansion 298-299
- gradient 380
- Keplerian 152, 154-155, 165, 169
- radial (see radial velocity)
- radius correlation 398-400, 428, 429
- stratification 393-394
viscosity 154-155, 165-166, 168-169, 170-183, 200-210, 214
VY Sculptoris star (see anti-dwarf nova)
white dwarf 4, 374, 556-558, 601
- CO 341, 562
- luminosity 406
- mass 374, 409
- O-Ne-Mg 341, 404, 408, 562
- pulsation (see coherent oscillations)
wind 385-387,393, 397
Wolf-Rayet stars 207, 373
WSagittae stars 17
W Ursae Majoris stars 42, 44-45, 149, 216, 228
X Leonis stars 16
X-ray source 268, 317, 336, 340-341, 342-346, 391, 634-638
- nova emission 342-346
- recurrent nova in outburst 346, 392-393
- symbiotics 634-636, 13/19-20
yellow symbiotic stars 608
Zanstra temperature (see temperature)
Z camelopardalis star 16-18, 20, 29, 48, 56, 146, 148, 172, 230, 234-235
Zeeman splitting 134, 139-140, 188, 190
Z-wave 79

STAR INDEX

Z And 4, 290, 584-587, 589, 592-593, 596-598, 607, 612-613, 621, 623, 626, 628, 631-632, 641-644, 648-649, 651, 660, 663-674, 729

RX And 55, 64-65, 68, 82, 89, 285, 287

AR And 222, 287

EG And 592, 598-599, 601-602, 608, 624, 641, 643-644, 651

R Aqr 598, 604, 606, 608-612, 616, 619, 632, 634, 635, 637-638, 641, 644, 648, 650-651, 656, 693-703

AE Aqr 64, 80, 95, 112-113, 117-119, 145, 148, 200, 234, 274-275, 290

FO Aqr 112, 123-124, 191

UU Aql 287

V 603 Aql = N Aql 1918 112, 193, 200, 263, 266, 277, 281-282, 284, 286, 299, 312, 316, 318-320, 322, 324-325, 327, 343-344, 348, 351-354, 356, 372, 381-382, 389, 393-398, 413, 426-438

V 605 Aql = N Aql 1919 310, 312-313

V 1301 Aql = N Aql 1975 304, 404

V 1370 Aql = N Aql 1982 304, 308-311, 314, 332-335, 342, 354, 366, 394, 562

TT Ari 35 103-108, 110, 112, 124, 187, 234, 274-275, 290

FS Aur 287

KR Aur 108, 110, 290

SS Aur 26, 28, 287

T Aur = N Aur 1891 277, 285-286, 314, 316, 320, 352, 357, 359, 375, 414, 487-490

UV Aur 593-595, 641, 643-644

V 363 Aur 98, 100

UZ Boo 73

AF Cam 222

Z Cam 18, 25-26, 28, 31, 34, 39, 64, 66, 90-91, 274, 287

HT Cas 288
AC Cnc 37

SY Cnc 57-58, 66, 274

YZ Cnc 55, 91, 274-275

HL CMa 77, 85-86

BG CMi 112

AM CVn 140-143, 227

TX CVn 601-602, 641, 643

OY Car 36-37, 39-43, 47-48, 50-53, 58, 77, 80, 82, 84, 90-91

HT Cas 32, 37, 55, 58, 70, 76, 79-80, 185, 274, 288

BV Cen 36, 55, 78

V 436 Cen 34, 36, 49-50, 73, 77, 274

V 442 Cen 274

V 803 Cen 140-141

V 834 Cen 130, 138-139

W Cep 602

IV Cep = N Cep 1971 366

VV Cep 648

WW Cet 26, 34, 76, 288

Omicron Ceti 619, 634, 638

Z Cha 37-38, 46-48, 50-52, 67, 76, 80, 84-87, 93, 185, 203, 203-206, 211-212, 274

SY Cnc 288

YZ Cnc 288

TV Col 112-113, 124

GP Com 140-142, 227

T Cor 314

V 394 CrA = N CrA 1949, 1987 328, 752

V 693 CrA = N CrA 1981 328, 332, 334, 562

T CrB = N CrB 1886, 1946 4, 230, 277, 285, 287, 296, 298-299, 311-313, 316, 319, 322, 326, 343, 348, 366, 368-369, 375, 391-392, 411, 511, 543-558, 561, 563, 565, 589, 598, 601-602, 609, 641, 644, 648, 651, 752

BI Cru 598-599, 610-611, 640, 641, 644

BF Cyg 583, 587-588, 596, 599, 639, 641, 644, 648

PRECEDING PAGE BLANK NOT FILMED

CH Cyg 587, 589, 593, 598, 601-604, 617-618, 620-621, 623, 625, 627, 631-632, 634, 637, 641, 643-644, 650-651, 663, 703-725, 728, 730

CI Cyg 64, 583, 587, 589-590, 592-593, 596, 598-599, 604-605, 607, 619, 626, 632, 641, 643-644, 648, 660, 727

EM Cyg 24-25, 40, 67, 69, 78, 80, 161, 217, 219, 274, 288

EY Cyg 8, 150

SS Cyg 15, 18-19, 22-26, 30, 32-34, 40, 42-43, 59, 60-61, 64, 66, 68-72, 74, 76, 79-83, 85-87, 128, 145-148, 150, 157, 159, 161, 176, 193, 213, 274-275, 288, 343

V 476 Cyg = N Cyg 1920 352, 354

V 503 Cyg 74

V 1016 Cyg = MH 328-116 585, 588, 595-596, 599, 601, 604, 606-607, 610, 612-617, 623, 628, 634-635, 641, 644, 651, 654, 683-684, 688-691, 693, 727, 752

V 1329 Cyg = HBV 475 584, 588, 593, 596-597, 599-600, 607, 613-614, 632, 641, 644, 654, 658, 683-684, 688-691, 693, 752

V 1500 Cyg = N Cyg 1975 263-264, 266, 277, 279, 297-300, 304-307, 347, 349-350, 352, 354, 366-368, 372, 392, 394, 401, 403, 405, 413-426, 753

V 1668 Cyg = N Cyg 1978 265-267, 294, 300, 303-305, 330-331, 334-335, 349, 354, 372, 403-404, 413, 460-470

CM Del 74

HR Del = N Del 1967 112, 261, 266, 269, 277-278, 280-281, 298, 300, 312-314, 316-320, 322-323, 325, 343, 350, 352, 354, 360, 366-368, 389, 401, 404-405, 414, 500-510, 561, 563

AB Dra 70, 288

AG Dra 584, 587, 591-594, 596, 598-602, 612, 622-628, 630, 632, 634, 636-637, 641, 643-645, 651, 655, 663, 674-683, 730-731

YY Dra 290

EF Eri 126-128, 130, 133-135, 138

DN Gem = N Gem 1912 277, 285-286, 299, 354, 389

IR Gem 288

U Gem 15, 19, 24-26, 30, 37, 40-42, 59-61, 64, 66, 68, 70-72, 74, 76, 78, 80, 145-147, 161, 187, 205, 213, 217, 219, 274-275, 288

AH Her 17, 34, 57-58, 64, 88-89, 176, 274, 289

AM Her 95, 125-126, 128-135, 137-140, 290

DQ Her = N Her 1934 112-117, 145, 148,187, 191, 205, 234, 262, 267-268, 274-275, 277, 286, 295, 299, 311-312, 314, 316, 320, 323, 345, 352, 354-355, 359, 361, 366, 373, 376, 378-379, 381, 393, 400-403, 413, 475-487

V 433 Her = N Her 1960 696, 641

V 446 Her = 262, 352

V 533 Her = Her 1963 112-113, 117, 262, 274-275, 277, 281-282, 286, 298, 316, 352, 354, 366

YY Her 641, 644

EX Hya 20, 112-113, 119-122, 124, 134, 289

R Hya 619

RW Hya 583, 592, 601-602, 641-644

BL Hyi 126, 131, 138

VW Hyi 16-18, 24-26, 29-31, 33-36, 40-41, 47-53, 60-64, 66-68, 71-72, 74-75, 84-85, 88-89, 176, 181-182, 213, 274-275, 282

WX Hyi 50, 68-69, 74-75, 88

CP Lac = N Lac 1936 348, 351-352, 355, 381-382

DI Lac = N Lac 1910 285-286, 348, 353

DK Lac = N Lac 1950 353, 381, 391

T Leo 80, 157-158, 289

X Leo 25-26, 274, 289

DP Leo 125-126, 128, 130

ST LMi 130, 132-135, 139

AY Lyr 26

CY Lyr 82

HR Lyr 353

MV Lyr 95, 103-104, 106-108

TU Men 20, 24, 26, 32, 52, 85-87, 93, 222, 235

BT Mon = N Mon 1939 202, 230, 262, 285-286, 294, 316, 320-321, 352, 409

BX Mon 591-593, 599, 602, 641, 644

GQ Mus = N Mus 1983 311-312, 314, 328, 337-338, 341-342, 345-346

SY Mus 591-592, 596, 641, 644

IL Nor = N Nor 1893 348, 375

RS Oph = N Oph 1898, 1933, 1958, 1967, 1985 4, 16, 277, 296, 285, 287, 300, 312-313, 316, 322, 327-328, 337, 339-341, 346, 355, 368-369, 391-392, 411-412, 511-512, 523-542, 563, 565, 589, 598, 602, 609, 641, 644, 752

V 426 Oph 64, 290

V 442 Oph 290

V 841 Oph = N Oph 1848 269, 284, 286, 316, 323, 343, 353

V 2051 Oph 37, 39, 55, 274, 290

V 2110 Oph = AS 239 290, 588, 684, 688

BI Ori 26

CN Ori 26, 35, 42-43, 46-48, 58, 68, 79, 82, 111, 124, 181-182, 235, 274, 289

CZ Ori 26, 289

AR Pav 587, 592, 601, 609, 641, 644, 727

BD Pav 40, 42, 44-45

RU Peg 26, 54, 57, 59, 78, 161, 274, 289

AG Peg 588-589, 591-592, 596, 598-599, 601, 603, 605, 613, 617, 619-620, 623, 628, 630, 641, 643-644, 649, 651, 654, 683-684, 688-690, 693, 729-730

IP Peg 37

TZ Per 73

UV Per 26, 74

AX Per 583-584, 591, 599, 601, 609, 619, 631, 641, 643-644, 648-649, 663, 730

GH Per 296, 343

GK Per = N Per 1901 28, 176, 222, 230, 261, 268-269, 274-275, 277, 285-286, 294, 316-317, 320, 344, 348, 352-353, 355, 359, 361, 368-369, 312, 375, 382, 389, 394-395, 397-399, 413, 443-459, 562-563, 753

KT Per 274, 289

V 471 Per 608

RR Pic = N Pic 1925 193, 231, 262, 269-275, 277-278, 284, 299, 314, 322, 325, 343-344, 348, 350, 352-353, 355, 357-363, 375, 382, 396, 398, 400, 414, 490-499, 561

AO Psc 113, 122-123, 191

TY Psc 50

CP Pup = N Pup 1942 9, 264-265, 277, 282, 284, 316, 343, 353, 359, 361, 392, 413-414, 438-443, 562

RX Pup 598-599, 607, 609-612, 615, 632-633, 641, 644

UY Pup 26

VV Pup 125-127, 129-132, 135-136, 138, 189, 290

T Pyx = N Pyx 1890, 1902, 1920, 1944, 1966 277, 284-285, 287, 298-300, 316, 326-327, 355, 359, 362, 412, 511, 519-523, 563, 565, 752

CL Sco 291

FQ Sco 26

HK Sco 291

KP Sco 312-313

T Sco 216, 352

U Sco = N Sco 1863, 1906, 1936, 1979, 1987 4, 300, 328, 334-335, 412, 511, 513-519, 563, 752

V 711 Sco 277

VZ Scl 103, 107

EU Sct 312

N Sct 1991 368

V 368 Sct = N Sct 1970 353, 366

V 373 Sct = N Sct 1975 298, 353

CT Ser 284

FH Ser 277, 279, 285, 287, 300, 302, 304-308, 310-314, 328, 348, 352-353, 355, 366-368, 384, 389, 397-399, 403-405, 413, 470-475, 561, 564

LW Ser = N Ser 1978 302, 304, 404

LX Ser 98, 103-104, 107, 110, 201

MR Ser 126, 135

MU Ser = N Ser 1983 310

RT Ser = N Ser 1909 296, 588, 601, 641, 644, 654, 684, 688-690, 693, 752

UX Ser 26, 69

UZ Ser 282

X Ser 287

RW Sex 274

SW Sex 97-98, 102, 201

HM Sge 585, 588, 596, 599, 604, 606-607, 609, 612-614, 616-617, 628, 634-636, 641, 644, 654, 683-684, 688, 690-691, 693, 730

RZ Sge 76-77

V Sge 16, 95, 291

WY Sge = N Sge 1783 231, 269, 274, 294-296, 353, 374, 414, 561, 751

WZ Sge = N Sge 1913 1, 17, 24, 29, 40, 42, 44-45, 50, 52-53, 63, 67, 91-94, 112-113, 122, 134, 268, 274, 289, 512

LG Sgr = N Sgr 1897 312-313

V 949 Sgr = N Sgr 1914 277, 312

V 1016 Sgr 312, 313

V 1017 Sgr = N Sgr 1919 (1901, 1973) 4, 8, 150, 285, 343, 369, 511, 542-543, 651, 752

V 1059 Sgr 343

V 1148 Sgr = N Sgr 1943 297

V 1223 Sgr 112-113, 123-124, 191

V 3885 Sgr 98, 100, 274, 282

V 3890 Sgr 291

V 4077 Sgr = N Sgr 1982 311-312, 314, 328, 335-336, 366, 368

RR Tel 4, 296, 312-313, 588, 591-592, 596-599, 601, 607, 608-611, 613-614, 621, 624, 627-629, 632, 634-635, 639, 641-642, 644, 654, 683-691, 693, 727, 729, 752

EK TrA 67,86

RW Tri 55, 64, 80, 97-99, 101-102, 128, 207, 212

AN UMa 125, 130, 291

SU UMa 17, 26, 32, 66-68, 73

SW UMa 148, 289

UX UMa 97-98, 100, 114-115, 149-150, 187, 192, 207, 274, 291

CQ Vel 313

IX Vel 97, 99-100, 102

KM Vel 611

TW Vir 40, 74, 289

CK Vul = N Vul 1670 231, 269, 294, 310, 314, 362, 364-366, 374, 414, 561, 751

LV Vul = N Vul 1968/1 277, 279, 352, 355

NQ Vul = N Vul 1976 277, 279, 303-305, 312-313, 355, 366, 368, 372, 403

PU Vul 588, 605, 612, 630, 632, 641, 644, 663, 684, 688-693, 728, 730

PW Vul = N Vul 1984/1 328, 336, 345-346

QQ Vul 126-127, 131-132, 136-137, 140

QU Vul = N Vul 1984/2 312, 328, 339, 345-346, 372, 404, 562

2A 0311-227 290

AS 201 608, 614

AS 239 see **V 2110 Oph**

AS 289 584

AS 296 601

AS 338 604, 606

BD -7 3007 = RW Sex

CD -42 14462 = X 3885 Sgr

CDP -48 1577 = IX Vel

E 2000 +223 314, 351

1E 0643.0 288

G 61-29 = GP Com 290

GD 1662 = VY Scl

GX 1+4 (4U1728-24) 634

2H 2215-086 291 291

H1-36 613-615, 617, 727

H2-38 596, 610

He 2-17 614

He 2-34 610, 612

He 2-38 596, 611, 614, 641

He 2-106 610-612

He 2-390 614

HD 149427 594, 608, 641

HD 330036 594, 641

HZ 29 = AM CVn

Lanning 10 = V 363 Aur

LMC S63 595-596, 641, 644

LMC SN 1987a 384

M1-2 594, 608, 641

PS 74 274

PS 141 = VY Sci

UKS Ce-1 595

Weaver star 595

X0139-608 = BL Hyi

X0311-277 (2A, 3A) = EF Eri

X0527-328 (2A, 3A) = TV Col

X0538+608 (H) 126, 135

X0643-1648 (1E) = HL CMa

X1729+103 (3A) = BG CMi

X1012-029 (PG) = SW Sex

X1013-477 (H) = KO Vel

X1103-254 (CW) = ST LMi

X1114+182 (1E) = DP Leo

X1140+719 (PG) = DO Dra

X1346+082 (PG) 140-142

X1405-451 (H) = V 834 Cen

X1550+191 (PG) = MR Ser

X2003+225 (H) = QQ Vul

X2215-086 (H) = FO Aqr

X2252-035 (H) = AO Psc

0623 +71 291, 351

LIST OF CONTRIBUTING AUTHORS

Antonio Bianchini

Osservatorio Astrofisico
Via Dell Osservatorio 8
I 36012 Asiago, Italy

Hilmar W. Duerbeck

Astronomishes Institut
Universitat Muenster
Domagkstrasse 75
D 4400 Muenster, Germany

Michael Friedjung

Institut d'Astrophysique
98 bis Boulevard Arago
F 75014 Paris, France

Margherita Hack

Osservatorio Astronomico
Via G. B. Tiepolo 11
I 34131 Trieste, Italy

Constanze la Dous

(preparation of Part I)
Osservatorio Astronomico
Trieste, and ...
Institute of Astronomy
University of Cambridge
(current)
EAS/IUE Observatory
Villafranca del Castillo
Apartado 50727
E 28080 Madrid, Spain

Pierluigi Selvelli

OAT
Box Succ Trieste 5
Via G. B. Tiepolo 11
I 34131 Trieste, Italy

Roberto Viotti

IAS
CNR
CP 67
I 00044 Frascati, Italy

PRECEDING PAGE BLANK NOT FILMED

END

DATE

FILMED

JUN 13 1995